





AERONAUTICS

THIRTEENTH ANNUAL REPORT

OF THE

NATIONAL ADVISORY COMMITTEE FOR AERONAUTICS



1927



UNITED STATES
GOVERNMENT PRINTING OFFICE
WASHINGTON
1928

ADDITIONAL COPIES

OF THIS PUBLICATION MAY BE PROCURED FROM
THE SUPERINTENDENT OF DOCUMENTS
U. S. GOVERNMENT PRINTING OFFICE
WASHINGTON, D. C.

AT

\$1.25 PER COPY (PAPER COVERS)

LETTER OF SUBMITTAL

To the Congress of the United States:

In compliance with the provisions of the act of March 3, 1915, establishing the National Advisory Committee for Aeronautics, I submit herewith the thirteenth annual report of the committee for the fiscal year ended June 30, 1927.

Attention is invited to the remarks of the committee on the death of its late chairman, Dr. Charles D. Walcott, on whose advice the committee was established by the Congress in 1915. At a time when there was but little appreciation of the value of aeronautics and but slight conception of its problems, Doctor Walcott had the vision to see the need for organized scientific research on the fundamental problems of flight. The establishment of the National Advisory Committee for Aeronautics, the development of its usefulness in the formulation of policies, and the results of its labors in the field of research are a tribute to the leadership of Doctor Walcott and stamp him as a great constructive force in the upbuilding of American aeronautics.

The technical improvement in the performance and efficiency of aircraft for all purposes, the policy of the Government in the regulation and encouragement of aviation, and the great impetus given to aeronautical development during the past year by the transoceanic flights of Lindbergh and others have combined to cause a broader recognition of the practicability of aircraft as a means of transportation that I believe is destined to play an ever increasing part in the advance of civilization.

The attention of the Congress is invited to Part V of the committee's report, presenting a summary of the present state of aeronautical development. It is gratifying to note the committee's opinion that aeronautical progress in the United States during the past year has surpassed the hopes of a year ago, and that the present governmental policy is primarily responsible. I concur in the committee's judgment that further substantial progress in aeronautics is dependent largely upon the continuous prosecution of scientific research.

CALVIN COOLIDGE.

THE WHITE HOUSE,
December 8, 1927.

LETTER OF TRANSMITTAL

NATIONAL ADVISORY COMMITTEE FOR AERONAUTICS,
Washington, D. C., November 26, 1927.

MR. PRESIDENT:

In compliance with the provisions of the act of Congress approved March 3, 1915 (Public, No. 271, 63d Cong.), I have the honor to transmit herewith the thirteenth annual report of the National Advisory Committee for Aeronautics for the fiscal year ended June 30, 1927.

During the past year the committee lost the services of its chairman, Dr. Charles D. Walcott, who died on February 9, 1927. He was the founder of the committee and for 12 years had served actively in the development of American aeronautics and in the framing of national policies. His services in the development of American aeronautics, especially during the war period, were of inestimable value to the Nation. Attention is invited to a brief summary of his major contributions to aeronautics presented in the beginning of the committee's report.

The year 1927 witnessed substantial and gratifying progress in the scientific study of the fundamental problems of flight and in the technical development of aircraft for all purposes. This year will always be noted for remarkable demonstrations of the uses of aircraft. Such failures as occurred emphasize the great necessity for adequate preparation and for further scientific research and development.

Attention is invited to Part V of the committee's report presenting an outline of the present state of aeronautical development. The report concludes with a summary of the factors that have contributed to the advancement of American aeronautics to the point where the development and use of American aircraft, military, civil, and commercial, are such as to meet the present demands or to indicate the lines of progress in the years to come.

In the opinion of the National Advisory Committee for Aeronautics the present gratifying position of American aeronautics and the growing rate of progress in its development are due primarily to the effective prosecution of the Government's sound aeronautical policy.

The committee reiterates its belief in the necessity of continuous fundamental research as the basis of continuous substantial progress.

Respectfully submitted.

JOSEPH S. AMES,
Chairman.

THE PRESIDENT,
The White House,
Washington, D. C.

CONTENTS

	Page
Letter of submittal.....	III
Letter of transmittal.....	V
Thirteenth annual report.....	1
The death of Dr. Charles D. Walcott, chairman.....	1
PART I. ORGANIZATION	
Functions of the committee.....	5
Organization of the committee.....	6
Meetings of the entire committee.....	6
The executive committee.....	7
Subcommittees.....	7
Quarters for committee.....	9
The Langley Memorial Aeronautical Laboratory.....	9
The Office of Aeronautical Intelligence.....	10
Financial report.....	11
PART II. GENERAL ACTIVITIES	
Consideration of aeronautical inventions.....	12
Relations with the aircraft industry.....	14
The committee's research program in relation to nonmilitary aircraft.....	14
The Daniel Guggenheim Fund for the Promotion of Aeronautics.....	15
Conference of representatives of educational institutions actively engaged in aeronautical education.....	16
Cooperation of Army and Navy.....	17
Investigations undertaken for the Army and the Navy.....	17
Use of nongovernmental agencies.....	18
Cooperation with British Aeronautical Research Committee.....	18
Exhibit at the National Sesquicentennial Exposition.....	19
International Congress on Aerial Navigation, Rome.....	19
The air mail service.....	19
PART III. REPORTS OF TECHNICAL COMMITTEES	
Report of committee on aerodynamics.....	21
Report of committee on power plants for aircraft.....	33
Report of committee on materials for aircraft.....	44
PART IV. TECHNICAL PUBLICATIONS OF THE COMMITTEE	
Summaries of technical reports.....	53
List of technical notes issued during the past year.....	62
List of technical memorandums issued during the past year.....	63
List of aircraft circulars issued during the past year.....	65
Bibliography of aeronautics.....	66
PART V. THE PRESENT STATE OF AERONAUTICAL DEVELOPMENT	
Progress in technical development.....	67
Aerodynamics.....	67
Airplane structures.....	70
Airships.....	72
Aircraft engines.....	74
Summary.....	75
Conclusion.....	76

TECHNICAL REPORTS

	Page
No. 257. Pressure Distribution Over a Wing and Tail Rib of a VE-7 and of a TS Airplane in Flight. By J. W. Crowley, jr.-----	77
No. 258. Some Factors Affecting the Reproducibility of Penetration and the Cut-off of Oil Sprays for Fuel-Injection Engines. By E. G. Beardsley-----	115
No. 259. Characteristics of Propeller Sections Tested in the Variable Density Wind Tunnel. By East- man N. Jacobs-----	125
No. 260. The Effect of a Flap and Ailerons on the N. A. C. A. M-6 Airfoil Section. By George J. Higgins and Eastman N. Jacobs-----	141
No. 261. Resistance and Cooling Power of Various Radiators. By R. H. Smith-----	161
No. 262. Friction of Aviation Engines. By S. W. Sparrow and M. A. Thorne-----	177
No. 263. Preliminary Flight Tests of the N. A. C. A. Roots Type Aircraft Engine Supercharger. By Arthur W. Gardiner and Elliott G. Reid-----	205
No. 264. Differential Pressures on a Pitot-Venturi and a Pitot-Static Nozzle over 360° Pitch and Yaw. By R. M. Bear-----	221
No. 265. A Full-Scale Investigation of Ground Effect. By Elliott G. Reid-----	231
No. 266. Air Force and Moment for N-20 Wing with Certain Cut-outs. By R. H. Smith-----	239
No. 267. Drag of Wings with End Plates. By Paul E. Hemke-----	251
No. 268. Factors in the Design of Centrifugal Type Injection Valves for Oil Engines. By W. F. Joachim and E. G. Beardsley-----	265
No. 269. Air Force Tests of Sperry Messenger Model with Six Sets of Wings. By James M. Shoemaker-----	281
No. 270. The Measurement of Pressure through Tubes in Pressure Distribution Tests. By Paul E. Hemke-----	301
No. 271. Pressure Distribution Tests on PW-9 Wing Models Showing Effects of Biplane Interference. By A. J. Fairbanks-----	313
No. 272. The Relative Performance Obtained with Several Methods of Control of an Overcompressed Engine Using Gasoline. By Arthur W. Gardiner and William E. Whedon-----	327
No. 273. Wind Tunnel Tests on Autorotation and the "Flat Spin." By Montgomery Knight-----	341
No. 274. The N. A. C. A. Photographic Apparatus for Studying Fuel Sprays from Oil Engine Injection Valves and Test Results from Several Researches. By Edward G. Beardsley-----	359
No. 275. The Effect of the Walls in Closed Type Wind Tunnels. By George J. Higgins-----	373
No. 276. Combustion Time in the Engine Cylinder and Its Effect on Engine Performance. By Charles F. Marvin, jr.-----	391
No. 277. The Comparative Performance of an Aviation Engine at Normal and High Inlet Air Tem- peratures. By Arthur W. Gardiner and Oscar W. Schey-----	407
No. 278. Lift, Drag, and Elevator Hinge Moments of Handley Page Control Surfaces. By R. H. Smith-----	427
No. 279. Tests on Models of Three British Airplanes in the Variable Density Wind Tunnel. By George J. Higgins and George L. DeFoe-----	449
No. 280. The Gaseous Explosive Reaction—The Effect of Inert Gases. By F. W. Stevens-----	477
No. 281. The Effects of Fuel and Cylinder Gas Densities on the Characteristics of Fuel Sprays for Oil Engines. By W. F. Joachim and Edward G. Beardsley-----	489
No. 282. The Performance of Several Combustion Chambers Designed for Aircraft Oil Engines. By William F. Joachim and Carlton Kemper-----	499

NATIONAL ADVISORY COMMITTEE FOR AERONAUTICS

3841 NAVY BUILDING, WASHINGTON, D. C.

JOSEPH S. AMES, Ph. D., *Chairman.*

Provost, Johns Hopkins University, Baltimore. Md.

DAVID W. TAYLOR, D. Eng., *Vice Chairman.*

Washington, D. C.

GEORGE K. BURGESS, Sc. D.,

Director, Bureau of Standards, Washington, D. C.

WILLIAM F. DURAND, Ph. D.,

Professor Emeritus of Mechanical Engineering, Stanford University, California.

WILLIAM E. GILLMORE, Brigadier General, United States Army, Chief, Matériel Division, Air Corps, Wright Field, Dayton, Ohio.

EMORY S. LAND, Captain, United States Navy,

Assistant Chief, Bureau of Aeronautics, Navy Department, Washington, D. C.

CHARLES F. MARVIN, M. E.,

Chief, United States Weather Bureau, Washington, D. C.

WILLIAM A. MOFFETT, Rear Admiral, United States Navy,

Chief, Bureau of Aeronautics, Navy Department, Washington, D. C.

MASON M. PATRICK, Major General, United States Army,

Chief of the Air Corps, War Department, Washington, D. C.

S. W. STRATTON, Sc. D.,

President, Massachusetts Institute of Technology, Cambridge, Mass.

ORVILLE WRIGHT, Sc. D.,

Dayton, Ohio.

Smithsonian Institution, Washington, D. C.

GEORGE W. LEWIS, *Director of Aeronautical Research.*

JOHN F. VICTORY, *Secretary.*

HENRY J. E. REID, *Engineer in Charge, Langley Memorial Aeronautical Laboratory, Langley Field, Va.*

JOHN JAY IDE, *Technical Assistant in Europe, Paris, France.*

EXECUTIVE COMMITTEE

JOSEPH S. AMES, *Chairman.*

DAVID W. TAYLOR, *Vice Chairman.*

GEORGE K. BURGESS.

WILLIAM E. GILLMORE.

EMORY S. LAND.

CHARLES F. MARVIN.

WILLIAM A. MOFFETT.

MASON M. PATRICK.

S. W. STRATTON.

ORVILLE WRIGHT.

JOHN F. VICTORY, *Secretary.*



CHARLES D. WALCOTT

1850-1927

Late Chairman National Advisory Committee for Aeronautics

THIRTEENTH ANNUAL REPORT

OF THE

NATIONAL ADVISORY COMMITTEE FOR AERONAUTICS

WASHINGTON, D. C., November 26, 1927.

To the Congress of the United States:

In accordance with the act of Congress approved March 3, 1915, establishing the National Advisory Committee for Aeronautics, the committee submits herewith its thirteenth annual report for the fiscal year 1927.

In Part I of this report the committee comments on the death of its late chairman, Dr. Charles D. Walcott, describes its organization, states its functions, outlines the facilities available under the committee's direction for the conduct of scientific research in aeronautics, explains the activities and growth of the Office of Aeronautical Intelligence in the collection, analysis and dissemination of scientific and technical data, and presents a financial report of its expenditures during the fiscal year ended June 30, 1927.

In Part II of this report the committee describes its general activities including those in connection with the consideration of aeronautical inventions and designs and the procedure followed by the committee in its relations with inventors and with the Aeronautical Patents and Design Board, which consists of the three assistant secretaries for aeronautics in the departments of War, Navy, and Commerce. The committee also reports on its relations with the aircraft industry and its cooperation with the Army and Navy and other American agencies, governmental and private, and with the British Aeronautical Research Committee.

In Part III the committee presents the reports of its standing technical subcommittees on aerodynamics, power plants for aircraft, and materials for aircraft, which include statements of the organization and the functions of each and of the progress of investigations conducted under their general cognizance in laboratories governmental and private.

In Part IV the committee presents summaries of the technical reports published during the past year and enumerates by title the technical notes, technical memorandums, and aircraft circulars issued.

In Part V the committee presents its views as to the present state of aeronautical development with special reference to the technical development of aircraft. The report closes with a summary of the progress made during the past year and of the factors that have contributed to the advancement of American aeronautics.

THE DEATH OF DR. CHARLES D. WALCOTT, CHAIRMAN

Dr. Charles D. Walcott, chairman of the National Advisory Committee for Aeronautics, died at his residence in Washington on February 9, 1927. He was one of the original 12 members appointed by President Wilson when the committee was established by law in 1915, and represented the Smithsonian Institution, of which he was the Secretary. Despite his activity in other fields, he was a leader in the development of aeronautics in America. His great foresight and genius for organization were brought to bear at a time when there was but little appreciation in America of the value of aeronautics and but little conception of its problems. Although the scientific world recognized him as preeminent in his chosen field in geology and had honored him accordingly, and although the public generally knew something of his career as Director of the Geological Survey, as Secretary of the Smithsonian Institution, as president of the National Academy of Sciences, and in other capacities, the American people knew little of his contributions to the development of aeronautics in America.

Shortly after succeeding the late Dr. Samuel P. Langley as Secretary of the Smithsonian Institution and before the outbreak of the World War, he secured from the Board of Regents of the Smithsonian Institution a resolution reopening the Langley Aerodynamical Laboratory and organized under the Smithsonian Institution an advisory committee of the Langley Aerodynamical Laboratory. That committee consisted of 12 members serving without compensation under the chairmanship of Doctor Walcott. It held several meetings but was soon disbanded because of the recognition of the need of public funds which it could not obtain, as it had not been created by law. In 1914, shortly after the outbreak of the war in Europe, Doctor Walcott presented to the Congress of the United States his views as to the need for organized scientific research in aeronautics and was successful in securing the establishment by law of the present National Advisory Committee for Aeronautics to study and investigate the fundamental problems of flight. The act establishing the committee was approved March 3, 1915. At the organization meeting held in the office of the Secretary of War, Lindley M. Garrison, Doctor Walcott was elected chairman of the executive committee. He was reelected annually until 1919, when he was elected chairman of the entire committee. The latter position he continued to fill by annual reelection until his death.

It was largely because of his personal responsibility for the results accomplished by the committee that official publicity during his lifetime was not given his constructive work for the upbuilding of American aeronautics. His colleagues on the committee at the present time, including four who have served since the establishment of the committee, feel that it is now a duty to state some of the facts regarding the influence of Doctor Walcott upon the development of aeronautics in America. The limitations of a public document preclude the presentation of the whole story in this report. Some day the historian or the biographer may place before the American people, and before American youth in particular, the whole romantic story of his life—of his start as a clerk in a hardware store, and of his rise on sheer personal merit and accomplishment to the very pinnacle of the scientific world. His colleagues on the committee, however, must rest content with the presentation in this report of the simple facts regarding his public service as a member and official of this committee. Accordingly his further major contributions to the progress of American aeronautics are briefly summarized chronologically as follows:

On June 8, 1916, there was held in Doctor Walcott's offices at the Smithsonian Institution a meeting of the executive committee of the National Advisory Committee for Aeronautics which was attended by representatives of the then existing aircraft and aircraft-engine industries. The purpose of that joint conference was to awaken American manufacturers to the need for the development of a more reliable and more efficient aircraft engine. It was the first general meeting of representatives of the American aircraft industry and many of them were reluctant to speak in the presence of each other. That meeting led directly to the formation of a subcommittee on power plants for aircraft and it is significant to note that within 12 months the first of the famous Liberty engines was undergoing tests.

In the fall of 1916 Doctor Walcott was a leader in securing the agreement of the Army and Navy to a plan for a joint Army and Navy experimental field and proving ground for aircraft upon which would be located the committee's research laboratory. He served as chairman of a special committee to select a site, which led directly to the selection of the site now known as Langley Field, Va. On this field is located the research laboratory of the committee known as the Langley Memorial Aeronautical Laboratory, where scientific research on the fundamental problems of flight is conducted under the committee's immediate control.

The progress of the war in Europe forced a realization of the increasing importance of aircraft in warfare, and in the fall of 1916 the Army and Navy began to expand their air organizations. This movement was only well started when in December, 1916, a patent war loomed in the American aircraft industry. The Wright-Martin Aircraft Corporation, holder of the basic Wright patents, served notice on the other aircraft manufacturers that they must take out licenses and pay royalties for the right to manufacture aircraft. The Curtiss Aeroplane & Motor Co. (Inc.), which held a number of important patents, including basic seaplane patents,

then served similar notice on the other members of the industry. The results were that the cost of aircraft to the Government advanced rapidly and to such an extent as to prevent the procurement of the number of airplanes desired by the Army and Navy within the limits of funds available; and the manufacturers who received orders in quantities which called for expansion of facilities were embarrassed by the pending or threatened patent litigation and were unable to obtain the necessary funds with which to expand, so that the Government, although contracting to pay higher prices, was not able to obtain deliveries of aircraft. In this state of affairs the War and Navy Departments officially called upon Doctor Walcott to have the Advisory Committee study the problem with a view to working out a solution. Doctor Walcott called several conferences with representatives of the various factions in the aircraft industry, and later appointed a subcommittee on patents of the National Advisory Committee. The result was the evolution of a "cross-license agreement" among the manufacturers, which put an end to the patent war and made it possible for the manufacturers to obtain capital to finance their expansion projects. Volumes have been written in criticism and in defense of the cross-license agreement in the aircraft industry. It has everywhere been upheld, first by the Attorney General, then by the courts, and lastly by the Comptroller General. Since its inception there has been no further patent warfare in the aircraft industry.

Coincident with the discussion and efforts to solve the perplexing patent situation was the imminent menace of America's entry into the World War. In March of 1917 Doctor Walcott called meetings of the aircraft manufacturers, acquainted them with the prospect of a greatly expanded aircraft building program, and urged upon them the necessity of expanding their facilities for production. He presented to the industry an outline of the first three-year American aircraft building program. In connection with this activity, Doctor Walcott conducted by telegraph a survey of the productive capacity of the industry as to aircraft and engines, with respect to the capacity at that time, capacity within six months, and capacity at the end of a year. The replies received were discouraging. He organized a subcommittee on production to work with the industry. Within a month he became convinced that the problem of aircraft production in quantities was so difficult as to require the attention of the ablest business and professional men that could be organized for the purpose. Accordingly he secured the adoption of a resolution by the National Advisory Committee for Aeronautics, recommending to the Council of National Defense that it organize an Aircraft Production Board to consider the situation in relation to the quantity production of aircraft and that a joint technical board of the Army and Navy for determining specifications and methods of inspection for aircraft be also organized. The Council of National Defense approved the committee's recommendations without delay, and Doctor Walcott turned over to the Aircraft Production Board all the records previously gathered by the National Advisory Committee for Aeronautics' subcommittee on production. The Congress of the United States within a few months enacted the famous \$640,000,000 appropriation act for aircraft and changed the status of the aircraft production board to that of an independent establishment known as the Aircraft Board.

Doctor Walcott called a conference to consider the problem of training aviators for the war which led to the calling of a conference of university presidents on April 30, 1917, to organize the training program.

While the foregoing policies were discussed and approved as actions of the National Advisory Committee for Aeronautics, their vital constructive force reflected primarily the broad vision and genius for organization of Doctor Walcott. In addition to those more important activities, he was an active leader in bringing about the following:

The inauguration of the air mail service, discussions on the subject beginning in committee meetings in December, 1916;

The establishment of the Office of Aeronautical Intelligence of the National Advisory Committee for Aeronautics in 1918;

The organization in 1919 of the Interdepartmental Committee on Aerial Photographic Surveying and Mapping, which led to the creation by Executive order of the present Board of Surveys and Maps of the Federal Government;

The formulation and approval by the Government of the first national aviation policy in 1920;

The encouragement of organized scientific research in cooperation with the Army and Navy;

The formulation of basic principles for the Federal control and encouragement of commercial aviation, beginning in 1919 and continuing to the enactment of the air commerce act of 1926.

He was a champion of progress and an inspiring leader. During the war period he rendered invaluable service to aeronautics in advising with and assisting the heads of the Army and Navy air organizations. He won for the committee the confidence and respect of the President, the Congress, the industry, and the public, and raised the dignity of membership on the committee to such a plane that no person has ever declined appointment on the main committee or on a subcommittee, although such service is without compensation.

At a special meeting of the members of the National Advisory Committee for Aeronautics, held in the city of Washington, D. C., on February 11, 1927, Dr. Joseph S. Ames, chairman of the executive committee, announced the death on February 9, 1927, of Dr. Charles D. Walcott, chairman of the National Advisory Committee for Aeronautics, whereupon by unanimous vote it was—

Resolved, That the members of the National Advisory Committee for Aeronautics do adopt and approve the following tribute to the memory of their late distinguished chairman.

Doctor Walcott was not only a great scientist; he was a great man. His mind was that of a true scientist, a skilled executive, and a trained diplomat, and withal he was an inspiring leader of men, and a man beloved by all his colleagues owing to his rare personal qualities. His broad interest extended to many branches of science and in his chosen field in geology he had no equal.

But we are met to-day in special session to praise his memory for his contributions to the new science of aeronautics. His was the vision that saw the need for organized scientific research on the fundamental problems of flight; his was the influence that caused the Congress of the United States to establish a National Advisory Committee for Aeronautics to supervise and direct the scientific study of the problems of flight. Appointed as one of the original 12 members of the committee in 1915, he served continuously until his death as our chief inspiration. From 1915 to 1919 he was chairman of the executive committee and from then until his death he was chairman of the entire committee. His was the leadership during the period of the Great War; then and since, his influence drew to the public service without compensation some of the best minds of the country and organized them into a cooperative effort for the advancement of the science of aeronautics. That he has in the field of aeronautics labored as successfully and as well as in other fields of his endeavor is attested not merely by the personal admiration and esteem of his associates on this committee, but more especially by the record of progress in American aeronautics, and by the character, stability, and standing of the research organization which has been developed by the committee under his guidance. If he had done no more for his country than he did in advancing the science of aeronautics alone, his fame would rest secure.

The world at large does but little appreciate the true greatness of this man. We who have had the privilege of serving with him as members of the National Advisory Committee for Aeronautics can only say that we are proud to have been associated with him, and we mourn his death as a loss to the entire scientific world and a distinct and irreparable loss to the science of aeronautics.

Resolved further, That a copy of these resolutions be engrossed and sent to the family of Doctor Walcott with an expression of our deep sympathy in their great loss.

In transmitting the engrossed memorial to the widow of Doctor Walcott, Dr. Joseph S. Ames, chairman of the executive committee, stated on behalf of the members that "Doctor Walcott was the father of the National Advisory Committee for Aeronautics and the chief constructive force in the upbuilding of American aeronautics" and that "The recollection of his wise counsel and inspiring leadership will serve to stimulate us in the future as it has in the past, to the end that our country may ever be in the vanguard of progressive nations in the development of aeronautics."

PART I

ORGANIZATION

FUNCTIONS OF THE COMMITTEE

The National Advisory Committee for Aeronautics was established by act of Congress approved March 3, 1915. The organic act charged the committee with the supervision and direction of the scientific study of the problems of flight with a view to their practical solution, the determination of problems which should be experimentally attacked, and their investigation and application to practical questions of aeronautics. The act also authorized the committee to direct and conduct research and experimentation in aeronautics in such laboratory or laboratories, in whole or in part, as may be placed under its direction.

Supplementing the prescribed duties of the committee under its organic act, its broad general functions may be stated as follows:

First. Under the law the committee holds itself at the service of any department or agency of the Government interested in aeronautics, for the furnishing of information or assistance in regard to scientific or technical matters relating to aeronautics, and in particular for the investigation and study of fundamental problems submitted by the War and Navy Departments with a view to their practical solution.

Second. The committee may also exercise its functions for any individual, firm, association, or corporation within the United States, provided that such individual, firm, association, or corporation defray the actual cost involved.

Third. The committee institutes research, investigation, and study of problems which, in the judgment of its members or of the members of its various subcommittees, are needful and timely for the advance of the science and art of aeronautics in its various branches.

Fourth. The committee keeps itself advised of the progress made in research and experimental work in aeronautics in all parts of the world, particularly in England, France, Italy, Germany, and Canada.

Fifth. The information thus gathered is brought to the attention of the various subcommittees for consideration in connection with the preparation of programs for research and experimental work in this country. This information is also made available promptly to the military and naval air organizations and other branches of the Government, and such as is not confidential is immediately released to university laboratories and aircraft manufacturers interested in the study of specific problems, and also to the public.

Sixth. The committee holds itself at the service of the President, the Congress, and the executive departments of the Government for the consideration of special problems which may be referred to it.

By act of Congress approved July 2, 1926 (Public, No. 446, 69th Cong.), and amended March 3, 1927 (Public, No. 748, 69th Cong.), the committee has been given an additional function. This legislation created and specified the functions of an Aeronautical Patents and Design Board, consisting of an Assistant Secretary of War, an Assistant Secretary of the Navy, and an Assistant Secretary of Commerce, and provided that upon favorable recommendation of the National Advisory Committee for Aeronautics the Patents and Design Board shall determine questions as to the use and value to the Government of aeronautical inventions submitted to any branch of the Government. The legislation provided that designs submitted to the board should be referred to the National Advisory Committee for Aeronautics for its recommendation and this has served to impose upon the committee the additional duty of considering on behalf of the Government all aeronautical inventions and designs submitted.

ORGANIZATION OF THE COMMITTEE

The committee has 12 members, appointed by the President. The law provides that the personnel of the committee shall consist of 2 members from the War Department, from the office in charge of military aeronautics; 2 members from the Navy Department, from the office in charge of naval aeronautics; a representative each of the Smithsonian Institution, the United States Weather Bureau, and the United States Bureau of Standards; and not more than 5 additional persons acquainted with the needs of aeronautical science, either civil or military, or skilled in aeronautical engineering or its allied sciences. The law further provides that all members as such shall serve without compensation.

In February of this year, the committee suffered irreparable loss in the death of its chairman, Dr. Charles D. Walcott, who represented the Smithsonian Institution in its membership. An account of Doctor Walcott's many activities in connection with aeronautics and the committee's work is given in another section of this report. At the semiannual meeting of the committee in April, 1927, Dr. Joseph S. Ames, who had served as chairman of the executive committee since 1919, was elected chairman to succeed Doctor Walcott, but the vacancy in the committee's membership caused by Doctor Walcott's death has not been filled.

During the past year as a result of reorganization of Army Air Corps activities, Maj. John F. Curry, formerly chief of the engineering division of the Air Corps, was relieved from membership and Brig. Gen. William E. Gillmore, chief of the newly organized matériel division, was appointed to succeed him.

With the approval of the President, the rules and regulations for the conduct of the work of the National Advisory Committee for Aeronautics were amended during the past year. The effects of the amendments were to create the new positions of vice chairman of the Advisory Committee and vice chairman of the executive committee to be filled by the election of members, and to change the secretaryship from an elective office filled formerly by a member to an appointive office to be filled by a paid official; the appointment to be made by the chairman with the approval of the executive committee. In accordance with these amendments Dr. David W. Taylor was elected vice chairman of the executive committee on June 22, 1927, and by letter ballot circulated under date of June 28, 1927, was also elected vice chairman of the Advisory Committee. On June 22, 1927, Mr. John F. Victory, who had been in the committee's service since its organization in 1915 and had served as assistant secretary since 1917, was appointed secretary of the committee.

The entire committee meets twice a year, the annual meeting being held in October and the semiannual meeting in April. The present report includes the activities of the committee between the annual meeting held on October 21, 1926, and that held on October 20, 1927.

The organization of the committee at the close of the past year was as follows:

Joseph S. Ames, Ph. D., chairman.
David W. Taylor, D. Eng., vice chairman.
George K. Burgess, Sc. D.
William F. Durand, Ph. D.
Brig. Gen. William E. Gillmore, United States Army.
Capt. Emory S. Land, United States Navy.
Charles F. Marvin, M. E.
Rear Admiral William A. Moffett, United States Navy.
Maj. Gen. Mason M. Patrick, United States Army.
S. W. Stratton, Sc. D.
Orville Wright, B. S.

MEETINGS OF THE ENTIRE COMMITTEE

The semiannual meeting of the entire committee was held on April 21, 1927, at the committee's headquarters in Washington, and the annual meeting on October 20, 1927, also at the committee's headquarters. At these meetings the general progress in aeronautical research was reviewed and the problems which should be experimentally attacked were discussed. Administrative reports were submitted by the secretary and by the Director of the Office of Aeronautical Intelligence.

At both the annual and the semiannual meetings Doctor Ames, as chairman of the executive committee, presented detailed reports of the research work being conducted by the committee at the Langley Memorial Aeronautical Laboratory, Langley Field, Hampton, Va., and exhibited charts and photographs showing the methods used and the results obtained in the more important investigations.

At the annual meeting on October 20 the members of the committee accepted an invitation from Admiral Moffett to inspect the aircraft carrier U. S. S. *Saratoga* at the Philadelphia Navy Yard in November, shortly after the carrier is placed in commission. At this meeting also the committee had as its guest Brig. Gen. James E. Fechet, Assistant Chief of the Army Air Corps.

The election of officers was the concluding feature of the annual meeting. The officers of the committee were reelected for the ensuing year, as follows: Chairman, Dr. Joseph S. Ames; vice chairman, Dr. David W. Taylor; chairman executive committee, Dr. Joseph S. Ames.

THE EXECUTIVE COMMITTEE

For carrying out the work of the Advisory Committee the regulations provide for the election annually of an executive committee, to consist of seven members, and to include in addition any member of the Advisory Committee not otherwise a member of the executive committee, but resident in or near Washington, and giving his time wholly or chiefly to the special work of the committee. The present organization of the executive committee is as follows:

Joseph S. Ames, Ph. D., chairman.

David W. Taylor, D. Eng., vice chairman.

George K. Burgess, Sc. D.

Brig. Gen. William E. Gillmore, United States Army.

Capt. Emory S. Land, United States Navy.

Charles F. Marvin, M. E.

Rear Admiral William A. Moffett, United States Navy.

Maj. Gen. Mason M. Patrick, United States Army.

S. W. Stratton, Sc. D.

Orville Wright, B. S.

The executive committee, in accordance with the general instructions of the Advisory Committee, exercises the functions prescribed by law for the whole committee, administers the affairs of the committee, and exercises general supervision over all its activities.

During the past year the executive committee accepted an invitation from General Patrick and General Gillmore to inspect the facilities and activities of the matériel division of the Army Air Corps in its new location at Wright Field, Dayton, Ohio, and visited the field on October 12, 1927.

The executive committee has organized the necessary clerical and technical staffs for handling the work of the committee proper. General responsibility for the execution of the policies and the direction of the activities as approved by the executive committee is vested in the director of aeronautical research, Mr. George W. Lewis. He has immediate charge of the scientific and technical work of the committee, being directly responsible to the chairman of the executive committee, Dr. Joseph S. Ames. The secretary, Mr. John F. Victory, is ex officio secretary of the executive committee, directs the administrative work of the organization, and exercises general supervision over the expenditures of funds and the employment of personnel.

SUBCOMMITTEES

In order to facilitate the conduct of its work the executive committee has organized seven standing subcommittees, as follows:

Governmental relations.

Publications and intelligence.

Personnel, buildings, and equipment.

Aeronautical inventions and designs.

Aerodynamics.

Power plants for aircraft.

Materials for aircraft.

The organization and work of the technical committees on aerodynamics, power plants for aircraft, and materials for aircraft are covered in the reports of those committees appearing in another part of this report, while the work of the committee on aeronautical inventions and designs is included under the subject of the consideration of aeronautical inventions.

During the past year the suggestion was made that the membership of the committees on aerodynamics and power plants for aircraft be enlarged to include representatives of the aircraft industry and of educational institutions offering courses in aeronautical engineering. Such representatives are already included in the membership of the committee on materials for aircraft. This suggestion was given careful consideration by the executive committee and a policy was adopted which will provide for the appointment in the future of special subcommittees organized from time to time under the standing subcommittees and including representatives of the aircraft industry, for the purpose of giving consideration to specific problems, as this plan was deemed more advisable and practicable than to appoint representatives of the industry on the aerodynamics and power plants committees.

A statement of the organization and functions of the administrative committees on governmental relations, publications and intelligence, and personnel, buildings, and equipment follows:

COMMITTEE ON GOVERNMENTAL RELATIONS

FUNCTIONS

1. Relations of the committee with executive departments and other branches of the Government.
2. Governmental relations with civil agencies.

ORGANIZATION

Prof. Charles F. Marvin, chairman.
Dr. David W. Taylor.
John F. Victory, secretary.

COMMITTEE ON PUBLICATIONS AND INTELLIGENCE

FUNCTIONS

1. The collection, classification, and diffusion of technical knowledge on the subject of aeronautics, including the results of research and experimental work done in all parts of the world.
2. The encouragement of the study of the subject of aeronautics in institutions of learning.
3. Supervision of the Office of Aeronautical Intelligence.
4. Supervision of the committee's foreign office in Paris.
5. The collection and preparation for publication of the technical reports, technical notes, technical memorandums, and aircraft circulars of the committee.

ORGANIZATION

Dr. Joseph S. Ames, chairman.
Prof. Charles F. Marvin, vice chairman.
Miss M. M. Muller, secretary.

COMMITTEE ON PERSONNEL, BUILDINGS, AND EQUIPMENT

FUNCTIONS

1. To handle all matters relating to personnel, including the employment, promotion, discharge, and duties of all employees.
2. To consider questions referred to it and make recommendations regarding the initiation of projects concerning the erection or alteration of laboratories and offices.
3. To meet from time to time on the call of the chairman, and report its actions and recommendations to the executive committee.
4. To supervise such construction and equipment work as may be authorized by the executive committee.

ORGANIZATION

Dr. Joseph S. Ames, chairman.
Dr. David W. Taylor, vice chairman.
Prof. Charles F. Marvin.
John F. Victory, secretary.

QUARTERS FOR COMMITTEE

The headquarters of the National Advisory Committee for Aeronautics are located in the Navy Building, Seventeenth and B Streets NW., Washington, D. C., in close proximity to the Army and Navy air organizations. The committee has recently moved the greater part of its administrative activities from the rear of the third wing, third floor of the Navy Building to larger quarters in the rear of the eighth wing, third floor. This space has been officially assigned for the use of the committee by the Public Buildings Commission. This move was necessitated by the growth in the committee's activities during the past year. The administrative office is also the headquarters of the various subcommittees and of the Office of Aeronautical Intelligence.

Field stations of the committee are the Langley Memorial Aeronautical Laboratory, at Langley Field, Hampton, Va., and the office of the technical assistant in Europe, located at the American Embassy in Paris.

The scientific investigations authorized by the committee are not all conducted at the Langley Memorial Aeronautical Laboratory, but the facilities of other governmental laboratories and shops are utilized, as well as the laboratories connected with institutions of learning whose cooperation in the scientific study of specific problems in aeronautics has been secured.

THE LANGLEY MEMORIAL AERONAUTICAL LABORATORY

The Langley Memorial Aeronautical Laboratory is operated under the direct control of the committee. It is located at Langley Field, Va., on a plot of ground set aside by the War Department for the committee's use. The laboratory was started in 1916 coincident with the establishment of Langley Field.

The laboratory is organized with four divisions, as follows: Aerodynamics division, power plants division, technical service division, and property and clerical division. The administration of the laboratory is under the immediate direction of an engineer in charge, Henry J. E. Reid, subject to the general supervision of the officers of the committee.

The laboratory consists of seven buildings: A research laboratory building, containing the administrative offices, the headquarters of the aerodynamics and power plants divisions, the technical library, and the photographic laboratory; two aerodynamical laboratories, one containing a wind tunnel of the standard type and the other a variable-density wind tunnel, each laboratory being complete in itself; two engine dynamometer laboratories of a semipermanent type, both equipped to carry on investigations in connection with power plants for aircraft; an airplane hangar with a repair shop and facilities for taking care of airplanes used in flight research; and a service building, containing an instrument laboratory, drafting room, machine and woodworking shops, and storeroom.

During the past year the committee put into operation a novel piece of apparatus known as the propeller research equipment, the construction of which was begun in June, 1925. This equipment is, in effect, a wind tunnel of the Eiffel type with a test chamber of sufficient size to accommodate the fuselage of a full-sized airplane. Full-sized propellers are tested, the propellers being mounted on the engine shaft and operated exactly the same as in free flight. The air stream in which the airplane is mounted is provided by two 1,000-horsepower Diesel engines which operate an eight-bladed propeller 28 feet in diameter. The throat of the test chamber is 20 feet in diameter and tests are conducted at air speeds up to 110 miles per hour. This piece of equipment is the largest wind tunnel in the world.

On August 1, 1927, a fire occurred in the variable-density wind tunnel which destroyed the interior of the structure, including the wind-tunnel cones, balance, propeller, and all instruments. It was necessary to remove entirely every piece of structure and apparatus from the interior of

the wind-tunnel tank, which is 32 feet long and 15 feet in diameter. The fire occurred during a test of an airplane model at 20 atmospheres and was caused by the bursting under pressure of an electric-light bulb which short circuited and caused an arcing that ignited the adjacent wood. Owing to the air circulation in the tunnel of about 50 miles per hour and the great amount of oxygen present in air under pressure of 300 pounds per square inch, the flames spread very rapidly. At the moment the fire was discovered the exhaust valves were opened and all current was cut off, but the equipment in the interior was destroyed because it was impossible to reach the fire inside the tank.

Plans were immediately made for rebuilding the interior of the structure, for making minor repairs to the steel tank housing the tunnel, and for repairing the damage to the building caused primarily by smoke. In rebuilding the tunnel, wood and other inflammable materials will be eliminated and the structure made fireproof.

The variable-density wind tunnel was the most important and valuable single piece of equipment in existence for the purpose of conducting aerodynamical research. It was being fully utilized in the prosecution of fundamental researches, a number of investigations on the program at the time of the fire having been requested by the Army and Navy air organizations.

Recognition by the Government of the necessity of satisfying the increasing demand for new and accurate knowledge on the fundamental problems of flight has made possible the development of the Langley Memorial Aeronautical Laboratory as an efficient research organization numbering 143 employees at the close of the fiscal year 1927. The work of the laboratory is conducted without interference with military operations at the field. In fact, there is a splendid spirit of cooperation on the part of the military authorities who, by their helpfulness in many ways, have aided the committee materially in its work.

THE OFFICE OF AERONAUTICAL INTELLIGENCE

The Office of Aeronautical Intelligence was established in the early part of 1918 as an integral branch of the committee's activities. Its functions are the collection, classification, and diffusion of technical knowledge on the subject of aeronautics to the military and naval air services, aircraft manufacturers, educational institutions, and others interested, including the results of research and experimental work conducted in all parts of the world. It is the officially designated Government depository for scientific and technical reports and data on aeronautics.

Promptly upon receipt, all reports are analyzed and classified, and brought to the special attention of the subcommittees having cognizance, and to the attention of other interested parties through the medium of public and confidential bulletins. Reports are duplicated where practicable, and distributed upon request. Confidential bulletins and reports are not circulated outside of Government channels.

To handle efficiently the work of securing and exchanging reports in foreign countries, the committee maintains a technical assistant in Europe, with headquarters at the American Embassy in Paris. It is his duty to visit the government and private laboratories, centers of aeronautical information, and private individuals in England, France, Italy, Germany, and other European countries, and endeavor to secure for America not only printed matter which would in the ordinary course of events become available in this country, but more especially to secure advance information as to work in progress, and any technical data not prepared in printed form, and which would otherwise not reach this country. John Jay Ide, of New York, has served as the committee's technical assistant in Europe since April, 1921.

The records of the office show that during the past year copies of technical reports were distributed as follows:

Committee and subcommittee members	1, 224
Langley Memorial Aeronautical Laboratory	2, 209
Paris office of the committee	4, 308
Army Air Corps	3, 012
Naval Air Service, including Marine Corps	3, 817
Manufacturers	6, 156
Educational institutions	5, 485
Bureau of Standards	579
Miscellaneous	26, 981
Total distribution	55, 636

Since the promulgation of the Air Navigation Regulations under the air commerce act of 1926 there has been a noticeable increase in requests for technical data. The flight of Colonel Lindbergh and the other transoceanic flights further stimulated interest in aeronautics which has been reflected in the greatly increased demand for the committee's publications. This is evidenced by a comparison of the distribution figures for the past two years. In 1926 the total distribution of technical documents numbered 35,884 and in 1927 it was 55,636, an increase of 55 per cent in one year.

The above figures include the distribution of 25,551 technical reports, 7,197 technical notes, 11,380 technical memorandums, and 5,627 aircraft circulars of the National Advisory Committee for Aeronautics. Part IV of this report presents the titles of the publications issued during the past year whose distribution is included in the foregoing figures. A total of 7,891 written requests for reports were received during the year in addition to innumerable telephone and personal requests, and 31,758 reports were distributed upon request.

FINANCIAL REPORT

The appropriation for the National Advisory Committee for Aeronautics for the fiscal year 1927, as carried in the independent offices appropriation act approved February 11, 1927, was \$500,000, under which the committee reports expenditures and obligations during the year amounting to \$491,920.80, itemized as follows:

Personal services	\$341, 574. 42
Supplies and materials	27, 569. 55
Communication service	1, 061. 75
Travel expenses	11, 595. 61
Transportation of things	1, 397. 28
Furnishing of electricity	8, 264. 34
Rent of office (Paris)	694. 62
Repairs and alterations	5, 953. 55
Special investigations and reports	37, 000. 00
Equipment	56, 809. 68
Expenditures	491, 920. 80
Reserve, "Two Per Cent Club"	6, 879. 16
Unobligated balance	1, 200. 04
Total	500, 000. 00

In addition to the above, the committee had a separate appropriation of \$13,000 for printing and binding, of which \$12,995.70 was expended.

PART II

GENERAL ACTIVITIES

CONSIDERATION OF AERONAUTICAL INVENTIONS

In its twelfth annual report for the year 1926 the committee presented a report on the organization of the Aeronautical Patents and Design Board, consisting of the three Assistant Secretaries for Aeronautics in the Departments of War, Navy, and Commerce. The report also presented an outline of the procedure followed by the committee in considering inventions and designs submitted to it. Under that procedure the committee has conducted the necessary correspondence with inventors to disclose clearly the ideas they have had in mind and made reports to the Aeronautical Patents and Designs Board, describing the inventions, analyzing the principles involved, and making definite recommendations. The number of designs submitted required frequent meetings of the board to consider the reports and recommendations of the National Advisory Committee for Aeronautics. The procedure under the law required careful consideration by the board of each report on a design submitted by the committee to the board, and the board had the sole responsibility for the final disposition of each invention or design submitted.

The act of Congress approved March 3, 1927, worked a change in the above procedure, for it amended the act creating the Patents and Design Board so as to limit the jurisdiction of the board in making awards to the consideration of those cases in which the National Advisory Committee for Aeronautics made favorable recommendations. One effect of this change was to make the National Advisory Committee a responsible agency of the Government for the final disapproval of the vast majority of applications for awards for aeronautical inventions or designs submitted to the Government, leaving to the Patents and Design Board the final decision only in those cases which received the favorable recommendation of the committee. Another effect of the amended legislation incident to relieving the board of the burden of considering cases unfavorably recommended by the committee was the loss by the inventor of his opportunity for a personal hearing before the board unless his invention were favorably recommended by the committee.

In view of the changed circumstances resulting from the legislation of March 3, 1927, the National Advisory Committee for Aeronautics on March 18, 1927, created a subcommittee on aeronautical inventions and designs, the organization and rules of procedure of which are as follows:

ORGANIZATION

Dr. D. W. Taylor, chairman.
Dr. George K. Burgess, vice chairman.
Capt. E. S. Land, United States Navy.
Prof. Charles F. Marvin.
Mr. J. F. Victory, secretary.

RULES OF PROCEDURE

1. The chairman will preside at meetings of the committee and will carry into effect the actions of the committee. In his absence the vice chairman will preside. Three members will constitute a quorum.
2. The secretary will issue notices of meetings, prepare an order of business for each meeting, arrange for the appearance of parties to be heard, record the minutes and transactions of the committee, and perform such other duties as may be assigned.
3. All inventions and designs shall be submitted in writing and be accompanied by descriptive matter sufficiently clear to present the idea.

4. The director of aeronautical research is designated to consider and dispose of inventions and designs submitted, and to conduct with inventors, with the Patents and Design Board, and with others, all correspondence up to the point where a case is taken up specifically for consideration by the committee.

5. The committee will take up specifically for consideration only those inventions or designs that have been recommended to it in writing by a member of the National Advisory Committee for Aeronautics not a member of the committee on aeronautical inventions and designs, or by the director of aeronautical research, and in any case only after preliminary consideration of the same by the director of aeronautical research. In such cases hearings will be granted upon request of the parties making such submissions.

6. The committee may, in its discretion, hear others in support or in denial of the claims of an inventor, and may obtain any information available bearing on the subject matter under consideration.

7. The proceedings before the committee will be informal.

8. The committee will not undertake to determine the validity of a patent nor will it consider claims for alleged infringement of a patent.

9. Inventions and designs will be considered by the committee only as to their technical merit, irrespective of whether they are patented or unpatented; but evidence of lack of novelty may be taken into consideration.

10. The findings and recommendations of the committee on all claims considered by it will be transmitted direct to the Patents and Design Board; provided that the committee may, in its discretion, refer any claim or question in connection therewith to the executive committee of the National Advisory Committee for Aeronautics.

In addition to the foregoing rules of procedure, the following general principles have been agreed upon:

(a) That favorable recommendations to the Patents and Design Board will be made only after consideration by the committee on aeronautical inventions and designs.

The effect of this is to limit the director of aeronautical research to the submission of unfavorable recommendations to the Patents and Design Board.

(b) That on favorable recommendation to the inventions committee from the director of aeronautical research the committee will not make an adverse report without giving the inventor an opportunity to be heard.

The first meeting of the Aeronautical Patents and Design Board was held in the conference room of the National Advisory Committee for Aeronautics on October 12, 1926. In the interests of economy and efficiency the board's records have been maintained by the committee but kept separate and distinct from the committee's records. During the first 12 months of the operation of the Aeronautical Patents and Design Board, approximately 1,000 inventions or designs were received by the committee, about one-half of which had been originally submitted by the applicants either directly or indirectly for the attention of the board. Of the number submitted for the attention of the board (approximately 500) the committee has submitted to the board reports and recommendations in 450 cases, which included favorable recommendations in only 3 cases. The remaining 500 cases submitted direct for the committee's consideration have been disposed of by direct correspondence with the inventors and no design included in this number was worthy of favorable recommendation to the board.

The volume of inventions and designs submitted has been increasing steadily since the summer of 1927, and the burden of this work has required additions to the engineering and clerical staffs of the committee.

Under the present procedure careful consideration is given to all inventions and designs submitted. The Aeronautical Patents and Design Board and the National Advisory Committee for Aeronautics are working in harmony and the burden of considering large numbers of inventions is placed so as to reduce the demands on the time of the members of the subcommittee on aeronautical inventions and designs and of the members of the Aeronautical Patents and Design Board to the consideration of submissions which have received competent preliminary examination and are deemed worthy of further consideration.

RELATIONS WITH THE AIRCRAFT INDUSTRY

In order to give to the manufacturers and operators of aircraft an opportunity to become more closely acquainted with the facilities of the committee's laboratory for the conduct of aeronautical research and to encourage the representatives of the industry to present to the committee research problems arising out of the development of civil and commercial aeronautics, with a view to the possible incorporation of such problems in the committee's research program, the committee in 1926 inaugurated the policy of holding annual conferences between its representatives and representatives of the industry.

In accordance with this policy the second general conference between representatives of the industry and of this committee was held at the Langley Memorial Aeronautical Laboratory, Langley Field, Hampton, Va., on May 24, 1927. In addition to the aircraft manufacturers and operators, aeronautical trade journals and educational institutions engaged in the teaching of aeronautical engineering were invited to send representatives to this conference. The National Advisory Committee for Aeronautics was represented by its subcommittees on aerodynamics and materials for aircraft and by members of its technical staff. Dr. Joseph S. Ames, chairman of the National Advisory Committee for Aeronautics and also at that time chairman of the subcommittee on aerodynamics, presided.

At a preliminary meeting held in the morning the functions and work of the committee were briefly outlined, following which the representatives of the industry were conducted on a tour of inspection of the laboratory and the investigations under way were explained. This occasion marked the formal opening of the committee's new propeller research equipment. In the afternoon the conference proper convened and after a brief statement by the chairman as to the purpose of the meeting, there was general discussion of the problems of commercial aviation in which the representatives of the industry participated. Among the problems which were mentioned as of importance to commercial aviation were the various factors relating to the comfort and convenience of passengers in airplanes and particularly the elimination of noise; the question of controllability at low speeds; and the effect of protuberances on an otherwise faired stream-line body. One of the problems suggested, the study of the effect of cowlings and fuselage shape on the resistance and cooling characteristics of air-cooled engines, was promptly incorporated in the committee's research program.

Following the conference proper, the subcommittee on materials for aircraft met in joint session with the other members of the conference, Dr. George K. Burgess, Director of the Bureau of Standards and chairman of the materials subcommittee, presiding. Doctor Burgess made a brief statement pointing out the importance to aeronautics of the light alloys of aluminum, particularly duralumin, and referring to the difficulties involved in the use of duralumin. Mr. E. H. Dix, jr., of the Aluminum Co. of America, presented a paper with slides, describing "Alclad," a newly developed corrosion-resistant aluminum product. This was followed by a general discussion of the problems in connection with aircraft materials, particularly aluminum alloys.

THE COMMITTEE'S RESEARCH PROGRAM IN RELATION TO NONMILITARY AIRCRAFT

At the semiannual meeting of the entire membership of the National Advisory Committee for Aeronautics held on April 21, 1927, Doctor Ames, the chairman, invited attention to the following extract from a report of the Committee of Experts on Civil Aviation to the Preparatory Commission for the Disarmament Conference assembled at Geneva:

The committee desires to state at the outset that civil aviation must in itself be regarded as one of the most important factors of civilization, and it is desirable that its free development should not be hampered by any consideration unconnected with the importance which that development possesses from the point of view of scientific, economic, and social progress and of the improvement of communications between peoples. The committee, regarding the question in this light, unanimously agreed that its examination of the subject should be based on the following principle:

In any limitation of air armaments it is essential to avoid hampering the development of civil aviation.

The chairman also invited attention to a recommendation of the Committee of Experts on Civil Aviation that international agreements proposing to limit military and civil aviation be made only for short terms.

Although the Geneva Conference adjourned in disagreement, it is believed that the principle involved in the above quoted report reflects accurately the state of enlightened international opinion regarding the development of civil aviation.

At the meeting referred to, the chairman next outlined the growth in aeronautical education in American universities during the past year which was largely made possible by gifts from the Daniel Guggenheim Fund for the Promotion of Aeronautics. He invited attention to the enlargement of aeronautical facilities at the Massachusetts Institute of Technology, New York University, the University of Michigan, Stanford University, and the California Institute of Technology. Numerous other colleges and institutions of learning had communicated with the committee requesting information as to equipment, such as small wind tunnels, which they contemplated incorporating as part of their experimental equipment for their regular engineering courses. The committee not only furnished the information requested but also gave advice in regard to the equipment and supplies necessary to make it possible for such institutions to offer elective courses to engineering seniors, and where practicable to incorporate aeronautical problems in engineering courses. The object was to acquaint engineering students generally with the fundamentals of aeronautics in much the same manner as they are now made acquainted in regular engineering courses with the fundamentals of hydrodynamics and hydraulics.

The chairman then noted the increased production of civil and commercial airplanes in America and observed that with the evidence of growth of commercial and private operation of aircraft it seems that the committee's research program may properly be so formulated as to include the fundamental problems presented by the development of civil and commercial aviation. Whereupon the following resolution was adopted:

Resolved, That in view of the enactment of the air commerce act of 1926 for the encouragement and regulation of commercial aeronautics, and of the increasing activity in the manufacture and operation of civil and commercial types of airplanes, the National Advisory Committee for Aeronautics directs the attention of its subcommittees to the desirability of considering those fundamental problems the solution of which in their judgment will tend to increase the safety and decrease the cost of construction and operation of such aircraft, and requests that the subcommittees submit recommendations to the executive committee for the approval of such research authorizations as in their judgment will serve best to solve these fundamental problems.

In accordance with the foregoing resolution, consideration of this problem was given by the subcommittees on aerodynamics, power plants for aircraft, and materials for aircraft, and a number of research authorizations were recommended to the executive committee which are now being carried into effect.

THE DANIEL GUGGENHEIM FUND FOR THE PROMOTION OF AERONAUTICS

The committee is pleased to note that the activities of the Daniel Guggenheim Fund for the Promotion of Aeronautics have been carefully planned so as to produce a maximum of immediately practical and substantial assistance to aviation in its commercial, industrial, and scientific aspects, while at the same time avoiding duplication with existing agencies, governmental and private.

The Daniel Guggenheim Fund for the Promotion of Aeronautics was established by Mr. Daniel Guggenheim on January 16, 1926. Its general purposes may be broadly defined as follows:

1. To promote aeronautical education both in higher institutions of learning and among the general public.
2. To assist in the extension of fundamental aeronautical science.
3. To assist in the development of commercial aircraft and aircraft equipment.
4. To further the application of aircraft in business, industry, and other economic and social activities of the Nation.

The major activities of the fund during the past year included the making of a study of the educational institutions of the country and especially those which had established courses in aeronautics, with a view to providing in different sections of the country adequately equipped schools giving courses in aeronautical engineering. As a result of this study grants of money were made by the fund to two California institutions, namely, Stanford University and the California Institute of Technology, at Pasadena; in the East funds were granted to the Massachusetts Institute of Technology, at Cambridge, and to New York University, in New York City; and in the Middle West funds were granted to the University of Michigan, at Ann Arbor.

The trustees of the fund announced that a primary aim of the fund would be the promotion of safety in flying. To this end the fund provided for a safe aircraft competition which for the first time in the history of American aviation caused concerted efforts to be made by manufacturers and designers in various countries to make safer airplanes. The rules and regulations of the competition are intended to encourage the design and construction of aircraft in which those characteristics which are considered most essential for safety shall be developed to a higher degree than exists in present types of aircraft.

The aerial tour of the United States by Col. Charles A. Lindbergh during the fall of 1927 was made possible by the Guggenheim Fund. In this tour Colonel Lindbergh visited every State in the Union and by public addresses before great numbers of the American people brought home to the municipalities a realization of the great need for providing municipal airports.

Among the other activities of the fund was the calling of a conference of representatives of universities engaged in aeronautical educational work. The fund was also active in studying the problems of aerology, fog flying, and navigational instruments.

CONFERENCE OF REPRESENTATIVES OF EDUCATIONAL INSTITUTIONS ACTIVELY ENGAGED IN AERONAUTICAL EDUCATION

The Daniel Guggenheim Fund for the Promotion of Aeronautics called a conference of representatives of educational institutions actively engaged in aeronautical educational work for the purpose of interchanging ideas relative to educational methods, coordinating research work, and developing specialized courses in aeronautical education. The following educational institutions were represented:

Massachusetts Institute of Technology.

New York University.

Stanford University.

California Institute of Technology.

University of Michigan.

University of Washington.

The matériel division of the Army Air Corps and the National Advisory Committee for Aeronautics were also represented.

Dr. William F. Durand, a member of the Daniel Guggenheim Fund for the Promotion of Aeronautics and a member and past chairman of the National Advisory Committee for Aeronautics, acted as chairman of the conference. Upon the request of the fund the committee gave the use of its conference room for the meetings, which were held on December 10 and 11, 1926. The conference was financed by the Guggenheim Fund.

The conference considered in particular the scope and the character of the courses of instruction in the various educational institutions and the possibility of developing specialized courses in aeronautics so that students wishing to specialize in any particular branch would have an opportunity of obtaining this instruction in one of the large universities.

The subject of aeronautical research was given careful consideration and the various institutions were requested to prepare and submit programs of aeronautical research to the Daniel Guggenheim Fund for the Promotion of Aeronautics.

The programs were later submitted to the National Advisory Committee for Aeronautics and brought to the attention of its standing technical subcommittees which have general cognizance of aeronautical research in the respective spheres of aerodynamics, power plants, and materials for aircraft. The programs referred to may be found under the report of the committee on aerodynamics.

COOPERATION OF ARMY AND NAVY

Through the personal contact of the heads of the Army and Navy air organizations serving on the main committee and the frequent personal contact on the subcommittees of their chief subordinates who have to do with technical matters in aeronautics, there has been accomplished in fact not only a coordination of aeronautical research, which is the major function of the committee, but also a coordination of experimental engineering activities of the services and an exchange of first-hand information, comment, and suggestions that have had beneficial effects in both services. The needs of each service in the field of aeronautical research are discussed and agreements invariably reached that promote the public interests. The cordial relations that usually follow from frequent personal contact are supplemented by the technical information service of the committee's Office of Aeronautical Intelligence, which makes available the latest scientific data and technical information secured from all parts of the world. Although there is a healthy rivalry between the Army and Navy air organizations, there is at the same time a spirit of cooperation and a mutual understanding of each other's problems that serve to prevent unnecessary duplication in technical developments in aeronautics.

Much of the fundamental research work of the committee has grown out of requests received from the Army and Navy for the study by the committee of particular problems encountered in the services, and in connection with this work the committee desires to give special recognition to the splendid spirit of cooperation of the two services with the committee. Each service has placed at the disposal of the committee airplanes and engines required for research purposes, and has otherwise aided in every practical way in the conduct of scientific investigations by the committee. Without this cooperation the committee could not have prosecuted successfully many of its investigations that have made for progress in aircraft development. The committee desires especially to acknowledge the many courtesies extended by the Army authorities at Langley Field, where the committee's laboratories are located, and by the naval authorities at the Hampton Roads Naval Air Station.

INVESTIGATIONS UNDERTAKEN FOR THE ARMY AND THE NAVY

As a rule research programs covering fundamental problems demanding solution are prepared by the technical subcommittees and recommended to the executive committee for approval. These programs supply the problems for investigation by the Langley Memorial Aeronautical Laboratory. When, however, the Army Air Corps or the Naval Bureau of Aeronautics desires special investigations to be undertaken by the committee, such investigations, upon approval by the executive committee, are added to the current research programs.

The investigations thus under conduct by the committee during the past year for the Army and the Navy may be outlined as follows:

FOR THE AIR CORPS OF THE ARMY

- Investigation of the flat spin of the Douglas O-2 airplane.
- Full-scale investigation of different wings on the Sperry messenger airplane.
- Investigation of the behavior of an airplane in landing and in taking off.
- Investigation of pressure distribution and accelerations in pursuit type airplane.
- Acceleration readings on the PW-9 airplane.

FOR THE BUREAU OF AERONAUTICS OF THE NAVY DEPARTMENT

- Investigation of pressure distribution on vertical tail surfaces fitted with balanced rudders.
- Investigation of methods of improving wing characteristics by control of the boundary layer.
- Development of a solid-injection type of aeronautical engine.
- Investigation of method of improvement in range of vision of pilot in an airplane.
- Investigation of maximum tail loads in dives.
- Investigation of the effect of fineness ratio on airship models.
- Design of accelerometers for determination of accelerations in catapulting.

Investigation of the forces on seaplane floats under landing conditions.
Investigation of water pressure distribution on seaplane hulls.
Study of design factors for metal propellers.
Investigation of application of compression ignition operation to air-cooled engine cylinders.
Investigation of flight path characteristics.
Effect of varying the aspect ratio and area of wings on performance of fighter airplane with supercharged air-cooled engine.
Investigation of aerodynamic loads on the U. S. S. *Los Angeles*.
Investigation of autorotation.
Investigation of spoiler aileron control.
Development of aircraft engine supercharger.
Investigation of performance of five propellers in flight.
Effect of various forms of cowling on performance and engine operation of fighter airplane with supercharged air-cooled engine.

USE OF NONGOVERNMENTAL AGENCIES

The various problems on the committee's approved research programs are as a rule assigned to governmental agencies for study and investigation. In cases where the proper study of a problem requires the use of facilities not available in any governmental establishment, or requires the talents of men outside the Government service, the committee contracts directly with the institution or individual best equipped for the study of each such problem to prepare a special report on the subject. Such special reports are published the same as other technical reports of the committee. In this way the committee makes effective use of the facilities of educational institutions and the services of specialists in the scientific study of the problems of flight.

COOPERATION WITH BRITISH AERONAUTICAL RESEARCH COMMITTEE

The cordial relations which have existed for a number of years between this committee and the Aeronautical Research Committee of Great Britain have been continued during the past year. In the summer of 1927 Dr. Joseph S. Ames, chairman of the National Advisory Committee for Aeronautics, visited Europe to observe recent progress and developments in aeronautical research in England and France, and while in England conferred with the Aeronautical Research Committee, representatives of the Air Ministry, and members of the staff of the National Physical Laboratory, and viewed the work in progress at the British laboratories. Many of the important problems of aeronautical research at the present time were discussed, and there was a free interchange of ideas. One of the points tentatively agreed upon was the exchange between the two committees of special instruments for use in flight research, in order that comparative tests on the same instruments might be made at different laboratories.

The program of comparative research for the standardization of wind tunnels carried on for the past several years by the two committees has been continued. This program included tests by this committee of models of airships, airplanes, and wing sections which had first been tested by the British committee. The results of tests in this committee's variable-density wind tunnel at Langley Field were of particular value in the subject of wind-tunnel standardization, and also in the study of scale effect on models. During the past year an agreement was reached between the two committees which provided for the publication separately by each committee as soon as practicable, of the results of the tests conducted by that committee, the comparative results from the two countries to be published at a later date. In accordance with this policy, papers covering the tests in this country of airship and airplane models will be published in the near future.

During the past year tests conducted in the variable-density wind tunnel at Langley Field as part of this program have been completed on three British airplane models with different wing sections. The models tested were a Bristol fighter with R. A. F. 15 wing section, a BE-2E with R. A. F. 19 wing section, and a Bristol fighter with R. A. F. 30 wing section. The results

of the tests on these models were forwarded to the British committee for analysis. The British committee is considering the question of constructing in England a variable-density wind tunnel similar in type to that at Langley Field for the study of scale effect.

On suggestion of the Aeronautical Research Committee, this committee last year forwarded to England for comparative tests a metal model propeller which had previously been tested in the open-type wind tunnel at Stanford University. This model is now undergoing test in the closed-type wind tunnel at the National Physical Laboratory.

EXHIBIT AT THE NATIONAL SESQUICENTENNIAL EXPOSITION

During the summer and fall of 1926 the committee maintained an exhibit in the Transportation Building of the National Sesquicentennial Exposition in Philadelphia, which exhibit was described in the committee's annual report for the year 1926. That exhibit proved to be very popular with all classes of visitors. Working models on exhibition depicted the methods employed in the conduct of scientific research in aeronautics. The exhibit closed on November 30, 1926. Shortly thereafter the jury of awards conferred a "grand prize certificate of award" upon the National Advisory Committee for Aeronautics for its "collective exhibit of working models used in scientific research on the fundamental problems of flight." The jury of awards also conferred a gold medal upon the National Advisory Committee for Aeronautics for its "exhibit of automatic recording instruments used in aeronautical research."

The diplomas of award have been framed and displayed at the committee's headquarters.

Mr. George W. Lewis, director of aeronautical research, was the contact officer between the committee and the Sesquicentennial Exposition Commission, and the committee's exhibit was installed under the personal supervision of Mr. John F. Victory, at that time assistant secretary of the committee.

INTERNATIONAL CONGRESS ON AERIAL NAVIGATION, ROME

In June, 1927, the Department of State requested an expression of opinion from the committee in regard to an invitation of the Italian Government that the United States be officially represented at an International Congress on Aerial Navigation to be held in Rome in October, 1927. In reply the committee offered the services of its technical assistant in Europe, Mr. John J. Ide, as a representative of the United States if the Department of State should so desire. In accordance with the committee's suggestion, and with the approval of the President, the Department of State designated Mr. Ide as one of the delegates on the part of the United States to the International Congress, which opened in Rome on October 24, 1927.

THE AIR MAIL SERVICE

On July 1, 1927, the air mail service officially passed from governmental operation into the hands of private carriers acting under contracts with the Post Office Department. The passing of the air mail service as a governmental activity closes a most interesting chapter in the history of aeronautical development and opens another, the significance of which it is difficult to visualize.

The air mail service was inaugurated in February, 1918, on the New York to Washington route. The National Advisory Committee for Aeronautics had been greatly interested in the project as discussions of the practicability and desirability of an air mail service had begun in committee sessions as early as December of 1916, and the committee had invited representatives of the Post Office Department to attend meetings from time to time for the purpose of encouraging the department to inaugurate such a service. The committee was largely responsible for the selection of the relatively safe route between New York and Washington for the first experiment. Gradually the air mail service was extended to connect the east and west coasts and also to serve other localities off the main transcontinental airway.

In December, 1922, questions of broad policy arose regarding the future of the air mail service and its fundamental purposes. In response to a request from President Harding the National Advisory Committee for Aeronautics made a study of the problem and submitted

a report dealing with the fundamental purposes of the air mail service, its accomplishments and what remained to be accomplished, and presenting a comparison of an operating with a development program and certain recommendations. In that report the committee stated that "The fundamental purpose of the air mail service is to demonstrate the safety, reliability, and practicability of air transportation of the mails, and incidentally of air transportation in general," and added that it should "Develop a reliable 36-hour service between New York and San Francisco, and make that service self-supporting by creating the necessary demand for it and charging a rate between ordinary postage rates and night-letter telegraph rates." The committee reported further that "In the present undeveloped state of the art, it would be wholly impracticable to operate an air mail service by contract."

The committee expressed the opinion that the most important objects remaining to be accomplished were to "demonstrate that night flying is practicable over a regular route and schedule," and to "bring about the development of an efficient type of airplane for this special purpose." The committee's report closed with recommendations that the air mail service be continued under the Post Office Department until it had—

- (1) Demonstrated the practicability of night flying in the mail service and actually established a regular service between New York and San Francisco in 36 hours or less;

- (2) Met the popular demand for a fast transcontinental service and made such service self-supporting by means of appropriate rates;

- (3) Demonstrated the exact cost and economic value of air transportation, using the most appropriate equipment, including airplanes specially designed for efficient performance.

The committee further recommended that "when the above program is once accomplished the further application of aircraft to the carrying of mail be effected by contracts with private enterprise."

The policy recommended by the National Advisory Committee for Aeronautics was approved by President Harding. How well it has been carried into effect is attested best by the record of progress of the air mail service. There has been no more valuable experiment in aeronautics and certainly none that contributed more directly to the demonstration of the practical value of air transportation and to the advancement of aeronautics generally.

Under the fundamental policy of the Post Office Department mail is bound to be carried eventually by the fastest means available, and the Post Office Department deserves recognition by the people of the United States of the important part it has played in demonstrating the practical use of aircraft in the transportation of the mail. The economic value of air transportation of the mails now that the service is operated by private contractors will continue to be tested and demonstrated until the air mail service is extended to serve communities in all parts of the country.

PART III

REPORTS OF TECHNICAL COMMITTEES

REPORT OF COMMITTEE ON AERODYNAMICS

ORGANIZATION

The committee on aerodynamics is at present composed of the following members:

Dr. David W. Taylor, chairman.

Capt. H. C. Richardson, United States Navy, vice chairman.

Dr. L. J. Briggs, Bureau of Standards.

Lieut. Ernest W. Dichman, United States Army, matériel division, Air Corps, Wright Field.

Lieut. W. S. Diehl, United States Navy.

Prof. Alexander Klemin, Department of Commerce.

George W. Lewis, National Advisory Committee for Aeronautics (ex officio member).

Maj. Leslie MacDill, United States Army, matériel division, Air Corps, Wright Field.

Prof. Charles F. Marvin, Weather Bureau.

Hon. Edward P. Warner, Assistant Secretary of the Navy for Aeronautics.

Dr. A. F. Zahm, construction department, Washington Navy Yard.

During the past year, Dr. Joseph S. Ames, who had for several years served as chairman of the committee on aerodynamics, submitted his resignation because of the additional demands on his time entailed by his election as chairman of the National Advisory Committee for Aeronautics. Dr. David W. Taylor was appointed to succeed him. The executive committee, in accepting Doctor Ames' resignation, recorded an expression of its sincere appreciation of the invaluable service rendered by Doctor Ames, who had presided at sessions of the committee on aerodynamics for over eight years.

FUNCTIONS

The functions of the committee on aerodynamics are as follows:

1. To determine what problems in theoretical and experimental aerodynamics are the most important for investigation by governmental and private agencies.

2. To coordinate by counsel and suggestion the research work involved in the investigation of such problems.

3. To act as a medium for the interchange of information regarding aerodynamic investigations and developments, in progress or proposed.

4. To direct and conduct research in experimental aerodynamics in such laboratory or laboratories as may be placed either in whole or in part under its direction.

5. To meet from time to time on call of the chairman and report its actions and recommendations to the executive committee.

The committee on aerodynamics, by reason of the representation of the various organizations interested in aeronautics, is in close contact with all aerodynamical work being carried out in the United States. In this way the current work of each organization is made known to all, duplication of effort being thus prevented. Also all research work is stimulated by the prompt distribution of new ideas and new results, which add greatly to the efficient conduct of aerodynamic research. The committee keeps the research workers in this country supplied with information on European progress in aerodynamics by means of a foreign representative who is in close touch with aeronautical activities in Europe. This direct information is supplemented by the translation and circulation of copies of the more important foreign reports and articles.

The committee on aerodynamics has direct control of the aerodynamical research conducted at Langley Field, certain propeller research conducted at Stanford University under the supervision of Dr. W. F. Durand, and a number of special investigations conducted at the Bureau of Standards. The aerodynamical investigations undertaken at the Washington Navy Yard, the matériel division of the Army Air Corps at Wright Field, and the Bureau of Standards are reported to the committee on aerodynamics.

SUBCOMMITTEE ON AIRSHIPS

In order that the committee on aerodynamics may be kept in closer touch with the latest developments in the field of airship design and construction, and that research on lighter-than-air craft may be fostered and encouraged to a greater extent, a subcommittee on airships was organized in September, 1927, under the committee on aerodynamics, with the following membership:

Hon. Edward P. Warner, Assistant Secretary of the Navy for Aeronautics, chairman.

Starr Truscott, National Advisory Committee for Aeronautics, vice chairman.

Dr. Karl Arnstein, Goodyear-Zeppelin Corporation.

Commander Garland Fulton, United States Navy.

George W. Lewis, National Advisory Committee for Aeronautics (ex officio member).

Capt. Edgar P. Sorenson, United States Army, matériel division, Air Corps, Wright Field.

R. H. Upson, Aircraft Development Corporation.

The initial meeting of this subcommittee was held during October, at which recent investigations in the field of lighter-than-air research were surveyed and problems for future investigation considered. Subsequently Captain Sorenson was relieved and Capt. William B. Mayer was appointed as a representative of the Army Air Corps.

LANGLEY MEMORIAL AERONAUTICAL LABORATORY

ATMOSPHERIC WIND TUNNEL.—*Pressure distribution.*—In continuation of tests requested by the Army Air Corps a half-span model of the biplane wing system of the Boeing pursuit airplane has been tested to obtain the distribution of pressure over each wing. The wings were also tested individually as monoplanes. In accordance with the practice now in effect in this tunnel, these wings were tested over a large range of angles of attack. The results showed that the air-flow modification mutually produced by the two wings in proximity to one another is confined chiefly to their adjacent surfaces. Reasons hitherto advanced for the difference between the air forces on monoplanes and biplanes at large angles of attack were confirmed by these tests.

Autorotation.—As a result of experience gained in spinning tests made on behalf of the Army and Navy air services, a study of the general subject of autorotation has been continued throughout the year.

A light airplane model, proportionate in weight as well as in size, was mounted in the tunnel free to pitch and to roll about its center of gravity. This model was found to be capable of autorotation as a monoplane up to 26° angle of attack, and as a biplane up to 80° . Four rectangular wing models (a biplane and three monoplanes) were then tested for autorotational characteristics. From these tests it was concluded that in flight a monoplane will not "flat spin," whereas an unstaggered biplane has inherent "flat-spinning" tendencies. These tests led to a general study of the unstable conditions occurring in the "stalled" flight of the orthodox airplane.

The impossibility of calculating accurately the autorotational characteristics of wing systems by the use of the conventional "strip method" led to pressure distribution tests on one of the wings used in the above-mentioned autorotation experiments. An analysis of these results is now being made with a view to improving the accuracy of autorotation calculations.

Tests are in progress to determine the autorotational characteristics of the various wing arrangements employed in modern airplanes. Every effort is being made to produce a non-spinning wing for the purpose of reducing the hazards of "stalled" flight.

Boundary layer control.—The possibility of important gains in airplane efficiency and performance by proper control of the so-called boundary layer has been investigated at this laboratory at the request of the Bureau of Aeronautics, Navy Department. Owing to the retardation of the air flow at the surface of a wing, as the angle of attack is increased the smooth flow over the upper surface ultimately breaks down completely and separates from it, thereby causing a loss of lift. By accelerating or by removing the “dead” air in this region of retarded flow (boundary layer) the breakdown may be delayed until greater angles of attack are reached, thus making available a greater lift.

A large number of pressure distribution tests have been made on a U. S. A. 27 airfoil fitted with various types and combinations of slots through which air has been blown or sucked for the purpose of controlling the boundary layer. The results of these tests have shown that the power required by an airplane may be reduced by the use of suitable slot arrangements in the wings. Removal of the boundary layer by suction has proved to be more economical than the acceleration of the layer by pressure.

The U. S. A. 27 airfoil was found to be unsatisfactory for this work by reason of its relatively sharp nose and consequently high nose pressures. The investigation is now being continued on a thick round-nosed airfoil having a theoretically derived profile of the Joukowsky type. Preliminary tests on this airfoil have shown satisfactory nose pressures.

Wind-tunnel apparatus.—A new apparatus for pressure distribution tests has been placed in service during the past year. It comprises a wood separation plane, a 115-tube photographic manometer, and a wing support permitting a 360° angle-of-attack range.

Several minor changes have been made in the force-test wire balance, resulting in more uniform operation and reduction of the personal factor in force testing.

Miscellaneous.—A mathematical analysis has been made of the problem of balancing flying models of airplanes for spinning tests. The study included the derivation of a method for giving the model the various known weight distributions for the purpose of determining their effect upon spinning.

At the inception of the recent series of long-distance flights a study was made of take-off conditions for heavily loaded airplanes. It has been suggested that the fact that an airplane can be made to take-off, even when so heavily loaded that it can not climb higher than the span of its wings, may account for several of the recent crashes.

A new study has been made of data obtained in this tunnel some years ago on an oscillating wing. As a result, it has been found that the lift of a wing while pitching is, in general, less than the lift of a stationery wing for the same angle of attack. A qualitative explanation of the phenomenon of the pitching airfoil has been derived from aerodynamic theory.

VARIABLE-DENSITY WIND TUNNEL.—This wind tunnel has been in continuous operation throughout the past year, during which three major researches and several minor ones have been conducted.

Three British airplane models.—In cooperation with the British Aeronautical Research Committee, an investigation was conducted in the variable-density wind tunnel on a series of airplane models which had been tested at the National Physical Laboratory and at the Royal Aircraft Establishment. Full-scale experiments had been made on the airplanes at Farnborough. The research consisted of tests to determine the scale effect on models of three British airplanes (BE-2E with R. A. F. 19 wings, Bristol fighter with R. A. F. 15 wings, and Bristol fighter with R. A. F. 30 wings). The scale effect on the maximum lift coefficient was the important item. Comparison was made with full-scale flight tests made in England on the original airplanes and a remarkably good agreement was obtained. A report has been written covering these tests.

R. A. F. 19 airfoil section, scale effect.—Three airfoil models of different sizes, having the R. A. F. 19 section and an aspect ratio of 6, were tested through the complete range of Reynolds Number of the tunnel to determine the effect of the size of the model and the density of the fluid on the aerodynamic characteristics of this section. The scale effect on the maximum lift coefficient agreed with previous data obtained on a model airplane using this section. The

effect of the size of the model in relation to the Reynolds Number was in accordance with the theory. This research is to be continued on another section and with variation of the velocity as well as the size of the model and the density.

N. A. C. A.—M6 airfoil with flap and ailerons.—At the first annual conference between the aircraft manufacturers and the committee on aerodynamics it was suggested that an investigation be undertaken to ascertain the effect of a flap and of ailerons at high angles of attack and at a Reynolds Number equivalent to full scale. A large model of the N. A. C. A.—M6 airfoil section fitted with a flap and ailerons, 20 per cent of the chord in width, was therefore tested at a density of 20 atmospheres up to high angles of attack for various settings of the flap and of the ailerons. Large changes in the values of the aerodynamic characteristics were obtained with changes in the flap setting. At a downward setting of 25° , a maximum lift coefficient of 1.71 was obtained. It is indicated from these tests that such a system may be used for decreasing the wing area of an airplane, or its landing speed. The travel of the center of pressure for the various conditions was determined. A report on these tests has been published.

Goodyear-Zeppelin airship tests.—At the request of the Navy Department, eight models of airships of different length-diameter ratios, of Goodyear-Zeppelin design, have been tested by means of the main balance through the full range of Reynolds Number obtainable, the tests including the determination of the lift, drag, and pitching moment at various angles of pitch. Further tests were then made by means of a more accurate drag balance to determine the resistance at zero pitch. The resistance of all the models showed a slight decrease in value as the scale was increased and it was found that on a basis of volume, a model of length-diameter ratio of near 6 has the least resistance coefficient. A comparison of the characteristics of these models was made with those of other models recently tested in this tunnel. A report has been written covering this investigation.

Miscellaneous.—Replicas of the long and short airship models constructed at the British National Physical Laboratory and used for wind-tunnel standardization research have been tested in this tunnel. A technical note has been published covering the results and their relation to previous data on these models.

Three N. A. C. A.—M6 biplane cellules of different staggers were tested up to an angle of attack of 48° to determine their characteristics at high angles and the effect of scale. A report has been written on the results of these tests.

A report covering tests mentioned in last year's report on the Sperry messenger airplane model equipped with six different sets of wings has been written. Comparison with similar tests in the committee's atmospheric wind tunnel was made.

An investigation of the relative thrusts obtainable from a reaction jet by the use of suitable augmentors of the Venturi type was made, the Melot system being used. A report has been drafted on this investigation.

A dynamic pressure survey by means of a minute Pitot tube was made very close to the tunnel wall to obtain data on the change in velocity head near the wall and further information on the "boundary layer." This work is covered in a report on an analysis of tunnel-wall effect.

PROPELLER RESEARCH EQUIPMENT.—The committee has realized for some time the need for an accurate means of making aerodynamic measurements on full-scale aircraft propellers. Tests on model propellers in wind tunnels are not entirely satisfactory because the deflection of the model is different from that of its full-sized propeller. This introduces a rather large error in some cases. The difference in scale effect and tip speed between the model and full scale propeller is also a cause of error. Full-scale flight tests have, of course, the correct conditions, but at the present time they can not be made with sufficient accuracy to be relied upon.

Two years ago the design and construction of a propeller research equipment to fill this need for full-scale tests was started by the committee. It has been completed during the past fiscal year and testing operations are now under way. This equipment consists of a wind tunnel of the open-jet type large enough to permit the mounting of a full-sized airplane fuselage with its engine and propeller. The diameter of the jet is 20 feet and an air velocity of 110

miles per hour has been obtained by means of a propeller fan 28 feet in diameter having eight cast aluminum alloy blades. The power to turn this propeller is furnished by two 1,000-horsepower Diesel engines.

The airplane under test is mounted on a balance which supports it in the center of the air stream. By means of this balance thrust, drag, lift, pitching moment, and rolling moment can be measured. There are also a special test fuselage, having a built-in dynamometer scale for measuring engine and propeller torque, and a device for measuring the deflection of propeller blades in operation.

This equipment makes it possible for the first time to make aerodynamic tests with laboratory accuracy on full-scale aircraft propellers. In addition tests may be made on fuselages, engine cowlings, cooling systems, landing gears, tail surfaces, and other airplane parts.

Air-flow survey.—A survey has been made of the velocity of the air through the test chamber, with gratifying results. It was found that the velocity was very uniform throughout a cross section of the jet.

Propeller tests, Sperry messenger airplane.—In order to provide for true corrections for the effect of the Sperry messenger propeller in flight tests on the airplane, tests were made in the propeller research equipment on the aerodynamic characteristics of the propeller near zero thrust. The tests were run at several air speeds between 50 and 100 miles per hour, corresponding to the actual velocities of the airplane in flight. The results of these tests are being used in a report now under preparation.

Drag tests, Sperry messenger airplane.—Full-scale tests on the drag of a Sperry messenger airplane with the wings removed have been completed for comparison with the drag of a model tested at the same Reynolds Numbers in the variable-density tunnel.

The full-scale drag of the Sperry messenger fuselage, tail surfaces, and landing gear has been measured, and also the drag due to the windshield, cockpit, and the radial air-cooled engine.

Air flow through the propeller plane.—In order to study the effect of the fuselage on the air flow through the propeller, a survey is being made in the plane of the Sperry messenger propeller with the propeller removed. The flow is being surveyed both with the engine in place and with the engine removed and the nose faired. The information from such tests will be of value to propeller designers in that it will allow them to take into account the effect of the fuselage upon the air flow through the propeller. At the present time this effect is not definitely known and is a source of error in the design of propellers.

FLIGHT RESEARCH.—*Airships.*—During the last year the extensive data on the loads and stresses experienced by the U. S. S. *Los Angeles* in maneuvering flight and in flight in gusty air have been worked up to completion, tabulated, and submitted in report form to the Navy Department. The data thus available cover the pressures experienced at 300 points on the hull and tail surfaces in addition to the air speeds, angular velocities, angles of yaw, and control positions at the time these pressures were encountered. As was indicated by the preliminary results mentioned in last year's report, the final results show quite conclusively that the loads in flight in rough air greatly exceed those resulting from maneuvering the airship. Since a knowledge of the character of gusts likely to be encountered in rough air is essential for the proper design of airships, the preliminary study of the instantaneous changes in wind velocity and direction, mentioned in last year's report, is being continued.

In conjunction with the Bureau of Aeronautics, Navy Department, an additional series of speed and deceleration tests has been conducted on the U. S. S. *Los Angeles*. These tests were made both with and without the water-recovery apparatus in place, for the purpose of determining its effect on the speed, drag, and shape coefficient of the airship.

Airplanes.—The load distribution on high-speed airplanes is a subject of particular importance at the present time, because the high speed and great maneuverability of present-day pursuit airplanes have made it advisable to revise the methods of load computations and the loading specifications now in use. In this connection, the major portion of the flight-research

work this year has been on the problems of determining the air loads experienced on airplanes in all conditions of flight. Pressure distribution and acceleration tests have been made on a modern pursuit airplane in which the pressures were measured over the complete supporting surfaces, i. e., wings and tail surfaces, and the accelerations measured at the wing tip, fuselage tail, and the center of gravity of the airplane in all types of maneuvers, in some of which the loadings approached the design load factor. The investigation has been completed for the pressures experienced on the wings, vertical tail surfaces, and one-half of the horizontal tail surfaces. The pressures in the slip-stream portion of the wings and the remaining horizontal surfaces are to be measured, after which the pressure distribution on the fuselage will be investigated. A somewhat similar research has been completed on the air loads on the tail surfaces of a pursuit airplane where the pressures on a balanced-type rudder were of special interest. These tests were made in very violent maneuvers, a load factor of $11\frac{1}{4}$ being attained in flight. Following the usual practice in this type of research, the pressures and accelerations were measured simultaneously and continuously throughout each maneuver, so that a time history of the pressures and accelerations is obtainable. The information obtained from previous tests on a wing and tail rib of two airplanes, a VE-7 and a TS, has been further analyzed and is being reported on in greater detail in a series of papers, each of which gives a time history of the pressures, air speed, and acceleration for a complete maneuver.

To investigate dangerous conditions in spinning flight the "dropping" tests instituted last year have been continued. In these tests flying models constructed to scale, both geometrically and with respect to loading and mass distribution, are dropped in a spin from a considerable altitude, and the rate of rotation and descent and the flight path are recorded by means of ultrarapid motion pictures. As yet only the effects of mass distribution have been investigated, but these show that the type of spin, flat or normal, can be controlled by the mass distribution, and indicate that dangerous spinning characteristics of an airplane may be avoided by proper apportioning of the weights. Tests on similar models are to be extended to include the effects of stagger, gap, and sweep back, and apparatus is being constructed to operate the controls after launching, in order to study control effectiveness in dangerous spins. To supplement the information on mass distribution obtained from the dropping tests, the full-scale moments of inertia of a number of airplanes, particularly those that evidenced unusual spinning characteristics, have been measured. For further information, the wing and tail pressures and loadings are being determined during spins in the pressure-distribution tests on a pursuit airplane, mentioned above.

A research on the water-pressure distribution on the bottom of a seaplane hull at landing and while taxiing has been completed for a single-float seaplane. The water pressures were measured in landings, take-offs, and in taxiing under a variety of wind and water conditions sufficient to assure obtaining the maximum pressures likely to be encountered in service. The pressure apparatus is now being prepared for a similar research on a boat-type seaplane.

Recent wind-tunnel experiments have indicated the possibility of improving the aerodynamic characteristics of wings by removing the boundary layer (the inert layer of air that clings to a wing section) either by sucking it into the interior of the wing or by blowing it off with air discharged under pressure. To determine the practicability of improving an airplane's performance by this means a series of flight tests was conducted in which the boundary layer of the upper wing of a biplane was removed by the pressure method. The tests were of a preliminary nature only, in that a wing already available was adapted to the purpose and an N. A. C. A. supercharger was used to supply air under pressure to the slots in the top of the wing. The tests indicated that the pressure method of boundary layer removal gave little promise of success, particularly on the type of wing section used. Further flight tests on boundary layer removal by suction methods are contemplated but will await more complete wind-tunnel data.

The subject of increased range of vision of the pilot in airplanes for combat purposes has received considerable attention lately from the services, and to demonstrate the effect of a cut-out center section on performance a series of tests was conducted on a training type biplane

with various types of cut-out center sections with and without wing tip shields at the cut-out portion of the wing. The tests show that a very considerable increase in forward and upward vision can be realized at a sacrifice of approximately 12 per cent in speed and climb. The cut-outs with shielding showed little improvement over a cut-out having elliptical tips at the open portion.

The lift and drag characteristics of the Sperry Messenger airplane equipped with R. A. F. 15, U. S. A. 5, U. S. A. 27, and Göttingen 387 wings, determined in flight tests last year, have been recomputed, using the information on propeller characteristics recently obtained in the propeller research equipment. The same propeller and airplane were used in the propeller tests as were used in flight. The corrections necessary are very slight and the results which have been held awaiting this confirmation are ready for publication.

Flight tests on five propellers on a VE-7 airplane have been completed and a report prepared.

Miscellaneous.—Preparations are being completed for a research on the comparative maneuverability of a number of modern airplanes of the pursuit and observation types, in which special attention is to be directed toward the determination of the flight path. Considerable study has been given to various methods of measuring an airplane's flight path in maneuvers, and one method showing considerable promise of success has been developed. By it, from measurements made in the airplane, the flight path may be determined to a greater degree of accuracy than has heretofore been possible. Another method incorporating motion pictures and triangulation from the ground has been partially developed.

Some time and study has been spent in assisting officials of the Guggenheim safe aircraft competition in formulating requirements of a safe airplane and prescribing methods of conducting the required flight tests.

INSTRUMENT RESEARCH AND DEVELOPMENT.—The attainment of high speed, greater maneuverability, and the resultant high acceleration of the modern military airplane used in connection with the various flight researches at the Langley Memorial Aeronautical Laboratory have called for greater refinements of the optical recording instruments which have been developed for the various flight researches. To meet these requirements a number of the former instruments have been remodeled and improved and several new instruments have been constructed. Among the remodeled and newly developed instruments are the following: A new recording turn meter, an airplane performance recorder, a new automatic observer, and a recording fuel flow meter.

In the study of the load on the PW-9 airplane during maneuvers it was found that turn meters used in previous tests where the angular accelerations were relatively low were subject to considerable error in cases of high angular accelerations. It was necessary, therefore, to make a complete analysis of the conditions under which the instrument would be required to operate and to so design one that the errors would be minimized. During this study the turn-meter calibrating table which was placed in operation last year was found to be invaluable in making the proper adjustments of sensitivity, natural period, and damping, and for the duplication of instruments with identical constants. It has also been found necessary to use the turntable for the adjustment of the three-component accelerometers to duplicate exactly sensitivity, natural frequency, and damping. This additional requirement has been found necessary for investigations on seaplanes to determine the loading on the landing structure during the take-off and landing periods. Along with the study of damping problems a new type of dashpot has been designed to prevent spilling and the evaporation of the damping fluid.

The increasing number of airplane performance tests conducted at this laboratory has made it necessary to incorporate the recording elements of three instruments into one. This new instrument, known as a performance recorder, consists of a standard N. A. C. A. instrument case in which are mounted a barometer, an air-speed meter, and a galvanometer. The galvanometer forms part of a resistance-type thermometer and records free-air temperature. Considerable study of the design of the strut element or bulb to minimize lag and at the same time to produce a rugged instrument has resulted in a recorder which operates very satisfactorily

and requires a minimum of service. The combination instrument makes a continuous record of barometric pressure, air speed, and air temperature, from which the airplane performance can readily be calculated.

Increased use of the automatic observer for flight tests and for laboratory tests has necessitated its redesign to eliminate service difficulties, increase the number of instruments which can be photographed, increase the frequency at which the pictures are taken, and reduce the space requirements. The new automatic observer meets these requirements and photographs the indications of as many as 12 standard instruments at the rate of 12 exposures per minute. The instrument has been found of value in laboratory tests where simultaneous readings are required from a number of indicating instruments, and through its use it is possible to complete a given series of tests in a much shorter time, with fewer personnel, and with an accurate definite record of the readings, unaffected by the personal element.

For some time there has been a definite need for an accurate fuel flow meter for use in flight researches on power plants, and the investigation of several types of instruments was reported last year. As a result of these investigations, an instrument has been built and given considerable service, and shows promise of fulfilling this need. It consists of a Venturi nozzle and two differential pressure bellows interconnected with a mechanism for operating a Wheatstone bridge in such a manner that the galvanometer registers rate of fuel flow. The instrument is not affected by the vibration of the airplane, and its installation may be made anywhere in the fuel line.

It was reported last year that an investigation was in progress to determine the practicability of the use of carbon disks in conjunction with the cathode ray oscillograph as an engine indicator for high-speed aircraft engines. Continuation of this investigation has shown that such an apparatus would be unduly complicated and would require much careful research before such equipment could be designed for practical use. Therefore it was decided to investigate the possibilities of a simple diaphragm type optical engine indicator, and very promising results have been obtained. One instrument has already been constructed which records upon a photographic film the pressure in the combustion chamber of a fuel injection engine during its operation. While the instrument is still in the experimental stage the results indicate that a very satisfactory indicator can be built upon this principle. It consists of an optical system attached to a small steel diaphragm, which is inserted directly through the spark plug hole of the engine cylinder head flush with the wall of the combustion chamber. The minute deflections of the diaphragm are optically amplified and recorded upon a moving film, thus resulting in a diagram of the pressures within the engine cylinder against time.

The new propeller research equipment recently put into operation was found to require some form of device for automatically controlling the air speed within close limits throughout the working range. To meet this need an instrument was constructed which is primarily a sensitive balance operated by small changes in pressure, electrical circuits being operated to maintain a constant air speed at any predetermined value by controlling the propeller speed. The instrument has been installed and used in connection with the 6-inch wind tunnel where experience has shown that it may be expected to operate very satisfactorily in controlling the air speed of the larger tunnel.

There have been numerous other investigations and instrument developments during the past year, such as a propeller protractor, a number of stop-watch control mechanisms, an automatic angle-of-attack mechanism for use in pressure-distribution investigations, and investigations of various oils suitable for instrument damping, which investigations are still in progress.

WASHINGTON NAVY YARD

Airplane models.—The 8-foot wind tunnel of the Washington Navy Yard has been used almost entirely for airplane model tests. During the past year 34 complete tests in pitch and yaw were made on 22 models representing 17 designs. Seventeen of the tests were of a research nature and an equal number were made on either design studies or existing service airplanes.

Following the usual practice, two models were tested in both landplane and seaplane arrangement, two models were tested with two wing sections, one model was tested with two tail surfaces, and two models were tested with three tail surfaces. These tests have supplied valuable data for the design requirements of the Bureau of Aeronautics. In this connection, it is to be noted that flight tests appear to confirm fully the wind-tunnel indications of high efficiency for the Göttingen 398 wing section and its modifications, excellent agreement having been obtained.

Two of the tests on tail surfaces are of general interest. The original PN-7 was found to have neutral static longitudinal stability for angles of attack between 5° and 12° , and this was verified by flight tests. Wind-tunnel tests with a new horizontal tail surface having the same area as the original but with an aspect ratio of 4.4 instead of 2.2 showed very satisfactory static stability which was also verified by flight tests. The original T3M-1 horizontal tail surfaces had a very thick section, and the control and stability were only fair according to both wind-tunnel and flight tests. A wind-tunnel test on this model fitted with tail surfaces of a comparatively thin section showed a considerable improvement in both control and stability. Flight tests have not yet been made to verify this, however.

Airfoils and wings.—Owing to an unusually large amount of urgent work it has not been practicable to carry out the airfoil testing program laid out several years ago. This work will be carried over until it can be done without holding up more important tests.

Control surfaces.—Two or more rudders or elevators are frequently tested on an airplane model as a part of the design research program, but occasional tests are made on control surfaces alone. During the past year three such models were tested for lift, drag, and hinge moments.

Lighter-than-air craft.—Drag tests have been made on a streamline form having for its longitudinal cross section one loop of the curve $r = K \cos (4.8\theta)$. The drag per unit area of the maximum cross section was very low, but the prismatic coefficient of the model was also low and the drag per unit volume not so favorable.

For more than two months the entire facilities of the wind tunnel were employed in research work on three rigid airship models fitted with various control surfaces. Drag readings were taken at 0° pitch and yaw and at a series of wind speeds with the models in various conditions ranging from the bare hull to complete appendages. Tests were made in pitch and yaw on one of the models fitted with various combinations of appendages and control surfaces. Damping coefficients were also measured.

Miscellaneous tests.—Tests have been made in the 4-foot wind tunnel on three float models and two fuselage models in addition to the series previously described. It has developed during these tests that the drag coefficient is quite sensitive to comparatively small changes in the lines and that further work is desirable. A variation of approximately 100 per cent in drag was found between two models of the same general appearance.

The pressure drop or resistance of wire screens of varying wire and mesh sizes is now being systematically investigated in the 4-foot wind tunnel.

BUREAU OF STANDARDS

Wind-tunnel investigations.—During the year the installation of apparatus at the Bureau of Standards for measurements of aerodynamic characteristics of airfoils at high speeds was completed. The equipment provides a continuous air stream 2 inches in diameter of speeds ranging from 0.5 to 1.08 times the speed of sound (375 to 825 miles per hour, approximately). The characteristics of 24 airfoil sections have been determined at speeds of 0.5, 0.65, 0.8, 0.95, and 1.08 times the speed of sound at angles of attack from the angle of zero lift to $+24^\circ$. The airfoils were of 1-inch chord, extending entirely across the air stream and represented members of the R. A. F. and Clark Y families commonly used in propeller design. The measurements form a part of a general program outlined by the conference on propeller research organized by the National Advisory Committee for Aeronautics and will be published as a technical report of the committee. The results show the Clark Y sections to have the greater efficiency at high speeds and indicate the desirability of moving the maximum ordinate back on airfoils intended for speeds equal to the speed of sound.

The investigation of turbulence in wind tunnels has been continued in cooperation with the National Advisory Committee for Aeronautics. The possibilities of the use of a hot wire have been extensively investigated and encouraging results have been obtained.

The subject of wind pressure on engineering structures has received further attention. The distribution of pressure over a model of a factory building has been measured and the results are being prepared for publication. The model experiments on chimneys are being supplemented by observations of the pressure distribution around an experimental chimney 10 feet in diameter and 30 feet high constructed on the roof of one of the buildings of the Bureau of Standards. Preliminary observations indicate that the model experiments carried out above the critical region give fairly reliable indications of the force on a full-scale chimney.

Aeronautic instrument investigations.—Progress has been made on the design of temperature elements having a small time lag for use in the electric-resistance type of air thermometers. These instruments were constructed for the National Advisory Committee for Aeronautics for use in performance tests of aircraft. Resistance elements have been constructed which have a thermometric time lag of 4 seconds when exposed in an air stream of 17 miles per hour, compared with a lag of 17 seconds at the same air speed for the elements previously built. This corresponds to a time lag of about 2 seconds at flying speeds, which reduces the lag error in the measurement of the air temperature during the climb of fast airplanes from about 0.9°C. to 0.2°C. A report entitled "Lag of thermometers and thermographs for aircraft," has been published in the Monthly Weather Review.

The development and construction of an altimeter corrected for air temperature has been completed during the year for the Bureau of Aeronautics of the Navy Department. The temperature correction feature relates to the application of a correction for the purpose of taking account of the temperature term in the altitude formula. The ground-level air temperature is set up in the instrument on a small drum showing through the dial. Altitudes are then indicated which take account of an average variation of temperature with altitude for the set value of ground-level temperature. The instrument also contains the usual devices which compensate for the effect on the reading due to the variation in temperature of the instrument. The altitude range is 15,000 feet.

Research relating to the properties of elastic materials used in instruments has been continued for the National Advisory Committee for Aeronautics. Three of the Ogilvie air-speed indicators containing special rubber diaphragms were returned for tests in May, 1927, from the Langley Memorial Aeronautical Laboratory. No appreciable change in the stiffness of the diaphragms was evident, covering a period of $1\frac{1}{2}$ years of use and three years since manufacture. Further progress has been made on the research relating to elastic hysteresis. The damping of a tuning fork of Armco iron was determined experimentally and a relation developed between the statical hysteresis modulus and the damping. Measurements on an Armco iron bar, loaded at one end and fixed at the other, have shown that the statical hysteresis is the same for cycles of equal load range, but different terminal loads. Reports are in preparation on this work. A large amount of experimental data has been accumulated on the change in the modulus of torsion of diaphragm and spring metals in the temperature range $+40^{\circ}\text{C.}$ to -20°C. A report on tension experiments on diaphragm metals was submitted to the National Advisory Committee for publication as a technical note.

An investigation is in progress for the National Advisory Committee for Aeronautics on suitable damping liquids for aircraft instruments. An ideal damping liquid of a required viscosity should be nonvolatile, nondrying, and chemically permanent and have a small temperature coefficient of viscosity in the temperature interval experienced by aircraft. Bearing in mind the above requirements the viscosity of a number of liquids and mixtures has been measured in the temperature range from $+40^{\circ}$ to -30°C.

Special emphasis was placed on the development and improvement of lighter-than-aircraft instruments and of flight-test instruments for the Bureau of Aeronautics. This has included the construction of an improved superheatmeter, the addition of an air-speed recorder to a barograph, the construction of a bimetallic element thermograph, and other refinements and improvements. Progress has also been made in the preparation for the Bureau of Aeronautics of the general report on capillary-type rate-of-climb indicators.

MATÉRIEL DIVISION, ARMY AIR CORPS

General.—During the past year the operation of the wind tunnels at McCook Field has been seriously handicapped by the necessity of moving the equipment to the new Wright Field. The 5-foot wind tunnel has been used almost exclusively for the various routine service tests of model airplanes. In the high-speed 14-inch wind tunnel a study of air flow was made by visual means. The surface-flow photographs were made by a method used by the General Electric Co., which consists of painting the model with a mixture of lampblack and kerosene; the air flow then records its direction by scoring fine channels in the pigment, resulting in "surface lines," which may be readily photographed. A further study was made in the 14-inch wind tunnel of air flow around airfoils at various angles of attack and around different bodies. The investigation also included a study of the effect upon the air flow of removing the boundary layer.

No major change has been made in the apparatus of the wind tunnels, but the mechanisms of the wire balance in the 5-foot wind tunnel has been refined by replacing the pulley in the "dead line" with levers mounted on knife edges.

Officers' school.—The usual period required by the McCook Field officers' school was devoted to the instruction of a class of 11 officers in the practice and technique of wind tunnel operation.

Service tests.—The majority of the airplane models were tested both on the N. P. L. balance at 40 miles per hour and on the wire balance at 100 miles per hour. This procedure was followed for tests on several models in order to study the effect of speed upon the burbling of the wing and to compare the two balances. The airplane model tests include the following:

Scale of model	Name of model	Method
	Light bombardment types:	
One-fortieth.....	Atlantic XLB-2.....	N. P. L. balance at 40 m. p. h.
One thirty-sixth.....	Keystone XLB-3.....	Do.
One forty-eighth.....	Glenn Martin XLB-4.....	Wire balance at 100 m. p. h. and N. P. L. balance at 40 m. p. h.
One thirty-sixth.....	Keystone XLB-5.....	N. P. L. balance at 40 m. p. h.
One-sixtieth.....	Woolsey bomber.....	Wire balance at 100 m. p. h.
	Heavy bombardment types:	
One-fiftieth.....	Keystone XB-1.....	Wire balance at 100 m. p. h. and N. P. L. balance at 40 m. p. h.
One-fortieth.....	Curtiss XB-2.....	N. P. L. balance at 40 m. p. h.
One forty-eighth.....	Atlantic XHB-2.....	Do.
One forty-fourth.....	Matériel division H. B.....	Wire balance at 100 m. p. h.
One-fortieth.....	Transport type: Fokker V-VII.....	Wire balance at 100 m. p. h. and N. P. L. balance at 40 m. p. h.
	Observation types:	
One-twelfth.....	Matériel division N. O.....	Wire balance at 100 m. p. h.
One twenty-fourth.....	Douglas XNO-2.....	Do.
One twenty-fourth.....	Thomas-Morse XO-6.....	N. P. L. balance at 40 m. p. h. and wire balance at 100 m. p. h.
One-twelfth.....	Ground attack type: Matériel division G. A.	Wire balance at 100 m. p. h.
One-eighteenth.....	Pursuit type: Curtiss P-1.....	N. P. L. balance at 40 m. p. h.

Two 6 by 36 inch airfoils (Clark Y and R. A. F. 15) with trailing edge flaps were tested. These airfoils were tested at 100 miles per hour on the wire balance. The N. A. C. A. 81-J airfoil was tested on the wire balance at 100 miles per hour. Several of the propeller series of airfoils which were tested in 1926 were retested to check the previous work.

Miscellaneous tests.—Tests were made upon $\frac{1}{24}$ -scale models of the Douglas O-2C and Curtiss O-1 airplanes and cellules at all angles of attack (0° to 360°). This work was done in connection with the study of the spinning characteristics of these airplanes.

An autogyro model of the la Cierva type was tested for lift and drag.

Preliminary "flutter" test on specially constructed airfoil was made.

Other miscellaneous tests included the tests of wind-driven generators and earth inductor compasses, tests on airplane fabric, a test of a commercial windmill, and a test of a model airplane wheel and tire.

EDUCATIONAL INSTITUTIONS

At a conference of representatives of educational institutions in this country engaged in the teaching of aeronautical engineering, held in Washington on December 10 and 11, 1926, under the auspices of the Daniel Guggenheim Fund for the Promotion of Aeronautics, at which conference the National Advisory Committee for Aeronautics, as well as the matériel division of the Army Air Corps, was represented, the programs of aerodynamic research to be carried on by the various educational institutions were discussed. As agreed upon at this conference, these research programs have since been submitted to the Daniel Guggenheim Fund.

Through the courtesy of the Guggenheim Fund, copies of these programs have been transmitted to the National Advisory Committee for Aeronautics. The principal items of aerodynamic investigation included in the research programs received from the educational institutions of the United States are as follows:

Massachusetts Institute of Technology:

1. Continuation of investigations of mutual interference effects of airplane propellers and other parts of the airplane. This is to include the effects of radical changes in fuselage form and location, effect of radical engine cylinders with different types of cowling, the effect of different propellers on performance, the effect of nacelles in multiengined airplanes, and the measurement of elevator and rudder hinge moments.
2. Measurements of flow around a model airplane as influenced by the propeller, particularly in the region near the tail.
3. Possible experimental determination of actual air flow near the blades of the propeller as opposed to the mean air flow.
4. Pressure distribution on the tail with slip stream.

New York University:

1. Corrections for calculations of performance test, with special reference to the Daniel Guggenheim Safe Aircraft Competition.
2. Wind-tunnel tests for comparative efficiency of an engine nacelle placed at different positions between the wings of a biplane.
3. Empirical design formulæ for downwash behind monoplane and biplane wings.

Stanford University:

1. An experimental investigation of the performance characteristics of a series of five metal model propellers in a free wind stream and in combination with a model of a VE-7 airplane.
2. An experimental investigation of air propellers in yaw. It is planned to conduct this investigation on a series of United States Navy standard models at angles of yaw from 0° to 20° .
3. An experimental investigation of the rotational velocity of the slip stream of air propellers. It is planned first to determine the rotation in the slip stream of a series of United States Navy standard model propellers and then to investigate the effect of straightening vanes upon the power absorbed and efficiency.
4. An experimental and theoretical investigation of the causes of discontinuous air flow. It is desired to formulate criteria which will enable the prediction of the departure of smooth flow from the surface of an airfoil or streamline body.
5. An experimental investigation of the induced drag of airfoils of high aspect ratio. It is intended to test airfoils having aspect ratios from 6 to 15 and to compare the results with the predictions of the Lanchester-Prandtl theory.

California Institute of Technology:

1. Theoretical investigations in boundary layer, heat conduction, and other aerodynamical subjects.
2. Full-scale construction and free flight-testing of a new model of the Merrill type stagger decalage biplane.
3. Installation and calibration of apparatus in the Daniel Guggenheim Laboratory of the institute.

REPORT OF COMMITTEE ON POWER PLANTS FOR AIRCRAFT

ORGANIZATION

The committee on power plants for aircraft is at present composed of the following members:

Dr. S. W. Stratton, Massachusetts Institute of Technology, chairman.
George W. Lewis, National Advisory Committee for Aeronautics, vice chairman.
Henry M. Crane, Society of Automotive Engineers.
Prof. Harvey N. Davis, Harvard University.
Dr. H. C. Dickinson, Bureau of Standards.
William F. Joachim, National Advisory Committee for Aeronautics.
Lieut. Commander James M. Shoemaker, United States Navy.
Prof. C. Fayette Taylor, Massachusetts Institute of Technology.
Capt. T. E. Tillinghast, United States Army, matériel division, Air Corps, Wright Field.

FUNCTIONS

The functions of the committee on power plants for aircraft are as follows:

1. To determine which problems in the field of aeronautic power-plant research are the most important for investigation by governmental and private agencies.
2. To coordinate by counsel and suggestion the research work involved in the investigation of such problems.
3. To act as a medium for the interchange of information regarding aeronautic power-plant research in progress or proposed.
4. To direct and conduct research on aeronautic power-plant problems in such laboratories as may be placed either in whole or in part under its direction.
5. To meet from time to time on call of the chairman and report its actions and recommendations to the executive committee.

By reason of the representation of the Army, the Navy, the Bureau of Standards, and the industry upon this subcommittee, it is possible to maintain close contact with the research work being carried on in this country and to exert an influence toward the expenditure of energy on those problems whose solution appears to be of the greatest importance, as well as to avoid waste of effort due to unnecessary duplication of research.

The committee on power plants for aircraft has direct control of the power-plant research conducted at Langley Field and also of special investigations authorized by the committee and conducted at the Bureau of Standards. Other power-plant investigations undertaken by the Army Air Corps or the Bureau of Aeronautics are reported upon at the meetings of the committee on power plants for aircraft.

LANGLEY MEMORIAL AERONAUTICAL LABORATORY

ENGINE RESEARCH.—*Fuel injection engine.*—The increased thermal efficiency and low fuel consumption theoretically obtainable with the high-speed oil engine as compared with the carburetor engine, make the use of the oil engine particularly attractive for both military and commercial aircraft. The use of an oil engine for this type of service requires, however, maximum engine reliability with high power output per pound of engine weight, and low fuel consumption.

As previously reported, the two factors of major importance in the design of an aircraft oil engine are, first, the complete preparation of the fuel charge to give practically instantaneous autoignition on injection into the combustion chamber and second, the efficient distribution of the fuel throughout the combustion chamber by use of proper oil sprays and the necessary degree and type of combustion chamber turbulence, which will give combustion of the fuel early in the power stroke. The amount of research work done in this country and abroad toward obtaining the solution of these problems has greatly increased within the last year. The committee's work has included the investigation of the effects of turbulence as produced by combustion chamber design, the analysis and testing of various types of fuel valves and injection

pumps by means of special spray photography apparatus and by engine tests, and the analysis of theoretical problems in connection with the calculation of oil engine cycle efficiencies.

Engine performance—Combustion chamber design.—The investigation of the effect on engine performance of the various degrees of turbulence brought about by combustion chamber design has been continued with a single-cylinder Liberty engine and the second bulb-type cylinder head. As previously reported, the engine performance of this type of cylinder head has been determined with a nine-sixteenth-inch orifice having sharp edges, rounded edges, and with the cylinder side of the orifice flared to discharge the burning gases over one-half the piston area. The orifice has now been flared on the bulb side to distribute the air more thoroughly in the bulb. All tests have been made at a compression ratio of 13.5. The corresponding compression pressure at 1,600 revolutions per minute is 440 pounds per square inch. The fuel injection system used includes a cam-operated impact-type fuel injection pump and a spring-loaded fuel injection valve designed to give a high degree of fuel atomization. The engine performance was determined for speeds from 600 to 1,800 revolutions per minute, with the orifice flared to distribute the gases from the bulb over one-half the piston area, and a constant fuel quantity equal to 83 per cent of the full-load fuel quantity. The indicated mean effective pressure throughout the entire range of speeds was approximately 110 pounds per square inch and the fuel consumption 0.39 pound per indicated horsepower per hour. The maximum cylinder pressure varied from 690 pounds per square inch at 600 revolutions per minute to 750 pounds per square inch at 1,800 revolutions per minute. Flaring the bulb side of the cylinder orifice resulted in increasing the indicated mean effective pressure at full load and 1,600 revolutions per minute from 109 pounds per square inch to 113 pounds per square inch. The corresponding fuel consumptions on an indicated basis were 0.48 and 0.46 pound per indicated horsepower per hour. This represents a gain in mean effective pressure of 3.6 per cent and a reduction in the fuel consumption of about 4 per cent. The maximum cylinder pressure at full load, as indicated by a diaphragm type maximum cylinder-pressure indicator, was 750 pounds per square inch for both series of tests. Along with this investigation on the effects of turbulence, many tests have been made with this engine to determine the effects of progressive piston alterations on the performance of special types of gas and oil piston rings.

Two additional cylinder heads have been designed and constructed under this investigation for the Universal test engine. The first cylinder head has a vertical disk-shaped combustion chamber located between the inlet and exhaust valve, with means for varying the amount and direction of the turbulence. This change in air turbulence is obtained by variations in large removable orifices connecting the cylinder with the disk-type combustion chamber. A wide range of cylinder-orifice areas and shapes has been selected to permit the determination of the engine performance for a complete range of air-fuel ratios. The fuel injection pump is cam-operated and equipped with means for timing the injection and determining the rate of fuel pressure rise and the point of injection cut-off. The fuel valve used is of the automatic, spring-loaded, stem type and can be fitted with nozzles having one or more orifices. An investigation on nozzles using various arrangements and sizes of small round orifices will be made sufficiently complete to make a comparison between engine performance with the multiple round orifices and with slotted and annular orifices. The minimum diameter of the orifices investigated will be 0.004 inch. This cylinder head will be tested at compression ratios from 11.7 to 13.6, speeds from 800 to 2,400 revolutions per minute, and a controlled maximum cylinder pressure of about 800 pounds per square inch. Preliminary tests of this cylinder head have included the determination of the volumetric efficiency for speeds from 1,200 to 2,000 revolutions per minute with four cylinder orifices having areas of 1.95, 2.60, 3.25, and 3.90 square inches.

The preliminary power tests made with this cylinder head and nozzles having from three to five orifices show that the performance to date is poorer than that previously reported for fuel injection valves having annular orifices. The decrease in engine performance obtained when using small round orifices in the injection valve nozzle indicates that the sprays are not sufficiently well atomized nor distributed for high-speed oil engines. This was expected from theoretical considerations, and was further indicated by spray distribution analyses made in

connection with certain fuel-spray photography investigations. The combinations of orifices which have been used to date with a single fuel injection valve have prevented the attainment of the variable fuel injection rates for which the injection-pump cam was designed.

The second cylinder head has a horizontal, disk-shaped combustion chamber designed to conform to fuel spray shapes and provided with openings for the use of one or more injection valves. Varying degrees of turbulence within the combustion chamber may be obtained with this cylinder head by varying the shape, height, and diameter of a short, large-diameter displacer on the piston. The performance of this cylinder head will be determined for various degrees of fuel preheating by using exhaust and electrical fuel preheating injection valves. The castings for this cylinder head are being machined.

One of the fundamental factors which control the performance of a high-speed oil engine is the rate at which the fuel and air are mixed and burned. If the combustion proceeds too rapidly or with shock, it results in excessive cylinder pressures. Too slow a combustion rate, giving low maximum cylinder pressures because of late ignition and after burning, results in poor engine performance. Consideration of these factors has led to the design of a cylinder unit which will control combustion in a high-speed oil engine by mechanical displacement of the vaporized and ignited oil charge and the air for its complete combustion from small cam-operated auxiliary cylinders into the power cylinder. This cylinder design will permit a considerable increase to be obtained in volumetric efficiency, and will have several desirable characteristics in connection with the construction of radial air-cooled engines because of its shorter cylinder length. The fuel-injection pump for this cylinder-head unit is cam-operated and the start and stop of injection are controlled by a poppet type by-pass valve. The pump-control levers will simulate the throttle and spark controls of a carburetor aircraft engine.

Engine performance—Engine variables.—Investigations conducted with standard Liberty-type aluminum-alloy pistons have indicated the necessity for a reduction in the friction of the rings and the pistons, and an increase in strength of the piston crown and bosses for oil engine operation. A skeleton-type piston has been designed for high-speed oil engine service to give maximum power transmission with minimum mechanical and thermal distortion. The pistons are constructed of "Y" alloy and weight nine-tenths as much as the standard Army Liberty type of aluminum-alloy piston. The loading on the piston crown is transmitted by a strut of large section directly to the mid-section of the piston-pin bosses. The skirt of the piston is insulated from the crown and ring belt by a slot. The thrust faces of the piston have been designed to operate at a loading of 250 pounds per square inch at a cylinder pressure of 1,000 pounds per square inch and an engine speed of 2,400 revolutions per minute. The thrust faces will be lubricated by oil under pressure from the wrist pin. These pistons will be tested in single-cylinder test engines with various piston-ring designs and assemblies for the determination of the major factors affecting power transmission and friction losses.

The investigation of factors influencing the mechanical efficiency of the oil engine has shown the need for reducing the friction mean effective pressure by reducing the wall pressure of piston rings. Special piston rings have been designed to permit flooding of the cylinder walls with oil under pressure. The inertia and friction of the ring against the cylinder wall, and the inertia, impact, and hydraulic pressure of the oil are used to seal the land and cylinder-wall surfaces against leakage. The normal wall pressure of the piston rings is practically zero. Progressive alterations to the piston have reduced the oil consumption of the engine with one autoseal oil ring to about one-third the initial oil consumption, and to about two-thirds the consumption obtained with three standard Liberty piston rings.

Indicators for engines which use diaphragms or disk valves to measure engine-cylinder pressures have inherent errors, because of the inertia of their moving parts and the difference in the area exposed to the cylinder gases and to the balancing gas pressures. Engine tests have been undertaken to determine the effect of varying the shape, mass, and displacement of the moving element in a diaphragm-type maximum-cylinder-pressure indicator.

Fuel-injection pumps and valves.—The relative amounts of fuel and the rates of fuel injection required to give the constant volume and constant pressure burning for theoretical dual-com-

bustion-cycle indicator cards have been calculated during the past year. These theoretical calculations have been used in the design of a cam for a fuel injection pump to deliver fuel at the rates required to control combustion so as to obtain the cylinder pressures as given by the theoretical indicator card. Injection, distribution, ignition, and combustion lags, as determined from bench tests and theoretical calculations, have been taken into account in the design of this cam to control the proportion of constant volume and constant pressure combustion. The injection valve used with this fuel injection pump is of the automatic, spring-loaded stem type, with a narrow conical seat at the end of the stem. Preliminary tests have been made with injection nozzles having combinations of from three to five round orifices in the cylinder head having a vertical disk-type combustion chamber. Test work now in progress will cover the range of efficient operation of multi orifice injection nozzles using small round orifices.

Tests made with the second N. A. C. A. bulb-type cylinder head indicated that there was only a slight increase in performance to be obtained by extending the fuel injection valve nozzle short distances into the bulb. The maximum length of extension previously tested was one-half inch. Since the $\frac{9}{16}$ -inch orifice has been flared on the bulb side, the fuel nozzle has been extended $1\frac{1}{2}$ inches into the bulb. This extension has been provided with a series of copper fins designed to increase the rate of vaporization of the fuel within the bulb. The orifice in the fuel-valve extension is designed to inject the fuel directly into the nine-sixteenths cylinder-to-bulb orifice which should give considerably improved mixing of the fuel and air. It is expected that the large surface area of the fins will reduce the time lag of autoignition of the fuel by acting as a hot surface within the precombustion chamber.

For successful high-speed oil engine operation, the time lag of autoignition must be reduced to a minimum. Two fuel injection valves have therefore been designed to study the effect of the thermal preparation of the fuel before injection on the lag of autoignition and engine performance. In the first valve design the heat required to prepare the fuel is taken from the exhaust gases by a series of fins. The second valve is provided with electric heating coils for heating the fuel. Fine wire thermocouples will be used to determine the progressive temperature rise of the fuel as it passes through the fuel injection valve. A direct comparison of the electric and exhaust heated valves will be made on the same cylinder heads.

FUEL-INJECTION RESEARCH.—The spray photography apparatus constructed and developed by the staff of the committee has permitted the extended photographic study of the characteristics of injection systems and the fuel sprays produced by them. Records of the start, development, cut-off, and distribution of the fuel sprays are obtained by photographing them at rates of from 2,000 to 4,000 per second with an exposure of less than one-millionth second. Injection pressures up to 12,000 pounds per square inch and spray chamber pressures up to 600 pounds per square inch are used. The spray-photography apparatus has been described in previous reports of the committee.

The time lags of an injection system are important in the design of high-speed oil engines. Additions to the spray-photography apparatus have made it possible to determine the time lags for the injection system used with the apparatus. In this system, oil under pressure is released by a cam and lever-operated timing valve to the injection valve tube to produce a spray from the injection valve. A record of the motion of the injection valve stem is obtained on a photographic film by means of an optical indicator. By coordinating this record with that of the series of spray photographs, the time lags for various test conditions for the pressure waves to travel the valve tube length can be obtained.

A research on the velocity of pressure waves and the time lags in an injection system between the instant the timing valve is lifted and the appearance of the spray from the injection valve has been completed. The factors investigated included the injection valve tube length and diameter, initial fuel pressure in the tube, injection pressure, and injection valve opening pressure. The effects of these factors on the lag of operation of the timing and injection valves and on the velocity of pressure waves in the systems have been investigated. It was found that the timing valve lag could be largely accounted for by the time required to release the timing valve stem from compression by the spring. The injection valve opening pressure had

the greatest effect on the injection valve lag, an increase in the opening pressure from 2,000 to 6,000 pounds per square inch causing the time lag of 0.0003 second for a 46-inch valve tube to increase 300 per cent. The velocity of the pressure waves was approximately that of a sound wave, but varied slightly with the initial tube pressure and the injection pressure. The injection valve tube length had the greatest effect on the wave velocity. Other results which can not be readily summarized here have been obtained.

Analyses of the experimental data obtained during the previous year have been completed. Reports have been prepared on the factors affecting the exact reproducibility of penetration and the cut-off of oil sprays, and on the factors in the design of centrifugal type injection valves for oil engines.

Analyses of experimental data have been completed for the investigation of the effects of fuel spray and spray-chamber gas densities and viscosities on the characteristics of fuel sprays. A logarithmic relation was found to exist between the chamber gas density and the spray volume at time intervals of from 0.002 to 0.004 second after the appearance of the sprays. An approximate application of the penetration data to the conditions of varying pressure and density in an engine during injection of the spray was made.

A complete description of the spray-photography apparatus in its present form has been published, together with representative spray photographs and curves. The effect on spray characteristics of injection pressure, chamber gas density, fuel-oil specific gravity, and of two factors in the design of a centrifugal type injection valve are given.

Both experimental investigations and mathematical analyses of the operation of the spray photography timing valve have been made. The effect of spring tension and of length of injection-valve tube on the time-lift diagram of the valve stem have been investigated and compared with the cam contour. The rates of fuel-pressure rise at the timing valve and in the injection valve tube have been computed and found to compare satisfactorily with the actual test results. The timing valve has been used as a positively operated injection valve, and records have been taken of the opening and closing of the valve.

A research has been undertaken to determine the effects of the weight of the moving parts, amount of movement, amount and type of operating forces, and the type of injection nozzle, on the lag of injection of the valve and on the characteristics of the fuel sprays. Injection valves already available will be used, and new valves designed to permit a comprehensive investigation of the above variables.

The design of various devices to be added to the present spray-photography apparatus has been undertaken in order to permit the study of the characteristics of combustion of atomized fuels for oil engines. No reliable data could be found from which the amount of heat which will be lost to the water jackets of the spray combustion chamber during the air heating and combustion periods could be computed. These data have been determined experimentally with a water-cooled cylinder in which the air was heated electrically. Heat transfer coefficients for this apparatus have been determined for a range of air temperatures up to 700° F., and for air pressures up to 50 pounds per square inch. The laws controlling the heat transfer for the conditions of these tests have been used for computing the size and capacity of the heating apparatus for the new spray combustion chamber.

The work to date indicates that the new apparatus will consist of a water-cooled chamber with fused quartz windows, a separate heating chamber, and apparatus for producing turbulence during injection of the fuel sprays. It will be possible to simulate the actual conditions of temperature, pressure, combustion-chamber shape, and turbulence in an engine. Analyses and computations for the various apparatus for this work are reaching a point where actual design can be started.

SUPERCHARGER DEVELOPMENT.—*Supercharger analysis.*—An investigation is now being made to determine the fundamental and practical requirements to be met by aircraft engine superchargers in military and commercial service. The adaptability and performance characteristics of all types of compressors are being studied to determine to what degree each meets the requirements of an ideal supercharger. It is believed that this analysis will lead to the proper selection and further development of the best compressor for each service.

Modifications to the Roots type supercharger.—A mathematical and analytical investigation is being made to determine the possibility of improving the performance characteristics of Roots type superchargers by means of a suitable type discharge valve. This valve will materially reduce the inherent disadvantages of a Roots blower, namely, the pulsating air flow, the lower volumetric efficiency at the higher critical altitudes, and the return flow of air which requires its redelivery. The latter disadvantage results in an inefficient increase in the carburetor air temperature and in the power required. Both oscillating and rotating valves have been studied. These valves will be synchronized with the impellers so that they close after each charge of air is delivered and do not open until the next charge is compressed and ready to be delivered.

Some difficulty has been experienced in maintaining the most efficient and best mechanical impeller clearances on the Roots type supercharger because of the expansion of the impellers at the high temperatures that accompany the pressure ratios obtained at high critical altitudes. Increasing the clearances sufficiently to eliminate the possibility of scoring the impellers at these high temperatures results in a decrease in the volumetric efficiency which necessitates a corresponding increase in impeller speed to maintain the same air delivery. A set of steel impellers is being constructed to replace the present magnesium alloy impellers now used. The steel impellers will have a weight equal to or less than the magnesium impellers, and because of their lower coefficient of expansion will not expand as much as the aluminum case. This will permit the use of smaller clearances at assembly without danger of scoring the impellers or the case at the higher temperatures.

Some difficulty has also been experienced with impeller end clearances because of the axial shift of the impellers caused by initial looseness and slight wear of the balls and races in the impeller-locating bearings. Precision-type ball bearings with much less looseness between the races have been obtained to eliminate this axial shift. The wear will be reduced by filtering out the carbon and foreign matter from the lubricating oil.

These several changes will permit the use of smaller impeller clearances with safety, and will result in increased supercharger efficiency and in net engine performance and power.

Effect of supercharger capacity on airplane performance.—This research was undertaken to determine the effect of various amounts of supercharging on the performance characteristics of an airplane. The investigation will be carried out on a modified DH-4 airplane with a steel fuselage. This airplane is now being partially rebuilt for this research. To obtain different degrees of supercharging the speed of the same supercharger will be varied by driving it at 1.615, 1.957, 2.4, and 3 times engine speed. These supercharger speeds will give critical altitudes of approximately 12,000, 16,000, 21,000, and 28,000 feet, respectively. The changes in power with altitude of a supercharged and unsupercharged engine, the effect of supercharging on volumetric efficiency, and the fuel consumption of a supercharged engine in flight will be determined in this research.

Problems incidental to supercharging.—The determination of engine power in flight has been attempted by several methods. The results obtained differ considerably, depending on the method used. The use of calibrated propellers is probably the most satisfactory method that has yet been tried, but this method may introduce errors as high as 10 per cent. These errors may be caused by bending and twisting of the propeller, which vary with changes in altitude; warping, which is caused by weathering or aging, and errors in correcting the power of a calibrated engine for changes in temperature and pressure. A Bendemann hub dynamometer has been used for determining engine power in flight and in calibrating two propellers in flight. The results obtained with the hub dynamometer were more satisfactory than the results which have been obtained with any other method used. Work is now in progress to determine the most suitable type hub dynamometer as a means of accurately measuring power in flight. The requirements to be met by a hub dynamometer have been formulated. A number of types have been studied to determine to what degree each meets these requirements. From several mechanical, hydraulic, and electrical methods considered, one mechanical and one hydraulic have been selected for further analysis.

The need for the determination of the effect of fuel consumption on engine performance in flight has led to the development of an experimental Venturi type fuel flow meter. This flow meter has been used on several flights with satisfactory results. A more serviceable flow meter embodying the same principles is now being designed.

Completed investigations.—Four investigations have been completed from last year. Three of these investigations were on problems directly pertaining to supercharging and the other on a problem incidental to supercharging.

The first investigation dealt with preliminary flight testing of the N. A. C. A. Roots type aircraft engine supercharger. The results show that the Roots type supercharger is inherently adaptable to commercial airplanes and to a number of military and naval airplanes, because of its low weight, mechanical simplicity, high efficiency, and low power requirements at moderate altitudes. Supercharging increased the ceiling, improved the climbing performance, and increased the air speed so that for a large range of altitudes it was higher than the normal sea-level maximum. The engine showed no detrimental effects which could be attributed to supercharging. This material has been prepared for publication.

The second investigation was conducted on a Wright E-4 and a Liberty-12 engine. The results obtained show the effect of high inlet air temperatures on power. In these tests the carburetor air temperature was varied from 45° to 180° F., and the speed from 1,400 to 1,800 revolutions per minute. Two fuels were used, domestic aviation gasoline and a mixture of 30 per cent benzol and 70 per cent gasoline. The blended fuel gave 5 to 6 per cent more power at the speeds giving maximum volumetric efficiency than did the domestic aviation gasoline. For a blended fuel the relation between temperature and power is linear. The indicated power decreases at a much faster rate with increase in temperature than that given by the square-root relation. For small variations in temperature, as occur for changes from one season to another, the square-root relation is sufficiently accurate, but where the change of temperature is very large and greater accuracy is desired, the temperature correction to be applied should be determined by testing the engine. The results of these tests have been prepared for publication.

The third investigation completed was on the comparative laboratory performance of three sizes of Roots superchargers. Compared on the basis of air delivered, the performance characteristics are similar except for the smaller superchargers, for which the power requirements are higher because the power required increases more rapidly than the speed. The difference between the actual and the theoretical power required to deliver the air in quantities and at pressures encountered in the range of ordinary supercharged flight varies with the speed raised to the 2.5 power. The ratio of discharge air temperature T_2 to the inlet air temperature T_1 depends upon the speed and may be evaluated by raising the ratio of the discharge pressure P_2 to the inlet pressure P_1 to the $n-1$ divided by n power, and multiplying this result by a constant C . The value of n in this relationship increases from 1.36 for an impeller length of 4 inches to 1.53 for an impeller length of 11 inches. The value of C varies from 1 at zero speed to 1.05 at 6,500 revolutions per minute. The results of these tests have been prepared for publication.

The fourth investigation completed includes the tests on a TS and a UO-1 airplane equipped with an air-cooled engine and an N. A. C. A. Roots type supercharger. In these tests the absolute ceiling of the UO-1 was increased from 19,400 to 32,000 feet by supercharging, and the time of climb to 16,000 feet was reduced 50 per cent. The average cylinder-head temperature obtained on several unsupercharged and supercharged flights was 325° and 470° F., respectively. The engine showed no detrimental effect that could be attributed to supercharging.

ENGINE ANALYSIS.—Fuel vapor pressure.—The performance of a high-speed oil engine is largely dependent upon the rate of vaporization of the fuel charge within the combustion chamber. The vapor pressure of fuels has been fairly well established up to approximately 300° C. but for temperatures greater than this the available data are incomplete. An investigation was therefore undertaken to determine the vapor pressures and temperatures of several fuels up to their autoignition temperatures. From the results of this investigation, the temperatures required to force rapid vaporization of these fuels in an engine cylinder could be determined.

The vapor pressures and temperatures of six fuels, various mixtures of these fuels, a lubricating oil, and water were determined up to 900° F. and 5,000 pounds per square inch pressure. A considerable amount of test data has been taken which indicates the stability and instability of the liquids tested. The test data are being analyzed and corrected for change in volume of the apparatus due to the high fuel vapor pressures and temperatures and to the diminishing quantity of the liquid fuel in the bomb of the test apparatus. The final results will be incorporated in a report for publication.

Analysis of cycle efficiency.—The performance of high-speed oil engines for aircraft is dependent upon the overall efficiency (which include cycle, combustion, volumetric, mechanical, and cooling efficiencies), maximum cylinder pressure, and the maximum overhaul period. Aircraft engine performance should be such that maximum power per pound engine weight, minimum fuel consumption per horsepower per hour, and maximum reliability are obtained.

The engine cycle that should be used in high-speed oil engines for aircraft is the dual cycle, a combination of constant volume and constant pressure combustion. Such a cycle would decrease the weight per horsepower and increase the reliability for the same power output obtained with the Otto cycle. Since it is important to compare various engines as to the efficiency with which the fuel is burnt and so compare engine designs, it is necessary to know the cycle efficiencies at which they operate.

A theoretical investigation is being made on the effects of compression pressure, air available for combustion, temperature of the induced air, temperature and pressure of the residual exhaust gases, explosion pressure, and point of cut-off on the efficiency of the dual cycle. This work involves calculations for the pressures and temperatures at all points on the indicator card, and these in turn require the use of the specific heats of gases for constant pressure and volume up to the highest temperatures of combustion, the Joule-Thomson effect, volumetric efficiencies versus compression ratio, chemical composition and weight of the working mixture at all points of the cycle, quantity of fuel required for various points of cut-off, and other factors. The completed results of this work will enable the rapid determination of the cycle and combustion efficiencies of an engine when the usual test data are known.

Calculations have been made to determine the effects of high residual exhaust gas temperature on the pressures and temperatures throughout the cycle for a compression ratio of 11. The results show that an increase of 300° F. in the temperature of the residual exhaust gases increased the temperatures and pressures throughout the cycle only slightly. The maximum increase in temperature obtained at the end of the suction stroke was 4° F. The pressure increase was 0.05 pounds per square inch.

Experiment and theoretical analyses have shown that the specific heat of gases varies with the temperature and pressure, especially with the temperature. It is therefore of importance in calculating the amount of work done on the compression and expansion stroke of an oil engine that the exponent for adiabatic changes of state in the fundamental equation for compression and expansion should be accurate for the temperature involved.

Calculations of pressures and temperatures have been made at several points on a compression curve, first by using a constant value for the exponent, and second by using a varying value for the exponent for adiabatic changes of state to determine the extent of error involved by using the constant value. The results show that the negative work done by using a constant exponent in the calculations was less than that obtained by using a varying exponent, although the difference was small. The greatest variation in pressure was of the order of 0.5 per cent. This result was expected on account of the small variation of the exponent with temperature for the compression stroke. Since the value of the specific heat of gases increases with temperature it is expected that on the expansion stroke the result of similar calculations will show an appreciable error in the work done, because of the higher temperatures involved.

A method of calculating the theoretical cycle efficiency of an oil engine has been practically completed. The data required for this work are the compression ratio, volumetric efficiency under power, temperature of the inlet air, temperature and pressure of the residual exhaust

gases, maximum cylinder pressure, and bore and stroke of the engine. The completion of this work will give a method for calculating the theoretical cycle and combustion efficiencies of an oil engine.

An investigation of the specific heats of the gases of combustion for temperatures up to 3000° C. is in progress. It was found by evaluating and plotting a large number of empirical formulæ developed by various investigators that there was a wide discrepancy in the results. The investigation has shown that the specific heats of the gases of combustion may be obtained by three methods—by considering the theoretical heat content of the molecule due to its translational, vibrational, and rotational energy, and by experimental methods involving the study of the velocity of sound and explosion. An attempt is being made to correlate the theoretical and experimental data for use in engine calculations.

Chromium-plated pistons.—Four Liberty pistons have been chromium-plated and tested to determine the wearing quality of chromium plating under both motoring and power conditions. The chromium plating on the crowns of the four pistons tested showed no material change, which indicates that temperature alone probably has little effect on the chromium plating. The excessive wear of the chromium plating on the piston skirt when under power in comparison to that when being motored, indicated that the failures of the chromium plating were apparently caused by the formation, growth, and breakage of blisters due to the lack of bond between the aluminum and chromium, and to the combination of rubbing and light and medium piston slap.

BUREAU OF STANDARDS

Supercharging of aircraft engines.—Tests have been made in the altitude laboratory of a Curtis D-12 engine equipped with a gear-driven centrifugal supercharger, installed between the carburetor and the intake manifold. This supercharger is designed for low-altitude work and for an engine speed of 2,000 revolutions per minute, its critical altitude is about 7,500 feet. Two types of manifold were used and about 5 per cent more power was obtained at all altitudes with one type of manifold than with the other. Up to the rated altitude, the power output with this supercharger and with the manifolds giving best distribution was from 5 to 10 per cent less than that obtained with the same engine under ideal supercharging conditions (i. e., with no power required to drive the supercharger). These tests were requested by the Army Air Corps and covered conditions corresponding to altitudes from sea level to 25,000 feet.

Phenomena of combustion.—The study of the gaseous explosive reaction by means of the constant-pressure bomb (soap bubble) has been continued and the thermodynamic as well as the kinetic possibilities of this method have been pointed out in several journal articles. That reaction velocity is proportional to the molecular concentration of the reacting gases has been verified for known mixtures of (1) carbon monoxide and methane with oxygen, and (2) carbon monoxide and hydrogen with oxygen. The effect of inert gases (nitrogen, helium, or carbon dioxide) on the carbon monoxide-oxygen reaction and on the methane-oxygen reaction has also been studied. A report to be published by the National Advisory Committee for Aeronautics shows that the effect of an inert gas on the reaction rate may be accounted for by an additive term, directly proportional to the concentration of the inert gas. The proportionality constants for different inert gases evidently depend on their thermal properties.

Combustion in an engine cylinder.—This project is concerned with obtaining information of a fundamental nature on the factors which influence combustion in actual engine cylinders. During the past year the effect of combustion time on engine performance has been analyzed on the basis of certain simplifying assumptions and the results compared with deductions from actual indicator cards. Technical Report No. 276 presents this discussion.

Automatic altitude control.—Runs were made with the Curtiss D-12 engine in the altitude laboratory to determine the proper opening of the carburetor control valve for various altitudes up to 25,000 feet. An automatic valve designed from the data thus obtained gave a constant fuel-air ratio from 5,000 to at least 20,000 feet. This work was done for the Army Air Corps.

At the request of the Navy, work has been started on the design of an automatic carburetor altitude-control device for the same engine, utilizing the multiplied pressure pump described in Technical Note No. 108 of the National Advisory Committee for Aeronautics.

Gaseous-fuel carburetor.—At the request of the Navy, an experimental gas carburetor was designed and data have been obtained on the relative performance of a given engine at various speeds and loads on aviation gasoline, on city illuminating gas, and on mixtures of the two. The results obtained will probably be used in the development of a gas carburetor for actual flight test on an airship engine. The object in view is the possibility of increasing the cruising range of lighter-than-air craft by the employment of natural gas or illuminating gas as an auxiliary fuel.

Fuels for high-compression engines.—The testing of fuels and fuel dopes in the single-cylinder Liberty engine has been continued. None of the fuel dopes submitted was found to affect power, economy, or antiknock value appreciably. While cracking and increased volatility both tend to raise the antiknock value of gasolines made from a given crude oil, the improvement due to cracking is often much less than the difference between straight-run gasolines from different crudes.

At the request of the Navy, work has been done on the development of a simple laboratory device for comparing the antiknock characteristics of aviation gasoline. An experimental bomb was built which had approximately the internal dimensions of the combustion chamber in a Liberty engine cylinder. This bomb gave average results which appeared to rate several fuels in the same order as does the routine engine test of the Bureau of Standards. However, successive observations with a given fuel under apparently identical conditions often showed considerable variation and a second bomb, having the same volume but different dimensions, is to be compared with the first bomb as regards reproducibility of results. Since the bomb test is rapid and requires only a small sample of fuel it has obvious advantages, provided that it can be shown to give consistent results which are uniformly in accord with the performance of fuels in aviation engines.

Lubrication under starting conditions.—Measurements of the rate of flow of about 35 commercial lubricating oils through the oil passages of a Wright J-4 engine, mounted in a cold chamber and slowly motored over, have been completed. These and other experiments on the flow of aircraft-engine oils at low temperatures form the basis of an extensive report now in preparation. The first conclusion of this work is that neither the pour point of an oil nor its viscosity at 210° F. is sufficient to determine its performance in the engine at temperatures below the ice point.

Starting of internal-combustion engines.—The analysis of laboratory data on fuel volatility and engine starting tests has made it possible to specify the fuel requirements for engine starting in terms of the usual A. S. T. M. distillation curve. It was also shown by bomb experiments with known mixtures of gasoline vapor and air that cracked gasolines do not differ in starting ability from straight-run gasolines of like distillation characteristics.

NEW ENGINE TYPES

The most striking developments of the year have been the advances made in air-cooled engines. These have included improvements in performance, increases in reliability, and reductions in the cost of maintenance. During the year no radical developments in the form of unconventional types of engines have appeared, with the exception of the Fairchild "Caminez" engine, which is now on the market.

The Fairchild "Caminez" engine is a 4-cylinder radial air-cooled engine, using a cam-type drive in place of the conventional crank shaft. The engine is the result of a number of years of intensive development, first by the engineering division of the Army Air Corps and later by the Fairchild Co. This engine is rated at 135 horsepower at 1,050 revolutions per minute and weighs approximately 340 pounds without starter and propeller hub.

Both the Bureau of Aeronautics and the Army Air Corps have assisted in the further development of air-cooled engines. The Army Air Corps is particularly interested in the

development of the Curtiss "Hex" engine, which is a 600-horsepower radial air-cooled engine having two banks of cylinders. This particular arrangement is the result of an effort to decrease the overall diameter and to eliminate the counterweight on the crank shaft.

The Army Air Corps has continued the development of the inverted air-cooled Liberty engine. The experimental engines of this type, built by the Allison Engineering Co. under the supervision of the Air Corps, have completed their tests and a number have been procured by the Air Corps for service use.

As an outgrowth of the air-cooled Liberty engine the Air Corps is sponsoring the development by the Wright Co. of a 12-cylinder air-cooled "V" engine of approximately 600 horsepower. The Air Corps is also sponsoring the development of a 24-cylinder "X" type engine which is being constructed by the Allison Engineering Co. This engine is expected to develop approximately 1,400 horsepower.

Air-cooled engines.—There are now available service-type air-cooled engines which can be substituted for the water-cooled aircraft engines of corresponding power, with the exception of the Packard 800-horsepower engine.

The air-cooled engines that have been developed are of two general types, the radial and the "V" type. Of the radial types the most prominent is the 9-cylinder Wright "Whirlwind" model J-5 engine. This engine is a further development of the J-4 type. It has a greatly improved cylinder construction and has fully inclosed valve gear. It also is equipped with a new "Eclipse" concentric impulse starter. The engine is in extensive use in military and commercial services.

The Wright "Cyclone" R-1750 type is a larger 9-cylinder radial air-cooled engine which has been flight-tested by the Navy Department and is still undergoing service tests. This engine is rated at 525 horsepower at 1,900 revolutions per minute.

The Pratt & Whitney "Wasp" 9-cylinder radial engine rated at 410 horsepower at 1,900 revolutions per minute has passed its service tests and is now in production. This engine is now considered standard equipment on a number of Navy service-type airplanes and has given a most satisfactory performance.

The Pratt & Whitney "Hornet," a 9-cylinder radial air-cooled engine, having a displacement of 1,690 cubic inches, is expected to develop 500 horsepower at 1,800 revolutions per minute. This engine was designed for use in heavy-duty types of aircraft and is now in the experimental development stage.

Water-cooled engines.—Continued development, as a result of service use, has been made on the Curtiss V-1550 engine, which is a further development of the Curtiss V-1400 and the very successful Curtiss D-12 engines. This development has been sponsored by the Army Air Corps. The new engine will develop 600 brake horsepower at 2,400 revolutions per minute and is available in both direct-drive and geared types. The weight of the direct-drive type is approximately 740 pounds. This engine has completed the experimental development stage and is now being given service tests.

The Packard 1A-1500 engine is being further developed as a result of experimental and service tests by the Army Air Corps. A new type, the 2A-1500, has successfully passed the experimental stage at a rating of 600 horsepower at 2,500 revolutions per minute. The 2A-1500 engine is made in the inverted direct-drive type and in the upright geared type. The large Packard 2500 engine has been further developed, and the latest type, the 3A-2500, is expected to develop 1,000 horsepower at 2,300 revolutions per minute. This engine has also been specially designed for use with superchargers.

Superchargers.—Superchargers have now passed from the experimental development stage to service use. The Roots type and the centrifugal type superchargers have been adapted successfully to the radial air-cooled engine, and superchargers of both types are in experimental development on the water-cooled types of engines in service.

REPORT OF COMMITTEE ON MATERIALS FOR AIRCRAFT

ORGANIZATION

The present organization of the Committee on Materials for Aircraft is as follows:

Dr. George K. Burgess, Bureau of Standards, chairman.
 H. L. Whittemore, Bureau of Standards, vice chairman and acting secretary.
 Lieut. R. S. Barnaby, United States Navy.
 S. K. Colby, American Magnesium Corporation.
 Henry A. Gardner, Institute of Paint and Varnish Research.
 Dr. H. W. Gillett, Bureau of Standards.
 Prof. George B. Haven, Massachusetts Institute of Technology.
 Zay Jeffries, Aluminum Co. of America.
 J. B. Johnson, matériel division, Army Air Corps, Wright Field.
 George W. Lewis, National Advisory Committee for Aeronautics (ex-officio member).
 Capt. H. C. Richardson, United States Navy.
 G. W. Trayer, Forest Products Laboratory, Forest Service.
 Starr Truscott, National Advisory Committee for Aeronautics.
 Hon. Edward P. Warner, Assistant Secretary of the Navy for Aeronautics.

FUNCTIONS

Following is a statement of the functions of the committee on materials for aircraft:

1. To aid in determining the problems relating to materials for aircraft to be solved experimentally by governmental and private agencies.
2. To endeavor to coordinate, by counsel and suggestion, the research and experimental work involved in the investigation of such problems.
3. To act as a medium for the interchange of information regarding investigation of materials for aircraft in progress or proposed.
4. To direct and conduct research and experiment on materials for aircraft in such laboratory or laboratories, either in whole or in part, as may be placed under its direction.
5. To meet from time to time on call of the chairman and report its actions and recommendations to the executive committee.

The committee on materials for aircraft, through its personnel acting as a medium for the interchange of information regarding investigations on materials for aircraft, is enabled to keep in close touch with research in this field of aircraft development. Much of the research, especially in the development of light alloys, must necessarily be conducted by the manufacturers interested in the particular problems, and both the Aluminum Co. of America and the American Magnesium Corporation are represented on the committee. In order to cover effectively the large and varied field of research on materials for aircraft, four subcommittees have been formed, as follows:

Subcommittee on metals:

Dr. H. W. Gillett, Bureau of Standards, chairman.
 Zay Jeffries, Aluminum Co. of America.
 J. B. Johnson, matériel division, Army Air Corps, Wright Field.
 George W. Lewis, National Advisory Committee for Aeronautics (ex officio member).
 Starr Truscott, National Advisory Committee for Aeronautics.
 H. L. Whittemore, Bureau of Standards.

Subcommittee on woods and glues:

G. W. Trayer, Forest Products Laboratory, Forest Service, chairman.
 H. S. Betts, Forest Service.
 George W. Lewis (ex officio member).
 H. L. Whittemore, Bureau of Standards.

Subcommittee on coverings, dopes, and protective coatings:

Henry A. Gardner, Institute of Paint and Varnish Research, chairman.
 Dr. W. Blum, Bureau of Standards.

Subcommittee on coverings, dopes, and protective coatings—Continued.

Warren E. Emley, Bureau of Standards.

Prof. George B. Haven, Massachusetts Institute of Technology.

Isadore M. Jacobsohn, Bureau of Standards.

George W. Lewis (ex officio member).

P. H. Walker, Bureau of Standards.

E. R. Weaver, Bureau of Standards.

Subcommittee on Aircraft Structures:

Starr Truscott, National Advisory Committee for Aeronautics, chairman.

Charles Ward Hall, Hall-Aluminum Aircraft Corporation.

Lieut. Lloyd Harrison, United States Navy.

G. W. Lewis (ex officio member).

Charles J. McCarthy, Chance Vought Corporation.

L. B. Tuckerman, Bureau of Standards.

John E. Younger, matériel division, Army Air Corps, Wright Field.

Most of the research in connection with the development of materials for aircraft is financed directly by the Bureau of Aeronautics of the Navy Department, the matériel division of the Army Air Corps, and the National Advisory Committee for Aeronautics.

The Bureau of Aeronautics and the matériel division of the Air Corps, in connection with the operation of tests in their own laboratories, apportion and finance research problems on materials for aircraft to the Bureau of Standards, the Forest Products Laboratory, and the industrial research laboratories.

MEETINGS OF THE COMMITTEE

As in past years the committee held several meetings during the year. The corrosion of the light alloys continues to be one of the subjects of great interest and has received much attention at each meeting. At the meeting which followed the second general aircraft conference at the Langley Memorial Aeronautical Laboratory Mr. E. H. Dix of the Aluminum Co. of America read a paper describing a new corrosion-resisting light alloy product of that company called "Alclad." This material consists of a sheet of aluminum alloy having a layer of very pure aluminum on each side. It appears to have remarkable resistance to corrosion. This paper has been issued by the committee as a technical note.

SUBCOMMITTEE ON METALS

Intercrystalline embrittlement of duralumin.—The subcommittee on metals has continued its experimental work on the study of the causes and prevention of intercrystalline embrittlement of duralumin. Corrosive attack starting at the surface and penetrating between the crystals may notably embrittle duralumin without the surface showing evidence of the extent of the attack below the surface. This embrittlement has been met in service to an extent sufficient to limit materially the application of duralumin in construction of aircraft for which long life is necessary, and has made it imperative that the deterioration be prevented.

During the period within which the problem has been studied sufficient advances have been made so that it is no longer a question whether or not the attack can be prevented, but it is instead merely a question of which one of several effective methods should be chosen in a particular case.

The laboratory methods of accelerated-corrosion testing chosen to indicate the propensity of the alloy toward intercrystalline embrittlement have so far shown good agreement with exposure tests.

The behavior of nonmetallic protective coatings is not so readily determined by laboratory tests and final choice among such coatings must await the completion of exposure tests.

The chief effective precaution, other than the use of some protective coating, is to quench the duralumin rapidly rather than slowly; that is, in cold water rather than in hot water or oil, since the former procedure gives material much less susceptible to embrittlement than the latter.

Age-hardening at room temperature rather than accelerated aging at elevated temperature also favors resistance to intercrystalline attack. These heat-treatment factors have much more to do with corrosion resistance than do any variations in chemical composition likely to be met commercially.

While dualumin suitably heat-treated is improved in corrosion resistance, embrittling corrosion is not thereby wholly avoided. Hence protection of the surface is also required.

It was stated in last year's report that protection of duralumin by a surface coating of pure aluminum was one of the surest methods. Further experiment and the results of exposure tests corroborate this, and justify the present conclusion that it is the most effective method yet available. The lead offered by the previous investigations of the subcommittee upon aluminum-coated duralumin has been followed by an American producer of duralumin, and duralumin sheet with an integral coating of aluminum on each side is now commercially available, so that this expedient is not one of merely academic interest, but is ready for application in practice. While the strength of the commercial aluminum-coated duralumin is not quite as high as that of plain duralumin, the initial strength and ductility will be retained with little loss so that after a period of service the initially weaker material will be the stronger.

The aluminum-coating process has not yet been commercially applied to tubing so that other methods of protection still need consideration. It is also advisable to make assurance doubly sure by using a nonmetallic protective coating over the aluminum surface since the aluminum coating, while not subject to the intercrystalline type of attack, is, like all other aluminum and aluminum alloys, subject to the less dangerous type of general corrosion whose advance is visible on the surface.

Nonmetallic protective coatings of the aluminized-varnish or bitumastic type, which have heretofore been largely used as protecting coatings, cling well on a mat surface, and poorly on a smooth metal surface. Hence where these coatings are to be used preliminary anodic treatment in chromic acid to produce the "anodic coating" or a chemical treatment producing a similar surface is advisable. The anodic coating in itself offers some protection but not enough to be a real solution. As a base for adherent coatings it is, however, of distinct value.

The chief trouble with coatings of the varnish type is their tendency to become brittle and to check and crack off. Flexibility of the coating is a very real advantage. Since any completely moisture-repellant coating which will "stay put" will defeat corrosion, covering the anodic coating with oil or lanolin gives very effective protection as long as the oil film remains. Oiled anodic coatings are finding much use here and abroad. They do not add as much weight as coatings of the varnish type and if the oil film is kept intact by periodic renewal offer much improved protection compared with a bare surface. Such coatings have some tendency to collect dirt, which may be decreased by the use of fairly thick coatings dusted with aluminum powder. A drawback to the oil coating is that visual inspection does not readily show whether the film is intact or not, so that recoiling on a definite schedule should be resorted to.

A recent development in the line of a flexible, water-repellant coating applicable to duralumin is a rubber cement which will stick tenaciously to metal and hence may be applied without previous anodic coating. The bare rubber cement breaks down rapidly in the atmosphere and by itself offers little real promise. Mixture of aluminum powder with the cement, or merely dusting aluminum powder on the tacky surface and brushing it down, raises the resistance of the cement to atmospheric influences almost immeasurably. While exposure tests of such a coating on duralumin have not yet progressed far enough to warrant final conclusions, the aluminized rubber coating deserves extended trial. It even offers promise for the protection of magnesium, a matter to which the subcommittee has given considerable attention and on which it can report continued activity and interest by producers of magnesium.

The foregoing shows that not only may duralumin itself be improved in corrosion resistance by suitable heat treatment, but that a variety of effective protective coatings are available which are applicable to most aircraft parts. Pontoons and tubing (especially the protection of the interior of tubing) still offer problems. It would appear that aluminized rubber coatings deserve trial on pontoons. Pending the availability of aluminum-coated duralumin tubing,

attention is being paid by the subcommittee, together with the subcommittee on aircraft structures, to high-chromium and other corrosion-resistant steel tubing. The fabrication and welding of such tubing appears feasible and may be expected to be better understood in the near future.

More advance has been made on the engineering angles of the protection of duralumin than on the clearing up of the mechanism by which embrittlement takes place, though unremitting effort has been put on the study of the cause of embrittlement. Metallographic and X-ray methods are being applied. The phenomenon of asterism, shown by "pin-hole" X-ray photographs of embrittled duralumin is being studied, but so far it appears that, while asterism usually accompanies embrittlement, intercrystalline attack can occur without asterism. Definite location of the cause of asterism may help in determining the cause of embrittlement.

There is some reason to believe that duralumin under the stresses of service is more subject to embrittlement than in unstressed exposure. On account of the importance of appraising the validity of exposure tests, experiments are under way to study the effect of both static and repeated stresses upon the progress of intercrystalline corrosion. Apparatus for this has been designed and constructed and the experiments are under way.

The exposure tests which will tend to verify or disprove the tentative conclusions given above as expressing the facts as far as they are at present known to the subcommittee are being continued, some 1,700 specimens being under exposure test, their properties being determined at appropriate intervals.

High-speed fatigue testing.—Continued work with the high-speed fatigue-testing machines has shown that the discrepancy between the results from the high-speed machines and the previously used crank-driven machines is not accounted for by incipient corrosion of the specimen. Check tests run in the old machines duplicated the previous results.

The major problem to be solved is the determination of the cause of this discrepancy. It may be due to adventitious stresses caused by the type of support, although the theoretical investigations made seem to preclude this. It seems more probable that it is due to an actual change of fatigue properties with the frequency of application of the load. With this question still unsettled it has not seemed desirable to start tests on magnesium and steel specimens as it is ultimately intended to do.

The investigation has been continued on the following lines:

(a) The method of supporting the specimen in the present air-driven machines has been changed from a pivot support to an air-jet support, thus freeing the specimen wholly from any possible longitudinal restraint, due to the pivots, which might introduce adventitious stresses. The machines with the new type of support are running smoothly but have not been in operation long enough to give definite results.

(b) Preliminary experiments and computations have been made on an electrically-driven machine with loaded specimens in order to close the gap in frequencies (200 per second to 20 per second) between the two types of machines. No conclusive results have as yet been obtained.

SUBCOMMITTEE ON WOODS AND GLUES

The Forest Products Laboratory of the Department of Agriculture conducts practically all the investigations on the application of woods and glues to aircraft construction. These investigations are undertaken at the request of the Bureau of Aeronautics of the Navy Department, the matériel division of the Army Air Corps, or the National Advisory Committee for Aeronautics. Some of the more important investigations completed during the past year or now in progress are outlined below.

The lateral buckling and twisting of deep beams.—The Bureau of Aeronautics, Navy Department, realized that it would be highly desirable to know the maximum load which could be carried by a wing beam under any condition of loading and fixity. Accordingly there has been carried on for some years a series of studies on the strengths of beams for the purpose of giving information to the designer. These have included researches into the behavior of continuous beams and into the design of detailed parts of various types of beams.

According to the commonly applied beam formulæ the strength of a beam increases more rapidly with depth than with thickness. Hence in aircraft, where weight is such an important item, designers usually use comparatively deep and narrow wing beams. The ratio of depth to breadth has usually been kept within certain arbitrary or conventional limits, since it is well known that a beam much deeper than wide may buckle laterally and twist before it will break by bending in a vertical plane. As a matter of fact there is for each condition of loading and support of a beam a critical buckling load just as there is a critical Euler load for a column. Under small loads a beam behaves according to the action assumed in the beam formula, but when the critical load is reached it buckles sideways, twists, and fails. Beyond the elastic limit, owing to a reduced modulus of elasticity, this twisting and buckling would cause a reduction in the ultimate load of practically all airplane wing beams of conventional size unless they were supported against it. When two wing beams are tied together with ribs lateral buckling may or may not be prevented. If the ribs are efficiently designed for their own loads alone they will have no reserve resistance for the extra load which any tendency of the beam to buckle would produce. On the other hand, if they are just a little stronger than necessary they may help to hold a quite deep beam in line until its maximum load is reached.

A study of this phenomenon was undertaken, using wood, which seemed to offer the best possibilities as test material because of the ease with which it could be worked into different shapes. So far as is known, very little experimental work had previously been done, although the problem of lateral stability had been investigated mathematically and several useful formulæ had been obtained, notably those by S. Timochenko.

The mathematical analysis by Timochenko was checked experimentally and found to be correct within the limits of accuracy of the experiments. Each of Timochenko's formulæ calls for certain constants dependent on the material. From this investigation have been derived the constants for stresses both within and beyond the elastic limit.

The bearing strength of wood under steel bolts.—This investigation covers quite completely such features of design as allowable bearing strength of wood under bolts subjected to a load acting at any angle to the grain, the allowable distance between bolts, the influence of cross bolts, the combined action of bolts of different diameters, the allowable bearing stress under washers, serviceability of different styles of fitting blocks, etc.

The first of a series of previous investigations of a generally similar character dealt with solid bolts and a condition of loading where the pull on the bolt was parallel to the grain of the wood. A second dealt with hollow bolts under the same conditions of loading, while a third covered the case where the pull was at an angle to the grain and in the plane determined by the grain and the axis of the bolt. This report covers the condition in which the axes of the bolts are perpendicular to the grain of the wood but not in or parallel to the plane determined by the line of action of the force and the grain of the wood.

The report covers many details involved in the design of fittings to be attached to wooden spars, including the spacing of the bolts, the use of bolts of different sizes, the fitting of bolts in laminated beams, and the design of fitting blocks for box beams, and gives certain factors to be applied to the design formulæ which have been used heretofore.

Preparation of manual for inspectors of aircraft wood and glue.—This work consisted of a compilation and digest of much of the perennially useful material developed in aircraft studies by the Forest Products Laboratory in the last 10 years and was done for the Bureau of Aeronautics, Navy Department. Separate chapters give descriptive material or instructions concerning inspection and process work under the following headings:

Structure and characteristic defects of wood.

Strength of wood.

Seasoning processes.

Steaming and bending.

Glues and gluing.

Common stains and decays in wood.

Identification of woods.

Specifications.

This manual, while primarily intended for the use of inspectors connected with the procurement of naval aircraft material, is expected to be of service to inspectors on similar work for the Army Air Corps or the Department of Commerce and for individual manufacturers. It also offers promise as a text for use in the instruction of aeronautical engineers, wood technicians, and mechanics who contemplate working in aircraft woods. This manual is now being printed by the Government Printing Office and will be available at a moderate cost for unrestricted distribution in this country.

Increasing durability of glued joints.—This work comprises an investigation into the effect upon mold formation and chemical dissolution (such as hydrolysis) of preservatives used with glues for aircraft use. The investigation has covered the study of the effects of application of various preservatives to the glue before use and also of the steeping of the completed joint in preservative material. No compound has been found to date whose addition to glue entirely inhibits molding. Beta naphthol and creosote when added in considerable quantities to water-resistant casein or animal glue and sodium chromate added to cold-pressed blood glue materially reduce molding and increase the durability of this glue film without affecting the other important properties of the glues beyond practical limits. They add considerably to weight, however.

Survey of gluing practice at naval aircraft establishments and contractors' plants.—At the request of the Bureau of Aeronautics, Navy Department, an inspection was made of the gluing practice followed at a number of naval aircraft establishments and contractors' plants. Individual inspection reports on the various plants visited were submitted and a final summary and report was also prepared. Many specific recommendations and suggestions were made to accompany a number of the general recommendations.

Permanence of glues.—Continued study has been devoted to the methods of handling casein glues in manufacturing processes. One of the most interesting features is the behavior of the glue during the period between mixture and final pressing. It is of great advantage to have a glue which retains its workability during this period but which does not require too great a time for setting after the working period is over. Accordingly experiments have been made to determine the influence of various factors on the viscosity of the glue during this period.

SUBCOMMITTEE ON COVERINGS, DOPES, AND PROTECTIVE COATINGS

Gas cell fabrics.—The work on the experimental gas cell fabrics made of materials intended to supply a substitute for goldbeater's skin has encountered difficulties due to the sensitiveness of these materials to outside influences. Both of the two types which have been developed to a point where they appear to have real promise are applied to a rubberized fabric having a very thin coat of spread rubber. The influence of the thin layer of rubber, and its compounding and curing, on one type was not suspected until difficulties were encountered due to variations in these factors. It was found that the material used in the original experiments was entirely satisfactory, but that a considerably larger quantity which was intended for use in a production order, had a composition and curing much different from the original. This resulted in the production of gas-cell material much inferior to the earlier samples.

The cause of the trouble was quickly located, but it was necessary to spend considerable time in making certain that a new supply of rubberized cloth should not possess the objectionable qualities found in the first one. The work is continuing with the confident expectation of ultimate success.

In connection with the development of the type of material using cellophane, the manufacture of a gas cell from fabric using the cellophane with high glycerine content has been delayed by the inability to obtain this material as promptly as was desired. It apparently is a special product and not produced regularly. When larger quantities are required it will undoubtedly be available as may be needed.

A most encouraging development has been the development of interest in this problem by one of the manufacturers of the raw materials used in the substitute for goldbeater's skin. This promises to lead to the taking over of the problem by them, when with the facilities available in their organization it should require only a comparatively short time before a satisfactory substitute fabric is available. This would be an arrangement very much to be desired, as it would

then be possible to purchase the fabric in yardage from the manufacturer and assemble the gas cells very much as is the case with rubberized fabric.

Coatings for duralumin to prevent corrosion.—While the anodic treatment apparently confers some degree of protection against corrosion in atmospheres which do not contain salt or other alkaline constituents, it certainly is relatively inefficient near the sea. Consequently the value of the process has been somewhat doubted. However, it is plain that the anodic treatment does improve the surface of aluminum alloys very much whenever it is intended to apply further coatings. Apparently a layer of infinitesimal thickness is produced which affords an almost ideal surface for the retention of grease or other coatings. Remarkably encouraging results have been reported from the use of the anodic treatment followed by a lanolin coating, or a grease, in which a proportion of aluminum powder has been mixed. Instead of the greasy surface which would naturally be expected, the coating results in a comparatively hard surface which does not easily rub off.

No paint and varnish coats which have been tried have been found to give any degree of protection comparable to that from the anodic treatment plus grease or to that conferred by the bituminous coatings. However, it has been definitely established that the bituminous paints must be given a light color by some pigment, preferably aluminum powder, or they will break down in the sunlight. Where not exposed to the sunlight this light color is not required.

The process by which a thin layer of gum rubber is built up on the surface of the material has been perfected to an extremely high degree. By the addition of powdered aluminum as a pigment the resistance to the deteriorating effect of sunlight has been much increased. Coatings applied by this method are extremely adhesive, and since they are repellent to water the degree of protection conferred is of a high order. However, the thickness of the coating which is required to give adequate protection is such that a distinct increase in weight is involved.

In the last report of this committee reference was made to the high degree of protection conferred by a thin coat of pure aluminum. It was then referred to as applied by means of the metal spray gun. The Aluminum Co. of America have now succeeded in producing a thin coat of very pure aluminum forming an integral part of the sheet of duralumin. Duralumin sheets protected on both sides by this method have shown remarkable resistance to corrosion, and the protection extends to uncoated duralumin, in the form of rivets, or bare spots of about one-half inch diameter, on the sheet. Although the final verdict can not be given without service tests, all the accelerated tests indicate that this material is the most successful in its protection which has so far been developed. If material of this character is anodically treated and then greased it is believed that the protection may be considered to be practically perfect.

The exposure tests on protective coatings for duralumin are still under way, and while some coatings have already broken down and others show signs of beginning to break down the tests are not yet completed. This was one of the purposes of making these tests, as it was hoped to obtain a scale by which to measure the results of accelerated corrosion tests.

The nitrocellulose lacquers for the protection of small metal fittings have come into wide use and afford a very useful method of rapidly applying a moderately effective protective coating by hand. With these, however, it is necessary to maintain the coating by constant inspection.

With the development of the method of protecting the aluminum alloys by means of a pure aluminum layer forming an integral part of the sheet it would appear that a very satisfactory solution for this problem has been obtained. It is confidently expected that this material will make possible the widespread use of duralumin in many places where it has heretofore been regarded with suspicion. By combining the pure aluminum coating with other methods, as described, the degree of protection can certainly be increased to far beyond anything which has been known heretofore. With the continuing development of this material and its introduction in the form of sections and tubing protected on both surfaces, as may be expected, aluminum alloys should become one of the most used materials in aircraft.

Airplane dopes.—During the past year semipigmented dopes have come into general use. These are nitrate dopes in which pigment has been incorporated in quantity approximately 25 per cent of that in the usual pigmented dopes. The doping schemes with these dopes contemplate the use of semipigmented dopes exclusively, no clear dopes being used.

Surfaces doped with semipigmented dope which have been in service for a considerable period of time have shown a marked increase in durability over surfaces using the old doping schemes where clear dopes were used and protected with a pigmented dope and pigmented varnish. Specifications covering this new material are being prepared by both Army and Navy.

Experiments on airplane dopes are still being conducted at the Naval Aircraft Factory. These include the older forms and the newer semipigmented dopes. An effort is also being made to develop some quantitative method for determining the tautness of a doped panel and some method for estimating the actual durability from an accelerated test. The Barnaby & Freymoyer tautness meter referred to in last year's report has now been superseded by the Mullen paper tester. The Naval Aircraft Factory is investigating the application of this tester and compiling coefficients for use in the interpretation of the results obtained with it.

Substitute for silk parachute cloth.—An American-made silk cloth to be used in place of the imported silk cloths which have been used in the manufacture of airplane parachutes has been developed and is now being incorporated in a production order.

The problem of finding a substitute for silk for this purpose has been attacked along the lines of treating cotton yarn by modified mercerization and doping processes. Gains in strength and elasticity as shown both in the yarn and in trial weavings using the treated yarns as the filling for the cloth have been accomplished.

The problem has now been shifted from the laboratory to a production scale. The difficulties experienced in the laboratory development work suggested the advisability of dividing the work into three different sections: Yarn treatment, cloth treatment, and a complete mill organization and finishing treatment.

In connection with the yarn treatment it has been found that domestic fine yarns with the desired properties are difficult to obtain. Most of the yarn used in the early work was made in England and even then had to be reprocessed in the laboratory to some extent. Arrangements have now been made for the supply of suitable yarns of American manufacture. These will be treated according to the methods which have been developed and will be woven in the experimental cotton mill.

In connection with the cloth treatment it appeared desirable to take advantage if possible of the light-weight cotton cloths which are used for other aeronautical purposes. For instance, a 2-ounce cloth of very high strength is regularly used in the manufacture of airship and balloon envelopes. Generous quantities of this material have been furnished by the Navy Department. Using the first pieces supplied a small scale mercerization apparatus for cloth was developed, which was designed and built at the Bureau of Standards. A large sample of material is now being put through this apparatus. It is planned to make small parachutes from the finished material. These will be tested in comparison with parachutes made of silk cloth and of untreated cotton cloth.

The complete organization for making the yarn on a production scale is being worked out in the experimental cotton mill. A bale of long staple "Arizona-Egyptian" cotton (grown in Arizona) has been purchased and is being processed in the cotton mill. When this yarn is spun it will be handled in the same manner and according to the processes which have been described above. This work will probably require eight months to a year to complete, but in the end will make available fairly complete information as to the possibilities of this method of processing.

SUBCOMMITTEE ON AIRCRAFT STRUCTURES

Welded joints.—Because of the possibility that metal aircraft structures can be fabricated by welding, at a lower cost and with a saving of weight, the metallurgical and fatigue properties of welds, with particular reference to the strength of specimens fabricated by this process, are being investigated.

Butt welds on sheets of duralumin, carbon steel, and chrome vanadium steel, in four thicknesses, and with three welding processes (atomic hydrogen, oxyacetylene, and electric arc) have been furnished for test.

Preliminary tensile tests on specimens in the "as received" condition, indentation tests, and metallurgical treatments, have been completed. The work has not advanced sufficiently to record any definite conclusions as to the efficiency of these methods of fabrication, but it is

expected that the investigation will ultimately furnish important information as to the availability of these welding processes for load-carrying members of aircraft structures.

Strength of flat plates.—The investigation of the column strength of flat plates of nickel, duralumin, stainless steel, and monel metal was decided upon as a result of the increasing use of metal construction in which the shell plating is required to carry part of the load. Very little information exists as to the manner in which the compressive loads in such a shell are carried, and as a preliminary step toward a solution of this problem the column strengths of flat plates of the different materials mentioned are being determined. In this investigation the effect of variations in width alone is being considered. The plates are always flat, and while the edges are fixed in position they are not fixed in direction.

Form factors for tubing of duralumin and steel under combined column and beam loads.—This research was undertaken to increase the amount of information available as to the loads which could be sustained by steel and duralumin tubing when used either in the fuselage or other structure of an airplane. Work on one size of duralumin tubing has been completed and curves prepared for the use of the designer. Work on the steel tubing in three sizes is still under way.

Structures for airships.—The compression tests made upon a *Shenandoah* type spiral latticed girder and a special girder with opposite latticing to determine the relative importance of the principal elastic constants of the chord members, i. e., the flexural stiffnesses (moments of inertia \times Young's modulus) in the directions of the two principal axes of inertia and the torsional stiffness (torsion constant \times shear modulus) showed that the characteristic wavy flexure of these girders under load was almost wholly a twist of the channel section; that restraining this twist without restraining the lateral deflections or spread of the flanges increased the carrying capacity of the girder by over 40 per cent; and that therefore the torsional stiffness of the channels was the major controlling factor in the strength of the girder.

Complete tests have been made upon nine specimens involving approximately 23,000 individual measurements. Those made upon *Shenandoah* type triangular spiral latticed girders having differing moments of inertia, area of channels, and character of restraints offered by the lattices, have confirmed these results within the range of girders tested. They have also been confirmed by tests on the square *Shenandoah* type girder, having angles for the chord members, where the load-carrying capacity of this type of girder was increased over 35 per cent upon restraint of the twist without in any way restraining the lateral deflection.

The results have also been confirmed by tests on four short sections of experimental girders with tubular chord members but otherwise identical with the Zeppelin type-55 series of *Shenandoah* girders. In these tubular type girders the moments of inertia and areas of the sections are not greatly different from those of the channel sections but the torsional stiffness is very much higher. The failure shows no effect of twisting, being of the mixed elastic and yielding flexural type characteristic of columns of medium slenderness (Karman range) with average stresses approaching the yield point of the material.

Like columns of medium slenderness the failure does not show the rapid collapse after the maximum load characteristic of the purely elastic flexural type of failure found with open channels. Each of the three was compressed a few tenths of an inch beyond the maximum, under decreasing load and increasing bending of the tubular chords. On release of load the girder lengthened with straightening of the bent chords, leaving only a small part of the curvature remaining as permanent deformation. There was, however, no evidence of the "pick up" found in certain ranges of solid columns.

Further tests are planned on two box girders such as are used in parts of the *Los Angeles* and upon several experimental box girders of similar design which have been fabricated at the Lakehurst Naval Air Station.

Fittings.—The Department of Commerce in administering the inspection and airworthiness provisions of the air commerce act of 1926, has found that there is great diversity in the manner in which fittings, for metal or wooden construction, are made in commercial practice. It accordingly requested the Bureau of Standards to investigate this subject with a view to improving the methods of design and construction and, if possible, introducing some simplification in the practice. The Bureau of Standards has referred the question to this subcommittee and recommendations are being prepared which will probably include a program of research.

PART IV

TECHNICAL PUBLICATIONS OF THE COMMITTEE

The National Advisory Committee for Aeronautics has issued technical publications during the past year covering a wide range of subjects. There are four series of publications, namely, Technical Reports, Technical Notes, Technical Memorandums, and Aircraft Circulars.

The Technical Reports present the results of fundamental research in aeronautics carried on in different laboratories in this country, including the Langley Memorial Aeronautical Laboratory, the aerodynamical laboratory at the Washington Navy Yard, the Bureau of Standards, the Weather Bureau, Stanford University, and the Massachusetts Institute of Technology. In all cases the reports were recommended for publication by the technical subcommittees having cognizance of the investigations. During the past year 26 Technical Reports were issued.

Technical Notes present the results of small research investigations and the results of studies of specific detail problems which form parts of long investigations. The committee has during the past year issued in mimeographed form 18 Technical Notes.

Technical Memorandums contain translations and reproductions of important aeronautical articles of a miscellaneous character. A total of 50 Technical Memorandums were issued during the past year.

Aircraft Circulars contain translations or reproductions of articles descriptive of new types of aircraft. During the past year 40 Aircraft Circulars were issued.

Summaries of the 26 Technical Reports and lists of the Technical Notes, Technical Memorandums, and Aircraft Circulars issued during the past year follow.

SUMMARIES OF TECHNICAL REPORTS

The first annual report of the National Advisory Committee for Aeronautics for the fiscal year 1915 contained Technical Reports Nos. 1 to 7; the second annual report, Nos. 8 to 12; the third annual report, Nos. 13 to 23; the fourth annual report, Nos. 24 to 50; the fifth annual report, Nos. 51 to 82; the sixth annual report, Nos. 83 to 110; the seventh annual report, Nos. 111 to 132; the eighth annual report, Nos. 133 to 158; the ninth annual report, Nos. 159 to 185; the tenth annual report, Nos. 186 to 209; the eleventh annual report, Nos. 210 to 232; the twelfth annual report, Nos. 233 to 256; and since the preparation of the twelfth annual report for the year 1926 the committee has authorized the publication of the following Technical Reports, Nos. 257 to 282.

Report No. 257, entitled "Pressure Distribution Over a Wing and Tail Rib of a VE-7 and of a TS Airplane in Flight," by J. W. Crowley, jr., National Advisory Committee for Aeronautics.—This investigation was made at the Langley Memorial Aeronautical Laboratory, to determine the pressure distribution over a rib of the wing and over a rib of the horizontal tail surface of an airplane in flight and to obtain information as to the time correlation of the loads occurring on these ribs. Two airplanes, VE-7 and TS, were selected in order to obtain the information for a thin and a thick wing section. In each case the pressure distribution was recorded for the full range of angle of attack in level flight and throughout violent maneuvers. Particular attention was given to the high and low angle of attack conditions. The results show: (a) That the present rib load specifications in use by the Army Air Corps and the Bureau of Aeronautics, Navy Department, are in fair agreement with the loads actually occurring in flight, but could be slightly improved; (b) that there appears to be no definite sequence in which wing and tail surface ribs reach their respective maximum loads in different maneuvers; (c) that in accelerated flight, at air speeds less than or equal to 60 per cent of the maximum speed, the

accelerations measured agree very closely with the theoretically possible maximum accelerations. In maneuvers at higher air speeds the observed accelerations were smaller than those theoretically possible.

Report No. 258, entitled "Some Factors Affecting the Reproducibility of Penetration and the Cut-off of Oil Sprays for Fuel Injection Engines," by E. G. Beardsley, National Advisory Committee for Aeronautics.—This investigation was undertaken at the Langley Memorial Aeronautical Laboratory, in connection with a general research on fuel-injection engines for aircraft. The purpose of the investigation was to determine the factors controlling the reproducibility of spray penetration and secondary discharges after cut-off.

The development of single sprays from automatic injection valves was recorded by means of special high-speed photographic apparatus capable of taking 25 consecutive pictures of the moving spray at a rate of 4,000 per second. The effects of two types of injection valves, injection-valve tube length, initial pressure in the injection-valve tube, speed of the injection control mechanism, and time of spray cut-off, on the reproducibility of spray penetration, and on secondary discharges were investigated.

It was found that neither type of injection valve materially affected spray reproducibility. The initial pressure in the injection-valve tube controlled the reproducibility of spray penetrations. An increase in the initial pressure or in the length of the injection-valve tube slightly increased the spray penetration within the limits of this investigation. The speed of the injection-control mechanism did not affect the penetration.

Analysis of the results indicates that secondary discharges were caused in this apparatus by pressure waves initiated by the rapid opening of the cut-off valve. The secondary discharges were eliminated in this investigation by increasing the length of the injection-valve tube.

Report No. 259, entitled "Characteristics of Propeller Sections Tested in the Variable Density Wind Tunnel," by Eastman N. Jacobs, National Advisory Committee for Aeronautics.—Tests were carried out in the variable density wind tunnel at the Langley Memorial Aeronautical Laboratory on six airfoil sections used by the Bureau of Aeronautics as propeller sections. The sections were tested at pressures of 1 and 20 atmospheres corresponding to Reynolds Numbers of about 170,000 and 3,500,000. The results obtained, besides providing data for the design of propellers, should be of special interest because of the opportunity afforded for the study of scale effect on a family of airfoil sections having different thickness ratios.

Report No. 260, entitled "The Effect of a Flap and Ailerons on the N. A. C. A. M6 Airfoil Section," by George J. Higgins and Eastman N. Jacobs, National Advisory Committee for Aeronautics.—This report contains the results obtained at the Langley Memorial Aeronautical Laboratory, on an N. A. C. A. M6 airfoil, fitted with a flap and ailerons, and tested in the variable-density wind tunnel at a density of 20 atmospheres. Airfoil characteristics are given for the model up to 48° angle of attack with the flap set at various angles, and also with the ailerons set at similar angles. The approximate lift distribution and the center of pressure variation along the span are determined with the model at 18° angle of attack and with the ailerons displaced 20° . Approximate rolling moment and yawing moment coefficients are determined for the various aileron settings.

A comparison of the calculated angles of zero lift and the calculated lift and moment coefficients with those observed is given in the appendix.

Report No. 261, entitled "Resistance and Cooling Power of Various Radiators," by R. H. Smith, construction department, Washington Navy Yard.—This report combines the wind-tunnel results of radiator tests made at the Navy aerodynamical laboratory in Washington during the summers of 1921, 1925, and 1926. In all, 13 radiators of various types and capacities were given complete tests for figure of merit. Twelve of these were tested for resistance to water flow and a fourteenth radiator was tested for air resistance alone, its heat-dissipating capacity being known. All the tests were conducted in the 8 by 8 foot tunnel, or in its 4 by 8 foot restriction, under conditions as nearly the same as possible. That is to say, as far as possible, the general arrangement and condition of the apparatus, the observation intervals, the ratio of water flow per unit of cooling surface, the differential temperatures, and the air speeds were the

same for all. Also, for reasons of comparison, the L/D value of 6, which was assumed in the 1921 tests as the L/D of the airplane using the radiator, was also used in the more recent tests.

No attempt is made to enter upon the theory of heat dissipation. Only the actual test results are given and reduced to coefficient form. The precision of the tests as representative of full-flight performance is definitely known only in the case of the HN-2. The McCook Field full-flight performance and the Navy tunnel performance of this radiator agree within about 3 per cent.

Since this full-flight test was made with unusual care and since the wind-tunnel tests on all the radiators were made not only accurately but also at almost full scale, it would seem probable that these tests represent quite accurately the full-flight performances in actual service.

Report No. 262, entitled "Friction of Aviation Engines," by S. W. Sparrow and M. A. Thorne, Bureau of Standards.—The first portion of this report discusses measurements of friction made in the altitude laboratory of the Bureau of Standards between 1920 and 1926 under research authorization of the National Advisory Committee for Aeronautics. These are discussed with reference to the influence of speed, barometric pressure, jacket-water temperature, and throttle opening upon the friction of aviation engines. It is concluded that: (1) Changes in friction due to changes in the temperature of the air entering the engine are negligible. (2) Changes in friction which result from changes in atmospheric pressure are due primarily to changes in pumping loss. An approximate figure for the engines mentioned in this report is that the friction mean effective pressure decreases about one-tenth of a pound per square inch for each decrease of 1 centimeter of mercury in the barometric pressure. (3) The increase in friction resulting from a decrease in throttle opening is due to the change in pumping loss. For the engines mentioned in this report, the change in friction mean effective pressure which accompanies a change in manifold suction of 1 inch (2.54 centimeters) of mercury ranges from 0.20 pound per square inch obtained at an engine speed of 1,200 revolutions per minute to 0.39 at 1,800 revolutions per minute. (4) For the range of speeds covered in this report, namely, from 1,000 to 2,200 revolutions per minute, the friction mean effective pressure increases with speed, but ordinarily the percentage increase is less than the corresponding percentage increase in speed. At low engine speeds the friction mean effective pressure changes much less with change in speed and in some instances remains practically constant. (5) Friction depends upon the viscosity of the oil upon the cylinder walls, which in turn depends upon the temperature of the jacket water. (6) While theoretical considerations would lead one to expect an increase in friction with increase in compression ratio the evidence at hand indicates that this effect is slight.

The second section of the report deals with measurements of the friction of a group of pistons differing from each other in a single respect, such as length, clearness, area of thrust face, location of thrust face, etc. Results obtained with each type of piston are discussed and attention is directed particularly to the fact that the friction chargeable to piston rings depends upon piston design as well as upon ring design. This is attributed to the effect of the rings upon the thickness and distribution of the oil film which, in turn, affects the friction of the piston to an extent which depends upon its design.

Report No. 263, entitled "Preliminary Flight Tests of the N. A. C. A. Roots Type Aircraft Engine Supercharger," by Arthur W. Gardiner and Elliott G. Reid, National Advisory Committee for Aeronautics.—An investigation of the suitability of the N. A. C. A. Roots type aircraft engine supercharger to flight-operating conditions, as determined by the effects of the use of the supercharger upon engine operation and airplane performance, is described in this report.

The supercharger has been previously described in N. A. C. A. Technical Report No. 230; the results of laboratory tests are also given there. The compressor has a displacement of 0.51 cubic foot per revolution and weighs 88 pounds.

The selection of a suitable propeller and the provision of satisfactory intake ducts and adequate engine cooling were preliminary problems. The supercharger was first tested in a modified DH-4 airplane with a 5.4-compression-ratio Liberty-12 engine. Two sets of drive

gears which enabled the maintenance of sea-level pressure at the carburetor intake up to 12,000 and 20,000 feet were provided. The higher gear ratio supercharger was next tested in a DT-2 landplane which was later converted into a twin-float seaplane; the DT-2 also had a Liberty engine. Loads up to 2,000 pounds were carried in the seaplane with normal and supercharged engines.

Attention was concentrated on the operation of the engine-supercharger unit and on the improvement of climbing ability; some information concerning high speeds at altitude was obtained.

The supercharger was found to be satisfactory under flight-operating conditions. Although two failures occurred during the tests, the causes of both were minor and have been eliminated. Careful examination of the engines revealed no detrimental effects which could be attributed to supercharging.

Marked improvements in climbing ability and high speeds at altitude were effected. It was also found that the load which could be carried to a given moderate or high altitude in a fixed time was considerably augmented. A slight sacrifice of low-altitude performance was necessitated, however, by the use of a fixed pitch propeller.

From a consideration of the very satisfactory flight performance of the Roots supercharger and of its inherent advantages, it is concluded that this type is particularly attractive for use in certain classes of commercial airplanes and in a number of military types.

Report No. 264, entitled "Differential Pressures on a Pitot-Venturi and a Pitot-Static Nozzle over 360° Pitch and Yaw," by R. M. Bear, construction department, Washington Navy Yard.—Measurements of the differential pressures on two Navy air-speed nozzles, consisting of a Zahm type Pitot-Venturi tube and a SQ-16 two-pronged Pitot-static tube, in a tunnel air stream of fixed speed at various angles of pitch and yaw between 0° and $\pm 180^\circ$, show for a range over -20° to $+20^\circ$ pitch and yaw, indicated air speeds varying very slightly over 2 per cent for the Zahm type and a maximum of about 5 per cent for the SQ-16 type from the calibrated speed at 0°.

For both types of air-speed nozzle the indicated air speed increases slightly as the tubes are pitched or yawed several degrees from their normal 0° attitude, attains a maximum around $\pm 15^\circ$ to 25° , declines rapidly therefrom as $\pm 40^\circ$ is passed, to zero in the vicinity of $\pm 70^\circ$ to 100° , and thence fluctuates irregularly from thereabouts to $\pm 180^\circ$. The complete variation in indicated air speed for the two tubes over 360° pitch and yaw is graphically portrayed in Figures 9 and 10.

For the same air speed and 0° pitch and yaw the differential pressure of the Zahm type Pitot-Venturi nozzle is about seven times that of the SQ-16 type two-pronged Pitot-static nozzle.

Report No. 265, entitled "A Full-Scale Investigation of Ground Effect," by Elliott G. Reid, National Advisory Committee for Aeronautics.—This report describes flight tests which were made with a Vought VE-7 airplane to determine the effects of flying close to the ground.

It is found that the drag of an airplane is materially reduced upon approaching the ground and that the reduction may be satisfactorily calculated according to theoretical formulas.

Several aspects of ground effect which have had much discussion are explained.

Report No. 266, entitled "Air Force and Moment for N-20 Wing with Certain Cut-Outs," by R. H. Smith, construction department, Washington Navy Yard.—The airplane designer often finds it necessary, in meeting the requirements of visibility, to remove area or to otherwise locally distort the plan or section of an airplane wing. This report, prepared for the Bureau of Aeronautics, January 15, 1925, contains the experimental results of tests on six 5 by 30-inch N-20 wing models, cut out or distorted in different ways, which were conducted in the 8 by 8-foot wind tunnel of the Navy Aerodynamical Laboratory in Washington in 1924.

The measured and derived results are given without correction for Vl/ν or for wall effect and for standard air density, $\rho = 0.00237$ slug per cubic foot.

Report No. 267, entitled "Drag of Wings with End Plates," by Paul E. Hemke, National Advisory Committee for Aeronautics.—In this report a formula for calculating the induced drag of multiplanes with end plates is derived. The frictional drag of the end plates is also

calculated approximately. It is shown that the reduction of the induced drag, when end plates are used, is sufficiently large to increase the efficiency of the wing.

Curves showing the reduction of drag for monoplanes and biplanes are constructed; the influence of gap-chord ratio, aspect ratio, and height of end plate are determined for typical cases. The method of obtaining the reduction of drag for a multiplane is described.

Comparisons are made of calculated and experimental results obtained in wind-tunnel tests with airfoils of various aspect ratios and end plates of various sizes. The agreement between calculated and experimental results is good.

Analysis of the experimental results shows that the shape and section of the end plates are important.

Report No. 268, entitled "Factors in the Design of Centrifugal Type Injection Valves for Oil Engines," by W. F. Joachim and E. G. Beardsley, National Advisory Committee for Aeronautics.—This research was undertaken at the Langley Memorial Aeronautical Laboratory, in connection with a general study of the application of the fuel injection engine to aircraft. The purpose of the investigation was to determine the effect of four important factors in the design of a centrifugal type automatic injection valve on the penetration, general shape, and distribution of oil sprays.

The general method employed was to record the development of single sprays by means of special high-speed photographic apparatus capable of taking 25 consecutive pictures of the moving spray at a rate of 4,000 per second. Investigations were made concerning the effects on spray characteristics of the helix angle of helical grooves, the ratio of the cross-sectional area of the orifice to that of the grooves, the ratio of orifice length to diameter, and the position of the seat. The sprays were injected at 6,000, 8,000, and 10,000 pounds per square-inch pressure into air at atmospheric pressure and into nitrogen at 200, 400, and 600 pounds per square-inch pressure. Orifice diameters from 0.012 to 0.040 inch were investigated.

It was found that decreasing the pitch of the helical grooves and thus increasing the centrifugal force applied to the spray increased the spray cone angle considerably, although the percentage increase was much less in dense air than in the atmosphere. On the other hand, the spray penetration decreased with increase in the amount of centrifugal force applied. About twice as much spray volume per unit oil volume was obtained with a high centrifugal spray as with a noncentrifugal spray. The spray cone angle increased, and the spray volume to oil volume ratio and spray penetration decreased with increase in the ratio of orifice area to groove area. Maximum spray penetration was obtained with a ratio of orifice length to diameter of about 1.5. Slightly greater penetration was obtained with the seat directly before the orifice.

Report No. 269, entitled "Air Force Tests of Sperry Messenger Model with Six Sets of Wings," by James M. Shoemaker, National Advisory Committee for Aeronautics.—The purpose of this test was to compare six well-known airfoils, the R. A. F. 15, U. S. A. 5, U. S. A. 27, U. S. A. 35-B, Clark Y, and Göttingen 387, fitted to the Sperry Messenger model at full-scale Reynolds Number as obtained in the variable-density wind tunnel of the National Advisory Committee for Aeronautics; and to determine the scale effect on the model equipped with all the details of the actual airplane. The results show a large decrease in minimum drag coefficient upon increasing the Reynolds Number from about one-twentieth scale to full scale. Maximum lift coefficient was increased with increasing scale for all the airfoils except the Göttingen 387, for which it was slightly decreased. A comparison is made between the results of these tests and those obtained from tests made in this tunnel on airfoils alone.

Report No. 270, entitled "The Measurement of Pressure through Tubes in Pressure Distribution Tests," by Paul E. Hemke, National Advisory Committee for Aeronautics.—The tests described in this report were made to determine the error caused by using small tubes to connect orifices on the surface of aircraft to central pressure capsules in making pressure-distribution tests.

Aluminum tubes of three-sixteenths inch inside diameter were used to determine this error. Lengths from 20 feet to 226 feet and pressures whose maxima varied from 2 inches to 140 inches

of water were used. Single-pressure impulses for which the time of rise of pressure from zero to a maximum varied from 0.25 second to 3 seconds were investigated.

The results show that the pressure recorded at the capsule on the far end of the tube lags behind the pressure at the orifice end and experiences also a change in magnitude. For the values used in these tests the time lag and pressure change vary principally with the time of rise of pressure from zero to a maximum and the tube length. Curves are constructed showing the time lag and pressure change. Empirical formulas are also given for computing the time lag.

Analysis of pressure-distribution tests made on airplanes in flight shows that the recorded pressures are slightly higher than the pressures at the orifice and that the time lag is negligible. The apparent increase in pressure is usually within the experimental error, but in the case of the modern pursuit type of airplane the pressure increase may be 5 per cent. For pressure-distribution tests on airships the analysis shows that the time lag and pressure change may be neglected.

Report No. 271, entitled "Pressure Distribution Tests on PW-9 Wing Models Showing Effects of Biplane Interference," by A. J. Fairbanks, National Advisory Committee for Aeronautics.—In this report tests are described in which the distribution of pressures over models of the wings of the PW-9 airplane was investigated. The wing models were tested individually and in the biplane combination. The investigation was conducted in the atmospheric wind tunnel of the National Advisory Committee for Aeronautics. It is concluded in this paper that the effect of biplane interference on the pressures on the wings is practically confined to the lower surface of the upper wing and the upper surface of the lower wing; that the overhanging portion of the upper wing is not greatly affected by the presence of the lower wing; and that a slight washin at the center section of the upper wing satisfactorily compensates for a reduced chord at this section (providing the airfoil section is not mutilated) and prevents a large reduction in the normal force over this portion of the wing.

Report No. 272, entitled "The Relative Performance Obtained with Several Methods of Control of an Overcompressed Engine Using Gasoline," by Arthur W. Gardiner and William E. Whedon, National Advisory Committee for Aeronautics.—This report presents some results obtained at the Langley Memorial Aeronautical Laboratory during an investigation to determine the relative performance characteristics for several methods of control of an overcompressed engine using gasoline and operating under sea-level conditions. For this work, a special single-cylinder test engine, 5-inch bore by 7-inch stroke, and designed for ready adjustment of compression ratio, valve timing and valve lift while running, was used. This engine has been fully described in N. A. C. A. Technical Report No. 250.

Tests were made at an engine speed of 1,400 revolutions per minute for compression ratios ranging from 4 to 7.6. The air-fuel ratios were on the rich side of the chemically correct mixture and were approximately those giving maximum power. When using plain domestic aviation gasoline, detonation was controlled to a constant, predetermined amount (audible), such as would be permissible for continuous operation, by (a) throttling the carburetor, (b) maintaining full throttle but greatly retarding the ignition, and (c) varying the timing of the inlet valve to reduce the effective compression ratio. For the first and third methods, the throttle opening and the valve timing, respectively, were adjusted so that the ignition timing could be advanced slightly beyond the advance, giving maximum power without exceeding the standard of permissible detonation. The optimum performance for the engine when using a nondetonating fuel, consisting of 80 per cent of commercial benzol and 20 per cent of aviation gasoline, was obtained as a basis for comparison.

The following comparative results are based on the optimum performance for the engine obtained with the nondetonating fuel at a compression ratio of 4.7. The power and fuel consumption with method (b) remained substantially constant at the higher compression ratios, the order of the ignition timing permitting full throttle operation ranging from 30° at 4.7 to 3° at 7.3; exhaust temperatures, heat loss to the cooling water, and explosion pressures at the higher ratios were normal. At a compression ratio of 7.5, the power obtained with method (a) was about 39 per cent less and the fuel consumption was considerably lower; with method

(b), time of inlet-valve opening constant and time of inlet-valve closing varied, the power was about 23 per cent less and the fuel consumption was greatly increased; with method (c), time of inlet opening and closing varied simultaneously, the power was about 29 per cent less and the fuel consumption was greatly increased.

From these results, it may be concluded that method (c) gives the best all-round performance and, being easily employed in service, appears to be the most practicable method for controlling an overcompressed engine using gasoline at low altitudes.

Report No. 273, entitled "Wind Tunnel Tests on Autorotation and the 'Flat Spin,'" by Montgomery Knight, National Advisory Committee for Aeronautics.—This report deals with the autorotational characteristics of certain differing wing systems as determined from wind-tunnel tests made at the Langley Memorial Aeronautical Laboratory. The investigation was confined to autorotation about a fixed axis in the plane of symmetry and parallel to the wind direction. Analysis of the tests leads to the following conclusions:

Autorotation below 30° angle of attack is governed chiefly by wing profile and above that angle by wing arrangement.

The strip method of autorotation analysis gives uncertain results between maximum C_L and 35° .

The polar curve of a wing system, and to a lower degree of accuracy the polar of a complete airplane model are sufficient for direct determination of the limits of rotary instability, subject to strip-method limitations.

The results of the investigation indicate that in free flight a monoplane is incapable of flat spinning, whereas an unstaggered biplane has inherent flat-spinning tendencies.

The difficulty of maintaining equilibrium in stalled flight is due primarily to rotary instability, a rapid change from stability to instability occurring as the angle of maximum lift is exceeded.

Report No. 274, entitled "The N. A. C. A. Photographic Apparatus for Studying Fuel Sprays from Oil Engine Injection Valves and Test Results from Several Researches," by Edward G. Beardsley, National Advisory Committee for Aeronautics.—Apparatus for recording photographically the start, growth, and cut-off of oil sprays from injection valves has been developed at the Langley Memorial Aeronautical Laboratory. The apparatus consists of a high-tension transformer by means of which a bank of condensers is charged to a high voltage. The controlled discharge of these condensers in sequence, at a rate of several thousand per second, produces electric sparks of sufficient intensity to illuminate the moving spray for photographing. The sprays are injected from various types of valves into a chamber containing gases at pressures up to 600 pounds per square inch.

Several series of pictures are shown. The results give the effects of injection pressure, chamber pressure, specific gravity of the fuel oil used, and injection-valve design upon spray characteristics.

Report No. 275, entitled "The Effect of the Walls in Closed Type Wind Tunnels," by George J. Higgins, National Advisory Committee for Aeronautics.—A series of tests has been conducted during the period 1925–1927 by the National Advisory Committee for Aeronautics in the variable density wind tunnel on several airfoil models of different sizes and sections to determine the effect of tunnel-wall interference and to determine a correction which can be applied to reduce the error caused thereby. The use of several empirical corrections was attempted with little success. The Prandtl theoretical corrections give the best results, and their use is recommended for correcting closed wind-tunnel results to the conditions of free air.

An appendix is attached wherein the experimentally determined effect of the walls on the tunnel velocity very close to their surface is given. This is of special interest because a "scale effect" was found in the boundary layer with a change in the density of the tunnel air.

Report No. 276, entitled "Combustion Time in the Engine Cylinder and Its Effect on Engine Performance," by Charles F. Marvin, jr., Bureau of Standards.—As part of a general program to study combustion in the engine cylinder and to correlate the phenomena of combustion with the observed performance of actual engines, this paper, which was outlined by

S. W. Sparrow, and the work undertaken at the request of the National Advisory Committee for Aeronautics, presents a sketchy outline of what may happen in the engine cylinder during the burning of a charge. It also suggests the type of information needed to supply the details of the picture and points out how combustion time and rate affect the performance of the engine.

A theoretical concept of a flame front which is assumed to advance radially from the point of ignition is presented, and calculations based on the area and velocity of this flame and the density of the unburned gases are made to determine the mass rate of combustion. From this rate the mass which has been burned and the pressure at any instant during combustion are computed.

This process is then reversed in an effort to determine actual rates of combustion and flame velocities from the pressures as recorded on indicator diagrams.

The effects of different rates of combustion on engine performance are then discussed and the importance of proper spark advance is emphasized.

Report No. 277, entitled "The Comparative Performance of an Aviation Engine at Normal and High Inlet Air Temperatures," by Arthur W. Gardiner and Oscar W. Schey, National Advisory Committee for Aeronautics.—This report presents some results obtained at the Langley Memorial Aeronautical Laboratory during an investigation to determine the effect of high inlet air temperature on the performance of a Liberty-12 aviation engine. The purpose of this investigation was to ascertain, for normal service carburetor adjustments and a fixed ignition advance, the relation between power and temperature for the range of carburetor air temperatures that may be encountered when supercharging to sea-level pressure at altitudes of over 20,000 feet and without intercooling when using plain aviation gasoline and mixtures of benzol and gasoline.

Laboratory tests were made at full throttle over the speed range from 1,400 to 1,800 revolutions per minute, in which the pressure at the carburetor and exhaust was maintained sensibly constant and the inlet air temperature varied from 45° to 180° F. The range of mixtures was that normally used in flight. Plain aviation gasoline, a mixture consisting of 30 per cent (by volume) of commercial benzol and 70 per cent gasoline, and a mixture of 65 per cent benzol and 35 per cent gasoline were used. Additional tests were made with a Wright E-4 aviation engine.

The results show that for the conditions of test, both the brake and indicated power decrease with increase in air temperature at a faster rate than given by the theoretical assumption that power varies inversely as the square root of the absolute temperature. On a brake basis, the order of the difference in power for a temperature difference of 120° F. is 3 to 5 per cent. The observed relation between power and temperature when using the 30 to 70 blend was found to be linear. But, although these differences are noted, the above theoretical assumption may be considered as generally applicable except where greater precision over a wide range of temperatures is desired, in which case it appears necessary to test the particular engine under the given conditions.

Report No. 278, entitled "Lift, Drag, and Elevator Hinge Moments of Handley-Page Control Surfaces," by R. H. Smith, construction department, Washington Navy Yard.—This report combines the wind-tunnel results of tests on four control surface models made in the two wind tunnels of the Navy aerodynamical laboratory, Washington Navy Yard, during the years 1922 and 1924. The purpose of the tests was to compare, first, the lifts and the aerodynamic efficiencies of the control surfaces from which their relative effectiveness as tail planes could be determined; then the elevator hinge moments upon which their relative ease of operation depended. The lift and drag forces on the control surface models were obtained for various stabilizer angles and elevator settings in the 8 by 8 foot tunnel by the writer in 1922; the corresponding hinge moments were found in the 4 by 4 foot tunnel by Mr. R. M. Bear in 1924.

Report No. 279, entitled "Tests on Models of Three British Airplanes in the Variable Density Wind Tunnel," by George J. Higgins and George L. DeFoe, National Advisory Committee for Aeronautics, and W. S. Diehl, Bureau of Aeronautics, Navy Department.—This report contains the results of tests made in the National Advisory Committee for Aeronautics

variable density wind tunnel on three airplane models supplied by the British Aeronautical Research Committee. These models, the BE-2E with R. A. F. 19 wings, the Bristol Fighter with R. A. F. 15 wings, and the Bristol Fighter with R. A. F. 30 wings, were tested over a wide range in Reynolds Numbers in order to supply data desired by the Aeronautical Research Committee for scale-effect studies.

The maximum lifts obtained in these tests are in excellent agreement with the published results of British tests, both model and full scale. No attempt is made to compare drag data, owing to the omission of tail surfaces, radiator, etc., from the model, but it is shown that the scale effect observed on the drag coefficients in these tests is due to a large extent to the parts of the models other than the wings.

Report No. 280, entitled "The Gaseous Explosive Reaction—The Effect of Inert Gases," by F. W. Stevens, Bureau of Standards.—(1) Attention is called in this report to previous investigations of gaseous explosive reactions carried out under constant volume conditions, where the effect of inert gases on the thermodynamic equilibrium was determined. The advantage of constant pressure methods over those of constant volume as applied to studies of the gaseous explosive reaction is pointed out and the possibility of realizing for this purpose a constant pressure bomb mentioned.

(2) The application of constant pressure methods to the study of gaseous explosive reactions, made possible by the use of a constant pressure bomb, led to the discovery of an important kinetic relation connecting the rate of propagation of the zone of explosive reaction within the active gases, with the initial concentrations of those gases: $s = k_1 [A]^{n_1} [B]^{n_2} [C]^{n_3}$.

(3) By a method analogous to that followed in determining the effect of inert gases on the equilibrium constant K , the present paper records an attempt to determine their kinetic effect upon the expression given above. It is found that this effect for the inert gases investigated— N_2 , He , and CO_2 —may be expressed as

$$s = k_1 [A]^{n_1} [B]^{n_2} [C]^{n_3} - - - + \beta G_1$$

where G_1 represents the initial concentration of the inert gas. From results obtained it seems probable that the value of β depends upon the combined effect of the thermal properties of the inert gas on the heat distribution of the reaction, the property of heat conductivity being predominant.

(4) An example of the utility of the constant pressure bomb for the study of the kinetics of the gaseous explosive reaction is offered in the results of the present paper.

Report No. 281, entitled "The Effects of Fuel and Cylinder Gas Densities on the Characteristics of Fuel Sprays for Oil Engines," by William F. Joachim and Edward G. Beardsley, National Advisory Committee for Aeronautics.—This investigation was conducted at the Langley Memorial Aeronautical Laboratory as a part of a general research on fuel-injection engines for aircraft. The purpose of the investigation was to determine the effects of fuel and cylinder gas densities upon several characteristics of fuel sprays for oil engines.

The start, growth, and cut-off of single fuel sprays produced by automatic injection valves were recorded on photographic film by means of special high-speed motion-picture apparatus. This equipment, which has been described in previous reports, is capable of taking 25 consecutive pictures of the moving spray at the rate of 4,000 per second.

The penetrations of the fuel sprays increased and the cone angles and relative distributions decreased with increase in the specific gravity of the fuel. The density of the gas into which the fuel sprays were injected controlled their penetration. This was the only characteristic of the chamber gas that had a measurable effect upon the fuel sprays. Application of fuel-spray penetration data to the case of an engine, in which the pressure is rising during injection, indicated that fuel sprays may penetrate considerably farther than when injected into a gas at a density equal to that of the gas in an engine cylinder at top center.

Report No. 282, entitled "The Performance of Several Combustion Chambers Designed for Aircraft Oil Engines," by William F. Joachim and Carlton Kemper, National Advisory Committee for Aeronautics.—Several investigations have been made on single-cylinder test engines

at the Langley Memorial Aeronautical Laboratory to determine the performance characteristics of four types of combustion chambers for aircraft oil engines. Two of the combustion chambers studied were bulb-type precombustion chambers, the connecting orifice of one having been designed to produce high turbulence by tangential air flow in both the precombustion chamber and the cylinder. The other two were integral combustion chambers, one being dome-shaped and the other pent-roof shaped. The injection systems used included cam and eccentric driven fuel pumps and diaphragm and spring-loaded fuel-injection valves. A diaphragm-type maximum cylinder pressure indicator has been used in part of these investigations with which the cylinder pressures were controlled to definite values. The performance of the engines when equipped with each of the combustion chambers is discussed. The data presented show the performance for speeds from 600 to 1,800 revolutions per minute.

The results obtained indicate that aircraft type oil engines with suitably designed combustion chambers and fuel-injection systems may be operated at speeds around 1,800 revolutions per minute without encountering excessive explosion pressures. At a speed of 1,600 revolutions per minute and with a fuel quantity giving 15 per cent excess air in the cylinder, a maximum indicated mean effective pressure of 119 pounds per square inch was obtained with a fuel consumption of 0.43 pound per indicated horsepower per hour. The maximum cylinder pressure was 740 pounds per square inch. A minimum fuel consumption of 0.26 pound per indicated horsepower per hour at an indicated mean effective pressure of 52 pounds per square inch and 1,600 revolutions per minute was obtained with a cylinder head having a bulb-type precombustion chamber. The maximum cylinder pressure was 560 pounds per square inch.

It is concluded that an increase in specific power output of the high-speed aircraft oil engine depends upon the ability to obtain higher mean effective pressures and an improvement in the mechanical efficiency of the engine. The best performance for the tests reported was obtained with a bulb-type combustion chamber designed to give a high degree of turbulence within the bulb and cylinder.

LIST OF TECHNICAL NOTES ISSUED DURING THE PAST YEAR

- | | |
|------|--|
| No. | |
| 248. | The Drag of Airships. By Clinton H. Havill, United States Navy. Part II. Drag of Bare Hulls. |
| 249. | Effect of Protruding Gasoline Tanks Upon the Characteristics of an Airfoil. By Eastman N. Jacobs. |
| 250. | Influence of the Orifice on Measured Pressures. By Paul E. Hemke. |
| 251. | The Effect of Tube Length Upon the Recorded Pressures from a Pair of Static Orifices in a Wing Panel. By T. Carroll and R. E. Mixon. |
| 252. | Resistance of a Fifteen-Centimeter Disk. By James M. Shoemaker. |
| 253. | Wind Tunnel Standardization Disk Drag. By Montgomery Knight. |
| 254. | Method of Correcting Wind Tunnel Data for Omitted Parts of Airplane Models. By R. H. Smith. |
| 255. | Precision of Wing Sections and Consequent Aerodynamic Effects. By Frank Rizzo. |
| 256. | Wall Interference in Closed Type Wind Tunnels. By George J. Higgins. |
| 257. | Technical Preparation of the Airplane "Spirit of St. Louis." By Donald A. Hall. |
| 258. | A Warning—Concerning the Take-Off with Heavy Load. By Elliott G. Reid and Thomas Carroll. |
| 259. | "Alclad"—A New Corrosion-Resistant Aluminum Product. By E. H. Dix, jr. |
| 260. | Study of Open Jet Wind Tunnel Cones. By Fred E. Weick. |
| 261. | Tension Experiments on Diaphragm Metals. By H. B. Henrickson. |
| 262. | The Installation and Correction of Compasses in Airplanes. By M. F. Schoeffel. |
| 263. | A Load Factor Formula. By Roy G. Miller. |
| 264. | Tests of the N. P. L. Airship Models in the Variable-Density Wind Tunnel. By George J. Higgins. |
| 265. | Measurement of the Moments of Inertia of Full-Scale Airplanes. By M. W. Green. |
| 266. | Airfoil Lift with Changing Angle of Attack. By Elliott G. Reid. |

LIST OF TECHNICAL MEMORANDUMS ISSUED DURING THE PAST YEAR

- No.
382. Experiments with Rotating Cylinders in Combination with Airfoils. By Kurt Frey. Translation from "Zeitschrift für Flugtechnik und Motorluftschiffahrt," August 28, 1926.
383. Spindled and Hollow Spars. By J. D. Blyth. From "Flight," August 26, 1926.
384. Experimental Investigation of the Physical Properties of Medium and Heavy Oils, Their Vaporization and Use in Explosion Engines. By Fritz Heinlein. Part III. Experimental Apparatus. Translation from "Der Motorwagen," June 30, 1926.
385. Cooling of Air-Cooled Engines by Forced Circulation of Air. Translation from "Les Ailes," September 9, 1926.
386. Central Aerohydrodynamic Institute of Moscow, Russia. By W. Margoulis. Translation from "L'Aeronautique," August, 1926.
387. Approximate Calculation of the Static Longitudinal Stability of Airplanes. By Theodor Bienen. Translation from "Zeitschrift für Flugtechnik und Motorluftschiffahrt," July 28, 1926.
388. Experiments with a Sphere from Which the Boundary Layer is Removed by Suction. By Oskar Schrenk. Translation from "Zeitschrift für Flugtechnik und Motorluftschiffahrt," September 14, 1926.
389. Devices for Prevention of Stalled Flight. By Paul Mazer. Translation from "L'Aeronautique," October, 1926.
390. Determining Size of Drops in Fuel Mixture of Internal-Combustion Engines. By J. Sauter. Translation from "Zeitschrift des Vereines deutscher Ingenieure," July 31, 1926.
391. Experiments on Self-Ignition of Liquid Fuels. By Kurt Neumann. Translation from "Zeitschrift des Vereines deutscher Ingenieure," August 7, 1926.
392. Experimental Investigation of the Physical Properties of Medium and Heavy Oils, Their Vaporization and Use in Explosion Engines. By Fritz Heinlein. Part IV. Translation from "Der Motorwagen," September 30 and November 10, 1926.
393. Stall-Proof Airplanes. By G. Lachmann. From Yearbook of "Wissenschaftlichen Gesellschaft für Luftfahrt," 1925.
394. Testing a Windmill Airplane ("Autogiro"). By R. Seiferth. Translation from "Zeitschrift für Flugtechnik und Motorluftschiffahrt," November 27, 1926.
395. Removing Boundary Layer by Suction. By J. Ackeret. Translation from "Zeitschrift des Vereines deutscher Ingenieure," August 28, 1926.
396. Determining the Efficiency of Atomization by Its Fineness and Uniformity. By J. Sauter. Translation from "Forschungsarbeiten auf dem Gebiete des Ingenieurwesens," No. 279, 1926.
397. High-Speed Oil Engines for Vehicles. By Ludwig Hausfelder. Part I. Engines with External Atomization of the Fuel; Engines with Internal Atomization of the Fuel; Hot-Bulb Engines; Diesel Engines. Translation from "Der Motorwagen," August 31, 1926.
398. Researches on Ailerons and Especially on the Test Loads to Which They Should be Subjected. By J. Sabatier. Translation from "La Technique Aeronautique," November 15 and December 15, 1926.
399. Duralumin Welding. By Wm. Nelson. From "Aviation," January 17, 1927.
400. On the Mutual Reaction of Wings and Body. By J. Lennertz. Translation from "Zeitschrift für Flugtechnik und Motorluftschiffahrt," January 14, 1927.
401. The Heat Treatment of Duralumin. By Wm. Nelson, From "Aviation," February 21, 1927.

- No.
402. Permanent Commission of Aeronautical Studies. Report No. 4.
 Part I. Determination of the Main Conditions Entailing Overload and Examination of the Existing Theoretical and Experimental Data.
 Part II. Reduction of the General Conditions of Calculation to Some Simple Cases.
 Part III. Load Factors.
 Translation from the French.
 403. High-Speed Oil Engines for Vehicles. By Ludwig Hausfelder. Part II. Translation from "Der Motorwagen," September 30 and December 10, 1926.
 404. The Protection of Duralumin from Corrosion. By Wm. Nelson. From "Aviation," November 8, 1926.
 405. Structural Details from 1926 Paris Aero Salon. By W. Rethel. Translation from "Zeitschrift für Flugtechnik und Motorluftschiffahrt," February 14, 1927.
 406. Flap Gear for Airplanes. A New Scheme in Which Variation is Automatic. By A. Hessell Tiltman. From "The Automobile Engineer," February, 1927.
 407. Some Impressions of the Paris Aero Show. By J. D. North. From "The Aircraft Engineer," supplement to "Flight," December 30, 1926.
 408. Duralumin and Its Corrosion. By Wm. Nelson. From "Aviation," November 1, 1926.
 409. Kinetographic Determination of Airplane Flight Characteristics. By P. Raethjen and H. Knott. Translation from "Zeitschrift für Flugtechnik und Motorluftschiffahrt," December 14 and 28, 1926.
 410. High-Speed Oil Engines for Vehicles. By Ludwig Hausfelder. Part III. Translation from "Der Motorwagen," December 20 and 31, 1926, and January 10, 1927.
 411. Determining the Velocity Distribution in the Boundary Layer of an Airfoil Fitted with a Rotary Cylinder. By B. G. Van der Hegge Zijnen. Translation from Report A 129 of the "Rijks-Studiedienst voor de Luchtvaart," Amsterdam. Reprint from "De Ingenieur," October 23, 1926, No. 43.
 412. Air Cooling. An Experimental Method of Evaluating the Cooling Effect of Air Streams on Air-Cooled Cylinders. By J. F. Alcock. From "The Automobile Engineer," April, 1927.
 413. Multiplicity of Solutions in Aerodynamics. By M. Dupont. Translation from "La Technique Aeronautique," December, 1926, and January, 1927.
 414. Aerodynamic Laboratory at Cuatro Vientos. By Moreno Caracciolo. Translation from "Boletin Oficial," Royal Aero-Club of Spain, 2d quarter, April-June, 1924, and "L'Aeronautique," September, 1926.
 415. Climbing Efficiency of Aircraft. By C. C. Walker. From "Flight," January 27, 1927.
 416. Effect of Streamline Curvature on Lift of Biplanes. By L. Prandtl. Translation from Report III, "Ergebnisse der Aerodynamischen Versuchsanstalt zu Göttingen," 1927.
 417. Drag Measurements of Two Thin Wing Sections at Different Index Values. By J. Ackeret. Translation from Report III, "Ergebnisse der Aerodynamischen Versuchsanstalt zu Göttingen," 1927.
 418. Investigation of a Wing with an Auxiliary Upper Part. By R. Seiferth. Translation from Report III, "Ergebnisse der Aerodynamischen Versuchsanstalt zu Göttingen," 1927.
 419. Experiments with Three Horizontal Empennages. By R. Seiferth. Translation from Report III, "Ergebnisse der Aerodynamischen Versuchsanstalt zu Göttingen," 1927.
 420. Some Notes on Gasoline-Engine Development. (A Résumé of a Paper by H. R. Ricardo.) From "The Automobile Engineer," April, 1927.
 421. Aero Dopes and Varnishes. By H. T. Britton. From "The Industrial Chemist," March, 1927.
 422. Systematic Investigation of Joukowsky Wing Sections. By O. Schrenk. Translation from "Zeitschrift für Flugtechnik und Motorluftschiffahrt," May 28, 1927.

- No.
423. Lindbergh's Flight. By August von Parseval. Translation from "Der Motorwagen," May 31, 1927.
 424. Discussion of the Results of the Boundary-Layer Tests of an Airfoil Fitted with a Rotary Cylinder. By E. B. Wolff and C. Koning. Translation of Report A.130 of the "Rijks-Studiedienst voor de Luchtvaart," Amsterdam. Reprint from "De Ingenieur," No. 52, December 25, 1926.
 425. Recent Suggestions in Diesel-Engine Construction. By F. Ernst Bielefeld. Translation from "Schiffbau," June 2, June 16, and July 7, 1926.
 426. Seaplane Floats and Hulls. By H. Herrmann. Translation from "Berichte und Abhandlungen der Wissenschaftlichen Gesellschaft für Luftfahrt," December, 1926.
 427. Seaplane Floats and Hulls. By H. Herrmann. Part II. Translation from "Berichte und Abhandlungen der Wissenschaftlichen Gesellschaft für Luftfahrt," December, 1926.
 428. Drag Measurements on a Junkers Wing Section. Application of the Betz Method to the Results of Comparative Tests Made on a Model and on an Airplane in Flight. By Hanns Weidinger. Translation from "Berichte und Abhandlungen der Wissenschaftlichen Gessellschaft für Luftfahrt," December, 1926.
 429. Building a Full-Size Glider. By F. J. Camm. From "The Air League Bulletin," of the Air League of the British Empire, London, No. 68, June, 1927.
 430. Effect of Roughness on Properties of Airfoils. By O. Schrenk. Translation from Report III, "Ergebnisse der Aerodynamischen Versuchsanstalt zu Göttingen," 1927.
 431. Experiments on Airfoils with Trailing Edge Cut Away. By J. Ackeret. Translation from Report III, "Ergebnisse der Aerodynamischen Versuchsanstalt zu Göttingen," 1927.

LIST OF AIRCRAFT CIRCULARS ISSUED DURING THE PAST YEAR

- No.
17. The Avro Avian Airplane. From "Flight," August 26, 1926.
 18. The De Havilland *Moth*. From "Flight," March 5, 1925.
 19. The Bristol *Badminton* Airplane. From "Flight," July 8, 1926.
 20. The Handley-Page *Hamlet* (Commercial Monoplane). From "The Aeroplane," October 13, 1926, and "Flight," October 14, 1926.
 21. The A. N. E. C. IV *Missel Thrush*, Light Airplane. From "Flight," September 9, 1926.
 22. Avia Pursuit Airplane *B. H. 21*. By J. Serryer. Translation from "Les Ailes," May 28, 1925.
 23. Albert *TE-1*, Training Airplane. Translation from the French.
 24. Rohrbach All-Metal Commercial Airplane *RO VIII*, "Roland." Translation from the German.
 25. The Supermarine *Southampton*, Seaplane (Observation or Bomber). From "Flight," November 18 and 25, 1926.
 26. The Boulton and Paul *Bugle*, Airplane (Day Bomber). From "Flight," April 23, 1925, and "The Aeroplane," April 29, 1925.
 27. Dyle and Bacalan Metal Monoplane *D. B. 10* (Night Bomber). Translation from "Les Ailes," December 2, 1926, and "L'Aerophile," November, 1926.
 28. Combat and Bombing Airplane, Amiot 120 *B3*. Translation from a circular issued by the S. E. C. M. ("Societe d'Etudes et de Constructions Mecaniques).
 29. Nieuport-Delage 48 *C1*, Pursuit Airplane ("Jockey" Type). Translation from the French.
 30. The *Dornier Mercury*, Commercial Airplane. From a circular issued by the Dornier Co.
 31. Dornier *Superwal*, Commercial Seaplane. From "I. F. W." No. 21, 1926, and from a circular issued by the Dornier Co.
 32. Macchi *M. 39*, Seaplane (Single Seat Racer). Translation from "L'Ala d'Italia," November, 1926.
 33. "Savoia" Seaplane *S. 55* (Military or Commercial). From a circular issued by the "S. I. A. I." and "Flight," April 9, 1925.

- No.
34. Vojenska-Smolik *S. 16*, Airplane (All-Metal Long-Distance Observation Biplane). From "Flight," January 13, 1927.
 35. Richard-Penhoet Commercial Seaplane. Translation from "Bulletin de la Chambre Syndicale des Industries Aeronautiques," September-December, 1926.
 36. The Rohrbach "Robbe" *RO VII*, Seaplane (Military or Commercial). From a circular issued by the Rohrbach Metal Aeroplane Co.
 37. The Francois Villiers Marine Pursuit Airplane. From a circular issued by Villiers Co., supplemented from article in "Les Ailes," November 25, 1926.
 38. Heinkel *H. E. 5*, Commercial Seaplane (Winner of the 1926 German Seaplane Contest at Warnemunde). From a circular issued by the Ernst Heinkel Airplane Co.
 39. Lioré-Olivier *LeO 194*, Seaplane. Translation from "L'Aéronautique," February, 1927.
 40. Training Airplane *Avia B. H. 11*. Translation from a circular issued by Milos Bondy A Spol, Czechoslovakia.
 41. *Meteore 63* Commercial Seaplane. From a circular issued by the S. P. C. A. with supplementary data from "Les Ailes," July 29, 1926.
 42. The Mureaux *Brunet 3C2*, Pursuit Airplane. By J. Serryer. Translation from "Les Ailes," March 24, 1927.
 43. Fiat *C. R. 20*, Pursuit Airplane. Translation from "L'Ala d'Italia," December, 1926.
 44. The Rohrbach *Rocco*, Seaplane (New German Commercial Seaplane). From "Flight," May 12, 1927.
 45. The Blackburn *Bluebird* (Two-Seat Training and Sport Airplane). From "The Aeroplane," March 16, 1927.
 46. Focke-Wulf *G. L. 18* (Commercial Airplane). By J. Serryer. Translation from "Les Ailes," September 23, 1926.
 47. Junkers Airplane *G. 24* (All-Metal Commercial Airplane). Translation from a circular issued by the "Junkers Flugzeugwerk, A. G.," of Dessau, Germany.
 48. The Gloster *Gambet*, Airplane (A Deck-Landing Ship's Fighter). From "The Aeroplane," June 1, 1927.
 49. The Avro "Gosport" *504 R* (A New Training Airplane). From "Flight," April 15, 1926.
 50. *Levasseur 8*, Transatlantic Airplane. Translation from "L'Aéronautique," June, 1927, and "L'Aerophile," June, 1927.
 51. Caproni Airplane *Ca 73* (Commercial) and *Ca 73 ter* (Military). Translation from a circular issued by the Caproni Co., Milan, Italy.
 52. The Boeing Mail Airplane. Prepared by the Boeing Airplane Co.
 53. The Westland *Widgeon III*. From "Flight," July 28, 1927.
 54. Junkers Commercial Airplane *G. 31*. Translation from "Zeitschrift des Vereines deutscher Ingenieure," May 7, 1927.
 55. *Travel Air*, Commercial Airplane—Type 5000. Prepared by Travel Air Manufacturing Co.
 56. Training Airplane *Arado SC 1*. Translation from "Flugwoche," June 22, 1927.

BIBLIOGRAPHY OF AERONAUTICS

During the past year the committee issued bibliographies of aeronautics for the years 1923 and 1924. It had previously issued bibliographies for the years 1909 to 1916, 1917 to 1919, 1920 to 1921, and 1922. A bibliography for the year 1925 is now in the hands of the printer, and should be ready for distribution during the coming year. An annual bibliography will be published hereafter by the committee.

Citations of the publications of all nations are included in the language in which the publications originally appeared. The arrangement is in dictionary form, with author and subject entry, and one alphabetical arrangement. Detail in the matter of subject reference has been omitted on account of cost of presentation, but an attempt has been made to give sufficient cross reference to make possible the finding of items in special lines of research.

PART V

THE PRESENT STATE OF AERONAUTICAL DEVELOPMENT

PROGRESS IN TECHNICAL DEVELOPMENT

AERODYNAMICS

The nature and results of the fundamental research carried out in the various laboratories during the past year emphasize the fact that the main theoretical foundation of this science has been laid and that new advances must be more in the nature of extensions or additions to existing theory rather than new fundamental conceptions. The majority of the aerodynamic problems investigated during the past year were closely identified either with particular design requirements or with the study of unusual phenomena. A well-balanced program should include as much fundamental research as possible, but continuing demands for answers to specific problems have made it impossible to give proper consideration to fundamental research. The work done during the past year and that laid out for the future may appear to contain only a small proportion of fundamental research, but careful analysis will show that almost every investigation, in addition to the possibility of some immediate practical application as one of its objects, has a bearing on some fundamental problem. It will readily be understood that the committee's research program must be arranged to suit the technical requirements of the services and the equipment and personnel available.

WIND TUNNELS.—*Airplane model tests.*—The wind tunnel continues to grow in the esteem of aeronautical engineers as its value becomes more generally recognized. Additional confirmation has recently been obtained of the necessity for either strict geometrical similarity or due allowance for lack of it. The first tests on the Sperry Messenger model in the variable-density wind tunnel gave drag coefficients very much less than the full-scale values obtained from flight tests. A comparison of the model with the full-scale airplane showed that a number of small parts and minor details had been omitted in the model. When these had been incorporated in the model a much better agreement was found. One of the first investigations in the new propeller research equipment was on the full-scale Sperry Messenger with wings removed, and the drag values were found to be about 10 per cent higher than those given by the variable-density wind tunnel for the same model condition.

It was found that the Sperry Messenger model did not have a fair representation of the landing-gear details, particularly in regard to the axle and shock absorbers. When these were faired in on the full-scale airplane in accordance with the model construction, excellent agreement in drag values was obtained. Several laboratories now allow for deviation from full scale in the model construction, and in particular the Washington Navy Yard wind tunnels have long made it a regular practice to apply a calculated drag correction for omitted detail, thereby securing consistent agreement between model and full-scale values.

Variable-density wind tunnel.—During the past year tests were made in the variable-density wind tunnel on three airplane models supplied by the British Aeronautical Research Committee. These models had previously been tested in various wind tunnels in England and the actual airplanes tested in free flight. The results obtained in the variable-density wind tunnel were in excellent agreement with the British data, both model and full scale. One of the most important lessons learned from these tests is that the scale effect on lift may be very large in airfoils which are very thick, very deeply cambered, or of symmetrical section. In particular, the high maximum lift at low Reynolds Number on a very thick or deeply cambered section is not likely to be obtained at high Reynolds Numbers.

Autorotation.—The research on autorotation has been continued with what appears to be definite results. After measuring rates of spin under various conditions it was found that they did not agree with the rates calculated by the "strip method." The angular ranges for spin instability were widely different as obtained by experiment and calculation. This feature was investigated thoroughly by means of pressure distribution studies and the variation of loading along the span was found to account for the differences. As a by-product of this investigation some very valuable load distribution data are being made available.

Included in the autorotation research were a number of tests on various airfoils in varying combinations leading to several conclusions worthy of note. The most important of these is that no monoplane model has been found which will "flat spin," and it does not appear likely that one will be found. The flat spin may be due either to the geometry of the wing cellule or to mass distribution in combination with the geometry (i. e., little or no stagger). An approximate criterion of spinning instability which is very easy to apply was developed during this research.

Boundary layer control.—A considerable amount of research work has been done on boundary layer control, both pressure and suction methods being used. In explanation of this research, Doctor Prandtl showed that the disturbance originating in a thin layer of air adjacent to the wing surface was the cause of the flow breaking away from the upper surface at high angles of attack and thus preventing the attainment of high lifts.

"Boundary layer control" is descriptive of the means employed to prevent the flow from breaking away. Air may be forced through small slots running across the upper surface of the wing and so formed that the jet is approximately parallel with the wing surface at the exit, or forward opening slots may be used with suction instead of pressure. From the standpoint of power absorbed the suction method has given the best results but slightly higher maximum lifts have been obtained with the pressure method. The greatest increase in maximum lift so far obtained is about 50 per cent but this was obtained on a wing section now known to be unsuited for the purpose, and further tests under way may be expected to show better results.

FREE FLIGHT TESTS.—Pressure distribution.—During the past year free flight work has followed the general program of the year before in that a large number of investigations have been completed and new projects initiated. The success of the studies made on the TS-1 and VE-7 airplanes led to an extension and expansion of program on pursuit airplanes in which an Army Boeing PW-9 and a Navy Curtiss F6C-4 have been used. Very complete records have been obtained in various maneuvers, giving linear and angular velocities and accelerations at various parts of the airplane, together with pressure distributions on wings and tail surfaces. Many important facts bearing on design requirements have been obtained. Special attention has been given to loads on the horizontal tail surfaces in diving and in quick pull-ups from diving at high speed, to the variation of loading along the span under various conditions, and to the distribution of loading over the two wings of a biplane. This work is made possible by the use of special photographic equipment so designed that continuous and simultaneous records are obtained for all desired factors in any maneuver. Engineers who are in touch with these developments are of the opinion that pressure distribution studies along these lines offer the most logical and promising method available for increasing our knowledge of design requirements.

Boundary layer control.—Free flight tests have been made on the TS-1 airplane fitted with the pressure system of boundary layer control in the upper wing only, the pressure being supplied by a supercharger blower. The results showed a rather small but quite definite improvement in climb without appreciable change in high speed. One feature of particular interest was that air speed for best climb was reduced about 10 miles per hour when the blower was operating. In view of the fact that the slots were installed on one wing only and that the wing section (U. S. A.-27) was shown by wind-tunnel tests to be unfavorable for this purpose, it is believed that boundary layer control may offer some promise and further work will be done.

Spinning.—One of the most important free flight investigations was carried out by the Army Air Corps at McCook Field during the past year. As a part of the general study of spinning, the effect of changing the location of the center of gravity in a systematic manner

ranging from about 17 to 39 per cent of the mean chord, together with the effect of various mass distributions was tried on two airplanes, the O-1 and the O2-E4. Spins were made in both directions under all conditions and the control position for recovery, altitude lost per turn, turns for recovery, etc., were noted in each case. Recovery in every case was assured by fitting the airplane with one or more boxes of lead shot which could be dropped so as to bring the center of gravity forward. It was found that as the center of gravity moved aft the airplane would spin slower and more down at the nose while the control forces increased. At a center of gravity location of approximately 38 per cent the control forces became so great and the response of the airplane so slow that the spin was considered dangerous and tests were discontinued. It was shown that mass distribution played a most important part in holding the airplane in a spin.

Landing and take-offs.—The study of the landing and take-off characteristics of various airplanes is being continued. At present tests are being made on a Douglas mail airplane to determine the effect of variations in the load and changes of the propeller characteristics on taking off and landing.

Pressure distribution on floats.—The water pressures over the bottom of the UO-1 seaplane float have been obtained in a great number of landings and this work is to be continued on a TS-1. The maximum intensity so far measured is less than 7 pounds per square inch. Readings are taken at a sufficient number of points to enable the drawing of an accurate load-contour map.

Improvement in visibility.—A VE-7 airplane with the center section of the upper wing cut away and the spars replaced by streamline struts for the purpose of improving the visibility was tested to determine the effect of the changes on the performance of the airplane. It was found that the rate of climb was reduced about 12 per cent which is in agreement with the increase in induced drag. As predicted, the high speed was affected less than 2 per cent. These values were but slightly improved by the use of "end planes" on the "inner" tips.

Control at low speeds.—Flight research on lateral control at low speeds was confined to the continuation of the spoiler-gear tests on the TS-1 airplane. Owing to the urgency of other work this research has not yet been completed. A number of additional tests on lateral control at low speeds have been proposed and it is probable that a definite program will be adopted during the present year.

PROPELLERS.—The recent completion of the propeller research equipment opens up an entirely new field of opportunity for propeller research. Preliminary tests on the Sperry messenger airplane indicate that a great number of problems involving power plant and fuselage design can now be solved. The testing program now under way includes check tests on the VE-7 propellers previously tested in flight, a study of propeller blade deflections under various flight conditions, a study of the effect of various forms of cowling on the resistance and cooling of air-cooled engines, and the determination of proper forms for wind shields and cowling.

Comparative tests on a model.—A metal model propeller supplied by Charles Ward Hall has been tested at Stanford University and will be tested in the wind tunnels at the Massachusetts Institute of Technology and the National Physical Laboratory, in order to obtain comparative data under different test methods and in open and closed types of wind tunnels. The matter of correction due to tunnel wall interference has received serious consideration in England and this series of tests will fit in with the general investigation.

LIGHTER-THAN-AIR CRAFT.—*Pressure distribution in flight.*—The most important lighter-than-air investigation completed during the past year was the flight pressure distribution runs on the rigid airship U. S. S. *Los Angeles*. It was found that the maximum loadings on tail surfaces due to gusts is greater than the maximum loadings obtained in maneuvers.

Fineness ratio.—The tests in the variable-density wind tunnel on a series of airship models of varying fineness ratio have been completed. In this research, each model was tested at various Reynolds Numbers, thus covering a very large range, previously unexplored. A special wire-type drag balance which was designed and installed for these tests gave such consistent results that several streamline models which had previously been tested on the regular balance

were retested with rather surprising results. One model in particular which had shown an extremely low drag in the original test was found to have a normal drag on the wire balance. The difference was easily shown to be due to spindle interference in the first tests.

FIELDS FOR FUTURE RESEARCH.—It is plain that continued progress in aerodynamics may be expected but that it will be largely along lines leading to refinements in design. Every detail of an airplane may be improved in this manner, both structurally and aerodynamically. The most promising fields of future research are those which increase our knowledge of the magnitude and distribution of the forces acting on an airplane. Research along these lines should lead to more efficient structures and greater safety, through better control, and to the development of better wing sections free from unstable flow characteristics. The study of the causes of discontinuous flow and of the effects of slots, flaps, and "boundary layer control" will also lead to better control at low speeds.

The immediate needs of the designer are for information which will promote this refinement of design. Important items in this information are the effects of the mutual interference between the propellers and other parts of the airplane in both single and multi-engined airplanes; the effect of the mutual interference between the wings, fuselage, and landing gear; and the effect of the cowling around the forward end of the fuselage on both the cooling of air-cooled engines and the drag of the airplane. The designer also requires more data on wings, especially data obtained in full-scale tests, including the distribution of pressure over the wings.

AIRPLANE STRUCTURES

TREND OF DESIGN.—*Standardization of types.*—The tendency toward the standardization of types for particular services has continued. The monoplane has definitely established itself for commercial service where air speeds are relatively low and efficiency is the prime requirement. It also has the advantages of easy maintenance and giving good visibility to passengers together with good ground clearance under the wing when on the landing field. In the lighter and faster types of commercial airplanes where moderate loads or only one or two passengers are carried the biplane continues to be preferred, as might be expected from the advantages it confers in the way of maneuverability and compactness of form.

For military airplanes the biplane combination continues in the lighter types where semi-internally braced and moderately thick wings are used. In pursuit airplanes a modification of the biplane, with the lower wing smaller than the upper, approximating the sesquiplane, appears to be the general practice. By this construction great compactness is obtained while the structural strength required by the demand for extreme speed and maneuverability is obtained with the lightest weight. The biplane cellule also continues for shipboard airplanes since the span of such an airplane can not exceed 50 feet owing to the limitations fixed by handling devices. While last year the biplane cellule was uniform in observation and bombing types the development of the monoplane type has been begun and a number of this type are now undergoing service tests.

Number and location of engines.—The use of several engines in large military aircraft is now standard practice. This is in general accord with the commercial practice for large airplanes which is definitely established as using several engines, generally three. A single engine continues to be used in commercial airplanes with a capacity of up to six passengers where a larger number of engines would be uneconomic or impracticable.

Amphibian airplanes.—Interest in the development of the amphibian type of airplane has been very much increased by the discovery that in many cases our lakes and rivers provide a series of favorable seaplane landing places, along traveled routes. The amphibian can take advantage of such a natural airway and also can land its passengers on a regular landing field. In addition it can propel itself from the water up a beach, either natural or artificial, thus doing away with both handling cradles and crews.

The successful development of the amphibian is due to the successful use of light alloys, which has made it possible to reduce the weight of structure, and to the use of the air-cooled engine. It is now possible to construct amphibians having a performance comparable with

that of other types. Several manufacturers are working on the development of amphibian airplanes for commercial purposes.

Differences between military and commercial types.—The differences in the fundamental requirements of military and commercial types of airplanes have been appreciated more clearly. This is evidenced by the fact that the construction of commercial airplanes in a plant entirely separate and distinct from that in which military airplanes are built has been proposed.

In the military types also an understanding of the differences between the fundamental requirements of aircraft for Army and Navy use is more apparent. Special equipment of Navy types enabling them to be projected from catapults and landed on arresting gear requires a considerably heavier structure and details in many parts than in the corresponding Army types. Consequently it is frequently found that a Navy airplane apparently identical with an Army type will weight several hundred pounds more than its Army duplicate.

The specialization which differentiates the military type so markedly from the commercial type of airplane has continued. It is now apparent that the great majority of commercial airplanes built in this country could not be adapted to any purely military use. Certain of the lighter and faster types might be used for preliminary training and some of the heavier ones might be used for transport purposes but neither would have a truly military character.

Landing gear—Shock absorbers.—Hydraulic shock absorbers are practically universal on military airplanes and have come into almost general use in commercial airplanes. As a rule it is only the smaller and lighter types of commercial airplanes which still retain the old rubber cord shock absorbers.

Brakes.—With the increasing appreciation of the necessity for proper handling of airplanes on the ground, both in taking-off and landing, brakes have undergone a very considerable further development and at present there are several good designs on the market. They are being generally applied to all types of airplanes, both military and commercial and are being used not only for landing but also in place of wheel chocks just before taking-off. Many pilots find it advantageous to run the engine up to full revolutions with the brakes on and then suddenly release them. This results in a shorter take-off run. The possibility of combining the use of brakes on the wheels of the regular landing gear with a wheel in place of the usual skid and the fitting of a brake on this wheel is engaging attention. This is particularly appreciated since the destructive effect of the ordinary skid on landing fields which handle much traffic has become apparent.

The combination of the shock absorbers and the brakes in the wheel has been proposed and has been tried out experimentally in military airplanes. This arrangement would be extremely desirable on account of the reduction in resistance and its development is being watched with interest.

STRUCTURAL MATERIALS.—*Metal construction.*—Even the smallest and lightest commercial airplanes now have a metal fuselage. In fact a wooden longéron fuselage is a comparative rarity.

The introduction of metal into the wing construction has not become so general, since it has been attended with considerable difficulties. Metal spars of aluminum alloy and steel have been constructed which show a very satisfactory weight as compared with wooden ones. However, the difficulties which have been experienced in the proper protection of the aluminum alloys against corrosion has prevented their full utilization especially in types of structures where inspection is difficult. With the introduction of aluminum alloys which are practically free from corrosion difficulties an expansion of this use is probable.

The most notable all-metal airplanes are usually original in design and details of construction. It should be noted that most of these airplanes use aluminum alloys and have done so for long periods with practically no serious difficulty regarding corrosion.

Steel tubing.—Corrosion in steel tubing has always been a disturbing factor. Many methods of protection have been proposed and tried but none has proved entirely satisfactory. The development of extremely high-strength and corrosion-resisting steel tubing has been proposed. This type of tubing will require special methods of welding, but great interest in the possibilities

has been displayed by the manufacturers of the material and by the manufacturers of the devices used in welding.

Duralumin tubing.—The use of duralumin tubing has decreased owing to the difficulties encountered in protecting the interior of the tubing from corrosion. Structural sections of **H** and **I** form have been substituted for tubing in many instances.

Floats.—The metal float has continued to gain in favor, particularly since the practical freedom from increase of weight caused by soakage means a permanent reduction in weight. With the development of a satisfactory method of protection against corrosion it is probable that this method of constructing floats will become standard.

Rubber protective coatings.—Considerable improvements in these coatings have been made and it is confidently expected that they will have an important place in the protection of aluminum and other parts of aircraft. The resistance of rubber to abrasion would appear to be particularly valuable in connection with floats on seaplanes and amphibians where the aircraft must be handled up and down on beaches.

AIRSHIPS

Technical development and present situation.—The technical development of airships continues to lag behind that of airplanes. This is only to be expected in view of the small numbers of airships which are built and the very limited opportunity for development of new ideas and methods of construction which are presented. No new airship construction has been begun in the United States. Attention has been confined to the replacement of parts of existing nonrigid airships.

A design competition was held by the Navy Department looking toward the procurement of the best designs for the 6,000,000-cubic-foot airships which have been authorized by Congress as a part of the Navy Department "five-year aviation program." A number of designs were submitted, among them a very satisfactory one, and negotiations toward a contract for the construction of one airship generally according to this design are under way. This design includes a number of features which, while novel as far as actual incorporation in airships is concerned, have been commonly discussed in that connection for many years.

Experimental investigation and research for the purpose of improving existing airships and providing improved materials and methods of construction for new airships whenever they are begun has continued although at a decreased rate. The satisfactory methods for the protection of duralumin against corrosion and progress made in the obtaining of substitutes for goldbeater's skin fabric are the most notable results.

Work with the "Los Angeles."—The *Los Angeles* has been maintained in splendid condition and undoubtedly has several years of useful and active life before it. It has been used frequently in research on problems connected with the design and operation of rigid airships. One of the most important problems was the determination of the effect on the speed of the airship of fitting water recovery apparatus. For this purpose a series of deceleration tests was carried out on the airship both with and without the water recovery apparatus. The resistance coefficients of the full-sized airship were thus determined and the effect of the added apparatus was accurately determined.

The operating personnel of the *Los Angeles* has been continuously active in the improvement of methods for handling airships on the ground and in and out of the shed. The enlisted and officer personnel engaged in this work have been very highly complimented by persons who have observed the manner in which this airship has been handled by the methods now in use. As a result of study by the personnel at Lakehurst there has been developed a method using a mobile telescopic mast and a large amount of mechanical equipment which it is expected will make it possible to reduce the number of men required for landing and handling the airship to a very notable degree. This equipment is now being constructed and it is expected will be tested in the coming year.

Work with "RS-1."—This airship has made several notable flights from its home station at Scott Field, including one to Langley Field and Lakehurst. It has been extremely active in spite of the handicap imposed on it by a very heavy power plant.

Steps are now being taken toward the redesign of the power plant, including the substitution of two new engines in place of the four now in use, together with the corresponding simplification and lightening in weight. No reverse gears are to be fitted but the propellers are to be made reversing.

The nose cone originally fitted, having shown indications of weakness, has been replaced by a new nose cone of an improved design which has operated with entire satisfaction. When the proposed modifications have been completed this airship should be very much improved in performance.

Metal-clad airship.—Progress on the design and construction of this airship, which is being supplied to the Navy Department by the Aircraft Development Corporation of Detroit, has been reported.

New mooring masts.—The mooring mast constructed at Scott Field, Belleville, Ill., by the Aircraft Development Corporation has been tried out and found to be very successful. The construction of this type of mast has been found to be very much simpler and to be capable of being carried out with much more rapidity than any previous type. At the same time it affords complete protection to the elevator and pipe lines inclosed within it. It also has a pleasing appearance, being a slender tube much like a smokestack.

Helium.—The Army has acquired an additional helium tank car and further tank cars are being considered by both the Army and the Navy. The savings from the use of these cars are very considerable and it is obvious that the tank cars are a very valuable help in the conservation of the helium supply.

A portable helium purification plant mounted upon railroad cars has been placed in service by the Army Air Corps. With this plant all that is necessary is to connect suitable openings on the car to electric leads, water, and helium lines from the impure helium and to storage. It has operated with great satisfaction and turned out helium of high purity.

A privately owned helium plant has been constructed and is now producing helium at a cost which compares favorably with the cost of helium produced in Government-owned plants. The Navy Department is taking practically the entire production of this plant. The owners propose to increase the capacity of the plant in the near future, which will make available a still greater quantity of helium. This plant draws its supply of gas from a field in Kansas. The supply of helium from this field will probably be limited but is large enough to be an important factor in the present available supply.

The gas production in the Petrolia field which supplies the Fort Worth plant has been somewhat improved by cleaning out wells. It has been found that many wells were badly filled and by the simple process of attaching orifice meters to each well it has been possible to select the wells to be cleaned. This has led to a very gratifying increase in the amount of raw gas supplied to the plant and a corresponding increase in the production of helium.

However, the necessity for the location of new supplies of helium and the adoption of proper measures for conservation and development still remained. Accordingly, steps have been taken by the Bureau of Mines leading toward the development of a large new field in northwest Texas. This field is practically untouched and if its entire supply can be exploited in an economical manner, as planned, processing all the gas, it is estimated that it contains a quantity of helium-bearing gas amply sufficient to serve the Nation's needs for several generations.

Progress in Great Britain.—Good progress has been made on the construction of the two 5,000,000-cubic-foot airships in Great Britain. These two airships have undergone numerous changes in design as work progressed, but it is understood that they are expected to be ready for flight in the first half of 1928.

The erection of an airship shed at Karachi, India, is well under way, while the mooring masts at Karachi; Ismallia, Egypt; and Cardington, England, are completed.

At the Imperial Conference held in England in October, 1926, emphasis was laid upon the importance of air transport and a system of imperial air communication. Airships were con-

sidered to play an important rôle in this matter and the data revealed by the report of the air delegates to the conference show that Great Britain has developed her airship program with great care and very thoroughly. An effort was made to interest several of the colonies in the establishment of mooring masts. Apparently Australia, Canada, and South Africa are showing considerable interest in establishing such masts. It was reported that a site for a mast has already been selected in Canada.

Progress in Germany.—The rigid airship having a capacity of about 3,500,000 cubic feet which has been under construction in Germany for the past year is reported to be near completion and may even take the air before the airships which are building in Great Britain.

Progress in Italy.—Information from Italy indicates that the large semirigid airship of about 53,000 cubic meters to which reference was made in last year's report has not been begun, although plans have been prepared for it. Just when its actual construction will be begun appears uncertain.

Standardization of mooring mast equipment.—In view of the probable international character of airship navigation efforts have been made looking toward the standardization of mooring masts. The amount of standardization required is not very great as it would involve primarily the mooring cone and the arrangement and method of operation of the mooring lines. With this accomplished an airship would be able to moor with facility to any mast which it might visit. This effort is still in the preliminary stages but it should lead to valuable results.

AIRCRAFT ENGINES

The greatly increased activity during the past year in the manufacture and operation of privately owned airplanes using engines originally designed and developed for the military services is evidence of the sound and farsighted policy of the Government services which have fostered and borne the expense of the development of new and better types of aircraft engines.

In the development of aircraft engines for military purposes particular stress has been laid on the reduction in weight and the improvement of the safety factor. The engines thus developed are well suited for use in commercial aviation. Light weight and a maximum of safety are most important aids in the economic success of commercial aviation. The one insures profitable loads and the other certainty of operation.

Several years ago the Navy Department decided to concentrate its efforts on the development of an air-cooled engine. As a result of this decision we now have an air-cooled engine combining light weight with extreme dependability and ruggedness.

Air-cooled engines which have been tested and have proved their value are now available in three powers, 200, 400, and 500 horsepower. The 200-horsepower Wright "Whirlwind" engine, which has been used on all the transoceanic flights from the United States, is now widely used in commercial activities throughout the country and has been one of the most important, if not the most important, contributing factor in the development of efficient, dependable, and comparatively moderate-priced commercial and privately owned aircraft.

The larger 400-horsepower radial air-cooled engine was designed for military purposes and is now finding its way in the commercially owned and operated aircraft, notably in the Chicago to the west coast air mail-service.

The still larger 500-horsepower radial air-cooled engine is now taking its place in flight service in the Navy and will be available for commercial purposes in the near future.

During the past year there has been a notable increase in the development by private capital of air-cooled engines especially adapted to commercial service. Several engines of 80 to 150 horsepower are under development. The Fairchild "Caminez" engine has passed the development stage and is now on the market.

These engines are being purchased for operation in commercial airplanes, notwithstanding the fact that there still remain a considerable number of war-time engines which may be purchased for a nominal sum. This is a most encouraging indication of the healthy condition of the commercial aircraft industry, as it shows that the industry has reached the stage where

private capital is building on its own initiative special types of airplanes and airplane engines without financial assistance from governmental agencies.

Further developments are being made, with the assistance of the Government, to decrease the weight per horsepower and increase the dependability and efficiency of aircraft engines. Higher compression ratios and improved fuels are being used with success in military service operation.

In the field of water-cooled aircraft engines no new types have been developed during the past year. Proved engines of from 200 to 800 horsepower are available and have been further developed by the addition of reduction gears and refinements permitting operation at high speeds. A number of engines of the water-cooled type are now designed so as to operate over long periods at speeds up to 3,000 revolutions per minute.

The past year has seen the beginning of the general service use of the supercharger, and it may now be said that the supercharger for aircraft engines has passed definitely out of the research stage and is in the engineering production stage. The development of light-weight and dependable reduction gears for propellers is progressing satisfactorily and they will no doubt be in extensive use on military types of aircraft engines in the near future. Following the supercharger, special engine fuels and reduction gears will no doubt be adapted to commercial purposes when they have shown their value in military types of aircraft.

SUMMARY

The year 1927 was notable in demonstrating the capabilities of aircraft. The transoceanic flights of Lindbergh and others led to the awakening of the American people to the possibilities of aviation and to the need for airports. Industrial capital was invested in aeronautical enterprises. The essential activities of the Department of Commerce in establishing airways and in regulating and encouraging commercial aviation were factors in this development. The success of the Army and Navy in developing and standardizing military types facilitated the procurement of aircraft and this, with the Government's support of the five-year aircraft programs for the two services, had a stabilizing effect on the industry. The Government provided air-mail service to the people and encouraged commercial air lines by making air-mail contracts with private carriers. Generally speaking, contract air-mail lines were operated on a sound economic basis.

The most significant characteristic of American aviation is the increase in the number of privately owned airplanes and the increase in the number of commercial flying enterprises which are operated without the cash subsidies that support commercial aviation in other countries.

The record of progress in the development of aeronautics for all purposes is the result of the coordinated effort of all interested, including the Congress, the Executive, the Army and Navy, the industry, the Daniel Guggenheim Fund for the Promotion of Aeronautics, educational institutions, the Weather Bureau, the Bureau of Standards, and the National Advisory Committee for Aeronautics. There is a splendid spirit of cooperation in scientific and technical matters in American aeronautics under the active leadership of the National Advisory Committee. The committee is continuing its scientific researches on the fundamental problems of flight and is distributing scientific and technical data resulting from its investigations and from investigations conducted in other countries. In this way the committee is marshalling the maximum effort of the Nation in the study of the basic problems of aeronautics. The year's record of substantial progress along rational lines is largely the result of the Government's sound aeronautic policy.

It is difficult adequately to draw a word picture of the effect that aeronautics is destined to have on the economic life of the Nation. Progress is being made steadily in the solution of the basic problems of greater safety and of reduction of cost. Where the radius of the average daily social life was once generally limited by walking distances, it has been successively increased by the horse, the street car, the railroad, and the automobile. In America the airplane is destined to play an important part in further enlarging this radius, and in creating new demands and new standards of life which it is hoped will lead to the development of a greater and a happier country.

CONCLUSION

It is with pleasure that the committee reports that aeronautical progress in the United States during the past year has surpassed the hopes of a year ago. This is particularly true with reference to the operation of aircraft for the transportation of mail and express on regular schedules; the increase in the private ownership and operation of aircraft; the establishment and equipment of airways; and the development of types of aircraft by the Army and Navy for military and naval purposes. It is our conviction that the present governmental policy in aeronautics is sound in principle and is primarily responsible for the progress that is being made. But the most striking evidence of the year's progress is that aviation is being accepted by the people as a means of transportation and as a business in which industrial capital is being invested.

It must be noted that further substantial progress is dependent largely upon the continuous prosecution of scientific research. The committee, therefore, recognizing its responsibility in this respect, recommends a continuation of the liberal support of its work in the fields of pure and applied research on the fundamental problems of flight.

Respectfully submitted.

NATIONAL ADVISORY COMMITTEE FOR AERONAUTICS,
JOSEPH S. AMES, *Chairman*.

REPORT No. 257

**PRESSURE DISTRIBUTION
OVER A WING AND TAIL RIB OF A VE-7 AND
OF A TS AIRPLANE IN FLIGHT**

**By J. W. CROWLEY, Jr.
Langley Memorial Aeronautical Laboratory**

REPORT No. 257

PRESSURE DISTRIBUTION OVER A WING AND TAIL RIB OF A VE-7 AND OF A TS AIRPLANE IN FLIGHT

By J. W. CROWLEY, Jr.

SUMMARY

This investigation was made by the National Advisory Committee for Aeronautics at Langley Field, to determine the pressure distribution over a rib of the wing and over a rib of the horizontal tail surface of an airplane in flight and to obtain information as to the time correlation of the loads occurring on these ribs. Two airplanes, VE-7 and TS, were selected in order to obtain the information for a thin and a thick wing section. In each case the pressure distribution was recorded for the full range of angle of attack in level flight and throughout violent maneuvers. Particular attention was given to the high and low angle of attack conditions. The results show: (a) That the present rib load specifications in use by the Army Air Corps and the Bureau of Aeronautics, Navy Department, are in fair agreement with the loads actually occurring in flight, but could be slightly improved; (b) that there appears to be no definite sequence in which wing and tail surface ribs reach their respective maximum loads in different maneuvers; (c) that in accelerated flight, at air speeds less than or equal to 60 per cent of the maximum speed, the accelerations measured agree very closely with the theoretically possible maximum accelerations. In maneuvers at higher air speeds the observed accelerations were smaller than those theoretically possible.

INTRODUCTION

The subject of load distribution on an airplane in accelerated flight is of the utmost importance for design purposes and is particularly so at the present time inasmuch as the high speeds and large accelerations occurring with the present airplanes make it advisable to improve the loading specifications and computation methods. Considerable work has been done previously on the subject of pressure distribution, but the knowledge of the loads in accelerated flight is still very incomplete. Wind tunnel tests have been devoted to steady flight conditions, and the previous flight work, while including both accelerated and steady flight, has not been extensive enough. In order to improve the present loading requirements, considerable additional investigation is necessary.

The present investigation was conducted primarily to determine the rib loads of the wing and of the horizontal tail surface in level and accelerated flight and the time correlation of these loads. It actually consisted of two series of tests—first, on the VE-7 training airplane with R. A. F. 15 wings and, secondly, on the TS fighter with U. S. A. 27 wings, neither airplane being in any way changed so as to affect the performance characteristics. On each airplane the pressure distribution over a rib of the upper wing and over a rib of the horizontal stabilizer and elevator was measured. Certain peculiarities, especially in the *C. P.* location, which was found in the first series of tests (VE-7 airplane) made it desirable on the second series (TS airplane) to investigate a rib of the lower wing also. The ribs chosen were located as far as possible from the slip stream and from the aileron, and where an upper and lower wing rib was investigated they were located in the same vertical plane. The tail surface rib locations were also chosen with the idea of keeping as far as possible from the fuselage and from the tip and at the same time maintaining a chord of somewhat near the average chord of the tail surface.

Since only single ribs in the span of the wing and tail surface were investigated, too close an application of the results must be avoided. It is quite probable that the load along the span varies considerably, particularly in the slip stream and at the ailerons, so that it is entirely possible that the loads on the ribs investigated were exceeded by those at other portions of the span. From the standpoint then of obtaining the maximum rib loads the results should be considered as indicative rather than conclusive.

A very important characteristic of this investigation is the determination of the time at which each load occurs and the resulting time correlation of the tail and wing loads. This, together with the knowledge of the variation of pressure distribution, air speed, and acceleration with time, is an important factor not only from the strength analysis standpoint, but also for the data they provide for the analysis of airplane maneuvers, and for the check of air flow theories applicable to accelerated flight.

METHOD AND APPARATUS

The pressures were measured at the points indicated in Figure 1 by means of orifices of the type shown in Figure 2, which were connected by three-sixteenth-inch diameter tubing to an N. A. C. A. multiple recording manometer (Reference 1). On the VE-7 the manometer was mounted in the front cockpit, and on the TS in approximately the same location under

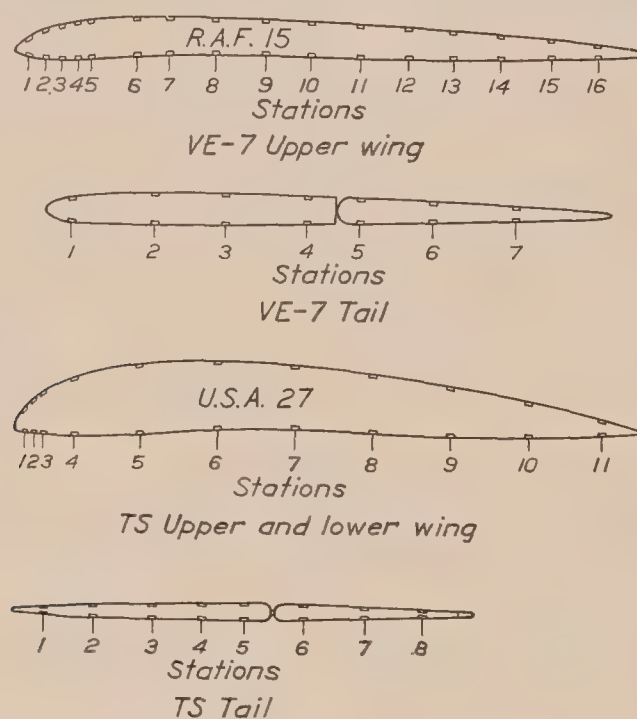


FIG. 1.—Location of orifices in ribs of VE-7 and TS airplanes

Station	VE-7 airplane				TS airplane			
	Wing		Tail		Wing		Tail	
	Inches from L. E.	Per cent chord	Inches from L. E.	Per cent chord	Inches from L. E.	Per cent chord	Inches from L. E.	Per cent chord
1.....	1.38	2.49	2.56	5.12	1.00	1.75	2.80	6.75
2.....	2.75	4.95	9.81	19.65	1.75	3.07	7.50	18.10
3.....	4.13	7.44	16.00	32.10	2.63	4.60	12.85	31.00
4.....	5.50	9.92	23.31	46.70	5.50	9.65	17.30	41.60
5.....	6.88	12.40	27.81	55.80	11.50	20.20	21.20	51.00
6.....	11.00	19.80	34.56	69.30	18.50	32.50	26.51	64.00
7.....	13.75	24.80	41.75	83.80	25.50	44.80	32.11	77.30
8.....	17.94	32.40	49.87	100.00	32.50	57.00	37.21	89.50
9.....	22.13	39.90			39.50	69.30	41.50	100.00
10.....	26.31	47.40			46.50	81.60		
11.....	30.50	55.00			53.00	93.00		
12.....	34.69	62.50			57.00	100.00		
13.....	38.88	70.00						
14.....	43.06	77.70						
15.....	47.25	85.20						
16.....	51.44	92.90						
Chord...	55.50	100.00						

the front cowling. At each station the orifices were attached directly opposite each other on the top and bottom of the rib and each pair was connected to the opposite sides of the same manometer capsule. The readings thus obtained on each capsule represent the resultant pressure normal to the chord line at a station, no attempt being made to record the pressures on the upper and lower surfaces separately. To avoid any permanent mutilation of the airplanes, false ribs with special cap strips (fig. 2) were used to which the orifices were attached. These false ribs were inserted at the positions shown in Figures 3 and 4. The orifices were installed so as to present a perfectly smooth surface, and the entire system was checked for possible leaks at frequent intervals throughout the tests. Figures 5, 6, and 7 are photographs of the orifice installation.

Besides the manometer, the following N. A. C. A. standard instruments were used on all the tests: Single component accelerometer (Reference 2); recording air-speed meter (Reference 3); recording yaw meter (Reference 4); and an electric contact making chronometer (Reference 5).

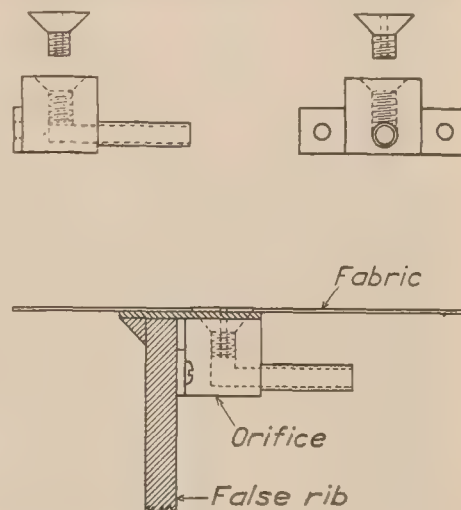


FIG. 2.—Type of orifice used and method of attachment

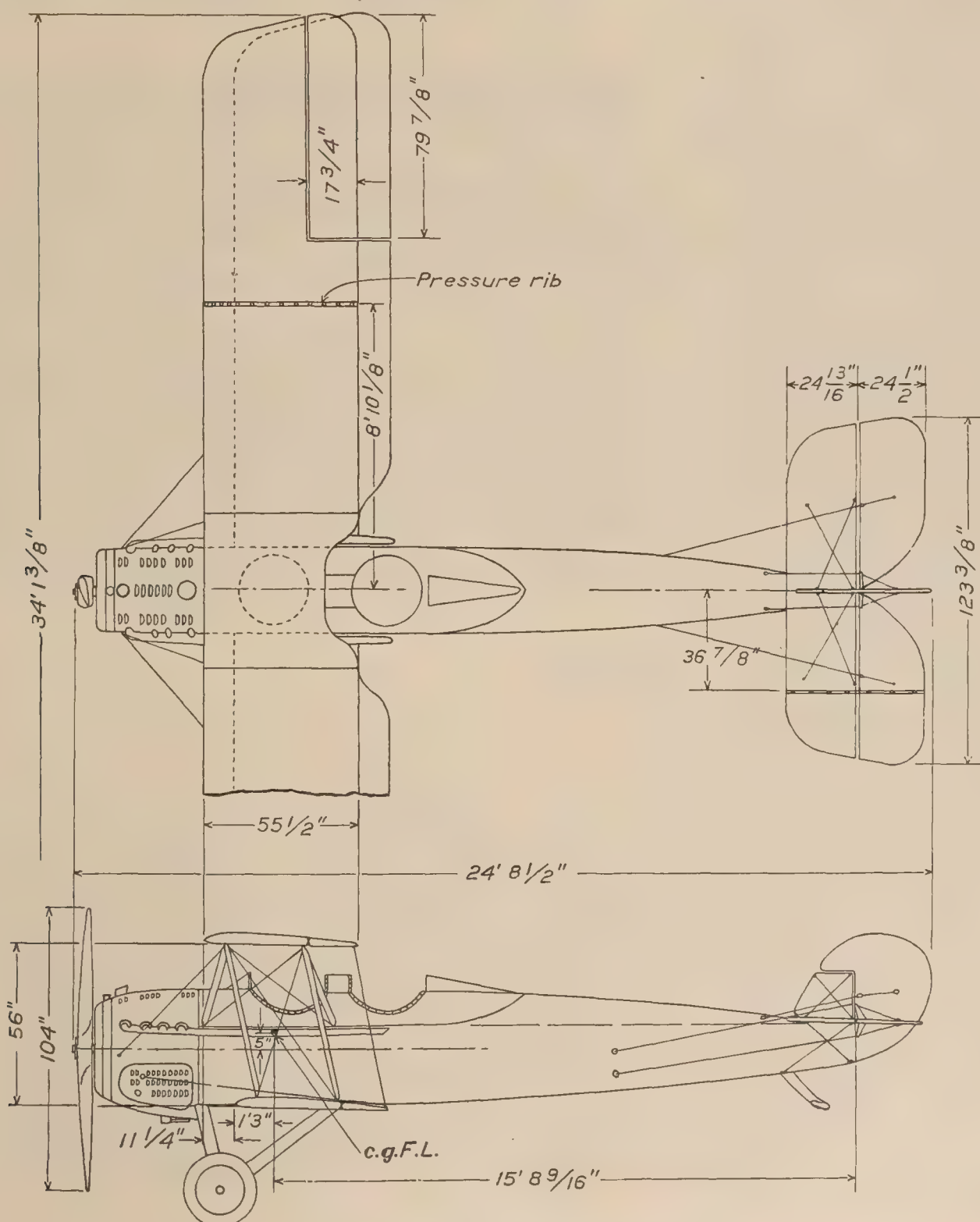


FIG. 3.—VE-7 airplane, showing location of false ribs

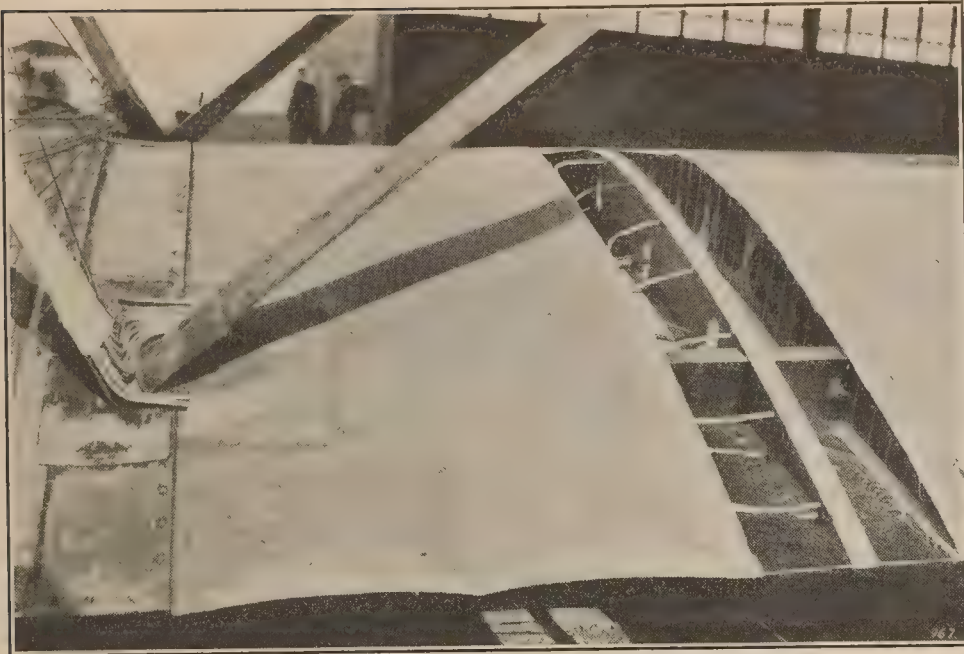


FIG. 5.—View showing orifice installation in wing

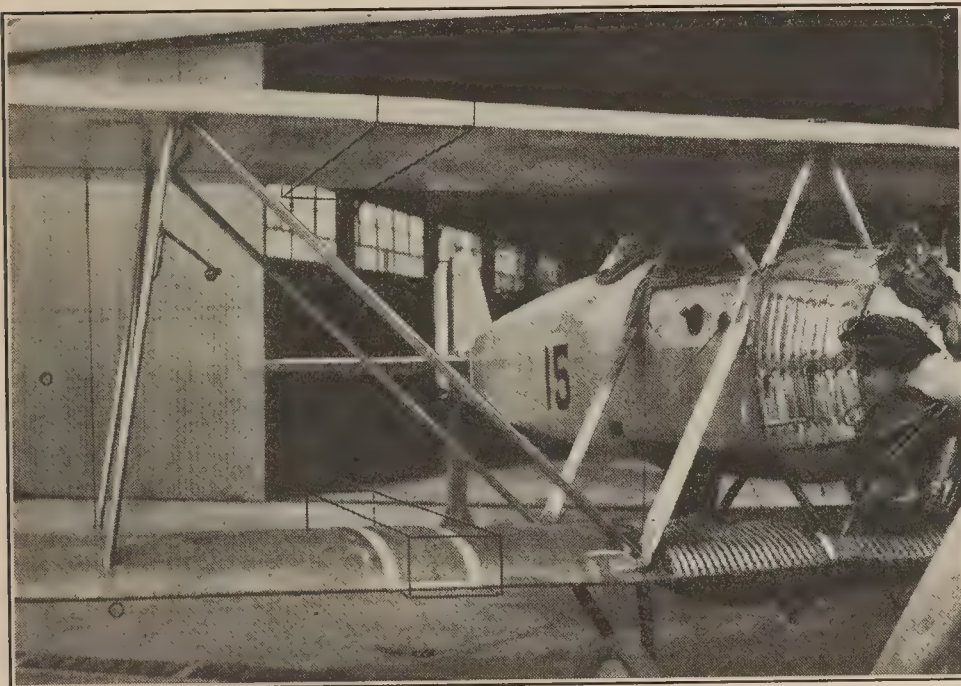


FIG. 6.—View showing finished orifice installation in wing

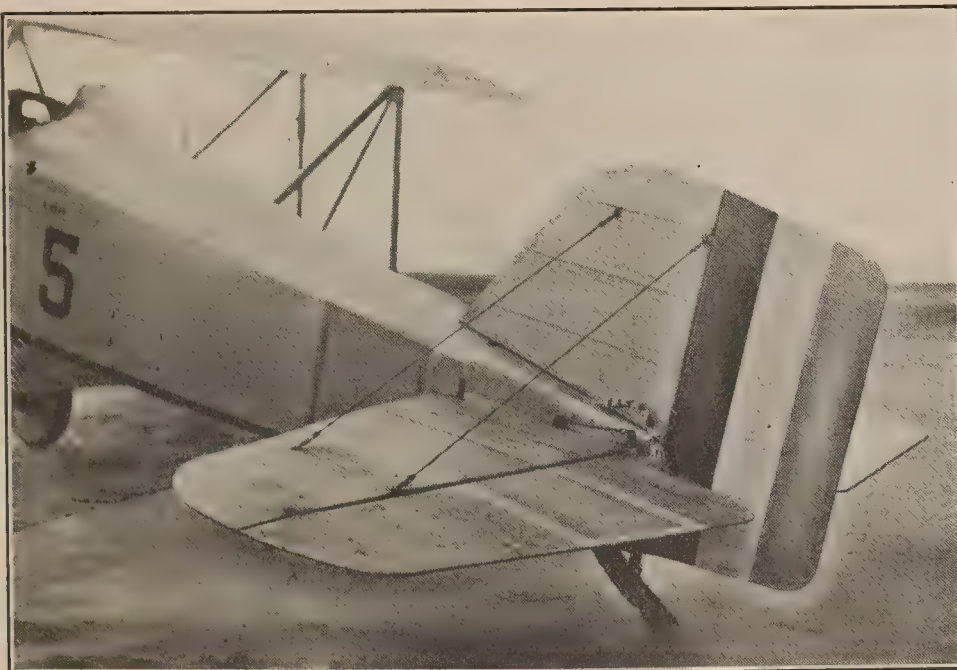


FIG. 7.—View showing finished orifice installation in tail surfaces of the TS-7 airplane



FIG. 8.—Multiple manometer record. Pressure distribution test on TS airplane

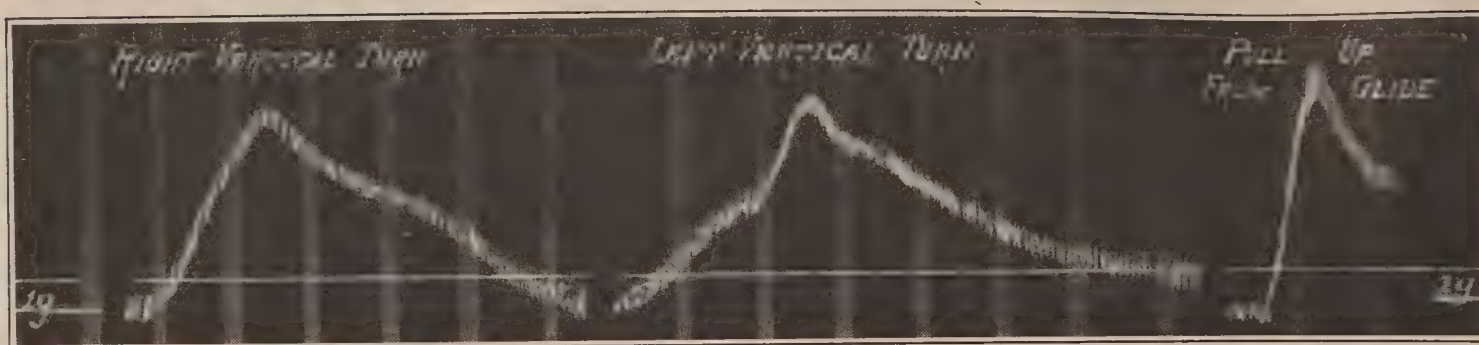


FIG. 9.—Accelerometer record. Pressure distribution test on TS airplane

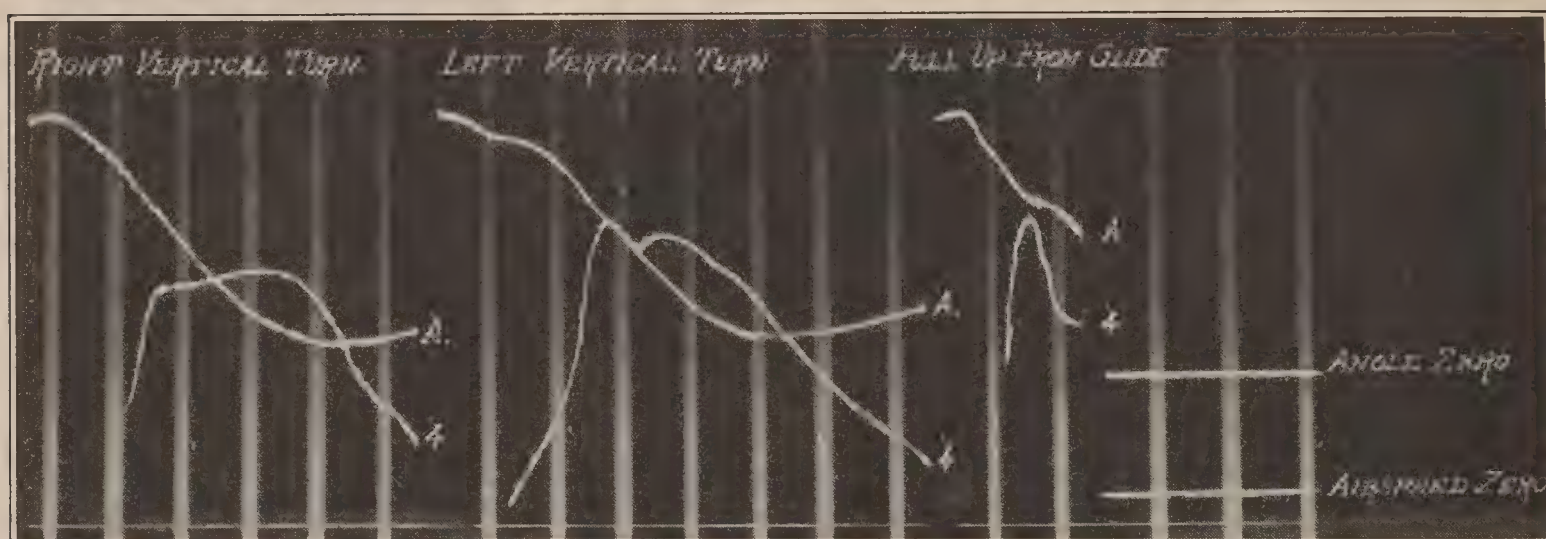


FIG. 10.—Air speed and angle of attack record. Pressure distribution test on TS airplane

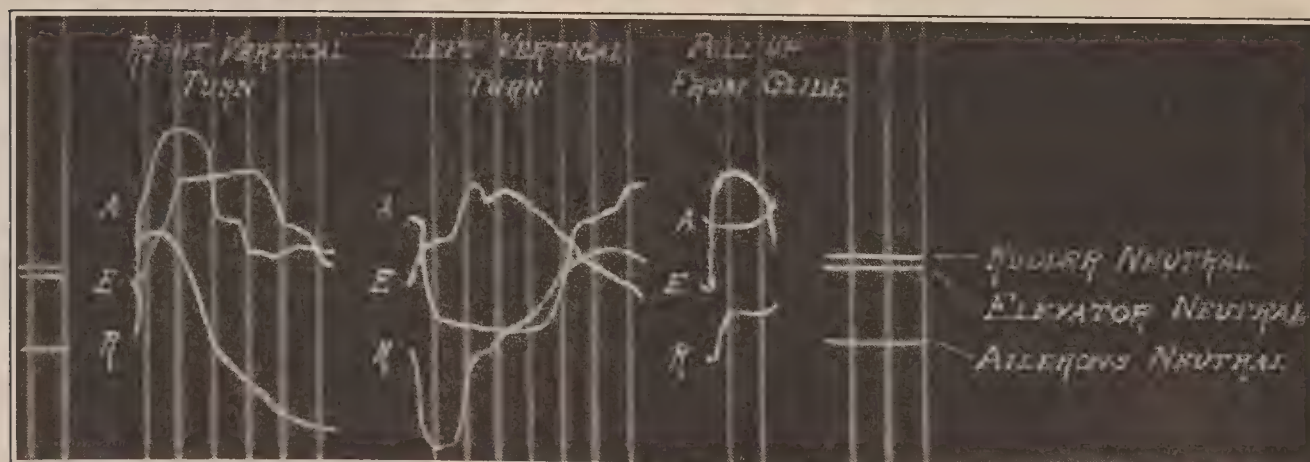


FIG. 11.—Control position record. Pressure distribution test on TS airplane

records were read at short-time intervals for each entire run, the proper synchronization of different records being obtained by means of the timing lines. These data were tabulated and the recorded normal pressures on the wing rib were plotted on the chord line, similar to those shown in Figures 13a to 13f.

The instantaneous load curves were planimeted, and from this the rib loads, centers of pressure, moments about the leading edge, and normal force coefficients were determined. The normal force coefficient is the coefficient of lift perpendicular to the chord line, and is obtained from the expression:

$$C_{NF} = \frac{L}{\frac{1}{2} \rho V^2},$$

Where L is the specific load found by planimeting the various distribution curves, and $\frac{1}{2} \rho V^2$ the dynamic pressure measured by the Pitot-static head. The various quantities enumerated, together with some of the original data read from the photographic records, were plotted against time, thus forming a complete time-history of each maneuver investigated (fig. 13). The loads as plotted on the time-history curves are the average loads along the chord in lb./sq. ft. Wing and tail-plane moments are given in inch pounds per foot of span.

In plotting loads on the elevator, this surface is shown in a neutral position at all times, whereas in reality, it is at a varying angle. There is a slight error in the tail-moment curves on account of this angle of the resultant elevator force being disregarded.

PRECISION

The estimated precision of the measurements is as follows:

1. Air speed.....	± 1 M. P. H.
2. Acceleration.....	± 0.1 g
3. Control position.....	$\pm 0.5^\circ$
4. Time synchronization.....	± 0.1 second
5. Individual normal pressures.....	± 2 per cent

In estimating the precision of the pressure measurements it is assumed that the errors introduced by the orifice and the inherent instrument errors are negligible. This is very probably true because care was taken to install the orifices flush with the surface of the ribs and the manometer was calibrated at frequent intervals throughout the tests. The pressure loss in the tubing is also small. A recent series of laboratory and flight tests conducted at the Langley Memorial Aeronautical Laboratory on the pressure loss in transmitting air pressure through tubes (Reference 7) has provided the basis of the above estimate of precision of the pressures. In the case of the loads, centers of pressure, moments and normal force coefficients, which are determined from an integration of the normal pressures along the rib, there is a possibility of further error. However, since the different sources of error cancel each other partially it can be assumed that these are exact to ± 3 per cent.

The measurement of angle of attack in accelerated flight was unsuccessful. This was probably due to the change of air flow in such flights and also to the fact that the angle of attack varies over the whole chord and span to some extent in all maneuvers. For this reason the angle of attack has been included in only a few of the curves and, except in the level flights, it should be regarded as the general trend of the angle rather than a specific value to be used in any calculations or comparisons. In level flight the angle of attack is precise to $\pm 0.5^\circ$.

DISCUSSION OF RESULTS

The results of this investigation are given in Tables I and II and in Figures 12 to 37. Table I contains the pressure measured at each station for each increment of air speed in level flight and for each interval of time in all the maneuvers. In Table II are given, for both the wing and tail surface, the load, normal force coefficient, and the center of pressure location or the moment about the leading edge (all of which are determined from an integration of the pressures along the rib) together with the air speed, acceleration, and control position. These values are also

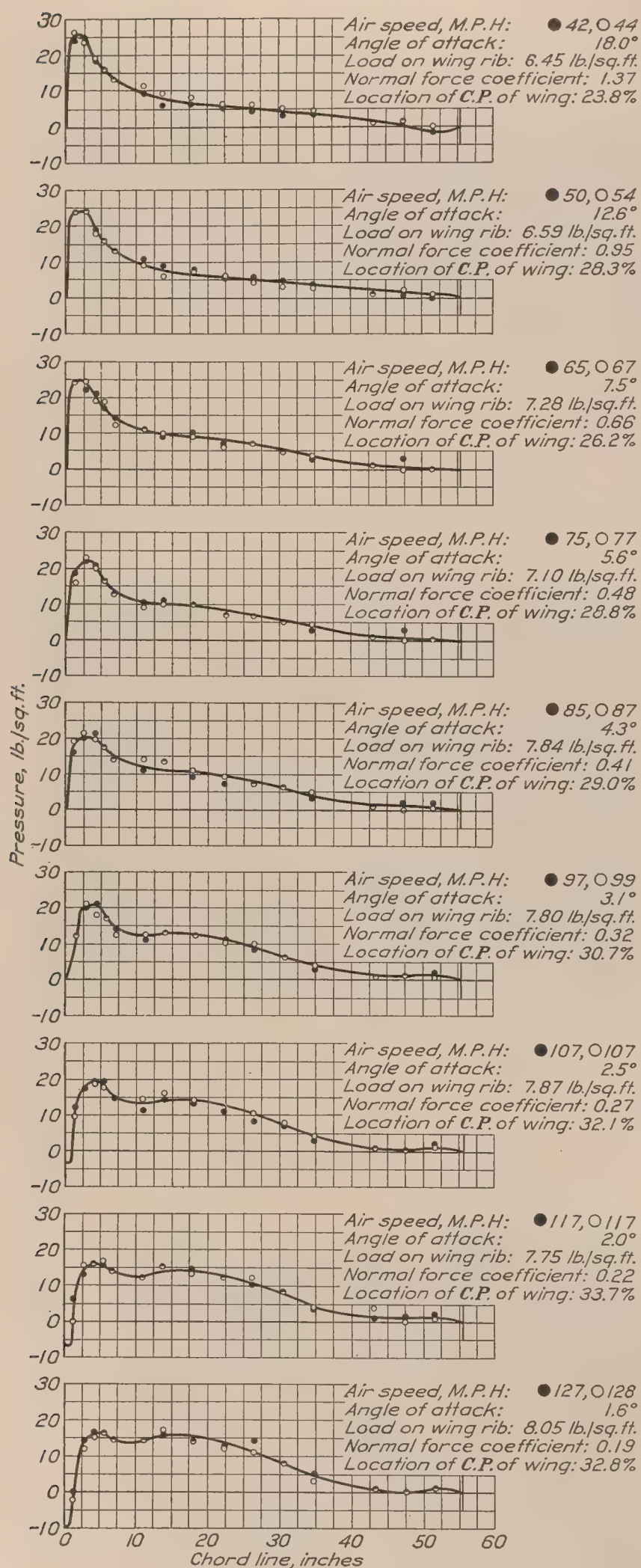


FIG. 12.—Pressure distribution on VE-7 airplane in level flight

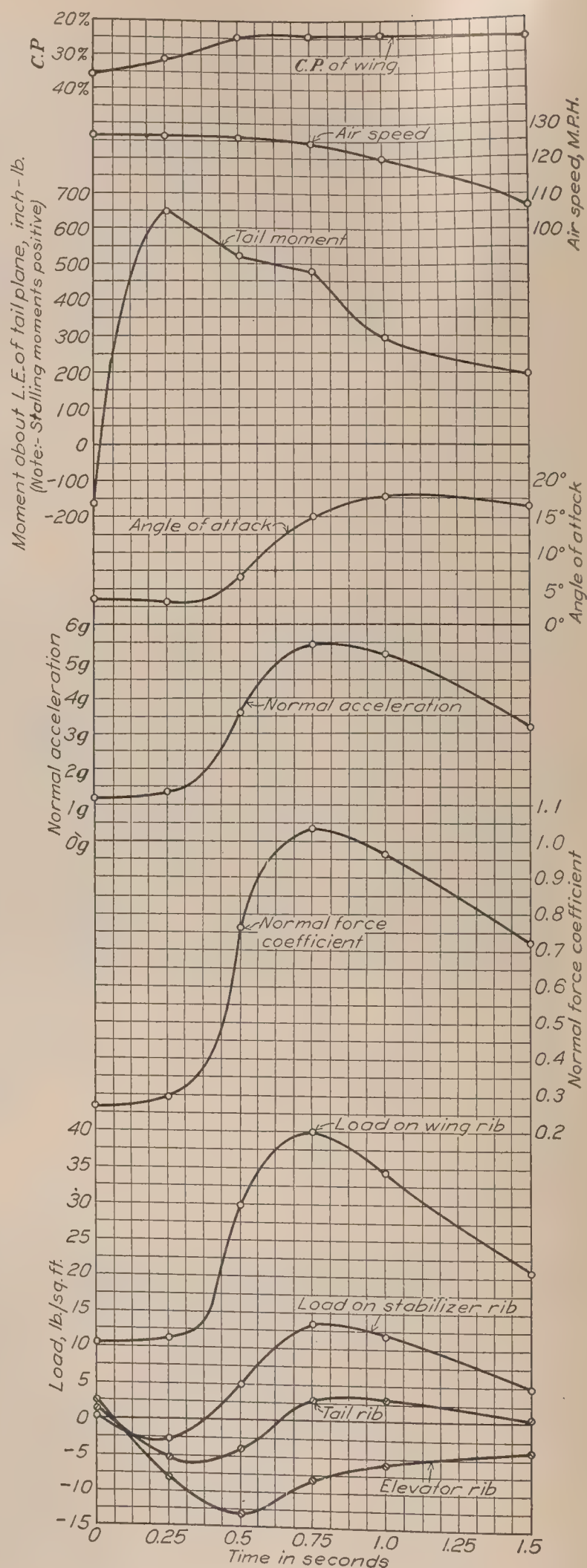


FIG. 13.—VE-7 airplane in a "pull-up" at 126 M. P. H.

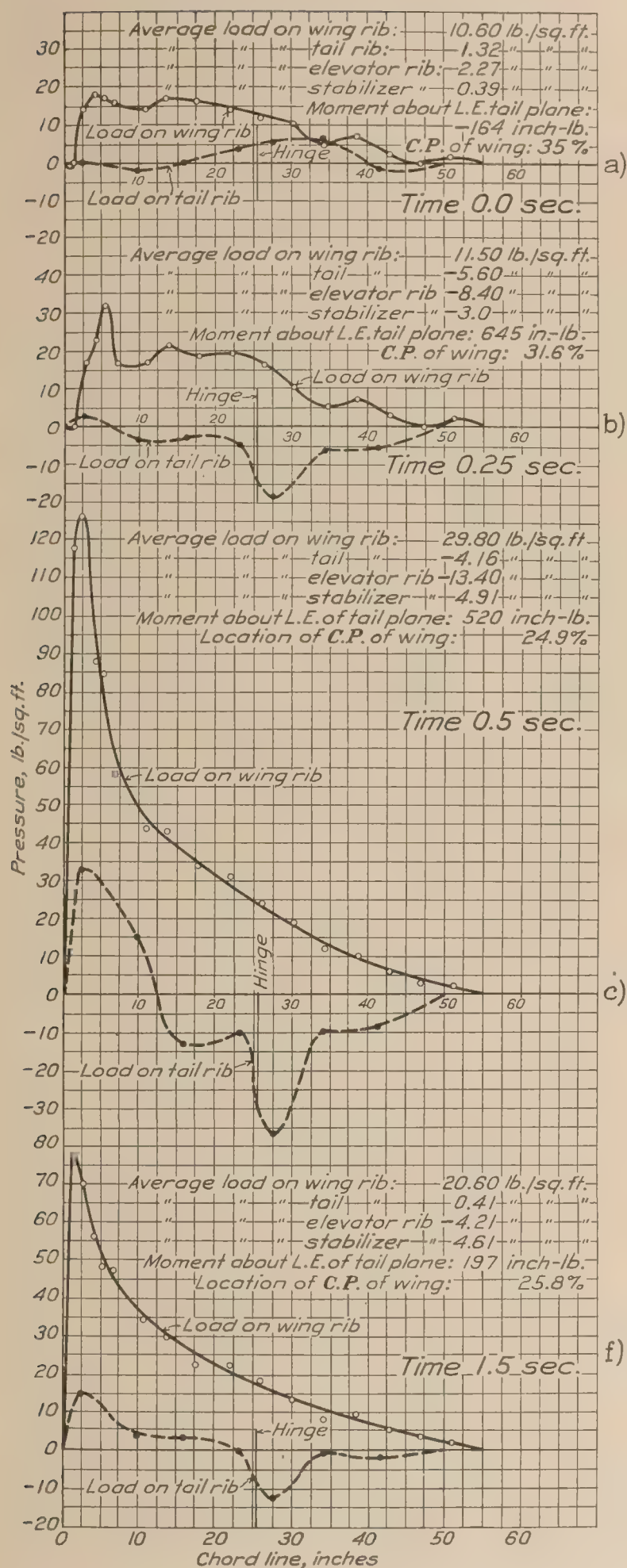


FIG. 13a, b, c, and f.—Pressure distribution on a VE-7 airplane in a "pull-up" at 126 M. P. H. for various intervals of time

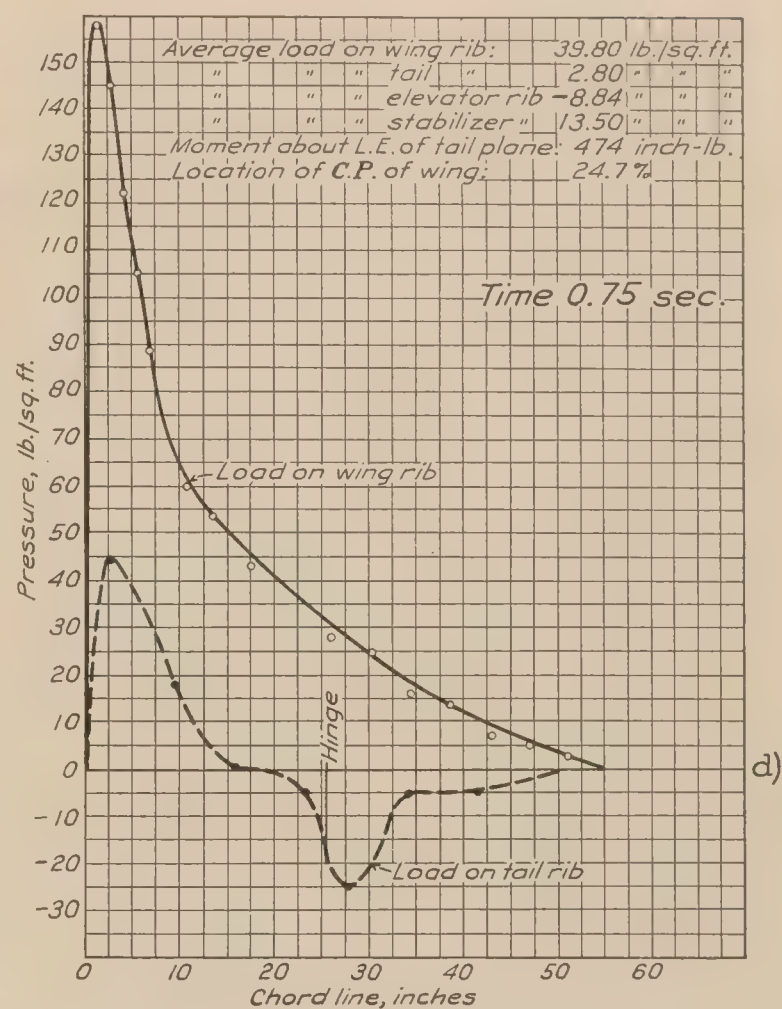


FIG. 13d.—Pressure distribution on VE-7 airplane in a "pull-up" at 126 M. P. H. for interval of 0.75 second

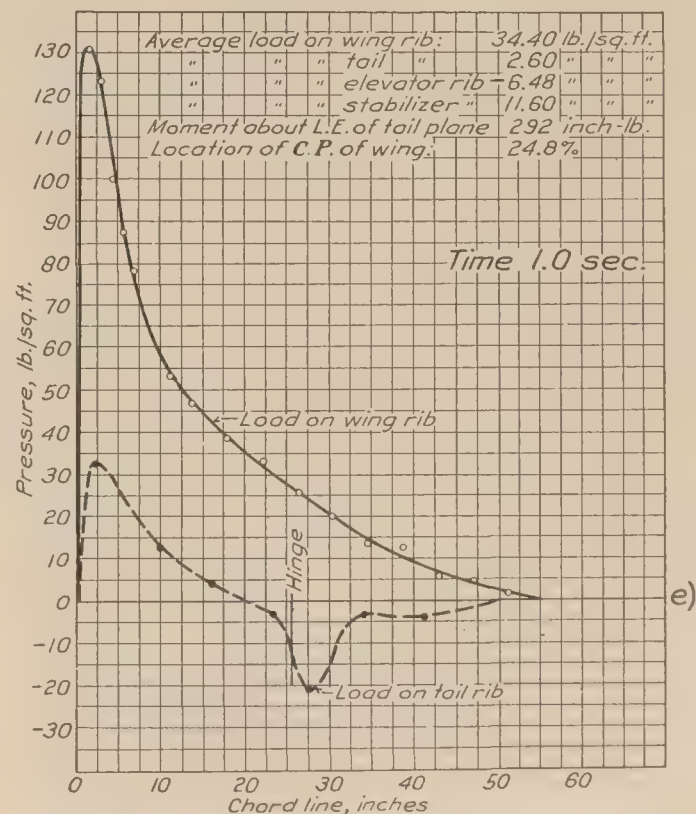


FIG. 13e.—Pressure distribution on VE-7 airplane in a "pull-up" at 126 M. P. H. for interval of 1.0 second

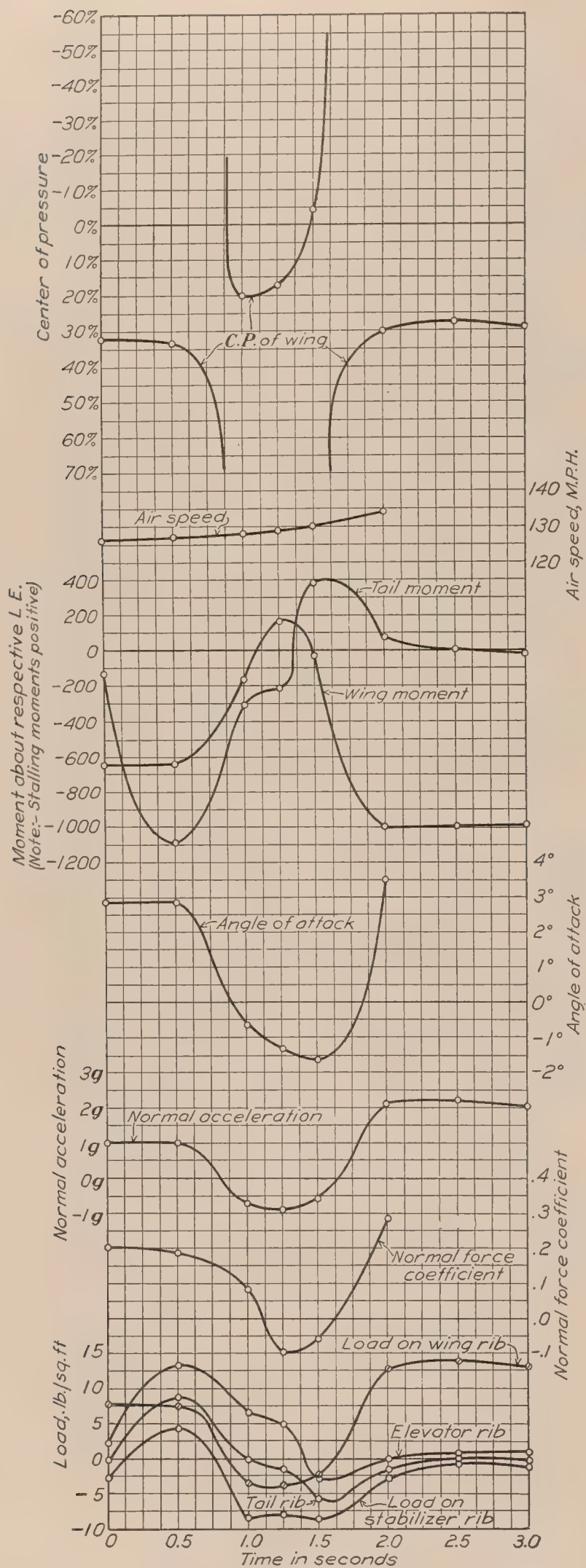


FIG. 14.—VE-7 airplane in a no lift condition (push-down) at high speed

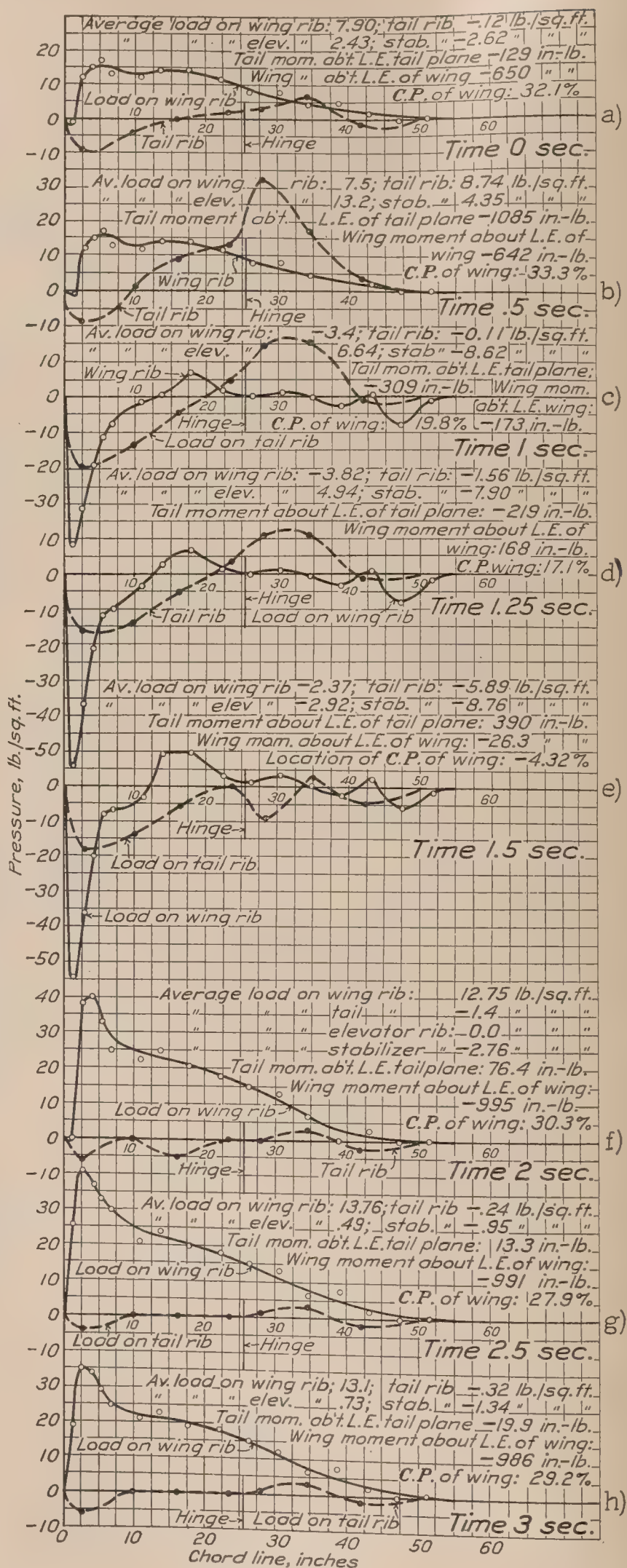


FIG. 14a, b, c, d, e, f, g, and h.—Pressure distribution on VE-7 airplane in a no lift condition at high speed for various intervals of time

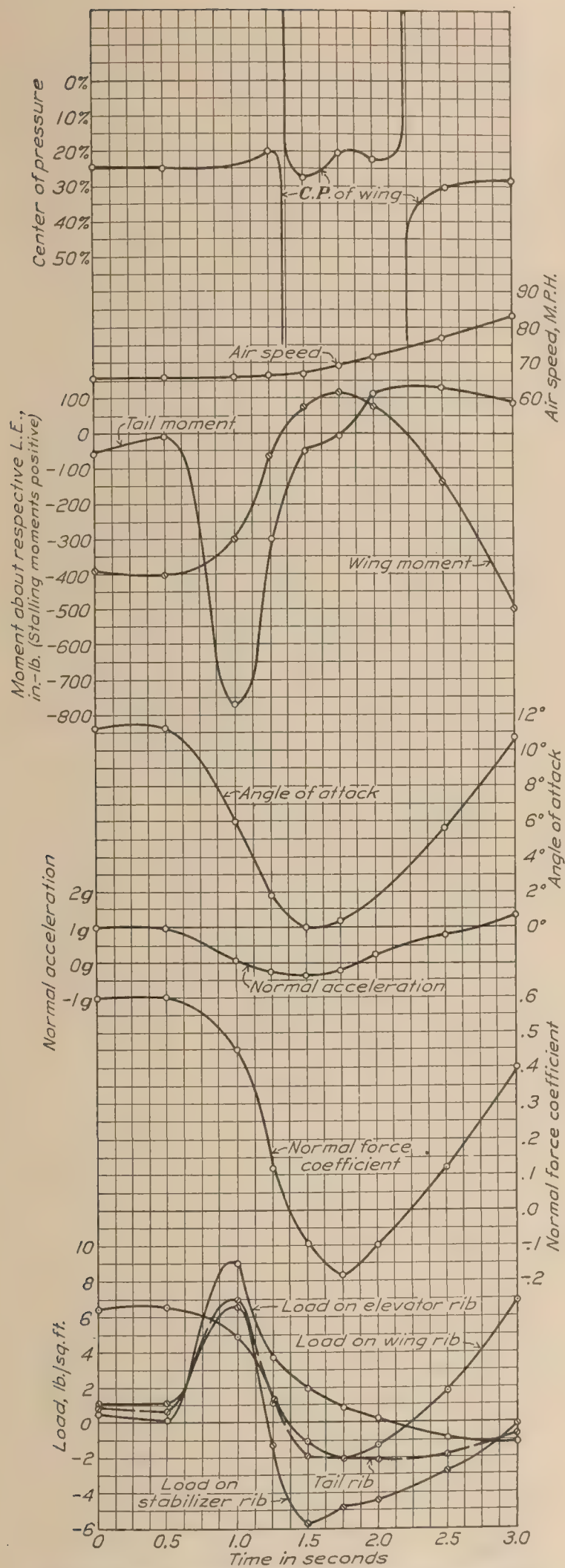


FIG. 15.—VE-7 airplane in a no lift condition (push-down) at low speed

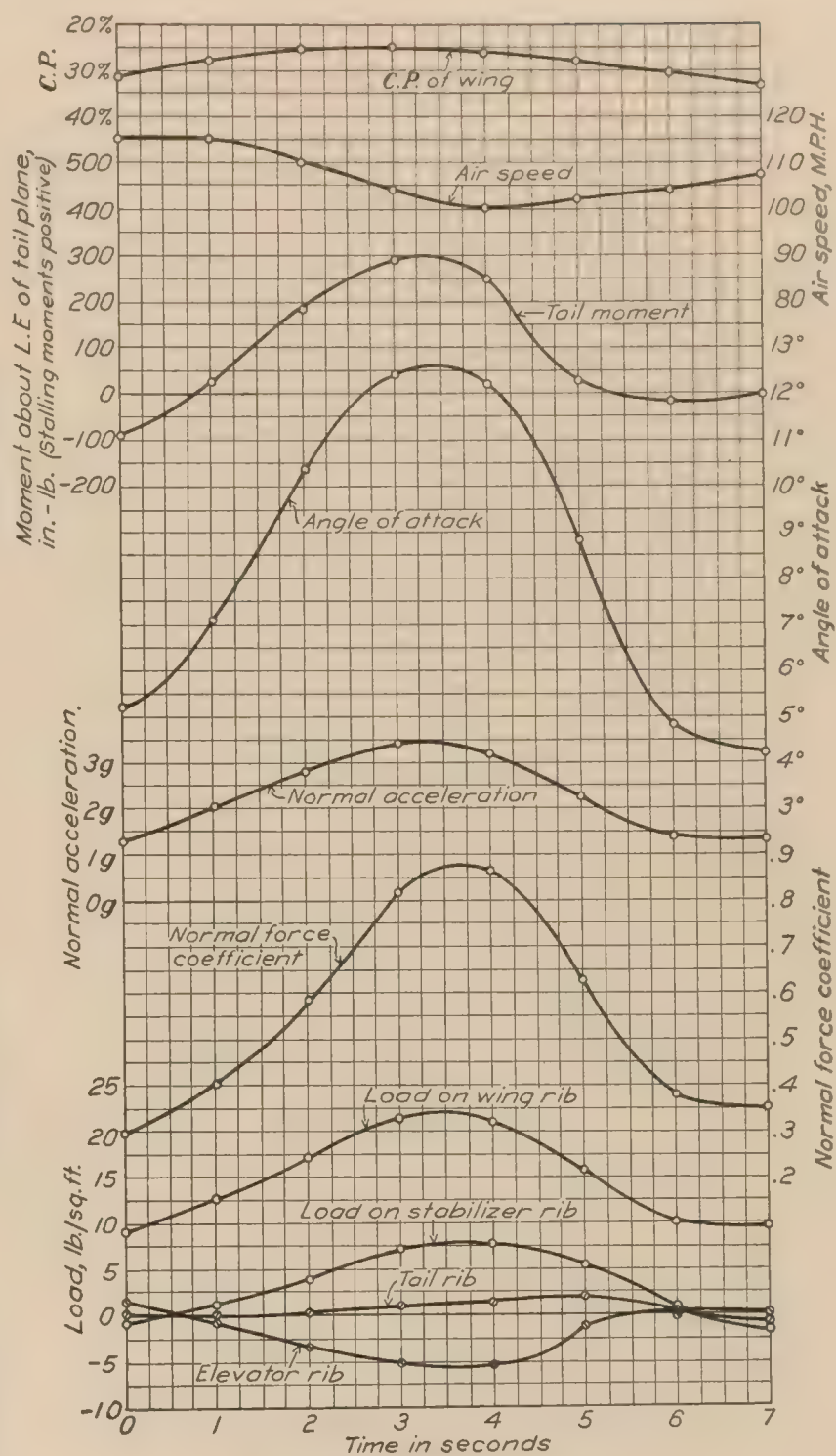


FIG. 16 —VE-7 airplane in a right turn

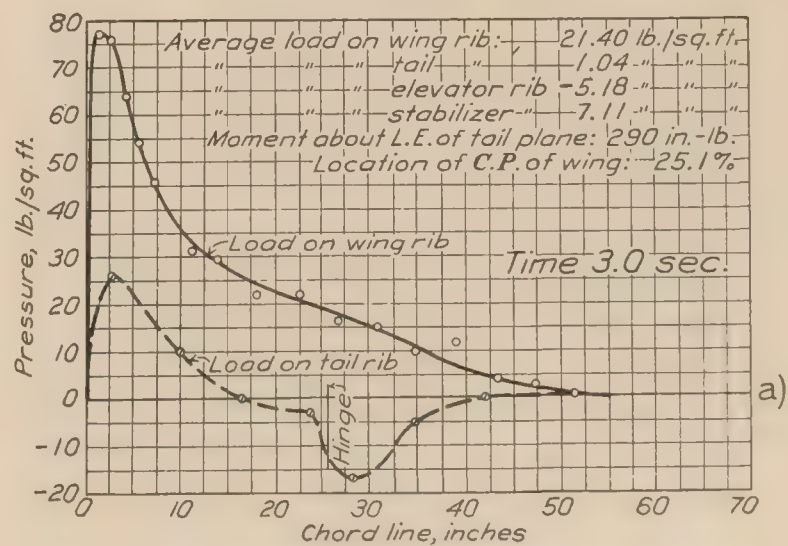


FIG. 16a.—Pressure distribution on VE-7 airplane in a right turn. Maximum wing loading

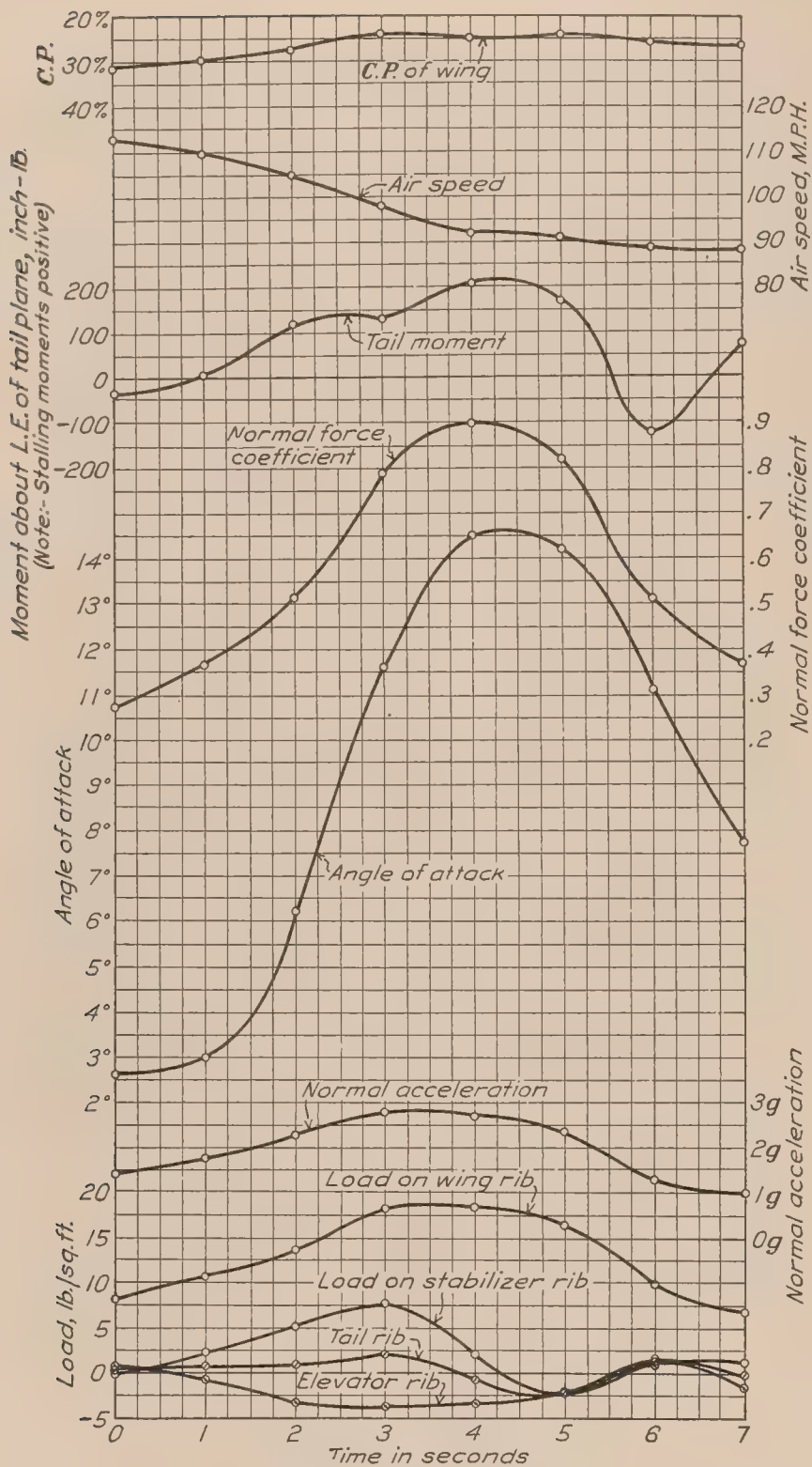


FIG. 17.—VE-7 airplane in a left turn

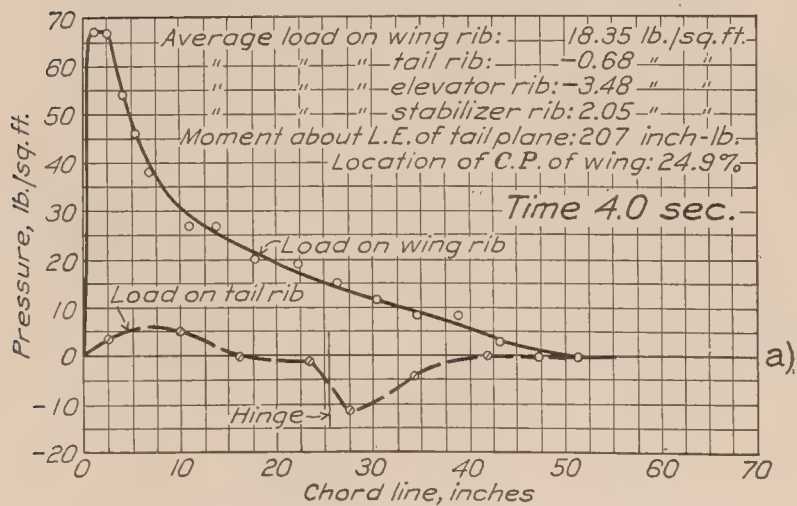
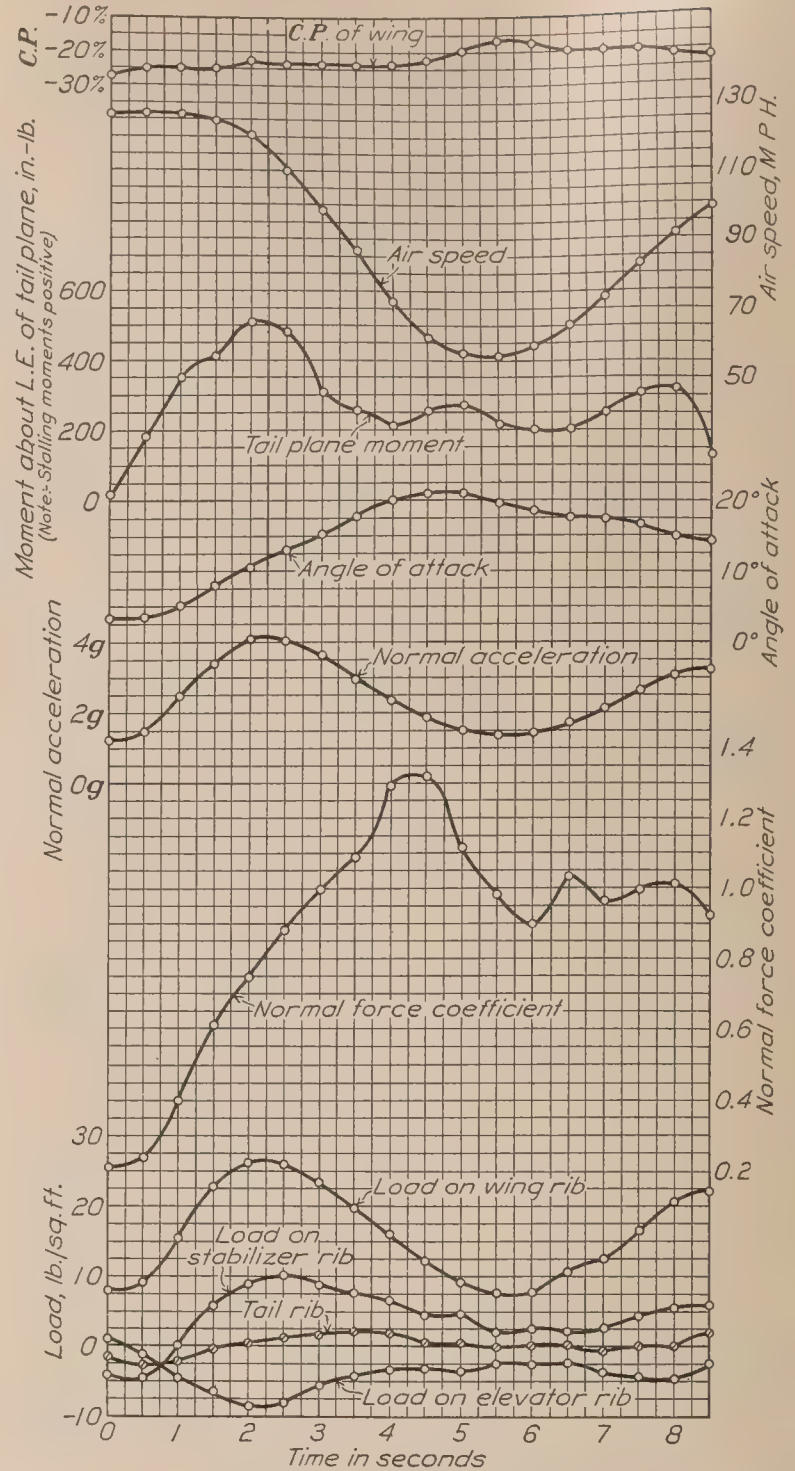
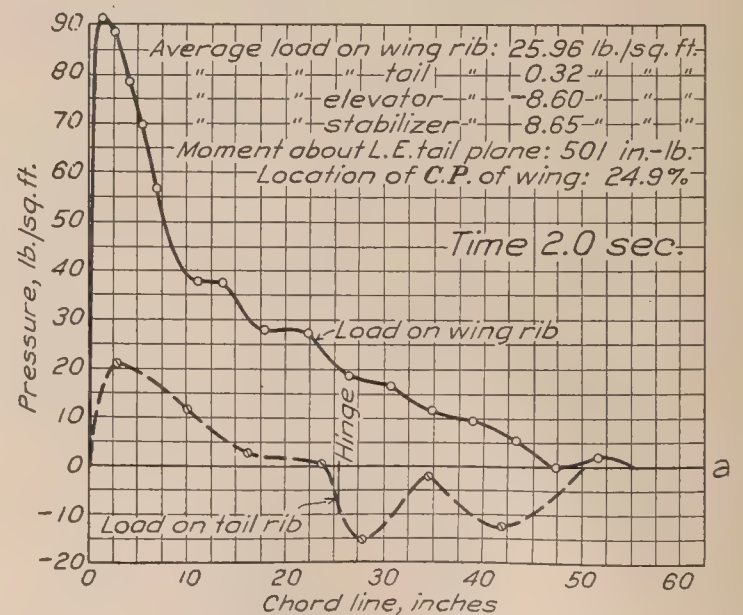
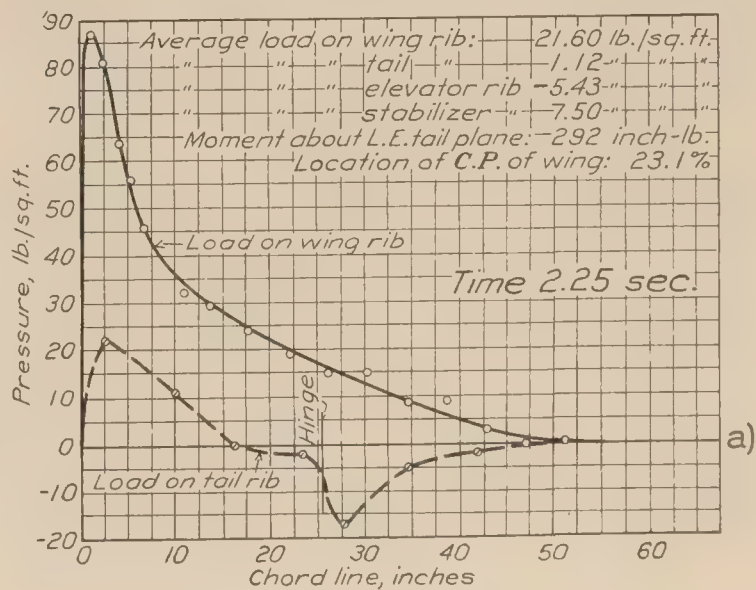
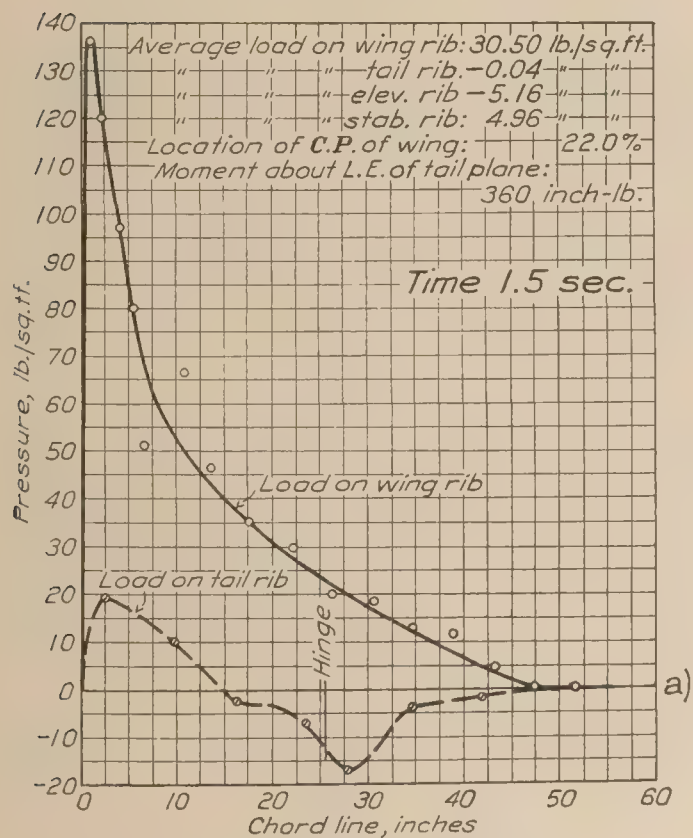
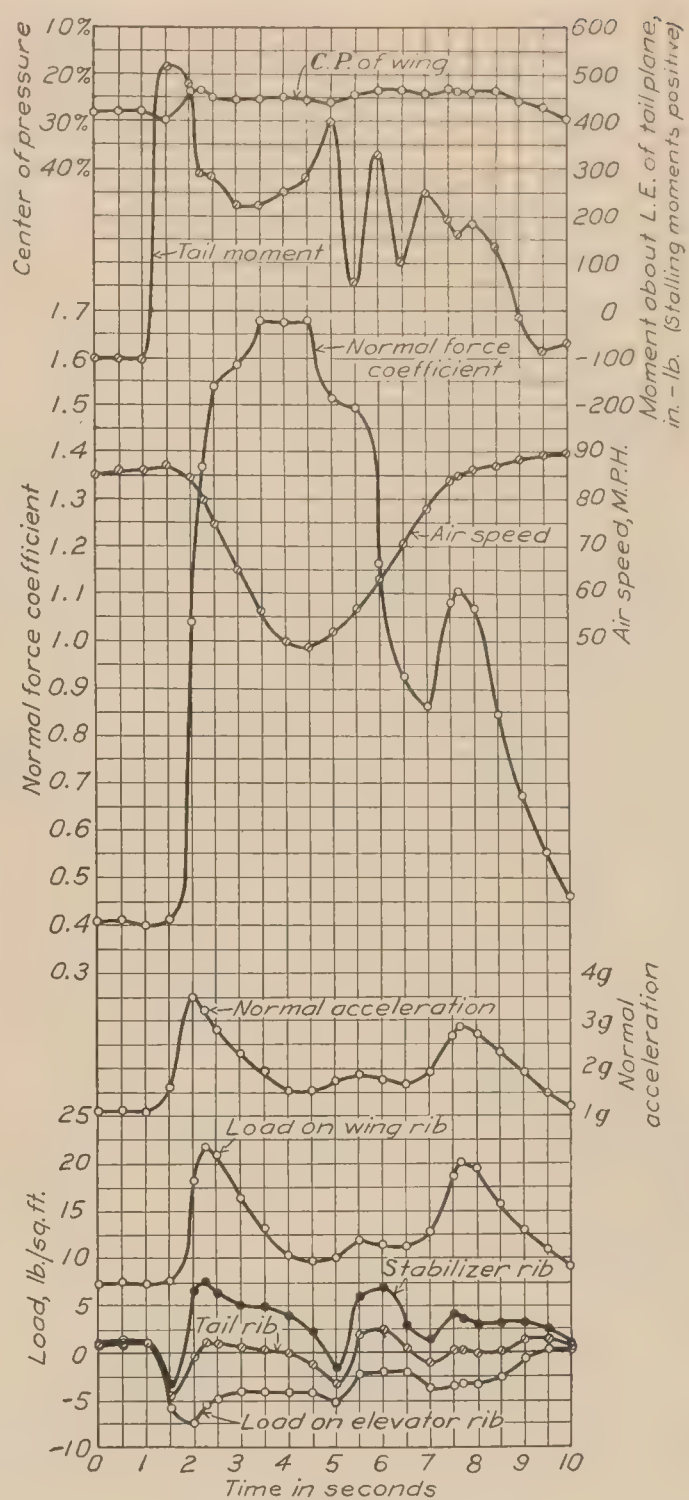
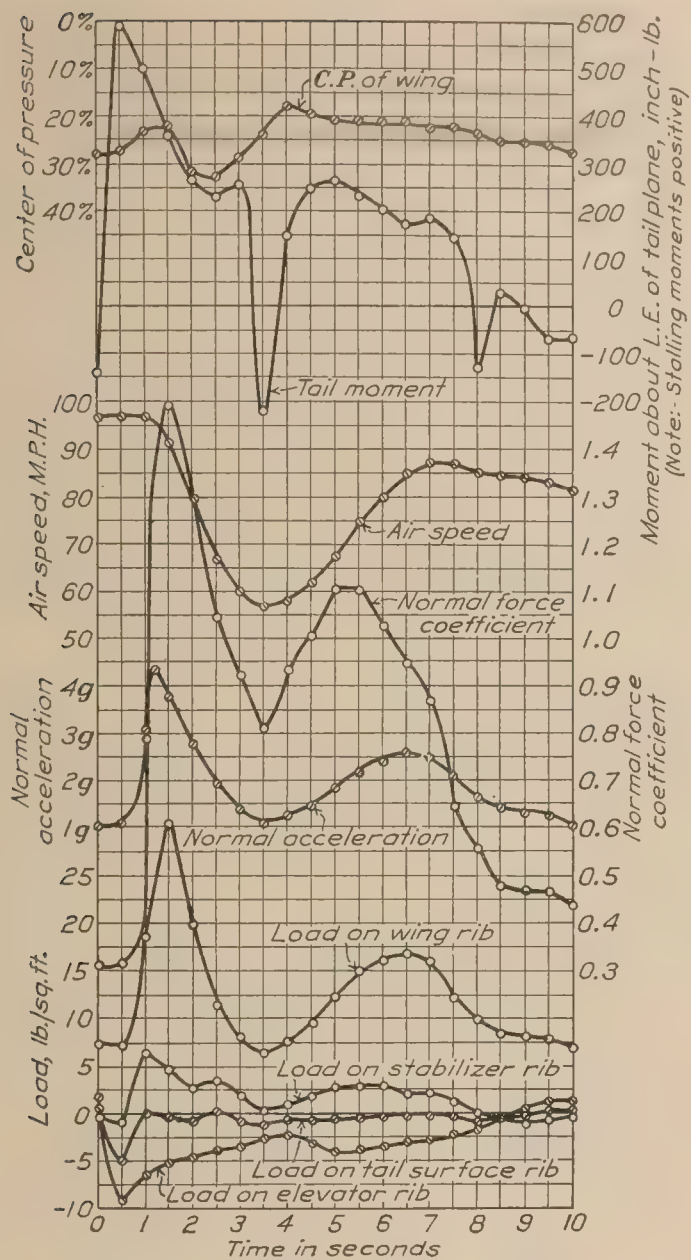
FIG. 17a.—Pressure distribution on VE-7 airplane in a left turn.
Maximum wing load

FIG. 18.—VE-7 airplane in a loop

FIG. 18a.—Pressure distribution on VE-7 airplane in a loop.
Maximum wing load



tabulated for each air-speed increment in level flight and each time interval of the maneuvers. In the past there has been some uncertainty concerning the moment acting on the wing when the *C. P.* approaches infinity. This has been remedied in this paper. In all such cases the moment has been determined in addition to the *C. P.* location. Three different kinds of curves showing the results are plotted: (a) Those showing the pressure distribution along the rib (figs. 12, 13a to 13f, etc.), which will be referred to hereinafter simply as pressure curves; (b) those representing a time history of the variables measured throughout a maneuver (figs. 13, 14, etc.); and (c) those showing a comparison of the loads obtained in flight with those specified for static load tests by the Army Air Corps and the Bureau of Aeronautics, Navy Department (figs. 29 to 36). There were a large number of pressure curves plotted to obtain the information necessary for the time histories, but only those of special interest are given in this report. The pressure curves for the pull-ups and push-downs are included complete, as these maneuvers give rise to the maximum loadings for the high and low angle of attack conditions, respectively, and these curves are also examples of the typical stages through which the rib loading builds up. For the other maneuvers only the pressure curve showing the largest load in each maneuver has been inserted.

In addition to the above, a curve is given showing the theoretical accelerations compared to those actually obtained (fig. 37).

Since the tables are rather extensive, another table has been added summing up the maximum average loads, maximum resultant pressures, and maximum normal force coefficients encountered, as follows:

TABLE III

	Maximum average positive load	Maximum average negative load	Maximum positive resultant pressure	Maximum negative resultant pressure	Maximum <i>C_{NF}</i>
VE-7 airplane:	<i>Lb./sq. ft.</i>	<i>Lb./sq. ft.</i>	<i>Lb./sq. ft.</i>	<i>Lb./sq. ft.</i>	
Wing rib.....	39.8	-3.8	158	-54	1.679
Tail rib.....	8.7	-5.9	44	-37	
Elevator rib.....	13.2	-13.4	32	-37	
Stabilizer rib.....	13.5	-8.8	44	-20	
TS airplane:					
Upper wing rib.....	52.3		164	-96.0	1.853
Lower wing rib.....	38.2		100	-129.5	1.770
Tail rib.....	2.3	-17.7	40	-53.0	
Elevator rib.....	17.7	-19.0	40	-37.0	
Stabilizer rib.....	7.9	-19.3	33	-53.0	

As previously stated, one of the two main objects of this investigation was to obtain some data as to the time correlation of the loads occurring on the wing and tail surfaces. This has been accomplished as the time-history curves indicate. A study of the results obtained shows that at least in so far as can be determined from an investigation of a single rib, there is no definite sequence in which the wing and tail ribs reach their maximum loads in different maneuvers. In general, the loads on the elevator start to build up sooner than the wing loads, but the latter appear to build up more rapidly and as a result may reach their maximum simultaneously with the tail loads or even before the tail loads.

The second main objective in the investigation was to determine the distribution of load on a wing rib and on a tail surface rib to check the rules for specifying rib loads for design purposes. Once again it should be pointed out that since only single ribs were investigated, the results can not be entirely conclusive. Figures 29 to 36 show the comparison of the rib loadings specified by the Army Air Corps (Reference 8) and the Bureau of Aeronautics, Navy Department (Reference 9), with those measured in these tests, the worst positive and negative loadings measured being given. It will be noted in general that the loadings for the high angle of attack condition are in fairly good agreement, the Navy specified loads more closely simulating the flight loads. In the low angle of attack condition there is a considerably greater discrepancy in the comparison, the Navy loading again agreeing better with the flight loads. The Army

specified loading in Figures 32, 33, and 34 is the loading for medium angle of attack condition, but is the loading used for low angle of attack as well and is therefore comparable to the flight tests and Navy low angle of attack loads. The Army loading to be applicable to low angle of attack, as shown particularly by the loads measured on the TS airplanes (figs. 33 and 34), should include a negative load on the leading edge. It will also be noted in these figures that there is a considerable difference in the pressure distribution on the two wings investigated in the low angle of attack condition. This indicates the desirability to further investigate the pressure distribution on other wing sections before suggesting a distribution satisfactorily applicable to all types of commonly used wing sections. Wind tunnel tests are now in preparation to find the characteristic distribution on several other standard wing sections. The specified total load on the horizontal tail surfaces (figs. 35 and 36) is much larger than was found in any of the maneuvers, but because of the irregularity of the tail surface load, some of the local loads exceeded the specified slightly.

The center of pressure location at high angle of attack is very interesting. On the VE-7, where only the upper wing was investigated, the *C. P.* location in level flight agrees with monoplane wind tunnel tests of the wing section, but in accelerated flight the measured *C. P.* is farther forward by approximately 4 per cent of the chord. On the TS, where both the upper and lower wings were measured, in level flight the *C. P.* location of the upper wing again agrees very closely with wind tunnel tests, but on the lower wing is about 1 per cent of the chord farther forward. In accelerated flight the *C. P.* of the upper wing is 2 per cent forward of tunnel results while the lower *C. P.* is 2 per cent back. (NOTE:—The comparisons of wind tunnel and flight center of pressure locations were made for the same normal force coefficient.) This variation is not at all serious with respect to rib design, but may be so with respect to the distribution of load between spars and with respect to the design of lift trusses. If, as is indicated here, there is a change in *C. P.* location caused by accelerations in flight the use of the usual wing section data for wing design might be dangerous. The present tests are not complete enough to definitely establish this. The variation of *C. P.* over the span might vary considerably so that the average *C. P.* location is farther back than found here, as was the case in a previous pressure distribution experiment (Reference 10). The problem warrants further and more complete research, which is at present in progress.

To determine the possible effect of engine power and slip stream on the loads experienced, pull-ups were made with "power on" and "power off" at the same air speed (figs. 22 and 23). The results show that while the same acceleration was obtained in each, the wing rib loads in the pull-up with "power off" exceeded those obtained in the "power on" condition. This seeming contradiction is explained by the fact that the rib investigated was outside of the slip stream and the "power on" flight, because of the slip stream, produces a larger loading on the portion of the wing in the slip stream with a consequent decrease on the portion outside. Thus, while the total loading for these two flights was equal, the distribution along the span was different in such a manner that the "power off" flight showed the largest wing rib load at the rib investigated. The "power on" flight indicates a much lower air speed drop between the start of the maneuver and point of maximum load.

Since it is easy to compute the theoretically possible maximum acceleration on an airplane when pulled up suddenly, it was considered of value to compare the theoretical and actual accelerations of each of the airplanes used. The flight tests were extended to include a series of pull-ups from level flight at speeds ranging from about 60 M. P. H., to the maximum speed. The actual accelerations were measured by the accelerometer and the theoretical calculated from the expression:

$$A = \frac{V^2}{V_s^2} \text{ (Reference 11),}$$

where A is the acceleration in terms of g ,

V_s is the minimum speed,

V is the speed at the pull-up.

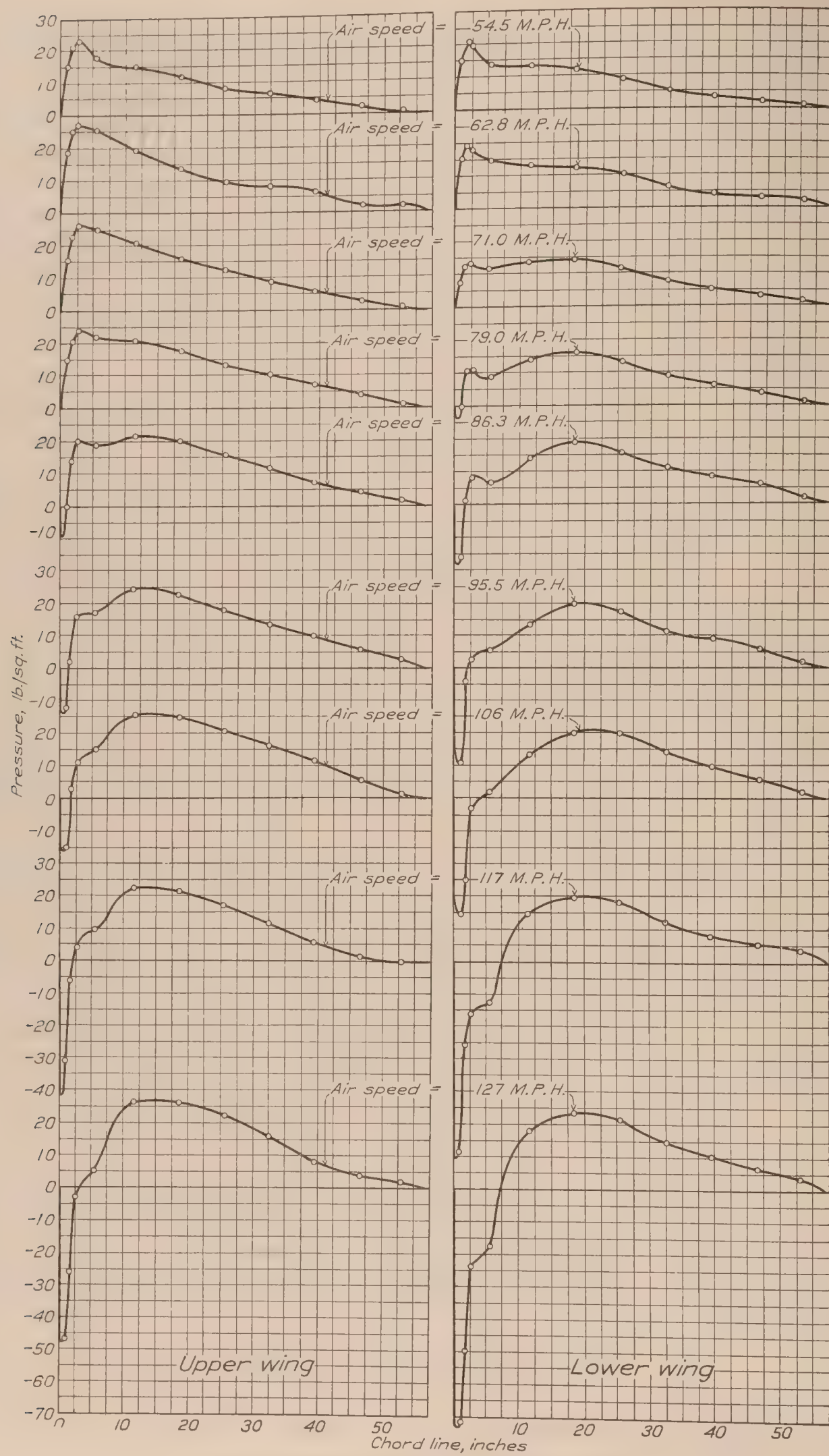


FIG. 21.—Pressure distribution on a TS airplane in level flight

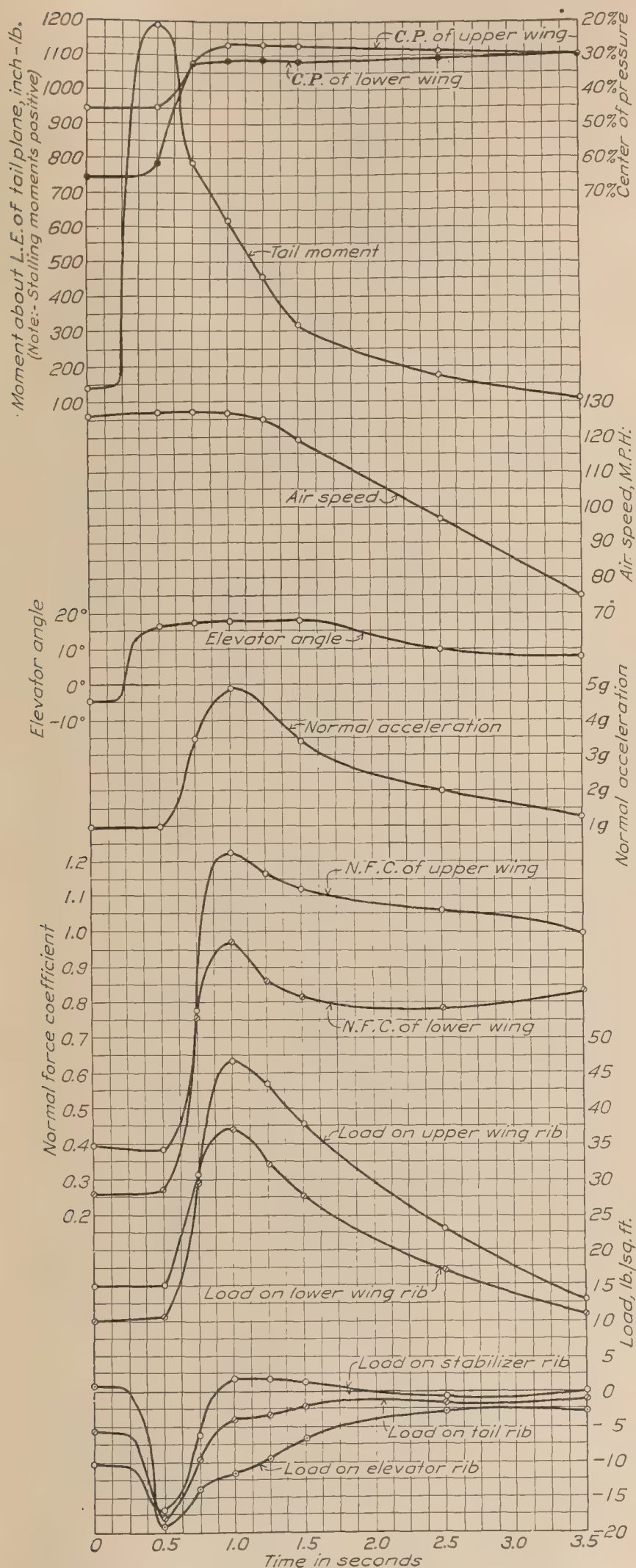


FIG. 22.—TS airplane in a "pull-up" with power on at 127 M. P. H.

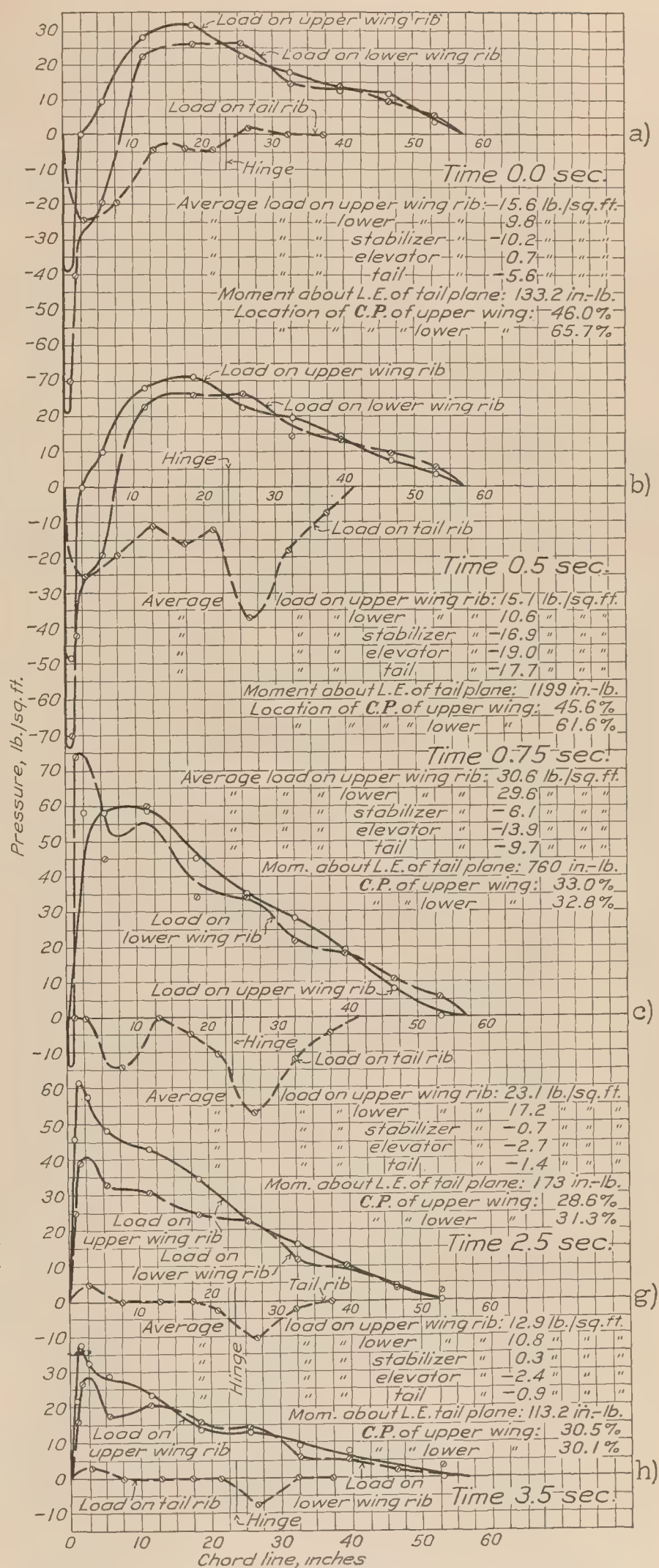


FIG. 22a, b, c, g, and h.—Pressure distribution on TS airplane in a "pull-up" with power on at 127 M. P. H. for various intervals of time

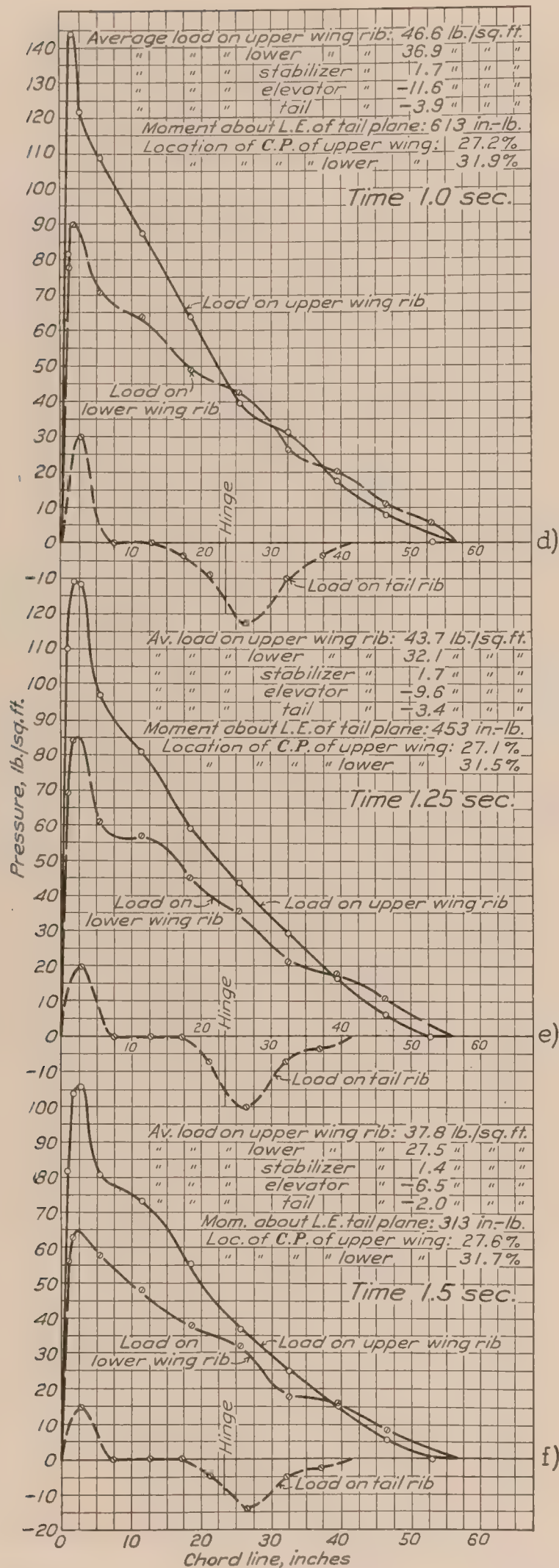


FIG. 22d, e, and f.—Pressure distribution on a "pull-up" with power on at 127 M. P. H. for various intervals of time

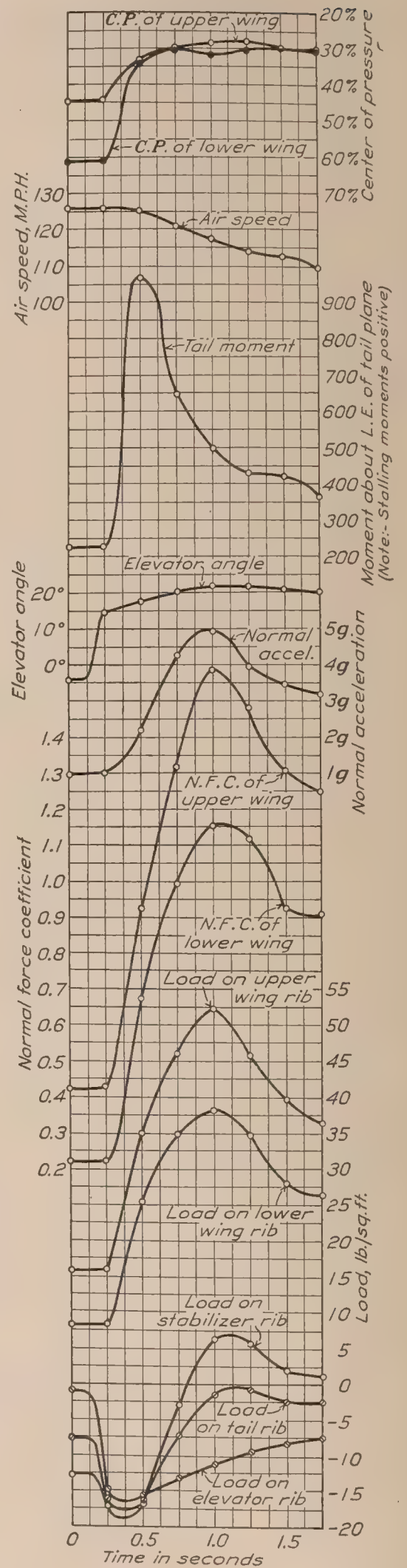


FIG. 23.—TS airplane in a "pull-up" with power off at 125 M. P. H.

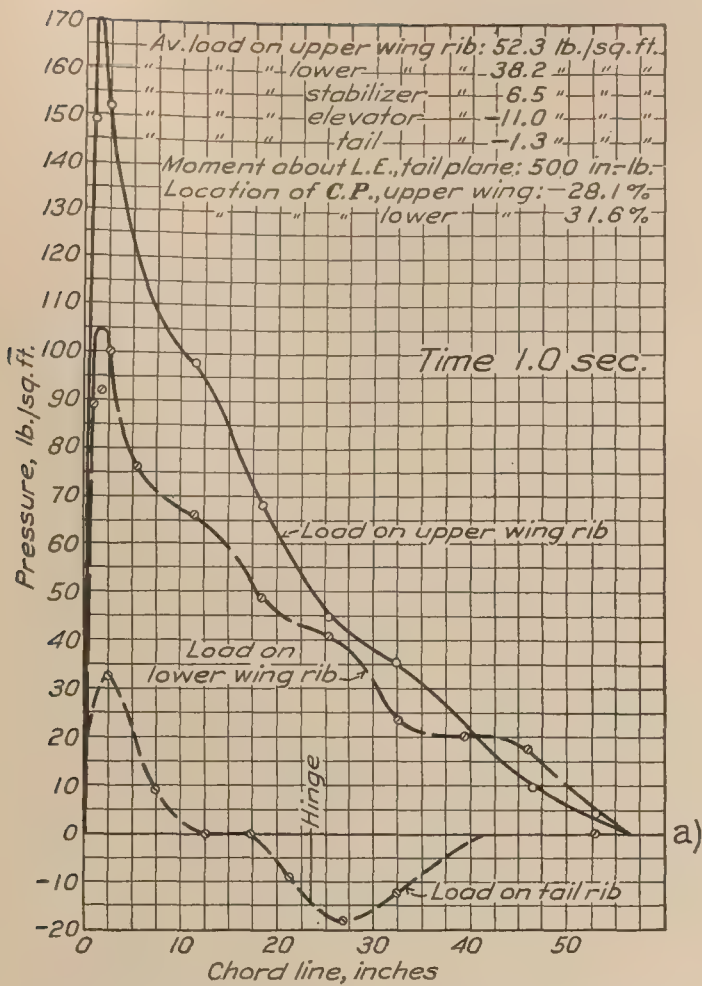


FIG. 23a.—Pressure distribution on a TS airplane in a "pull-up" with power off at 125 M. P. H. Maximum load, upper and lower wings

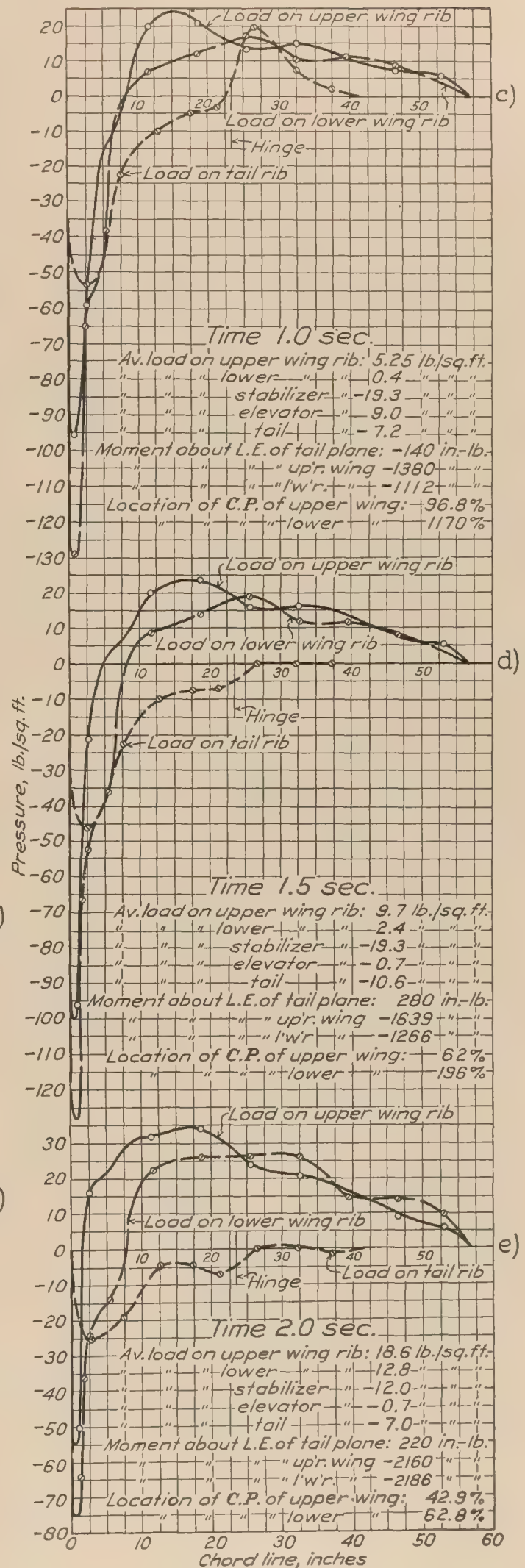


FIG. 24c, d, and e.—Pressure distribution on TS airplane in a no lift condition (push-down) at high speed for various intervals of time

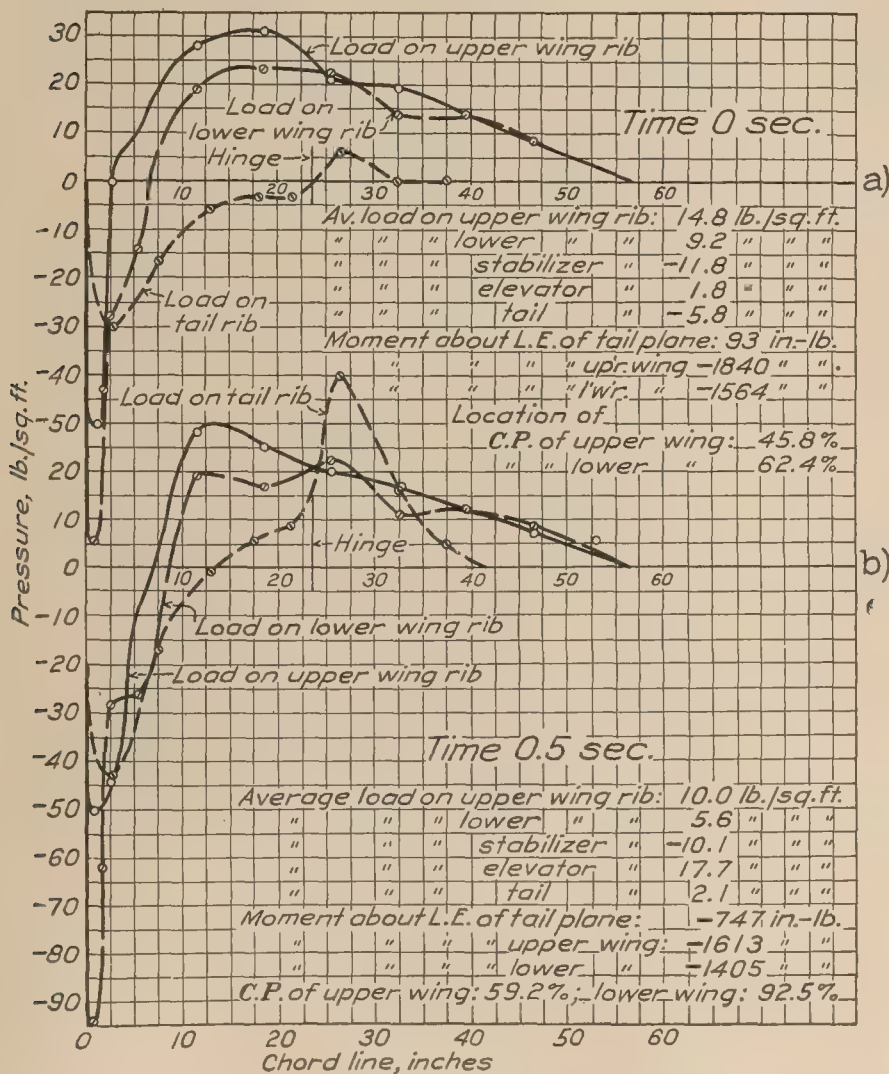


FIG. 24a and b.—Pressure distribution on TS airplane in a no lift condition (push-down) at high speed for various intervals of time

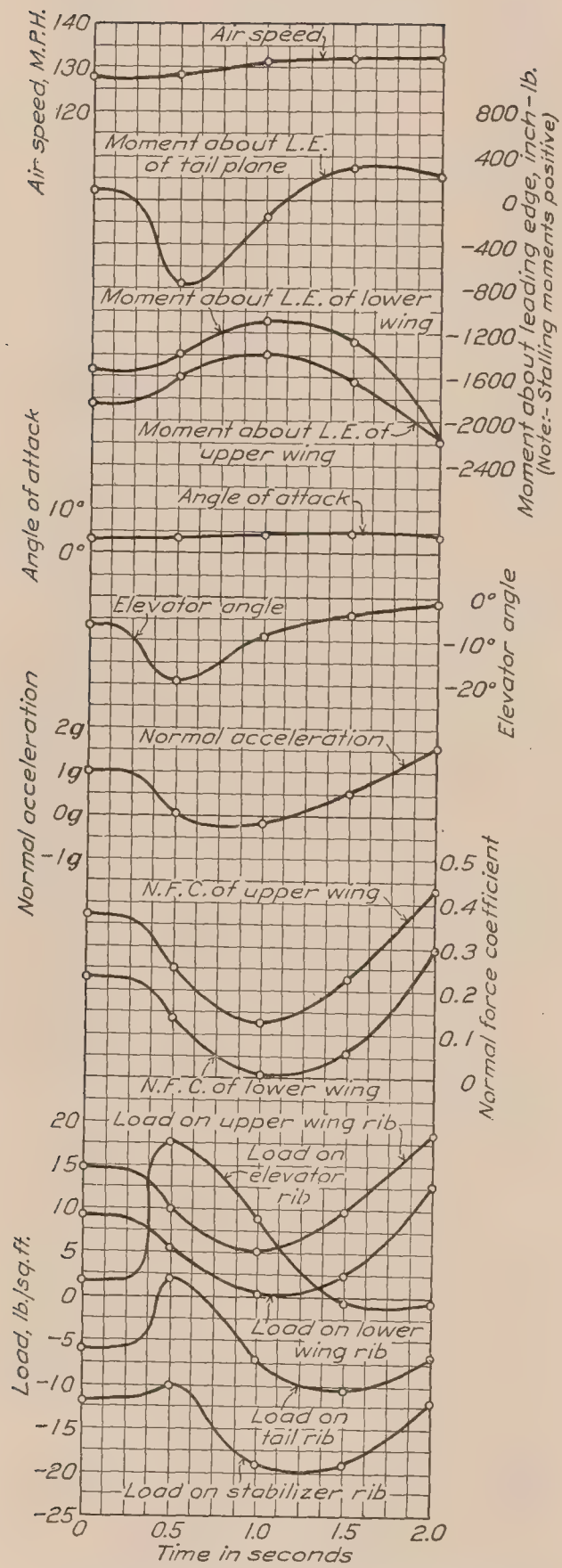


FIG. 24.—TS airplane in a no lift condition (push-down) at high speed

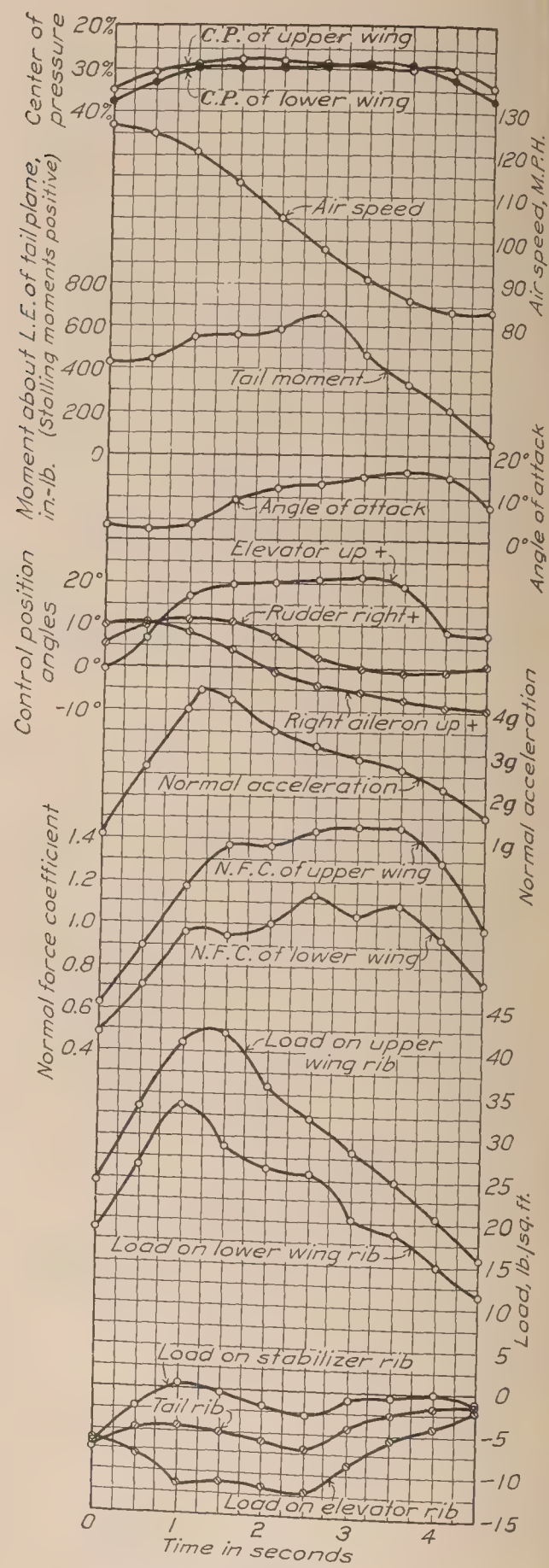


FIG. 25.—TS airplane in a right turn

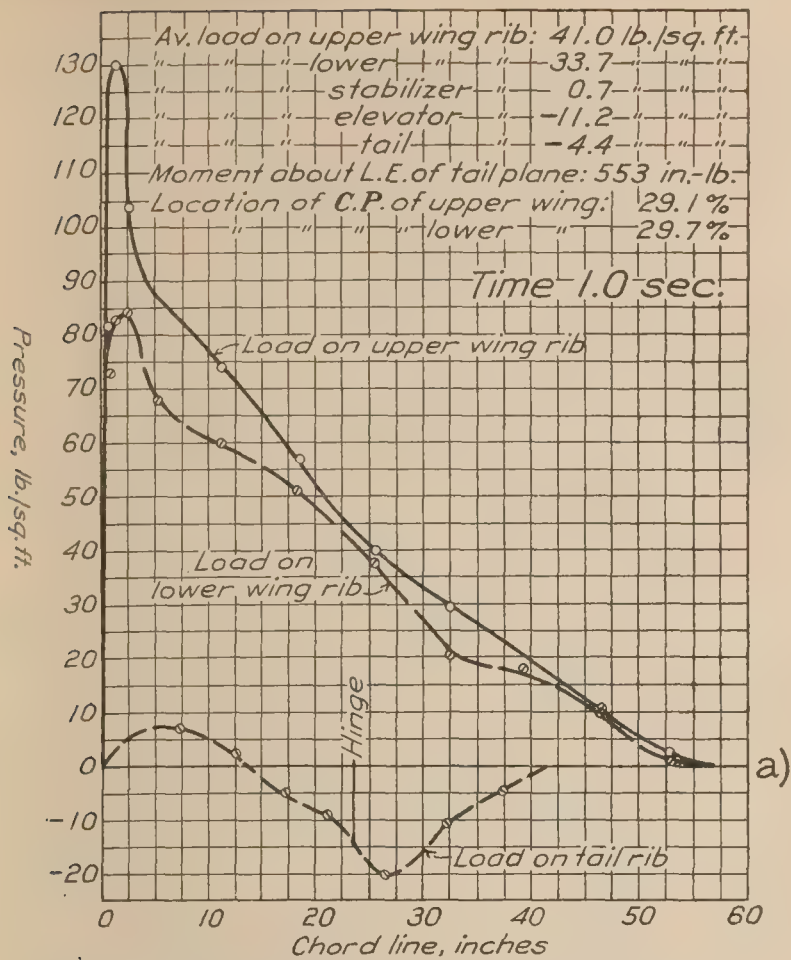


FIG. 25a.—Pressure distribution on TS airplane in a right turn.
 Maximum load lower wing

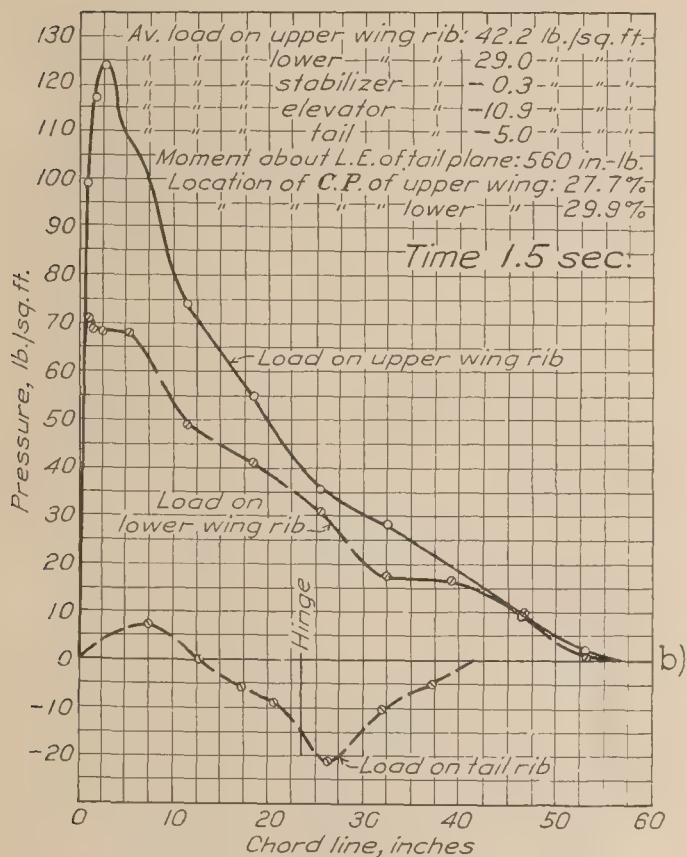


FIG. 25b.—Pressure distribution on TS airplane in a right turn.
 Maximum load upper wing

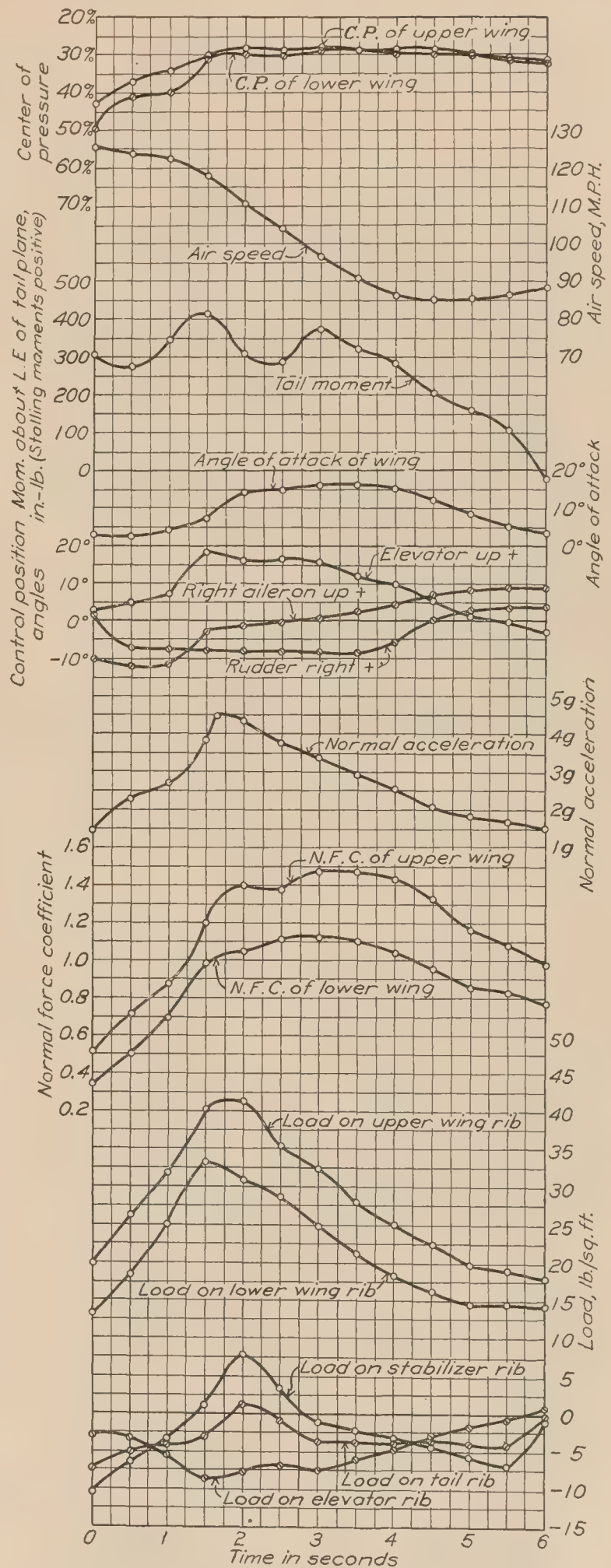


FIG. 26.—TS airplane in a left turn

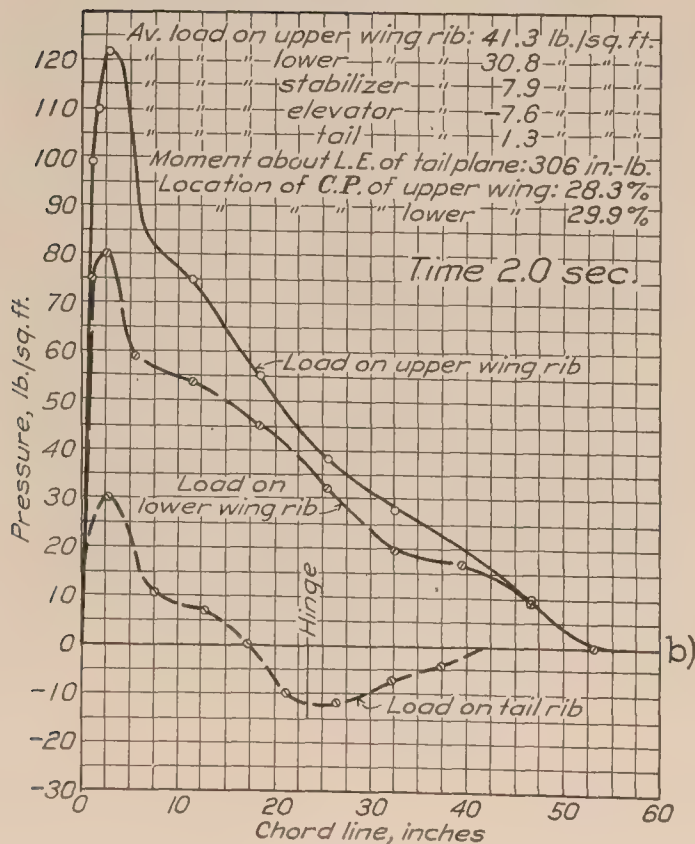
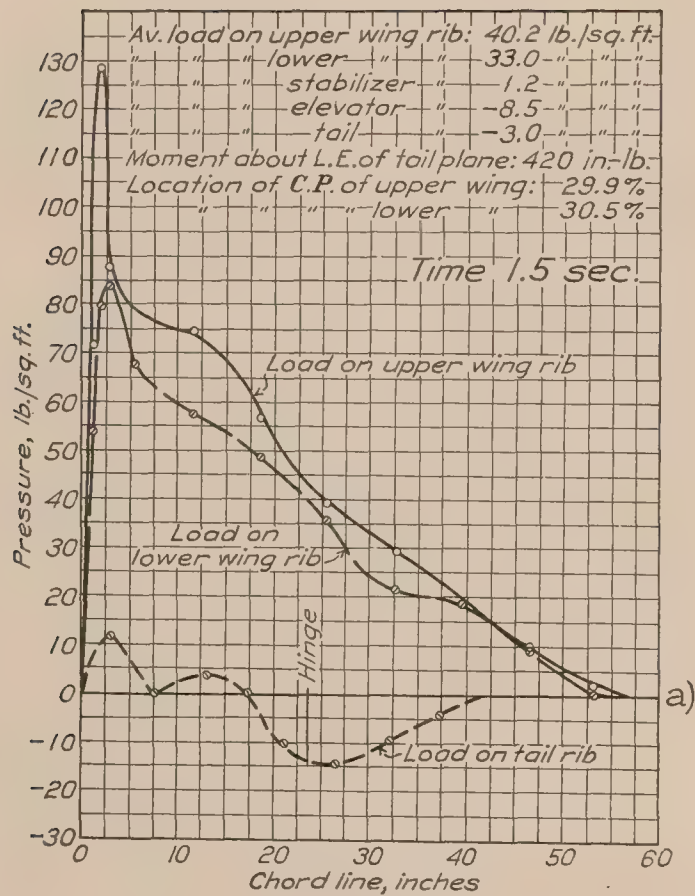


FIG. 26a and b.—Pressure distribution on TS airplane in a left turn. Maximum loads, (a) lower, (b) upper wings

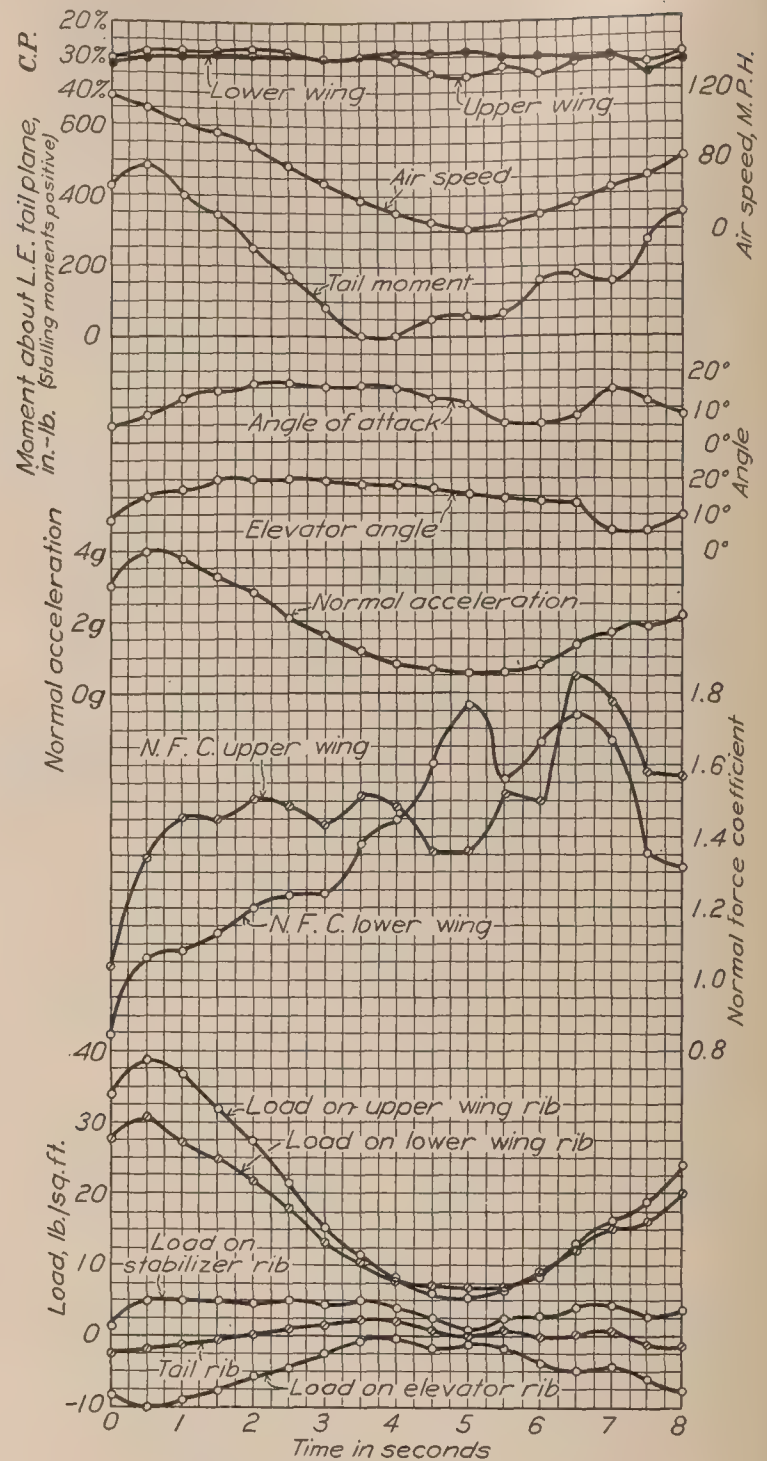


FIG. 27.—TS airplane in a loop

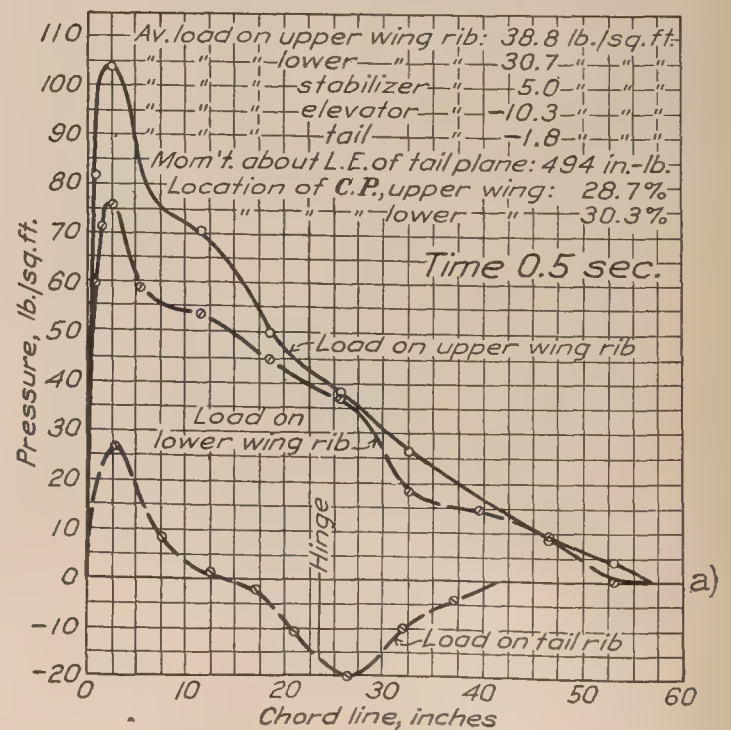


FIG. 27a.—Pressure distribution on TS airplane in a loop. Maximum loads, upper and lower wings

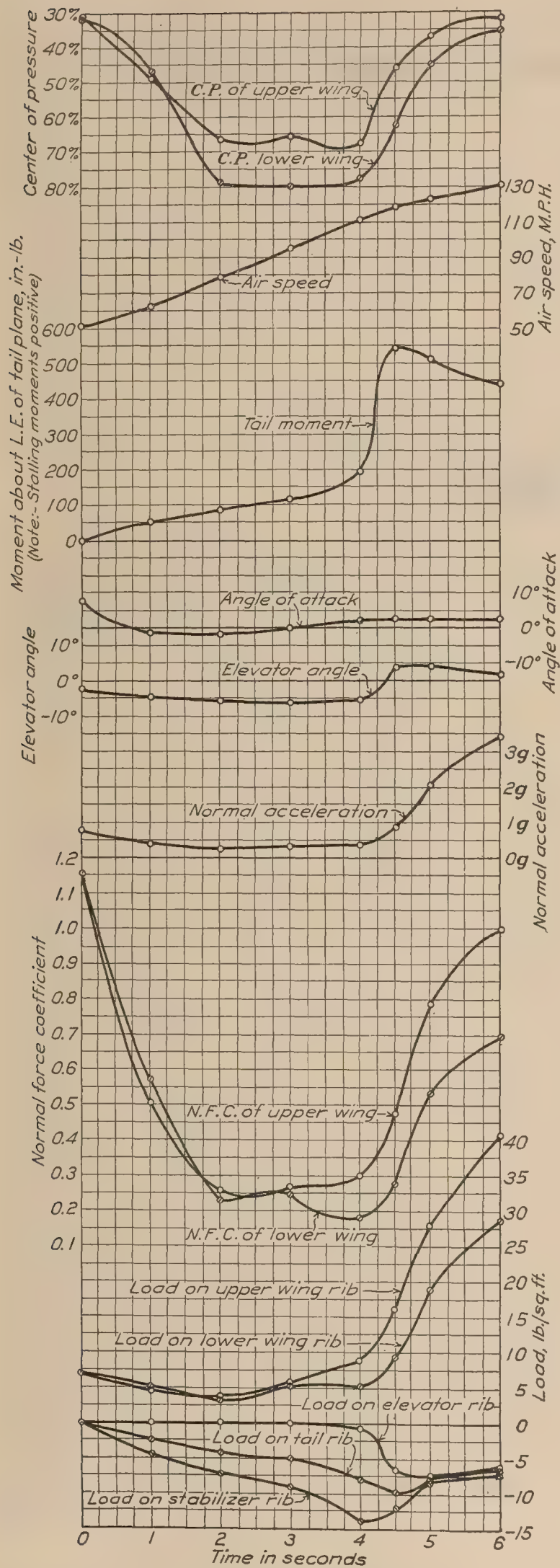


FIG. 28.—TS airplane in a dive

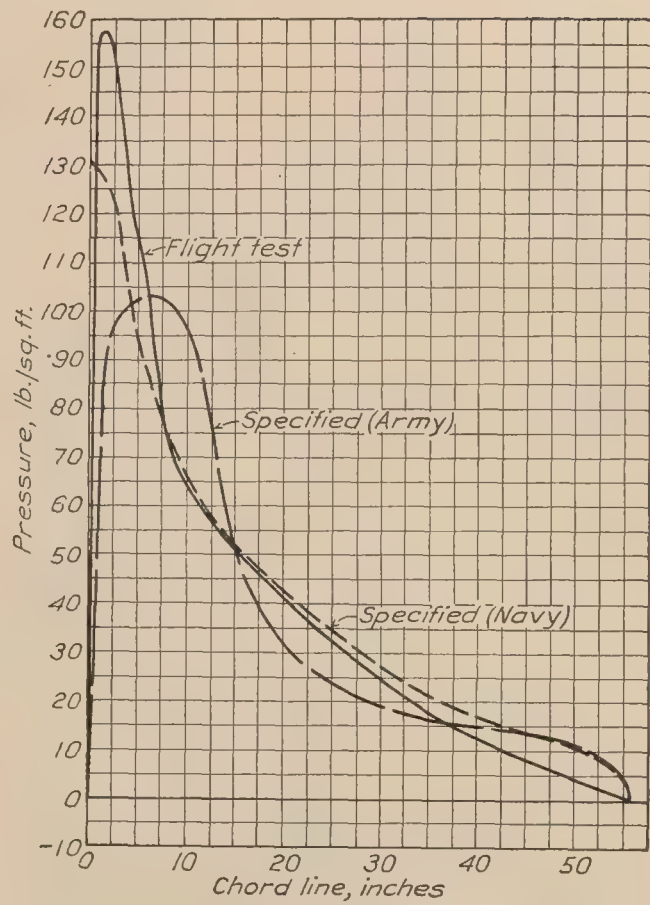


FIG. 29.—Maximum loading encountered on upper wing of VE-7 compared with specified static test loads

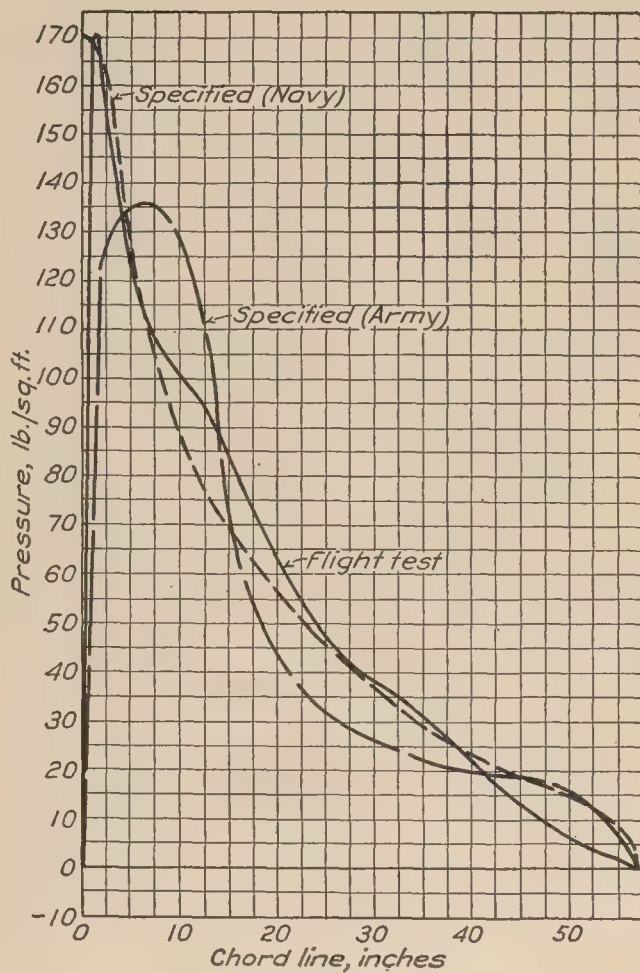


FIG. 30.—Maximum loading encountered on upper wing of TS compared with specified static test loads

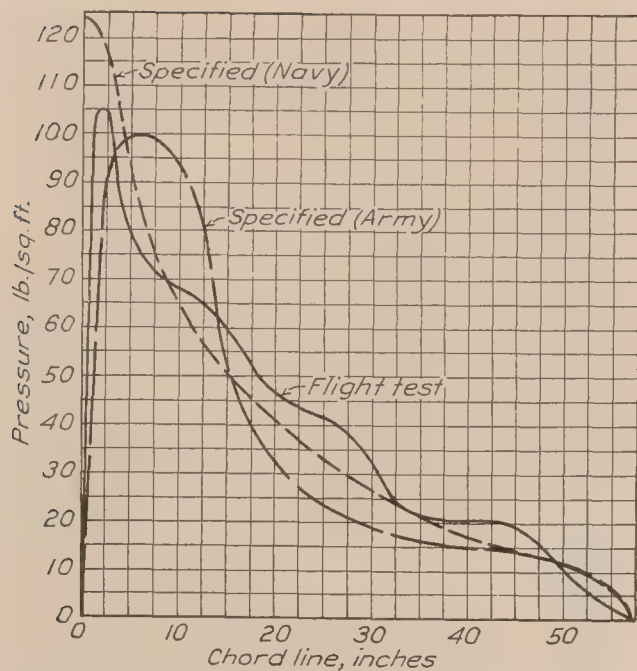


FIG. 31.—Maximum loading encountered on lower wing of TS compared with specified static test loads

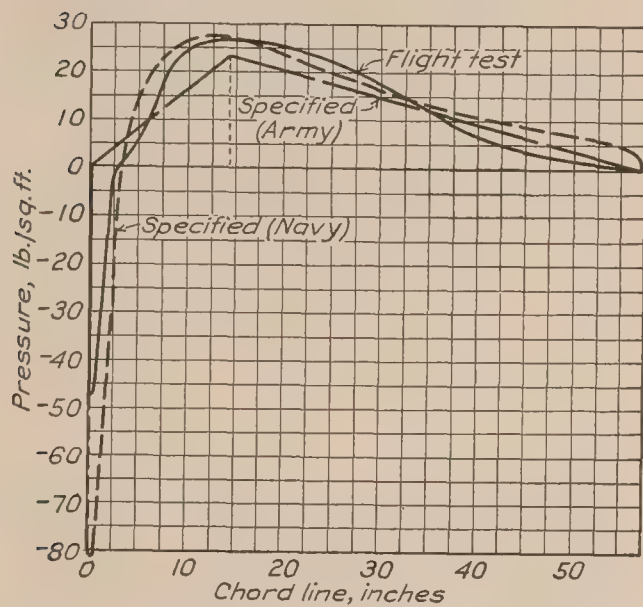


FIG. 33.—Low incidence (angle of attack) load on TS upper wing compared with medium incidence static test load specified by Army Air Corps and low incidence static test load specified by Bureau of Aeronautics, Navy Department

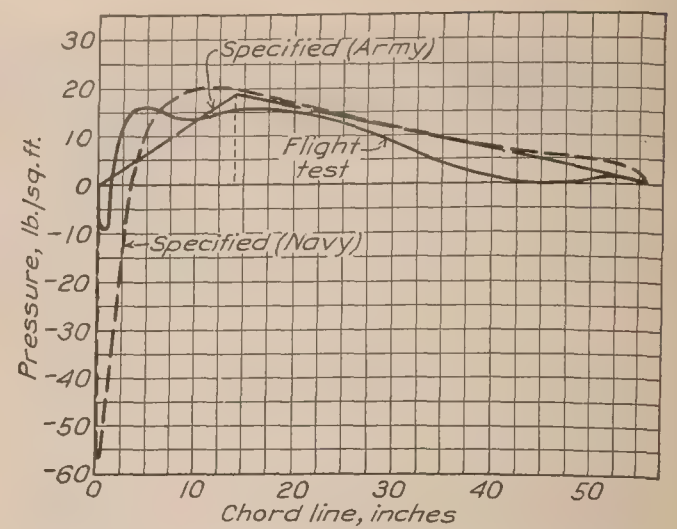


FIG. 32.—Low incidence (angle of attack) load on VE-7 upper wing compared with medium incidence static test load specified by Army Air Corps and low incidence static test load specified by Bureau of Aeronautics, Navy Department

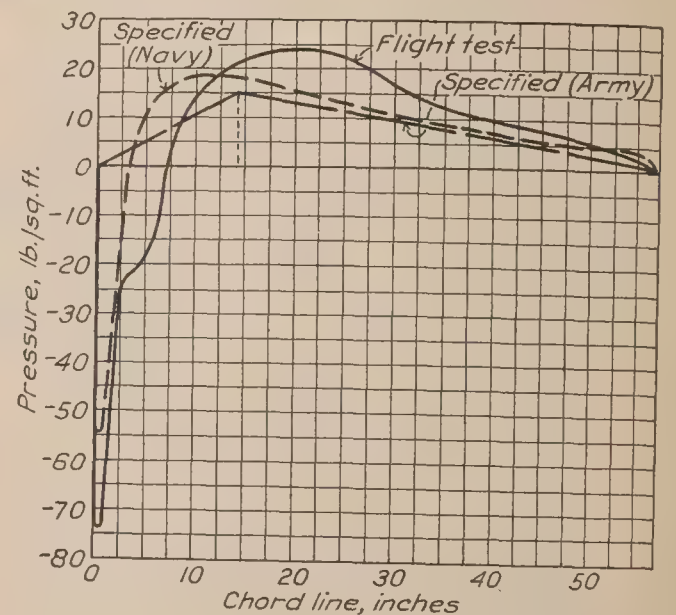


FIG. 34.—Low incidence (angle of attack) load on TS lower wing compared with medium incidence static test load specified by Army Air Corps and low incidence static test load specified by Bureau of Aeronautics, Navy Department

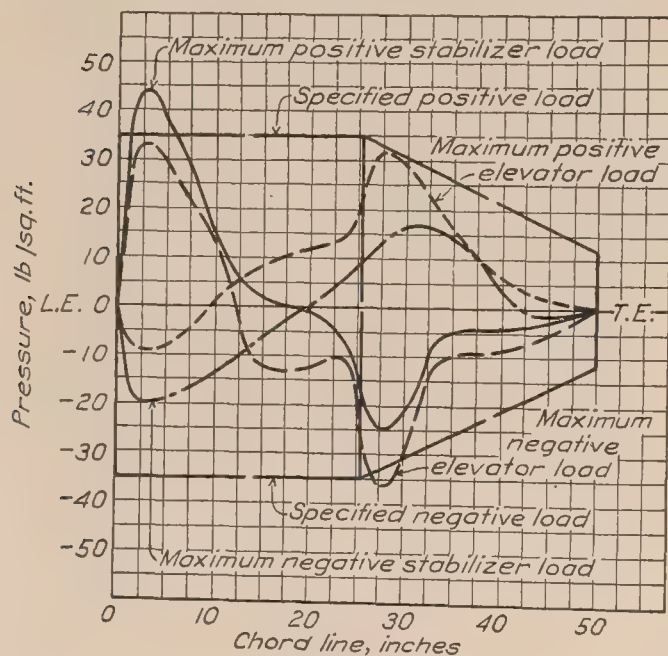


FIG. 35.—Maximum load on horizontal tail surfaces of VE-7 compared with static test load specified by Army Air Corps

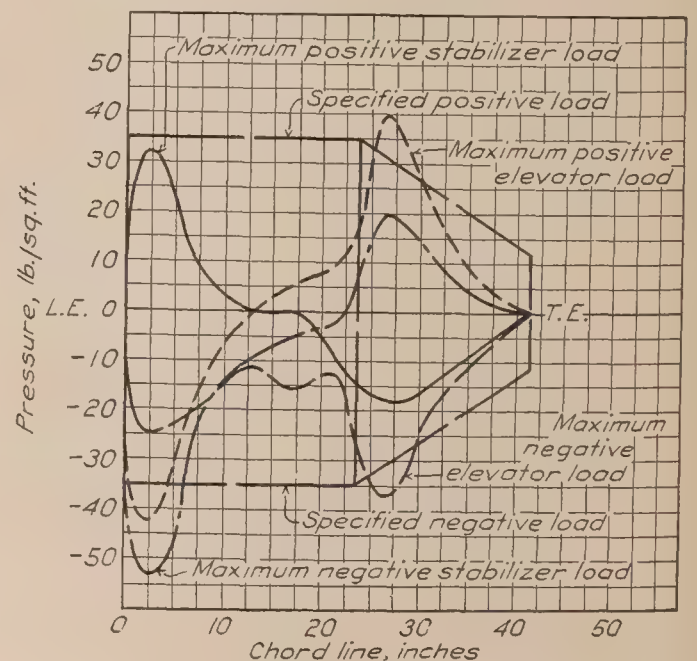


FIG. 36.—Maximum load on horizontal tail surfaces of TS compared with static test load specified by Army Air Corps

The accelerations are plotted for comparison in Figure 37. Uncertainty as to the exact value of V_s makes the computed values liable to some error. It appears though that on these two airplanes it is possible to obtain the theoretical maximum accelerations in flight below and up to speeds that are approximately 60 per cent of the maximum speed in level flight and that "power on" and "power off" does not affect this. In all cases the control stick was pulled full back practically instantaneously. The falling off of the actual accelerations from the theoretical at higher speeds must be due to lack of maneuverability and there may be derived therefrom a maneuverability factor.

In attempting to obtain the no lift or low angle of attack conditions in flight, several maneuvers were attempted before the push-down was decided upon. The most promising method of passing through zero lift apparently was in a dive at high speeds. However, it was found

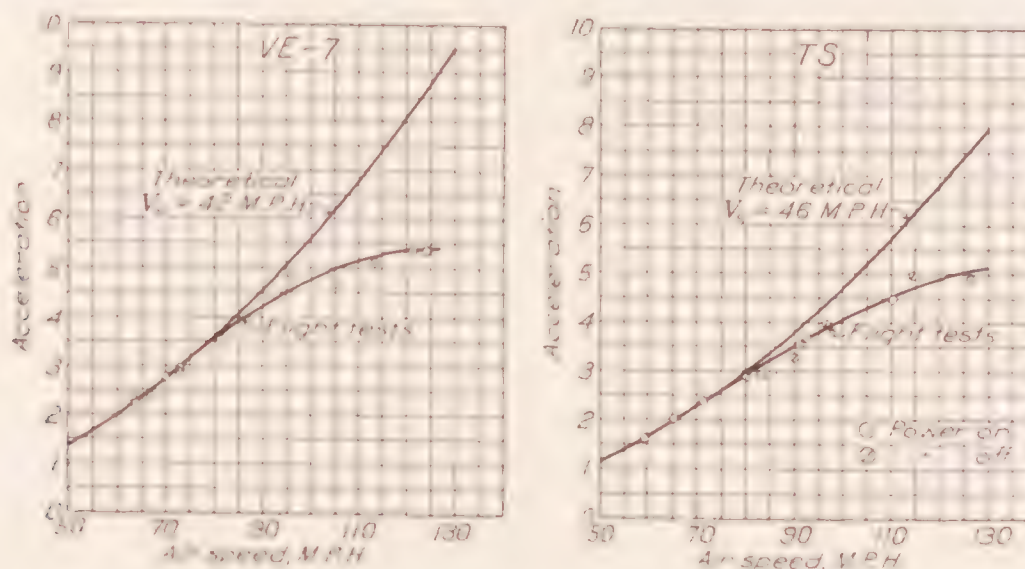


FIG. 37.—Theoretical accelerations compared with accelerations obtained in flight

that neither airplane had sufficient elevator control to reach the desired attitude, i. e., partly over on the back in a dive. A second method employed, that of "hanging" on the top of a slow loop, gave the desired result, but at such a low air speed that the pressure readings were very small and consequently indeterminate. The push-down method proved entirely satisfactory, the negative accelerations obtained indicating conclusively that the no lift condition was obtained and at the same time the air speed was large enough to eliminate the error caused by small pressure readings.

In some of the time-history figures of maneuvers made at low speeds, such as the loops, it will be noted that the shape of the normal force coefficient curves appears to be erratic. This is because at low air speeds the accuracy of the pressure measurements is poor and also because the errors of integrating the load curves, when the load is small, introduces a large percentage error in these results.

REFERENCES

1. NORTON, F. H., and BROWN, W. G. The Pressure Distribution Over the Horizontal Tail Surfaces of an Airplane—III. N. A. C. A. Technical Report No. 148. 1922.
2. NORTON, F. H., and WARNER, E. P. Accelerometer Design. N. A. C. A. Technical Report No. 100. 1921.
3. NORTON, F. H. N. A. C. A. Recording Airspeed Meter. N. A. C. A. Technical Note No. 64. 1921.
4. FREEMAN, R. G. Air Flow Investigation for Location of Angle of Attack Head on a JN4H Airplane. N. A. C. A. Technical Note No. 222. 1925.
5. BROWN, W. G. The Synchronization of N. A. C. A. Flight Records. N. A. C. A. Technical Note No. 117. 1922.

6. NORTON, F. H. N. A. C. A. Control Position Recorder. N. A. C. A. Technical Note No. 97. 1922.
7. CARROLL, T., and MIXON, R. E. The Effect of Tube Length upon the Recorded Pressures from a Pair of Static Orifices in a Wing Panel. N. A. C. A. Technical Note No. 251.
8. ENGINEERING DIVISION, ARMY AIR CORPS. Handbook of Instructions for Airplane Designers. 1925.
9. BUREAU OF CONSTRUCTION AND REPAIR, NAVY DEPARTMENT. Load Distribution for Wing Rib Tests. April 1, 1921. (SD-19.) General Specifications for the Design of Airplanes for the U. S. Navy. April 1, 1926. (SD-24B.)
10. NORTON, F. H. Pressure Distribution Over the Wings of an MB-3 Airplane in Flight. N. A. C. A. Technical Report No. 193. 1924.
11. DOOLITTLE, J. H. Accelerations in Flight. N. A. C. A. Technical Report No. 203. 1925.

TABLE I
PRESSURE IN POUNDS PER SQUARE FOOT ON VE-7 AIRPLANE

Station No.	Wing																Tail surface						
	1	2	3	4	5	6	7	8	9	10	11	12	13	14	15	16	1	2	3	4	5	6	7
Level flight																							
Air speed (M. P. H.):																							
42.....	24	24	18	16	13	9	6	6	5	4	3	3	-----	1	1.5	-2							
44.....	26	24	19	16	13	11	9	8	8	8	5	4	-----	1	1.5	0							
50.....	24	24	19	16	13	11	9	8	8	8	5	4	-----	1	1	0							
54.....	24	24	18	16	13	9	6	7	6	4	3	3	-----	1	2	1							
65.....	24	22	21	17	14	11	9	10	7	7	5	3	-----	1	3	.5							
67.....	24	24.5	19	19	12.5	10.5	10	9	6	7	5	4	-----	1	0	0							
75.....	19	22	21	17	13	11	11	10	7	7	5	3	-----	1	3	1							
77.....	16	23	20	17	13	9	10	10	7	7	5	4	-----	1	0	.2							
85.....	16	20	21	17	14	11	13	9	7	7	8	3	-----	1	2	1.5							
87.....	19	21	19	17	14	14	13	11	9	7	8	4.5	-----	1	0	.5							
97.....	12	20	21	17	14	11	13	12	11	8	6	3	-----	1	1	1.5							
99.....	12	21	18	17	12.5	12.5	13	12	10	10	8	4	-----	1	.5	.5							
107.....	11	17	18	17	14	14	15.5	13.5	11	10	7.5	4	-----	1	0	1							
107.....	12	17	19	19	14	11	14	13	11	8	7	3	-----	1	0	2							
117.....	11	15.5	16	17	14	12.5	15.5	13.5	12.5	12	8	4	-----	4	0	1							
117.....	6	13	16	16	14	12	15	14	12	10	8	3	-----	1	1	1.5							
127.....	11	14	16	16	14	14	15.5	14	12.5	14	8	5	-----	1	0	1							
128.....	-2	12	15	16	14	14	17	15	12	11	8	3	-----	1	0	1							
Pull-up																							
Time (seconds):																							
0.....	0	14	18	17	16	14	17	16	14	12	10	4.5	7	2	0	1.5	0	-2	0	3	5	6	-1.5
0.25.....	0	16	22	32	16	16	21	18	19	16	10	4.5	7	3	0	1.5	2	-4	-3.5	-5	-19	-6.5	-5.5
0.50.....	118	126	88	85	58	44	43	34	31	24	19	12	10	6	11	2	33	15	-13	-10	-37	-10	-9
0.75.....	158	145	122	105	89	60	53.5	43	39	28	24.5	16	14	7	5	2.5	44	18	0	-5	-25	-5	-5
1.00.....	132	124	101	88	79	54	47.5	39	33.5	26	20.5	14	13	5	5	2	33	13	4	-3	-21	-3	-4
1.50.....	77	70	56	48	47	34	29.5	22	22	18	13	8	9	5	3	1.5	14	3	3	-1	-13	-1	-2
Push-down—high speed																							
0.....	-1	12	15	17	13	12	14	14	11.5	8	8	4.5	5	2	0	.25	-9	-4	0	2	3	7	-1.5
0.50.....	-1	12	15	17	13	12	14	14	11.5	8	8	4.5	5	2	0	.25	-9	1	9	13	32	17	3.5
1.00.....	-42	-32	-20	-12	-8	-2	0	6.5	1.5	0	1	-5	-3	0	-8	-1.5	-20	-14	-5	4	14	15	-1.5
1.25.....	-54	-37	-21	-12	-10	-3.5	2.5	6.5	1.5	0	1	-5	-3	1	-8	-1.75	-16	-14	-5	3	10.5	11	-1.5
1.50.....	-54	-36	-20	-8	-7	-3.5	9	9	2.5	1	3	0	-3	2	-6	-1.75	-18	-14	-6	0	-9	2	-5
2.00.....	0	38	40	33	25	22.5	25	20.5	18	15	13	7	0	3	0	0	-6	0	-5	0	0	3	-2
2.50.....	26	41	37	33	30	21	24	20	18	15	13	6.5	7.5	2	0	.5	-4	0	0	0	1	3	-2
3.00.....	19	35	34	29	25	21	22.5	19	18	15	12	6.5	7.5	2	0	.5	-6	0	0	0	1	3	-2

TABLE I—Continued
PRESSURE IN POUNDS PER SQUARE FOOT ON THE VE-7 AIRPLANE—Continued

		Wing															Tail surface								
Station No.-----		1	2	3	4	5	6	7	8	9	10	11	12	13	14	15	16	1	2	3	4	5	6	7	
Push-down—low speed																									
Time (seconds)—Contd.		19	23	18	14	13	11	9	9	6	6	4	3	3	1	0	0	2	1	1.5	0	0	1	—	5
0-----		19	23	18	14	13	11	9	9	6	6	4	3	3	1	0	0	2	1	1.5	0	0	1	—	5
0.50-----		16	18	18	10	8	9	6.5	8	5	6	2	1	0	0	0	0	0	5	9	0	17.5	8	4.5	
1.00-----		0	0	9	0	0	3	4	5	2	3	1	0	—1	0	—2	—1.5	—14	0	—2.5	10	9	4	1	
1.25-----		—10	—9	0	—8	—8	0	0	2	0	2	0	0	—1	0	—3	—2	—16	—7	—2.5	2	3	4	0	
1.50-----		—16	—10	—7	—6	—8	—	—2	2	—1	0	0	0	—1	0	—3	—2	—12	—7	—2.5	0	2	2	—	
1.75-----		—14	—9	—6	—4	—4	0	0	3	0	—2	1	1	0	1	—3	—2	—7	—7	—2	—1	0	1	—1	
2.00-----		—2	0	3	8	2	3	4	6	2	0	3	3	3	1	—2	—1.5	—4	—4	—1.5	—1	—3	0	—1	
2.50-----		19	20	19	17	13	11	9	10	6	4	5.5	4	3	1	0	0	0	0	0	—1	—3	0	—1	
Right turn																									
0-----		12	24	23	21	16	12	17	13	12.5	9	8.5	4.5	7	3	0	0	—3	0	0	0	1.5	3	0	
1.00-----		30	41	34	31	27	21	20	15	15	12	10.5	5.5	9	3	0	0	2	3	0	0	—7	2	0	
2.00-----		52	59	48	42	36	27	25	18	19	14	13	7	10	3	0	.5	14	5	0	—2	—13	—2	0	
3.00-----		77	76	64	54	46	31	29.5	22	22	16	15	10	11.5	4	3	.5	26	10	0	—3	—17	—5	0	
4.00-----		72	72	62	50	44	27	28	21	20	16	15	9	11.5	4	3	.5	24	10	0	—3	—15	—5	0	
5.00-----		38	49	48	36	32	19	24	20	16	15	12	7	10	4	3	.5	16	8	0	—2	—5	0	0	
6.00-----		14	26	25	19	18	12	15.5	13	12.5	11	8.5	4.5	9	3	3	.5	0	3	0	0	—3	2	0	
7.00-----		9	23	22	17	18	12	15.5	13	12.5	11	8.5	4.5	9	2	3	.5	—8	0	0	0	—3	2	0	
Left turn																									
0-----		8	19	18	18.5	15	12.5	14	12	12.5	9	6	4.5	5	2	0	0	0	0	0	0	0	1	0	
1.00-----		19	29	26	24	20	16	17	15	14	10.5	9	6	7	2	0	0	6	3	1.5	0	—3	0	0	
2.00-----		36	42	36	32	25	19.5	21	17	16	13	11.5	7	8.5	3	0	0	14	6	3	—1	—11	—2	0	
3.00-----		62	65	54	46	38	27	27	20	19	15	11.5	8.5	8.5	3	0	0	21	8	3	—1	—11	—4	0	
4.00-----		67	67	54	46	38	27	27	20	19	15	11.5	8.5	8.5	3	0	0	4	5	0	—1	—11	—4	0	
5.00-----		57	56	50	44	37	24	22	17	16	14	10	7	7	2	0	0	—9	1.5	—2.5	0	—7	—2	0	
6.00-----		26	33	28	24	22	14	15	11	11	10.5	8	4.5	5	.5	0	0	—1	1.5	1.5	1	3	3	0	
7.00-----		14	23	19	18.5	15	9.5	11.2	9	7	8	5	2.5	5	0	0	0	0	1.5	1.5	1	—3	—3	0	
Loop																									
0-----		0	16	19	21	14	12.5	15	15	12	10	8	4	3	3	—6	1	—14	—4	—2.5	3	2	6	—5	
0.50-----		2	22	25	24	16	14	15	18	12	12	10	4.5	3	3	—6	1	—12	—4	—3.5	2	0	4	—7	
1.00-----		38	53	49	41	28	22.5	21	22	18	15	13	8.5	7	4	—2	1.5	0	1	—2.5	1	—9	1	—8	
1.50-----		75	80	70	58	46	29	34	28	24	19	15	9	10	6	0	2	16	6	2	0	—13	0	—12	
2.00-----		92	89	79	70	57	37	37	28	28	19	17	12	10	6	0	2	21	12	3	1	—15	—2	—12	
2.50-----		92	89	76	68	57	37	37	26	27	19	17	12	10	6	3	2	24	13	2	2	—15	—3	—12	
3.00-----		87	81	66	64	53	35.5	34	23	23	16	15	10	10	4	5	2	26	13	0	—3	—17	—3	—3	
3.50-----		74	68	53	52	44	29	26.5	20	20	15	13	9	9	3	3	1.5	23	11	0	—4	—15	—2	—2	
4.00-----		60	58	43	39	34	24	22	15	18	12	11	8.5	7	3	0	1.5	21	11	—1	—3	—13	—2	—1.5	
4.50-----		43	41	32	30	25	17.5	17	11	12	10	7.5	6.5	7	3	0	1	19	8	—2.5	—3	—13	—1	—1.5	
5.00-----		36	34	28	24	18	14	11	10	11	5	5	5.5	5	2	—4	.5	19	6	—3.5	—4	—13	—1	—1.5	
5.50-----		31	28	25	21	18	11	10	9	7	4	4	4	3	2	—6	.5	12	4	—2.5	—3	—11	0	—1.5	
6.00-----		30	29	25	23	18	11	10	10	6	6	5	4.5	3	3	—6	.5	10	3	—1	—2	—9	0	—1.5	
6.50-----		40	37	36	30	24	16	13	13	10	8	6	5.5	5	4	—6	1	10	3	—1	—2	—9	0	—1.5	
7.00-----		52	49	43	35	29	21	17	14	12	8	7.5	6.5	7	4	—4	1	10	4	—1	—3	—13	—1	—2	
7.50-----		64	61	53	46	34	26	22	18	16	12	10	7	7	4	—4	1.5	14	6	0	—4	—13	—2	—2	
8.00-----		80	74	62	56	44	29	28	21.5	19	14	13	10	9	6	—2	1.8	18	8	0	—3	—15	—2	—3	
8.50-----		85	76	68	58	49	30.5	31	23	23	18	13	10	10	6	0	2	18	8	0	0	—9	0	—1.5	

Right roll																							
0	9	19	18	17	14	14	13	11	8.5	8	6	4	3	1	0	0	-3	0	-1.5	3	0	5	-5
0.50	12	19	18	17	16	14	13	11	8.5	7	6	4	3	1	0	0	-3	0	-1.5	3	-35	5	-6
1.00	82	58	62	39	38	37	26.5	19	19	14	14	7	8.5	2	0	0	32	12	-1.5	-12	-24.5	-5	-3.5
1.50	136	120	97	80	51	66	46	35	29.5	20	18	12.5	11.5	4.5	0	0	19	10	-2.5	-7	-17	-4	-2
2.00	50	44	35	38	45	29	34	25	22	16	14	11	13	14	5	3	14	6	-3.5	-4	-15	-4	-1.5
2.50	16	19	17	24	20	14	25	13	11	12	11	7	7.5	6	0	0	14	6	-2.5	-3	-13	-3	-5
3.00	16	19	15	17	16	14	14	11	8.5	10	7.5	4.5	3	2	1	0	9	3	-3.5	-2	-13	-2	-5
3.50	24	17	14	14	11	12.5	10	9	6	7	5	4	2	1	-1	-1.5	7	1	-2.5	-2	-11	-1	0
4.00	36	33	25	21	18	14	10	9	6	7	5	3	0	0	-1	-2	9	1	-2.5	-1	-9	-1	0
4.50	40	40	31	26	22	16	13	11	8.5	7	6	4	2	0	-1	-2	11	1	-2.5	-1	-11	-2	-5
5.00	50	50	37	31	29	22.5	17	13	10	10	7.5	5	4	1	-1	-1.5	12	4	-2.5	-1	-13	-2.5	-1
5.50	64	60.5	46	39	34	27	19	16	14	11	10	6	5	1	-1	-1	11	4	-2.5	-1	-13	-3	-1
6.00	67	64	48	44	38	27	22.5	18	15	12	10	6	5	1	-1	-1	11	4	-2.5	-1	-13	-2.5	-1
6.50	70	67	53	44	38	27	24	19	15	12	10	5	5	1	0	0	9	3	-2.5	0	-11	-2.5	-1
7.00	62	62	48	44	34	26	22.5	19	14	11	10	5	5	2	0	0	7	5	-2.5	0	-9	-2	-1
7.50	46	44	40	35	28	21	17	18	11	8	9	4.5	4	1	0	0	4	3	-2.5	0	-7	-1	-5
8.00	33	34	31	28	23.5	17.5	14	15	10	8	6.5	3.5	3	.5	0	0	0	1	-2.5	1	-7	0	-5
8.50	24	26	25	22	18	14	14	13	8.5	7	5.5	3.5	3	.5	0	0	-1	0	-2.5	1	-5	1	0
9.00	21	28	25	21	18	12.5	13	12	8.5	7	5.5	3.5	3	.5	0	0	-3	0	-2.5	1	-3	0	0
9.50	19	28	23	21	16	12.5	13	12	8.5	7	5.5	3.5	3	.5	0	0	-3	.5	-1.5	1.5	0	3	0
10.00	14	21	19	17	14	11	11.5	11	8.5	7	5.5	3.5	3	.5	0	0	-3	1	-1.5	2	0	4	0
Left roll																							
0	12	22	20	17	14	11	11.5	11	8.5	8	6	3	3	1	0	.5	0	1	0	3	0	3	0
0.50	14	22	20	17	16	12	11.5	11	8.5	8	6	3	3	1	0	.5	0	1	0	3	0	3	0
1.00	12	22	20	17	14	11	11.5	11	8.5	8	6	3	3	1	0	.5	0	1	0	3	0	3	0
1.50	12	22	20	15	14	11	11.5	11	8.5	8	6	5	3	1	0	1	0	1	-6	-6	-25	3	-4
2.00	74	75	49	48	42	22	25	17	17.5	15	11	10	9	3	0	1	28	5	0	-2	-21	-5	-3
2.25	87	81	64	56	46	32	29.5	24	19	15	15	9	9	3	0	.5	22	11	0	-2	-17	-5	-2
2.50	79	68	60	56	44	32	28	24	19	14	15	8	7	3	0	.5	21	8	0	-2	-15	-4	-2
3.00	60	53	48	42	34	27	22	20	15	12	12	6	7	3	0	.5	18	6	0	-2	-13	-3	-1.5
3.50	48	44	38	33	28	21	17	18	12	10	10	5	5	2	0	.5	16	6	0	-2	-13	-3	-1.5
4.00	36	35	31	26	22	17.5	13	12	10	8	7	4.5	5	1	0	.5	12	6	0	-2	-13	-3	-1.5
4.50	33	34	26	22	20	16	11.5	13	10	8	6	4.5	5	1	0	.5	6	6	0	-2	-15	-3	-1.5
5.00	35	37	29	26	22	16	13	13	10	8	6	4.5	5	1	0	.5	-6	3	-3.5	-2	-17	-4	-2
5.50	46	46	35	31	25	19	14	13	10	10	7	4.5	5	1	0	.5	16	6	4	-2	-11	-3	2
6.00	48	44	35	31	25	19	14	13	10	10	7	4.5	5	1	0	.5	12	12	5.5	-2	-9	0	0
6.50	41	41	34	28	25	17.5	14	16	10	10	7	4.5	5	1	0	.5	7	6	0	-2	-9	-1	0
7.00	48	47	38	31	28	19	14	20	12.5	10	7	6	5	2	0	.5	7	1	-1	-2	-11	-3	-1
7.50	81	70	51	46	42	24	22	23	17.5	11	11	8	7	3	0	.5	16	5	0	-2	-11	-4	-1
7.66	81	75	60	51	45	32	23	19	14	13	8	9	9	3	0	.5	12	5	0	-2	-11	-3	-1
8.00	75	70	60	50	42	32	25	20	17.5	14	12	7	7	3	0	.5	9	5	0	0	-11	-3	-1
8.50	58	59	51	42	36	26	22	17	16.5	12	11	6	7	2	0	.5	9	3	0	1	-9	-2	-1
9.00	38	46	40	32	20	21	19.5	16	14	11	10	5	5	1	0	.5	9	3	0	2	-2	0	-5
9.50	24	33	32	26	24	17.5	15	13	12.5	10	9	4.5	3	1	0	.5	4	3	0	2	0	2	-5
10.00	16	26	23	21	18	12	13	12	11	8	8	3.5	3	1	0	.5	0	1	0	2	0	2	-5

TABLE I—Continued
PRESSURE IN POUNDS PER SQUARE FOOT ON THE TS AIRPLANE

	Upper wing											Lower wing											Tail surface								
Station No.-----	1	2	3	4	5	6	7	8	9	10	11	1	2	3	4	5	6	7	8	9	10	11	1	2	3	4	5	6	7	8	
Level flight																															
Air speed (M. P. H.):																															
54.5-----	15	21	23	18	15	12	8	6.5	4	2	0.5	15	20.5	20	14	13.5	12	9	5.5	3.5	2.5	1.5									
62.8-----	19	25	27	25.5	19	13.5	9.5	8	6.5	2	2	15	19	18	14.5	13	12	10	6	4	3	2									
71.0-----	16	23	26.5	25	21	16	12.5	9	6	3	1	8	12.5	13	12	13.5	14	11.5	8	5	3	1.5									
79.0-----	15	21	24	22	21	18	13.5	10.5	7.5	4.5	1.5	0	11	11	9	14	16	13	9	6	4	1.5									
86.3-----	0	14	20	19	21.5	20	16	12	7.5	4.5	2	-16	1	8	6.5	14	18.5	15.5	11	8	6	2									
95.5-----	-12	2	16	17.5	24.5	23	18	13.5	10	6	3	-29.5	-4	2.5	5.5	13	19.5	17	11	9	6	2									
106.0-----	-15	3	11	15	26	25	21	16.5	12	6	2	-36	-25	-3	2	13	20	20	14	10	6	2									
117.0-----	-31	-6	4	9.5	22	21.5	17	11.5	6	1.5	0	-59	-26	-16.5	-13	14	19	18	12	7.5	5	3.5									
127.0-----	-47	-26	-3	5	26	25.5	22	15.5	8	3.5	2	-72	-50	-24	-18	17.5	23	21	14.5	10	6.5	3.5									
Pull-up—power on																															
Time (seconds):																															
0-----			0	10	28	31	22.5	18	12.5	11.5	3.5	-70	-40		-19	22.5	26	26	14.5	13.5	9.3	5.5	-24	-19	-3.5	-3.4	-4	2	0	0	
0.50-----	-48		0	10	28	31	22.5	19.5	14	7	3.5	-70	-42		-19	22.5	26	26	14.5	13.5	9.3	5.5	-25	-19	-11	-16	-12	-37	-18	-7.5	
0.75-----	0		58	58	59	45	34.5	28	19	8	0	0	74		45	60	34	34	21.6	18	10.2	5.5	0	-14	0	-5	-10.2	-27	-12	-5	
1.00-----	82	144	122	109	87.5	64	39.5	31	17.3	7.5	0	78	90		71	64	49	42.5	26	20	11	5.5	30	0	0	-3.4	-9	-23	-10.5	-4	
1.25-----	110	129	128	97	81	59	43.5	29.5	16.5	6.5	0	69	84		61	57	45	36	21.6	18	11		20	0	0	0	-7	-20	-6.5	-3.5	
1.50-----	82	104	106	81	73.5	55.5	37	25	15	5.5	0	56	63		58	48	38	32.5	17.5	16	9.5		15	0	0	0	-5	-14	-5	-2.5	
2.50-----	46	62	58	48	43	35	22.5	16	10	4	0	25	39		33	31	25	22.5	11.4	10	3.5	3	5	0	0	0	-2	-10.2	-2	0	
3.50-----	22	38	33	29	24	14	13.5	9	7.7	2	0	16	27		18	21	16	14	6	5	2	3	3	0	0	0	0	-7	0	0	
Pull-up—power off																															
0-----	-40	-12	0		29	30	24	19.5		7.5	5.5		-48	-28	-16	19	26.5	22.5	12.2	12.5	5.5	0	-31.5	-16.5	-4.5	-6	-5	-4	0		
0.25-----	-40	-12	0		29	30	24	19.5		7.5	5.5		-48	-28	-16	19	26.5	22.5	12.2	12.5	5.5	0	-30	-20	-5.5	-9	-13	-35	-15		
0.50-----			68		64.5	55	39.5	28		9.5	4		42	48	38	36.5	47	34	17.5	18	8.5	0	-36	-20	-5.5	-9	-12	-31	-15.5		
0.75-----	92	164	104		86	66	46	32.5		10	4		94	76	76	48	54	41	20.5	21	10	0	0	-2	0	0	-10	-23	-14		
1.00-----	149		152		98	68	44.8	35.5		9.5	4	89	92	100	76	66	49	41	23.5	20	17.5	0	33	9	0	0	-9	-18	-12.5		
1.25-----	109	128	143		88	64	42	29.5		8.5	4		78	93	66	69	47	37.5	20.5	18	10	0	28	7.5	0	0	-9	-16	-10.5		
1.50-----	82	108	111		75	57	37	28		8	4		65	80	54	55	39	32.5	17.5	17	7.5	0	25	-4	0	0	-9	-12	-9		
1.75-----	72	98	94		67	50	33	26.5	17	8	4		56	68	50	51	39	29	16.5	14.5	7.5	0	14	0	0	0	-7	-11	-9		
Push-down																															
0-----	-50		0		28	31	21	19.2		8.5		-74	-43	-28	-14	19	23	22.3	13.4	13.5	8.3		-30	-16.5	-5.5	-3.2	-3.5	0	0	0	
0.50-----	-50		-44		28	25	20	16.4		7	5.5	-94	-62	-28	-26	19	17	22.3	11.3	12.3	8.3		-43	-16.5	-5	5.5	8.5	40	15.5	4.4	
1.00-----	-96		-59		20	21	13.3	15		7	5.5	-129		-65	-38	7	12	17	10.2	11	8.3		-53	-22.5	-9.8	-4.7	-3.5	19.4	7	1.8	
1.50-----	-96		-21		20	24	16	16.4		8	5.5		-66	-52	-36	9	14	19	12.2	12.3	8.3		-46	-22.5	-9.8	-7.5	-7	0	0	0	
2.00-----	-50		16		32	34	23.8	20.6		9	5.5	-64	-36	-24	-14	-22.5	26	28	26	14.3	13.5	9.3	-25	-19	-4.5	-4.7	-7	0	0	-1.6	
Right turn																															
0-----	0		40		43	40	29	22		8.5	2	-21	0	28	17	40	38	27.5	16.5	12.4	7.5	0		-15	-1.4	-5	-7	-9	-7	-3.5	
0.50-----	36	100	67		59	48	37	26.5		9.5	2	26	56	60	35	48	43	34	18.5	15.7	9.3	0		0	0	-5	-7	-12	-9	-4.5	
1.00-----	82	131	104		74	57	39.5	29.5		9.5	2	73	83	84	68	60	51	37.5	20.5	18	10	0		7.5	2.5	-5	-9	-20	-10.5	-5	
1.50-----	98	117	124		74	55	35.5	28		9	2	71	69	68	68	49	41	30.5	17.5	16.8	10	0		7.5	0	-6	-9	-21	-10.5	-5	
2.00-----	82	95	106		63	47	30.5	23.5		8.5	2	62	68	64	57	44	38	27.5	14.5	14.7	9.3	0		3.5	-5	-6	-10	-21	-10.5	-4.5	
2.50-----	72	86	88		55.5	42	29	22		8.5	2	56	61	60	52	50	34	26	11.3	12.4	7.5	0		0	-5	-5	-9	-18	-10.5	-3.5	
3.00-----	62	76	79		49	37	26.5	20.5		8.5	2	50	61	52	44	35	32	22.5	11.3	10	4.5	0		3.5	0	-3	-7	-16	-9	-3.5	
3.50-----	58	69	69		43	32	24	18		8	2	44	50	44	40	33	28	20.5	10.3	10	3.5	0		5.5	0	-4	-5	-9	-7	-3.5	
4.00-----	30	38	54		36	27	20	15		7	2	24	29	28	26	25	19	10.3	10	4.5	0			3.5	0	-2	-4	-5	-5	-2.5	
4.50-----	12	24	30		28	24	17	13.5		6.5	2	0	14	15	14	21	21	17	9.2	10	4.5	0		0	0	-2	-2	-2	-2	-2	

Left turn																														
0	-28	0	12		36	38	28	22		10	5.5	-53	-28	0	-1.2	26	30	26	15.5	15.8	8.4	0	-19	-12.5	-4.5	-5	-9	-2	-2	-3.5
0.50	0	38	36		48	43	33	25		10.5	4	-12	0	17	14	35	34	29	17.5	17	9.3	0	-10	-9	-2.5	-2	-10	-3	-2	-3.5
1.00	30	58	58		56	50	34.5	28		10.5	4	0	24	30	31	40	39	30.5	28.5	29	9.3	0	0	-4	-1.4	-2	-10	-7	-7	-3.5
1.50	72	129	88		75	57	39.5	29.5		10	2	54	80	84	68	58	49	36	21.5	19	9.3	0	12	0	4	0	-10	-14	-9	-4
2.00	98	110	122		75	55	38	28		9	0	75	80	59	54	45	32.5	32.5	19.5	17	9.3	0	30	10.5	7	0	-10	-12	-7	-4
2.50	82	110	100		65	46	32	25		8	0	62	71	80	59	48	41	30.5	17.5	15.7	8.4	0	15	0	4	0	-7	-12	-9	-1
3.00	72	95	100		57	41	29	22		7	0	56	61	68	47	42	35	26	15.5	12.4	5.5	0	4	0	0	0	-7	-12	-9	-1
3.50	52	84	81		50	37	25	19.5		6.5	0	46	54	60	40	35	30	24	14.4	11	3.5	0	0	-2	0	0	-7	-11	-7	-1
4.00	52	72	72		45	34	21	16.5		8	0	38	45	48	35	29	28	20.5	11.2	10	3.5	0	-3	-6	0	0	-7	-9	-5	-2
4.50	47	62	64		40	31	18.5	15		5.5	0	32	36	44	28	28	26	17	9.2	9	3.5	0	-10	-7.5	0	0	-5	-5	-2	-2.5
5.00	36	50	52		36	28	17	15		5.5	0	23	28	40	24	26	24	17	9.2	7.5	3.5	0	-18	-7.5	0	0	-4	-2	0	-2.5
5.50	30	46	48		34	28	17	15		5.5	0	18	26	40	24	26	24	17	9.2	9	3.5	0	-24	-7.5	0	0	-2	0	0	-2
6.00	23	38	42		32	28	17	15		5.5	0	12	24	36	19	26	24	17	9.2	9	3.5	0	0	-4	0	0	0	4	0	-1
Loop																														
0	58	77		65	47	35	26.5		9	4	32	54	60	50	51	41	34	20.7	14.7	9.3	0	20	0	0	-1.7	-10.5	-14	-9	-3.5	
0.5	82	104		71	50	38.2	26.5		8.5	4	60	71	76	59	54	45	37.5	18.5	14.7	9.3	0	27	9.4	1.6	-1.7	-10.5	-19.6	-9	-3.5	
1.00	76	98	102		67	48	33	25		7.5	4	62	71	72	56	46	41	27.5	16.5	14.7	8.4	0	25	11	1.6	-1.7	-10.5	-16	-9	-3.5
1.50	72	86	89		60	41	30.5	22		6	4	60	64	50	45	36	25.8	15.3	13.5	6.5	0	23	11	1.6	-1.7	-10.5	-14	-6.5	-3.5	
2.00	56	72	79		50	34	25	18		5	4	56	60	52	42	38	30	22.5	14.4	12.3	5.5	0	20	11	1.6	0	-8.6	-10	-6.5	-2.5
2.50	52	55	62		40	27	20	15		4	4	56	50	44	35	31	25	17	11.3	11	4.5	0	19	11	1.6	0	-7	-7	-4.5	-1
3.00	36	36	38		28	19	13.4	10.7		3.2	4	32	38	32	26	23	19	12	7.2	9	3.5	0	17	9.4	1.6	0	-5	-5	-2	0
3.50	30	29	27		21	14	12	7.8		2.7	2	24	26	28	21	20	14	8.6	8	8	2.7	0	15	9.4	1.6	0	-2	-1	-1	0
4.00	24	22	20		15	10	6.8	6.5		2.2	2	20	22	24	14	17	10	7	5	4	1.8	0	14	7.5	1.6	0	-2	0	-1	0
4.50	12	14	14		11	8	5.5	5		2.2	2	14	17	20	12	15	8	7	5	2.5	1.8	0	12	4	1.6	0	-3.6	-1	-2	0
5.00	0	10	10		10	8	5.5	5		2.2	2	12	14	20	12	15	8	7	5	2.5	1.8	0	11	3.5	1.6	0	-3.6	-1.6	-2	0
5.50	0	10	12		11	9	5.5	5		2.2	2	12	14	20	12	15	8	7	5	4	1.8	0	11	3.5	1.6	0	-3.6	-3	-2	0
6.00	12	14	18		15	12	8	7.8		3.2	2	14	17	24	14	17	12	10.5	8	5.3	2.7	0	14	3.5	1.6	0	-3.6	-7	-4.5	0
6.50	24	29	30		23	16	12	10.7		3.6	2	21	29	28	24	23	15	14	8.2	8	3.5	0	15	7.5	1.6	0	-3.6	-8.7	-6.5	0
7.00	30	40	42		30	21	14.5	13.5		4	2	30	38	40	28	28	21	17	10.3	9	4.5	0	17	9.4	1.6	0	-3.6	-8.7	-4.5	0
7.50	36	43	44		36	27	18.5	15		5	2	38	36	36	28	30	23	19	12	10	4.5	0	19	3.5	1.6	-2	-5	-8.7	-9	-1.6
8.00	47	60	60		44	32	22.5	18		6	2	42	45	40	40	37	28	24	14.3	11	5.5	0	22	3.5	1.6	0	-7	-14	-9	-1.6
Dive																														
0	7	18		13	10	5.5	5		2.2	0	10	15	20	12	13	8	7	4	5.2	2.7	0	0	0	0	0	0	0	0	0	0
1.00	-9	0		7	8	5.5	5		3	0	-10	-2	4	0	11	8	7	5	6.5	3.5	0	-10	-7.5	0	0	0	0	0	0	0
2.00	-28	-14		7	9	6.8	8		4	2	-38	-23	-16	-10	9	8	8.5	8	7.5	5.5	0	-17.5	-12.5	-3.5	-2	0	0	0	0	0
3.00	-55	-16		13	15	12	10.8		6	5.5	-56	-35	-20	-16	13	12	14	18	10	6.5	0	-25	-14	-4.5	-3.5	0	0	0	0	0
4.00	-70	-16		17	21	16	15		7	7	-74	-48	-32	-21	15	17	17	10.2	12.5	7.5	0	-34.5	-18	-6.5	-5	-7	0	0	0	0
4.50	-42	0		30	29	22.5	19		8.5	7	-69	-51	-32	-12	19	25	26	14.5	14.5	8.2	0	-17.5	-18	-8.5	-7.5	-7	-12	-6.5	-6.5	
5.00	0	40	38		53	43	33	26.5		10.5	7	-27	0	18	31	36	32.5	19.5	19	9.2	0	-8	-14	-3.5	-5	-8.5	-14	-6.5	-2.5	
6.00	40	70	77		75	51	50	29.5		12	9	7	27	28	33	51	56	39	22.7	21	10.2	0	-6.5	-10.5	-2.5	-3	-10.5	-10.5	-6.5	-2.5

TABLE II
VE-7 AIRPLANE

Air speed (M.P.H.)	Normal accelera- tion (in terms of <i>g</i>)	Upper wing			Angle of attack (degrees)
		Average load (lb./ sq. ft.)	<i>C_{NP}</i>	Center of pressure (per cent chord)	
		Level flight			
42	1	6.5	1.370	23.8	18
44					
50	1	6.6	.950	28.3	12.6
54					
65	1	7.3	.660	26.2	7.5
67					
75	1	7.1	.480	28.8	5.6
77					
85	1	7.8	.410	29.0	4.3
87					
97	1	7.8	.320	30.7	3.1
99					
107	1	7.9	.270	32.1	2.5
117	1	7.7	.220	33.7	2.0
127	1	8.0	.190	32.8	1.6
128					

Time (seconds)	Air speed (M.P.H.)	Normal accelera- tion (in terms of <i>g</i>)	Upper wing			Tail surface			
			Average load (lb./ sq. ft.)	<i>C_{NP}</i>	Moment about leading edge (in. lb.)	Average load on stabilizer (lb./ sq. ft.)	Average load on elevator (lb./ sq. ft.)	Average load on tail (lb./ sq. ft.)	Moment about leading edge (in. lb.)
			Push-down—high speed						
0	126	1.00	7.9	0.203	—650	—2.6	2.4	—0.1	—129
.50	127	1.03	7.5	.189	—642	4.3	13.2	8.7	—1085
1.00	128	— .75	—3.4	.084	—173	—8.6	6.6	— .1	—309
1.25	129	— .90	—3.8	— .093	168	—7.9	4.9	—1.5	—219
1.50	130	— .60	—2.4	— .057	—26	—8.8	—2.9	—5.8	390
2.00	134	2.10	12.8	.288	—995	—2.7	0	—1.4	76
2.50		2.20	13.8		—991	— .9	.5	— .2	13
3.00		2.05	13.1		—986	—1.3	.7	— .3	—20
Push-down—low speed									
0	66	1.00	6.3	0.593	—393	1.1	.5	.8	—60
.50	66	1.00	6.4	.601	—407	1.1	.2	.6	—13
1.00	66	.05	4.8	.451	—299	6.5	8.9	7.0	—766
1.25	66.5	— .25	1.2	.115	—64	—1.3	3.6	1.1	—297
1.50	67	— .35	—1.1	— .097	77	—5.7	1.9	—1.9	—50
1.75	69	— .20	—2.1	— .180	111	—4.8	.8	—2.0	—10
2.00	72	.25	—1.2	— .096	70	—4.4	.2	—2.1	110
2.50	77	.80	1.8	.127	—143	—2.7	— .9	—1.8	125
3.00	83	1.35	6.9	.404	—496	— .2	—1.1	— .6	83

Time (seconds)	Air speed (M.P.H.)	Normal accelera- tion (in terms of <i>g</i>)	Upper wing			Tail surface			
			Average load (lb./ sq. ft.)	<i>C_{NP}</i>	Center of pressure (per cent chord)	Average load on stabilizer (lb./ sq. ft.)	Average load on elevator (lb./ sq. ft.)	Average load on tail (lb./ sq. ft.)	Moment about leading edge (in. lb.)
				Pull-up					
0	126	1.10	10.6	0.269	35.0	0.4	2.3	1.3	-164
.25	126	1.25	11.5	.292	31.6	-3	-8.4	-5.6	645
.50	125	3.50	29.8	.766	24.9	4.9	-13.4	-4.1	520
.75	124	5.40	39.8	1.040	24.7	13.5	-8.3	2.8	474
1.00	120	5.10	34.4	.965	24.8	11.6	-6.4	2.6	292
1.50	107	3.15	20.6	.726	25.8	4.6	-4.2	.4	197
				Right turn					
0	115	1.30	9.4	0.295	31.7	-.6	1.5	.4	-90
1	115	2.05	12.8	.403	28.1	1.3	-.6	.3	26
2	110	2.80	17.1	.584	25.9	4.0	-3.3	.5	186
3	104	3.45	21.4	.820	25.1	7.1	-5.2	1.0	290
4	100	3.20	20.8	.863	26.7	7.8	-5.3	1.3	246
5	102	2.25	15.7	.628	28.3	5.4	-1.3	2.0	30
6	104	1.40	9.8	.376	30.4	.8	0	.4	-16
7	107	1.35	9.7	.350	33.3	-1.7	.1	-.8	0

TABLE II—Continued
VE-7 AIRPLANE—Continued

Time (seconds)	Air speed (M.P.H.)	Normal accelera- tion (in terms of <i>g</i>)	Upper wing			Tail surface			
			Average load (lb./ sq. ft.)	<i>CNF</i>	Center of pressure (per cent chord)	Average load on stabilizer (lb./ sq. ft.)	Average load on elevator (lb./ sq. ft.)	Average load on tail (lb./ sq. ft.)	Moment about leading edge (in. lb.)
Left turn									
0	113	1.45	8.4	0.274	31.4	0	.9	.4	-33
1	110	1.80	10.8	.368	29.5	2.4	-.6	.8	13
2	105	2.30	13.7	.517	27.4	5.1	-3.2	1.0	120
3	98	2.80	18.2	.790	24.1	7.6	-3.6	2.0	130
4	92	2.70	18.3	.900	24.9	2.0	-3.5	-.7	207
5	91	2.35	16.3	.819	24.0	-2.2	-2.0	-2.1	170
6	89	1.30	9.7	.511	25.8	.8	1.5	1.2	-124
7	88	1.00	6.8	.366	26.5	1.2	-1.5	-.2	76
Loop									
0	126	1.20	7.8	0.204	29.4	-4.0	1.0	-1.7	20
.5	126	1.40	8.9	.232	28.1	-4.5	-1.2	-2.9	181
1.0	126	2.45	15.3	.397	27.8	-.1	-4.5	-2.2	348
1.5	124	3.35	22.6	.605	25.9	5.6	-6.4	-.5	407
2.0	120	4.05	26.0	.744	24.9	8.7	-8.6	.3	501
2.5	109.5	4.00	25.6	.876	25.1	10.0	-8.0	1.0	476
3.0	98	3.60	23.2	.991	25.2	8.6	-5.7	1.5	305
3.5	86	2.90	19.4	1.080	25.8	7.5	-4.5	1.8	252
4.0	71.5	2.30	16.0	1.285	25.4	6.3	-3.5	1.5	210
4.5	61	1.80	11.8	1.310	25.7	4.2	-3.4	.4	254
5.0	57	1.45	8.8	1.110	22.4	4.3	-3.7	.2	269
5.5	56	1.30	7.5	.980	18.3	2.0	-2.7	-.4	212
6.0	59	1.40	7.5	.892	21.4	2.2	-2.8	-.3	200
6.5	65	1.70	10.5	1.028	23.0	2.1	-2.5	-.2	200
7.0	73	2.05	12.4	.958	24.4	2.3	-3.9	-.7	256
7.5	82.5	2.55	16.4	.992	22.6	4.0	-4.5	-.3	308
8.0	91.5	3.05	20.5	1.005	24.4	5.4	-4.8	.1	322
8.5	99	3.20	22.0	.919	25.4	5.8	-2.2	1.8	136
Right roll									
0	97	1.05	7.5	0.317	27.9	-.3	1.7	.6	-133
.5	97	1.10	7.4	.314	27.6	-.9	-9.1	-4.9	584
1.0	97	3.10	18.6	.792	23.0	6.5	-6.4	.1	500
1.5	91.5	3.80	30.5	1.495	22.0	4.9	-5.1	0	360
2.0	79	2.80	19.8	1.294	31.6	2.9	-4.6	-.8	266
2.5	67	1.95	11.5	1.045	32.9	3.6	-3.7	0	230
3.0	60	1.40	8.1	.922	28.6	1.9	-3.5	-.8	256
3.5	57	1.10	6.4	.815	24.0	.5	-2.6	-1.0	-219
4.0	58	1.25	7.7	.938	17.9	1.0	-2.3	-.6	150
4.5	62	1.45	9.5	1.006	19.6	1.8	-3.1	-.6	249
5.0	67.5	1.85	12.3	1.105	20.9	2.9	-4.0	-.5	262
5.5	75	2.20	15.1	1.101	20.9	2.8	-3.8	-.5	232
6.0	80	2.40	16.1	1.025	21.1	2.8	-3.6	-.4	203
6.5	85	2.60	16.8	.946	21.1	2.1	-3.0	-.4	173
7.0	87	2.50	16.0	.865	22.3	2.1	-2.9	-.4	186
7.5	87	2.10	12.0	.649	22.2	1.1	-2.0	-.4	143
8.0	85	1.65	9.9	.559	23.4	-.1	-1.8	-.9	-126
8.5	84.5	1.40	8.3	.479	25.2	-.5	-.5	-.4	30
9.0	84	1.30	8.1	.471	25.4	-1.1	.2	-.4	-7
9.5	83	1.25	7.9	.468	25.6	-.8	1.3	.2	-70
10.0	81.5	1.05	7.1	.439	27.1	-.6	1.2	.3	-66
Left roll									
0	85	1.10	7.3	0.412	27.6	.9	1.1	1.0	-101
.5	86	1.10	7.5	.419	27.7	.9	1.1	1.0	-101
1.0	86	1.05	7.2	.402	27.6	.9	1.1	1.0	-101
1.5	87	1.60	7.7	.416	29.6	-3.2	-5.9	-4.6	514
2.0	84.5	3.45	18.1	1.040	23.6	6.6	-7.4	-.4	480
2.25	79.5	3.20	21.6	1.368	23.1	7.5	-5.4	1.1	292
2.5	74.5	2.80	20.8	1.541	25.0	6.3	-4.9	.8	286
3.0	65	2.30	16.3	1.583	25.3	5.1	-4.1	.6	226
3.5	56.5	1.90	13.1	1.679	25.4	4.8	-4.2	.3	226
4.0	50	1.50	10.2	1.673	24.9	3.9	-4.2	-.1	253
4.5	48.5	1.50	9.6	1.679	25.6	2.1	-4.4	-1.1	282
5.0	52	1.70	10.0	1.515	25.9	-1.6	-5.2	-3.4	397
5.5	57	1.85	11.8	1.494	24.3	5.8	-2.3	1.8	63
6.0	63	1.75	11.3	1.165	23.2	6.8	-2.1	2.4	332
6.5	70.5	1.65	11.2	.926	23.1	2.8	-2.1	.4	107
7.0	78	1.90	12.7	.862	24.0	1.4	-3.7	-1.1	252
7.5	84	2.65	18.6	1.082	23.0	4.1	-3.6	.3	196
7.7	85	2.85	20.0	1.105	23.3	3.6	-3.2	.2	164
8.0	86.5	2.70	19.5	1.071	23.8	3.2	-3.4	-.1	187
8.5	87	2.30	15.6	.848	23.5	3.2	-2.7	.2	140
9.0	88.5	1.90	12.9	.675	25.6	3.2	-.6	1.3	-10
9.5	89.5	1.45	10.9	.559	26.9	2.5	.3	1.4	-40
10.0	90.0	1.20	9.1	.466	29.2	.9	.5	.7	-36

TABLE II—Continued

TS AIRPLANE

Air speed (M. P. H.)	Normal accelera- tion (in terms of <i>g</i>)	Upper wing			Lower wing			Angle of attack (degrees)
		Average load (lb./sq. ft.)	<i>C_{NF}</i>	Center of pressure (per cent chord)	Average load (lb./sq. ft.)	<i>C_{NF}</i>	Center of pressure (per cent chord)	
Level flight								
54.5	1	8.2	1.210	29.0	8.1	1.199	28.4	10.95
62.7	1	10.7	1.175	29.8	8.6	.945	31.4	8.3
71	1	12.0	1.039	29.2	8.8	.760	35.4	5.9
79	1	12.3	.845	32.0	9.0	.617	37.6	4
86.7	1	12.3	.711	36.1	9.5	.549	42.3	2.48
95.5	1	13.3	.631	38.5	9.2	.436	46.5	1
106	1	14.5	.541	39.5	9.2	.343	53.0	-1.45
117	1	10.0	.304	41.7	6.7	.204	61.3	-1.5
127	1	11.8	.301	43.7	7.8	.199	67.3	-1.8

Time (sec- onds)	Air speed (M. P. H.)	Normal accelera- tion (in terms of <i>g</i>)	Upper wing			Lower wing			Tail surface				
			Average load (lb./sq. ft.)	<i>C_{NF}</i>	Moment about leading edge (in lb.)	Average load (lb./sq. ft.)	<i>C_{NF}</i>	Moment about leading edge (in lb.)	Average load on stabilizer (lb./sq. ft.)	Average load on elevator (lb./sq. ft.)	Average load on tail (lb./sq. ft.)	Moment about leading edge (in lb.)	Elevator angle (degrees)
					Push-down								
0	128	1.00	14.8	0.373	-1,840	9.2	0.230	-1,564	-11.8	1.8	-5.8	93	-6.5
.50	128.5	.05	10.00	.248	-1,613	5.6	.139	-1,405	-10.1	17.7	2.1	-747	-19
1.00	131.5	-.15	5.3	.124	-1,380	.4	.009	-1,112	-19.3	9.0	-7.2	-140	-9
1.50	132	.55	9.7	.225	-1,639	2.4	.055	-1,266	-19.3	-.7	-10.6	280	-4
2.00	132.5	1.55	18.6	.429	-2,160	12.8	.295	-2,186	-12.0	-.7	-7.0	220	-1.5

Time (sec- onds)	Air speed (M. P. H.)	Normal accel- eration (in terms of <i>g</i>)	Upper wing			Lower wing			Tail surface							
			Average load (lb./ sq. ft.)	<i>C_{NF}</i>	Center of pres- sure (per cent chord)	Average load (lb./ sq. ft.)	<i>C_{NF}</i>	Center of pres- sure (per cent chord)	Average load on stabi- lizer (lb./sq. ft.)	Average load on elevator (lb./sq. ft.)	Average load on tail (lb./sq. ft.)	Moment about leading edge (in lb.)	Elevator angle (degrees)	Rudder angle (de- grees)	Aileron angle (de- grees)	
							Pull-up—power on									
0	126	1.00	15.0	0.412	46.0	9.8	0.258	65.7	−10.2	.7	−5.6	133	−5			
.50	126.5	1.00	15.1	.387	45.6	10.6	.272	61.6	−16.9	−19.0	−17.7	1,199	16			
.75	127	3.45	30.6	.779	33.0	29.6	.754	32.8	−6.1	−13.9	−9.7	760	16.5			
1.00	126	4.90	46.6	1.225	27.2	36.9	.966	31.9	1.7	−11.6	−3.9	613	18			
1.25	124.5	4.35	43.4	1.160	27.1	32.1	.858	31.5	1.7	−9.6	−3.4	453	18			
1.50	119	3.40	37.8	1.119	27.6	27.5	.814	31.7	1.4	−6.5	−2.0	313	18			
2.50	96.5	2.00	23.1	1.057	28.6	17.2	.786	31.3	−.7	−2.7	−1.4	173	9			
3.50	75	1.25	12.9	.993	30.5	10.8	.832	30.1	.3	−2.5	−.9	113	7.5			
							Pull-up—power off									
0	126	1.00	16.1	.427	44.2	8.5	.226	61.0	−12.6	−.7	−7.4	226	−4			
.25	126	1.00	16.1	.427	44.2	8.5	.226	61.0	−17.0	−14.6	−16.0	226	15			
.50	125	2.2	35.0	.929	33.0	25.6	.679	34.2	−16.6	−15.5	−16.2	965	18			
.75	121	4.3	46.2	1.317	29.5	34.9	.995	31.2	−2.7	−13.0	−7.0	646	20.5			
1.00	117.5	4.95	52.3	1.585	28.1	38.2	1.157	31.6	6.5	−11.0	−1.3	500	22			
1.25	114	3.95	45.7	1.480	27.8	34.6	1.120	30.3	5.8	−9.2	−.6	426	22			
1.50	112.5	3.45	39.4	1.305	29.7	27.9	.924	29.7	2.0	−8.3	−2.3	419	21			
1.75	109.5	3.15	36.1	1.250	29.8	26.2	.908	31.0	1.2	−7.4	−2.3	366	20.5			

TABLE II—Continued
TS AIRPLANE—Continued

Time (sec- onds)	Air speed (M. P. H.)	Normal accel- eration (in terms of <i>g</i>)	Upper wing			Lower wing			Tail surface							
			Aver- age load (lb./ sq. ft.)	<i>C_{NP}</i>	Center of pres- sure (per cent chord)	Aver- age load (lb./ sq. ft.)	<i>C_{NP}</i>	Center of pres- sure (per cent chord)	Average load on stabi- lizer (lb./sq. ft.)	Average load on elevator (lb./sq. ft.)	Average load on tail (lb./sq. ft.)	Moment about leading edge (in lb.)	Elevator angle (degrees)	Rudder angle (de- grees)	Aileron angle (de- grees)	
Right turn																
0	127	1.15	24.5	.624	35.2	19.1	.486	37.6	-7.0	-6.3	-6.7	433	0	5.5	10	
.50	125	2.75	33.4	.894	31.3	26.5	.709	33.3	-2.2	-7.8	-4.7	447	7	10.5	11	
1.00	120.5	4.05	41.0	1.170	29.1	33.7	.960	29.7	.7	-11.2	-4.4	553	17	11.5	8.5	
1.50	113.5	4.30	42.2	1.375	27.7	28.9	.944	29.9	-.3	-10.9	-5.0	560	19.5	11.0	4.5	
2.00	105.5	3.55	35.8	1.363	28.2	26.4	1.005	29.3	-1.7	-11.4	-5.9	593	20	7.5	-1	
2.50	98	3.25	32.2	1.439	28.8	25.6	1.142	29.3	-2.9	-12.1	-6.9	550	20.5	2.5	-4	
3.00	91	2.90	28.4	1.456	29.9	20.4	1.046	28.5	-.9	-8.7	-4.2	460	21.5	0	-5.5	
3.50	86	2.65	25.0	1.455	30.4	18.7	1.090	29.1	-.5	-5.6	-2.6	320	19	-1	-7	
4.00	83.5	2.20	20.6	1.282	30.4	14.9	.925	32.8	0	-4.0	-1.7	206	8.5	-1	-9	
4.50	83.5	1.55	15.7	.978	34.4	11.5	.718	37.6	-.9	-1.8	-1.4	60	8	1	-9.5	
Left turn																
0	126	1.45	20.0	.520	42.8	13.4	.348	49.2	-10.3	-2.7	-7.0	313	3	2	-10	
.5	124	2.30	26.4	.716	37.0	18.5	.502	41.0	-6.2	-3.1	-4.9	280	5	-7	-11.5	
1.0	123	2.70	31.7	.870	34.2	25.1	.690	40.0	-3.3	-5.4	-4.1	353	7	-7.5	-11.5	
1.5	118.5	3.85	40.2	1.200	29.9	33.0	.985	30.5	1.2	-8.5	-3.0	420	18.5	-7.5	-2.5	
2.0	111	4.35	41.3	1.393	28.3	30.8	1.040	29.9	7.9	-7.6	1.3	306	16	-8	-1.5	
2.5	104.5	3.75	35.3	1.372	28.6	28.5	1.109	30.3	3.6	-6.7	-.8	293	17	-8	0	
3.0	97	3.40	32.4	1.468	27.7	24.7	1.118	28.8	-1.0	-7.4	-3.7	386	16	-8	1	
3.5	91	2.90	27.9	1.450	28.8	21.1	1.096	28.6	-2.1	-6.0	-3.7	320	12	-8	2.5	
4.0	86.5	2.55	24.8	1.425	28.4	18.1	1.040	29.8	-3.2	-4.7	-4.0	293	10	5.5	4.5	
4.5	85.5	2.10	22.4	1.327	28.6	16.1	.954	29.8	-4.3	-2.9	-3.7	207	5.5	.5	7.5	
5.0	85.5	1.80	19.6	1.160	30.1	14.3	.845	29.9	-5.6	-1.8	-4.0	160	1.5	3	8.5	
5.5	86.5	1.70	18.8	1.080	30.9	14.4	.827	31.3	-6.7	-.7	-4.1	113	0	3.5	9	
6.0	88.5	1.55	17.8	.978	31.4	14.0	.769	32.3	-1.0	.9	-.2	-20	-2.5	4	9	
Loop																
0	117.5	3.00	34.1	1.040	30.8	27.7	.845	32.0	1.4	-8.3	-2.4	434	8.5	-----	-----	
.5	110.5	3.95	38.8	1.342	28.7	30.7	1.062	30.3	5.0	-10.3	-1.8	494	15	-----	-----	
1.0	102	3.75	36.7	1.459	28.1	27.2	1.080	29.9	5.1	-9.0	-1.0	400	17	-----	-----	
1.5	97	3.25	31.9	1.444	28.6	25.0	1.130	29.1	5.0	-7.6	-.5	361	19.5	-----	-----	
2.0	88	2.85	27.4	1.505	27.7	21.8	1.199	29.7	4.6	-5.6	.2	247	19.5	-----	-----	
2.5	77.5	2.10	21.6	1.483	28.7	18.0	1.236	29.1	5.1	-4.5	1.0	173	19.5	-----	-----	
3.0	68	1.65	15.2	1.428	30.6	13.2	1.239	30.5	4.4	-2.5	1.5	87	19	-----	-----	
3.5	57.5	1.15	11.4	1.512	29.9	10.4	1.380	29.9	5.0	-.7	2.3	0	18	-----	-----	
4.0	51	.80	8.1	1.483	31.1	7.9	1.448	28.9	3.9	-.4	2.0	0	18	-----	-----	
4.5	45	.65	6.0	1.359	35.0	7.1	1.608	28.9	2.6	-1.6	.9	50	17	-----	-----	
5.0	41	.55	5.3	1.360	36.0	6.9	1.770	28.3	.9	-1.1	0	67	15.5	-----	-----	
5.5	45	.60	6.7	1.518	33.2	6.9	1.561	30.4	2.6	-1.6	.8	67	14.5	-----	-----	
6.0	50	.75	8.2	1.500	35.4	9.1	1.666	30.0	2.9	-3.8	0	160	13.5	-----	-----	
6.5	56	1.35	13.0	1.853	31.9	12.2	1.740	30.9	4.1	-4.7	.3	173	13.5	-----	-----	
7.0	64	1.65	16.2	1.780	31.5	15.2	1.670	30.6	4.6	-4.3	.8	153	5.5	-----	-----	
7.5	70	1.85	18.9	1.580	32.9	16.2	1.355	35.4	2.9	-6.0	-1.0	280	5.5	-----	-----	
8.0	81.5	2.20	24.1	1.571	29.8	20.2	1.319	30.9	3.8	-7.6	-1.3	347	10	-----	-----	
Dive																
0	52	.75	6.9	1.154	31.2	6.9	1.154	31.9	0	0	0	0	-2.5	-----	-----	
1.0	63	.40	4.6	.506	48.5	5.2	.571	46.5	-4.3	0	-2.4	53	-4.5	-----	-----	
2.0	79.5	.25	3.7	.254	66.3	3.3	.227	78.4	-7.3	0	-4.3	86	-6	-----	-----	
3.0	95.5	.30	5.7	.268	65.8	5.3	.249	79.5	-9.1	0	-5.1	113	-6	-----	-----	
4.0	111	.35	8.8	.299	67.7	5.3	.180	78.0	-13.7	-.7	-8.0	193	-5.5	-----	-----	
4.5	119	.85	16.1	.473	46.5	9.3	.273	62.7	-12.0	-6.7	-9.8	540	3.5	-----	-----	
5.0	122.5	2.05	28.2	.786	37.1	19.0	.529	45.1	-8.2	-7.4	-7.9	507	3.5	-----	-----	
6.0	130	3.40	41.0	.994	32.3	28.6	.693	36.0	-7.3	-6.3	-6.6	440	1.5	-----	-----	

REPORT No. 258

SOME FACTORS AFFECTING THE REPRODUCIBILITY OF PENETRATION AND THE CUT-OFF OF OIL SPRAYS FOR FUEL-INJECTION ENGINES

By E. G. BEARDSLEY
Langley Memorial Aeronautical Laboratory

REPORT No. 258

SOME FACTORS AFFECTING THE REPRODUCIBILITY OF PENETRATION AND THE CUT-OFF OF OIL SPRAYS FOR FUEL-INJECTION ENGINES

By E. G. BEARDSLEY

SUMMARY

This investigation was undertaken at the Langley Memorial Aeronautical Laboratory at Langley Field, Virginia, in connection with a general research on fuel-injection engines for aircraft. The purpose of the investigation was to determine the factors controlling the reproducibility of spray penetration and secondary discharges after cut-off.

The development of single sprays from automatic injection valves was recorded by means of special high-speed photographic apparatus capable of taking 25 consecutive pictures of the moving spray at a rate of 4,000 per second. The effects of two types of injection valves, injection-valve tube length, initial pressure in the injection-valve tube, speed of the injection control mechanism, and time of spray cut-off, on the reproducibility of spray penetration, and on secondary discharges were investigated.

It was found that neither type of injection valve materially affected spray reproducibility. The initial pressure in the injection-valve tube controlled the reproducibility of spray penetrations. An increase in the initial pressure or in the length of the injection-valve tube slightly increased the spray penetration within the limits of this investigation. The speed of the injection-control mechanism did not affect the penetration.

Analysis of the results indicates that secondary discharges were caused in this apparatus by pressure waves initiated by the rapid opening of the cut-off valve. The secondary discharges were eliminated in this investigation by increasing the length of the injection-valve tube.

INTRODUCTION

During an investigation of the characteristics and development of the sprays from several types of automatic fuel injection valves, designed for use in high-speed fuel-injection engines, considerable difficulty was experienced in obtaining the same spray penetrations, when using the same injection valve under seemingly similar conditions. Also spray discharges, of much smaller mass and at lower pressure than the main sprays, took place after cut-off. These small spray discharges will be referred to in this report as "secondary discharges." These and similar phenomena are undoubtedly present in many injection systems, but have generally remained undiscovered because there has been no apparatus available capable of recording them.

To obtain smooth operation in high-speed fuel-injection engines, running at constant speed and load, it is necessary that a constant quantity of fuel be injected each cycle, and that the sprays produced be alike in all respects. The spray cut-off must take place quickly and in most cases there must be no secondary discharges if the highest efficiency is to be obtained. The work presented in this report deals with the effects of two types of injection valve designs, injection-valve tube length, initial pressure in the injection-valve tube, speed of the injection control mechanism, and time of spray cut-off, on the reproducibility of spray penetration, and

by the curves A and B in Figure 2. The divergence of the points from the mean curves indicates that the reproducibility of the sprays is not appreciably different for either of these two

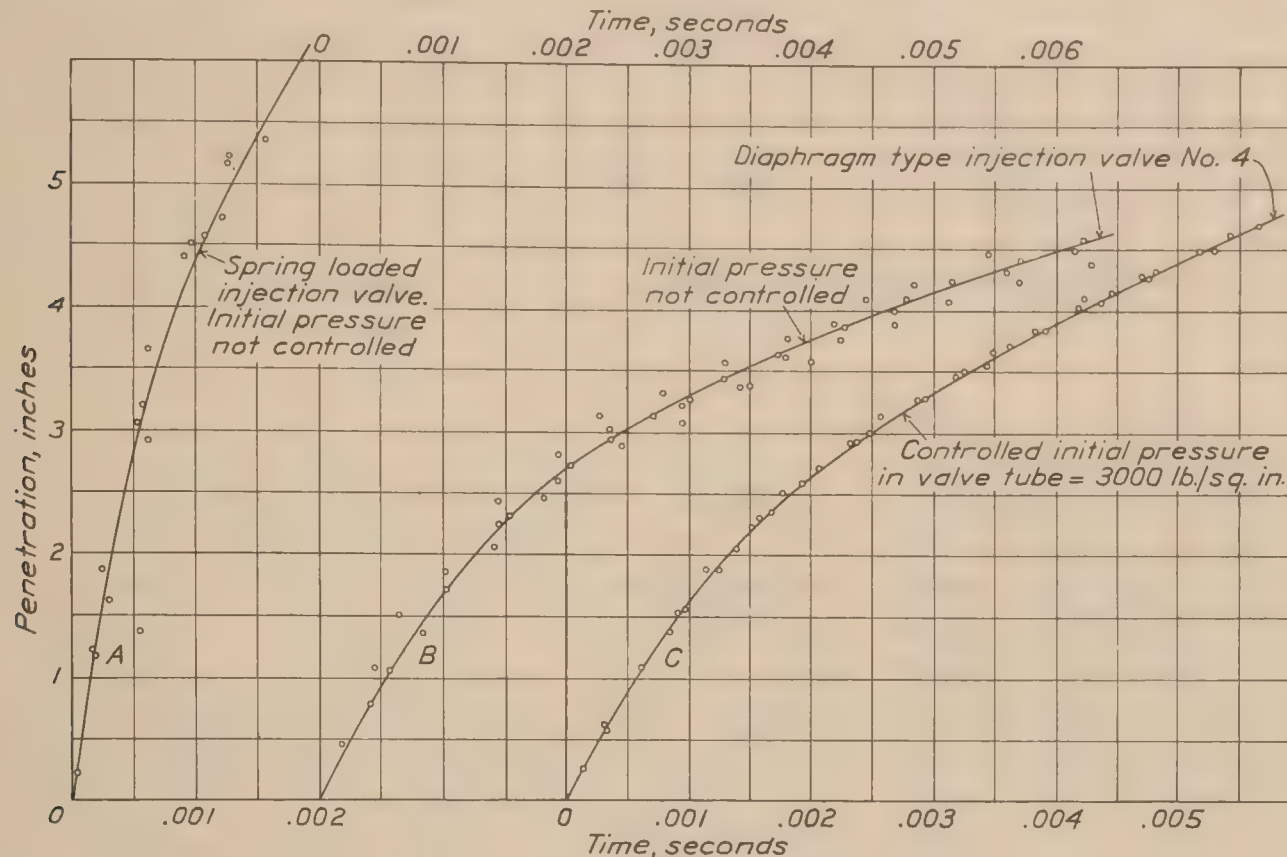


FIG. 2.—Effect of controlling initial pressure in injection-valve tube. Each curve is the result of four experiments. Injection pressure, 8,000 lb./sq. in.; chamber pressure, 400 lb./sq. in. No cut-off. Valve tube length, 7 inches

types of injection valves. Difference in the design of the two valves caused the different penetration of the spray from one as compared with the other.

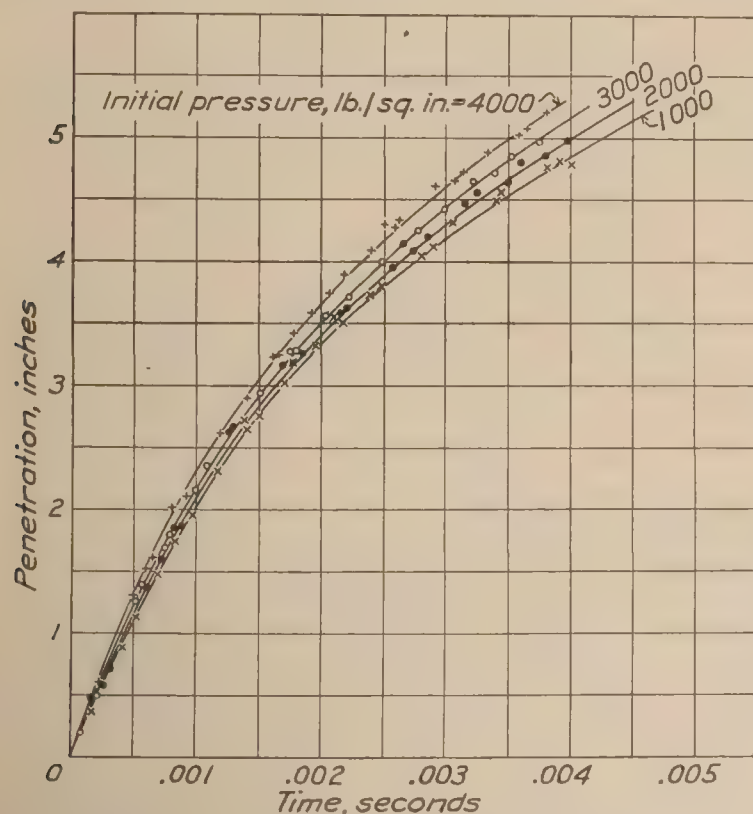


FIG. 3.—Effect of initial pressure in injection-valve tube. Each curve is the result of three experiments. Injection pressure, 8,000 lb./sq. in.; chamber pressure, 200 lb./sq. in. Injection valve No. 4. Injection valve tube length, 41 in. Cut-off after 0.003 seconds

The effect of controlling the initial pressure in the injection-valve tube is shown, for the diaphragm-type injection valve, by curves B and C in Figure 2. These results indicate that when the initial pressure in the injection-valve tube is controlled to a definite value good reproducibility is obtained.

The initial pressure in the injection-valve tube may vary in successive tests if not controlled. The amount of this variation depends upon the pressure at which the injection valve closes after discharge, upon the rate of leakage in the system, and upon the time interval between tests. Accordingly, tests were made with several controlled initial pressures to determine their effect upon the spray penetration.

The results of these tests, in which the initial pressure was controlled to 1,000, 2,000, 3,000, and 4,000 pounds per square inch are shown in Figure 3. The penetration was found to increase about 3 per cent with each 1,000 pounds per square inch increase in the initial pressure.

The initial pressure in the injection-valve tube acts directly against the end of the timing-valve needle. The effects of the intensity of this pressure upon the rate of opening of the timing

valve and the rate of pressure rise in the injection-valve tube have been considered in analyses of the results. Although these factors have some effect upon the penetration, a consideration of the characteristics of pressure waves seems to offer the best explanation of this phenomenon. The behavior of pressure waves, such as are initiated when the timing valve is opened, may be compared to the behavior of sound waves in a liquid. Merriman's *Hydraulics* (Reference 2) gives the velocity of sound in a liquid, as

$$V = \sqrt{\frac{Eg}{W}} \quad (1)$$

E is equal to $\frac{P}{\theta}$, which, substituted in (1) gives

$$V = \sqrt{\frac{Pg}{W\theta}} \quad (2)$$

The notation used is as follows:

V = Velocity of sound.

E = Modulus of elasticity of the liquid.

P = Pressure on the liquid.

θ = Coefficient of cubical compression of liquid.

W = Weight of a cubical unit of the liquid.

g = The acceleration of gravity.

The values of g and θ are constant, and W varies only slightly for a liquid, with change in pressure. From formula (2) it can be seen that the velocity of a sound wave varies almost

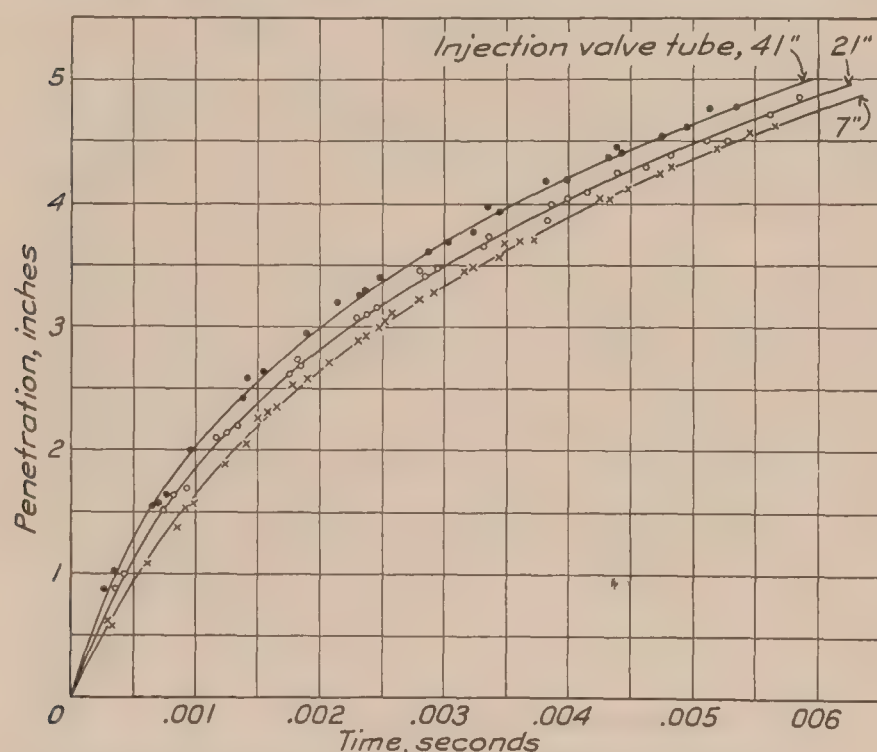


FIG. 4.—Effect of injection-valve tube length. Each curve is the result of three experiments. Injection pressure, 8,000 lb./sq. in. Chamber pressure, 400 lb./sq. in. Injection-valve No. 4. Cut-off after 0.003 seconds. Initial pressure, 3,000 lb./sq. in.

pressure wave. The discharge caused by the pressure impulse occurred at the beginning of injection and was of very short duration in comparison with the total discharge, which explains why only slightly increased penetration was obtained for large increases in the initial pressure in the injection-valve tube.

The results for the tests with the 7-inch, 21-inch, and 41-inch injection-valve tube lengths are shown in Figure 4. The spray penetration was increased slightly, with increase in the injection-valve tube length, within the limits investigated.

Experiments have been made relating to the behavior of pressure waves in air contained in small tubes by the Aeronautical Research Committee of Great Britain, the results of which are given in their reports and memoranda No. 957. (Reference 3.) The results of these tests

directly with the square root of the pressure. Thus the velocity of a sound wave in a liquid at 4,000 pounds per square inch pressure will be about twice the velocity for 1,000 pounds per square inch pressure. This analysis indicates that the velocity of a pressure wave in the injection-valve tube would increase with the initial pressure on the liquid.

Since equal injection pressures were used for all tests, the pressure impulses released by the timing valve to the injection-valve tube were of approximately the same magnitude for the several initial pressures used. The impact energy of the pressure impulse at the injection valve was, however, approximately equal to $\frac{1}{2} MV^2$. Thus the instantaneous pressure available for impulse discharge increased directly with the square of the velocity of the

show that in some cases the pressures, recorded at the far end of a closed tube, increased considerably as the length of the tube was increased. An effect similar to that indicated by these results might well have existed in the injection system and produced the greater spray penetrations recorded.

In order to determine the effect of the rate of opening of the timing valve on the spray penetration, tests were made with cam-shaft speeds of 550, 750, 900, and 1,100 revolutions per minute. The results of these tests show that the spray penetration was the same for the four rates of opening of the timing valve investigated. The rate of pressure rise in the injection-valve tube was not controlled, therefore, by the rate of opening of the timing valve in these tests. This indicates that the maximum rate of pressure rise at the injection valve was obtained with the slowest cam-shaft speed.

SECONDARY DISCHARGES

The results for the investigation of the effect of the type of injection valve used, the time of cut-off, and injection-valve tube length on the occurrence of secondary discharges and the time at which they appeared are shown in Table I. The results in Table I are given to the nearest hundred-thousandth second. By measurement to a hundredth of an inch on the film records, time computations can be made to 0.000003 second, so it can be seen that the results given in the table are within the limit of accuracy. Spray pictures taken during the investigation are shown in Figures 5 and 6. Figure 5 shows two sprays with typical secondary discharges, and Figure 6 two similar sprays with no secondary discharges. The secondary discharges may be seen to have their start in the third or fourth spray from the left in both pictures of Figure 5. Although a series of 25 pictures were taken of each spray, it was not thought necessary to show all of them in this report. The sprays are one-third actual size.

The start of the cut-off of the spray and of the secondary discharges are not always recorded by the films, since these events often occur in the time interval between consecutive illuminations. The variation in the time of the spray reappearance after cut-off as given in Table I is probably caused by the necessity for estimating the exact beginning of the cut-off, and of the secondary discharge by extrapolating slightly, curves plotted from measurements of the film.

The results of the tests with the spring-loaded and diaphragm-type injection valves show that similar secondary discharges were obtained with both valves. Also the time of appearance of the secondary discharges after cut-off of the spray was approximately the same.

Tests were made with cut-off approximately 0.0018, 0.0034, and 0.0048 second after the start of the spray, using an injection-valve tube 7 inches long. The results of the tests with cut-off after 0.0018 and 0.0034 second show that the secondary discharges took place at approximately the same time interval after spray cut-off. This indicates that these secondary discharges were controlled by the cut-off valve and not by the timing valve. No secondary discharge appeared with cut-off after 0.0048 second. In this case the timing valve was nearly closed and the pressure impulse of any oil which passed through it was too low to open the automatic injection valve.

Bouncing of the moving parts of the injection valves after their impact at cut-off has been considered in analyses of the secondary discharge phenomena. For example, the nozzle-diaphragm unit of the diaphragm-type injection valve might vibrate according to its natural period, or might rebound because of its impact upon the fixed stem. However, the results of the investigation show that no secondary discharge appeared when a 41-inch injection valve tube was used in place of the 7-inch tube. It is probable that the length of the injection-valve tube would have little effect upon the vibration of the moving parts of the injection valve. If bouncing of the moving parts caused secondary discharges, the discharges would undoubtedly have taken place at different time intervals after cut-off for the two types of valve used. Table I shows, however, that the intervals were approximately the same for both valves. For these reasons, the results indicate that bouncing of the moving parts did not cause secondary discharges.



Injection pressure, 8,000 lb./sq. in., chamber pressure, atoms



Injection pressure, 8,000 lb./sq. in., chamber pressure, 400 lb./sq. in.

FIG. 5.—Oil spray with secondary discharge



Injection pressure, 8,000 lb./sq. in., chamber pressure, atoms



Injection pressure, 8,000 lb./sq. in., chamber pressure, 400 lb./sq. in.

FIG. 6.—Oil spray without secondary discharge

A brief analysis of pressure wave phenomena and of the operation of the apparatus in relation to the secondary discharge phenomena has been made. When the cut-off valve was opened, the pressure in the injection-valve tube was released so that the injection valve closed and cut off the spray. It is probable that the pressure on the oil in the injection-valve tube was so rapidly released that although the timing valve was still open the inertia of the oil in the supply system made increased flow through the timing valve impossible for an instant. When increased flow through the timing valve took place, its impact on the oil in the injection-valve tube, which was directly in line with the timing valve, may have created a pressure wave which caused a small spray to discharge from the injection valve.

No secondary discharges appeared in any of the tests with the 41-inch injection-valve tube length. In this case it is probable that the pressure wave was damped out by the resistance of the long tube, or absorbed by the compression of the oil and expansion of the tube. The pressures which caused the secondary discharges were never much above the opening pressure of the injection valve. It would not, therefore, have taken much resistance to damp out the pressure waves sufficiently to have prevented them from opening the valve and causing secondary discharges.

Although the secondary discharges were controlled in this investigation by increasing the length of the injection-valve tube, there are undoubtedly other ways to control these phenomena. Thus, rearrangement of the injection-control apparatus, change in the relative size and shape of various parts, or the use of other injection pressures, might govern secondary discharges.

CONCLUSIONS

The results of these experiments indicate that the initial pressure in the injection-valve tube must be controlled to obtain spray reproducibility. The spray penetration is slightly increased by increasing the length of, or the initial pressure in, the injection-valve tube.

Secondary discharges may be caused by pressure waves in the injection system during and after spray cut-off. Though secondary discharges were eliminated in this investigation by increasing the length of the injection-valve tube, they could probably be controlled by changing the location or size of various parts of the spray production and control apparatus, and by using different injection pressures.

TABLE I.—Effect of cut-off, injection valve tube length, and type of valve on secondary discharges

Test No.	Valve No.	Valve type	Angle of spiral grooves	Orifice diameter	Valve tube length	Cut-off time	Spray reappearance time	Reappearance time after cut-off
			Degrees	Inches	Inches	Second	Second	Second
1.....	4	Diaphragm.....	30	0.022	7	0.00178	0.00213	0.00035
1.....	4	do.....	30	.022	7	.00190	.00220	.00030
1.....	4	do.....	30	.022	7	.00180	.00219	.00039
2.....	4	do.....	30	.022	7	.00336	.00375	.00039
2.....	4	do.....	30	.022	7	.00345	.00377	.00034
2.....	4	do.....	30	.022	7	.00337	.00367	.00030
3.....	4	do.....	30	.022	7	.00490	None.	-----
3.....	4	do.....	30	.022	7	.00485	None.	-----
3.....	4	do.....	30	.022	7	.00480	None.	-----
4.....	4	do.....	30	.022	41	.00199	None.	-----
4.....	4	do.....	30	.022	41	.00180	None.	-----
4.....	4	do.....	30	.022	41	.00184	None.	-----
5.....	3a	Spring loaded.....	23	.029	7	.00275	.00312	.00037
5.....	3a	do.....	23	.029	7	.00275	.00310	.00035
5.....	3a	do.....	23	.029	7	.00272	.00307	.00035

The effect of time of cut-off is shown by tests 1, 2, and 3.
The effect of injection-valve tube length is shown by tests 1 and 4.
The effect of type of valve is shown by tests 2 and 5.

REFERENCES AND BIBLIOGRAPHY

REFERENCE 1. HAROLD E. MILLER, and EDWARD G. BEARDSLEY. Spray Penetration with a Simple Fuel Injection Nozzle. N. A. C. A. Technical Report No. 222. 1926.

REFERENCE 2. MANSFIELD MERRIMAN. Treatise on Hydraulics, 1916, 10th Ed. New York, John Wiley and Son (Inc.).

REFERENCE 3. L. F. G. SIMMONS, and F. C. JOHANSEN. Experiments on Transmission of Air Waves Through Pipes. British Aeronautical Research Committee Reports and Memoranda No. 957. 1925.

K. J. E. HESSELMAN. Hesselman Heavy Oil High-Compression Engine. N. A. C. A. Technical Memorandum No. 312. 1924.

REPORT No. 259

**CHARACTERISTICS OF PROPELLER SECTIONS
TESTED IN THE VARIABLE DENSITY
WIND TUNNEL**

**By EASTMAN N. JACOBS
Langley Memorial Aeronautical Laboratory**

REPORT No. 259

CHARACTERISTICS OF PROPELLER SECTIONS TESTED IN THE VARIABLE DENSITY WIND TUNNEL

By EASTMAN N. JACOBS

SUMMARY

Tests were carried out in the variable density wind tunnel of the National Advisory Committee for Aeronautics on six airfoil sections used by the Bureau of Aeronautics as propeller sections. The sections were tested at pressures of 1 and 20 atmospheres corresponding to Reynolds Numbers of about 170,000 and 3,500,000. The results obtained, besides providing data for the design of propellers, should be of special interest because of the opportunity afforded for the study of scale effect on a family of airfoil sections having different thickness ratios.

DESCRIPTION OF TESTS

A description of the tunnel and of the general methods of testing airfoils may be found in Reference 1. The usual 5 by 30-inch duralumin airfoils were used. The models have flat lower surfaces and the maximum thickness at one-third of the chord from the leading edge. The radius of the leading edge is one-tenth of the maximum ordinate. The maximum ordinates are: 0.04, 0.08, 0.10, 0.12, 0.16, and 0.20 of the chord. The ordinates of all of the sections may be obtained from those of the thickest section by reducing all of the ordinates in the same ratio as the maximum ordinate. The ordinates of all of the upper surfaces are given in Table I.

Tests were carried out on each airfoil to determine the lift, drag, and moment coefficients at different angles of attack. The tests were made at pressures of approximately 1 and 20 atmospheres, giving Reynolds Numbers of about 170,000 and 3,500,000.

RESULTS AND DISCUSSION

Figures 1 and 2 are the curves of lift coefficients plotted against angle of attack for all sections. Those in Figure 1 are from the 1 atmosphere tests and those in Figure 2, from the 20 atmosphere tests. These curves show the effect of changing the thickness of a section at a low Reynolds Number and at a high Reynolds Number.

Figures 3 and 4 are the curves of lift coefficients plotted against drag coefficients for all sections, from the 1 and 20 atmosphere tests, respectively. These curves show that the profile drag increases uniformly with thickness, over the range where it is fairly constant, for both the small and the large Reynolds Number tests. However, the range of constant profile drag is greater at the large Reynolds Number. The extremely low drag measured for the thinnest airfoil may be erroneous since it was set up differently.

In the same manner, curves of drag per unit lift (D/L) are drawn in Figures 5 and 6. The straight line representing the induced drag per unit lift for aspect ratio 6 is plotted on the same sheets.

The next set of curves, Figures 7 to 12, show the complete characteristics and also the scale effect on each section by means of the drag (polar curves), and moment coefficient plotted against lift coefficient. The solid curves represent the 20-atmosphere tests and the dotted curves the 1-atmosphere tests. The same data will be found in tabular form in the Tables numbered III to XIV.

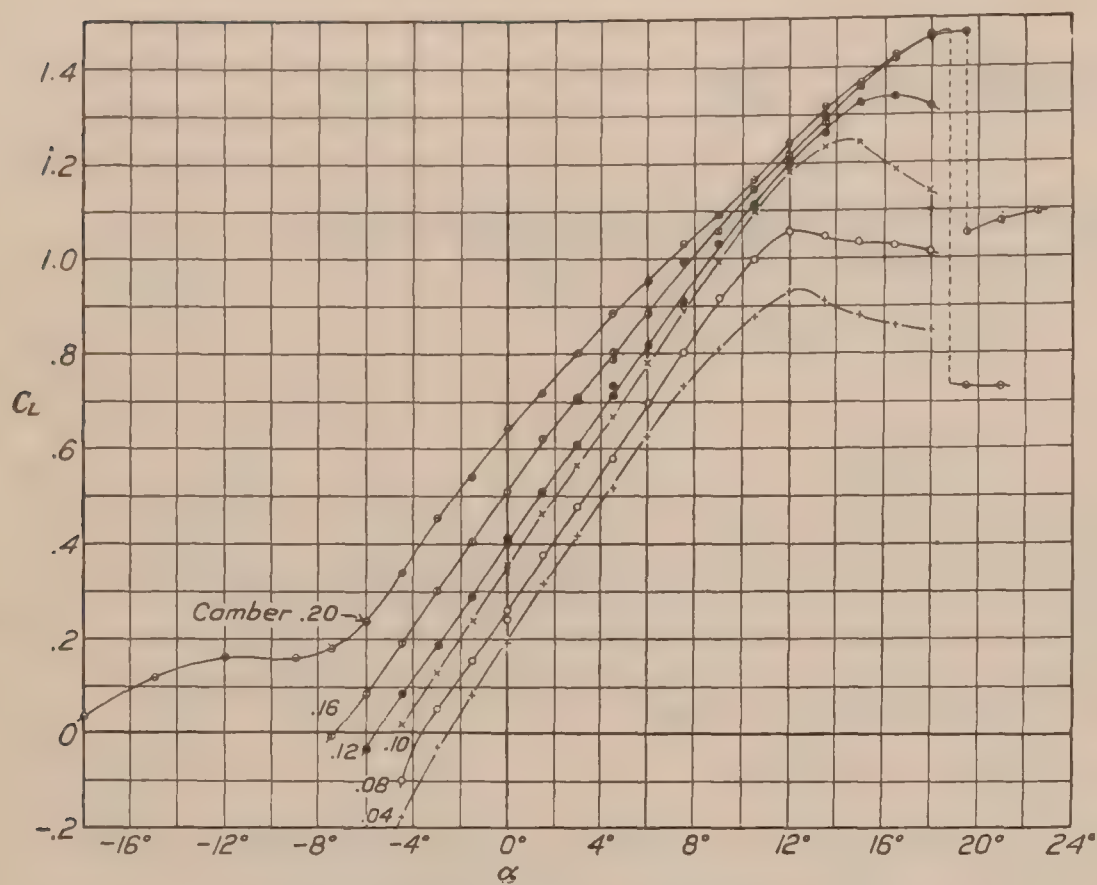


FIG. 1.—Lift curves from tests at 1 atmosphere

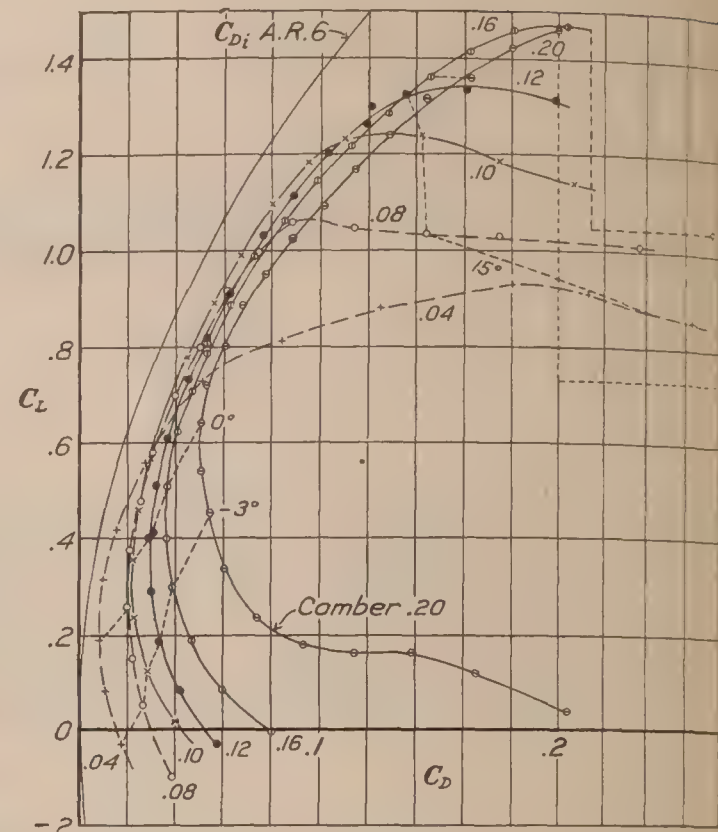


FIG. 3.—Polar curves from tests at 1 atmosphere

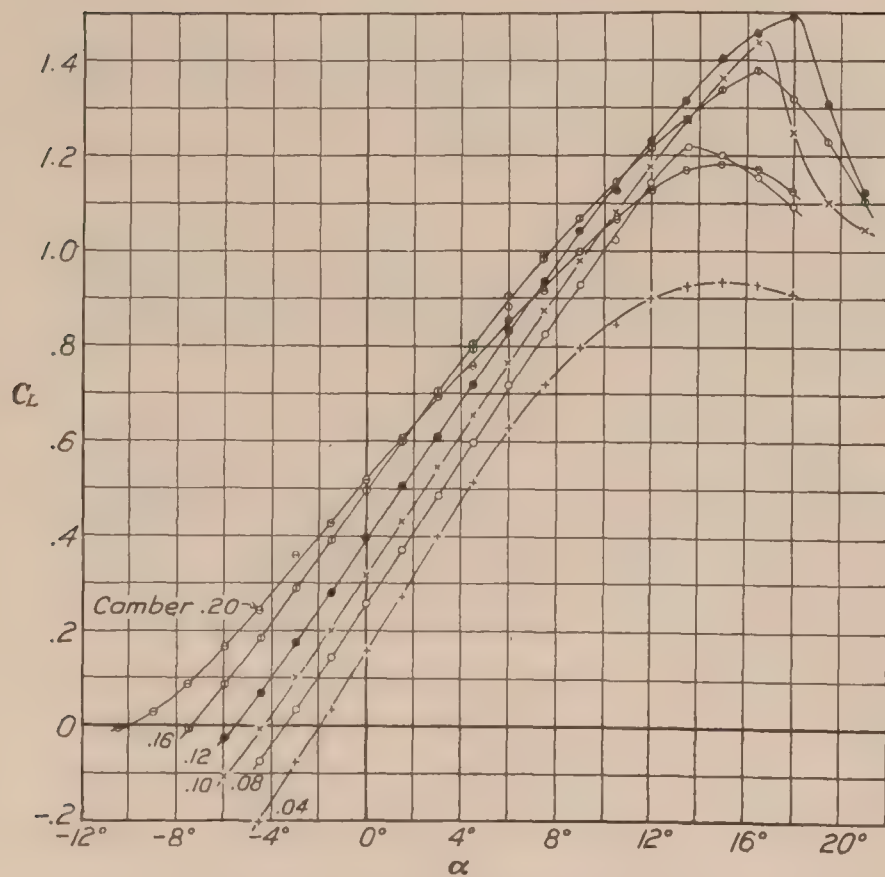


FIG. 2.—Lift curves from tests at 20 atmospheres

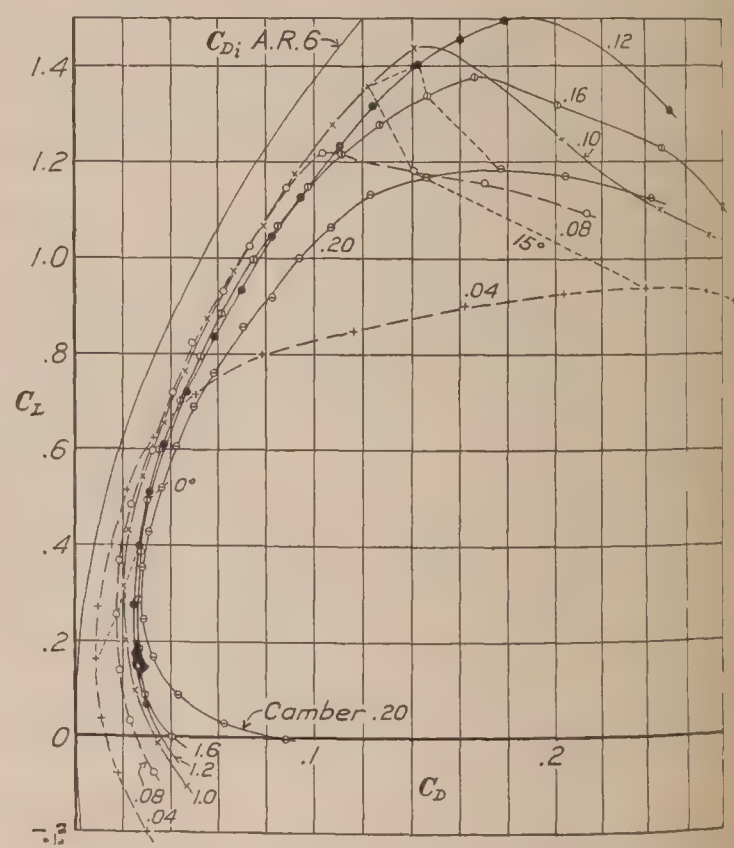


FIG. 4.—Polar curves from tests at 20 atmospheres

The remaining curves, Figures 13 to 18, represent the variation of lift coefficient, drag coefficient, and $\frac{L}{D}$ with angle of attack. The results from both the high and low Reynolds Number tests are plotted on the same sheet in order to show the scale effect on each section. We may conclude from these curves that there is little scale effect on either slope of the lift curve or angle of zero lift except for the thickest section where the slope of the lift curve is considerably below normal and the angle of zero lift is effected by burbling, which probably exists at all angles of attack. The two thickest sections at one atmosphere show a discontinuity of flow at maximum lift and give a lower maximum lift without the discontinuity at 20 atmospheres. The moderately thick airfoils all give a higher maximum lift at the higher Reynolds Number.

As regards scale effect on the drag, it may be concluded that, below maximum lift, the drag at any angle of attack is either reduced or not changed at all as the Reynolds Number is increased from 170,000 to 3,500,000. There is an exception for the two thickest sections at angles just below the discontinuity of flow at maximum lift where the drag is lower at the lower Reynolds Number. In general, the scale effect is small for efficient sections over the range of angles where the sections have a low profile drag.

Previous tests have been made to determine the characteristics and scale effect for these propeller sections. In the tests covered by References 3 and 4 the dynamic scale was increased by increasing the velocity to very high values. However, the range of Reynolds Numbers was not as great and the conditions of the tests were so different that a comparison of the results here is not justified.

The tendency of the drag to increase at low and negative angles of attack indicates a breaking away of the flow from the lower surface of the airfoil. Although the effect is less at the higher Reynolds Number, it could probably be eliminated altogether by the substitution of a leading edge similar to that of the Clark Y.

Before the models were tested some of their characteristics were calculated from their sections. The moment coefficient about the quarter chord point from the leading edge and the angle of zero lift were calculated by a method based on Munk's integrals and outlined in

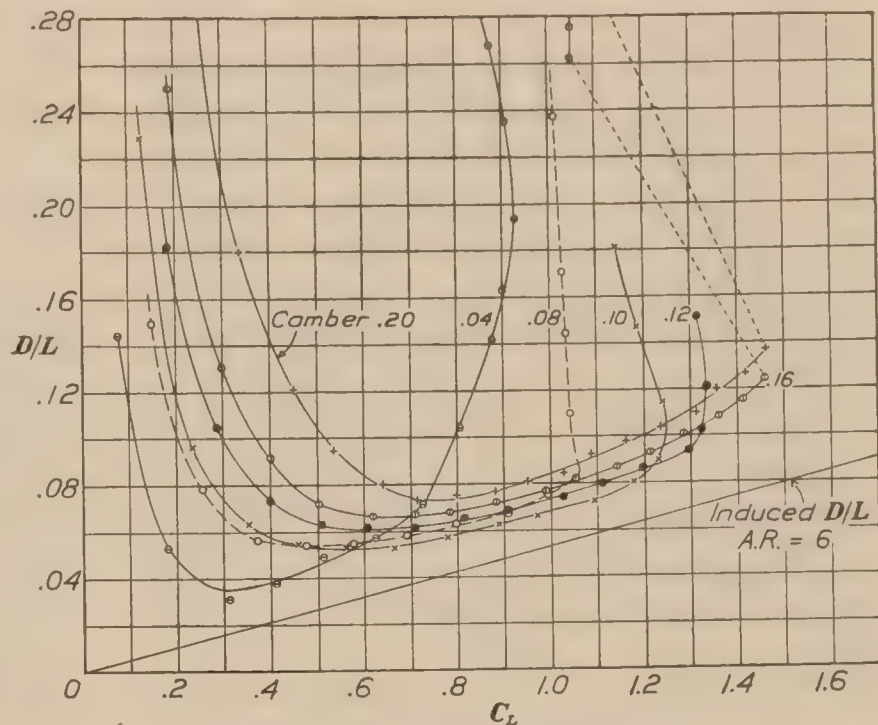


FIG. 5.— D/L curves from tests at 1 atmosphere

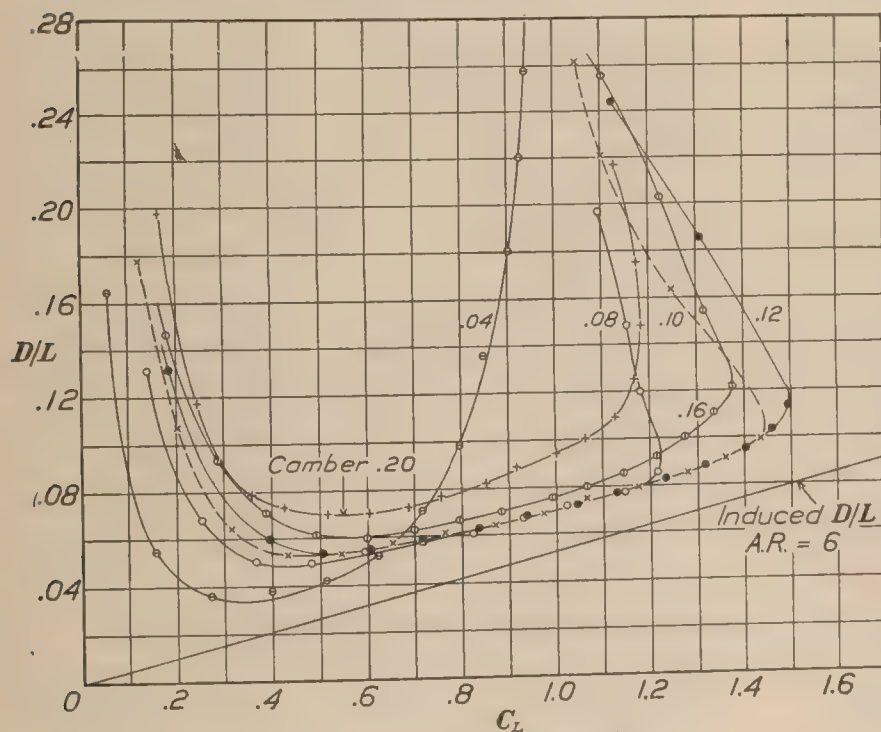


FIG. 6.— D/L curves from tests at 20 atmospheres

moment coefficient about the quarter chord point from the leading edge and the angle of zero lift were calculated by a method based on Munk's integrals and outlined in

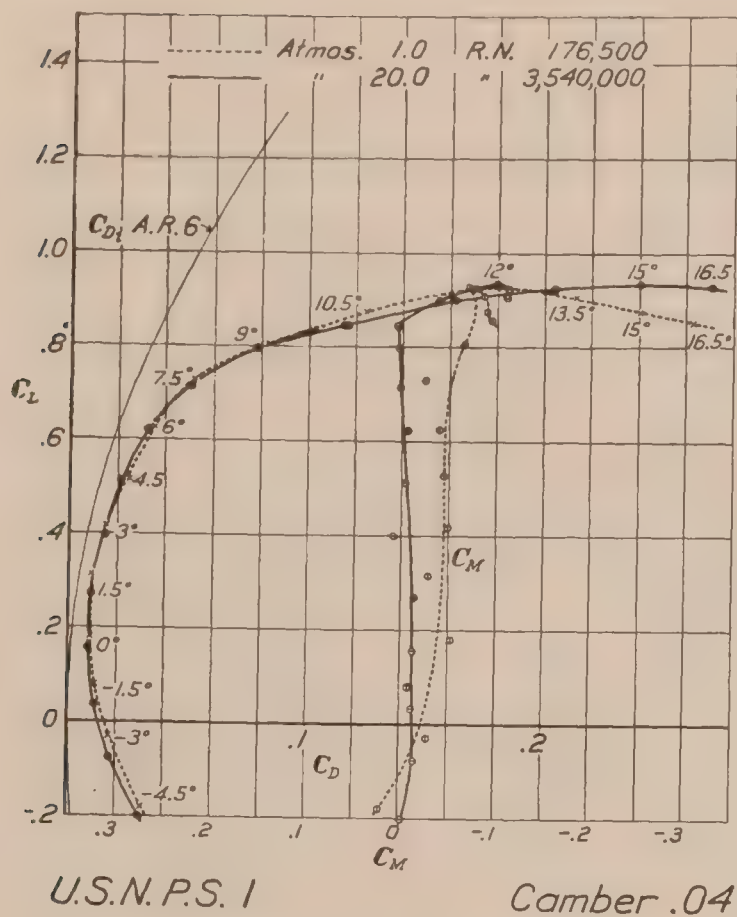


FIG. 7.—Polar and moment curves of U. S. N. P. S. 1 at different values of R. N.

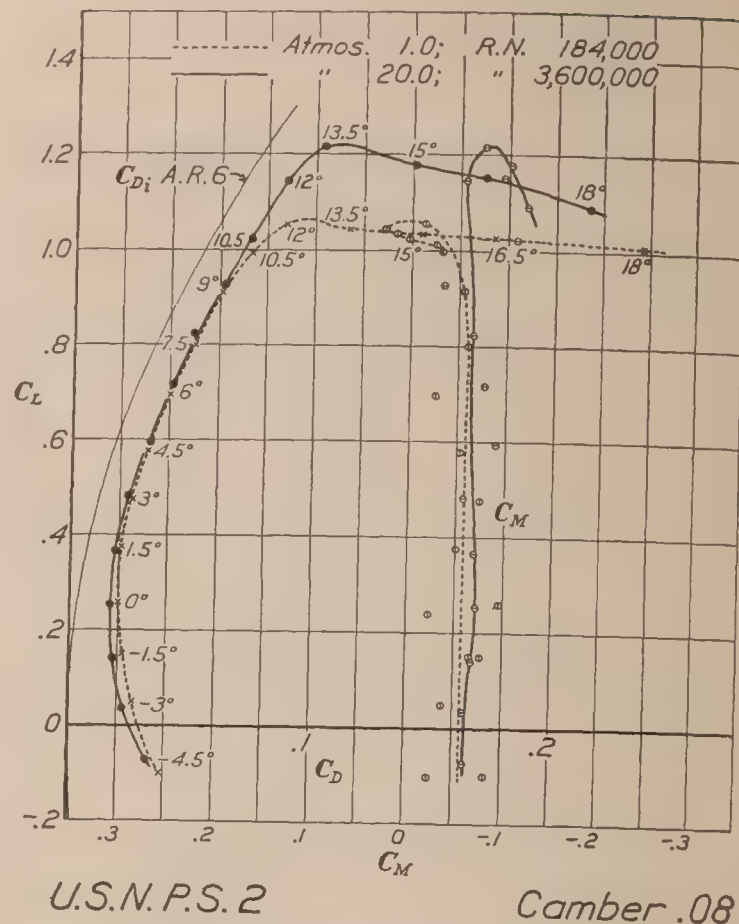


FIG. 8.—Polar and moment curves of U. S. N. P. S. 2 at different values of R. N.

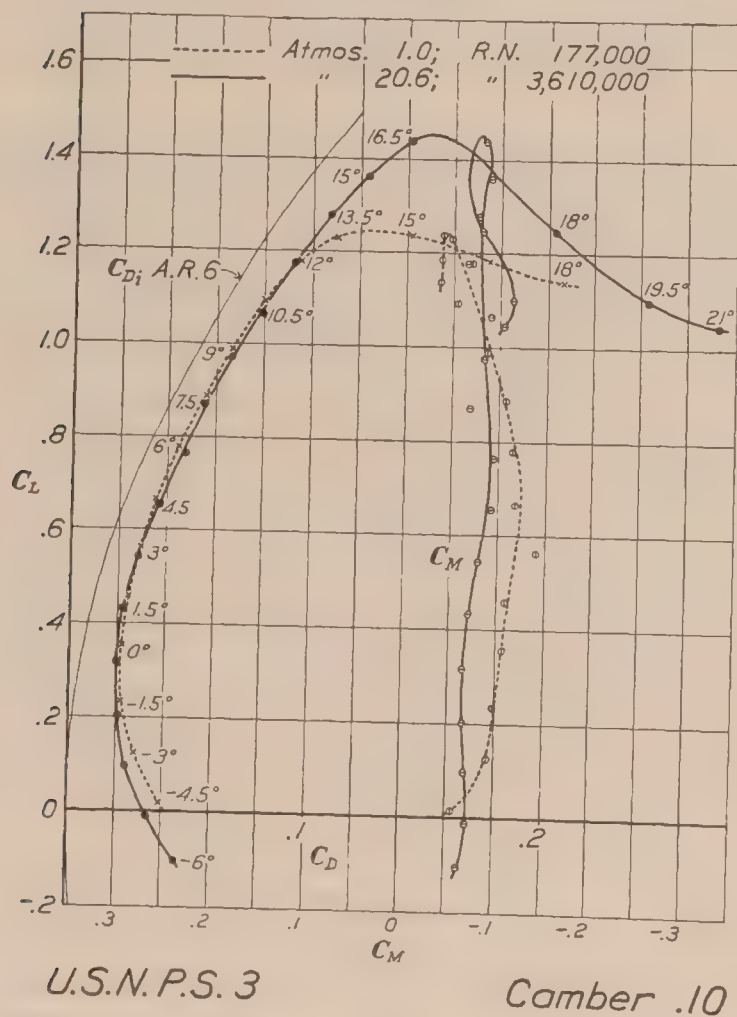


FIG. 9.—Polar and moment curves of U. S. N. P. S. 3 at different values of R. N.

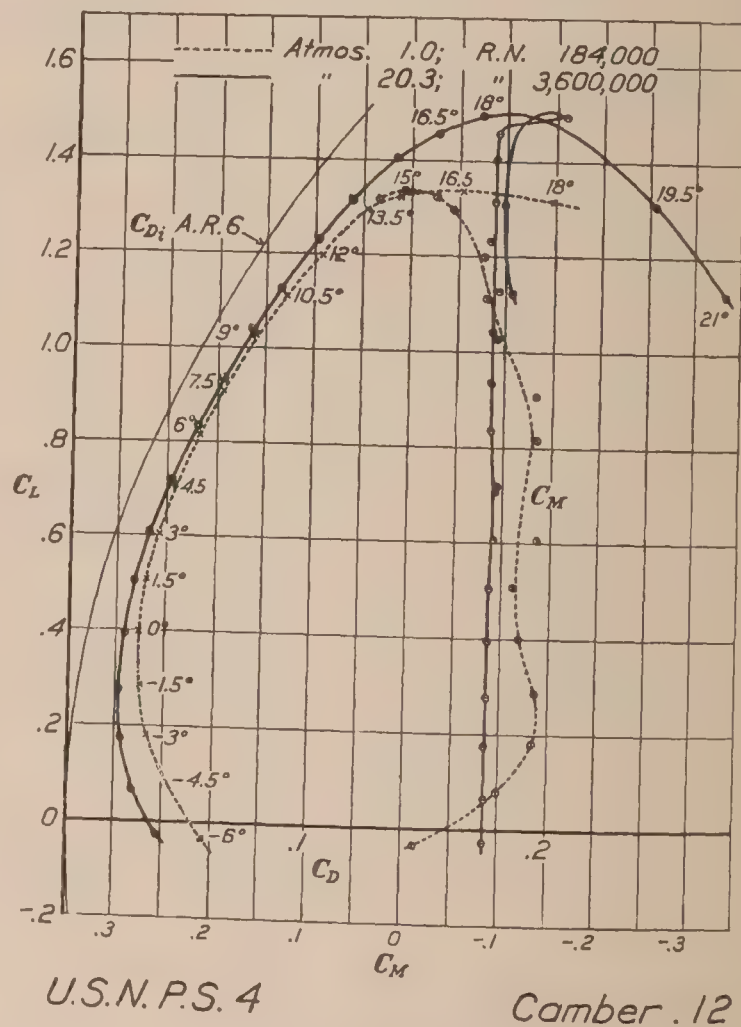
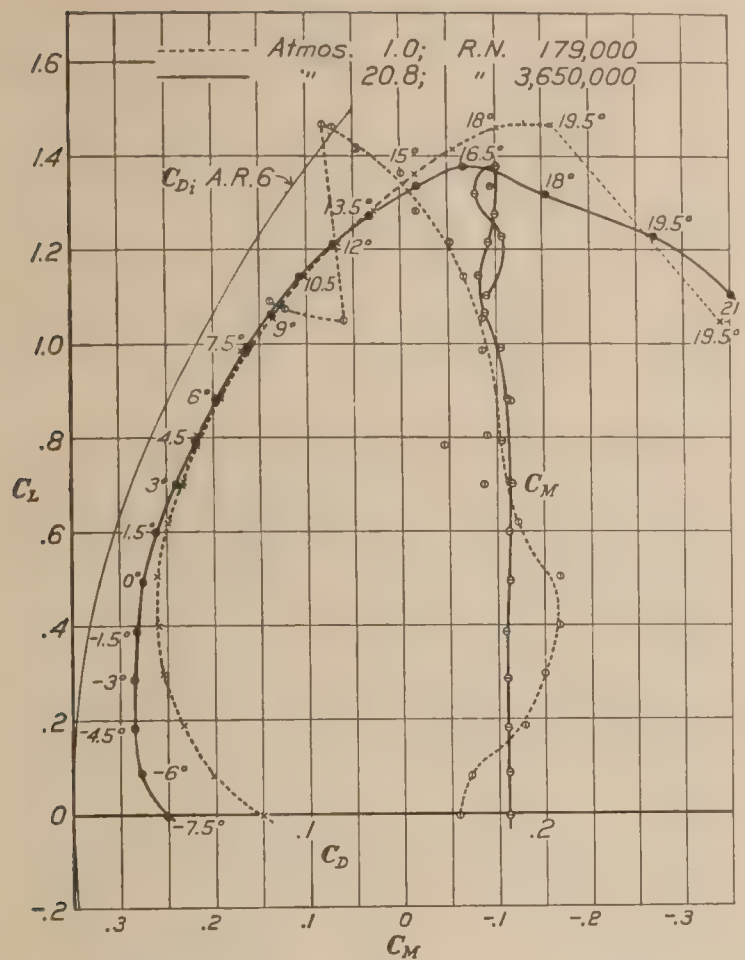
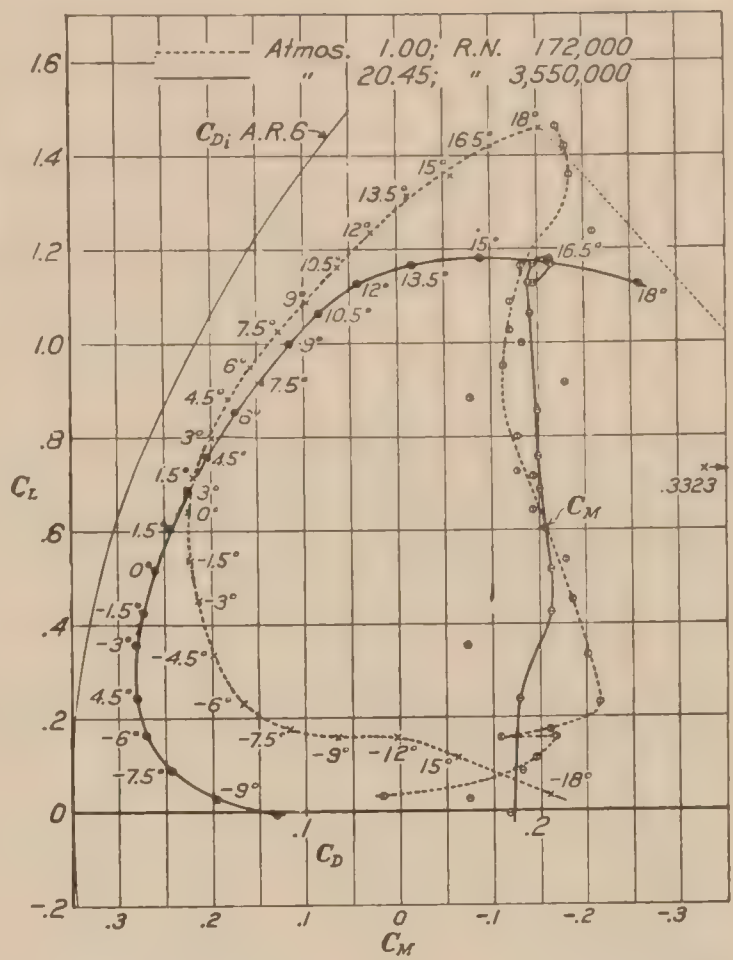


FIG. 10.—Polar and moment curves of U. S. N. P. S. 4 at different values of R. N.



U.S.N.P.S. 5 Camber .16

FIG. 11.—Polar and moment curves of U. S. N. P. S. 5 at different values of R. N.



U.S.N.P.S. 6 Camber .20

FIG. 12.—Polar and moment curves of U. S. N. P. S. 6 at different values of R. N.

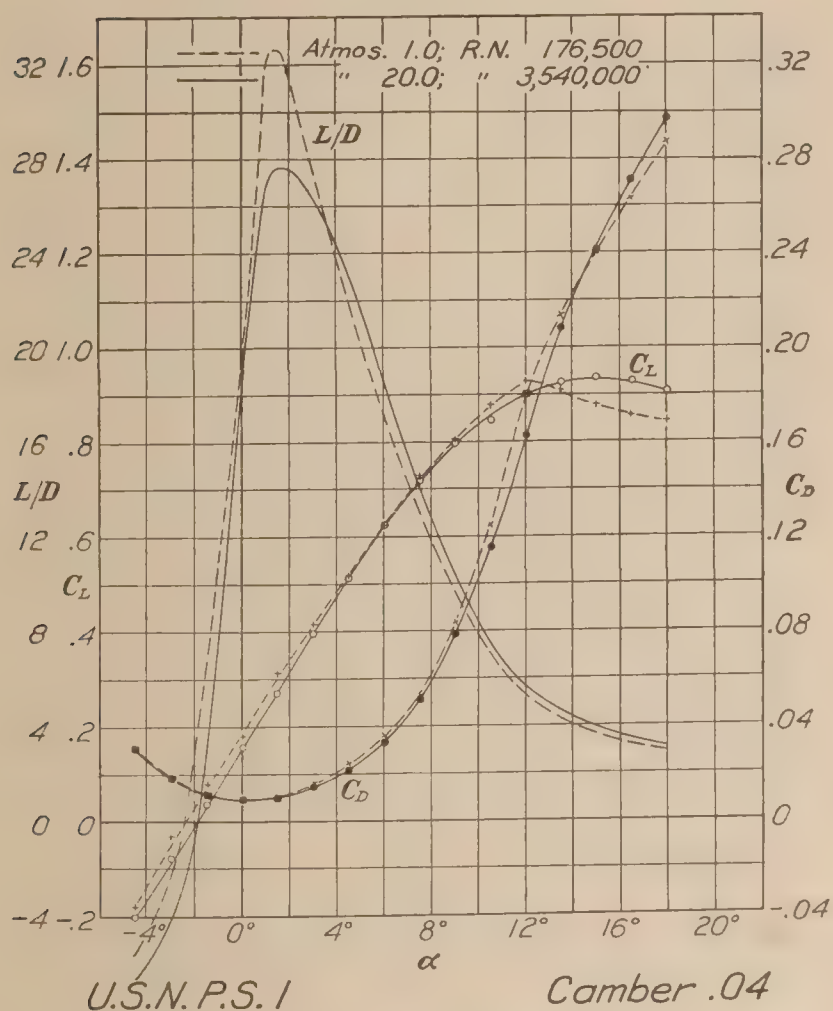


FIG. 13.—Characteristic curves of U. S. N. P. S. 1 at different values of R. N.

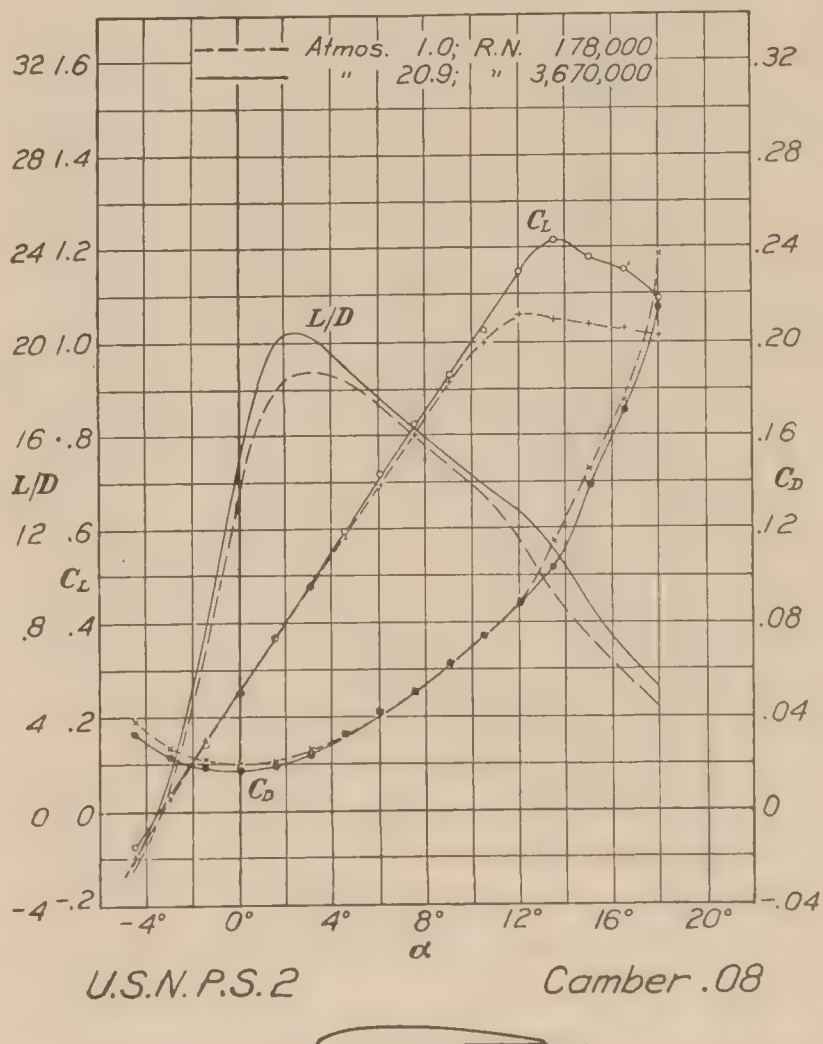


FIG. 14.—Characteristic curves of U. S. N. P. S. 2 at different values of R. N.

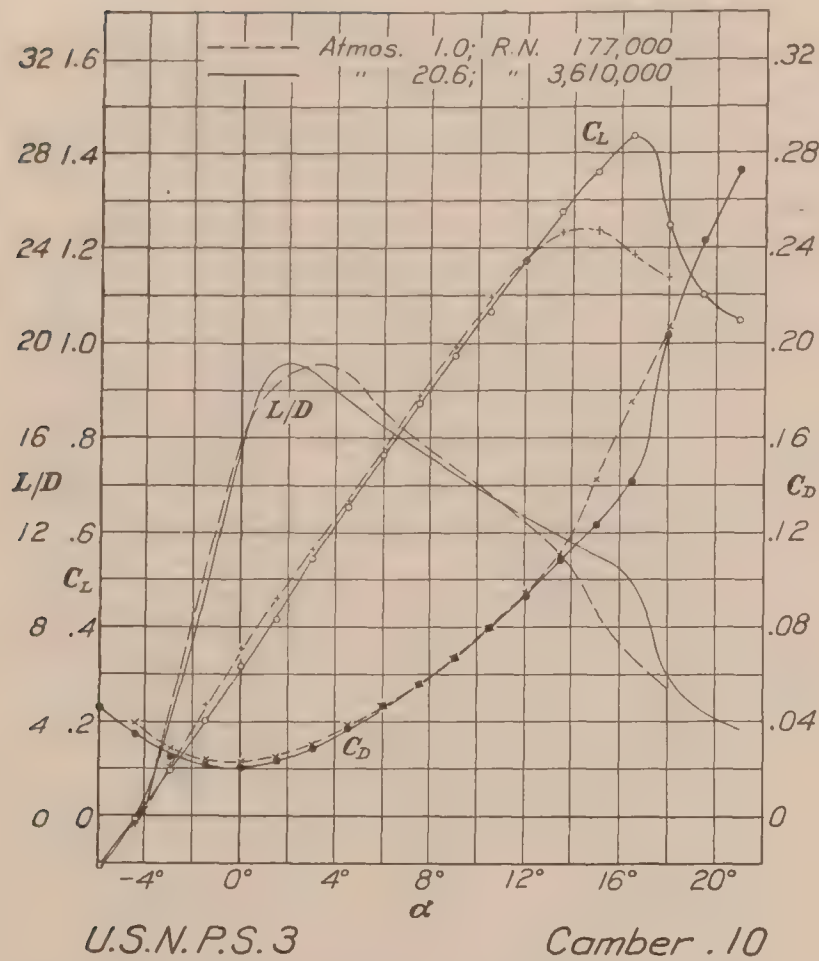


FIG. 15.—Characteristic curves of U. S. N. P. S. 3 at different values of R. N.

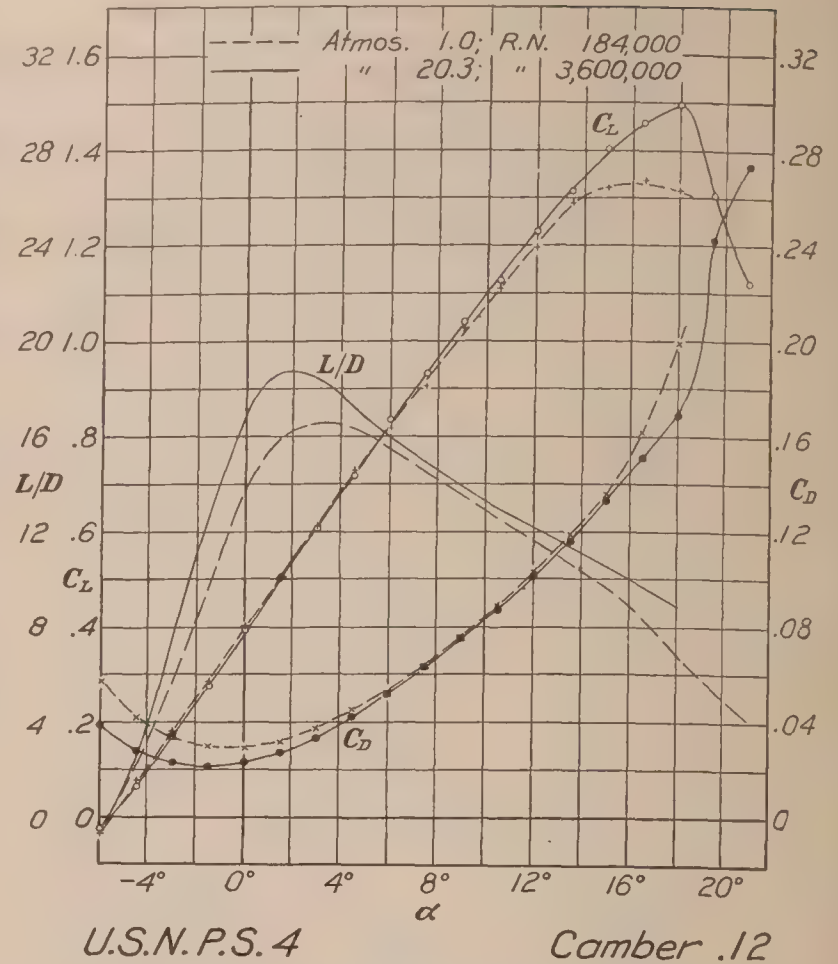


FIG. 16.—Characteristic curves of U. S. N. P. S. 4 at different values of R. N.

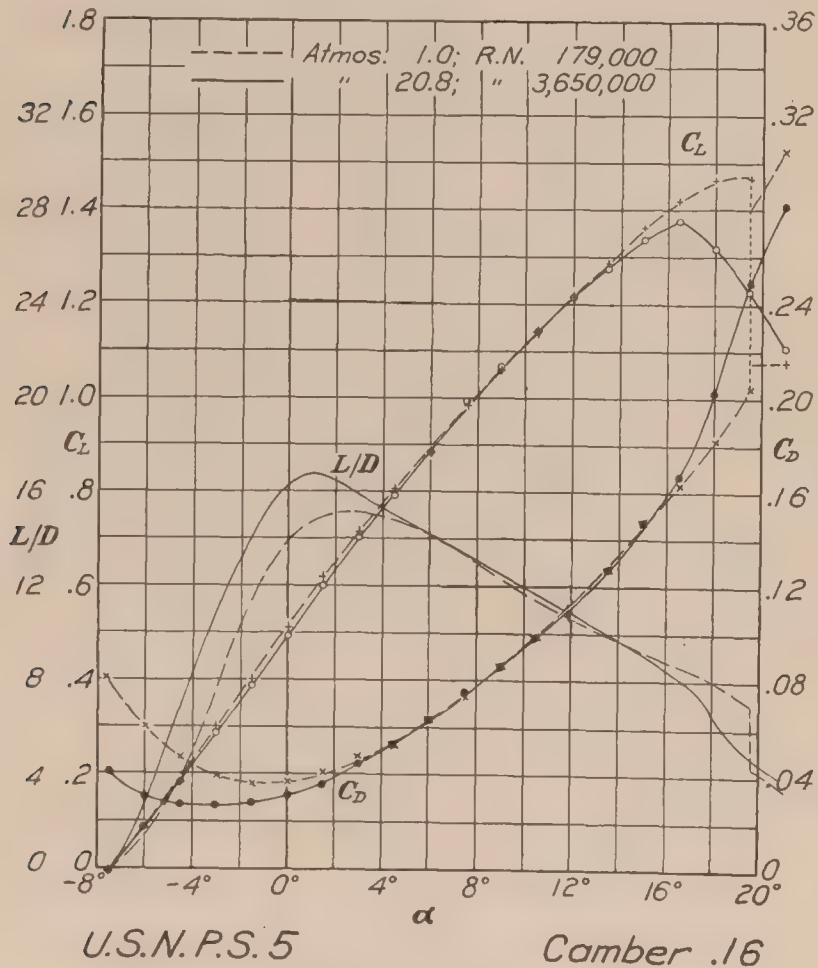


FIG. 17.—Characteristic curves of U. S. N. P. S. 5 at different values of R. N.

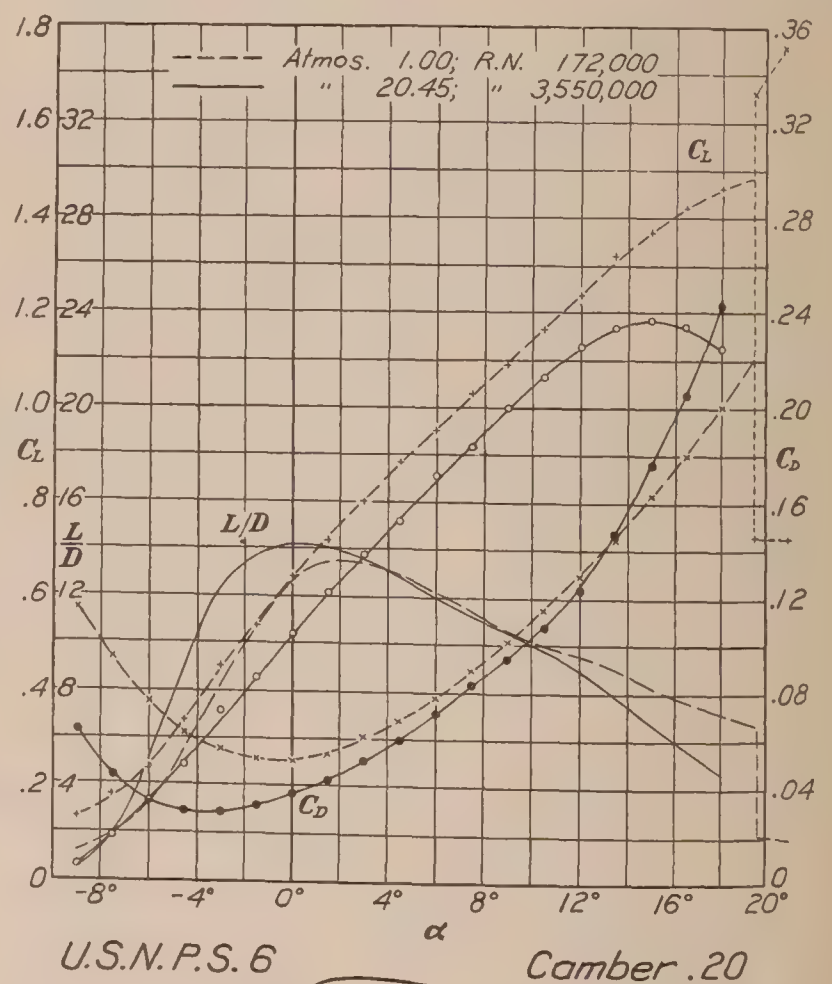


FIG. 18.—Characteristic curves of U. S. N. P. S. 6 at different values of R. N.

Reference 2. The results of these calculations, together with the data as found from the experiments, for comparison, are given in Table II. The agreement is certainly very striking if allowance is made for the errors of measurement and for the assumptions and approximations made in the derivation of the theory. It would appear from Table II that the moment coefficient and the angle of zero lift may be calculated from the ordinates of a section to an accuracy sufficient for most engineering work. The slope of the lift curve, however, departs noticeably from the computed values and in such a way as to be consistent with all other measurements made in this tunnel. This subject will be taken up in a technical note.

REFERENCES

No. 1. Munk, Max M., and Miller, Elton W.: The Variable Density Wind Tunnel of the National Advisory Committee for Aeronautics. N. A. C. A. Technical Report No. 227, 1926.

No. 2. Munk, Max M.: The Determination of the Angles of Attack of Zero Lift and of Zero Moment, Based on Munk's Integrals. N. A. C. A. Technical Note No. 122, 1923.

No. 3. Caldwell, F. W., and Fales, E. N.: Wind Tunnel Studies in Aerodynamic Phenomena at High Speed. N. A. C. A. Technical Report No. 83, 1920.

No. 4. Briggs, L. J., and Dryden, H. L., Aerodynamic Characteristics of Airfoils at High Speed. N. A. C. A. Technical Report No. 207, 1925.

TABLE I

SPECIFIED ORDINATES OF UPPER SURFACE OF PROPELLER SECTIONS IN FRACTIONS OF CHORD

Lower Surfaces are Flat

Section.....	1	2	3	4	5	6
Camber.....	0. 04	0. 08	0. 10	0. 12	0. 16	0. 20
L. Edge Rad.....	0. 0040	0. 0080	0. 0100	0. 0120	0. 0160	0. 0200
0. 025 Sta.....	. 0164	. 0328	. 0410	. 0492	. 0656	. 0820
. 05 Sta.....	. 0236	. 0472	. 0590	. 0708	. 0944	. 1180
. 075 Sta.....	. 0283	. 0566	. 0708	. 0850	. 1133	. 1416
. 10 Sta.....	. 0316	. 0632	. 0790	. 0948	. 1265	. 1580
. 15 Sta.....	. 0358	. 0716	. 0895	. 1074	. 1432	. 1790
. 20 Sta.....	. 0380	. 0760	. 0950	. 1140	. 1520	. 1900
. 30 Sta.....	. 0399	. 0798	. 0998	. 1198	. 1597	. 1996
. 40 Sta.....	. 0396	. 0792	. 0990	. 1188	. 1584	. 1980
. 50 Sta.....	. 0380	. 0760	. 0950	. 1140	. 1520	. 1900
. 60 Sta.....	. 0348	. 0696	. 0870	. 1044	. 1392	. 1740
. 70 Sta.....	. 0296	. 0592	. 0740	. 0888	. 1184	. 1480
. 80 Sta.....	. 0224	. 0448	. 0560	. 0672	. 0896	. 1120
. 90 Sta.....	. 0142	. 0282	. 0352	. 0423	. 0563	. 0704
. 95 Sta.....	. 0098	. 0197	. 0246	. 0295	. 0394	. 0492
T. Edge Rad.....	. 0031	. 0062	. 0092	. 0077	. 0123	. 0154

TABLE II
COMPUTED ANGLE OF ZERO LIFT AND MOMENT COEFFICIENT

Section No.	Maximum thickness	Angle of zero lift		Moment coefficient	
		Predicted	Found from experiment	Predicted	Average value from experiment
		<i>Degrees</i>	<i>Degrees</i>		
1	0.04	-1.6	-2.0	-0.024	-0.012
2	.08	-3.3	-3.4	-.052	-.065
3	.10	-4.1	-4.3	-.064	-.075
4	.12	-5.2	-5.5	-.080	-.088
5	.16	-7.0	-7.4	-.108	-.110
6	.20	-8.6	-10.0	-.131	-.145

TABLE III

Section No. U. S. N. P. S. 1.
Average pressure, 1 atmos.
Average dynamic pressure, 28 kg/m².
Average temperature, 24° C.
Average Reynolds Number 176,500.

Test No. 176-7.
Chord, 5 in. (12.7 cm).
Span, 30 in. (76.2 cm).
Aspect ratio, 6.
Area, 0.0968 m².

Angle of attack degrees	Lift coefficient C_L	Drag coefficient C_D	Ratio $\frac{L}{D}$	Moment coefficient C_M
-4.5	-0.180	0.0319	-5.64	+0.021
-3.0	-.030	.0178	-1.68	-.029
-1.5	+.078	.0114	6.84	-.009
0	.181	.0096	18.85	-.055
+1.5	.313	.0096	32.60	-.029
3	.417	.0152	27.43	-.049
4.5	.515	.0249	20.68	-.045
6	.626	.0354	17.68	-.038
7.5	.729	.0517	14.10	-.024
9	.806	.0837	9.63	-.063
10.5	.877	.1244	7.05	-.087
12	.929	.1798	5.17	-.069
13.5	.907	.2136	4.25	-.086
15	.877	.2404	3.65	-.089
16.5	.855	.2631	3.25	-.098
18	.844	.2873	2.94	-.085

TABLE IV

Section No. U. S. N. P. S. 1.

Test No. 146-4.

Average pressure, 20.0 atmos.

Chord, 5 in. (12.7 cm).

Average dynamic pressure, 618 kg/m².

Span, 30 in. (76.2 cm).

Average temperature, 35° C.

Aspect ratio, 6.

Average Reynolds Number 3,540,000.

Area, 0.0968 m².

Angle of attack degrees	Lift coefficient C_L	Drag coefficient C_D	Ratio $\frac{L}{D}$	Moment coefficient C_M
-4.5	-0.202	0.0300	-6.73	-0.004
-3	-.078	.0179	-4.36	-.017
-1.5	+.035	.0112	3.12	-.013
0	.155	.0086	18.02	-.014
+1.5	.270	.0098	27.55	+.020
3	.397	.0152	26.12	+.007
4.5	.512	.0216	23.70	-.005
6	.623	.0328	18.99	-.007
7.5	.713	.0507	14.06	+.002
9	.797	.0787	10.13	+.004
10.5	.845	.1154	7.32	+.005
12	.898	.1624	5.53	-.038
13.5	.924	.2035	4.54	-.072
15	.933	.2410	3.87	-.100
16.5	.930	.2715	3.42	-.111
18	.908	.2971	3.06	-.111

TABLE V

Section No. U. S. N. P. S. 2.

Test No. 151-2.

Average pressure, 1 atmos.

Chord, 5 in. (12.7 cm).

Average dynamic pressure, 28.5 kg/m².

Span, 30 in. (76.2 cm).

Average temperature, 24° C.

Aspect ratio, 6.

Average Reynolds Number 178,000.

Area, 0.0968 m².

Angle of attack degrees	Lift coefficient C_L	Drag coefficient C_D	Moment coefficient C_M	Ratio $\frac{L}{D}$
-4.5	-0.101	0.0388	-0.084	-2.60
-3	+.051	.0268	-.040	1.90
-1.5	.149	.0223	-.067	6.68
0	.258	.0202	-.096	12.77
+1.5	.374	.0210	-.051	17.81
3	.477	.0258	-.075	18.49
4.5	.578	.0314	-.053	18.41
6	.694	.0402	-.027	17.26
7.5	.799	.0504	-.061	15.85
9	.912	.0615	-.055	14.83
10.5	.995	.0740	-.033	13.45
12	1.054	.0880	-.013	11.98
13.5	1.043	.1140	+.029	9.15
15	1.032	.1443	+.015	7.15
16.5	1.028	.1748	+.003	5.88
18	1.010	.2369	-.024	4.26

TABLE VI

Section No. U. S. N. P. S. 2.
 Average pressure, 20.9 atmos.
 Average dynamic pressure 650 kg/m².
 Average temperature, 38° C.
 Average Reynolds Number, 3,670,000.

Test No. 151-3.
 Chord, 5 in. (12.7 cm).
 Span, 30 in. (6.2 cm).
 Aspect ratio, 6.
 Area, 0.0968 m².

Angle of attack degrees	Lift coefficient C_L	Drag coefficient C_D	Moment coefficient C_M	Ratio $\frac{L}{D}$
-4.5	-0.075	0.0331	-0.064	-2.27
-3	+0.033	.0230	-.061	1.43
-1.5	.140	.0185	-.068	7.57
0	.252	.0173	-.072	14.57
+1.5	.367	.0185	-.068	19.84
3	.481	.0238	-.056	20.21
4.5	.594	.0324	-.088	18.33
6	.717	.0415	-.076	17.28
7.5	.822	.0496	-.064	16.57
9	.927	.0622	-.034	14.90
10.5	1.021	.0737	-.107	13.85
12	1.143	.0880	-.054	12.99
13.5	1.215	.1033	-.072	11.76
15	1.178	.1411	-.101	8.35
16.5	1.151	.1701	-.093	6.77
18	1.090	.2141	-.118	5.09

TABLE VII

Section No. U. S. N. P. S. 3.
 Average pressure, 1 atmos.
 Average dynamic pressure, 28.4 kg/m².
 Average temperature, 27° C.
 Average Reynolds Number 177,000.

Test No. 152-1.
 Chord, 5 in. (12.7 cm).
 Span, 30 in. (76.2 cm).
 Aspect ratio, 6.
 Area, 0.0968 m².

Angle of attack degrees	Lift coefficient C_L	Drag coefficient C_D	Ratio $\frac{L}{D}$	Moment coefficient C_M
-4.5	0.018	0.0399	0.45	-0.058
-3	.125	.0287	4.35	-.096
-1.5	.236	.0228	10.35	-.099
0	.353	.0225	15.69	-.109
+1.5	.459	.0252	18.21	-.111
3	.564	.0301	18.74	-.143
4.5	.666	.0349	19.08	-.119
6	.779	.0449	17.35	-.116
7.5	.889	.0561	15.85	-.108
9	.990	.0669	14.80	-.087
10.5	1.095	.0801	13.67	-.054
12	1.179	.0950	12.41	-.069
13.5	1.230	.1101	11.17	-.047
15	1.237	.1420	8.71	-.038
16.5	1.183	.1751	6.76	-.038
18	1.139	.2069	5.50	-.036

TABLE VIII

Section No. U. S. N. P. S. 3.

Test No. 152-2.

Average pressure, 20.6 atmos.

Chord, 5 in. (12.7 cm).

Average dynamic pressure, 640 kg/m².

Span, 30 in. (76.2 cm).

Average temperature, 38° C.

Aspect ratio, 6.

Average Reynolds Number 3,610,000.

Area, 0.0968 m².

Angle of attack degrees	Lift coefficient C_L	Drag coefficient C_D	Ratio $\frac{L}{D}$	Moment coefficient C_M
-6	-0.106	0.0461	-2.30	0.066
-4.5	-.011	.0341	-0.32	-.073
-3	+.098	.0253	3.87	-.072
-1.5	.202	.0217	9.31	-.068
0	.317	.0204	15.54	-.067
+1.5	.431	.0227	18.99	-.073
3	.543	.0288	18.85	-.082
4.5	.652	.0374	17.43	-.095
6	.762	.0467	16.32	-.097
7.5	.870	.0557	15.62	-.070
9	.972	.0663	14.66	-.085
10.5	1.065	.0792	13.45	-.090
12	1.174	.0923	12.72	-.066
13.5	1.277	.1079	11.83	-.077
15	1.359	.1231	11.04	-.089
16.5	1.438	.1416	10.15	-.083
18	1.247	.2034	6.13	-.081
19.5	1.100	.2430	4.53	-.114
21	1.047	.2730	3.83	-.106

TABLE IX

Section No. U. S. N. P. S. 4.

Test No. 153-1.

Average pressure, 1 atmos.

Chord, 5 in. (12.7 cm).

Average dynamic pressure, 29.34 kg/m².

Span, 30 in. (76.2 cm).

Average temperature, 22° C.

Aspect ratio, 6.

Average Reynolds Number 184,000.

Area, 0.0968 m².

Angle of attack degrees	Lift coefficient C_L	Drag coefficient C_D	Ratio $\frac{L}{D}$	Moment coefficient C_M
-6	-0.035	0.0576	-0.610	-0.015
-4.5	+.081	.0422	1.92	-.101
-3	.182	.0332	5.48	-.137
-1.5	.288	.0301	9.57	-.138
0	.400	.0292	13.70	-.121
+1.5	.509	.0320	15.90	-.113
3	.607	.0375	16.19	-.137
4.5	.710	.0432	16.43	-.093
6	.816	.0531	15.37	-.136
7.5	.908	.0631	14.39	-.134
9	1.028	.0759	13.54	-.092
10.5	1.110	.0888	12.50	-.079
12	1.198	.1033	11.60	-.076
13.5	1.296	.1218	10.64	-.043
15	1.322	.1357	9.74	-.025
16.5	1.336	.1612	8.29	+.007
18	1.315	.1991	6.60	+.035

TABLE X

Section No. U. S. N. P. S. 4.
 Average pressure, 20.3 atmos.
 Average dynamic pressure, 635 kg/m².
 Average temperature, 36° C.
 Average Reynolds Number 3,600,000.

Test No. 153-2.
 Chord, 5 in. (12.7 cm).
 Span, 30 in. (76.2 cm).
 Aspect ratio, 6.
 Area, 0.0968 m².

Angle of attack degrees	Lift coefficient C_L	Drag coefficient C_D	Ratio $\frac{L}{D}$	Moment coefficient C_M
-6	-0.028	0.0383	-0.73	-0.086
-4.5	+0.067	.0280	2.39	-.088
-3	.173	.0228	7.59	-.086
-1.5	.276	.0218	12.66	-.088
0	.393	.0235	16.72	-.089
+1.5	.506	.0272	18.60	-.088
3	.607	.0330	18.39	-.093
4.5	.718	.0420	17.09	-.095
6	.833	.0522	15.90	-.087
7.5	.932	.0633	14.72	-.088
9	1.041	.0748	13.92	-.088
10.5	1.127	.0865	13.03	-.094
12	1.230	.1017	12.09	-.083
13.5	1.314	.1158	11.35	-.087
15	1.403	.1331	10.54	-.088
16.5	1.456	.1506	9.67	-.090
18	1.492	.1689	8.83	-.160
19.5	1.308	.2424	5.40	-.097
21	1.121	.2734	4.10	-.106

TABLE XI

Section No. U. S. N. P. S. 5.
 Average pressure, 1 atmos.
 Average dynamic pressure, 28.8 kg/m².
 Average temperature, 25° C.
 Average Reynolds Number 179,000.

Test No. 154-1.
 Chord, 5 in. (12.7 cm).
 Span, 30 in. (76.2 cm).
 Aspect ratio, 6.
 Area, 0.0968 m².

Angle of attack degrees	Lift coefficient C_L	Drag coefficient C_D	Ratio $\frac{L}{D}$	Moment coefficient C_M
-7.5	-0.007	0.0803	-0.09	-0.059
-6	+0.082	.0599	1.37	-.073
-4.5	.189	.0473	4.00	-.130
-3	.299	.0389	7.70	-.150
-1.5	.401	.0358	11.20	-.167
0	.508	.0365	13.92	-.167
+1.5	.620	.0409	15.16	-.123
3	.709	.0478	14.83	-.114
4.5	.805	.0532	15.13	-.090
6	.885	.0633	13.98	-.115
7.5	.988	.0727	13.59	-.085
9	1.056	.0859	12.29	-.086
10.5	1.142	.0985	11.59	-.067
12	1.215	.1131	10.74	-.062
13.5	1.282	.1286	9.97	-.016
15	1.361	.1460	9.32	-.001
16.5	1.415	.1621	8.73	+0.046
18	1.461	.1809	8.08	+0.073
19.5	1.468	.2041	7.19	+0.084
21	1.074	.3048	3.52	+0.123

TABLE XII

Section No. U. S. N. P. S. 5. Test No. 154-2.
 Average pressure, 20.8 atmos. Chord, 5 in. (12.7 cm).
 Average dynamic pressure, 643 kg/m². Span, 30 in. (76.2 cm).
 Average temperature, 45° C. Aspect ratio, 6.
 Average Reynolds Number 3,650,000. Area, 0.0968 m².

Angle of attack degrees	Lift coefficient C_L	Drag coefficient C_D	Ratio $\frac{L}{D}$	Moment coefficient C_M
-7.5	-0.005	0.0406	-0.01	-0.113
-6	+0.086	.0295	2.91	-.113
-4.5	.182	.0267	6.82	-.112
-3	.287	.0266	10.79	-.111
-1.5	.389	.0277	14.04	-.110
0	.492	.0303	16.24	-.116
+1.5	.599	.0357	16.78	-.113
3	.701	.0442	15.86	-.117
4.5	.792	.0526	15.06	-.106
6	.883	.0614	14.38	-.112
7.5	.992	.0744	13.33	-.106
9	1.065	.0849	12.54	-.088
10.5	1.143	.0973	11.75	-.082
12	1.212	.1114	10.88	-.093
13.5	1.274	.1271	10.02	-.100
15	1.338	.1469	9.11	-.095
16.5	1.376	.1663	8.27	-.102
18	1.319	.2019	6.53	-.079
19.5	1.228	.2482	4.95	-.107
21	1.103	.2810	3.92	-.090

TABLE XIII

Section No. U. S. N. P. S. 6. Test No. 155-2.
 Average pressure, 1 atmos. Chord, 5 in. (12.7 cm).
 Average dynamic pressure, 27.3 kg/m². Span, 30 in. (12.7 cm).
 Average temperature, 27° C. Aspect ratio, 6.
 Average Reynolds Number 172,000. Area, 0.0968 m².

Angle of attack degrees	Lift coefficient C_L	Drag coefficient C_D	Ratio $\frac{L}{D}$	Moment coefficient C_M
-18	0.034	0.2042	0.17	+0.015
-15	.117	.1656	.71	-.148
-12	.159	.1383	1.15	-.168
-9	.159	.1141	1.39	-.110
-7.5	.178	.0936	1.90	-.162
-6	.232	.0742	3.13	-.216
-4.5	.337	.0607	5.55	-.203
-3	.452	.0547	8.26	-.187
-1.5	.538	.0509	10.57	-.181
0	.642	.0503	12.76	-.145
+1.5	.717	.0529	13.55	-.144
3	.800	.0606	13.20	-.128
4.5	.883	.0675	13.08	-.078
6	.951	.0770	12.35	-.114
7.5	1.029	.0890	11.56	-.121
9	1.089	.1012	10.76	-.120
10.5	1.164	.1146	10.16	-.132
12	1.238	.1286	9.63	-.110
13.5	1.315	.1443	9.11	-.155
15	1.357	.1629	8.33	-.184
16.5	1.420	.1799	7.89	-.179
18	1.462	.2004	7.29	-.170
19.5	.728	.3323	2.19	-.129
21	.727	.3585	2.03	-.082

TABLE XIV

Section No. U. S. N. P. S. 6.
 Average pressure, 20.45 atmos.
 Average dynamic pressure, 628 kg/m².
 Average temperature, 39° C.
 Average Reynolds Number 3,550,000.

Test No. 155-3.
 Chord, 5 in. (12.7 cm).
 Span, 30 in. (76.2 cm).
 Aspect ratio, 6.
 Area, 0.0968 m².

Angle of attack degrees	Lift coefficient C_L	Drag coefficient C_D	Ratio $\frac{L}{D}$	Moment coefficient C_M
-10.5	-0.006	0.0880	-0.01	-0.119
-9	+.028	.0624	0.45	-.077
-7.5	.088	.0433	2.03	-.134
-6	.164	.0325	5.05	-.128
-4.5	.241	.0284	8.49	-.131
-3	.356	.0281	12.67	-.075
-1.5	.426	.0314	13.57	-.114
0	.517	.0363	14.24	-.115
+1.5	.604	.0426	14.18	-.108
3	.688	.0502	13.70	-.102
4.5	.758	.0587	12.91	-.100
6	.853	.0705	12.10	-.099
7.5	.916	.0824	11.12	-.129
9	.999	.0939	10.64	-.083
10.5	1.062	.1067	9.95	-.092
12	1.129	.1232	9.16	-.091
13.5	1.168	.1464	7.98	-.095
15	1.181	.1755	6.73	-.113
16.5	1.170	.2053	5.70	-.112
18	1.124	.2432	4.62	-.094

REPORT No. 260

THE EFFECT OF A FLAP AND AILERONS ON THE N. A. C. A. M-6 AIRFOIL SECTION

By GEORGE J. HIGGINS and EASTMAN N. JACOBS

Langley Memorial Aeronautical Laboratory

REPORT No. 260

THE EFFECT OF A FLAP AND AILERONS ON THE N. A. C. A. M-6 AIRFOIL SECTION

By GEORGE J. HIGGINS and EASTMAN N. JACOBS

SUMMARY

This report contains the results obtained at the Langley Memorial Aeronautical Laboratory on an N. A. C. A. M-6 airfoil, fitted with a flap and ailerons, and tested in the variable density wind tunnel at a density of 20 atmospheres. Airfoil characteristics are given for the model up to 48° angle of attack with the flap set at various angles, and also with the ailerons set at similar angles. The approximate lift distribution and the center of pressure variation along the span are determined with the model at 18° angle of attack and with the ailerons displaced 20° . Approximate rolling moment and yawing moment coefficients are determined for the various aileron settings.

A comparison of the calculated angles of zero lift and the calculated lift and moment coefficients with those observed is given in the appendix.

INTRODUCTION

The N. A. C. A. M-6 is a good airfoil section, stable in pitch and with very small center of pressure travel. Consequently in its adoption in airplane design, some knowledge of its behavior under the action of ailerons or of a flap seems desirable. This is particularly true in regard to the center of pressure travel. As no similar tests have been conducted under full-scale conditions, this series was undertaken by the Aerodynamics Staff of the Langley Memorial Aeronautical Laboratory in their variable density wind tunnel. To obtain, at the same time, the effect of controls; that is, flap or ailerons, at high angles, the range of investigation was made to extend from zero lift to an angle of attack of $+48^\circ$.

THE TEST

The model was a 6-inch by 36-inch duralumin airfoil of the N. A. C. A. M-6 section. A flap and two ailerons were constructed along the trailing edge, see Figures 1 to 4. The ailerons were one-quarter span each in length; and the flap consisted of the remaining portion of the trailing edge between the ailerons. In the tests with the flap, the ailerons were set in line as if integral with the flap. In the aileron tests, the flap was set neutral and the ailerons were set both up or both down. Consequently, in these latter tests, the balance readings were approximately equivalent to double those for a semispan.

The airfoil was mounted in the tunnel in the usual manner except that slight modifications were necessary in some parts of the apparatus to obtain a range of angle of attack from -20° to $+48^\circ$.

The tests consisted in setting the flap or ailerons to the desired angle and, after compressing the air in the tank to 20 atmospheres, making a normal test, recording data for lift, drag, and pitching moment. Because of the limited counterweight on the standard drag balance, 40 kilograms, the tests had to be run in two parts, the second of which was run with an additional counterweight of 50 kilograms added. Consequently, observations in which the gross drag amounted to between 40 and 50 kilograms had to be omitted.

RESULTS

The results of this series of tests are given in Tables I to XVII and in charts, Figures 5 to 20. The general airfoil characteristics, C_L , C_D , C_M (about the quarter chord), and L/D are given in Tables I to VIII, inclusive, at all angles of attack, one table for each flap setting, -20° , -10° ,

-5° , 0° , $+5^\circ$, $+10^\circ$, $+20^\circ$, and $+25^\circ$. Similarly, Tables IX to XV contain the characteristics for the model with different aileron settings, both ailerons at -20° , -10° , -5° , 0° , $+5^\circ$, $+10^\circ$, and $+20^\circ$. No corrections have been made for tunnel wall interference. Applying the Prandtl formula, the data given herein are correct for an effective aspect ratio of 7.318, whereas the geometrical aspect ratio of the model was 6.00.

Figures 5 and 6 show the true polar (lift and drag coefficient to the same scale) curves for the tests with the flap and with the ailerons, respectively; Figures 7, 8 and 9, 10 show the lift and drag coefficients plotted against the angle of attack. The effect of flap or aileron setting is seen to be uniform in regard to both the lift and the drag. The angle of zero lift varies uniformly with the flap angle through its main range. The rate of change of the lift coefficient, C_L ,

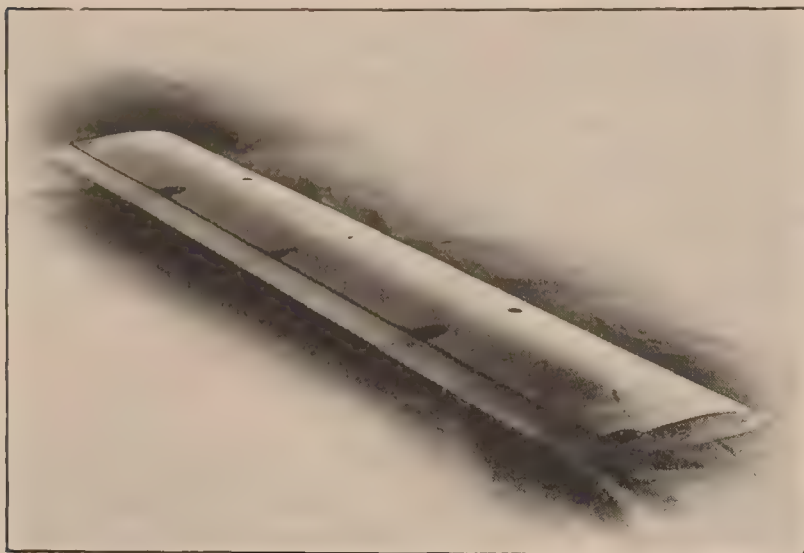


FIG. 1.—N. A. C. A. M-6 airfoil with 20 per cent flaps

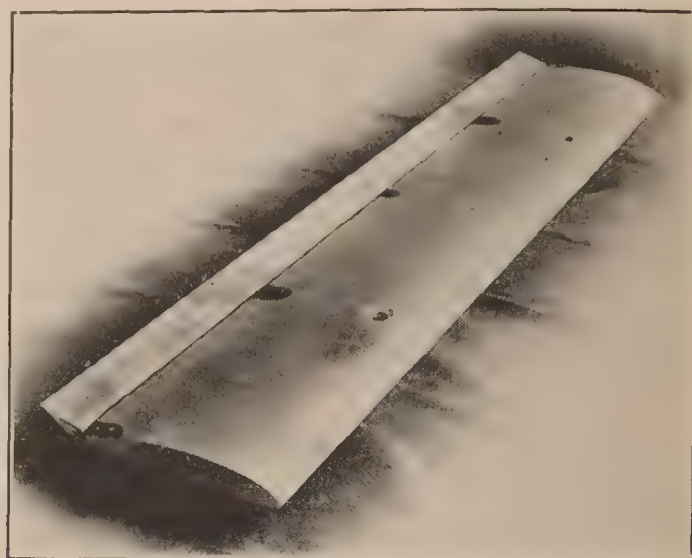


FIG. 2.—N. A. C. A. M-6 airfoil with flaps 20° up

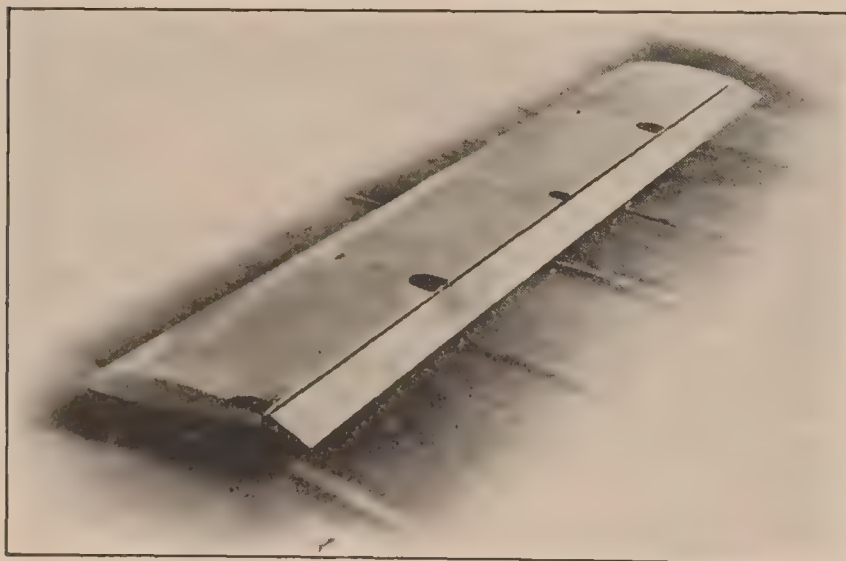


FIG. 3.—N. A. C. A. M-6 airfoil with flaps 20° down

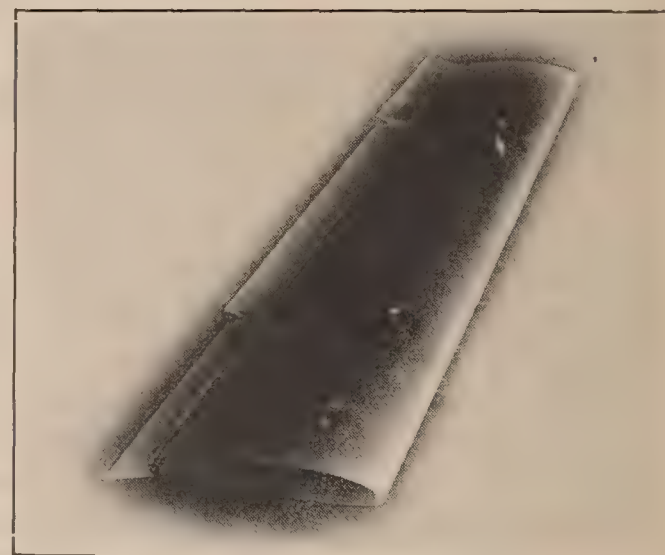


FIG. 4.—N. A. C. A. M-6 airfoil with ailerons displaced 20°

with angle of attack, α , $\frac{dC_L}{d\alpha}$, for the various conditions is practically constant, verifying that the $\frac{dC_L}{d\alpha}$ of an airfoil is independent, or nearly independent of the shape of the section. Figure 18 shows the variation with flap angle of the maximum lift coefficient, the angle of zero lift, and the total lift angle from zero lift to the burble point.

The pitching moment coefficients, about the quarter chord, and the curves of center of pressure travel are given in Figures 11, 12 and 13, 14, respectively, plotted against α for all the various flap and aileron settings.

Figure 15 shows the variation of the center of pressure across the span for the angle of attack of 18° (immediately before the burble point) and an aileron displacement of 20° . It was determined by first assuming a lift distribution along the span, see Figure 16; then computing

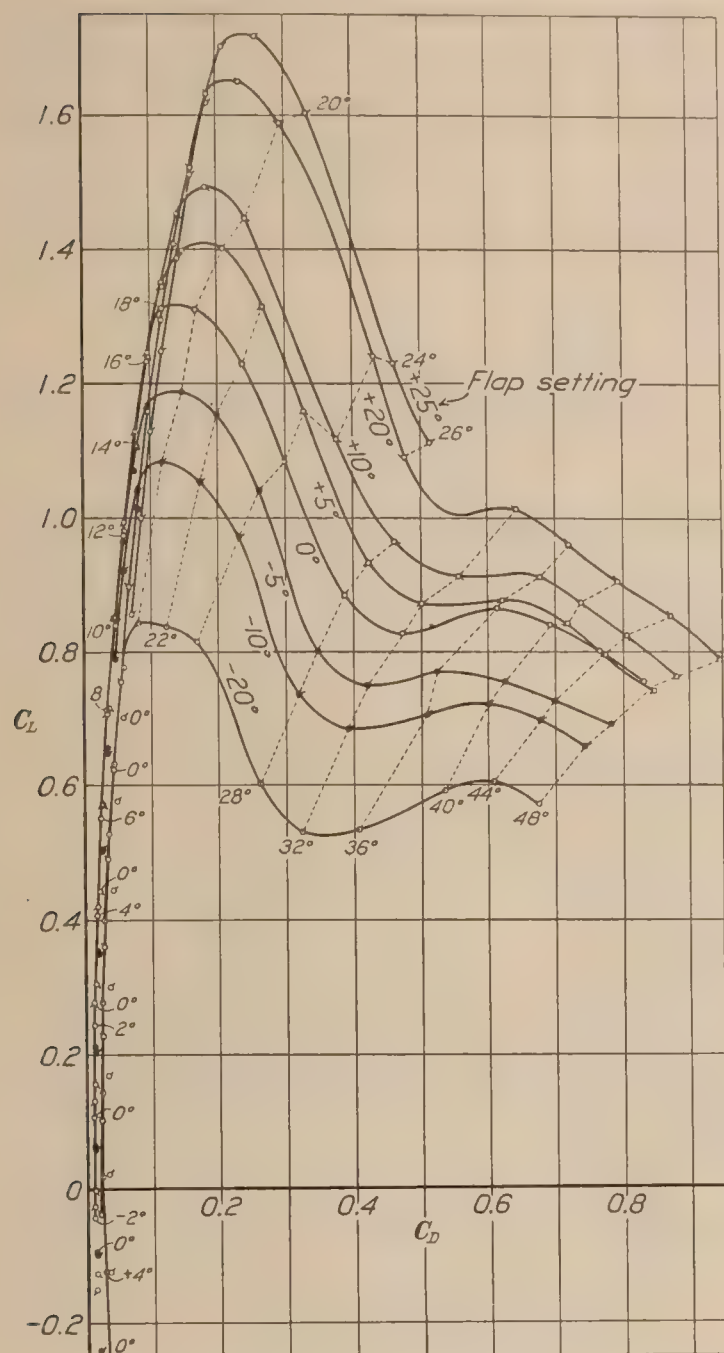


FIG. 5.—Polar curves of N. A. C. A. M-6 airfoil with different flap settings

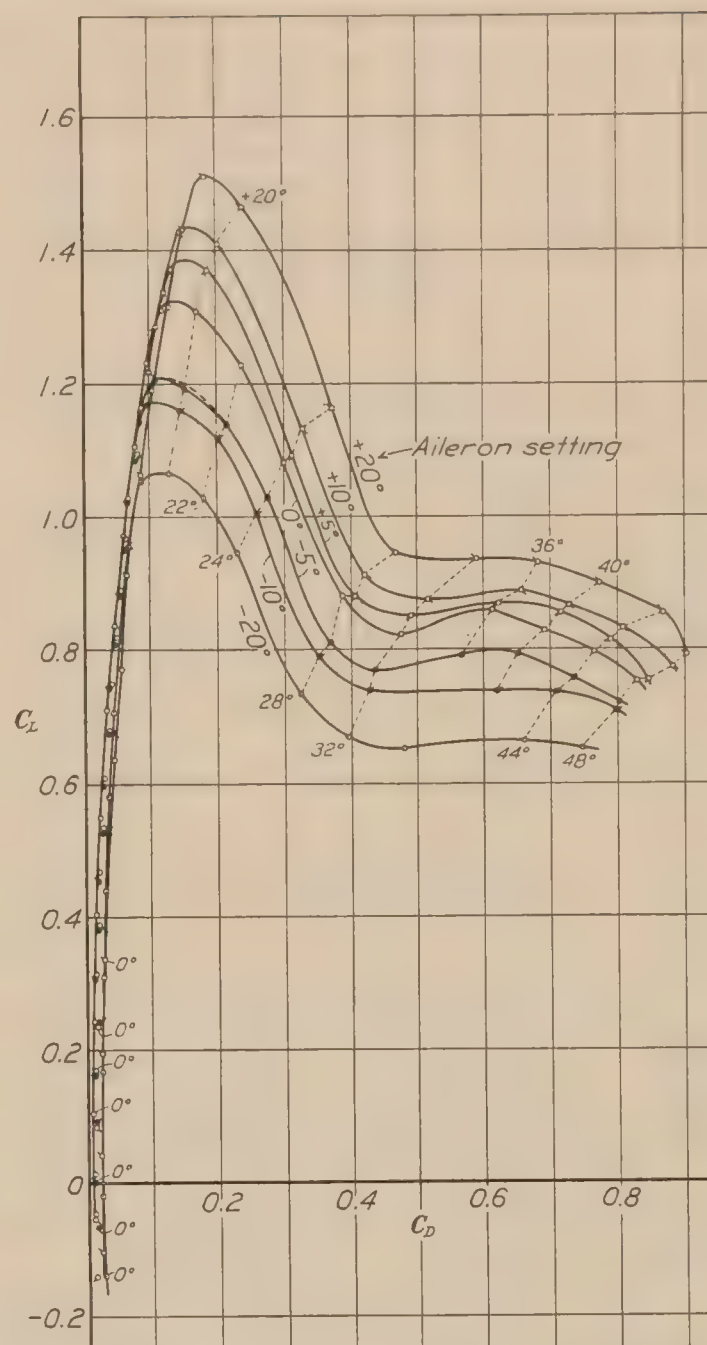


FIG. 6.—Polar curves of N. A. C. A. M-6 airfoil with different aileron settings

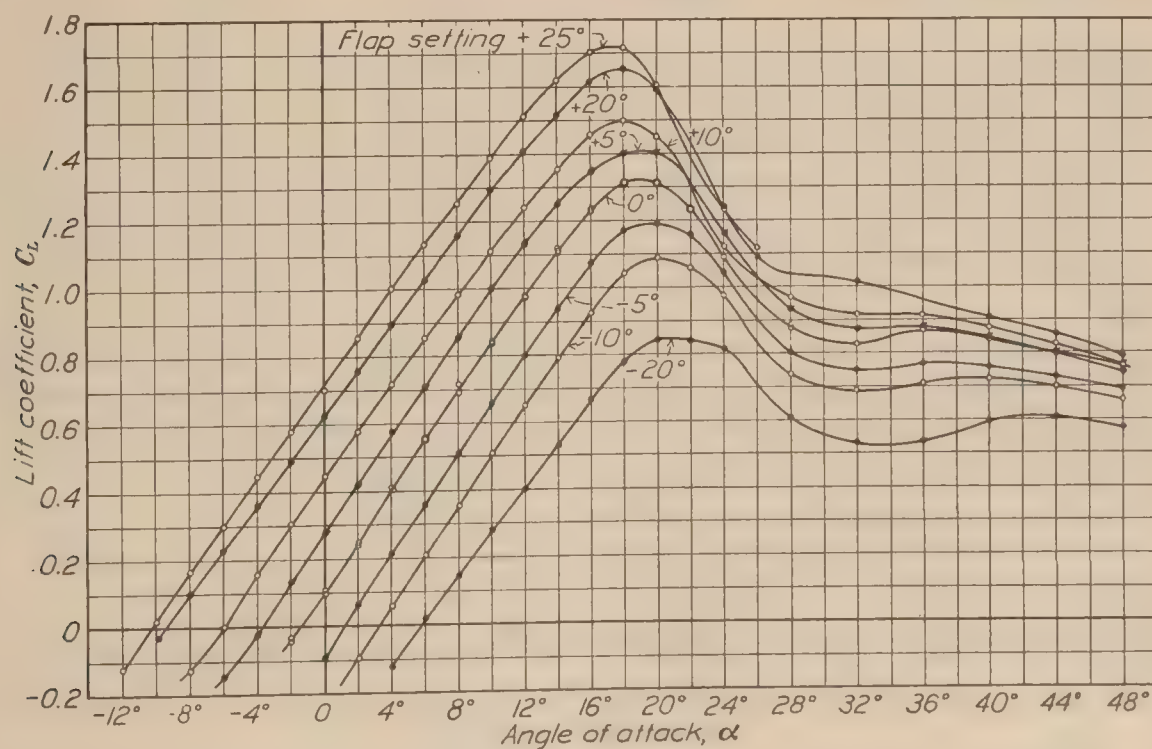


FIG. 7.—Lift coefficient versus angle of attack of N. A. C. A. M-6 airfoil with different flap settings

the lift distribution with the ailerons displaced. This was done by assuming that the total lift of the semispan equals one-half that determined from the aileron tests; and that the lift coefficient at the center is equal to the lift coefficient of the airfoil with the flap neutral, and the lift coefficient at the extreme tip equals that of the model with the flap at $+20^\circ$ or -20° as the case may be. The pitching moment coefficient, C_M , was also treated in a similar manner, see Figure 17. The $C. P.$ curve was then determined from these curves by the use of the formula:

$$C. P. = 25\% - \frac{C_M}{C_L} \cdot 100\%$$

The above formula holds approximately true for the usual range of lift. The $C. P.$ travel is also given (fig. 15) for neutral ailerons. The aileron effect is seen to be large at the outer portion of the airfoil.

Curves showing the variation of rolling and yawing moment coefficients with aileron angle are given in Figures 19 and 20. In each case these values were determined by taking one-half of the difference of the lift and drag values for the up and the down aileron tests and multiplying this quantity by a lever arm equal to the distance from the center of the aileron to the center of the airfoil in terms of the span, or:

$$\text{Rolling moment coefficient, } C_L' = \frac{C_L(+20^\circ) - C_L(-20^\circ)}{2} \times 3/8 \text{ (spans)}$$

$$\text{Yawing moment coefficient, } C_N = \frac{C_D(+20^\circ) - C_D(-20^\circ)}{2} \times 3/8 \text{ (spans)}$$

DISCUSSION

The N. A. C. A. M-6 airfoil section is a stable section in its original form, but when equipped with a flap, its stability characteristics are greatly altered by any change of the position of the flap. The center of pressure travel varies considerably for various flap settings and should be taken into account in designs where ailerons or flaps are used.

From the polar curves and also from the curves of rolling moment coefficient it may be seen that there is still adequate lateral control available at high angles by the use of ailerons provided the yawing tendency can be overcome.

The results given herein have been obtained at 20 atmospheres density and are therefore approximately equivalent to full dynamic scale.

APPENDIX

COMPARISON OF THE MEASURED AND COMPUTED CHARACTERISTICS OF THE M6 AIRFOIL WITH FLAPS

The preceding report contains information about the air forces on an airfoil with a flap, obtained for the first time from force measurement tests simulating full scale conditions. It is of special interest to use such particularly valuable information to throw further light on the aerodynamic theory, and in turn to use the theory to interpret the experimental information. Accordingly, the angle of attack of zero lift and angle of attack of zero moment were computed by means of Munk's integrals. (Reference 2.) These angles were then compared with the observed values.

For this computation the chord is chosen so that it passes through the trailing edge at the point $x = +1$, $\xi = 0$, and its length, so that the leading edge is on the line $x = -1$. ξ denotes the ordinates of the mean curve; that is, the curve which is equidistant from the upper and lower curves of the section. The angle of zero lift is then given by:

$$\alpha_0 = -\frac{1}{\pi} \int_{-1}^{+1} \frac{\xi dx}{(1-x)\sqrt{1-x^2}}$$

The angle at which the moment about the origin (50 per cent chord) is zero is given by:

$$\alpha'_0 = -\frac{2}{\pi} \int_{-1}^{+1} \frac{x\xi dx}{\sqrt{1-x^2}}$$

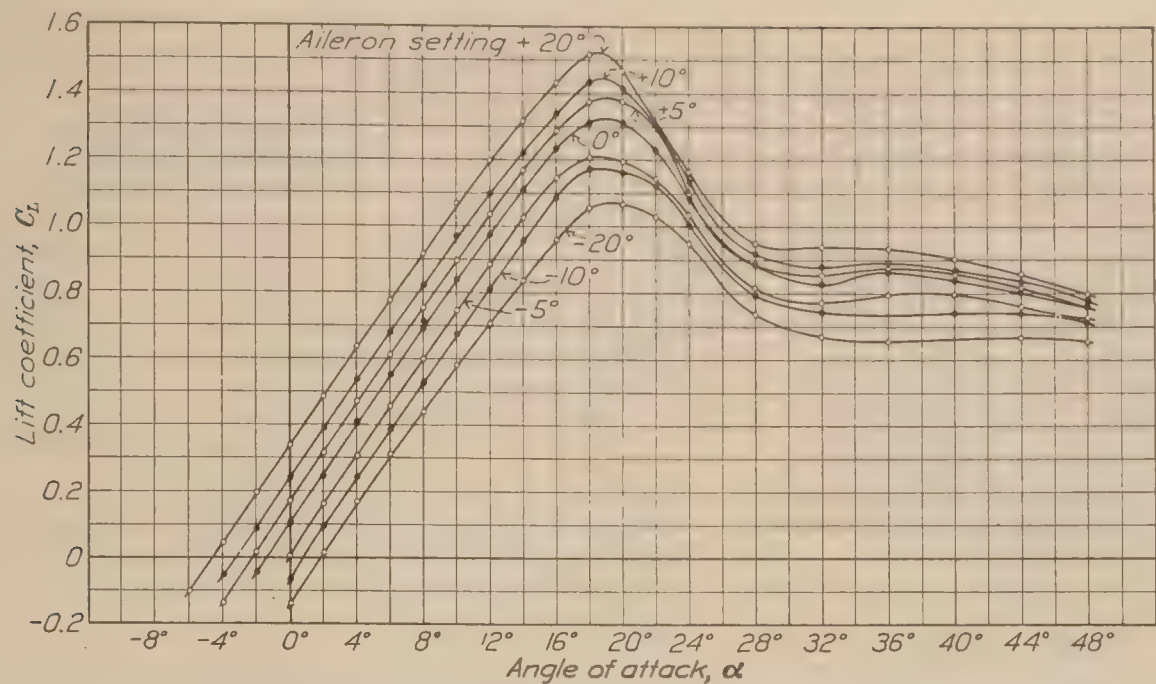


FIG. 8.—Lift coefficient versus angle of attack of N. A. C. A. M-6 airfoil with different aileron settings

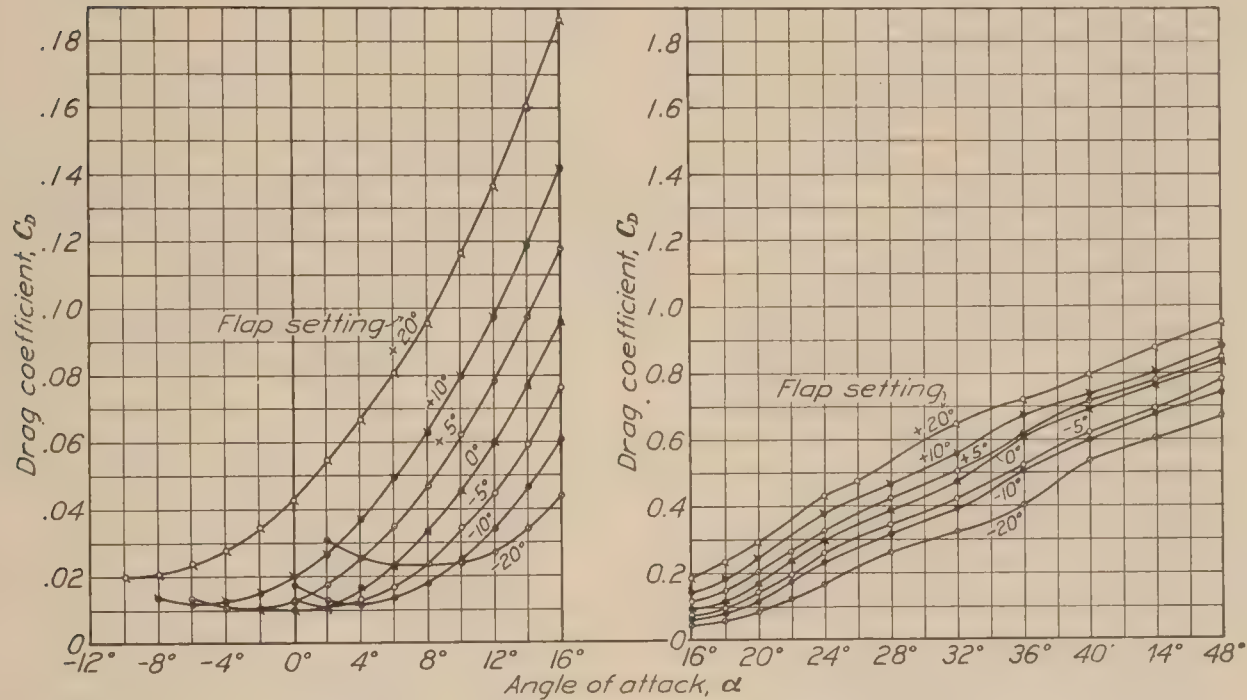


FIG. 9.—Drag coefficient versus angle of attack of N. A. C. A. M-6 airfoil with different flap settings

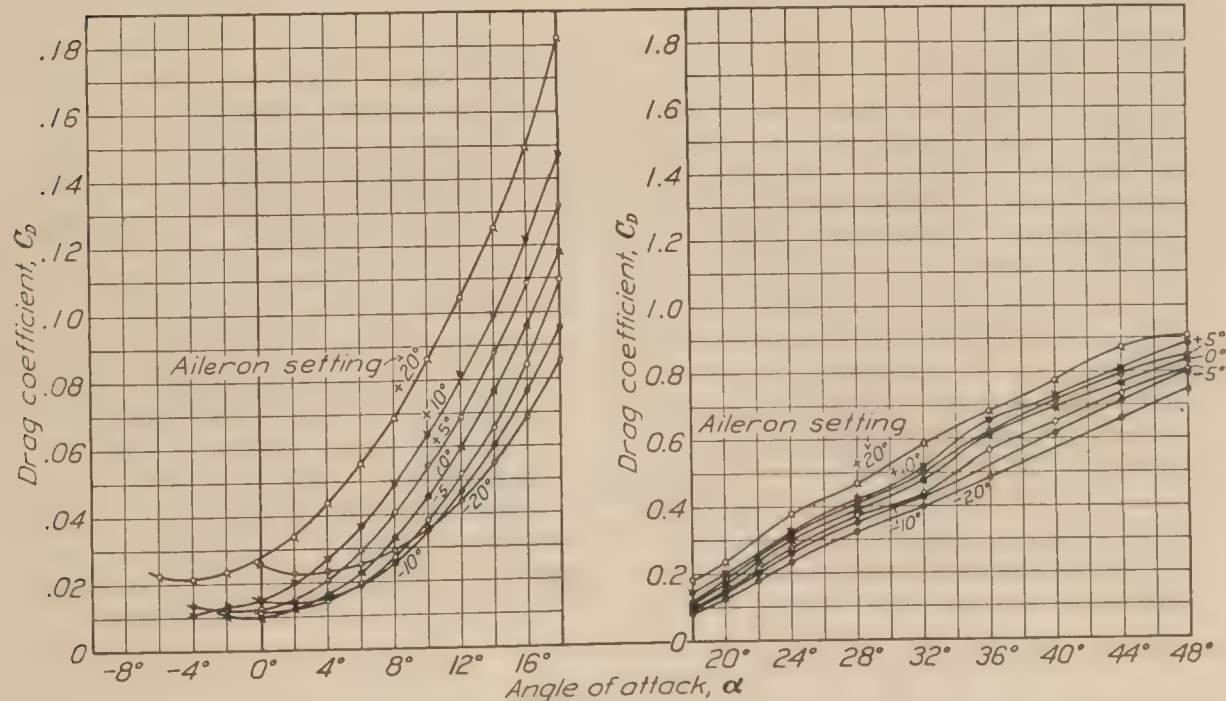


FIG. 10.—Drag coefficient versus angle of attack of N. A. C. A. M-6 airfoil with different aileron settings

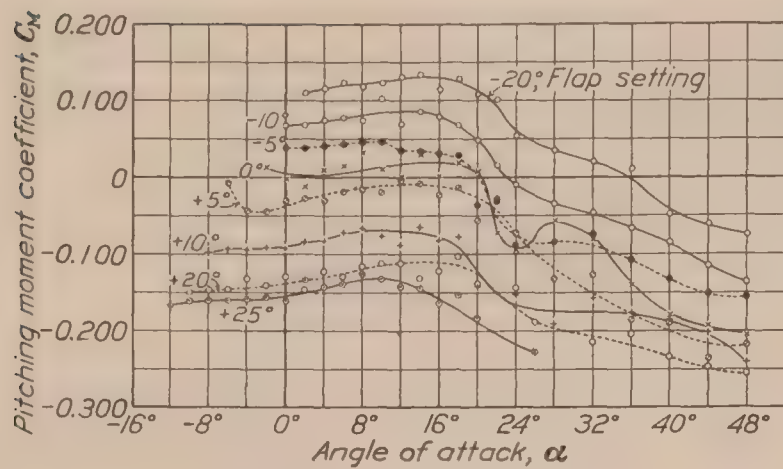


FIG. 11.—Moment coefficient versus angle of attack of N. A. C. A. M-6 airfoil with different flap settings

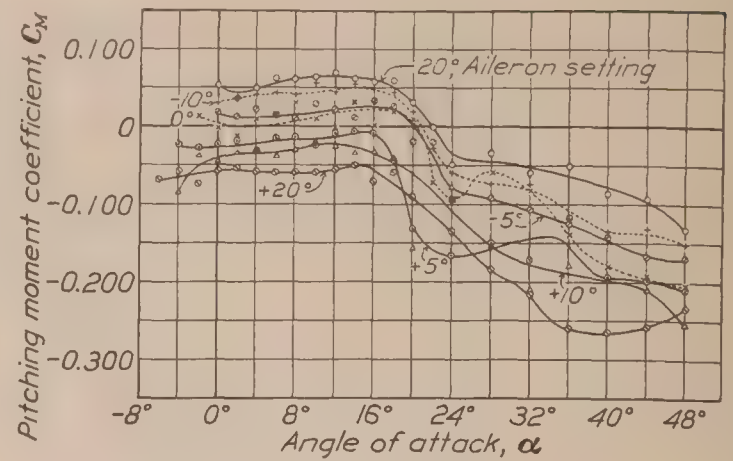


FIG. 12.—Moment coefficient versus angle of attack of N. A. C. A. M-6 airfoil with different aileron settings

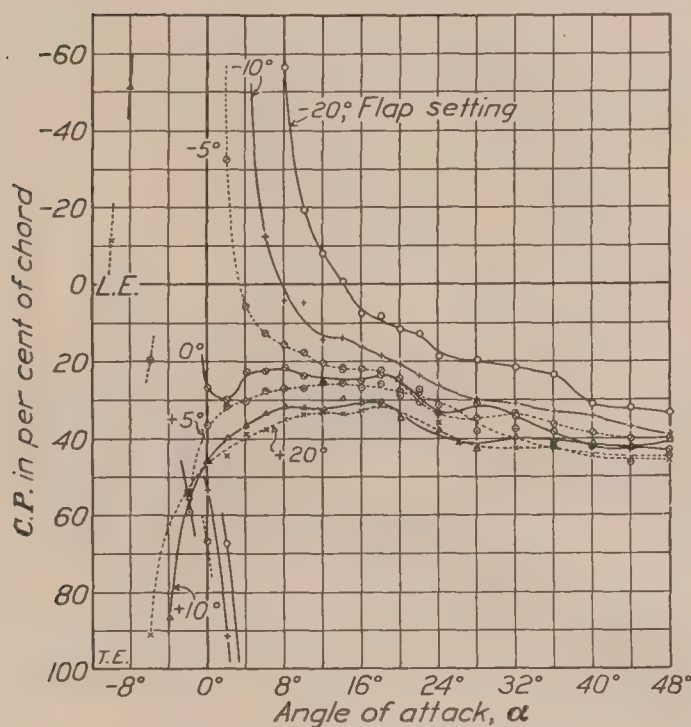


FIG. 13.—Center of pressure versus angle of attack of N. A. C. A. M-6 airfoil with different flap settings

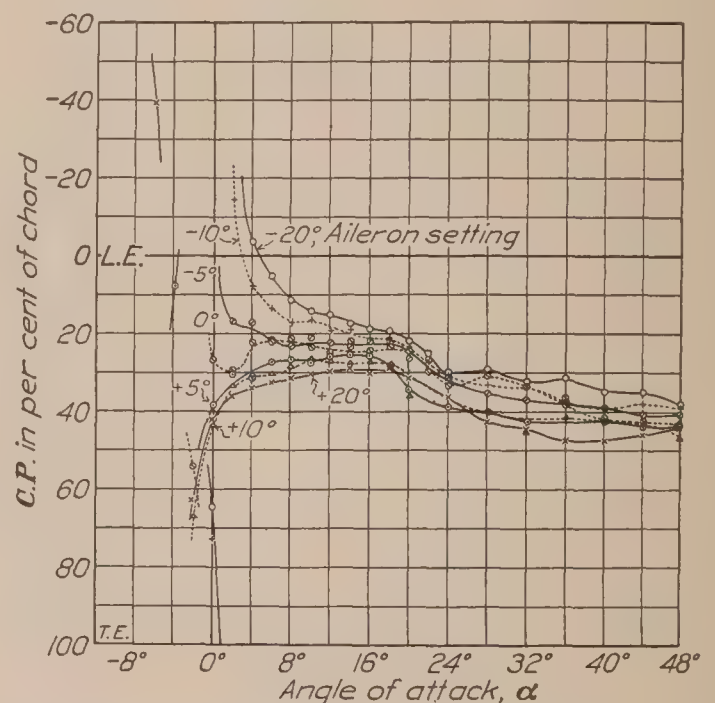


FIG. 14.—Center of pressure versus angle of attack of N. A. C. A. M-6 airfoil with different aileron settings

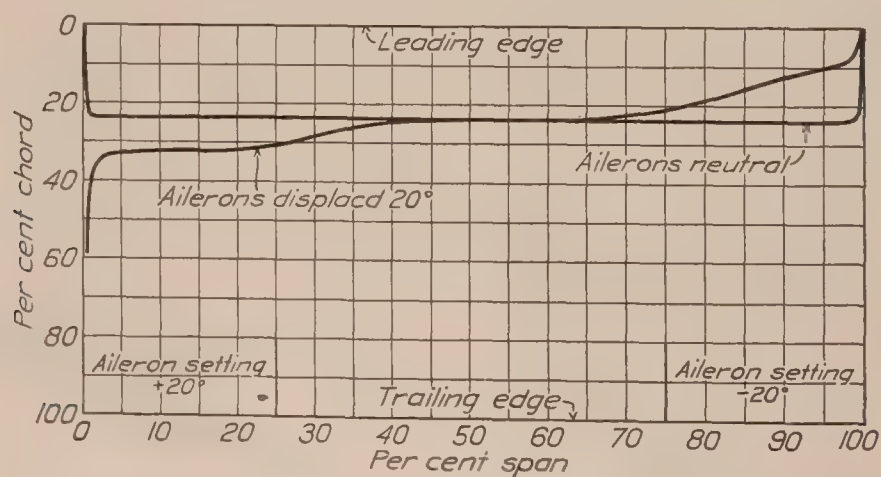


FIG. 15.—Center of pressure variation along span of N. A. C. A. M-6 airfoil with different aileron settings

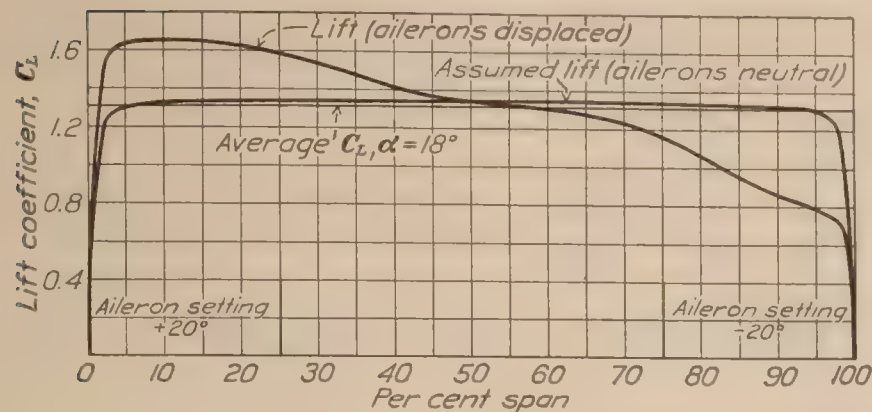


FIG. 16.—Lift distribution along span of N. A. C. A. M-6 airfoil with different aileron settings

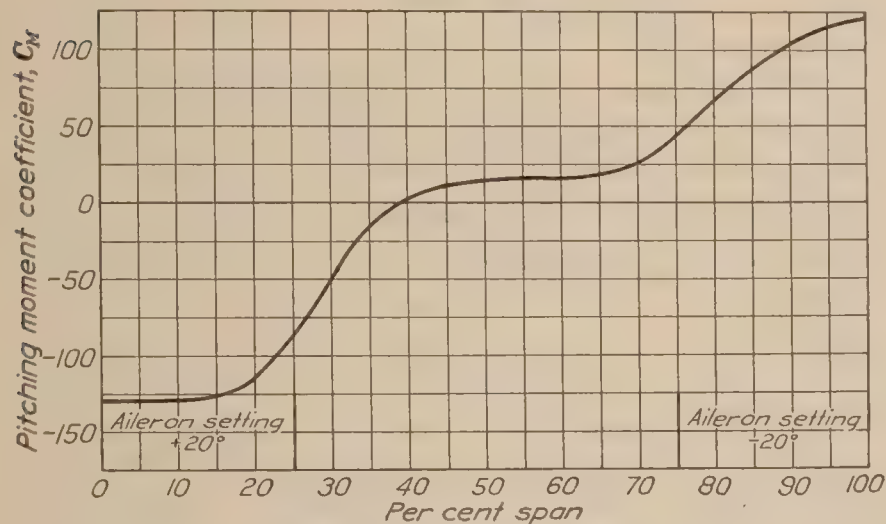


FIG. 17.—Variation of moment along span of N. A. C. A. M-6 airfoil at 18° angle of attack

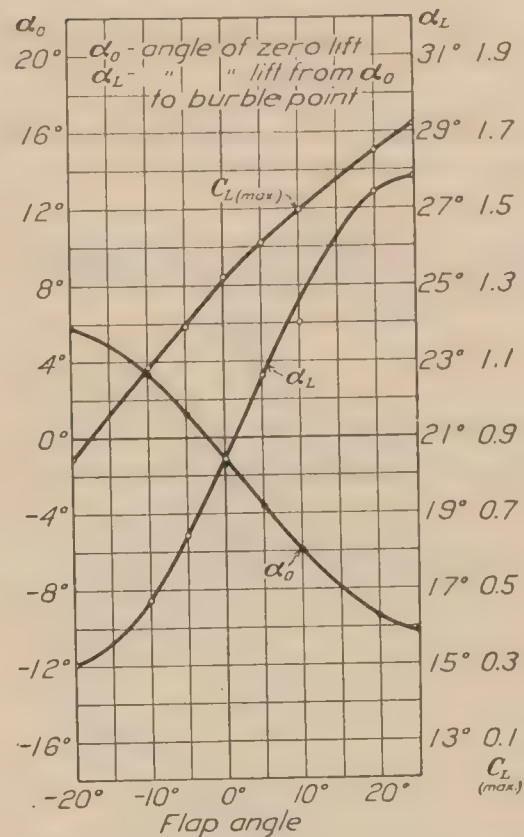


FIG. 18.—Maximum C_L , α_0 and α_L versus flap angle of N. A. C. A. M-6 airfoil

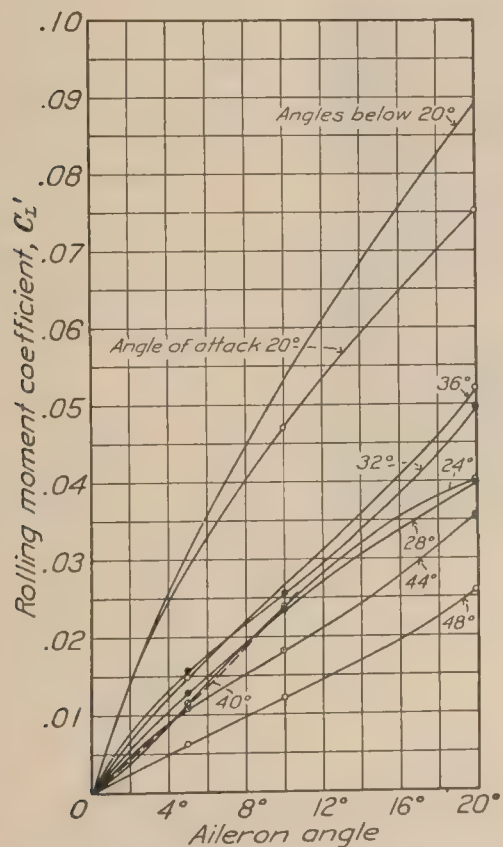


FIG. 19.—Rolling moment versus aileron angle at different angles of attack of N. A. C. A. M-6 airfoil

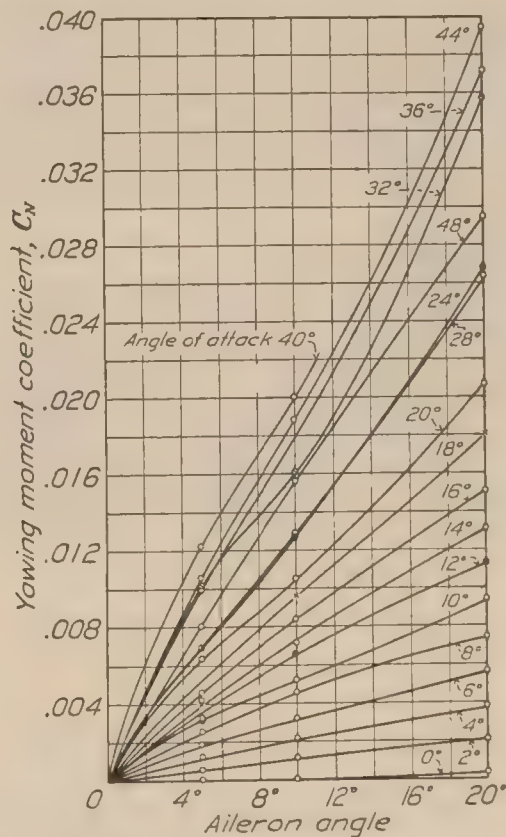


FIG. 20.—Yawing moment versus aileron angle at different angles of attack of N. A. C. A. M-6 airfoil

In the case of a symmetrical section with a flap the mean curve is a broken line as shown in Figure 21.

The value of the angles of zero lift and moment are then

$$\alpha_0 = -\frac{\cos^{-1} h + \sqrt{1-h^2}}{\pi} \tan \beta$$

$$\alpha'_0 = -\frac{\cos^{-1} h - h\sqrt{1-h^2}}{\pi} \tan \beta$$

where β is the angle of displacement of the flap and h is the abscissa of the hinge as shown in the figure, or:

$$h = \frac{S - E \cos \beta}{S + E \cos \beta}$$

where S and E are the lengths of the chords of the stabilizer and elevator, respectively, or in the present case, the fixed part of the airfoil and the flap.

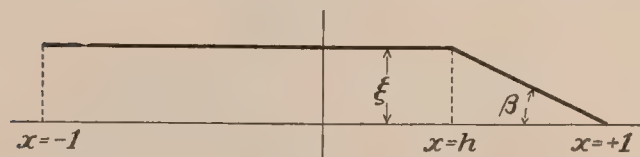


FIG. 21

If the mean curve of the base section is not a straight line it is necessary to correct the angles as given above by adding to them the corresponding angles computed for the undeformed section. These angles were determined by the method given in Reference 1.

TABLE XVIII

1	2	3	4	5	6	7	8
Flap displacement	Computed angle of zero lift	Measured angle of zero lift	K exp.	$\frac{K \text{ exp.}}{K \text{ theor.}}$	Computed effective angle of zero moment	Measured effective angle of zero moment	C_M (Theor.)
-20°	10.67°	5.7°	1.70	0.62	2.33°	-----	0.229
-10°	4.99°	3.3°	2.25	.82	.96°	0.0°	.111
-5°	2.24°	1.2°	2.30	.84	.26°	-.6°	.054
0°	-0.53°	-1.4°	-----	-----	-.45°	-----	-.002
+5°	-3.30°	-3.7°	2.50	.91	-1.16°	-----	-.059
10°	-6.05°	-6.0°	2.40	.87	-1.86°	-2.0°	-.115
20°	-11.73°	-9.5°	2.08	.76	-3.23°	-2.3°	-.233
25°	-14.58°	-10.3°	1.82	.66	-3.84°	-2.7°	-.295

Table XVIII gives the computed angles of zero lift and moment, and also the measured angles, for comparison. Columns giving the value of K and the ratio of its measured to its computed value are also given. K is the coefficient which gives the effect of elevator turning (Reference 2) according to the equation:

$$\alpha \text{ effective} = \frac{E}{E+S} K\beta$$

α effective is the angle of attack of the whole undeformed airfoil which has the same effect as turning the flap by an angle β ; as before, E denotes the chord of the elevator and S , the chord of the stabilizer. For small values of β , the theoretical value of K is

$$K = \frac{E+S}{E} \cdot \frac{\cos^{-1} h + \sqrt{1-h^2}}{\pi}$$

$$h = \frac{S-E}{S+E}$$

From this expression the theoretical value of K is 2.75 for 20 per cent flaps. The ratio of the value of K deduced from the experiments to the above theoretical value is given in column 5 of Table XVIII as a measure of the efficiency of the elevator. These ratios indicate that the efficiency of the elevator is greatest for small displacements and larger when the displacement is down rather than up. The fact that the elevator effect, as compared with the effect as given by the theoretical calculation, falls off rapidly when the displacement angle is over 10°, is shown by both the figures in Table XVIII and the curve in Figure 22.

From the computed angles of zero moment and zero lift, the theoretically constant value of the moment coefficient, C_M , about the quarter chord point was found. (Reference 1.)

$$C_M = \frac{2\pi}{4} (\alpha_0 - \alpha_0^1)$$

where 2π is the theoretical slope of the lift curve for two dimensional flow. The computed values of C_M are plotted in Figure 23 together with the values as determined from the experiments.

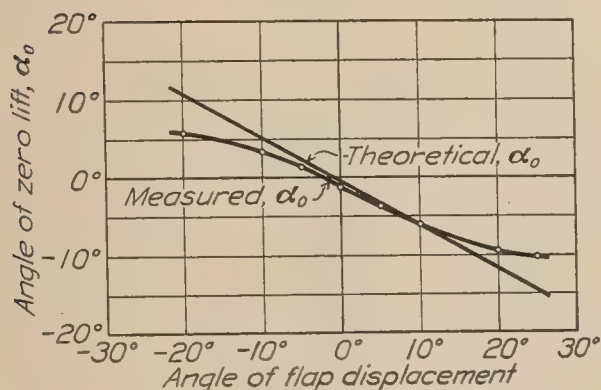


FIG. 22.—Comparison of the theoretical with the measured angles of zero lift in relation to the flap displacement angle

As in the case of the lift, displacing the flap produced a smaller change in the moment coefficient than the change indicated by the theoretical calculation, especially for large flap displacement angles. The moment coefficient as determined from the tests is in agreement with the theory inasmuch as it is approximately independent of the angle of attack below the burble point. Above this point the theory, of course, does not apply so it is not surprising to find that the value of the moment coefficient falls off.

In order to throw some light on what was considered a rather large discrepancy between observed and computed angles of zero lift, the flow pattern around the airfoil was studied near the angle of zero lift. The flap was set down 20° and the airfoil placed in a 6-inch wind tunnel so that the end of the wing rested on a plate which was coated with lamp black and kerosene. The airfoil was set at an angle with the air stream corresponding to the computed angle of zero lift. The resulting pattern, a photograph of which will be found in Figure 24, reveals at once the reason for the discrepancy between the observed and computed angles of zero lift.

The burble region arising at the hinge and extending back over the upper surface of the flap destroys the smooth flow and the lift on the flap so that the total experimental lift is negative in this position instead of zero as indicated by the theory, which assumes a potential flow. If there were no irregularity in the upper surface curve at the hinge the flow would undoubtedly approach more nearly the potential flow assumed by the theory and a better agreement with the theory would result. In every case investigated where the drag has been low at the angle of zero lift, indicating a close approach to a potential flow, the measured angle of zero lift has been found to be very near its theoretical value. The theory then shows in this case that a considerable part of the elevator effect from the flap is lost because of the surface irregularity between the wing and the flap.

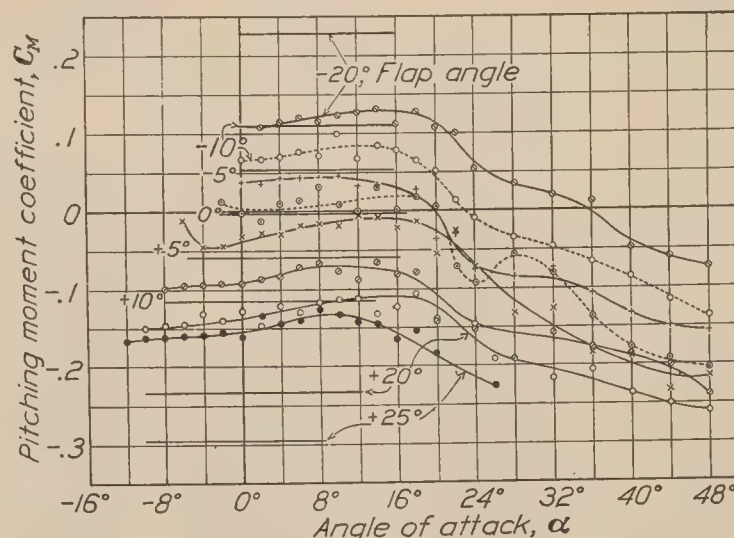


FIG. 23.—Comparison of the theoretical with the measured values of moment coefficient for various flap displacement angles

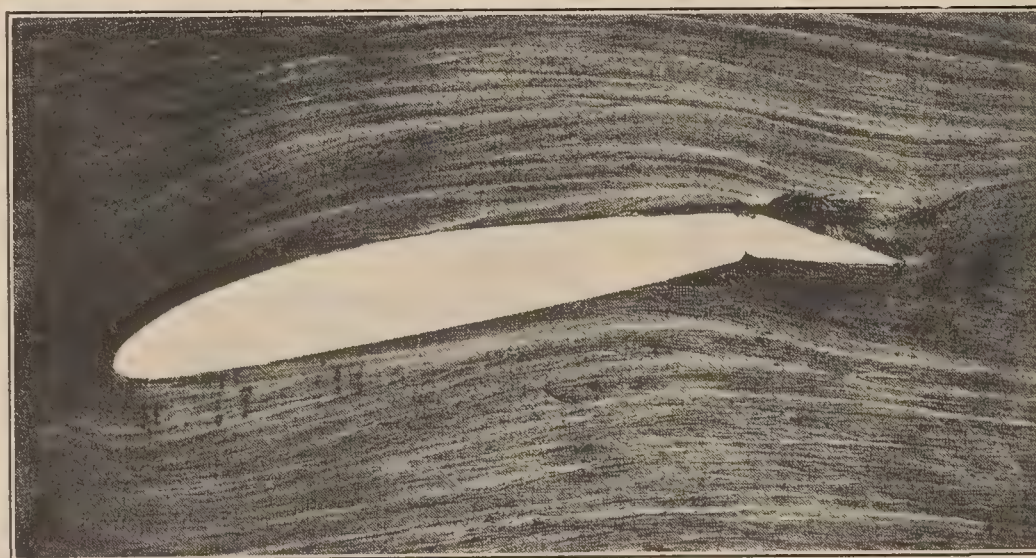


FIG. 24.—Flow pattern around airfoil at theoretical angle of zero lift

REFERENCES

1. MUNK, MAX M. General Theory of Thin Wing Sections. N. A. C. A. Technical Report No. 142. 1922.
2. MUNK, MAX M. The Determination of the Angles of Attack of Zero Lift and of Zero Moment Based on Munk's Integrals. N. A. C. A. Technical Note No. 122. 1923.

TABLE I

Span.....	91.44 cm.	Test No. 202.
Chord.....	15.24 cm.	Airfoil N. A. C. A. M-6 (6'' by 36'') with 20 per cent
Area.....	.1393 m ² .	c flaps.
		Average tank pressure, 20.6 atmospheres.
		Average dynamic pressure, 590 kg/m ² .
		Average Reynolds Number, 3,890,000.

FLAPS SET 20° UP

α Degrees	C_L	C_D	L/D	C_M	$C. P.$ per cent chord
2	-0.262	0.0308	-8.51	+0.110	+67.2
4	-.124	.0257	-4.82	.117	+120.9
6	+.018	.0233	+.77	.123	-586.5
8	.143	.0235	6.08	.117	-55.7
10	.277	.0238	11.64	.123	-19.4
12	.398	.0270	14.74	.131	-8.2
14	.526	.0340	15.47	.134	-.9
16	.662	.0437	15.15	.114	+7.4
18	.775	.0588	13.18	.128	8.1
20	.842	.0804	10.47	.109	11.7
22	.835	.1227	6.80	.101	12.6
24	.813	.1676	4.85	.054	18.3
28	.602	.2612	2.30	.035	19.6
32	.530	.3229	1.64	.020	21.8
36	.533	.4061	1.31	.011	23.3
40	.592	.5534	1.11	-.048	31.0
44	.605	.6062	1.00	-.060	32.0
48	.572	.6736	.85	-.074	33.3

TABLE II

Span.....	91.44 cm.	Test No. 201.
Chord.....	15.24 cm.	Airfoil N. A. C. A. M-6 (6'' by 36'') with 20 per cent
Area.....	.1393 m ² .	c flaps.
		Average tank pressure, 20.6 atmospheres.
		Average dynamic pressure, 610 kg/m ² .
		Average Reynolds Number, 4,130,000.

FLAPS SET 10° UP

α Degrees	C_L	C_D	L/D	C_M	$C. P.$ per cent chord
0	-0.242	0.0172	-14.07	0.068	+53.1
2	-.099	.0129	-7.67	.065	+91.0
4	+.058	.0115	+5.04	.074	-101.0
6	.204	.0136	15.00	.077	-12.7
8	.349	.0178	19.61	.073	+4.0
10	.505	.2520	20.04	.102	4.6
12	.647	.0339	19.09	.069	14.2
14	.787	.0461	17.07	.086	13.9
16	.920	.0609	15.11	.079	16.2
18	1.040	.0809	12.86	.066	18.5
20	1.084	.1162	9.33	.048	20.5
22	1.054	.1743	6.05	.015	23.6
24	.971	.2306	4.21	-.010	26.0
28	.735	.3179	2.31	-.034	29.7
32	.684	.3909	1.75	-.045	30.9
36	.705	.5088	1.39	-.067	32.8
40	.721	.6002	1.20	-.084	34.0
44	.697	.6773	1.03	-.115	36.8
48	.659	.7443	.88	-.137	38.9

TABLE III

Span.....	91.44 cm.	Test No. 200.
Chord.....	15.24 cm.	Airfoil N. A. C. A. M-6 (6'' by 36'') with 20 per cent
Area.....	.1393 m ² .	c flaps.
		Average tank pressure, 20.5 atmospheres.
		Average dynamic pressure, 615 kg/m ² .
		Average Reynolds Number, 4,150,000.

FLAPS SET 5° UP

α Degrees	C_L	C_D	L/D	C_M	$C. P.$
0	-0.094	0.0130	-7.23	0.039	+66.5
2	+.064	.0108	+5.93	.037	-32.5
4	.211	.0131	16.11	.041	+5.6
6	.353	.0165	21.39	.044	12.5
8	.502	.0234	21.45	.046	15.7
10	.655	.0341	19.21	.046	17.9
12	.795	.0444	19.90	.035	20.5
14	.936	.0590	15.86	.034	21.3
16	1.070	.0761	14.06	.032	21.9
18	1.168	.0972	12.02	.029	22.4
20	1.187	.1426	8.32	-.036	28.1
22	1.153	.1984	5.81	-.031	27.7
24	1.040	.2608	3.99	-.088	33.4
28	.800	.3472	2.30	-.083	34.6
32	.748	.4215	1.78	-.074	33.6
36	.767	.5242	1.46	-.106	36.3
40	.754	.6240	1.21	-.132	38.5
44	.726	.6977	1.04	-.151	40.0
48	.690	.7834	.88	-.154	39.7

TABLE IV

Span.....	91.44 cm.	Test No. 194.
Chord.....	15.24 cm.	Airfoil N. A. C. A. M-6 (6'' by 36'') with 20 per cent
Area.....	.1393 m ² .	c flaps.
		Average tank pressure, 20.8 atmospheres.
		Average dynamic pressure, 620 kg/m ² .
		Average Reynolds Number, 4,180,000.

FLAPS SET AT 0°

α Degrees	C_L	C_D	L/D	C_M	$C. P.$ per cent chord
-2	-0.044	0.0103	-4.27	+0.013	54.4
0	+.106	.0099	+10.71	-.002	26.9
2	.243	.0107	22.71	-.012	29.9
4	.407	.0165	24.67	+.010	22.5
6	.550	.0228	24.12	.015	22.3
8	.690	.0326	21.17	.032	21.4
10	.836	.0451	18.54	.010	23.8
12	.972	.0597	16.28	-.001	25.1
14	1.107	.0765	14.47	+.031	22.1
16	1.233	.0958	12.87	.001	24.9
18	1.310	.1178	11.12	.018	23.6
20	1.308	.1692	7.73	.008	24.4
22	1.227	.2374	5.17	-.072	30.9
24	1.082	.2991	3.62	-.094	33.5
28	.882	.3868	2.28	-.057	31.0
32	.824	.4751	1.73	-.080	33.4
36	.863	.6134	1.41	-.139	38.1
40	.838	.6925	1.21	-.179	41.7
44	.800	.7660	1.04	-.191	42.3
48	.755	.8315	.91	-.203	43.1

TABLE V

Span	91.44 cm.	Test No. 196.
Chord	15.24 cm.	Airfoil N. A. C. A. M-6 (6'' by 36'') with 20 per cent c
Area	.1393 m ² .	flaps.
		Average tank pressure, 20.6 atmospheres.
		Average dynamic pressures, 620 kg/m ² .
		Average Reynolds Number, 4,205,000.

FLAPS SET 5° DOWN

α Degrees	C_L	C_D	L/D	C_M	$C. P.$ per cent chord
-6	-0.150	0.0134	-11.19	-0.008	+19.6
-4	-.027	.0103	-2.62	-.043	-145.4
-2	+.130	.0102	+12.74	-.045	+59.4
0	.277	.0123	22.52	-.032	36.5
2	.418	.0174	24.02	-.027	31.5
4	.573	.0256	22.38	-.030	30.2
6	.707	.0346	20.43	-.019	27.7
8	.851	.0464	18.34	-.016	26.9
10	.991	.0621	15.96	-.020	27.0
12	1.127	.0780	14.45	-.003	25.3
14	1.250	.0971	12.87	-.008	25.6
16	1.344	.1179	11.40	-.024	26.9
18	1.401	.1496	9.36	-.013	25.9
20	1.402	.2090	6.71	-.056	29.0
22	1.317	.2682	4.91	-.027	27.1
24	1.158	.3282	3.53	-.073	31.2
28	.931	.4227	2.02	-.132	38.0
32	.872	.5028	1.73	-.126	37.5
36	.875	.6208	1.41	-.185	42.3
40	.841	.7190	1.17	-.188	41.9
44	.794	.7793	1.02	-.235	46.1
48	.740	.8476	.87	-.216	44.3

TABLE VI

Span	91.44 cm.	Test No. 197.
Chord	15.24 cm.	Airfoil N. A. C. A. M-6 (6'' by 36'') with 20 per cent
Area	.1393 m ² .	c flaps.
		Average tank pressure, 20.7 atmospheres.
		Average dynamic pressure, 623 kg/m ² .
		Average Reynolds Number, 4,320,000.

FLAPS SET 10° DOWN

α Degrees	C_L	C_D	L/D	C_M	$C. P.$
-8	-0.127	0.0136	-9.34	-0.098	-51.6
-6	-.002	.0118	-.17	-.094	+1765.0
-4	+.155	.0122	+12.70	-.094	86.3
-2	.304	.0148	20.54	-.092	55.2
0	.442	.0201	21.99	-.092	45.8
2	.574	.0264	21.74	-.085	39.8
4	.715	.0369	19.38	-.082	36.5
6	.852	.0491	17.35	-.071	33.3
8	.980	.0627	15.63	-.066	31.7
10	1.106	.0796	13.89	-.077	32.0
12	1.238	.0971	12.75	-.088	32.2
14	1.350	.1186	11.38	-.065	29.8
16	1.453	.1420	10.22	-.081	30.7
18	1.494	.1838	8.13	-.077	30.3
20	1.447	.2424	5.97	-.142	34.8
24	1.116	.3752	2.97	-.152	38.0
28	.964	.4621	2.09	-.190	42.9
32	.912	.5561	1.64	-.157	39.8
36	.910	.6757	1.35	-.176	40.5
40	.874	.7389	1.18	-.186	41.3
44	.824	.8052	1.02	-.200	42.3
48	.761	.8816	.86	-.239	40.5

TABLE VII

Span.....	91.44 cm.	Test No. 198.
Chord.....	15.24 cm.	Airfoil N. A. C. A. M-6 (6'' by 36'') with 20 per cent
Area.....	.1393 m ² .	<i>c</i> flaps.
		Average tank pressure, 20.8 atmospheres.
		Average dynamic pressure, 620 kg/m ² .
		Average Reynolds Number, 4,170,000.

FLAPS SET 20° DOWN

α Degrees	C_L	C_D	L/D	C_M	$C. P.$ per cent chord
-10	-0.038	0.0197	-1.93	-0.150	-11.8
-8	+.100	.0203	+4.93	-.147	+178.4
-6	.226	.0237	9.54	-.147	91.0
-4	.359	.0273	13.15	-.131	62.0
-2	.490	.0344	14.24	-.141	53.8
0	.624	.0424	14.72	-.130	45.8
2	.754	.0549	13.73	-.146	44.4
4	.896	.0665	13.47	-.123	38.6
6	1.027	.0807	12.73	-.130	37.7
8	1.157	.0953	12.14	-.116	35.0
10	1.293	.1168	11.07	-.112	33.7
12	1.408	.1363	10.33	-.112	33.0
14	1.521	.1606	9.47	-.132	33.7
16	1.631	.1866	8.74	-.123	32.6
18	1.650	.2343	7.04	-.103	31.2
20	1.589	.2945	5.40	-.140	33.8
24	1.240	.4311	2.88	-.144	35.9
26	1.090	.4775	2.28	-.189	41.0
28					
32	1.012	.6410	1.58	-.214	42.7
36	.959	.7133	1.34	-.203	42.0
40	.904	.7931	1.14	-.233	44.4
44	.852	.8729	.98	-.245	45.1
48	1.787	.9463	.83	-.254	45.6

TABLE VIII

Span.....	91.44 cm.	Test No. 199.
Chord.....	15.24 cm.	Airfoil N. A. C. A. M-6 (6'' by 36'') with 20[per cent <i>c</i>
Area.....	.1393 m ² .	flaps.
		Average tank pressure, 20.6 atmospheres.
		Average dynamic pressure, 613 kg/m ² .
		Average Reynolds Number, 4,110,000.

FLAPS SET 25° DOWN

α Degrees	C_L	C_D	L/D	C_M	$C. P.$ per cent chord
-12	-0.124	0.0327	-3.79	-0.167	-105.3
-10	+.020	.0314	+.64	-.162	+1161.0
-8	.169	.0317	5.33	-.161	+124.4
-6	.298	.0351	8.49	-.161	80.3
-4	.442	.0408	10.83	-.159	61.3
-2	.576	.0484	11.90	-.146	50.5
0	.702	.0570	12.32	-.162	48.1
2	.855	.0705	12.13	-.134	40.6
4	1.001	.0851	11.76	-.144	39.3
6	1.129	.1009	11.19	-.140	37.3
8	1.250	.1180	10.59	-.127	35.2
10	1.389	.1405	9.89	-.133	34.6
12	1.510	.1613	9.36	-.143	34.5
14	1.619	.1849	8.76	-.144	33.9
16	1.703	.2098	8.12	-.165	34.7
18	1.718	.2581	6.65	-.153	33.9
20	1.605	.3336	4.81	-.184	36.4
24	1.231	.4608	2.67	-.337	51.6
26	1.112	.5144	2.16	-.227	43.6

TABLE IX

Span.....	91.44 cm.	Test No. 208.
Chord.....	15.24 cm.	Airfoil N. A. C. A. M-6 (6'' by 36'') with 20 per cent <i>c</i>
Area.....	.1393 m ² .	flaps.
		Average tank pressure, 20.4 atmospheres.
		Average dynamic pressure, 602 kg/m ² .
		Average Reynolds Number, 4,100,000.

AILERONS SET 20° DOWN

α Degrees	C_L	C_D	L/D	C_M	$C. P.$ per cent chord
-6	-0.103	0.0223	-4.62	-0.068	-39.5
-4	+.043	.0213	+2.02	-.057	+162.5
-2	.195	.0233	8.37	-.074	63.0
0	.336	.0275	12.22	-.057	42.0
2	.483	.0337	14.33	-.053	36.0
4	.637	.0437	14.58	-.058	34.1
6	.772	.0552	13.99	-.059	32.6
8	.914	.0686	13.32	-.059	31.5
10	1.063	.0862	12.33	-.059	30.5
12	1.193	.1044	11.43	-.055	29.6
14	1.315	.1252	10.50	-.053	29.0
16	1.429	.1494	9.56	-.071	30.1
18	1.512	.1819	8.31	-.059	28.9
20	1.468	.2384	6.16	-.092	31.3
24	1.163	.3741	3.11	-.134	36.1
28	.948	.4659	2.04	-.183	42.5
32	.936	.5863	1.60	-.215	44.4
36	.932	.6804	1.37	-.258	47.4
40	.901	.7746	1.16	-.263	47.2
44	.856	.8698	.98	-.256	46.0
48	.792	.9042	.88	-.233	44.4

TABLE X

Span.....	91.44 cm.	Test No. 207.
Chord.....	15.24 cm.	Airfoil N. A. C. A. M-6 (6'' by 36'') with 20 per cent <i>c</i>
Area.....	.1393 m ² .	flaps.
		Average tank pressure, 20.6 atmospheres.
		Average dynamic pressure, 610 kg/m ² .
		Average Reynolds Number, 4,130,000.

AILERONS SET 10° DOWN

α degrees	C_L	C_D	L/D	C_M	$C. P.$ per cent chord
-4	-0.051	0.0108	-4.72	-0.084	-138.0
-2	+.087	.0131	+6.64	-.037	+67.3
0	.240	.0147	16.33	-.044	43.3
2	.390	.0201	19.40	-.034	33.7
4	.536	.0270	19.85	-.031	30.8
6	.679	.0363	18.70	-.039	30.8
8	.821	.0491	16.72	-.030	28.7
10	.969	.0635	15.26	-.018	26.9
12	1.097	.0816	13.44	-.025	27.3
14	1.219	.0990	12.31	-.034	27.8
16	1.339	.1219	10.98	-.031	27.3
18	1.431	.1472	9.72	-.042	28.0
20	1.413	.2011	7.03	-.156	36.1
24	1.135	.3280	3.46	-.078	31.7
28	.916	.4206	2.18	-.152	40.2
32	.878	.5146	1.71	-.208	45.5
36	.891	.6552	1.36	-.179	41.2
40	.868	.7283	1.19	-.197	42.4
44	.835	.8095	1.03	-.208	42.9
48	.775	.8819	.88	-.252	46.4

TABLE XI

Span.....	91.44 cm.	Test No. 206.
Chord.....	15.24 cm.	Airfoil N. A. C. A. M-6 (6'' by 36'') with 20 per cent c
Area.....	.1393 m ² .	flaps.
		Average tank pressure, 20.7 atmospheres.
		Average dynamic pressure, 622 kg/m ² .
		Average Reynolds Number, 4,200,000.

AILERONS SET 5° DOWN

α degrees	C_L	C_D	L/D	C_M	$C. P.$ per cent chord
-4	-0.135	0.0135	-10.00	-0.023	7.8
-2	+.015	.0122	+1.23	-.027	209.0
0	.170	.0122	13.93	-.023	38.5
2	.315	.0151	20.86	-.018	30.7
4	.469	.0207	22.66	-.031	31.6
6	.610	.0294	20.75	-.015	27.5
8	.751	.0407	18.45	-.013	26.7
10	.892	.0545	16.37	-.025	27.8
12	1.032	.0687	15.02	-.009	25.9
14	1.166	.0880	13.25	-.007	25.6
16	1.285	.1086	11.83	-.008	25.6
18	1.372	.1319	10.40	-.043	28.2
20	1.372	.1862	7.37	-.132	34.7
24	1.095	.3130	3.50	-.166	39.0
28	.882	.4075	2.16	-.149	40.4
32	.853	.4904	1.74	-.171	42.7
36	.872	.6208	1.41	-.119	36.1
40	.858	.7159	1.20	-.193	42.3
44	.816	.7902	1.03	-.198	42.4
48	.755	.8465	.89	-.210	43.5

TABLE XII

Span.....	91.44 cm.	Test No. 194.
Chord.....	15.24 cm.	Airfoil N. A. C. A. M-6 (6'' by 36'') with 20 per cent
Area.....	.1393 m ² .	c flaps.
		Average tank pressure, 20.8 atmospheres.
		Average dynamic pressure, 620 kg/m ² .
		Average Reynolds Number, 4,180,000.

AILERONS SET AT 0°

α Degrees	C_L	C_D	L/D	C_M	$C. P.$ per cent chord
-2	-0.044	0.0103	-4.27	+0.013	54.4
0	+.106	.0099	+10.71	-.002	26.9
2	.243	.0107	22.71	-.012	29.9
4	.407	.0165	24.67	+.010	22.5
6	.550	.0228	24.12	+.015	22.3
8	.690	.0326	21.17	+.032	21.4
10	.836	.0451	18.54	+.010	23.8
12	.972	.0597	16.28	-.001	25.1
14	1.107	.0765	14.47	+.031	22.1
16	1.233	.0958	12.87	+.001	24.9
18	1.310	.1178	11.12	+.018	23.6
20	1.308	.1692	7.73	+.008	24.4
22	1.227	.2374	5.17	-.072	30.9
24	1.082	.2991	3.62	-.094	33.5
28	.882	.3868	2.28	-.057	31.0
32	.824	.4751	1.73	-.080	33.4
36	.863	.6134	1.41	-.139	38.1
40	.838	.6925	1.21	-.179	41.7
44	.800	.7660	1.04	-.191	42.3
48	.755	.8315	.91	-.203	43.1

TABLE XIII

Span.....	91.44 cm.	Test No. 205.
Chord.....	15.24 cm.	Airfoil N. A. C. A. M-6 (6'' by 36'') with 20 per cent
Area.....	.1393 m ² .	c flaps.
		Average tank pressure, 20.6 atmospheres.
		Average dynamic pressure, 600 kg/m ² .
		Average Reynolds Number, 3,990,000.

AILERONS SET 5° UP

α Degrees	C_L	C_D	L/D	C_M	$C. P.$ per cent chord
0	0.002	0.0113	0.18	0.019	-925.0
2	.162	.0122	13.28	.013	+17.0
4	.308	.0144	21.39	.023	17.5
6	.455	.0196	23.21	.014	21.9
8	.596	.0273	21.83	.010	23.3
10	.744	.0380	19.58	.029	21.1
12	.883	.0520	16.98	.021	22.5
14	1.024	.0654	15.66	.011	23.9
16	1.144	.0840	13.62	.033	22.0
18	1.207	.1098	10.99	.026	22.7
20	1.192	.1521	7.84	-.020	26.7
22	1.141	.2162	5.28	-.020	26.8
24	1.033	.2758	3.74	-.095	32.0
28	.813	.3701	2.20	-.093	35.3
32	.770	.4359	1.77	-.106	37.0
36	.793	.5673	1.40	-.126	37.9
40	.796	.6508	1.22	-.141	38.7
44	.758	.7335	1.03	-.167	40.8
48	.722	.8037	.90	-.168	40.6

TABLE XIV

Span.....	91.44 cm.	Test No. 204.
Chord.....	15.24 cm.	Airfoil N. A. C. A. M-6 (6'' by 36'') with 20 per cent
Area.....	.1393 m ² .	c flaps.
		Average tank pressure, 20.6 atmospheres.
		Average dynamic pressure, 610 kg/m ² .
		Average Reynolds Number, 4,150,000.

AILERONS SET 10° UP

α Degrees	C_L	C_D	L/D	C_M	$C. P.$ Per cent chord
0	-0.065	0.0150	-4.33	0.031	72.7
2	+.095	.0140	+6.79	.037	-14.2
4	.241	.0153	15.75	.041	+8.0
6	.383	.0191	20.05	.043	13.8
8	.526	.0254	20.71	.041	17.2
10	.676	.0353	19.15	.056	16.6
12	.810	.0465	17.42	.043	19.6
14	.953	.0608	15.67	.055	19.1
16	1.086	.0769	14.12	.031	22.0
18	1.171	.0955	12.26	.043	21.2
20	1.163	.1451	8.02	.019	23.4
22	1.121	.2015	5.56	-.028	27.5
24	1.008	.2600	3.88	-.059	30.8
28	.793	.3519	2.25	-.074	33.5
32	.742	.4286	1.73	-.074	33.7
36					
40	.739	.6196	1.19	-.134	38.9
44	.738	.7091	1.04	-.131	37.8
48	.710	.7988	.89	-.150	39.0

TABLE XV

Span.....	91.44 cm.	Test No. 203.
Chord.....	15.24 cm.	Airfoil N. A. C. A. M-6 (6'' by 36'') with 20 per cent
Area.....	.1393 m ² .	c flaps.
		Average tank pressure 20.6 atmospheres.
		Average dynamic pressure, 611 kg/m ² .
		Average Reynolds Number, 4,110,000.

AILERONS SET 20° UP

α Degrees	C_L	C_D	L/D	C_M	C. P. per cent chord
0	-0.137	0.0258	-5.31	0.054	64.4
2	+.018	.0227	+.79	.031	205.6
4	.169	.0234	7.22	.048	-3.6
6	.311	.0252	12.34	.062	+5.1
8	.440	.0291	15.12	.060	11.4
10	.581	.0358	16.23	.063	14.2
12	.707	.0438	16.14	.068	15.3
14	.835	.0550	15.18	.061	17.6
16	.958	.0688	13.92	.057	19.0
18	1.055	.0853	12.37	.059	19.3
20	1.067	.1279	8.34	.030	22.1
22	1.030	.1800	5.72	-.001	25.1
24	.949	.2312	4.10	-.050	30.3
28	.736	.3254	2.26	-.035	29.4
32	.672	.3958	1.70	-.059	32.5
36	.654	.4821	1.36	-.052	31.4
40					
44	.665	.6595	1.01	-.093	34.9
48	.654	.7471	.88	-.132	38.3

TABLE XVI

VARIATION OF C_L' , C_M , and C. P. ALONG SPAN $\alpha=+18^\circ$

Per cent span	Ailerons—Neutral			Ailerons—20°*		
	C_L'	C_M	C. P. per cent chord	C_L'	C_M	C. P. per cent chord
0.0	0.00	0.14	$+\alpha$	0.0	-0.130	$-\alpha$
.5	.62	.14	22.74			
1.0	.88	.14	23.41			
2.5	1.24	.14	23.87	1.56	-.130	33.3
5.0	1.29 ₅	.14	23.92	1.62 ₅	-.129	32.9
10.0	1.32	.14	23.94	1.65	-.128	32.7
20.0	1.33	.14	23.95	1.62	-.114	32.0
30.0	1.33 ₅	.14	23.95	1.53 ₅	-.052	28.4
40.0	1.34	.14	23.96	1.41	+.002	24.9
50.0	1.34	.14	23.96	1.34	.014	24.0
60.0	1.34	.14	23.96	1.30	.016	23.8
70.0	1.33 ₅	.14	23.95	1.23	.027	22.8
75.0				1.15 ₅	.046	21.0
80.0	1.33	.14	23.95	1.06	.067	18.7
85.0				.95 ₅	.088	15.8
90.0	1.32	.14	23.94	.86	.104	12.9
95.0	1.29 ₅	.14	23.92	.79	.115	10.4
97.5	1.24	.14	23.87	.73 ₅	.118	9.0
99.0	.88	.14	23.41			
99.5	.62	.14	22.74			
100.0	.00	.14	$+\alpha$.00	.121	$+\alpha$

* Down aileron, 0 to 25 per cent of span.
Up aileron, 75 to 100 per cent of span.

TABLE XVII

MOMENTS CAUSED BY AILERONS

$$C_{L'} = \frac{L'}{qbS} \quad C_N = \frac{N}{qbS}$$

α Degrees	Rolling moment coefficient $C_{L'}$			Yawing moment coefficient C_N		
	Ailerons 5°	Ailerons 10°	Ailerons 20°	Ailerons 5°	Ailerons 10°	Ailerons 20°
0	0. 0315	0. 0572	0. 0885	0. 00017	0. 00006	0. 00032
2	. 0287	. 0553	. 0870	. 00054	. 00114	. 00206
4	. 0302	. 0553	. 0877	. 00118	. 00219	. 00380
6	. 0291	. 0555	. 0862	. 00184	. 00322	. 00562
8	. 0291	. 0553	. 0889	. 00251	. 00461	. 00740
10	. 0278	. 0550	. 0904	. 00309	. 00529	. 00945
12	. 0279	. 0538	. 0911	. 00313	. 00656	. 01136
14	. 0266	. 0499	. 0900	. 00424	. 00716	. 01316
16	. 0264	. 0474	. 0881	. 00461	. 00843	. 01510
18	. 0309	. 0488	. 0855	. 00414	. 00965	. 01810
20	. 0337	. 0469	. 0750	. 00639	. 01050	. 02070
24	. 0116	. 0238	. 0401	. 00696	. 01275	. 02680
28	. 0129	. 0231	. 0398	. 00700	. 01286	. 02635
32	. 0156	. 0255	. 0495	. 01020	. 01610	. 03570
36	. 0148		. 0521	. 01002		. 03717
40	. 0116	. 0242		. 01220	. 02040	
44	. 0109	. 0182	. 0356	. 01062	. 01885	. 03945
48	. 0062	. 0122	. 0259	. 00802	. 01560	. 02945

REPORT No. 261

RESISTANCE AND COOLING POWER OF VARIOUS RADIATORS

By R. H. SMITH

**Aerodynamical Laboratory, Bureau of Construction and Repair,
United States Navy**

REPORT No. 261

RESISTANCE AND COOLING POWER OF VARIOUS RADIATORS

By R. H. SMITH

INTRODUCTION

This report combines the wind-tunnel results of radiator tests made at the Navy Aerodynamical Laboratory in Washington during the summers of 1921, 1925, and 1926, and submitted for publication to the National Advisory Committee for Aeronautics, November 29, 1926. In all, 13 radiators of various types and capacities were given complete tests for figure of merit. Twelve of these were tested for resistance to water flow and a fourteenth radiator was tested for air resistance alone, its heat-dissipating capacity being known. All the tests were conducted in the 8 by 8 foot tunnel, or in its 4 by 8 foot restriction, by the writer and under conditions as nearly the same as possible. That is to say, as far as possible, the general arrangement and condition of the apparatus, the observation intervals, the ratio of water flow per unit of cooling surface, the differential temperatures, and the air speeds were the same for all. Also, for reasons of comparison, the L/D value of 6, which was assumed in the 1921 tests as the L/D of the airplane using the radiator, was also used in the more recent tests.

No attempt is made to enter upon the theory of heat dissipation. Only the actual test results are given and reduced to coefficient form. The precision of the tests as representative of full-flight performance is definitely known only in the case of the *HN-2*. The McCook Field full-flight performance and the Navy tunnel performance of this radiator agree within about 3 per cent.

Since this full-flight test was made with unusual care and since the wind-tunnel tests on all the radiators were made not only accurately but also at almost full scale, it would seem probable that these tests represent quite accurately the full-flight performances in actual service.

DESCRIPTION OF RADIATORS

Nine radiators of the 13 had cores of the cartridge type whose frontal areas were uniformly 1 foot square. Figure 1 gives the external appearance of one of these radiators and Figures 2 and 3 are close views of core segments of each. Six of these 9 are known as G. and O., 2 as U. S. Cartridge, and 1 as Rome Turney. For the heat-dissipation tests each was equipped with headers of equal frontal area.

With these nine was tested a tenth radiator, known as the Lamblin, composed of evenly spaced radial planes, whose outline was roughly that of a spheroid. The air flowing along the major axis entered at the front end and passed out between the planes. Stream-lined hoops, placed at the front and back, served as water headers as well as strengthening members. Structural data for this radiator as well as for the first nine are given in Table I.

The other three radiators tested for figure of merit were manufactured by the Heinrich Engineering Corporation. One, known as type *HN-2* and illustrated in Figure 4, consisted of 230 flat parallel fins three-eighths inch apart, each composed of tubes of 0.007 inch hard drawn copper, flattened to about 0.50 inch by 0.07 inch and tack soldered edge to edge. These fins were supported and connected with the main headers by thin branch headers into which the flat tubes of the fins emptied. At the leading edge there was a shutter so constructed as to fold

into the streamline form of the headers when closed, as in the figure, or to spread over the ends of the fins when open. The approximate external dimensions of this radiator are 30 inches length, 44 inches height, and 9 inches width. It contained about 206 square feet of radiating surface and had empty and full weights of 113 and 173 pounds, respectively.

The other two Heinrich radiators, known as the Heinrich wing radiators, are illustrated in Figures 5 and 6. They consisted of several thin fins extending vertically from the under surface of the wing, each constructed in similar fashion and of like material to those used in the Heinrich stream-line radiator described above. The over-all dimensions of the wing radiator fin was 5 inches width and 31.75 inches length. The two wing radiators differed only in the spacing and the number of the fins; one had 9 fins spaced 1 inch, the other 6, spaced 1.5 inches. Both were attached to a 40 by 36 inch wing of R3C3 section.

The fourteenth radiator, which was tested for air resistance alone, was a Curtis radiator having a 9-inch cartridge core and over-all dimensions of 40 by 12 by 10.75 inches. This radiator is illustrated by Figure 7. Its full and empty weights were 159.8 and 105.6 pounds, respectively.

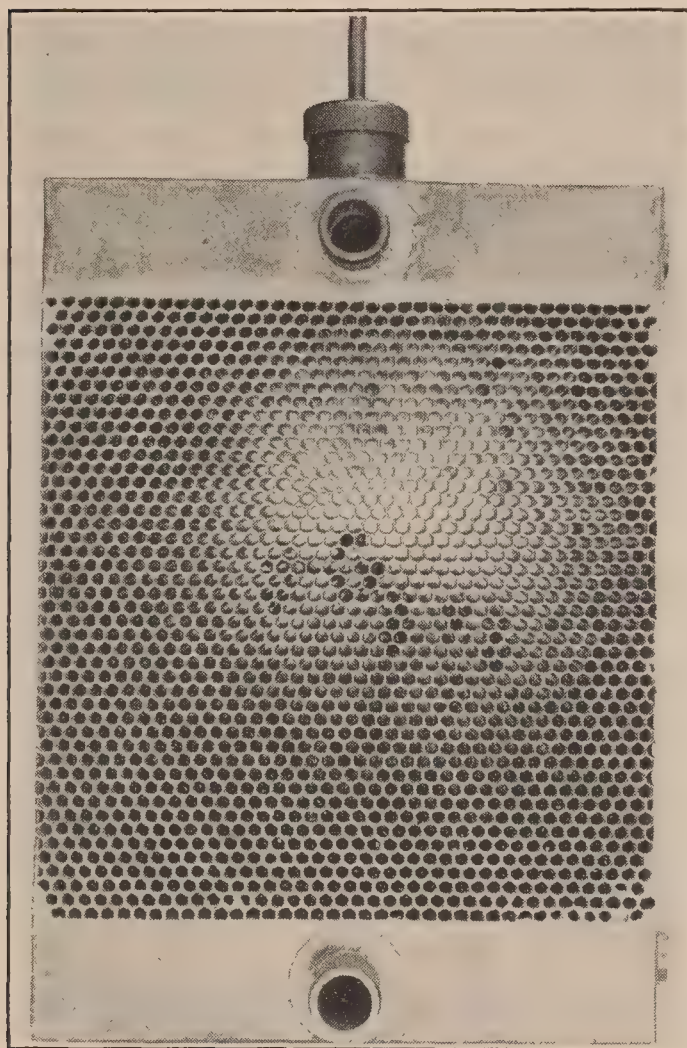


FIG. 1.—Typical test radiator

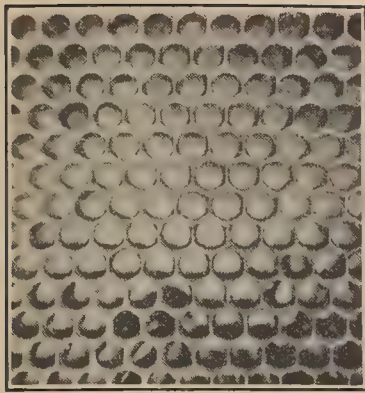
METHOD OF MEASURING AIR RESISTANCE

The air resistance of the radiator or radiator core was determined, in most cases, by suspending it by two or more wires attached to its upper edges and running either to the tunnel, ceiling, or through it to the ceiling of the laboratory above. The radiator was then displaced downstream until the displacing force exceeded the maximum air resistance to be measured, then connected to the balance shank by a horizontal tension wire. Lateral motion of the radiator was prevented by two taut cross-tunnel wires with eyelets through which two guide pins, projecting upstream from the upper and lower edges of the radiator, had only slight lateral freedom. The downstream movement of the radiator due to the wind was negligible, hence no correction of the measured resistance for gravity was required. To determine the correction required to reduce the measured resistance by the resistance of the suspending wires, a second run was made with double wires, the additional wires being placed beside the permanent ones and 10 or more

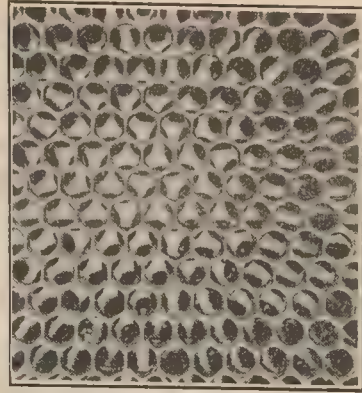
diameters away. The increments of resistance thus found, due to the additional wires, was taken as the resistance of the permanent ones and was subtracted from the radiator and single-wire resistance as the wire correction. The resistance of the horizontal wire was negligible.

Figures 7 and 8 illustrate the Curtis radiator mounted in the tunnel ready for an air-resistance test. All the radiators or radiator cores were tested for air resistance in a similar manner excepting the two wing radiators, for which the method of mounting was necessarily a little different.

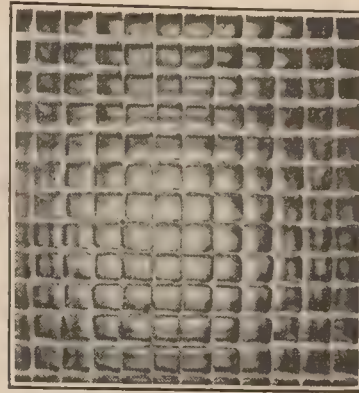
The two Heinrich wing radiators were given air-resistance tests assembled to a wing segment. This wing segment was supported in the inverted position at zero degrees angle of attack by four vertical suspension wires, as shown in Figure 5. The wing was restrained from downstream movement in the wind by a compression rod running horizontally from the balance shank to the trailing edge of the wing, and from lateral motion by cross-tunnel wires, both vertical and



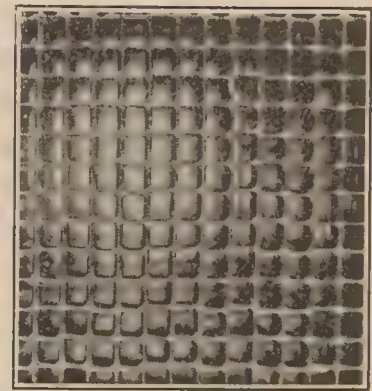
9-inch U. S. Cartridge



4-inch U. S. Cartridge

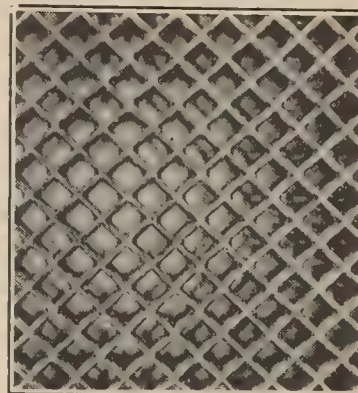


5-inch G. & O. 176503

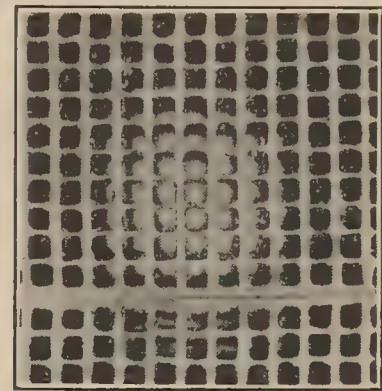


5-inch Rome Turney

FIG. 2.—Radiator cores

2-inch G. & O.
1765062-inch G. & O.
1765053-inch G. & O.
176507

5-inch G. & O. 176502



5-inch G. & O. 176504

FIG. 3.—Radiator cores

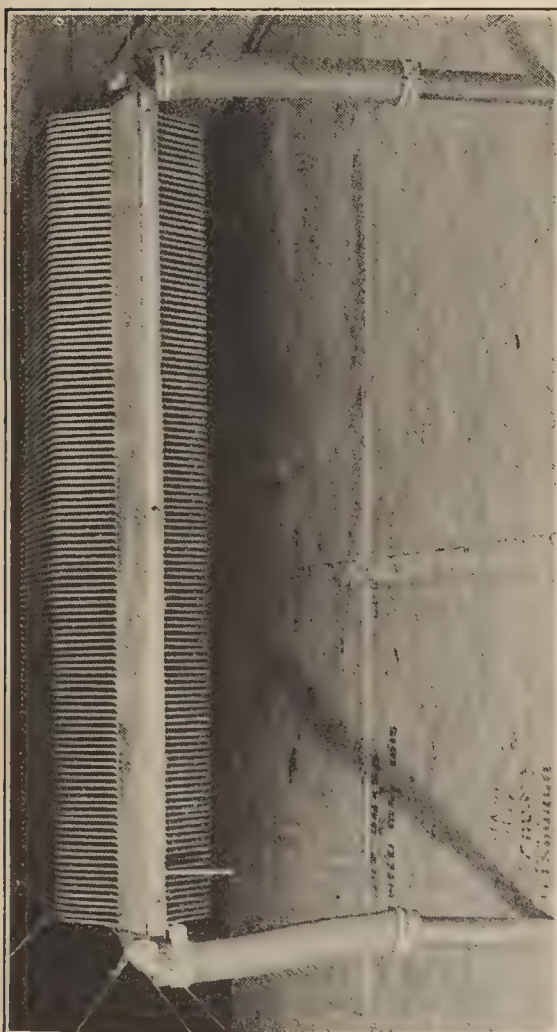


FIG. 4.—Heinrich radiator. Shutter flaps closed

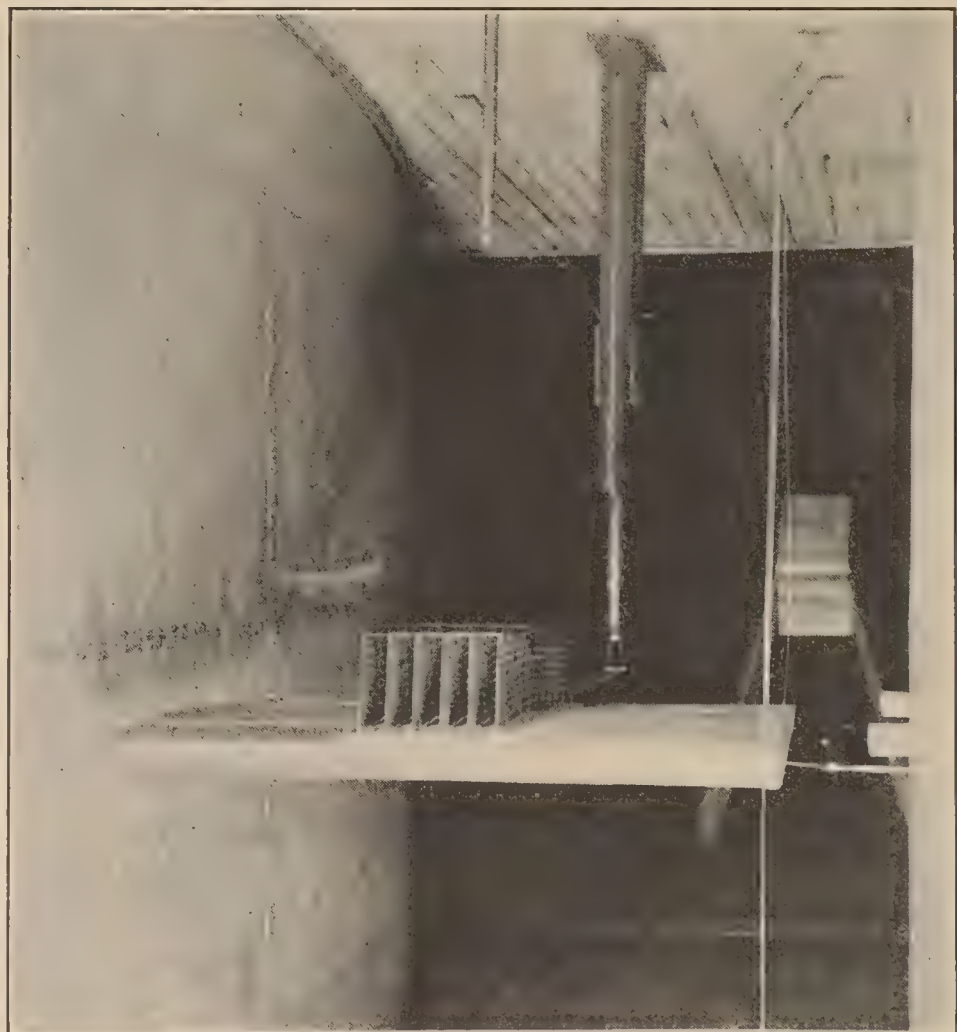


FIG. 5.—Heinrich wing radiator (Resistance mounting)

horizontal, with eyelets at the intersections, through which guide pins, projecting from the leading edge of the wing had only small lateral or vertical freedom. The wing lift, being downward, was borne by the four suspension wires, the drag by the compression rod and the balance shank. The resistance of the radiator was determined from two tests, one made on the radiator and wing assembled as in Figure 5 and the other made on the wing alone. The difference of the resistances was taken as the radiator resistance.

METHOD OF MEASURING RATE OF COOLING

The general appearance of the apparatus for a cooling test is portrayed in Figure 9. The radiator was supported symmetrically in the tunnel throat by 8 taut stay wires, 4 at the top running obliquely up to the tunnel ceiling and 4 at the bottom running obliquely down to the tunnel floor. Hot water pumped from the supply tank, shown to the right, was passed through the Venturi meter, thence through the radiator and the return pipe to the same tank, which was kept at nearly constant temperature by means of a steam-heating coil. Thermometers which were accurately calibrated were carefully inserted to the same depth in the supply and return pipes to measure the temperature of the water upon entering and leaving the radiator, and a third was inserted through the wind-tunnel ceiling to measure the temperature of the general air stream. The rate of flow of the water through the radiator was measured with the standard Venturi. The speed of the undisturbed air approaching the radiator was measured in the usual way with a Pitot tube and manometer, the Pitot tube being placed sufficiently upstream to avoid blanketing by the radiator. The manometer and Pitot tube in this position were calibrated to read the air speeds in the position occupied by the radiator.

MEASUREMENT OF WATER PRESSURE-DROP INSIDE RADIATORS

The pressure difference of the water on entering and leaving the radiator due to various rates of flow was measured by two U-tube manometers, one in each header.

RESULTS OF THE TESTS

Tables I to V, inclusive, show, for the various air speeds noted, the heat dissipation and air resistance, both as measured and in coefficient form, and the ratio of the two expressed in terms of power, which is defined as the figure of merit. Table I contains the results of 13 tests on 10 radiators—the Lamblin radiator was tested at four rates of water flow—the data given for each test being condensed from data as observed and recorded in Tables II, III, and IV. These latter three tables give the data in uncondensed form on the three Heinrich radiators. The six observations for each air speed were taken at two-minute intervals after fairly steady air speed and water flow were obtained and thermal equilibrium was established. Each observation given in Table I is the average of six like observations. Various definitions, constants, and radiator dimensions are supplied in the tables.

The air resistance of the radiators or the radiator cores, as given in the five tables and plotted in Figures 10, 11, and 12 is expressed by the general equation $R = KV^n$ where n varies from 1.84 for the Heinrich wing radiators to 2.13 for the Heinrich stream-line radiator. For the cartridge core types n varies from 1.95 to 2.02.

The figure of merit, which is the final object of the tests, diminishes continuously with increase of velocity. For the cartridge core types the figure of merit decreases roughly with the increase of the velocity squared, while for the wing radiator types it decreases nearly with the increase of the velocity. In the case of the cartridge core types the short tube radiators have greatest merit at low speeds, the long ones at high speeds. This is clearly shown by the U. S. Cartridge radiator with 9-inch tubes. This radiator has the least merit of the nine at low speeds, but is the most efficient at speeds above 130 miles per hour. The figure of merit of the parallel fin type radiator, such as the Heinrich wing radiators, is about the same as that of the best cartridge core at airplane landing speeds, but is distinctly better at the higher air speeds. Figure of merit plots are given in Figures 13, 14, and 15.

The pressure heads required to maintain different mass rates of water flow through the various radiators are given in Tables VI and VII and are plotted in Figures 16 and 17 for all 13 radiators except the Heinrich stream-line radiator, upon which these measurements were omitted. The pressure heads have the general form $p = K v^n$ where, for all cases measured, n varies from 1.86 to 2.00. The formula for pressure drop in terms of turbulent flow speed, commonly given in works on fluid dynamics, is $p = K v^{2.00}$.

The tables and diagrams given in this report may be analyzed in different ways, depending upon the experimental facts desired. No attempt is made here to enter upon such analyses, although the material is presented in a form as complete as possible for this purpose. Likewise no expression of opinion is given touching the suitability of any radiator or type of radiator for any particular use.

REFERENCES

DICKINSON, H. C.; JAMES, W. S.; and KLEINSCHMIDT, R. V. General analysis of airplane radiator problems. National Advisory Committee for Aeronautics. Technical Report No. 59, 1920. (A useful reference for definitions.)

DICKINSON, H. C.; JAMES, W. S.; and KLEINSCHMIDT, R. V. General discussion of test methods for radiators. National Advisory Committee for Aeronautics. Technical Report No. 60, 1920. (A good account of the technique, laboratory apparatus, and working formula used in a thorough radiator test at ground pressure.)

DICKINSON, H. C.; JAMES, W. S.; and KLEINSCHMIDT, H. C. Heat dissipation and other properties of radiators. National Advisory Committee for Aeronautics. Technical Report No. 63, 1920. (This reference considers how the head resistance and the heat transfer of a radiator are affected by such items as air speed, type of core, and rate of water flow.)

HARPER (3d), D. R., and BROWN, W. B. Mathematical equations for heat conduction in fins of air-cooled engines. National Advisory Committee for Aeronautics. Technical Report No. 158, 1923. (This report gives the mathematics required in a theoretical treatment of heat flow.)



FIG. 6.—Heinrich wing radiator. (Heat dissipation mounting)

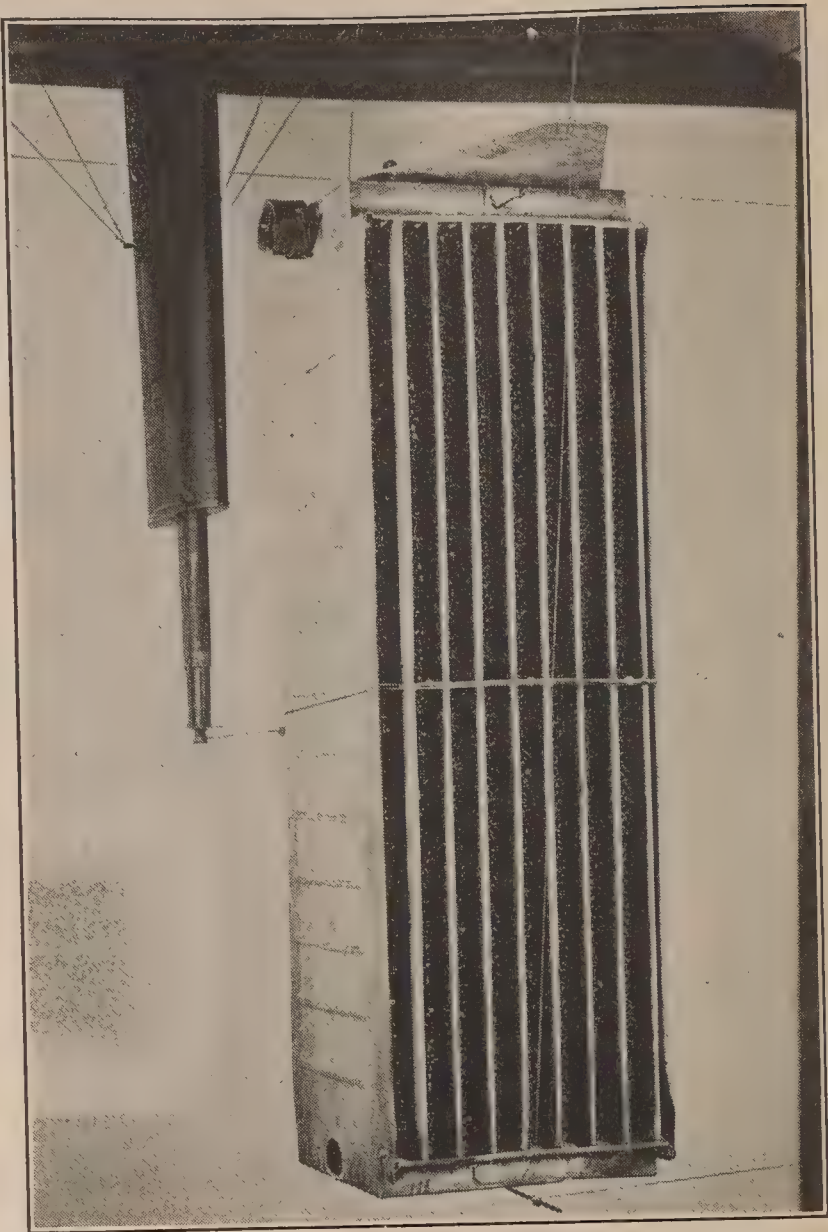


FIG. 7.—Curtiss radiator. Shutter open

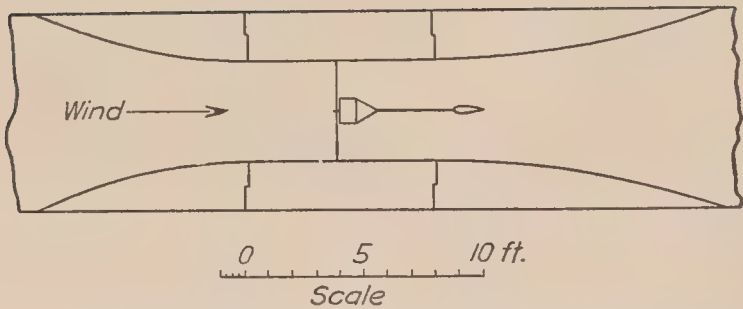


FIG. 8.—Plan view of 4 by 8 foot wind tunnel and radiator mounting

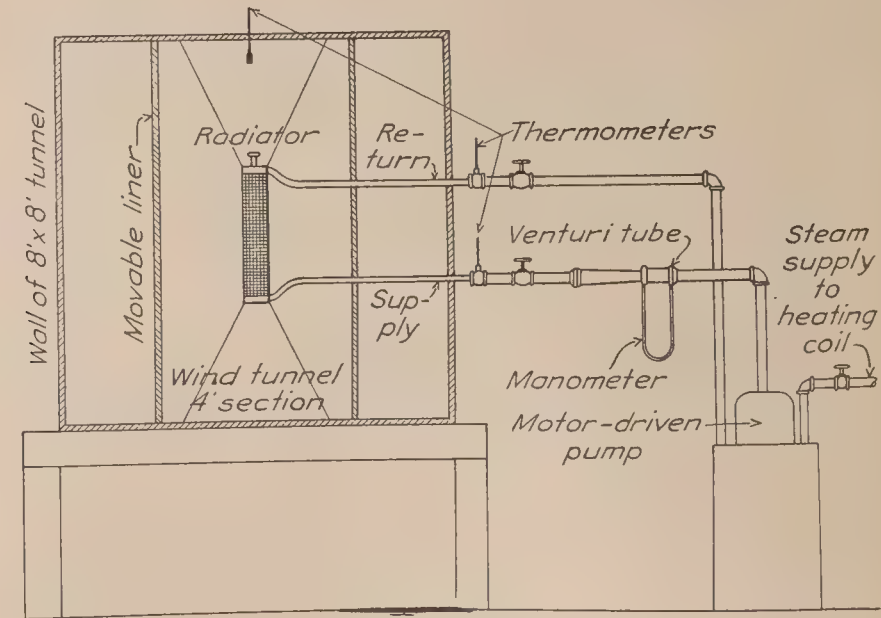


FIG. 9.—Apparatus for thermal test of radiators

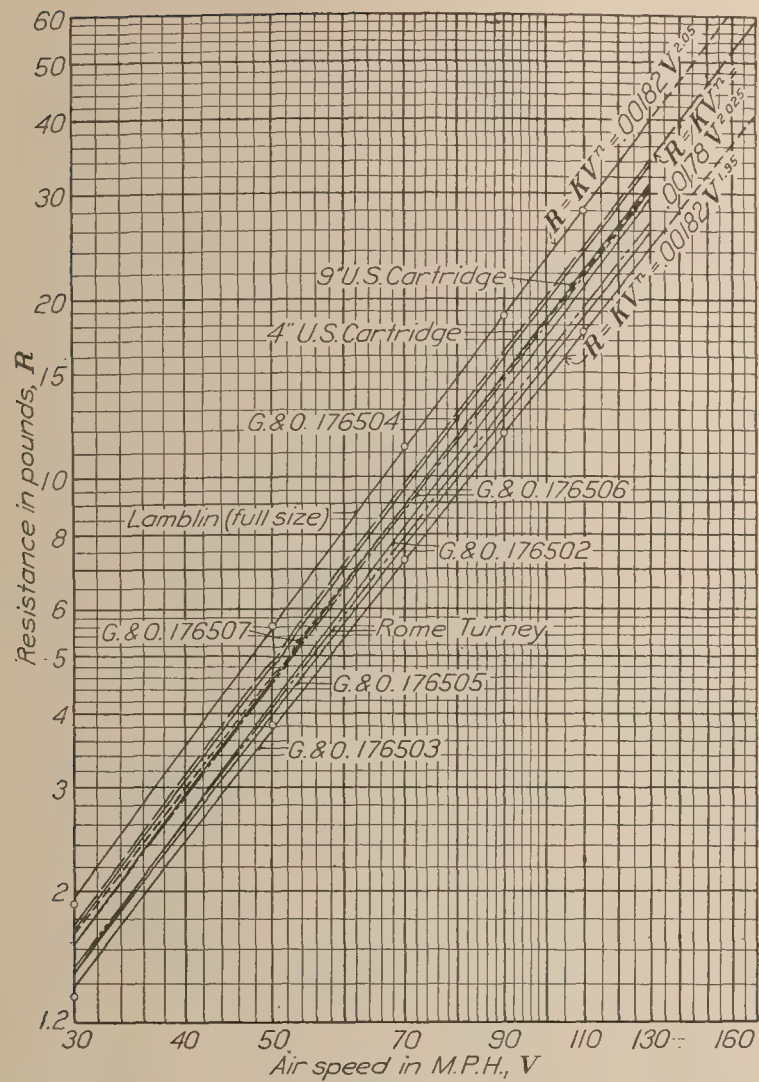


FIG. 10.—Resistance of radiator cores in pounds per square foot frontal area

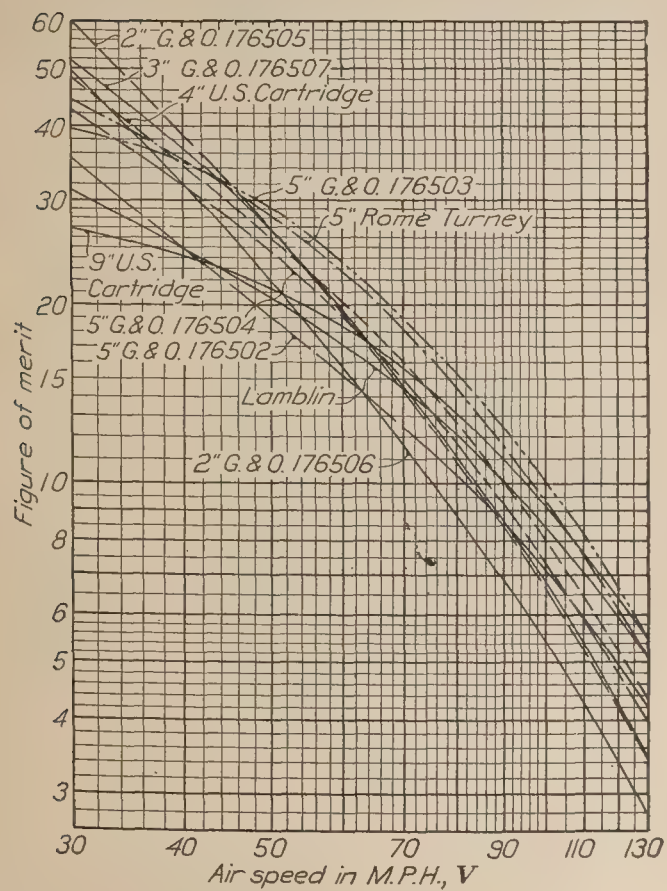


FIG. 13.—Figure of merit versus air speed for various radiator cores

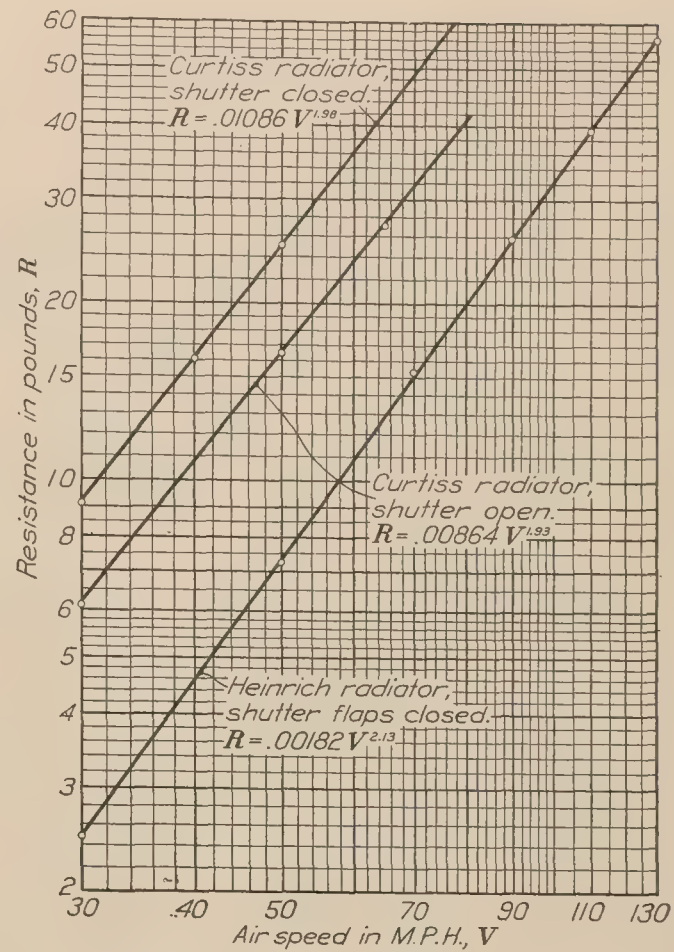


FIG. 11.—Resistance versus air speed of Heinrich and Curtiss radiators

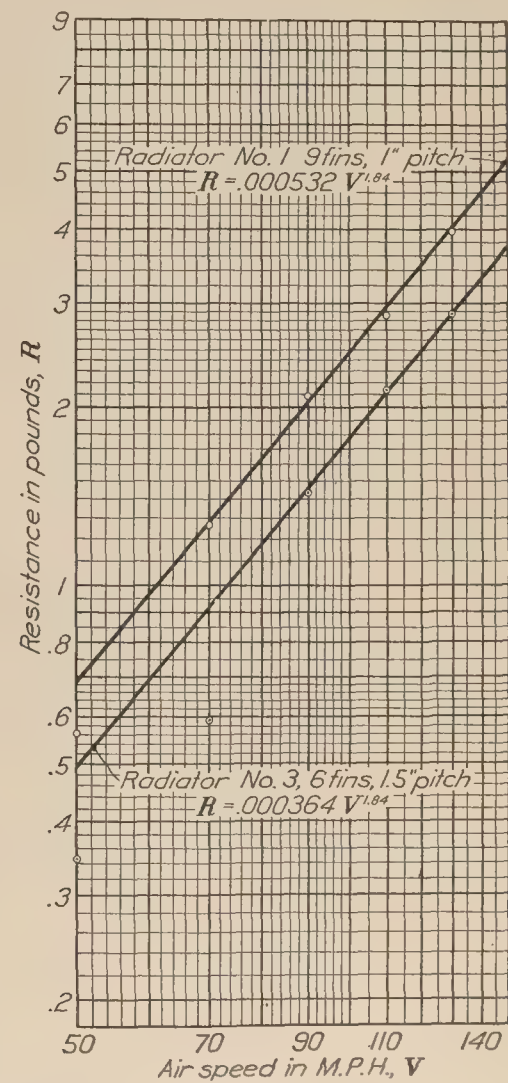


FIG. 12.—Resistance versus air speed of Heinrich wing radiators

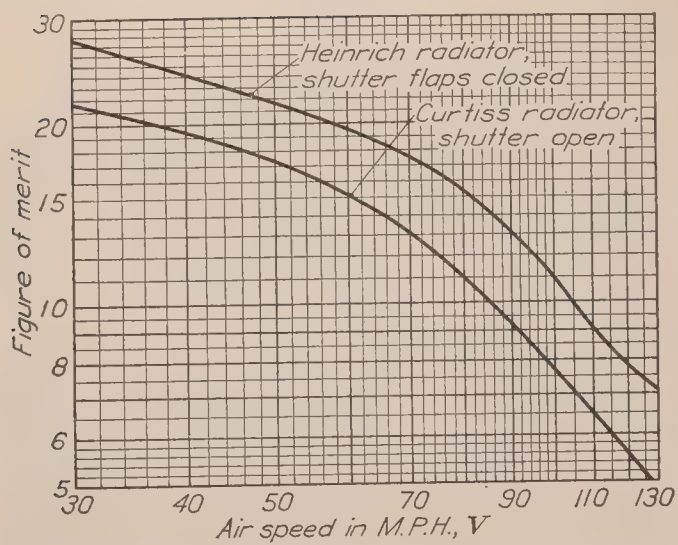


FIG. 14.—Figure of merit versus air speed for Heinrich and Curtiss radiators

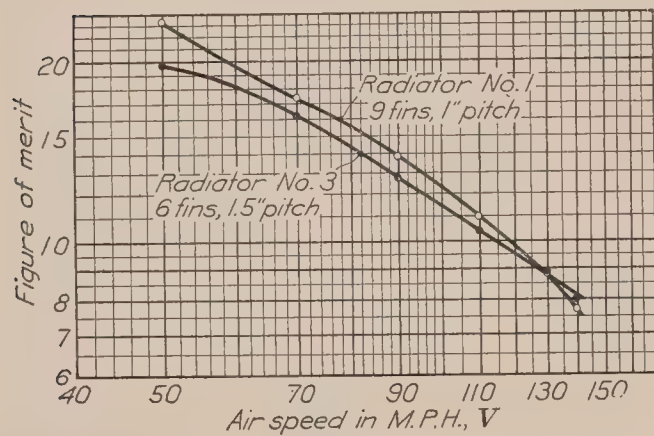


FIG. 15.—Figure of merit versus air speed for Heinrich wing radiator

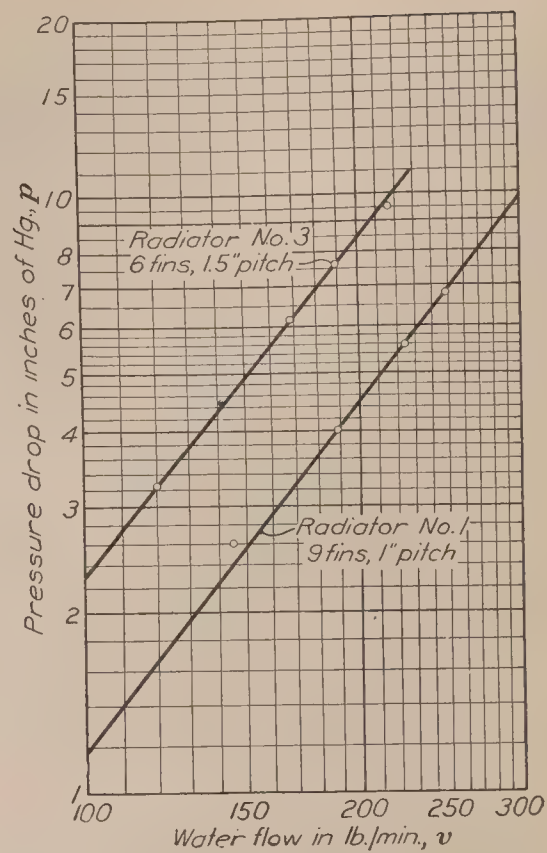


FIG. 17.—Pressure drop versus water flow for Heinrich wing radiator

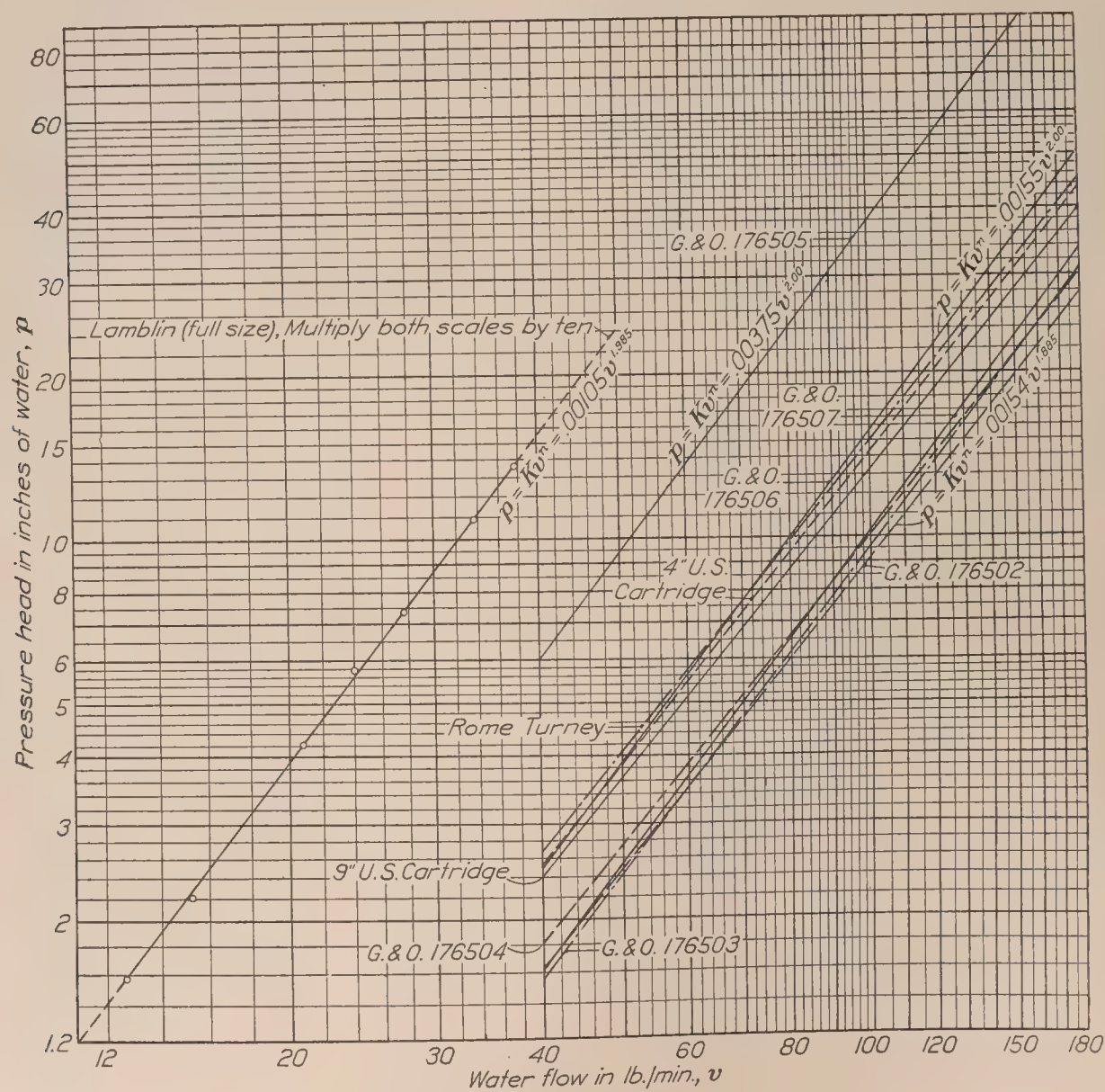


FIG. 16.—Pressure head versus water flow for various radiators

TABLE I.—FIGURE OF MERIT

Name of radiator with miscellaneous data ¹	Air speed M. P. H.	Temperature in degrees F.							B. t. u. dissipated per minute for 1 square foot frontal area of core only = C (°)	C per 100° difference between mean water and air	Total resistance of radiator core, in pounds	Total resistance per square foot of frontal area = R	HP. dissipated per 100° difference of temperature per square foot of frontal area = H	HP. absorbed per square foot of frontal area = P	Figure of merit = H/P
		Air in tunnel	Water inlet	Water outlet	Mean	Difference	Mean difference, air and water	Rate of flow, pounds of water per minute							
9-inch U. S. Cartridge--- W=43.17 pounds. A=1.00 square foot. D=3.35 per cent.	30	97	185.5	178.5	182	7	85	101.5	687	808	1.635	1.635	18.97	0.706	26.88
	50	98	189.5	177	183.2	12.5	85.2	99.5	1,202	1,411	4.544	4.544	33.13	1.563	21.21
	70	101	184.5	168.5	176.5	16	75.5	98	1,515	2,008	8.927	8.927	47.15	3.007	15.67
	90	103	186	168	177	18	74	106	1,844	2,491	14.920	14.920	58.48	5.303	11.01
	110	106	184	165	174.5	19	68.5	104.5	1,919	2,800	22.120	22.120	65.74	8.591	7.65
4-inch U. S. Cartridge--- W=21.25 pounds. A=0.98 square foot. D=4.76 per cent.	130	115	181.6	164	172.8	17.6	57.8	105	1,786	3,090	31.170	31.170	72.55	13.285	5.46
	30	92	184.5	177	180.7	7.5	88.7	105.8	772	870	1.715	1.749	20.43	.422	48.41
	50	93.5	188	176.5	182.2	11.5	88.7	102.8	1,150	1,296	4.814	4.915	30.43	1.126	27.01
	70	96	182.5	169.5	176	13	80	107.5	1,358	1,697	9.567	9.758	39.85	2.480	16.06
	90	98	186.5	170.5	178.5	16	80.5	104.5	1,625	2,019	15.820	16.150	47.41	4.722	10.04
5-inch Rome Turney--- W=22.84 pounds. A=1.00 square foot. D=3.27 per cent.	110	104	179	164	171.5	15	67.5	105	1,530	2,267	23.820	24.310	53.23	8.163	6.52
	130	112	180.4	166	173.2	14.4	61.2	105	1,470	2,402	33.470	34.150	56.40	13.054	4.32
	30	96	183.5	177	180.2	6.5	84.2	106.7	671	797	1.485	1.485	18.71	.423	44.25
	50	97	182	172	177	10	80	105.2	1,018	1,273	4.094	4.094	29.89	1.053	28.38
	70	100	183	170	176.5	13	76.5	103.5	1,302	1,702	7.897	7.897	39.96	2.182	18.30
5-inch G. & O. 176504--- W=24.77 pounds. A=0.98 square foot. D=3.98 per cent.	90	104	183	169	176	14	72	105.5	1,429	1,984	12.900	12.900	46.58	4.008	11.62
	110	105	188.5	172.5	180.5	16	75.5	106.7	1,651	2,188	19.200	19.200	51.37	6.743	7.61
	130	113	186.8	172	179.4	14.8	66.4	105.2	1,506	2,270	26.570	26.570	53.30	10.520	5.07
	30	91	181.4	175	176.6	7.3	85.6	102.5	725	847	1.695	1.713	19.89	.467	42.58
	50	92.5	182	171.5	176.7	10.5	84.5	104	1,059	1,253	4.784	4.835	29.42	1.194	24.65
3-inch G. & O. 176507--- W=14.75 pounds. A=1.00 square foot. D=3.22 per cent.	70	96	175	163.5	169.2	11.5	73.3	106.8	1,191	1,625	9.447	9.54	38.16	2.55	14.96
	90	99	179.5	166	172.7	13.5	73.7	107	1,401	1,903	15.74	15.89	44.68	4.801	9.29
	110	103	181.5	167.5	174.5	14	71.5	103	1,399	1,955	23.52	23.75	45.9	8.171	5.62
	130	113	185	170	177.5	15	64.5	100	1,414	2,192	33.07	33.40	51.47	13	3.96
	30	100	184.5	178.5	181.5	60	81.5	102.5	595	730	1.675	1.675	17.14	.331	51.8
5-inch G. & O. 176503--- W=22.89 pounds. A=0.989 square foot. D=3.25 per cent.	50	101	189	180	184.5	9	83.5	103.8	904	1,082	4.594	4.594	25.41	.94	27.04
	70	102.5	187.4	177	182.2	10.4	79.7	104	1,046	1,312	8.977	8.977	30.81	2.133	14.44
	90	106.5	185	174	179.5	11	73	105	1,118	1,532	14.82	14.82	25.97	4.142	8.68
	110	111	187.2	175.5	181.3	11.7	70.3	103	1,166	1,658	22.02	22.02	38.93	7.173	5.43
	130	120	182	172.5	177.3	9.5	57.3	103.8	954	1,665	30.87	30.87	39.09	11.543	3.39
2-inch G. & O. 176505--- W=11.90 pounds. A=1.00 square foot. D=6.46 per cent.	30	101	183.9	191	187.4	7.1	86.4	103	721	834	1.355	1.369	19.58	.494	39.65
	50	101	175.5	185.5	180.5	10	79.5	101.2	1,000	1,258	3.674	3.78	29.54	1.012	29.18
	70	102	177.8	191	184.4	13.2	82.4	103.5	1,351	1,641	7.087	7.162	38.53	2.047	18.82
	90	104	175	190	182.5	15	78.5	104.5	1,550	1,975	11.64	11.77	46.38	3.736	12.41
	110	108	174.7	190.5	182.6	15.8	74.6	105	1,640	2,198	17.22	17.400	57.61	6.218	8.3
Lamblin radiator----- W=66.3 pounds. A=full size. D=0.	130	111	174.1	189.3	181.7	15.2	70.7	106	1,592	2,250	23.87	24.14	52.83	9.682	5.46
	30	91	197.8	190.5	194.1	7.3	103.1	105.6	721	699	1.445	1.445	16.41	.271	60.6
	50	92	190	181	185	9	93	99	834	896	3.964	3.964	21.04	.788	26.71
	70	95	188	178	183	10	88	101	945	1,062	7.587	7.587	24.94	1.778	14.02
	90	98	180.4	170.5	175.4	9.9	77.4	100.2	928	1,198	12.42	12.42	28.13	3.445	8.17
Lamblin radiator----- W=66.3 pounds. A=full size. D=0.	110	101	195.5	183	189.2	12.5	88.2	101	1,182	1,341	18.42	18.42	31.49	5.97	5.28
	130	110	185.2	175.2	180.2	10	70.2	102.2	956	1,362	25.57	25.57	31.98	9.532	3.36
	30	92	191.5	181	186.2	10.5	94.3	106.1	³ 1,114	1,182	1.955	-----	27.75	1.039	26.72
	50	94	186.2	173	179.6	13.2	85.6	106.4	1,404	1,640	5.614	-----	38.51	2.22	17.35
	70	96.5	185	169	177	16	80.5	106.1	1,698	2,110	11.167	-----	49.54	4.144	11.96
Lamblin radiator----- W=66.3 pounds. A=full size. D=0.	90	100	179.2	163	171.1	16.2	71.1	106.1	1,719	2,418	18.72	-----	56.77	7.139	7.94
	110	103	187	168	177.5	19	74.5	106.9	2,031	2,729	28.12	-----	64.07	11.477	5.58
	130	109	184.5	166	175.2	18.5	66.3	105.7	1,956	2,950	39.67	-----	69.26	17.564	3.94
	30	96	181.4	177	179.2	4.4	83.2	198	871	1,048	1.955	-----	24.61	1.038	23.71
	50	97	186.5	179.5	183	7	86	199	1,393	1,620	5.614	-----	38.04	2.219	17.15
Lamblin radiator----- W=66.3 pounds. A=full size. D=0.	70	100	184.5	176	180.2	8.5	80.2	203	1,725	2,150	11.167	-----	50.48	4.144	12.18
	90	002	181.3	172	176.5	9.3	74.6	205	1,906	2,558	18.72	-----	60.06	7.137	8.43
	110	109	180.8	171.5	176.1	9.3	67.1	200	1,860	2,770	28.12	-----	65.04	11.477	5.67
	130	115	177	168.5	172.7	8.5	57.7	203	1,726	2,990	39.67	-----	70.21	17.564	3.99

¹ W=weight of 1 square foot frontal area of core with water; A=frontal area of core tested; D=percentage. B. t. u. deduction due to header area considered as equivalent to core area.

² Note area correction and deduction of percentage due to headers.

³ Headers were not removed; results not comparable with other tests.

HP. absorbed = $(R V + \frac{1}{6} W V) 0.002664$, where V=air speed in M. P. H.; R=resistance per unit frontal area-pounds; W=weight of full radiator per unit frontal area-pounds; $\frac{1}{6} = L/D$ of airplane—assumed.

HP. dissipated = $0.02348 \times (\text{B. t. u.})$.

TABLE I.—FIGURE OF MERIT—Continued

Name of radiator with miscellaneous data	Air speed M.P. H.	Temperature in degrees F.							B. t. u. dissipated per minute for 1 square foot frontal area of core only = C (2)	C per 100° difference between mean water and air	Total resistance of radiator core, in pounds	Total resistance per square foot of frontal area = R	HP. dissipated per 100° difference of temperature per square foot of frontal area = H	HP. absorbed per square foot of frontal area = P	Figure of merit = H/P
		Air in tunnel	Water inlet	Water outlet	Mean	Difference	Mean difference, air and water	Rate of flow, pounds of water per minute							
Lamblin radiator----- W=66.3 pounds. A=full size. D=0.	30	89	185.5	182	183.7	3.5	94.7	298	1,043	1,104	1.955	-----	25.92	1.038	24.95
	50	90	188.3	183	185.6	5.3	95.6	297	1,574	1,646	5.614	-----	38.65	2.219	17.42
	70	93.5	181.2	175	178.1	6.2	84.6	302	1,872	2,215	11.167	-----	52	4.144	12.54
	90	98	180.5	173.5	177	7	79	302	2,114	2,680	18.72	-----	62.93	7.137	8.82
	110	102	189.5	181	185.2	8.5	83.2	302	2,567	3,085	28.12	-----	72.44	11.477	6.31
	130	108	178	171	174.5	7	66.5	302	2,114	3,180	39.67	-----	74.67	17.564	4.25
Lamblin radiator----- W=66.3 pounds. A=full size D=0.	30	96.8	179.5	176.5	178	3	81.2	372	1,116	1,374	1.955	-----	32.26	1.038	31.05
	50	97.7	180	175.8	177.9	4.2	80.2	368	1,546	1,930	5.614	-----	45.32	2.219	20.45
	70	101.2	178.5	173.4	175.9	5.1	74.7	375	1,913	3,560	11.167	-----	60.11	4.144	14.51
	90	96.8	183.8	177	180.4	6.8	83.6	378	2,571	3,080	18.720	-----	72.32	7.137	10.13
	110	102.2	180.2	173.2	176.7	7	74.5	368	2,576	3,455	28.120	-----	81.12	11.477	7.06
	140	113	184	177	180.5	7	67.5	367	2,569	3,805	39.67	-----	89.34	17.564	5.08
2-inch G. & O. 176506-- W=9.02 pounds. A=1.00 square feet. D=8.7 per cent.	30	91	182	177	179.5	5	88.5	102.4	467	528	1.635	1.635	12.39	.251	49.4
	50	92.5	188.8	182	185.4	6.8	92.9	112	696	749	4.514	4.514	17.59	.801	21.95
	70	95	189.5	180.5	185	9	90	104	854	949	8.757	8.757	22.28	1.913	11.65
	90	97	186	176	181	10	84	102.4	934	1,112	14.42	14.42	26.11	3.818	6.85
	110	105	182.5	173	177.7	9.5	72.7	104.5	907	1,248	21.52	21.52	29.3	6.747	4.35
	140	108	187.5	177.2	182.8	10.3	74.8	101.2	951	1,271	30.17	30.17	29.84	10.969	2.72
5-inch G. & O. 176502-- W=24.4 pounds. A=0.988 square feet. D=4.11 per cent.	30	96	188.5	182.5	185.5	4	89.5	101	588	657	1.435	1.453	15.43	.44	35.05
	50	98	185.5	178	181.7	7.5	83.7	100.5	739	883	4.114	4.166	20.73	1.097	18.91
	70	100	183.8	174	178.9	9.8	78.9	101.5	963	1,220	8.157	8.25	28.65	2.297	12.48
	90	103	187	174.5	180.7	12.5	77.7	101.2	1,230	1,584	13.57	13.73	37.19	4.267	8.72
	110	108	184.5	171.5	178	13	70	101.6	1,282	1,832	20.52	20.78	43.02	7.281	5.91
	140	114	185	172	178.5	13	64.5	103.5	1,308	2,029	28.68	29.02	47.64	11.459	4.16

TABLE II.—FIGURE OF MERIT FOR HEINRICH STREAMLINE RADIATOR¹

Shut- ter flaps	Air speed, M. P. H.	Temperature in degrees F.						Rate of flow, pounds of water per minute	B. t. u. dissi- pated per minute for 1 square foot of radiat- ing sur- face = C	C per 100° differ- ence between mean water and air	Total resist- ance of radiator, in pounds	Total resist- ance per square foot of radiat- ing sur- face = R	HP. dissi- pated per 100° differ- ence of tempera- ture per square foot of radiat- ing sur- face = H ²	HP. absorbed per square foot of radiat- ing sur- face = P ²	Figure of merit = H/P	
		Air in tunnel	Water inlet	Water outlet	Mean	Differ- ence	Mean differ- ence, air and water									
Closed	8 by 8 foot tunnel	30	100.0	183.0	176.5	179.7	6.5	79.7	358	11.3	14.2	2.483	0.0120	0.333	0.0122	27.3
			98.0	168.0	161.5	164.7	6.5	66.7	366	11.5	17.2			.404		33.1
			98.2	173.0	166.0	169.5	7.0	71.3	364	12.4	16.9			.397		32.5
			98.6	181.0	173.9	177.5	7.1	78.9	363	12.5	15.9			.373		30.6
			99.0	181.0	174.5	177.7	6.5	78.7	362	11.4	14.5			.341		28.0
			99.7	182.2	176.0	179.1	6.2	79.4	362	10.9	13.8			.324		26.6
		50	100.6	183.5	174.5	178.7	9.0	72.7	365	15.9	21.9	7.269	.0353	.515	.0232	22.2
			107.0	184.5	175.5	180.0	9.0	73.0	364	15.9	21.8			.512		22.1
			110.0	185.0	176.0	170.5	9.0	60.5	365	15.9	26.3			.618		26.6
			112.0	186.0	177.0	171.5	9.0	59.5	366	15.9	26.7			.627		27.1
			114.0	187.0	178.1	182.6	8.9	68.6	366	15.8	23.2			.545		23.5
			115.0	187.4	179.2	183.3	8.3	68.3	376	15.1	23.3			.547		23.6
		70	115.0	182.0	173.1	177.6	8.9	62.6	364	15.7	25.2	15.410	.0749	.592	.0397	14.8
			116.0	179.0	170.2	174.6	8.8	58.6	363	15.5	26.5			.623		15.7
			120.0	181.0	171.9	176.5	9.1	56.5	365	16.1	28.5			.669		16.8
			123.0	181.7	173.5	177.6	8.2	54.6	364	14.5	26.6			.625		15.7
			128.0	183.0	175.0	179.0	8.0	51.0	362	14.2	27.9			.655		16.5
			130.0	184.0	176.0	180.0	8.0	50.0	365	14.2	28.5			.670		16.9
	4 by 8 foot tunnel	30	90.0	183.0	176.0	179.5	7.0	89.5	370	12.6	14.1	2.483	0.0120	.331	.0122	27.1
			92.0	183.5	176.5	180.0	7.0	88.0	371	12.6	14.3			.336		27.5
			92.1	180.0	173.3	176.7	6.7	84.6	372	12.1	14.3			.336		27.5
			92.2	180.0	173.0	176.5	7.0	84.3	373	12.7	15.1			.355		29.1
			92.5	181.0	174.0	177.5	7.0	85.0	373	12.7	14.9			.350		28.1
			92.5	182.5	175.6	179.0	6.9	86.5	373	12.5	14.5			.341		27.9
50		94.0	181.5	172.0	176.7	9.5	82.7	377	17.4	21.1	7.269	.0353	.496	.0232	21.4	
		94.5	180.2	170.1	175.1	10.1	80.6	376	18.4	22.8			.535		23.1	
		95.0	181.1	171.5	176.3	9.6	81.3	376	17.5	21.5			.505		21.8	
		95.5	180.0	170.8	175.4	9.2	79.9	376	16.8	21.0			.493		21.3	
		96.0	182.0	172.2	177.1	9.8	81.1	376	17.9	22.1			.519		22.3	
		96.5	183.7	175.1	179.4	8.6	82.9	376	15.7	19.0			.446		19.3	
70		102.0	184.0	172.0	178.0	12.0	76.0	379	22.1	29.1	15.410	.0749	.684	.0401	17.1	
		102.5	184.2	171.8	178.0	12.4	76.5	380	22.9	30.0			.705		17.6	
		103.0	183.0	171.0	177.0	12.0	74.0	379	22.1	29.9			.702		17.5	
		103.5	181.2	169.1	175.1	12.1	71.6	378	22.2	31.0			.727		18.1	
		104.0	181.2	169.5	175.3	11.7	71.3	378	21.5	30.2			.709		17.7	
		104.5	180.7	169.8	175.3	10.9	70.7	378	20.0	28.3			.665		16.6	
90	106.1	180.1	167.5	173.8	12.6	67.7	378	23.1	34.2	25.950	.1260	.803	.0638	12.6		
	108.0	180.0	167.1	173.6	12.9	65.6	380	23.8	36.3			.852		13.4		
	108.4	179.2	166.5	172.8	12.7	64.4	381	23.5	36.5			.858		13.4		
	110.0	179.0	167.0	173.0	12.0	63.0	381	22.2	35.3			.829		13.0		
	111.3	179.8	168.0	173.9	11.8	62.6	381	21.8	34.8			.818		12.8		
	111.6	181.7	169.1	175.4	12.6	63.8	380	23.3	36.6			.859		13.5		
110	114.0	182.0	169.3	175.6	12.7	61.6	377	23.3	37.8	39.650	.1926	.888	.0976	9.1		
	116.2	182.0	169.9	175.8	12.1	59.6	378	22.2	37.3			.876		9.0		
	118.0	181.7	170.0	175.8	11.7	57.8	392	22.3	38.6			.907		9.3		
	119.3	181.5	170.0	175.7	11.5	56.4	393	22.0	39.0			.916		9.4		
	120.3	182.0	171.0	176.5	11.0	56.3	393	21.0	37.3			.876		9.0		
	120.2	183.0	171.8	177.4	11.2	57.2	392	21.3	37.3			.876		9.0		
130	114.1	178.0	164.1	171.1	13.9	57.0	384	25.9	45.5	56.750	.2755	1.068	.1437	7.4		
	118.2	186.0	170.0	178.0	10.0	59.8	385	29.9	50.0			1.173		8.2		
	121.1	184.2	172.2	178.2	12.0	57.1	385	22.4	39.3			.923		6.4		
	124.0	182.0	170.2	176.1	11.8	52.1	385	22.1	42.5			.999		6.9		
	126.3	181.2	169.9	175.6	11.3	49.3	385	21.1	42.8			1.005		7.0		
	128.4	181.5	171.0	176.2	10.5	47.8	386	19.7	41.3			.970		6.7		
Open	130	100.0	184.2	176.0	180.1	8.2	81.1	388	15.4	19.2						
		104.0	180.7	172.5	176.6	8.2	72.6	385	15.3	21.1						
		108.0	182.2	174.0	178.1	8.2	70.1	390	15.5	22.1						
		112.0	182.0	175.2	178.6	7.8	66.6	387	14.6	21.9						
		114.0	182.5	176.0	179.2	6.5	65.2	388	12.2	18.7						
		116.0	182.7	176.5	179.6	6.2	63.6	388	11.7	18.4						

¹ Supplied data: Radiating surface=206 square feet. Weight of radiator, dry=113 pounds; weight of radiator, full=173 pounds.² Horsepower dissipated=0.02348×(B. t. u.).³ Horsepower absorbed=0.002664 (R V+1/6 W V) where V=air speed in M. H. P. R=resistance per square foot of radiating surface—pounds. W=weight of full radiator per square foot of radiating surface—pounds. 6=L/D of airplane—assumed.

TABLE III.—FIGURE OF MERIT FOR HEINRICH WING RADIATOR NO. 1¹

[9 fins, 1-inch pitch]

Air speed M. P. H.	Temperature in degrees F.						Rate of flow in pounds of water per minute	B. t. u. dissi- pated per minute per square foot of radiating surface = C	C per 100° difference between water and air	Total re- sistance of radi- ator in pounds ²	Total resistance per square foot of radiating surface = R	HP. dis- sipated per 100° difference of tem- perature per square foot of radiating surface = H ³	HP. absorbed per square foot of radiating surface = P ⁴	Figure of merit = H/P
	Air in tunnel	Water inlet	Water outlet	Mean	Differ- ence	Mean differ- ence air and water								
50-----	90.0	181.8	180.0	180.9	1.8	90.9	217	20.2	22.2	0.686	0.0355	0.519	0.0228	22.8
	90.0	182.2	180.2	181.5	2.0	91.5	217	21.4	23.4			.549		24.1
	90.0	182.3	180.5	181.4	1.8	91.4	212	19.7	21.6			.507		22.2
	90.0	182.7	180.8	181.8	1.9	91.8	213	20.9	22.8			.535		23.5
	90.5	183.0	181.0	182.0	2.0	91.5	217	22.4	24.5			.575		25.2
	90.5	183.0	181.2	182.1	1.8	91.6	217	20.2	22.1			.519		22.8
70-----	92.0	182.7	180.5	181.6	2.2	89.6	217	24.7	27.6	1.275	.0659	.648	.0376	17.2
	92.5	182.4	180.1	181.3	2.3	88.8	213	25.3	28.5			.669		17.8
	93.0	182.2	179.9	181.1	2.3	88.1	213	25.3	28.8			.677		18.0
	93.5	181.8	179.6	180.7	2.2	86.7	217	24.7	28.5			.669		17.8
	94.0	181.5	179.4	180.5	2.1	86.5	218	23.7	27.4			.643		17.1
	94.5	181.0	179.0	180.0	2.0	85.5	219	22.6	26.4			.620		16.5
90-----	96.0	180.7	178.2	179.5	2.5	83.5	219	28.3	33.9	2.030	.1049	.796	.0577	13.8
	97.0	180.3	177.8	179.1	2.5	82.1	217	23.0	34.2			.803		13.9
	98.0	180.4	177.9	179.2	2.5	81.2	217	28.0	34.6			.813		14.1
	99.5	180.7	178.2	179.5	2.5	80.0	211	27.3	34.1			.801		13.9
	100.5	181.0	178.5	179.8	2.5	79.3	212	27.4	34.6			.813		14.1
	101.0	180.9	178.5	179.7	2.4	78.7	212	26.3	33.4			.785		13.6
110-----	106.0	181.0	178.5	179.8	2.5	73.8	217	28.0	38.0	2.935	.1517	.893	.0843	10.6
	107.5	181.1	178.6	179.9	2.5	72.4	217	28.0	38.7			.909		10.8
	109.0	181.0	178.5	179.8	2.5	70.8	217	28.0	39.6			.930		11.0
	109.5	180.8	178.3	179.6	2.5	70.1	217	28.0	40.0			.939		11.1
	110.0	180.8	178.3	179.6	2.5	69.6	217	28.0	40.3			.946		11.2
	110.5	181.0	178.5	179.8	2.5	69.3	219	28.3	40.9			.961		11.4
130-----	117.0	180.9	178.4	179.7	2.5	62.7	219	28.3	45.2	4.000	.2068	1.061	.1187	8.9
	118.5	181.0	178.5	179.8	2.5	61.3	219	28.3	46.2			1.083		9.1
	120.0	180.9	178.5	179.7	2.4	59.7	217	26.9	45.1			1.058		8.9
	121.5	181.0	178.8	179.9	2.2	58.4	219	24.9	42.6			1.000		8.4
	123.5	181.2	179.0	180.1	2.2	56.6	219	24.9	44.0			1.033		8.7
	125.0	181.4	179.2	180.3	2.2	55.3	219	24.9	45.1			1.058		8.9
140-----	112.0	183.0	180.2	181.6	2.8	69.6	219	31.7	45.6	4.580	.2363	1.070	.1388	7.7
	117.0	182.8	180.0	181.4	2.8	64.4	217	31.4	48.8			1.146		8.2
	122.0	182.2	179.8	181.0	2.4	59.0	217	26.9	45.6			1.070		7.7
	125.0	182.2	180.0	181.1	2.2	56.1	217	24.7	44.0			1.033		7.4
	127.5	182.4	180.2	181.3	2.2	53.8	213	24.2	45.0			1.057		7.6
	129.0	182.6	180.5	181.6	2.1	52.6	213	23.1	43.9			1.030		7.4

¹ Weight of radiator, dry =10.90 pounds; weight of radiator, wet =15.78 pounds. Radiating surface =19.35 square feet.
² Faired resistance values.
³ HP. dissipated = 0.02348 × B. t. u.
⁴ HP. absorbed = 0.002664 (R V + $\frac{1}{6}$ W V). V = air speed in M. P. H. R = resistance per square feet. of radiating surface in pounds. W = weight of full radiator per square foot of radiating surface in pounds. $\frac{6}{L}$ = L/D of airplane, assumed.

TABLE IV.—FIGURE OF MERIT FOR HEINRICH WING RADIATOR NO. 3¹

[6 Fins, 1½" pitch]

Air speed M.P.H.	Temperature in degrees F.						Rate of flow in pounds of water per minute	B. t. u. dissipated per min- ute per square foot of radiating surface C	C per 100° differ- ence between mean water and air	Total resist- ence of radiator in pounds ²	Total resistance per square foot of radiating surface = R	HP. dis- sipated per 100° differ- ence of tempera- ture per square foot of radiating surface = H ³	HP. absorbed per square foot of radiating surface = P ⁴	Figure of merit = H/P
	Air in tunnel	Water inlet	Water outlet	Mean	Differ- ence	Mean differ- ence, air and water								
50	87.0	175.5	173.8	174.7	1.7	87.7	161	21.2	24.2	0.493	0.0382	0.568	0.259	21.9
	87.0	176.9	175.1	176.0	1.8	89.0	155	21.6	24.3			.571		22.1
	87.5	180.6	179.1	179.9	1.5	92.4	155	18.0	19.5			.458		17.7
	88.0	180.0	178.6	179.3	1.4	91.3	158	17.2	18.8			.441		17.0
	88.0	180.9	179.3	180.1	1.6	92.1	158	19.6	21.3			.500		19.3
	88.5	182.1	180.4	181.2	1.7	91.9	158	20.8	22.6			.531		20.5
70	90.0	183.3	181.0	182.2	2.3	92.2	155	27.7	30.1	.917	.711	.707	.0425	16.6
	90.5	183.9	181.7	182.8	2.2	92.3	155	26.5	28.7			.674		15.9
	91.0	183.8	181.5	182.7	2.3	91.7	155	27.7	30.2			.709		16.7
	91.5	183.7	181.5	182.6	2.2	91.1	151	25.8	28.3			.664		15.6
	92.0	183.6	181.3	182.5	2.3	90.5	155	27.7	30.6			.719		16.9
	92.5	183.0	180.9	182.0	2.1	89.5	155	25.2	28.2			.662		15.6
90	94.5	182.4	179.9	181.2	2.5	86.7	155	30.1	34.7	1.459	.1131	.815	.0646	12.6
	96.0	181.9	179.4	180.7	2.5	84.7	155	30.1	35.6			.836		12.9
	97.0	181.2	178.8	180.1	2.4	83.1	155	28.9	34.8			.817		12.6
	97.5	180.6	178.2	179.5	2.4	82.0	155	28.9	35.3			.829		12.8
	98.0	180.4	178.0	179.3	2.4	81.3	155	28.9	35.6			.836		12.9
	98.5	180.0	177.0	178.3	3.0	79.8	151	35.2	44.1			1.035		16.1
110	102.0	180.0	177.2	178.6	2.8	76.6	155	33.7	44.0	2.114	1.639	1.033	.939	11.0
	103.5	179.5	177.0	178.3	2.5	74.8	155	30.1	40.3			.946		10.1
	104.5	179.0	176.7	177.9	2.3	73.4	155	27.7	37.8			.887		9.4
	106.0	179.0	176.5	177.8	2.5	71.8	155	30.1	41.9			.984		10.5
	107.5	178.8	176.3	177.6	2.5	70.1	155	30.1	43.0			1.010		10.8
	108.5	178.6	176.2	177.4	2.4	68.9	155	28.9	42.0			.986		10.5
130	112.5	179.5	176.8	178.2	2.7	65.7	155	32.5	49.5	2.879	.2231	1.162	.1315	8.8
	115.0	182.0	179.1	180.6	2.9	65.6	155	34.9	53.2			1.248		9.5
	119.0	183.2	180.5	181.9	2.7	62.9	155	32.5	51.7			1.214		9.2
	120.5	184.4	181.8	183.1	2.6	62.6	155	31.3	50.0			1.173		8.9
	122.0	183.7	181.3	182.5	2.4	60.5	155	28.9	47.8			1.122		8.5
	124.0	183.7	181.3	183.5	2.4	59.5	148	28.9	48.6			1.141		8.7
140	127.0	184.4	182.0	183.2	2.4	55.2	155	28.9	52.4	3.290	.2550	1.230	.1535	8.0
	130.0	184.6	182.1	183.4	2.5	53.4	144	27.9	52.3			1.228		8.0
	132.0	185.0	182.6	183.8	2.4	51.8	158	29.4	56.8			1.333		8.7
	133.5	185.8	183.5	184.7	2.3	51.2	158	28.2	55.1			1.293		8.4
	135.5	185.9	183.9	184.9	2.0	49.4	158	24.5	49.6			1.154		7.5
	137.0	185.8	183.9	184.9	1.9	47.9	158	23.3	48.7			1.143		7.4

¹ Weight of radiator, dry=8.03 pounds, weight of radiator, wet=12.09 pounds. Radiating surface=12.90 square feet.
² Faired resistance values.
³ HP. dissipated=0.02348×B.t.u.
⁴ HP. absorbed=0.002664 (R V+½ W V). V=air speed in M.P.H. R=resistance per square foot of radiating surface in pounds. W=weight of full radiator per square foot. of radiating surface in pounds. 6=L/D of airplane, assumed.

TABLE V.—FIGURE OF MERIT FOR CURTISS RADIATOR¹

[Shutter open]

Air speed (M. P. H.)	Total re- sistance of radiator ² (pounds)	HP. dissi- pated per 100° of tem- perature = H ³	HP. ab- sorbed = P	Figure of merit of = H/P
30	6.11	56.91	2.62	21.71
50	16.50	99.39	5.74	17.31
70	31.43	141.45	10.84	13.05
90	51.05	175.44	18.63	9.42
110	75.19	197.22	29.87	6.61
130	103.79	217.65	45.21	4.81

¹ Weight of radiator, dry=105.6 pounds; weight of radiator, wet=159.8 pounds; frontal core area=3 square feet.
² Resistance values were computed from the equation of the faired curve.
³ Values for H were taken from 9-inch U₁ S. Cartridge core tests in Report No. 183, and increased in proportion to the change in core area, neglecting effect of header area.

TABLE VI.—WATER-PRESSURE DROP INSIDE RADIATOR FOR DIFFERENT RATES OF FLOW

[Pressure head—inches of water]

Water flow pounds per minute	U. S. Cartridge, 9-inch	U. S. Cartridge, 4-inch	G. & O. 176504	Rome Turney	G. & O. 176503	G. & O. 176507	G. & O. 176506	G. & O. 176505	G. & O. 17502
40-----	2.38	2.52	1.80	2.65	1.55	1.60	2.47	6.0	1.62
60-----	5.05	5.45	3.86	5.65	3.45	3.60	5.55	13.5	3.48
80-----	8.62	9.35	6.60	9.75	6.10	6.45	9.90	24.0	6.00
100-----	13.10	14.25	10.00	14.80	9.50	10.10	15.50	37.5	9.10
120-----	18.40	20.10	14.00	21.00	13.60	14.50	22.40	54.0	12.90
140-----	24.50	27.00	18.80	28.00	18.60	20.00	30.50	73.8	17.20
160-----	31.50	34.50	24.00	36.00	24.20	26.00	39.50	96.0	22.00
180-----	39.30	43.00	29.80	44.80	30.50	33.00	50.00	-----	-----

FOR LAMBLIN RADIATOR

Water flow-----	125	150	175	200	250	300	350	400	450
Pressure drop-----	15.3	21.9	30.0	38.8	60.5	87.0	118	145	195

TABLE VII.—PRESSURE DROP IN RADIATOR FOR VARIOUS RATES OF FLOW

Rate of flow in pounds of water ¹ per minute	Pressure drop in radiator in inches of mercury
HEINRICH RADIATOR NO. 1 (9 FINS, 1-INCH PITCH)	
0	0
145	2.60
189	4.00
224	5.45
248	6.80
HEINRICH RADIATOR NO. 3 (6 FINS, 1½-INCH PITCH)	
0	0
84	1.90
120	3.26
155	5.40
168	6.14
189	7.60
216	9.50

¹ Temperature of water=180° F.

REPORT No. 262

FRICTION OF AVIATION ENGINES

By S. W. SPARROW and M. A. THORNE
Bureau of Standards

REPORT No. 262

FRICITION OF AVIATION ENGINES

By S. W. SPARROW and M. A. THORNE

SUMMARY

The first portion of this report discusses measurements of friction made in the altitude laboratory of the Bureau of Standards between 1920 and 1926 under research authorization of the National Advisory Committee for Aeronautics. These are discussed with reference to the influence of speed, barometric pressure, jacket-water temperature, and throttle opening upon the friction of aviation engines. It is concluded that: (1) Changes in friction due to changes in the temperature of the air entering the engine are negligible. (2) Changes in friction which result from changes in atmospheric pressure are due primarily to changes in pumping loss. An approximate figure for the engines mentioned in this report is that the friction mean effective pressure decreases about one-tenth of a pound per square inch for each decrease of 1 centimeter of mercury in the barometric pressure. (3) The increase in friction resulting from a decrease in throttle opening is due to the change in pumping loss. For the engines mentioned in this report, the change in friction mean effective pressure which accompanies a change in manifold suction of 1 inch (2.54 centimeters) of mercury ranges from 0.20 pound per square inch obtained at an engine speed of 1,200 revolutions per minute to 0.39 at 1,800 revolutions per minute. (4) For the range of speeds covered in this report, namely, from 1,000 to 2,200 revolutions per minute, the friction mean effective pressure increases with speed, but ordinarily the percentage increase is less than the corresponding percentage increase in speed. At low engine speeds the friction mean effective pressure changes much less with change in speed and in some instances remains practically constant. (5) Friction depends upon the viscosity of the oil upon the cylinder walls, which in turn depends upon the temperature of the jacket water. (6) While theoretical considerations would lead one to expect an increase in friction with increase in compression ratio the evidence at hand indicates that this effect is slight.

The second section of the report deals with measurements of the friction of a group of pistons differing from each other in a single respect, such as length, clearance, area of thrust face, location of thrust face, etc. Results obtained with each type of piston are discussed and attention is directed particularly to the fact that the friction chargeable to piston rings depends upon piston design as well as upon ring design. This is attributed to the effect of the rings upon the thickness and distribution of the oil film which in turn affects the friction of the piston to an extent which depends upon its design.

INTRODUCTION

In connection with tests of aviation engines in the altitude laboratory of the Bureau of Standards considerable attention has been paid to measurements of engine friction. Part I of this report presents and discusses some of these measurements with a view to showing the influence of changes in speed, barometric pressure, jacket-water temperature, and throttle opening upon the friction of aviation engines.

Part II discusses experiments made to obtain information on the influence which certain features of piston design have upon friction. For these experiments several groups of pistons originally of the same dimensions within manufacturing tolerances were modified with respect to length, clearance, area of thrust face, location of thrust face, etc. The friction of pistons thus modified was compared with the friction of the unmodified pistons, under several conditions of engine operation.

Both parts of the report are admittedly incomplete, presenting results with comments as to their probable significance rather than with explanations based upon definite knowledge. Nevertheless it is believed that the information will prove useful as indicating the effect of a change in altitude upon engine friction and suggesting how such friction may be affected by various factors.

PART I

FRICITION HORSEPOWER, DEFINITION AND METHOD OF MEASUREMENT

For the purpose of this paper friction horsepower is defined as the difference between indicated horsepower¹ and brake horsepower. As thus defined it includes the power expended in drawing in and exhausting the charge, known as the pumping loss, and in driving the auxiliaries such as pump, magneto, etc., as well as the power expended in what can strictly be termed engine friction. Measurements of friction were made in the usual manner, namely by driving the engine by the dynamometer with ignition and fuel turned off but with oil and water temperatures maintained as nearly as possible at their normal operating values.

Numerous objections may be raised to this method of measuring friction horsepower. For example the pumping loss, the power expended in drawing in and expelling the charge, under such conditions is slightly lower than when the engine is operating under its own power as the pressure at the beginning of the exhaust stroke is approximately atmospheric when making friction measurements whereas it may be 20 or 30 pounds per square inch above atmospheric when the engine is operating under its own power. Moreover the side thrust of the piston obviously is greater under explosion pressures than under compression pressures. This, however, is of importance only to the extent to which it affects the thickness of the oil film, as fluid friction is practically independent of pressure² so long as the film thickness remains constant. Of course, if for any portion of the stroke there is metal to metal contact the friction for that portion will increase with increase in pressure. The influences mentioned thus far tend to make the friction under load greater than when the engine is being driven by the dynamometer. One would expect the temperature of the oil film upon the cylinder wall to be slightly higher than the jacket-water temperature and that this difference would be greater when the engine is operating under its own power. This effect in its influence upon friction is in the opposite direction to, and tends to compensate for, those that have been mentioned. Presumably the magnitude of these influences is small, as available evidence confirms the belief that friction as measured by the method described is approximately equal to the friction of the engine when it is operating under its own power. Ricardo, in Great Britain, reached the same conclusion after a painstaking study of the subject in which several methods of measuring friction were employed. (See bibliography.) Records of engine tests in the altitude laboratory furnish many examples where the change of indicated horsepower (brake horsepower + friction horsepower) agrees with what would be expected from theoretical considerations to an extent very difficult to explain were the friction measurements appreciably in error.

¹ Indicated horsepower is understood to be the net work done on the piston during the compression and expansion strokes. While it may be obtained from an indicator card, sufficiently accurate indicator cards are not generally available in connection with high-speed internal-combustion engine operation, and it is normally figured back from measurements of the brake horsepower and the various losses (the pumping loss, power to drive auxiliaries, etc.).

² This is not strictly true, as Hersey has shown that viscosity changes slightly with pressure. See third report on "Viscosity of Lubricating Oils at High Pressure," *Mechanical Engineering*, Vol. 45, May, 1923, p. 315.

FRICTION MEAN EFFECTIVE PRESSURE, DEFINITION

In most of the curves in this report the quantity plotted is friction mean effective pressure (F. M. E. P.). This may be defined as the pressure per unit area of piston head which, if applied and maintained constant through each working stroke, would produce an amount of power equivalent to the friction horsepower. Friction does not manifest itself as a pressure nor does it necessarily or probably remain constant, and from this standpoint the term F. M. E. P. has little excuse for existence. The reason for its use in preference to horsepower will be evident from an examination of the following general equation:

$$\text{Mean effective pressure} = \frac{\text{horsepower} \times 792,000}{\text{R. P. M.} \times \text{piston displacement}}$$

where mean effective pressure is given in pounds per square inch and piston displacement in cubic inches. It will be observed that the mean effective pressure is proportional to the horsepower of an engine of unit piston displacement operated at unit speed and hence forms a convenient basis for comparing the friction of engines which differ as to size and speed.

ATMOSPHERIC TEMPERATURE AND FRICTION

There appears to be no reason to expect that seasonal or climate changes in the temperature of the air entering the engine will be of sufficient magnitude to produce a measurable change of friction horsepower. Moreover, tests have shown no indication of such an effect. Results have been plotted, therefore, against barometric pressure rather than against air density, as the effect upon friction of a change of air density would depend upon whether the change was due to a change in pressure or temperature.

ATMOSPHERIC PRESSURE AND FRICTION

Figures 1 to 7 show relations between F. M. E. P. and barometric pressure as determined from tests of several engines operating at various speeds and jacket-water temperatures. Figures 1 to 5 were derived from groups of curves such as are shown in Figure 8. Such groups were obtained from tests under conditions corresponding to sea level and altitudes of 5,000, 10,000, 15,000, 20,000, and 25,000 feet. The engine was operated at several speeds and at several jacket-water temperatures, and because of the consistency and large number of the measurements it is believed that the results merit considerable confidence. Figures 6 and 7 are based upon a much smaller number of measurements and for that reason are somewhat less trustworthy.

It is well at this point to emphasize the statement made previously to the effect that the information presented in these curves was obtained at intervals covering a long period of time and with engines differing in piston design and many other respects. It is entirely possible that oils of different viscosities were used with the different engines. For this reason one should use considerable caution in comparing the friction of one engine with the friction of another or the friction at one compression ratio with the friction at another compression ratio. Fortunately this limitation is not likely to be of major importance in comparing engines from the standpoint of changes in friction with change of barometric pressure, which is one of the objects of this paper. This results from the fact that the change of friction with change of barometric pressure is primarily due to a change in pumping loss and should not be materially affected by piston design or oil viscosity provided these are such as to insure an adequate oil seal between the piston and cylinder wall.

WHY ATMOSPHERIC PRESSURE AFFECTS PUMPING LOSS

There is no intention of discussing fully the factors which affect the pumping loss and the reasons why this loss should be proportional to the barometric pressure. In this report the intention is merely to point out that measurements of friction indicate that such relation does exist and to suggest why it would reasonably be expected.

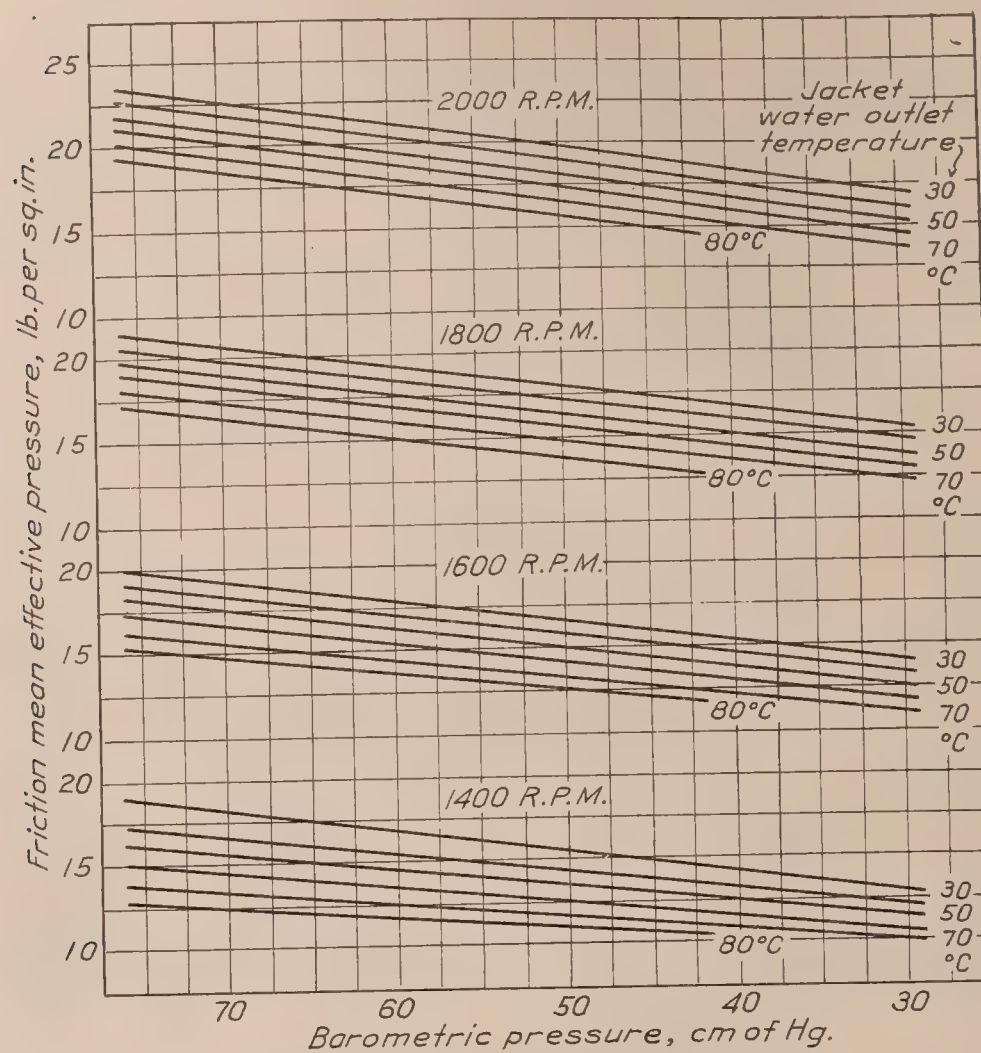


FIG. 1.—Compression ratio, 6.5. Engine A, 8 cylinders

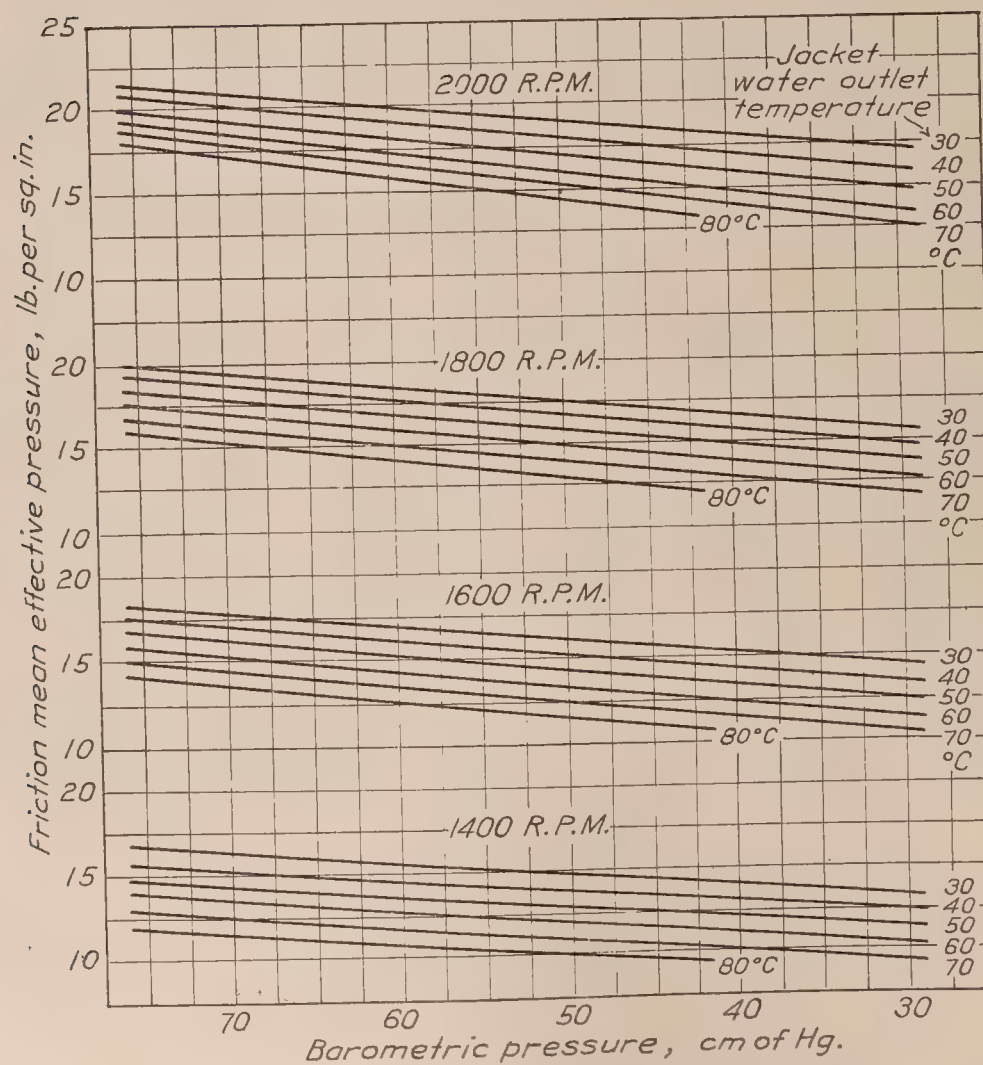


FIG. 2.—Compression ratio, 5.4; bore, 5.51 inches; stroke, 5.91 inches

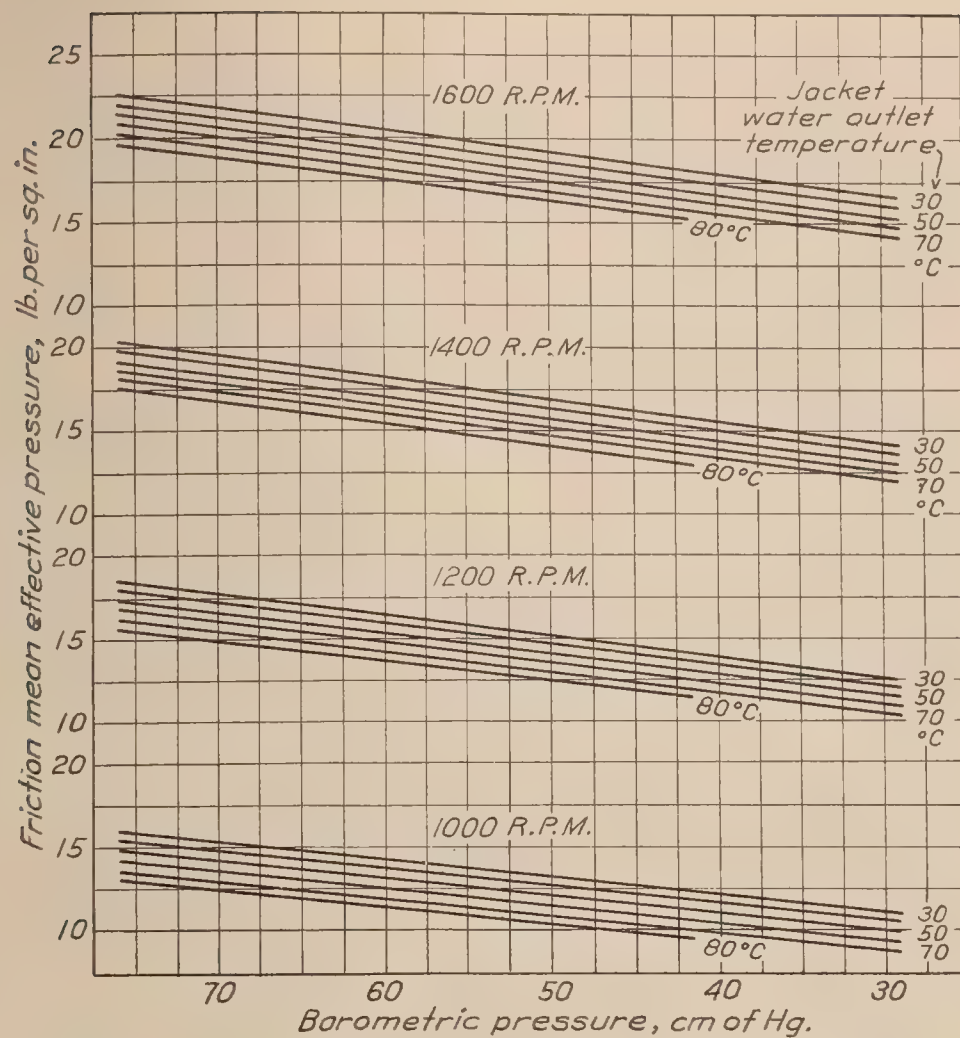


FIG. 3.—Compression ratio, 6.5. Engine B, 6 cylinders

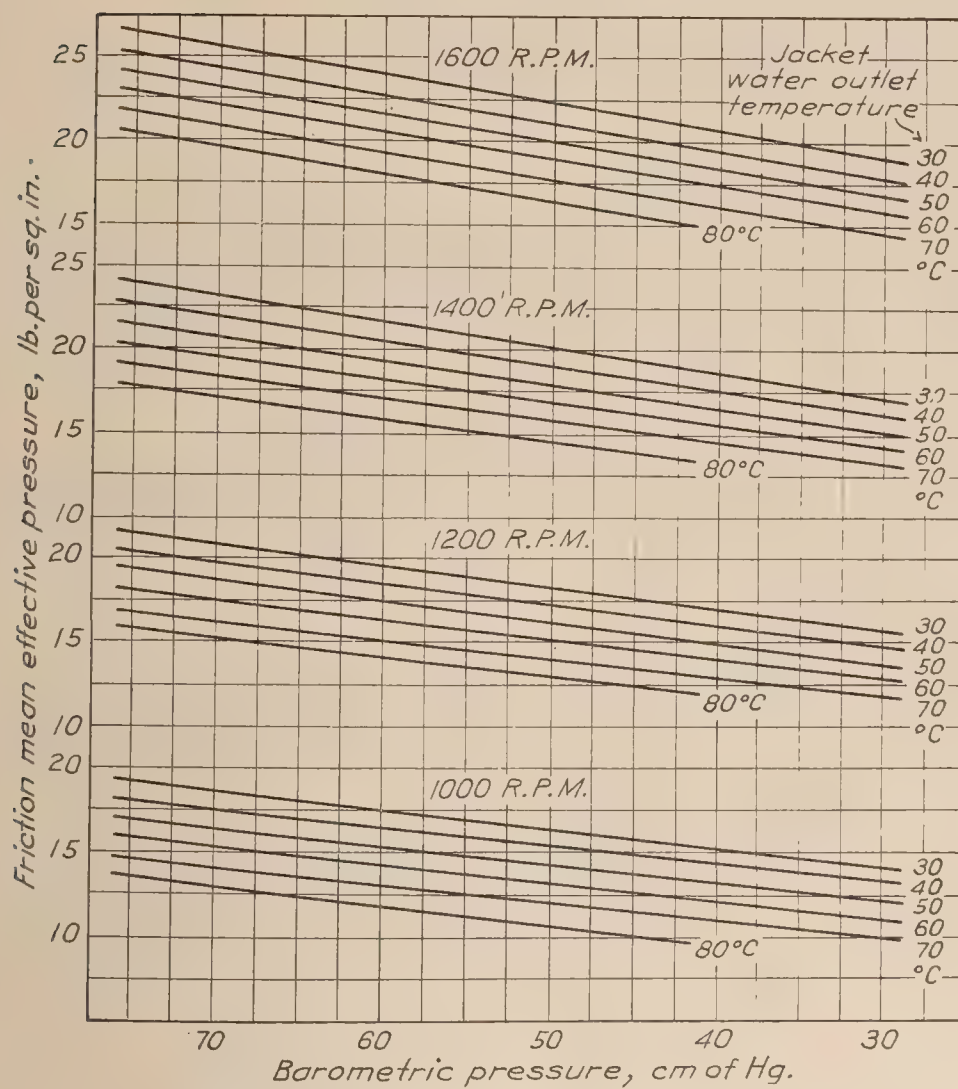


FIG. 4.—Compression ratio 5.5; bore, 6.62 inches; stroke, 7.5 inches

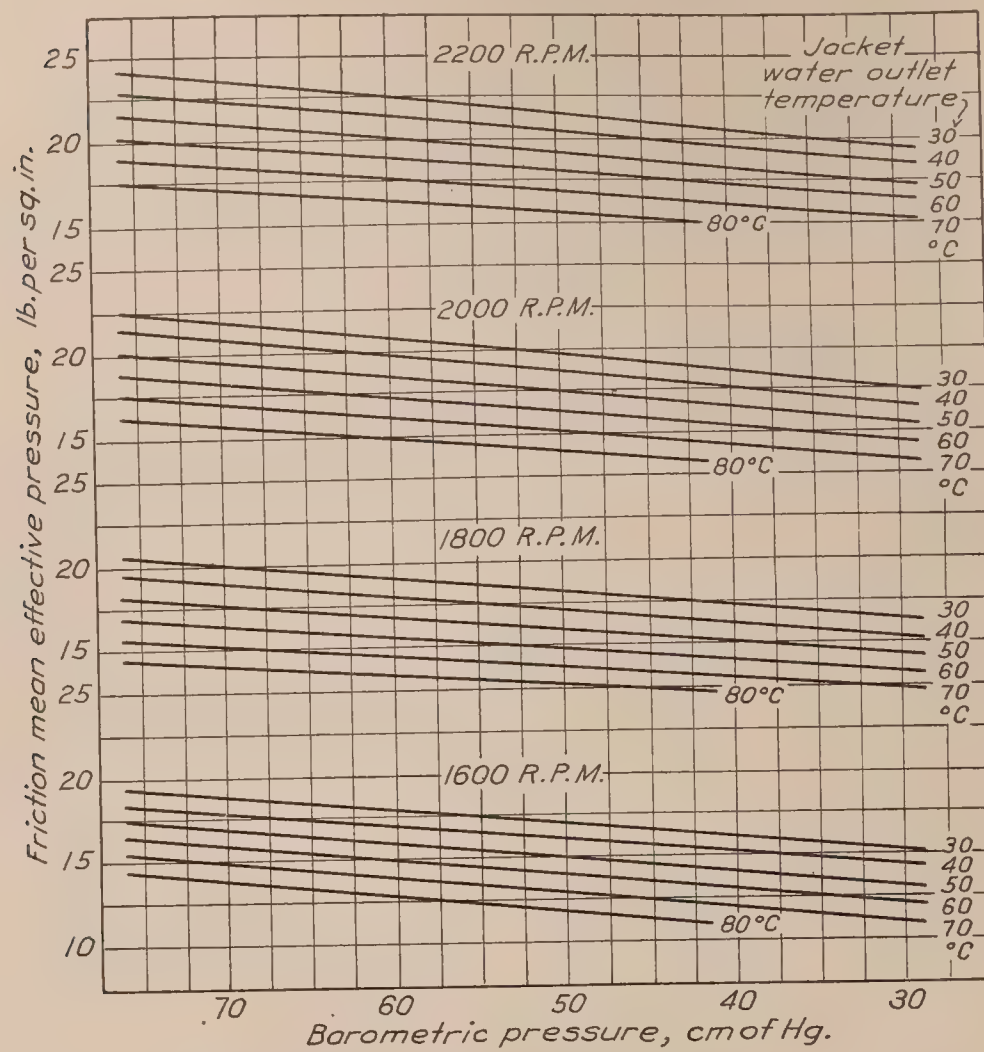


FIG. 5.—Compression ratio, 5.3. Engine C: 12 cylinders; bore, 4.5 inches; stroke, 6 inches

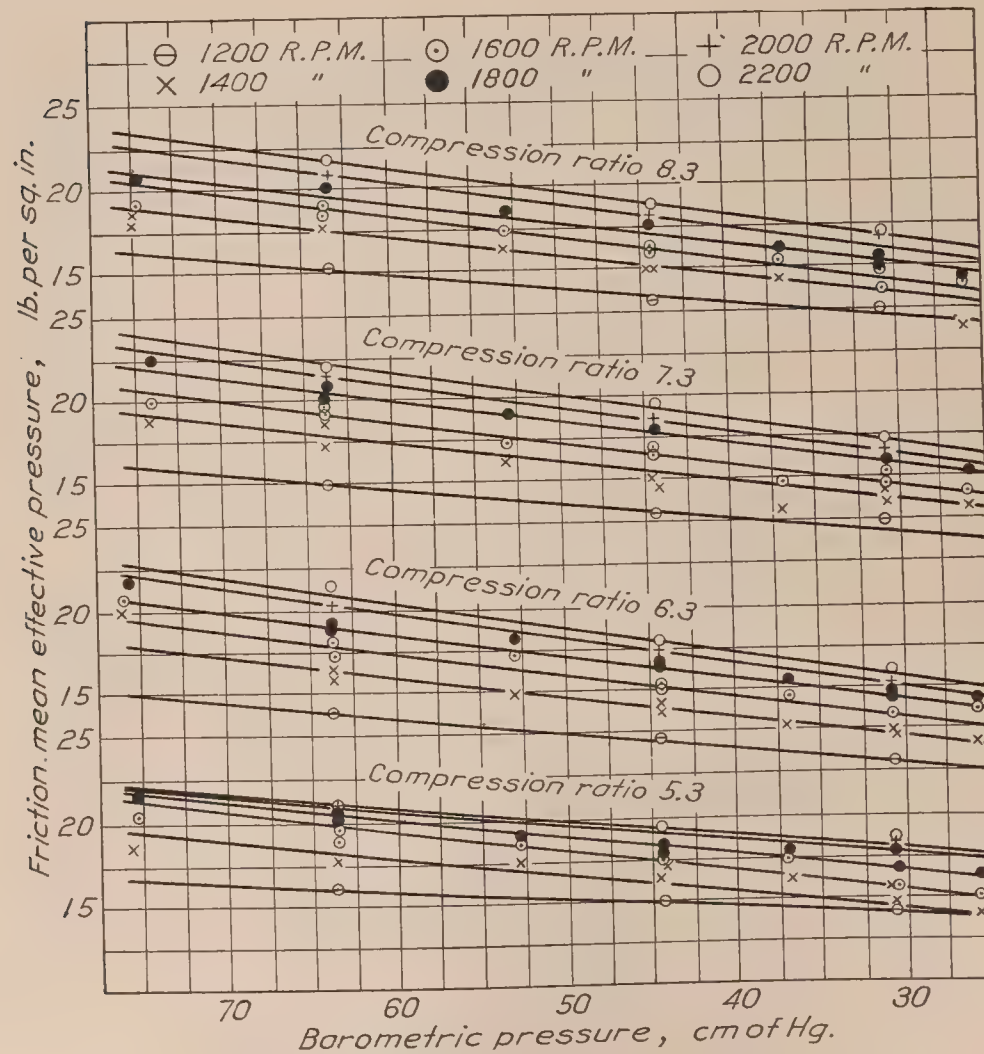
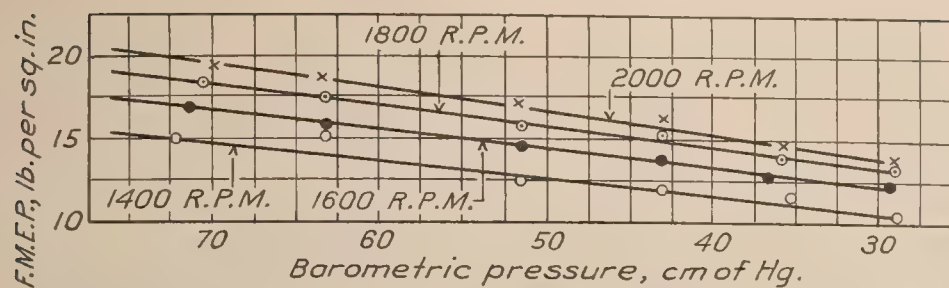
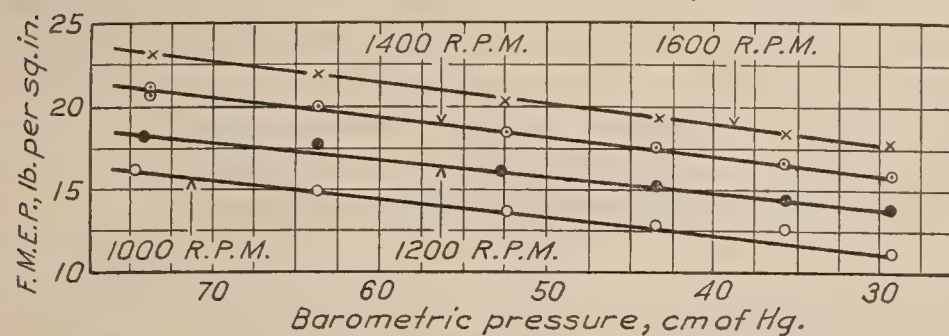


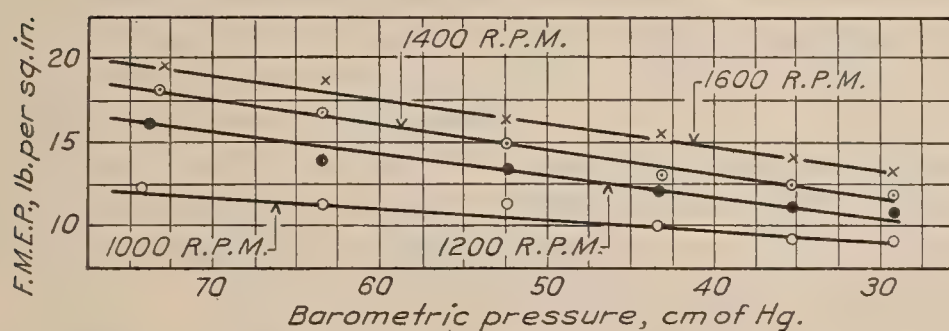
FIG. 6.—Engine D: 8 cylinders; bore, 4.72 inches; stroke, 5.12 inches



Engine G: 12 cylinders; bore, 5 inches; stroke, 5.25 inches; compression ratio, 6.5



Engine E: 6 cylinders; bore, 6.5 inches; stroke, 7.09 inches; compression ratio, 5.9



Engine F: 6 cylinders; bore, 5.9 inches; stroke, 7.09 inches; compression ratio, 6.7

FIG. 7 (a, b, c)

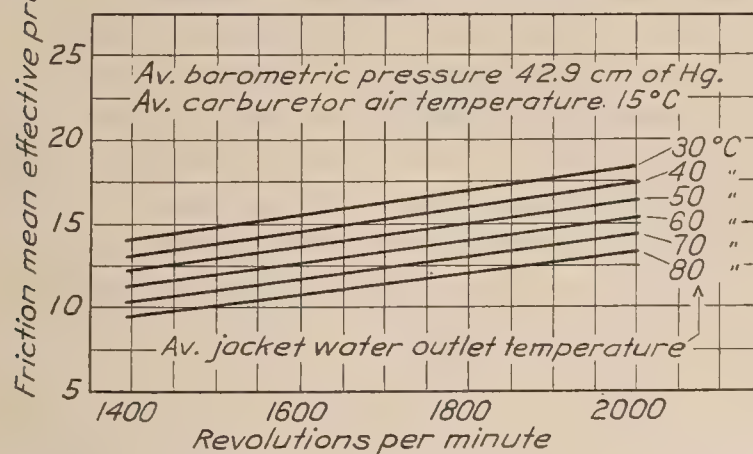
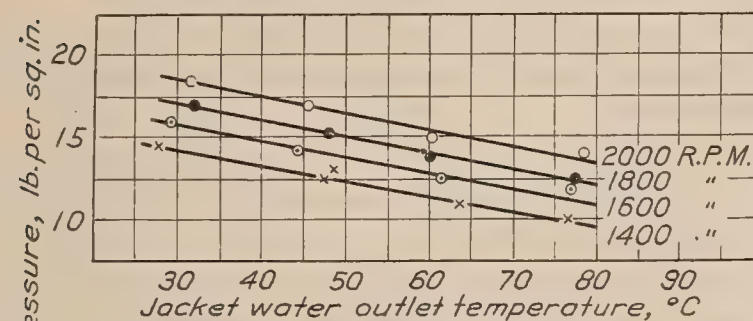


FIG. 8.—Engine A: 8 cylinders; bore, 5.51 inches; stroke, 5.91 inches; compression ratio, 6.5

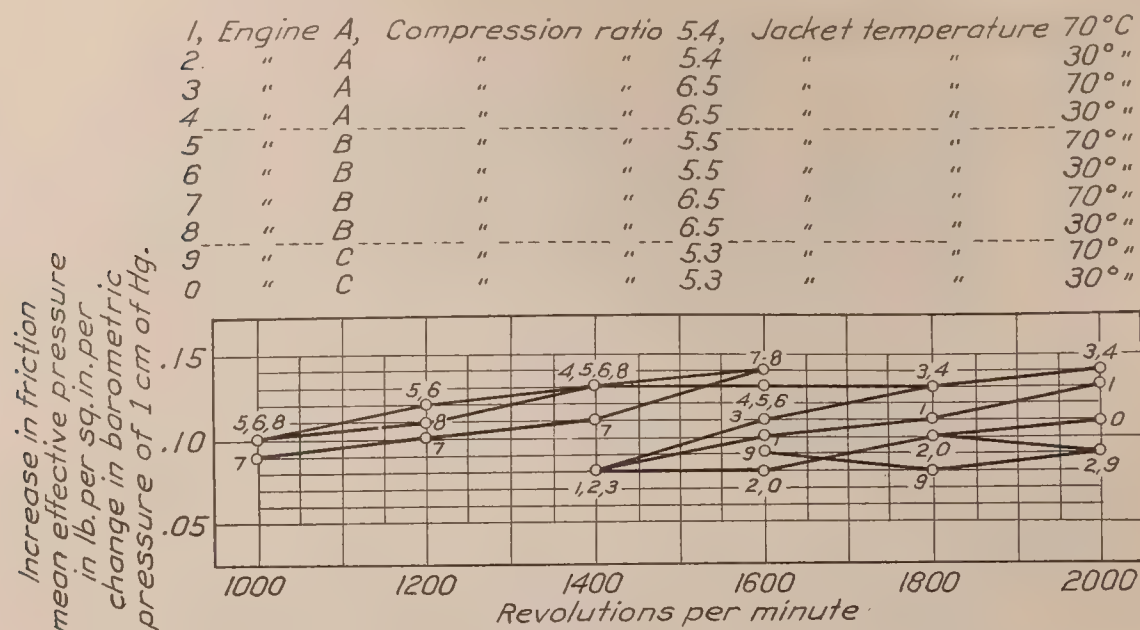


FIG. 9.—Change in friction with change in barometric pressure

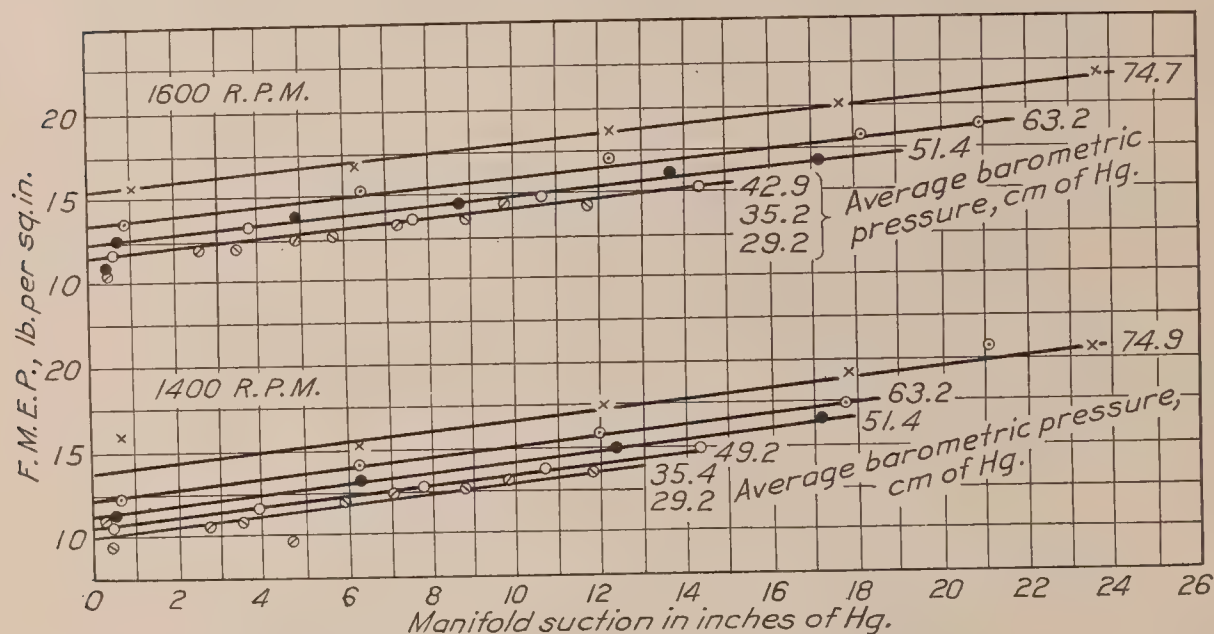


FIG. 10.—Engine A: 8 cylinders; bore, 5.51 inches; stroke, 5.91 inches; compression ratio, 5.4; change in F. M. E. P. per change in manifold suction of 1 centimeter (2.54 inches) Hg, 0.26 lb./sq. in. at 1,600 R. P. M., 0.29 lb./sq. in. at 1,400 R. P. M.

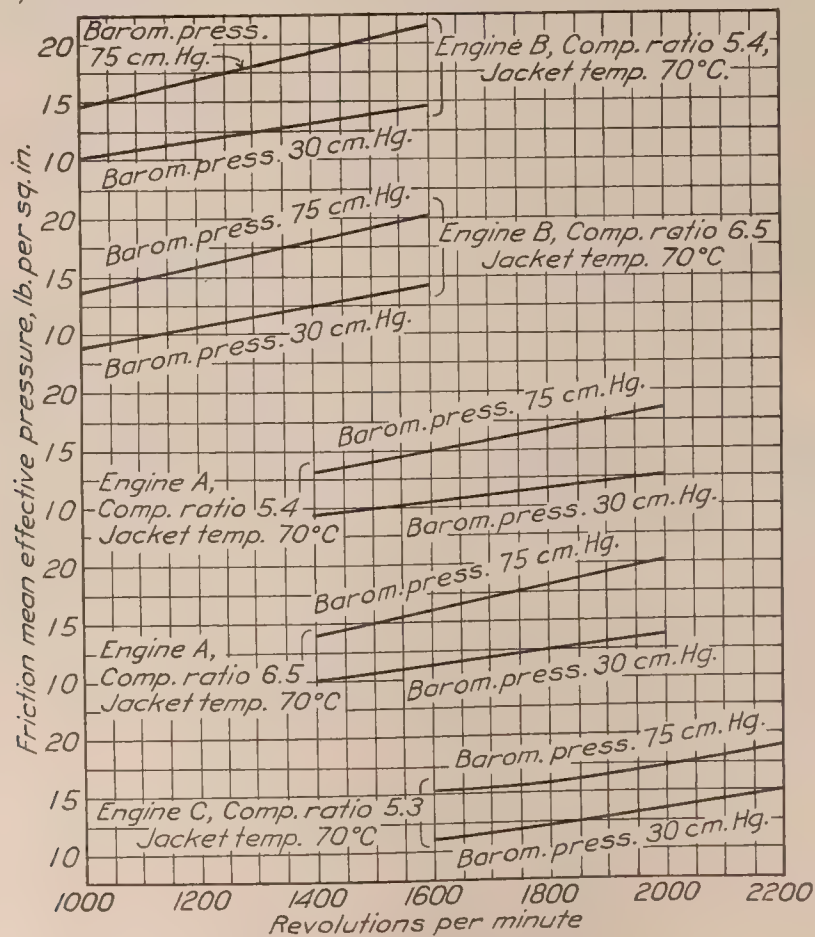


FIG. 11.—Friction versus engine speed

Tests in the altitude laboratory have shown that volumetric efficiency is not affected by changes in barometric pressure. The term volumetric efficiency as here used may be defined as the ratio between the volume of charge received per cycle measured at the temperature and pressure existing at the entrance to the carburetor and the piston displacement. In other words the volume of charge entering the engine per cycle when the barometric pressure is 38 centimeters of mercury is the same as the volume when the pressure is 76 centimeters of mercury. The weight of air entering the engine per cycle at the lower pressure is, of course, only one-half as great. Volumetric efficiency is determined by the conditions governing flow into the cylinder on the intake stroke and out from the cylinder on the exhaust stroke. That the rate of flow is not affected by changes of barometric pressure is indicated by the fact that the volumetric efficiency remains constant. If for any portion of the cycle the volume rate of flow is to be the same for two different barometric pressures, the relation between the pressure differences producing flow in the two cases must be such as to make the heads producing flow the same when measured at the temperature and pressure of the fluid flowing. To accomplish this the actual pressure differences must be directly proportional to the barometric pressure. Since these pressure differences govern the pumping losses, such losses therefore should vary directly as the barometric pressure.

In Report No. 190 of the National Advisory Committee for Aeronautics, which is entitled "Correcting Horsepower Measurements to a Standard Temperature" it is pointed out that the volumetric efficiency changes with change of atmospheric temperature. As has been stated, experiments indicate that changes in atmospheric temperature have a negligible influence upon friction. These facts are not inconsistent with the discussion in the previous paragraph since the change in volumetric efficiency with change in atmospheric temperature is due primarily to a change in the volume rate of flow with a given pressure difference which does not change appreciably with change in atmospheric temperature rather than to changes in such pressure differences and consequently in the pumping losses.

ENGINE SPECIFICATIONS

Before discussing the actual changes in friction with change in barometric pressure shown in Figures 1 to 7 it will be well to furnish sufficient information concerning the engines to serve as a basis for their identification. Table I furnishes such information. It will be noted that tests were made with two compression ratios with engines A and B and with four compression ratios with engine D. In each case the difference in compression ratio was obtained by changing pistons.

CHANGE IN FRICTION PER UNIT CHANGE IN BAROMETRIC PRESSURE

Table II was derived from Figures 1 to 7 and shows changes in F. M. E. P. per unit change of barometric pressure. As a matter of interest, mean piston speed has been tabulated in addition to revolutions per minute. While the table shows a rather wide range of values to have been obtained, it at least gives an idea as to the probable accuracy with which the change of friction with altitude can be predicted and may serve as a basis for such predictions.

Figure 9 shows data from the engines which have been tested most completely. In this figure the points are taken from the plotted curves and not from original data. Elsewhere in the report the conventional practice of using points only to indicate original data is followed. As would be expected, there is a tendency for the values to increase with speed. Since these are values of actual rather than percentage change, the increase with speed merely indicates that pumping losses are greater for high speeds than for low. From Figure 9 it would appear that the F. M. E. P. decreases about one-tenth of a pound per square inch for a decrease in barometric pressure of 1 centimeter of mercury.

THROTTLE OPENING AND FRICTION

When an engine is operated with partly closed throttle the friction is higher than at full throttle because of the higher pumping loss. Figure 10 shows a typical group of measurements made in connection with the altitude laboratory test of engine A. In such tests the friction

at various jacket water temperatures is measured only at full throttle. In order to obtain the friction at part throttle, there is added to the appropriate full throttle value an amount determined by means of (1) such information as is shown in Figure 10 and (2) knowledge as to the difference between the manifold suction at full and part throttle.

For the engines tested thus far it has been found that friction varies almost linearly with manifold suction and that the magnitude of this variation is approximately the same for various altitudes. As is shown in Figure 10, with engine A and a compression ratio of 5.4, a change in manifold suction of 1 inch (2.54 centimeters) of mercury changes the F. M. E. P. at 1,600 R. P. M. by about 0.26 pound per square inch, whereas at 1,400 R. P. M. the change is 0.29 pound. The same values were obtained in tests of this engine with the 6.5 compression ratio. With engine B and a compression ratio of 5.5, values of 0.20 and 0.24 were obtained for speeds of 1,200 and 1,000 R. P. M., respectively, while for a compression ratio of 6.5 a value of 0.19 was obtained at 1,200 R. P. M. and 0.18 at 1,000 R. P. M. For engine C a value of 0.39 was obtained for a speed of 1,800 R. P. M. and 0.38 for 1,600 R. P. M.

These values have been quoted as being of interest rather than as being of major importance in a general analysis of engine friction. This arises from the fact that the pumping losses are dependent upon the pressures and the distance through which they act whereas the manifold suction depends upon the *time* during which these pressures act. Moreover the manifold pressure is dependent upon the volume of the intake system, the number of cylinders which draw from it, etc., and its relation to the pressures in the cylinder depends upon valve areas, valve timing, piston speed, etc.

ENGINE SPEED AND FRICTION

Figure 11 shows values of F. M. E. P. over the normal operating range of speeds of engines A, B, and C. It will be noted that in this range the F. M. E. P. increases with speed and that in most instances the percentage increase is less than the corresponding percentage increase in speed. At very low speeds the F. M. E. P. changes to a much less extent with change of speed and in some instances remains almost constant over a considerable range. If the F. M. E. P. increases with speed then the friction horsepower will increase more than in proportion to the speed. This is chiefly responsible for the decrease in mechanical efficiency that ordinarily results from an increase in speed.

JACKET-WATER TEMPERATURE AND FRICTION

The influence of jacket-water temperature upon friction is clearly evidenced in Figures 1 to 5. The reason for this influence is, of course, that the temperature of the jacket water governs the temperature of the oil film upon the cylinder walls and consequently its viscosity. Thus far in the work with aviation engines the temperature of the circulating oil has not appeared to affect friction materially, the influence of the temperature of the jacket water being dominant. There are indications, however, that the temperature of the circulating oil does have an appreciable effect upon the friction of certain motor car engines. It is possible that in these engines the friction of main and connecting rod bearings or the power required to drive the oil pump may constitute a greater percentage of the total engine friction than is usually the case.

The oil used in the tests of engines A and B had the following viscosities:

Temperature (°C.)	Viscosity (seconds), Saybolt Universal
30	6,700
40	2,415
50	1,105
60	579
70	327
80	191
90	128
100	91

Engines must operate, during the starting period at least, with jacket-water temperatures below normal. To prevent abnormally high-friction losses during such periods, it is desirable that the change in the viscosity of an oil with change in temperature be small. This is desirable also for the reason that an oil should be of high enough viscosity to maintain a lubricating film at maximum pressures and temperatures and yet of low enough viscosity to flow freely under cold starting conditions.

These curves (figs. 1 to 5) emphasize the importance of reducing to a minimum the amount of engine operation at jacket-water temperatures *other than normal*. If the normal operating temperature is high, then operation at lower jacket temperatures will result in unduly high friction losses and consequently lower brake thermal efficiencies. On the other hand, if the normal operating temperature is low, then operation at high jacket temperatures may be dangerous, as the viscosity of the oil may not be adequate to prevent metal-to-metal contact.

One should not conclude from these curves, however, that friction losses are necessarily high for engines which normally operate at low jacket-water temperatures. Such engines ordinarily permit the use of an oil of comparatively low viscosity and hence have friction losses no greater than those of engines whose normal operating temperature is high. Friction is therefore ultimately more dependent upon the *range* of operating temperatures than upon the actual temperatures.

COMPRESSION RATIO AND FRICTION

In tests of engine A it was found that with a jacket-water temperature of 80° C., practically the same friction was obtained with compression ratios of 5.4 and 6.5, whereas with a jacket-water temperature of 30° C. the friction was materially higher for the lower compression ratio. With engine B, conditions were somewhat reversed, the friction with a compression ratio of 6.5 being higher at all jacket-water temperatures than with a compression ratio of 5.5. Although, for reasons already given, the results obtained from engine D are somewhat less dependable, it is of interest to note that the highest values of friction were obtained with the 5.3 ratio and the lowest with the 6.3, the values for ratios of 7.3 and 8.3 being between these two. In tests with a single-cylinder engine having a bore of 5 inches and a stroke of 7 inches no changes in friction with change in compression ratio were noted over a range of ratios extending from 5.4 to 14.

Hence while there are theoretical grounds for expecting a slight increase in friction with increase in compression ratio, from the evidence at hand it appears that the magnitude of this effect is ordinarily so small as to be masked by accidental differences in the pistons used to obtain the different compression ratios.

CONCLUSIONS

(1) Changes in friction due to changes in the temperature of the air entering the engine are negligible.

(2) Changes in friction which result from changes in atmospheric pressure are due primarily to changes in pumping loss. There is a wide difference between engines in the extent to which the friction changes with a given change of barometric pressure. An approximate figure for the engines mentioned in this report is that the F. M. E. P. decreased about one-tenth of a pound per square inch for each decrease of 1 centimeter of mercury in the barometric pressure.

(3) The increase in friction resulting from a decrease in throttle opening is also the effect of a change in pumping loss. For the engines mentioned in this report changes in throttle opening cause the mean effective pressure to vary in an almost linear relation to manifold suction. Values are quoted which show that for these engines the change in F. M. E. P. which accompanies a change in manifold suction of 1 inch (2.54 centimeters) of mercury ranges from 0.20 pound per square inch, obtained at an engine speed of 1,200 R. P. M., to 0.39 at 1,800 R. P. M.

(4) Nearly all of the data presented in this report were obtained for engine speeds ranging from 1,000 to 2,200 R. P. M. Over this range the F. M. E. P. increases with speed, but ordinarily the percentage increase is less than the corresponding percentage increase in speed. At low engine speeds the F. M. E. P. changes to a much less extent with change in speed, in some instances remaining practically constant over a considerable range.

(5) Friction depends very greatly upon the viscosity of the oil upon the cylinder walls, which in turn depends upon the temperature of the jacket water. It does not follow that the friction of an engine which normally operates at a low jacket-water temperature will necessarily be high, but it is important to take this temperature into consideration when selecting the oil and to reduce to a minimum the amount of operation that takes place at temperatures other than normal.

(6) From theoretical considerations one would expect that friction would increase with increase in compression ratio, but from the evidence at hand this effect appears to be slight.

TABLE I
SPECIFICATIONS OF ENGINES USED IN FRICTION TESTS

Engine	Bore (in inches)	Stroke (in inches)	Number of cylinders	Compression ratio
A	5.51	5.91	8	{ 6.5 5.4
B	6.62	7.50	6	{ 6.5 5.5
C	4.50	6.00	12	{ 5.3 5.3
D	4.72	5.12	8	{ 6.3 7.3 8.3
E	6.50	7.09	6	5.9
F	5.90	7.09	6	6.7
G	5.00	5.25	12	6.5

TABLE II
CHANGE IN F. M. E. P. FOR CHANGE IN BAROMETRIC PRESSURE OF 1 CENTIMETER Hg

R. P. M.	1,200	1,400	1,600	1,800	2,000	2,200	
Mean piston speed feet per minute..	1,024	1,195	1,365	1,536	1,707	1,877	
	0.06 .10 .10 .10	0.12 .13 .13 .13	0.13 .14 .14 .14	0.11 .14 .14 .13	0.09 .16 .15 .15	0.09 .16 .15 .15	Engine D, compression ratio, 5.3. Engine D, compression ratio, 6.3. Engine D, compression ratio, 7.3. Engine D, compression ratio, 8.3.
R. P. M.		1,000	1,200	1,400	1,600		
Mean piston speed feet per minute..		1,182	1,418	1,654	1,891		
		0.07	0.13	0.15	0.14		Engine F.
R. P. M.		1,400	1,600	1,800	2,000		
Mean piston speed feet per minute..		1,225	1,400	1,575	1,750		
		0.10	0.11	0.12	0.14		Engine G.
R. P. M.		1,000	1,200	1,400	1,600		
Mean piston speed feet per minute..		1,182	1,418	1,654	1,891		
		0.11	0.10	0.12	0.13		Engine E.

CHANGE IN F. M. E. P. FOR CHANGE IN BAROMETRIC PRESSURE OF 1 CENTIMETER Hg—Continued

R. P. M. Mean piston speed feet per minute..	1,400 1,379	1,600 1,576	1,800 1,773	2,000 1,970	
	0.13	0.13	0.13	0.14	Engine A, compression ratio, 6.5; jacket-water temperature, 30° C.
	.11	.12	.13	.14	Engine A, compression ratio, 6.5; jacket-water temperature, 40° C.
	.10	.12	.13	.14	Engine A, compression ratio, 6.5; jacket-water temperature, 50° C.
	.09	.12	.13	.14	Engine A, compression ratio, 6.5; jacket-water temperature, 60° C.
	.08	.11	.13	.14	Engine A, compression ratio, 6.5; jacket-water temperature, 70° C.
	.07	.10	.18	.14	Engine A, compression ratio, 6.5; jacket-water temperature, 80° C.
	.08	.08	.10	.09	Engine A, compression ratio, 5.4; jacket-water temperature, 30° C.
	.07	.09	.10	.10	Engine A, compression ratio, 5.4; jacket-water temperature, 40° C.
	.07	.09	.10	.11	Engine A, compression ratio, 5.4; jacket-water temperature, 50° C.
	.08	.09	.11	.12	Engine A, compression ratio, 5.4; jacket-water temperature, 60° C.
	.08	.10	.11	.13	Engine A, compression ratio, 5.4; jacket-water temperature, 70° C.
	.07	.10	.11	.14	Engine A, compression ratio, 5.4; jacket-water temperature, 80° C.
R. P. M. Mean piston speed feet per minute..	1,000 1,250	1,200 1,500	1,400 1,750	1,600 2,000	
	0.10	0.12	0.13	0.13	Engine B, compression ratio, 5.5; jacket-water temperature, 30° C.
	.10	.12	.13	.13	Engine B, compression ratio, 5.5; jacket-water temperature, 40° C.
	.11	.12	.13	.13	Engine B, compression ratio, 5.5; jacket-water temperature, 50° C.
	.11	.12	.13	.13	Engine B, compression ratio, 5.5; jacket-water temperature, 60° C.
	.10	.12	.13	.13	Engine B, compression ratio, 5.5; jacket-water temperature, 70° C.
	.10	.12	.13	.13	Engine B, compression ratio, 5.5; jacket-water temperature, 80° C.
	.10	.11	.13	.14	Engine B, compression ratio, 6.5; jacket-water temperature, 30° C.
	.09	.11	.12	.14	Engine B, compression ratio, 6.5; jacket-water temperature, 40° C.
	.09	.11	.12	.14	Engine B, compression ratio, 6.5; jacket-water temperature, 50° C.
	.09	.10	.12	.14	Engine B, compression ratio, 6.5; jacket-water temperature, 60° C.
	.09	.10	.11	.14	Engine B, compression ratio, 6.5; jacket-water temperature, 70° C.
	.10	.09	.11	.14	Engine B, compression ratio, 6.5; jacket-water temperature, 80° C.
R. P. M. Mean piston speed feet per minute..	1,600 1,600	1,800 1,800	2,000 2,000	2,200 2,200	
	0.08	0.10	0.11	0.10	Engine C, jacket-water temperature, 30° C.
	.08	.09	.10	.10	Engine C, jacket-water temperature, 40° C.
	.09	.09	.10	.09	Engine C, jacket-water temperature, 50° C.
	.09	.08	.09	.09	Engine C, jacket-water temperature, 60° C.
	.09	.08	.09	.08	Engine C, jacket-water temperature, 70° C.
	.09	.07	.08	.08	Engine C, jacket-water temperature, 80° C.

PART II

FRICTION OF PISTONS

GENERAL COMMENT

This section of the report is to present the results of the measurements of friction obtained with the group of pistons shown in Figures 12 to 19. These pistons as originally received were all the same within close manufacturing tolerances. In modifying them as regards length, clearance, area of thrust face, location of thrust face, etc., the sole object sought was the obtaining of information as to the influence of the changes upon piston friction. No attempt was made to obtain piston designs which would be satisfactory from the standpoint of gas tightness, strength, wear, or freedom from noise. In fact, the changes made were usually far greater than would be permissible in service but, being large, the effects of the changes were much less likely to be masked by other influences than would have been the case had the pistons been modified only to the extent which would be feasible in normal operation.

It has not been possible to carry this work far enough to justify definite predictions as to the magnitude of the changes in friction which would result from a given change in piston design. Nevertheless although the information obtained thus far is qualitative and incomplete it is believed to be of sufficient value to warrant its publication at this time.

Measurements of friction were obtained, as is customary, by driving the engine by the dynamometer, with ignition and fuel turned off and with temperatures of oil and water maintained at predetermined values. Friction as thus measured includes not only piston friction but also the friction of main, connecting rod, and piston pin bearings, the power expended in driving the auxiliaries such as water pump, oil pump, magneto, etc., and the pumping loss, which is the term applied to the power utilized in drawing in and expelling the charge.³ As only pistons were changed in these experiments, any changes found in the total engine friction could reasonably be ascribed to differences between pistons.

The engine used in these experiments was designed for use in a truck and is of the rugged construction essential to such service. It is water-cooled and has a bore of $4\frac{3}{4}$ inches and a stroke of 6 inches. The cylinders are cast in blocks of two and are bolted to the upper half of the crankcase. This construction permits the cylinders to be removed for the installation of pistons and rings and makes it unnecessary to disturb connecting rod big-end bearings. Changes in the bearings during these tests were therefore limited to the slight increase in clearance which resulted from wear.

For many of the experiments it was considered highly desirable to eliminate the pumping loss or rather to reduce it to a negligible value. This was accomplished by removing the spark plugs and holding the valves open by means of wedges. From the standpoint of reducing pumping losses it would have been simpler to remove the cylinder head, but this would have complicated the problem of maintaining the circulation and hence of controlling the temperature of the jacket water.

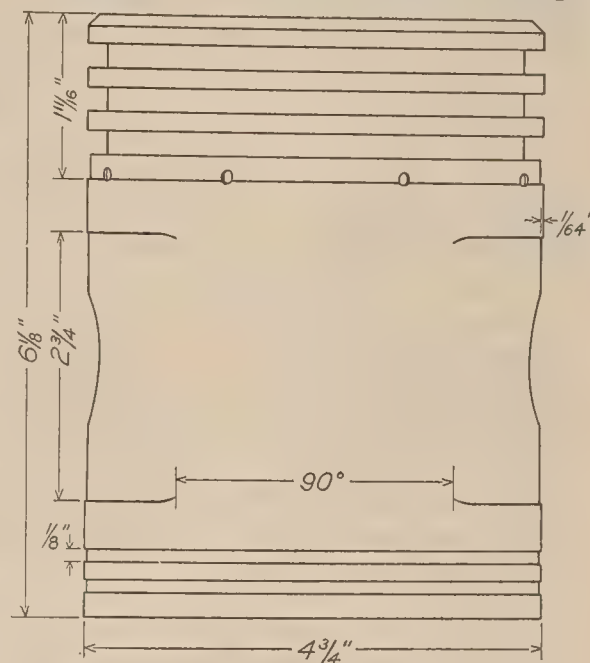


FIG. 12.—Standard piston; total area of piston bearing not in relieved portion, 41 square inches

³ The slight heat loss to the cylinder walls during the compression stroke is also included in the term "pumping loss."

In this engine, as in all others which have been tested at the Bureau of Standards, the condition of operation which has the chief effect upon piston friction is the temperature of the jacket water, the reason being that this governs the viscosity of the oil upon the cylinder walls. The friction of this particular engine was appreciably influenced also by the temperature of the circulating oil, which has not been the case with most of the engines—of the aviation type, at least—tested at the bureau. Probably the viscosity of the circulating oil has an influence upon the power required to drive the pump and upon bearing friction, gear friction, cam friction, etc. It is not probable that the temperature of the oil thrown on the cylinder wall will materially affect piston friction in view of the rapidity with which a temperature approximating

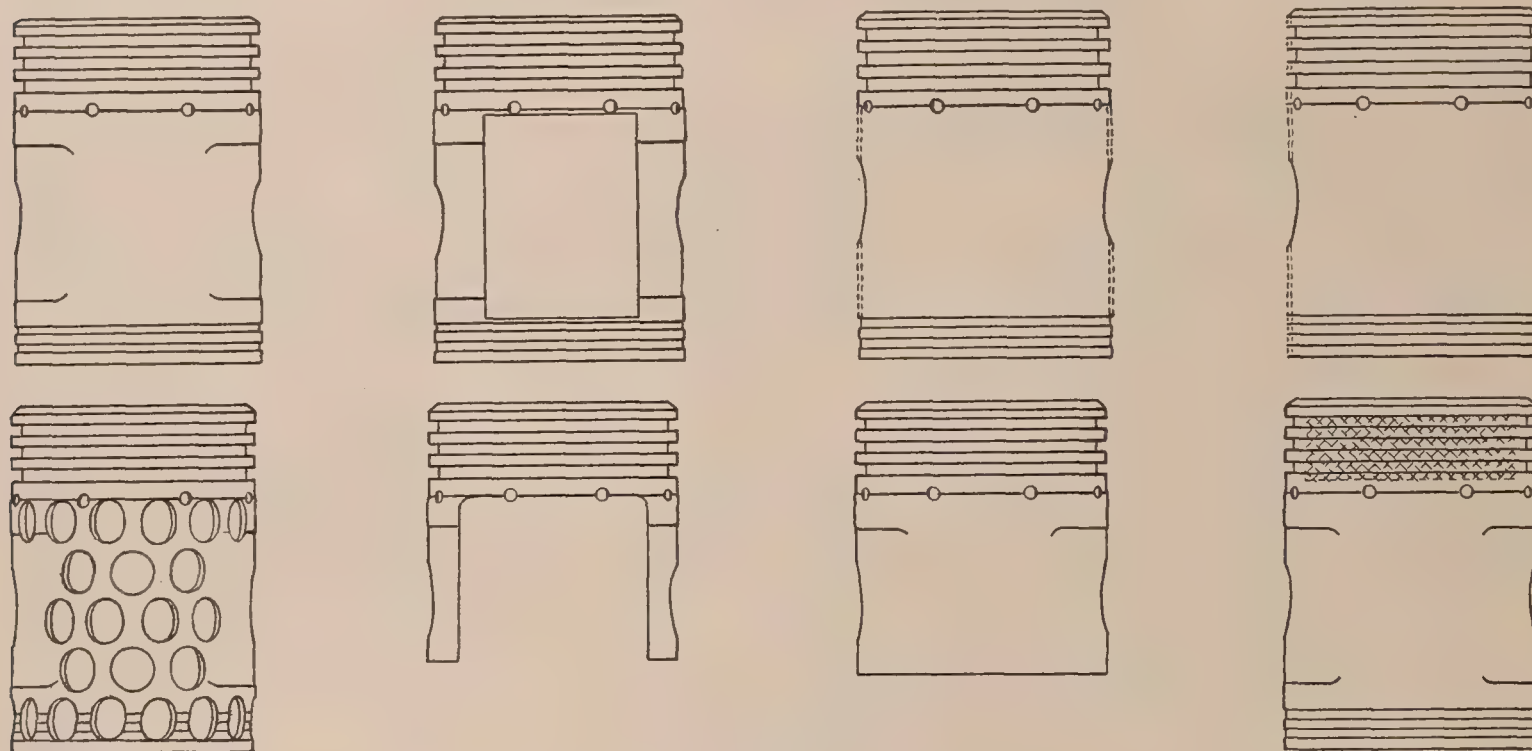


FIG. 13

Piston S: Standard; clearance, 0.005 inch; bearing area, 41 square inches; weight, 5 pounds 12 ounces.

Piston F: Forty-six 0.75-inch holes through skirt; clearance 0.005 inch; bearing area, 23 square inches.

Piston B: Thrust faces milled out; clearance, 0.005 inch; bearing area, 12.5 square inches.

Piston G: Skirt milled away; bearing area, 3 square inches.

Piston C: Clearance, part length, increased to 0.050 inch; bearing area, 4.5 square inches.

Piston H: Skirt shortened; clearance, 0.005 inch; bearing area, 25 square inches.

Piston D: Increased clearance, full length; clearance, 0.037 inch.

Piston E: Lead cast in head; clearance, 0.005 inch; bearing area, 41 square inches; weight, 12 pounds 8 ounces.

that of the cylinder wall is attained. In so far as these tests were concerned the influence of circulating oil temperature upon engine friction was of importance only because it necessitated careful control of this temperature. In most of this work, the temperature of the oil in the sump was maintained at approximately 60° C.

The standard piston and its important dimensions are shown in Figure 12. In this and other figures the designation "bearing area" is not applied to projected area but to the entire rubbing surface. This ordinarily includes all of the ground portion of the piston but of course does not include ring grooves, oil grooves, or the relieved portion around the end of the piston pin. Figure 13 shows the manner in which each piston was modified and the letter by which each piston is designated in the report.

CONDITIONS OF TEST

In general tests were made with each type of piston under the four following conditions of operation: (1) Pistons with full set of three rings and with valves held open so that cylinder pressures varied only a negligible amount from atmospheric; (2) pistons without rings and with valves held open so that cylinder pressure varied only a negligible amount of atmospheric;

(3) pistons with full set of three rings and with cylinder pressures varying normally; and (4) pistons without rings and with cylinder pressures varying normally. In each group of tests, measurements were made at engine speeds of 400, 600, 800, 1,000, and 1,200 R. P. M. and at jacket-water temperatures of 20, 45, 70, and 95° C. (68, 113, 158, and 203° F.).

Runs were made both with atmospheric and normal pressures in the cylinder in order that the pistons might be compared under different conditions of loading, the differences in friction presumably being the same except as affected by loading. When the pistons were operated at normal pressures and without rings, the differences in the amount of leakage past the pistons affected the pumping losses to such an extent as to mask the differences in actual friction. The information obtained in this particular group of tests though of interest deals with a phase of the problem of piston design somewhat outside the scope of this report and for this reason has not been included. The results obtained under the other three conditions of operation, however, have been plotted for each type of piston which received a complete test.

PISTON-RING FRICTION

Before proceeding to a discussion of the results obtained with each group of pistons it will be well to make a few comments on the subject of piston-ring friction. It has been stated that friction measurements were obtained both for pistons with and without rings. The difference in these measurements is the friction *due* to the rings but not necessarily, or probably, the friction *of* the rings. This is borne out by the fact that while the same rings were used with each group of pistons, the increase in friction which resulted from the addition of the rings was far from being the same. A probable explanation of this is that the rings affect the thickness and distribution of the oil film between the pistons and cylinder walls, which in turn affects the friction of the piston to an extent which depends upon its design.

COMPARISON OF PISTON B AND STANDARD PISTON

Piston B, as is shown by Figure 13 and Figure 14, was obtained by removing a large portion of the thrust faces of the standard piston, thus decreasing the area of the rubbing surface from about 41 square inches to about 12 square inches.

The results are shown in Figure 20 and the lower part of Figure 25. When no rings are used and the viscosity of the oil upon the cylinder walls is low, because of the high jacket-water temperature, the difference in the friction of the two pistons is negligible. At the higher viscosities, however, the friction of piston B is much less than that of the standard piston. In this connection it is of interest to note that the friction of piston B when the jacket-water temperature is 20° C. is approximately the same as that of the standard piston when the jacket-water temperature is 45° C. In other words, the effect of the change in piston construction in this particular instance was equivalent to a definite change in oil viscosity. It should be mentioned that in all of these experiments measurements of the friction at 600 R. P. M. are questionable, as there frequently was excessive engine vibration at that speed.

When the pistons were equipped with their full complement of three rings, however, the friction of piston B was higher than that of the standard piston under all of the conditions of test. From these results it would appear that with pistons of this type, reducing the thrust face area while permitting a narrow band of bearing surface to extend completely around the base of the piston tends to increase rather than decrease friction.

COMPARISON OF PISTON C AND STANDARD PISTON

In this piston, as is shown by Figures 13 and 15, the outside diameter of a considerable portion of the skirt was reduced, increasing the clearance to about 0.050 inch and decreasing the area of rubbing surface to about 4 square inches. Only a few measurements were made with this particular type of piston because of failure due to the reduction in the cross section of the skirt necessitated by the increase in clearance. The few measurements which had been obtained at the time of the failure of the pistons did not show anything of particular interest.

COMPARISON OF PISTON D AND STANDARD PISTON

This piston is shown in Figures 13 and 16. A cut was taken over the entire surface of this piston, increasing the clearance to 0.037 inch over the entire length.

Results are shown in Figures 21 and 25. When no rings are employed piston D gives much less friction than the standard piston. When the pistons are equipped with a full set of rings and compared at approximately atmospheric cylinder pressures the differences in friction are much less, and the differences are smaller yet when the comparisons are made at normal cylinder pressures.

The only conclusion that appears to be justified by this comparison is that differences in clearance may have a marked effect on friction but that with the customary ring arrangement one would not expect the effect to be large.

COMPARISON OF PISTON E AND STANDARD PISTON

The changes made in the various pistons altered their weight and therefore the inertia forces at any given speed. It appeared probable, however, that under the conditions of test the change in the inertia forces would have a negligible effect upon friction. As a rough means of checking the reasonableness of this assumption, friction measurements were made, using pistons E. This type of piston, differed from the standard only in the matter of weight, but in this respect it differed much more than any of the other types of piston. Vibration with these pistons was so excessive that it was not deemed advisable to make more than a brief series of tests. These tests, however, failed to show significant differences between the friction of the heavy and standard pistons. It does not appear probable, therefore, that the differences in weight of the other pistons tested had an appreciable effect upon their friction.

COMPARISON OF PISTON F AND STANDARD PISTON

This piston is shown in Figures 13 and 17. It differs from the standard piston only in that the rubbing surface has been reduced by the drilling of 46 holes of $\frac{3}{4}$ -inch diameter.

Results are shown in Figures 22 and 25. Without rings, piston F gives somewhat less friction than the standard piston. When equipped with rings and operating at approximately atmospheric cylinder pressures the differences in the friction of the two pistons were rather small. With normal cylinder pressures, however, the friction of piston F was somewhat higher than that of the standard piston.

On the basis of the data here presented, it is not possible to predict whether the reduction of bearing surface by the addition of holes will increase or decrease the friction, but it does not appear probable that the magnitude of the change in friction will be great.

COMPARISON OF PISTON G AND STANDARD PISTON

This piston is shown in Figures 13 and 18. It will be observed that the thrust faces have been cut away to an even greater extent than in piston B and that there is no band of rubbing surface extending entirely around the base of the piston as in piston B.

Results are plotted in Figures 23 and 25. It will be noted that practically all of the comparisons show the friction to be lower for piston G than for the standard piston. In this connection it is of interest to recall that the friction of piston B was lower than that of the standard piston only when no rings were used.

As far as piston G is concerned, the conclusion appears warranted that a reduction in rubbing surface in conjunction with the removal of the band of bearing surface completely surrounding the base is likely to reduce considerably the friction both when the rings are in place and when they are removed. In this connection one should not forget the statement made earlier in the paper to the effect that the changes made in the pistons used in these experiments were usually much greater than would be permissible in service. Piston G, for example, would very likely be unsatisfactory from the standpoint of wear and gas tightness.



FIG. 14.—Piston B



FIG. 15.—Piston C

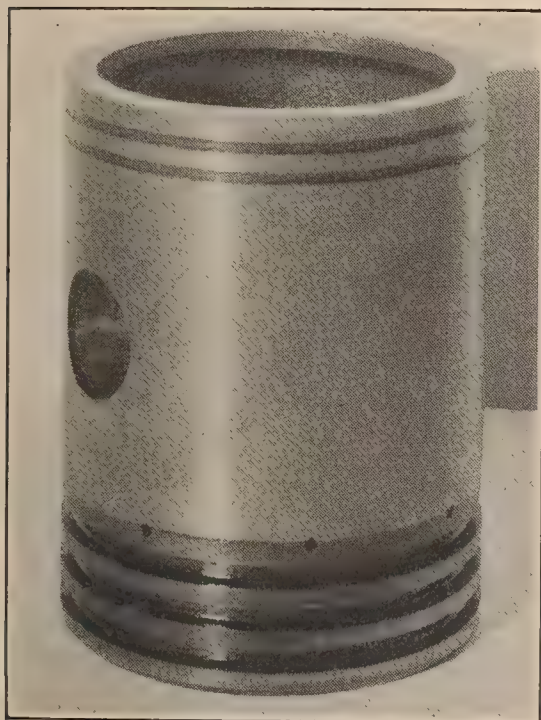


FIG. 16.—Piston D

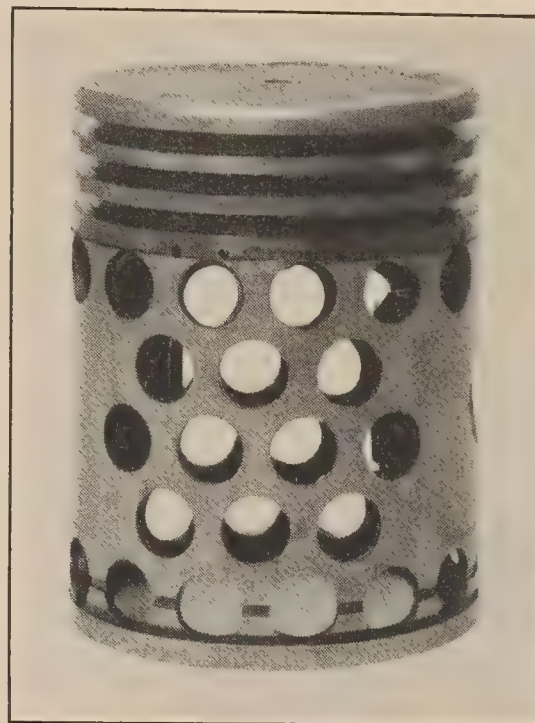


FIG. 17.—Piston F



FIG. 18.—Piston G

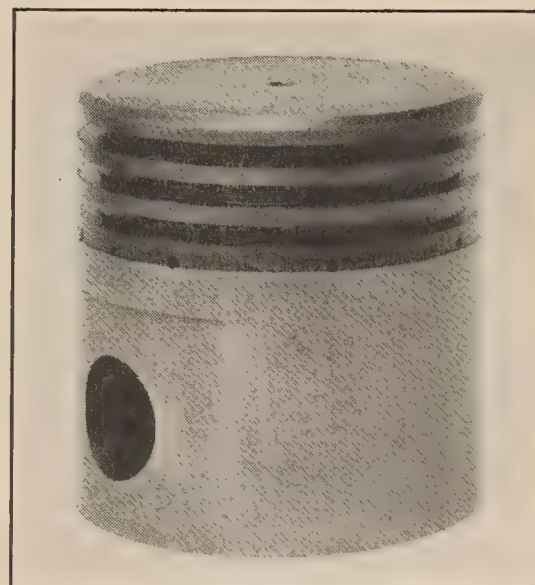


FIG. 19.—Piston H

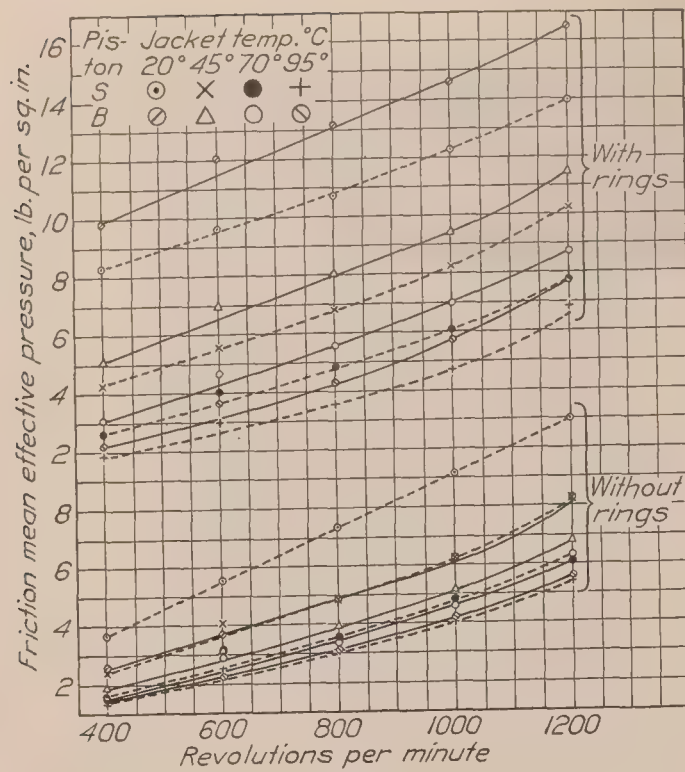


FIG. 20.—Pistons S and B

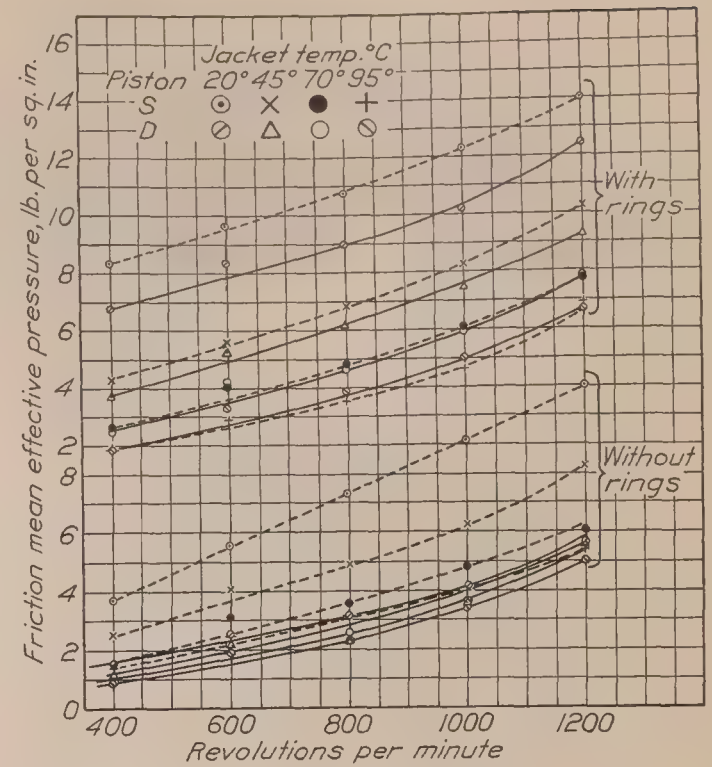


FIG. 21.—Pistons S and D

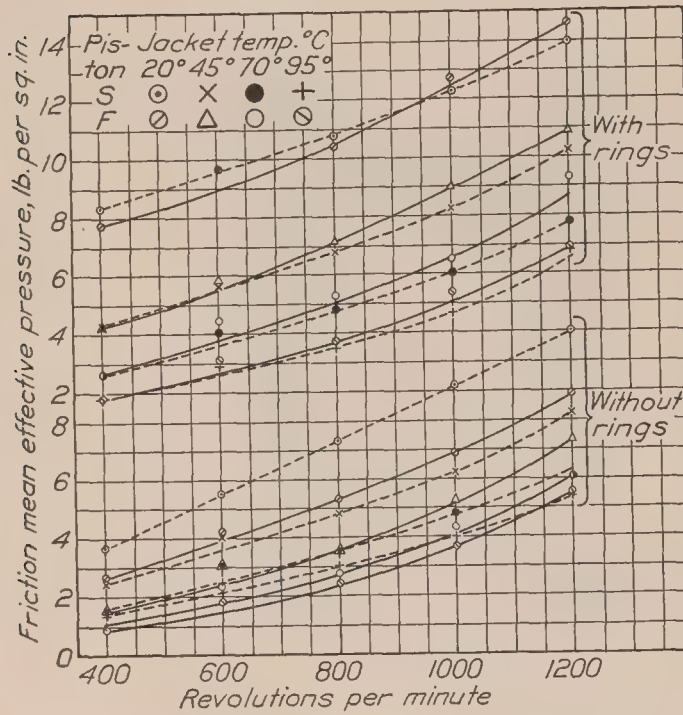


FIG. 22.—Pistons S and F

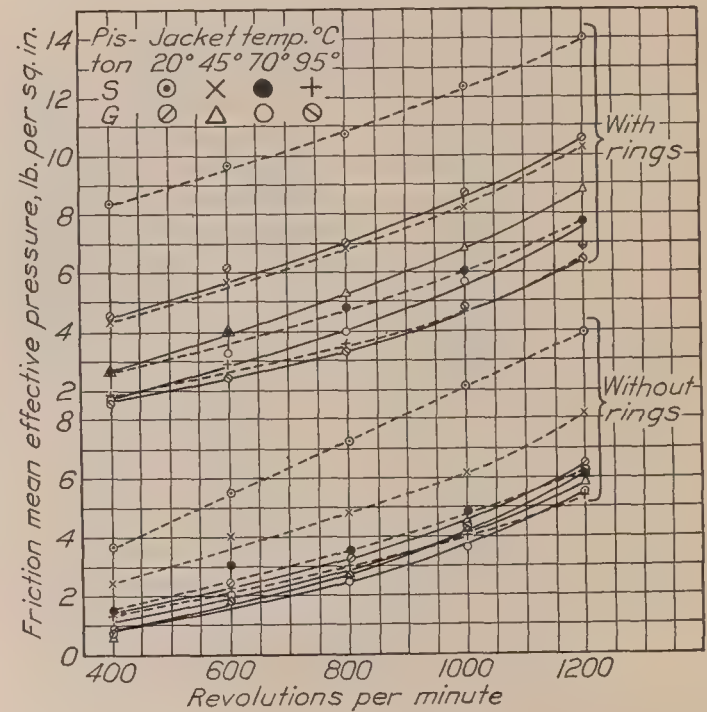


FIG. 23.—Pistons S and G

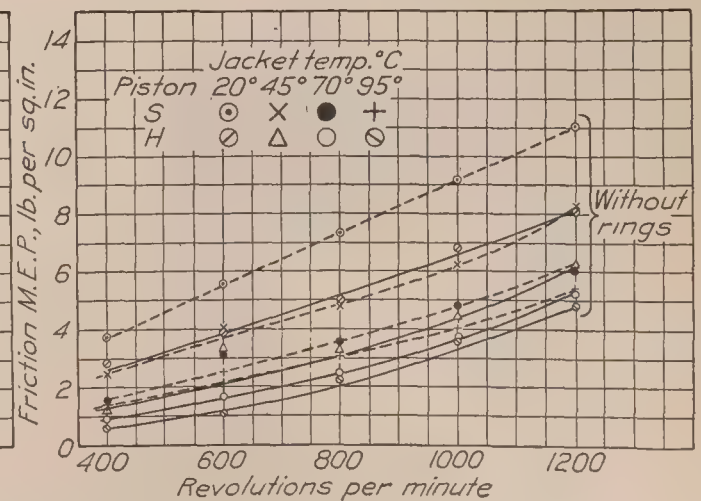
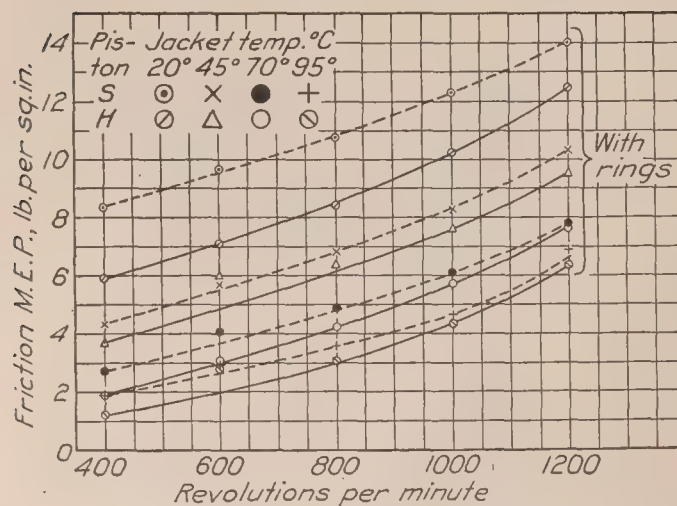


FIG. 24.—Pistons S and H: Friction mean effective pressure versus revolutions per minute; cylinder pressure nearly constant. ("No pumping loss")

COMPARISON OF PISTON H AND STANDARD PISTON

This piston is shown in Figures 13 and 19. It is considerably shorter than the standard piston but does not differ otherwise. Results are shown in Figures 24 and 25. In general the friction is less than with the standard piston, but when rings are used and the cylinder pressures are normal the difference is rather small. The results obtained with this type of piston lead to the conclusion that a reduction in the over-all length of pistons is likely to reduce friction but that the magnitude of the change may be rather small even though the change in the area of rubbing surface is rather large.

COMPARISON OF ALL PISTONS

Figures 26, 27, and 28 show comparisons of all the pistons for three conditions of operation and for the highest and lowest temperature of jacket water. It is not proposed to discuss in detail these comparisons but merely to point out that the employment of piston rings changes the order of the pistons as regards friction and to draw attention to the much greater friction and differences in friction at a jacket-water temperature of 20°C . than of 95°C . While the latter fact is not at all surprising, it emphasizes the folly of taking great pains to secure a piston design which will give low friction and then neglecting to use an oil of suitable viscosity or to maintain the temperature of the jacket water close to the desired value.

GENERAL COMMENTS ON PISTON FRICTION

As was stated at the outset, this work has not been carried far enough to permit definite predictions as to the effect a given change in piston design will have upon friction. It seems desirable, however, to discuss briefly some of the factors which would appear to influence this friction and which should therefore receive attention in any further work on the subject. The magnitude of the friction undoubtedly depends upon whether there is or is not a complete film of lubricant between the cylinder walls and the piston and rings. Where there is no film one would expect the friction to be proportional to the load but independent of the area of rubbing surface. If, however, there is a complete film, then the friction will be due to the shearing of the oil and will be affected by the load on the piston only to the extent that load governs the thickness of the film. A reduction in thrust face area increases the unit pressure. An increase in unit pressure increases the rate at which the lubricant flows out from between the rubbing surfaces and hence decreases the average thickness of the lubricating film. This decrease in film thickness causes an increase in friction which counteracts to some extent the decrease in friction due to the reduction in the area of the rubbing surfaces.

Friction under conditions of complete film lubrication and the conditions essential to the maintenance of such film have been discussed on numerous occasions since attention was directed to the problem by the work of Tower as reported to the Institute of Civil Engineers (British) in 1884. It is proposed here merely to call attention to some of the respects in which piston friction differs from the simple problem of sliding friction between two flat surfaces. The piston at any instant bears only upon one side of the cylinder whereas the piston rings are intended at least to bear over their entire circumference. Loads, proportion of total surface which is bearing, film thickness, etc., are not the same for pistons and piston rings. This would offer no particular difficulty if the friction and lubrication of the piston were unaffected by the presence of the rings, and vice versa, and if conditions remained constant throughout the stroke. That such is not the case will be evident from a single illustration. Figure 29 shows a piston in four positions A, B, C, and D. At the beginning of the stroke, position A, there is clearance between the side of the piston opposite to the thrust face and the oil film on the cylinder wall. By the time that the piston has reached position B, however, a considerable amount of the space between the piston and cylinder wall is filled with a film of oil which must be sheared if the piston is to move farther. When the piston reaches position C practically the entire space between the piston and cylinder is filled with oil. It is evident that the force required to move the piston at a given rate from A to B will be different from that required to move it from B to C and still different from that required to move it from C to D. In an actual engine the force required to move

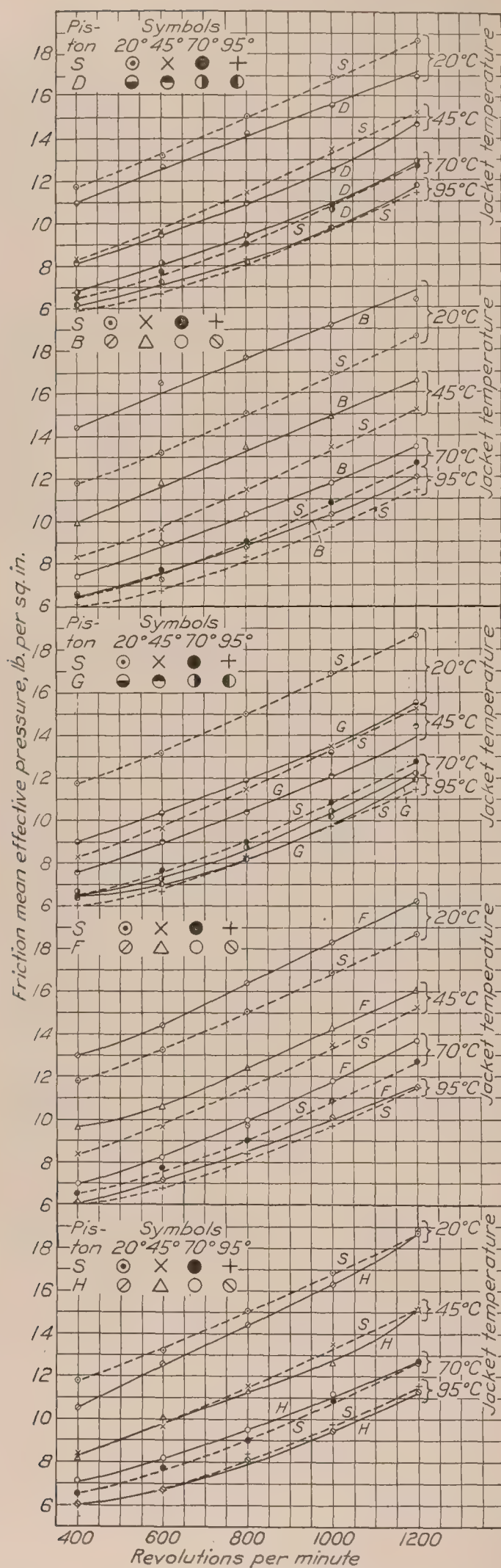


FIG. 25.—Pistons with rings; cylinder pressure varying normally. ("With pumping loss")

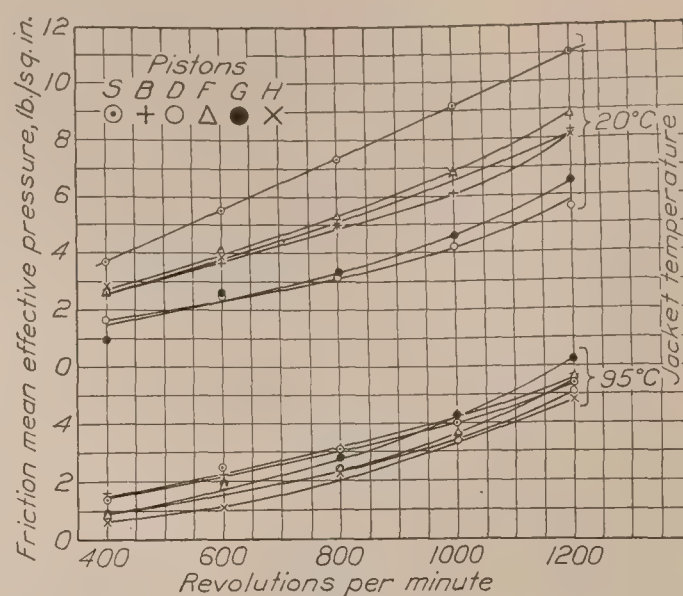


FIG. 26.—Pistons without rings; cylinder pressure nearly constant. ("No pumping loss")

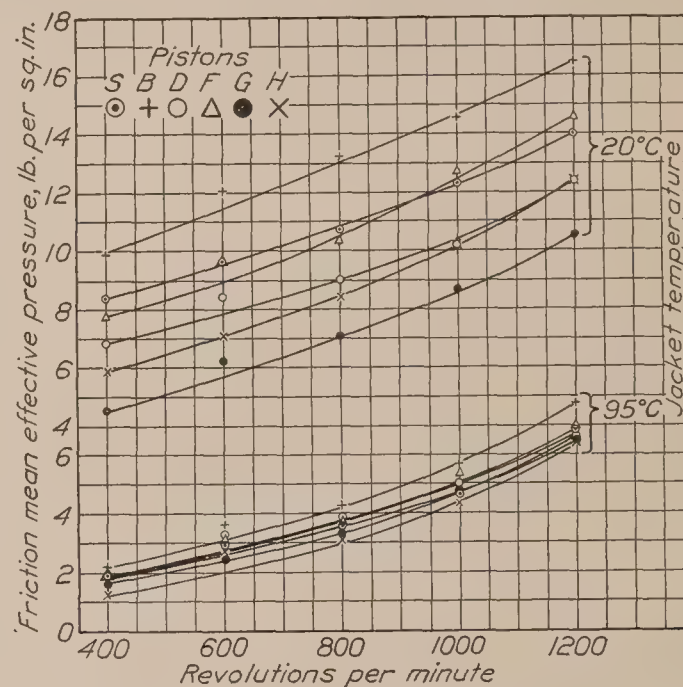


FIG. 27.—Pistons with rings; cylinder pressure nearly constant. ("No pumping loss")

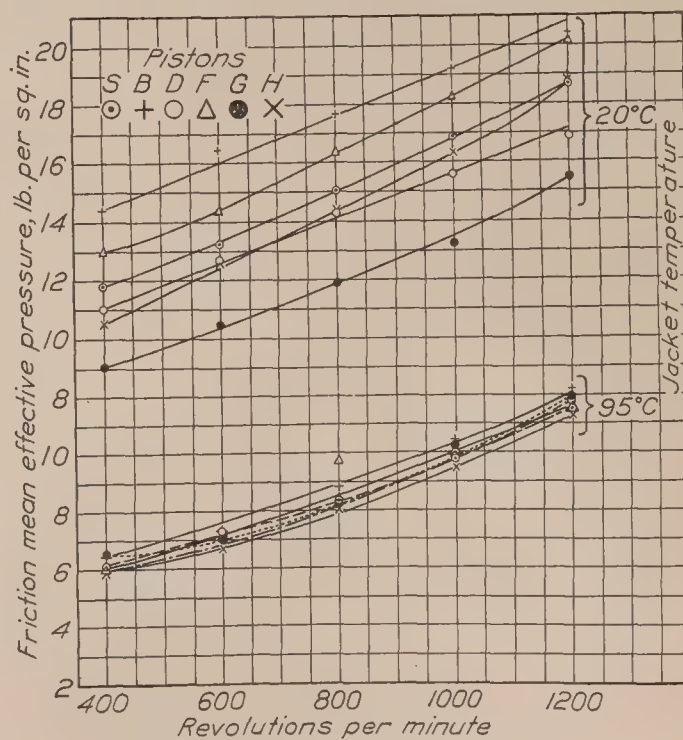


FIG. 28.—Pistons with rings; cylinder pressure varying normally. ("With pumping loss")

the piston is affected by the fact that the piston speed varies throughout the stroke. Piston design and ring design govern the distribution of the lubricant as well as the extent to which it can collect between the piston and cylinder walls. These remarks will serve to indicate the complexity of the relation between piston design and piston friction and the danger of drawing conclusions from two brief a series of tests.

Figures 30 and 31 present relations of considerable interest, although the numerical values shown are not generally applicable. The friction values are the same as given in Figures 20 to 24 for the condition of minimum pressure variation in the cylinder—that is to say, with valves held open and spark plugs removed. The friction is plotted against viscosity on the assumption that the oil film on the cylinder wall is at the same temperature as the jacket water. In all probability the actual difference between these two temperatures is small.

As has been stated already, the temperature of the oil entering the engine was maintained constant so that the temperature of the jacket water affected only the viscosity of the oil upon the cylinder walls and hence only the friction of pistons and rings. As the viscosity of the oil film between two rubbing surfaces is decreased the friction is decreased and in the unobtainable ideal condition of complete film lubrication with an oil of zero viscosity the friction would be

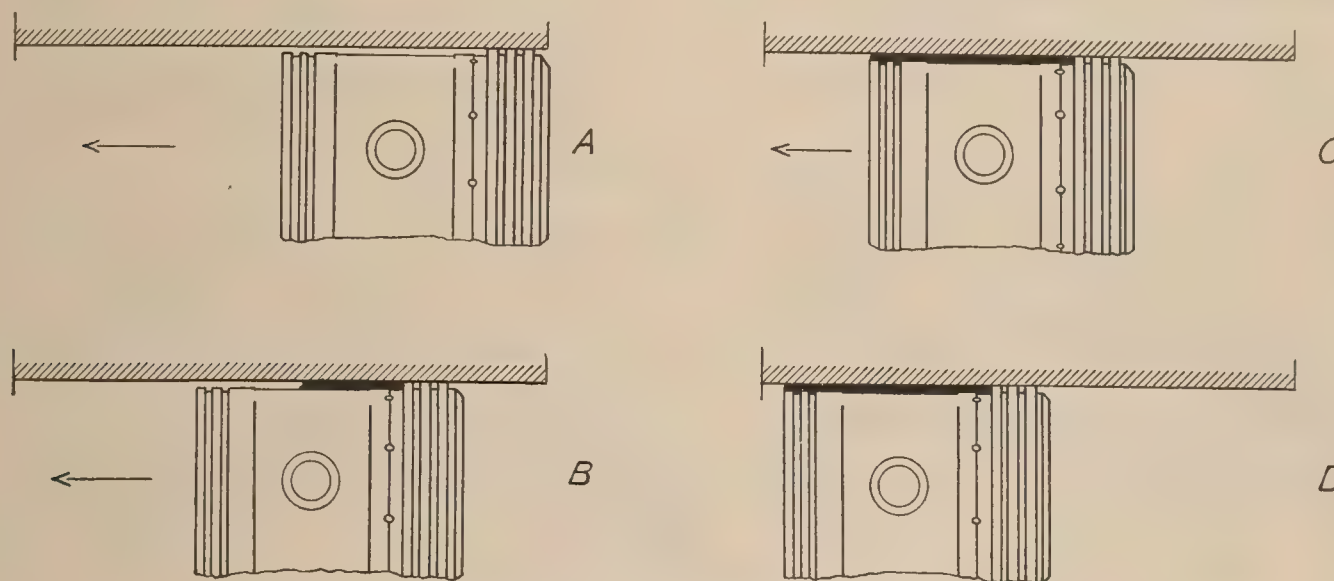


FIG. 29.—Illustrating the collection of oil on the unloaded side of piston

zero. The fact that, in actual operation, the film breaks down and the friction increases long before the viscosity becomes zero must be recognized. However, complete film lubrication is believed to obtain over a wide range of viscosities and, from measurements of friction within this range, it is possible to plot a curve showing the relation between viscosity and friction. It seems a justifiable assumption to project this curve back to zero viscosity. This has been done in Figures 30 and 31, although measurements were not made for a sufficient number of viscosities to make the exact location of the curves definite. It is believed, however, that the intersection of the curves with the line of zero viscosity is an approximate measure at least of the friction of the engine minus the friction of pistons and rings. It is not the actual friction value which is of particular interest in connection with these curves but the fact that at a given speed nearly the same friction was obtained at zero viscosity with all the pistons tested both with and without rings. This suggests at least that conditions of complete film lubrication prevailed during practically all the tests.

Figure 32 has also been presented more as an illustration than because of any particular significance in the actual values of friction as plotted. The lower curve represents zero piston friction as taken from Figures 30 and 31. The curve immediately above it shows the lowest values of friction with pistons and rings obtained in this group of tests, whereas the third curve shows the highest values. These curves do not represent limiting values but merely suggest the extent to which piston and ring friction may vary. They emphasize also the importance of such further research as will make it possible to predict definitely the effect of a given change in piston design upon piston friction.

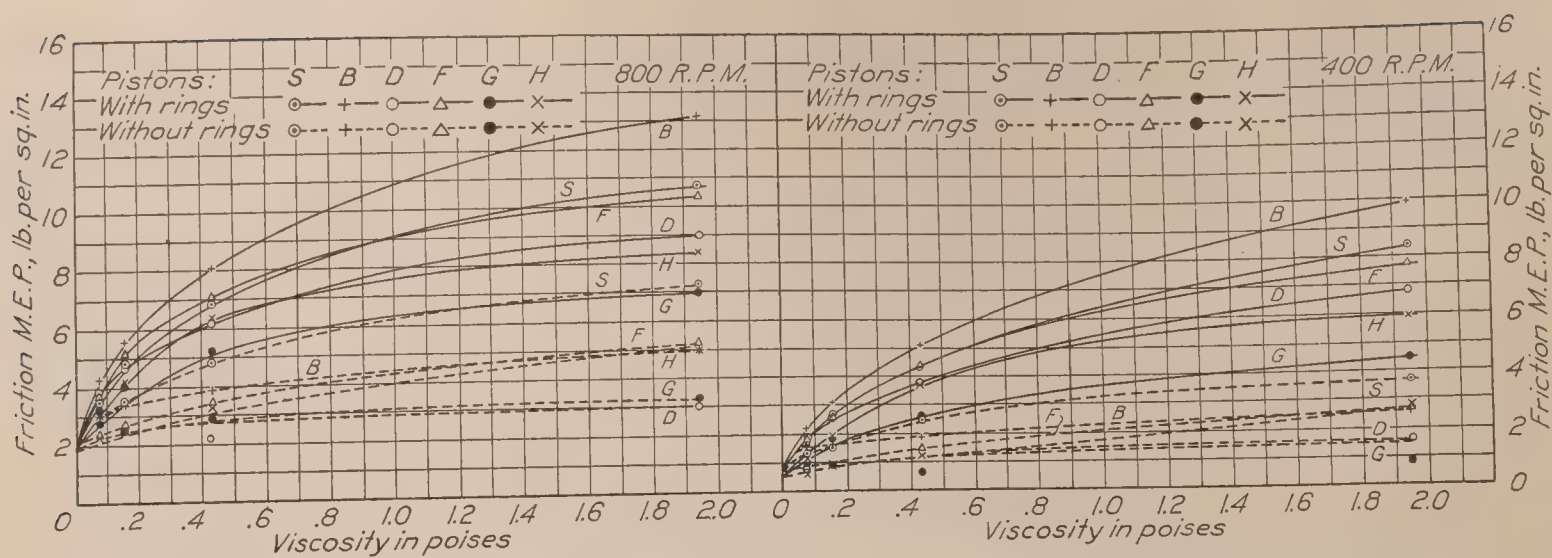


FIG. 30.—Pistons with and without rings; cylinder pressures nearly constant; ("no pumping loss"); 400 and 800 revolutions per minute

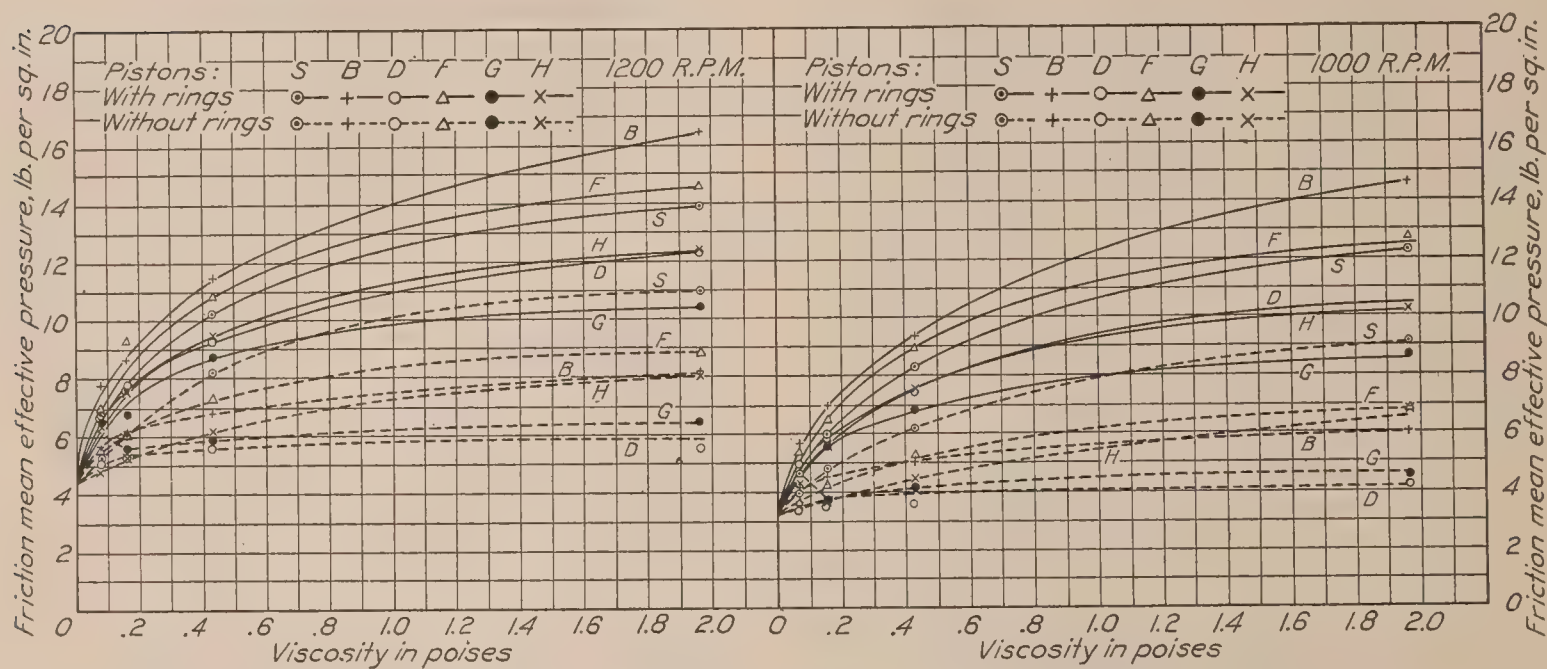


FIG. 31.—Pistons with and without rings; cylinder pressures nearly constant; ("no pumping loss"); 1,000 and 1,200 revolutions per minute

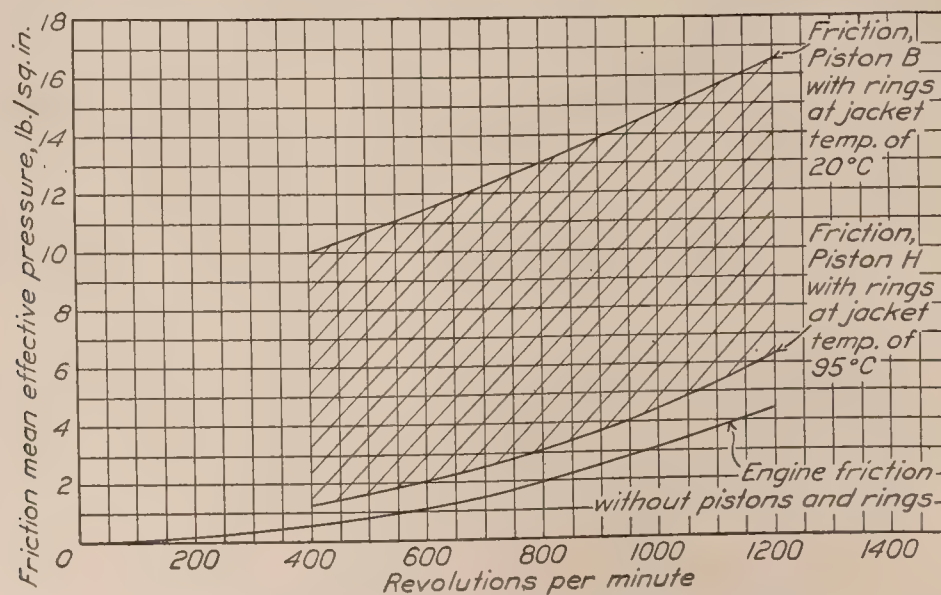


FIG. 32.—High and low values of friction of pistons and rings

CONCLUSIONS

This report has shown over a wide range of conditions the differences in friction produced by various changes in piston design. From this work the following conclusions may be drawn: (1) With pistons of the type tested, reducing the thrust face area while permitting a narrow band of bearing surface to extend completely around the base of the piston tends to increase rather than to decrease friction. (2) A reduction in rubbing surface in conjunction with the removal of the band of bearing surface completely surrounding the base is likely to reduce friction very materially. (3) Differences in the clearance between the piston and cylinder walls may have a marked effect on friction, but with the usual ring arrangement one would not expect the effect to be large. (4) It is not probable that the presence of a large number of holes in the skirt of a piston will reduce its friction to any great extent. (5) Reducing the over-all length of a piston is likely to reduce friction, but the magnitude of the change may be small even though the change in the area of rubbing surface is rather large. While these experiments covered a wide range of conditions it is entirely possible that some of these conclusions might not hold for radically different designs or conditions of operation.

One fact strikingly shown in these tests is that the friction chargeable to piston rings depends upon piston design as well as upon ring design. This is probably due to the effect of the rings upon the thickness and distribution of the oil film, which in turn affects the friction of the piston to an extent which depends upon its design.

BIBLIOGRAPHY

- SPARROW, S. W. Correcting Horsepower Measurements to a Standard Temperature. N. A. C. A. Technical Report No. 190. 1924.
- GAGE, VICTOR R. A Study of Airplane Engine Tests. N. A. C. A. Technical Report No. 46. 1920.
- GAGE, VICTOR R. Some Factors of Airplane Engine Performance. N. A. C. A. Technical Report No. 108. 1921.
- RICARDO, HARRY R. The High Speed Internal Combustion Engine. The Automobile Engineer, July, 1925.
- MOSS, H. and STERN, W. J. The Mechanical Efficiency of an Internal Combustion Engine. The Automobile Engineer, March, 1925.
- RICARDO, HARRY R. Piston Design, with Special Reference to Aluminum Pistons. The Automobile Engineer, March, 1917.
- RICARDO, HARRY R. Piston Design. The Automobile Engineer October, 1918.
- RICARDO, HARRY R. High Speed Internal Combustion Engines. The Automobile Engineer, July, 1918.
- STANTON, T. E. The Friction of Pistons and Rings. The Engineer, January 16, 1925.

REPORT No. 263

**PRELIMINARY FLIGHT TESTS
OF THE N. A. C. A. ROOTS TYPE AIRCRAFT ENGINE
SUPERCHARGER**

**By ARTHUR W. GARDINER and ELLIOTT G. REID
Langley Memorial Aeronautical Laboratory**

REPORT No. 263

PRELIMINARY FLIGHT TESTS OF THE N. A. C. A. ROOTS TYPE AIRCRAFT ENGINE SUPERCHARGER

By ARTHUR W. GARDINER and ELLIOTT G. REID

SUMMARY

An investigation of the suitability of the N. A. C. A. Roots type aircraft engine supercharger to flight-operating conditions, as determined by the effects of the use of the supercharger upon engine operation and airplane performance, is described in this report.

The supercharger has been previously described in N. A. C. A. Technical Report No. 230; the results of laboratory tests are also given there. The compressor has a displacement of 0.51 cubic foot per revolution and weighs 88 pounds.

The selection of a suitable propeller and the provision of satisfactory intake ducts and adequate engine cooling were preliminary problems. The supercharger was first tested in a modified DH-4 airplane with a 5.4 compression ratio Liberty-12 engine. Two sets of drive gears which enabled the maintenance of sea-level pressure at the carburetor intake up to 12,000 and 20,000 feet were provided. The higher gear ratio supercharger was next tested in a DT-2 landplane which was later converted into a twin-float seaplane; the DT-2 also had a Liberty engine. Loads up to 2,000 pounds were carried in the seaplane with normal and supercharged engines.

Attention was concentrated on the operation of the engine-supercharger unit and on the improvement of climbing ability; some information concerning high speeds at altitude was obtained.

The supercharger was found to be satisfactory under flight-operating conditions. Although two failures occurred during the tests, the causes of both were minor and have been eliminated. Careful examination of the engines revealed no detrimental effects which could be attributed to supercharging.

Marked improvements in climbing ability and high speeds at altitude were effected. It was also found that the load which could be carried to a given moderate or high altitude in a fixed time was considerably augmented. A slight sacrifice of low-altitude performance was necessitated, however, by the use of a fixed-pitch propeller.

From a consideration of the very satisfactory flight performance of the Roots supercharger and of its inherent advantages, it is concluded that this type is particularly attractive for use in certain classes of commercial airplanes and in a number of military types.

INTRODUCTION

The function of an aircraft engine supercharger is to prevent or reduce the diminution of power output which is experienced with engines of the conventional type as altitude is gained and the air pressure and density are correspondingly reduced. This is effected by compressing the air charge before it enters the engine cylinders.

It is known that the performance of an airplane at altitude may be improved by the addition of a supercharger to the power plant. Improvements in climbing ability and in maximum speed at altitude have the greatest practical importance. However, these practical advantages have not become generally appreciated. The mere attainment of extreme altitudes

is of little importance except under special and unusual circumstances. Moreover, the maximum altitude to which an airplane can climb is not a measure of its performance at lower altitudes. In fact, the provision of supercharger and propeller equipment suitable for flight at very high altitudes occasions a reduction of the performance at lower altitudes.

The potentialities of a special Roots type blower as an aircraft engine supercharger have been dealt with in Reference 1. The laboratory tests described therein led to the conclusion that this type of blower could be advantageously used to effect improvements in the important characteristics mentioned above because its outstanding features are high efficiency, durability, mechanical simplicity, and small power requirements at low altitudes.

This report deals with the first flight tests of the Roots type supercharger in conjunction with standard Liberty engines of 5.4 compression ratio. The purpose of the investigation was to ascertain the suitability of the supercharger to flight-operating conditions, to observe the effect of supercharging on engine operation, and to determine, in a preliminary way, what improvements in airplane performance may be effected by this means.

INSTALLATION AND PRELIMINARY TRIALS

The principal features of the experimental installation of the Roots type supercharger in conjunction with a Liberty engine are illustrated by Figure 1; the airplane is a DT-2 land-

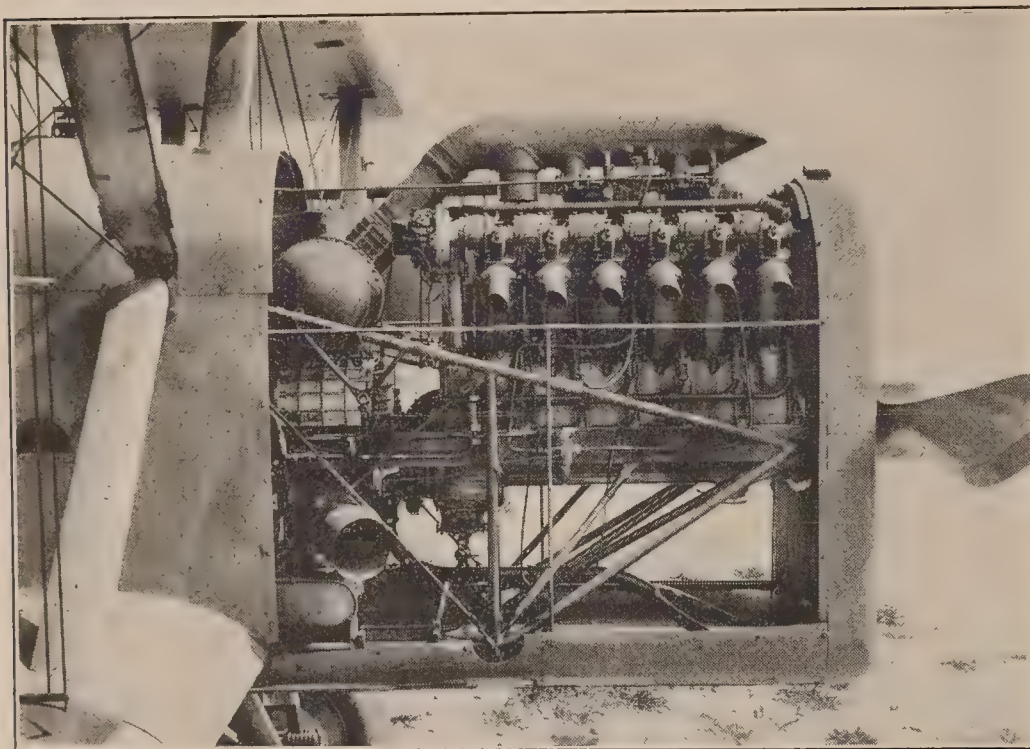


FIG. 1

plane. The supercharger is mounted on the engine bearers and is driven by the crank shaft through a flexible coupling. Below the supercharger are the intake ducts which open outside the engine cowling; directly above it is the cylindrical receiver which, though used in these tests, has been subsequently found unnecessary. There are two outlets from this receiver. One is the short open-end pipe which will be seen on the top of the receiver; a butterfly valve in this pipe is the supercharger control. The other is the duct which ex-

tends along the top of the engine and communicates with the intake passages of the carburetors (inverted Stromberg, Model NAL-5A). The pressure in this duct depends on the amount of air which is allowed to escape into the atmosphere through the by-pass valve. Attached to the underside of the duct, just behind the rear carburetor, is the auxiliary air-intake valve. This is a large spring-loaded, poppet valve which was used in the experimental work to insure continuous engine operation in the event of supercharger failure with the by-pass valve closed.

The fuel system is necessarily somewhat different from that used on unsupercharged engines. Wind-driven fuel pumps were used on both the DH-4 and DT-2 airplanes. The ordinary spring-loaded fuel pressure relief valve is replaced by a spring-loaded Sylphon valve (fig. 3.); the pressure on the fuel supplied to the carburetors is made to exceed that of the air entering the carburetors by the amount of the spring load, regardless of atmospheric pressure, by providing an air line which connects the Sylphon to the carburetor duct. The usual mixture-control mechanism, which, in the Stromberg carburetor, is a valve through which

atmospheric air is admitted to the float chamber, is replaced by a valve in a short air line of relatively large diameter which leads from the carburetor duct to the float chamber. Free flow through this line is necessary for the instantaneous balancing of pressures.

An ordinary Bourdon tube gage is used to indicate the differential fuel pressure. The Bourdon tube is connected to the fuel supply line and an air line is led from the carburetor duct to the gage case which is carefully sealed. The carburetor air pressure, or amount of supercharging, is indicated by an altimeter of the aneroid type; its ordinary atmospheric vent is connected by a tube to the carburetor duct and its case is also sealed to prevent leakage into the atmosphere. To maintain sea-level pressure at the carburetors, the pilot has but to regulate the by-pass valve until the sealed altimeter indicates zero.

A threaded rod, which could be pulled or screwed through a fitting which was anchored in the pilot's instrument board, was provided for the regulation of the supercharger by-pass valve. A hand lubricator was used to provide the necessary oil. These features are, of course, characteristic of experimental

installations only, as a combined engine throttle and by-pass control and lubrication by the engine oiling system would be incorporated in a service installation.

A complete description of the supercharger is given in Reference 1; its displacement was 0.51 cubic foot per revolution and the rotor speed was 1.5 times crank-shaft speed. The supercharger was first installed in a modified DH-4 airplane. Air was taken directly into the compressor from the engine section; no supercharger intake header was used. This arrangement was found to be unsatisfactory as the "critical altitude" (maximum altitude at which sea-level

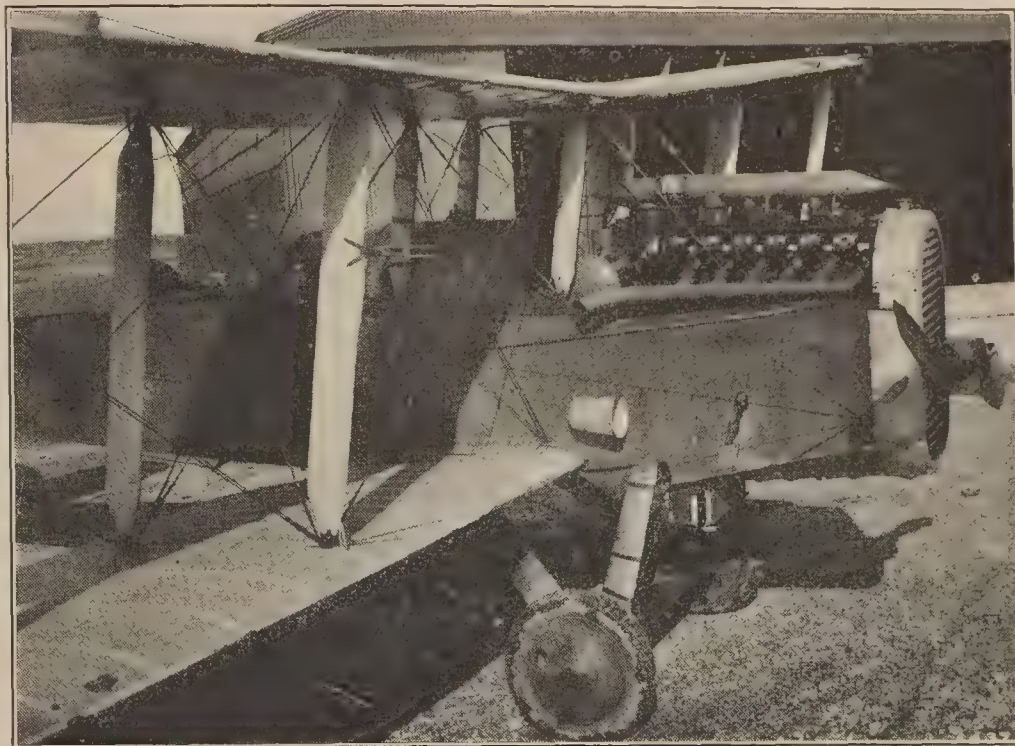


FIG. 2

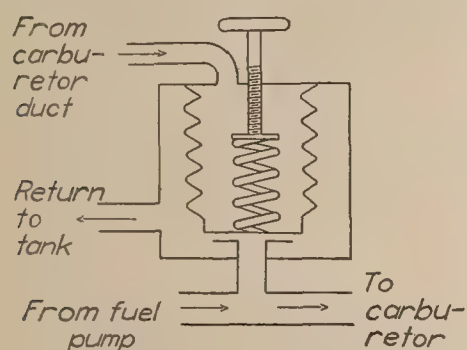


FIG. 3

pressure can be maintained at the carburetors) obtained in flight was much less than that predicted from the results of laboratory tests. Removal of the bottom cowling of the engine section produced very little improvement. Satisfactory operation was first obtained with the forward opening scoops shown in Figure 2. The ducts were later modified to the form which may be seen in Figure 1, which was also satisfactory.

The selection of a suitable propeller was the next problem encountered. Propellers designed for use on normal Liberty engines would not limit the speed of the supercharged engine to the arbitrary "maximum allowable R. P. M." with the airplane in level flight at any considerable altitude. Propellers for higher-powered engines which might have been suitable for this work were not available. A propeller designed for use on the supercharged Liberty engines of Martin bombers was obtained and found to meet the requirements reasonably well. Its pitch and diameter are 6.35 feet and 10.67 feet, respectively.

It had been anticipated that the radiator provided for the normal engine would be insufficient for the supercharged engine at high altitudes. Such was found to be the case and a booster radiator was connected in series with the nose radiator. (See fig. 2.) When, in later tests, the supercharger was fitted with a drive of higher gear ratio, thus increasing the critical

altitude, the radiation was further augmented by the substitution of a pressure-type nose radiator having a slightly deeper core than that of the normal one.

TESTS

The preparatory work on the DH-4 was followed by tests of the supercharger with two drive gear ratios, 1.5 and 1.94, in that airplane. Comparative tests were then made with a DT-2 landplane equipped with normal and supercharged engines; a 1.94 drive gear ratio supercharger was used. The work was concluded by making a series of similar comparative tests on the DT-2 seaplane with nominal useful loads up to 2,000 pounds. The 1.94 drive ratio was used for these tests, but the performance characteristics of the seaplane were such that the critical altitude of the supercharger-engine unit was attained only in the flight with no load.

The principal characteristics of the DH-4 and DT-2 airplanes are given in Appendix I. Incidental information including weights, propellers used, etc., is also given.

Attention was concentrated on the climbing characteristics of the airplanes throughout this work. Determinations of maximum speed were made only in the case of the DH-4 with the 1.5 ratio supercharger. In all landplane tests, the climbs were carried above the critical altitude of the supercharger but only a few were extended far toward the absolute ceilings of the airplanes because of the small importance of this particular characteristic.

Continuous climbs were made rather than resorting to the "saw-tooth" method, which is frequently used in determining the climbing characteristics of an airplane. The former method was adopted in order that the results might be representative of service operating conditions, rather than ideal ones which can not be duplicated in service, and to demonstrate the adequacy of the engine-cooling system under the most severe conditions to be met in service. This demonstration is not conclusive if the saw-tooth method is used because the duration of engine operation at maximum output is very short and there is a considerable lag between the variations of engine output and cooling-water temperature.

Considerable information relating to the conditions of engine operation and the data required for the reduction of the performance to standard atmospheric conditions were obtained.

RESULTS

The supercharger was found to be mechanically satisfactory under flight operating conditions. Smooth engine operation was obtained with all degrees of supercharging.

No indication was found that the use of this type of supercharger is more injurious to the engine than is full throttle, unsupercharged operation near sea level. Valves, spark plugs, and pistons were in as good condition as would be expected after an equal period of full throttle operation of the normal engine at low altitude.

The results of the flight tests are presented in graphical form in Figures 4 to 9. Lesley's method (Reference 2) was used for the reduction of the flight data to the conditions of the standard atmosphere.

DISCUSSION

The curves of Figures 4, 5, and 7 picture the conditions under which the supercharged engine operates. A few general comments relative to the curves themselves are inserted to preface the discussion of this information.

It may be noted that the curve of carburetor air pressure in Figure 4 has fewer irregularities than those of Figures 5 and 7; this difference is the result of less frequent observations having been made in first tests than in the later ones during which recording instruments were carried in place of an observer. The curve of carburetor air temperature is omitted from Figure 4 because it was discovered, some time after completion of the tests, that the thermometer readings were erroneous. Erratic behavior of the strut thermometer at low temperatures gave rise to the double curves of Figure 5. It was found that the readings of this thermometer were unreliable below -22° F. The continuous curve of atmospheric temperature passes through

the observed points; the broken curve is extended, from the last reliable point, parallel to the curve of temperature versus altitude for the standard atmosphere. The other curves of this figure have been correspondingly modified and are shown as broken lines.

Upon inspection of the carburetor air-pressure curves of Figures 4, 5, and 7, it may be seen that sea-level pressure is approximately maintained up to considerable altitudes and that

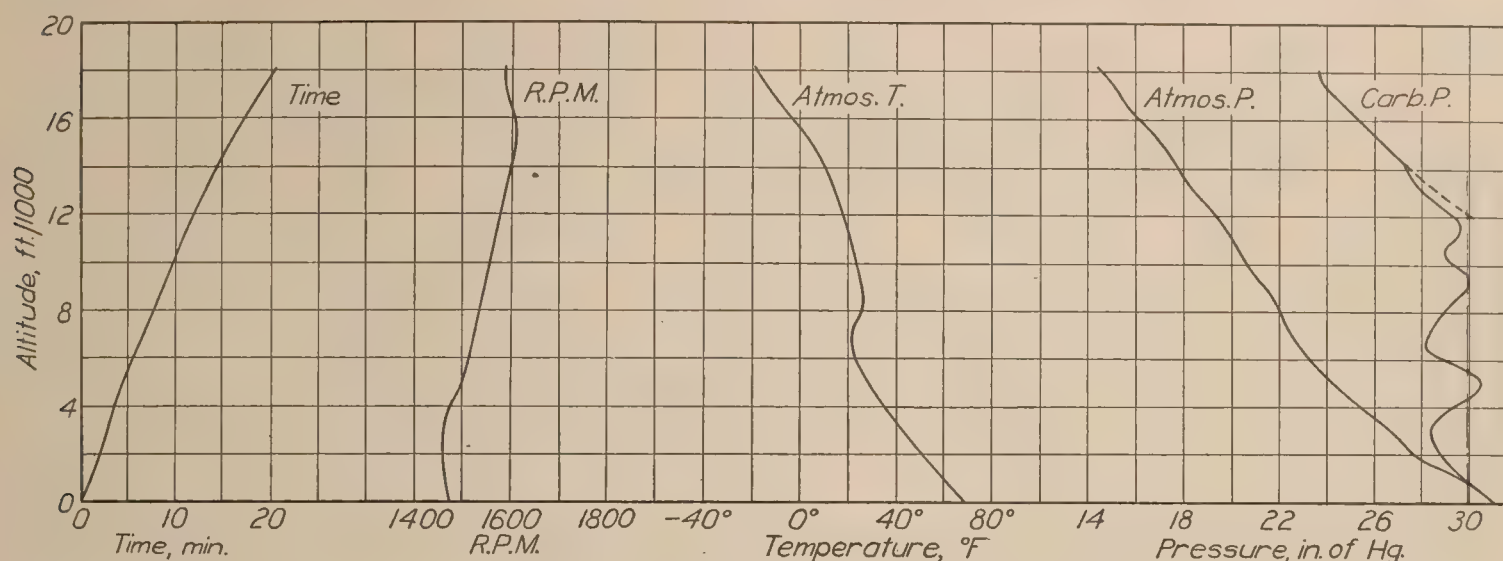


FIG. 4.—DH-4 with 1.5 gear ratio supercharger

beyond the point at which this is possible the pressure at the carburetor stays well above atmospheric pressure. The intersection of the sloping upper branch of the curve, which represents operation with the supercharger by-pass valve completely closed, with the sea-level pressure line defines the critical altitude of the engine-supercharger unit. The effect of changing the drive gear ratio of the supercharger is evident in the difference between the critical altitudes shown in Figures 4 and 5.

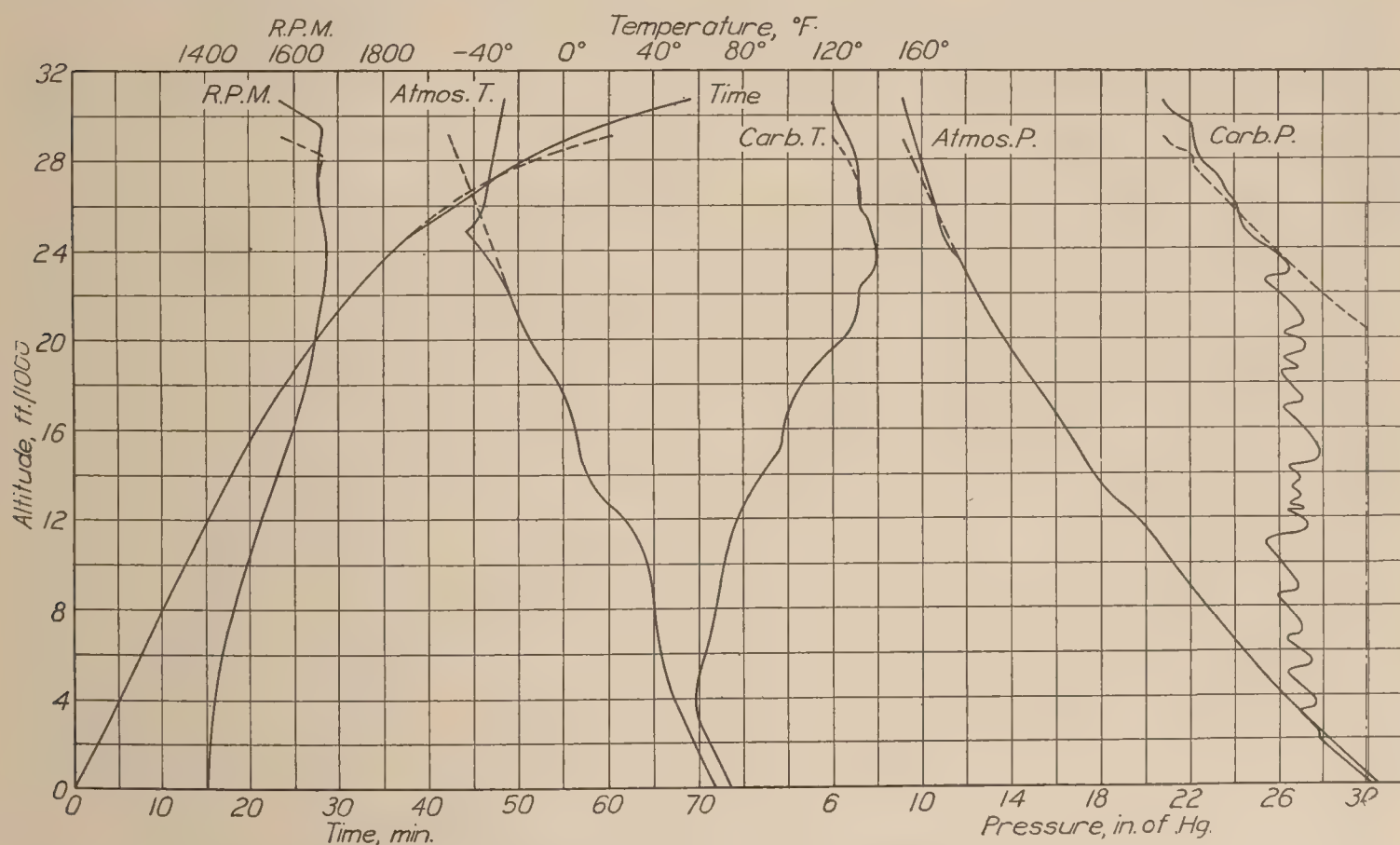


FIG. 5.—DH-4 with 1.94 gear ratio supercharger

The carburetor air temperatures (figs. 5 and 7) are of particular interest from the standpoint of engine operation. These temperatures differ very little from the atmospheric temperatures at low altitudes. This condition is a result of using the by-pass method of control as, at the low altitudes, there is very little compression of the air passing through the supercharger.

At higher altitudes the carburetor air temperatures increase with the amount of compression and reach a maximum near the critical altitude, but do not reach excessive values because of the low atmospheric temperatures. Knowledge of this fact prompted the very desirable omission of the usual air intercooler from the experimental installations, thus saving considerable weight and parasite resistance. However, the temperatures at the carburetors are abnormal at high

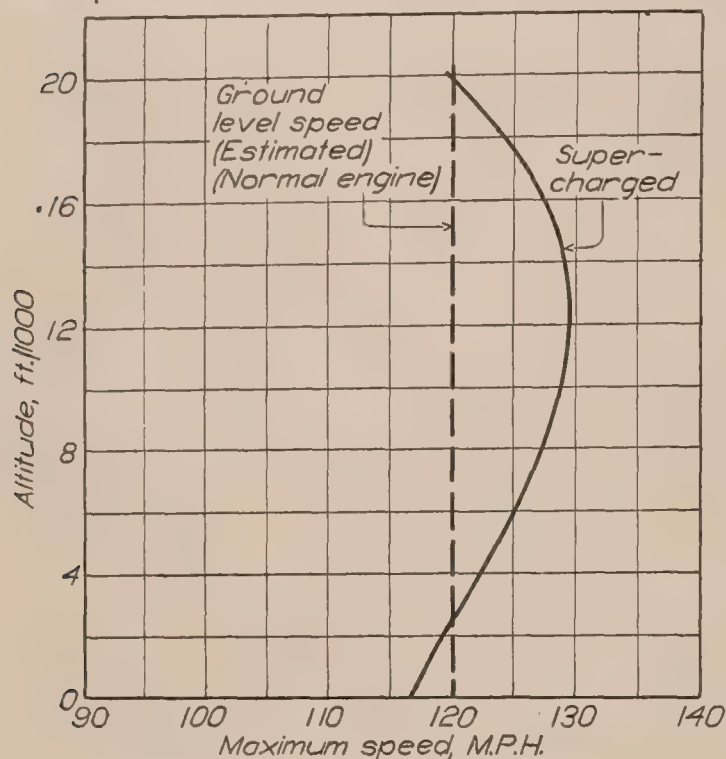


FIG. 6.—DH-4 with 1.5 gear ratio supercharger

altitudes and, to combat the increased tendency for detonation under this condition, a 30-70 benzol-gasoline blend was used as fuel during the tests made with the DH-4. Plain domestic aviation gasoline was used in the DT-2 tests, but no unusual detonation was encountered. It has been found in subsequent laboratory tests that the normal Liberty engine suffers a loss of power which is caused by detonation even at ordinary inlet temperatures when straight gasoline is used as fuel. However, as inlet temperatures increase, the ratio of the power obtained with gasoline to that obtained with the 30-70 benzol-gasoline blend remains practically constant. From these results, it appears that the Roots supercharger with a critical altitude of at least 20,000 feet may be satisfactorily used without an air intercooler and without resorting to the use of special fuels.

It had been anticipated that this type of supercharger would be unusually free from mechanical troubles in flight. However, as an extra precaution, the clearances between rotors, and between rotors and case, were enlarged from the average value of 0.006 inch which existed during laboratory tests to 0.009 inch before flight tests were begun. Two failures occurred in flight; the causes of both were easily eliminated. The first failure was caused by seizure of the rotors against one end of the case which resulted from the use of a brass part in the assembly

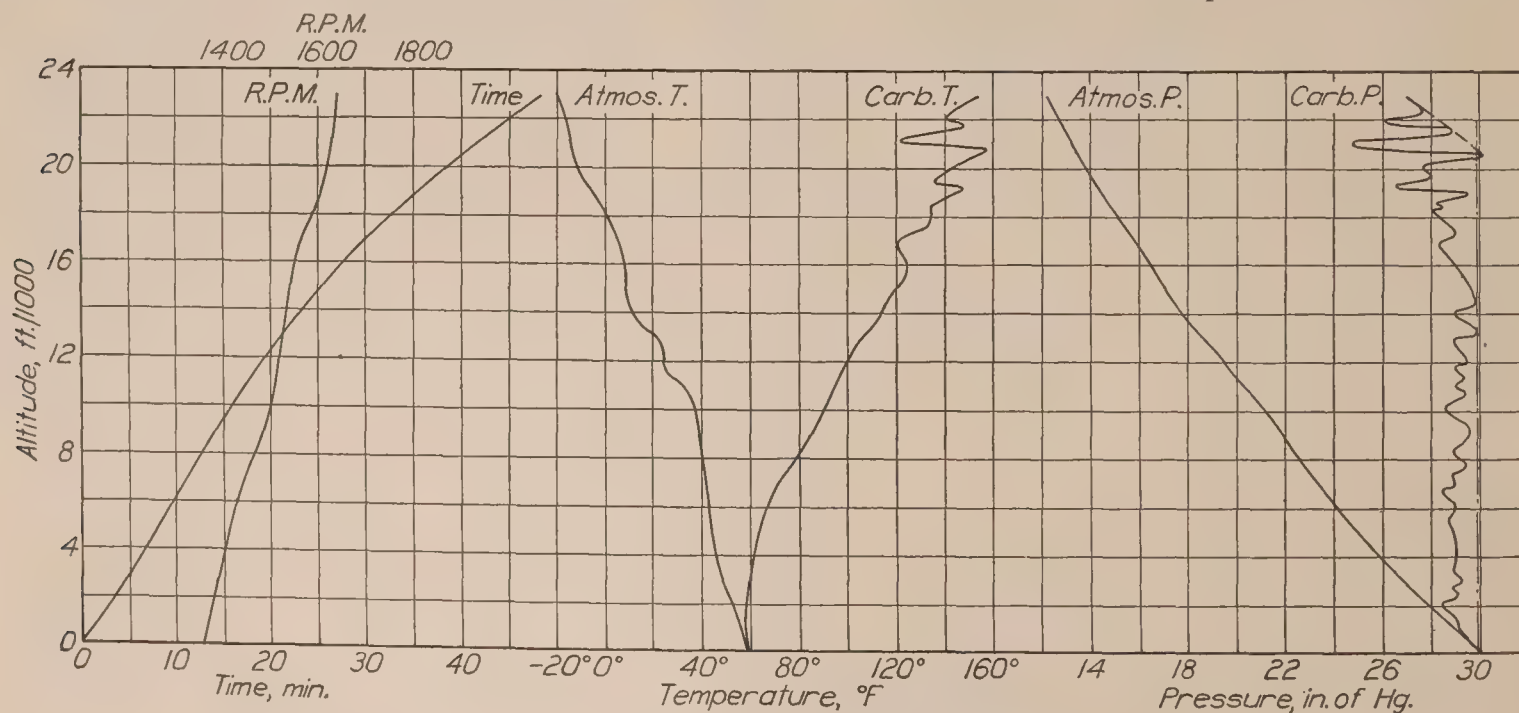


FIG. 7.—DT-2 landplane with 1.94 gear ratio supercharger

used for maintaining endwise location of the rotors. This part has been replaced by a similar one of hardened steel. The second failure was brought about by improper operation; the engine was partially throttled while the supercharger by-pass valve was closed. This gave rise to very high pressures and excessive heating in the system and consequent damage to the supercharger. A combined engine throttle and by-pass valve control which makes it impos-

sible to throttle the engine while supercharging has been found satisfactory. This system of control would be suitable for service operation.

With the incorporation of this form of control and the maintenance of proper compression chamber clearances, the Roots type supercharger should have greater durability than that of any existing aircraft engine, because the only wearing parts are moderately loaded gears and ball bearings.

Some representative examples of the improvements of airplane performance which are made possible by the use of the supercharger are illustrated by Figures 6, 8, and 9.

Let us consider the time required to reach given altitudes and the rates of climb at various heights. In the case of the DT-2 landplane without useful load (fig. 8), the use of the supercharger results in reducing the time required to reach altitudes in excess of 9,000 feet, but for lower altitudes the time required with the supercharged engine is slightly greater.

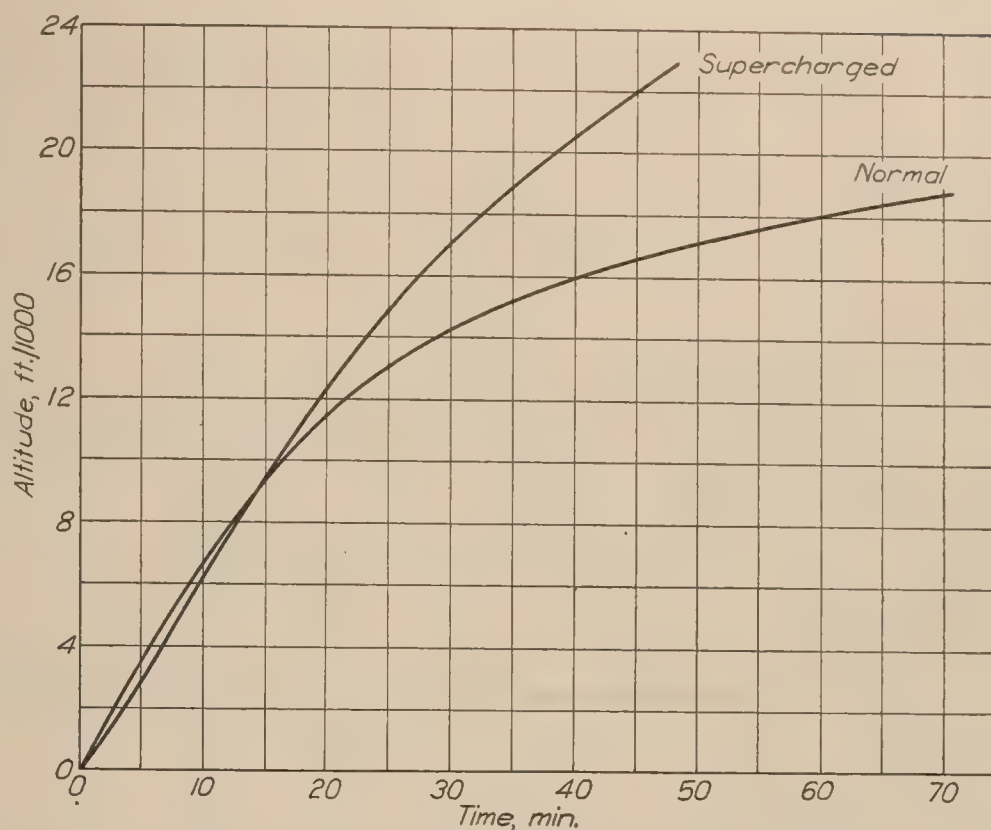


FIG. 8.—DT-2 landplane—normal and supercharged (1.94 gear ratio) engines

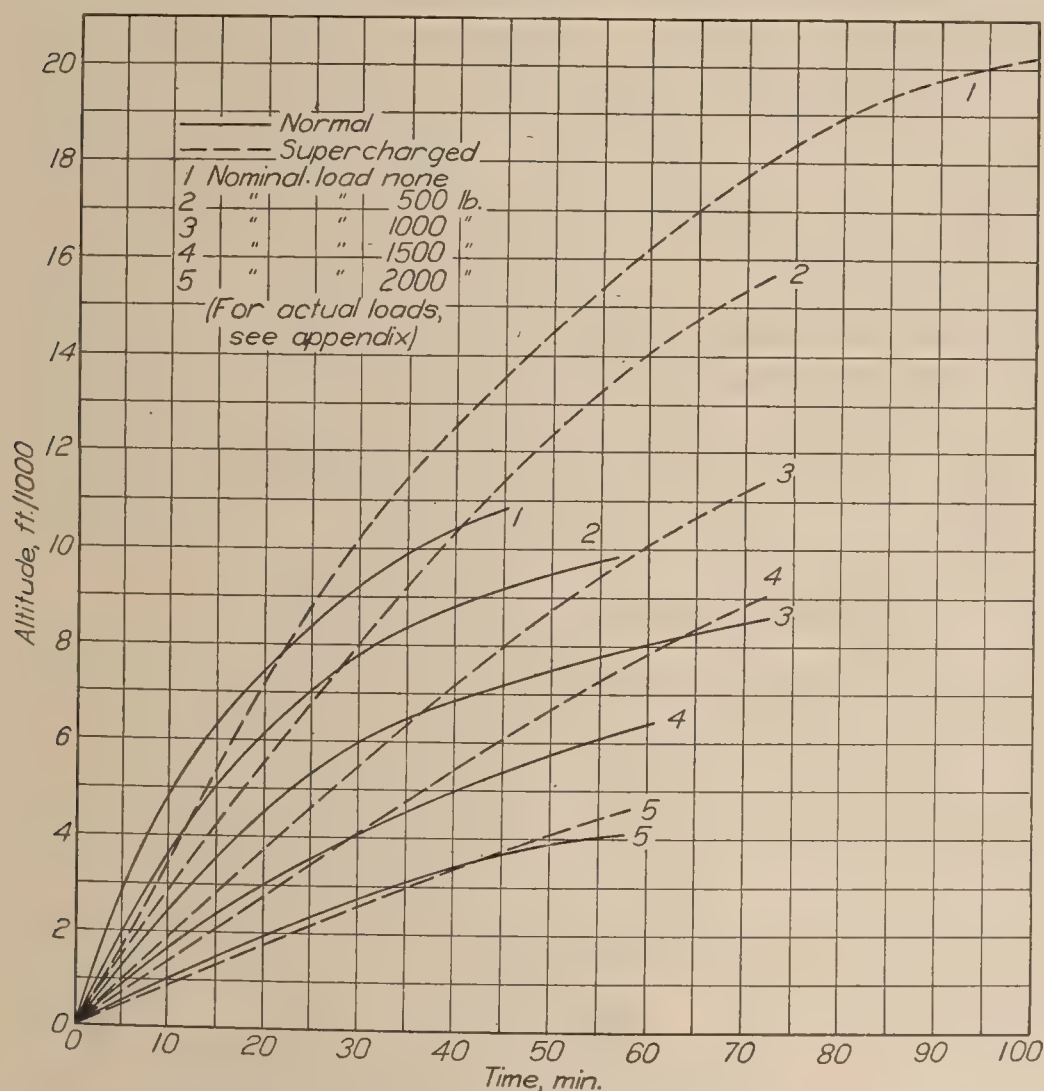


FIG. 9.—DT-2 seaplane—normal and supercharged (1.94 gear ratio) engines

At this point attention is called to the fact that the initial inferiority of the supercharged engine is also evident, although to a smaller degree, in both rates of climb and maximum horizontal speeds. (See fig. 6.) This is the result of having to fit the supercharged engine with a propeller which will limit the engine speed in level flight at high altitudes to the arbitrary "maximum allowable R. P. M." stipulated for the unsupercharged engine. Consequently, at low altitudes, the engine speed and power output are limited to relatively low values by the heavy propeller load. (Note the maximum values of R. P. M. in Figures 4, 5, and 7.)

Returning to the consideration of the DT-2 time-altitude curves, it is interest-

ing to see that the initial inferiority of the supercharged engine disappears at about 3,500 feet altitude. That is to say, as the curves are parallel at that height, the rates of climb are the same with both types of engine. Above that altitude, the advantage of supercharging increases. As a rather extreme example, the normal DT-2 climbs to 18,000 feet in 59.5 minutes while with the supercharged engine it reaches the same altitude in 32.5 minutes; the time is reduced by 45 per cent. For the climb from 5,000 to 15,000 feet, the reduction is from 26.5 to 17.1 minutes, or 35 per cent. Corresponding figures for 10,000 to 18,000 feet are 43.1 and 16.7 minutes, a reduction of 61 per cent.

It has been mentioned above that in the case of the DT-2 landplane with no useful load, improved rates of climb are obtained above 3,500 feet altitude by using the supercharged engine. By comparing the slopes of the curves of Figure 8, it is found that equal rates of climb are obtained at 5,000 and 10,000 feet with normal and supercharged engines, respectively. Extending the comparison to higher altitudes, it will be seen that supercharging makes it possible for the DT-2 to climb as rapidly at 23,000 feet as it can at 13,000 feet with the normal engine.

The consideration of the time required to reach given altitudes is also of particular interest in the case of an airplane carrying a considerable useful load. The curves of Figure 9 are illustrative of the advantages of supercharging in this case. Let us compare the time-altitude curves corresponding to a nominal useful load of 1,000 pounds. With the normal engine, one hour is required for the climb to 8,000 feet, whereas only 45 minutes are required when the engine is supercharged. With the normal engine, a rate of climb of 100 feet per minute can not be maintained above 6,300 feet altitude, while the corresponding limit with the supercharged engine was 11,500 feet. Attention is also called to the fact that the time-altitude curves corresponding to nominal useful loads of 500 and 1,000 pounds with the normal and supercharged engines, respectively, intersect at about 10,000 feet altitude.

One of the most important assets of the airplane having a supercharged power plant is its ability to maintain, at high altitudes, speeds in excess of the maximum attainable at ground level without the supercharger. This characteristic is illustrated by Figure 6, which refers to the DH-4 landplane fitted with the 1.5 gear ratio supercharger. The highest speed is attained at 12,000 feet, which is approximately the critical altitude. Accurate determinations of maximum horizontal speed were not made while this airplane was fitted with the supercharger of larger capacity but, from the few observations made, it is believed that 140 M. P. H. could be attained at the critical altitude of the 1.94 gear ratio supercharger, or approximately 20,000 feet. The estimated sea level maximum speed shown in Figure 6 for the unsupercharged DH-4 is believed to be slightly optimistic as it is considerably higher than the best value obtained with the airplane used in these tests; it should be mentioned though that a somewhat unsuitable propeller, the Liberty "club," was used for this test. The estimated speed was selected as a compromise between the speed actually obtained and that determined with a DH-4 Corps observation airplane at McCook Field.

ADVANTAGES AND LIMITATIONS OF ROOTS TYPE SUPERCHARGER

The preceding discussion has been limited to the suitability of the Roots type supercharger to flight-operating conditions and the effects of its use on engine operation and on the performance of representative airplanes. It seems advisable before drawing any general conclusions relative to the merits of the type, to set forth the advantages and limitations inherent in its application. The following questions are pertinent and will be discussed in the order stated below:

How will the reliability and durability of a normal airplane engine be affected by the addition of a supercharger of this type?

How much weight will be added?

How much power will be required to drive the supercharger at various altitudes?

Can the engine be operated with or without supercharging at the will of the pilot and, if so, to what extent is the normal operation complicated by the presence of the supercharger?

Is it necessary to build entirely different superchargers to meet different operating conditions or for engines of different displacements operating under like conditions?

How complicated is the control of the supercharged engine?

To what extent must the aerodynamic characteristics of the airplane be modified to accommodate the supercharger?

How is airplane performance improved or impaired by the use of the supercharger?

RELIABILITY AND DURABILITY

A positive drive through a system of amply proportioned parts is provided for the supercharger. A simple fabric coupling gives satisfactory protection against possible damage by angular accelerations. As the only wearing parts are moderately loaded gears and ball bearings, pure mechanical failure within a life equal to that of an airplane engine is improbable in a Roots type supercharger having adequate compression chamber clearances. Maltreatment of the supercharger can be prevented and possible failure averted by the use of the combined throttle and by-pass control. It appears that the reliability and durability of a present-day airplane engine when equipped with a properly designed Roots type supercharger will be in no way inferior to those of the same engine under the conditions of unsupercharged, full load operation.

WEIGHT

The compressor unit which was used in the present tests weighed 88 pounds. The total weight chargeable to the supercharger installation in the DH-4, exclusive of the weight of the added radiator, was 185 pounds. This figure includes the weights of the supercharger complete with intake pipes, receiver, ducts, and drive coupling, and of all attachment fixtures. In the case of the DT-2, the total weight of the supercharger installation was reduced to 166 pounds; no additional radiator had to be provided, as removal of the top engine cowling gave sufficient cooling. (The figures given in Appendix I indicate a difference of 191 pounds between the normal and supercharged engine weights. This apparent discrepancy was brought about by the substitution of instruments for an observer and the addition of oxygen equipment.) It must be considered that these weights represent the weights added in experimental adaptations to normal power plants. It is conservatively estimated that a 400-horsepower V-type engine can be fitted with a Roots type supercharger giving a critical altitude of at least 20,000 feet without adding more than 110 pounds plus the weight of the addition to the engine cooling system that may be required. Further reductions could be obtained in a power plant designed to incorporate the supercharger as an integral part. While the value 110 pounds, or 0.275 pound per horsepower, may seem somewhat excessive, the values of weight per horsepower with and without supercharging, at 20,000 feet altitude illustrate the advantage of the supercharged engine. Consider a 400-horsepower engine which weighs 600 pounds dry. At 20,000 feet it will develop not more than 200-horsepower; the weight per horsepower is 3 pounds. When supercharged, the engine will develop its full 400-horsepower at 20,000 feet, and the weight per horsepower becomes 1.775 pounds. For larger V-type engines, the value 0.275 pound per horsepower can be improved, while for radial engines the supercharger installation will weigh less than that for a V-type of the same power.

POWER REQUIRED

The power required to drive either the 1.5 or the 1.94 gear ratio supercharger at sea level is less than 5 horsepower; at the critical altitudes of 12,000 and 20,000 feet, the requirements are 33 and 60 horsepower. Between these points, the power required varies linearly with the pressure difference across the supercharger. Above the critical altitude the supercharger will operate at an approximately constant pressure ratio. The pressure difference across the supercharger will therefore decrease as altitude increases and the power required will decrease with the pressure difference.

FLEXIBILITY

The supercharger can be made inoperative as such and its power requirement reduced to practically that of friction alone at any time in flight; the engine will continue to operate as it would without a supercharger. No complicated manipulation of controls is involved; the supercharger bypass valve has merely to be opened.

ADAPTABILITY

A single Roots type supercharger may be adapted to various conditions of operation, i. e., to supercharge a given engine to various critical altitudes or to supercharge engines of various displacements to the same critical altitude, by merely changing the drive gear ratio.

CONTROL

The supercharger has but one control—a by-pass valve on the delivery side. The combined form of control which has been designed for service installations is a linkage by which the forward movement of a lever successively opens the carburetor throttle and closes the supercharger by-pass valve. In operating the control, to which the engine responds instantly, the pilot refers to a sealed altimeter which indicates the altitude corresponding to the pressure of the air entering the carburetor. This altimeter serves principally as a danger signal; any throttle setting which does not give rise to a subsea level pressure is permissible.

AERODYNAMICS

As a suitable supercharger delivery duct can be inclosed, in most cases, within the normal engine cowling, the use of a supercharger involves only two questions of aerodynamics. The first and least important one is that of engine cooling. It is necessary to provide more cooling capacity for the supercharged water-cooled engine than is necessary for the normal one. The amount of this excess varies with the critical altitude of the engine-supercharger unit, but is rather small in any case. If the critical altitude is 20,000 feet, it will be necessary to augment the cooling capacity by approximately 10 per cent. This is not a serious item when the drag of the entire airplane is considered. The use of a retractable radiator for at least part of the cooling is suggested.

The most serious limitation of the usefulness of the supercharged power plant is imposed by the use of a propeller suitable for high altitude level flight. A small sacrifice of performance at low altitudes is unavoidable so long as propellers of fixed pitch must be used, unless it is permissible to overspeed the engine in level flight at high altitudes, i. e., to increase the engine speed above the "maximum allowable R. P. M." fixed for normal operation.

AIRPLANE PERFORMANCE

It has been demonstrated in the tests which are described above that the use of the Roots type supercharger materially improves the rates of climb of an airplane with a given engine and brings about marked reductions of the time required to reach high altitudes. It enables the attainment of higher speeds, throughout a considerable range of altitudes, than are possible with the unsupercharged power plant at any altitude and also augments the useful load which may be carried to a given altitude in a fixed time.

The price of these advantages is a small sacrifice of low-altitude performance, but this is far outweighed by the gains realized. It must be added that if an airplane is so heavily loaded that its ceiling is relatively low even when the engine is supercharged, the relative advantage of supercharging decreases. The effect of supercharging the engine of a given airplane upon the radius of action at altitude has not been investigated as yet but it is expected that the overdimensioned engines with supercompression will find their greatest usefulness and probably be somewhat superior to supercharged engines at moderate altitudes because of their characteristic economy.

CONCLUSIONS

The N. A. C. A. Roots type supercharger for aircraft engines is satisfactory under flight operating conditions and its use enables the realization of greatly improved climbing performance and the attainment of speeds in excess of the normal sea level maximum throughout a considerable range of altitudes. A slight sacrifice of low-altitude performance results from the use of a fixed pitch propeller suitable for high-altitude flight.

This supercharging equipment, as compared with other types, is efficient, simple, and durable; it is readily adaptable to diversified operating conditions, and may be successfully used without an air intercooler and, for moderate amounts of supercharging, without resorting to special fuels; it effects its purpose with a minimum of harm to the engine.

The advantages of this type of supercharger make it particularly attractive for use in certain classes of commercial airplanes and in a number of military types.

LANGLEY MEMORIAL AERONAUTICAL LABORATORY,
NATIONAL ADVISORY COMMITTEE FOR AERONAUTICS,
LANGLEY FIELD, VA., *December 29, 1926.*

APPENDIX I

DH-4 AIRPLANE

This airplane has been termed the DH-4 throughout the report because it is not a standard DH-4B Corps Observation airplane although it resembles the latter more than it does the original DH-4. The wing cellule, tail surfaces, and landing gear are those of the DH-4B except in the detail of wheels and tires; these were of the small size used on the DH-4. The fuselage is externally that of a DH-4B except that the pilot and observer are seated in a single long cockpit; the inside arrangement is slightly different because the engine compartment had to be lengthened to accommodate the supercharger. However, the resulting position of the center of gravity was such that satisfactory longitudinal balance was obtained by small changes of rigging and adjustment of the horizontal stabilizer.

The principal characteristics of the airplane are:

Span (both wings)	42.46 feet
Chord (both wings)	5.5 feet
Gap	5.5 feet
Stagger	1 foot
Dihedral (both wings)	3 degrees
Total wing area	440 square feet
Engine, Liberty-12, 420 horsepower at	1,700 R. P. M.
Flying weight with supercharger	3,960 pounds.
Propeller	Martin Bomber (Supercharger).
Air Service Part No. 065323.	
Diameter	10.67 feet
Pitch	6.35 feet

DT-2 LANDPLANE

This is a service type airplane. The only changes which had to be made were lengthening of the engine compartment and extending the engine bearers. The principal characteristics are:

Span (both wings)	50.0 feet.
Chord (both wings)	7.5 feet.
Gap (at center)	8.5 feet.
Stagger	None.
Dihedral (lower only)	2 degrees.
Total wing area	707 square feet.
Engine, Liberty-12, 420 horsepower at	1,700 R. P. M.
Flying weight—normal	5,020 pounds.
Flying weight—supercharged	5,211 pounds.
Propeller—normal—DT-2:	
Navy Drawing No. X-4987.	
Diameter	10 feet.
Pitch	5.13 feet.
Propeller—supercharged. Same as for DH-4.	

DT-2 SEAPLANE

Same airplane as above with landing gear replaced by twin floats. The total flying weights and the useful loads carried were:

Nominal useful load	Actual disposal load carried ¹		Gross weight	
	Normal	Super-charged	Normal	Super-charged
	<i>Pounds</i>	<i>Pounds</i>	<i>Pounds</i>	<i>Pounds</i>
None.....	234	203	6,021	6,159
500 pounds.....	609	601	6,396	6,557
1,000 pounds.....	1,109	1,101	6,896	7,057
1,500 pounds.....	1,609	1,601	7,396	7,557
2,000 pounds.....	2,109	2,101	7,896	8,057

¹ Disposal load is obtained by subtracting the weight of the airplane with fuel, oil, water, and pilot (and supercharging equipment when used) from the gross weight.

For these tests the long-distance cruising type fuel tank, which is similar to a torpedo in shape and size, was slung in the torpedo tunnel in the underside of the fuselage. Water loads were carried in this tank.

The standard DT-2 propeller (X-4987) was used for all flights with the normal engine. The supercharged engine was equipped with a Martin bomber supercharger propeller (065323) which had been cut down to 10.33 feet diameter for the flight with zero nominal useful load. A plain Martin bomber propeller (Air Service part No. 047815, diameter 10.33 feet, pitch 5.74 feet) was used in the other load tests.

BIBLIOGRAPHY

- REFERENCE 1. WARE, MARSDEN. Description and Laboratory Tests of a Roots Type Aircraft Engine Supercharger. N. A. C. A. Technical Report No. 230, 1925.
- REFERENCE 2. DIEHL, WALTER S., and LESLEY, E. P. The Reduction of Airplane Flight Test Data to Standard Atmosphere Conditions. N. A. C. A. Technical Report No. 216, 1925.
- GARDINER, ARTHUR W. A Roots Type Aircraft Engine Supercharger. Journal of the Society of Automotive Engineers, September, 1926.

REPORT No. 264

DIFFERENTIAL PRESSURES ON A PITOT-VENTURI AND A PITOT-STATIC NOZZLE OVER 360° PITCH AND YAW

By R. M. BEAR

**Aerodynamical Laboratory, Bureau of
Construction and Repair, U. S. Navy**

REPORT No. 264

DIFFERENTIAL PRESSURES ON A PITOT-VENTURI AND A PITOT-STATIC NOZZLE OVER 360° PITCH AND YAW

By R. M. BEAR

SUMMARY

Measurements of the differential pressures on two Navy air-speed nozzles, consisting of a Zahm type Pitot-Venturi tube and a SQ-16 two-pronged Pitot-static tube, in a tunnel air stream of fixed speed at various angles of pitch and yaw between 0° and $\pm 180^\circ$, show for a range over -20° to $+20^\circ$ pitch and yaw, indicated air speeds varying very slightly over 2 per cent for the Zahm type and a maximum of about 5 per cent for the SQ-16 type from the calibrated speed at 0°.

For both types of air-speed nozzle the indicated air speed increases slightly as the tubes are pitched or yawed several degrees from their normal 0° attitude, attains a maximum around $\pm 15^\circ$ to 25° , declines rapidly therefrom as $\pm 40^\circ$ is passed, to zero in the vicinity of $\pm 70^\circ$ to 100° , and thence fluctuates irregularly from thereabouts to $\pm 180^\circ$. The complete variation in indicated air speed for the two tubes over 360° pitch and yaw is graphically portrayed in Figures 9 and 10.

For the same air speed and 0° pitch and yaw the differential pressure of the Zahm type Pitot-Venturi nozzle is about seven times that of the SQ-16 type two-pronged Pitot-static nozzle.

INTRODUCTION

The data presented in this report were obtained in tests made for the Navy Bureau of Aeronautics at different times on a Zahm type and a SQ-16 type of air-speed nozzle in the 4 by 4 foot wind tunnel of the Bureau of Construction and Repair, Washington Navy Yard.

The present text and figures, submitted for publication to the National Advisory Committee for Aeronautics, November 29, 1926, have been compiled with some revision from C. & R. Aeronautical Reports Nos. 295 and 300 prepared by the aeronautics staff for the Bureau of Aeronautics.

Other N. A. C. A. reports on air-speed nozzles are Nos. 31, 110, 127, and 156. (References 1-4.)

DESCRIPTION OF NOZZLES

Photographs of the Zahm and SQ-16 air-speed nozzles mounted in the tunnel for testing constitute Figures 1, 2, 3, and 4, and drawings of the two nozzles with their chief dimensions are presented in Figures 5 and 6.

The Zahm Pitot-Venturi nozzles are manufactured by the American Instrument Company, of Washington, D. C.; the SQ-16 two-pronged Pitot-static nozzles, by the Pioneer Instrument Company, of Brooklyn, N. Y.

The two sample nozzles tested were stamped with the factory serial Nos. 1041 and 066239, respectively.

The Venturi of the Zahm type nozzle is made and assembled in three parts; namely, a short forward cone, a long trailing cone with spun trumpet flare, and an accurately reamed short cylinder connecting the two cones and forming the Venturi throat. The small boss visible

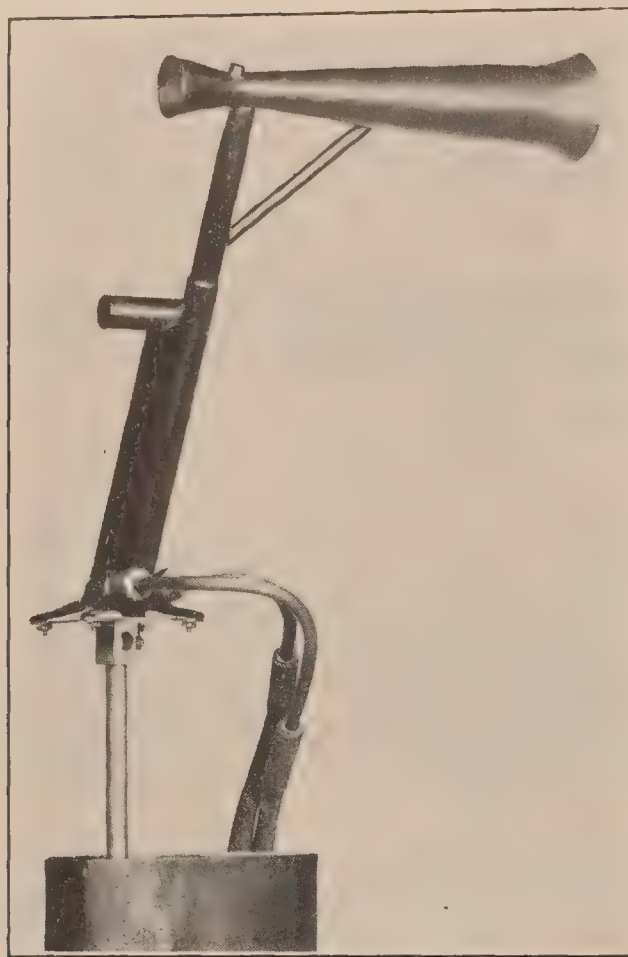


FIG. 1.—Zahm nozzle. Pitch mounting

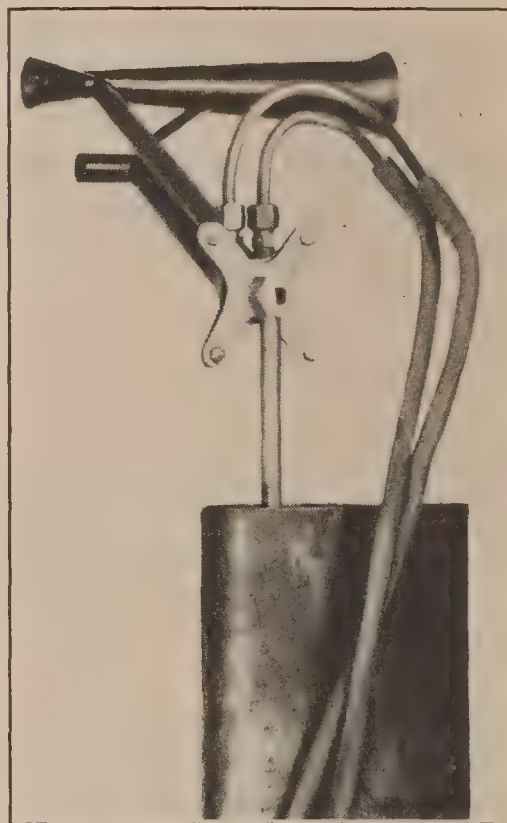


FIG. 2.—Zahm nozzle. Yaw mounting



FIG. 3.—SQ-16 nozzle. Pitch mounting



FIG. 4.—SQ-16 nozzle. Yaw mounting

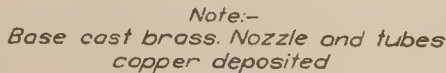


FIG. 5.—Navy-Zahm.—Pitot-Venturi nozzle



FIG. 6.—Navy SQ-16. Pitot-static nozzle

in Figure 1 on the throat section opposite the Venturi duct, holds a standard 6-32 brass screw (fig. 5), which projects into the Venturi throat in the form of a 60° cone, slightly but uniformly truncated. By a slight adjustment of this screw in each of a given lot of nozzles it is possible to compensate for small factory variations in cone and throat dimensions causing variable differential pressures for the nozzles at the same air speed, and thus bring all into conformity with a standard calibration.

As seen from the illustrations of Figures 3 and 4, the SQ-16 Pitot-static nozzle differs essentially from an ordinary Pitot-static tube only in being shorter and having static and impact openings on separate prongs.

METHOD OF TESTS

In order that the nozzles could be rotated in both pitch and yaw on the vertical shaft of the wind tunnel balance, thereby facilitating accurate incidence setting, each of the two types was mounted on a small metal block, in which two three-eighths inch holes were drilled with axes at right angles to each other and to the nozzle axis. Thus fitted, the nozzle was mounted in the tunnel for testing on the end of a three-eighths-inch drill rod clamped in the balance-shaft chuck, as shown in Figures 1 to 4.

The nozzle incidences were set in the usual way for models, on the horizontal graduated plate encircling the balance shaft below the tunnel. All angular displacements of the nozzles were

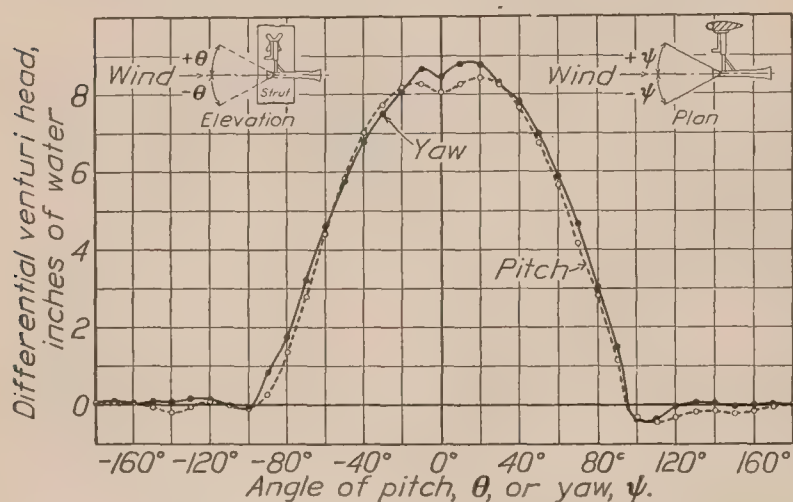


FIG. 7.—Zahm nozzle. Differential head versus angle of pitch or yaw at 50 M. P. H.

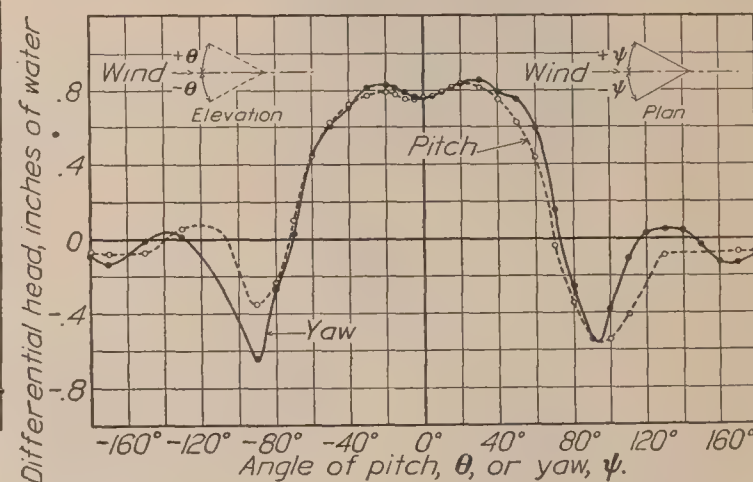


FIG. 8.—SQ-16 nozzle. Differential head versus angle of pitch or yaw at 40 M. P. H.

made in an air stream of fixed test speed, and with a sequence of incidence settings progressing from 0° to -180° and 0° to $+180^\circ$.

The test speed for the Zahm nozzle was 50 miles an hour; for the SQ-16 40 miles an hour.

The differential pressure heads were read on an inclined alcohol manometer fixed below the tunnel at such a slope as to indicate pressures directly in inches of water.

RESULTS OF TESTS

Tables I and II give the observed differential heads in vertical inches of water for the two nozzles in both pitch and yaw, and Figures 7 and 8 portray these same data graphically.

The discrepancy in the observed differential pressures on the Zahm nozzle for the pitch and yaw mountings at 0° is probably due to the fact that the nozzle occupied different positions in the tunnel for the two mountings, and was thus possibly subjected to different types of air flow or interference effects.

Differential pressures observed on the Zahm nozzle with the calibration set-screw cone removed from the Venturi throat give a pressure versus incidence curve for -20° to $+20^\circ$ yaw and pitch, having less depression near the center than the curves of Figure 7.

Table III gives comparative data for the two types of nozzle in the form of velocity ratios or "correction factors," based on the 0° pitch and yaw differential pressure heads. These data are plotted for graphical comparison in Figures 9 and 10.

Assuming the indicated velocity V to vary as the square root of the nozzle differential pressure, the factor K , tabulated and plotted, is defined as follows:

$$K = \frac{V \text{ at pitch, } \theta^\circ, \text{ yaw } 0^\circ; \text{ or yaw } \psi^\circ, \text{ pitch } 0^\circ}{V \text{ at } 0^\circ \text{ pitch and yaw}}$$

In the above form, K always has small finite values, which are hence better adapted for comparative plotting over the complete test range, than the larger values obtained at high angles

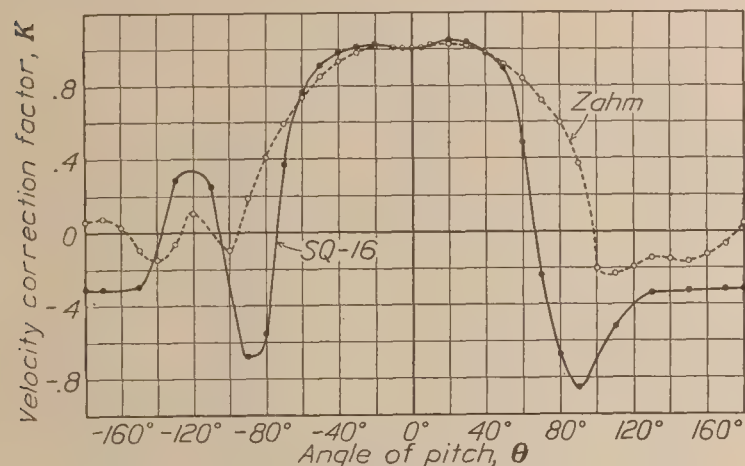


FIG. 9.—Velocity correction factor versus angle of pitch

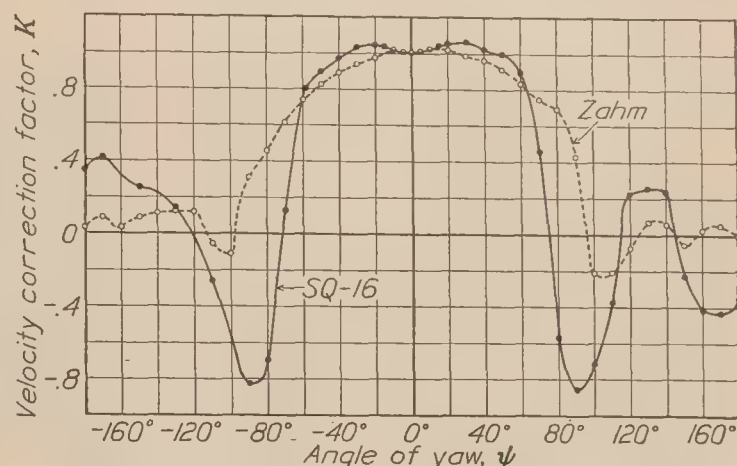


FIG. 10.—Velocity correction factor versus angle of yaw

from the inverse relation. The reciprocal $1/K$, however, is more convenient for use, as a multiplier, in the conversion of the indicated speed to the true one, and hence is given in Table IV for all angles of the test, and plotted in Figure 11 for a limited but ample range of pitch and yaw angles, including the practical flying attitudes. The percentage correction to be added algebraically to the indicated speed to obtain the true value is also here clearly shown for any practical nozzle attitude.

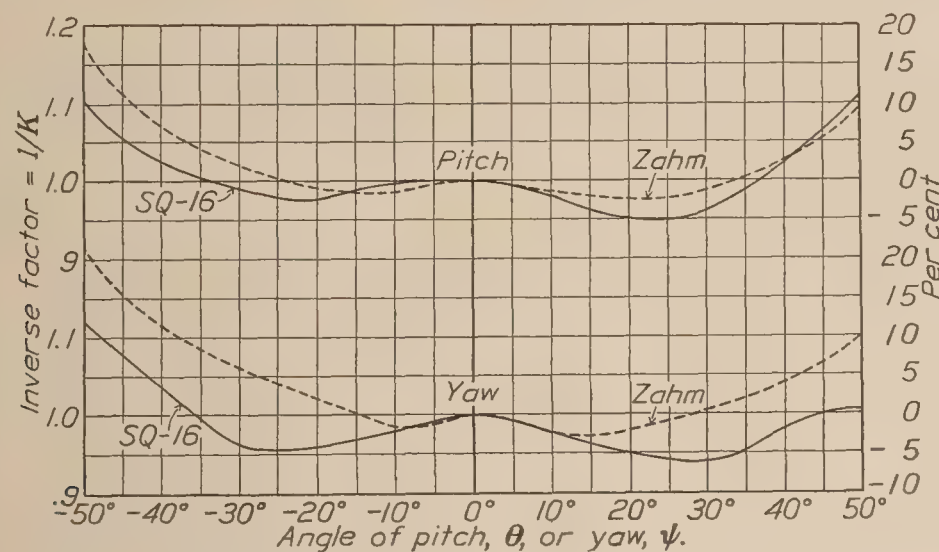


FIG. 11.—Inverse factor versus angles of pitch and yaw

REFERENCES

1. National Advisory Committee for Aeronautics. Development of Air-Speed Nozzles. N. A. C. A. Technical Report No. 31, 1919.
2. National Advisory Committee for Aeronautics. The Altitude Effect on Air-Speed Indicators. N. A. C. A. Technical Report No. 110, 1920.
3. National Advisory Committee for Aeronautics. Aircraft Speed Instruments. N. A. C. A. Technical Report No. 127, 1921.
4. National Advisory Committee for Aeronautics. The Altitude Effect on Air-Speed Indicators-II. N. A. C. A. Technical Report No. 156, 1922.

TABLE I
DIFFERENTIAL HEAD ON ZAHM NOZZLE AT 50 M. P. H.

Angle of pitch or yaw (degrees)	Differential head ¹ (inches of water)		Angle of pitch or yaw (degrees)	Differential head ¹ (inches of water)	
	Nozzle yawed	Nozzle pitched		Nozzle yawed	Nozzle pitched
0	+8.43	+8.03	0	+8.40	+8.02
+10	8.80	8.23	-10	8.67	8.23
20	8.77	8.41	-20	8.07	8.17
30	8.27	8.23	-30	7.48	7.71
40	7.81	7.64	-40	6.77	7.00
50	6.96	6.71	-50	5.72	5.78
60	5.87	5.64	-60	4.60	4.40
70	4.63	4.13	-70	3.22	2.78
80	3.02	2.83	-80	1.75	1.31
90	+1.51	+1.13	-90	+0.84	+0.28
100	-0.39	-0.32	-100	-0.09	-0.08
110	-0.34	-0.42	-110	-0.02	0.00
120	-0.04	-0.30	-120	+0.13	+0.09
130	+0.05	-0.16	-130	0.13	-0.03
140	+0.04	-0.16	-140	0.09	-0.19
150	-0.02	-0.21	-150	0.08	-0.07
160	+0.01	-0.12	-160	0.01	+0.01
170	+0.03	-0.03	-170	0.08	0.05
+180	0.00	+0.02	-180	+0.01	+0.03

¹ Tabulated differential head is mean of 10 readings

TABLE II
DIFFERENTIAL HEAD ON SQ-16 NOZZLE AT 40 M. P. H.

Angle of pitch or yaw (degrees)	Differential head ¹ (inches of water)		Angle of pitch or yaw (degrees)	Differential head ¹ (inches of water)	
	Nozzle pitched	Nozzle yawed		Nozzle pitched	Nozzle yawed
0	+0.757	+0.757	0	+0.757	+0.757
-5	.758	.767	5	.766	.767
-10	.758	.787	10	.788	.789
-15	.778	.808	15	.817	.815
-20	.794	.822	20	.836	.838
-30	.771	.816	30	.817	.857
-40	.721	.706	40	.751	.784
-50	.623	.615	50	.615	.748
-60	.440	.447	60	+ .428	.595
-70	+ .104	+ .011	70	- .042	+ .157
-80	- .236	- .367	80	- .345	- .253
-90	- .356	- .646	90	- .545	- .544
-100			100		- .383
-110	+ .046	- .250	110	- .200	- .106
-120			120		+ .038
-130	+ .060	+ .015	130	- .083	+ .049
-140			140		+ .045
-150	- .068	- .005	150	- .078	- .038
-160			160		- .125
-170	- .076	- .133	170	- .071	- .129
-180	- .073	- .091	180	- .073	- .092

¹ Tabulated differential head is mean of five readings.

TABLE III
VELOCITY CORRECTION FACTOR ¹

Angle of pitch or yaw (degrees)	SQ-16 nozzle		Zahm nozzle		Angle of pitch or yaw (degrees)	SQ-16 nozzle		Zahm nozzle	
	In pitch	In yaw	In pitch	In yaw		In pitch	In yaw	In pitch	In yaw
0	+1.000	+1.000	+1.000	+1.000	0	+1.000	+1.000	+1.000	+1.000
-5	1.001	1.007			5	1.006	1.007		
-10	1.001	1.020	1.013	1.015	10	1.021	1.021	1.013	1.022
-15	1.014	1.033			15	1.039	1.038		
-20	1.024	1.043	1.009	.979	20	1.051	1.052	1.024	1.020
-30	1.009	1.038	.980	.942	30	1.039	1.064	1.013	.991
-40	.976	.965	.934	.897	40	.978	1.017	.976	.963
-50	.907	.894	.849	.824	50	.901	.994	.914	.909
-60	.762	.769	.741	.739	60	+.492	.886	.838	.835
-70	+.371	+.121	.590	.618	70	-.236	+.455	.717	.742
-80	.559	-.697	.406	.456	80	-.675	-.578	.594	.599
-90	-.686	-.924	+.187	+.316	90	-.848	-.848	+.375	+.424
-100			-.100	-.103	100		-.711	-.200	-.215
-110	+.247	-.575	.000	-.049	110	-.514	-.375	-.229	-.201
-120			+.106	+.124	120		-.224	-.193	-.069
-130	+.282	+.141	-.061	.124	130	-.331	-.254	-.141	+.077
-140			-.154	.103	140		-.244	-.141	+.069
-150	-.300	-.257	-.094	.098	150	-.321	-.224	-.162	-.049
-160			+.035	.034	160		-.407	-.122	-.034
-170	-.317	-.420	.079	.098	170	-.307	-.413	-.061	-.060
-180	-.310	-.347	+.061	+.034	180	-.310	-.348	+.050	.000

¹ Data of Tables I and II used in computing these factors.

TABLE IV
INVERSE VELOCITY CORRECTION FACTOR ¹

Angle of pitch or yaw (degrees)	SQ-16 nozzle		Zahm nozzle		Angle of pitch or yaw (degrees)	SQ-16 nozzle		Zahm nozzle	
	In pitch	In yaw	In pitch	In yaw		In pitch	In yaw	In pitch	In yaw
0	+1.000	+1.000	+1.000	+1.000	0	+1.000	+1.000	+1.000	+1.000
-5	.999	.993			5	.994	.993		
-10	.999	.980	.987	.985	10	.979	.979	.987	.978
-15	.986	.968			15	.962	.963		
-20	.977	.959	.991	1.021	20	.951	.951	.977	.980
-30	.991	.963	1.020	1.062	30	.962	.940	.987	1.009
-40	1.025	1.036	1.071	1.114	40	1.022	.983	1.025	1.038
-50	1.103	1.119	1.178	1.214	50	1.110	1.006	1.094	1.100
-60	1.312	1.300	1.350	1.353	60	+2.033	1.129	1.193	1.198
-70	+2.695	+8.264	1.695	1.618	70	-4.237	+2.198	1.395	1.348
-80	-1.789	-1.435	2.463	2.193	80	-1.481	-1.730	1.684	1.669
-90	-1.458	-1.082	+5.348	+3.165	90	-1.179	-1.179	+2.667	+2.358
-100			-10.000	-9.709	100		-1.406	-5.000	-4.651
-110	+4.049	-1.739	∞	-20.408	110	-1.946	-2.667	-4.367	-4.975
-120			+9.434	+8.065	120		-4.464	-5.181	-14.493
-130	+3.546	+7.092	-16.393	8.065	130	-3.021	-3.937	-7.092	+12.987
-140			-6.494	9.709	140		-4.098	-7.092	+14.493
-150	-3.333	-3.891	-10.638	10.204	150	-3.115	-4.464	-6.173	-20.408
-160			+28.571	29.411	160		-2.457	-8.197	-29.412
-170	-3.155	-2.381	12.658	10.204	170	-3.257	-2.421	-16.393	-16.667
-180	-3.226	-2.882	+16.393	+29.412	180	-3.226	-2.874	+20.000	∞

¹ Reciprocal of value in Table III.

REPORT No. 265

**A FULL-SCALE INVESTIGATION OF
GROUND EFFECT**

By ELLIOTT G. REID
Langley Memorial Aeronautical Laboratory

REPORT No. 265

A FULL-SCALE INVESTIGATION OF GROUND EFFECT

By ELLIOTT G. REID

SUMMARY

This report describes flight tests which were made with a Vought VE-7 airplane to determine the effects of flying close to the ground.

It is found that the drag of an airplane is materially reduced upon approaching the ground and that the reduction may be satisfactorily calculated according to theoretical formulas.

Several aspects of ground effect which have had much discussion are explained.

INTRODUCTION

It is a well-known fact that the aerodynamic characteristics of an airplane undergo marked changes near the surface of the earth. However, little has been definitely known concerning either the nature or the magnitude of these changes. Although model tests which appear to substantiate a certain well-founded theory of "ground effect" have been made, the theory has been neither well known nor generally accepted. The lack of general acceptance is probably explained by the fact that no full scale test results have been published and that the methods used in some of the model tests have been questioned on the ground of incomplete or incorrect simulation of the conditions of flight close to the ground.

The above-mentioned theory of ground influence on airfoil characteristics is developed in a paper by C. Wieselsberger (Reference 1); it is an extension of the Lanchester-Prandtl theory and in it are utilized the basic concepts of the induced drag of multiplanes (Reference 2). Wieselsberger presents monoplane model test results which agree very well with his theoretical calculations. The results of other model tests (References 3, 4, and 5), when plotted in polar form, closely resemble those of Reference 1.

The tests which form the subject of this report were made to determine the effects of proximity of the ground upon the aerodynamic characteristics of a full-scale airplane. The experimental results are compared with theoretical calculations.

METHOD OF TESTING

The tests consisted in determining the lift and drag characteristics of an airplane under two conditions: (1) At an altitude sufficient to avoid any possibility of ground influence, and (2) close to the ground.

A Vought VE-7 airplane was selected for the tests. The aerodynamic characteristics of this airplane had been previously determined by glide tests which are described in Reference 6 but, in order to make certain that the normal aerodynamic characteristics of the airplane had not changed, check tests were made at approximately 500 feet altitude. In these tests the R. P. M. of a propeller which had been tested as described in Reference 6 were determined in level flight at several speeds. These values were then compared with the ordinates of the R. P. M. versus air-speed curve obtained from the original propeller test results.

The other tests consisted in measuring the R. P. M. and air speed in level flights made very close to the ground (height of lower wing 5 to 9 feet). The lift and drag characteristics of the airplane were calculated from these data by use of the previously established propeller thrust coefficients. It is assumed that there is no ground effect upon the propeller characteristics as the production of thrust involves only horizontal acceleration of the air.

The details of the method of obtaining the R. P. M. versus air-speed values in level flight at some distance from the ground are given here because the process may be applied to other work in which the same problem exists. This method has the great advantage of eliminating the necessity of maintaining horizontal flight. Three or four runs were made at the same air speed but with different throttle settings. The gain or loss of altitude during 30 seconds and the engine revolutions for the same period were recorded by an observer who read the first from a

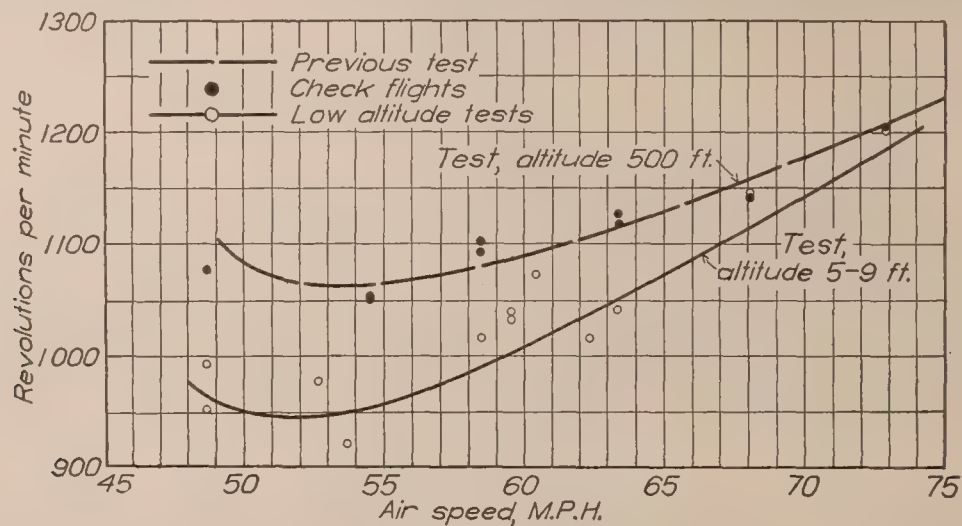


FIG. 1

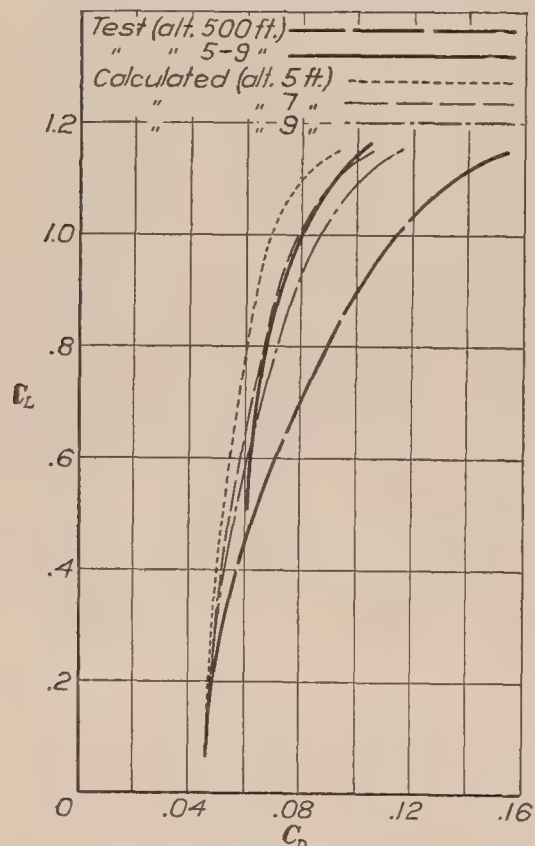


FIG. 2

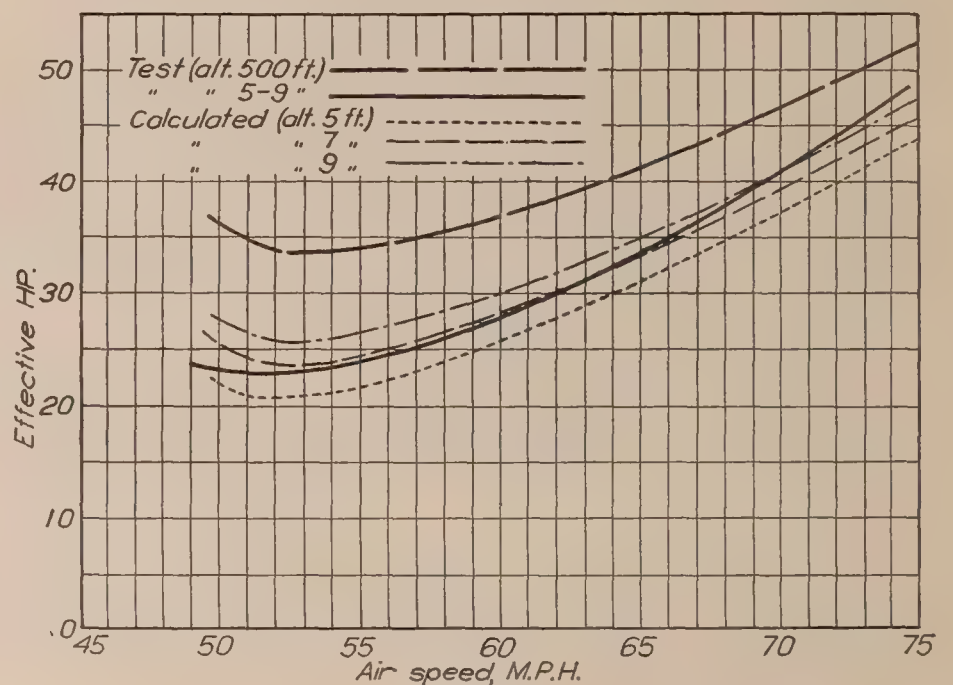


FIG. 3

very sensitive altimeter and the second from a direct-driven revolution counter. The R. P. M. for level flight was obtained from a plot of altitude change versus R. P. M.

RESULTS

The results of the tests are presented in Figures 1-3.

In Figure 1 will be seen the curve of R. P. M. versus air speed for 500 feet altitude which was obtained from the propeller test data, the corresponding check points, and the R. P. M. versus air-speed curve of the low-altitude tests.

The normal polar curve of the VE-7 airplane, as determined by the glide tests of Reference 6 and confirmed by the present experiments, is shown in Figure 2. In the same illustration are the polar which was derived from the low-altitude tests results and the polars which were

derived from the normal one by application of the theoretical formulas. The formulas are summarized in the appendix.

The curves of required thrust horsepower versus air speed, which constitute Figure 3, correspond to the polar curves of Figure 2.

DISCUSSION

It should be understood, before comparing the experimental and theoretical results, that the low-altitude curves are representative of flight at approximately 7 feet from the ground. Only the results of flights in which the height of the lower wing had been estimated by the observers to be between 5 and 9 feet (wheels 2 to 6 feet above the ground) are plotted in Figure 1. In this figure the curve is faired to represent an average of the data and, therefore, an average height of about 7 feet. The fairing at the higher speeds may be criticized on first inspection, but it is felt that this fairing is justifiable as the high-speed flights were made at consistently greater heights than the low-speed ones. This is only natural, as the danger connected with striking the ground increases with the air speed.

The ordinates of the curve for 500 feet altitude vary 5 R. P. M. or less, at speeds above 60 M. P. H., from those of the previously established curve. At the lower speeds the curve represents a mean between the previous and present results.

The agreement of the experimental and theoretical curves, both in absolute value and in shape, is so good at the low speeds that the apparent discrepancies at higher speeds are ascribed to experimental errors. This conclusion is substantiated by the fact that a careful comparison failed to reveal any measurable difference between the maximum speeds of the VE-7 at approximately 10 and 500 feet altitude. The experimental polar for low altitudes is thus shown to be practically coincident with the normal one at low lift coefficients. In view of the excellent correspondence over that range in which the experimental results are considered to be most accurate, and the previously demonstrated agreement of model test results with theory in the range not covered in the present tests, the conclusion that the theory is satisfactorily accurate appears well justified.

Several phases of ground effect can now be explained. The possibility of obtaining an increased maximum speed by flying very close to the ground has frequently been suggested. If the induced power is an appreciable portion of the total power required by an airplane at maximum speed, then an appreciable increase of maximum speed may be obtained by flying close to the ground. This will be the case only when the speed range of the airplane is comparatively small. The case of the VE-7 is treated in the appendix.

"Floating" during the landing glide is obviously caused by the increase of the lift-drag ratio which occurs upon approaching the ground. The tests show this ratio to be increased from 9 to 12.5 for the VE-7 airplane.

The reduction of the power required for level flight, as shown in Figure 3, may become of considerable importance. The climbing ability is affected to a large extent when the airplane is close to the ground, particularly if the available power is only slightly greater than the required power. Demonstrations of this condition are frequently seen. It has been noticed that light airplanes having large power loadings climb rapidly upon leaving the ground, but soon suffer a rapid reduction of climbing speed. A striking example was recently observed at Langley Field when a heavily-loaded seaplane was taken off and kept in the air, although at a low air speed, for about 10 miles, at the end of which distance some of the load had to be discharged because it had not been possible to gain enough altitude to allow a turn to be made safely.

Although both theory and experiment indicate a reduction of induced drag as the ground is approached, there seems to be a critical altitude, or combination of altitude and air speed, at which some radical change of air flow takes place. It was found that the VE-7, when flying very low, would sometimes drop to the ground without any warning such as a sudden change of angle or of air speed. Pilots report that this is a frequent occurrence in landing; an airplane will "float" for some distance, the air speed gradually decreasing, and then "pancake" for no

apparent reason. Discussions with several pilots have not made it clear whether this characteristic is common to all types of airplanes, or to only a few. It would be interesting to know whether the stall is more abrupt close to the ground than at altitude, and to what extent the tendency to "pancake" depends on design.

As the extent of the disturbance created by the wings of an airplane, i. e., the quantity of air given downward momentum in producing the lift, is directly connected with the induced drag, an alternative explanation of the cause of ground effect could be made if the extent of the disturbance could be determined at altitude and close to the ground. An attempt to obtain such information was made by photographing the pattern left in a smoke screen through which the airplane was flown. Satisfactory pictures have not yet been obtained at altitude, but in Figure 4 are some which were taken close to the ground. These pictures, which are the first of their kind, are presented here as an interesting side-light only. However, as the photographic study of air flow is now being pursued at numerous laboratories, it is possible that this method may prove very useful.

CONCLUSIONS

The induced drag of an airplane is reduced upon approaching the ground and the theory of Wieselsberger offers a satisfactory explanation and method of calculation of the reduction.

LANGLEY MEMORIAL AERONAUTICAL LABORATORY,
NATIONAL ADVISORY COMMITTEE FOR AERONAUTICS,
LANGLEY FIELD, VA., *October 19, 1926.*

APPENDIX

The following formulas and explanation are summarized from Reference 1. A comment on a practical simplification of the biplane computations is added.

The induced drag coefficient of a monoplane at height $h/2$ above the ground is

$$C_{Di} = (1 - \sigma) \frac{C_L^2 S}{\pi b^2} \quad (1)$$

wherein

σ is the "influence coefficient."

C_L is the lift coefficient.

S is the wing area.

b is the span.

The value of σ may be computed from the formula

$$\sigma = \frac{1 - 0.66 \frac{h}{b}}{1.05 + 3.7 \frac{h}{b}} \quad (2)$$

which applies over the range of h/b from $1/15$ to $1/2$. Values of σ for $\frac{h}{b} > \frac{1}{2}$ which occurred in the computations of this report were taken from a graphical extrapolation of the curve computed from (2).

To compute the ground effect upon the characteristics of a biplane, Wieselsberger divides the reduction of induced drag into four parts—i. e., each wing is considered as a monoplane which is influenced by the action of its own image in the ground plane as well as by that of the other wing. The components all have the same sign and two are considered to be of equal value. These are the reductions of the drag of the upper and lower wings brought about by the action of the images of lower and upper wings, respectively.

To be strictly accurate, the lift coefficients of the individual wings should be taken into account. However, the reduction of induced drag which is calculated for a biplane with



From ground

Complete pattern

From cockpit of airplane

Half pattern

FIG. 4.—Photographs of pattern left in smoke screen by VE-7 airplane

97297—28. (Face p. 236.)

wings of equal span under the assumption that the average lift coefficient applies to both wings is in error by only about 2 per cent if the lift coefficients of the individual wings differ by 20 per cent at $\frac{h}{b} = 0.3$. The theoretical calculations for the VE-7 are based on the average (or cellule) lift coefficient.

The increase of maximum speed obtainable by flying the VE-7 with its lower wing 5 feet from the ground is calculated below. The following values are assumed to be true in the absence of ground influence:

$$V_{max} = 120 \text{ M. P. H.}$$

$$\text{B. HP.} = 180.$$

$$\text{Propeller efficiency} = 76 \text{ per cent.}$$

The total power required is therefore,

$$\text{HP}_r = 180 \times .76 = 136.8$$

and the induced power is

$$\text{HP}_i = \frac{W^2}{3k^2b^2V} = \frac{(2075)^2}{3 \times 1.37 \times (34.11)^2 \times 120} = 7.5$$

$$W = \text{weight, } b = \text{span, } k^2 = \text{Munk biplane constant.}$$

According to the theory, the coefficient of induced drag of this airplane with its lower wing 5 feet above the ground is 0.27 of that without ground effect. Hence, at 120 M. P. H. the induced power is

$$\text{HP}_{(5')} = 7.5 \times .27 = 2.0$$

and the total power required is

$$\text{HP}_{r(5')} = 136.8 - (7.5 - 2.0) = 131.3.$$

Assuming that the power required varies with the cube of the speed, the maximum speed at 5 feet height is

$$V_{max(5')} = 120 \sqrt[3]{\frac{136.8}{131.3}} = 121.6 \text{ M. P. H.}$$

The increase of maximum speed is therefore only 1.6 M. P. H., or 1.3 per cent.

REFERENCES AND BIBLIOGRAPHY

- REFERENCE 1. WIESELSBERGER, C. Wing Resistance Near the Ground. N. A. C. A. Technical Memorandum No. 77. 1922.
- REFERENCE 2. PRANDTL, L. The Induced Drag of Multiplanes. N. A. C. A. Technical Note No. 182. 1924.
- REFERENCE 3. RAYMOND, A. E. Ground Influence on Aerofoils. N. A. C. A. Technical Note No. 67. 1921.
- REFERENCE 4. COWLEY, W. L., and C. N. H. LOCK. Cushioning Effect on Aeroplanes Close to the Ground. B. A. C. A. Reports and Memoranda No. 754. 1920.
- REFERENCE 5. ZAHM, A. F., and R. M. BEAR, Washington Navy Yard. Ground Plane Influence on Airplane Wings. Construction Department, United States Navy, Report No. 173. 1921.
- REFERENCE 6. DURAND, W. F., and E. P. LESLEY. Comparison of Tests on Air Propellers in Flight with Wind Tunnel Model Tests on Similar Forms. N. A. C. A. Technical Report No. 220. 1926.
- BETZ, A. The Lift and Drag of a Wing in Proximity to the Ground. McCook Field Memorandum Report No. 167. 1925.
- MERRILL, A. A. Ground Effect on Wings. "The Ace." December, 1920.

REPORT No. 266

AIR FORCE AND MOMENT FOR N-20 WING WITH CERTAIN CUT-OUTS

By R. H. SMITH
**Aerodynamical Laboratory, Bureau of Construction
and Repair, U. S. Navy**

REPORT No. 266

AIR FORCE AND MOMENT FOR N-20 WING WITH CERTAIN CUT-OUTS

By R. H. SMITH

INTRODUCTION

The airplane designer often finds it necessary, in meeting the requirements of visibility, to remove area or to otherwise locally distort the plan or section of an airplane wing. This report, prepared for the Bureau of Aeronautics January 15, 1925, and submitted for publication to the National Advisory Committee for Aeronautics November 29, 1926, contains the experimental results of tests on six 5 by 30 inch N-20 wing models, cut out or distorted in different ways, which were conducted in the 8 by 8 foot wind tunnel of the Navy Aerodynamical Laboratory in Washington in 1924.

The measured and derived results are given without correction for Vl/ν or for wall effect and for standard air density, $\rho = 0.00237$ slug per cubic foot.

DESCRIPTION OF MODELS

The principal dimensions and specified offsets of the six models are given in Figure 1; their full-scale section views in Figure 4. They were made of dry mahogany and varnished, then satisfactorily verified by application of their steel templates. The two wings, composing model N-20_A, were assembled by means of two streamlined steel members in the position of the spars. The other models were made completely of wood.

RESULTS

Tables I to XIII give the numerical results of the tests, all of which were made at 40 miles per hour; the first three containing test data, the next four the lift and drag coefficients, and the next six the speed and power factors, efficiencies, and center of pressure coefficients. The data, excepting for K_x and K_y coefficients, are plotted in Figures 2, 3, and 4. Table XIV gives the chief structural and aerodynamic characteristics of the models.

While no analysis of the results is attempted, a few conclusions are outstanding. Although the N-20 wing with no cut-out or distortion has the largest values of L/D maximum, C_L maximum and maximum speed ratio, some of the distorted forms outperform it in other items. The N-20_C, for instance, has the lowest minimum C_D ; the largest L/D at $1/8$ C_L maximum and the largest C_L maximum/ C_D minimum. Likewise N-20_E is the best of the six for minimum power and maximum ceiling, and N-20_D is best for effectiveness in climbing. On the other hand the performance of N-20_B, and particularly N-20_A, is less favorable in every item.

REFERENCE

POWELL, C. H.: On the Effects of Cutting a Hole in the Top Plane of a Biplane. British Reports and Memoranda No. 419. 1918.

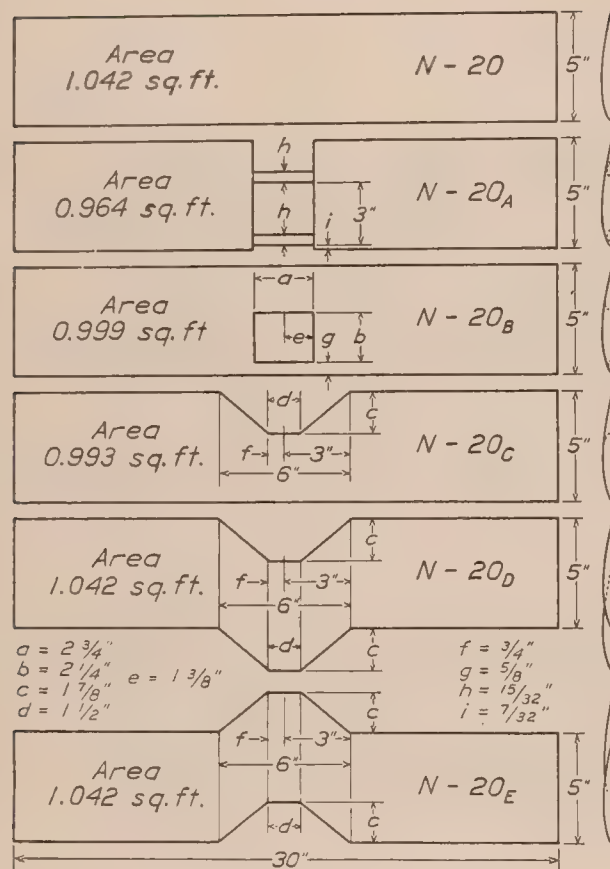
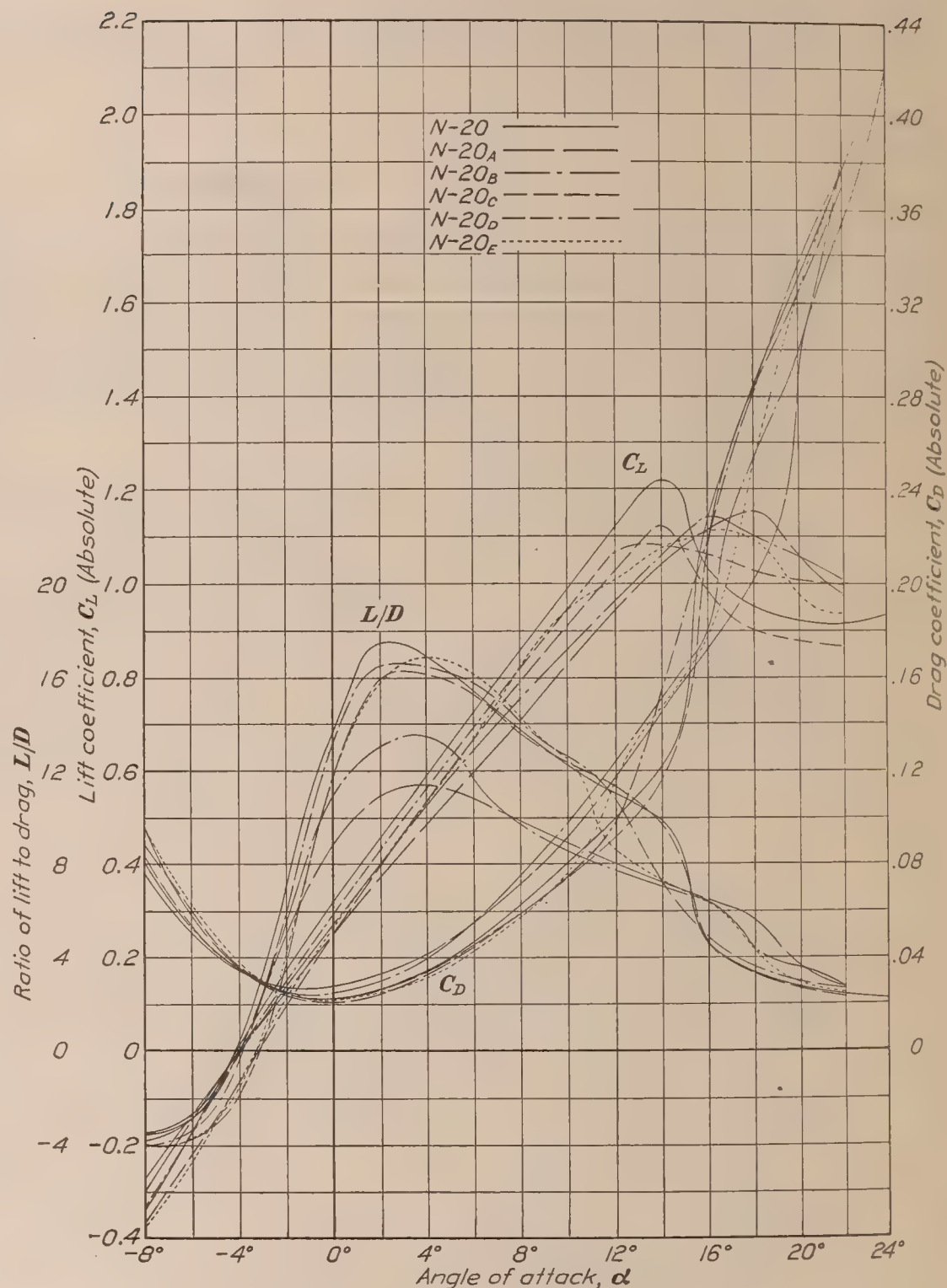


FIG. 1.—Principal dimensions of models

CAMBERS OF N-20 AIRFOIL

From L. E.-----	0	0.0125	0.0250	0.0500
Upper-----	.0107	.0300	.0390	.0510
Lower-----	.0107	0	0	0
From L. E.-----	.0750	.1000	.1500	.2000
Upper-----	.0590	.0650	.0732	.0770
Lower-----	0	0	0	0
From L. E.-----	.3000	.4000	.5000	.6000
Upper-----	.0817	.0806	.0761	.0694
Lower-----	0	0	0	0
From L. E.-----	.7000	.8000	.9000	1.0000
Upper-----	.0593	.0451	.0271	.0160
Lower-----	0	0	0	.0025

All dimensions given as decimal parts of chord length.
 Rad. L. E.=0.0107. Rad. T. E.=0.0025.

FIG. 2.— C_L , C_D , and L/D versus α . Air speed $V=40$ M. P. H.

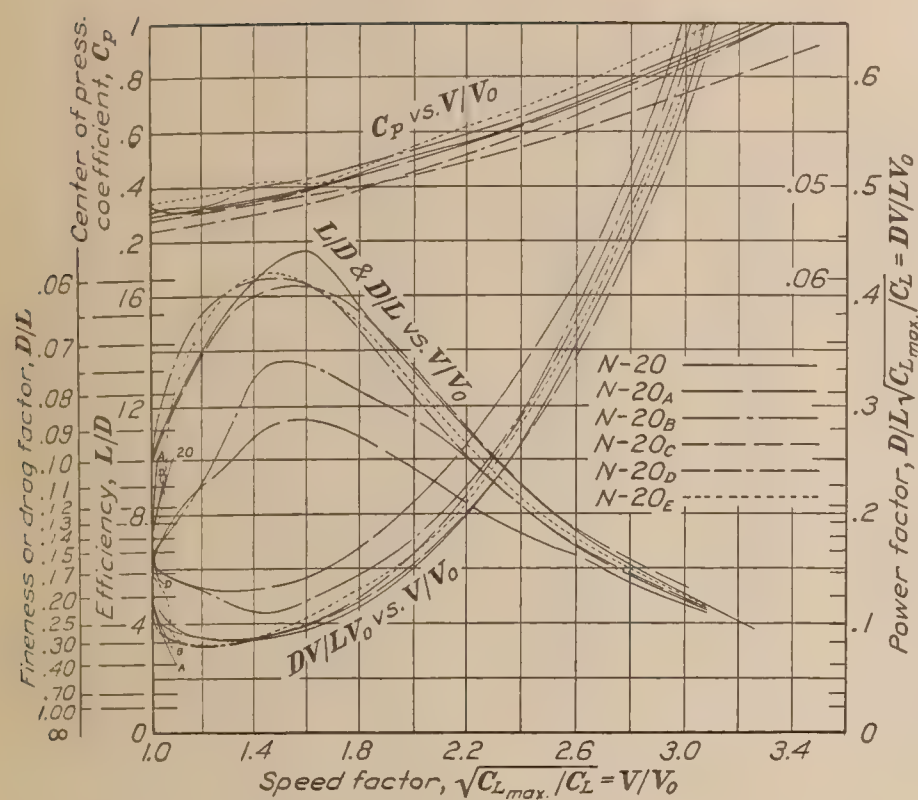


FIG. 3.—Functions of speed factor

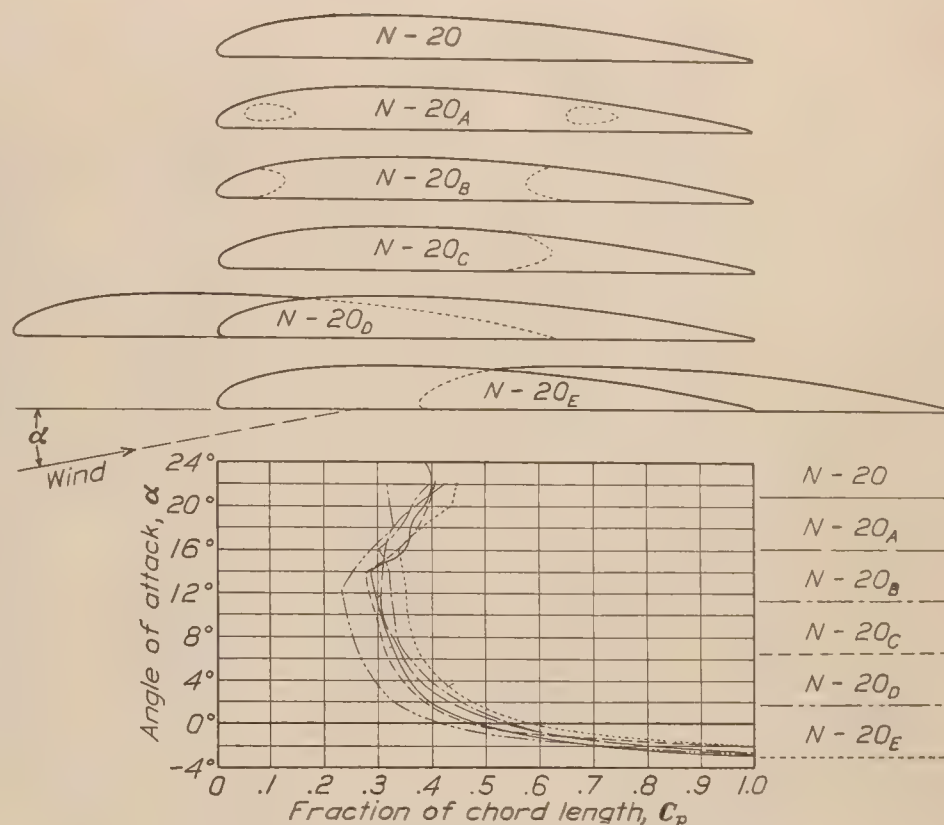
FIG. 4.—Sections and α versus C_p at $V=40$ M. P. H.

TABLE I
NET MEASURED LIFT, IN POUNDS, AT 40 M. P. H.

Angle of attack (degrees) α	N-20	N-20 _A	N-20 _B	N-20 _C	N-20 _D	N-20 _E
-8	-1.440	-1.067	-1.242	-1.485	-1.388	-1.560
-6	-.716	-.548	-.612	-.935	-.750	-.987
-5	-.318	-.273	-.297	-.598	-.382	-.609
-4	+.067	+.005	+.015	-.267	-.027	-.230
-3	.415	.291	.310	+.065	+.323	+.139
-2	.740	.547	.585	.383	.607	.494
-1	1.047	.783	.850	.695	.962	.812
0	1.343	1.011	1.130	.999	1.259	1.124
+2	1.947	1.440	1.605	1.602	1.835	1.687
4	2.527	1.872	2.249	2.217	2.418	2.270
6	3.077	2.371	2.662	2.750	2.987	2.847
8	3.651	2.816	3.082	3.255	3.502	3.488
10	4.201	3.283	3.516	3.755	4.031	4.028
12	4.678	3.740	3.963	4.212	4.538	4.279
14	5.118	4.150	4.384	4.625	4.601	4.583
16	4.379	4.435	4.740	4.037	4.523	4.824
18	4.038	4.610	4.536	3.703	4.372	4.665
20	3.919	4.239	4.410	3.611	4.272	4.141
22	3.868	+3.902	+4.170	+3.561	+4.229	+3.975
+24	+3.957					

TABLE II
NET MEASURED DRAG IN POUNDS AT 40 M. P. H.

Angle of attack (degrees) α	N-20	N-20 _A	N-20 _B	N-20 _C	N-20 _D	N-20 _E
-8	0.401	0.297	0.325	0.363	0.346	0.396
-6	.243	.203	.217	.247	.222	.260
-5	.191	.163	.173	.186	.170	.209
-4	.155	.136	.142	.149	.140	.160
-3	.123	.116	.121	.114	.115	.127
-2	.104	.109	.106	.100	.099	.109
-1	.096	.109	.098	.088	.095	.099
0	.098	.115	.102	.086	.095	.095
+2	.111	.132	.124	.100	.111	.107
4	.150	.164	.167	.138	.147	.135
6	.201	.220	.230	.179	.189	.176
8	.266	.287	.312	.241	.250	.244
10	.343	.368	.412	.305	.319	.323
12	.425	.466	.511	.373	.414	.503
14	.515	.576	.627	.473	.657	.625
16	.966	.685	.743	.902	.928	.755
18	1.210	.802	1.052	1.165	1.198	1.064
20	1.415	1.170	1.240	1.338	1.432	1.406
22	1.610	1.422	1.579	1.528	1.598	1.602
+24	1.780					

TABLE III
NET MEASURED PITCHING MOMENT ABOUT *M* AXIS* OF MODEL HOLDER IN POUND-
INCHES AT 40 M. P. H.

Angle of attack (degrees) α	N-20	N-20 _A	N-20 _B	N-20 _C	N-20 _D	N-20 _E
-8	+0.289	+0.202	+0.240	+0.342	+1.073	-1.677
-6	-.246	-.046	-.083	-.117	+.331	-1.360
-5	-.256	-.117	-.162	-.180	+.033	-1.038
-4	-.229	-.164	-.199	-.188	-.233	-.744
-3	-.190	-.232	-.243	-.157	-.516	-.182
-2	-.167	-.235	-.305	-.107	-.659	+.274
-1	-.145	-.200	-.334	-.039	-.693	.729
0	-.148	-.158	-.318	-.035	-.804	1.153
+2	-.199	-.243	-.433	-.176	-1.208	1.787
4	-.466	-.398	-.719	-.523	-2.021	2.207
6	-1.062	-.807	-.903	-1.064	-2.903	2.434
8	-1.913	-1.375	-1.292	-1.853	-4.086	2.393
10	-2.873	-2.182	-1.918	-2.860	-5.448	2.083
12	-4.096	-3.080	-2.852	-4.048	-6.888	2.261
14	-5.387	-4.265	-3.974	-5.277	-6.852	1.914
16	-2.982	-5.335	-4.948	-2.609	-6.428	1.491
18	-1.481	-6.536	-3.976	-1.573	-6.029	2.152
20	-1.205	-4.805	-4.260	-1.339	-4.936	3.416
22	-.868	-4.043	-2.483	-1.058	-5.038	+3.915
+24	-.920					

**M* axis, N-20, is 32.6 per cent of chord length aft of L. E. and 183 per cent of chord length below the chord.
M axis, N-20_A, is 29.8 per cent of chord length aft of L. E. and 180.4 per cent of chord length below the chord.
M axis, N-20_B, is 26.1 per cent of chord length aft of L. E. and 180.8 per cent of chord length below the chord.
M axis, N-20_C, is 25.6 per cent of chord length aft of L. E. and 183.4 per cent of chord length below the chord.
M axis, N-20_D, is 14.2 per cent of chord length aft of L. E. and 183.4 per cent of chord length below the chord.
M axis, N-20_E, is 62.8 per cent of chord length aft of L. E. and 183.8 per cent of chord length below the chord.

TABLE IV
LIFT COEFFICIENTS AT 40 M. P. H.

Angle of attack (degrees) α	C_L (absolute)					
	N-20	N-20 _A	N-20 _B	N-20 _C	N-20 _D	N-20 _E
-8	-0.3388	-0.2674	-0.3003	-0.3613	-0.3266	-0.3671
-6	-.1685	-.1373	-.1480	-.2275	-.1765	-.2322
-5	-.0748	-.0684	-.0718	-.1455	-.0899	-.1433
-4	+.0158	+.0012	+.0036	-.0650	-.0635	-.0541
-3	.0976	.0729	.0750	+.0158	+.0760	+.0327
-2	.1741	.1371	.1415	.0932	.1428	.1162
-1	.2464	.1962	.2055	.1691	.2264	.1911
0	.3160	.2534	.2732	.2430	.2962	.2645
+2	.4581	.3609	.3881	.3897	.4318	.3970
4	.5946	.4691	.5438	.5394	.5690	.5341
6	.7240	.5942	.6437	.6690	.7028	.6699
8	.8591	.7057	.7453	.7919	.8240	.8207
10	.9885	.8227	.8502	.9135	.9485	.9478
12	1.1007	.9372	.9583	1.0247	1.0678	1.0068
14	1.2043	1.0400	1.0601	1.1252	1.0826	1.0784
16	1.0304	1.1114	1.1462	.9821	1.0643	1.1351
18	.9501	1.1553	1.0969	.9009	1.0287	1.0977
20	.9221	1.0623	1.0664	.8785	1.0052	.9744
22	.9101	+.9778	+1.0083	+.8663	+.9951	+.9353
+24	+.9311					

TABLE V
LIFT COEFFICIENTS AT 40 M. P. H.

Angle of attack (degrees) α	K_v (lb./ft. ² /mi. ² /hr. ²)					
	N-20	N-20 _A	N-20 _B	N-20 _C	N-20 _D	N-20 _E
-8	-0.000864	-0.000682	-0.000766	-0.000921	-0.000833	-0.000930
-6	-.000430	-.000350	-.000377	-.000580	-.000450	-.000592
-5	-.000101	-.000174	-.000183	-.000371	-.000229	-.000365
-4	+.000402	+.000031	+.000009	-.000166	-.000162	-.000138
-3	.000249	.000186	.000191	+.000040	+.000194	-.000083
-2	.000444	.000350	.000361	.000024	.000364	-.000030
-1	.000628	.000500	.000524	.000043	.000577	+.000487
0	.000806	.000646	.000697	.000062	.000755	.000674
+2	.001168	.000920	.000990	.000099	.001101	.001012
4	.001516	.001196	.001387	.000138	.001451	.001362
6	.001846	.001515	.001641	.000170	.001792	.001708
8	.002191	.001800	.001900	.000202	.002101	.002093
10	.002521	.002098	.002168	.000232	.002419	.002417
12	.002807	.002390	.002444	.000261	.002722	.002567
14	.003071	.002652	.002703	.000287	.002761	.002750
16	.002628	.002834	.002923	.000250	.002714	.002894
18	.002423	.002946	.002797	.000230	.002623	.002799
20	.002351	.002709	.002719	.000224	.002563	.002485
22	.002323	+.002493	+.002571	+.000221	+.002534	+.002385
+24	+.002374					

TABLE VI
DRAG COEFFICIENTS AT 40 M. P. H.

Angle of attack (degrees) α	C_D (absolute)					
	N-20	N-20 _A	N-20 _B	N-20 _C	N-20 _D	N-20 _E
-8	0. 0944	0. 0744	0. 0786	0. 0883	0. 0814	0. 0932
-6	. 0572	. 0509	. 0525	. 0601	. 0522	. 0612
-5	. 0449	. 0408	. 0418	. 0452	. 0400	. 0492
-4	. 0365	. 0341	. 0343	. 0362	. 0329	. 0378
-3	. 0289	. 0291	. 0293	. 0277	. 0270	. 0299
-2	. 0245	. 0273	. 0256	. 0243	. 0233	. 0256
-1	. 0226	. 0273	. 0237	. 0214	. 0224	. 0233
0	. 0230	. 0288	. 0247	. 0209	. 0224	. 0224
+2	. 0261	. 0331	. 0300	. 0243	. 0261	. 0252
4	. 0353	. 0411	. 0404	. 0336	. 0346	. 0318
6	. 0472	. 0551	. 0556	. 0435	. 0445	. 0414
8	. 0626	. 0719	. 0754	. 0586	. 0588	. 0574
10	. 0807	. 0922	. 0996	. 0742	. 0751	. 0760
12	. 1000	. 1168	. 1236	. 0907	. 0974	. 1184
14	. 1212	. 1443	. 1516	. 1151	. 1546	. 1471
16	. 2273	. 1717	. 1797	. 2194	. 2184	. 1776
18	. 2847	. 2010	. 2544	. 2834	. 2819	. 2504
20	. 3329	. 2932	. 2999	. 3255	. 3369	. 3308
22	. 3788	. 3564	. 3818	. 3717	. 3760	. 3770
+24	. 4188					

TABLE VII
DRAG COEFFICIENTS AT 40 M. P. H.

Angle of attack (degrees) α	K_X (lb./ft. ² /mi. ² /hr. ²)					
	N-20	N-20 _A	N-20 _B	N-20 _C	N-20 _D	N-20 _E
-8	0. 0002407	0. 0001894	0. 0002004	0. 0002252	0. 0002076	0. 0002377
-6	. 0001459	. 0001298	. 0001339	. 0001532	. 0001331	. 0001561
-5	. 0001145	. 0001040	. 0001069	. 0001153	. 0001020	. 0001255
-4	. 0000931	. 0000870	. 0000875	. 0000923	. 0000839	. 0000959
-3	. 0000737	. 0000742	. 0000747	. 0000706	. 0000688	. 0000762
-2	. 0000625	. 0000696	. 0000653	. 0000620	. 0000594	. 0000653
-1	. 0000576	. 0000696	. 0000604	. 0000546	. 0000571	. 0000594
0	. 0000587	. 0000734	. 0000630	. 0000533	. 0000571	. 0000571
+2	. 0000666	. 0000844	. 0000765	. 0000620	. 0000666	. 0000643
4	. 0000900	. 0001048	. 0001030	. 0000858	. 0000882	. 0000811
6	. 0001204	. 0001405	. 0001418	. 0001109	. 0001135	. 0001056
8	. 0001596	. 0001833	. 0001923	. 0001494	. 0001499	. 0001464
10	. 0002058	. 0002351	. 0002539	. 0001892	. 0001915	. 0001938
12	. 0002550	. 0002978	. 0003151	. 0002313	. 0002484	. 0003019
14	. 0003091	. 0003680	. 0003866	. 0002935	. 0003942	. 0003751
16	. 0005796	. 0004378	. 0004582	. 0005595	. 0005569	. 0004529
18	. 0007260	. 0005126	. 0006487	. 0007227	. 0007188	. 0006385
20	. 0008489	. 0007477	. 0007646	. 0008300	. 0008591	. 0008435
22	. 0009659	. 0009088	. 0009737	. 0009478	. 0009588	. 0009614
+24	. 0010679					

TABLE VIII

SPEED FACTOR, POWER FACTOR, EFFICIENCY, AND CENTER OF PRESSURE COEFFICIENT
AT 40 M. P. H. FOR N-20 WING

Angle of attack (degrees) α	Efficiency L/D	Speed factor $\sqrt{C_{Lmax}/C_L}$	Power factor $\frac{D}{L} \sqrt{C_{Lmax}/C_L}$	Center of pressure coefficient C_p
-8	-3.59			0.132
-6	-2.94			
-5	-1.66			
-4	+.43	8.751	20.335	
-3	3.37	3.521	1.049	1.098
-2	7.11	2.636	.371	.706
-1	10.91	2.214	.203	.564
0	13.71	1.957	.143	.494
+2	17.54	1.625	.093	.392
4	16.85	1.427	.085	.354
6	15.31	1.293	.084	.334
8	13.72	1.187	.087	.320
10	12.24	1.101	.110	.302
12	11.01	1.048	.095	.294
14	9.93	1.003	.101	.284
16	4.53	1.084	.239	.350
18	3.34	1.128	.338	.358
20	2.77	1.146	.414	.388
22	2.40	1.159	.483	.400
+24	+2.22	1.140	.514	.386

TABLE IX

SPEED FACTOR, POWER FACTOR, EFFICIENCY, AND CENTER OF PRESSURE COEFFICIENT
AT 40 M. P. H. FOR N-20_A WING

Angle of attack (degrees) α	Efficiency L/D	Speed factor $\sqrt{C_{Lmax}/C_L}$	Power factor $\frac{D}{L} \sqrt{C_{Lmax}/C_L}$	Center of pressure coefficient C_p
-8	-3.60			0.098
-6	-2.70			
-5	-1.67			
-4	+.04	8.978	224.200	
-3	2.51	3.992	1.590	1.291
-2	5.02	2.909	.580	.810
-1	7.19	2.431	.338	.634
0	8.80	2.141	.243	.534
+2	10.91	1.793	.165	.434
4	11.41	1.573	.138	.372
6	10.78	1.398	.130	.346
8	9.82	1.282	.131	.326
10	8.93	1.187	.133	.306
12	8.03	1.113	.139	.306
14	7.21	1.057	.137	.308
16	6.47	1.022	.158	.310
18	5.75	1.002	.174	.326
20	3.62	1.044	.288	.372
+22	+2.75	1.089	.396	.426

TABLE X

SPEED FACTOR, POWER FACTOR, EFFICIENCY, AND CENTER OF PRESSURE COEFFICIENT
AT 40 M. P. H. FOR N-20_B WING

Angle of attack (degrees) α	Efficiency L/D	Speed factor $\sqrt{C_{Lmax}/C_L}$	Power factor $\frac{D}{L} \sqrt{C_{Lmax}/C_L}$	Center of pres- sure coefficient C_p
-8	-3.83			0.150
-6	-2.82			
-5	-1.72			
-4	+.11	17.873	178.680	
-3	2.56	3.927	1.530	1.297
-2	5.52	2.851	.516	.822
-1	8.67	2.366	.273	.640
0	11.08	2.053	.185	.542
+2	12.94	1.722	.133	.456
4	13.47	1.454	.108	.394
6	11.57	1.337	.116	.360
8	9.89	1.244	.126	.332
10	8.53	1.164	.136	.328
12	7.76	1.096	.141	.322
14	7.00	1.042	.149	.318
16	6.38	1.002	.157	.301
18	4.31	1.024	.238	.342
20	3.56	1.039	.292	.362
+22	+2.64	1.063	.404	.394

TABLE XI

SPEED FACTOR, POWER FACTOR, EFFICIENCY, AND CENTER OF PRESSURE COEFFICIENT
AT 40 M. P. H. FOR N-20_C WING

Angle of attack (degrees) α	Efficiency L/D	Speed factor $\sqrt{C_{Lmax}/C_L}$	Power factor $\frac{D}{L} \sqrt{C_{Lmax}/C_L}$	Center of pres- sure coefficient C_p
-8	-4.09			0.174
-6	-3.78			.000
-5	-3.22			
-4	-1.79			
-3	+.57	8.471	14.856	
-2	3.83	3.483	.910	.918
-1	7.90	2.568	.325	.588
0	11.62	2.155	.186	.474
+2	16.02	1.704	.106	.384
4	16.06	1.448	.090	.346
6	15.36	1.300	.085	.316
8	13.51	1.195	.088	.306
10	12.31	1.125	.091	.294
12	11.29	1.065	.094	.282
14	9.78	1.002	.102	.280
16	4.48	1.072	.239	.334
18	3.18	1.121	.353	.374
20	2.70	1.134	.420	.392
+22	+2.33	1.143	.491	.406

TABLE XII

SPEED FACTOR, POWER FACTOR, EFFICIENCY, AND CENTER OF PRESSURE COEFFICIENT
AT 40 M. P. H. FOR N-20_D WING

Angle of attack (degrees) α	Efficiency L/D	Speed factor $\sqrt{C_L \max/C_L}$	Power factor $\frac{D}{L} \sqrt{C_L \max/C_L}$	Center of pressure coefficient C_p
-8	-4.01			0.104
-6	-3.38			
-5	-2.25			
-4	-.19			
-3	+2.81	3.778	1.344	1.223
-2	6.13	2.764	.452	.728
-1	10.13	2.194	.217	.504
0	13.25	1.913	.144	.412
+2	16.53	1.587	.096	.322
4	16.45	1.384	.084	.292
6	15.80	1.246	.079	.264
8	14.01	1.151	.082	.252
10	12.64	1.072	.085	.242
12	10.96	1.011	.085	.232
14	7.02	1.004	.143	.252
16	4.88	1.013	.208	.284
18	3.65	1.030	.282	.328
20	2.98	1.042	.350	.322
22	+2.64	1.050	.398	.316

TABLE XIII

SPEED FACTOR, POWER FACTOR, EFFICIENCY, AND CENTER OF PRESSURE COEFFICIENT
AT 40 M. P. H. FOR N-20_E WING

Angle of attack (degrees) α	Efficiency L/D	Speed factor $\sqrt{C_L \max/C_L}$	Power factor $\frac{D}{L} \sqrt{C_L \max/C_L}$	Center of pressure coefficient C_p
-8	-3.94			0.216
-6	-3.80			.080
-5	-2.91			
-4	-1.44			
-3	+1.09	5.909	5.421	
-2	4.53	3.118	.688	1.000
-1	8.20	2.443	.298	.704
0	11.83	2.077	.176	.578
+2	15.77	1.695	.107	.410
4	16.81	1.462	.087	.416
6	16.18	1.305	.081	.380
8	14.30	1.178	.082	.364
10	12.47	1.098	.088	.352
12	8.51	1.065	.125	.352
14	7.33	1.028	.140	.344
16	6.40	1.002	.157	.338
18	4.38	1.019	.235	.376
20	2.94	1.082	.368	.438
22	+2.48	1.080	.436	.446

TABLE XIV
DATA AND CHARACTERISTICS

Data and characteristics	N-20	N-20 _A	N-20 _B	N-20 _C	N-20 _D	N-20 _E	Significance for air- planes of same weight and pro- pulsive system
SPECIFICATIONS							
Source of design-----	(1)	(1)	(1)	(1)	(1)	(1)	
General shape-----	(2)	(2)	(2)	(2)	(2)	(2)	
Per cent chord length:							
Maximum top cam- ber.	8. 17	8. 17	8. 17	8. 17	8. 17	8. 17	
Thickness 10 per cent from nose.	6. 50	6. 50	6. 50	6. 50	6. 50	6. 50	} Front spar depth.
Thickness 15 per cent from nose.	7. 32	7. 32	7. 32	7. 32	7. 32	7. 32	
Thickness 60 per cent from nose.	6. 94	6. 94	6. 94	6. 94	6. 94	6. 94	} Rear spar depth.
Thickness 70 per cent from nose.	5. 93	5. 93	5. 93	5. 93	5. 93	5. 93	
Maximum thickness--	8. 17	8. 17	8. 17	8. 17	8. 17	8. 17	
DIRECT WIND TUNNEL DATA							
Size of tunnel-----	(3)	(3)	(3)	(3)	(3)	(3)	
Speed <i>V</i> of test ft./sec----	58. 67	58. 67	58. 67	58. 67	58. 67	58. 67	
<i>V</i> of test, ft. ² /sec-----	24. 44	24. 44	24. 44	24. 44	24. 44	24. 44	
No lift angle <i>α</i> -----	-4. 2°	-4. 0°	-3. 9°	-3. 2°	-3. 8°	-3. 4°	
Main slope of <i>C_L</i> curve--	. 069	. 057	. 052	. 075	. 069	. 066	
<i>C_L</i> maximum-----	1. 209	1. 158	1. 150	1. 125	1. 089	1. 135	Minimum speed.
<i>C_L</i> at maximum <i>L/D</i> -----	. 482	. 471	. 540	. 451	. 478	. 540	
<i>C_D</i> minimum-----	. 023	. 027	. 024	. 021	. 022	. 022	
Range of <i>C_p</i> for 2 <i>V_o</i> < <i>V</i> < 3 <i>V_o</i> in per cent chord length.	. 356	. 347	. 360	. 301	. 387	. 402	
COMPUTED RATIOS							
<i>L/D</i> maximum-----	17. 69	11. 41	13. 47	16. 40	16. 72	16. 81	Minimum wing drag; maximum speed re- gardless of mini- mum; flattest glide; maximum radius; maximum lb.- miles/lb. fuel.
<i>L/D</i> at 1/8 <i>C_L</i> maximum--	5. 8	4. 4	4. 6	6. 2	5. 8	6. 0	Effectiveness for speed.
<i>L/D</i> at 2/3 <i>C_L</i> maximum--	14. 3	12. 8	10. 2	14. 8	15. 4	15. 0	Effectiveness for climb.
(<i>C_L³/C_D²)</i> maximum-----	171. 0	69. 6	98. 3	158. 2	118. 0	175. 4	Minimum power; maximum rate of climb; maximum absolute ceiling; maximum duration. (All with constant loading.)
<i>C_L</i> maximum/ <i>C_D</i> mini- mum.	52. 6	42. 9	47. 9	53. 6	49. 5	51. 6	Maximum speed with given minimum.
<i>C_L³/C_D²</i> maximum/ <i>C_D²</i> mini- mum.	3, 340	2, 130	2, 644	3, 228	2, 665	3, 016	Maximum speed ratio <i>V/V_o</i> .

¹ Navy Department.² See fig. 1.³ 8 by 8 feet.

REPORT No. 267

DRAG OF WINGS WITH END PLATES

By PAUL E. HEMKE
Langley Memorial Aeronautical Laboratory

REPORT No. 267

DRAG OF WINGS WITH END PLATES

By PAUL E. HEMKE

SUMMARY

In this report a formula for calculating the induced drag of multiplanes with end plates is derived. The frictional drag of the end plates is also calculated approximately. It is shown that the reduction of the induced drag, when end plates are used, is sufficiently large to increase the efficiency of the wing.

Curves showing the reduction of drag for monoplanes and biplanes are constructed; the influence of gap-chord ratio, aspect ratio, and height of end plate are determined for typical cases. The method of obtaining the reduction of drag for a multiplane is described.

Comparisons are made of calculated and experimental results obtained in wind tunnel tests with airfoils of various aspect ratios and end plates of various sizes. The agreement between calculated and experimental results is good.

Analysis of the experimental results shows that the shape and section of the end plates are important.

INTRODUCTION

The end plates which are dealt with in this report are fins or shields which are attached to the tips of airfoils; the plane of the fin is perpendicular to the span of the airfoil. The purpose of this device is to serve as a barrier to the flow along the span and around the tips of the airfoil. This flow in a vertical plane containing the span is usually called the transverse flow. By obstructing this transverse flow its kinetic energy is diminished and as a consequence the induced drag of the airfoil is thereby reduced.

From wind tunnel tests made at Göttingen (Reference 1) and at the Langley Memorial Aeronautical Laboratory (Reference 2), it has been learned that the induced drag may be materially reduced by the use of end plates. The reduction of the induced drag exceeds the additional frictional drag of the end plates which were used in these tests for all but small values of the lift coefficients.

The German tests were analyzed but the method of analysis gives no direct information on the value of the frictional drag of the end plates. The American tests have not been previously analyzed.

In this report a formula for calculating the induced drag of multiplanes with end plates is derived. The induced drag is calculated by finding the kinetic energy of the transverse flow using the method of conformal transformation. The induced drags of the monoplane and biplane with end plates are found as special cases of this general formula.

The formula for the monoplane is used to calculate the reductions of drag for the airfoils tested at Göttingen and the Langley Memorial Aeronautical Laboratory. Comparison of calculated and experimental results for airfoils of various aspect ratios with end plates of various sizes are made. Curves illustrating the total reduction of drag for monoplanes and biplanes are constructed; the influence of such major factors as gap-chord ratio, aspect ratio, and height of end plates is determined. In all cases the frictional drag of the end plates is considered in calculating the total drag.

INDUCED DRAG OF A MULTIPLANE WITH END PLATES

The longitudinal projection of the multiplane consists of equal, parallel straight lines. The same projection of the end plates will also be considered as straight lines whose directions are at right angles to the projection of the multiplane elements.

The induced angle of attack and consequently the induced drag depend upon the induced downwash. It is sufficient then for the purpose in hand to consider the transverse flow in a vertical plane at right angles to the air stream.

This two-dimensional transverse flow may be determined in several ways. In this report it has been obtained by using the method of conformal transformation. The rectilinear polygon bounding the longitudinal projection of the wings and end plates is transformed into a single straight line. The flow around such a line is well known.

Let the plane of the lines with end pieces be the plane of a complex variable z as shown in Figure 1. The mid-point of the system of lines is at the origin and the direction of the lines

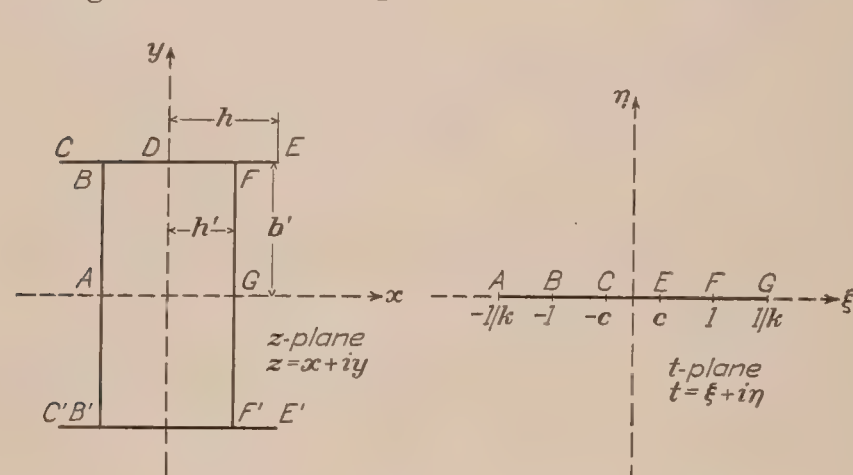


FIG. 1.—Conformal representation of biplane with end plates

coincides with that of the axis of imaginaries. The end pieces CE and C'E' are then parallel to the real axis and are each of length $2h$. The bounding rectangle BFF'B' has dimensions $2b' \times 2h'$. It is assumed that $h \geq h'$.

The transformation to an auxiliary t -plane is effected by means of the theorem usually called the Schwarz-Christoffel theorem. According to this theorem, if $z = x + iy$ and $t = \xi + i\eta$ then any polygon bounded by straight lines in the z -plane can be transformed into

the axis of ξ , points inside the polygon corresponding to points on one side of the axis of ξ . The transformation is

$$\frac{dz}{dt} = A(t - \xi_1)^{\frac{\alpha_1 - 1}{\pi}} (t - \xi_2)^{\frac{\alpha_2 - 1}{\pi}} \cdots (t - \xi_n)^{\frac{\alpha_n - 1}{\pi}} \quad (1)$$

where $\alpha_1, \alpha_2, \dots, \alpha_n$ are internal angles of the polygon in the z -plane and $\xi_1, \xi_2, \dots, \xi_n$ are the points on the axis of ξ that correspond to the angular points of the polygon in the z -plane and A is a real constant.

In our application we shall consider the polygon $-\infty A B C D E F + \infty$ in the z -plane as transformed into the upper half of the t -plane. By the theory if the point $\xi = \infty$ be taken to correspond with one corner of the polygon the corresponding factor in the expression for dz/dt is omitted. Also we may choose three values of ξ arbitrarily since a polygon similar to a given polygon of n sides may be constructed by means of $n - 3$ relations between the sides.

We shall accordingly choose the three points as follows:

	D	F	∞
z	ib'	$h' + ib'$	∞
t	0	1	∞

Then to the points E and G will correspond the values $\xi = c$ and $\xi = \frac{1}{k}$, respectively. The transformation is then found in the form

$$\frac{dz}{dt} = a \frac{(t^2 - c^2)}{\sqrt{(t^2 - 1)\left(t^2 - \frac{1}{k^2}\right)}}, \quad (2)$$

where a is a real constant.

We may integrate (2) by substituting $t = sn\omega \pmod{k}$. $sn\omega$ denotes an elliptic function and from the relations given in textbooks on these functions we find,

$$z = \frac{\alpha}{k} \left[Z(\omega) - \omega \left(1 - \frac{E}{K} - k^2 c^2 \right) \right] + \beta \quad (3)$$

Here $Z(\omega)$ is Jacobi's zeta-function.

The correspondence between the various points is exhibited in the following table:

A	B	C	D	E	F	G	∞
$z, -h'$	$-h' + ib'$	$-h + ib'$	ib'	$h + ib'$	$h' + ib'$	h'	∞
$t, -1/k$	-1	$-c$	0	c	1	$1/k$	∞
$\omega, -K + iK'$	$-K$	$-\omega_0$	0	ω_0	K	$K + iK'$	iK'

K and E are the complete elliptic integrals of the first and second kind, K' being the complete elliptic integral of the first kind for the comodulus k' ($k'^2 = 1 - k^2$).

Since $c = sn \omega_0$ we may now use the relation $1 - \frac{E}{K} - k^2 sn^2 \omega_0 = Z'(\omega_0)$. This relation is also found in textbooks on elliptic functions. The prime accent indicates differentiation with respect to the variable ω . We then have

$$z = \frac{\alpha}{k} [-\omega Z'(\omega_0) + Z(\omega)] + \beta, \alpha \text{ and } \beta \text{ constants.} \quad (4)$$

Using (4) and the correspondence given in the table we have the following equations:

$$\frac{\alpha}{k} [-\omega_0 Z'(\omega_0) + Z(\omega_0)] + \beta = h + ib' \quad (5)$$

$$\frac{\alpha}{k} [-K Z'(\omega_0)] + \beta = h' + ib' \quad (6)$$

$$\frac{\alpha}{k} [-(K + iK') Z'(\omega_0)] - \frac{i\pi}{2K} + \beta = h' \quad (7)$$

Solving these we have:

$$h = \frac{\alpha}{k} [Z(\omega_0) - \omega_0 Z'(\omega_0)]; \quad ib' = \beta$$

$$h' = -\frac{\alpha}{k} [(K) Z'(\omega_0)]$$

$$b' = \frac{\alpha}{k} \left[K' Z'(\omega_0) + \frac{\pi}{2K} \right]$$

$$\frac{h}{b'} = \frac{Z(\omega_0) - \omega_0 Z'(\omega_0)}{K' Z'(\omega_0) + \frac{\pi}{2K}} \quad (8)$$

$$\frac{h'}{b'} = \frac{-K Z'(\omega_0)}{K' Z'(\omega_0) + \frac{\pi}{2K}} \quad (9)$$

$$\text{If } \frac{h'}{b'} = \gamma, \quad Z'(\omega_0) = \frac{-\pi\gamma}{2K(K + \gamma K')} \quad (10)$$

$$\frac{\alpha}{k} = \frac{2b'(K + K'\gamma)}{\pi} \quad (11)$$

$$z = b' \left[\frac{2(K + \gamma K')}{\pi} Z(\omega) + \frac{\omega b'\gamma}{K} + i \right] \quad (12)$$

The transverse flow around the lines with end pieces is parallel to the real axis at infinity in the z -plane, the direction of flow at infinity being in the direction of the positive x -axis. The potential function for this flow is more easily expressed in terms of t . It is $\Phi_1 = \varphi_1 + i\psi_1 = \alpha Vt$, where V is the velocity of the flow in the z -plane at a great distance from the origin.

If we superimpose on this flow one whose potential function is $\Phi_2 = -Vz$ we shall have the potential function for the flow set up by the motion of the lines in a fluid otherwise at rest. The lines will move in the direction of the positive real axis in the z -plane with a constant velocity V .

To find the kinetic energy we evaluate the integral

$$-\frac{1}{2} \rho \int_L \varphi \frac{\partial \varphi}{\partial n} ds \quad (\text{Reference 3, p. 44}).$$

The path of integration, L , is the complete boundary of the wing, φ is the real part of $(\alpha Vt - Vz)$, $\frac{\partial \varphi}{\partial n}$ is the normal velocity component along the boundary and ds is the element of length of the boundary. We have

$$T = 2\rho V^2 \alpha^2 \frac{\pi}{2} \left[\frac{1}{2} \left(1 + \frac{1}{k^2} \right) - c^2 \right]$$

By using again the relation $1 - \frac{E}{K} - k^2 c^2 = Z'(\omega_0)$ as well as equations (10) and (11), we have

$$T = \frac{1}{2} \rho V^2 \frac{4b' (K + K'\gamma)^2}{\pi} \left[\frac{2E}{K} - k'^2 - \frac{\pi\gamma}{K(K + \gamma K')} \right] \quad (13)$$

This may be written $T = \frac{1}{2} \rho V^2 A_M$ where

$$A_M = \frac{4b'^2 (K + K'\gamma)^2}{\pi} \left[2 \frac{E}{K} - k'^2 - \frac{\pi\gamma}{K(K + K'\gamma)} \right] \quad (14)$$

Prandtl (Reference 4, p. 48) has shown that, if it is assumed that all air particles within an air stream of cross sectional area A_M are uniformly deflected downward by the wing and all outside are not deflected, then the correct lift and the correct work due to the induced drag are obtained by application of the impulse theorem and the energy theorem. Doctor Zahm has suggested that A_M be called the *area of the equivalent air stream* and this term will be used throughout the report.

As the minimum induced drag of the wing system is known to be $D_i = \frac{L^2}{4q A_M}$, where L is the lift and q the dynamic pressure, it may be computed by using equation (14).

THE MONOPLANE WITH END PLATES

The area of the equivalent air stream of the monoplane with end plates is found from (14) by setting $\gamma = 0$.

$$A_M = \frac{4b'^2 K^2}{\pi} \left(\frac{2E}{K} - k'^2 \right)$$

If the span is b we have

$$A_M = \frac{K^2 b^2}{\pi} \left[\frac{2E}{K} - k'^2 \right] \quad (15)$$

This reduces when $h' = h = 0$ to

$$A_M = \frac{\pi b^2}{4} \text{ which is known to be correct.}$$

The ratio of the area of the equivalent air stream of the monoplane to that of the monoplane with end plates is

$$R = \frac{\pi^2}{4K^2 \left(\frac{2E}{K} - k'^2 \right)} \quad (16)$$

Values of R were calculated in the following manner: When $\gamma = 0$, $Z'(\omega_0) = 0$, and ω_0 was then found from a table of elliptic functions (Reference 5) after the modulus k had been arbitrarily assigned. k is usually expressed as the sine of a modular angle, θ . Then $2h/b$ and R were calculated using equations (8) and (16).

Table I contains the values of R for various values of $2h/b$. The quantity J as given by Nagel (Reference 2) is related to R by the equation

$$R = \frac{\pi}{8J}$$

The value of R obtained by using the approximate formula

$$J = \frac{\pi}{8} + 0.6515 \left(\frac{2h}{b} \right) \text{ is also given in Table I.}$$

Let us consider now an airfoil whose span is b and chord c . We shall assume that the longitudinal projection of the airfoil is a straight line. The width of the end plate is taken as a chord length where no statement to the contrary is made. The coefficient of minimum induced drag is then

$$C_{Di} = \frac{C_L^2 S}{4A_M}$$

$C_L = \text{lift coefficient}$
 $S = \text{area of wing.}$

Using (16) this may be written

$$C_{Di} = \frac{C_L^2 R S}{\pi b^2} \quad (17)$$

The use of end plates introduces an additional frictional drag. This frictional drag may be designated D_F and is given by

$$D_F = C_F q S'$$

The end plates act as airfoils so that C_F is a drag coefficient and S' is the area of the two end plates.

The difference of total drag coefficient, C_D , and profile drag coefficient, C_{DP} , is

$$C_D - C_{DP} = \frac{C_L^2 R S}{\pi b^2} + C_F \frac{S'}{S}$$

The same expression for a wing without end plates is $\frac{C_L^2 S}{\pi b^2}$. To determine the actual gain with a given set of end plates we subtract these two expressions. If we call this difference ΔC_D , we have

$$\Delta C_D = \frac{C_L^2 S}{\pi b^2} (1 - R) - C_F \frac{S'}{S} \quad (18)$$

If the width of the end plate is a chord length and the height $2h$, then

$$\frac{S'}{S} = \frac{4ch}{cb} = \frac{4h}{b}$$

Then

$$\Delta C_D = \frac{C_L^2 S}{\pi b^2} (1 - R) - 2C_F \left(\frac{2h}{b} \right) \quad (19)$$

If we use

$$R = \frac{\pi}{8J} = \frac{1}{1 + 1.66 \left(\frac{2h}{b} \right)},$$

we have

$$\Delta C_D = \frac{C_L^2 S}{\pi b^2} \frac{1.66 \left(\frac{2h}{b} \right)}{1 + 1.66 \left(\frac{2h}{b} \right)} - 2C_F \left(\frac{2h}{b} \right) \quad (20)$$

From this the reduction of drag for a given end plate may be easily found. Figure 2 shows parabolas obtained from (20) by using a fixed value of b^2/S , C_F , and different sizes of end plates. For smaller values of b^2/S the slopes of the parabolas increase but the intersection points on the vertical axis are not altered. There is consequently a greater average reduction of drag for the smaller values of b^2/S over the usual range of values of the lift coefficient.

ANALYSIS OF WIND TUNNEL RESULTS

The Göttingen tests (Reference 1) were made with single airfoils. The end plates were flat and of various shapes and sizes. Two aspect ratios were used, 8/3 and 4/3. In the analysis made of these tests the frictional drag of the end plates was not actually calculated. In this report this quantity has been calculated approximately.

Figures 3, 4, and 5 show the results of the Göttingen tests, for aspect ratio 8/3, in the form of polar curves. In each case except for end plate 3, Figure 4, the reduction of drag was computed from formula (19) using the appropriate value of aspect ratio, ratio of length of end plate to span and area of end plates. In the case of end plate 3, since the end of the wing was only partially shielded, an average height of the plate, over the chord, was used. The value of C_F which gave the best agreement for the frictional drag of the end plates is 0.0140.

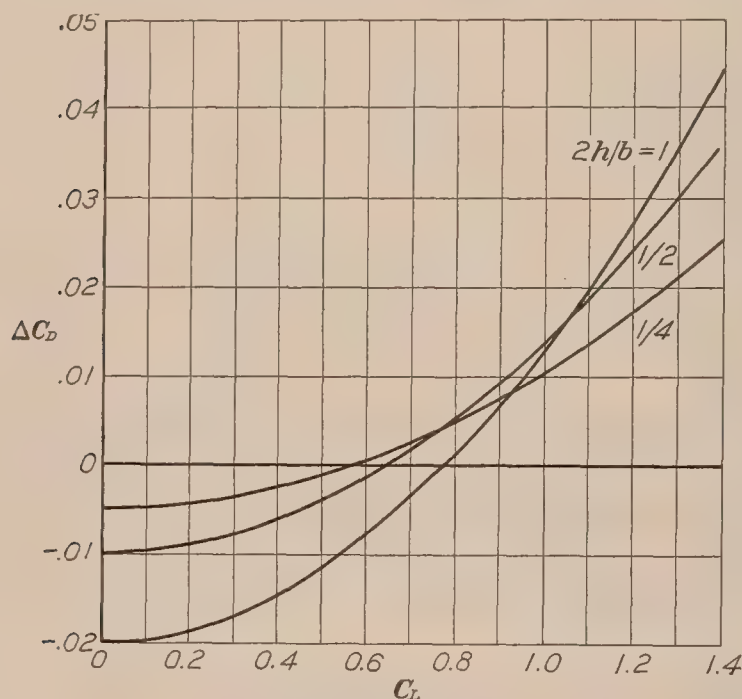


FIG. 2.—Monoplane with end plates. Calculated reduction of drag, ΔC_D , against lift coefficient for various values of $2h/b$. $2h$ =height of end plate. b =span. Aspect ratio, 6. Drag coefficient, $C_F=0.01$

Laboratory. Single airfoils, wing section N. A. C. A. 73, with aspect ratio 6 were used in these tests. Only two plates, one circular, the other trapezoidal, were tried. These plates were streamlined and consequently the value of C_F to be used in making the calculations is different. The value 0.008 (Reference 1) proved satisfactory.

The results of these tests are shown graphically in Figures 6 and 7. The reduction of drag was calculated as before, C_F only being changed in value. Since tabular values are available much closer comparison could be made. The calculated and observed reductions of drag are shown in tabular form in Table II, and graphically in Figures 6, 7, and 8. The agreement is good, considering that we have only an approximation to the actual reduction in consequence of the simplifying assumptions made in the calculations.

Comparing the two series of tests we see that theory and experiment show a larger reduction of drag for smaller aspect ratios. The use of end plates with good aerodynamical profile sections is preferable since this reduces the drag for all values of C_L . This is illustrated by the two series of tests studied; in one the coefficient is 0.014, and in the other 0.008.

The agreement between calculated and observed reductions of drag in the American tests suggests using an end plate of given area in the best possible way. Since the use of the entire height of the trapezoidal end plate (fig. 6) in the formula gave calculated results agreeing very

This calculated reduction of drag was then laid off on each diagram starting from the polar obtained when using the wing without end plates. Unfortunately, no tabular values of drag and lift coefficients were given in the Göttingen report. Consequently, no accurate comparisons of calculated and observed reduction of drag could be made.

On the whole, the agreement between calculated and observed reductions of drag is good for that portion of the polar curve where the angles of attack are smaller than the burbling angle. The use of a partial end plate such as end plate 3 is not satisfactory. In this instance the disturbance of flow around the end of the wing apparently increases the frictional drag at low values of C_L and the reduction of drag is not as great at the higher values of C_L .

The American tests (Reference 2) were made at the Langley Memorial Aeronautical

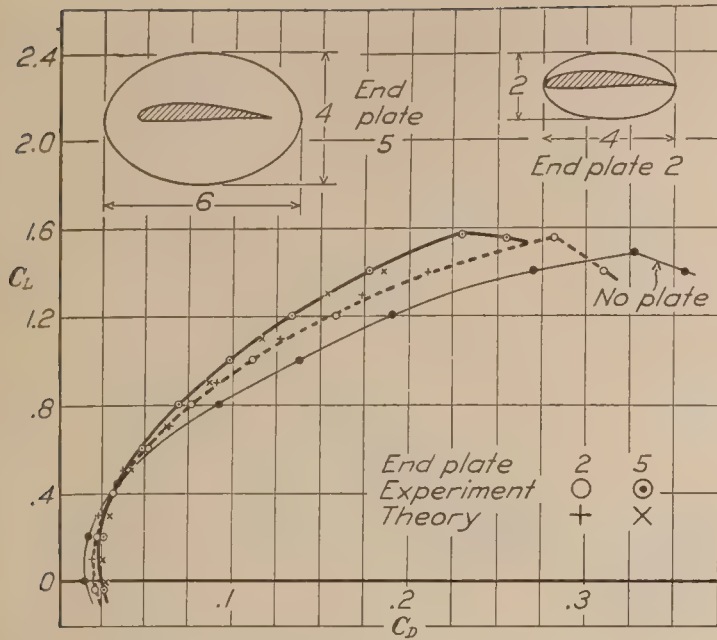


FIG. 3.—Polar curves of Göttingen tests showing reduction of drag due to end plates 2 and 3. Aspect ratio 8/3

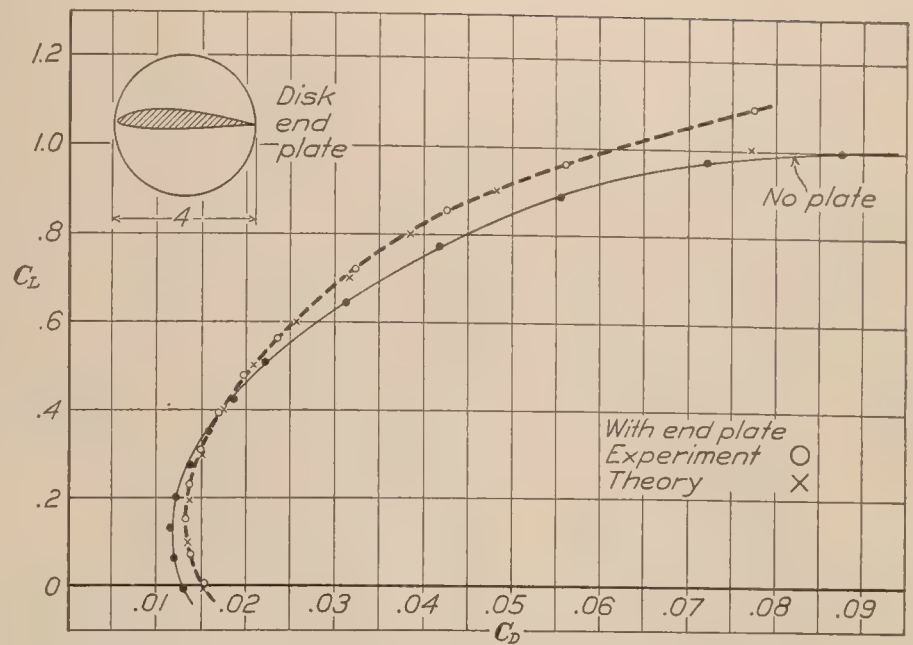


FIG. 6.—Polar curves of N. A. C. A. tests showing reductions of drag due to disk end plates. N. A. C. A. 73 airfoil. Aspect ratio, 6

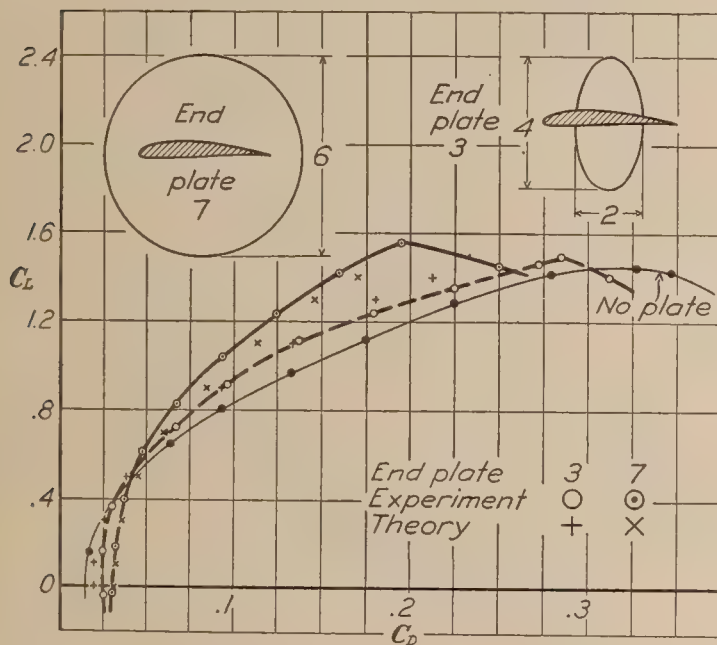


FIG. 4.—Polar curves of Göttingen tests showing reduction of drag due to end plates 3 and 7. Aspect ratio, 8/3

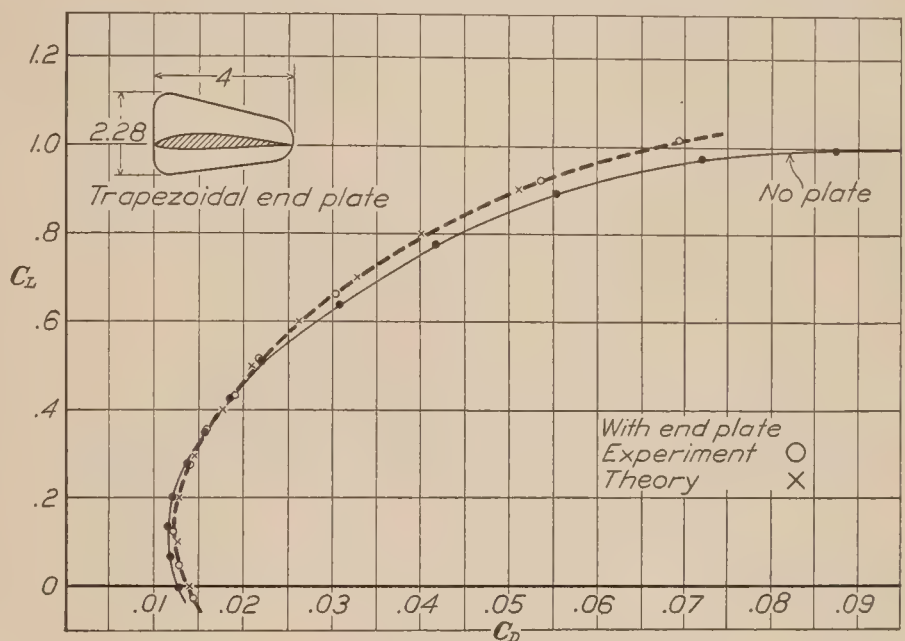


FIG. 7.—Polar curves of N. A. C. A. tests showing reductions of drag due to trapezoidal end plates. N. A. C. A. 73 airfoil. Aspect ratio, 6

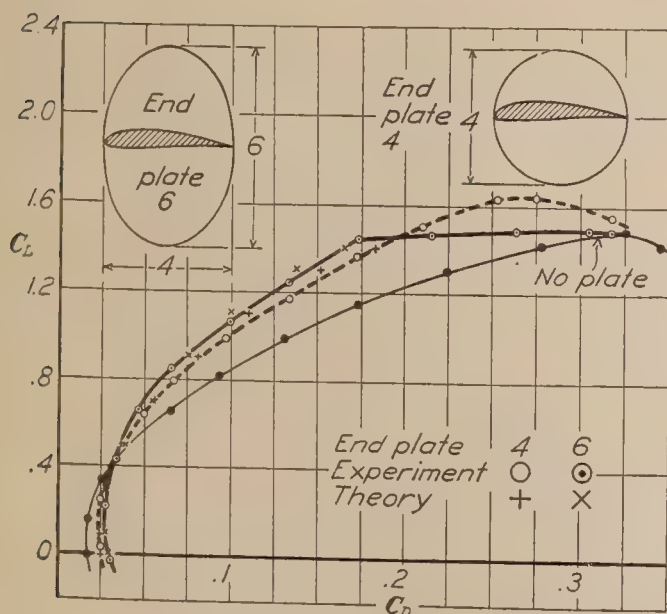


FIG. 5.—Polar curves of Göttingen tests showing reduction of drag due to end plates 4 and 6. Aspect ratio, 8/3

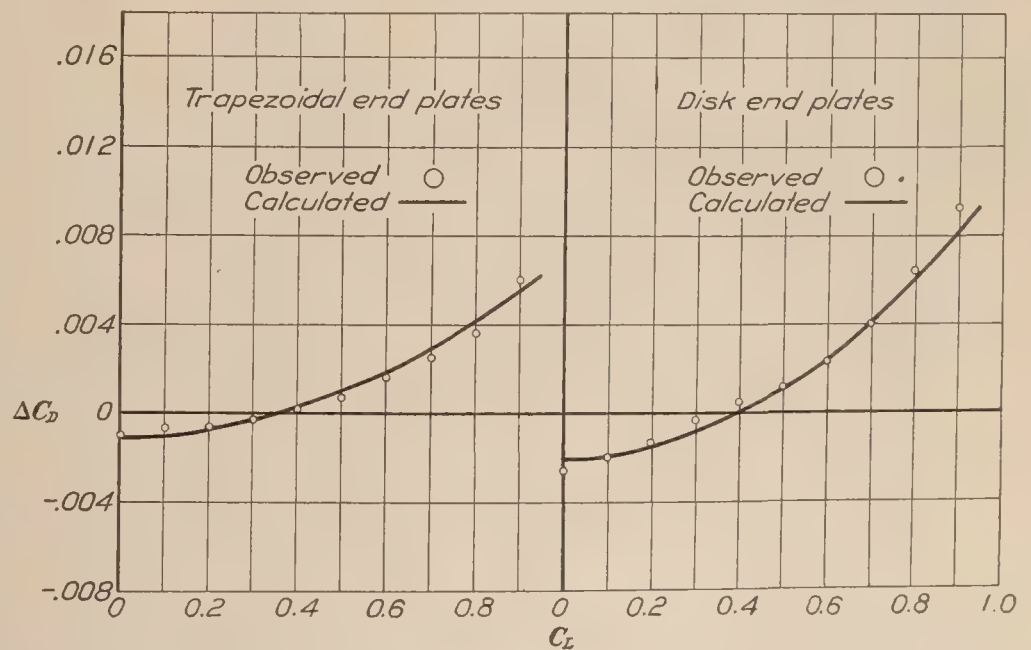


FIG. 8.—Calculated and observed differences of drag of wings with different end plates. N. A. C. A. 73 airfoil. Aspect ratio, 6

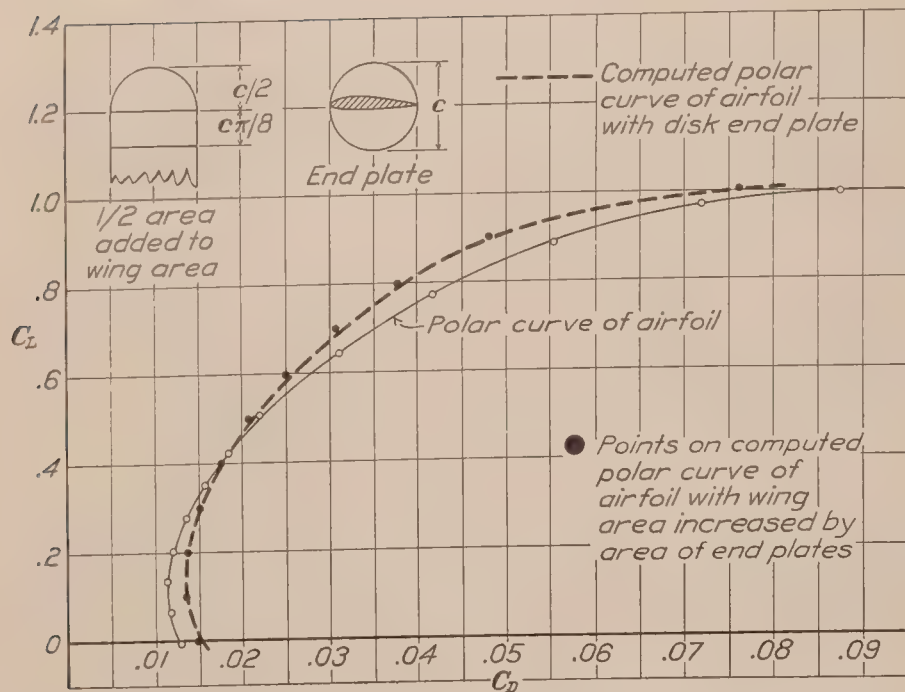


FIG. 9.—Calculated reduction of drag using disk end plates and increasing wing area by an amount equal to area of end plates. N. A. C. A. 73 airfoil. Aspect ratio, 6

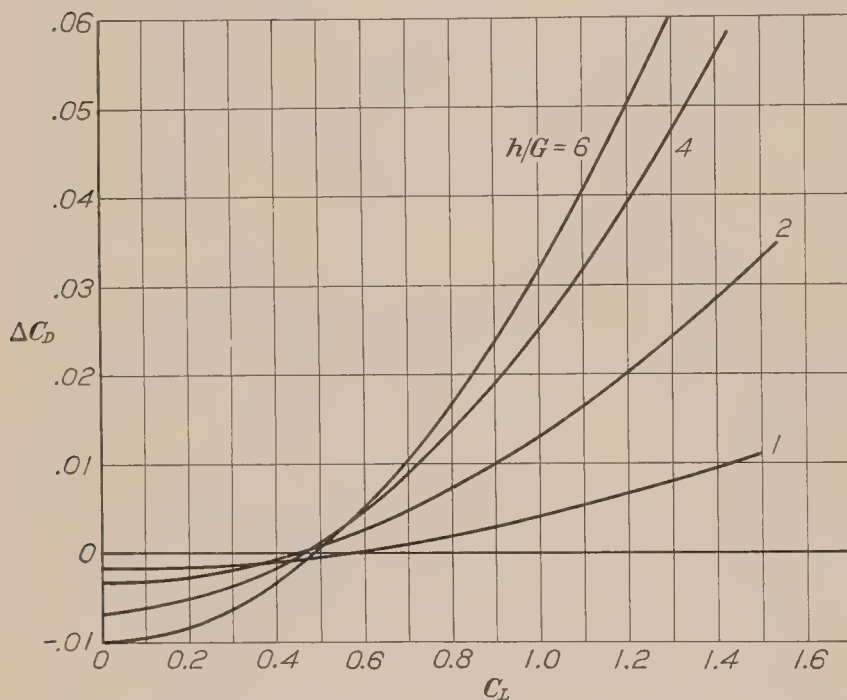


FIG. 10.—Biplanes with end plates. Calculated reduction of drag, ΔC_D , plotted against lift coefficient for various values of h/G . $2h$ =height of end plate. $2G$ =gap. Span/chord=6. Gap/chord=0.6. Drag coefficient, $C_F=0.01$

well with observed results, it appears that an end plate of a given area, and therefore having a fixed frictional drag, may have a greater effect on the drag in one shape than in another. In particular, the tests and calculations with this end plate make it seem plausible that the greater part of the restriction of the transverse flow occurs over the forward portion of the span and that a shape which has greater height in the portion nearer the leading edge is advantageous to use.

Nagel (Reference 1) has stated that the reduction of drag when using end plates, does not equal the corresponding reduction obtained when the span is increased by an amount equal to the sum of the heights of the end plates. The reason for adding to the span an amount equal to the total height of end plates is not quite evident. The addition to the span might also be made, with as good reason, by adding to the wing area the sum of the areas of the two end plates. Such a comparison is shown graphically in Figure 9. The polar curve of an airfoil is shown compared with the computed polar curves when end plates are added to the wing and

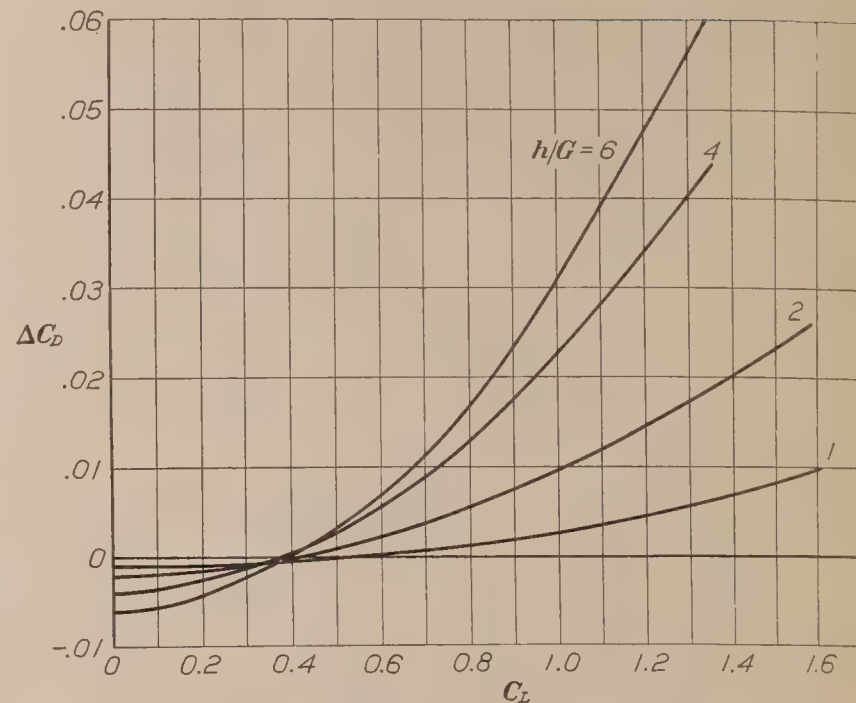


FIG. 11.—Biplanes with end plates. Calculated reduction of drag, ΔC_D , plotted against lift coefficient for various values of h/G . $2h$ =height of end plate. $2G$ =gap. Span/chord=6. Gap/chord=1.00. Drag coefficient, $C_F=0.01$

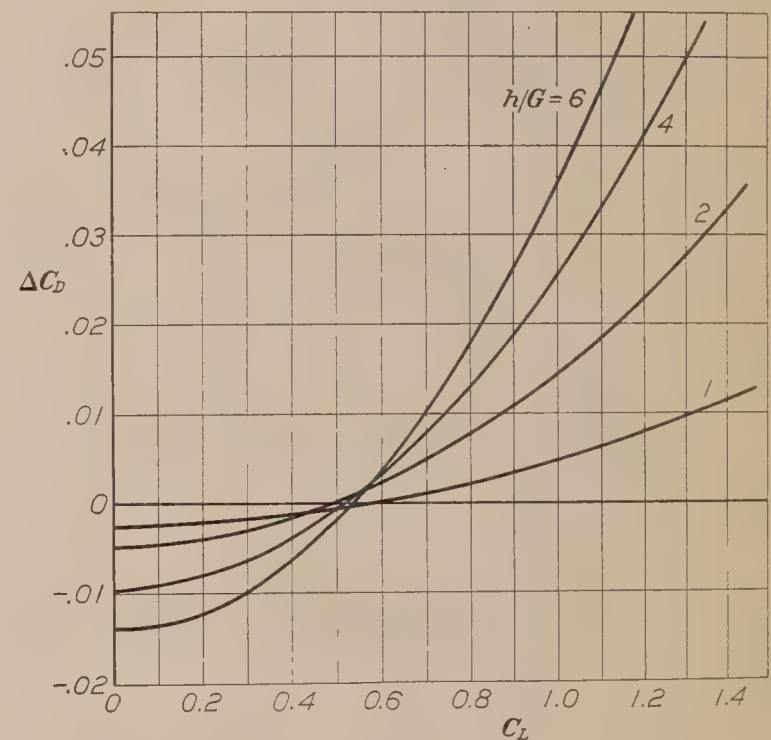


FIG. 12.—Biplanes with end plates. Calculated reduction of drag, ΔC_D , plotted against lift coefficient for various values of h/G . $2h$ =height of end plate. $2G$ =gap. Span/chord=6. Gap/chord=1.40. Drag coefficient, $C_F=0.01$

when the wing area is increased by an amount equal to the total area of the end plates. The comparison was made using the same drag coefficient for the end plates as for the additional wing area. The results do not differ much.

CALCULATED REDUCTION OF DRAG FOR MULTIPLANES WITH END PLATES

The method will be used to calculate first the reduction of drag for a biplane. The area of the equivalent air stream for a biplane with end plates is given by equation (14). The end plates must have heights equal to or greater than the gap of the biplane, for otherwise the flow would change to such an extent that (14) would no longer hold. This formula reduces when $h = h'$, that is, when the end plate has a height equal to the gap of the biplane, to one which has been previously derived (Reference 6). It is evident from the correspondence of values between z , t and ω that when

$$h = h', \quad \omega_0 = K, \quad Z(\omega_0) = 0 \quad \text{and} \quad Z'(\omega_0) = 1 - \frac{E}{K} - k^2.$$

From (10) we find then

$$\gamma = \frac{E - K k'^2}{E' - K' k^2} \quad \text{and} \quad A_M = \pi b^2 \cdot \frac{k'^2}{E' - k^2 K'}.$$

For a span b this reduces to

$$A_M = \frac{\pi b^2}{4} \cdot \frac{k'^2}{E' - k^2 K'}$$

which is the value previously found.

The expression for reduction of drag is derived in a manner quite similar to that used for the monoplane. We find

$$\Delta C_D = \frac{C_L^2}{2} \left(\frac{c}{b} \right) \left(\frac{b^2}{A_M} - \frac{b^2}{A_{M_1}} \right) - C_F \left(\frac{2h}{b} \right).$$

b = span of biplane.

c = chord.

C_L = lift coefficient.

A_M = area of the equivalent air stream of a biplane without end plates.

A_{M_1} = area of the equivalent air stream of a biplane with end plates.

C_F = drag coefficient of end plates.

$2h$ = height of end plate (width assumed to be c).

If we introduce Prandtl's ratio $x = \frac{\pi b^2}{4 A_M}$ and a similar ratio

$$x_1 = \frac{\pi b^2}{4 A_{M_1}} \quad \text{we have}$$

$$\Delta C_D = \frac{2 C_L^2}{\pi} \frac{c}{b} (x - x_1) - C_F \left(\frac{2h}{b} \right) \quad (22)$$

The value of x_1 depends on both the gap/chord ratio and the ration of height of end plate to gap. The former ratio is γ and has been chosen in each calculation. The calculations were made in the following manner:

(a) $Z'(\omega_0)$ was found from $Z'(\omega_0) = \frac{\pi \gamma}{2 K (K + \gamma K')}$, after γ has been arbitrarily assigned.

(b) From $dn^2 \omega_0 = \frac{E}{K} + Z'(\omega_0)$, ω_0 was found using the table of elliptic functions (Reference 4).

(c) The value of $\frac{2h}{b} = \frac{Z(\omega_0) - \omega_0 Z'(\omega_0)}{\frac{\pi}{2 K} + K' Z'(\omega_0)}$ was calculated next.

(d) $A_{M_1} = \frac{b^2 (K + K' \gamma)^2}{\pi} \left[2 \frac{E}{K} - k'^2 - 2 Z'(\omega_0) \right]$ was evaluated then quite easily.

Figures 10, 11, and 12 show the calculated reductions of drag for span/chord of 6 and gap/chords of 0.6, 1.0, and 1.4. In each case the following values of h/h' were used; $h/h' = 1, 2, 4, 6$ and, as in Figure 2, the value $C_F = .01$ was used as it represents an average value of C_F .

The curves illustrate how properties of end plates affect biplanes of various proportions. The increase of drag at lower values of C_L is considerably less than it is for larger values of gap/chord while the reduction of drag, especially when larger plates are used, is relatively large.

The reduction of drag persists at the higher values of C_L for plates which are quite large, so large as to be useless in practice.

The method used in calculating the effect of end plates for biplanes may be used for multiplanes. Formula (22) would differ only as far as x is concerned. This quantity may be calculated, however (Reference 7), and the reductions of drag for multiplanes may be calculated in precisely the same manner as that just described and carried out for biplanes.

CONCLUSIONS

Calculations show that the induced drag of monoplanes and multiplanes may be decreased by attaching end plates to the ends of the wing. The frictional drag of the end plates may be calculated approximately. The reduction of the induced drag exceeds the additional frictional drag due to the end plates at all but small values of the lift. For given dimensions of wings and end plates the reduction of drag less the frictional drag of the end plates varies directly as the square of the absolute lift coefficient. The average reduction of drag increases as the aspect ratio decreases. Calculations and experiments agree quite satisfactorily for single wings equipped with end plates.

Wind tunnel tests show that the coefficient used in calculating the frictional drag of the end plates may be reduced materially by fairing the end plates. The shape of the end plate determines to some extent the reduction of induced drag. Further tests would be necessary to find end plates of good shape and having at the same time a low drag coefficient.

Recent experiments have shown that much higher lift coefficients can be obtained than has been the case up to now with the conventional airfoils. Since the reduction of drag due to end plates is much greater at the higher values of the lift coefficient, the use of end plates together with the use of means for increasing the lift will result in a material improvement of the efficiency of the present-day airplane.

LANGLEY MEMORIAL AERONAUTICAL LABORATORY,
NATIONAL ADVISORY COMMITTEE FOR AERONAUTICS,
LANGLEY FIELD, VA., *January 20, 1927.*

REFERENCES

1. NAGEL, F.: Flügel mit seitlichen Scheiben. "Vorläufige Mitteilungen der Aerodynamischen Versuchsanstalt zu Göttingen," No. 2, July, 1924.
2. REID, E. G.: The Effect of Shielding the Tips of Airfoils. N. A. C. A. Technical Report No. 201, 1925.
3. LAMB, H.: Hydrodynamics—Fifth edition, 1924.
4. PRANDTL, L.: Applications of modern Hydrodynamics to Aeronautics. N. A. C. A. Technical Report No. 116, 1925.
5. HIPPISEY, R. L.: Smithsonian Mathematical Formulae and Tables of Elliptic Functions. Smithsonian Miscellaneous Collections. Volume 74, No. 1, 1922.
6. Tragflügel Theorie, zweite Mitteilung. (Nachrichten der Königlichen Gesellschaft der Wissenschaften zu Göttingen. Mathematische-Physikalische, 1919.)
7. PRANDTL, L.: Induced Drag of Multiplanes. N. A. C. A. Technical Note No. 182, 1924.

TABLE I

Values of R and $2h/b$ for given values of θ .
 $R = (\text{area of the equivalent air stream of a monoplane})/(\text{area of the equivalent air stream of a monoplane with end plates})$.
 $2h/b = (\text{height of end plate})/(\text{span of wing})$.

θ degrees	$2h/b$	R	Nagel's formula	Per cent difference
15	0. 0173	0. 971	0. 974	+0. 33
20	. 0311	. 948	. 951	. 32
25	. 0493	. 909	. 925	1. 76
30	. 0721	. 877	. 895	2. 05
35	. 0996	. 844	. 859	1. 78
40	. 133	. 800	. 820	2. 50
45	. 173	. 751	. 777	3. 47
50	. 222	. 704	. 731	3. 83
55	. 285	. 653	. 678	3. 80
60	. 349	. 610	. 633	3. 77
65	. 433	. 562	. 582	3. 56
70	. 541	. 508	. 527	3. 74
75	. 686	. 452	. 468	3. 15
80	. 897	. 395	. 401	+1. 52
85	1. 27	. 323	. 321	-. 62
88	1. 78	. 261	. 252	-3. 45
89	2. 17	. 227	. 217	-4. 40

TABLE II

OBSERVED AND CALCULATED REDUCTION OF DRAG

[Tests made at Langley Memorial Aeronautical Laboratory. Monoplane, 4 by 24 inches; wing section, N. A. C. A. 73]

C_L	C_D (disk end plates)		Difference of observed and calculated reduction as per cent of drag	C_D (trapezoidal end plates)		Difference of observed and calculated reduction as per cent of drag
	Observed	Calculated		Observed	Calculated	
0	-0. 0026	-0. 00210	+3. 90	-0. 0010	-0. 00113	-0. 18
. 1	-. 0020	-. 00196	+. 35	-. 0007	-. 00105	-3. 50
. 2	-. 0013	-. 00159	-2. 40	-. 0007	-. 0008	-. 83
. 3	-. 0003	-. 00095	-4. 60	-. 0003	-. 00039	-. 63
. 4	+. 0005	-. 00005	+3. 15	+. 00020	-. 00018	+. 11
. 5	+. 0012	+. 00110	+. 95	. 0007	+. 00092	-1. 00
. 6	+. 0023	+. 00250	-. 72	+. 0016	+. 00183	-. 82
. 7	+. 0038	. 00412	-. 90	+. 0027	+. 00289	-. 54
. 8	+. 0064	. 00604	+. 82	+. 0036	+. 00413	-1. 21
. 9	+. 0093	. 00826	+1. 82	+. 0060	+. 00553	+. 83
1. 0	+. 0180	. 01060	+8. 22	+. 0162	+. 00708	+10. 10

REPORT No. 268

**FACTORS IN THE DESIGN
OF CENTRIFUGAL TYPE INJECTION VALVES
FOR OIL ENGINES**

**By W. F. JOACHIM and E. G. BEARDSLEY
Langley Memorial Aeronautical Laboratory**

REPORT No. 268

FACTORS IN THE DESIGN OF CENTRIFUGAL TYPE INJECTION VALVES FOR OIL ENGINES

BY W. F. JOACHIM and E. G. BEARDSLEY

SUMMARY

This research was undertaken at the Langley Memorial Aeronautical Laboratory, at Langley Field, Va., in connection with a general study of the application of the fuel injection engine to aircraft. The purpose of the investigation was to determine the effect of four important factors in the design of a centrifugal type automatic injection valve on the penetration, general shape, and distribution of oil sprays.

The general method employed was to record the development of single sprays by means of special high-speed photographic apparatus capable of taking 25 consecutive pictures of the moving spray at a rate of 4,000 per second. Investigations were made concerning the effects on spray characteristics, of the helix angle of helical grooves, the ratio of the cross-sectional area of the orifice to that of the grooves, the ratio of orifice length to diameter, and the position of the seat. The sprays were injected at 6,000, 8,000, and 10,000 pounds per square-inch pressure into air at atmospheric pressure and into nitrogen at 200, 400, and 600 pounds per square-inch pressure. Orifice diameters from 0.012 to 0.040 inch were investigated.

It was found that decreasing the pitch of the helical grooves and thus increasing the centrifugal force applied to the spray increased the spray cone angle considerably, although the percentage increase was much less in dense air than in the atmosphere. On the other hand, the spray penetration decreased with increase in the amount of centrifugal force applied. About twice as much spray volume per unit oil volume was obtained with a high centrifugal spray as with a noncentrifugal spray. The spray cone angle increased, and the spray volume to oil volume ratio and spray penetration decreased with increase in the ratio of orifice area to groove area. Maximum spray penetration was obtained with a ratio of orifice length to diameter of about 1.5. Slightly greater penetration was obtained with the seat directly before the orifice.

INTRODUCTION

The centrifugal type injection valve is used to-day in a considerable number of oil-injection engines. Also, the centrifugal type oil burner, which employs the same principle, is used successfully with steam boilers burning fuel oil. In both cases the rotation of the oil is usually accomplished by passing it through helical grooves.

Oil sprays from injection valves, which depend entirely upon forcing the oil through small cylindrical holes to break it up, are finely atomized near the spray surface, especially at the spray tip, but have a core which is but little atomized. The possibility of obtaining more complete atomization and greater distribution of the oil particles by the use of centrifugal force has been studied by many investigators. (References 1 to 6.) The performance of engines operating with centrifugal-type injection valves often differs from that which was expected from observation of the sprays from these valves in the atmosphere. The explanation is presumably that the dense air of the engine cylinder has unexpected effects upon the sprays. Some knowledge of the behavior of centrifugal sprays in dense air should facilitate the successful application of this type of injection valve to engine service.

Computations have been made by several investigators of the penetration of single oil drops of small size when injected at high initial velocity into dense air. (References 1 and 2.) While these computations may show the approximate penetration of single oil drops, the behavior of sprays composed of millions of such drops is considerably different from that of single drops.

There are many variables in the design of a centrifugal injection valve and each variable may have a considerable effect upon spray characteristics. The purpose of this research was to investigate the effect of four important factors in the design of a centrifugal-type automatic injection valve upon the penetration, general shape, and distribution of oil sprays. The factors investigated were the helix angle of the grooves, the ratio of the cross-sectional area of the orifice to that of the grooves, the ratio of orifice length to diameter, and the position of the seat.

A high-grade Diesel engine fuel oil of specific gravity 0.85 at 80° F. was used in all tests. It was injected at pressures of 6,000, 8,000, and 10,000 pounds per square inch into a chamber containing air at atmospheric pressure and nitrogen at pressures of 200, 400, and 600 pounds per square inch. The injection period was 0.003 second. The opening pressure of the automatic injection valve was maintained at 5,000 pounds per square inch throughout the tests.

Although the density of the gases in an engine cylinder seldom exceeds the density of air at room temperature and 250 pounds per square inch, the results presented cover a range of conditions permitting extended physical analysis. The effects of cylinder air temperature on the fuel spray may also lead to results comparable with those for the high chamber pressures.

This investigation was carried out at the Langley Memorial Aeronautical Laboratory of the National Advisory Committee for Aeronautics, at Langley Field, Va.

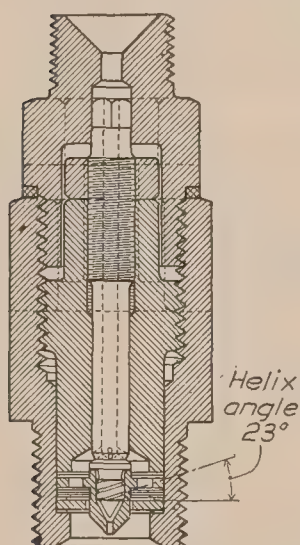


FIG. 1.—Diaphragm type automatic injection valve used with various stem and nozzle assemblies throughout this investigation

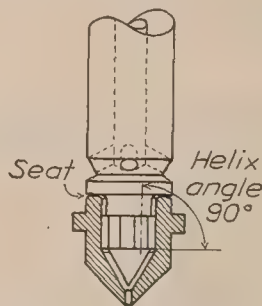


FIG. 2.—Stem with seat at top of nozzle

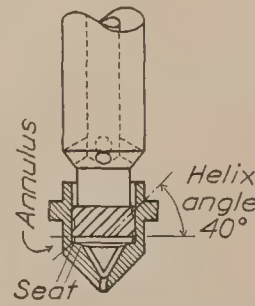


FIG. 3.—Stem with seat inside of nozzle

METHODS AND APPARATUS

The general method employed in this investigation was to record the development and cut-off of single sprays produced by an automatic injection valve, by means of special high-speed photographic apparatus capable of taking 25 consecutive pictures of the moving spray at a rate of 4,000 per second. Descriptions of the spray photography apparatus which was used for this work have been published by the National Advisory Committee for Aeronautics. (References 7 and 8.)

Cross sections of the assembled injection valve and of the two types of stem and nozzle used are shown in Figures 1, 2, and 3. A diaphragm-type automatic injection valve (Reference 8) was used for all tests and was fitted with the stem and nozzle which each test required. The type of stem and the nozzle used in all but one test are shown in Figure 2. The flat surface of the projecting ledge near the end of the stem seats on the V-shaped top edge of the nozzle. The other type of stem and the nozzle used are shown in Figure 3. In this case the stem seats on a 15° ledge inside of the nozzle. With the seat at the top of the nozzle the oil passed through the helical grooves after it passed through the seat. With the second seat position the pressure on the oil which passed through the grooves was not materially throttled until it reached the seat directly before the orifice. Table I gives the injection valve assemblies used in this investigation.

TABLE I

INJECTION VALVE ASSEMBLIES USED FOR INVESTIGATION OF EFFECT OF VALVE DESIGN

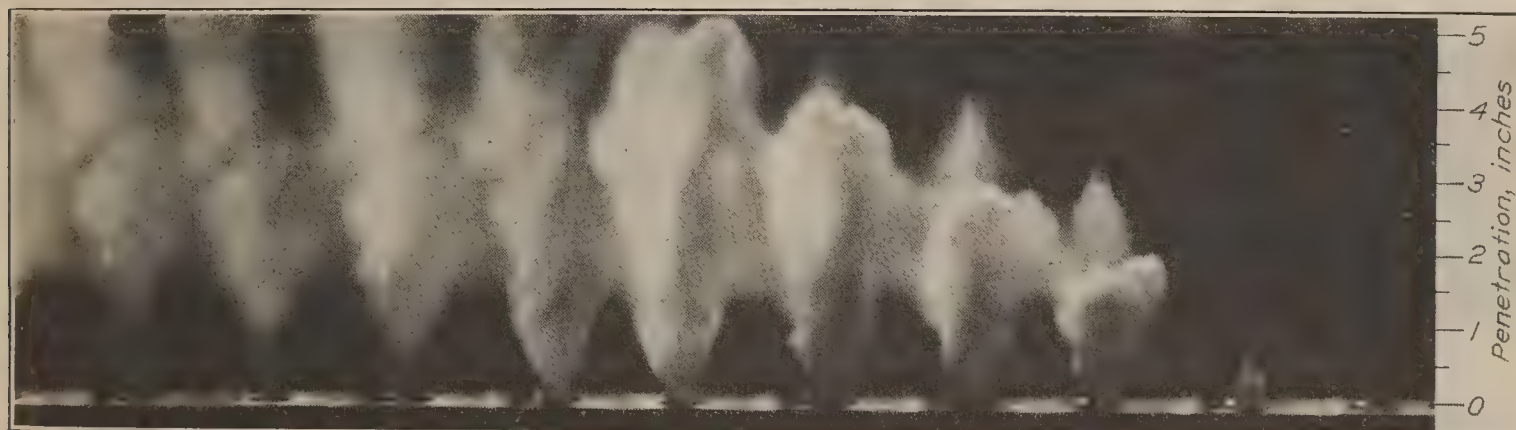
Assem- bly No.	Orifice diameter	Ratio orifice length to di- ameter	Groove helix angle	Num- ber of grooves	Total groove area	Ratio orifice area to groove area	Nozzle seat posi- tion	Remarks
	<i>Inch</i>		<i>°</i>		<i>Square inch</i>			
1	0.022	2	23	4	0.00060	0.63	Top----	{ Effect of groove helix angle.
2	.022	2	40	6	.00060	.63	---do---	
3	.022	2	90	4	.00060	.63	---do---	
4	.012	2	23	4	.00060	.19	---do---	{ (A) Effect of constant groove area.
5	.022	2	23	4	.00060	.63	---do---	
6	.040	2	23	4	.00060	2.05	---do---	{ (B) Effect of constant orifice area.
7	.022	2	23	4	.00060	.63	---do---	
8	.022	2	23	4	.00205	.19	---do---	{ Effect of ratio of ori- fice area to groove area.
9	.022	2.6	40	6	.00060	.63	---do---	
10	.022	1.7	40	6	.00060	.63	---do---	
11	.022	.2	40	6	.00060	.63	---do---	{ Effect of ratio of ori- fice length to di- ameter.
12	.022	2	40	6	.00060	.63	---do---	
13	.022	2	40	6	.00060	.63	Inside--	{ Effect of seat posi- tion.

In order to obtain information concerning the actual spray characteristics, measurements were made of the spray images on photographic films. Time-penetration curves were plotted from data computed from these measurements taking into account the film speed and photographic reduction. Spray volumes were computed by summation of the volumes of a number of disks into which each spray was divided for volume measurements. It was assumed that the sprays were symmetrical in their cross sections.

RESULTS

EFFECT OF GROOVE HELIX ANGLE

The results of the tests in which the 90°, 40°, and 23° helical grooves were used are given in Figures 4 to 15. This range of groove angles gives at one extreme a noncentrifugal spray and at the other a high-centrifugal spray.



Injection pressure, 8,000 pounds per square inch

Chamber pressure, atmospheric



Injection pressure, 8,000 pounds per square inch

Chamber pressure, 200 pounds per square inch

FIG. 4.—Spray photographs for stem and nozzle assembly No. 1, 0.022 inch diameter orifice, 23° helix and ratio of orifice area to groove area 0.63



Injection pressure, 8,000 pounds per square inch

Chamber pressure, atmospheric



Injection pressure, 8,000 pounds per square inch

Chamber pressure, 200 pounds per square inch

FIG. 5.—Spray photographs for stem and nozzle assembly No. 2, 0.022 inch diameter orifice and 40° helix



Injection pressure, 8,000 pounds per square inch

Chamber pressure, atmospheric



Injection pressure, 8,000 pounds per square inch

Chamber pressure, 200 pounds per square inch

FIG. 6.—Spray photographs for stem and nozzle assembly No. 3, 0.022 inch diameter orifice and 90° helix

Figures 4, 5, and 6 are reproductions of actual photographs taken during the investigations. Each figure contains two series of pictures of the development of single sprays injected at 8,000 pounds per square inch pressure into atmospheric and into 200 pounds per square inch chamber pressure. The pointed sprays seen advancing ahead of the main sprays in

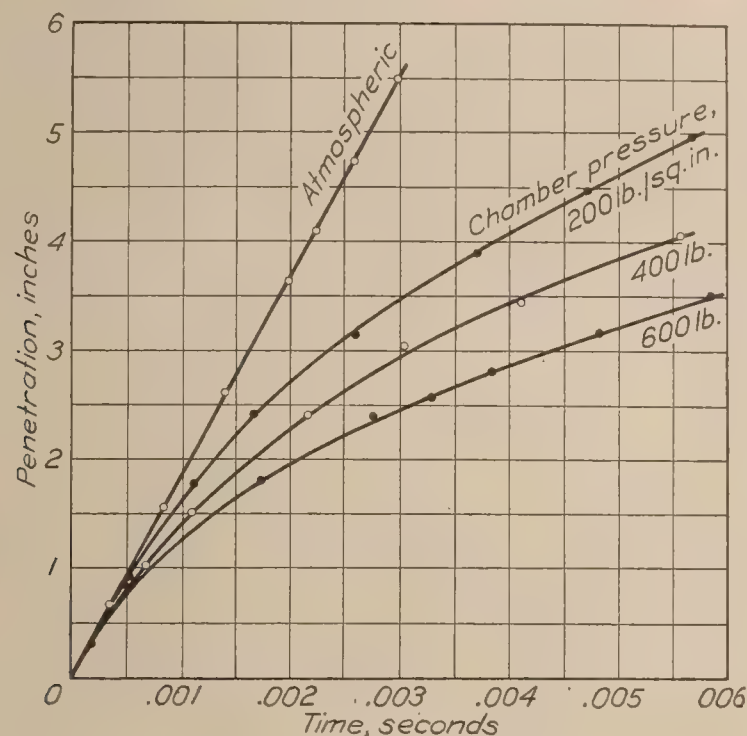


FIG. 7.—Effect of chamber pressure on spray penetration. Orifice diameter 0.022 inch. Groove helix angle 23°. Injection pressure, 8,000 pounds per square inch. Cut-off after 0.003 second. Stem and nozzle assembly No. 1

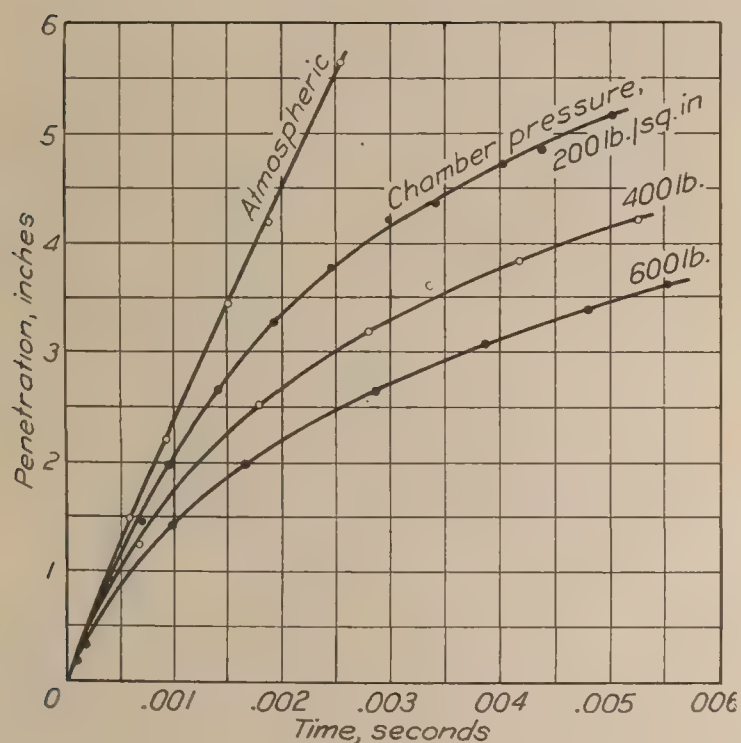


FIG. 8.—Effect of chamber pressure on spray penetration. Orifice diameter 0.022 inch. Groove helix angle 40°. Injection pressure 8,000 pounds per square inch. Cut-off after 0.003 second. Stem and nozzle assembly No. 2

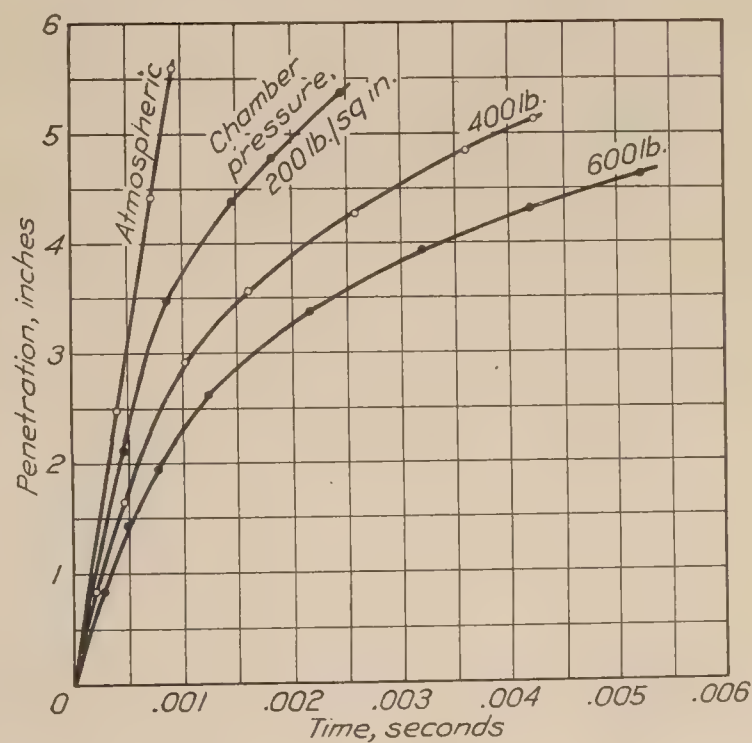


FIG. 9.—Effect of chamber pressure on spray penetration. Orifice diameter 0.022 inch. Groove helix angle 90°. Injection pressure, 8,000 pounds per square inch. Cut-off after 0.003 second. Stem and nozzle assembly No. 3.

Figures 4 and 5 are formed by oil trapped between the seat and the orifice which receives no rotation.

Figures 7, 8, and 9 are graphs showing the variation of penetration with time for a valve using each of the three-groove helix angles investigated, all other details of valve design and

of testing being maintained constant. The sprays were injected at 8,000 pounds per square inch pressure into the atmosphere and also into a chamber containing nitrogen at 200, 400, and 600 pounds per square inch pressures. Other pictures were taken using 6,000 and 10,000 pounds per square inch injection pressures and the four chamber pressures mentioned. In each case the penetration of the sprays increased with the injection pressure.

The effects of three-groove helix angles on the velocity and deceleration of the sprays in dense air at 200 pounds per square inch pressure are shown in Figures 10 and 11. Although the initial velocity of the sprays (fig. 10) was very much greater when the straight or 90° grooves were used, the velocity after 0.0025 second was the same for all three-groove angles. Thus the deceleration was more rapid for the spray produced with the straight grooves than for the 40° and 23° grooves, as is clearly shown by Figure 11. This rapid deceleration was accompanied by a rapid loss of kinetic energy by the spray. This energy presumably went

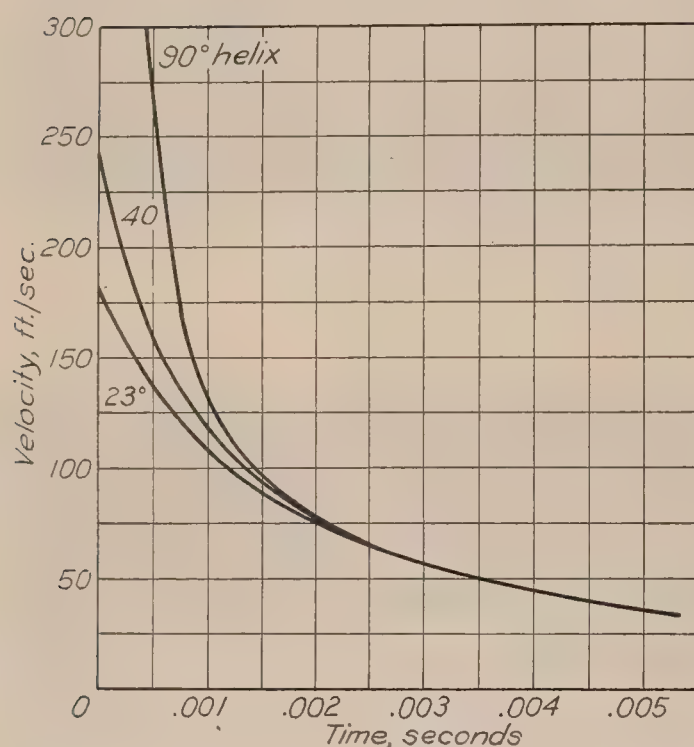


FIG. 10.—Effect of groove helix angle on spray tip velocity. Orifice diameter 0.022 inch. Injection pressure, 8,000 pounds per square inch. Chamber pressure, 200 pounds per square inch. Cut-off after 0.003 second. Stem and nozzle assemblies, Nos. 1, 2, and 3

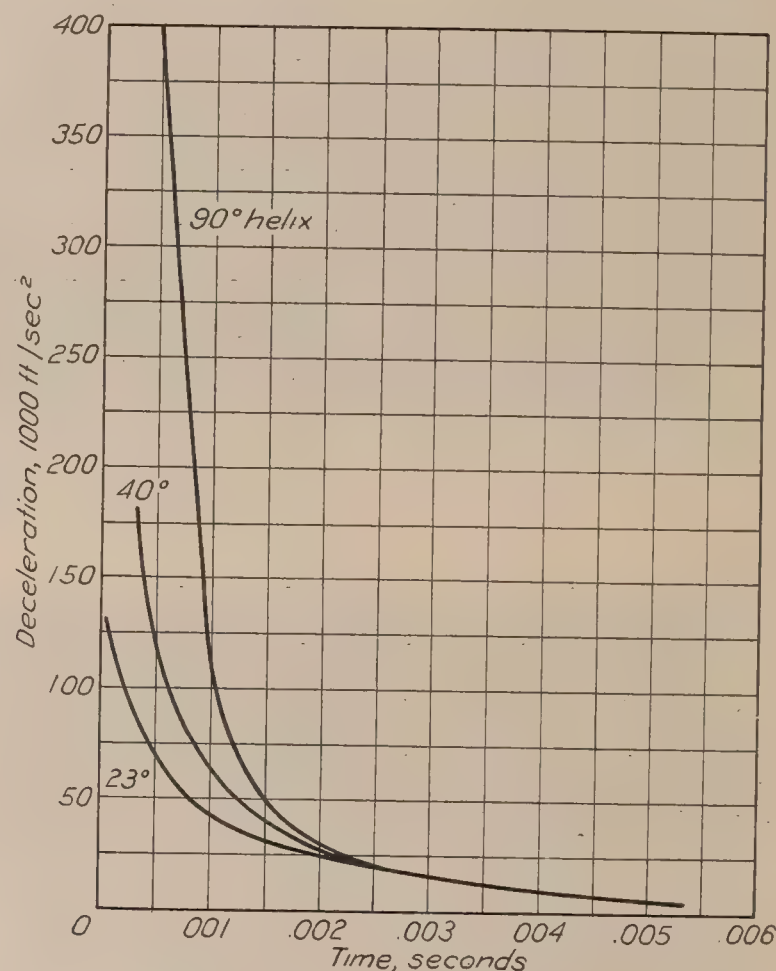


FIG. 11.—Effect of groove helix angle on spray tip deceleration. Orifice diameter 0.022 inch. Injection pressure, 8,000 pounds per square inch. Chamber pressure, 200 pounds per square inch. Cut-off after 0.003 second. Stem and nozzle assemblies, Nos. 1, 2, and 3

into breaking up and atomizing the spray and setting some of the surrounding gaseous medium into motion. The sprays from the 40° and 23° helical grooves were well atomized by centrifugal force as they emerged from the nozzle. The initial velocities of these sprays were therefore much less than that of the noncentrifugal spray, and the deceleration was also much less, because impact on the air did not cause much further atomization with the resultant rapid loss of energy.

The effects of the groove helix angle on the cone angle of the spray injected into the atmosphere and into nitrogen at 200, 400, and 600 pounds per square inch pressure are shown by Figure 12. The spray cone angle decreased with increase in the chamber pressure in the case of the high-centrifugal spray, while the spray cone angle of the noncentrifugal spray increased. In this latter case the spray was atomized and spread out by impact on the dense gas which resulted in the slightly increased spray cone angle. The curves indicate that the spray cone

angle would remain practically unchanged with a groove helix angle of about 80° for any chamber gas pressure, other conditions being the same as given in Figure 12.

The spray cone angle for 600 pounds per square inch chamber pressure was in the case of the high-centrifugal spray reduced to approximately one-half of the value attained for atmospheric pressure. This was because the oil particles thrown out centrifugally from the injection valve are extremely small and therefore have too little inertia to penetrate far into the dense gas. (Reference 2.) Thus the velocity of the oil particles at the outside of the spray falls to practically zero, while those near the core have a considerable forward velocity. The small clouds of oil particles appearing as bumps on the sides of the sprays (figs. 6 and 15) show no forward motion, and this fact seems to indicate that the other particles on the outside of the spray are practically at a standstill.

The volumes of spray produced by the same injection valve during equal elapsed time intervals and for the same test conditions but using three different groove helix angles are shown

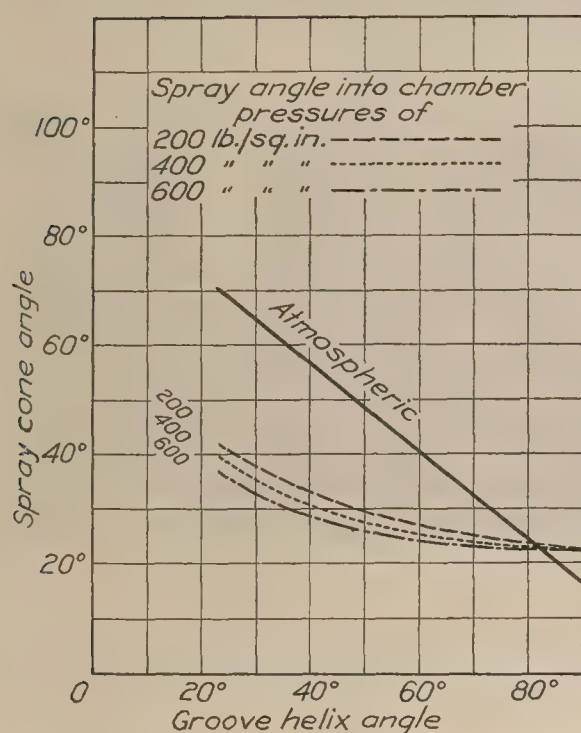


FIG. 12.—Effect of groove helix angle on spray cone angle of centrifugal sprays. Orifice diameter 0.022 inch. Injection pressure, 8,000 pounds per square inch. Cut-off after 0.003 second. Stem and nozzle assemblies, Nos. 1, 2, and 3

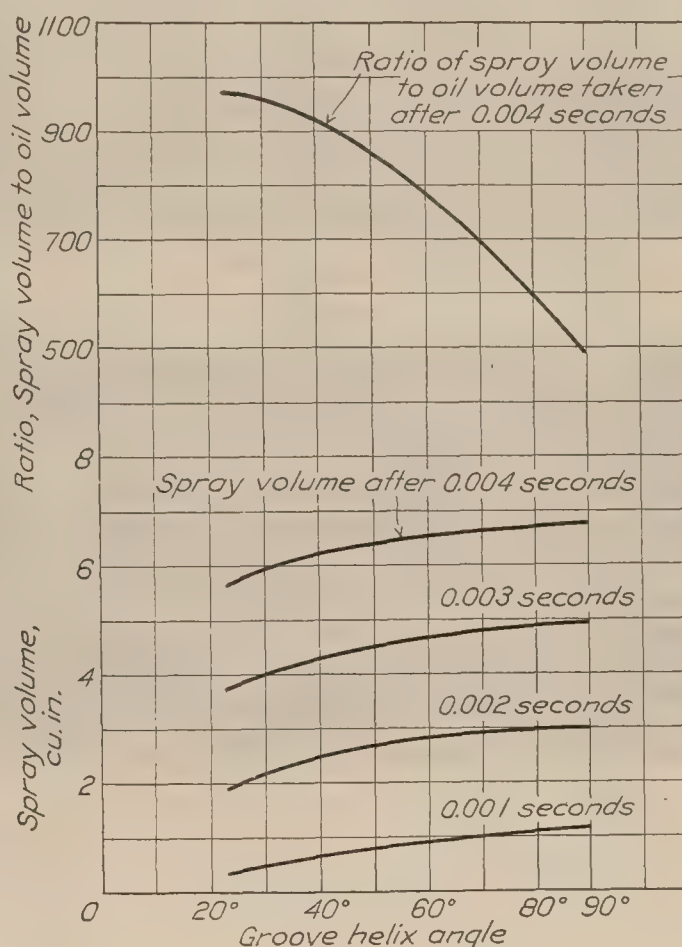


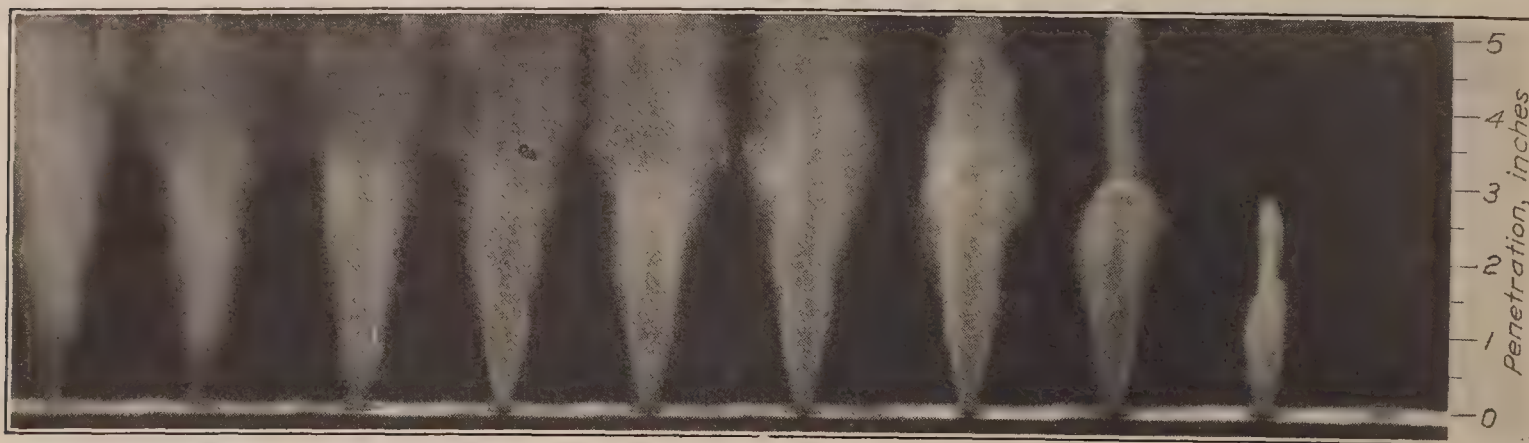
FIG. 13.—Effect of groove helix angle on spray volume, and ratio of spray volume to oil volume. Orifice diameter, 0.022 inch. Injection pressure, 8,000 pounds per square inch. Chamber pressure, 200 pounds per square inch. Cut-off after 0.003 second. Stem and nozzle assemblies, Nos. 1, 2, and 3

in Figure 13. The spray volumes increased with increase in the groove helix angle, but the volumes of oil, which produced each spray, also increased. In order to obtain a true measure of the spray distribution and possibly atomization, the ratio of the spray volume produced in a given time to the oil volume injected during that time must be considered. The curve at the top of Figure 13 shows the effect of groove helix angle on the ratio of spray volume to oil volume.

If it is assumed that a drop of oil one-fourth inch in diameter having a volume of 0.00817 cubic inch is injected from an injection valve such as was used in this investigation, the spray volume after 0.004 second would be, from Figure 13, approximately one thousand times the original oil volume, or 8.17 cubic inches. This would occupy about two-thirds the compression space of an engine of 5-inch bore by 7-inch stroke operating with a 12 to 1 compression ratio.

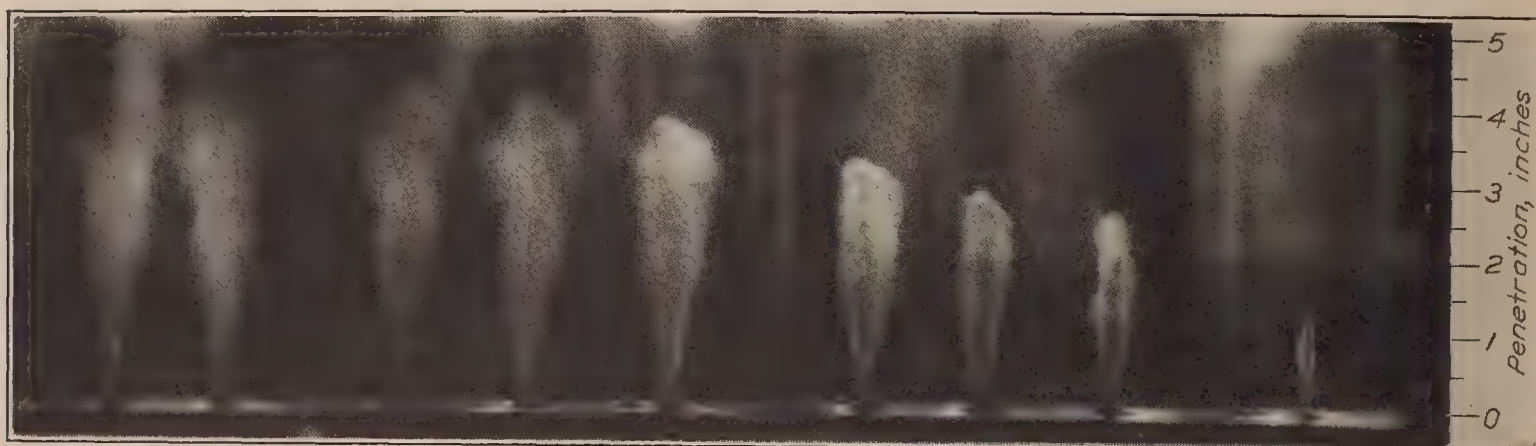
It is interesting to compare a drop of oil one-fourth inch in diameter with the spray, of volume equal to that of a sphere $2\frac{1}{2}$ inches in diameter, which can be produced from it. The

outer surface of this sphere would be one hundred times that of the original oil drop. The spray would, however, be composed of millions of minute oil particles. The total surface area of a number of spheres of the same diameter and of a given total volume varies inversely as the sphere diameter selected. Also the diameter of the particles is inversely proportional to the cube root of the number of particles. Assume a particle diameter of 0.0004 inch (Reference 2), which would be one six hundred and twenty-fifth of the diameter of the $\frac{1}{4}$ -inch drop. The total surface of all the oil particles would be six hundred and twenty-five times the surface area of a single $\frac{1}{4}$ -inch drop and the number of particles the cube of 625, or slightly over 244,000,000. As the



Injection pressure, 8,000 pounds per square inch

Chamber pressure, atmospheric



Injection pressure, 8,000 pounds per square inch

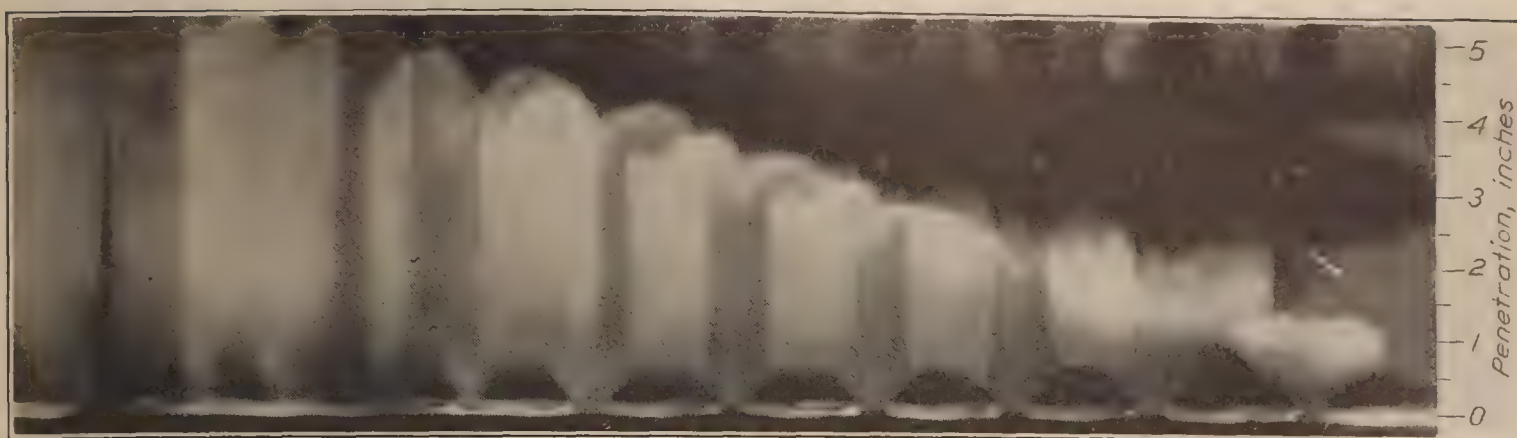
Chamber pressure, 200 pounds per square inch

FIG. 14.—Spray photographs for stem and nozzle assembly No. 4, 0.012 inch diameter orifice and 23° helix

particle diameter approaches zero the total area and the number of particles will approach infinity. This discussion gives an indication of what it is possible to do with a small drop of oil by passing it through a centrifugal-type injection valve.

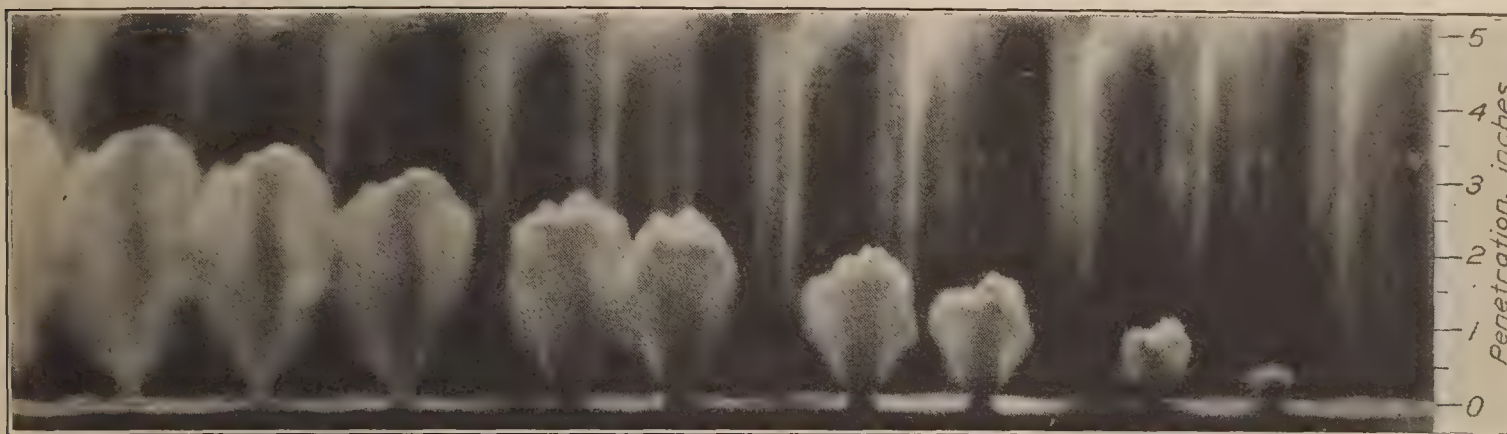
RATIO OF ORIFICE AREA TO GROOVE AREA

The results of the tests, in which the ratio of the cross-sectional area of the orifice to that of the grooves was varied from 0.19 to 2.05 are shown in Figures 14 to 20. The areas of the orifices controlled the flow with the first two ratios, while the area of the grooves controlled the flow with the third ratio. Figures 14 and 15 are series of pictures at two chamber pres-



Injection pressure, 8,000 pounds per square inch

Chamber pressure, atmospheric



Injection pressure, 8,000 pounds per square inch

Chamber pressure, 200 pounds per square inch



Injection pressure, 8,000 pounds per square inch

Chamber pressure, 400 pounds per square inch



Injection pressure, 8,000 pounds per square inch

Chamber pressure, 600 pounds per square inch

FIG. 15.—Spray photographs for stem and nozzle assembly No. 6, 0.040 inch diameter orifice and 23° helix

tures using the same injection valve stem with large and small diameter orifices of such size as to give orifice to groove area ratios of 0.19 and 2.05. The time-penetration curves for the tests with these ratios are given in Figures 16 and 17. The pictures for the third ratio—namely, 0.63—have already been given in Figure 4 and the time-penetration curves in Figure 7.

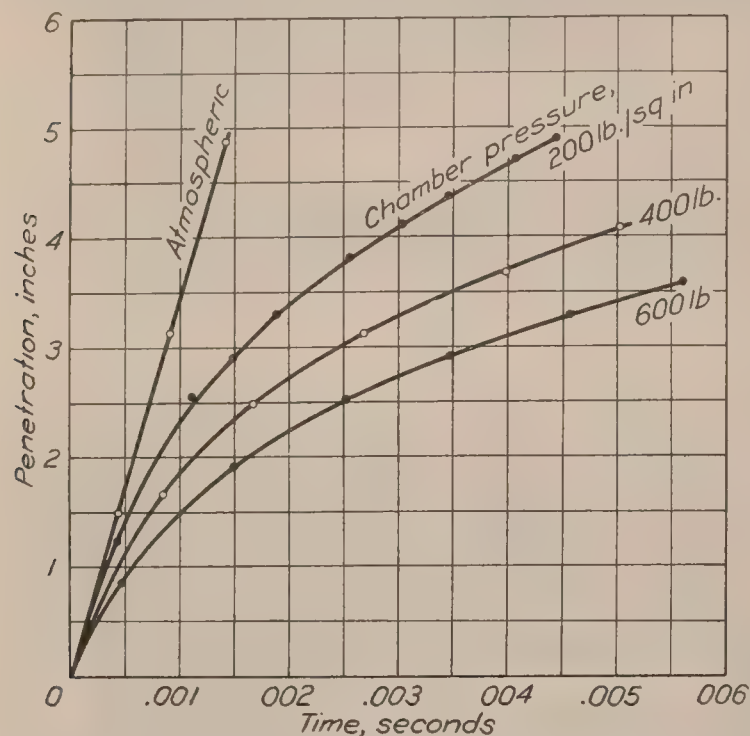


FIG. 16.—Effect of chamber pressure on spray penetration. Orifice diameter, 0.012 inch. Groove helix angle 23° . Injection pressure, 8,000 pounds per square inch. Cut-off after 0.003 second. Stem and nozzle assembly No. 4

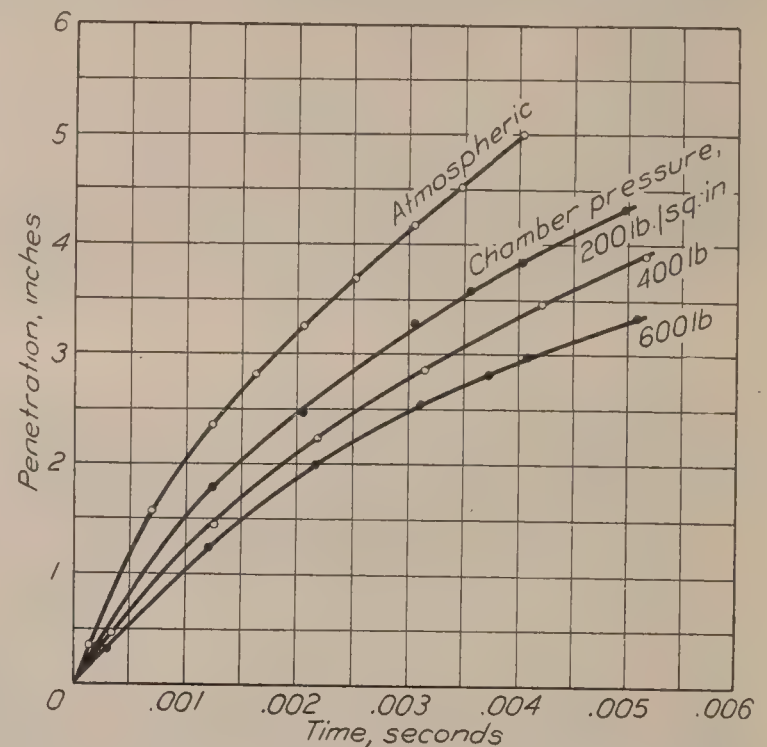


FIG. 17.—Effect of chamber pressure on spray penetration. Orifice diameter, 0.040 inch. Groove helix angle 23° . Injection pressure, 8,000 pounds per square inch. Cut-off after 0.003 second. Stem and nozzle assembly No. 6

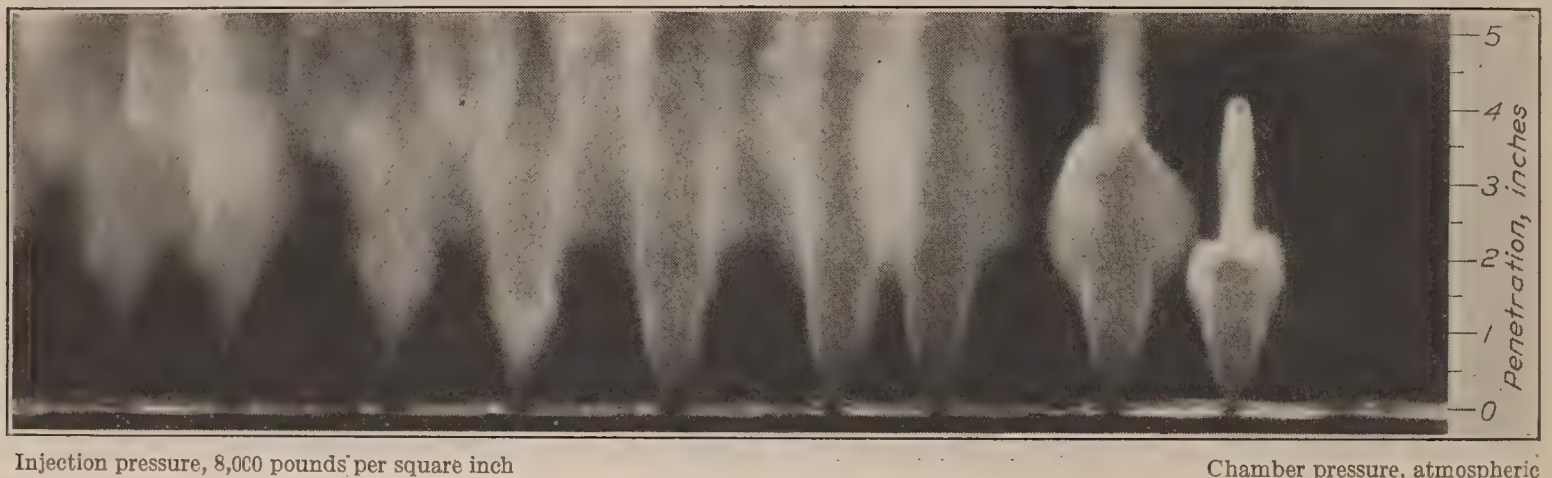


FIG. 18.—Spray photographs for stem and nozzle assembly No. 8, 0.022 inch diameter orifice, 23° helix and ratio of orifice area to groove area 0.19

In order to determine the effect of varying the orifice-groove area ratio by increasing the groove area, the orifice area was kept constant and the groove area was increased so as to change the ratio from 0.63 to 0.19. Thus the same ratio of 0.19 was obtained with two orifice diameters. A series of pictures for this test are shown in Figure 18.

The effect of the ratio of orifice area to groove area upon the spray cone angle and penetration in the atmosphere, after 0.002 second, is shown in Figure 19. The general trend of the spray cone-angle curve indicates that the spray cone angle would not be greatly increased by increase in the ratio of orifice area to groove area beyond 2.05. A narrow spray was obtained with the 0.012-inch orifice and ratio of 0.19. This was chiefly due to two causes. First, because the orifice area was very much smaller than the groove area, the velocity of the oil through the grooves was necessarily low. Thus the amount of centrifugal force applied to the oil passing through the orifice was small. Second, the small bore of the orifice did not allow much of the rotation of the oil to continue through it. Thus the spray emerging from the orifice was practically noncentrifugal. This fact accounts for the penetration being greater than that obtained with the larger orifices.

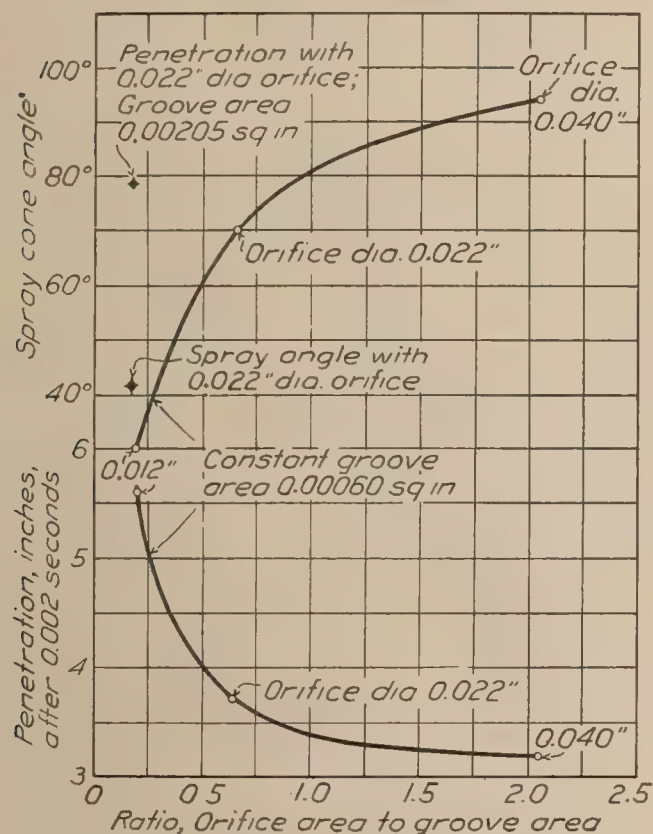


FIG. 19.—Effect of ratio of orifice area to groove area upon spray cone angle and penetration. Groove helix angle, 23°. Injection pressure, 8,000 pounds per square inch. Chamber pressure, atmospheric. Cut-off after 0.003 second. Stem and nozzle assemblies, Nos. 4, 5, and 6

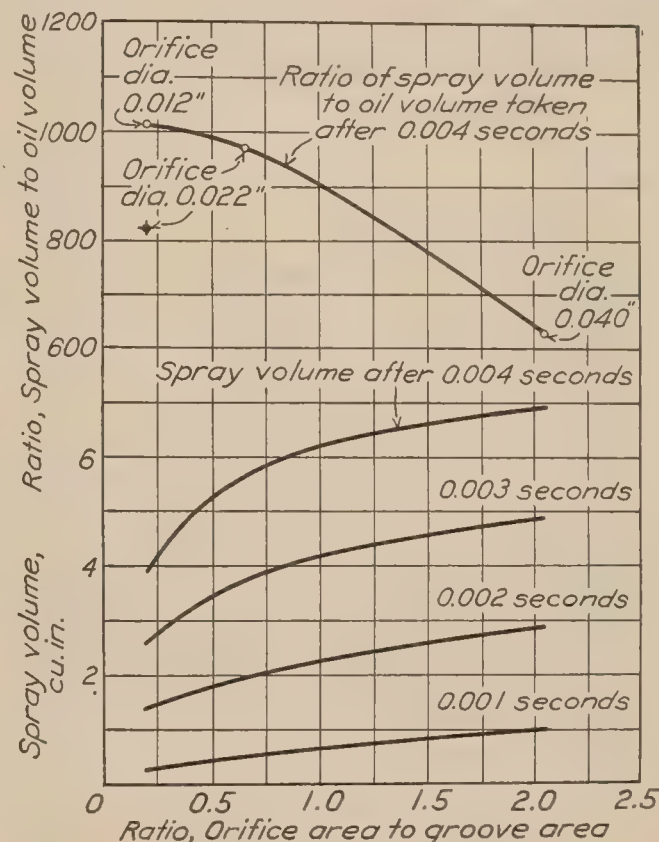


FIG. 20.—Effect of ratio of orifice area to groove area on spray volume, and ratio of spray volume to oil volume. Groove helix angle, 23°. Groove area, 0.00060 square inch. Injection pressure, 8,000 pounds per square inch. Chamber pressure, 200 pounds per square inch. Cut-off after 0.003 second. Stem and nozzle assemblies, Nos. 4, 5, and 6

The two points in Figure 19 labeled 0.022 inch, which are not on the curves, were obtained with a 0.022-inch orifice and ratio of orifice area to groove area of 0.19. The penetration was increased 50 per cent as compared with that for a 0.012-inch orifice and ratio of 0.19, and the spray angle was increased 30 per cent. The increase in penetration is explained by the greater inertia of the larger quantity of oil injected, and the increase in spray angle by increased jet rotation as a result of the larger orifice.

The effect of ratio of orifice area to groove area on the actual spray volume is shown in Figure 20. The quantity of oil injected increased with the ratio, so that the volume curves are not a measure of the spray distribution. The curve at the top of Figure 20 shows the variation of the ratio of spray volume to oil volume, with three ratios of orifice area to groove area. This curve gives an estimate of the relative spray distribution. The ratio of spray volume to oil volume for 0.19 ratio and 0.022-inch orifice is shown by a point below the curve. The spray distribution was not as great with the larger orifice and grooves as with the smaller orifice and grooves.

RATIO OF ORIFICE LENGTH TO DIAMETER

The results of the tests in which only the orifice length was varied, giving orifice length to diameter ratios of 2.6, 1.7, and 0.2, are shown in Figure 21. The same stem and nozzle were used in all three tests, the end of the nozzle being ground off to reduce the orifice length as desired for successive tests. This eliminated any variation in the sprays caused by slight differences in workmanship on similar nozzles.

The effects of the ratio of orifice length to diameter, on the spray cone angle and penetration after 0.003 second, in 200 pounds per square inch, chamber pressure, are shown in Figure 21. The spray angle increased with decrease in the orifice length. The shorter the orifice the less tendency it has to direct the spray axially and decrease the jet rotation because of friction. The result is, therefore, a larger spray cone angle. The spray angle seems to approach the angles of the stem tip and nozzle, both of which are 60° . (See fig. 2.) The maximum spray penetra-

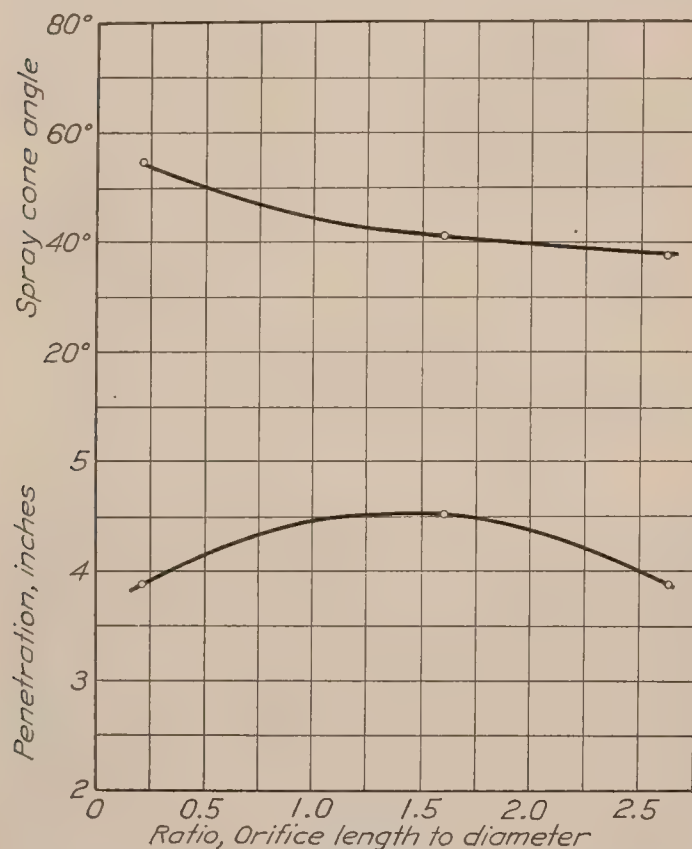


FIG. 21.—Effect of ratio of orifice length to orifice diameter on centrifugal sprays. Orifice diameter, 0.022 inch. Groove helix angle, 40° . Injection pressure, 8,000 pounds per square inch. Chamber pressure, 200 pounds per square inch. Cut-off after 0.003 second. Stem and nozzle assemblies, Nos. 9, 10, and 11

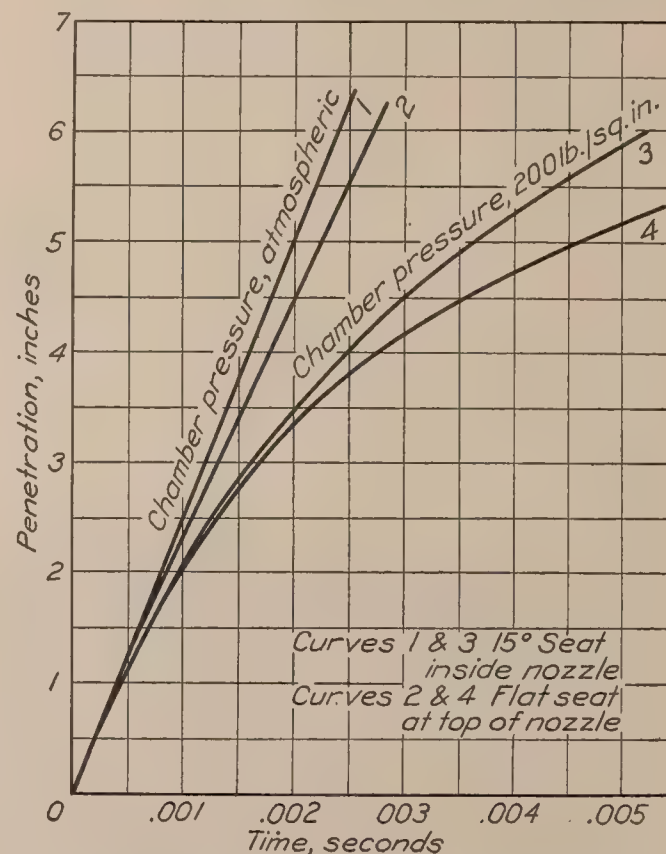


FIG. 22.—Effect of valve seat position on spray penetration. Orifice diameter, 0.022 inch. Groove helix angle, 40° . Injection pressure, 8,000 pounds per square inch. Cut-off after 0.003 second. Stem and nozzle assemblies, Nos. 12 and 13

tion is attained with a ratio of length to diameter of about 1.5. The decrease in penetration beyond this ratio may be caused by the reexpansion of the jet within the orifice which probably takes place with increased orifice length. This causes an increase in the cross section of the jet sufficient to fill the orifice at its outer end which produces an energy loss due to friction. The velocity is therefore reduced and likewise there is a decrease in the spray penetration.

EFFECT OF SEAT POSITION

The data presented in Figure 22 show that somewhat greater penetration was obtained with the injection valve stem seating on a ledge inside of the nozzle and directly before the orifice. The spray angle in the atmosphere was, however, decreased from 58° to 53° . It is probable that locating the seat directly before the orifice and after the helical grooves materially reduced the jet rotation produced by the helical grooves. This would tend to decrease the spray angle and increase the penetration. It is much easier and more economical to have the valve made with a flat seat, and much more accurately fitting surfaces are assured than if the seat is located inside of the nozzle.

CONCLUSIONS

This investigation has shown that although the application of centrifugal force to an oil spray does reduce the penetration, the spray may still maintain a relatively high degree of penetration into dense air. It has shown that examination of centrifugal sprays injected into the atmosphere may lead to incorrect conclusions as to their characteristics when injected into dense air.

The results obtained show that the penetration decreases with reduction in the pitch of the helical grooves, while the spray angle and distribution increase. The spray penetration and distribution increase with a reduction in the ratio of orifice area to groove area, while the spray-cone angle decreases. The spray-cone angle and penetration were increased, in the two tests made, by increase in the size of both orifice and grooves, keeping their ratio of areas constant. A ratio of orifice length to diameter of about 1.5 gave best penetration, although a smaller ratio gives a wider spray. Slightly greater penetration was obtained with the seat directly before the orifice, but the spray-cone angle was slightly less than with the seat at the top of the nozzle.

LANGLEY MEMORIAL AERONAUTICAL LABORATORY,
NATIONAL ADVISORY COMMITTEE FOR AERONAUTICS,
LANGLEY FIELD, VA., *January 27, 1927.*

REFERENCES

1. KUEHN, Dr. R. Atomization of Liquid Fuels. Part II. N. A. C. A. Technical Memorandum No. 330, 1925. Figures 2-23.
2. HESSELMAN, K. J. E. Hesselman Heavy-Oil High-Compression Engine. N. A. C. A. Technical Memorandum No. 312, 1925. Pp. 10-15. Figures 11 and 12.
3. NICHOLSON, A. I. Some Oil Engine Experiments. "Transactions of the Institution of Engineers and Shipbuilders in Scotland," April, 1923, Vol. LXVI, pp. 66 and 67. Figures 9 and 10.
4. BUCHNER, Doctor. The Fundamental Principles of High-Speed Semi-Diesel Engines. Part I. N. A. C. A. Technical Memorandum No. 356, 1926. Pp. 19-23. Figures 10, 13-15.
5. BIRD, A. L. Oil Engines, 1923. vii+281 pages. VII, 103 figures. Methuen & Co. (Ltd.), London.
6. SHEPHERD, H. F. The Solid Injection Oil Engine. "Transactions of the American Society of Mechanical Engineers," vol. 45, pp. 487-488.
7. MILLER, H. E., and BEARDSLEY, E. G. Spray Penetrations with a Simple Fuel Injection Nozzle. N. A. C. A. Technical Report No. 222, 1926. Pp. 4-5. Figures 1 and 2.
8. BEARDSLEY, E. G. Some Factors Affecting the Reproducibility of Penetration and the Cut-Off of Oil Sprays for Fuel Injection Engines. N. A. C. A. Technical Report No. 258, 1927. P. 4. Figure 1.

REPORT No. 269

AIR FORCE TESTS OF SPERRY MESSENGER MODEL WITH SIX SETS OF WINGS

By JAMES M. SHOEMAKER
Langley Memorial Aeronautical Laboratory

REPORT No. 269

AIR FORCE TESTS OF SPERRY MESSENGER MODEL WITH SIX SETS OF WINGS

By JAMES M. SHOEMAKER

SUMMARY

The purpose of this test was to compare six well-known airfoils, the R. A. F. 15, U. S. A. 5, U. S. A. 27, U. S. A. 35-B, Clark Y, and Göttingen 387, fitted to the Sperry Messenger model, at full scale Reynolds Number as obtained in the variable density wind tunnel of the National Advisory Committee for Aeronautics; and to determine the scale effect on the model equipped with all the details of the actual airplane. The results show a large decrease in minimum drag coefficient upon increasing the Reynolds Number from about one-twentieth scale to full scale. Maximum lift coefficient was increased with increasing scale for all the airfoils except the Göttingen 387, for which it was slightly decreased. A comparison is made between the results of these tests and those obtained from tests made in this tunnel on airfoils alone.

INTRODUCTION

This test was made to compare six well-known airfoils, the R. A. F. 15, U. S. A. 5, U. S. A. 27, U. S. A. 35-B, Clark Y, and Göttingen 387, fitted to the Sperry Messenger model, at full-scale Reynolds Number as obtained in the variable density wind tunnel of the National Advisory Committee for Aeronautics. The scale effect on the model equipped with all the details of the actual airplane was determined. Previous tests on this model conducted in the same tunnel have already been reported (Reference 1). The tests were made at the request of the Army Air Corps.

THE TEST

A one-tenth scale model, reproducing all the details of external construction which could be considered as contributing drag, was tested at tank pressures of one and of twenty atmospheres for the model equipped with each set of wings. By "tank pressure" is meant the pressure of the air within the steel shell of the tunnel. This is used as the simplest means of indicating the scale of the test. Thus a tank pressure of twenty atmospheres means that the Reynolds Number of the test is approximately twenty times as great as that of a one atmosphere test of the same model in this tunnel.

In addition, the model fitted with U. S. A. 5 wings was equipped with a propeller, made very accurately to scale, which was mounted on a bearing having little friction and allowed to turn as a windmill. This combination was tested at five tank pressures ranging from one to twenty atmospheres to determine the effect of the propeller.

A photograph and dimensioned drawing of the model will be found in Figures 1 and 2, respectively. The small streamlined object suspended beneath the fuselage in Figure 2 was used to represent the trailing-bomb type flight path recorder used in the flight tests of the airplane. Figure 3 is a photograph of the model in position for test. The fuselage is made of mahogany with metal fittings. The empennage is of brass and the wings are of dural, with steel struts. The dimensions of the biplane cellule are the same for all sets of wings. As will be seen from the drawing, the angle of incidence is $+2^\circ$, while that of the stabilizer is $+1\frac{1}{2}^\circ$. These angles were used for all sets of wings, the elevators remaining neutral.

A description of the tunnel and its balance mechanism will be found in Reference 2. The model was mounted in a manner similar to that used in the previous tests described in Reference 1. Two airplane streamline wires of sufficient stiffness to support the model were attached to



FIG. 1.—Model of Sperry Messenger airplane

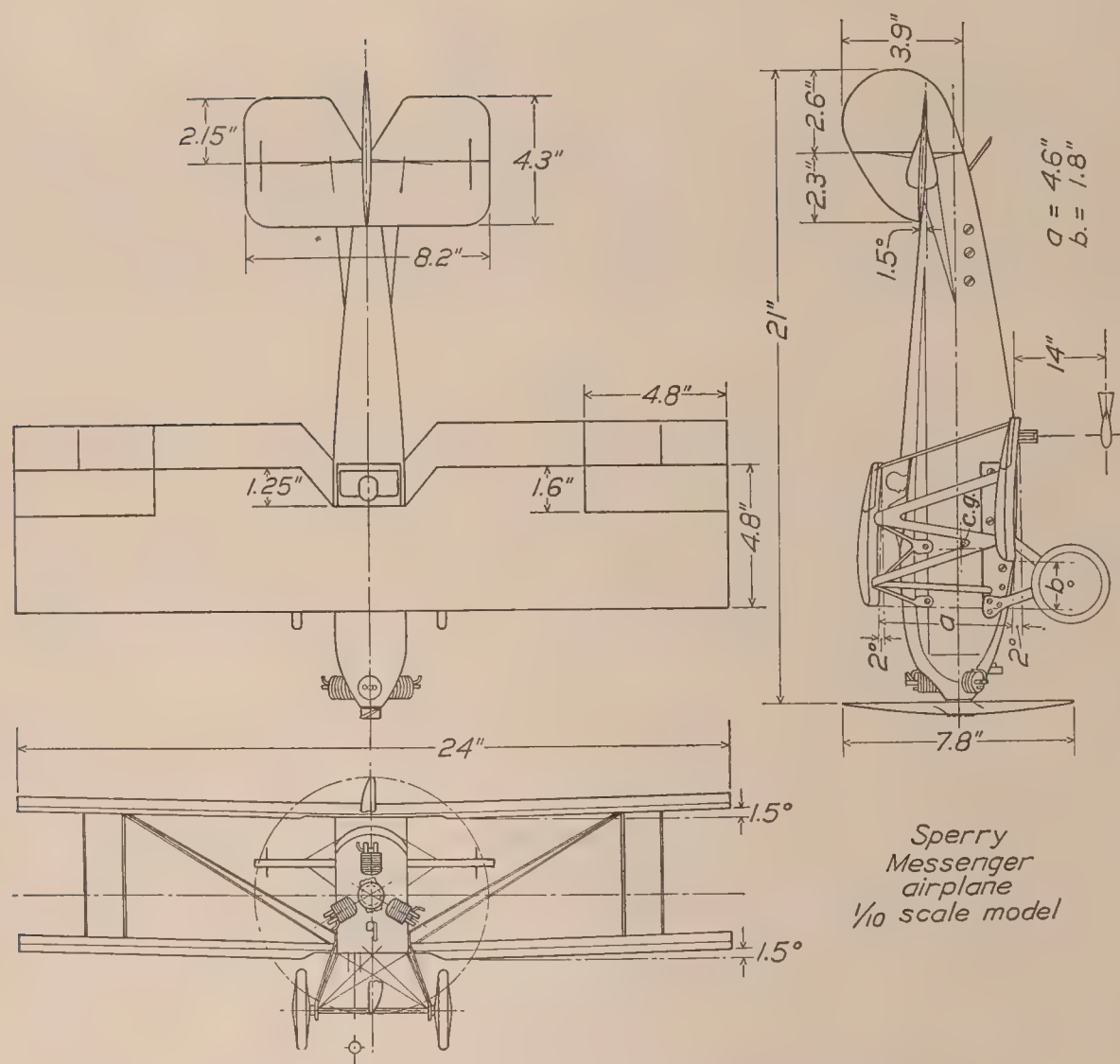


FIG. 2.—Plan, elevations, and dimensions of the Sperry Messenger model

the lower wing at the quarter-chord point and fixed at their lower end to the balance ring. A skid pivoting in the after part of the fuselage was attached to the vertical bar by which the angle of attack was changed. This set-up differed from that described in Reference 1 only in that faired shields were used over the streamline wires to within approximately 10 inches of the model to reduce the wire drag.

RESULTS AND DISCUSSION

The results of the tests, with drag coefficient and angle of attack corrected for tunnel-wall interference by the Prandtl formulas (Reference 3), will be found in Tables I to XVII. The

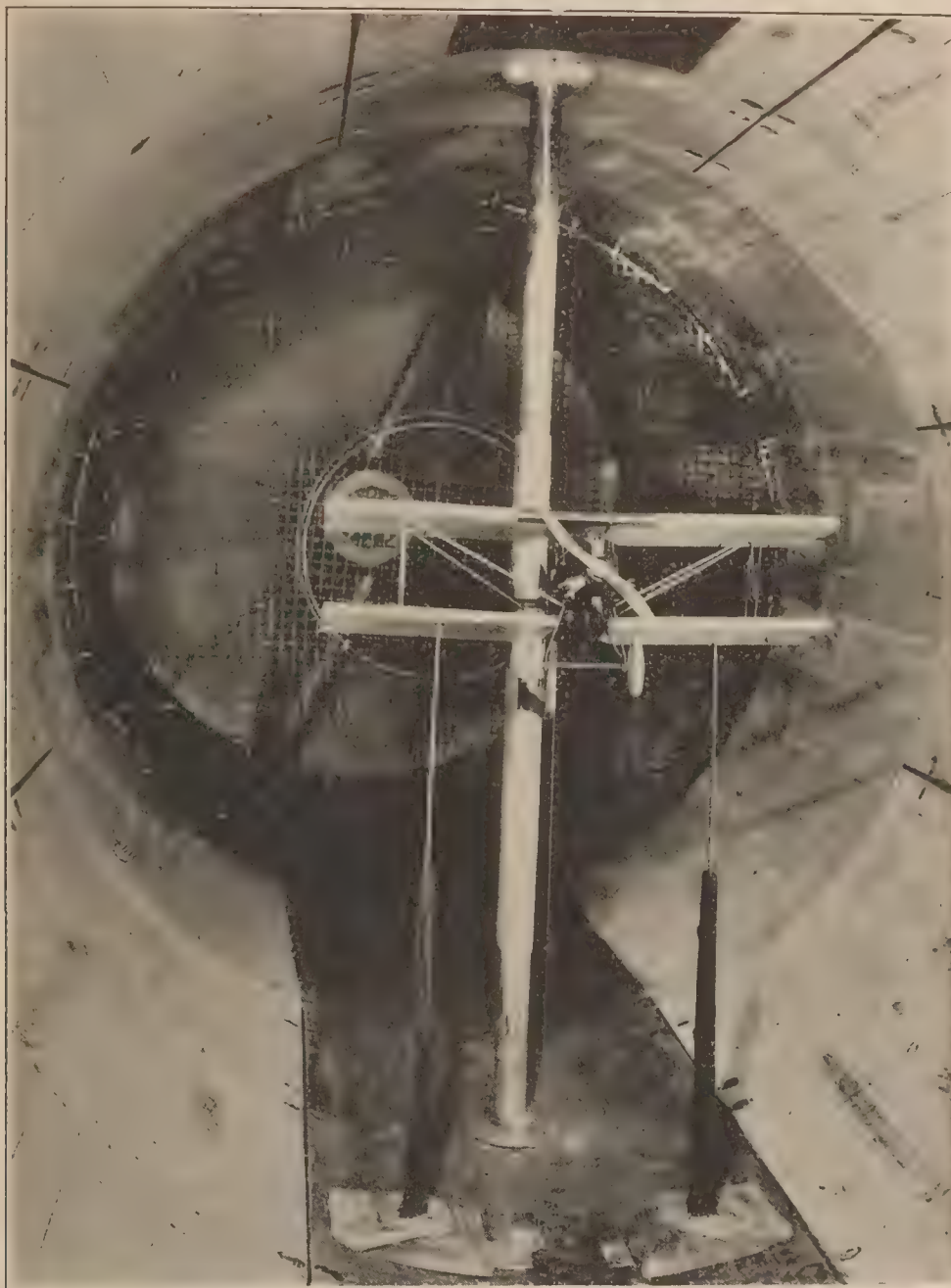


FIG. 3.—The model in the variable density wind tunnel

moment coefficients taken about the center of gravity of the airplane are given as measured. No correction for the effect of tunnel walls upon the moment was made.

The curves of C_D and C_M plotted against C_L as an ordinate are given in Figures 4 to 11. The value of the angles spotted on the polar curves is that measured in the tunnel and is not corrected for tunnel-wall effect. For the corresponding angles in free air, refer to the tabulated data. The curves for the model fitted with U. S. A. 5 wings and propeller are shown for five tank pressures in Figure 4. The spacing of these curves shows that the scale effect is large at the lower Reynolds Numbers, particularly that on minimum drag coefficient. There is very little difference between the drag coefficient at 10 and at 20 atmospheres. Figures 5 and 6 are from the 1 and 20 atmosphere tests, respectively, each showing the curves for the model with and without propeller. The ratio between minimum drag with and without propeller seems to

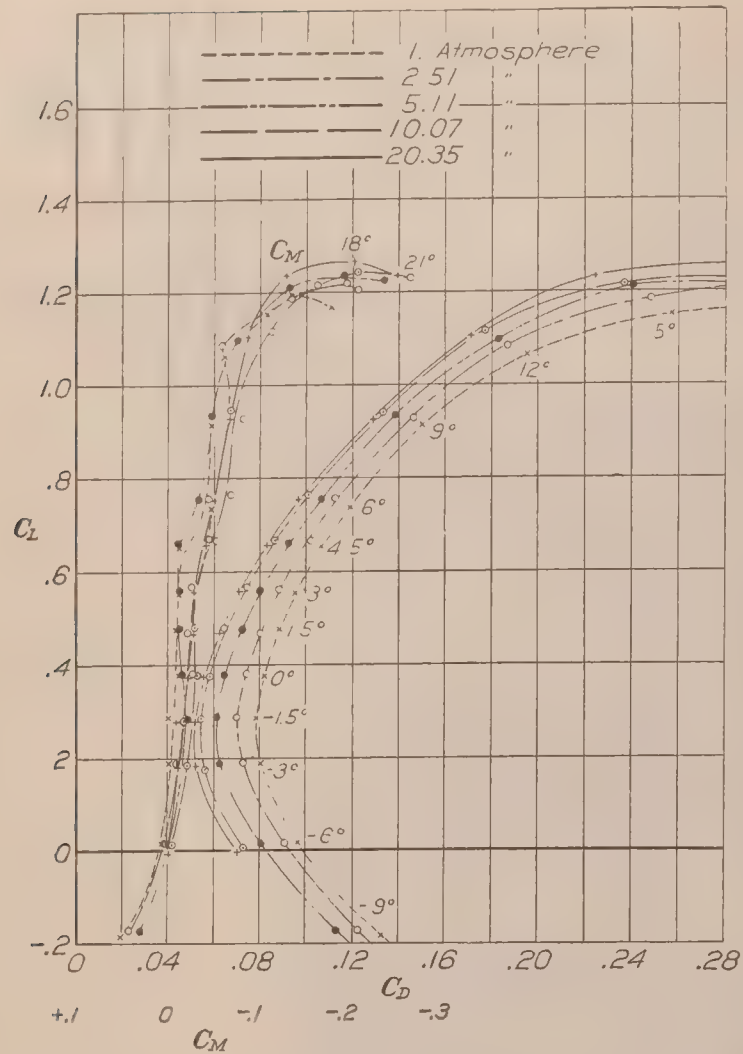


FIG. 4.—Polar curves of S. M. model with U. S. A. 5 wings and propeller

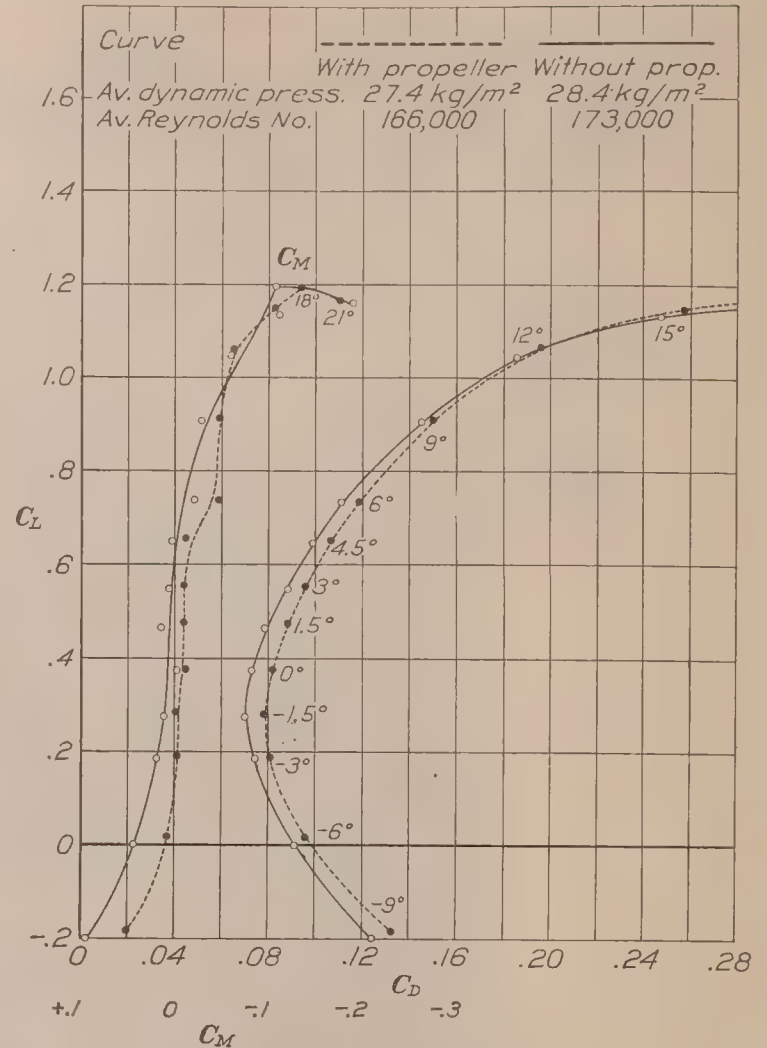


FIG. 5.—Polar curves of S. M. model with U. S. A. 5 wings at one atmosphere

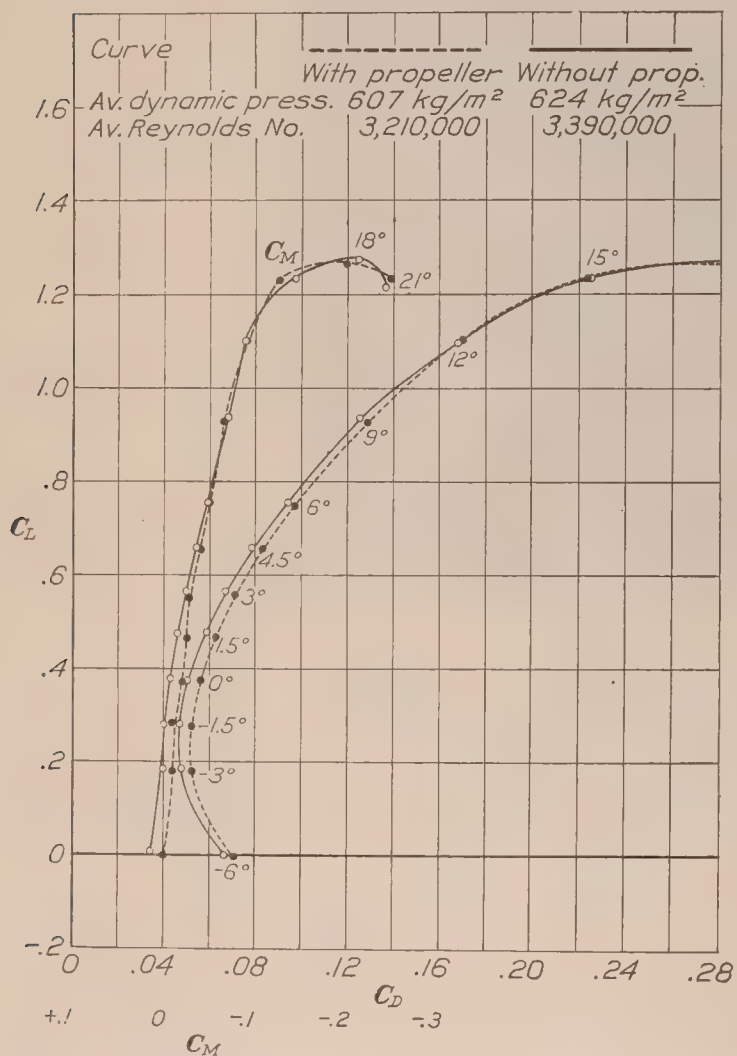


FIG. 6.—Polar curves of S. M. model with U. S. A. 5 wings at 20 atmospheres

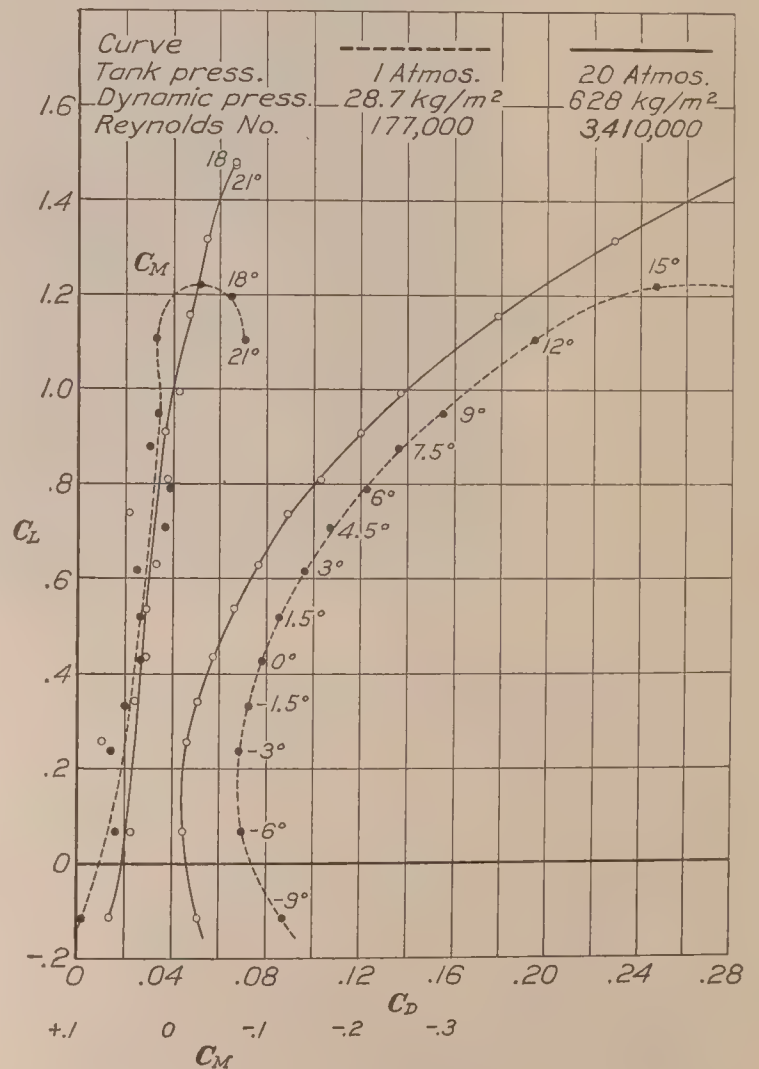


FIG. 7.—Polar curves of S. M. model with U. S. A. 35B wings and no propeller

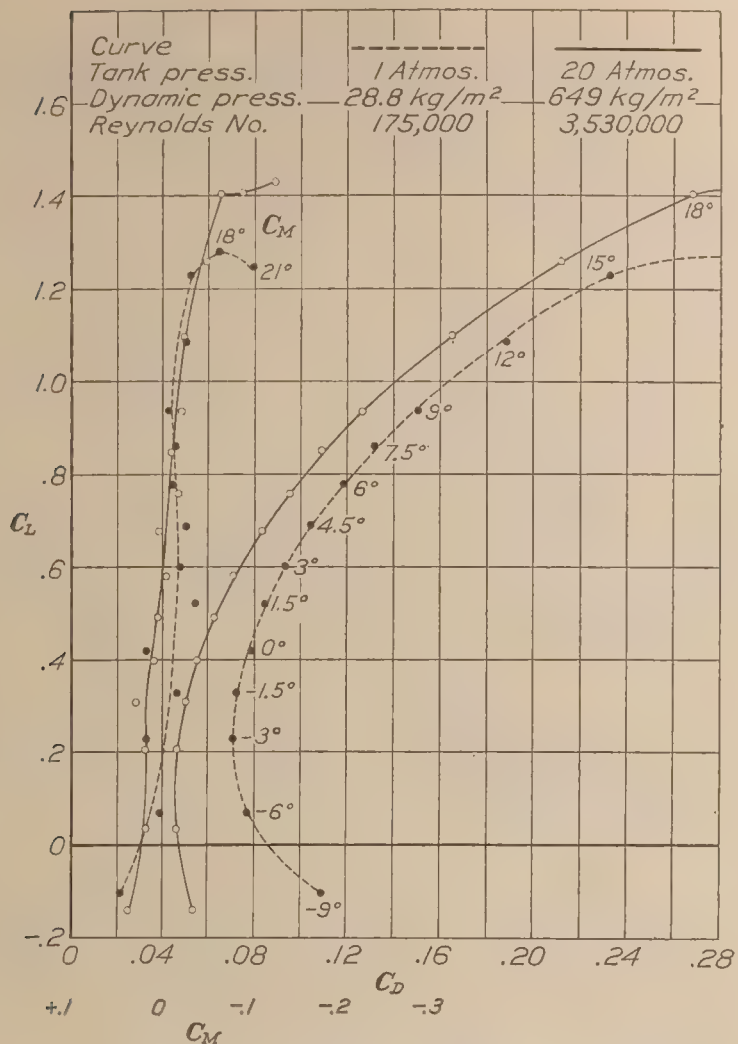


FIG. 8.—Polar curves of S. M. model with U. S. A. 27 wings and no propeller

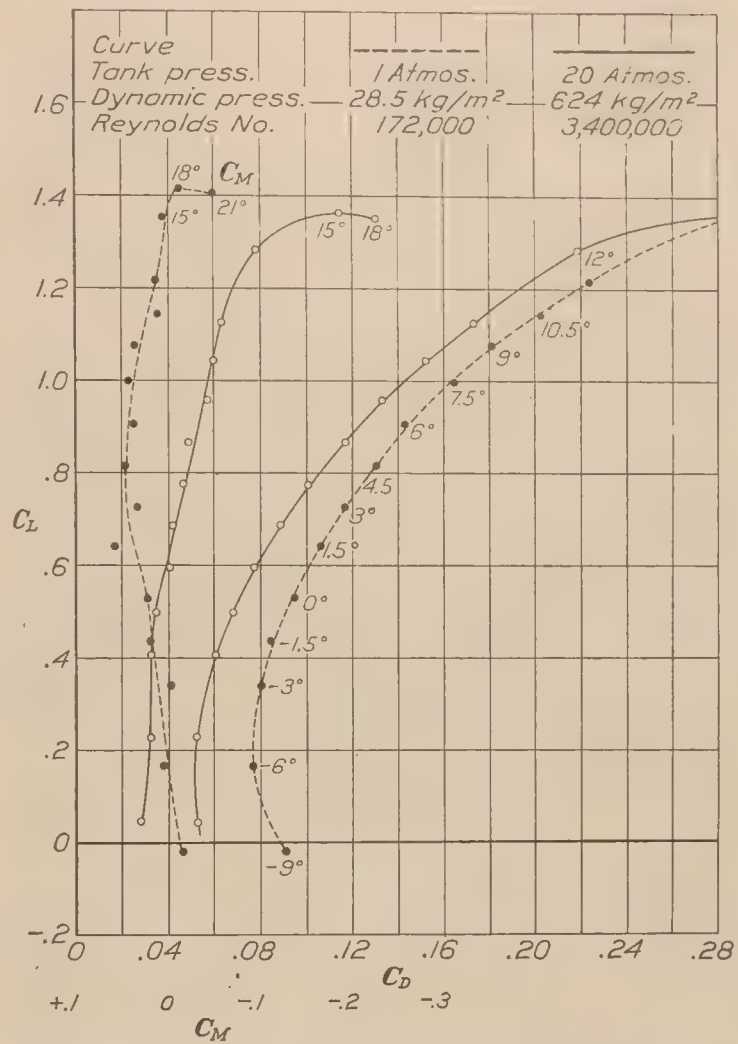


FIG. 9.—Polar curves of S. M. model with Göttingen 387 wings and no propeller

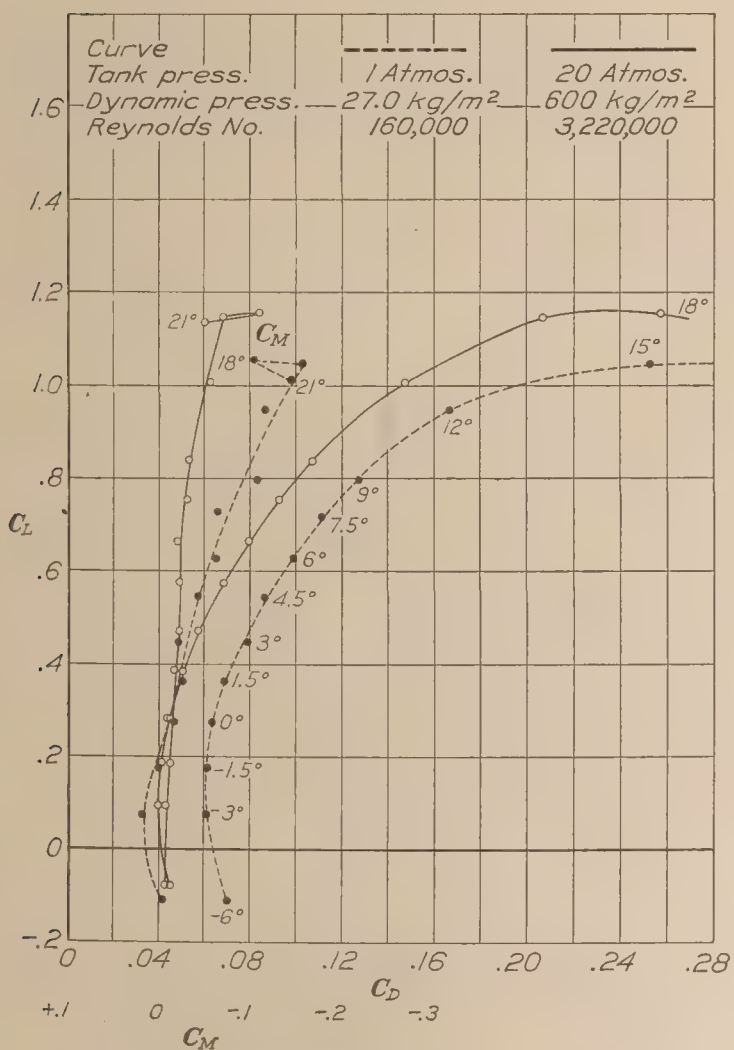


FIG. 10.—Polar curves of S. M. model with R. A. F. 15 wings and no propeller

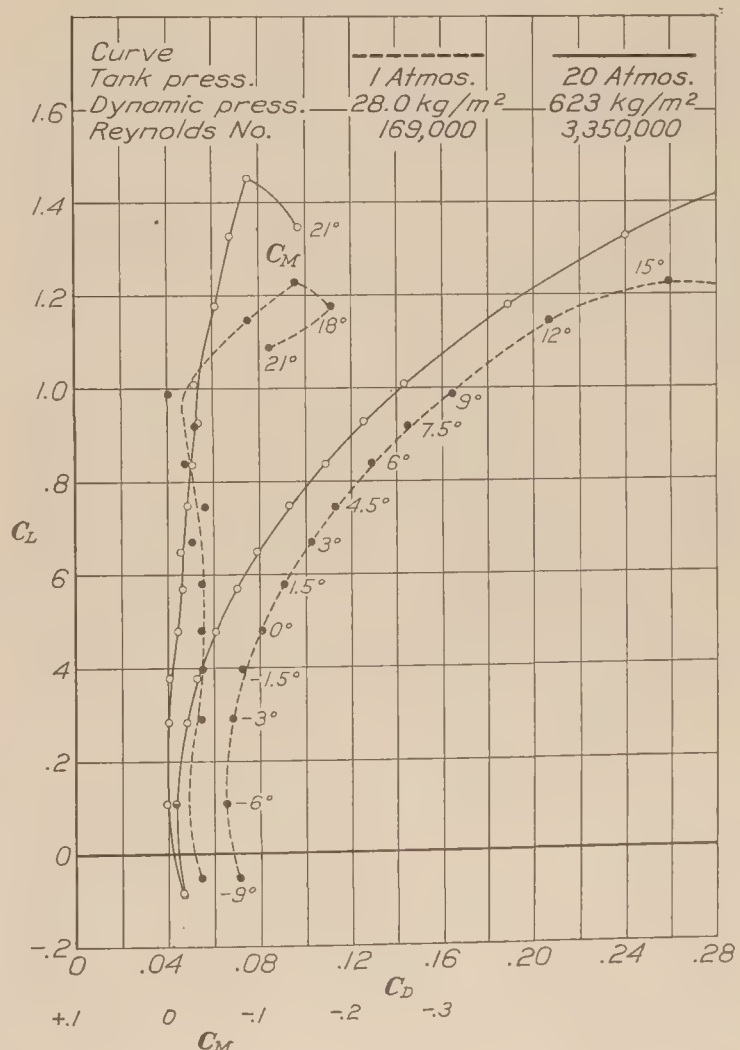


FIG. 11.—Polar curves of S. M. model with Clark Y wings and no propeller

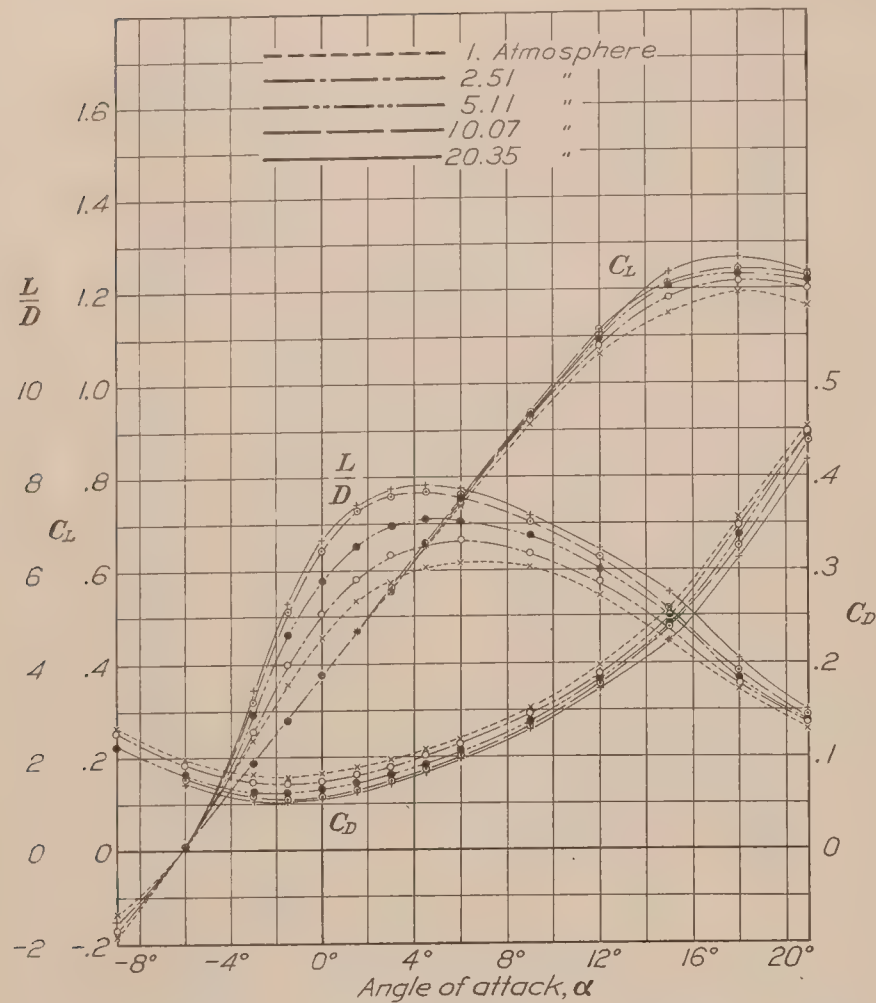


FIG. 12.—Characteristic curves of S. M. model with U. S. A. 5 wings and propeller

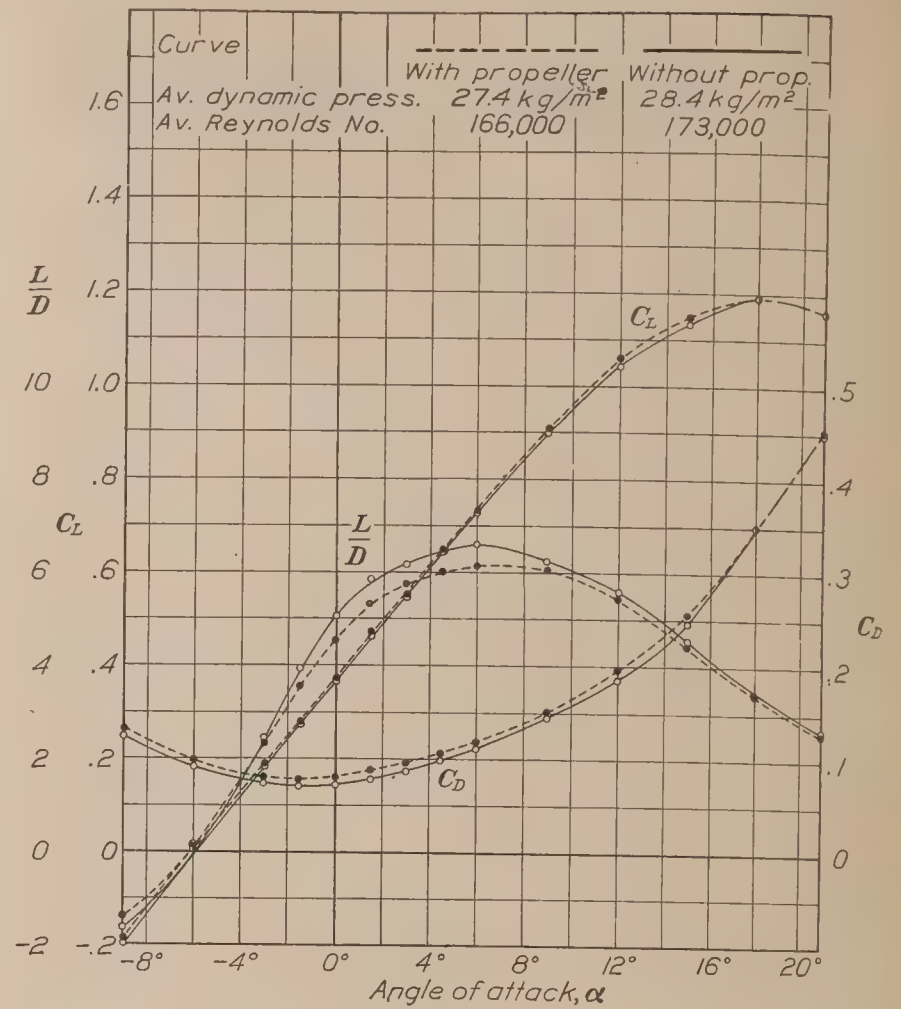


FIG. 13.—Characteristic curves of S. M. model with U. S. A. 5 wings at one atmosphere

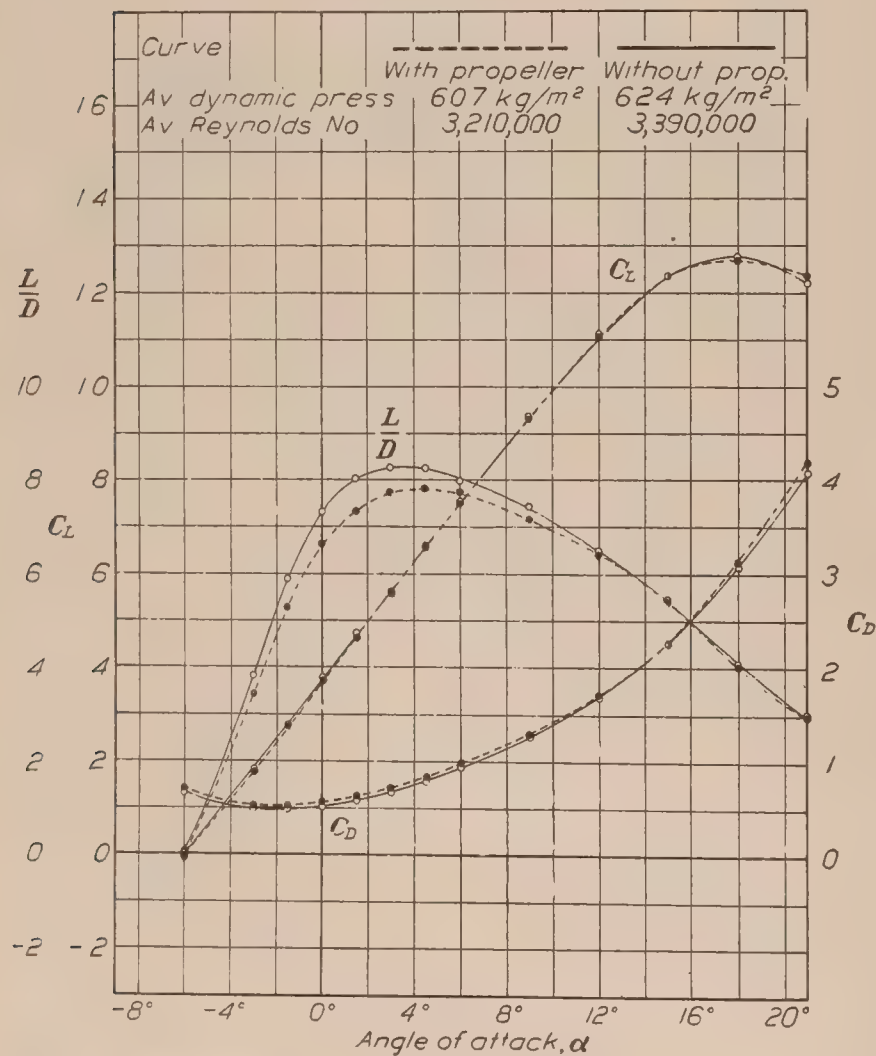


FIG. 14.—Characteristic curves of S. M. model with U. S. A. 5 wings at 20 atmospheres

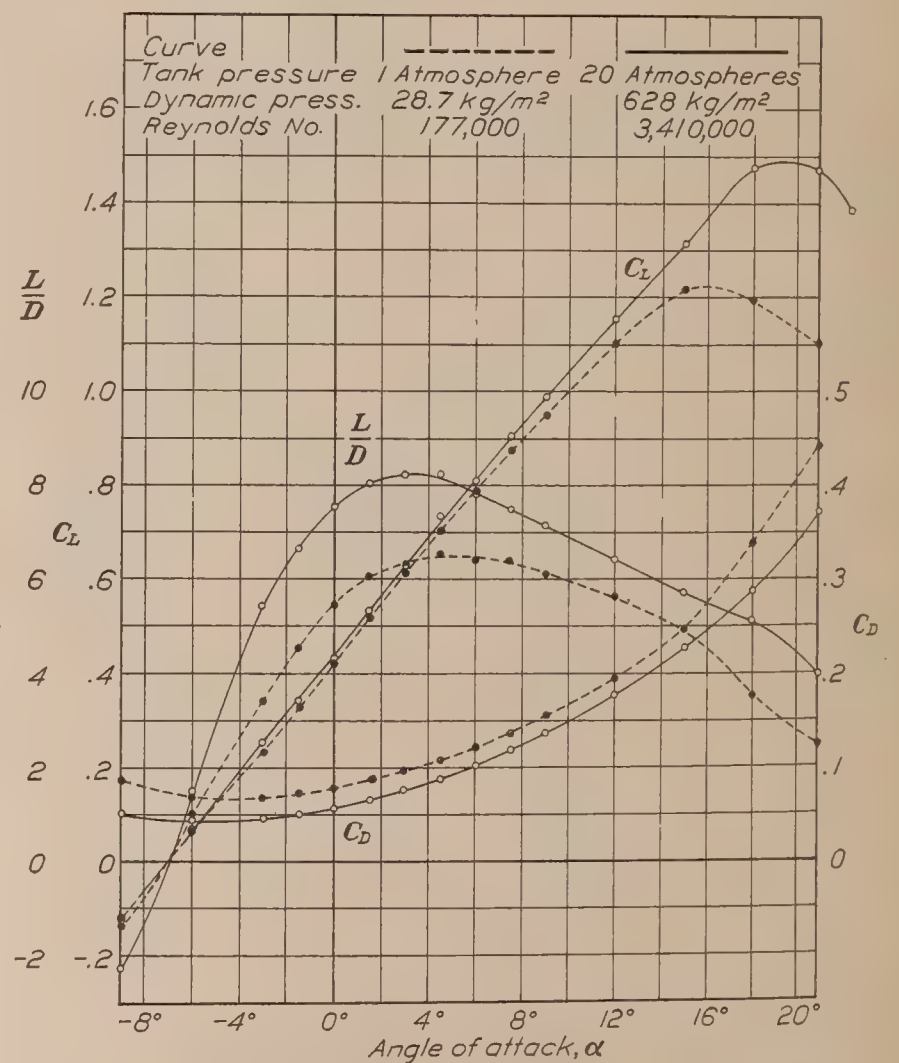


FIG. 15.—Characteristic curves of S. M. model with U. S. A. 35B wings and no propeller

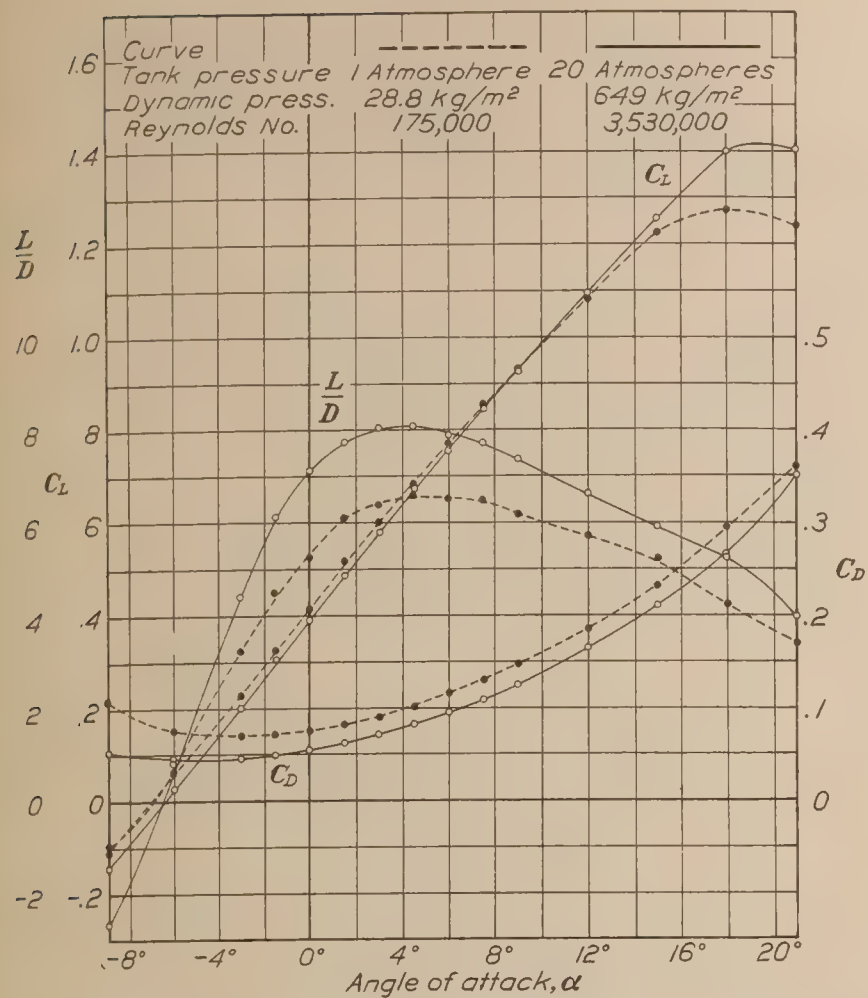


FIG. 16.—Characteristic curves of S. M. model with U. S. A. 27 wings and no propeller

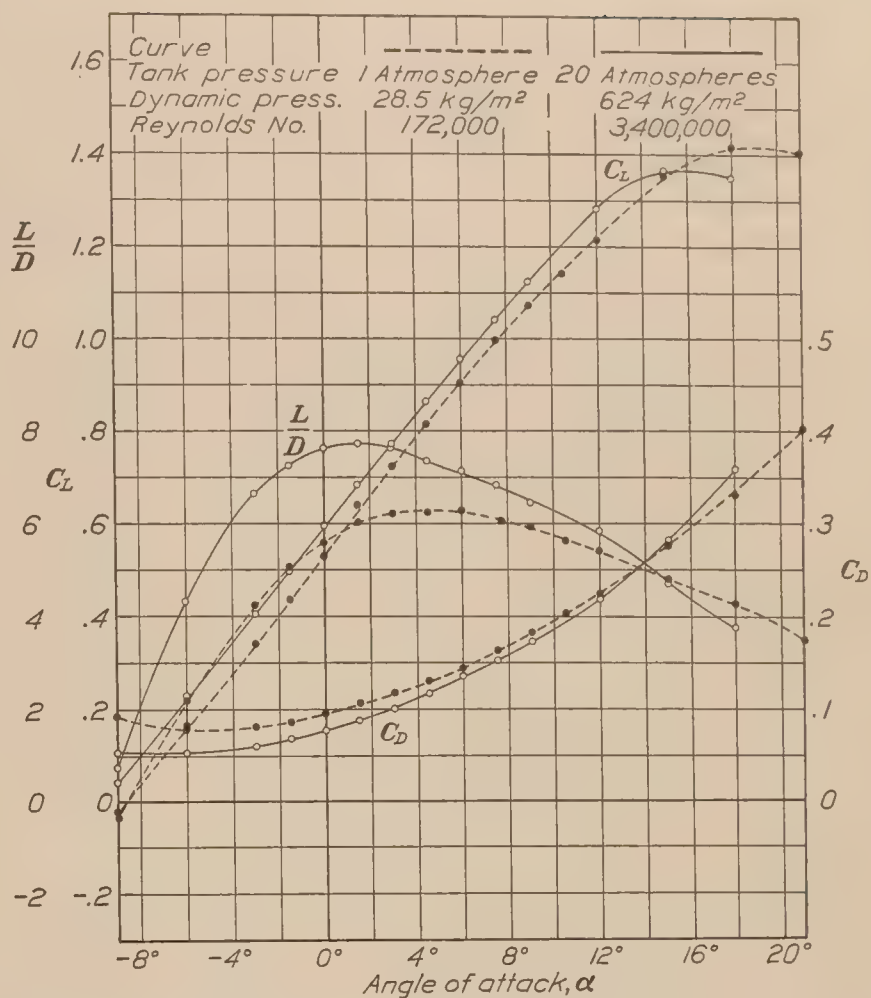


FIG. 17.—Characteristic curves of S. M. model with Göttingen 387 wings and no propeller

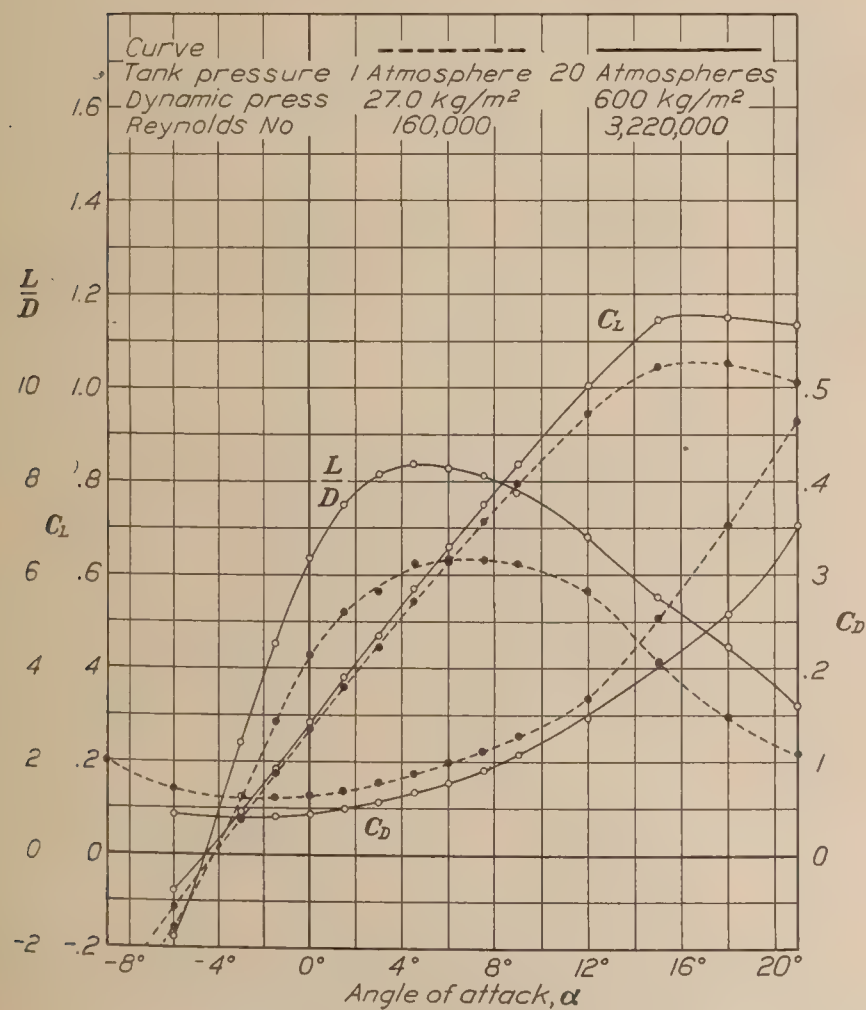


FIG. 18.—Characteristic curves of S. M. model with R. A. F. 15 wings and no propeller

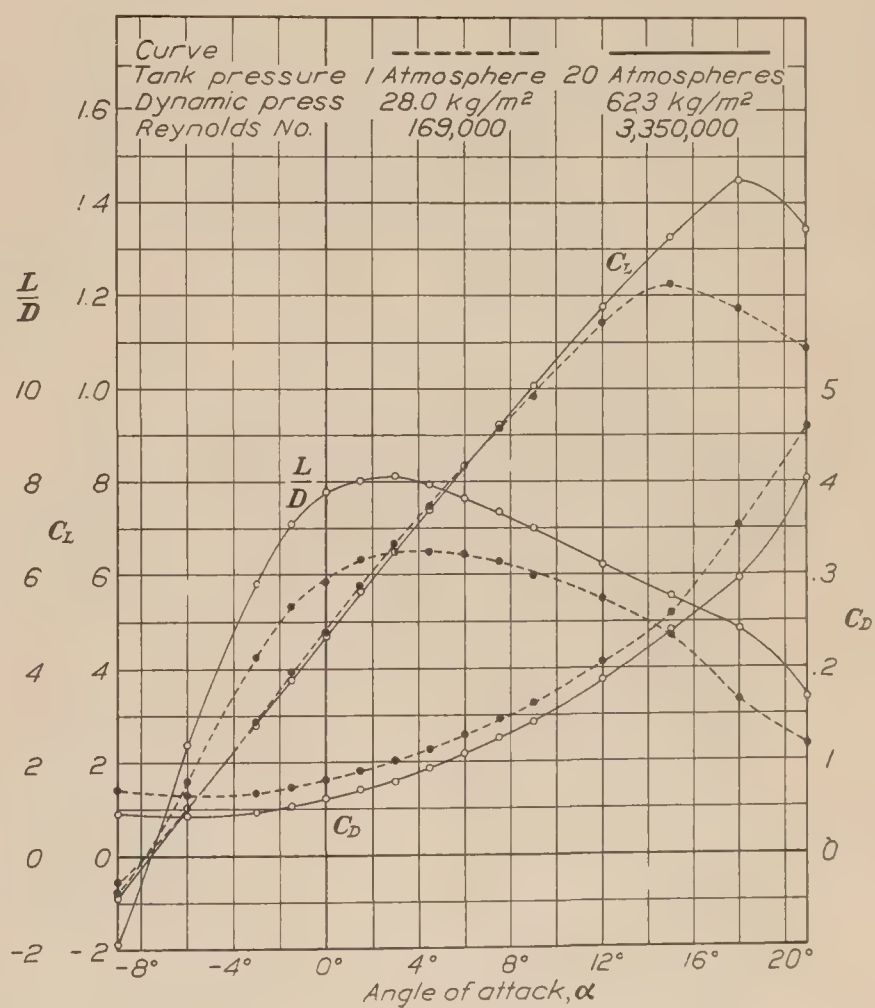


FIG. 19.—Characteristic curves of S. M. model with Clark Y wings and no propeller

be about the same regardless of scale. In these tests the propeller was running practically at condition of zero torque, since the bearing friction was very slight. In Figures 6 to 11 are plotted the results from the 1 and the 20 atmosphere tests for each set of wings. In every case there is a large reduction in drag coefficient with increased Reynolds Number. All the airfoils except the Göttingen 387 show also a considerable increase in maximum lift for the runs at 20 atmospheres.

In Figures 12 to 19 lift coefficient, drag coefficient, and lift-drag ratio are plotted against the angles of attack measured in the tunnel. As explained above the corresponding angles for free air will be found in the tables. These figures show that the scale effect on the lift-drag ratio is large and practically the same for all the airfoils. The maximum L/D averages about 8 for the 20-atmosphere and about 6.5 for the 1-atmosphere tests.

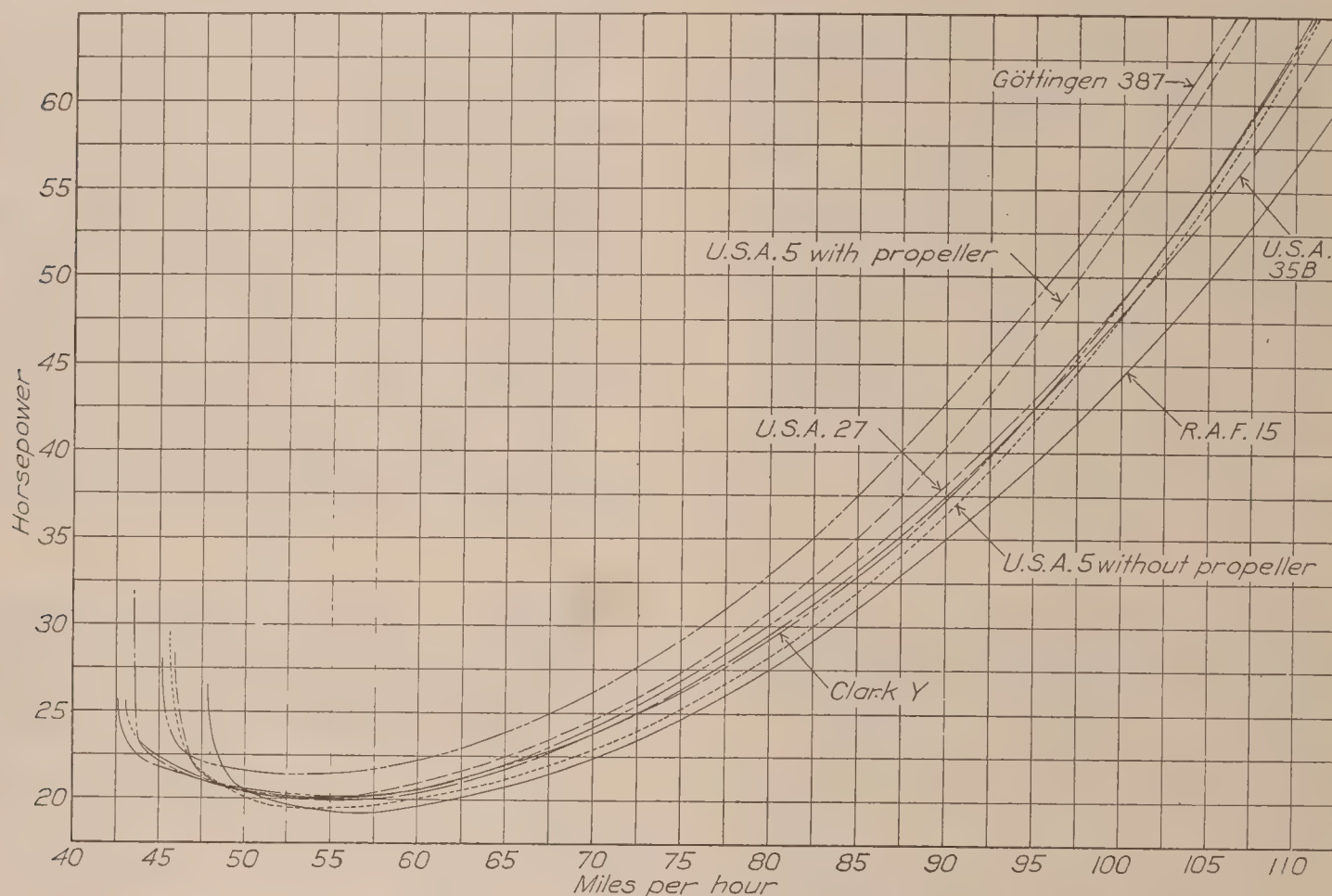


FIG. 20.—Curves of power required by Sperry Messenger airplane. Tests at 20 atmospheres

The curves of power required are plotted against speed in miles per hour in Figure 20. The tests at 20 atmospheres, corrected for tunnel wall, were used in computing this data. On account of the large difference in landing speed with the various airfoils it is difficult to make any direct comparison of merit. The Clark Y, U. S. A. 35-B, and U. S. A. 27 all combine low power over most of the range with comparatively low landing speed. The U. S. A. 5 and R. A. F. 15, while showing lower power over most of the flying range, have considerably higher landing speeds. The curve for the U. S. A. 5 with propeller is also plotted for comparison. The Göttingen 387 shows very large power consumption and comparatively high landing speed, and is evidently the poorest airfoil of the group.

A summary of the data from these tests is given in Table XVIII. Since the actual power curves are given in Figure 20, no figures of merit involving power were computed. The values of maximum L/D and the ratio of maximum C_L to minimum C_D are given as being of some interest for comparison. The order of merit of the sections based on these items is given in Table XIX for both the 1-atmosphere and the 20-atmosphere tests. The order for the airfoils alone, taken from variable density tunnel tests (Reference 4) are also given in this table. It will be seen that the order obtained from the 20-atmosphere airfoil tests is, with minor exceptions, the same as that from the 20-atmosphere Sperry model tests. On the other

hand, the one-atmosphere tests, both of airfoils and model, are very misleading when compared with the model tests at full-scale Reynolds Number.

LANGLEY MEMORIAL AERONAUTICAL LABORATORY,
NATIONAL ADVISORY COMMITTEE FOR AERONAUTICS,
LANGLEY FIELD, VA., *January 20, 1927.*

REFERENCES

1. MUNK, MAX M., and DIEHL, WALTER S. The Air Forces on a Model of the Sperry Messenger Airplane Without Propeller. N. A. C. A. Technical Report No. 225, 1925.
2. MUNK, MAX M., and MILLER, ELTON W. The Variable Density Wind Tunnel of the National Advisory Committee for Aeronautics. N. A. C. A. Technical Report No. 227, 1926.
3. PRANDTL, L. Application of Modern Hydrodynamics to Aeronautics. N. A. C. A. Technical Report No. 116, 1921.
4. MUNK, MAX M., and MILLER, ELTON W. The Aerodynamic Characteristics of Seven Frequently Used Wing Sections at Full Reynolds Number. N. A. C. A. Technical Report No. 233, 1926.

TABLE I

Sperry Messenger.
U. S. A. 5 wings without propeller.
Av. tank pres.=1 atm.
Av. dynamic pres., $q=28.4$ kg/m².
Av. Reynolds Number=173,000.
Av. temperature=24° C.

Span=24 in. (61.0 cm).
Chord=4.8 in. (12.2 cm).
Aspect ratio=5.
Area=0.1377 m².
Date, October 1, 1925.

Angle of attack, degrees α	Lift coefficient C_L	Corrected C_D	L/D	Moment coeffi- cient C_M	Corrected angle of attack, degrees
-9	-0.201	+0.1245	-1.61	+0.094	-9.11
-6	.000	.0913	0	.043	-6.00
-3	+.184	.0746	+2.47	.018	-2.90
-1.5	.275	.0702	3.92	.011	-1.35
0	.371	.0735	5.05	-.004	+ .20
+1.5	.463	.0790	5.86	+.014	1.75
3	.546	.0885	6.17	.005	3.29
4.5	.648	.0999	6.49	.000	4.85
6	.734	.1110	6.61	-.022	6.40
9	.906	.1455	6.23	-.030	9.49
12	1.046	.1861	5.62	-.060	12.56
15	1.133	.2476	4.58	-.113	15.61
18	1.194	.3503	3.41	-.109	18.64
21	1.160	.4568	2.54	-.190	21.63

TABLE II

Sperry Messenger.
U. S. A. 5 wings without propeller.
Av. tank pres.=20.3 atm.
Av. dynamic pres., $q=624$ kg/m².
Av. Reynolds Number=3,390,000.
Av. temperature=39° C.

Span=24 in. (61.0 cm).
Chord=4.8 in. (12.2 cm).
Aspect ratio=5.
Area=0.1377 m².
Date, October 1, 1925.

Angle of attack, degrees α	Lift coefficient C_L	Corrected C_D	L/D	Moment coeffi- cient C_M	Corrected angle of attack, degrees
-6	+0.007	+0.0662	+0.11	+0.014	-6
-3	.184	.0480	3.83	.000	-2.90
-1.5	.280	.0476	5.88	-.001	-1.35
0	.379	.0518	7.32	-.008	+ .20
+1.5	.475	.0592	8.02	-.016	1.76
3	.563	.0680	8.28	-.026	3.30
4.5	.659	.0796	8.28	-.036	4.86
6	.752	.0941	7.99	-.049	6.41
9	.936	.1260	7.43	-.071	9.50
12	1.100	.1689	6.52	-.089	12.59
15	1.237	.2261	5.46	-.145	15.67
18	1.279	.3076	4.16	-.214	18.69
21	1.220	.4093	2.98	-.244	21.66

TABLE III

Sperry Messenger.
U. S. A. 5 wings with propeller.
Av. tank pres.=1 atm.
Av. dynamic pres. $q=27.4$ kg/m².
Av. Reynolds Number=166,000.
Av. temperature=26° C.

Span=24 in. (61.0 cm).
Chord=4.8 in. (12.2 cm).
Aspect ratio=5.
Area=0.1377 m².
Date, October 5, 1925.

Angle of attack, degrees α	Lift coefficient C_L	Corrected C_D	L/D	Moment coeffi- cient C_M	Corrected angle of attack, degrees
-9	-0.184	+0.1327	-1.39	+0.050	-9.10
-6	+.013	.0962	+.14	+.007	-5.99
-3	.189	.0804	2.35	-.004	-2.90
-1.5	.282	.0789	3.57	-.002	-1.35
0	.375	.0827	4.53	-.013	+.20
+1.5	.472	.0886	5.33	-.011	1.75
3	.551	.0960	5.74	-.013	3.30
4.5	.652	.1072	6.08	-.013	4.85
6	.737	.1197	6.16	-.049	6.40
9	.911	.1502	6.07	-.049	9.49
12	1.061	.1955	5.43	-.064	12.57
15	1.150	.2577	4.46	-.109	15.62
18	1.193	.3511	3.40	-.135	18.64
21	1.161	.4536	2.56	-.177	21.63

TABLE IV

Sperry Messenger.
U. S. A. 5 wings with propeller.
Av. tank pres.=2.51 atm.
Av. dynamic pres. $q=69.9$ kg/m².
Av. Reynolds Number=417,000.
Av. temperature=30° C.

Span=24 in. (61.0 cm).
Chord=4.8 in. (12.2 cm).
Aspect ratio=5.
Area=0.1377 m².
Date, October 5, 1925.

Angle of attack, degrees α	Lift coefficient C_L	Corrected C_D	L/D	Moment coeffi- cient C_M	Corrected angle of attack, degrees
-9	-0.171	+0.1227	-1.39	+0.041	-9.09
-6	+.014	.0916	+.15	+.005	-5.99
-3	.189	.0737	2.56	-.010	-2.90
-1.5	.283	.0709	3.99	-.023	-1.35
0	.380	.0748	5.08	-.029	+.20
+1.5	.467	.0804	5.80	-.022	1.75
3	.560	.0884	6.32	-.029	3.30
4.5	.664	.1025	6.48	-.046	4.86
6	.753	.1127	6.68	-.045	6.41
9	.929	.1461	6.36	-.083	9.50
12	1.082	.1871	5.78	-.059	12.58
15	1.183	.2485	4.76	-.133	15.64
18	1.219	.3463	3.52	-.195	18.66
21	1.201	.4433	2.71	-.206	21.65

TABLE V

Sperry Messenger.
 U. S. A., 5 wings, with propeller.
 Av. tank pres. = 5.11 atm.
 Av. dynamic pres. $q = 148.2 \text{ kg/m}^2$.
 Av. Reynolds Number = 867,000.
 Av. temperature = 29° C .

Span = 24 in. (61.0 cm).
 Chord = 4.8 in. (12.2 cm).
 Aspect ratio = 5.
 Area = 0.1377 m^2 .
 Date, October 6, 1925.

Angle of attack, degrees α	Lift coefficient C_L	Corrected C_D	L/D	Moment coeffi- cient C_M	Corrected angle of attack, degrees
-9	-0.174	+0.1138	-1.53	+0.030	-9.09
-6	+.007	.0806	+.09	-.001	-6.00
-3	.187	.0632	2.96	-.015	-2.90
-1.5	.287	.0620	4.63	-.023	-1.35
0	.379	.0654	5.80	-.016	+.20
+1.5	.473	.0723	6.54	-.012	1.75
3	.558	.0803	6.95	-.014	3.30
4.5	.660	.0929	7.10	-.012	4.86
6	.751	.1064	7.06	-.035	6.40
9	.933	.1385	6.74	-.048	9.50
12	1.098	.1830	6.00	-.076	12.59
15	1.210	.2406	5.03	-.132	15.65
18	1.232	.3352	3.67	-.191	18.66
21	1.221	.4471	2.73	-.235	21.66

TABLE VI

Sperry Messenger.
 U. S. A. 5 wings with propeller.
 Av. tank pres. = 10.07 atm.
 Av. dynamic pres. $q = 296 \text{ kg/m}^2$.
 Av. Reynolds Number = 1,670,000.
 Av. temperature = 36° C .

Span = 24 in. (61.0 cm).
 Chord = 4.8 in. (12.2 cm).
 Aspect ratio = 5.
 Area = 0.1377 m^2 .
 Date, October 6, 1925.

Angle of attack, degrees α	Lift coefficient C_L	Corrected C_D	L/D	Moment coeffi- cient C_M	Corrected angle of attack, degrees
-6	+0.007	+0.0737	+0.09	-0.005	-6
-3	.182	.0569	3.20	-.021	-.290
-1.5	.281	.0550	5.11	-.020	-1.35
0	.376	.0586	6.42	-.034	+.20
+1.5	.479	.0658	7.28	-.030	1.76
3	.564	.0742	7.60	-.028	3.30
4.5	.664	.0865	7.68	-.055	4.86
6	.762	.1016	7.50	-.070	6.41
9	.940	.1335	7.04	-.069	9.51
12	1.115	.1772	6.29	-.113	12.60
15	1.213	.2371	5.11	-.162	15.65
18	1.243	.3242	3.83	-.207	18.67
21	1.228	.4351	2.82	-.263	21.66

TABLE VII

Sperry Messenger.
U. S. A. 5 wings with propeller.
Av. tank pres.=20.35 atm.
Av. dynamic pres. $q=607\text{ kg/m}^2$.
Av. Reynolds Number=3,210,000.
Av. temperature=49° C.

Span=24 in. (61.0 cm).
Chord=4.8 in. (12.2 cm).
Aspect ratio=5.
Area=0.1377 m².
Date, October 6, 1925.

Angle of attack, degrees α	Lift coefficient C_L	Corrected C_D	L/D	Moment coeffi- cient C_M	Corrected angle of attack, degrees
-6	-0.002	+0.0709	-0.03	-0.000	-6
-3	+.180	.0524	+3.43	-.011	-2.90
-1.5	.276	.0523	5.28	-.010	-1.35
0	.372	.0562	6.62	-.023	+.20
+1.5	.465	.0633	7.34	-.028	1.75
3	.556	.0719	7.73	-.029	3.30
4.5	.656	.0839	7.82	-.042	4.85
6	.751	.0971	7.74	-.051	6.40
9	.929	.1295	7.17	-.066	9.50
12	1.106	.1706	6.48	-.087	12.60
15	1.237	.2247	5.50	-.128	15.67
18	1.268	.3122	4.06	-.200	18.68
21	1.236	.4188	2.96	-.248	21.67

TABLE VIII

Sperry Messenger.
U. S. A. 35-B wings.
Av. tank pres.=1 atm.
Av. dynamic pres. $q=28.7\text{ kg/m}^2$.
Av. Reynolds Number=177,000.
Av. temperature=20° C.

Span=24 in. (61.0 cm).
Chord=4.8 in. (12.2 cm).
Aspect ratio=5.
Area=0.1377 m².
Date, April 13, 1926.

Angle of attack, degrees α	Lift coefficient C_L	Corrected C_D	L/D	Moment coeffi- cient C_M	Corrected angle of attack, degrees
-9	-0.119	+0.0869	-1.37	+0.095	-9.06
-6	+.066	.0699	+.94	.059	-5.96
-3	.235	.0689	3.41	.064	-2.88
-1.5	.330	.0727	4.54	.049	-1.33
0	.426	.0781	5.46	.032	+.23
+1.5	.519	.0856	6.06	.034	1.78
3	.613	.0965	6.35	.036	3.33
4.5	.706	.1078	6.55	.007	4.87
6	.789	.1229	6.42	.001	6.42
7.5	.876	.1364	6.42	.024	7.97
9	.949	.1554	6.11	.014	9.51
12	1.105	.1950	5.66	.017	12.60
15	1.220	.2475	4.93	-.030	15.66
18	1.193	.3397	3.51	-.062	18.64
21	1.101	.4427	2.49	-.077	21.59

TABLE IX.

Sperry Messenger.
 U. S. A. 35-B wings.
 Av. tank pres.=20.2 atm.
 Av. dynamic pres., $q=628$ kg/m².
 Av. Reynolds Number=3,410,000.
 Av. temperature=38° C.

Span=24 in. (61.0 cm).
 Chord=4.8 in. (12.2 cm).
 Aspect ratio=5.
 Area=0.1377 m².
 Date, April 13, 1926.

Angle of attack, degrees α	Lift coefficient C_L	Corrected C_D	L/D	Moment coeffi- cient C_M	Corrected angle of attack, degrees
-9	-0.115	+0.0512	-2.25	+0.066	-9.06
-6	+.066	.0444	+1.49	.043	-5.96
-3	.254	.0462	5.50	.073	-2.86
-1.5	.340	.0510	6.66	.038	-1.32
0	.433	.0575	7.53	.026	+.23
+1.5	.536	.0665	8.06	.026	1.79
3	.629	.0765	8.22	.017	3.34
4.5	.737	.0892	8.26	.045	4.90
6	.809	.1034	7.82	.003	6.44
7.5	.908	.1202	7.55	.007	7.99
9	.991	.1379	7.18	-.007	9.53
12	1.154	.1785	6.46	-.019	12.62
15	1.317	.2285	5.76	-.037	15.71
18	1.478	.2889	5.12	-.067	18.79
21	1.472	.3708	3.97	-.066	21.79
22.5	1.384				

TABLE X

Sperry Messenger.
 U. S. A. 27 wings.
 Av. tank pres.=1 atm.
 Av. dynamic pres., $q=28.8$ kg/m².
 Av. Reynolds Number=175,000.
 Av. temperature=22° C.

Span=24 in. (61.0 cm).
 Chord=4.8 in. (12.2 cm).
 Aspect ratio=5.
 Area=0.1377 m².
 Date, April 16, 1926.

Angle of attack, degrees α	Lift coefficient C_L	Corrected C_D	L/D	Moment coeffi- cient C_M	Corrected angle of attack, degrees
-9	-0.104	+0.1093	-0.95	-0.045	-9.06
-6	+.068	.0777	+.87	+.001	-5.96
-3	.229	.0711	3.22	+.017	-2.88
-1.5	.328	.0727	4.51	-.017	-1.32
0	.418	.0788	5.30	+.017	+.23
+1.5	.519	.0846	6.14	-.036	1.78
3	.600	.0938	6.40	-.019	3.32
4.5	.687	.1041	6.60	-.027	4.87
6	.775	.1186	6.54	-.012	6.42
7.5	.858	.1320	6.50	-.014	7.96
9	.935	.1509	6.20	-.007	9.50
12	1.083	.1885	5.74	-.026	12.58
15	1.228	.2337	5.25	-.031	15.66
18	1.277	.2986	4.28	-.062	18.69
21	1.242	.3635	3.42	-.099	21.67

TABLE XI

Sperry Messenger.
U. S. A. 27 wings.
Av. tank pres.=20.5 atm.
Av. dynamic pres., $q=649$ kg/m².
Av. Reynolds Number=3,530,000.
Av. temperature=37° C.

Span=24 in. (61.0 cm).
Chord=4.8 in. (12.2 cm).
Aspect ratio=5.
Area=0.1377 m².
Date, April 16, 1926.

Angle of attack, degrees α	Lift coefficient C_L	Corrected C_D	L/D	Moment coeffi- cient C_M	Corrected angle of attack, degrees
-9	-0.141	+0.0534	-2.64	+0.037	-9.08
-6	+.032	.0463	+.69	.017	-5.98
-3	.206	.0465	4.43	.018	-2.89
-1.5	.307	.0501	6.13	.027	-1.33
0	.395	.0555	7.12	.009	+.21
+1.5	.489	.0631	7.75	.005	1.76
3	.579	.0719	8.05	-.005	3.31
4.5	.674	.0832	8.10	+.004	4.86
6	.755	.0957	7.89	-.017	6.41
7.5	.849	.1099	7.72	-.010	7.96
9	.932	.1266	7.36	-.022	9.50
12	1.099	.1655	6.64	-.024	12.59
15	1.258	.2121	5.93	-.049	15.68
18	1.401	.2682	5.22	-.064	18.76
21	1.404	.3509	4.00	-.086	21.76
22.5	1.428	.3891	3.67	-.122	23.27

TABLE XII

Sperry Messenger.
Göttingen 387.
Av. tank pres.=1 atm.
Av. dynamic pres., $q=28.5$ kg/m².
Av. Reynolds Number=172,000.
Av. temperature=26° C.

Span=24 in. (61.0 cm).
Chord=4.8 in. (12.2 cm).
Aspect ratio=5.
Area=0.1377 m².
Date, May 28, 1926.

Angle of attack, degrees α	Lift coefficient C_L	Corrected C_D	L/D	Moment coeffi- cient C_M	Corrected angle of attack, degrees
-9	-0.021	+0.0908	-0.23	-0.016	-9.01
-6	+.164	.0764	+.2.15	+.005	-5.91
-3	.339	.0801	4.23	-.003	-2.82
-1.5	.434	.0859	5.05	-.019	-1.27
0	.529	.0946	5.59	.022	+.28
+1.5	.640	.1062	6.03	.057	1.83
3	.724	.1168	6.20	.033	3.39
4.5	.815	.1309	6.22	.046	4.95
6	.904	.1436	6.29	.037	6.49
7.5	.999	.1641	6.08	.042	8.04
9	1.074	.1815	5.92	.035	9.58
10.5	1.142	.2033	5.62	.010	11.12
12	1.216	.2240	5.43	.012	12.66
15	1.352	.2822	4.79	.005	15.73
18	1.416	.3303	4.28	-.013	18.76
21	1.404	.4040	3.47	-.050	21.76

TABLE XIII

Sperry Messenger.
 Göttingen 387 wings.
 Av. tank pres.=20.3 atm.
 Av. dynamic pres. $q=624$ kg/m².
 Av. Reynolds Number=3,400,000.
 Av. temperature=39° C.

Span=24 in. (61.0 cm).
 Chord=4.8 in. (12.2 cm).
 Aspect ratio=5.
 Area=0.1377 m².
 Date, May 10, 1926.

Angle of attack, degrees α	Lift coefficient C_L	Corrected C_D	L/D	Moment coeffi- cient C_M	Corrected angle of attack, degrees
-9	+0.041	+0.0523	+0.78	+0.029	-8.98
-6	.228	.0526	4.33	.019	-5.88
-3	.404	.0609	6.63	.018	-2.78
-1.5	.497	.0685	7.26	.012	-1.23
0	.594	.0778	7.64	-.002	+.32
+1.5	.687	.0891	7.71	-.006	1.87
3	.772	.1010	7.64	-.017	3.42
4.5	.865	.1176	7.36	-.023	4.97
6	.957	.1337	7.16	-.044	6.52
7.5	1.041	.1521	6.84	-.050	8.06
9	1.124	.1735	6.47	-.059	9.61
12	1.282	.2185	5.87	-.096	12.69
15	1.362	.2856	4.77	-.182	15.73
18	1.350	.3593	3.76	-.227	18.73

TABLE XIV

Sperry Messenger.
 R. A. F. 15 wings.
 Av. tank pres.=1 atm.
 Av. dynamic pres., $q=27.0$ kg/m².
 Av. Reynolds Number=160,000.
 Av. temperature=53° C.

Span=24 in. (61.0 cm).
 Chord=4.8 in. (12.2 cm).
 Aspect ratio=5.
 Area=0.1377 m².
 Date, June 15, 1926.

Angle of attack, degrees α	Lift coefficient C_L	Corrected C_D	L/D	Moment coeffi- cient C_M	Corrected angle of attack, degrees
-9	-0.281	+0.1003	-2.80	-0.036	-9.15
-6	-.110	.0700	-1.57	-.004	-6.06
-3	+.076	.0607	+1.25	+.018	-2.96
-1.5	.176	.0618	2.85	.004	-1.41
0	.273	.0637	4.28	-.017	+.15
+1.5	.360	.0691	5.21	-.026	1.69
3	.446	.0788	5.66	-.021	3.24
4.5	.543	.0867	6.26	-.044	4.79
6	.626	.0991	6.32	-.064	6.34
7.5	.714	.1117	6.39	-.066	7.88
9	.794	.1278	6.21	-.109	9.43
12	.945	.1662	5.68	-.116	12.51
15	1.044	.2530	4.13	-.156	15.56
18	1.051	.3523	2.98	-.105	18.57
21	1.010	.4643	2.18	-.145	21.54

TABLE XV

Sperry Messenger.
 R. A. F. 15 wings.
 Av. tank pres.=20.2 atm.
 Av. dynamic pres., $q=600$ kg/m².
 Av. Reynolds Number=3,220,000.
 Av. temperature=47° C.

Span=24 in. (61.0 cm).
 Chord=4.8 in. (12.2 cm).
 Aspect ratio=5.
 Area=0.1377 m².
 Date, June 15, 1926.

Angle of attack, degrees α	Lift coefficient C_L	Corrected C_D	L/D	Moment coeffi- cient C_M	Corrected angle of attack, degrees
-6	-0.078	+0.0445	-1.75	-0.006	-6.04
-3	+.096	.0399	+2.41	-.007	-2.95
-1.5	.187	.0411	4.55	-.013	-1.40
0	.286	.0449	6.37	-.008	+.15
+1.5	.381	.0508	7.50	-.018	1.71
3	.470	.0577	8.15	-.024	3.25
4.5	.572	.0683	8.38	-.024	4.81
6	.662	.0798	8.29	-.022	6.36
7.5	.751	.0925	8.12	-.032	7.91
9	.838	.1079	7.77	-.034	9.45
12	1.007	.1478	6.82	-.058	12.54
15	1.146	.2071	5.53	-.072	15.62
18	1.151	.2573	4.47	-.110	18.62
21	1.135	.3545	3.20	-.051	21.61

TABLE XVI

Sperry Messenger.
 Clark Y wings.
 Av. tank pres.=1 atm.
 Av. dynamic pres., $q=28.0$ kg/m².
 Av. Reynolds Number=169,000.
 Av. temperature=27° C.

Span=24 in. (61.0 cm).
 Chord=4.8 in. (12.2 cm).
 Aspect ratio=5.
 Area=0.1377 m².
 Date, June 11, 1926.

Angle of attack, degrees α	Lift coefficient C_L	Corrected C_D	L/D	Moment coeffi- cient C_M	Corrected angle of attack, degrees
-9	-0.054	+0.0710	-0.76	-0.035	-9.03
-6	+.105	.0657	1.60	-.009	-5.94
-3	.289	.0682	4.24	-.036	-2.84
-1.5	.392	.0730	5.37	-.038	-1.29
0	.477	.0815	5.86	-.037	+.26
+1.5	.578	.0910	6.35	-.037	1.81
3	.668	.1029	6.49	-.027	3.36
4.5	.740	.1138	6.50	-.041	4.90
6	.836	.1293	6.46	-.020	6.45
7.5	.916	.1454	6.30	-.030	7.99
9	.983	.1641	5.99	-.002	9.53
12	1.142	.2070	5.52	-.088	12.62
15	1.226	.2597	4.72	-.140	15.66
18	1.172	.3530	3.32	-.179	18.63
21	1.086	.4593	2.36	-.111	21.58

TABLE XVII

Sperry Messenger.
Clark Y wings.
Av. tank pres.=20 atm.
Av. dynamic pres., $q=623 \text{ kg/m}^2$.
Av. Reynolds Number=3,350,000.
Av. temperature=42° C.

Span=24 in. (61.0 cm).
Chord=4.8 in. (12.2 cm).
Aspect ratio=5.
Area=0.1377 m².
Date, June 11, 1926.

Angle of attack, degrees α	Lift coefficient C_L	Corrected C_D	L/D	Moment coeffi- cient C_M	Corrected angle of attack, degrees
-9	-0.088	+0.0465	-1.89	-0.017	-9.05
-6	+.103	.0431	2.39	+.001	-5.94
-3	.280	.0481	5.82	-.001	-2.85
-1.5	.375	.0528	7.10	-.002	-1.30
0	.474	.0608	7.79	-.012	+.26
+1.5	.566	.0703	8.05	-.017	1.81
3	.647	.0797	8.12	-.015	3.35
4.5	.744	.0937	7.94	-.023	4.90
6	.835	.1091	7.66	-.026	6.45
7.5	.925	.1259	7.35	-.035	8.00
9	1.009	.1438	7.02	-.030	9.54
12	1.177	.1884	6.25	-.054	12.63
15	1.328	.2400	5.54	-.068	15.72
18	1.450	.2974	4.87	-.088	18.78
21	1.344	.4030	3.33	-.144	21.73

TABLE XVIII
SUMMARY OF DATA

Airfoil section	Tank pressure in atmospheres	Reynolds Number	C_L max.	C_D min.	Ratio $\frac{C_L \text{ max.}}{C_D \text{ min.}}$	Max. L/D
U. S. A. 5 without propeller--	1	173,000	1.194	0.0702	16.7	6.61
	20.3	3,390,000	1.279	.0476	26.9	8.28
U. S. A. 35-B-----	1	177,000	1.220	.0689	17.7	6.55
	20.2	3,410,000	1.490	.0440	33.8	8.26
U. S. A. 27-----	1	175,000	1.277	.0706	18.1	6.60
	20.5	3,530,000	1.428	.0460	31.0	8.10
Göttingen 387-----	1	172,000	1.416	.0764	18.5	6.29
	20.3	3,400,000	1.362	.0515	26.4	7.71
R. A. F. 15-----	1	160,000	1.051	.0607	17.3	6.39
	20.2	3,220,000	1.151	.0399	28.8	8.38
Clark Y-----	1	169,000	1.226	.0657	18.7	6.50
	20.2	3,350,000	1.450	.0431	32.9	8.12

TABLE XIX
ORDER OF MERIT OF AIRFOILS

Order of merit	From Sperry Messenger tests			
	C_L max. / C_D min.		Max. L/D	
	1 atm.	20 atm.	1 atm.	20 atm.
1	Clark Y-----	U. S. A. 35-B-----	U. S. A. 5-----	R. A. F. 15.
2	Gött. 387-----	Clark Y-----	U. S. A. 27-----	U. S. A. 5.
3	U. S. A. 27-----	U. S. A. 27-----	U. S. A. 35-B-----	U. S. A. 35-B.
4	U. S. A. 35-B-----	R. A. F. 15-----	Clark Y-----	Clark Y.
5	R. A. F. 15-----	U. S. A. 5-----	Gött. 387-----	U. S. A. 27.
6	U. S. A. 5-----	Gött. 387-----	R. A. F. 15-----	Gött. 387.

Order of merit	From airfoil tests			
	C_L max. / C_D min.,		Max. L/D	
	1 atm.	20 atm.	1 atm.	20 atm.
1	R. A. F. 15-----	U. S. A. 35-B-----	Clark Y-----	R. A. F. 15.
2	Clark Y-----	R. A. F. 15-----	U. S. A. 5-----	U. S. A. 5.
3	U. S. A. 5-----	Clark Y-----	R. A. F. 15-----	Clark Y.
4	U. S. A. 27-----	U. S. A. 27-----	U. S. A. 27-----	U. S. A. 27.
5	U. S. A. 35-B-----	Gött. 387-----	U. S. A. 35-B-----	U. S. A. 35-B.
6	Gött. 387-----	U. S. A. 5-----	Gött. 387-----	Gött. 387.

TABLE XX
ORDINATES OF SECTIONS

Per cent chord	U. S. A. 5		U. S. A. 35-B		U. S. A. 27	
	Upper	Lower	Upper	Lower	Upper	Lower
0	0. 73	0. 33	2. 76	2. 76	1. 77	1. 77
1. 25	2. 10	. 17	5. 15	1. 03	3. 80	. 50
2. 5	3. 03	. 03	6. 10	. 61	5. 07	. 33
5	4. 40	. 03	7. 53	. 27	6. 93	. 17
7. 5	5. 40	. 25	8. 65	. 14	8. 22	. 10
10	6. 20	. 57	9. 47	. 07	9. 17	. 00
15	7. 16	1. 10	10. 57	. 00	10. 50	. 10
20	7. 92	1. 55	11. 28	. 05	11. 33	. 35
30	8. 30	2. 02	11. 74	. 16	11. 90	. 95
40	8. 14	2. 17	11. 37	. 28	11. 57	1. 17
50	7. 55	1. 96	10. 29	. 41	10. 77	. 80
60	6. 75	1. 55	8. 86	. 41	9. 52	. 25
70	5. 63	1. 16	7. 08	. 41	8. 00	. 10
80	4. 24	. 76	5. 02	. 37	6. 03	. 05
90	2. 52	. 55	2. 76	. 21	3. 65	. 15
95	1. 50	. 35	1. 52	. 12	2. 00	. 47
100	. 50	. 00	. 28	. 00	. 67	. 65

Per cent chord	Gött. 387		R. A. F. 15		Clark Y	
	Upper	Lower	Upper	Lower	Upper	Lower
0	3. 61	3. 61	0. 20	0. 20	3. 50	3. 50
1. 25	6. 74	1. 35	1. 90	— . 45	5. 45	1. 93
2. 5	7. 98	. 81	2. 80	— . 73	6. 50	1. 47
5	9. 87	. 36	3. 90	— . 90	7. 90	. 93
7. 5	11. 32	. 18	4. 60	— 1. 00	8. 85	. 63
10	12. 40	. 13	5. 05	— 1. 00	9. 60	. 42
15	13. 83	. 00	5. 58	— . 80	10. 69	. 15
20	14. 77	. 08	5. 76	— . 50	11. 36	. 03
30	15. 36	. 22	5. 80	— . 10	11. 70	. 00
40	14. 88	. 38	5. 58	— . 05	11. 40	. 00
50	13. 48	. 54	5. 17	— . 28	10. 52	. 00
60	11. 59	. 54	4. 68	— . 47	9. 15	. 00
70	9. 16	. 54	4. 07	— . 62	7. 35	. 00
80	6. 58	. 50	3. 28	— . 67	5. 22	. 00
90	3. 61	. 27	2. 24	— . 35	2. 80	. 00
95	1. 99	. 16	1. 63	— . 20	1. 49	. 00
100	. 37	. 00	. 30	+ . 30	. 12	. 00

REPORT No. 270

**THE MEASUREMENT OF PRESSURE THROUGH TUBES
IN PRESSURE DISTRIBUTION TESTS**

By PAUL E. HEMKE
Langley Memorial Aeronautical Laboratory

REPORT No. 270

THE MEASUREMENT OF PRESSURE THROUGH TUBES IN PRESSURE DISTRIBUTION TESTS

By PAUL E. HEMKE

SUMMARY

The tests described in this report were made by the National Advisory Committee for Aeronautics to determine the error caused by using small tubes to connect orifices on the surface of aircraft to central pressure capsules in making pressure distribution tests.

Aluminum tubes of $\frac{3}{16}$ -inch inside diameter were used to determine this error. Lengths from 20 feet to 226 feet and pressures whose maxima varied from 2 inches to 140 inches of water were used. Single-pressure impulses for which the time of rise of pressure from zero to a maximum varied from 0.25 second to 3 seconds were investigated.

The results show that the pressure recorded at the capsule on the far end of the tube lags behind the pressure at the orifice end and experiences also a change in magnitude. For the values used in these tests the time lag and pressure change vary principally with the time of rise of pressure from zero to a maximum and the tube length. Curves are constructed showing the time lag and pressure change. Empirical formulas are also given for computing the time lag.

Analysis of pressure-distribution tests made on airplanes in flight shows that the recorded pressures are slightly higher than the pressures at the orifice and that the time lag is negligible. The apparent increase in pressure is usually within the experimental error, but in the case of the modern pursuit type of airplane the pressure increase may be 5 per cent. For pressure-distribution tests on airships the analysis shows that the time lag and pressure change may be neglected.

INTRODUCTION

The air pressure acting on an aircraft in flight is usually measured by providing an orifice at the point to be investigated and connecting this orifice to a manometer by means of a tube of comparatively small diameter. During steady rectilinear motions of the aircraft the pressure in the tube at the manometer end differs from the pressure at the orifice end only by the amount due to the differences in level of the two ends of the tube. This difference of pressure is usually quite small but may easily be computed.

While maneuvering the aircraft, however, the pressure at the orifice end of the tube changes more or less rapidly and a pressure wave is then propagated along the tube to the manometer. If now a second manometer is connected with the tube, at or very near the orifice, records of the pressure wave given by the two manometers show both a time displacement and a change of amplitude. This error in the reading of the manometer at the far end of the tube is due to the viscosity, elasticity, and mass of the air inclosed in the tube, to the inertia of the manometer parts, to the material of which the tube is made, and to the condition of the inside surface of the tube.

The error caused by the mass forces of the air inside the tube may be easily computed. This error can be avoided by using two tubes approximately equal in length and diameter to connect two orifices on opposite sides of a wing or fin to the same manometer. The mass forces due to the air inside the two tubes will be equal and will cancel each other in the difference of the two pressures. In the instruments now used the mass forces of the manometer

parts affect the readings to such a small extent that this error can be neglected. The material of which the tubes are made will not yield sufficiently, in the range of pressures encountered in aeronautical research, to cause any appreciable error unless the tubes are made of rubber.

The error due to the viscosity and elasticity of the air depends chiefly on the length and diameter of the tube and the time rate of change of pressure at the orifice. This error has not yet been computed, and extensive analysis has shown that the phenomenon giving rise to it is quite complicated. It is likely that our present knowledge of the mechanism of air flow very near solid boundaries must be considerably extended before this error can be calculated.

The Aeronautical Research Committee (British) has published a preliminary report describing experiments dealing with the transmission of air waves through pipes (Reference 1). A test to determine the effect of tube length upon the recorded pressure has been made on an airplane in flight (Reference 2). The tests described in this report were made concurrently with and independently of the experiments made by the British (Reference 1) and previous to the flight tests described in Reference 2. Two series of experiments were made as follows:

(a) *Experiments with tubes of very small diameter using pressures changing periodically:*

These tests were undertaken to determine the suitability of tubes of very small diameter for transmitting pressures acting at various points on the surface of an aircraft. Both time displacement and change in amplitude of a pressure wave as recorded by two manometers, one at the near or orifice end of the tube and the other at the far end, were studied. Frequencies and amplitudes were used which would permit comparison with a previously derived theoretical formula due to Rayleigh (Reference 3).

The experiments with these very small tubes soon showed that condensation on the inner surface of the tubes due to atmospheric conditions and other slight obstructions in the tubes would very seriously affect the correct interpretation of the results obtained.

(b) *Experiments with larger tubes using single pressure waves:*

In this series of tests aluminum tubes of $\frac{3}{16}$ -inch inside diameter were used. Single-pressure impulses of various rates of pressure rise and of various amplitudes were used exclusively. Time displacement and change in amplitude, as previously described, were investigated. Results could be reproduced under varying atmospheric conditions with sufficient accuracy to warrant continuing the tests.

It is not claimed that the empirical information obtained in these tests is an exhaustive study of the transmission of pressure waves through tubes. The tests reproduced conditions as they exist in what is now standard practice at the Langley Memorial Aeronautical Laboratory in making pressure distribution tests—i. e., using aluminum tubes of $\frac{3}{16}$ -inch inside diameter to connect orifices to standard manometer capsules. The information obtained is useful to the flight-research engineer in enabling him to foresee when large errors are likely to be encountered and what the approximate errors actually are in tests with known tube lengths and known rates of pressure rise.

METHODS AND APPARATUS

(a) *Experiments with pressures changing periodically:*

The first series of experiments were made with round brass tubes, 0.040 and 0.048 inch inside diameter. The lengths of the tubes varied from 15 to 35 feet.

As shown in Figure 2, the two ends of each tube used were connected to pressure-measuring capsules similar to those described in N. A. C. A. Technical Note No. 233 (Reference 4). These capsules are closed by thin metallic diaphragms, deflecting elastically under the action of a pressure difference on the two sides of the diaphragm. These deflections are transferred mechanically to a small mirror, which reflects a light beam to a sensitive photographic film. In this way a record is created on the film indicating the pressure at each moment of the interval. One film was exposed to the light beams of two such capsules. Figure 1 represents a record so obtained. The film moved from right to left at uniform speed, so that the length of a horizontal line represents a time. The two horizontal lines AA' and BB' represent the zero pressure readings for

the two capsules. Two curves M and M' indicate the deflections of the diaphragms, and points of the two curves lying on the same vertical line give the pressures at the two ends of the tube at the same moment.

At one end of the tube a periodically changing pressure was created by means of a "pressure oscillator," diagrammatically represented in Figure 2. At the other end of the tube the pressure changed periodically also, but pressures at the two ends did not necessarily agree. The photo-

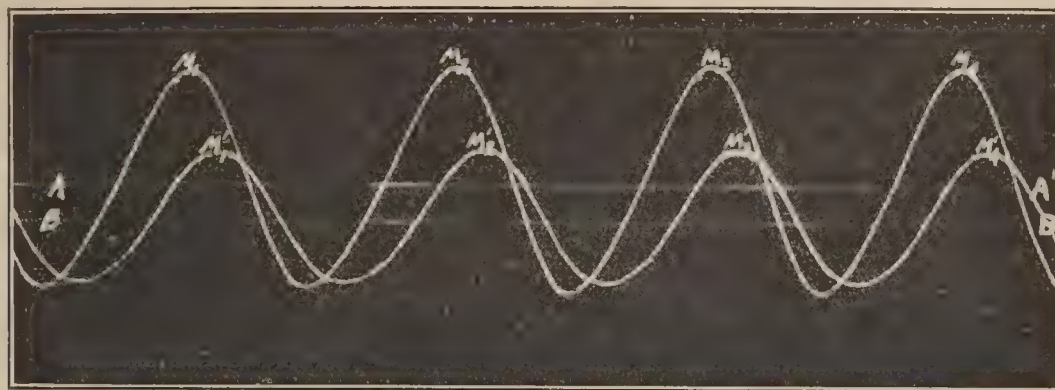


FIG. 1.—A photographic record from the tests with very small tubes using pressures changing periodically

graphic records obtained give the differences of pressures at the two ends, and thus furnish experimental data for studying the physical laws governing the magnitude of such pressure differences.

The pressure oscillator shown in Figure 2 consisted of a cylinder in which a piston was made to reciprocate by an eccentric cam. This motion was so regulated that a maximum air pressure of about $1\frac{1}{2}$ inches of water was reached. The pressure wave traversing the tube H leading from the cylinder was recorded at a point near the origin by means of a pressure-recording

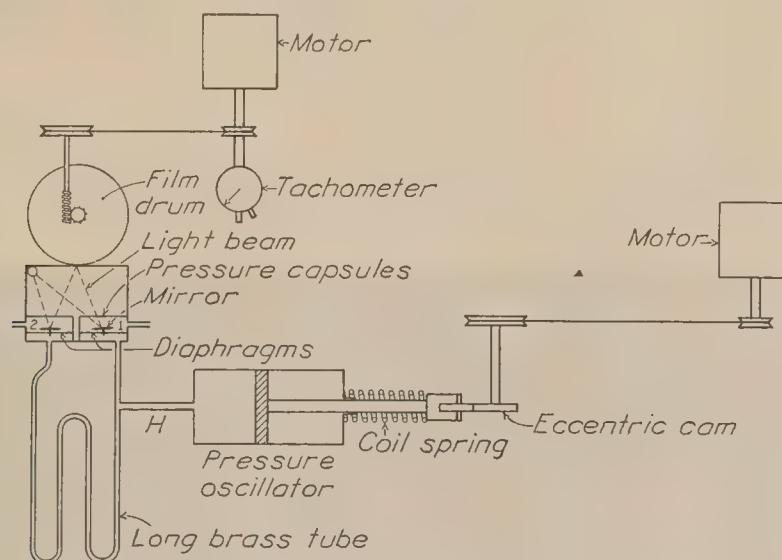


FIG. 2.—Apparatus used in tests with tube of very small diameter, pressure changing periodically

device or "capsule" 1, which was attached to the tube by a tee joint. After traversing the full length of the tube the pressure was recorded on capsule 2.

(b) *Tests with single-pressure waves:*

The second series of tests were made with aluminum tubes of $\frac{3}{16}$ -inch internal diameter. Lengths from 20 to 226 feet, and pressures whose maxima varied from 2 to 140 inches of water, were used. The time of rise of pressure from zero to a maximum varied from 0.25 to 3 seconds.

The piston type of pressure oscillator was not well adapted for securing a wide pressure range. Accordingly, a valve arrangement shown in the sketch at the lower right-hand corner of Figure 3 was substituted.

A tank of large volume containing air at a known, constant pressure was connected by a pipe to the pressure-control valve. Air from the tank flowed into the chamber A and into the tubes when the poppet valve B opened. This made the pressure in the tubes equal to that in

the tank. At any desired time thereafter valve B was quickly closed and valve C opened. The air in the tubes was thereby again reduced to atmospheric pressure through the vent D. By altering the shapes and the relative settings of the cams, various kinds of pressure variations were obtained. A wider latitude for variation of pressure maxima and rate of change of pressure was allowed with this system than with the piston type of oscillator.

In this manner a single pressure wave was propagated through the tube. It was recorded on the film by capsule 1 when it entered the tube and by capsule 2 when it reached the end.

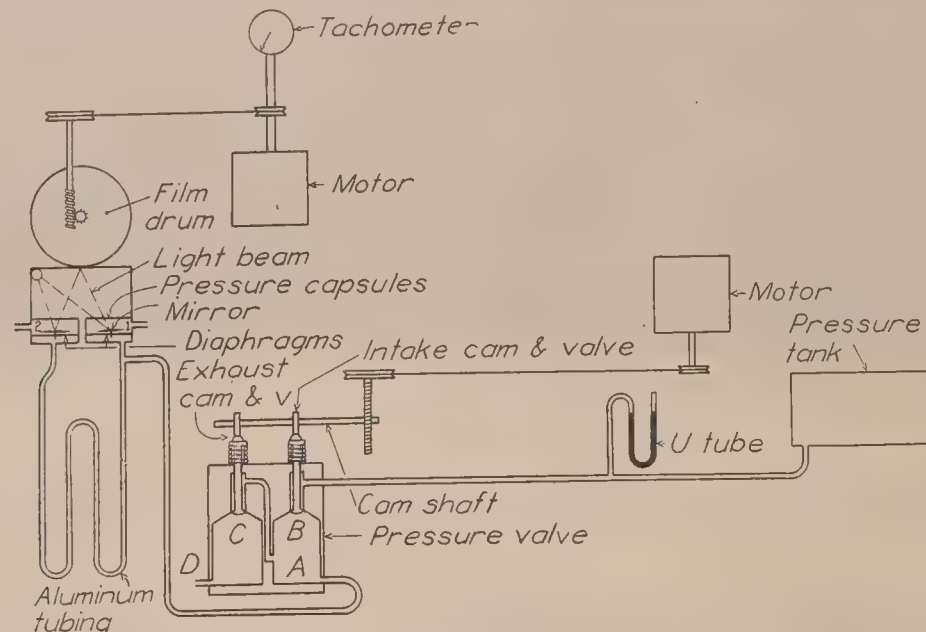


FIG. 3.—Apparatus used in tests with tubes of $\frac{3}{16}$ inch inside diameter single pressure waves

The tachometer gave the film drum speed and the calibration of the capsules gave the pressures obtained. By starting the film drum at different positions a mean of four readings at the same pressure and for the same rate of pressure rise was obtained.

Figure 4 shows a typical record. The zero pressure lines AA' and BB' were obtained by making an exposure of the photographic film when both capsules registered atmospheric pressure. This is called the zero pressure in the text and on the curves. In order to get full-scale deflections of the capsules, the zero pressure line BB' for capsule 2 was placed at the top of the film and the

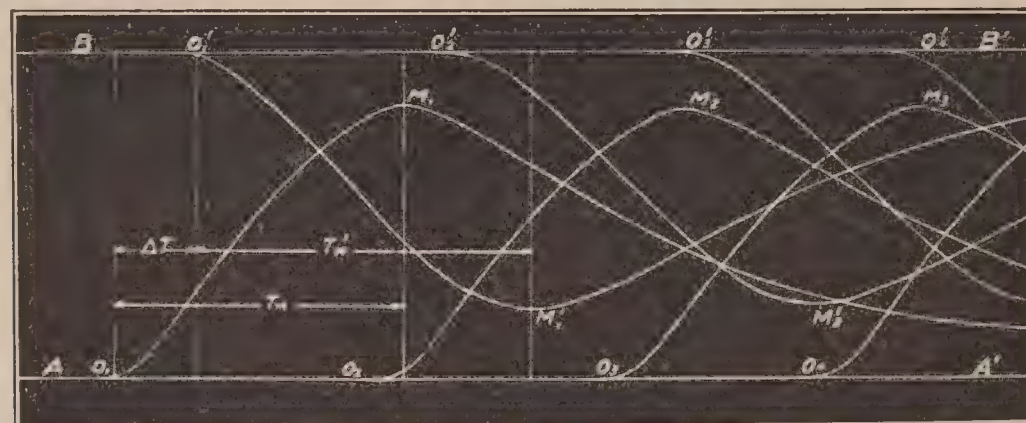


FIG. 4.—A photographic record from the tests with tubes of $\frac{3}{16}$ inch inside diameter using single pressure waves

records as obtained from this capsule were $O_1' M_1'$, $O_2' M_2'$, etc. AA' similarly represents the zero line for capsule 1 and $O_1 M_1$ and $O_2 M_2$, etc., the records of this capsule. Points $O_1, O_2, \dots, M_1, M_2$, etc. were marked on the film with great care. Very fine lines were drawn by means of a stylus through the points thus located. These lines are perpendicular to AA' and BB' in direction. The time displacement of the pressure wave was studied by measuring the following quantities:

- (1) T_M , the time of rise of pressure, from zero to a maximum, of the pressure wave at the orifice.

(2) T_M' , the time of rise of pressure, from zero to a maximum, of the pressure wave after it had traversed the tube.

(3) ΔT , the time required for the front of the pressure wave to traverse the tube.

The time displacement, T_L , of the peaks of the two waves is of interest and was determined in each case by means of the equation $T_L = T_M' + \Delta T - T_M$. This quantity is called time lag in the report.

Figure 5 shows a record where the loss in pressure as well as the time displacement were greater, due to a more rapid rate of pressure rise.

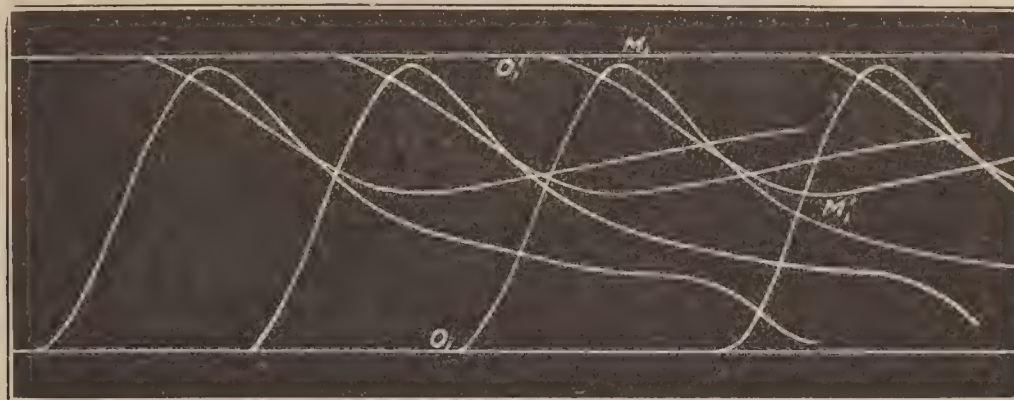


FIG. 5.—A photographic record from the tests with tubes of $\frac{1}{16}$ inch inside diameter showing a rapid rate of pressure rise

RESULTS

(a) Experiments with pressures changing periodically:

The tests with sine waves show a regular time lag. In Figure 6 the observed time lag is plotted in seconds per foot as ordinate against the frequency of oscillation per second as abscissa.

Lamb has published (Reference 3) a formula derived by Rayleigh from theory only. It enables us to find the time lag for small oscillations and small tubes in the form,

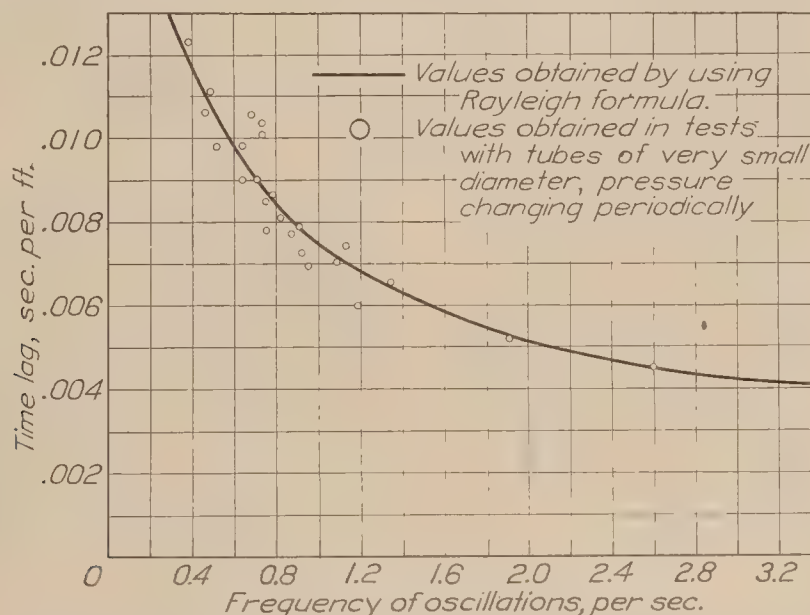


FIG. 6.—Comparison of results obtained in tests using tubes of very small diameter, pressure changing periodically with Rayleigh formula

$$T_L = \frac{r}{2} \sqrt{\frac{2\pi p_o N}{\mu}} \quad (1)$$

where

T_L = time lag

r = internal radius of tube

p_o = zero pressure

N = frequency of oscillation

μ = coefficient of viscosity of air.

The value obtained from the lag when the Rayleigh formula is used is plotted in Figure 6, together with the values found in the experiments.

(b) *Experiments with single pressure waves:*

Analysis of the results showed that T_M , T_M' and ΔT (fig. 4) could be readily expressed by means of empirical formulas. These formulas, which hold in the range of values used for tube length, rate of pressure rise and maximum pressure, are as follows:

$$T_M' = k T_M^m$$

$$k = 1 + (P^{4.84} \times 10^{-15}) L^{4.94} - .0542P + .000227P^2 \quad (2)$$

$$m = 1 - .000796 L - .000393 P$$

$$T = k_1 T_M^{m_1} \quad (3)$$

$$k_1 = (9.50 - .016P) \times 10^{-4} L^{1.1}$$

$$m_1 = (1.30 - .00311P) \times 10^{-3} L$$

From these the time lag T_L was found by means of

$$T_L = \Delta T + T_M' - T_M \quad (4)$$

Figures 7 and 8 are curves of T_L and T_M' plotted against T_M for the shortest and longest tube lengths used. In Figure 7 the maximum pressure is 5 inches of water, in Figure 8 it is 140 inches of water.

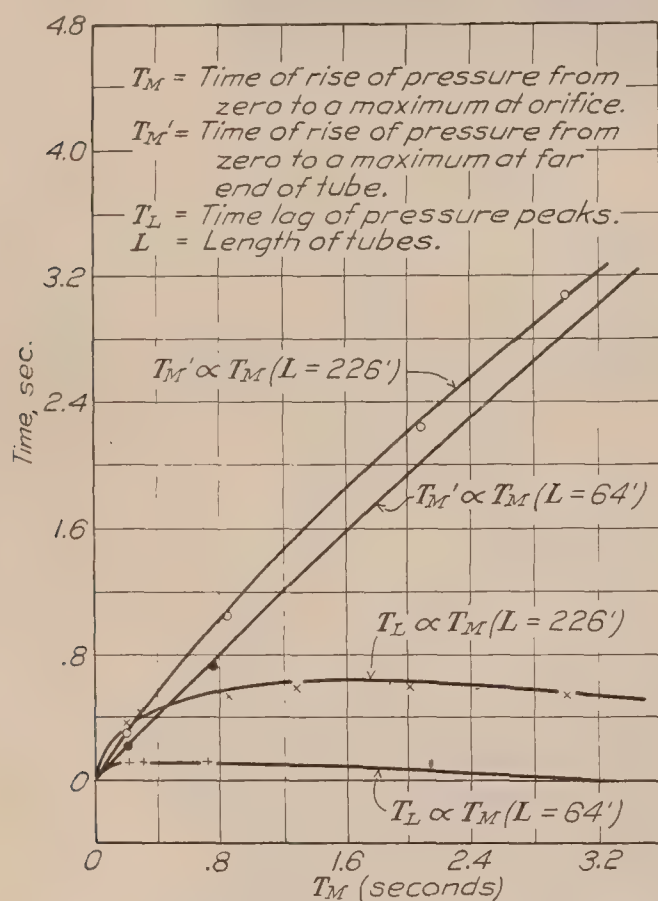


FIG. 7.—Maximum pressure 5 inches of water. Aluminum tubes $\frac{3}{16}$ inch inside diameter

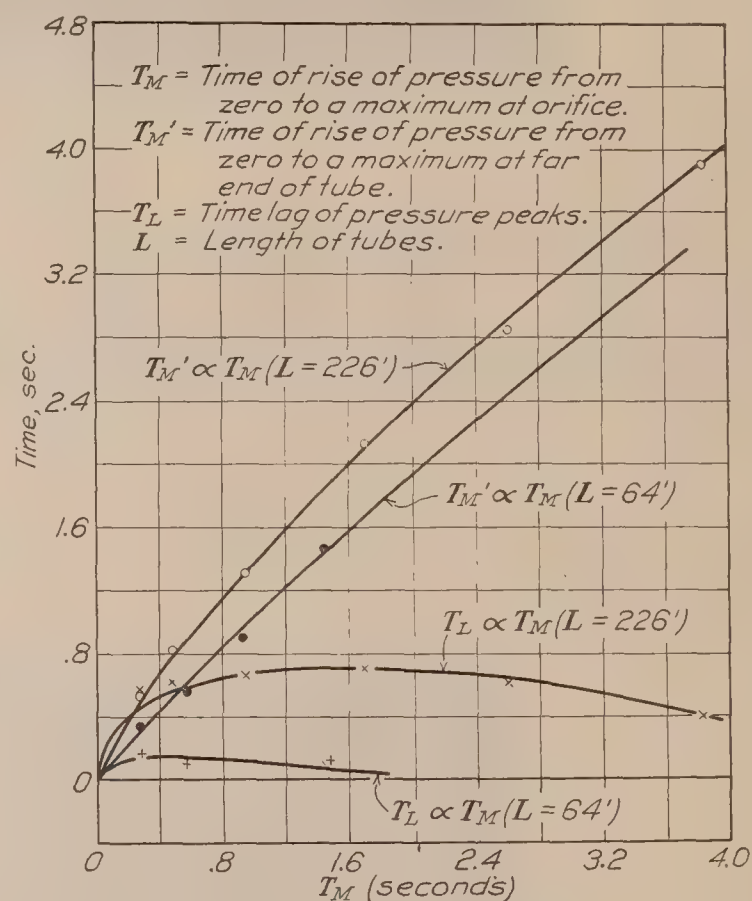


FIG. 8.—Maximum pressure 140 inches of water. Aluminum tubes $\frac{3}{16}$ inch inside diameter

Effect of change of maximum pressure and tube length on time lag of pressure peaks and time of use of pressure at end of tubes.

The maximum time lag or time displacement of pressure peaks is 0.7 second and occurs when $T_M' = 1.9$ seconds, the pressure maximum being 140 inches of water. This maximum time lag, however, occurs for only the longest tube. The time lag is affected principally by the tube length, the increased pressure not having a very large effect. This small change due to the increased pressure is not surprising inasmuch as the pressure range extends only from 1 to 1.34 atmospheres.

Analysis of the results revealed no simple formulas for the pressure loss or change in amplitude due to the frictional and other losses in the tubes. Figures 9, 10, 11, and 12 show in graphical form the pressure loss for maximum pressures of 2, 10, 60, and 140 inches of water as plotted against tube length. The pressure loss is expressed as a per cent of loss of the pressure at the orifice. Several values of the time required for the pressure to rise from zero to a maximum are shown for each maximum pressure.

In the tests with long tubes and slow rates of pressure rise the pressure maximum at the end of the tube proved to be smaller than the pressure maximum at the orifice end. For the shorter tubes and the more rapid rates of pressure rise the reverse was true, the phenomenon being very similar to that known as "water hammer."

At the time of writing no analytical formula has been discovered which may be used to compute the change of amplitude and time lag. The Rayleigh formula previously cited does not give results agreeing with the results obtained in the second series of experiments. The British tests which were restricted to pressures whose maximum value did not exceed 0.59 inch (15 mm.) of water did not yield results agreeing with analytical formulas.

APPROXIMATE ERRORS DUE TO THE USE OF TUBES FOR MEASURING AIR PRESSURES ON AIRCRAFT IN FLIGHT

The discussion will be limited to those errors caused by the viscosity and elasticity of the air. The results obtained in the laboratory tests with aluminum tubes of $\frac{3}{16}$ -inch internal diameter are used to determine the approximate error in the manometer readings. These results include the error due to the inertia of the manometer parts and the error caused by the slight expansion of the tubes.

A comparison was first made with a flight test (Reference 2) where a direct measurement had been made of the error due to the use of tubes of different length leading from an orifice on the surface of the wing of a JNS-1 airplane to the manometers. The rate of pressure rise was comparatively slow and consequently no appreciable errors could be expected. The most rapid rate of observed pressure rise was 4 inches of water in 1 second. The tube length used was 25 feet. The empirical formula for time lag gives a very small value which may be neglected. Figures 9 and 10 show that the change in pressure is negligible. The flight tests verified this as no measurable errors were observed.

The determination of the approximate error in flight tests which have been made previously is complicated by the fact that it is common practice to connect two orifices on opposite sides of a wing, fin, or tail surface to the two sides of a manometer and in this way measure the resultant pressure. The error is then a resultant of the errors of the two sets of orifices and tubes. Flight tests made recently with a VE-7 airplane (Reference 5) were used in determining the approximate errors. R. A. F. 15 wing sections are used on this airplane and pressure distribution tests (Reference 6) on a biplane model with this wing section gave some information about the pressures on the upper and lower surfaces of the wing. These tests showed that the average value of the magnitude of the maximum pressures on the lower surface was 75 per cent of the maximum resultant pressure and on the upper surface 25 per cent of the maximum resultant pressure while the angle of attack was being changed from that of zero lift to maximum lift. The maneuver in which large pressures occur and in which the rate of pressure rise is also fairly rapid is a pull up at high speed. As the principal changes in the aerodynamic forces in this maneuver are those due to the change in angle of attack it was assumed that the maximum pressures on the lower and upper surfaces are 75 per cent and 25 per cent, respectively, of the maximum resultant pressure. With this assumption the maximum errors found for the pressures on the upper wing of the VE-7 in a pull up at 126 M. P. H. were pressure gains of 1 per cent and time lags of 0.025 second. For pressures on the tail surface where the tubes were longer the pressure gain did not exceed 1.5 per cent and the time lag 0.03 second. The longest tube used was about 20 feet in length, the maximum pressure was 30 inches of water, and the minimum value of the recorded time of rise of pressure ($T_{M'}$) was 0.50 second. In flight tests now being made with a PW-9 airplane the maximum pressures will be higher and the values of $T_{M'}$ will probably be less than those in the VE-7 tests. Tube lengths do not exceed 25 feet and from the curves in Figures 9, 10, 11, 12 it is seen that the maximum error is a pressure gain of 3 per cent (approximately) if $T_{M'}$ is not less than 0.5 second. If $T_{M'}$ should be as low as 0.25 second the maximum pressure gain would be approximately 8 per cent. This comparatively large pressure gain would occur only for the smaller pressures, so that the total wing load would not be recorded 8 per cent higher than it really is.

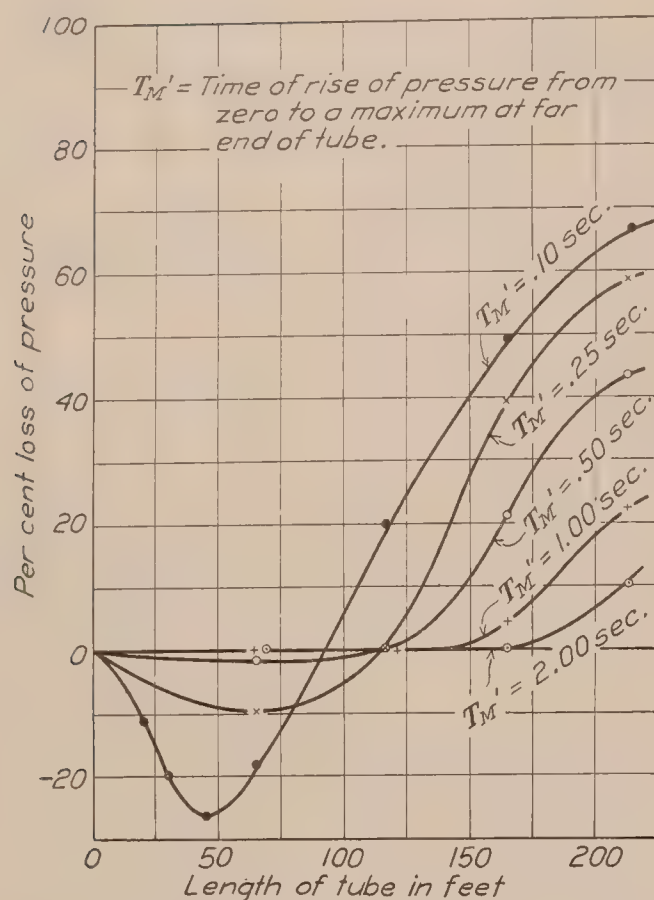


FIG. 9.—Maximum pressure 2 inches of water. Aluminum tubes $\frac{1}{8}$ inch inside diameter

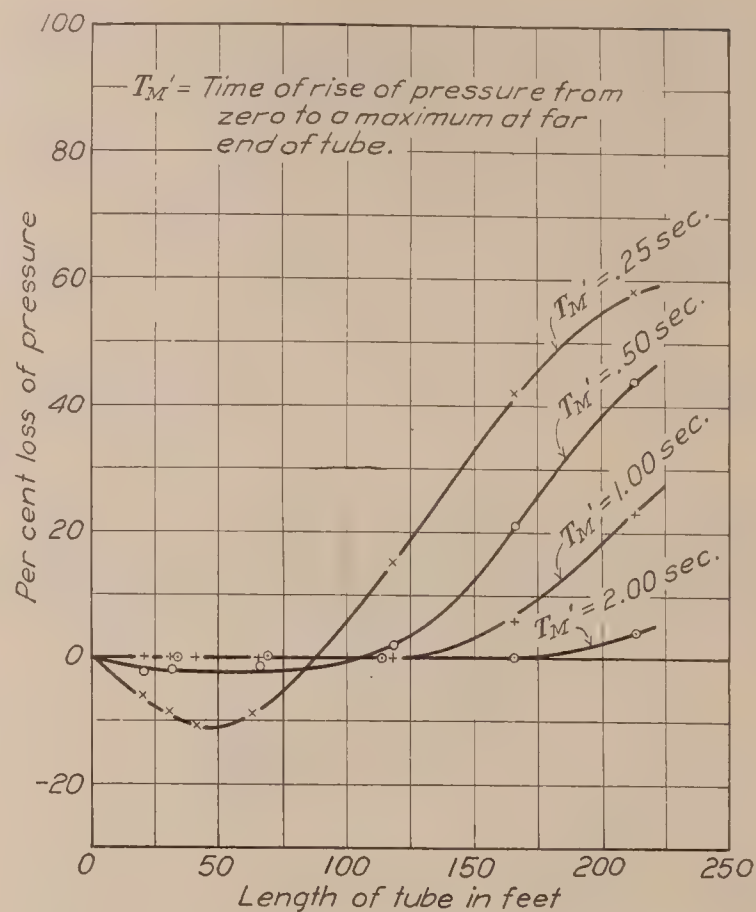


FIG. 10.—Maximum pressure 10 inches of water. Aluminum tubes $\frac{1}{8}$ inch inside diameter

Effect of the tube length and rate of pressure rise on the maximum pressure at the far end of the tube for various maximum pressures at the orifice end of the tube.

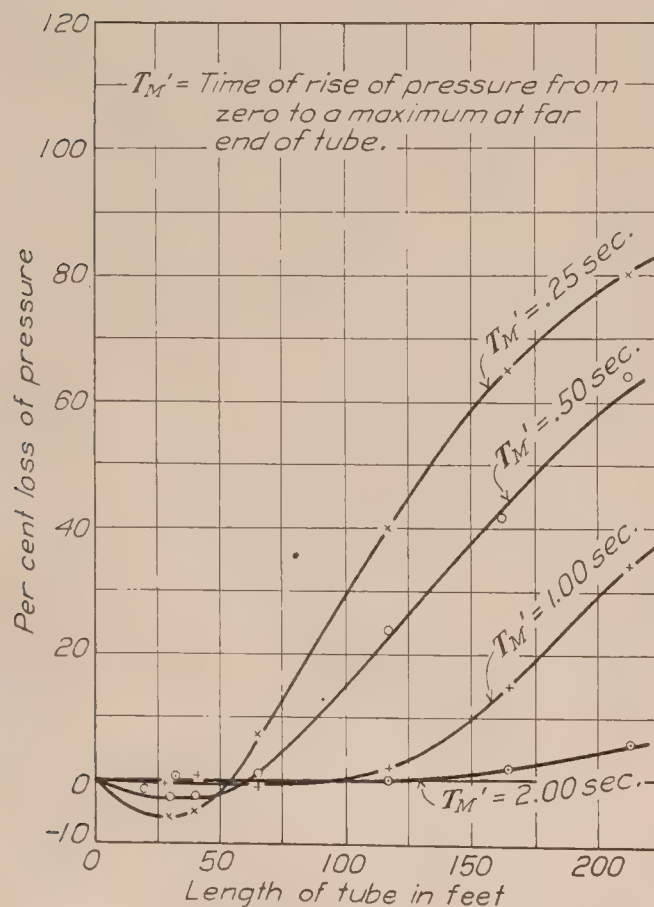


FIG. 11.—Maximum pressure 60 inches of water. Aluminum tubes $\frac{1}{8}$ inch inside diameter

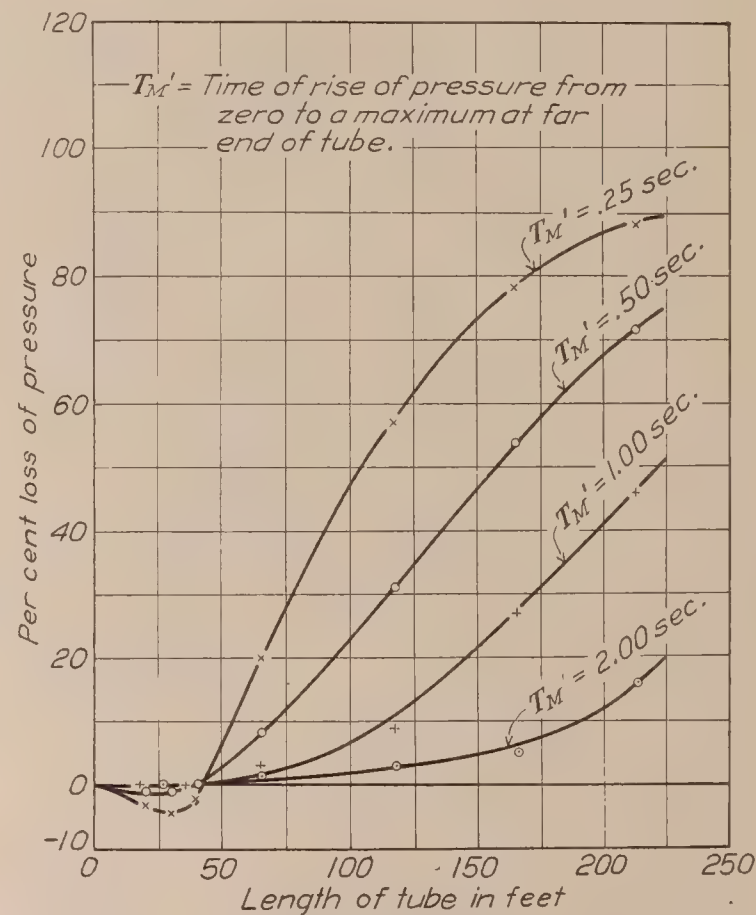


FIG. 12.—Maximum pressure 140 inches of water. Aluminum tubes $\frac{1}{8}$ inch inside diameter

Effect of the tube length and rate of pressure rise on the maximum pressure at the far end of the tube for various maximum pressures at the orifice end of the tube.

It appears then that even for modern high-speed airplanes the pressure losses are nil when tubes under 40 feet in length are used. The pressure errors are of such a nature that the designer using the records of pressure distribution tests without making corrections for possible tube errors is on the safe side.

In pressure distribution tests on airships in maneuvers the tubes are longer, the maximum pressures are smaller, and the rates of pressure rise much less than in tests with airplanes. In flight tests made recently on the airship U. S. S. *Los Angeles*, the most rapid rise of pressure was from zero to 3 inches of water in 16 seconds in a tube 100 feet in length. From the curves of pressure loss it is seen that this maneuver is so slow that the conditions may be considered as steady with a negligible pressure error and time lag.

CONCLUSIONS

These tests indicate that the pressure distribution measurements previously made and those now being made in flight research on aircraft, using aluminum tubes ($\frac{3}{16}$ -inch inside diameter) for connecting pressure capsules to orifices are on the whole quite accurate.

The error caused by the viscosity and elasticity of the air in the tubes is, for conditions approximating those of actual flight of airplanes, such as to make the recorded pressures higher than the actual pressures. For the types which have already been tested this apparent pressure gain is about 1 per cent in magnitude and is less than the experimental errors. For an airplane of the modern pursuit type the apparent pressure gain may reach 5 per cent. In pressure distribution tests on airships the time of rise of pressure is so slow that, even with the longer tubes necessary, the pressure loss or gain is negligible.

The magnitude of the time lag is so small that it does not affect the pressure distribution measurements made in flight research on aircraft.

LANGLEY MEMORIAL AERONAUTICAL LABORATORY,
NATIONAL ADVISORY COMMITTEE FOR AERONAUTICS,
LANGLEY FIELD, VA., *February 23, 1927.*

REFERENCES

1. SIMMONS, L. F. G., and JOHANSEN, F. C. Experiments on the Transmission of Air Waves through Pipes. British Reports and Memoranda No. 957, 1925.
2. CARROLL, T., and MIXSON, R. E. The Effect of Tube Length upon the Recorded Pressures from a Pair of Static Orifices in a Wing Panel. N. A. C. A. Technical Note No. 251, 1927.
3. LAMB, H. The Dynamical Theory of Sound. 1910.
4. COLEMAN, D. G. N. A. C. A. Flight-Path-Angle and Air-Speed Recorder. N. A. C. A. Technical Note No. 233, 1926.
5. CROWLEY, JR., J. W. Pressure Distribution over a Wing and Tail Rib of a VE-7 and of a TS Airplane in Flight. N. A. C. A. Technical Report No. 257, 1927.
6. IRVING, B. H., POWELL, C. H., and JONES, C. N. The Distribution of Pressure on the Upper and Lower Wings of a Biplane. British Reports and Memoranda No. 355, 1917.

REPORT No. 271

PRESSURE DISTRIBUTION TESTS ON PW-9 WING MODELS SHOWING EFFECTS OF BIPLANE INTERFERENCE

By A. J. FAIRBANKS
Langley Memorial Aeronautical Laboratory

REPORT No. 271

PRESSURE DISTRIBUTION TESTS ON PW-9 WING MODELS SHOWING EFFECTS OF BIPLANE INTERFERENCE

By A. J. FAIRBANKS

SUMMARY

In this report tests are described in which the distribution of pressures over models of the wings of the PW-9 airplane was investigated. The wing models were tested individually and in the biplane combination. The investigation was conducted in the atmospheric wind tunnel of the National Advisory Committee for Aeronautics. It is concluded in this paper that the effect of biplane interference on the pressures on the wings is practically confined to the lower surface of the upper wing and the upper surface of the lower wing; that the overhanging portion of the upper wing is not greatly affected by the presence of the lower wing; and that a slight washin at the center section of the upper wing satisfactorily compensates for a reduced chord at this section (providing the airfoil section is not mutilated) and prevents a large reduction in the normal force over this portion of the wing.

INTRODUCTION

At the request of the Army Air Corps, the distribution of pressures over the wings and the tail surfaces of a modern pursuit airplane (PW-9) is being investigated by the National Advisory Committee for Aeronautics. In order to study some of the phases of the problem which can not be undertaken in flight and to further correlate the results of wind tunnel and flight tests, pressure distribution tests have been made in the atmospheric wind tunnel on models of the wings of the PW-9. The models were tested individually and together in the mutual relation they have in the airplane.

In this paper the results of the model tests are presented and discussed.

TESTS

The wings of the PW-9 airplane are of the Göttingen 436 airfoil section throughout (fig. 1). The details of the models and the arrangement of the cellule are illustrated by Figure 2. The most unusual features of the cellule are the difference between the plan forms of the two wings and the washin of the center section of the upper wing.

Half span, laminated wooden models with inlaid pressure tubes, similar to those used in previous pressure distribution tests (reference 1) were employed in this investigation (fig. 3). The effect of the missing half span was reproduced by the use of a reflecting plane (fig. 4).

A new liquid multiple manometer (fig. 5) which has 117 tubes of approximately 15 inches clear height, was developed for and used in these tests. A photographic record obtained with this manometer is reproduced as Figure 6.

Static and dynamic pressure surveys were made two chord lengths ahead of the models (fig. 7). The integrated means of the survey values were used as a reference static pressure and the effective dynamic pressure, respectively.

The tests, which were made at approximately 30 meters per second air stream velocity, covered the range from -6 degrees through $+24$ degrees angle of attack.

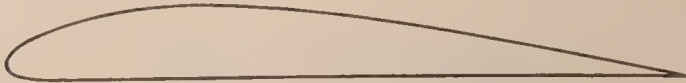


FIG. 1.—Göttingen 436 airfoil section

Airfoil ordinates

Station per cent chord	Upper per cent chord	Lower per cent chord
0	2.85	2.85
1¼	4.59	1.21
2½	5.54	0.69
5	6.86	0.37
7½	8.02	0.21
10	8.92	0.05
15	10.03	0.00
20	10.82	0.00
30	11.08	0.00
40	10.55	0.00
50	9.60	0.00
60	8.28	0.00
70	6.60	0.00
80	4.70	0.00
90	2.59	0.00
95	1.43	0.00
100	0.26	0.00

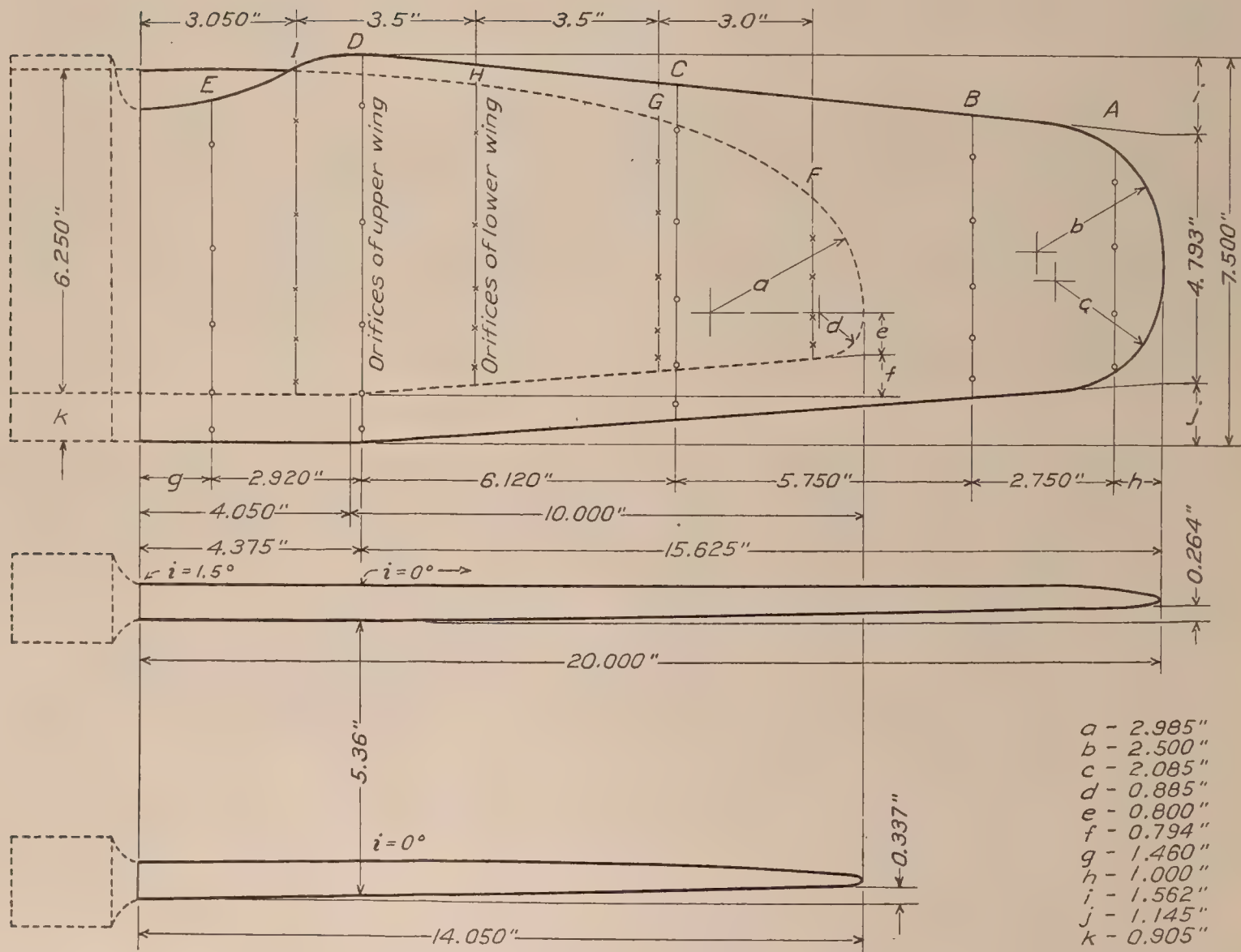


FIG. 2.—Plan and front elevation of PW-9 wing models



FIG. 3.—PW-9 pressure distribution wing models

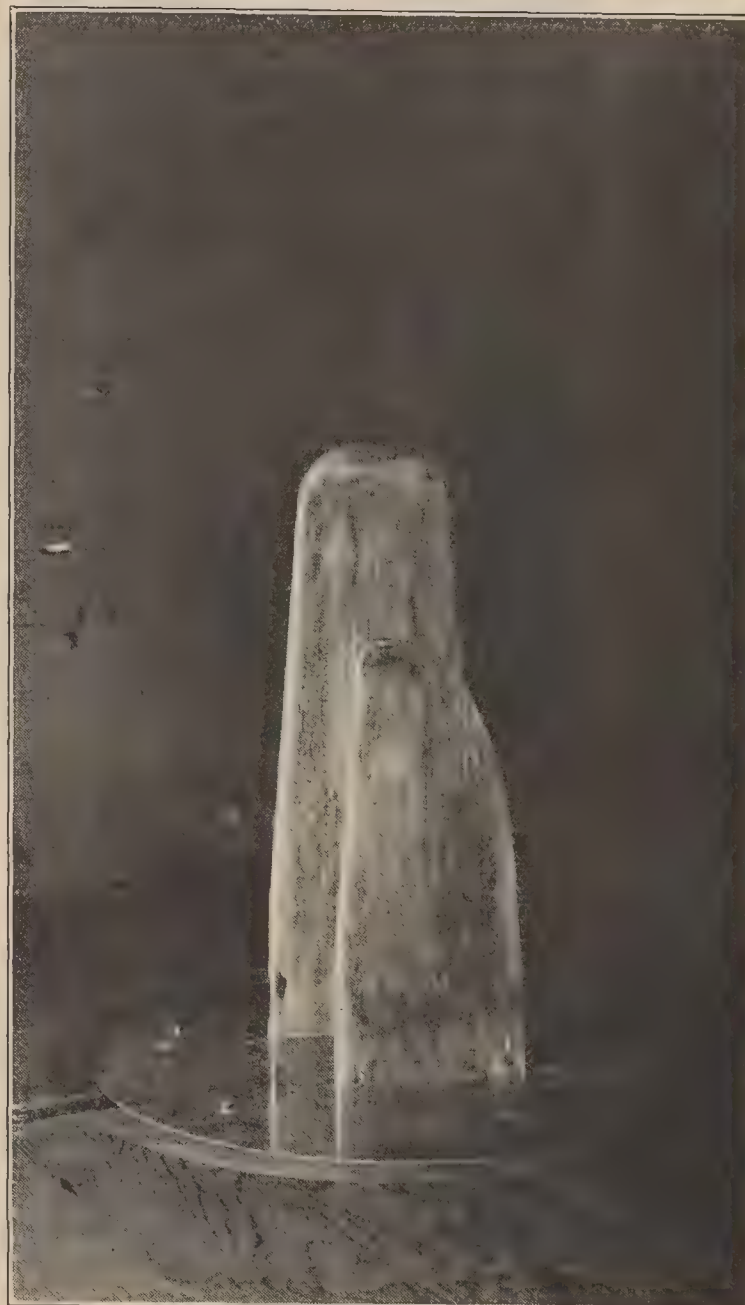


FIG. 4.—PW-9 wing models in wind tunnel

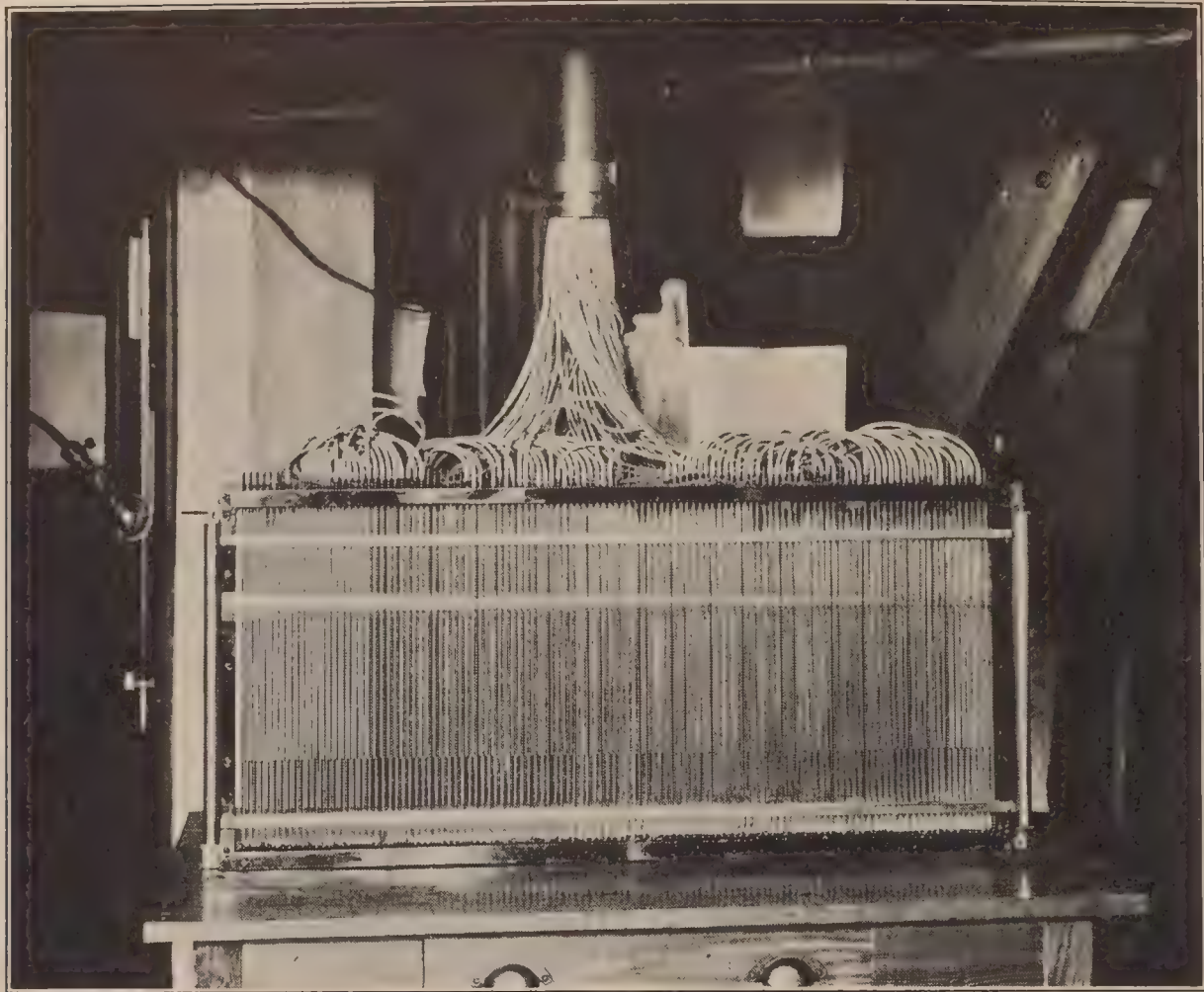


FIG. 5.—Multiple liquid manometer

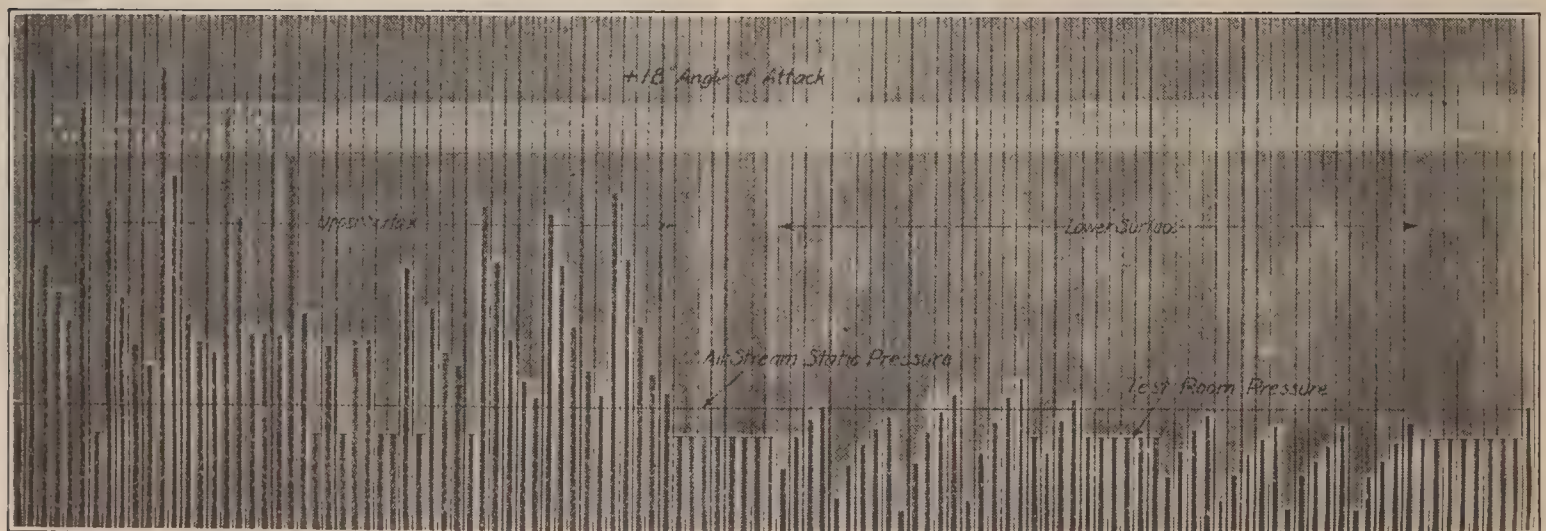


FIG. 6.—Reduced photograph of a manometer record

RESULTS

The results of the tests are presented in Figures 8 through 14. Five forms of representation are used, namely, pressure diagrams for the test sections, curves of normal force vs. span, normal force coefficient vs. span, normal force coefficient vs. angle of attack, and plots of centers of pressure on plan-view drawings of the wings. In each case the results of the tests of the wings in the biplane combination are compared with those of tests of the individual airfoils.

The diagrams of Figures 8 and 9 illustrate the variation of pressure along the test section chords. The pressures are given in terms of the dynamic pressure, $q = \frac{\rho V^2}{2}$.

The distribution of the normal force along the span is illustrated by Figure 10. The ordinates of these curves represent the magnitude of the normal force per unit span per unit q . The nondimensional coefficient K is defined by the equation

$$\text{Normal force per unit span} = K \times q \times \text{upper wing span}$$

or

$$K = C_{NF} \times \frac{\text{chord}}{\text{upper wing span}}$$

Figure 11 illustrates the variation of the normal force coefficient (C_{NF}) across the span. C_{NF} is usually defined as normal force divided by $q \times S$ but this may be transformed into

$$C_{NF} = \frac{\text{average pressure}}{q}$$

It will be seen that C_{NF} may, therefore, be interpreted as the ratio of the average normal pressure along a chord to the dynamic pressure.

Curves of normal force coefficient vs. angle of attack for each of the wings are presented in Figure 12. Similar curves for the entire cellule appear in Figure 13.

Curves showing the variation of the positions of centers of pressure along the spans of the wings are presented in Figure 14. The lateral positions of the centers of pressure are indicated.

DISCUSSION

In Figures 8 and 9 the effect of combining the wings to form the biplane can be seen in the change of pressures. The greatest change appears on the interior surfaces of the combination, i. e., the lower surface of the upper wing and the upper surface of the lower wing. The positive pressures on the lower surface of the upper wing and the negative pressures on the upper surface of the lower wing are reduced. It appears that the increased pressure below the upper wing partially neutralizes, and is neutralized by, the reduced pressure above the lower wing.

There is a small but consistent reduction of the pressures on the whole upper wing. The reverse is true of the lower wing. This may be explained as a result of placing the upper wing in the region of increased velocity and reduced static pressure which exists above the lower wing. Then by similar reasoning the lower wing is in a region of reduced velocity and increased static pressure.

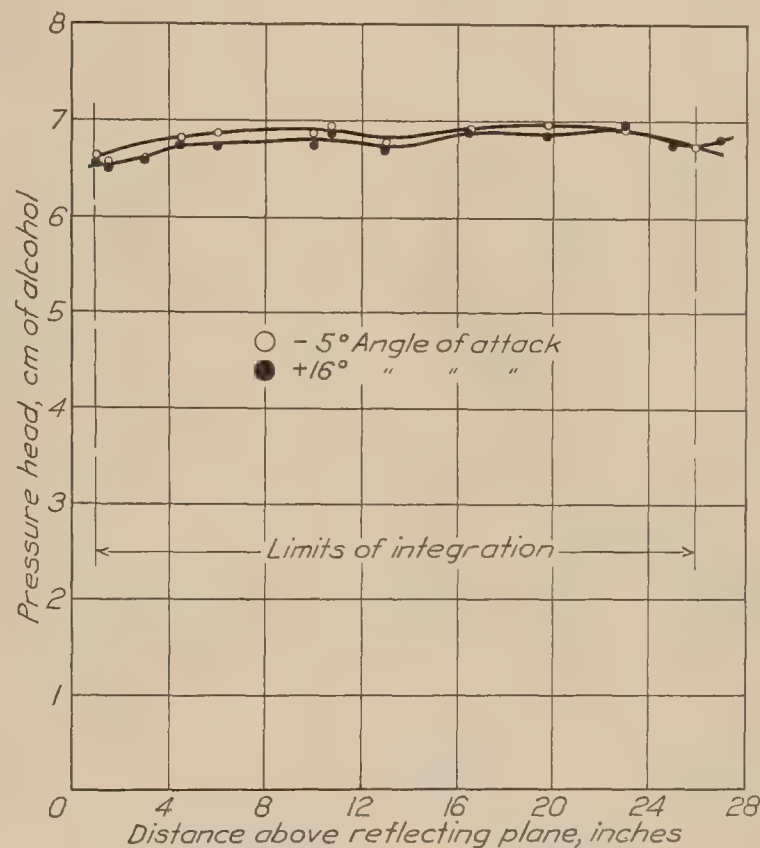


FIG. 7.—Dynamic pressure surveys. (Average dynamic head 6.805 c. m.)

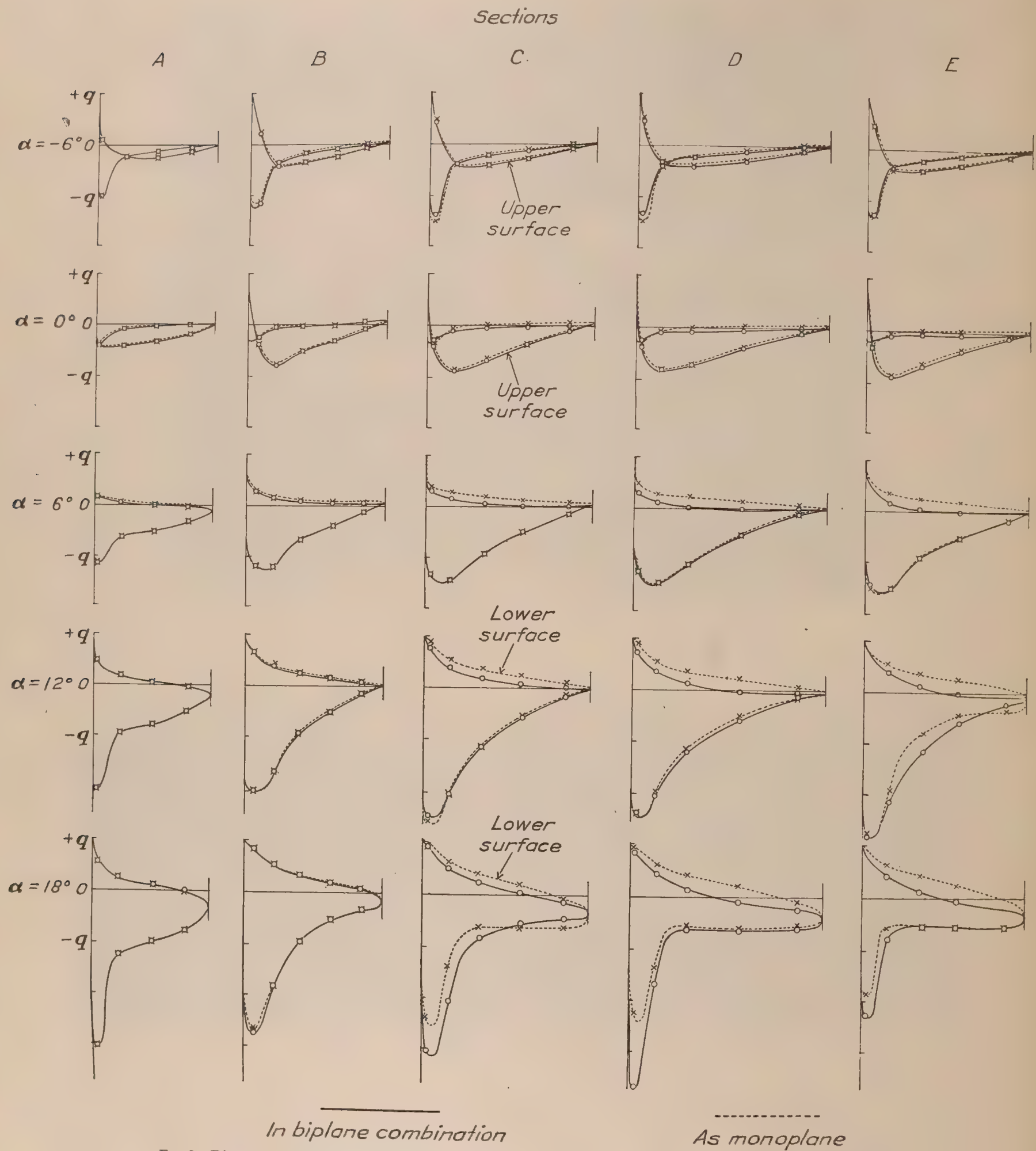


FIG. 8.—Diagrams of pressures at test sections of upper wing. Comparison as monoplane and in biplane combination

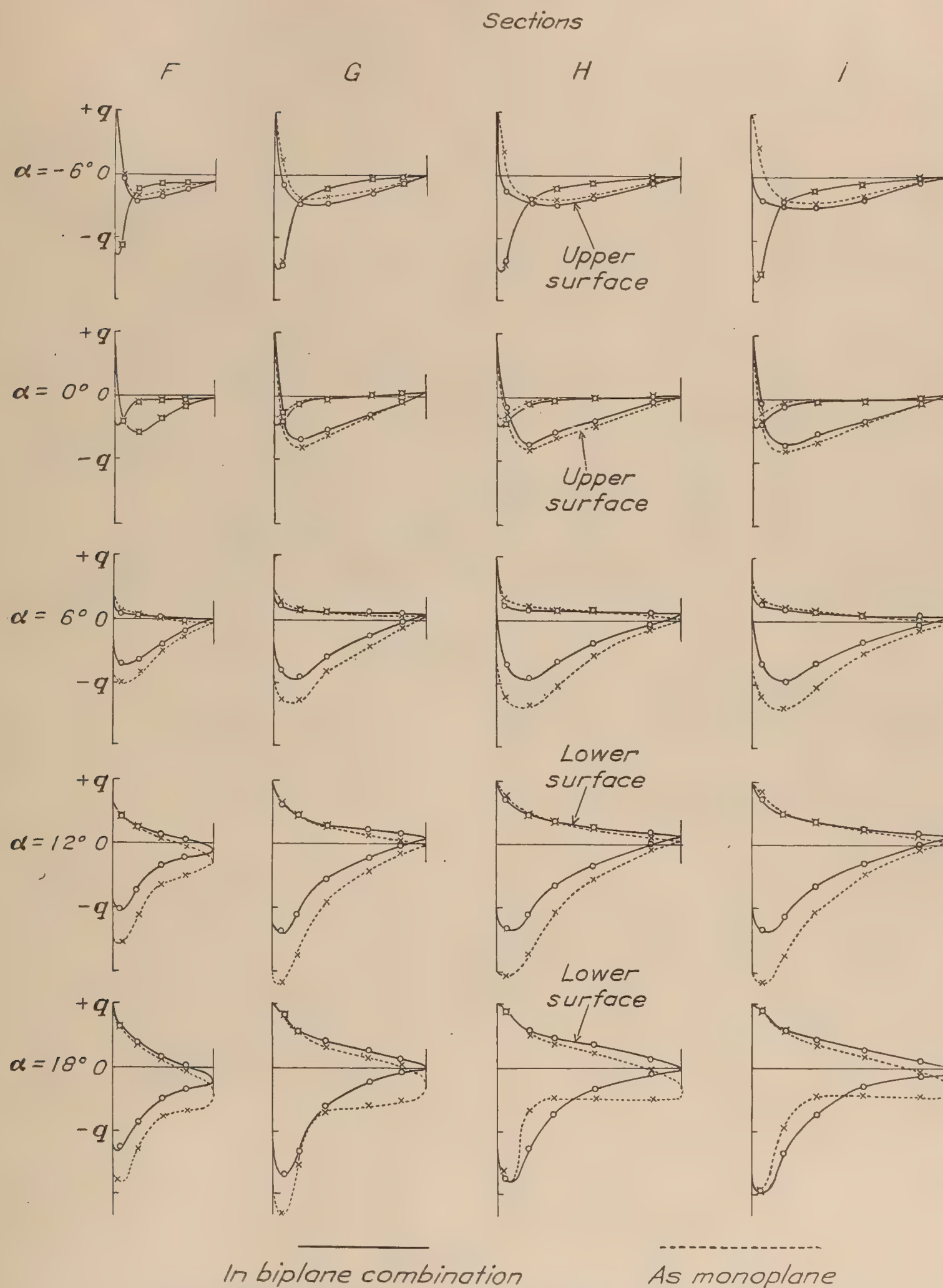


FIG. 9.—Diagrams of pressures at test sections of lower wing. Comparison as monoplane and in biplane combination

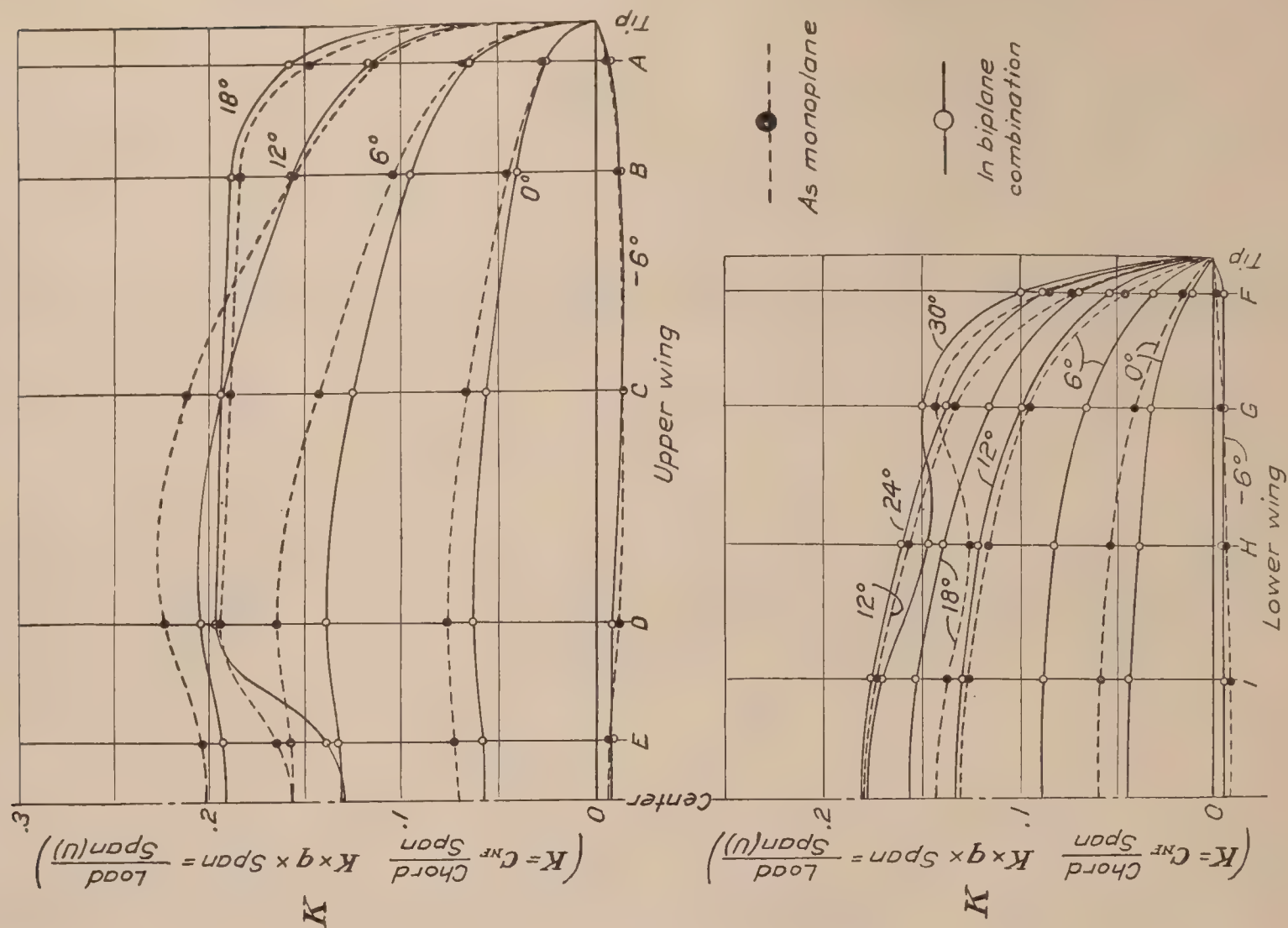


FIG. 10.—Lateral load distribution

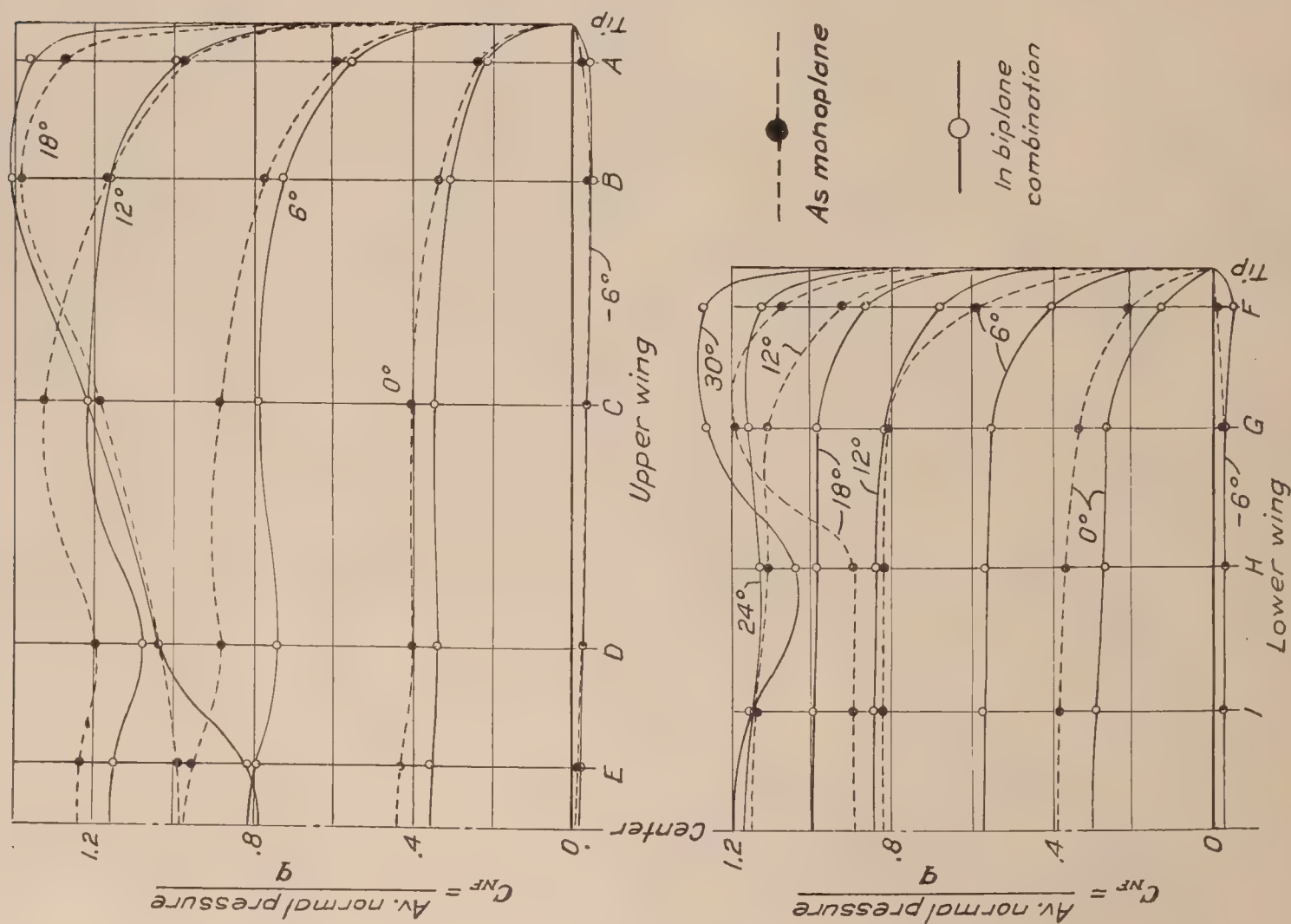


FIG. 11.—Normal force coefficient

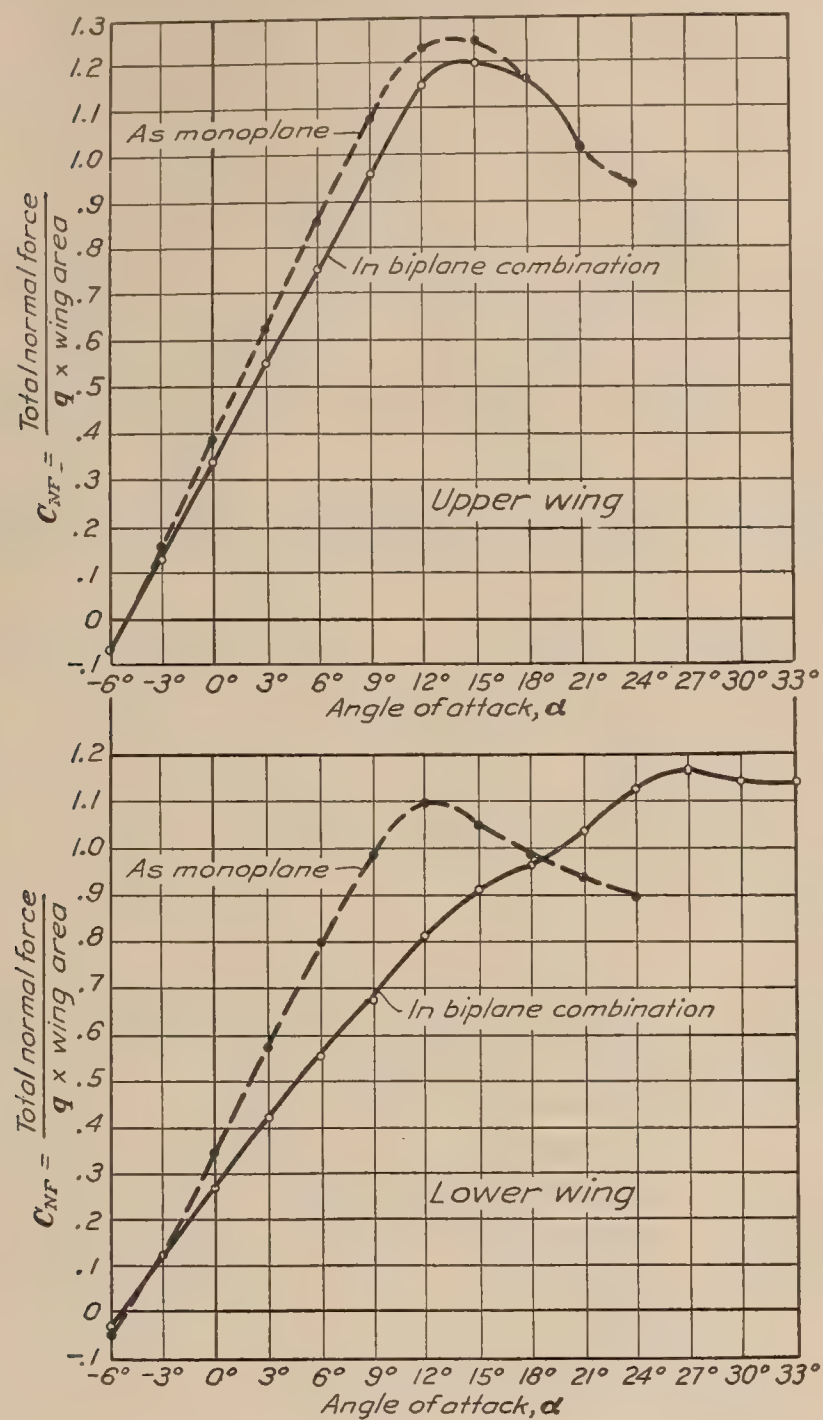


FIG. 12.—Normal force coefficient for wing

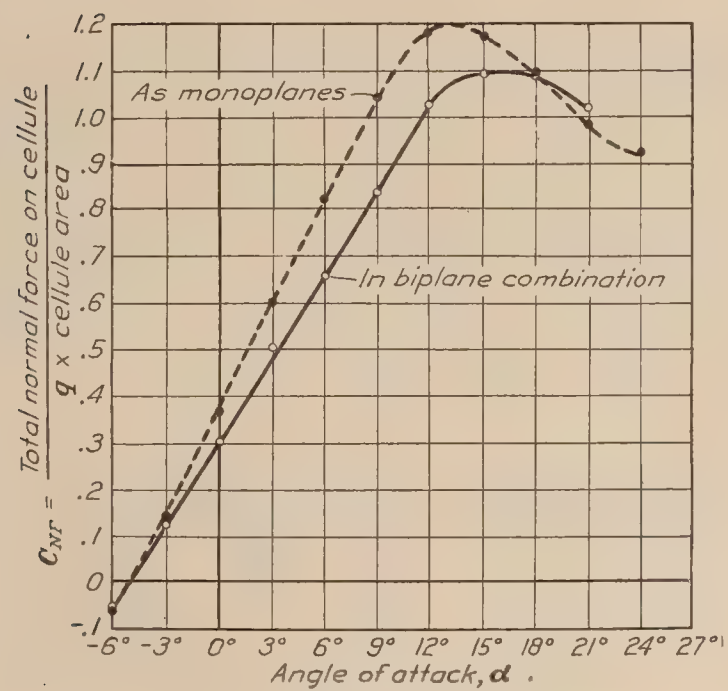


FIG. 13.—Cellule normal force coefficient

In Figure 10 it can be seen that, although the normal forces are not equal for the same angles of attack, their distribution along the span is not greatly affected. The upper wing with its less influenced overhanging portion has a somewhat more uniform distribution in the biplane combination. The distributions along the span of the lower wing are similar.

The washout of the center section of the upper wing serves to prevent a large reduction in the load per unit span over the section in which the chord is reduced. Although the chord is but 87 per cent of the maximum chord, the washout of but $1\frac{1}{2}$ degrees is sufficient.

The curves of Figure 11 show that, with the exception of the tips, the normal force varies along the span in practically the same manner that the chords vary. At 18 degrees angle of attack the flow has begun to burble and the normal force distribution has become irregular.

The maximum ordinates of the curves for the upper wing in Figure 12 occur at practically the same angles of attack. The effect of reduction of pressure on the lower surface of the upper wing of the biplane is apparent. The air flow over the upper surface of the upper wing, being practically uninfluenced by the lower wing, breaks away at the same angle of attack

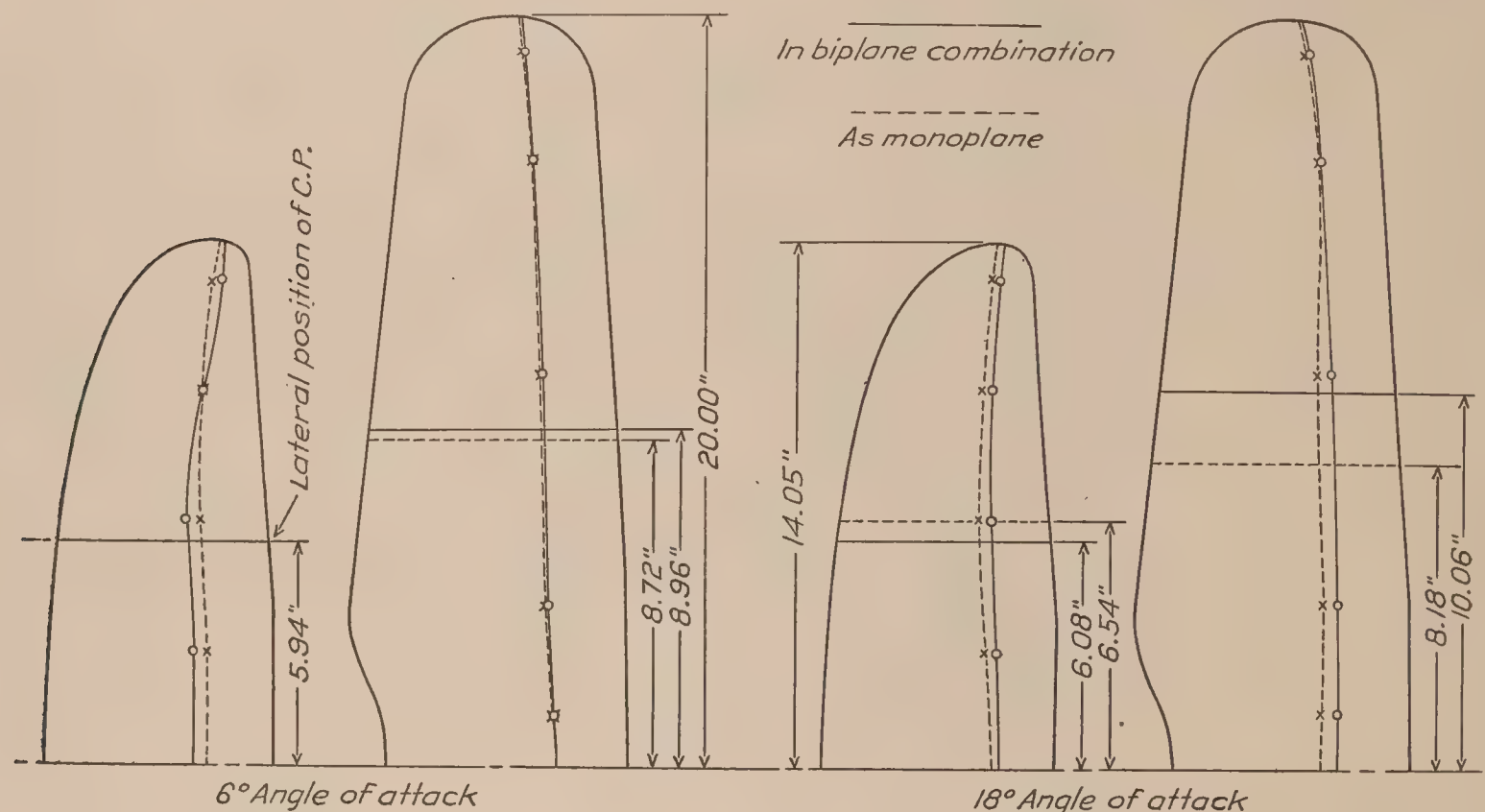


FIG. 14.—Center of pressure

whether the wing is in the biplane combination or by itself. The maximum normal force on the lower wing occurs at a much greater angle of attack when the wing is in the biplane combination. The air flow over the upper surface of the lower biplane wing is restricted by the upper wing and the burbling delayed. The maximum normal force on the lower wing of the biplane is slightly greater than the maximum normal force on the same wing as a monoplane. The normal force on the lower wing of the biplane does not break down suddenly.

The slope of the curve of normal-force coefficient vs. angle of attack (fig. 13) for the complete biplane cellule is less than would be obtained by a summation of the results of the individual monoplane tests. The maximum normal force is also less than that derived from the monoplane tests.

At large angles of attack the centers of pressure are farther forward on both wings of the biplane than they are when the wings are not in combination (fig. 14). At small angles of attack the upper wing appears to be but little influenced, whereas the lower wing has its centers of pressure farther to the rear.

The lateral position of the center of pressure is but little affected at small angles, but at large angles of attack is changed considerably. On the lower wing it is moved inward. The

biplane interference on the inner portion of the upper wing and the relatively small influence on the overhanging tip shift the lateral position of the center of pressure outward a considerable amount.

CONCLUSIONS

The conclusions of this paper may be summarized as follows:

1. The effect of the biplane interference on the pressures on the individual wings is almost entirely restricted to the lower surface of the upper wing and the upper surface of the lower wing.
2. The distribution of the normal force along the span of the individual biplane wings is not greatly different from that along the span of the same wings when tested individually. That variation which is apparent is caused by the fact that the overhanging tip of the upper wing is relatively little influenced.
3. The washin of the center section of the upper wing, where the chord is reduced, prevents a large reduction of the normal force across this portion of the wing, providing the airfoil section is not mutilated.
4. The upper wing of the biplane burbles at the same angle of attack at which it burbles when tested individually. The burble of the lower wing of the biplane occurs at an increased angle of attack relative to that at which it burbles when tested as a monoplane.
5. The overhanging tip of the upper wing causes the lateral center of pressure to be farther out along the span than it is when the wing is tested as a monoplane. At large angles of attack the centers of pressure are moved forward by the biplane interference.

LANGLEY MEMORIAL AERONAUTICAL LABORATORY,
NATIONAL ADVISORY COMMITTEE FOR AERONAUTICS,
LANGLEY FIELD, VA., *April 7, 1927.*

REFERENCES AND BIBLIOGRAPHY

- Reference 1.—Reid, Elliott G.: Pressure Distribution over Thick Tapered Airfoils, N. A. C. A. 81, U. S. A. 27C Modified and U. S. A. 35. N. A. C. A. Technical Report No. 229. 1926.
University of Toronto: Pressure Distribution over U. S. A. 27 Aerofoil with Square Wing Tips. Aeronautical Research Paper No. 18. 1926.
University of Toronto: Pressure Distribution Over Göttingen 387 Aerofoil with Square Wing Tips. Aeronautical Research Paper No. 18a. 1926.

REPORT No. 272

**THE RELATIVE PERFORMANCE
OBTAINED WITH SEVERAL METHODS OF CONTROL
OF AN OVERCOMPRESSED ENGINE
USING GASOLINE**

**By ARTHUR W. GARDINER and WILLIAM E. WHEDON
Langley Memorial Aeronautical Laboratory**

REPORT No. 272

THE RELATIVE PERFORMANCE OBTAINED WITH SEVERAL METHODS OF CONTROL OF AN OVERCOMPRESSED ENGINE USING GASOLINE

By ARTHUR W. GARDINER and WILLIAM E. WHEDON

SUMMARY

This report presents some results obtained at the Langley Memorial Aeronautical Laboratory of the National Advisory Committee for Aeronautics, during an investigation to determine the relative performance characteristics for several methods of control of an overcompressed engine using gasoline and operating under sea-level conditions. For this work, a special single cylinder test engine, 5-inch bore by 7-inch stroke, and designed for ready adjustment of compression ratio, valve timing and valve lift while running, was used. This engine has been fully described in N. A. C. A. Technical Report No. 250.

Tests were made at an engine speed of 1,400 R. P. M. for compression ratios ranging from 4.0 to 7.6. The air-fuel ratios were on the rich side of the chemically correct mixture and were approximately those giving maximum power. When using plain domestic aviation gasoline, detonation was controlled to a constant, predetermined amount (audible), such as would be permissible for continuous operation, by (a) throttling the carburetor, (b) maintaining full throttle but greatly retarding the ignition, and (c) varying the timing of the inlet valve to reduce the effective compression ratio. For the first and third methods, the throttle opening and the valve timing, respectively, were adjusted so that the ignition timing could be advanced slightly beyond the advance giving maximum power without exceeding the standard of permissible detonation. The optimum performance for the engine when using a nondetonating fuel, consisting of 80 per cent of commercial benzol and 20 per cent of aviation gasoline, was obtained as a basis for comparison.

The following comparative results are based on the optimum performance for the engine obtained with the nondetonating fuel at a compression ratio of 4.7. The power and fuel consumption with method (b) remained substantially constant at the higher compression ratios, the order of the ignition timing permitting full throttle operation ranging from 30° at 4.7 to 3° at 7.3; exhaust temperatures, heat loss to the cooling water and explosion pressures at the higher ratios were normal. At a compression ratio of 7.5, the power obtained with method (a) was about 39 per cent less and the fuel consumption was considerably lower; with method (b), time of inlet-valve opening constant and time of inlet-valve closing varied, the power was about 23 per cent less and the fuel consumption was greatly increased; with method (c), time of inlet opening and closing varied simultaneously, the power was about 29 per cent less and the fuel consumption was greatly increased.

From these results, it may be concluded that method (b) gives the best all-round performance and, being easily employed in service, appears to be the most practicable method for controlling an overcompressed engine using gasoline at low altitudes.

INTRODUCTION

Owing to the inherent advantages of higher specific output and reduced fuel consumption resulting therefrom, considerable attention has been directed toward increasing the expansion ratio of the carbureted engine, particularly the engines used in aircraft, as it is in this field that the above advantages are in greatest demand. However, coincidentally with an increase in the expansion ratio, there is, in conventional engines, a corresponding increase in the compression ratio with consequent aggravation of those conditions within the engine inducing detona-

tion and preignition. For this reason, compression ratios have been limited by the detonation characteristics of the fuels available for general service use and, where higher compressions have been employed, it has been necessary to resort to the use of special fuels, which have not been, and are not now, at once cheap and generally available. Thus, the employment of higher compression ratios in aircraft engines has not been generally adopted.

However, as conditions inducing detonation in the high-compression engine become less severe at high altitudes, a compromise has been sought, in which relatively high-compression ratios are employed in conjunction with throttling at low altitudes to reduce the density of the charge and thus suppress detonation until sufficient altitude has been gained to permit full-throttle operation. This scheme has received approval because it permits the use of fuels that are generally available, results in increased fuel economy (greater expansion ratio) at all altitudes, and gives an altitude range of constant power output. For operation below the altitude permitting full-throttle operation, the maximum permissible output, compared to the maximum obtainable with the same engine using a nondetonating fuel, is considerably reduced, and the specific weight of the engine, even when designed especially for the reduced stresses accompanying the reduced power, is increased. Thus, the questions arise: How much throttling is required to suppress detonation at low altitudes, does the performance under this condition compare favorably with that of a normal engine permitting full-throttle operation with the common fuel, and is this method of control, by throttling, the most advantageous? In this connection, Ricardo has shown (Reference 1) that the specific output of an overcompressed engine throttled to prevent detonation is relatively low. But information showing the relative performance obtained with other methods of control is, apparently, not available.

The present investigation was undertaken, therefore, at the Langley Memorial Aeronautical Laboratory of the National Advisory Committee for Aeronautics in connection with a research program involving the determination of the comparative flight performance of normal, overcompressed, and supercharged engines. The immediate object was to determine the relative performance of a single-cylinder, four-stroke-cycle, high-compression engine using domestic aviation gasoline with detonation controlled to a constant, predetermined, and permissible amount by throttling, retarding the ignition timing and varying the inlet valve timing. The full-throttle performance for optimum conditions when using a nondetonating fuel consisting of 80 per cent of commercial benzol and 20 per cent aviation gasoline was also obtained for comparison. The range of compression ratios used was from 4.0 to 7.6.

The tests herein reported were conducted under the immediate supervision of Clyde R. Paton.

DESCRIPTION

For the present investigation a special, single-cylinder, four-stroke-cycle test engine, 5-inch bore and 7-inch stroke, connected to a 40/100 HP. electric cradle dynamometer was used. This engine, a transverse cross section of which is shown in Figure 1, has been fully described in Reference 2. Briefly, the following adjustments can be made while the engine is running: A change in compression ratio from 4 to 14; a variation in the time of opening and closing of both the inlet and exhaust valves of 50° measured in terms of crank travel, the opening and closing being controlled independently, and a variation in the lift of both the inlet and exhaust valves from $\frac{1}{4}$ inch to $\frac{1}{2}$ inch. Overhead valves are used, the two inlet and the two exhaust valves being operated by independent cam shafts. The water jackets for the cylinder head and cylinder barrel are separate, so that the temperature of the cooling water for each may be controlled independently. For the present tests the compression ratio was varied from 4 to 7.5, and for all tests except those involving a varied timing the following valve adjustments were used:

Inlet open.....	10 degrees after top center.
Inlet closed.....	45 degrees after bottom center.
Inlet-valve lift.....	$\frac{7}{16}$ inch.
Exhaust open.....	50 degrees before bottom center.
Exhaust closed.....	10 degrees after top center.
Exhaust-valve lift.....	$\frac{3}{8}$ inch.

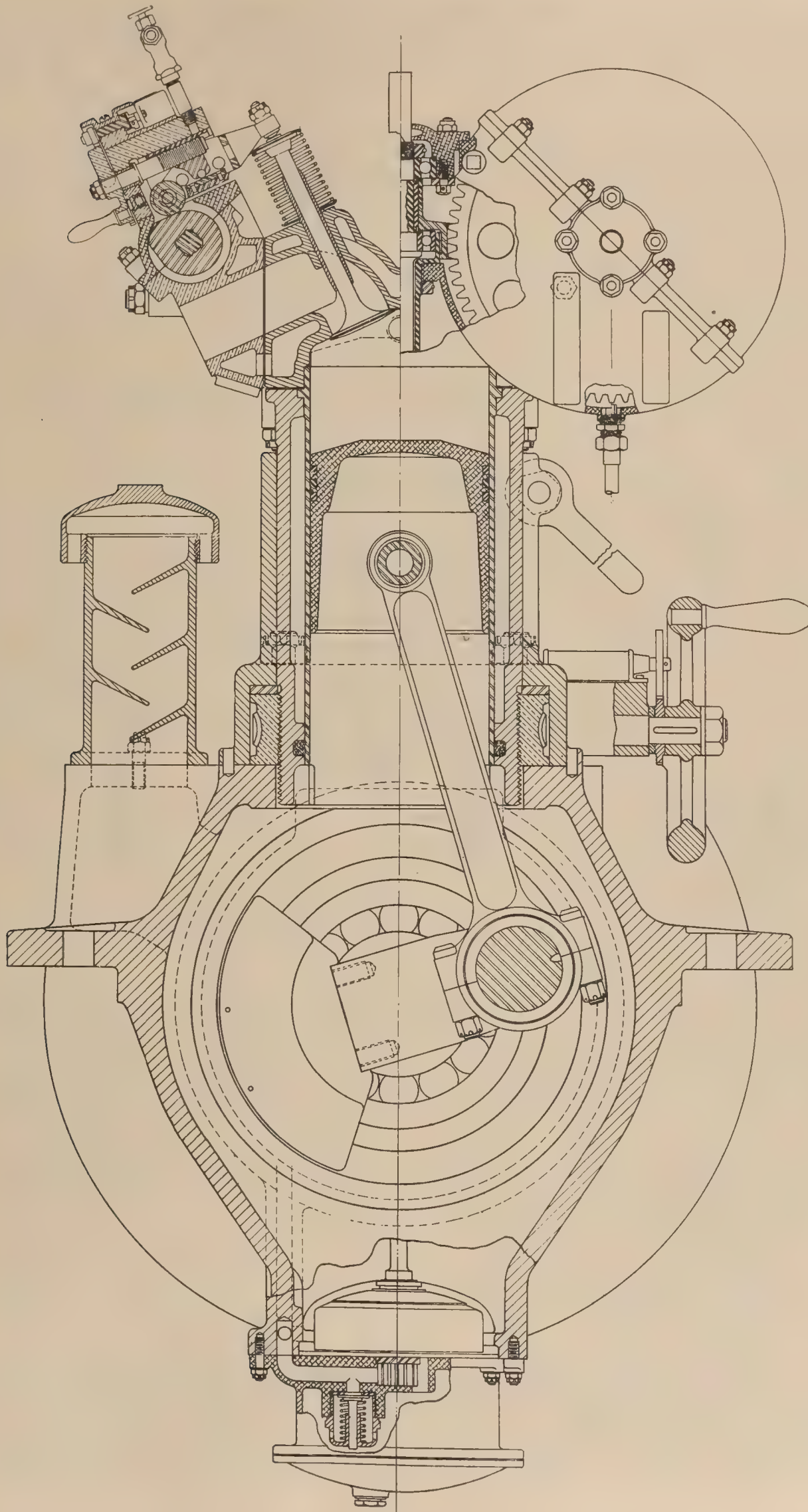


FIG. 1.—Transverse section through single-cylinder test engine, showing adjustment for varying the compression ratio while running

For the tests with constant inlet-valve opening and late closing, the latter was varied from 45° to 108° after bottom center. For the tests with the total inlet phase displaced in the cycle, the phase was maintained at 125° and the time of opening varied from 10° to 60° after top center.

Two porcelain-insulated spark plugs located diametrically opposite on the longitudinal axis of the cylinder were used; these were timed synchronously.

A standard Liberty engine duplex carburetor was used, one Venturi being completely closed and the main metering jet for the remaining Venturi being provided with a needle valve for ready adjustment of the fuel flow. Some tests were made with a small fixed metering jet, the needle valve being omitted.

Fuel consumption was measured by timing the rate of flow from a 400 cm.³ tank.

Domestic aviation gasoline, conforming to Army specifications, was used as the detonating fuel. A mixture of 80 per cent of benzol (commercial 90 per cent) and 20 per cent aviation gasoline (80-20 blend) was used as the nondetonating fuel.

A diagrammatic layout of the induction system is shown on Figure 2. Air measurements were made with a gasometer having a displacement volume of 10 cubic feet; the gasometer bell

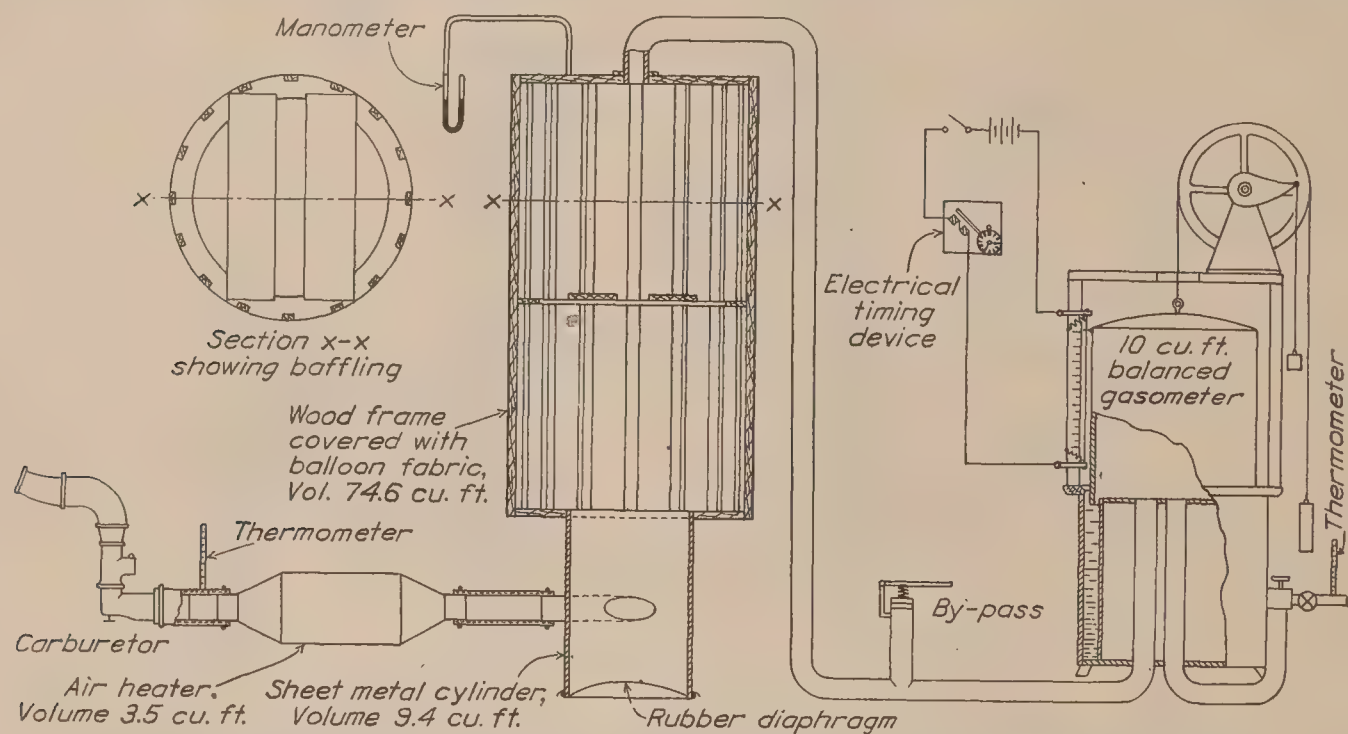


FIG. 2.—Diagrammatic layout of induction system used with single-cylinder test engine, showing the gasometer with the moving bell counterbalanced for weight and flotation, the large receiver, and the electric heater for temperature regulation

was counterbalanced for weight and flotation. Time was measured by a stop watch operated through an electric relay and contacts located on the gasometer bell. The pulsating flow was damped by providing a large-volume receiver between the gasometer and engine. An air heater, located between the receiver and carburetor, was used for temperature regulation.

Engine speed was measured with a revolution counter and stop watch, both operated synchronously by means of an electric switch. Torque was measured on a platform scale.

Exhaust temperatures were measured with a thermocouple and an indicating pyrometer. All other temperatures were measured with mercury thermometers. The following temperatures were maintained practically constant by manual control:

	° F.
Water in.....	140
Water out of cylinder head.....	180
Water out of cylinder barrel.....	170
Oil out.....	130
Air to carburetor.....	95

A spring-loaded piston element proved unsatisfactory for measurement of combustion-chamber pressures, and this was replaced with a maximum-pressure gauge unit, in which the chamber pressures acting on the under side of a $\frac{1}{8}$ inch steel ball-check-valve were balanced by gas pressure introduced on the upper side from a storage tank. An indicating gauge was in

direct communication with the space above the check valve. The method of operation consisted in adjusting the gas pressure in the valve chamber, by means of an admission and a bleeder valve, to the point where the gauge needle ceased vibrating. Compression pressures were measured in the same manner.

In adjusting the engine settings to give a constant, predetermined, and permissible amount of detonation, several instruments for measuring the amount of detonation were tried but found unsatisfactory. During this preliminary testing, it was found that the amount of detonation obtaining under given conditions could be more readily and more accurately determined by the ear of an experienced observer, so that, for the tests herein reported, an arbitrary standard of audible detonation was determined upon as the criterion in adjusting the engine. In order to minimize errors due to the personal factor, two experienced observers checked each other in estimating that the amount of detonation existing during any particular run was in accordance with the standard.

METHODS OF TESTING

The tests herein reported were made at a constant engine speed of 1,400 R. P. M., although, in some cases, additional tests were made at 1,200 and 1,600 R. P. M. to check the general trend of the data obtained at the intermediate speed. For any given test, after conditions were stabilized, a power run was made extending over a time interval averaging from two to three minutes, during which readings were taken of engine speed, torque scale, rate of fuel and air consumption, exhaust temperatures, and explosion pressures, and the water from both the cylinder head and cylinder barrel diverted into containers and weighed for the determination of heat dissipation to the cooling water. Immediately following each power run, and for the same engine settings used during the power run, the circulation of cooling water was shut off and a friction run was made by motoring the engine with the dynamometer. Compression pressures were measured during these friction runs.

The testing methods employed with the several schemes of operation are thought to be of sufficient interest to merit a detailed description:

1. Effect of ignition advance on the performance of a high-compression engine when using (a) a detonating fuel and (b) a nondetonating fuel (fig. 3): In this case, the compression ratio was fixed arbitrarily at 6.3, the carburetor needle-valve was maintained at a constant setting, and full-throttle performance obtained at progressively increasing ignition advances ranging from top center to 50° advance.

2. Optimum performance with a nondetonating fuel: Full-throttle performance was obtained for the range of compression ratios from 4 to 7.3. At each compression ratio, the ignition setting and air-fuel ratio were adjusted to give maximum power.

3. Throttled performance using a detonating fuel:

- (a) With a fixed ignition advance: In these tests, the ignition advance was fixed arbitrarily, the air-fuel ratio was adjusted for each run to an approximately constant value of 12.2. Full-throttle runs were made at low compression ratios, and, as the compression ratio was increased, the throttle was adjusted to give the standard of detonation.

- (b) Throttled performance with normal optimum ignition advance: In these tests, the arbitrary criterion for the permissible amount of throttle opening selected was the greatest opening that permitted the ignition to be advanced slightly beyond the advance giving maximum power without exceeding the standard of detonation. At a given compression ratio, the throttle opening was fixed arbitrarily and several preliminary runs made at increasing ignition advances until the standard of detonation was obtained; the throttle was reset at a lesser opening and preliminary runs made as above, until the arbitrary condition had been fulfilled, following which a run was taken for this throttle opening and the optimum ignition advance. Tests for compression ratios from 4.5 to 7.5 were made with a fixed carburetor jet giving an approximate air-fuel ratio of 12.2.

4. Full-throttle performance with greatly retarded ignition: In these tests, full throttle was maintained and the ignition timing was retarded sufficiently to give the standard of detonation at compression ratios of 5.3, 6.3, and 7.3. The air-fuel mixture was adjusted to give approximately maximum power.

5. Full-throttle performance with varied timing for the inlet valve: Tests were made with fixed carburetor metering jets giving an approximate air-fuel ratio of 12.2. For a given compression ratio, the valve timing was set arbitrarily and the ignition adjusted to give the standard of detonation; the valve timing was readjusted and the ignition advance varied until a valve timing was determined that permitted the ignition timing to be advanced slightly ahead of the advance giving maximum power without exceeding the standard of detonation. A run was then made for the valve timing so determined and with the optimum ignition advance. Two methods of varying the inlet valve timing were used:

(a) With the time of opening fixed, and the time of closing varied; range of compression ratios from 6 to 7.5.

(b) With the time of opening and closing varied simultaneously; range of compression ratios from 5.1 to 7.6.

PRECISION

Changes in atmospheric conditions caused relatively large variations in the amount of detonation, as evidenced, for instance, by the fact that, for otherwise constant engine conditions, the amount of throttle opening permissible without exceeding the standard of detonation varied somewhat on successive days. This caused some discrepancies in the engine settings necessary to fulfill given requirements, and introduced unknown errors in the comparative results. As these variations affected the results probably to a greater extent than any instrumental or personal errors, a discussion of the latter is thought to be unnecessary.

For the above reason, precise comparisons of the relative performances can not be made. However, the data are sufficiently precise to permit of making some general comparisons.

RESULTS

The results are presented in the form of curves on Figures 3 and 4; the comparative performance being presented as plots on a percentage basis for ready comparison. The base values are for the optimum performance of the engine using a nondetonating fuel at a compression ratio of 4.7 to 1; these base values are given on the several curves. Power has been corrected to a standard pressure of 29.92 inches mercury. Some comparative results taken from Reference 1 are also shown.

DISCUSSION

For the reason that some detonation is permissible, and that maximum power for a given fuel is usually obtained when a small amount of detonation is present, a criterion of "some" detonation rather than "no perceptible" detonation was selected. Moreover, many service engines are operated under such conditions; that is, with a certain permissible amount of detonation present during full-throttle operation. The amount of detonation selected as permissible in the present tests had no perceptible effect on power or heat losses to the cooling water, and was such as would be permissible in an engine for continuous operation.

Preliminary tests with gasoline at a compression ratio of 7.3 to 1 showed that, for a given ignition advance, the amount of throttling required to limit detonation to the permissible amount was dependent to a great extent on the quality of the fuel mixture. In one test at a compression ratio of 7.3, increasing the air-fuel ratio from 14.7 to 17.4, with a fixed ignition advance of 30°, permitted a greater throttle opening and resulted in an increase in power of more than 14 per cent. On the lean side, the mixture permitting the greatest throttle opening, and consequently giving maximum power, varied considerably with a change in ignition advance; for one test, at a compression ratio of 7.3, the air-fuel ratio giving maximum power changed from 15.8 to 18.7 for a change in ignition advance from 5° to 20°. The range of air-fuel ratios giving maximum power

on the rich side also varied with the ignition advance but, in general, it was found that these ratios ranged from 11.7 to 12.3 for all compression ratios. For the results presented herein, the air-fuel ratios were approximately those giving maximum power on the rich side, thus simulating, approximately, flight service conditions. However, some variations in these ratios have entered to influence the results, and to prevent obtaining precise comparisons.

The information given in Figure 3 is presented to indicate the effect of ignition advance on engine performance at a compression ratio of 6.3 when operating at full throttle with plain aviation gasoline, and with a nondetonating fuel. The carburetor needle-valve adjustment was slightly different for the two fuels, but was maintained constant for each fuel; these settings

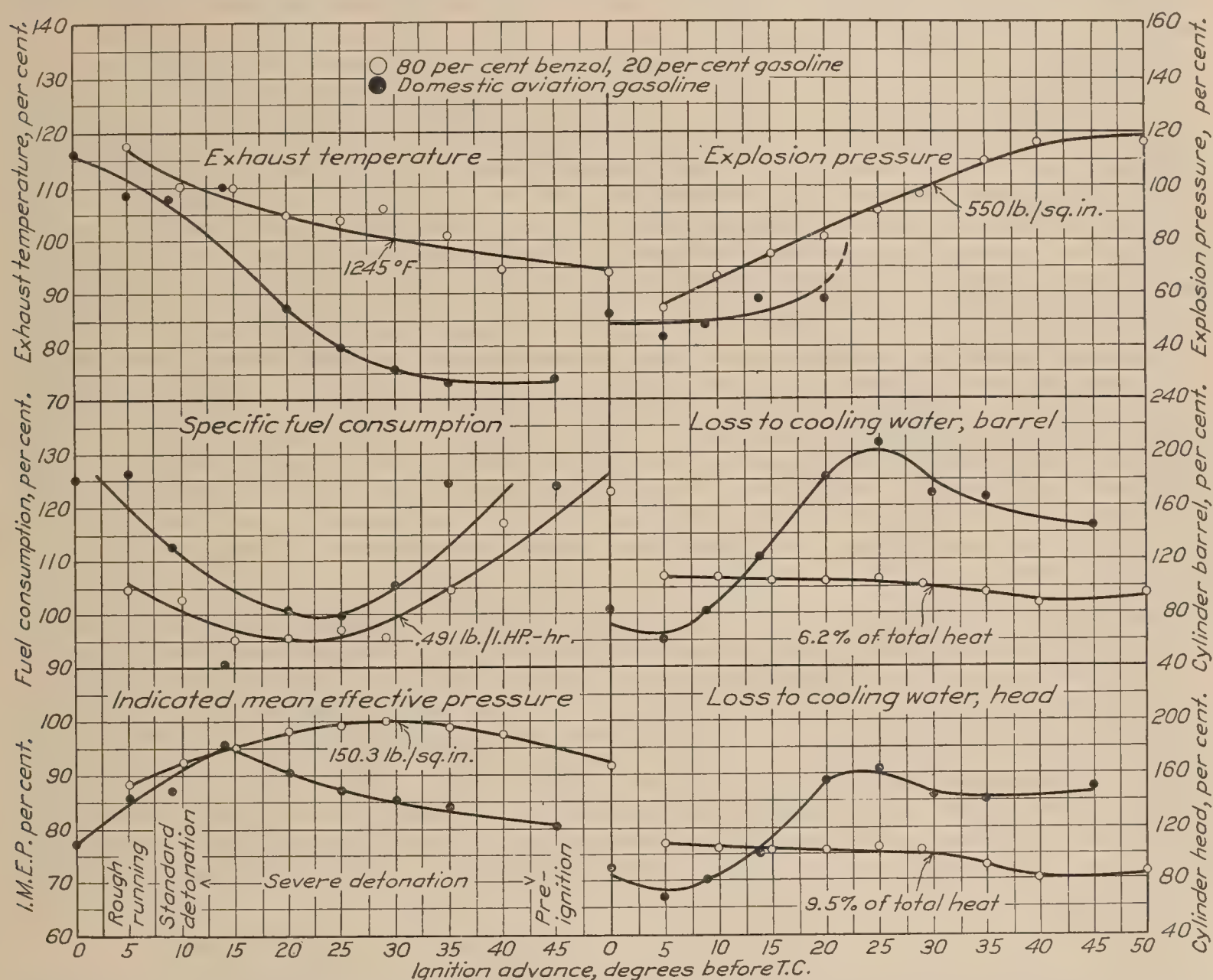


FIG. 3.—Effect of ignition advance on engine performance at a constant speed of 1,400 R. P. M. and a constant compression ratio of 6.3:1 when using gasoline and a nondetonating fuel. Percentages are based on values obtained with the nondetonating fuel for optimum power at 30° ignition advance. These base values are noted on the several curves. The notes on detonation refer to operation with gasoline

did not necessarily give maximum power. There were wide variations (from 12 to 13.5 for gasoline and from 10 to 12.5 for the 80–20 blend), in the air-fuel ratios, which caused some irregularities in performance. From these data, it is seen that, when using gasoline, there is a marked increase in the severity of detonation as the ignition timing is advanced beyond 10°, resulting finally, for an advance of 45°, in excessive preignition and fused spark-plug electrodes. Under these severe detonation conditions, there is a marked decrease in power and an increase in the heat losses to the cooling water. When using the 80–20 blend, there is a normal reduction in power for ignition advances beyond the optimum of 30°, but the heat losses remain fairly constant, or even decrease slightly, and the explosion pressures increase uniformly. Attention is called to the fact that maximum power with gasoline was obtained at an advance slightly greater than the advance giving the arbitrary standard of detonation; also, that the extreme detonation did not

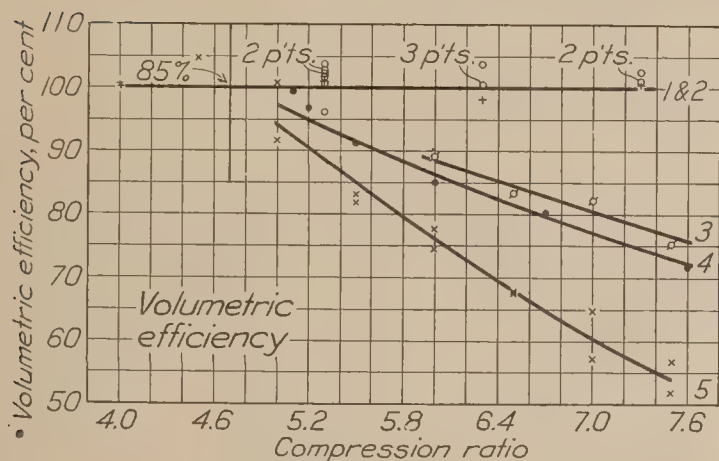
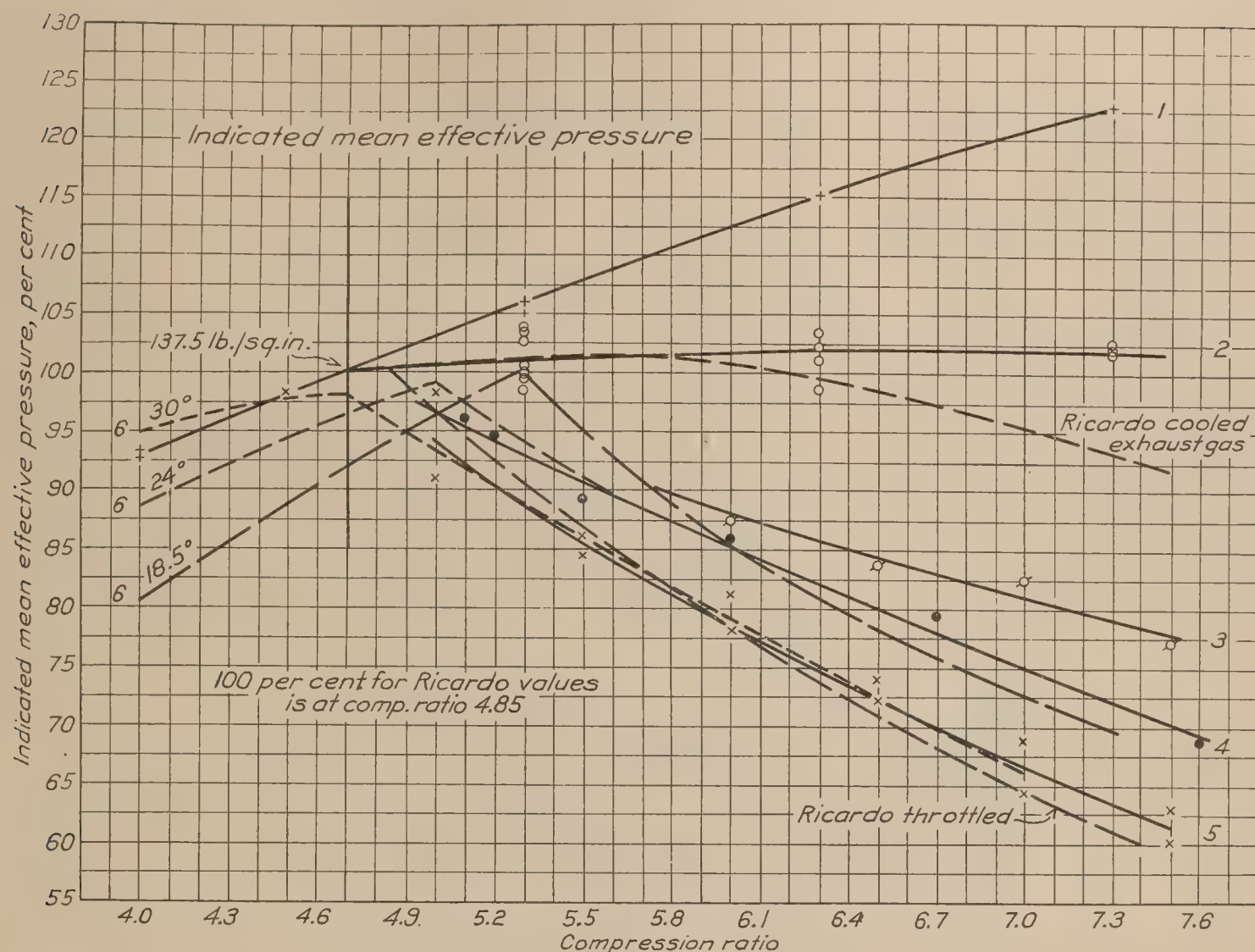
tend to increase the exhaust temperatures. The explosion pressures when using gasoline increased rapidly for ignition advances above 20° . Although the maximum-pressure gage was not reliable for measurements under these conditions, the indication was that pressures of the order of 1,600 pounds per square inch existed. For the range of ignition timing resulting in severe detonation, there was probably some power lost as negative work on the piston due to incipient preignition. The power runs in this region were maintained only for a period of about two minutes. From these results, it is apparent that full-throttle operation with gasoline at this compression ratio could not be maintained continuously for ignition advances greater than $9-10^{\circ}$.

The optimum performance when using the 80-20 blend and the comparative performance obtained by the several methods of control when using gasoline are shown on Figure 4. The performance curves are numbered in accordance with the test conditions enumerated in the title for this figure.

Considering the optimum performance of the engine using the 80-20 blend, it is found that the variation in indicated power and indicated specific fuel consumption with change in compression ratio is approximately that given by the ratio of air-cycle efficiencies. There is an indication that power increases with compression ratio at a faster rate than given by the cycle efficiencies, but this slight discrepancy may be attributed to small errors introduced by the method of obtaining friction power. It is seen that the optimum ignition advance decreases slightly with increase in compression ratio, a decrease from 37° to 26° being noted for a change in compression ratio from 4 to 7.3. The observed optimum air-fuel ratios for the different compression ratios varied (from 11 to 12.5) more than would be expected, but, as the direction was not consistent and as power was not very sensitive to changes of mixture in this range, an average value of 12 may be considered as representing the optimum for all ratios. In this connection it should be kept in mind that the chemically correct air-fuel ratio for this fuel is less than for gasoline. The variations in air-fuel ratios have caused some irregularities in the observed values for specific fuel consumption.

Tests made with gasoline at a fixed ignition advance and throttling to suppress detonation will next be considered. In this case it was found that, for a fixed advance of 30° , full-throttle operation could be maintained up to a compression ratio of 4.7 without exceeding the standard of detonation, but that at the higher ratios considerable throttling was necessary, with a resultant sharp decrease in power. Values for power at the higher ratios were obtained from cross plots, and no data points are shown. For an advance of 24° full throttle could be maintained up to a compression ratio of 5, and for 18.5° , up to 5.3. For these lower advances the full-throttle power at the lower compression ratios was reduced, as the timing used was less than the optimum, but at the higher ratios the permissible power increased as the timing was retarded. This comparison points clearly to the sensitiveness of ignition timing in its influence on detonation, and hence to the amount of throttling necessary and the permissible power output at the higher ratios.

The above discussion leads logically to a consideration of the results obtained when the ignition timing was retarded sufficiently to permit full-throttle operation at all compression ratios investigated. From the above discussion it was seen that permissible power increased with decrease in ignition timing at the higher ratios. Thus it would be expected that maximum power at these ratios would be obtained by carrying this procedure to the limit. Such was found to be the case, and of those methods investigated retarding the ignition timing to permit full-throttle operation proved to be the most advantageous from the standpoint of power. With this method of control, the permissible power remained substantially constant for all ratios from 4.7 to 7.3, whereas for the other methods the power decreased at the higher ratios. It is noted that the power obtained by this method at the intermediate ratios approximates that obtained by Ricardo (Reference 1, p. 92) when admitting cooled exhaust gases with the intake charge to suppress detonation in an overcompressed engine using fuel having a low toluene value. (Fig. 4.) Fuel consumption with retarded ignition was not excessive, but remained practically constant at the value of 0.532 pound per I.H.P. per hour, obtained with the non-detonating fuel at a compression ratio 4.7. Heat losses to the cooling water and the exhaust temperatures also remained normal. The ignition advance found necessary to give these



1 Full-throttle; 80 per cent benzol - 20 per cent aviation gasoline; best mixture and ignition advance.

2 Full-throttle; aviation gasoline; ignition timing retarded to limit detonation to a predetermined amount; approximately best power mixture.

3 Full-throttle; gasoline; time of inlet-valve opening fixed, time of inlet-valve closing adjusted to permit ignition timing to be advanced slightly beyond the advance giving best power without exceeding permissible detonation.

4 Full-throttle; gasoline; time of inlet-valve opening and closing varied simultaneously to permit best ignition advance (see 3).

5 Throttled operation; gasoline; throttle adjusted to permit ignition timing to be advanced slightly beyond advance giving best power without exceeding permissible detonation.

6 Throttled; gasoline; throttled to limit detonation with fixed ignition timing.

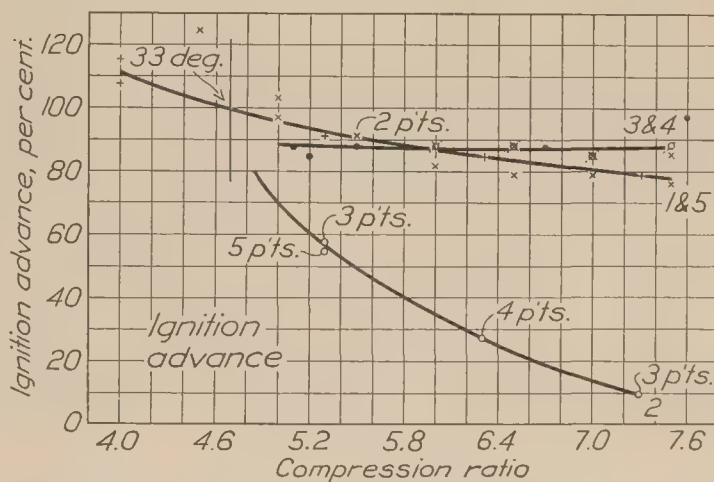
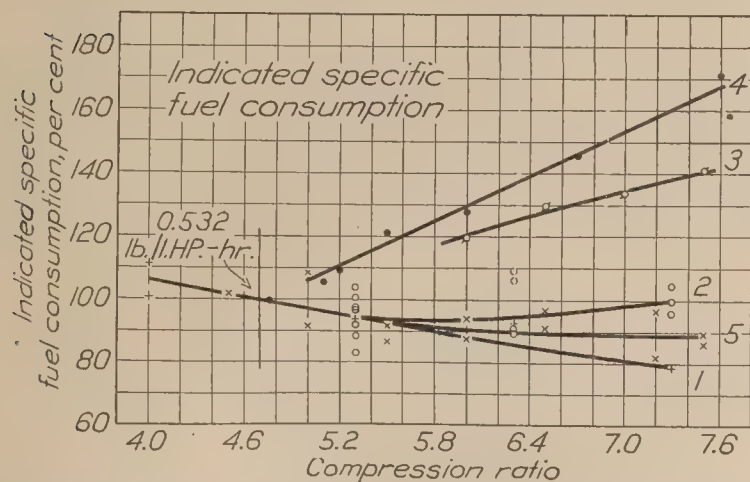


FIG. 4.—Comparative performance obtained with several methods of control of an overcompressed engine. Performances shown as percentages based on values obtained with a nondetonating fuel at a compression ratio of 4.7. Base values are shown on the various curves. The curves are numbered to correspond to the conditions of operation as given

results varied from 30° at 4.7 to 3° at 7.3 compression ratio. Ignition timing at the higher ratios was very critical, small changes in timing causing considerable variation in the amount of detonation. This is probably the greatest disadvantage of this method for service use. The present tests do not show to what extent the compression ratio may be increased with this method of control, but apparently this method may be used advantageously up to a compression ratio of at least 8:1.

The performance obtained when throttling the carburetor just sufficiently to permit the ignition timing to be advanced, for each compression ratio, slightly beyond the advance giving maximum power will next be considered. The condition stipulated in these tests is, admittedly, an arbitrary one, but it fulfills, in general, the service condition where the ignition advance at low altitudes is maintained constant at the adjustment giving maximum performance for altitudes above that permitting full-throttle operation. It may be seen from Figure 4 that the optimum ignition timing for this method of control, and also for the method discussed below in which the inlet-valve timing was varied, approximates, for the various compression ratios, the optimum ignition timing determined for the nondetonating fuel. The power obtained by throttling under these conditions approximates, at the higher ratios, that obtained for the fixed ignition timing of 30° . This would be expected, as the optimum timing determined with

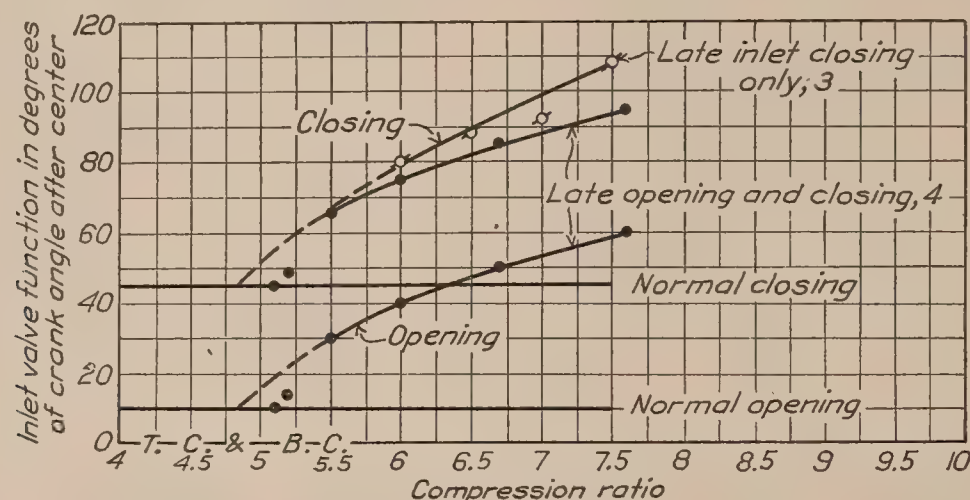


FIG. 5.—Inlet-valve timing used for conditions (3) and (4), Figure 4

this method varied but slightly from 30° . The permissible power output at a compression ratio of 7.3 is seen to be about 40 per cent less than obtained by maintaining full throttle and retarding the ignition. The indicated specific fuel consumption is, however, somewhat lower, although the variations in the quality of the fuel mixture have caused a scattering of the data and have thus obscured the advantage of the throttling method from this standpoint. It would be expected that the indicated fuel consumption with this method would be but little different from that obtained with the nondetonating fuel. This method would suffer somewhat by comparison on a brake basis owing to the higher friction losses with the engine throttled. It is worthy of note that the percentage decrease in indicated power is less than the percentage decrease in volumetric efficiency at the higher ratio. This method of control, although giving the best fuel consumption, gives the least power. The general trend of the power curves obtained with this method approximates that found by Ricardo (Reference 1, p. 94) when employing the throttling method to give no detonation with a fuel having detonation characteristics similar to gasoline, although it is not stated in the reference whether a fixed ignition timing or a variable timing was employed.

Varying the inlet-valve timing has been employed in England in connection with the use of higher compression ratios in the Bristol Jupiter air-cooled engine. For this reason it seemed pertinent to investigate the relative performance to be obtained with this method of control. From Figure 4 it is seen that when the time of inlet opening and closing was varied simultaneously and the ignition maintained in the optimum position noted in the preceding discussion the permissible power output decreased with increase in compression ratio, the decrease at a compression ratio of 7.5 being about 29 per cent. Under these conditions there was considerable reversed flow through the inlet valve and, as a consequence, the fuel consumption

with the single-cylinder engine increased considerably as the valve timing was varied from the normal. No account has been taken of the fuel that was deposited in the air heater as a result of the reversed air flow. Considerable improvement in fuel economy would be expected in a multi-cylinder engine, where several cylinders are connected to a common manifold. Some improvement in power and fuel consumption was obtained by maintaining the time of opening constant and varying only the time of closing, but the gain is not considerable and the method would not be practical for service use. The disadvantage of complexity more than offset the advantage of slightly better power obtained with this method as compared to the throttling method. Figure 5 shows the inlet-valve settings employed.

For all conditions, the heat loss to the cooling water in the head remained below 10.5 per cent of the total heat in the fuel; and for the cooling water in the cylinder barrel, below 7.5 per cent. When the variable valve timing was used, these losses were considerably reduced at the higher compression ratios.

Exhaust temperatures remained below 1,425° F. for all conditions of operation above 4.7 compression ratio. For the variable valve-timing method, these temperatures were likewise reduced considerably at the higher compression ratio.

A detailed discussion of the underlying conditions influencing detonation in these tests has been purposely omitted, as the data are not sufficiently precise to permit of making a detailed analysis.

CONCLUSIONS

From these comparative tests, it may be concluded that, of those methods investigated for controlling an overcompressed engine using gasoline under sea-level conditions, maximum power is obtained by maintaining full throttle and greatly retarding the ignition timing. Also, as the fuel consumption, exhaust temperatures, and heat loss to the cooling water are normal, and as this method of control is easily accomplished without adding to the complexity of the power plant, it may be considered the most practicable method for service use.

Throttling the carburetor with, approximately, full normal ignition advance gives the best economy of the various methods but the least power. Varying the timing of the inlet valve with, approximately full normal ignition advance gives somewhat greater power than obtained by the throttling method, but the fuel consumption is excessive, although the values for the latter given in this report are higher than would be obtained with a multi-cylinder engine.

LANGLEY MEMORIAL AERONAUTICAL LABORATORY,
NATIONAL ADVISORY COMMITTEE FOR AERONAUTICS,
LANGLEY FIELD, VA., *February 25, 1927.*

REFERENCES AND BIBLIOGRAPHY

- REFERENCE 1. RICARDO, HARRY R.: Report of the Empire Motor Fuels Committee, Session 1923-24. The Institution of Automobile Engineers (London), Vol. XVIII, Part I, pp. 1-352.
2. WARE, MARSDEN: Description of the N. A. C. A. Universal Test Engine and Some Test Results. N. A. C. A. Technical Report No. 250, 1926.
3. RICARDO, HARRY R.: The Internal Combustion Engine, Vol. II, pp. 1-366, 1923.
4. RICARDO, HARRY R.: The High-Speed Internal Combustion Engine. The Automobile Engineer (London), Vol. XV, No. 204, pp. 206-210, 1925.
5. SPARROW, STANWOOD W.: The Effect of Changes in Compression Ratio upon Engine Performance. N. A. C. A. Technical Report No. 205, 1925.
6. SPARROW, STANWOOD W.: Fuels for High-Compression Engines. N. A. C. A. Technical Report No. 232, 1925.
7. HORNING, H. L.: Effect of Compression Ratio on Detonation and Its Control. Transactions of Society of Automotive Engineers (N. Y.), Vol. XVIII, Part II, pp. 49-67, 1923.
8. HOLLOWAY, J. H., HUEBOTTER, H. A., and YOUNG, G. A. Engine Characteristics under High Compression. Transactions of the Society of Automotive Engineers (N. Y.), Vol. XVIII, Part I, pp. 131-159, 1923.
9. UPTON, G. B.: Spark Advance in Engines. Transactions of the Society of Automotive Engineers (N. Y.), Vol. XVIII, Part II, pp. 98-159, 1923.
10. SPARROW, S. W.: The Background of Detonation. N. A. C. A. Technical Note No. 93, 1922.

REPORT No. 273

**WIND TUNNEL TESTS ON AUTOROTATION
AND THE "FLAT SPIN"**

**By MONTGOMERY KNIGHT
Langley Memorial Aeronautical Laboratory**

REPORT No. 273

WIND TUNNEL TESTS ON AUTOROTATION AND THE "FLAT SPIN"

By MONTGOMERY KNIGHT

SUMMARY

The following report deals with the autorotational characteristics of certain differing wing systems as determined from wind tunnel tests made at the Langley Memorial Aeronautical Laboratory. The investigation was confined to autorotation about a fixed axis in the plane of symmetry and parallel to the wind direction. Analysis of the tests leads to the following conclusions:

Autorotation below 30° angle of attack is governed chiefly by wing profile, and above that angle by wing arrangement.

The strip method of autorotation analysis gives uncertain results between maximum C_L and 35° .

The polar curve of a wing system, and to a lower degree of accuracy the polar of a complete airplane model are sufficient for direct determination of the limits of rotary instability, subject to strip method limitations.

The results of the investigation indicate that in free flight a monoplane is incapable of flat spinning, whereas an unstaggered biplane has inherent flat-spinning tendencies.

The difficulty of maintaining equilibrium in stalled flight is due primarily to rotary instability, a rapid change from stability to instability occurring as the angle of maximum lift is exceeded.

INTRODUCTION

Autorotation may be explained by a consideration of the torques brought into play by the rotation of a wing or combination of wings about an axis in the plane of symmetry and parallel to the wind direction. This phenomenon is recognized as a vital factor in the "spin" of an airplane.

The so-called "flat spin" may be defined as a spin in which the longitudinal axis of the airplane is more nearly horizontal than vertical in contradistinction to the "normal spin" in which the reverse is true. The flat spin is a characteristic of certain unstaggered biplanes, notably the British B. A. T. *Bantam* and Short *Springbok*, and the American Boeing *NB-1*. This type of spin is considered dangerous owing to the difficulty of returning to normal flight, and means of insuring against its occurrence are being sought.

Autorotation has been studied for several years with the aid of wind tunnel rotational experiments and mathematical analyses based on force tests. Spinning tests of airplanes in free flight have also been made, and these have been supplemented by tests upon light models dropped from a height.

The present investigation was instituted for a further study of autorotation with emphasis laid upon the flat spin. Three airfoils of widely differing characteristics were tested as monoplanes, and tests were also made on an unstaggered biplane cell.

The experiments, which consisted of both force and rotation tests from zero lift to 90° angle of attack, were conducted in the 5-foot, circular-throat, atmospheric wind tunnel (Reference 1) of the Langley Memorial Aeronautical Laboratory.

In this report three terms are used with reference to rotation about a fixed axis in the plane of symmetry and parallel to the wind direction. They are defined as follows:

1. "Stable autorotation" signifies a state of equilibrium in autorotation to which the model returns whenever disturbed therefrom.

2. "Unstable autorotation" signifies a state of equilibrium in autorotation such that a small disturbance aiding the rotation causes stable autorotation, while an opposing disturbance brings the model to rest.

3. "Rotary instability" signifies a state of equilibrium in rectilinear motion such that a small rotary disturbance causes stable autorotation.

APPARATUS AND TESTS

Three airfoil profiles were used in the tests. These were Göttingen 387-FB (flat bottom), R. A. F. 15, and N. A. C. A.-M1. Rectangular wings, 5 by 30 inches in plan, having these profiles were tested as monoplanes. An unstag-

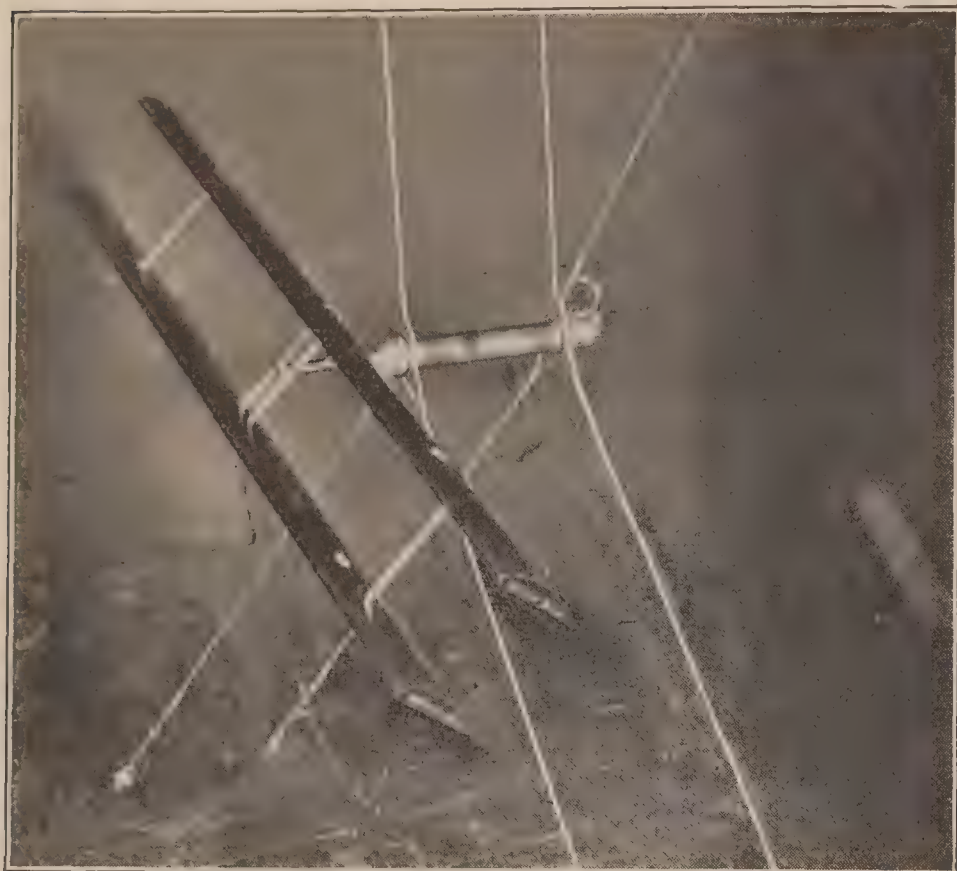


FIG. 1.—Biplane mounted on autorotation apparatus

gered biplane cell of Göttingen 387-FB profile was also tested.

The autorotation apparatus, illustrated in Figures 1 and 2, consisted of a barrel containing ball bearings supporting a shaft upon which the models were mounted as shown. A simple screw adjustment permitted locking of the model at any desired angle of attack. A reduction gear and electrical contact at the down-wind end of the barrel operated a light outside the tunnel for determining rates of rotation.

The average rates of rotation in opposite directions for a given mean angle of attack α_m gave the results presented below. The limits of rotary instability were obtained merely by noting the angles of attack between which stable autorotation was induced when the model was disturbed slightly from rest.

The force tests were made on the regular wire balance of the tunnel (Reference 1). Lift and drag were measured from approximately zero lift to 90° angle of attack. The biplane drag coefficients are corrected for strut drag.

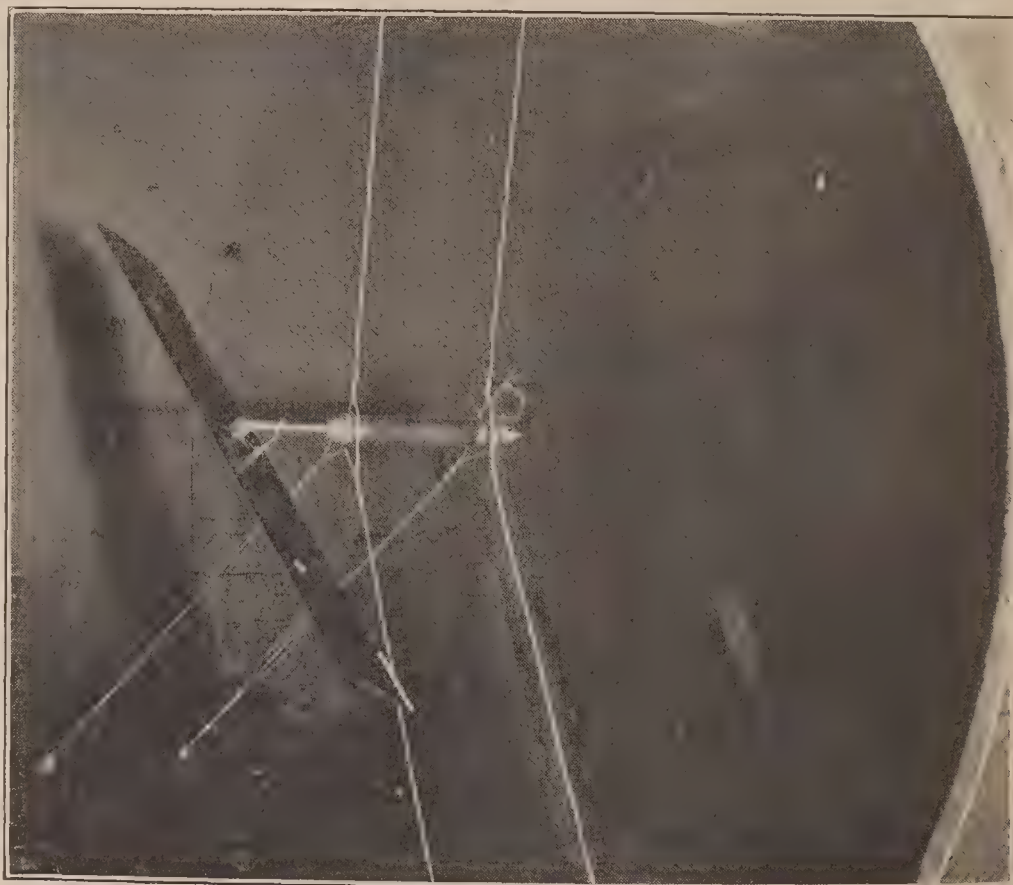


FIG. 2.—Monoplane mounted on autorotation apparatus

All tests were run at a dynamic pressure of 20.2 kg/m² (4.13 lb./sq. ft.), representing an average air speed of 18 m/s (40.3 M. P. H.), and an average Reynolds Number of 153,000.

Rates of rotation were checked to within ± 1 per cent. Limits of rotary instability may be relied upon to $\pm 1^\circ$ and angles of attack to $\pm 0.1^\circ$. The lift and drag data are accurate to ± 1.5 per cent. The dynamic pressure showed a maximum variation of ± 0.5 per cent.

RESULTS

TESTS

The results of the autorotation tests may be found in Tables I-IV and Figures 3-7, inclusive. Rates of stable autorotation are plotted against mean angles of attack in the curves. Rates of rotation are expressed nondimensionally in terms of the linear and angular velocities u and p , respectively, as

$$\tan \Phi = \frac{pb}{2u}$$

where b = span. This expression is merely the ratio of the wing tip speed to forward speed, and is analogous to the tangent of the effective helix angle of a propeller tip.

Force test results are given in Tables V-VIII and Figures 8-12. Lift and drag are plotted against one another in the polar curves, the customary absolute coefficients being used.

$$C_L = \frac{L}{qS}$$

$$C_D = \frac{D}{qS}$$

where L and D are the lift and drag, respectively, S the area, and q the test dynamic pressure ($q = \frac{1}{2} \rho V^2$, where ρ = density, V = air speed) all in consistent units.

No corrections are made for tunnel wall effects, and hence these results are not "free air" data for the models tested.

AUTOROTATION CALCULATIONS

The strip method as applied to the analysis of autorotation consists in treating individual wing elements (parallel to the plane of symmetry) separately, and computing the torque due to each on the basis of their helical motions. Summation then gives the resultant torque for the entire wing which must be zero for the condition of stable autorotation. Ordinary force tests carried to high angles of attack (assuming uniform distribution of resultant force across the span) furnish the data for these computations. In the present work no account is taken of the modification of force distribution by the tip form of the model, by centrifugal force and scale effect due to rotation, or by the tunnel walls. This is the usual practice, but as demonstrated later, these factors are by no means negligible under certain conditions.

The customary analysis, first made by Glauert, utilizes the curves of lift and drag against angle of attack. (References 2, 3, 4, and 5.) However, the work done at this laboratory has shown that the polar curve furnishes a simpler basis for the analysis. In addition, the polar itself is a means for the direct determination of the limits of rotary instability, subject to the same limitations as the strip method.

Expressions for torque and force coefficients in rotation and the corresponding criterion for rotary instability are derived on the basis of resultant force in the Appendix. The criterion is

$$\frac{d(C_R)}{d\alpha} < 0$$

where C_R is the absolute coefficient of resultant force, and α , the angle of attack of the wing. This criterion is an approximation but, for all practical purposes, it gives the same results as

Glauert's exact expression. (See Appendix.) Both criteria are subject to strip method limitations.

The new criterion makes the polar a sufficient means of determining the ranges of rotary instability, since the relation signifies a decreasing resultant force with increasing angle of attack. For this purpose it is essential that the true polar (equal ordinates and abscissas) be used. The limits of instability may be found merely by noting the angles of attack at which

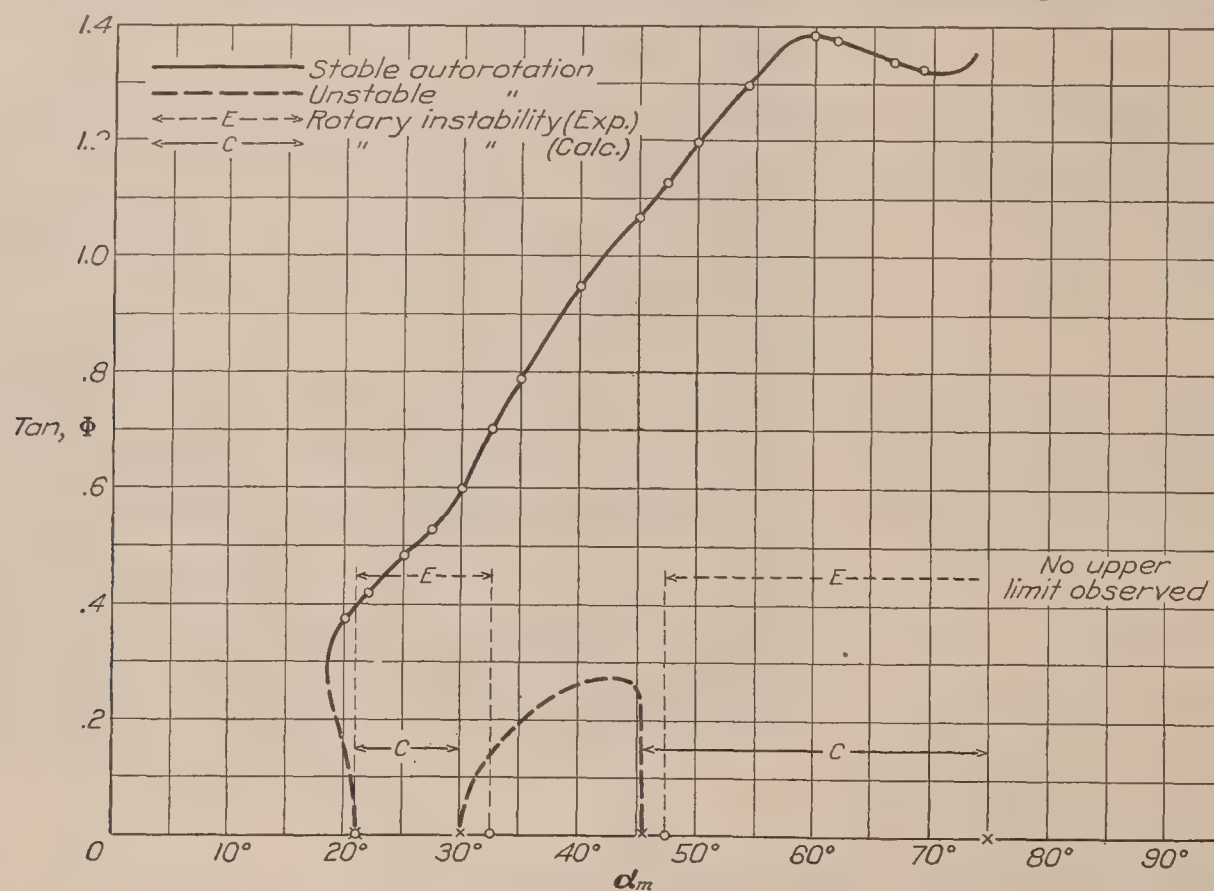


FIG. 3.—Autorotation test on Göttingen 387-FB biplane (5 by 30 inches), $G/c=1$, stagger=0, $q=20.2 \text{ kg/m}^2$, Reynolds No. = 155,000

the polar curve is perpendicular to a line drawn from the origin. The relative degree of stability or instability at various angles (α_m) is indicated roughly by $\cos \alpha_m \frac{dC_R}{d\alpha}$. (See fig. 15.)

The calculated ranges of rotary instability are included in Figures 3-6 and 8-11 for comparison with the experimental results.

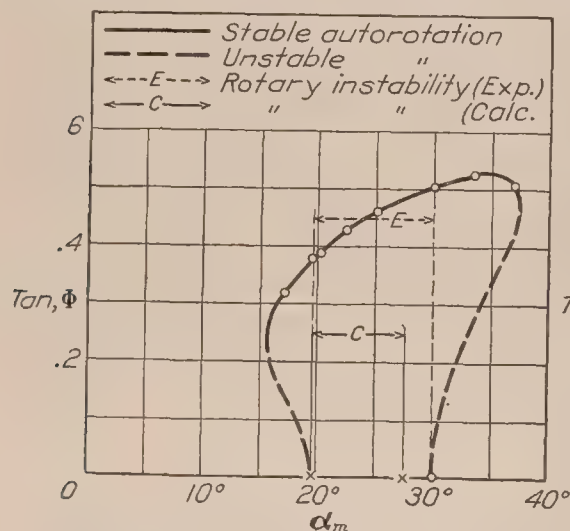


FIG. 4.—Göttingen 387-FB monoplane (5 by 30 inches), $q=20.2 \text{ kg/m}^2$, Reynolds No. = 153,000

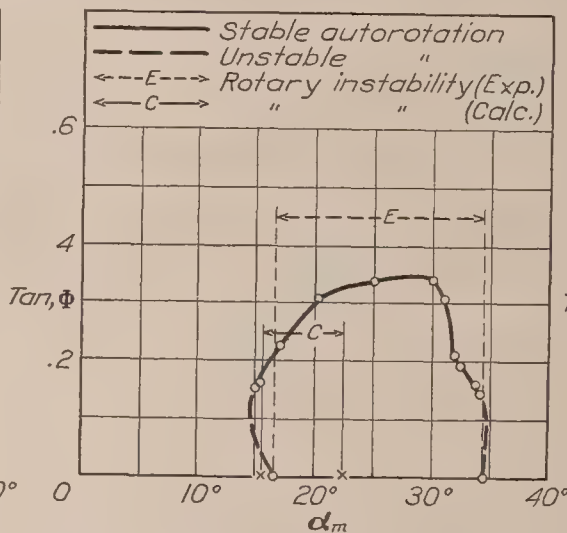


FIG. 5.—R. A. F. 15 monoplane (5 by 30 inches), $q=20.2 \text{ kg/m}^2$, Reynolds No. = 152,000

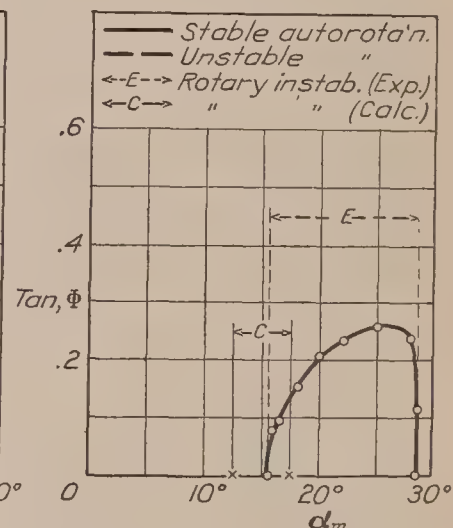


FIG. 6.—N. A. C. A. M1 monoplane (5 by 30 inches), $q=20.2 \text{ kg/m}^2$, Reynolds No. = 153,000

DISCUSSION OF RESULTS

AUTOROTATION TESTS

The test results shown in Figure 7 furnish a striking demonstration of the possible variation in autorotational characteristics of common types of airfoils and airfoil combinations. An outstanding feature is the wide difference, both in range and in magnitude, between monoplane and biplane results, illustrating the already recognized effect of multiplane interference.

The differing rates and ranges of autorotation up to 45° furnish a means of comparing the effects of different airfoil profiles upon autorotation.

Another and unanticipated feature is the well-defined autorotation of the symmetrical M1 airfoil, for which strip method calculations predicted but a slight degree of instability.

The experimental autorotation curves are merely interpolated for unstable autorotation (shown by dotted lines in Figures 3, 4, and 5) since the apparatus did not permit of obtaining these values experimentally. In Figure 3 is included also a calculated curve of the values of $\tan \Phi$ at which unstable autorotation occurs for the biplane. These additions are intended only as a rough indication of existing conditions.

FORCE TESTS AND AUTOROTATION CALCULATIONS

The polar diagrams in Figure 12 afford another illustration of the marked difference between the characteristics of the monoplane and the unstaggered biplane. This difference has previously been attributed to the shielding of the upper wing of a biplane by the lower (References 6

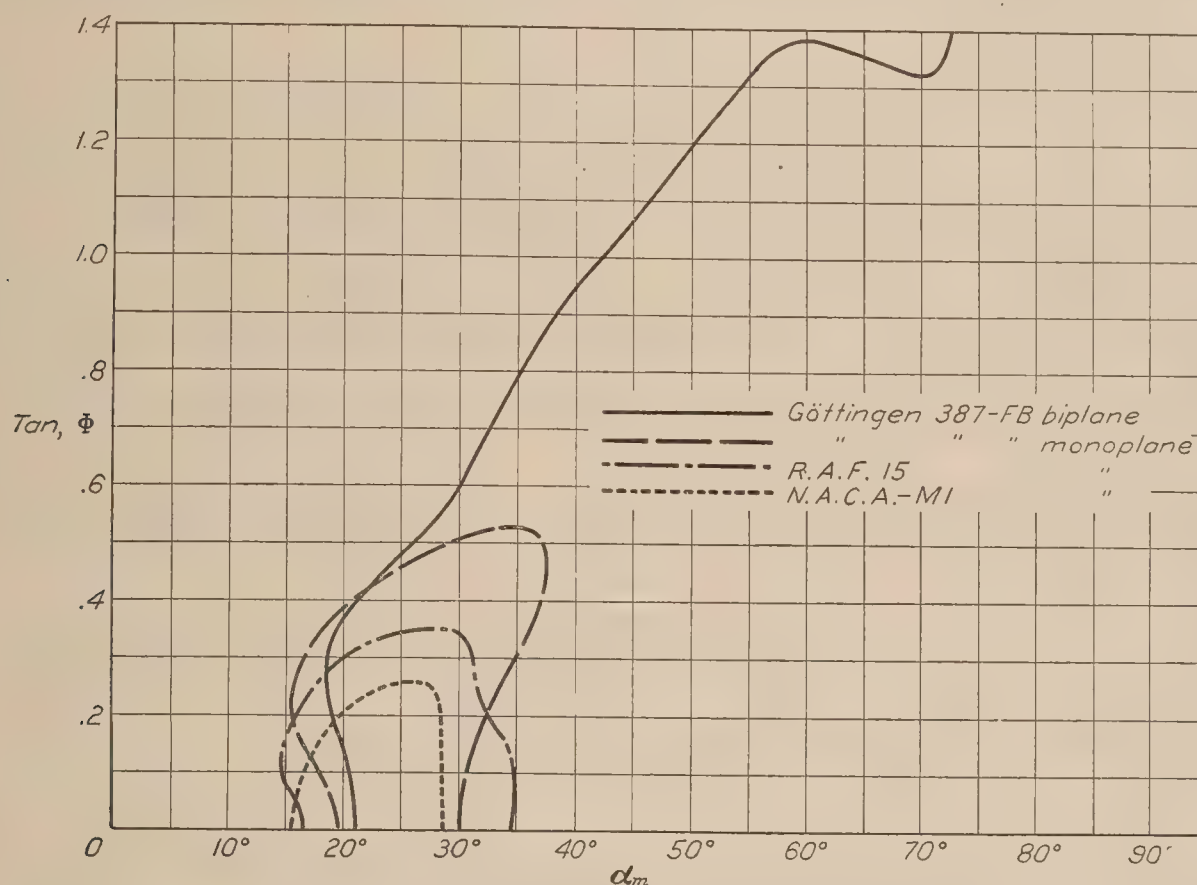


FIG. 7.—Autorotation tests on four models

and 7), and recent biplane pressure distribution experiments carried to 90° angle of attack (conducted at this laboratory), proved this fact conclusively. Positive stagger or upper wing overhang may be expected to reduce biplane autorotational tendencies by reducing this shielding, thereby approaching the monoplane condition. (Reference 8.) The same may be said for an increase in gap, except that for practical gap-chord ratios the reduction in shielding due to gap increase will probably be small compared with that for stagger increase, or for overhang. However, it was not possible at the time of test to include an investigation of the effects of stagger, overhang, and gap throughout the first quadrant, and very little data of this nature for angles of attack above 30° has been made available elsewhere up to this time.

In Figures 8–11 the calculated and experimental ranges of rotary instability are shown to demonstrate the use of the polar as a criterion. These curves show that, with the exception of the M1 wing, the lower limits of instability are in good agreement and for each wing are practically at the point of maximum C_L . None of the monoplanes show, either by experiment or calculation, any definite tendency to rotate above 35° , while the biplane has distinct autorotational tendencies in the region above 45° .

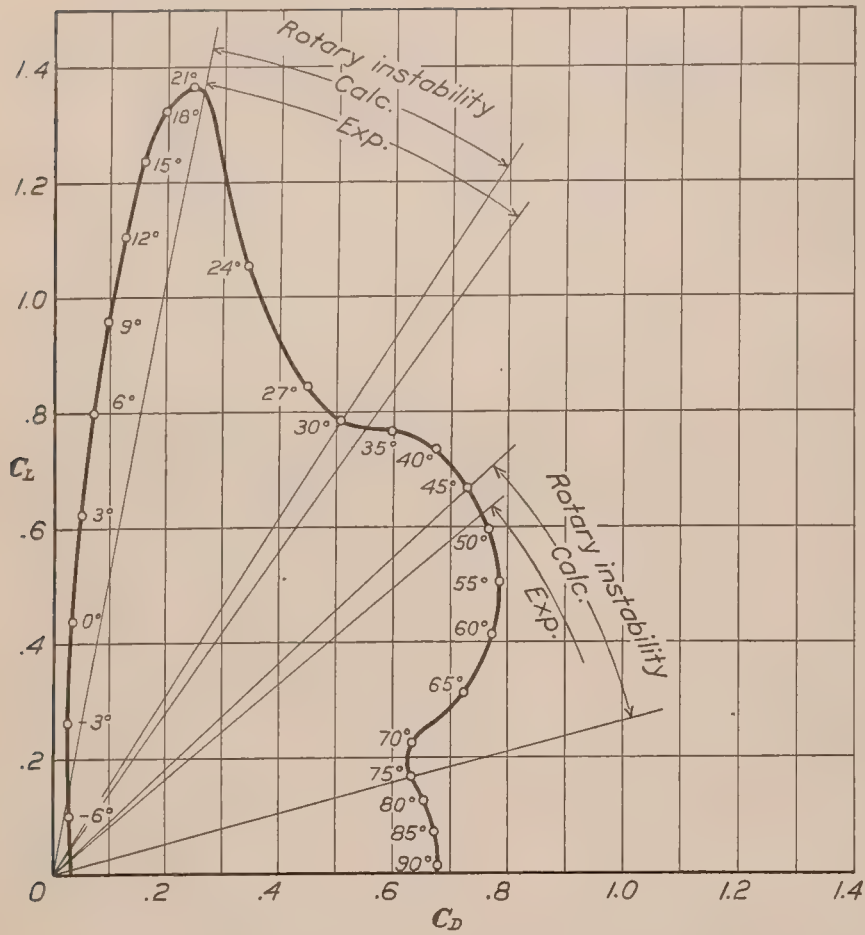


FIG. 8.—Force test on Göttingen 387-FB biplane (5 by 30 inches) $G/c=1$, stagger=0, $q=20.2$ kg/m², Reynolds No.=156,000

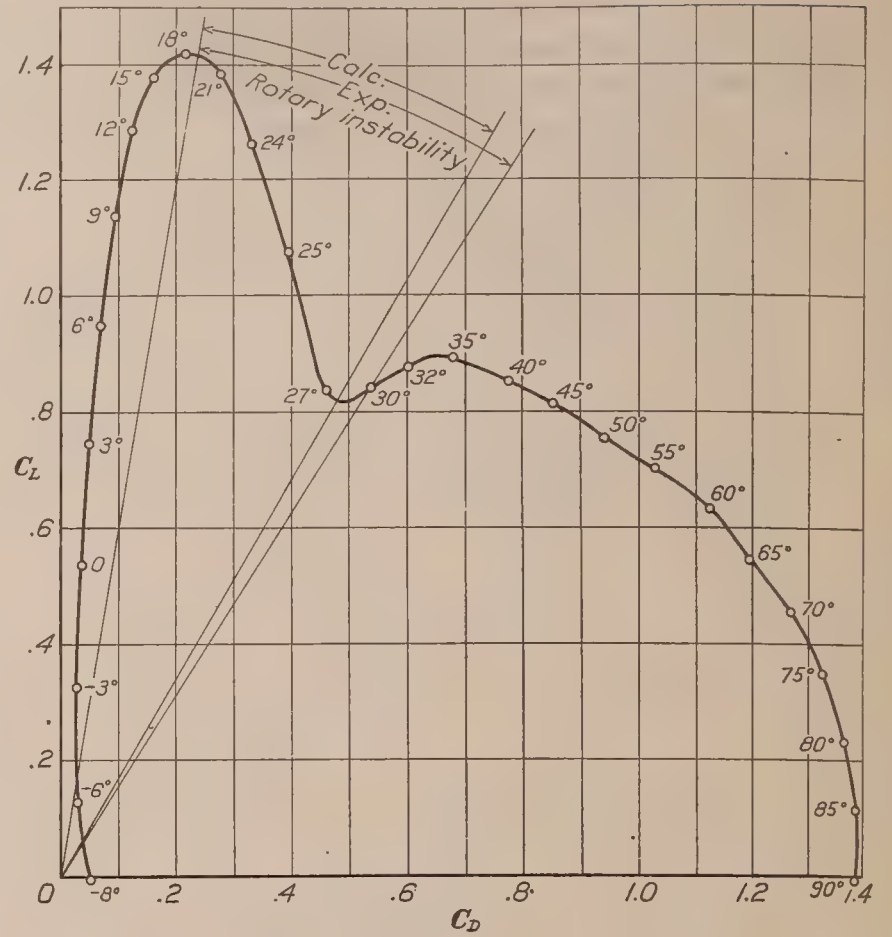


FIG. 9.—Force test on Göttingen 387-FB monoplane (5 by 30 inches), $q=20.2$ kg/m², Reynolds No.=155,000

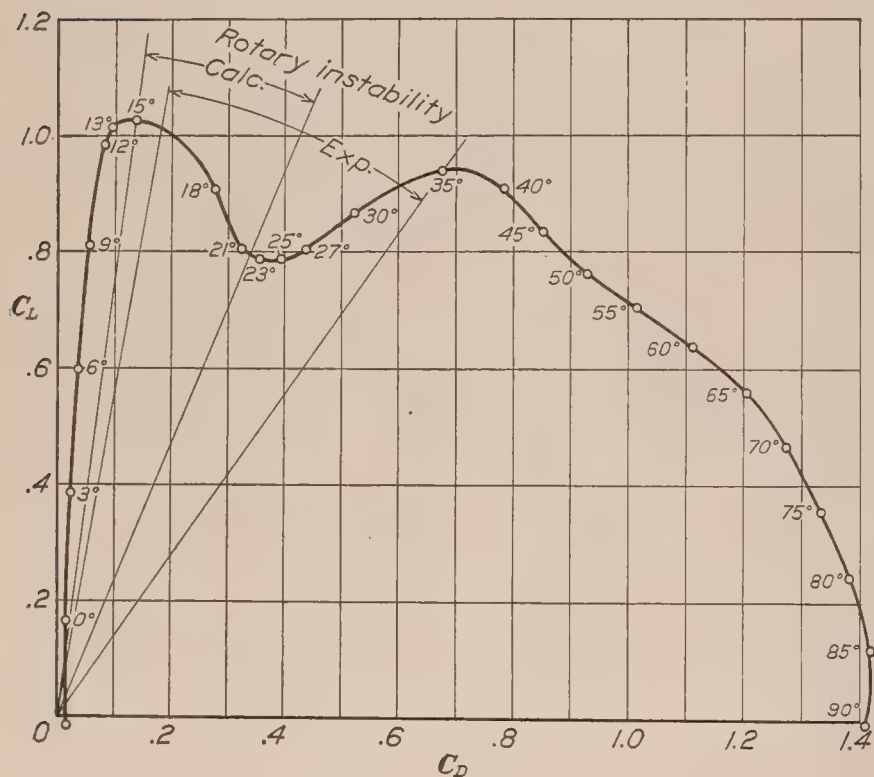


FIG. 10.—Force test on R. A. F. 15 monoplane (5 by 30 inches), $q=20.2$ kg/m², Reynolds No.=155,000

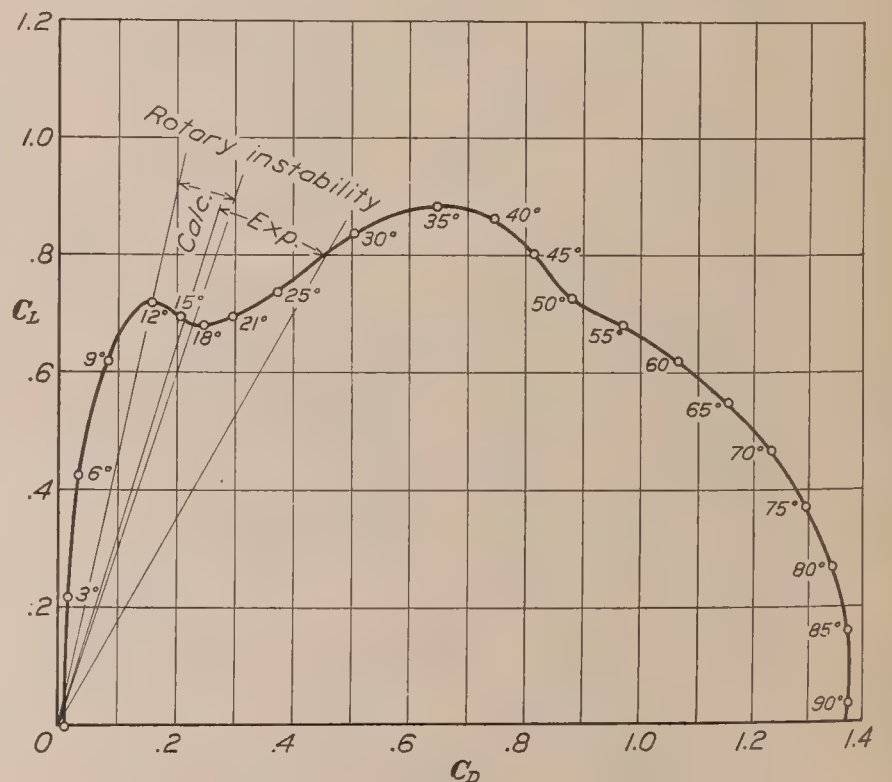


FIG. 11.—Force test on N. A. C. A. M1 monoplane (5 by 30 inches), $q=20.2$ kg/m², Reynolds No.=156,000

Figures 10 and 11 show that the accuracy of the strip method is to be questioned between the angles of maximum C_L and 35° , though it may be relied on reasonably well beyond these limits. Doubtless the discrepancies may be attributed largely to the basic assumption of uniform force distribution across the span.

The very apparent similarity of the monoplane polars from 30° to 90° , and the wide differences between monoplane and biplane in Figure 12, indicate that wing arrangement and not wing profile is the controlling factor over this range.

The radial lines drawn in Figure 12 together with the points shown on the curves indicate the relative positions of the normal to the chord and the resultant force vectors for 30° , 45° , and 90° angle of attack. Figure 17 shows this relationship more completely, and it is evident that between 30° and 90° departure of the resultant force vector from the normal to the chord is less than $\pm 3^\circ$, for any of the models tested.

Figures 13 and 14 are included in this report to demonstrate the feasibility of using the first quadrant polar of complete airplane models for determining roughly their limits of rotary instability. Figure 13 is taken from force tests made at the Washington Navy Yard upon a 1/16 scale model of the Boeing NB-1 seaplane. (Reference 9.) Similar results for a 1/24 scale model of the Douglas XO-2 landplane are given in Figure 14, as obtained from tests recently made at this laboratory at the request of the Army Air Corps. Calculated ranges of rotary instability are shown on these curves. Experimental ranges for the XO-2 are given in Figure 14.

The criterion for rotary instability is developed from the strip method analysis of wing systems only. Therefore the presence in the complete model polars of the forces upon body, tail, and landing gear may be expected to introduce errors in determining the limits of rotary instability. However, in spite of these spurious effects, flat-spinning tendencies are distinctly indicated for the models in Figures 13 and 14, and in the latter figure the calculated ranges of instability are in fair agreement with experiment.

In Figure 15 are shown curves of the complete criterion for rotary instability, $\frac{d(C_L)}{d\alpha}$, against angle of attack. (See Appendix for derivation.) This criterion indicates not only the state of equilibrium, but also the degree of stability or instability. The points shown are values of $\cos \alpha_m \frac{d(C_R)}{d\alpha}$ and are included to show that the simpler expression may be used with good accuracy. The following deductions may be made from these curves:

Maximum damping (stable) tendencies occur at or near zero angle of attack and are of practically the same magnitude for all the models tested.

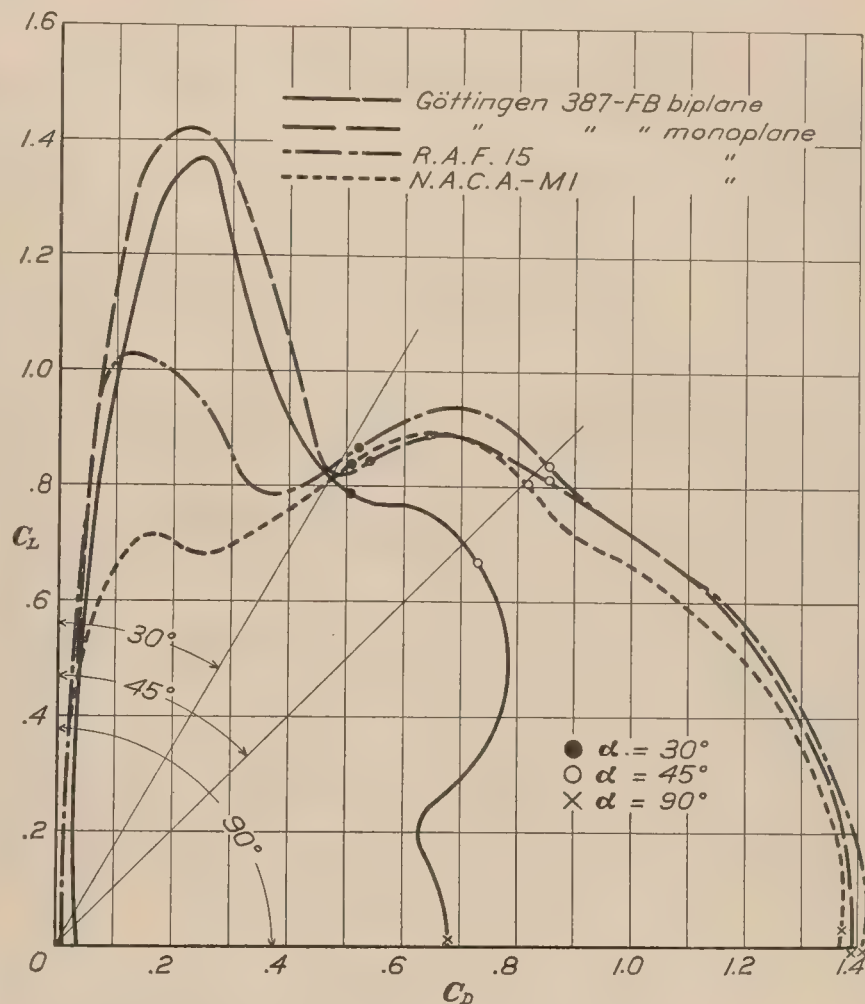


FIG. 12.—Force tests on four models

Maximum autorotational (unstable) tendencies occur in each case just beyond maximum lift, and vary widely in magnitude for the different models.

Beyond 35° the characteristics of the monoplanes are practically identical, with small stable tendencies between 45° and 75° , and practically neutral equilibrium at 45° and between 75° and 90° .

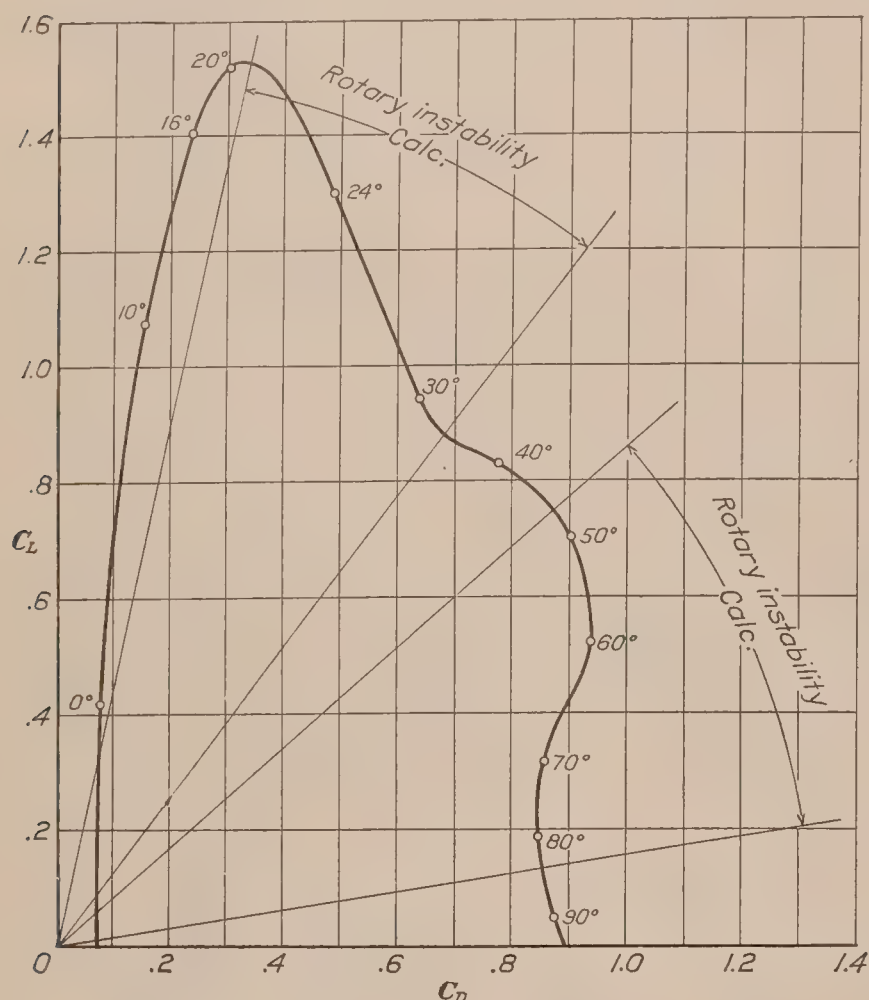


FIG. 13.—Force test on Boeing NB-1 seaplane, $1/16$ scale model. $V=40$ M. P. H.

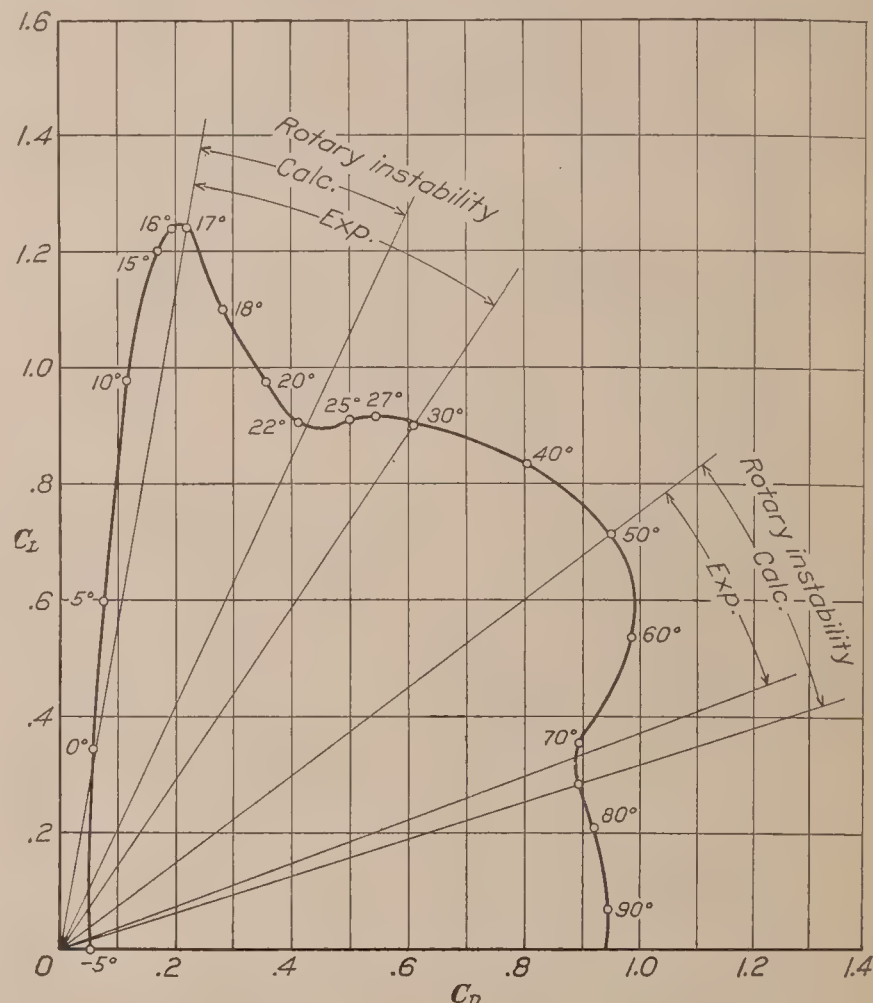


FIG. 14.—Force test on Douglas XO-2 airplane, $1/24$ scale model. $q=55.5$ kg/m²

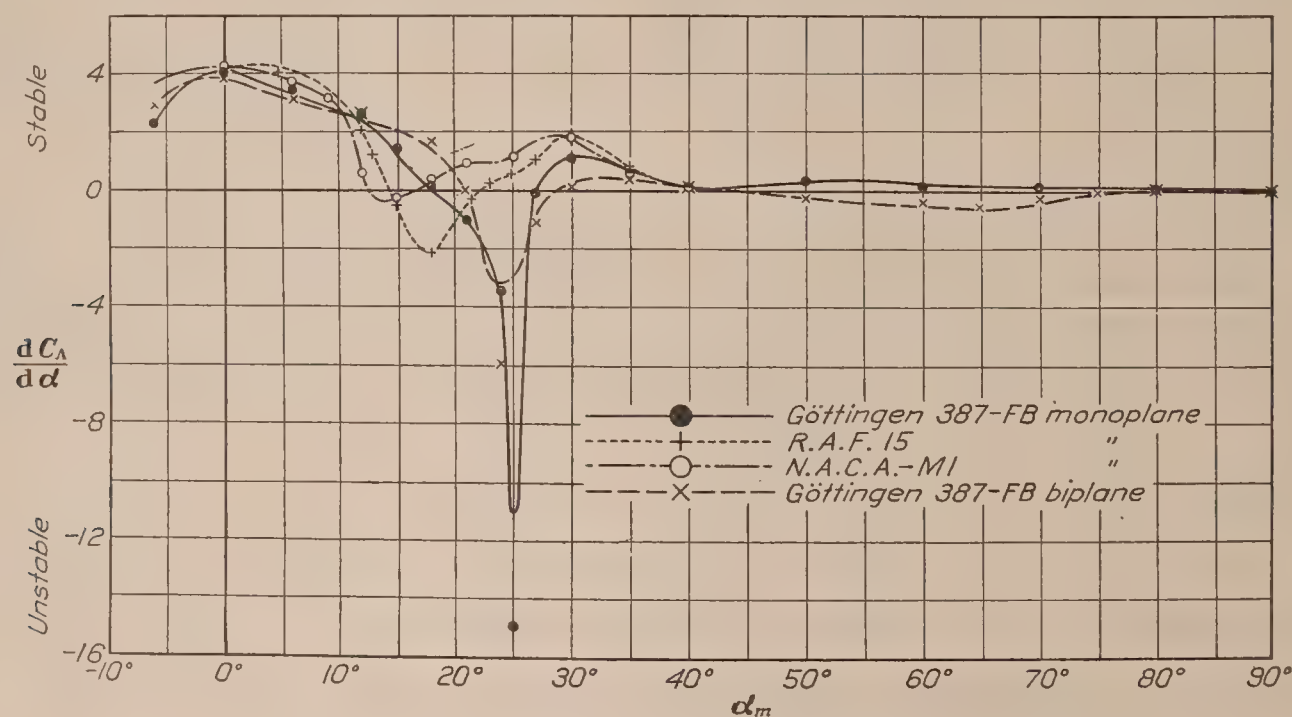


FIG. 15.—Rotary stability curves, $\frac{dC_A}{d\alpha}$

Beyond 45° the biplane shows instability, and neutral equilibrium between 75° and 90° .

As the angle of maximum lift is exceeded, strip method and test results begin to diverge, agreement being reached again at 35° . Due to this divergence no attempt can safely be made to interpret the curves between these limits.

By far the most important deduction to be made relates to stalled flight. The curves show that in the vicinity of maximum lift there is for each model a rapid change from rotary stability to instability. This means that the orthodox airplane in flight suddenly becomes laterally unstable as maximum lift is passed, and if small rotary disturbances are not promptly corrected for by ailerons and rudder, the rapidly increasing autorotational forces may become large enough to overcome the control forces, and a spin ensues.

For greater safety in flight every effort should be made in the direction of maintaining rotary stability and improving lateral control above the stall. Especially should rotary instability be an immediate object of investigation in wind tunnel and free flight research.

CONCLUSIONS

Although this investigation is far from being exhaustive, the following general conclusions may safely be drawn from it:

1. Autorotation below 30° angle of attack is governed largely by wing profile, and above that angle by wing arrangement.

2. The strip method of analysis furnishes a criterion for rotary instability which is in good agreement with experiment above 35° and also in the vicinity of maximum C_L .

3. Strip method results are to be questioned between maximum C_L and 35° , and this fact calls for further investigation of that region.

4. The polar curve of a wing system furnishes means for the direct determination of the limits of rotary instability and, for a rough indication, the polar of a complete airplane model may be used similarly, subject in both cases to strip method limitations.

The following statements relative to the airplane in free flight may now be made with reasonable assurance:

1. An airplane with a monoplane wing is not capable of flat spinning.

2. An airplane with unstaggered biplane wings has inherent flat-spinning tendencies.

3. Positive stagger or upper wing overhang may be expected to reduce flat-spinning tendencies.

4. The difficulty of maintaining equilibrium in stalled flight is due primarily to rotary instability, a rapid change from stability to instability occurring as the angle of maximum lift is exceeded.

LANGLEY MEMORIAL AERONAUTICAL LABORATORY,
NATIONAL ADVISORY COMMITTEE FOR AERONAUTICS,
LANGLEY FIELD, VA., *April 21, 1927.*

REFERENCES AND BIBLIOGRAPHY

1. REID, ELLIOTT G. Standardization Tests of N. A. C. A. No. 1 Wind Tunnel. N. A. C. A. Technical Report No. 195. 1924.
2. GLAUERT, H. The Rotation of an Aerofoil about a Fixed Axis. B. A. C. A. Reports and Memoranda No. 595. March, 1919.
3. GLAUERT, H. The Investigation of the Spin of an Aeroplane. B. A. C. A. Reports and Memoranda No. 618. June, 1919.
4. BRADFIELD, F. B. Lateral Control of Bristol Fighter at Low Speeds. Measurement of Rolling and Yawing Moments of Model Wings, Due to Rolling. B. A. C. A. Reports and Memoranda No. 787. January, 1921.
5. ANDERLIK, E. Experiments on Autorotation. N. A. C. A. Technical Memorandum No. 380. 1926. (Translated from "Zeitschrift für Flugtechnik und Motorluftschiffahrt," August 28, 1926.)
6. BRADFIELD, F. B., and SIMMONDS, O. E. Rolling and Yawing Moments Due to Roll of Model Avro Wings with Standard and Interplane Ailerons, and Rudder Moments for Standard and Special Large Rudder. B. A. C. A. Reports and Memoranda No. 848. November, 1922.
7. TOWNEND, H. C. H., and KIRKUP, T. A. Some Experiments on a Model of a B. A. T. Bantam Aeroplane with Special Reference to Spinning Accidents. B. A. C. A. Reports and Memoranda No. 976. November, 1925.
8. IRVING, H. B., and BATSON, A. S. Preliminary Note on the Effect of Stagger and Decalage on the Autorotation of a R. A. F. 15 Biplane. B. A. C. A. Reports and Memoranda No. 733. September, 1920.
9. AERONAUTICS STAFF. Air Force and Moment for NB-1 Airplane. Construction Department, Washington Navy Yard. Aeronautical Report No. 282. June, 1925.
10. THOMSON, G. P. Calculations on the Spinning of an Aeroplane. B. A. C. A. Reports and Memoranda No. 211. November, 1915.
11. LINDEMANN, F. A., GLAUERT, H., and HARRIS, R. G. The Experimental and Mathematical Investigation of Spinning. B. A. C. A. Reports and Memoranda No. 411. March, 1918.
12. RELF, E. F., and LAVENDER, T. The Autorotation of Stalled Aerofoils and Its Relation to the Spinning Speed of Aeroplanes. B. A. C. A. Reports and Memoranda No. 549. October, 1918.
13. RELF, E. F., and LAVENDER, T. A Continuous Rotation Balance for the Measurement of L_p at Small Rates of Roll. B. A. C. A. Reports and Memoranda No. 828. August, 1922.
14. BRADFIELD, F. B., and COOMBES, L. P. Autorotation Measurements on a Model Aeroplane with Zero Stagger. B. A. C. A. Reports and Memoranda No. 975. April, 1925.
15. OFSTIE, RALPH A. The Flat Spin of the Boeing N. B. Training Airplane. Bureau of Aeronautics, Navy Department. Technical Note No. 164. May, 1926.
16. LACHMANN, G. Stall-Proof Airplanes. N. A. C. A. Technical Memorandum No. 393. 1927. (Translation from the Yearbook of the "Wissenschaftlichen Gesellschaft für Luftfahrt," 1925.)
17. BRYANT, L. W., and GATES, S. B. The Spinning of Aeroplanes. "The Journal of the Royal Aeronautical Society." July, 1927.

APPENDIX

STRIP METHOD ANALYSIS

Following is the strip method derivation of the expressions for torque and force coefficients in rotation, and also the development of a criterion for rotary instability.

The symbols used are illustrated in Figure 16. C_R is the resultant force coefficient (absolute) for the angle of attack α , while C_A and C_N are its components, respectively, along and normal to the axis of rotation. The angle of the wing chord to this axis is α_m . The effective wind velocity V_E is the vector sum of the velocity V along the axis and the tangential velocity V_R . The wing chord and span are represented by c and b , respectively, and, in this derivation, c is a constant.

Therefore the torque increment due to a given wing element of width Δy at a distance y from the axis of rotation may be written

$$\Delta\Lambda = C_A q' y c (\Delta y) \quad (1)$$

where

$$\begin{aligned} q' &= \frac{1}{2} \rho V_E^2 \\ &= \frac{1}{2} \rho (V \sec \Delta\alpha)^2 \\ &= q (\sec^2 \Delta\alpha) \end{aligned} \quad (2)$$

$\Delta\alpha$ being the algebraic sum of the angle of attack of the element in question and α_m . The total torque for the wing is therefore

$$\Lambda = qc \int_{-b/2}^{b/2} C_A y (\sec^2 \Delta\alpha) dy \quad (3)$$

and reduced to nondimensional coefficient form

$$\begin{aligned} C_\Lambda &= \frac{\Lambda}{qbS} = \frac{\Lambda}{qb^2c} \\ &= \frac{1}{b^2} \int_{-b/2}^{b/2} C_A y (\sec^2 \Delta\alpha) dy \end{aligned} \quad (4)$$

where C_Λ is the coefficient of autorotational moment. The lift coefficient (force normal to axis) is

$$C_L = \frac{1}{b^2} \int_{-b/2}^{b/2} C_N (\sec^2 \Delta\alpha) dy \quad (4a)$$

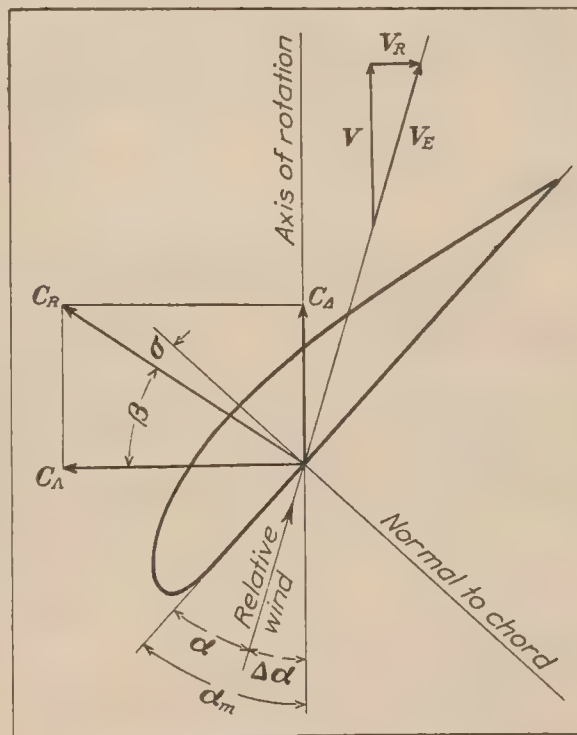


FIG. 16.—Wing element in autorotation

The corresponding equation for moment about an axis in the plane of symmetry and normal to that of autorotation is similarly

$$C_\delta = \frac{1}{b^2} \int_{-b/2}^{b/2} C_\Delta y (\sec^2 \Delta \alpha) dy \quad (4b)$$

while the drag coefficient in rotation is

$$C_D = \frac{1}{b^2} \int_{-b/2}^{b/2} C_\Delta (\sec^2 \Delta \alpha) dy \quad (4c)$$

If we now consider very small angular velocities we may determine the criterion of rotary instability for the model at rest. The angular velocity is to be taken sufficiently small that variations in C_Δ along the span may be considered linear. For this condition equation (1) shows that, for a given wing element, the increment of torque

$$\Delta \Lambda = K C_\Delta$$

where

$$K = q' y c (\Delta y).$$

If we consider two wing-tip elements (1, 2) such that 1 is on the up-going or small-angle-of-attack tip, and 2 the down-going or large-angle tip, we have from Figure 16

$$\begin{aligned} C_{\Delta 1} &= C_{R_1} \cos \beta_1 = C_{R_1} \cos (\alpha_m - \sigma_1) \\ &= C_{R_1} (\cos \alpha_m \cos \sigma_1 + \sin \alpha_m \sin \sigma_1) \\ C_{\Delta 2} &= C_{R_2} \cos \beta_2 = C_{R_2} \cos (\alpha_m - \sigma_2) \\ &= C_{R_2} (\cos \alpha_m \cos \sigma_2 + \sin \alpha_m \sin \sigma_2) \end{aligned}$$

On the basis of linear variation of force between tips, the initial condition for rotary instability is that

$$C_{\Delta 1} > C_{\Delta 2}$$

or

$$C_{\Delta 2} - C_{\Delta 1} < 0.$$

We may write

$$\begin{aligned} C_{\Delta 2} - C_{\Delta 1} &= C_{R_2} (\cos \alpha_m \cos \sigma_2 + \sin \alpha_m \sin \sigma_2) - C_{R_1} (\cos \alpha_m \cos \sigma_1 + \sin \alpha_m \sin \sigma_1) \\ &= \cos \alpha_m (C_{R_2} \cos \sigma_2 - C_{R_1} \cos \sigma_1) + \sin \alpha_m (C_{R_2} \sin \sigma_2 - C_{R_1} \sin \sigma_1). \end{aligned}$$

Dividing both sides by $2\Delta\alpha$ we note that in the limit

$$\begin{aligned} \frac{C_{\Delta 2} - C_{\Delta 1}}{2\Delta\alpha} &= \frac{d(C_\Delta)}{d\alpha} \\ \frac{C_{R_2} \cos \sigma_2 - C_{R_1} \cos \sigma_1}{2\Delta\alpha} &= \frac{d(C_R \cos \sigma)}{d\alpha} \\ \frac{C_{R_2} \sin \sigma_2 - C_{R_1} \sin \sigma_1}{2\Delta\alpha} &= \frac{d(C_R \sin \sigma)}{d\alpha} \end{aligned}$$

and the criterion becomes

$$\frac{d(C_\Delta)}{d\alpha} = \cos \alpha_m \frac{d(C_R \cos \sigma)}{d\alpha} + \sin \alpha_m \frac{d(C_R \sin \sigma)}{d\alpha} < 0 \quad (7)$$

Figure 17 shows the variation of σ with angle of attack for the models tested. Since $\sigma < 10^\circ$ the following approximations may be made, the criterion becoming

$$\cos \alpha_m \frac{d(C_R)}{d\alpha} + \sin \alpha_m \frac{d(C_R \sigma)}{d\alpha} < 0$$

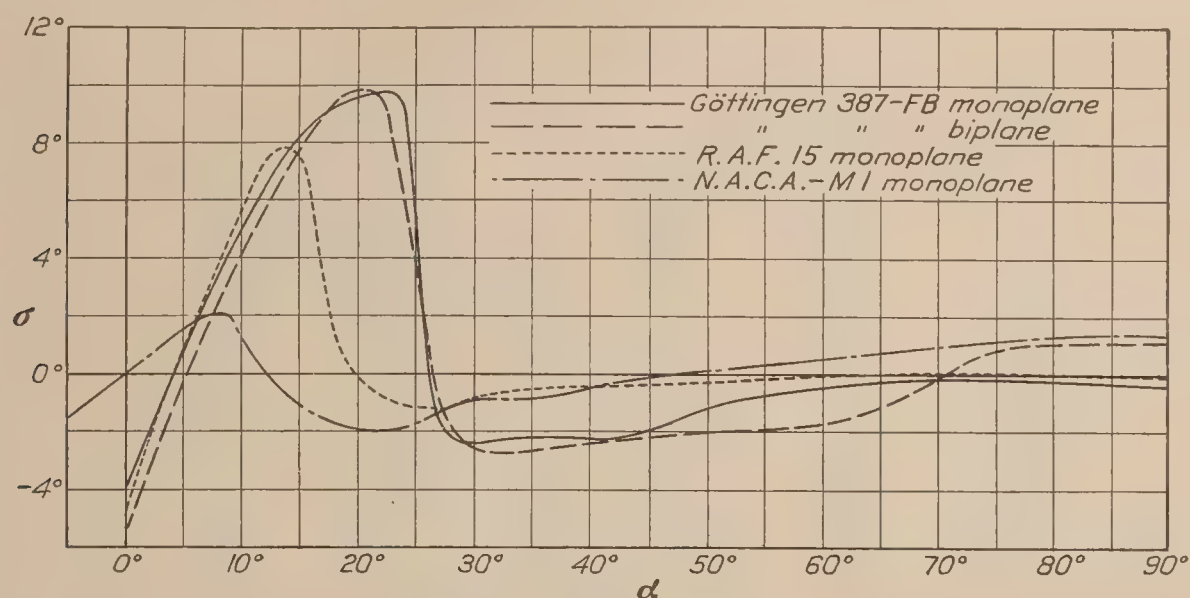


FIG. 17.—Curves of σ vs. α

Figure 15 shows that with the exception of the maximum negative values of $\frac{d(C_A)}{d\alpha}$ the second term of equation (7) is negligible and since $\cos \alpha_m$ is always positive in the first quadrant, our criterion becomes

$$\frac{d(C_R)}{d\alpha} < 0 \quad (8)$$

Glauert's criterion is

$$\frac{d(C_L)}{d\alpha} + C_D < 0$$

which is exact, but equation (8), in spite of its approximate nature, for all practical purposes, gives the same results.

TABLE I

Autorotation Test

Göttingen 387—FB biplane (5 by 30 inches)

$G/c=1$, stagger=0

$q=20.2 \text{ kg/m}^2$

Reynolds Number=155,000

α_m degrees	$\tan \phi$	α_m degrees	$\tan \phi$
20	0.373	47.5	1.125
22	.417	50	1.197
25	.482	54.3	1.293
27.5	.528	59.9	1.382
30	.593	61.8	1.373
32.5	.696	66.7	1.338
35	.787	69.2	1.322
40	.945	74.7	1.930
45	1.063		

TABLE II

Autorotation Test

Göttingen 387—FB monoplane (5 by 30 inches)

$$q=20.2 \text{ kg/m}^2$$

Reynolds Number=153,000

α_m degrees	$\tan \phi$	α_m degrees	$\tan \phi$
17. 1	0. 319	25	0. 458
19. 5	. 376	30	. 503
20. 2	. 389	33. 5	. 526
22. 5	. 429	37	. 509

TABLE III

Autorotation Test

R. A. F. 15 monoplane (5 by 30 inches)

$$q=20.2 \text{ kg/m}^2$$

Reynolds Number=152,000

α_m degrees	$\tan \phi$	α_m degrees	$\tan \phi$
15	0. 152	31	0. 308
15. 4	. 161	32	. 214
17	. 228	32. 5	. 196
20. 2	. 307	33. 8	. 161
25	. 338	34. 1	. 147
30	. 341		

TABLE IV

Autorotation Test

N. A. C. A.—M1 monoplane (5 by 30 inches)

$$q=20.2 \text{ kg/m}^2$$

Reynolds Number=153,000

α_m degrees	$\tan \phi$	α_m degrees	$\tan \phi$
16	0. 078	22. 1	0. 236
16. 5	. 093	25	. 257
18. 1	. 152	28	. 238
20	. 208	28. 6	. 115

TABLE V

Force Test

Göttingen 387-FB biplane (5 by 30 inches)

 $G/c=1$, stagger=0 $q=20.2$ kg/m²

Reynolds Number=156,000

α degrees	C_L	C_D	α degrees	C_L	C_D
-8	-0.006	0.046	30	0.784	0.509
-6	+.100	.030	35	.766	.598
-3	.262	.028	40	.734	.676
0	.438	.037	45	.669	.730
+3	.620	.051	50	.596	.769
6	.798	.072	55	.505	.788
9	.958	.098	60	.415	.776
12	1.104	.126	65	.312	.728
15	1.236	.160	70	.226	.634
18	1.324	.198	75	.170	.633
21	1.365	.244	80	.128	.656
24	1.052	.344	85	.072	.676
27	.842	.450	90	.014	.682

TABLE VI

Force Test

Göttingen 387-FB monoplane (5 by 30 inches)

 $q=20.2$ kg/m²

Reynolds Number=155,000

α degrees	C_L	C_D	α degrees	C_L	C_D
-8	-0.005	0.052	30	0.840	0.538
-6	+.127	.030	32	.876	.602
-3	.323	.029	35	.892	.680
0	.534	.036	40	.851	.776
+3	.744	.050	45	.811	.854
6	.948	.070	50	.751	.941
9	1.136	.095	55	.700	1.028
12	1.285	.124	60	.631	1.124
15	1.377	.162	65	.544	1.195
18	1.418	.217	70	.452	1.270
21	1.378	.283	75	.347	1.328
24	1.260	.331	80	.232	1.356
25	1.075	.395	85	+.113	1.390
27	.836	.461	90	-.009	1.389

TABLE VII

Force Test

R. A. F. 15 monoplane (5 by 30 inches)

$q=20.2 \text{ kg/m}^2$

Reynolds Number=155,000

α degrees	C_L	C_D	α degrees	C_L	C_D
-2	-0.015	0.016	30	0.866	0.523
0	+.163	.015	35	.938	.679
+3	.383	.021	40	.908	.786
6	.597	.035	45	.834	.854
9	.810	.055	50	.760	.929
12	.981	.081	55	.703	1.016
13	1.011	.094	60	.637	1.111
15	1.025	.138	65	.558	1.205
18	.907	.279	70	.463	1.276
21	.804	.324	75	.353	1.335
23	.789	.355	80	.241	1.382
25	.789	.391	85	+.119	1.420
27	.804	.438	90	-.008	1.409

TABLE VIII

Force Test

N. A. C. A.-M1 monoplane (5 by 30 inches)

$q=20.2 \text{ kg/m}^2$

Reynolds Number=155,000

α degrees	C_L	C_D	α degrees	C_L	C_D
0	-0.006	0.011	40	0.863	0.746
3	+.216	.015	45	.802	.816
6	.422	.032	50	.725	.881
9	.619	.081	55	.680	.970
12	.717	.159	60	.619	1.066
15	.694	.207	65	.546	1.153
18	.680	.248	70	.463	1.233
21	.695	.298	75	.369	1.296
25	.735	.374	80	.266	1.345
30	.837	.508	85	.155	1.375
35	.883	.648	90	.031	1.377

REPORT No. 274

**THE N. A. C. A. PHOTOGRAPHIC APPARATUS FOR
STUDYING FUEL SPRAYS FROM OIL ENGINE INJECTION
VALVES AND TEST RESULTS FROM
SEVERAL RESEARCHES**

**By EDWARD G. BEARDSLEY
Langley Memorial Aeronautical Laboratory**

REPORT No. 274

THE N. A. C. A. PHOTOGRAPHIC APPARATUS FOR STUDYING FUEL SPRAYS FROM OIL ENGINE INJECTION VALVES AND TEST RESULTS FROM SEVERAL RESEARCHES

By EDWARD G. BEARDSLEY

SUMMARY

Apparatus for recording photographically the start, growth, and cut-off of oil sprays from injection valves has been developed at the Langley Memorial Aeronautical Laboratory of the National Advisory Committee for Aeronautics. The apparatus consists of a high-tension transformer by means of which a bank of condensers is charged to a high voltage. The controlled discharge of these condensers in sequence, at a rate of several thousand per second, produces electric sparks of sufficient intensity to illuminate the moving spray for photographing. The sprays are injected from various types of valves into a chamber containing gases at pressures up to 600 pounds per square inch.

Several series of pictures are shown. The results give the effects of injection pressure, chamber pressure, specific gravity of the fuel oil used, and injection-valve design, upon spray characteristics.

INTRODUCTION

The first successful compression-ignition oil engine, using air injection, was built about 1897, by Doctor Diesel. About 1912, McKechnie constructed a practicable so-called solid or hydraulic injection engine. Since that time the solid-injection engine has been gradually developed and the demand for it has so increased that to-day a large number of engine builders are manufacturing this type. Much progress has been made, and a great deal of knowledge has been gained concerning solid-injection engines.

The part of the engine about whose operation we have the least information thus far, is probably one of the most important parts, namely, the injection valve. Sprays from injection valves have been examined in the atmosphere as to their cone angle, fineness of atomization, and rapidity of combustion when ignited. They have been injected into water and the penetration noted visually. However, the complete behavior of a spray injected into dense air has always been a matter for conjecture and theoretical computation. (Reference 1.) Yet it is something which is very important, and because of this lack of definite knowledge, the design of an injection valve to give the best results in a particular combustion chamber has been to a large degree a process of cut and try.

A study of the compression-ignition, solid-injection type of engine, with regard to its possible development for aircraft use was started at the Langley Memorial Aeronautical Laboratory at Langley Field, Va., in 1921. The general problem was analyzed and an attempt made to attack it from all angles. Actual knowledge about the characteristics of sprays from injection valves was desired. While the adaptability of the spray to the combustion chamber is not of so much importance in the case of a low-speed, low-capacity engine, it is vital for the high-speed, high-capacity engine useful for aircraft. The spray was therefore to be studied with regard to its penetration, general shape, and atomization when injected into dense air.

It was concluded that the method by which it would be possible to obtain the greatest amount of information about oil sprays was to take high-speed motion pictures of their start,

development, and cut-off, which would show their penetration, general shape, and possibly their atomization. With this end in view, preliminary apparatus was designed, built, and tested during the summer of 1921. However, it was found impossible to obtain a series of pictures of oil sprays with this apparatus. Finally, in the fall of 1924, the photography of oil sprays in dense air became a reality. From that time to the present day much improvement has been made in the apparatus and methods, and considerable knowledge has been gained concerning the several factors governing the characteristics of oil sprays.

DESCRIPTION OF THE N. A. C. A. SPRAY PHOTOGRAPHY APPARATUS

DEVELOPMENT OF THE APPARATUS

The problems involved in taking moving pictures of oil sprays from injection valves presented numerous difficulties. The two outstanding problems were: The necessity of having a duration of exposure of about a millionth of a second; and the production of photographic records, with this short exposure, at a rate of several thousand a second. The extremely short

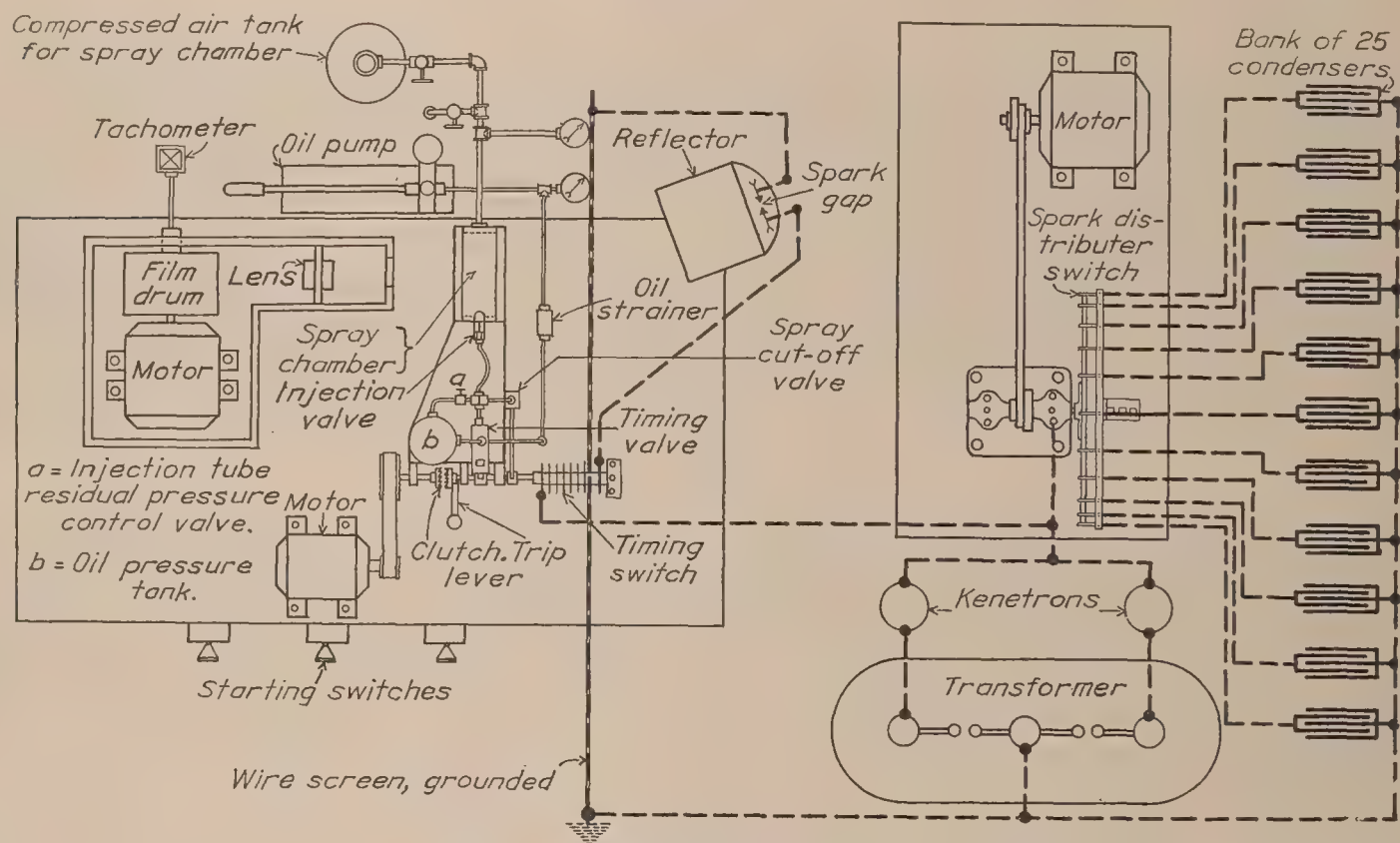


FIG. 1.—Diagrammatic arrangement of spray-photography apparatus

duration of exposure necessary can be computed by assuming that the spray has an initial velocity of 500 feet per second, or 6,000 inches per second, and permitting a distortion of one one-hundredth inch of the spray image recorded on a photographic film. For these conditions the duration of exposure must not be more than one six-hundred-thousandth second. It is evident that it would be practically impossible to build a mechanically operated shutter which would give such a brief exposure. Also, with this infinitesimal duration of exposure, the illumination must be very intense in order to produce a satisfactory record on the film. The only solution of the problem seemed to be to use the discharge of electrical condensers, the duration of the spark from a condenser discharge being known to be of the short time required, thus eliminating mechanical shutters.

The next requirement was that the series of pictures of the spray be taken at a rate of several thousand per second. This necessitated the use of a number of condensers arranged so that they could be discharged at the required frequency.

The first electrical system investigated consisted of 15 Leyden jars, which were charged by a static machine. Because of the dampness of the climate the machine failed to charge satisfactorily.

A 100,000-volt transformer and kenotron rectifying tubes were next installed. Fifteen 30 by 30 inch glass-plate condensers were built, but were unsuccessful because of excessive surface leakage and frequent puncturing of the glass plates. Twenty-five condensers were then built with Micanite plates for dielectrics. These have proved to be successful.

The present spray-photography apparatus, so far as is known, was the first apparatus ever built capable of recording by a series of pictures the growth of oil sprays. A diagrammatic layout of the apparatus is shown in Figure 1, and a general view is shown in Figure 2. The electrical apparatus consists of a high-tension transformer, two kenotron rectifying tubes, a bank of 25 condensers, a rotating distributor switch, a timing switch, and a spark gap in front of a

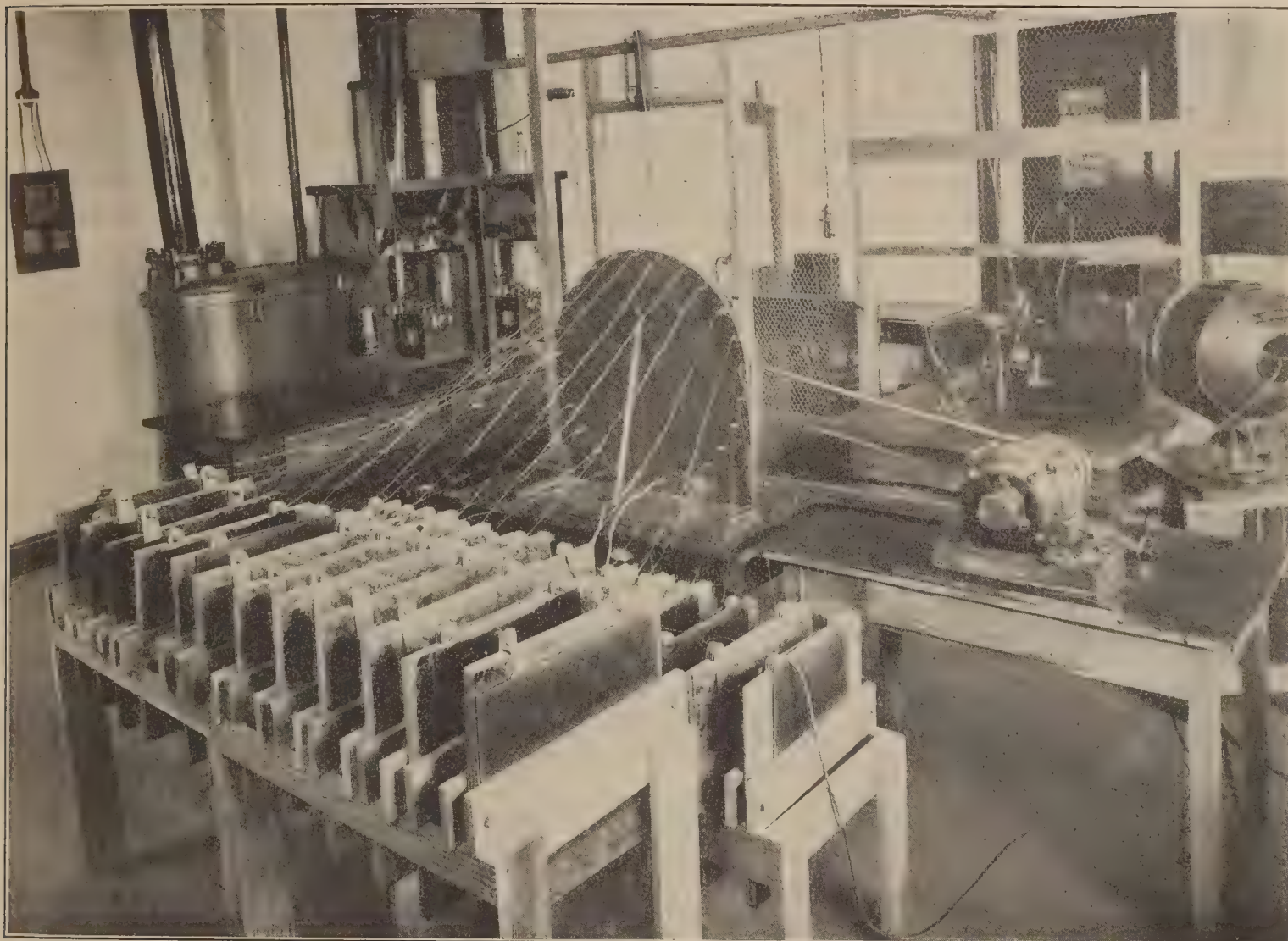


FIG. 2.—GENERAL VIEW OF SPRAY-PHOTOGRAPHY APPARATUS

reflector for focusing the light on the moving oil spray. Figures 1 and 2 show the transformer and kenotron rectifying tubes, by means of which the 25 condensers are charged to 30,000 volts through the rotating distributor switch. One terminal of each condenser is connected to a contact on the switch panel, and the other is grounded. Discharge across the spark gap can not take place until the timing switch operated by the cam shaft is rotated, when each condenser is discharged in sequence across the gap. The frequency of the discharges is controlled by the speed of rotation of the distributor switch. This switch is of the rotating, multiple-break type, by means of which it is possible to make and break a high-tension circuit without serious arcing.

THE INJECTION SYSTEM

The apparatus for the production and control of sprays is shown diagrammatically in the left-hand half of Figure 1. It consists of a high-pressure, hydraulic hand pump, a pressure tank, timing valve, cut-off valve, initial-pressure control valve, motor-driven cam shaft, and spray chamber.

The hydraulic hand pump used is of the ordinary plunger type and is capable of delivering oil at pressures up to 12,000 pounds per square inch. The pressure tank provides a sufficient volume of oil to insure a practically constant pressure on the oil during the whole injection period. The timing valve consists of a spring-loaded needle valve which is lifted from its seat by a cam-operated lever. The cut-off valve is a poppet valve actuated by another cam-operated lever. The duration of injection is controlled by adjusting the lever along the cam so as to obtain earlier or later operation of the cut-off valve with respect to the timing valve. The mechanism is so designed that the amount and rate of opening of the valve is practically constant for all cut-off positions of the lever. The initial-pressure control valve, when opened, allows oil to be pumped directly into the injection-valve tube, either for testing the opening pressure of the valve or to provide the correct initial pressure in the injection-valve tube before injection.

The shaft carrying one-half of the jaw clutch is driven at 900 revolutions per minute by a motor. The clutch is similar to the type used on punch presses, and is so arranged that when the trip lever is struck the two halves of the clutch engage and the hollow shaft carrying the cams is given one revolution. The timing switch is connected to the cam shaft by means of a serrated coupling and can be turned so that it will make contact at the proper time to synchronize the beginning of the sparks with the beginning of the spray.

The spray chamber is of cast iron, two sides of which are formed by frames holding optical-glass windows 1 inch thick supported on rubber. The window frames are bolted on and sealed with rubber gaskets. Gas pressures up to 600 pounds per square inch are used in the chamber.

THE RECORDING APPARATUS

The recording apparatus consists of a camera box containing a lens and a motor-driven film drum. To concentrate the light of the spark upon the spray a reflector is used. It will be noted from Figure 1 that it is offset from the line of the chamber and film drum. Only the light refracted and reflected by the spray itself passes in through the lens and records the series of pictures of the moving spray upon the film. The film is fastened around a drum 30 inches in circumference, which is mounted on the shaft of an electric motor. The speed of rotation of the film, together with the rate of discharge of the condensers, determine the spacing of pictures. An F:2 lens is used. All pictures of the sprays are taken half-size on commercial photographic roll film.

Apparatus, not shown in Figure 1, is used to determine the time lag between the opening of the timing valve and the opening of the injection valve, as shown by the appearance of the spray. It consists of a mirror which is rotated by the opening of the timing valve and deflects a light beam reflected by it onto a moving film. The time lag between the start of opening of the timing valve and the start of the spray is obtained by means of timing lines marked on the film by a one sixty-fourth-inch spark gap in series with the main spark gap.

OPERATION OF APPARATUS

The operation of the apparatus is as follows: The initial pressure in the injection valve tube is adjusted, after which the control valve is closed. Oil is pumped into the pressure tank to the test pressure, and the air pressure in the spray chamber is adjusted. All test conditions being obtained, the clutch trip lever is struck. The timing valve opens, allowing oil under high pressure to pass to the injection valve and open it, causing a spray to shoot across the chamber. The cut-off valve then opens after the required time interval, releases the pressure, and causes the injection valve to close and cut off the spray. The timing switch is closed when the timing valve is opened and the condensers are discharged across the gap, a series of 25 pictures being taken of the start, development, and cut-off of the spray.

TEST RESULTS FROM SEVERAL RESEARCHES WITH THE SPRAY PHOTOGRAPHY APPARATUS

RANGE OF INVESTIGATIONS

Various researches have been carried on with the present apparatus to determine the effects of injection pressure, chamber pressure, and gas density, fuel oil used, and injection-valve design, on oil sprays. Thus the development of single sprays with time, their velocities, penetrations, distribution, form, spray-cone angles, actual volumes, and relative atomization are determined for various types and designs of injection valves. Several phenomena connected with injection hydraulics also have been investigated.

The injection valves studied include mechanically operated valves, and automatic-injection valves especially developed for high-speed operation. The sprays are discharged from round orifices with or without directing impact surfaces and through annular orifices. Spiral grooves with helix angles of from 23° to 90° have been used to break up the spray by means of centrifugal force. The former groove angle gives a spray to which about the maximum amount of centrifugal force practicable has been applied, while the latter gives a noncentrifugal spray.

Descriptions of the injection valve and the valve assemblies used in obtaining Figures 3 to 7 are given in Reference 1.

SPRAY PHOTOGRAPHS

Figure 3 shows a complete spray from an injection valve employing medium centrifugal force. The injection pressure was 8,000 pounds per square inch, and the chamber-air pressure was 200 pounds per square inch. The actual penetration of the moving spray in inches and the time in thousandths of a second from the start of injection are given by the scales. The start of cut-off is marked.

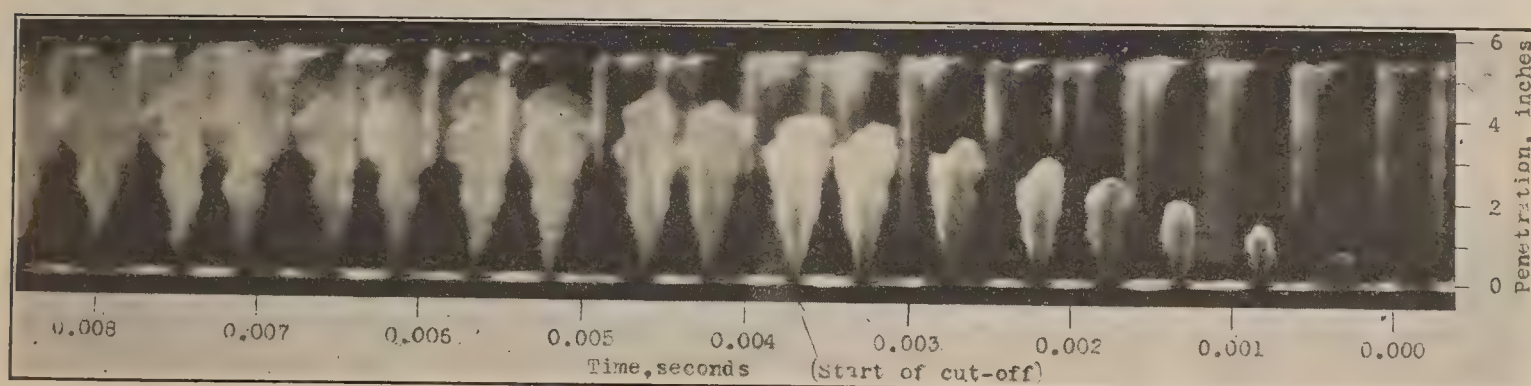


FIG. 3. MEDIUM CENTRIFUGAL SPRAY FROM INJECTION VALVE No. 7

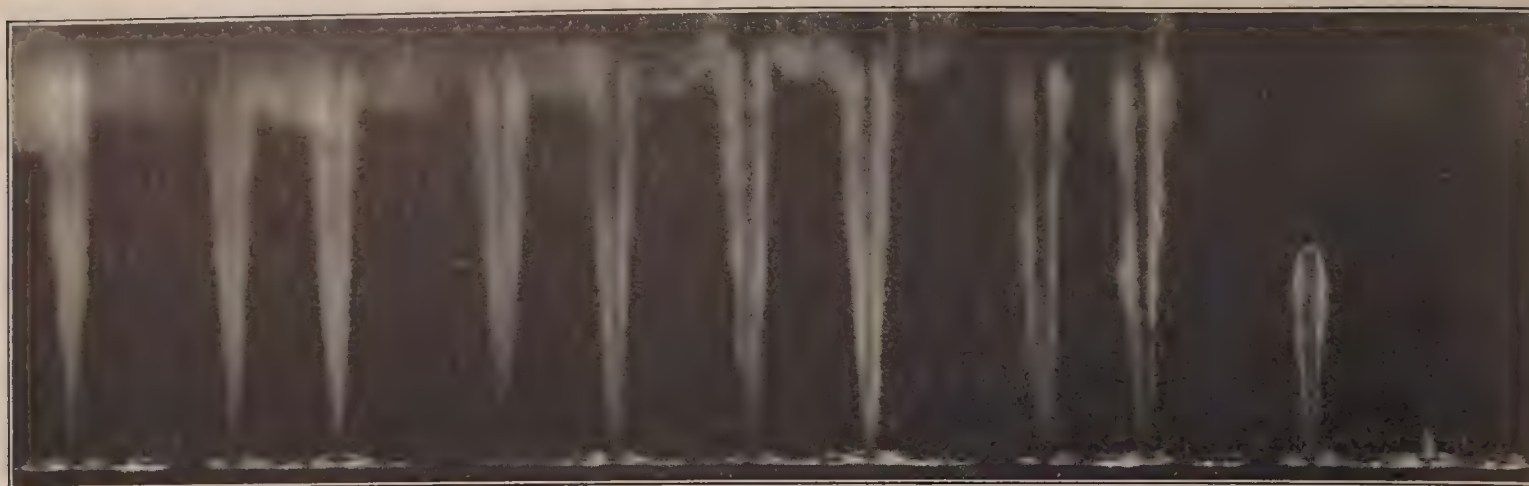
Diesel oil of 0.85 specific gravity injected at 8,000 pounds per square inch into compressed air at 200 pounds per square inch

The following information is obtained from series of pictures similar to the above:

Visual studies	Measurements and computations	Effects of variables
General spray form.....	Spray penetration with time.....	Effects of injection pressure.
Peculiarities in spray form.....	Time of cut-off after spray starts.....	Effect of chamber gas density.
Cut-off.....	Spray cone angle.....	Effects of specific gravity of fuel oil.
Phenomena occurring after cut-off.....	Volumetric growth of spray.....	Effect of injection valve design.
Atomization of spray.....	Spray distribution.....	Effect of injection system.

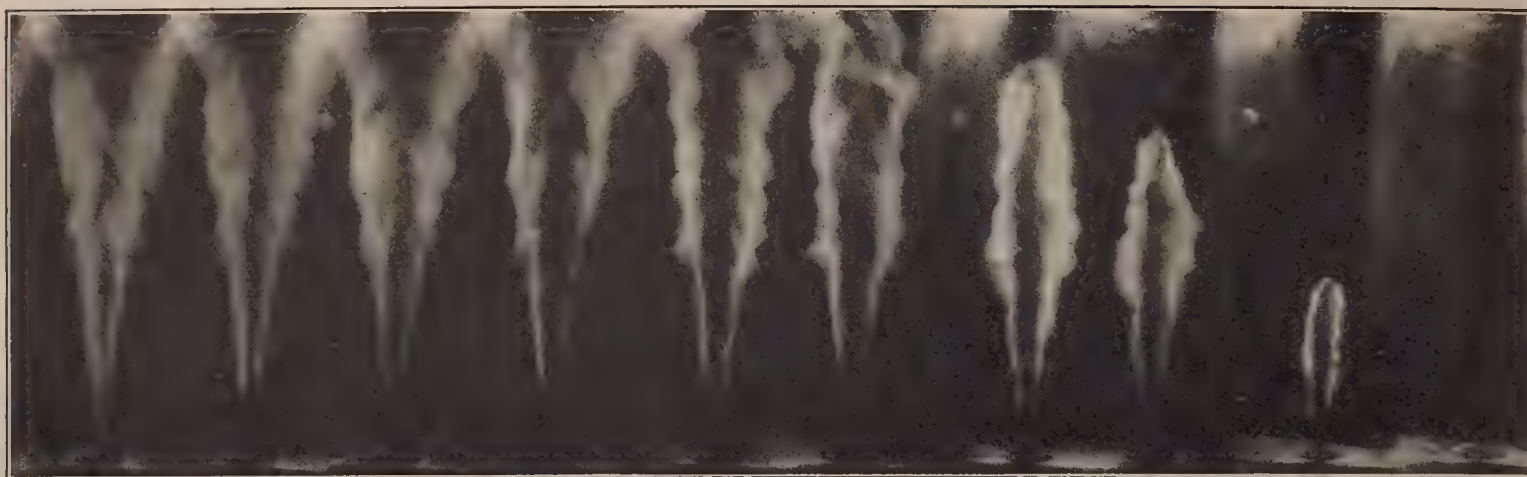
The end of the spray after cut-off appears somewhat like a corkscrew. This spiral appearance is probably caused by whirling of the oil drops which have passed around spiral grooves inside the valve, and continues after the oil has left the valve in spray form. It will be noted that the spray seems to have lost its motion in the last few pictures, especially at the nozzle where the spray is practically hanging motionless in mid-air.

In Figure 4 are shown noncentrifugal sprays from a cylindrical orifice injected at 8,000 pounds per square inch pressure into the atmosphere and into 200 pounds per square inch air pressure. The sprays appear somewhat like fir trees with drooping branches. This is because the velocity of the drops of oil is practically zero at the outside of the spray and increases toward the center. The oil seems to shoot out through the center and spill over on the sides, much like a fountain of water. On the sides of the sprays clouds of oil particles appear as bumps,



Injection pressure, 8,000 pounds per square inch

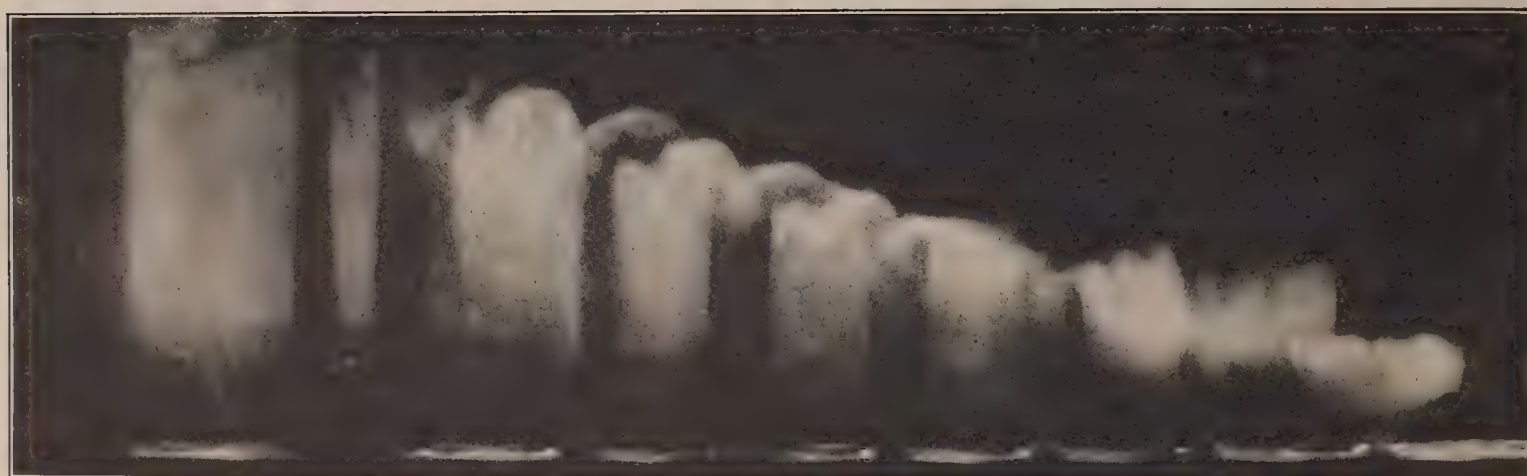
Chamber pressure, atmospheric



Injection pressure, 8,000 pounds per square inch

Chamber pressure, 200 pounds per square inch

FIG. 4.—EFFECT OF CHAMBER PRESSURE ON NONCENTRIFUGAL SPRAY



Injection pressure, 8,000 pounds per square inch

Chamber pressure, atmospheric



Injection pressure, 8,000 pounds per square inch

Chamber pressure, 200 pounds per square inch

FIG. 5.—EFFECT OF CHAMBER PRESSURE ON HIGH CENTRIFUGAL SPRAY

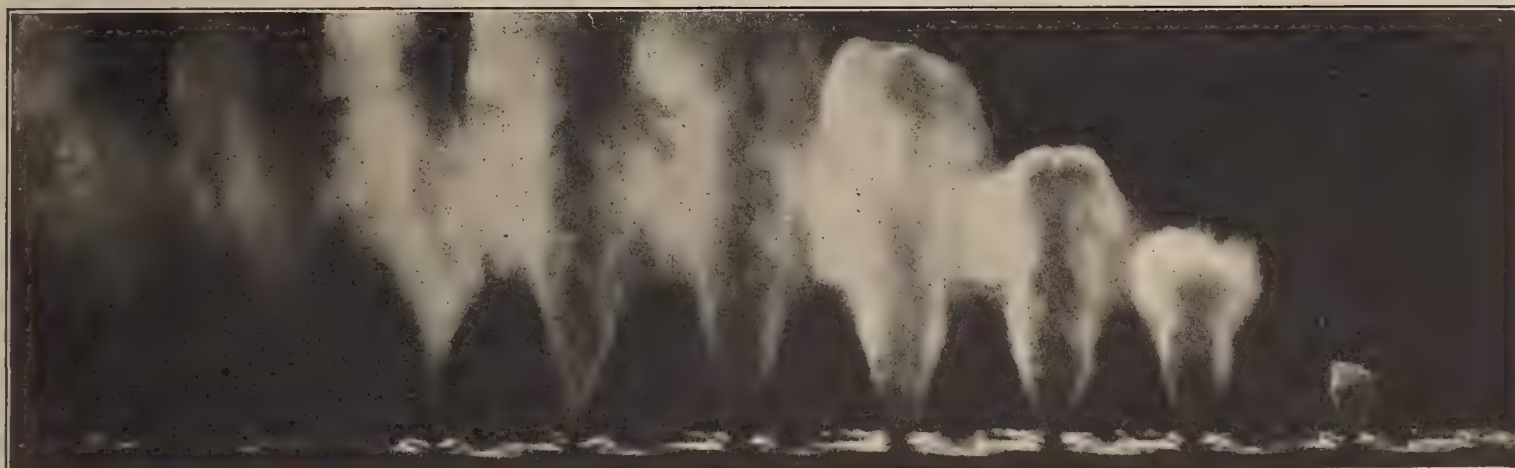


Injection pressure, 8,000 pounds per square inch
 Chamber pressure, 200 pounds per square inch
 Ratio of orifice area to groove area, 0.19
 Orifice area, 0.000113 square inch



Injection pressure, 8,000 pounds per square inch
 Chamber pressure, 200 pounds per square inch
 Ratio of orifice area to groove area, 0.19
 Orifice area, 0.00038 square inch

FIG. 6.—EFFECT OF VALVE SIZE UPON CENTRIFUGAL SPRAY



Injection pressure, 8,000 pounds per square inch
 Chamber pressure, atmospheric
 Centrifugal spray with secondary discharge after cut-off



Injection pressure, 8,000 pounds per square inch
 Chamber pressure, atmospheric
 Centrifugal spray with no secondary discharge after cut-off

FIG. 7.—CENTRIFUGAL SPRAYS WITH AND WITHOUT DISCHARGE AFTER CUT-OFF

which do not change their position from one picture to another. They show that the oil particles at the outside of the sprays are motionless. The spray-cone angle was increased 50 per cent by injection into dense air. The atomization also appears to be increased, as shown by the pictures.

High-centrifugal sprays injected into the atmosphere and into 200 pounds per square inch air pressure are shown in Figure 5. The reduction in the spray angle with the spray injected into dense air is about 40 per cent. This may well explain the failure of some centrifugal valves to operate successfully in an engine when the spray appeared well suited for the engine combustion chamber from observations made in the atmosphere. This decrease of spray-cone angle is characteristic of all centrifugal sprays.

In Figure 6 are two sprays injected into 200 pounds per square inch air pressure, which show what might be called scale effect; that is to say, the ratio of orifice area to groove area is the same for both, but a larger orifice and corresponding grooves were used for the second spray, and as a result the quantity of oil injected was over three times as great.

Figure 7 shows a spray which has a small secondary spray discharge taking place after cut-off. This phenomenon is thought to be caused by a pressure wave in the oil line, and was eliminated in the second series of pictures by increasing the length of the injection-valve tube, thus damping out the pressure wave.

The penetration-time curves are plotted from data computed from measurements of the spray images on each film, taking into account the film speed and photographic reduction as has been done in computing the scales on the pictures in Figure 3. The spray volumes are computed by summation of the differential cylinders making up each spray.

EFFECT OF INJECTION PRESSURE

Figure 8 shows the effect of injection pressures of from 2,000 to 8,000 pounds per square inch on the penetration of sprays, from a 0.0155 inch diameter round orifice, injected into 200 pounds per square inch air pressure. The curves are almost straight and parallel, which shows that the penetration increased nearly in proportion to the injection pressure. This is a charac-

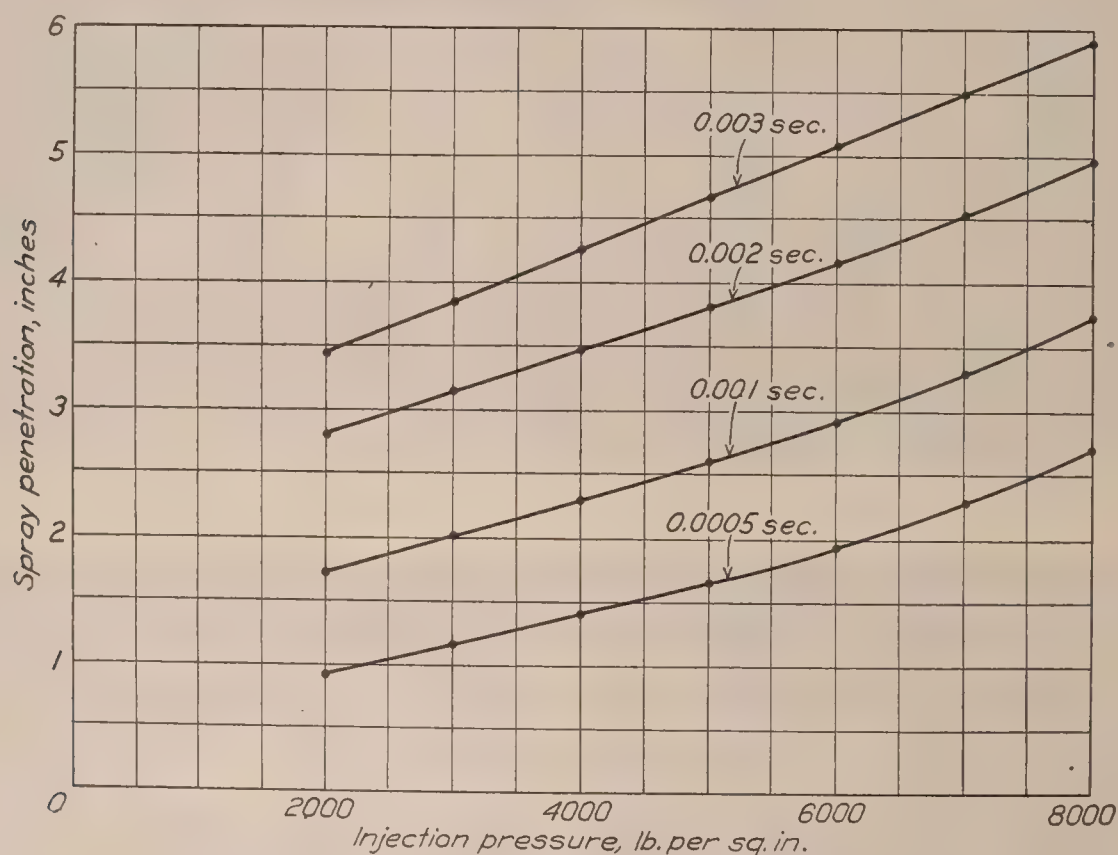


FIG. 8.—Effect of injection pressure on spray penetration

Cylinder orifice, 0.0155 inch diameter.
 Fuel oil used, Diesel oil of 0.85 specific gravity.
 Nitrogen in spray chamber at 200 pounds per square inch.

teristic result. There is a limit beyond which increase in the injection pressure would not increase the penetration and might even decrease it. This limit is reached when the drops are atomized so finely as to be too light to penetrate the dense air. The injection pressure affects the spray-cone angle as well as the penetration. Increase in the injection pressure causes a narrower spray-cone angle with a noncentrifugal valve, and a wider spray-cone with a high-centrifugal valve.

EFFECT OF GAS DENSITY

Figure 9 shows the effect of chamber-gas pressure and density upon the spray penetration after 0.001, 0.002, and 0.003 seconds. The main curves were cross-plotted from the curves shown in the insert, which are for nitrogen gas, and from similar curves obtained with helium and carbon dioxide gas in the chamber. Each point is labeled as to the gas which was used in obtaining it. The points obtained by injection into the various gases were all plotted on a basis

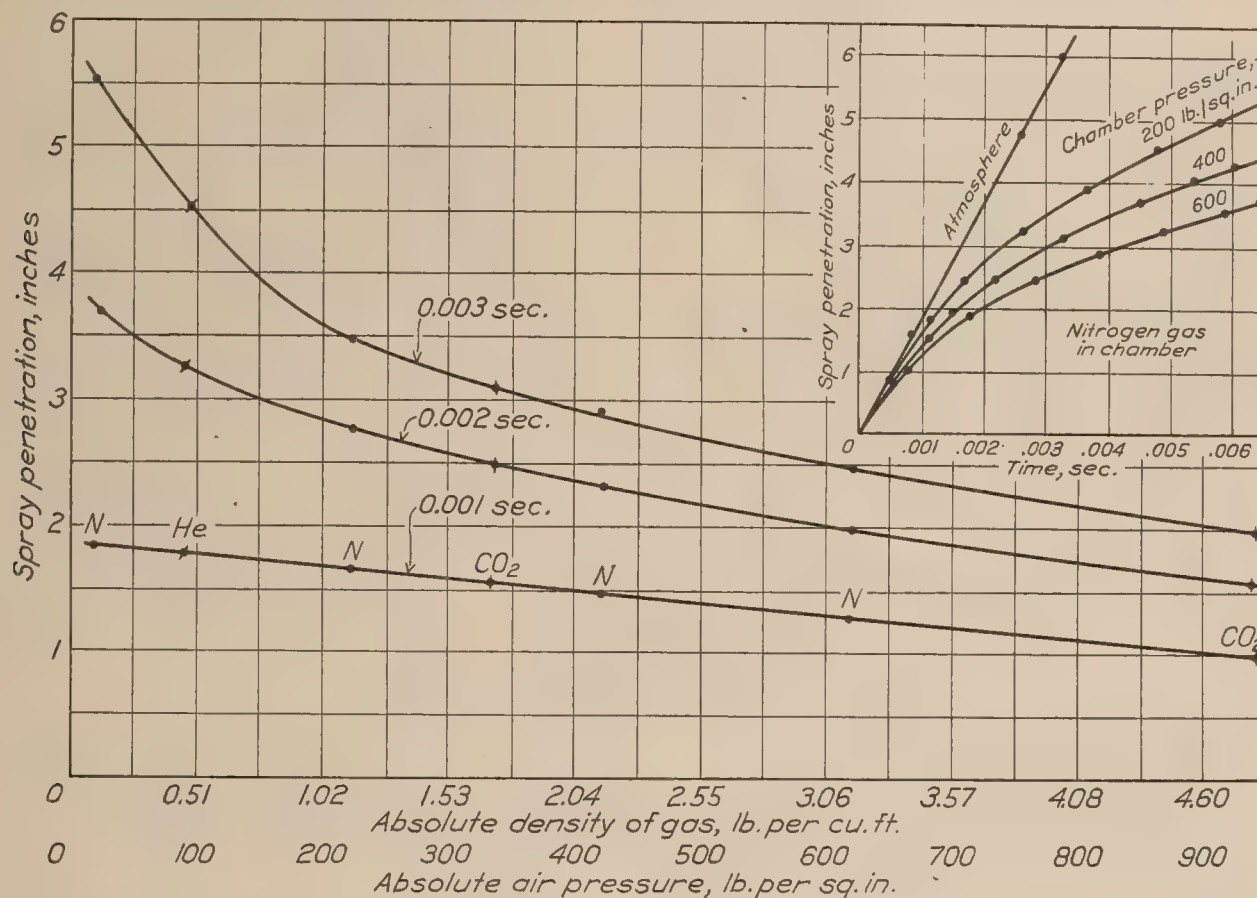


FIG. 9.—Effect of gas density on spray penetration

Injection valve No. 7; 23° spiral grooves.
Cylinder orifice, 0.022 inch diameter.
Injection pressure, 8,000 pounds per square inch.
Fuel used, Diesel oil of 0.85 specific gravity.
Gas in spray chamber, nitrogen, carbon dioxide, or helium.

of absolute gas density. As all of the points lie on the curves, this shows that it is the absolute density of the gas which controls spray penetration, that the viscosity of the gases has no appreciable effect, and pressure affects the penetration only in so far as it controls the density. This indicates that it is the density of the gas which controls spray penetration in an engine cylinder and not the compression pressure.

EFFECT OF SPECIFIC GRAVITY OF FUEL OIL

Figure 10 shows the effect of the specific gravity of the fuel used upon the spray penetration after 0.001, 0.002, 0.003, and 0.004 seconds, with a high-centrifugal valve spraying into 200 pounds per square inch chamber pressure. The points for the curves were cross-plotted from the curves for heavy fuel oil shown in the insert, and from similar curves for the other fuel oils.

The penetration is seen to increase with the specific gravity and the upward trend of the curves indicates that oils of greater specific gravity than those tested would have still greater effects. From the curves, a heavy oil of 0.90 specific gravity would have 10 per cent greater penetration after 0.003 second than an ordinary Diesel oil of a specific gravity of 0.85. The heavy oil is more viscous than the others, and is not as readily atomized. This makes the spray angle narrower and helps to produce greater penetration.

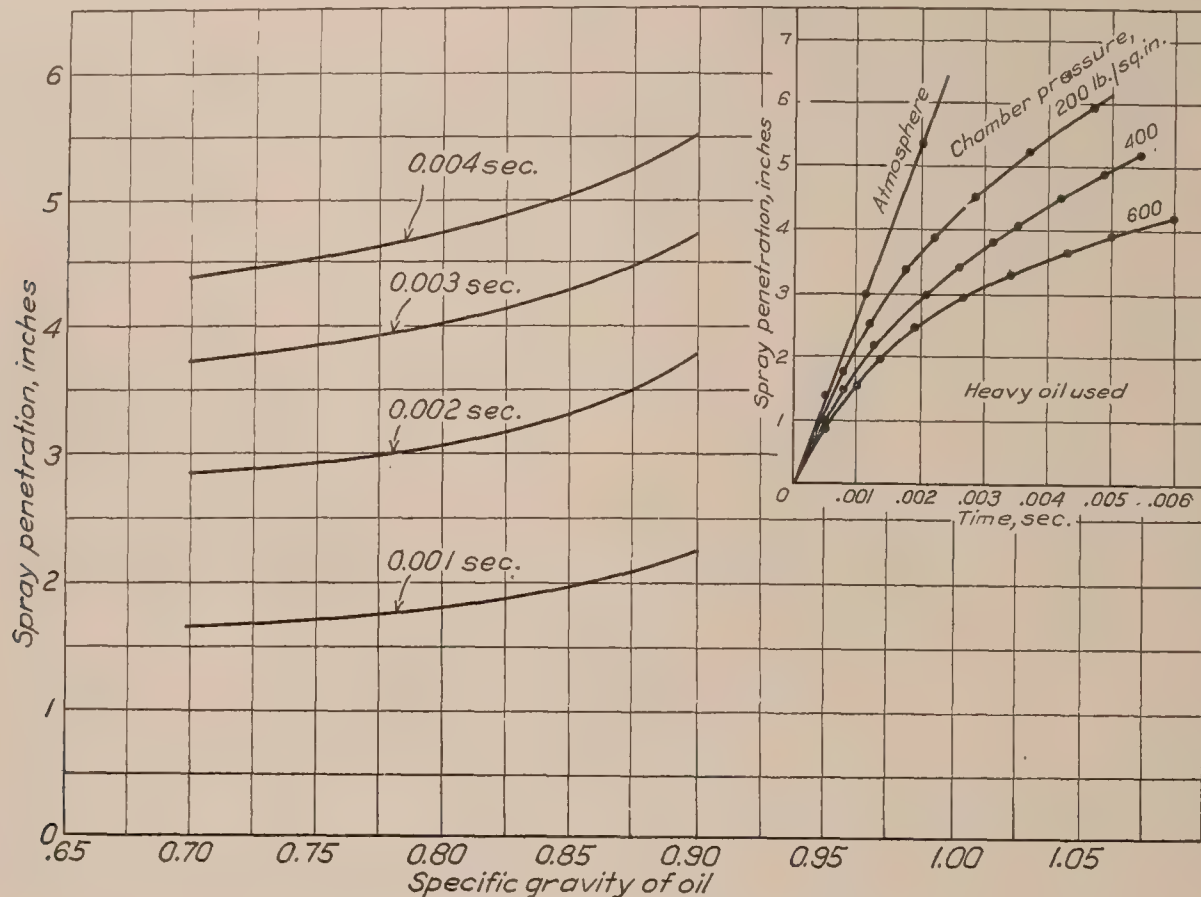


FIG. 10.—Effect of specific gravity of oil on spray penetration

Injection valve No. 7; 23° spiral.

Cylinder orifice, 0.022 inch diameter.

Injection pressure, 8,000 pounds per square inch.

Fuel oil used, gasoline, kerosene, Diesel, and heavy fuel oil of specific gravity 0.705, 0.799, 0.85, and 0.90, respectively.

Air in spray chamber at 200 pounds per square inch

EFFECT OF VALVE DESIGN

The effect of the groove-helix angle on the penetration, cone angle, and ratio of spray volume to oil volume with a valve injecting into 200 pounds per square inch air pressure is shown in Figure 11. The penetration increases considerably with increase in the angle of the spiral grooves, the 90° or noncentrifugal spray having 60 per cent greater penetration after 0.003 second than does the 23° high-centrifugal spray. The spray angle was decreased from 53° to 23° by this same increase in the groove-helix angle.

To find the relative distribution, and to obtain an indication of the atomization of the spray, the actual spray volumes were computed. The quantities of oil injected with each valve assembly were different; therefore, to put them all on the same basis, the ratios of spray volume to oil volume were computed. These are plotted in Figure 11, and indicate the spray distribution. The distribution was 100 per cent greater for the high-centrifugal than for the noncentrifugal spray.

The effects of varying the ratio of orifice area to groove area from 0.19 to 2.05 upon the spray penetration, cone angle, and the ratio of spray volume to oil volume, with 200 pounds per square inch air pressure, are shown in Figure 12. The penetration increases rapidly as the ratio becomes very small. The ratio was decreased by decreasing the size of the orifice, the groove area being kept constant. Thus the orifice became very small with a small ratio and the rotation

of the jet initiated by the spiral grooves could not continue effectively through this small orifice. The energy which, with a larger orifice, was consumed in rotating the oil went into giving the spray axial penetration in the case of the very small orifice. The spray angle was therefore reduced, as shown by the spray-angle curve. The shape of this curve indicates that the spray angle would not be greatly increased by increase in the ratio beyond 2.0.

The curve at the top of Figure 12 shows the effect of the ratio of orifice area to groove area upon the spray distribution. This curve would indicate that the orifice size has considerable effect upon the spray distribution and possibly atomization.

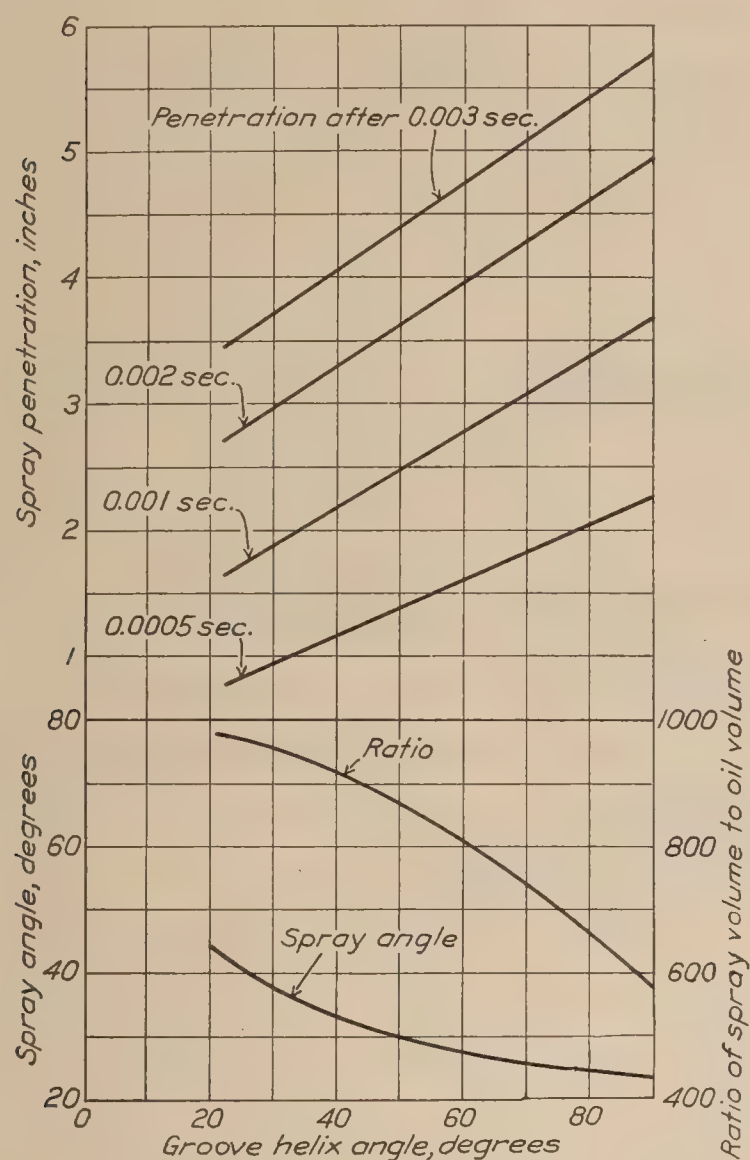


FIG. 11.—Effect of groove helix angle on spray characteristics.

Injection valve No. 7.
Cylinder orifice, 0.022 inch diameter.
Injection pressure, 8,000 pounds per square inch.
Fuel oil used, Diesel oil of 0.85 specific gravity.
Gas in spray chamber, nitrogen at 200 pounds per square inch.

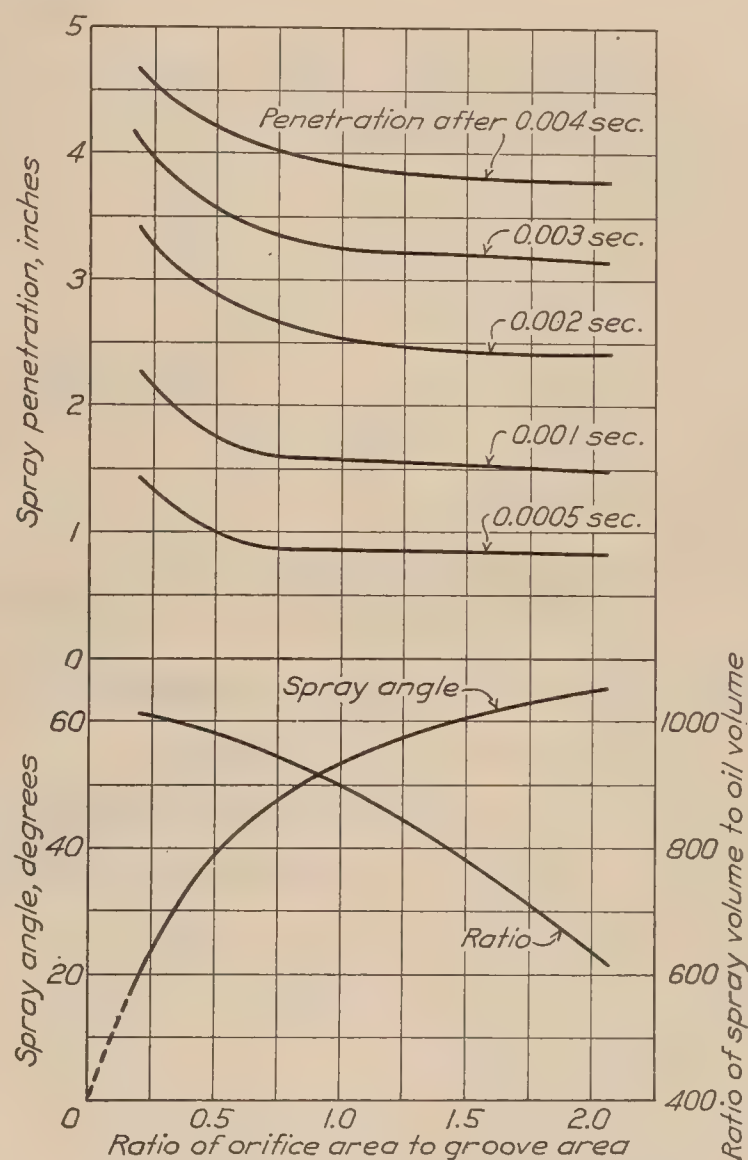


FIG. 12.—Effect of ratio of orifice area to groove area on spray characteristics

Injection valve No. 7; 23° spiral grooves.
Cylinder orifices, 0.012, 0.022, and 0.040 inch diameter.
Injection pressure, 8,000 pounds per square inch.
Fuel oil used, Diesel oil of 0.85 specific gravity.
Nitrogen in spray chamber at 200 pounds per square inch.

CONCLUSIONS

The test results presented in this report are examples of the information which it is possible to obtain by means of the apparatus described. The results show some fundamental effects of the variables investigated. The spray penetration increased directly with the injection pressures. The absolute gas density in the chamber was found to control spray penetration. The spray penetration increased with increase in the specific gravity of the fuel oil used. The spray penetration increased with increase in the groove-helix angle, while the spray angle and ratio of spray to oil volume decreased. On the other hand, the spray penetration and ratio of spray to oil volume decreased with increase in the ratio of orifice area to groove area, but the spray angle increased. By means of these and other investigations, data are obtained which

make possible the design of injection valves to produce sprays for various sizes and shapes of engine combustion chambers.

LANGLEY MEMORIAL AERONAUTICAL LABORATORY,
NATIONAL ADVISORY COMMITTEE FOR AERONAUTICS,
LANGLEY FIELD, VA., *May 25, 1927.*

REFERENCE

1. JOACHIM, W. F., and BEARDSLEY, E. G. Factors in the Design of Centrifugal Type Injection Valves for Oil Engines. N. A. C. A. Technical Report No. 268, 1927.

REPORT No. 275

**THE EFFECT OF THE WALLS IN CLOSED TYPE
WIND TUNNELS**

By GEORGE J. HIGGINS

Langley Memorial Aeronautical Laboratory

REPORT No. 275

THE EFFECT OF THE WALLS IN CLOSED TYPE WIND TUNNELS

By GEORGE J. HIGGINS

SUMMARY

A series of tests has been conducted during the period 1925-1927 by the National Advisory Committee for Aeronautics in the variable-density wind tunnel on several airfoil models of different sizes and sections to determine the effect of tunnel-wall interference and to determine a correction which can be applied to reduce the error caused thereby. The use of several empirical corrections was attempted with little success. The Prandtl theoretical corrections give the best results, and their use is recommended for correcting closed wind tunnel results to the conditions of free air.

An appendix is attached wherein the experimentally determined effect of the walls on the tunnel velocity very close to their surface is given. This is of special interest because a "scale effect" was found in the boundary layer with a change in the density of the tunnel air.

INTRODUCTION

When tests are made on models in wind tunnels to determine their aerodynamic characteristics, the results obtained are not truly representative because of the limited air jet of the tunnel. The boundary of the jet, whether free or inclosed by walls, affects the flow to a considerable extent. This effect has been considered theoretically and a method devised for correcting the results from wind-tunnel tests.

Experimental confirmation of this correction is extremely desirable, and though such confirmation has been obtained in wind tunnels in Europe, tests for that purpose had not been made in wind tunnels of the National Advisory Committee for Aeronautics. A series of tests was therefore authorized for the variable-density wind tunnel.

This investigation consisted of force tests on several airfoil models of the N. A. C. A.-M6 section having a constant chord and a varying span. From these tests some idea of the effect of the tunnel walls can be ascertained.

Data from previous tests on models of the M6 airfoil section of different sizes, aspect ratio 6, were available and were used in the analysis. For further confirmation, and in conjunction with another investigation, tests were made on three airfoil models of the R. A. F. 19 section, each having the same aspect ratio but different areas.

TESTS

The tests on the N. A. C. A.-M6 airfoils in this investigation were conducted after the usual method employed for force tests in the variable-density wind tunnel, as described in reference 1. The angle of attack was varied from -3° to $+21^\circ$; runs were made at three densities or Reynolds Numbers, corresponding to tank pressures of about 1, 15, and 20 atmospheres. The R. A. F. 19 series was similarly tested, but at different values of the Reynolds Number.

The N. A. C. A.-M6 section model was $4\frac{1}{2}$ inches by 36 inches in plan. It was tested in this form, of aspect ratio 8, and then cut off on the ends so that the span became 32 inches, giving the model an aspect ratio of 7.12. This procedure was repeated, making tests on the model with aspect ratios of 6, 5.33, and 4.44. The R. A. F. 19 models were all of aspect ratio 6 with plan form dimensions of 4 inches by 24 inches, 5 inches by 30 inches, and 6 inches by 36 inches. All models were made of duralumin and machined to within ± 0.002 inch of the specified ordinates.

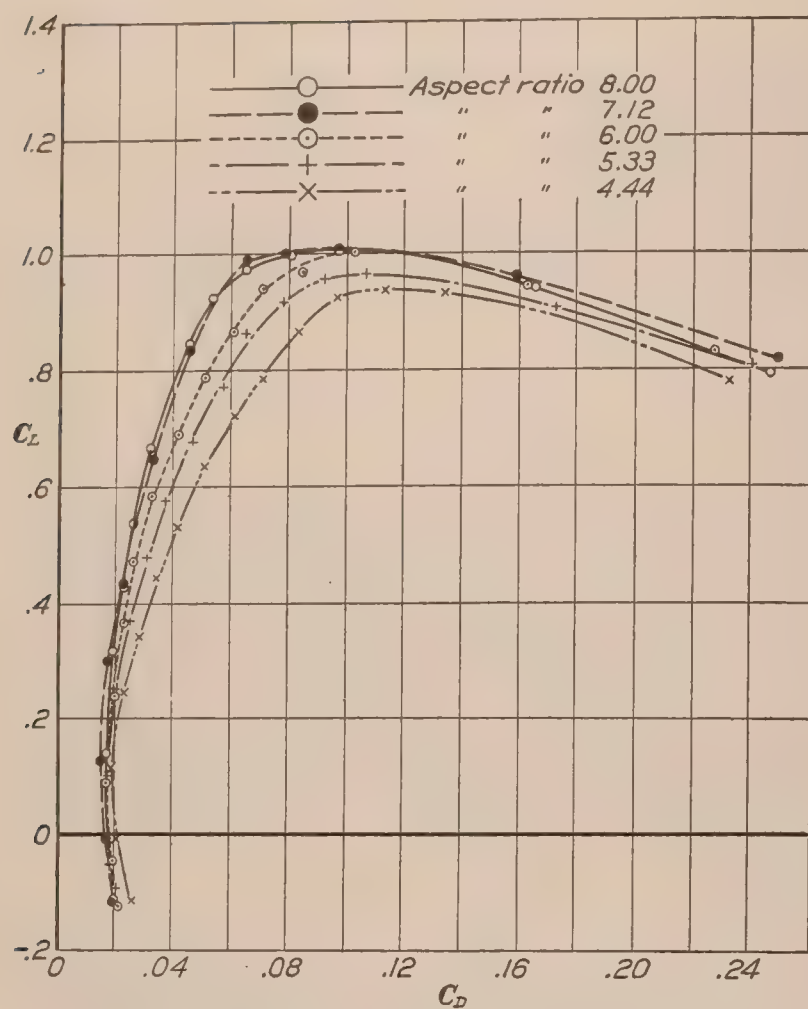


FIG. 1.—N. A. C. A.-M6 airfoil of various aspect ratios, as observed in tunnel, 1 atmosphere

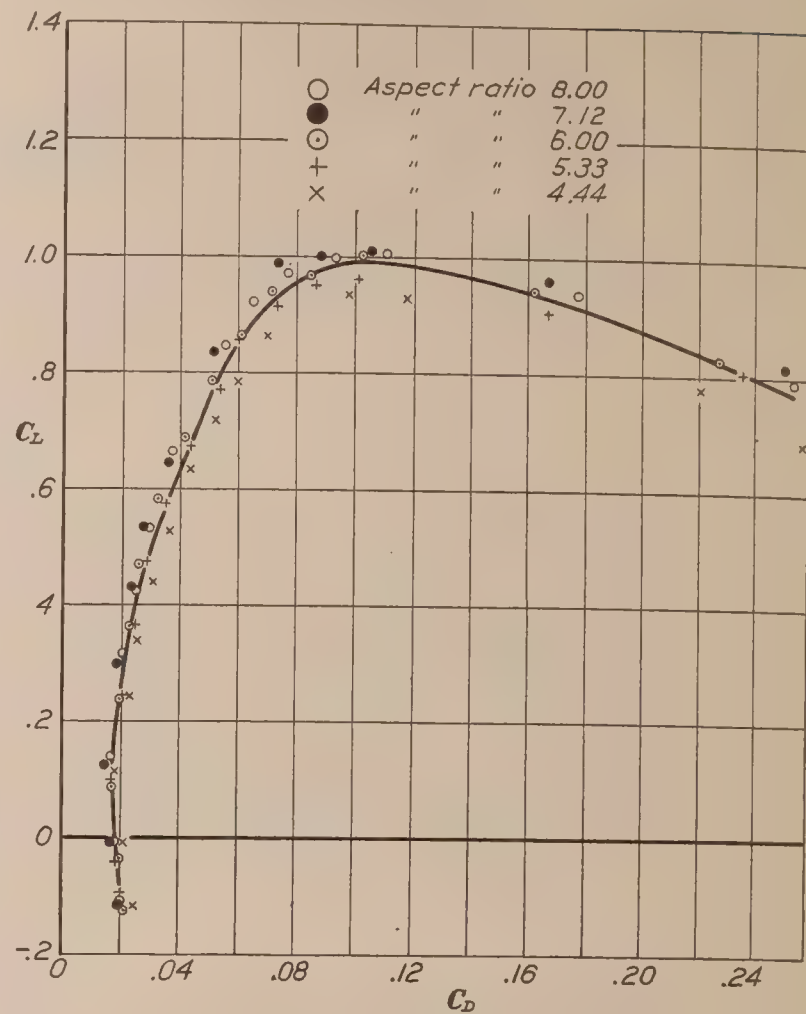


FIG. 2.—N. A. C. A.-M6 airfoil of various aspect ratios, corrected to aspect ratio 6.00; no correction for tunnel wall; 1 atmosphere

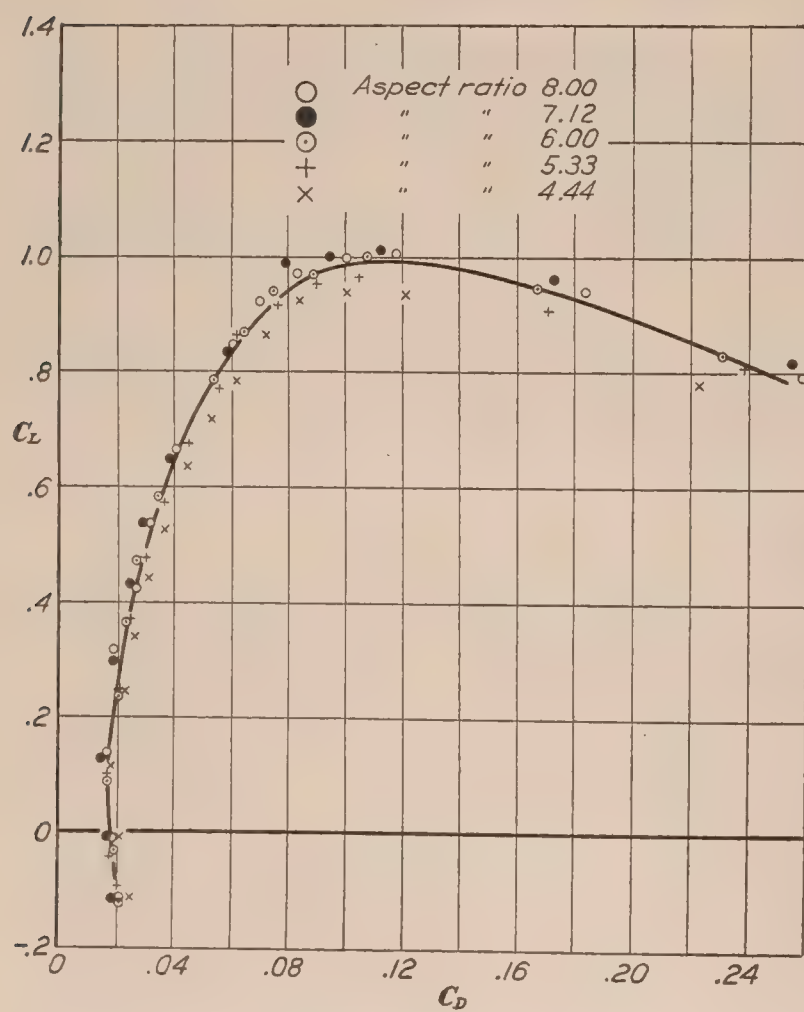


FIG. 3.—N. A. C. A. M-6 airfoil of various aspect ratios, corrected to aspect ratio 6.00 in free air, 1 atmosphere

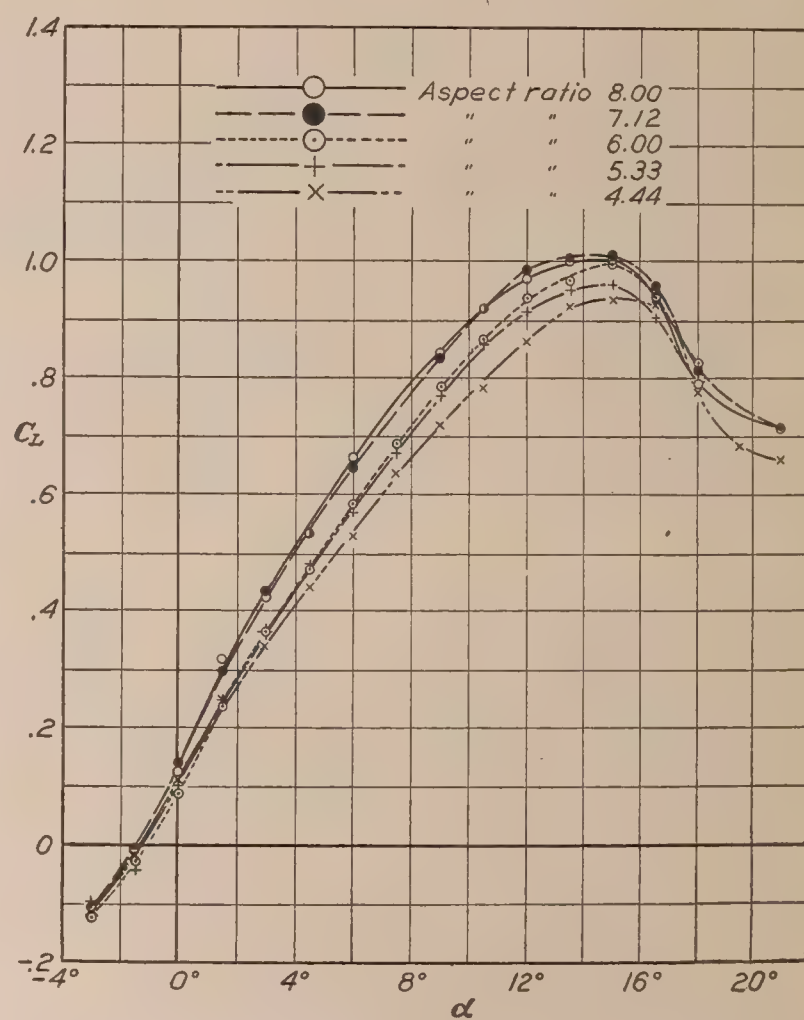


FIG. 4.—N. A. C. A.-M6 airfoil of various aspect ratios, as observed in tunnel, 1 atmosphere

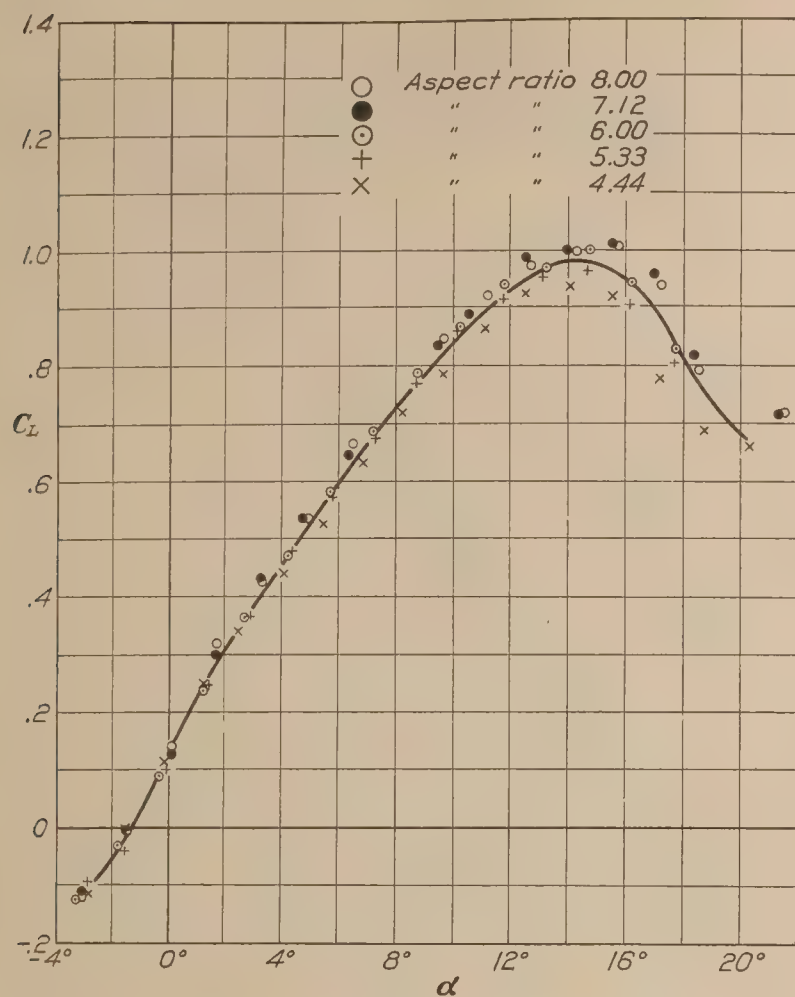


FIG. 5.—N. A. C. A.-M6 airfoil of various aspect ratios, corrected to aspect ratio 6.00; no correction for tunnel wall; 1 atmosphere

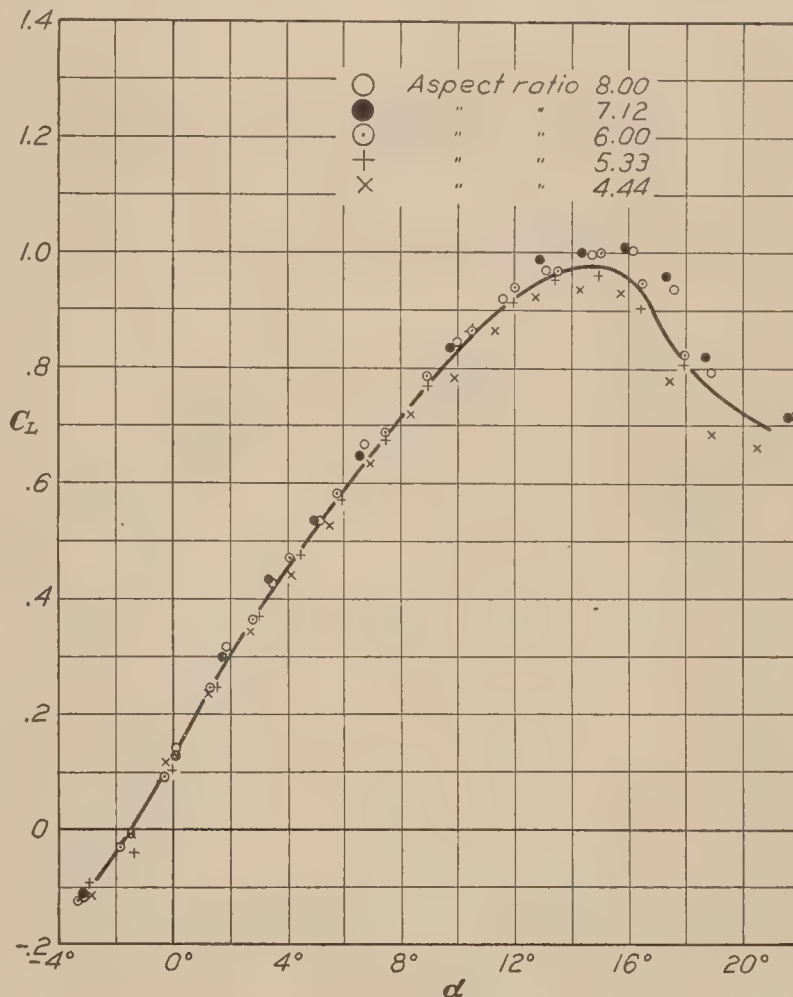


FIG. 6.—N. A. C. A.-M6 airfoil of various aspect ratios, corrected to aspect ratio 6.00 in free air, 1 atmosphere

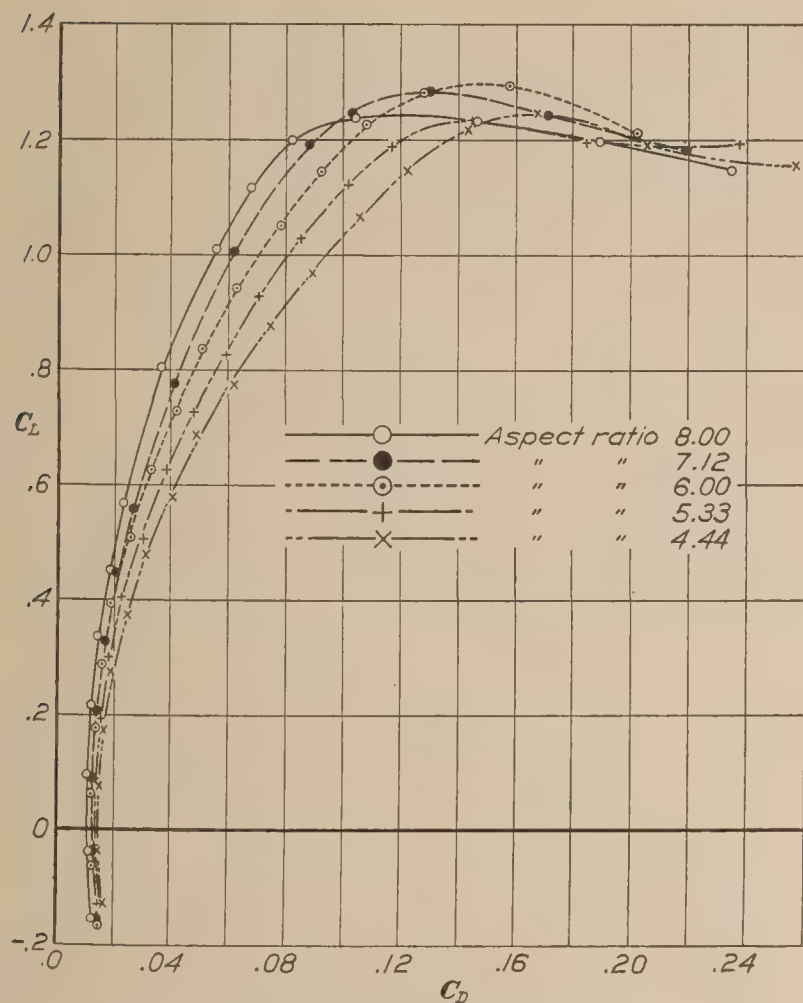


FIG. 7.—N. A. C. A.-M6 airfoil of various aspect ratios, as observed in tunnel, 15 atmospheres

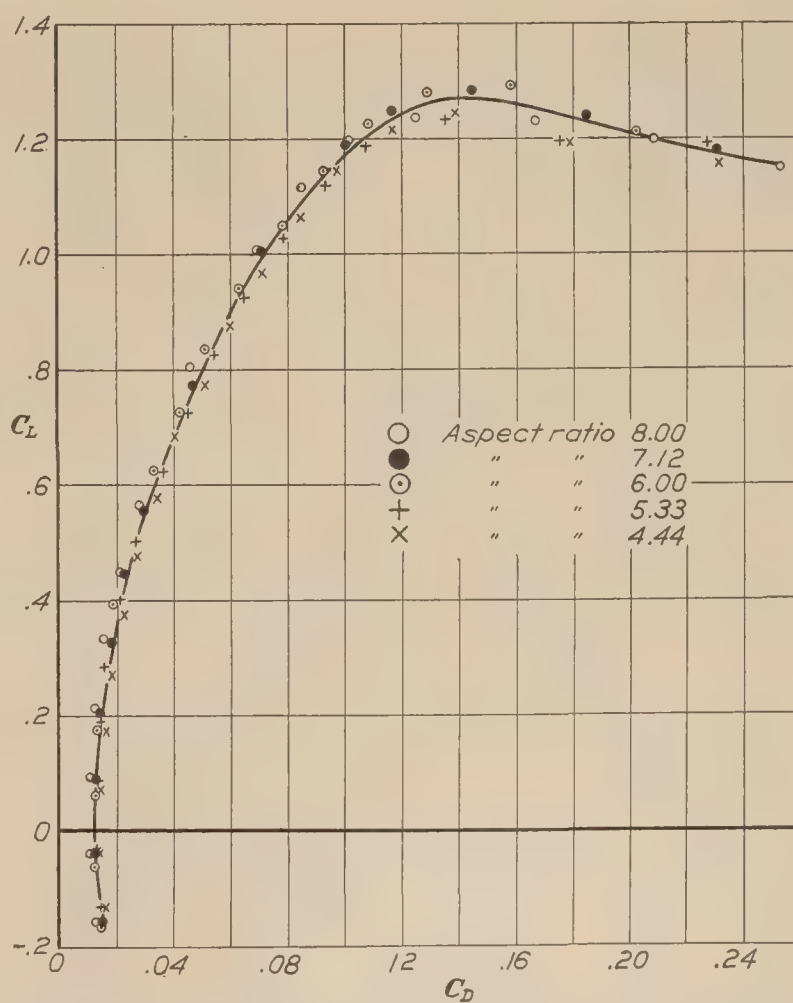


FIG. 8.—N. A. C. A.-M6 airfoil of various aspect ratios, corrected to aspect ratio 6.00; no correction for tunnel wall; 15 atmospheres

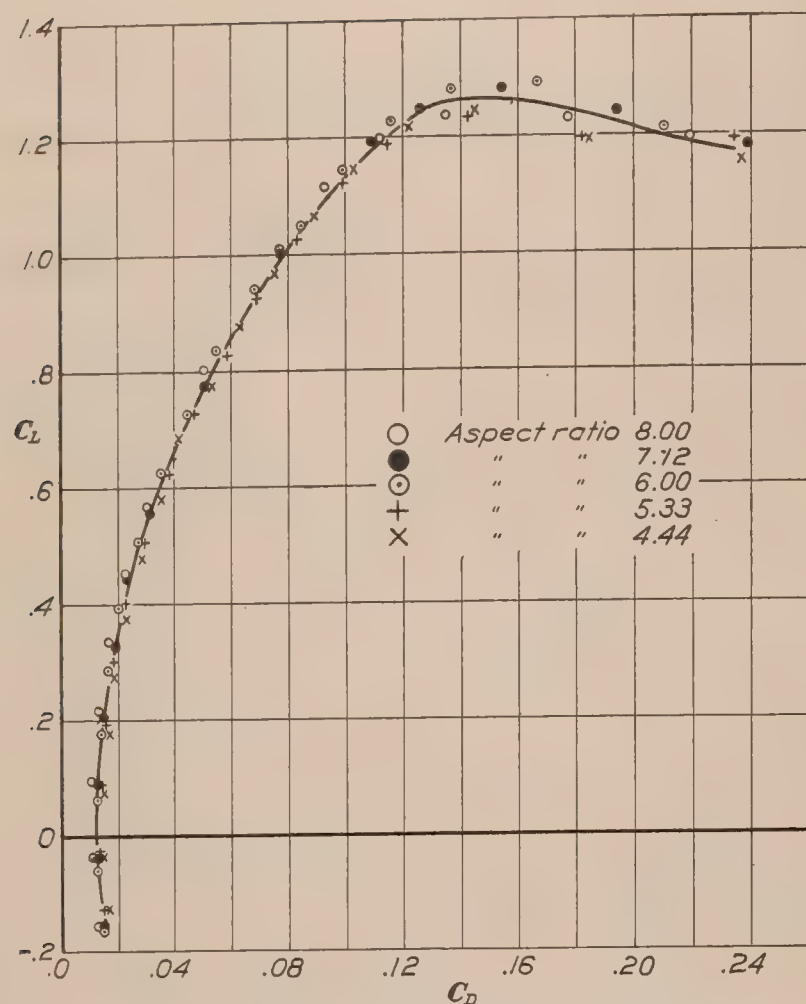


FIG. 9.—N. A. C. A.-M6 airfoil of various aspect ratios, corrected to aspect ratio 6.00 in free air, 15 atmospheres

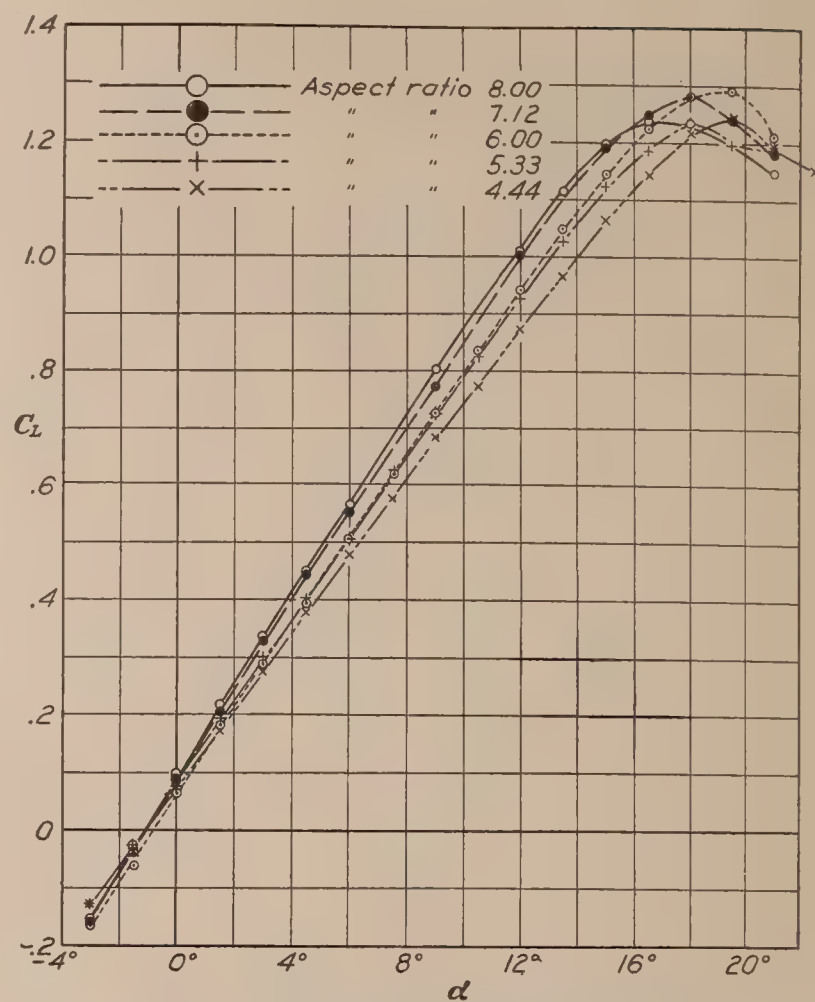


FIG. 10.—N. A. C. A.-M6 airfoil of various aspect ratios, as observed in tunnel, 15 atmospheres

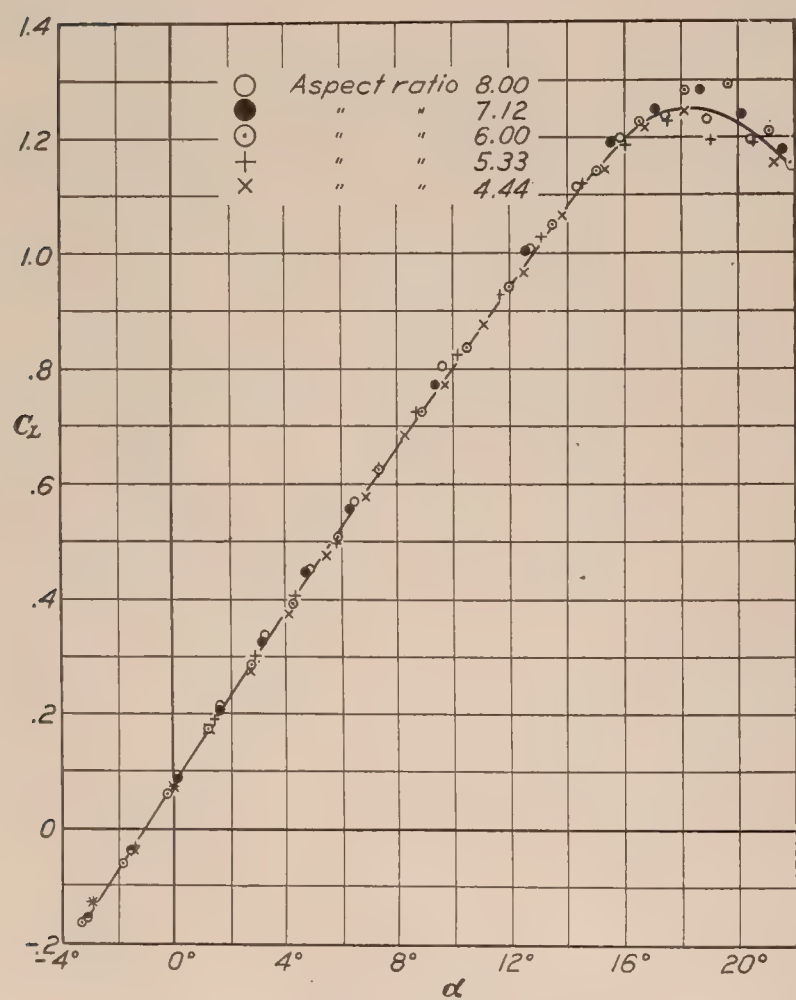


FIG. 11.—N. A. C. A.-M6 airfoil of various aspect ratios, corrected to aspect ratio 6.00; no correction for tunnel wall; 15 atmospheres

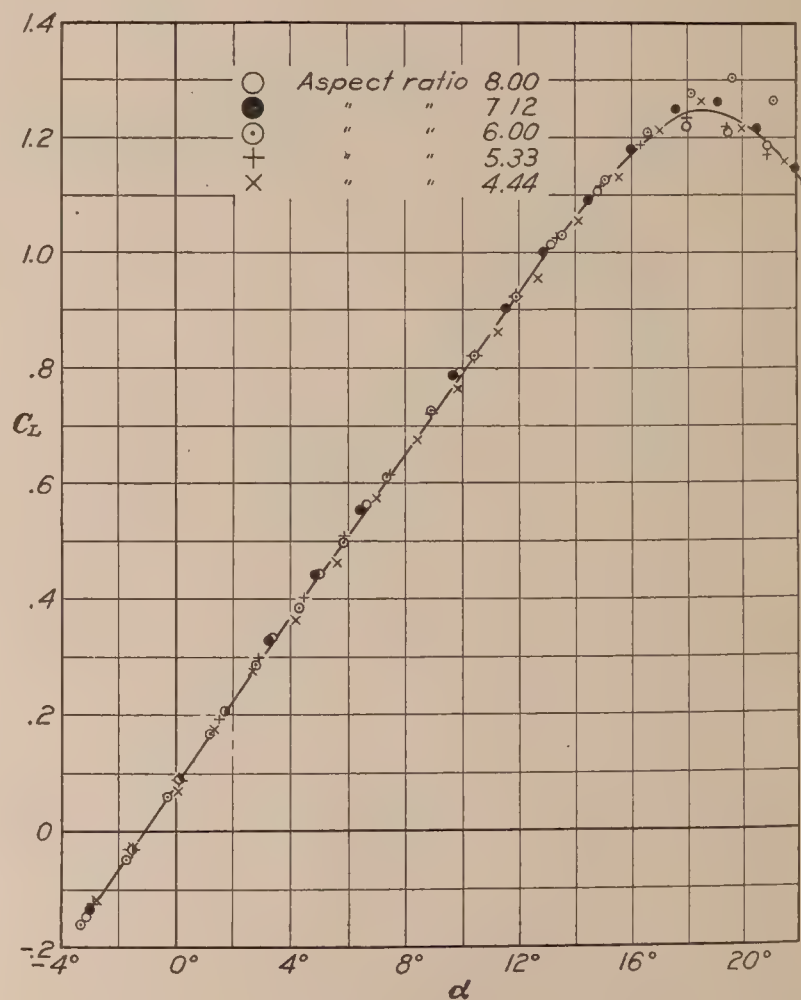


FIG. 12.—N. A. C. A.-M6 airfoil of various aspect ratios, corrected to aspect ratio 6.00 in free air, 15 atmospheres

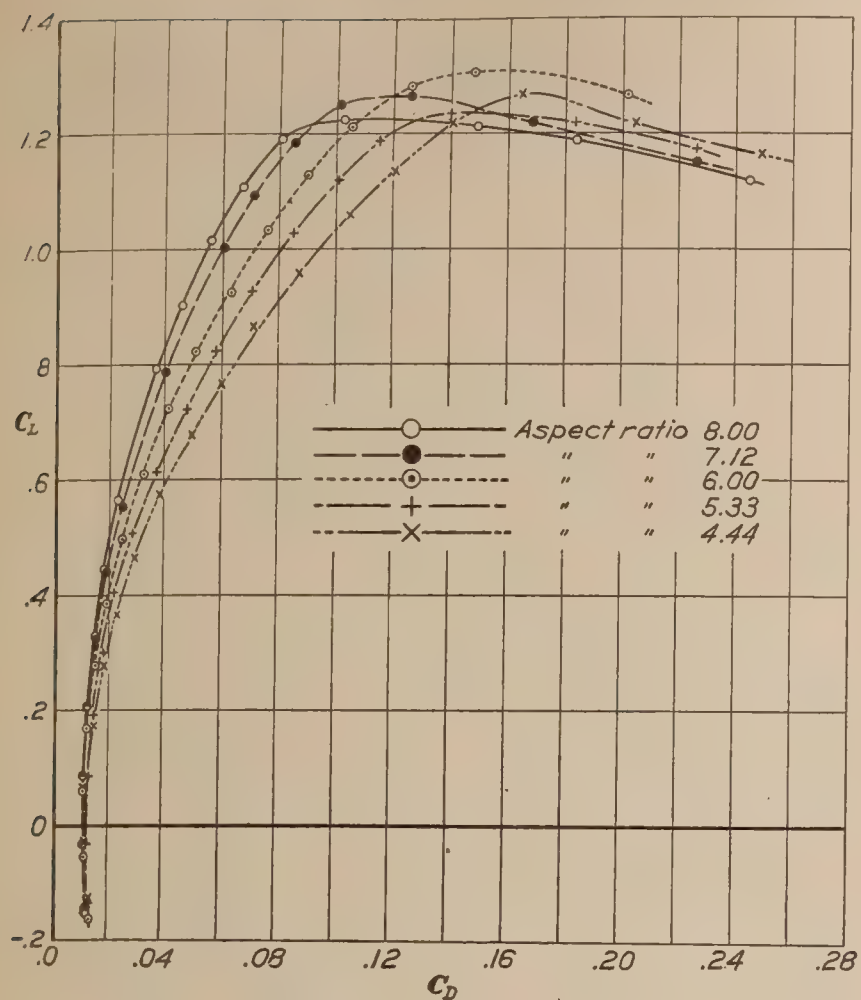


FIG. 13.—N. A. C. A.-M6 airfoil of various aspect ratios, as observed in tunnel, 20 atmospheres

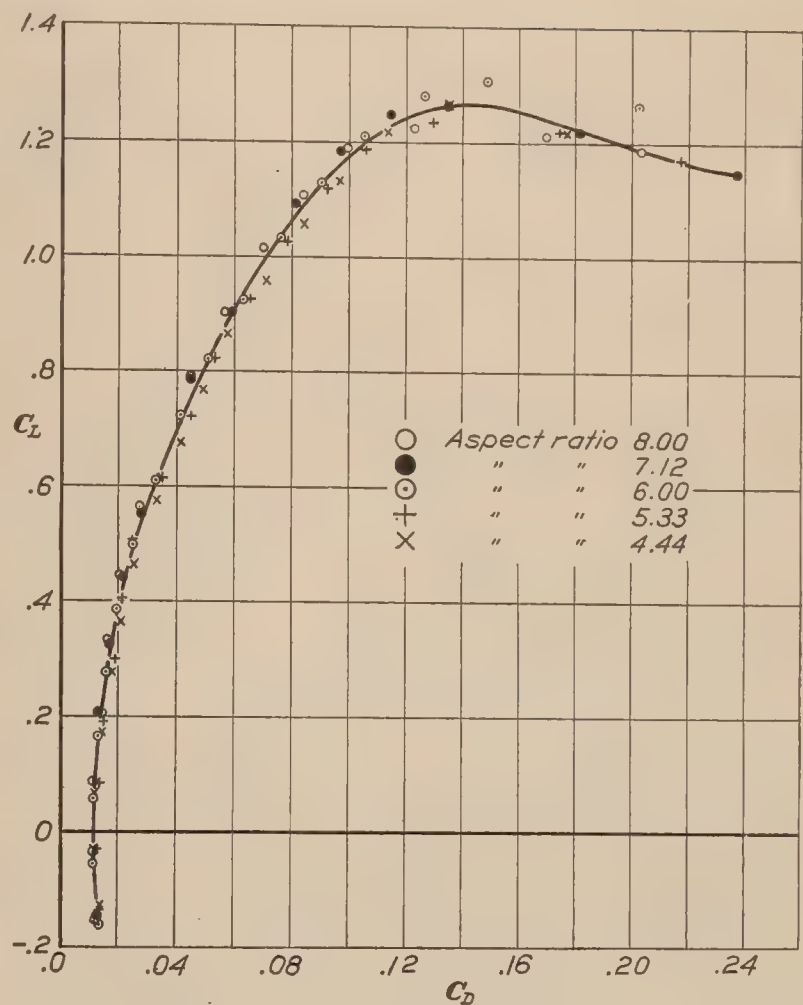


FIG. 14.—N. A. C. A.-M6 airfoil of various aspect ratios, corrected to aspect ratio 6.00; no correction for tunnel walls; 20 atmospheres

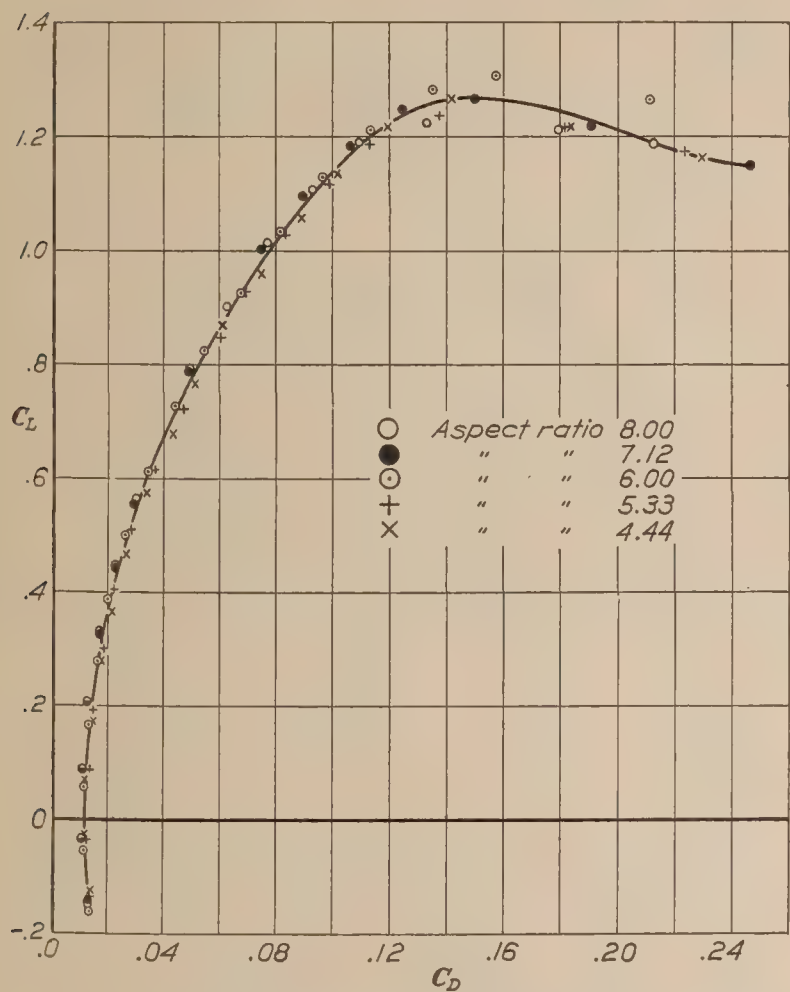


FIG. 15.—N. A. C. A.-M6 airfoil of various aspect ratios, corrected to aspect ratio 6.00 in free air, 20 atmospheres

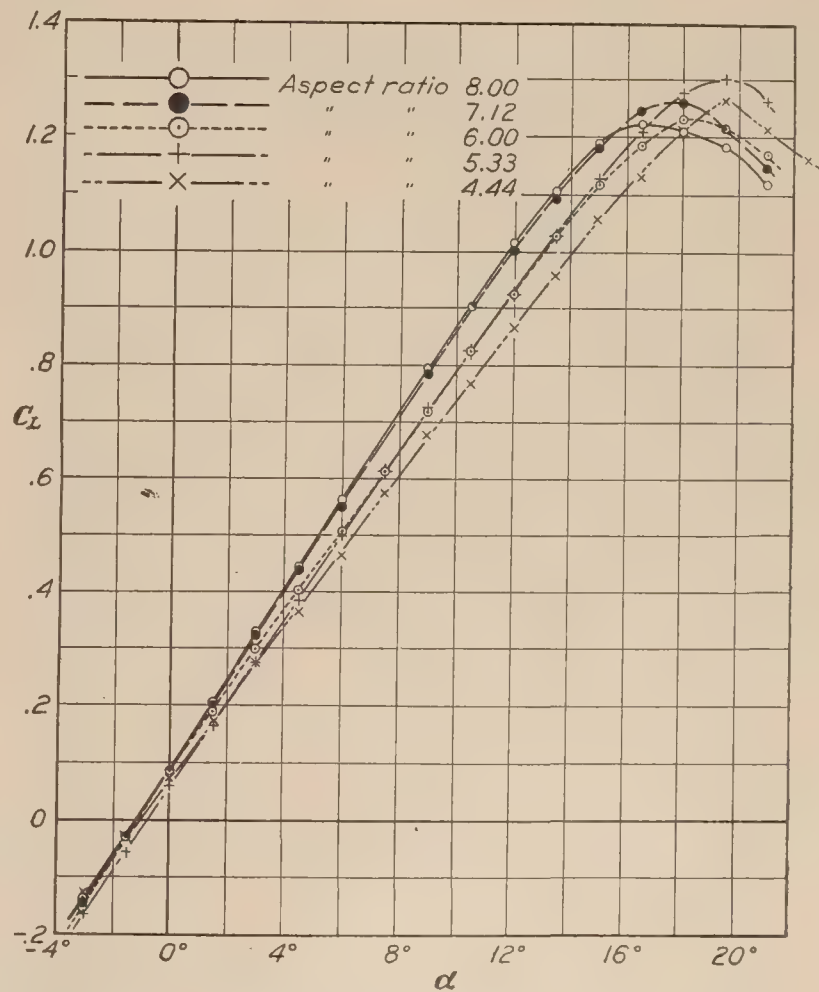


FIG. 16.—N. A. C. A.-M6 airfoil of various aspect ratios, as observed in tunnel, 20 atmospheres

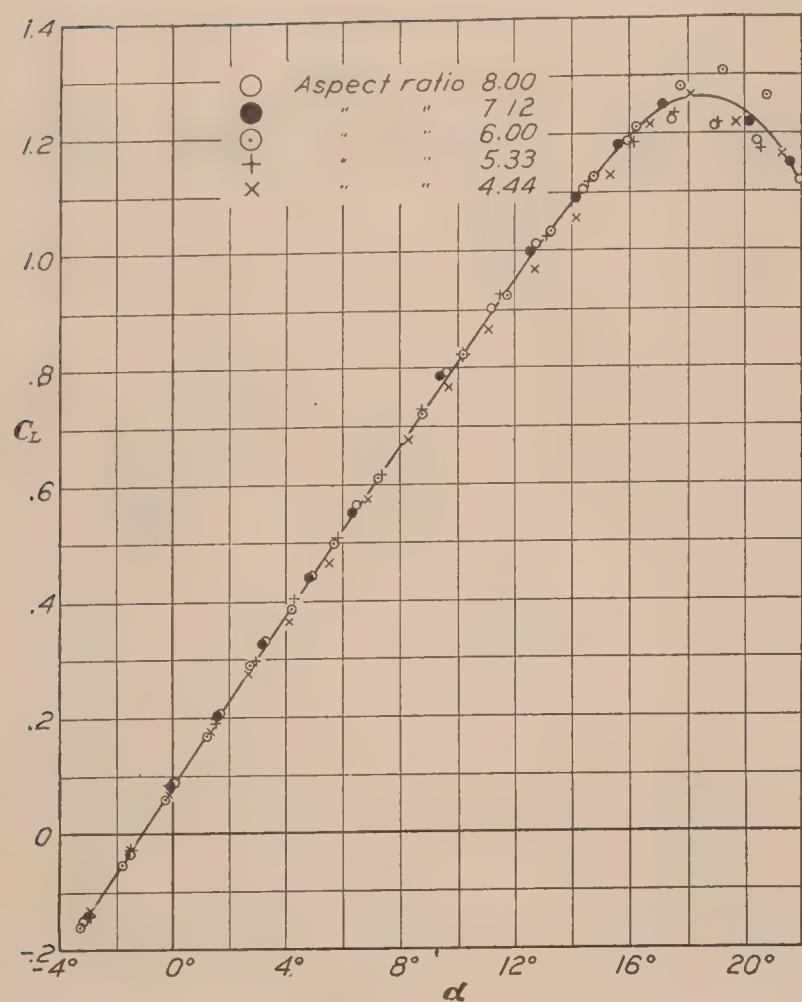


FIG. 17.—N. A. C. A.-M6 airfoil of various aspect ratios, corrected to aspect ratio 6.00; no correction for tunnel walls; 20 atmospheres

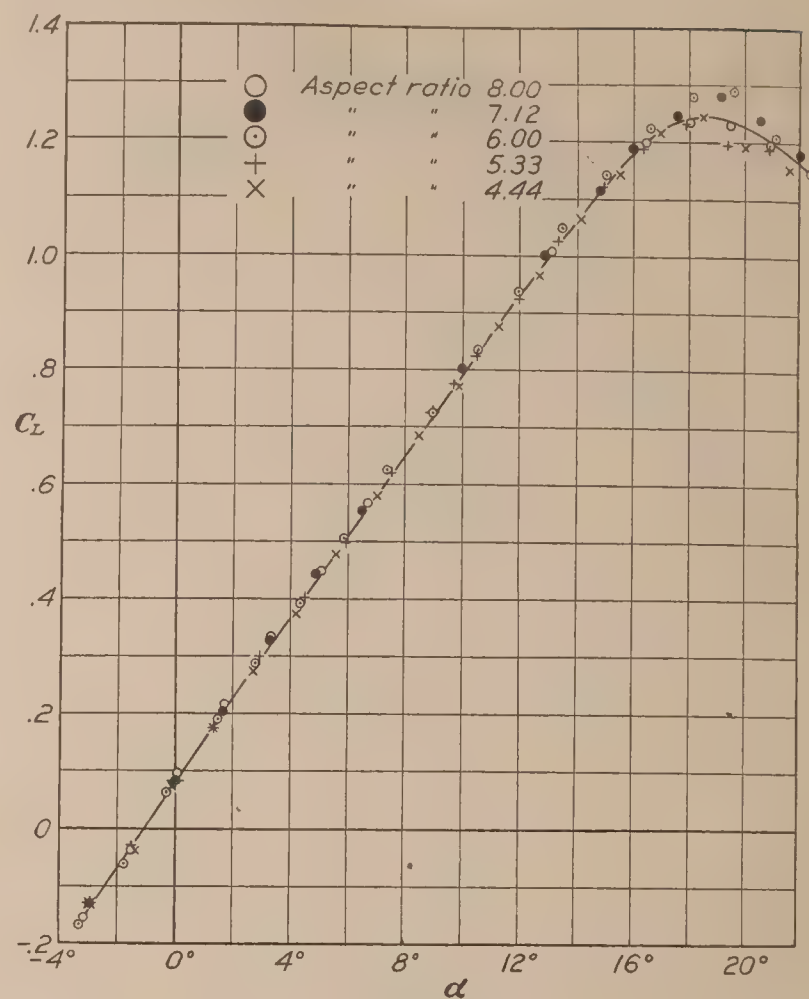


FIG. 18.—N. A. C. A.-M6 airfoil of various aspect ratios, corrected to aspect ratio 6.00 in free air, 20 atmospheres

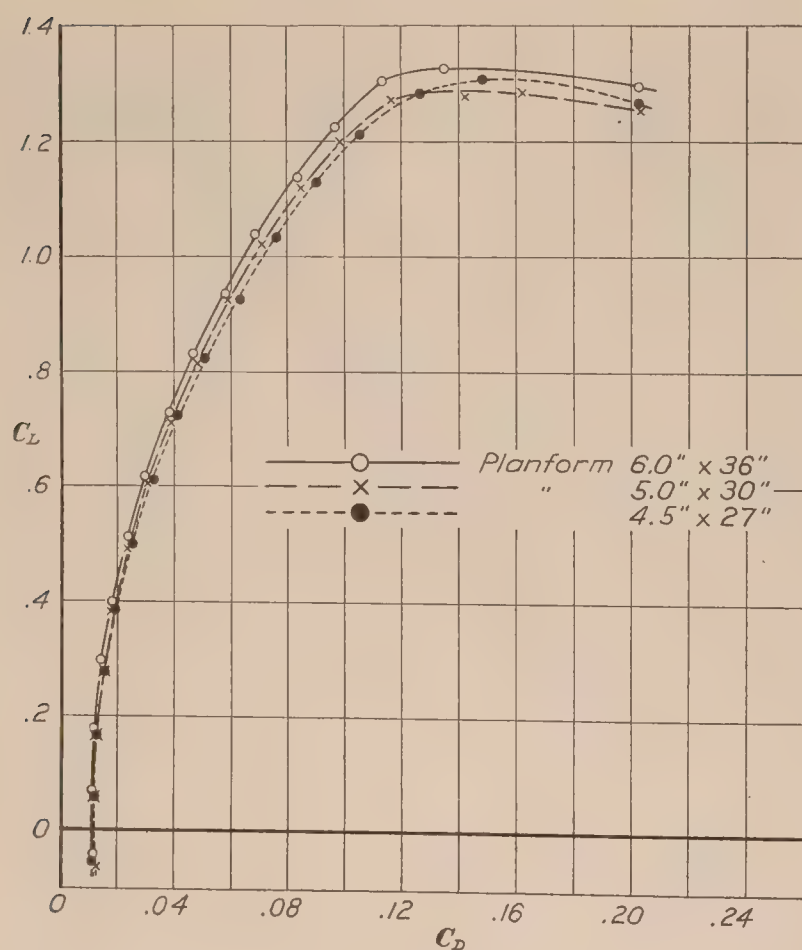


FIG. 19.—As observed in tunnel

N. A. C. A.-M6 airfoils of various sizes; aspect ratio 6.00; 20 atmospheres

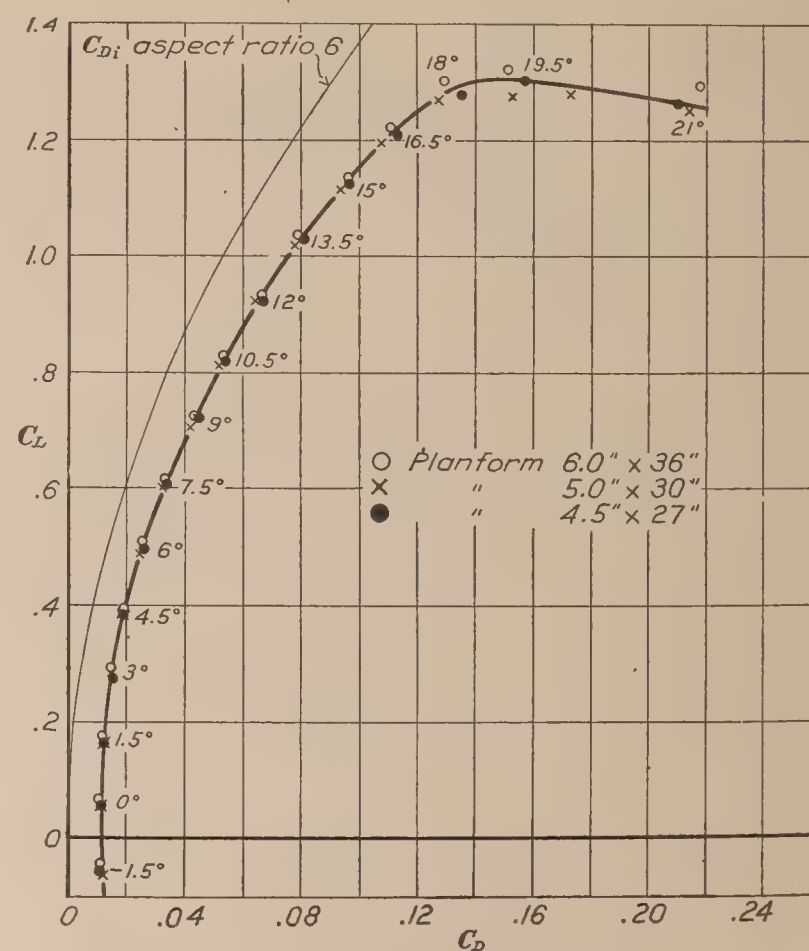


FIG. 20.—Corrected for wall interference

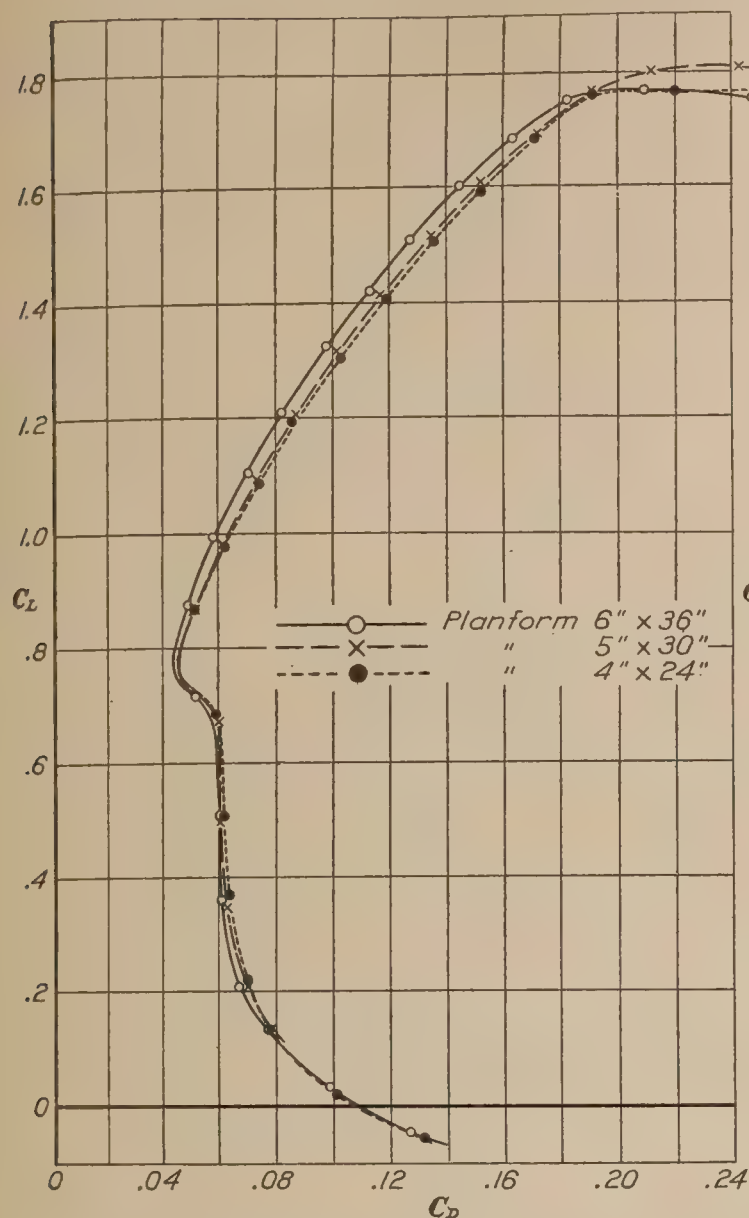


FIG. 21.—As observed in tunnel

R. A. F. airfoils of various sizes; aspect ratio 6.00; average Reynolds Number 530,000

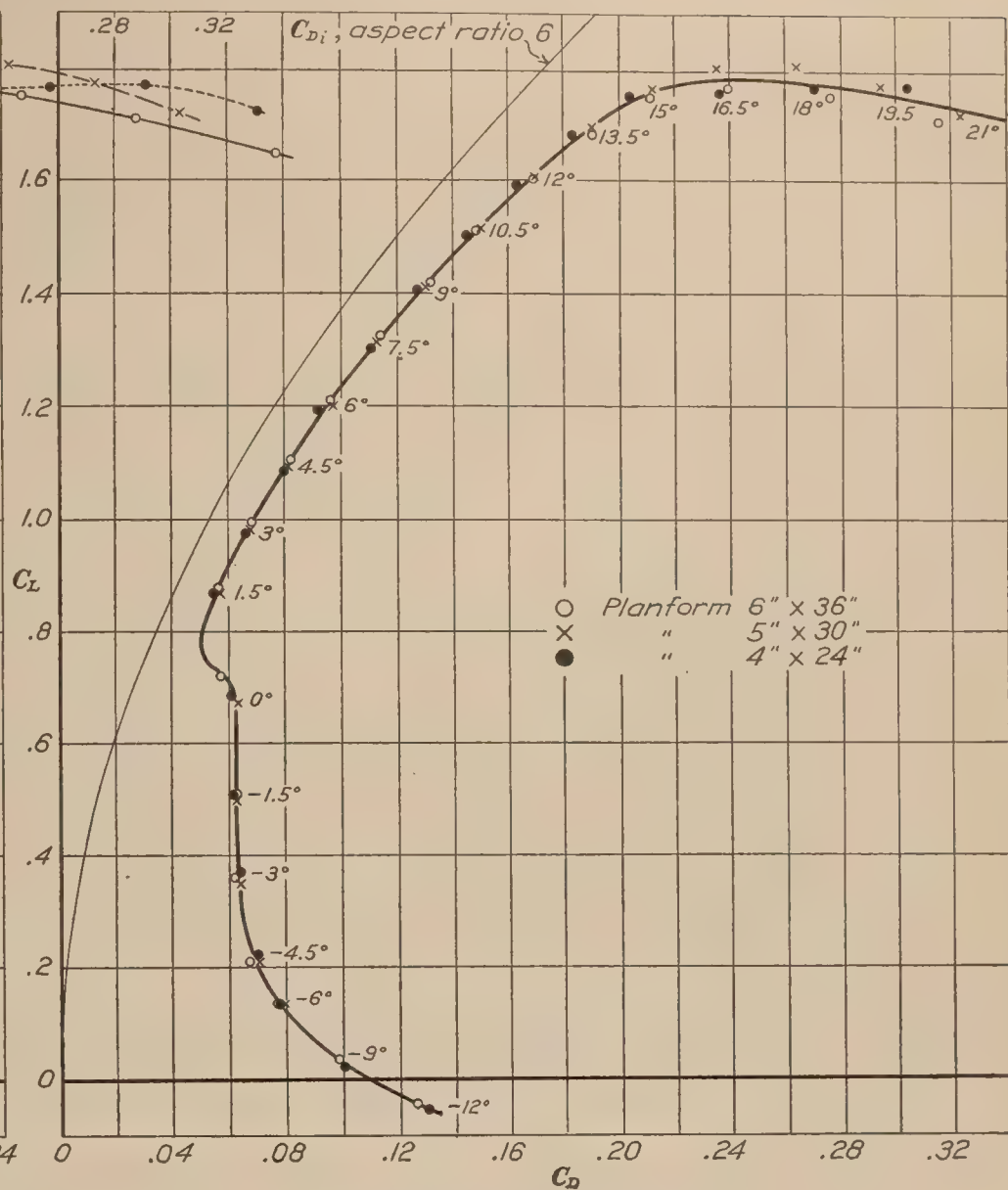


FIG. 22.—Corrected for wall interference

RESULTS AND DISCUSSION

Readings of lift and drag at various angles of attack were obtained and reduced to absolute coefficients. Those obtained from the tests on models of aspect ratios other than 6 were reduced to coefficients for that aspect ratio as noted in the figures, using the Prandtl induced drag equation. These data were then plotted in various forms to determine the existence of any effects that might possibly be attributed to the interference of the walls. Numerous empirical corrections and the Prandtl theoretical corrections (references 2 and 3) were applied to find whether better agreement between the results from the different models could be obtained.

None of the empirical corrections tried was very satisfactory, while the theoretical corrections of Prandtl gave results which were in good agreement. These corrections are:

$$\Delta C_{D_i} = \frac{C_L^2 S}{2\pi D^2}$$

and

$$\Delta \alpha_i = \frac{C_L S}{2\pi D^2}$$

to be added to C_D and α , respectively,
where

- C_L = lift coefficient.
- C_{D_i} = induced drag coefficient.
- α_i = induced angle.
- S = area of the airfoil.
- D = diameter of the tunnel.

A comparison of the results may be had by referring to the figures which are listed below:
 FIGURE 1.—N. A. C. A.—M6 airfoil of various aspect ratios— C_L vs. C_D —1 atm., as observed in tunnel.

FIGURE 2.—N. A. C. A.—M6 airfoil of various aspect ratios— C_L vs. C_D —1 atm., corrected to aspect ratio 6 (assuming no wall correction necessary).

FIGURE 3.—N. A. C. A.—M6 airfoil of various aspect ratios— C_L vs. C_D —1 atm., corrected to aspect ratio 6 with the Prandtl wall interference correction.

FIGURE 4. }
 FIGURE 5. } Same as above, C_L vs. α —1 atm.
 FIGURE 6. }

FIGURE 7. }
 FIGURE 8. } Same as above, C_L vs. C_D —15 atm.
 FIGURE 9. }

FIGURE 10. }
 FIGURE 11. } Same as above, C_L vs. α —15 atm.
 FIGURE 12. }

FIGURE 13. }
 FIGURE 14. } Same as above, C_L vs. C_D —20 atm.
 FIGURE 15. }

FIGURE 16. }
 FIGURE 17. } Same as above, C_L vs. α —20 atm.
 FIGURE 18. }

FIGURE 19.—N. A. C. A.—M6 airfoils of three sizes, A. R. 6, C_L vs. C_D —20 atm., as observed in tunnel.

FIGURE 20.—Same as above, C_L vs. C_D , corrected for wall interference.

FIGURE 21.—R. A. F. 19 airfoils of three sizes, A. R. 6, C_L vs. C_L , R. N. 530,000, as observed in the tunnel.

FIGURE 22.—Same as above, C_L vs. C_D , corrected for wall interference.

It may be seen from an inspection of the above figures that in every case there is better agreement between the results from the different models after the Prandtl corrections have been applied. The improved agreement is found not only for the drag coefficient but also for the angle of attack. The corrections are valid for any airfoil section and for any plan form.

CONCLUSION

Test data from closed wind tunnels on airfoil models of a given section, but having various plan forms, show better agreement when corrected for tunnel wall interference by the Prandtl formulas. The use of these formulas is therefore recommended for correcting wind-tunnel data to the conditions of free air.

LANGLEY MEMORIAL AERONAUTICAL LABORATORY.
 NATIONAL ADVISORY COMMITTEE FOR AERONAUTICS,
 LANGLEY FIELD, VA., May 5, 1927.

APPENDIX

PITOT TUBE SURVEY CLOSE TO WALL

INTRODUCTION

A dynamic pressure and velocity survey has been made across the throat of the variable density wind tunnel for the purpose of determining the variation, particularly near the walls of the tunnel. The results were to be used for further theoretical consideration of the "tunnel wall effect" in which the transverse velocity variation is taken into account.

METHOD OF MEASUREMENT

The survey was made by means of two bars built on the principle of a Pitot-static tube with one bar for impact pressures and one for static pressures. (See figs. 23 and 24.) Pressures were obtained at 31 points on each bar, spaced more closely near the walls, the closest point being at one-fourth inch from the wall surface. The bars were mounted in the tunnel as shown in Figure 25; and the survey was made on three different diameters. Readings were taken simultaneously at the 31 points by means of a large photomanometer.

It developed later that readings closer to the wall were necessary. For this purpose a minute Pitot tube was constructed from 0.051 inch outside diameter hypodermic tubing. Differential pressures were read between this Pitot tube and a static plate flush with the wall, 2 inches to one side and in the same transverse plane, as shown in Figure 26. Observations were taken with this arrangement at several tank pressures at distances of 1, $\frac{1}{2}$, $\frac{1}{4}$, $\frac{1}{8}$, and $\frac{1}{16}$ inch from the wall. Due to mutual interference between the Pitot tube and the wall, the 0.051-inch tube was changed to one of 0.019 inch outside diameter, and further observations were taken at $\frac{1}{8}$, $\frac{1}{16}$, $\frac{1}{32}$, and $\frac{1}{64}$ inch.

RESULTS

The results from the survey using the bars were not unusual, and for this reason the data from this portion of the survey will be omitted; an average curve for three radii, shown in Figure 30, will indicate the general character of the dynamic pressure distribution. The survey using the small Pitot tube, however, will be discussed more fully, particularly because of the information obtained in regard to the conditions close to the wall.

The observations are recorded in Tables I and II. Here also are given readings for a standard Pitot-static tube at the center of the tunnel throat, which is 60 inches in diameter. The ratios of velocities at the two points v/V_c are plotted on logarithmic scales in Figure 27, a separate curve for each tank pressure, against x , the distance from the wall. Figure 28 shows curves that have been deduced from Figure 27, plotted against the tank pressure, which is proportional to the density.

The indicated points in Figures 29 and 30 show the observations p/P_c the ratio of the dynamic pressure at the point to that at the center of the tunnel throat, plotted against x and compared with empirical curves derived from the data. Figure 30 also shows an average curve of the dynamic pressure taken by means of the bars extending across the tunnel for comparison.

DISCUSSION

The walls of a tube or wind tunnel are known to have an effect on the flow adjacent. Theoretical consideration has been given to this effect, which has also been previously studied experimentally. In general, it has been found that the velocity at the center is maintained at approximately full value within the immediate neighborhood of the wall, the so-called region of the "boundary layer." Prandtl, Blasius, v. Karman (reference 4), Van der Hegge Zijnen (reference 5), and others have made a study of this boundary layer.

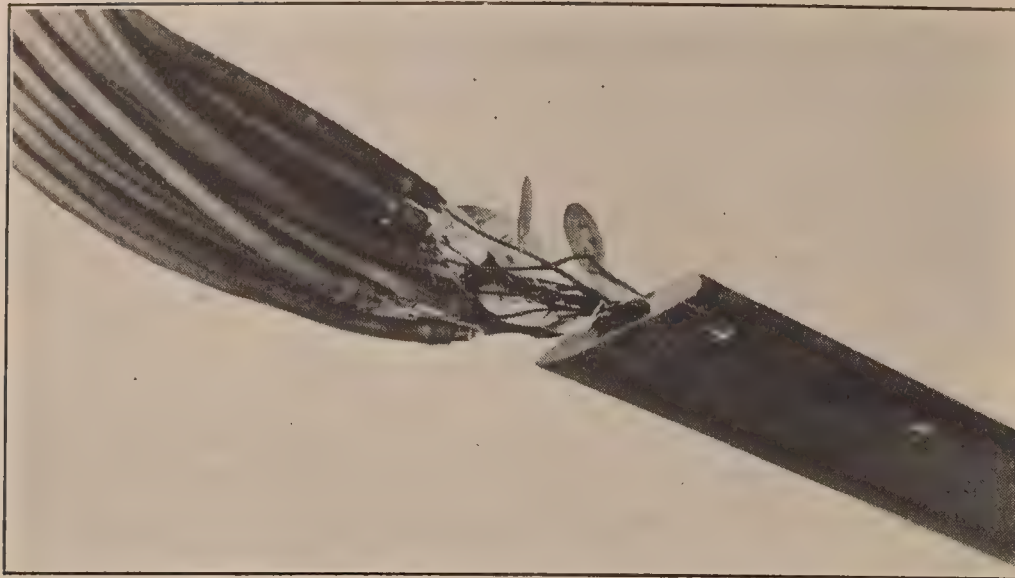


FIG. 23.—Survey bar with impact openings

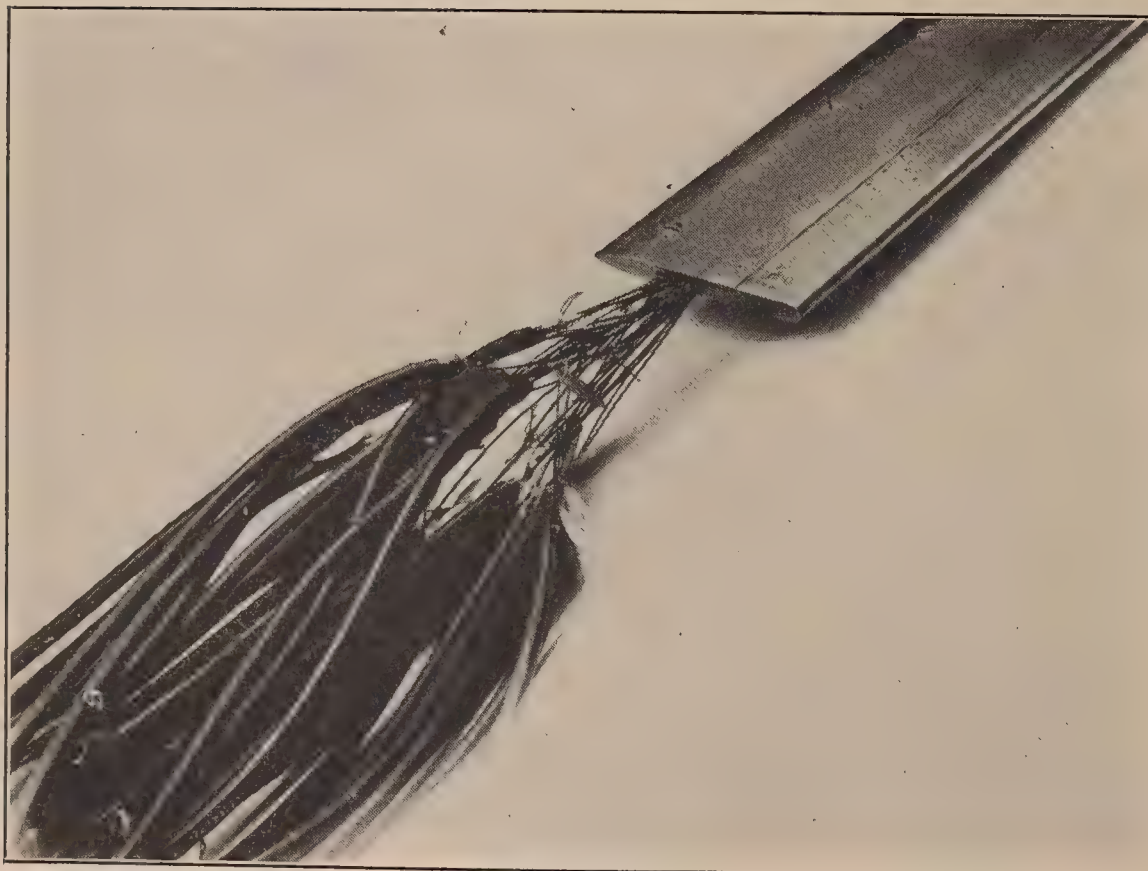


FIG. 24.—Survey bar with static openings

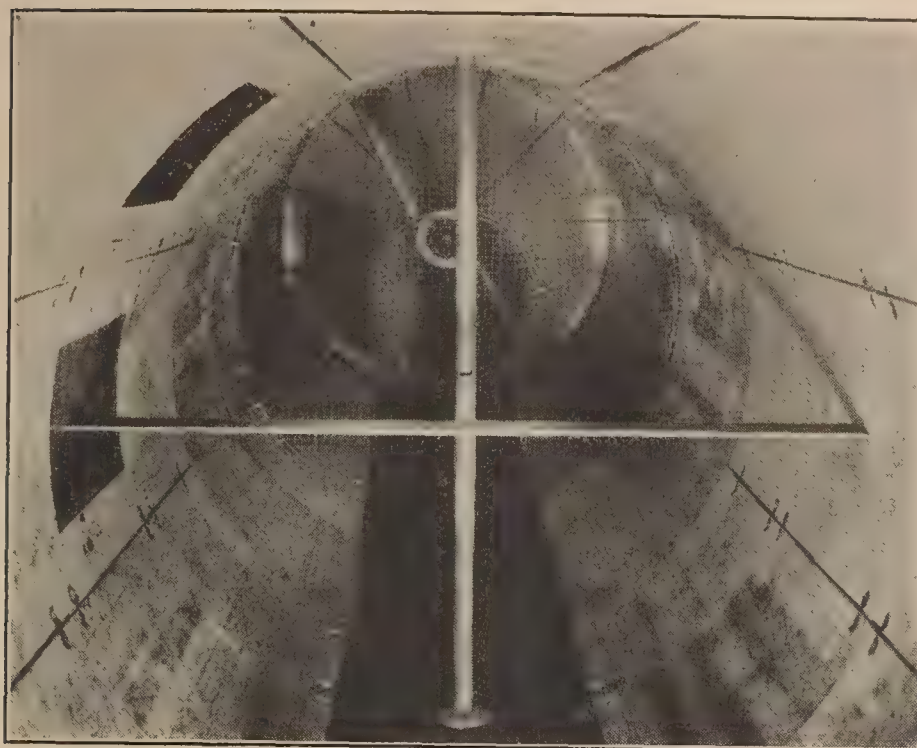


FIG. 25.—Survey bar mounted in tunnel

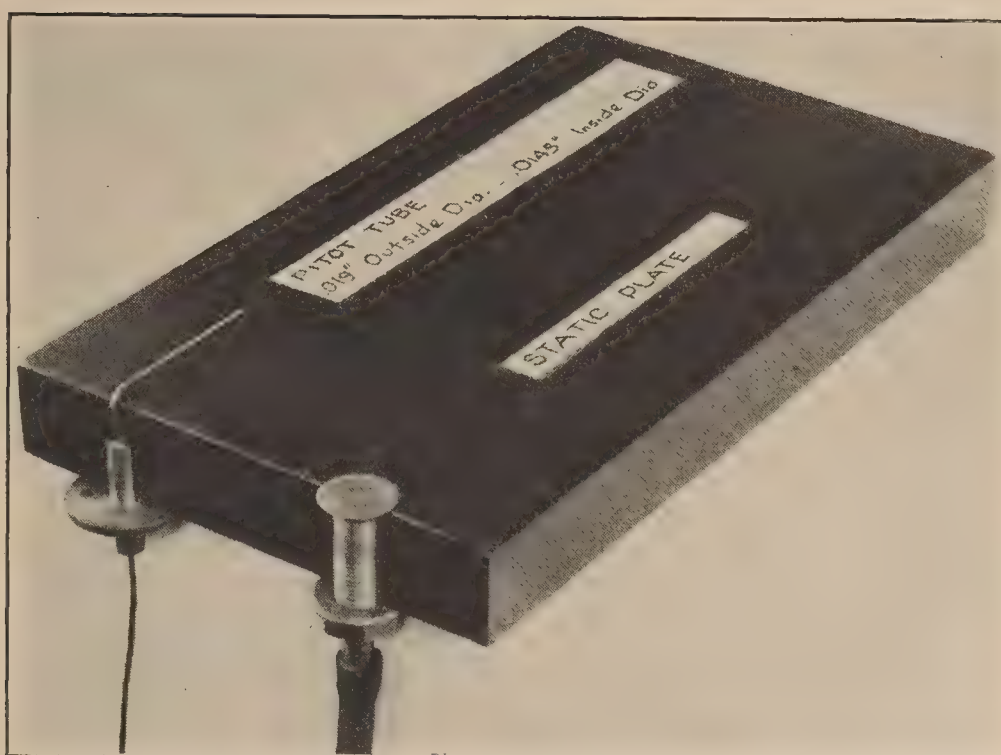
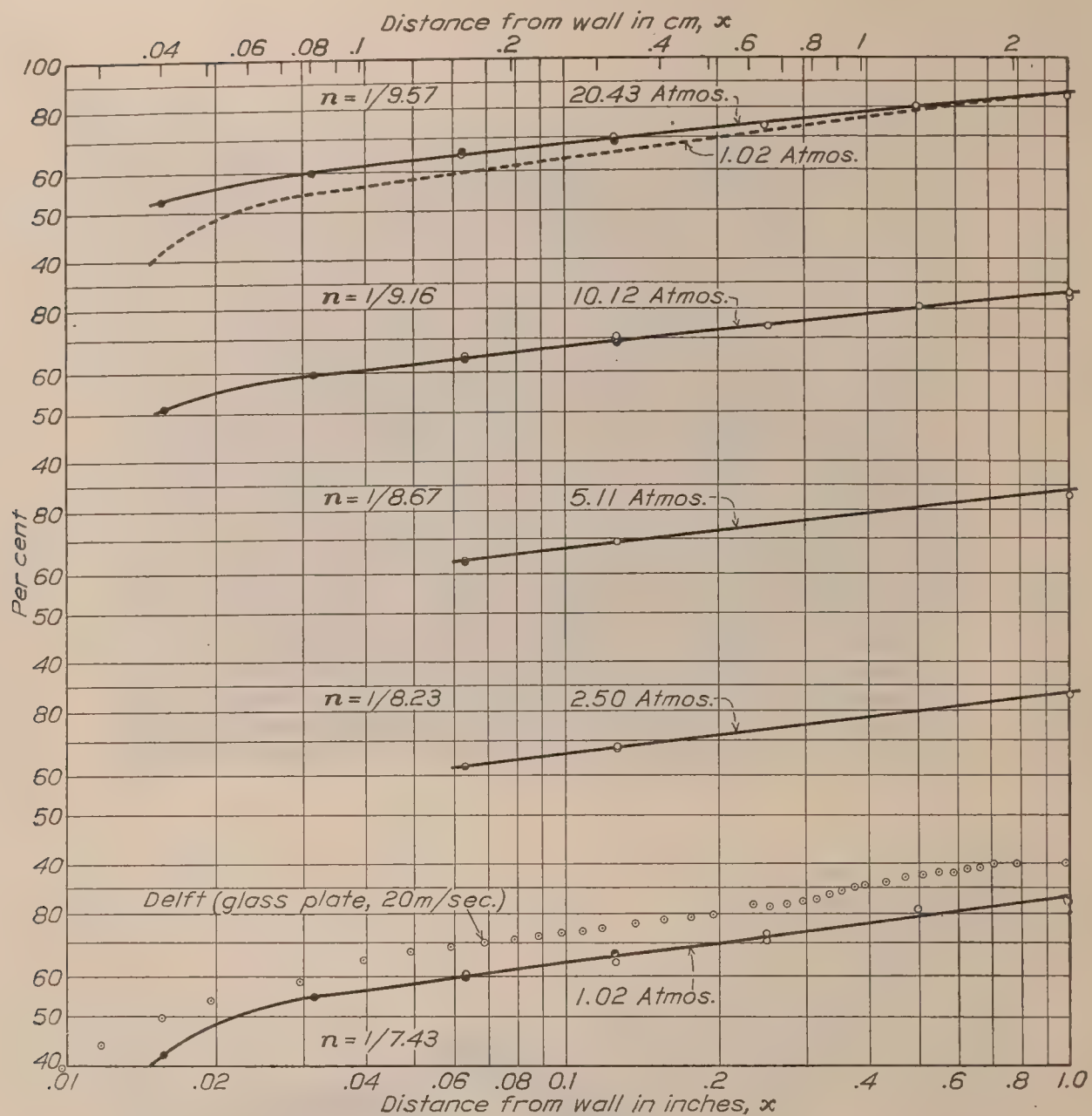
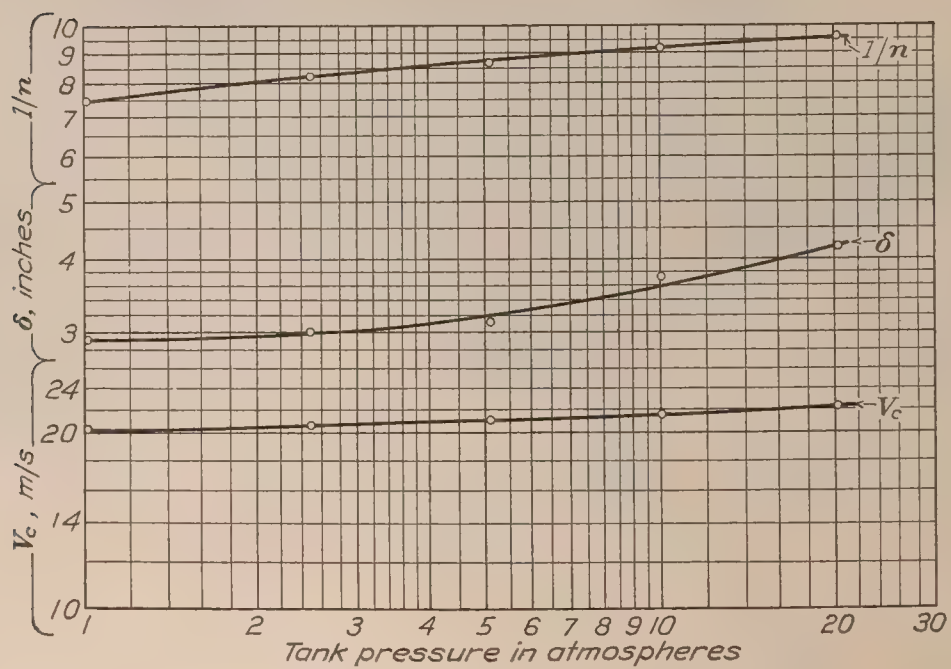
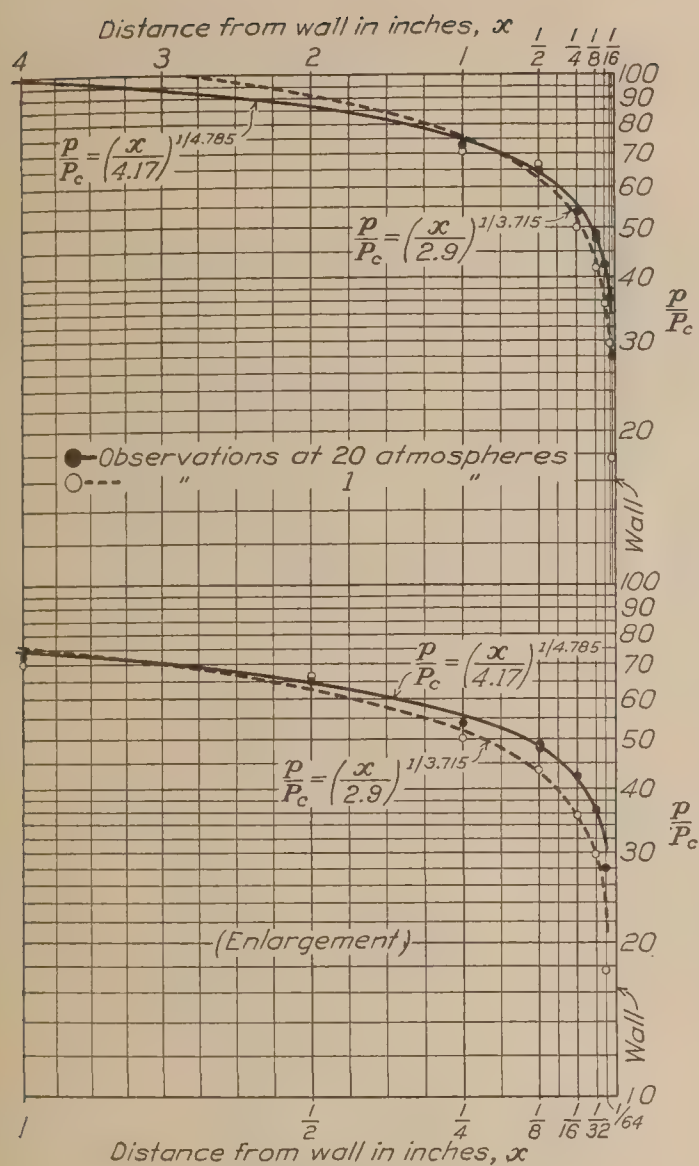
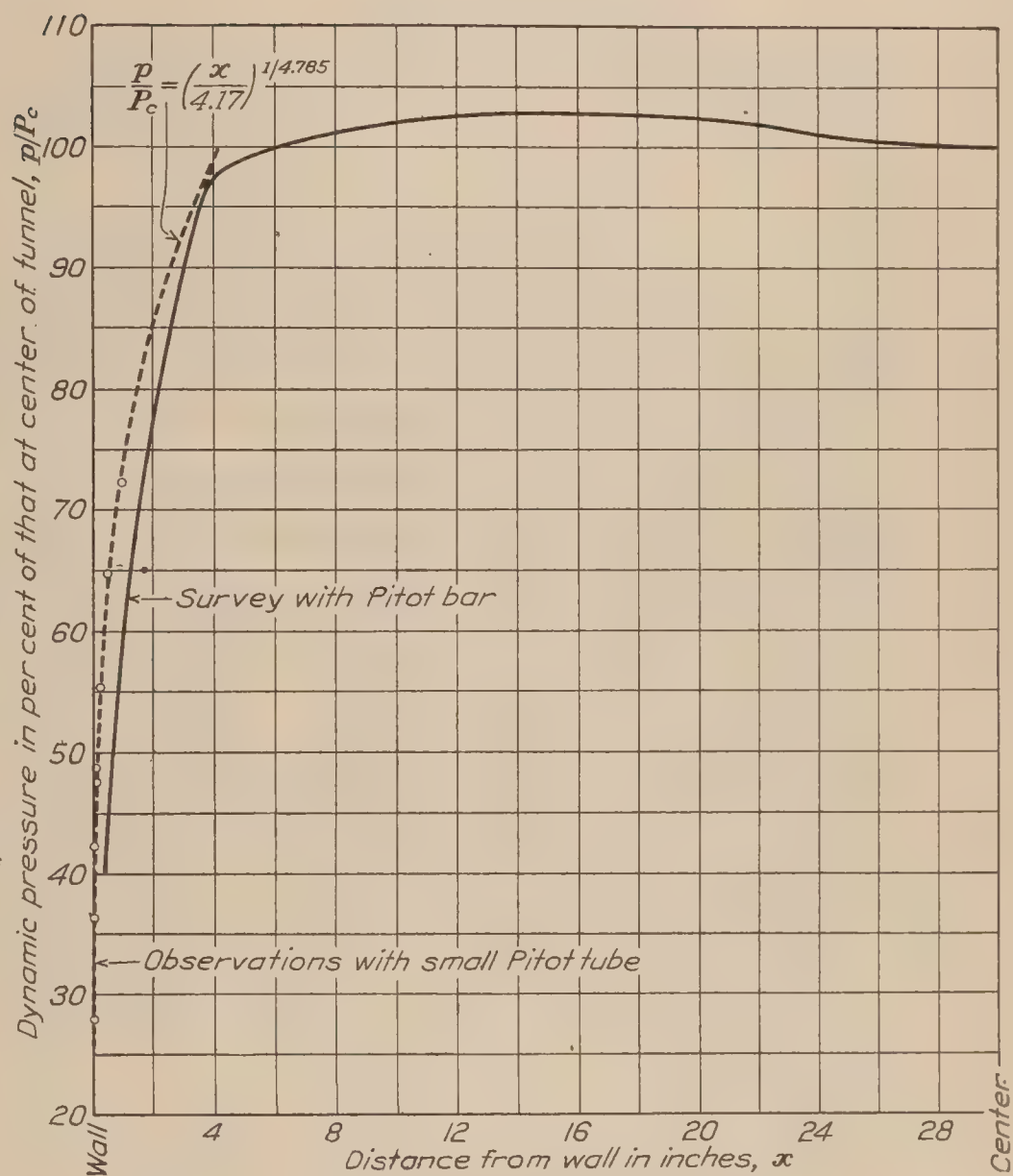


FIG. 26.—Installation of small Pitot tube and static plate

FIG. 27.—Values of v/V_c .FIG. 28.—Variation of V_c , δ and $1/n$ with tank pressure

FIG. 29.—Variation of p/P_c with x FIG. 30.—Variation of p/P_c with x , 20 atmospheres

Von Karman divides this layer into two regions, one of laminar flow close to the wall and the second of turbulent flow outside of the first. For these conditions he has derived equations for the variation of the velocity near the wall. For the laminar region, he gives:

$$v = \frac{\tau_o}{\mu} x,$$

where v = velocity at the point parallel to the wall.

τ_o = shearing stress at the surface $\mu \left(\frac{\partial v}{\partial x} \right)_{x=0}$

μ = viscosity of the air.

x = distance from the wall or surface.

For the turbulent flow, the following equation is given:

$$v = V_c \left(\frac{x}{\delta} \right)^{1/7}$$

where V_c = velocity at the center of the tunnel.

δ = total thickness of the boundary layer in the direction of x .

The experimental work at Delft of Van der Hegge Zijnen (reference 5) on the boundary layer close to a smooth glass plate, gives an excellent opportunity for comparison with the above theoretical equations. Such a comparison shows very good agreement.

In view of the above, it is interesting to note the agreement that is obtained between the results from Delft and those of this investigation at 1 atmosphere. In Figure 27 there are plotted values of v/V_c for respective values of x with curves drawn for each pressure or density. The velocity in the center of the tunnel for the condition of 1 atmosphere tank pressure is, from Figure 28, 20.2 m/s; on the same plot (fig. 27) there is given the data obtained at Delft for 20 m/s. When plotted on logarithmic scales the straight portion of the curve corresponds to the turbulent region wherein the relation $v/V_c = \left(\frac{x}{\delta} \right)^n$ holds and the curved portion, to the laminar region (reference 5). In each case the laminar flow region extends to about the same distance from the wall, point A. In the remaining portion the two curves are about parallel, though displaced from one another. The large boundary layer shown by the results of this research is no doubt due to the comparative roughness of the tunnel wall and to the continuous (longitudinal) surface of the wall.

The effect of the change in density may be seen in Figures 27, 28, and 29. The depth of the boundary layer, which was found by extrapolation, increases as the density becomes greater. The reciprocal of the exponent n of the equation $\frac{v}{V_c} = \left(\frac{x}{\delta} \right)^n$ has been plotted in Figure 28, where its variation with density may be seen. At 20 atmospheres a value of n of $\frac{1}{9.57}$ was obtained, a considerable change from the 1 atmosphere value of $\frac{1}{7.43}$. The latter figure is in the neighborhood of the values obtained by other experimenters at a density of 1 atmosphere. One might conclude from an inspection of the above figures that as the density is increased the mass of inertia effect becomes more prominent in comparison to the viscosity effect; at the high densities the velocity gradient in the turbulent portion of the boundary layer is less and in the laminar portion greater.

CONCLUSION

This investigation has shown good agreement with previous researches, and has shown that there is a "scale effect" as the density of the fluid is increased; the "scale effect" found is, primarily, a decrease in the exponent n of the Von Karman formula,

$$\frac{v}{V_c} = \left(\frac{x}{\delta} \right)^n$$

which defines the flow of a fluid in the boundary layer at the surface (in this case, of the wind tunnel).

REFERENCES

1. MUNK, MAX M., and MILLER, ELTON W. The Variable Density Wind Tunnel of the National Advisory Committee for Aeronautics. N. A. C. A. Technical Report No. 227, 1925.
2. PRANDTL, L. Applications of Modern Hydrodynamics to Aeronautics. Part II, section F. N. A. C. A. Technical Report No. 116, 1921.
3. GLAUERT, H. The Interference of Wind Channel Walls on the Aerodynamic Characteristics of Airfoil. Reports and Memoranda No. 867, March, 1923. British Aeronautical Research Committee.
4. VON KARMAN, TH. "Zeitschrift für angewandte Mathematik und Mechanik" I, 1921.
5. ZIJNEN, B. G., Van der Hegge. Measurements of the Velocity Distribution in the Boundary Layer Along a Plane Surface. Mededeeling No. 6. "Uit het Laboratorium voor Aerodynamica en Hydrodynamica der Technische Hoogeschool te Delft," 1924.

TABLE I

VELOCITIES CLOSE TO WALL OF TUNNEL IN PLANE OF MODEL

[0.051 inch hypodermic tube used as pitot]

Pressure atm.	Density ρ	Pitot at center		Pitot at wall		Distance from wall		v/V_∞ %
		P_c kg/m ²	V_c m/s	p kg/m ²	v m/s	x in.	x cm	
1. 012	0. 1234	25. 45	20. 31	18. 1	17. 10	1. 00	2. 54	84. 2
2. 495	. 3095	67. 3	20. 85	49. 5	17. 88	1. 00	2. 54	85. 8
5. 10	. 6270	139. 5	21. 09	102. 0	18. 04	1. 00	2. 54	85. 6
10. 27	1. 235	290. 0	21. 68	212. 2	18. 55	1. 00	2. 54	85. 6
9. 92	1. 202	278. 0	21. 50	204. 0	18. 43	1. 00	2. 54	85. 7
20. 36	2. 480	613. 0	22. 34	442. 0	18. 88	1. 00	2. 54	84. 5
10. 34	1. 261	287. 0	21. 35	205. 2	18. 04	1. 00	2. 54	84. 5
5. 24	. 6470	142. 8	21. 00	104. 8	17. 99	1. 00	2. 54	85. 7
2. 57	. 3145	66. 6	20. 58	49. 5	17. 74	1. 00	2. 54	86. 2
1. 01	. 1228	25. 0	20. 19	17. 4	16. 84	1. 00	2. 54	83. 4
1. 026	. 1281	26. 5	20. 34	17. 52	16. 54	1/2	1. 27	81. 3
10. 20	1. 240	286. 0	21. 48	187. 4	17. 40	1/2	1. 27	81. 0
20. 20	2. 390	594. 0	22. 30	384. 0	17. 92	1/2	1. 27	80. 4
1. 025	. 1265	25. 5	20. 07	12. 78	14. 21	1/4	. 635	70. 8
10. 20	1. 222	282. 0	21. 49	153. 2	15. 85	1/4	. 635	73. 8
20. 75	2. 475	598. 0	22. 00	320. 7	16. 10	1/4	. 635	73. 2
1. 008	. 1247	25. 1	20. 05	13. 35	14. 63	1/4	. 635	72. 9
1. 020	. 1280	25. 6	20. 01	11. 2	13. 23	1/8	. 318	66. 6
2. 515	. 3105	66. 1	20. 65	30. 8	14. 08	1/8	. 318	68. 2
4. 90	. 6000	133. 1	21. 07	63. 6	14. 57	1/8	. 318	69. 2
10. 20	1. 230	280. 2	21. 35	137. 2	14. 95	1/8	. 318	70. 0
9. 04	1. 132	262. 2	21. 52	126. 6	14. 96	1/8	. 318	69. 4
20. 55	2. 478	612. 0	22. 26	298. 5	15. 53	1/8	. 318	69. 8
20. 55	2. 478	611. 0	22. 22	295. 0	15. 43	1/8	. 318	69. 4
5. 24	. 6300	142. 0	21. 22	68. 0	14. 69	1/8	. 318	69. 2
2. 31	. 2870	60. 8	20. 58	27. 8	13. 93	1/8	. 318	67. 7
1. 020	. 1258	25. 76	20. 22	10. 5	12. 93	1/8	. 318	63. 9
1. 021	. 1249	25. 5	20. 21	9. 14	12. 10	1/16	. 159	59. 9
1. 021	. 1249	25. 5	20. 21	9. 06	12. 04	1/16	. 159	59. 6
2. 525	. 3070	65. 6	20. 67	25. 74	12. 96	1/16	. 159	62. 7
2. 525	. 3070	65. 8	20. 70	25. 74	12. 96	1/16	. 159	62. 6
5. 10	. 6130	137. 6	21. 17	55. 8	13. 50	1/16	. 159	63. 8
10. 35	1. 229	286. 2	21. 60	119. 4	13. 94	1/16	. 159	64. 5
20. 30	2. 380	580. 0	22. 07	239. 9	14. 21	1/16	. 159	64. 4
20. 20	2. 375	582. 0	22. 14	246. 1	14. 39	1/16	. 159	65. 0
20. 40	2. 400	581. 0	22. 00	246. 9	14. 34	1/16	. 159	65. 2

TABLE II

VELOCITIES CLOSE TO WALL OF TUNNEL IN PLANE OF MODEL

[0.019 inch Dural tube used as pitot]

Pressure atm.	Density ρ	Pitot at center		Pitot at wall		Distance from wall		v/V_c %
		P_c kg/m ²	V_c m/s	p kg/m ²	v m/s	x in.	x cm	
1. 015	. 1253	25. 6	20. 21	11. 23	13. 39	1/8	. 318	66. 2
10. 20	1. 222	284. 5	21. 58	135. 6	14. 90	1/8	. 318	69. 1
10. 20	1. 222	284. 5	21. 58	132. 8	14. 74	1/8	. 318	68. 3
20. 47	2. 405	596. 0	22. 27	277. 0	15. 17	1/8	. 318	68. 4
20. 47	2. 393	588. 0	22. 18	279. 5	15. 27	1/8	. 318	68. 3
1. 017	. 1250	25. 6	20. 33	9. 0	12. 00	1/16	. 159	59. 3
2. 535	. 3070	65. 5	20. 66	25. 1	12. 78	1/16	. 159	61. 9
5. 10	. 6090	135. 8	21. 11	55. 3	13. 48	1/16	. 159	63. 9
10. 27	1. 242	290. 0	21. 60	123. 3	14. 10	1/16	. 159	65. 3
20. 60	2. 420	604. 0	22. 34	259. 5	14. 64	1/16	. 159	65. 5
1. 015	. 1238	25. 5	20. 30	7. 6	11. 08	1/32	. 0795	54. 6
10. 20	1. 211	281. 0	21. 54	99. 0	12. 79	1/32	. 0795	59. 4
20. 50	2. 395	586. 0	22. 20	211. 0	13. 27	1/32	. 0795	59. 8
1. 020	. 1231	25. 1	20. 01	4. 4	8. 45	1/64	. 040	41. 8
10. 20	1. 198	274. 0	21. 60	72. 4	11. 00	1/64	. 040	50. 9
20. 25	2. 360	580. 0	22. 16	162. 2	11. 72	1/64	. 040	52. 9

REPORT No. 276

**COMBUSTION TIME IN THE ENGINE CYLINDER
AND ITS EFFECT ON ENGINE PERFORMANCE**

**By CHARLES F. MARVIN, Jr.
Bureau of Standards**

REPORT No. 276

COMBUSTION TIME IN THE ENGINE CYLINDER AND ITS EFFECT ON ENGINE PERFORMANCE

By CHARLES F. MARVIN, Jr.

SUMMARY

As part of a general program to study combustion in the engine cylinder and to correlate the phenomena of combustion with the observed performance of actual engines, this paper, which was outlined by Mr. S. W. Sparrow, and the work undertaken at the request of the National Advisory Committee for Aeronautics, presents a sketchy outline of what may happen in the engine cylinder during the burning of a charge. It also suggests the type of information needed to supply the details of the picture and points out how combustion time and rate affect the performance of the engine.

A theoretical concept of a flame front which is assumed to advance radially from the point of ignition is presented, and calculations based on the area and velocity of this flame and the density of the unburned gases are made to determine the mass rate of combustion. From this rate the mass which has been burned and the pressure at any instant during combustion are computed.

This process is then reversed in an effort to determine actual rates of combustion and flame velocities from the pressures as recorded on indicator diagrams.

The effects of different rates of combustion on engine performance are then discussed and the importance of proper spark advance is emphasized.

INTRODUCTION

When the intake valve of a gasoline engine closes, it traps a definite weight of charge in the engine cylinder. If leakage by the piston and valves is neglected, this weight remains constant until the exhaust valve opens. During the short interval between these two events, the trapped gases undergo extremely rapid chemical and physical changes which enable them to do work on the piston. The amount of this work can be determined with fair accuracy and many tests show that it varies considerably for different engine designs and operating conditions.

Determinations of just what happens in the cylinder during the burning of a charge to cause the observed variations in engine performance are rendered very difficult and uncertain because of the complexity and speed of the chemical reactions and the presence of a number of operating variables, such as fuel characteristics, pressure, temperature, turbulence, and piston movement, all of which influence combustion and complicate its study.

Experiments with simple explosive mixtures under controlled conditions in bombs of various sorts have yielded important information regarding the phenomena of combustion, but there is need for supplementary data which will correlate the fundamentals of combustion with the observed performance of actual engines.

FLAME PROPAGATION IN THE ENGINE CYLINDER

As a first step in the visualization of what might happen in an engine cylinder when a charge is burned, a series of sectional views through the cylinder at the spark plug may be taken during combustion as shown in Figure 1. To make the picture as simple as possible it is assumed that the charge is homogeneous, that there is no turbulence or piston movement, and that the combustion chamber is a thin disk.

The small dotted portion of **A** (fig. 1) represents the original volume of that portion of the charge which burns during the first short interval of time " t " after the occurrence of the spark. As this increment of charge burns, its temperature rises and it therefore expands, pushing the flame front ahead of it, compressing the unburned charge, and causing a uniform increase in pressure throughout the cylinder. At the end of the time " t " the volumes of the burned and unburned gas, separated by the flame front, are shown at **B**.

For the sake of simplicity, it is assumed that during the second time interval " t " the flame proceeds into the unburned mixture at the same constant rate as during the first time interval. The amount of gas to be burned during the second time interval may be represented, before the flame front enters it, by the dotted section of **C**. After the second increment has burned and expanded, the position of the flame front and the relative volumes of burned and unburned gas are shown at **D**. Similar calculations give the position of the flame front after each successive equal interval of time.

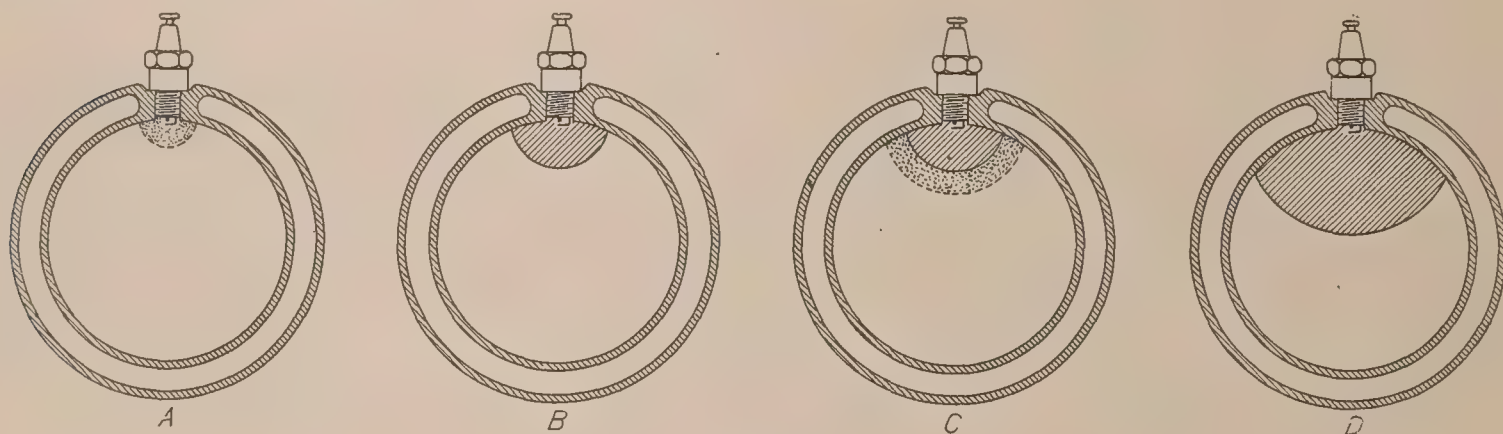


FIG. 1

RATE OF BURNING—MASS BURNED—PRESSURE RISE

The mass rate R_m at which the charge burns at any instant during combustion will be equal to the area, A , of the flame front multiplied by the velocity, V , with which the flame front is advancing into the unburned charge multiplied by the density, D , of the unburned charge or—

$$R_m = A V D \quad (1)$$

It is apparent that in Figure 1 the area of the flame front increases from zero to a maximum and then decreases to zero again as the flame advances across the cylinder from the spark plug to the opposite wall. It is also evident that the shape of the combustion chamber and the location of the ignition point may have a considerable effect on the area of the flame front and consequently on the mass rate of burning and the pressure rise. Consider, for example, the extreme cases of a spherical bomb ignited at the center, and a long thin tube of the same volume ignited at one end. In the spherical bomb, the flame can spread radially in all directions without interference, its area increasing as the square of the radial spread, until it reaches the walls of the bomb and the charge is entirely burned. In the tube, however, the flame can travel in only one direction and its area remains at a constant small value throughout the combustion. A much more rapid pressure rise and a shorter combustion time would be expected in the case of the bomb. In a somewhat similar manner, the number of ignition points would also affect the area of the flame front and hence the rate of burning.

Of course, the flame may not advance as a spherical surface in the actual engine cylinder. Its shape may be distorted from true sphericity by turbulence or stratification of the charge, by reflected pressure or sound waves, or by the movement of the piston. Under certain conditions or at some stage in the combustion, the whole of the unburned portion of the charge may be ignited simultaneously by compression or by incandescent particles. These possibilities invite further investigation.

The velocity at which the flame front advances into the unburned charge is known to be different for different fuels and mixture ratios. It also depends in some way on the pressure, temperature, and density of the burning gases. The presence of catalyzers or inert gases in the charge would also be expected to affect the velocity.

During combustion the unburned charge is undergoing continual compression by the increasing amount of burned charge so that its density increases steadily.

By making certain simple assumptions in regard to A , V , and D , it is possible to compute the mass rate of burning, R_m , and the total amount which has been burned at any instant during combustion for the simple case shown in Figure 1.¹ These quantities are plotted in Figure 2. Since the pressure rise is almost proportional to the mass burned, the solid curve in Figure 2 also indicates the type of pressure rise to be expected.

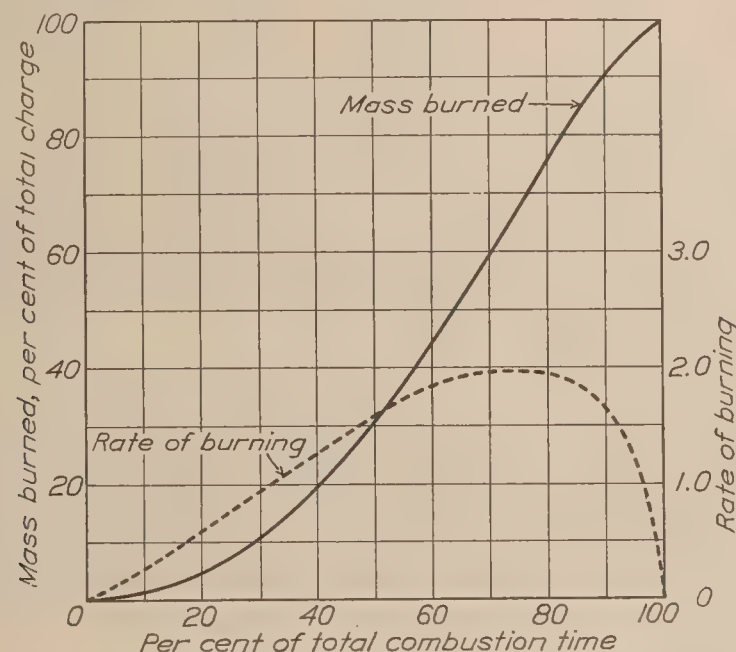


FIG. 2

ANALYSIS OF INDICATOR DIAGRAM

The fact that calculations of pressure rise can be made from a concept of an advancing flame front suggests that this process might be reversed and that the pressure rise as recorded on an indicator diagram might be made to yield information in regard to flame propagation in the actual engine cylinder.

A portion of a typical indicator diagram is shown plotted on logarithmic coordinates in Figure 3. The solid line shows actual pressures as measured by the indicator and the dotted line represents the pressures which would have been expected had the charge been instantly burned at upper dead center as in the theoretical Otto cycle. Theoretically and actually, compression is represented on the logarithmic plot by a straight line to the point where the spark occurs. Here the actual diagram begins to rise more sharply due to the burning of the charge. By the time the piston has reached upper dead center the actual pressure is at "c" instead of at "b" where it would have been had there been no burning. If it is assumed that the pressure rise above the straight compression line is proportional to the mass of charge burned, then the fraction of the total charge which is actually burned at upper center would be equal to $\frac{c-b}{d-b}$. In a similar manner the fraction burned at any other instant during combustion can be computed from a similar ratio of pressures. At "e" combustion is complete and expansion of the burned gases is represented by a straight line.

Seven indicator diagrams,² taken under different operating conditions as listed in Table I, were analyzed by this method and the results are plotted in Figures 4-7. The engine

¹ Details of these calculations are given in Appendix I.

² These diagrams were made in the "altitude chamber" at the Bureau of Standards with a balanced diaphragm pressure indicator described in N. A. C. A. Report No. 107.

on which these indicator cards were taken has a cylindrical combustion chamber similar to that pictured in Figure 1 except that in the engine two plugs are used, one on each side of the cylinder. As would be expected, the general shape of the curves, Figures 4-7, is similar to that of the theoretical curve shown as a solid line in Figure 2, but because of the various operating conditions there are variations in the rate of burning and the total time required for complete combustion.

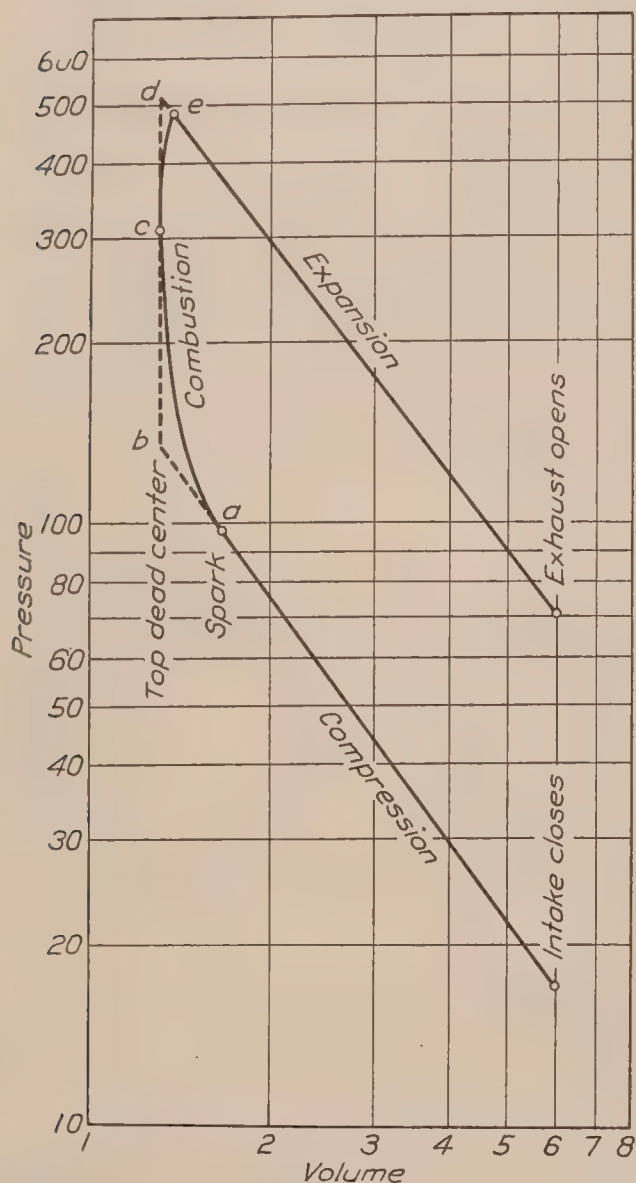


FIG. 3

Returning to Figure 4, an attempt was made to estimate approximately, by means of Formula (1), the actual flame velocities at different instants during combustion.

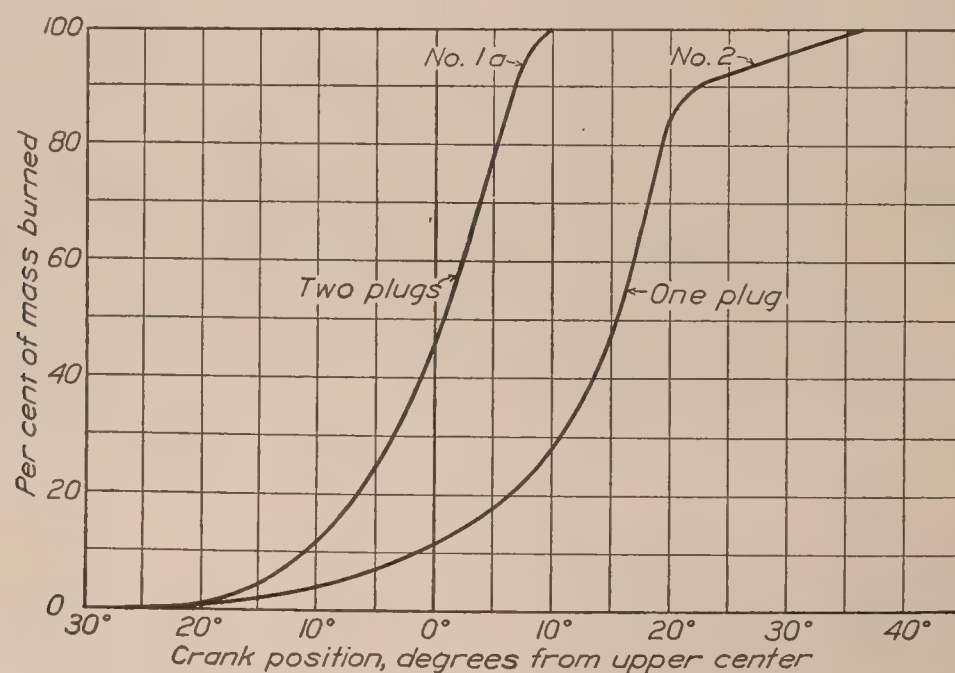


FIG. 4

As shown in Figure 4, combustion is more rapid when the charge is fired by two plugs than when one plug only is used. This is the natural result of having two flame fronts originating at opposite sides of the cylinder.

Figure 5 compares a lean mixture with a mixture producing maximum power. In this case the more rapid burning of the maximum power mixture must be due to a higher velocity of flame propagation rather than to a difference in the flame area, since two plugs were fired in both cases.

The curves in Figure 6 were made at different "altitudes," the density of the charge being the chief operating variable. The velocity of flame propagation is evidently higher for the denser charges. The very slow burning as represented by the curve for 25,000 feet altitude is partly accounted for by the fact that the mixture ratio in this case happened to be very lean.

The load, speed, charge density, and mixture ratio were all different for the two runs shown in Figure 7, and it would be difficult to isolate the effects of these various factors on the curves.

Prior to ignition, conditions in the engine cylinder were almost identical for the two runs represented by the two curves in Figure 4. The weights, pressures, temperatures, and compositions of the two charges were practically the same and the engine was operated at the same

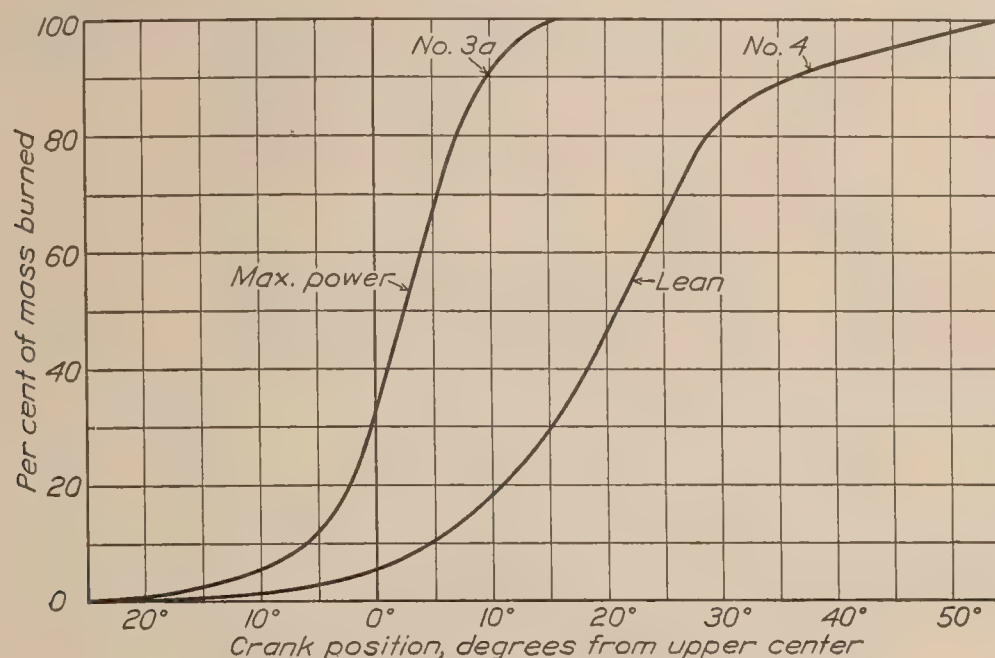


FIG. 5

speed and with the same spark advance in both runs. The flame velocities in the two cases should therefore be equal at the start of combustion and would be expected to vary only with temperature, pressure, and charge density as the burning progressed. For an appreciable time near top dead center the volume change is negligible and pressure, temperature, and charge density are proportional. During this period it would be expected that flame velocities in both

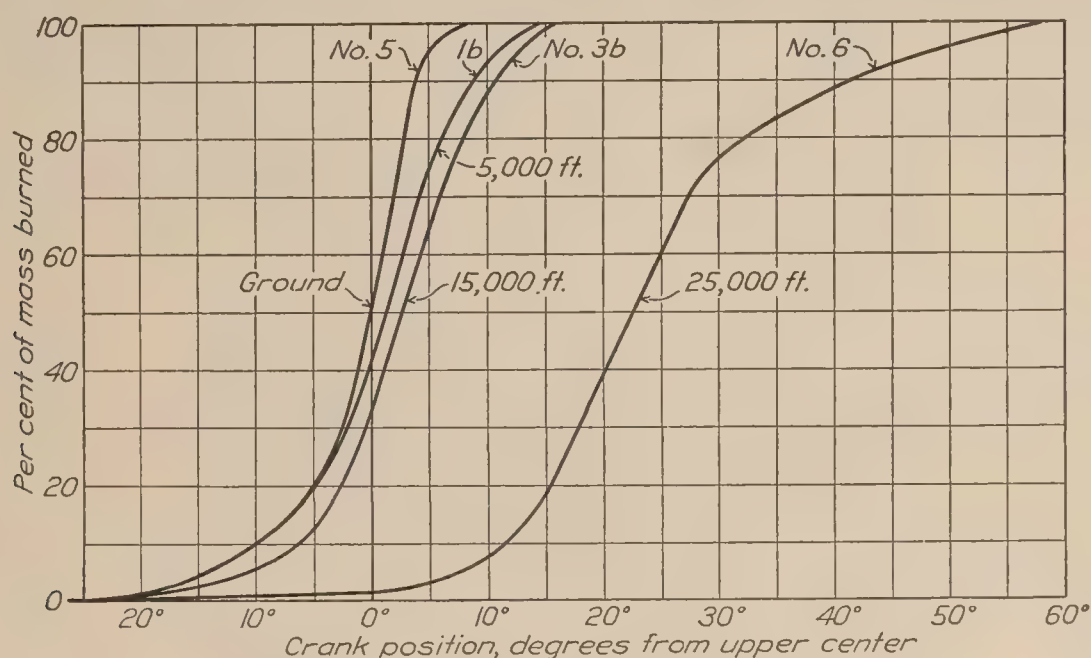


FIG. 6

runs would vary in the same manner with pressure. If it is assumed that the flame advances radially from the point of ignition, flame velocities can be estimated for the two cases by means of Formula 1.³ The calculated velocities are plotted in Figure 8, and contrary to expectations, do not vary in the same manner with pressure for the two cases. The most plausible explanation for the fact that all of the points plotted in Figure 8 do not fall on the same smooth curve would seem to be that the areas of the flame fronts in the actual engine are not such as would be

³ The method of calculating velocity is given in detail in Appendix II.

expected from the theoretical picture in Figure 1, and that the estimated velocities therefore reflect the errors involved in assuming this radial advance.

COMBUSTION TIME

It is obvious that the time required to completely burn the charge must affect the power and specific fuel consumption of an internal-combustion engine. Data have been presented

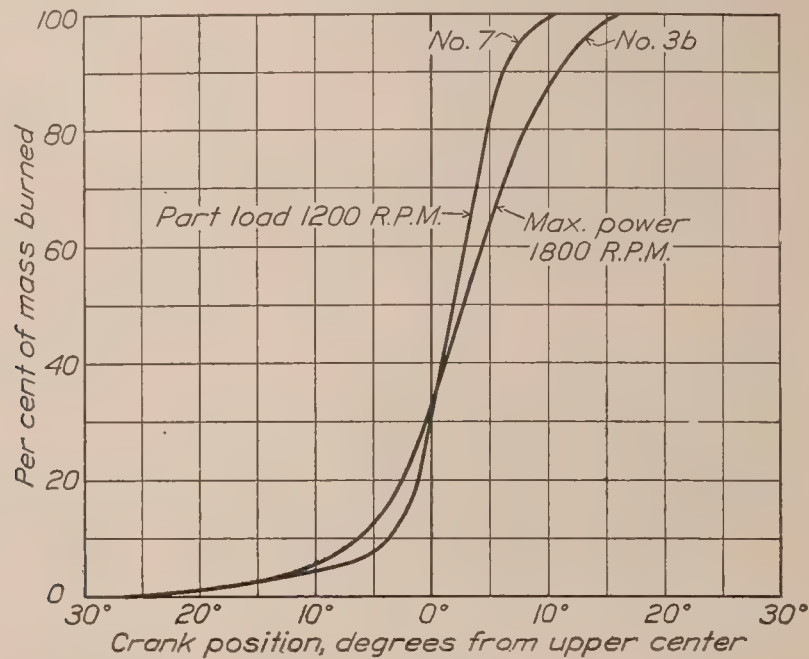


FIG. 7

from time to time showing this effect to be surprisingly small. For the most part these presentations have dealt with what happened and have assumed that the reader knew why it happened. While, in general, this assumption may be justified, it is believed that a somewhat detailed discussion of the reasons underlying this effect may be of value.

In the theoretical Otto cycle, it is assumed that the charge is completely burned at upper

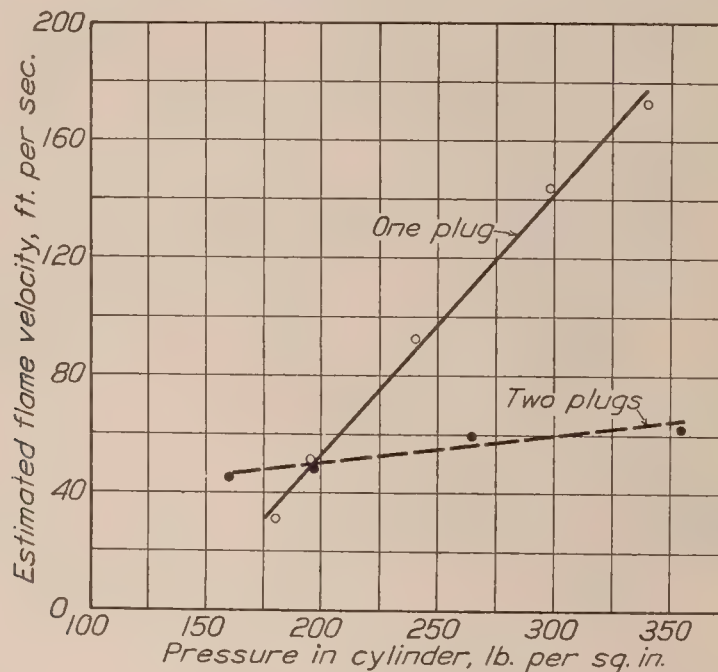


FIG. 8

dead center. The efficiency under such conditions depends only on the expansion ratio which is the ratio between the volumes above the piston at the end and at the beginning of the power stroke. The efficiency is given by the expression

$$E = 1 - \frac{1}{r^{n-1}}$$

where E is what is commonly known as the air cycle efficiency, r is the expansion ratio and n is the ratio between the specific heats at constant pressure and constant volume, which for air is approximately 1.4.

If the ignition of the charge is delayed, but the charge is still assumed to burn completely in a single instant, the efficiency obtainable will be less than was the case when the charge was burned at top center, as the volume above the piston will be greater at the time of combustion than when the charge is burned at top center, and hence the expansion ratio will be less.

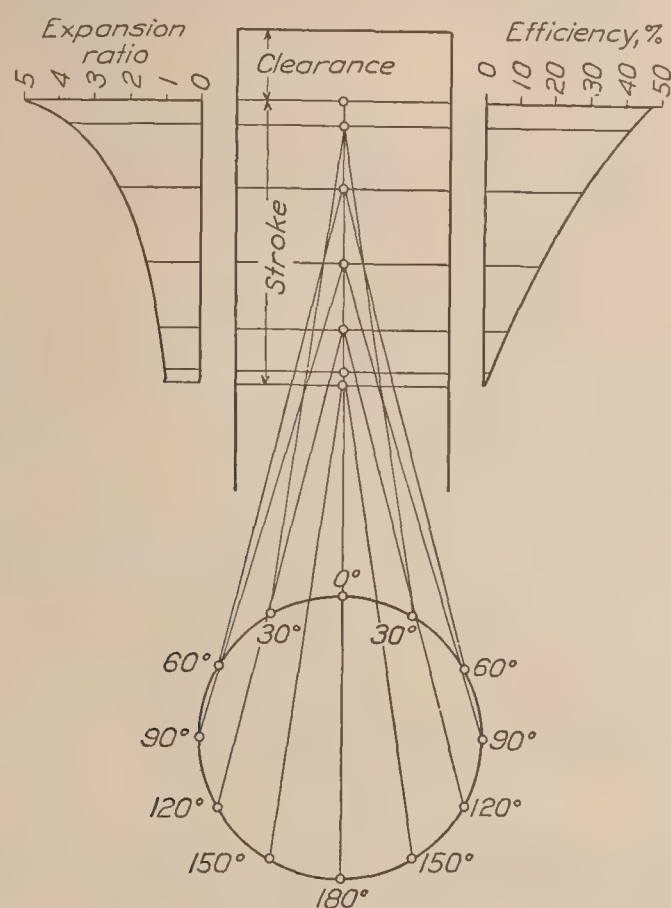


FIG. 9

If now the charge is burned—again instantly—with the piston in the position last considered but before center instead of after center, additional work will be required to compress the burned charge to dead center. However, in the absence of heat loss, this energy will be returned on the power stroke and the effect on engine performance will be the same as in the previous case where the charge was burned after center.

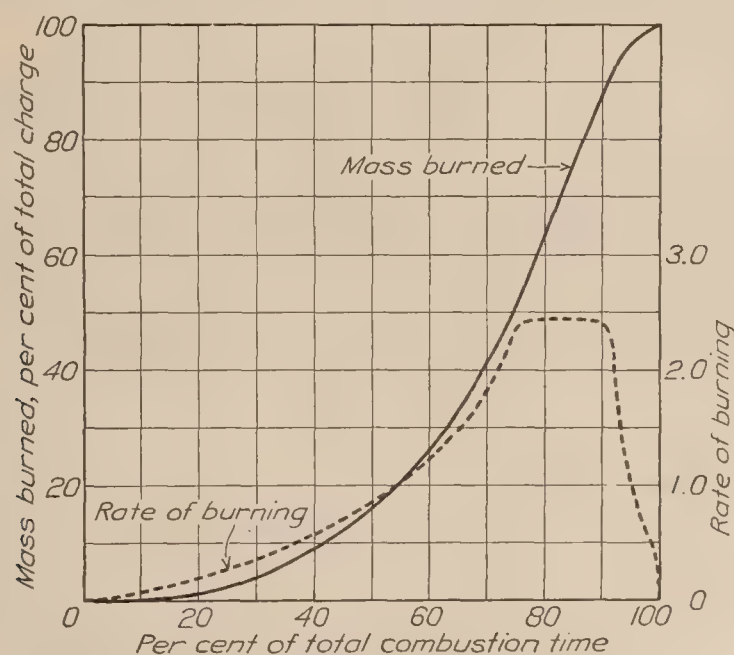


FIG. 10

In the actual engine the charge is, of course, not burned instantly but combustion continues over an appreciable part of the cycle. However, the efficiency obtainable from any small portion of the charge may be calculated as outlined above from the position of the piston at the time that portion is burned.

Figure 9 shows the positions of the top of the piston corresponding to several crank positions for a typical engine. If the expansion ratio based on upper dead center is 5 to 1, then the expansion ratios for portions of the charge burned at other positions of the piston are shown on the left in Figure 9. The air cycle efficiencies corresponding to these expansion ratios are plotted on the right in the same figure.

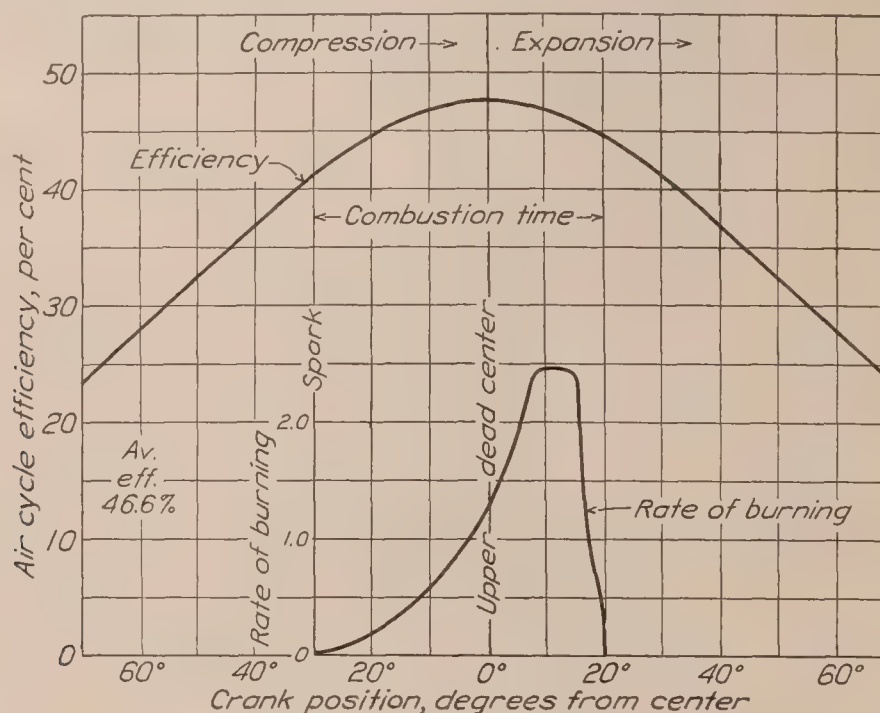


FIG. 11

It is now necessary to determine how much of the charge is burned at each position of the crank, or, in other words, the rate of burning at various stages of the combustion. This information can be obtained from the curves in Figures 4-7. Curve No. 1a in Figure 4 is typical of normal combustion, and to make the case perfectly general this curve has been replotted as the

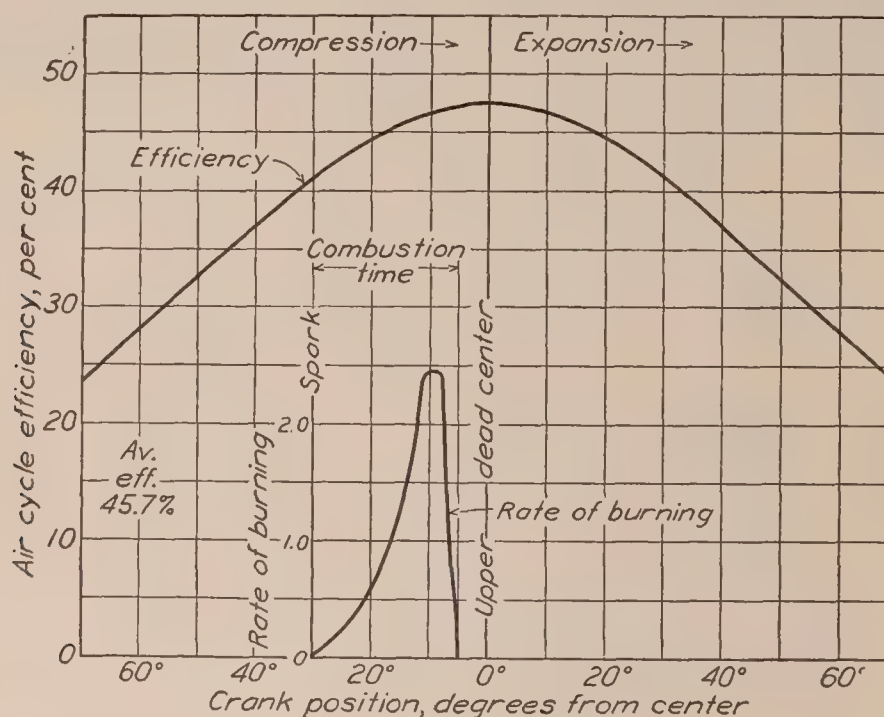


FIG. 12

solid line in Figure 10. The slope of this line is plotted as a dotted line in the same figure and represents the mass rate of burning at each instant during combustion. From this curve the amount of charge burned during any small increment of crank travel may be determined.

From the information in Figures 9 and 10 the average air cycle efficiency for the whole combustion can be computed, as illustrated in Figure 11. The upper curve in the figure gives the air cycle efficiencies corresponding to different crank positions as obtained from Figure 9.

The lower curve is the rate of burning taken from Figure 10, it being assumed that the charge is completely burned during 50° of crank travel and that the spark advance is 30° . The average efficiency for this particular operating condition is obtained by multiplying the amounts of charge burned during successive small increments of crank travel by the corresponding efficiencies and dividing the sum of the products so obtained by the total amount of charge burned, the result in the case being 46.6 per cent.

Assume now that the total time required to burn the charge is only one-half as great as before; that is, combustion is completed in 25° of crank travel instead of 50° . With a 30° spark advance the efficiency and rate curves would be as shown in Figure 12, and the average efficiency for this case is 45.7 per cent.

If combustion required 100° of crank travel and a spark advance of 30° was still retained, the curves would appear as in Figure 13 and the average efficiency would be only 35.7 per cent. So far as this analysis is concerned the reduction or increase in the combustion time as shown in Figures 12 and 13 may result from either a change in actual time of burning due to a change in fuel, mixture ratio, or operating conditions, or merely from a change in engine speed.

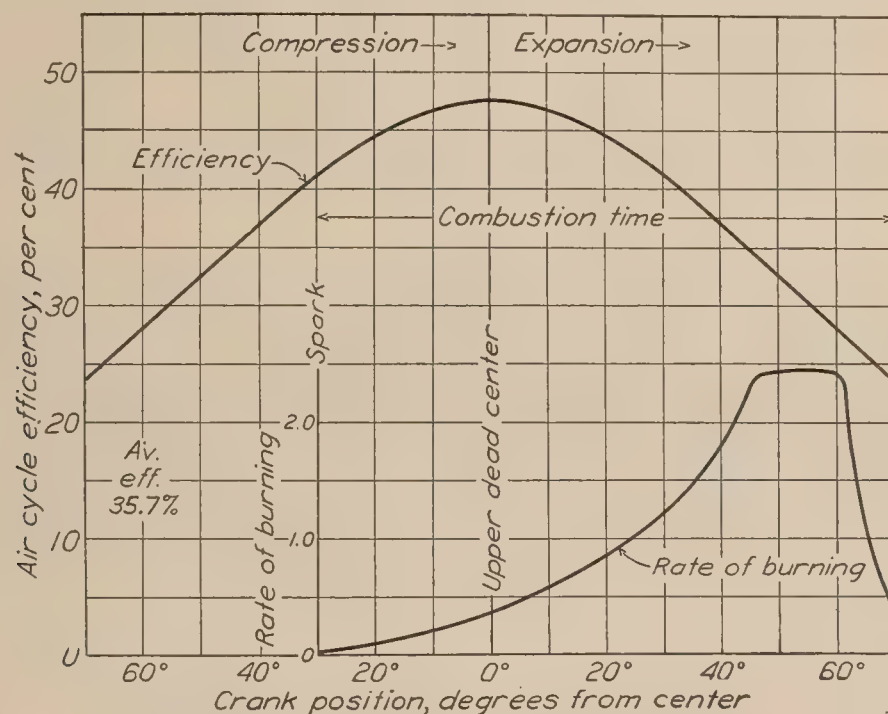


FIG. 13

SPARK ADVANCE

It is quite evident that 30° is too much spark advance for the rapid combustion shown in Figure 12 and not enough for the slow combustion shown in Figure 13. These two figures demonstrate clearly the need for a variable spark advance which can be adjusted to obtain the greatest power and economy possible with each different rate of combustion. As the spark advance does not affect the amount of charge that enters the cylinder, the spark advance that gives the highest average air cycle efficiency will give both maximum power and minimum specific fuel consumption.

Average efficiencies for values of spark advance other than 30° can be determined by shifting the rate curves along the horizontal axes of the charts to each desired spark advance and repeating the calculations described above. For example, Figure 14 shows the rate curve for the 50° combustion time set for values of spark advance of 60° , 40° , 20° , and 0° . The average efficiency for each setting is plotted as a circle against the corresponding spark advance. The peak of the curve drawn through these points gives the optimum spark advance and the maximum efficiency obtainable with this combustion time. This average efficiency curve is reproduced in Figure 15 where it may be compared with similar curves computed for combustion times of 25° and 100° of crank travel and for the theoretical case of instantaneous combustion.

The optimum spark advance and the maximum efficiency corresponding to each of the several combustion times have been taken from the curves in Figure 15 and plotted as circles against combustion time in Figure 16. It will be observed that the spark advance required for

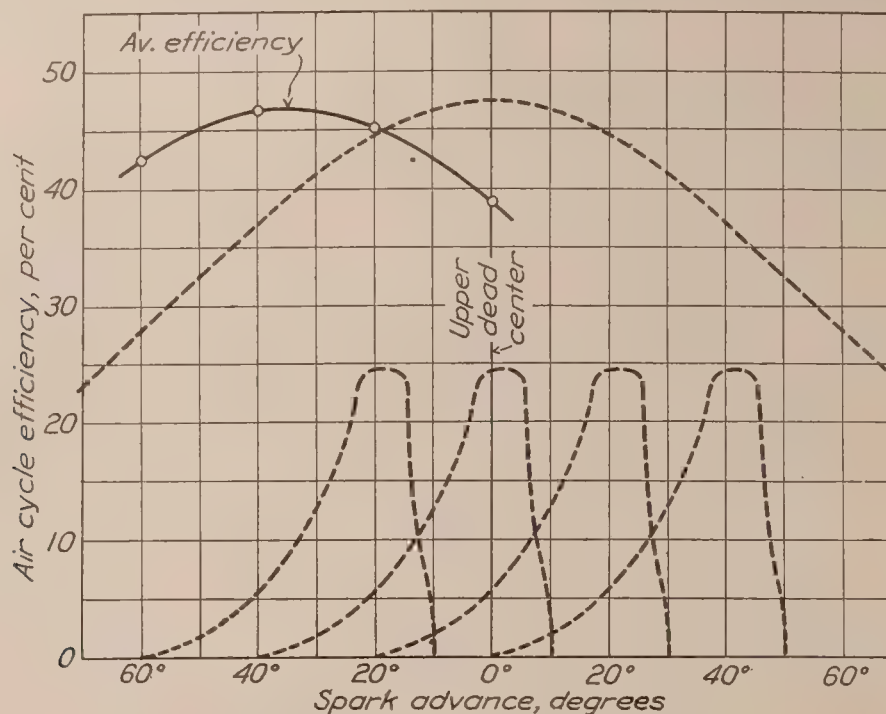


FIG. 14

highest efficiency is radically different for the different combustion times and agrees very well with Upton's rule (Reference 1), based on experimental data, viz: "The optimum spark advance is such that the half pressure rise occurs at the dead center, and that this stage of the pressure rise occurs practically at 75 per cent of the explosion time after ignition." This rule is represented by the dotted line in Figure 16. This figure also shows that the efficiencies obtainable with widely different combustion times are not greatly different, provided the optimum spark advance is used in each case. This also is in agreement with experimental results.

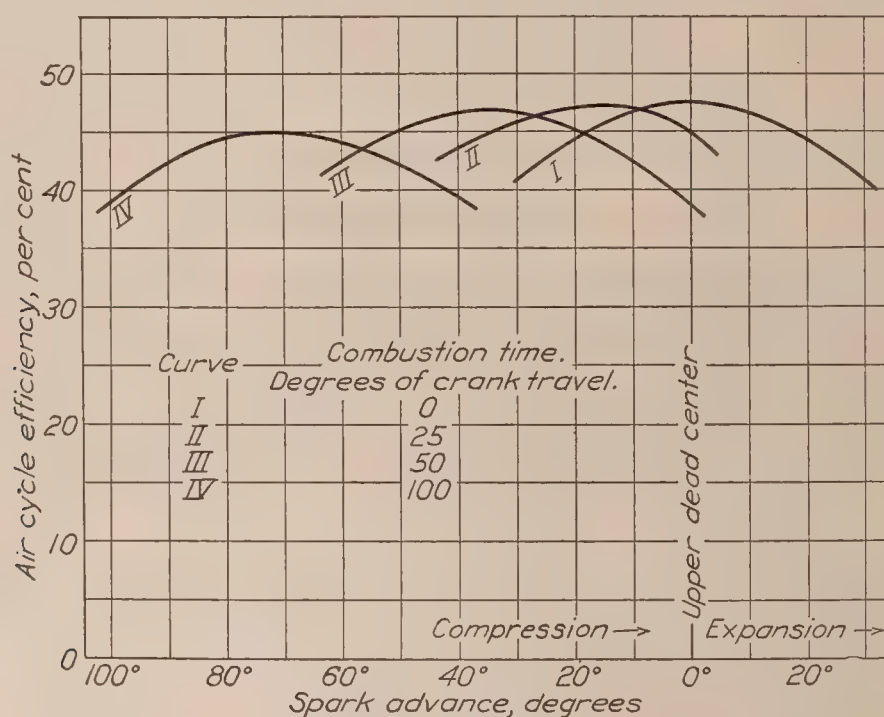


FIG. 15

RATE OF BURNING

Throughout the foregoing discussion of the effect of combustion time and spark advance on engine performance the charge was assumed to burn at a rate represented by the dotted curve in Figure 10. For actual engines the shape of this rate curve will vary somewhat, depend-

ing on engine design and operating conditions. However, it may be demonstrated by substituting a different rate curve in Figures 11-14, that considerable difference in the shape of the rate curve will have very little effect on engine performance provided the proper spark advance is maintained. Thus the rate curve shown in Figure 2 is quite different in shape from the one shown in Figure 10, but the maximum efficiencies computed on the basis of these two curves differ by less than 1 per cent.

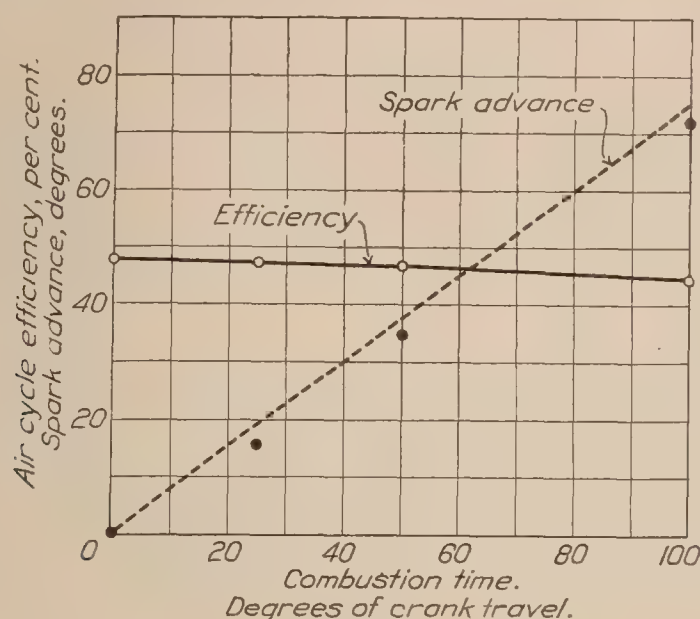


FIG. 16

CONCLUSIONS

From a theoretical standpoint, from the analysis of indicator cards, and from observation of actual engines, it is evident that the time required for complete combustion of a charge varies considerably with different engine designs and operating conditions. It is also known that the rate of burning at any particular instant after ignition may differ even in cases where the total combustion time is the same. Both the rate of combustion and the time required for complete burning of the charge have an effect on the power and economy of the engine. The greatest power and economy are, of course, attained in the theoretical case of instantaneous combustion at upper dead center. The slower combustions obtainable in practice may result in considerably reduced efficiencies if improperly timed with respect to piston position. However, the maximum theoretical performance may be approached very closely with a wide range of combustion times and rates, provided the proper spark advance is maintained for each particular condition.

REFERENCE

1. The Society of Automotive Engineers, Transactions, Vol. 18, Part II, p. 117.

BUREAU OF STANDARDS,
Washington, D. C., April 2, 1927.

TABLE I.—Operating conditions during test of 300-horsepower, 8-cylinder aviation engine in the altitude chamber at the Bureau of Standards

Curve numbers	1 (a & b)	2	3 (a & b)	4	5	6	7
"Altitude"—ft	5,000	5,000	15,000	15,000	Ground.	25,000	15,000
Speed—R. P. M.	1,800	1,800	1,800	1,800	1,800	1,800	1,200
Load	Maximum.	Maximum.	Maximum.	Maximum.	Maximum.	Maximum.	Part.
Spark advance—deg.	26.5	26.5	26.5	26.5	26.5	26.5	26.5
Number of plugs firing	2	1	2	2	2	2	2
Air density at carburetor, lb./cu. ft.	0.068	0.066	0.047	0.048	0.081	0.034	0.048
Mixture ratio	12.25:1	12.8:1	12.9:1	14.7:1	12.6:1	15.4:1	8.2:1
Weight of charge per hour—lb.	2,293	2,288	1,550	1,553	2,757	1,094	624

APPENDIX I

METHOD OF CALCULATING RATE OF BURNING FOR RADially ADVANCING FLAME FRONT SHOWN IN FIGURE 1

A circle 10 inches in diameter was drawn and was divided into sections one-tenth of an inch wide by circular arcs of increasing radius drawn about an "ignition point" on the circumference of the 10-inch circle. The area of each of these sections was determined by measuring the average length of the section and multiplying by one-tenth inch. A curve was then plotted showing the area (or volume) behind the flame for each different flame position or radius from the point of ignition.

It was assumed that the cylinder was filled with a homogeneous charge at 600° C. absolute and that during the first interval of time "*t*" after the occurrence of the spark the first one-tenth inch section of the charge was burned. For purposes of calculation this portion of the charge was assumed to burn at constant volume, its temperature being raised 2,700° in the process, the final temperature being 600 + 2,700 = 3,300°. The ratio of pressures before and after burning will be equal to the ratio of temperatures or

$$\frac{p_u}{p_b} = \frac{600}{3,300}$$

where—

p_u = original pressure in the cylinder before ignition
 p_b = pressure of burned gases before expansion

The burned gases are then assumed to expand, compressing the unburned gases ahead of them, according to the equation $pv^{1.3} = \text{constant}$, until the pressure throughout the cylinder is uniform. (The exponent 1.3 was selected because it is the approximate mean between an exponent for compression of 1.39 and an exponent for expansion of 1.22 as determined from indicator cards.) The following equations will then apply:

$$p_b v_b^{1.3} = P V_b^{1.3} \text{ expansion of burned gases.} \quad (1)$$

$$p_u v_u^{1.3} = P V_u^{1.3} \text{ compression of unburned gases.} \quad (2)$$

where—

v_b = original volume of burned gases before expansion.
 v_u = original volume of unburned gases before compression = $V - v_b$.
 V = total volume of cylinder.
 V_b = final volume of burned gases after expansion.
 V_u = final volume of unburned gases after compression = $V - V_b$.
 P = final uniform pressure throughout the cylinder.

The simultaneous equations (1) and (2) may be reduced to the following general form:

$$\log \left(\frac{V}{V_b} - 1 \right) = \log \left(\frac{V}{v_b} - 1 \right) + \frac{\log \frac{p_u}{p_b}}{1.3}$$

This equation may be solved for V_b the volume of the burned gases after expansion, and the position of the flame front after the first interval of time "*t*" may thus be determined.

In the next equal interval of time the flame will proceed into the unburned mixture another one-tenth of an inch, constant volume burning being assumed. The increment of volume corresponding to this second one-tenth of an inch of movement can be found from the curve

of volumes and flame positions. Since this new increment of volume contains compressed gas, its density must be known before its mass can be calculated. The total mass of unburned gas before the second increment is burned is $V - v_b$, mass being proportional to volume in the charge at original conditions. The volume of this total mass of unburned charge after compression by the first burn is $V - V_b$, and its density will therefore be $\frac{V - v_b}{V - V_b}$. Multiplying this density by the second increment of volume will give the mass burned during the second time interval. Adding this to the mass burned during the first interval will give the total mass burned after two intervals of time. In the calculations it is now assumed that this total mass is burned as a single unit. It thus becomes the new v_b in the equation and its volume after expansion is determined as in the case of the original increment. The computations are repeated for equal time intervals until the flame has traveled entirely across the cylinder. Such computations supply the data for plotting both the total mass burned and the mass rate of burning.

APPENDIX II

METHOD OF ESTIMATING FLAME VELOCITIES AT ANY INSTANT DURING COMBUSTION

$$R_m = A V D$$

R_m = mass rate of burning in pounds per second.

A = area of flame front in square feet.

V = velocity of flame front with respect to unburned gas in feet per second.

D = density of unburned gas in pounds per cubic foot.

Take, for example, curve No. 2 (fig. 4). Data taken during the engine test make it possible to transpose the values of per cent of mass burned to pounds burned and to express crank position as seconds of time after ignition. If curve No. 2 is replotted on these coordinates, its slope at any point will be the mass rate of burning (R_m) in pounds per second at that point.

The density of the unburned charge at any instant will be equal to the weight of the unburned charge divided by its volume. Consider, for example, the point at which 80 per cent of the charge is burned, the crank position at this point being given in Figure 4. The weight of the unburned portion is 20 per cent of the total weight of charge in the cylinder. If no burning had taken place this portion would occupy 20 per cent of the total volume above the piston, and its pressure would be the engine compression pressure for the given piston position as determined from the straight compression line on the indicator card. The burning of 80 per cent of the charge has, however, compressed the unburned 20 per cent to a smaller volume and a higher pressure according to the equation $pv^{1.4}$ constant.* This higher pressure is found on the indicator card and the final volume can therefore be calculated.

With the relative volumes of burned and unburned gas known, the position of the flame front in the cylinder can be determined and its area computed from the cylinder dimensions. In making these calculations the flame is assumed to advance across the cylinder in the manner illustrated in Figure 1. In the case of curve No. 1a, this advance takes place simultaneously from both ends of the diameter.

With values of R_m , D , and A thus determined the equation $R_m = A V D$ is solved for V .

* An average exponent of 1.39 for compression has been determined from indicator cards.

REPORT No. 277

THE COMPARATIVE PERFORMANCE OF AN AVIATION ENGINE AT NORMAL AND HIGH INLET AIR TEMPERATURES

By ARTHUR W. GARDINER and OSCAR W. SCHEY
Langley Memorial Aeronautical Laboratory

REPORT No. 277

THE COMPARATIVE PERFORMANCE OF AN AVIATION ENGINE AT NORMAL AND HIGH INLET AIR TEMPERATURES

By ARTHUR W. GARDINER and OSCAR W. SCHEY

SUMMARY

This report presents some results obtained at the Langley Memorial Aeronautical Laboratory of the National Advisory Committee for Aeronautics during an investigation to determine the effect of high inlet air temperature on the performance of a Liberty 12 aviation engine. The purpose of this investigation was to ascertain, for normal service carburetor adjustments and a fixed ignition advance, the relation between power and temperature for the range of carburetor air temperatures that may be encountered when supercharging to sea level pressure at altitudes of over 20,000 feet and without intercooling when using plain aviation gasoline and mixtures of benzol and gasoline.

Laboratory tests were made at full throttle over the speed range from 1,400 to 1,800 R. P. M., in which the pressure at the carburetor and exhaust was maintained sensibly constant and the inlet air temperature varied from 45° to 180° F. The range of mixtures was that normally used in flight. Plain aviation gasoline, a mixture consisting of 30 per cent (by volume) of commercial benzol and 70 per cent gasoline, and a mixture of 65 per cent benzol and 35 per cent gasoline were used. Additional tests were made with a Wright E-4 aviation engine.

The results show that for the conditions of test, both the brake and indicated power decrease with increase in air temperature at a faster rate than given by the theoretical assumption that power varies inversely as the square root of the absolute temperature. On a brake basis, the order of the difference in power for a temperature difference of 120° F. is 3 to 5 per cent. The observed relation between power and temperature when using the 30-70 blend was found to be linear. But, although these differences are noted, the above theoretical assumption may be considered as generally applicable except where greater precision over a wide range of temperatures is desired, in which case it appears necessary to test the particular engine under the given conditions.

INTRODUCTION

In conducting flight research with supercharged engines equipped with a gear-driven Roots type supercharger, no air intercooler has been employed, thus giving rise to a condition where, with full supercharging maintained to 20,000 feet, air temperatures before the carburetor as high as 160° F. have been observed. As a result of these high temperatures the power of the engine is obviously impaired, owing to a reduction in the weight of charge inducted and, possibly, to the existence of temperature conditions within the engine conducive to appreciable detonation with a consequent further loss in power. A blended fuel, consisting of 30 per cent benzol and 70 per cent gasoline, has been used to obviate this latter possibility.

In view of the above conditions it was desirable to determine the reduction in power at this high air temperature and thus obtain information of aid in ascertaining the advisability of providing an intercooler and to ascertain the gain, if any, that is obtained by using the special fuel.

It is generally conceded that, for a given compression ratio, the character of combustion obtained with a given fuel is dependent to some extent upon the particular engine in which it

is used. Moreover, there is some disagreement among investigators regarding the magnitude of the influence of temperature on the tendency for detonation. For the condition of normal combustion, White (Reference 3) and Sparrow (Reference 4) favor the application of a general law for correcting horsepower measurements for changes in air temperature. Sparrow has considered in detail the various factors affecting the density of the induced charge and has arrived at the conclusion "that the assumption that the indicated horsepower of an engine varies inversely as the square root of the absolute temperature has sufficient justification to warrant its adoption as a basis for correcting horsepower measurements to a standard temperature." The tests on which this conclusion was based covered a temperature range from -20° to $+40^{\circ}$ C. and were made at a time when higher temperatures were of comparatively little practical importance. A review of available information indicated that the application of a general law for the variation of power with air temperature, especially for a wide range of temperature and air-fuel ratios, may not give the precision desired.

Investigations have shown that the air-fuel ratio employed has a marked effect on the power variation with temperature. Brown found (Reference 6) that the power was actually increased at high temperatures when using very lean mixtures; that the power remained practically constant from 80° to 250° F. when using a mixture ratio slightly richer than the chemical combining ratio, and that the power decreased with increase in temperature when using still richer mixtures, the decrease being greater the richer the mixture. Berry obtained (Reference 5) that an appreciable decrease in power resulted from an increase in temperature for mixture proportions equal to and richer than that for the chemical combining ratio. In both of these investigations, maximum power occurred with air-fuel ratios between 12 and 12.5 at all temperatures. Sparrow states (Reference 7) that the maximum power of aviation engines is usually obtained with air-fuel ratios between 12.5 and 14.3 for the range of pressures and temperatures encountered in flight and that the mixture ratio giving maximum power is sensibly constant for all entrance air temperatures. Gibson found (Reference 8) that the power of an engine, without water-jacketing on the manifolds, decreased most rapidly with increase in entrance air temperatures when using lean mixtures, and least rapidly when using over-rich mixtures.

Therefore the present investigation was undertaken at the Langley Memorial Aeronautical Laboratory of the National Advisory Committee for Aeronautics to determine, for normal service carburetor adjustments and a fixed ignition advance, the performance of a Liberty 12 aviation engine over a wide range of air temperatures, and to ascertain the comparative performance under these conditions when using plain gasoline and two fuel mixtures of benzol and gasoline. Some tests were also made with a Wright E-4 aviation engine.

DESCRIPTION OF APPARATUS AND METHODS

A standard Liberty 12 aviation engine, 5-inch bore by 7-inch stroke, having a compression ratio of 5.4 to 1, was used for the major part of the investigation. It was equipped with two Stromberg inverted carburetors, Model NA-L5A, of the duplex type, having fixed main metering jets, No. 44 drill. The manifolds used with these carburetors are water-jacketed, so that a portion of the internal surface is backed by water at approximately the temperature of the water discharged from the engine, in this case about 160° F.

A standard Wright E-4 aviation engine, 4.72-inch bore by 5.12-inch stroke, having a compression ratio of 5.3 to 1, was also used. It was equipped with a single Stromberg carburetor, Model NA-U5A, also of the duplex type, having fixed main metering jets, No. 47 drill. The intake manifolds on this engine are also water-jacketed.

In each case the engine was coupled to a 300/400 HP. electric cradle dynamometer, which was used to absorb the engine output and to motor the engine during friction tests.

Two methods were employed for heating the air supplied the engine. For all tests with the Wright engine and for some tests with the Liberty engine, a separately driven Roots supercharger was used, but for the major part of the tests with the latter engine, a lagged heating box, housing several large-size steam radiators, was used. When using the supercharger, the

air was heated by throttling the intake. In making tests at low temperatures, air was piped from outside the building.

Plain domestic aviation gasoline, conforming to standard Army specifications, a mixture of 30 per cent benzol (commercial, 90 per cent) and 70 per cent gasoline (30-70 blend) and a mixture of 65 per cent benzol and 35 per cent gasoline (65-35 blend) were used during tests of the Liberty engine. The 30-70 blend was used in the Wright engine tests.

Inlet air temperatures were measured at a point directly before the carburetors. The temperature of the discharge water was maintained about 160° F. for both engines.

Friction power was measured by motoring the engine, with the throttle open and fuel and ignition off, immediately following a series of power runs; the air pressure, and the air, water, and oil temperatures were held practically the same as for the preceding power runs.

The test procedure consisted in determining the engine performance, with a given fuel and mixture condition and with a fixed spark advance of 30° for the Liberty and 27° for the Wright engine, over the interesting speed range at several nominally constant air temperatures from 45° to 180° F. After conditions were stabilized, a run was made extending over a one-minute interval, during which two complete sets of readings were taken, one at the beginning and another near the end of the interval; the average of the two readings was taken as the average for the run. Timing of the rate of fuel flow was started at the beginning of the run and extended somewhat over the one-minute interval, but conditions were stabilized sufficiently to obviate introducing appreciable error in the fuel measurements from this cause.

Two carburetor settings were used—i. e., with the mixture control maintained in the full-rich position (rich) and with the control adjusted to give the approximate condition of maximum power with best economy (best setting).

Observed power and mean effective pressures were corrected to the standard pressure of 29.92 inches of mercury; the average correction was considerably less than 1 per cent. Specific fuel consumption was based on the observed power and rate of consumption.

RESULTS

The results of the tests are presented in the form of curves (figs. 1 to 14, inclusive).

Due to the test procedure employed, it was difficult to duplicate the air temperatures in the various series of tests, so that cross plots are relied upon to give comparative information at any given temperature and also to determine the variations with temperature. Values for mean effective pressure, friction power, hourly fuel consumption, and manifold depressions taken from the faired curves of the original plots are shown on the cross plots to indicate the precision with which the latter are determined. The most probable values at the arbitrary base temperatures, 59° F. for the Liberty tests and 70° F. for the Wright tests, have been used in establishing the percentage ratios for the performance at other temperatures; these base values are given on the several curves.

Fuel consumption data were not obtained for the Wright engine. Also, only a few friction power tests were made with this engine, and as these did not indicate any consistent variation between friction power and air temperature, one curve has been drawn averaging all data. (Fig. 3.)

As the power with a given fuel was practically the same for both mixture adjustments, the cross-plot curves of mean effective pressure against air temperature for several engine speeds have been drawn averaging all data for each fuel irrespective of mixture adjustment. (Figs. 6 and 7.) Likewise, on the cross plots showing the percentage variation in mean effective pressure with change in temperature (figs. 8 and 9), the plotted point at a given temperature represents the average of the individual percentages for the several speeds.

Data on fuel consumption were, in some cases, erratic, due to the short time intervals during which the rate of fuel flow was measured and the probability of errors in timing, but the information obtained is sufficiently precise to indicate the order of the variation with air temperature.

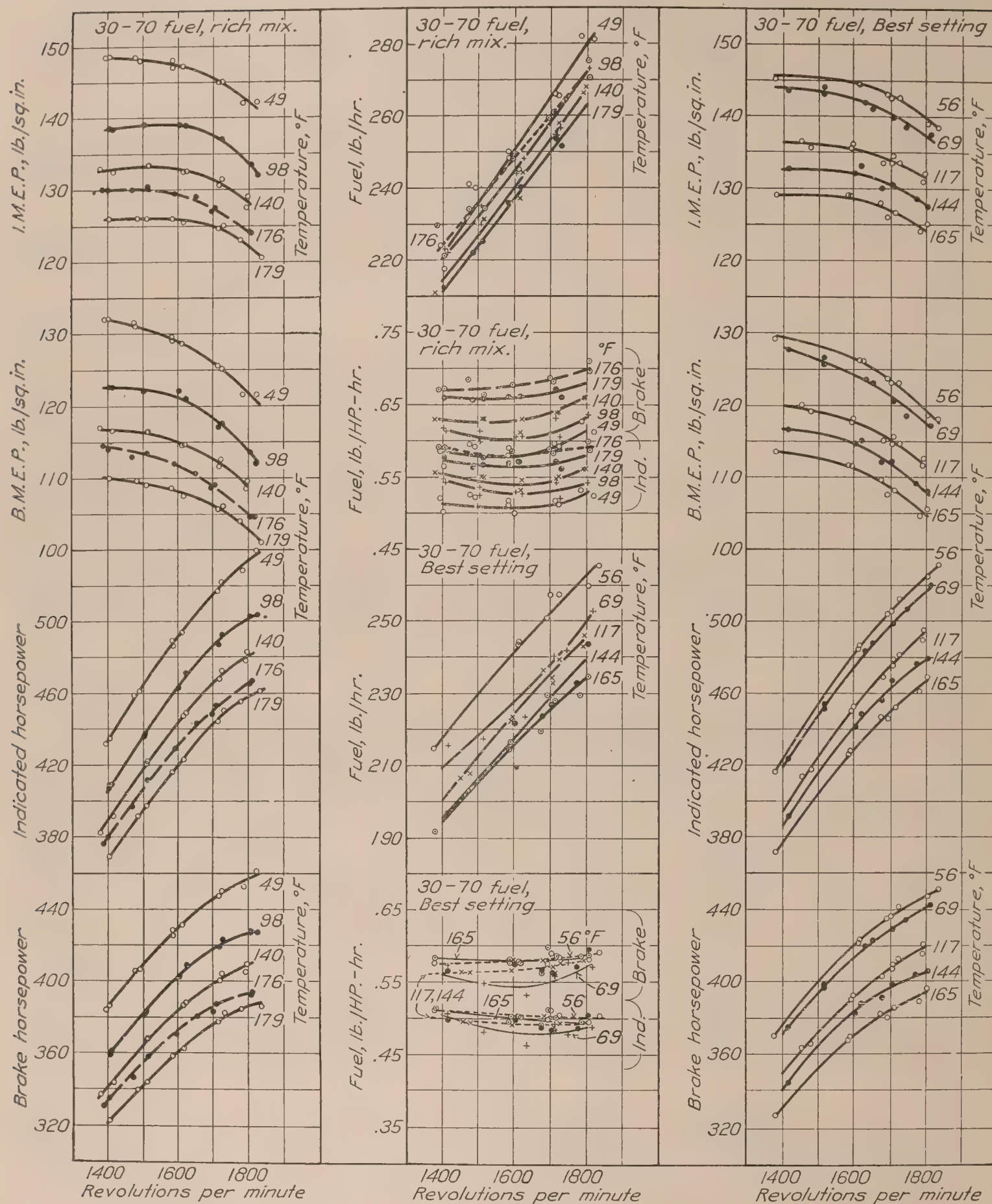


FIG. 1.—Liberty 12 engine. Full throttle power and fuel consumption at various air temperatures using a fuel mixture containing 30 per cent benzol and 70 per cent aviation gasoline. Full rich mixture and best setting. Stromberg inverted carburetors, Model NA-L5A with 1½ in. Venturi and No. 44 drill main metering jets. Fixed ignition advance 30°. Dash curves for fuel mixture containing 65 per cent benzol and 35 per cent gasoline with full rich mixture. Figures on curves denote average air temperatures for individual series of tests

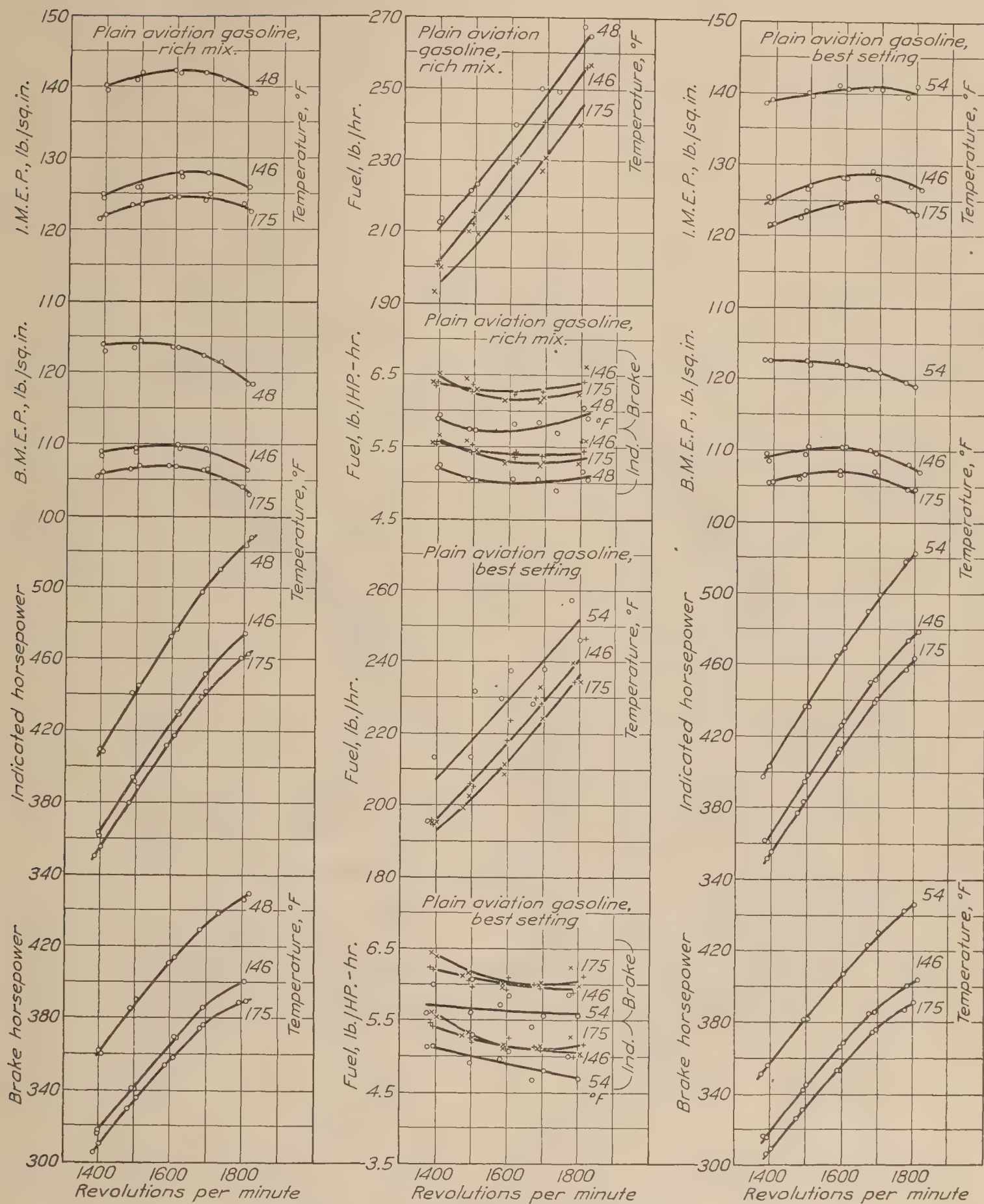


FIG. 2.—Liberty 12 engine. Full throttle power and fuel consumption at various air temperatures using plain domestic aviation gasoline. Full rich mixture and best setting. Same carburetor, carburetor settings, and ignition advance as given under Figure 1. Figures on curves denote average air temperatures for individual series

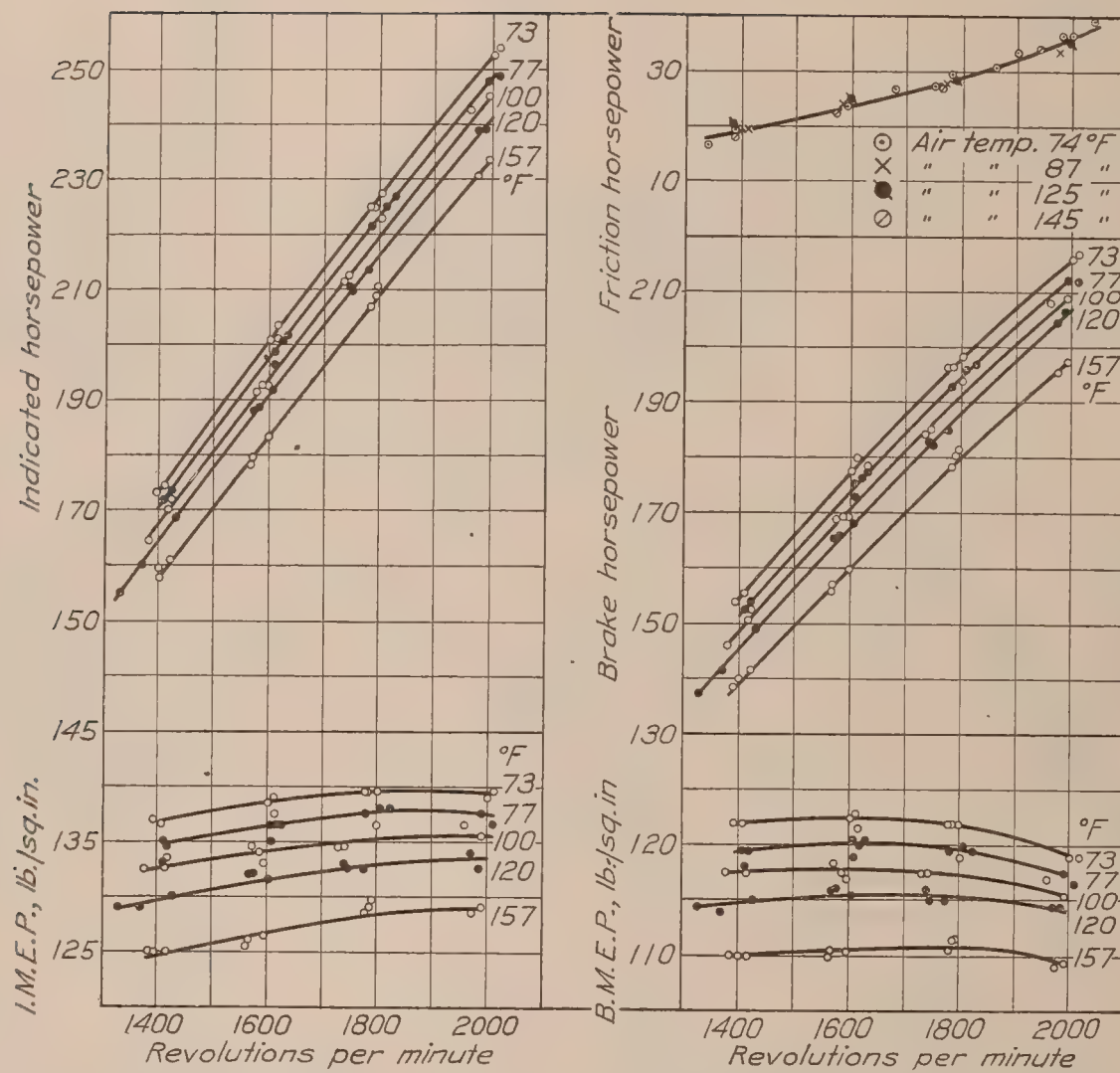


FIG. 3.—Wright E-4 engine. Full throttle power at various air temperatures using a fuel mixture containing 30 per cent benzol and 70 per cent aviation gasoline. Full rich mixture. Stromberg carburetor Model NA-U5A, No. 47 main metering jets. Fixed ignition advance 27°. Friction power curve at upper right. Figures on curves denote average air temperatures for individual series

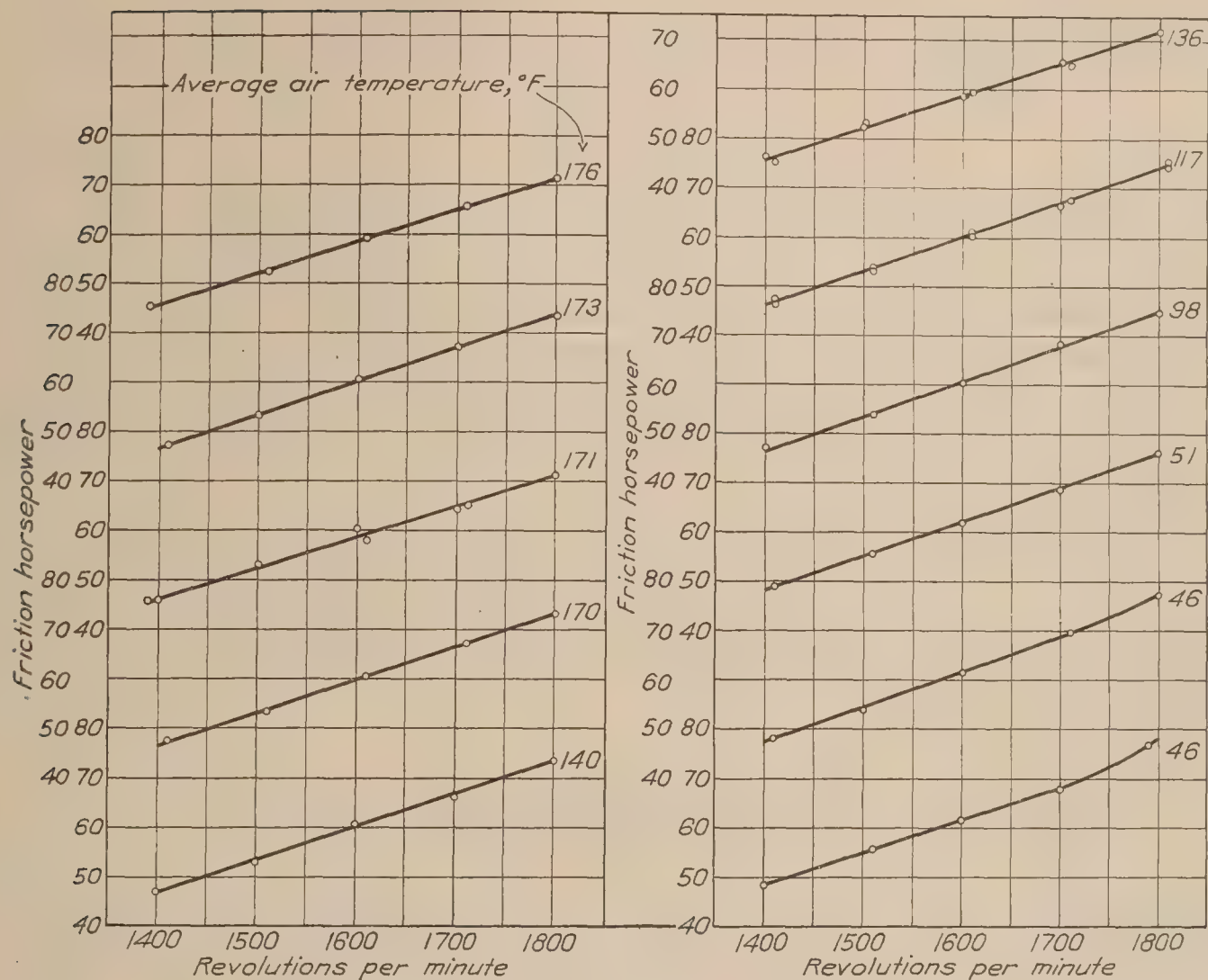


FIG. 4.—Friction power of Liberty 12 engine at various air temperatures

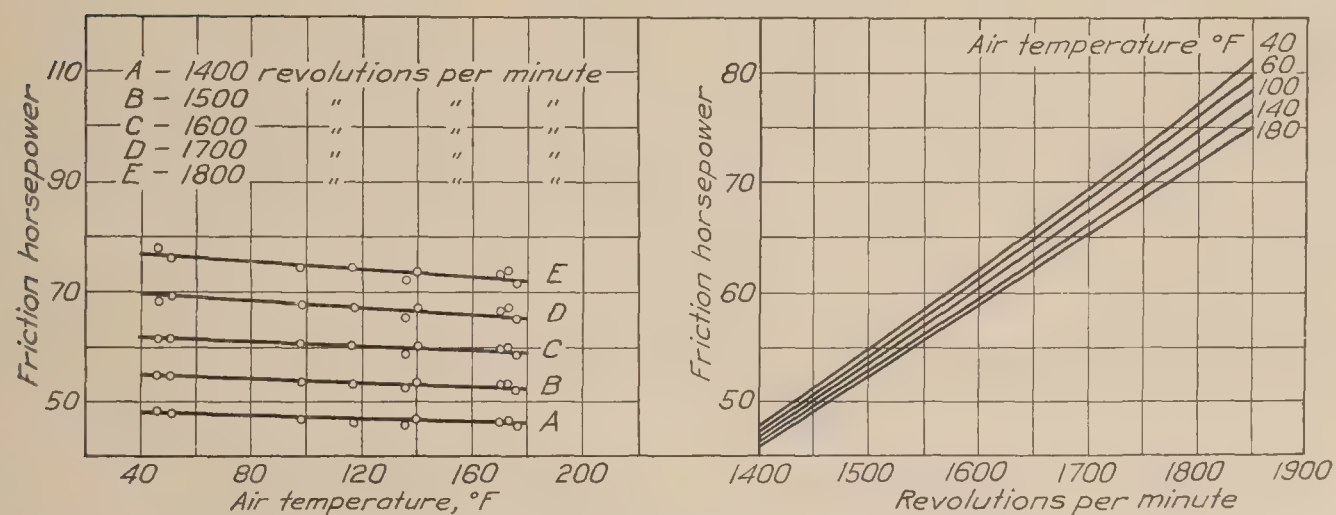


FIG. 5.—Variation in friction power of Liberty engine with temperature (cross plot of curves, fig. 5) and composite curves of friction vs. R. P. M. at various temperatures (cross plot of upper group, this figure)

The power obtained with the Liberty engine at normal temperatures when using the 30-70 blend was appreciably greater than that obtained with average service engines. The power obtained with gasoline was about normal for this engine, but detonation was encountered at all temperatures, as evidenced by free carbon in the exhaust and the fact that leaks developed in practically all of the cylinder jackets during the period of testing with this fuel.

Fuel consumption for the Liberty engine was above the average.

The power developed by the Wright engine at normal temperature when using the 30-70 blend was about normal.

DISCUSSION

TEST CONDITIONS

In this investigation the flight conditions of the supercharged engine were simulated, especially with regard to the fuel flow conditions existing at the carburetors. Air pressure at the entrance to the carburetors and in the float chambers was maintained sensibly constant, as for the condition in flight with sea-level pressure maintained at the carburetors and the float chambers balanced by the supercharging pressure. Tests were not made to simulate flight conditions above the critical altitude of the supercharger-engine unit, where the pressure at the carburetors is reduced below the sea-level standard. Air-fuel ratios were on the rich side of the chemically correct mixture, and probably slightly on the rich side of maximum power mixtures.

In these tests the engine exhausted into air at approximately sea-level pressure. Therefore the effect of the differential pressure existing in flight, between intake and exhaust, on the scavenging of the cylinders, the amount of residual gases left in the cylinders and the combined effect of more complete scavenging coupled with high temperatures on the character of the combustion was not ascertained. The present data are only applicable in showing the independent effect of air temperature.

EFFECT OF FUEL USED ON THE PERFORMANCE OF THE LIBERTY ENGINE AT NORMAL AND HIGH TEMPERATURES

Comparison of the performance of the Liberty engine obtained with the various fuels and mixture conditions at 59° and 176° F. are given below. These temperatures have been chosen because they lie within the extremes of the range of temperatures for most of the tests; the higher temperature is the average of the single series of tests made with the 65-35 blend.

For the tests with the 30-70 blend at 59° F., it appears that, in leaning the mixture to obtain the best setting, there resulted a slight decrease in power at all speeds (figs. 6 and 7), probably caused by leaning too far. However, the power obtained with both mixture conditions for this fuel did not vary appreciably at the higher temperatures, and for this reason the cross-plot curves for mean effective pressure have been drawn averaging all data for this fuel irrespective of mixture condition. Although no air measurements were made during the present investigation, by assuming the volumetric efficiencies for the Liberty engine given in Reference 9 as an approximation, it is found that the probable air-fuel ratios obtaining with the 30-70 blend, rich mixture, range from 11.8 to 12.2, or but slightly richer than mixtures giving maximum power. (References 7 and 11.) Values for volumetric efficiencies given in this reference are for the Liberty engine equipped with Zenith carburetors having a common air intake, and as the power obtained with the inverted Stromberg carburetors and separate intake stacks for each carburetor is somewhat greater (Reference 10) than that obtained with the standard Zenith carburetors, the volumetric efficiency with the Stromberg carburetors is probably higher; and the above values for air-fuel ratios should be increased. Assuming the same efficiencies, corresponding values for the 30-70 blend, lean mixture, lie between 12.9 and 13.2, or well within the range of mixtures normally giving maximum power. From the standpoint of fuel mixtures, then, values of mean effective pressure at 59° F. taken from the curves on the above figures should represent fairly closely the maximum power obtainable with this fuel, and as it has been found (References 12 and 13) that a 30-70 blend may be used at normal air temperature

in a single cylinder Liberty test engine for compression ratio up to 6 to 1 without encountering detonation, it may be further reasonably assumed that these values represent the maxima for the engine at this temperature.

The power obtained with plain domestic aviation gasoline at 59° F. departs but little from that obtained with the best Stromberg carburetor adjustments determined in Reference 10. In leaning the mixture to obtain best power and economy with this fuel, the power remained unchanged. Based on the assumed volumetric efficiencies, the air-fuel ratios for the rich mixture lie between 12.5 and 13 and for the best setting, between 13 and 13.3. Even at this low temperature there was considerable detonation, especially at the lower speeds. The brake power obtained with this fuel at this temperature at 1,800 R. P. M. is 1.5 per cent lower than the assumed maximum power for the engine obtained with the 30-70 blend, but there is a marked reduction, about 6 per cent, in the relative power at 1,400 R. P. M. This indicates the loss in power resulting from the use of plain aviation gasoline in this engine under conditions of full throttle at ground level at the lower range of the usual operating speeds, where the volumetric efficiency is a maximum and the higher density of the fuel charge induces considerable detonation. The decrease in detonation at the higher speeds is in accordance with common experience, the primary cause in the case of the Liberty engine being attributable to the marked decrease in volumetric efficiency and the greater proportion of residuals at the higher speeds. That there is a certain amount of detonation in this particular engine at ground level when using gasoline is generally known, but it is not believed that the order of the loss in power at normal temperatures resulting from detonation is generally appreciated.

It is known that gasolines obtained from different sources have varying influences on detonation even though they comply with the same specifications, and it may be that the loss in power caused by detonation was greater in these tests than would occur with a different lot of gasoline.

Comparisons of the performance at a temperature of 176° F. when using the 30-70 blend, the 65-35 blend, and plain gasoline are given below. For the 30-70 blend, reducing the hourly fuel rate 10 to 11 per cent by leaning resulted in no change in power. Maximum power at this temperature was obtained with the 65-35 blend (fig. 8); only the rich mixture was used with this fuel. The brake power with the 30-70 blend was about 2.3 per cent lower than this maximum, ranging from 1.7 per cent lower at 1,800 R. P. M. to 2.5 per cent lower at 1,400 R. P. M. This difference is, apparently, not accounted for on the basis of differences in air-fuel mixtures. Optimum ignition advance was not determined for each fuel; the ignition advance remained fixed at 30°—a service condition. This may have influenced the results to give erroneous general comparisons. However, the indication is that a certain amount of detonation attended the use of the 30-70 blend at this temperature. An estimation of the probable air-fuel ratios at this temperature may be made by assuming that the weight of air charge inducted varies proportionally with the ratio of the indicated mean effective pressure obtained with the 65-35 blend at 176° F. to the indicated mean effective pressure obtained with the 30-70 blend at 59° F., and using the previous air weights determined for the low temperature. If this be permitted for the sake of making a rough approximation, it is found that the air-fuel ratios for the 30-70 blend lie between 11.2 and 11.4 for the rich condition and between 12.4 and 12.6 for the best setting; between 10.7 and 10.9 for the 65-35 blend, rich condition; between 11.7 and 12.2 for gasoline, rich mixture; and between 12.2 and 12.7 for gasoline, best setting. These values are at least comparative among themselves. It may be seen that the mixture for the 65-35 blend is apparently somewhat overrich to give maximum power, but the gain to be realized with an optimum mixture would probably not be very great, and it has been found (Reference 6) that power is less sensitive to mixture adjustment at the higher temperatures. For this reason, and for the additional reason that the high benzol content gives reasonable assurance of freedom from detonation, the power obtained with this fuel may be assumed to be the approximate maximum for the engine at this temperature.

The air-fuel ratios for gasoline given above are approximately those giving maximum power. Compared with the 30-70 blend, the relative power is slightly greater than observed at 59° F.;

in fact, at 1,800 R. P. M. (fig. 8), the power obtained with gasoline is actually greater. From the trend of the cross-plot curves, it may be seen that the power with gasoline tends to approach that for the 30-70 blend at all speeds. As the range of air-fuel ratios for the two fuels overlap this can not be readily explained on the basis of mixture differences. The fixed ignition advance and differences in the amount of vaporization taking place in the manifold may be cited as factors having a possible influence on the comparative results. The power with gasoline is from 1 per cent at 1,800 R. P. M. to 7 per cent at 1,400 R. P. M. less than that obtained with the 65-35 blend.

Thus the conclusion may be made that, as aviation gasoline does not give the maximum M. E. P. for the normal engine at speeds giving maximum volumetric efficiency, and as the volumetric efficiency under supercharged conditions is greater than for any condition of the normal engine, the loss in power resulting from the use of this fuel in the supercharged engine would probably be greater than evidenced by the present results. Also, unlike the normal engine, the conditions inducing detonation in the supercharged engine are encountered at all altitudes. For these reasons, the use of the 30-70 blend instead of plain aviation gasoline in the supercharged engine gives an appreciable gain in power.

THE EFFECT OF AIR TEMPERATURE ON POWER

Owing to the variation in the character of the combustion as influenced by varying degrees of detonation, no laws of general applicability can be promulgated from these tests for the variation in engine power with air temperature. Also, in the matter of air-fuel mixtures and ignition advance, the data are incomplete, and do not show definitely that the power obtained at each temperature was the maximum possible for the particular fuel used. The lack of complete data at several air temperatures in the case of the 65-35 blend, which might be considered suitable from the standpoint of detonation suppression, precludes the possibility of comparing the observed performance obtained with the other two fuels with the optimum performance of the engine. However, the power obtained with each fuel was probably within 1 per cent of the maximum obtainable with the given fuel, and the data are valuable as showing the variation in power with temperature of two representative engines for normal carburetor adjustments encountered in service, where overrich mixtures are usually employed to secure safe operation under all flight conditions and where the mixture is adjusted neither to give the absolute maximum power nor the best fuel economy. With this in mind, the following empirical relations determined from the present tests are submitted.

The ratios of the mean effective pressure at high temperatures to the mean effective pressure at a low base temperature, with comparative curves showing the ratios that would exist were the power to vary directly with air density or inversely as the square root of the inlet temperature, are plotted in Figures 8 and 9. As the magnitude of the differences in the values for relative power at high and low speeds was, in the present tests, small, average percentage values have been used instead of the individual values for each speed. The average values for brake power represent the observed values for all speeds within less than 1 per cent, and, in most cases, within less than 0.5 per cent.

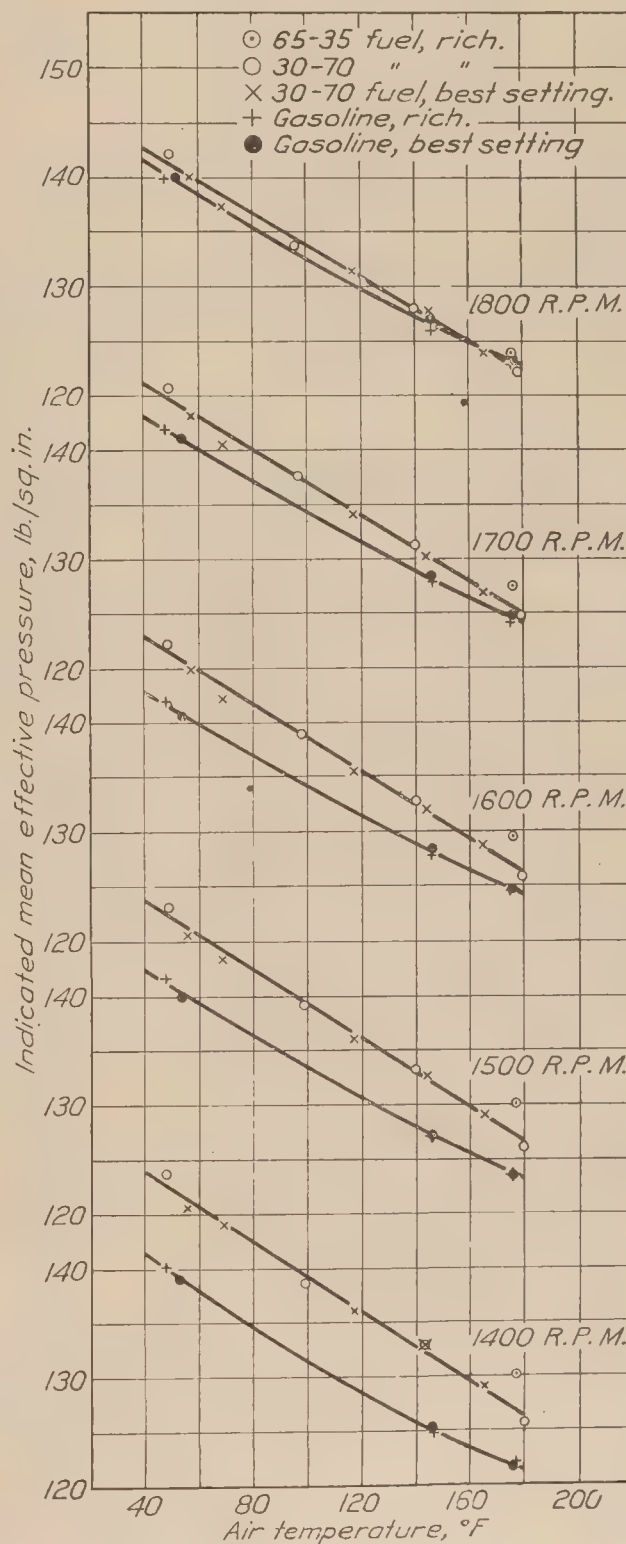
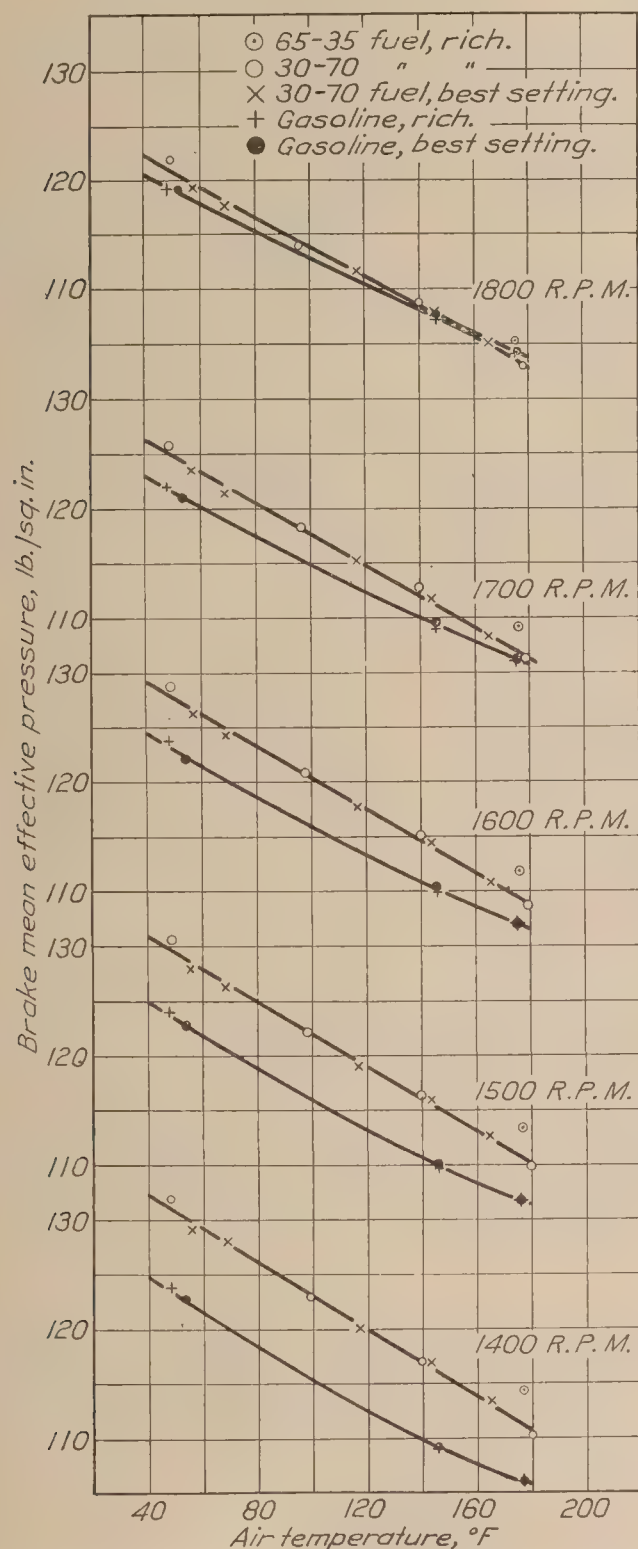
Considering first the performance of the Liberty engine when using the 30-70 blend, it is found that the cross plots at several engine speeds show the variation in mean effective pressure with air temperature to be linear. The relation between power ratio and air temperature may be thus given by general equation,

$$\text{Power ratio} = 1 \pm mt,$$

where m is the slope of the line and t the difference in temperature in degrees Fahrenheit. The straight lines determined by the average ratios for all speeds (fig. 8) have a slope, m , of 0.00115 for brake power and 0.00108 for indicated power. At the highest temperature, 180° F., temperature difference of 121° F., the brake power is about 5 per cent higher than given by straight density proportion, and about 4 per cent lower than given by the square root relation; corresponding values for indicated power are 6 per cent and 3 per cent, respectively.

As mentioned previously, there is a greater tendency for detonation with this fuel under flight conditions, but the above relation, and the given values of m , may be considered as more nearly representing the power variation with temperature for the supercharged Liberty engine, for the range of mixtures used with the 30-70 blend in flight, than would be given by the square root relation.

For a constant speed, data for both the rich and lean mixtures for plain gasoline lie on a single curve. Sufficient data were not taken to determine the exact trend of the mean effective pressure-temperature curves for this fuel, and no equation for the observed relation is submitted, but the indication is that the relation is not quite linear as was the case for the 30-70 blend (fig. 8). Also, the decrease in power with increase in temperature is not as great as observed for the 30-70 blend. The brake power at 180° F. is seen to be 2.5 per cent lower, and the indicated power 1.5 per cent lower than that given by the square root relation; the trend of the curve against air temperature approximates that given by the theoretical relation.



FIGS. 6 and 7.—Liberty 12 engine. Variation in mean effective pressure with air temperature for various speeds from 1,400 to 1,800 R. P. M. for all fuel conditions (cross plot of faired curves, figs. 1 and 2)

The ratios of the mean effective pressure obtained with the 65-35 blend at 176° F., the assumed maximum at this temperature, to the assumed maximum mean effective pressure obtained with the 30-70 blend at 59° F. are also shown on Figure 8, from which it is seen that the single points for this fuel closely approximate the percentage variation in power observed for plain gasoline.

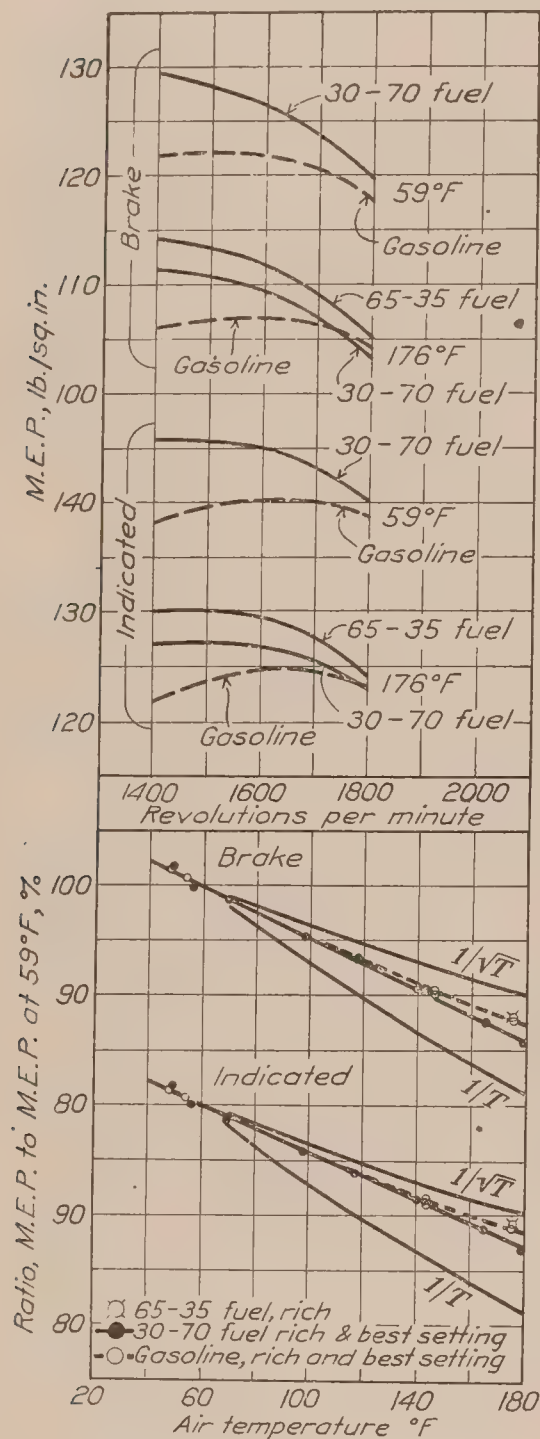


FIG. 8.—Liberty 12 engine. Mean effective pressure at 59° F. and 176° F. with various fuels (from faired curves of figs. 6 and 7) and percentage variation in mean effective pressure with air temperature. (Points on percentage plots are average of percentage decrease for five speeds)

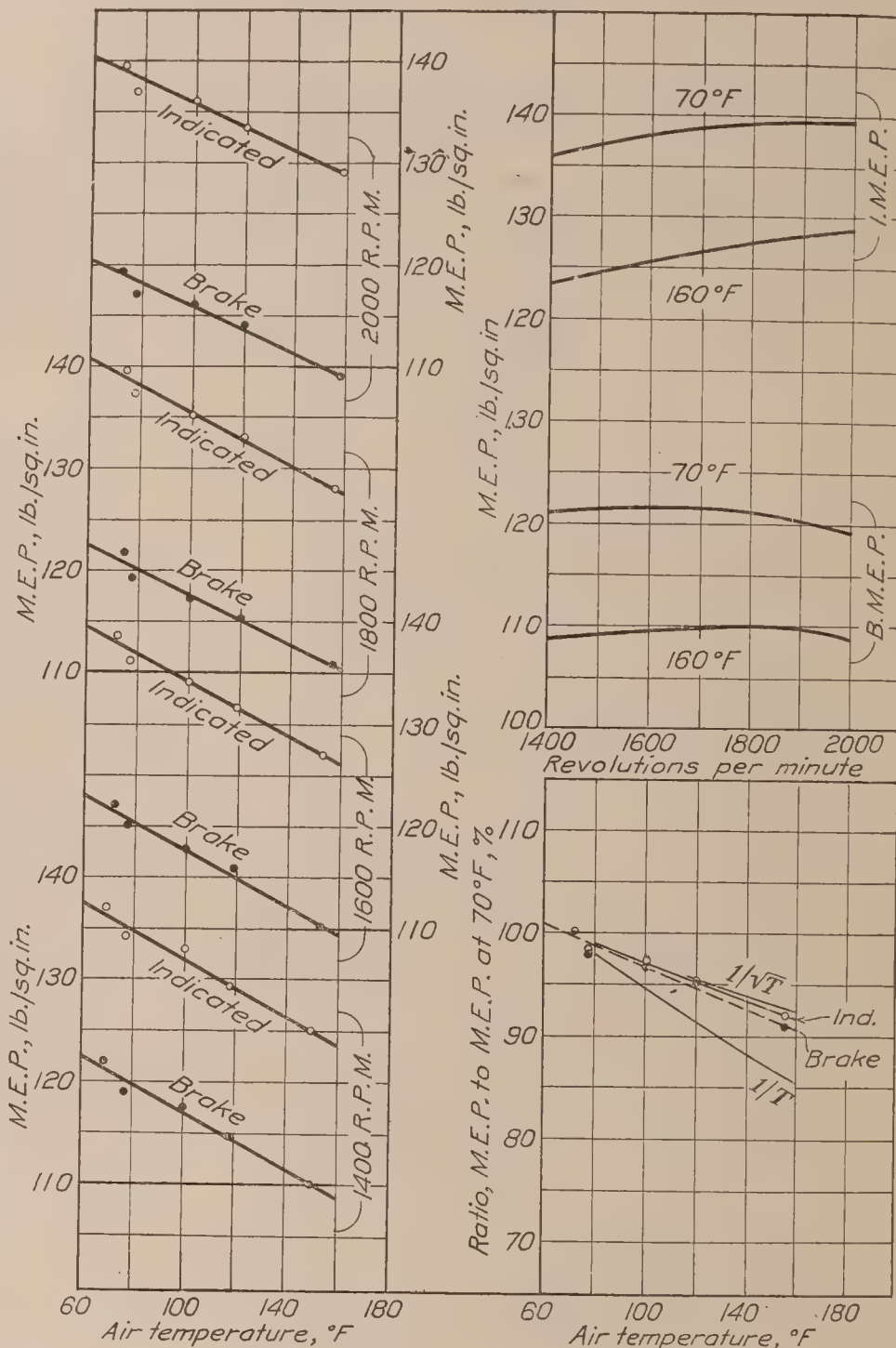


FIG. 9.—Wright E-4 engine. Variation in mean effective pressure with air temperature for various speeds (cross plot of curves, fig. 4), mean effective pressure at 70° and 160° F. and percentage variation in mean effective pressure with air temperature. (Points on percentage plots are average of four speeds)

The variation in power with temperature for the Wright engine using the 30-70 blend, rich mixture, is shown on Figure 9. The average ratios of mean effective pressure for all speeds determine a linear relation, as for the case of the same fuel in the Liberty engine, but in this case, the decrease in power is not as rapid, and approaches more nearly the variation given by the square-root relation. For a temperature difference of 90° F., the brake power is only 1.8 per

cent, and the indicated power is only 0.8 per cent, below that given by the theoretical square-root relation, as compared to 2.8 per cent and 2 per cent for the same fuel and the same temperature difference for the Liberty engine. This comparison serves to indicate the differences that may exist in the variation in power with temperature between two different types of engines using the same fuel and approximately the same air-fuel mixtures. Again, it is noted that power decreased more rapidly with temperature at speeds giving the maximum volumetric efficiency. Using the average percentage for all speeds, values of m in the general relation,

$$\text{Power ratio} = 1 \pm mt,$$

are 0.00104 for brake and 0.00093 for indicated power.

The results given in References 1, 5, 6, 8, 11, and 13 do not agree in all respects, but, in the main, the brake power obtained at high temperatures when using rich fuel mixtures is less than that given by the theoretical square-root relation. On a basis of indicated power, the results probably would have been in closer agreement with this relation, but the indications are that for overrich mixtures the indicated power would still be less, as found in the present tests.

From the present results, it may be concluded that, for normal service carburetor adjustments, both the brake and indicated power at high temperatures is less than given by the square-root relation, but that the square-root relation may be considered as generally applicable except when greater precision over wide range of temperatures is desired, in which case it appears that the particular engine should be tested under the given conditions.

EFFECT OF AIR TEMPERATURE ON FRICTION POWER

From theoretical considerations it is indicated that an increase in air temperature results in an increase in the absolute pressure during the suction stroke. (Reference 4.) As a result the pumping loss, and consequently the friction power, would decrease with an increase in temperature. Such an effect was noted in the present investigation.

Although the friction power was obtained by motoring the engine with the dynamometer, which method, it has been shown (Reference 15), may give values for friction power that may be in serious error compared to the friction actually existing with the engine under power, and although the volumetric efficiency with and without the engine firing would probably be different, the results obtained are comparative. Friction power curves for the Liberty engine are shown on Figure 5. Cross plots for constant engine speeds (fig. 6) show a measurable decrease in friction power with increase in temperature, the decrease over the temperature range from 40° to 180° F., being about 7 per cent at 1,800 R. P. M. and 3.5 per cent at 1,400 R. P. M.

Only a few friction power determinations were made with the Wright engine, and these data did not show a consistent variation with air temperature. (Fig. 3.)

EFFECT OF TEMPERATURE ON FUEL CONSUMPTION

The hourly fuel rates for the Liberty engine have been cross-plotted against temperature on Figure 10. Figure 11 presents curves showing the percentage change in the hourly rate with temperature; the points shown on this figure are the average of the percentages for the several speeds.

It is noted that for the condition with the mixture control in the full-rich position, the hourly rate for both the 30-70 blend and plain gasoline decreases about 5 per cent for the temperature change from 59° to 180° F., but as the decrease in air weight for this range of tempera-

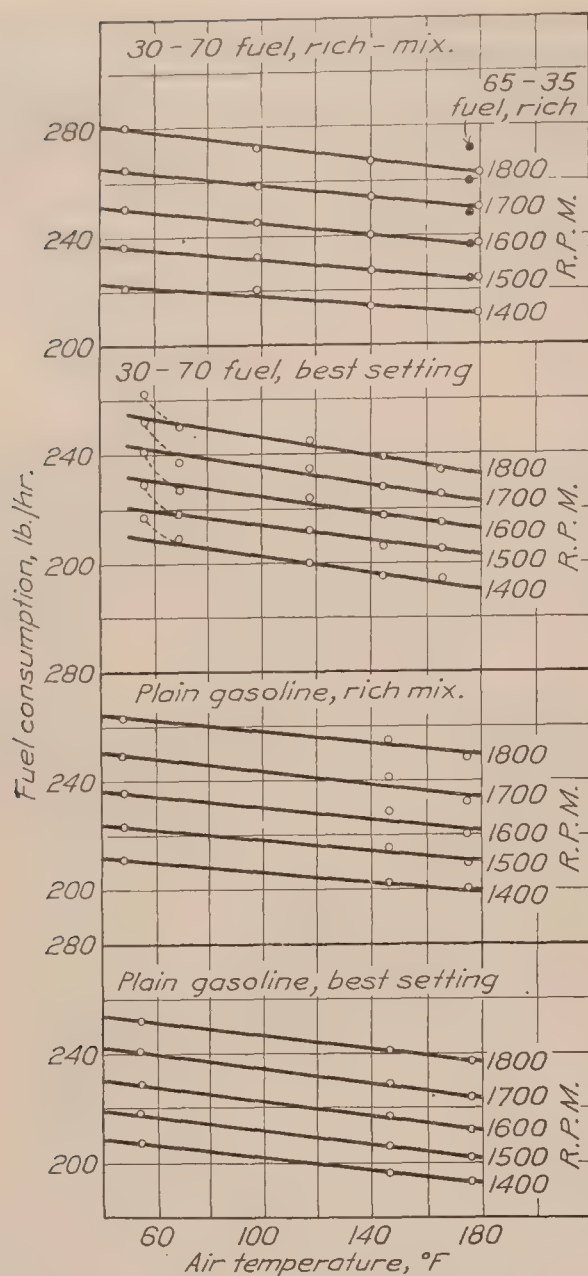


FIG. 10.—Liberty 12 engine. Variation in hourly fuel rate with air temperature for all fuels and mixture conditions (cross plot of faired curves, figs. 1 and 2)

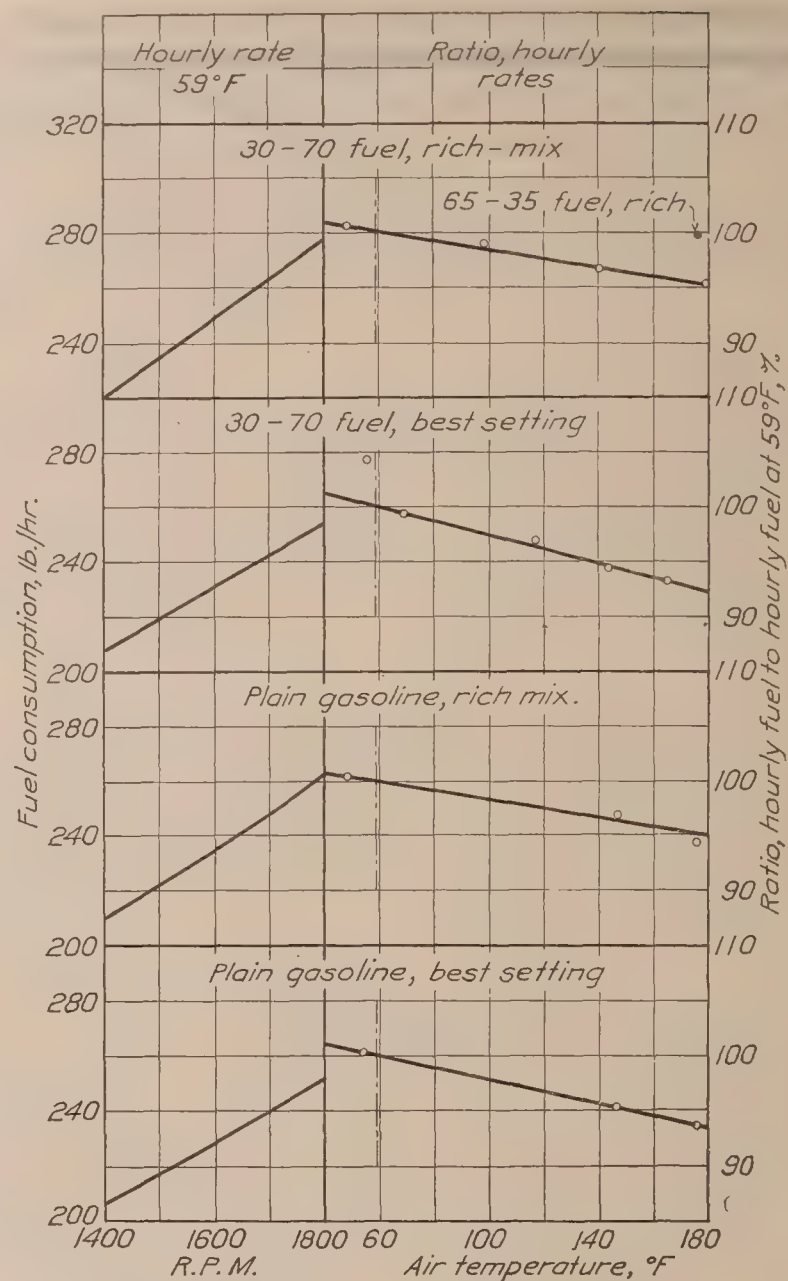


FIG. 11.—Liberty 12 engine. Hourly fuel rate at 59° F. (from faired curves, fig. 10) and percentage variation in fuel rate with air temperature. (Points are average of percentages for five speeds)

ture is considerably greater, the mixture is enriched at the higher temperature. Likewise, as the power decreases at a faster rate than the hourly consumption, the specific consumption is increased. For the leaned condition, the data are not very consistent, but the indication is that the indicated specific consumption is increased at the higher temperatures, either because the leaning was not carried far enough or because the loss in power due to detonation at the higher temperatures served to increase the specific consumption. These results point to the advisability of leaning as the temperature is increased, in order to effect a saving in fuel.

EFFECT OF TEMPERATURE ON MANIFOLD PRESSURES

With a constant pressure maintained at the entrance to the carburetor, it would be expected that some change in the friction loss through the carburetor would result from the change in air density caused by a change in temperature, and that this effect coupled with a variation in the amount and kind of fuel carried in the air stream, with consequent changes in the amount of vaporization taking place in the manifolds, would have some effect on the manifold pressures. Such an indication of the influence of air density was found during these tests.

Data for the Liberty engine, giving the average depressions in two manifolds below the existing carburetor pressure, are shown on Figures 12 and 13, and for the Wright engine, on Figure 14. From the average of the many observations taken, it was found that a measurable decrease in the depression in the manifold occurred with increase in air temperature. The order of the increase in the absolute manifold pressure, about 0.5 per cent for 140° F. temperature

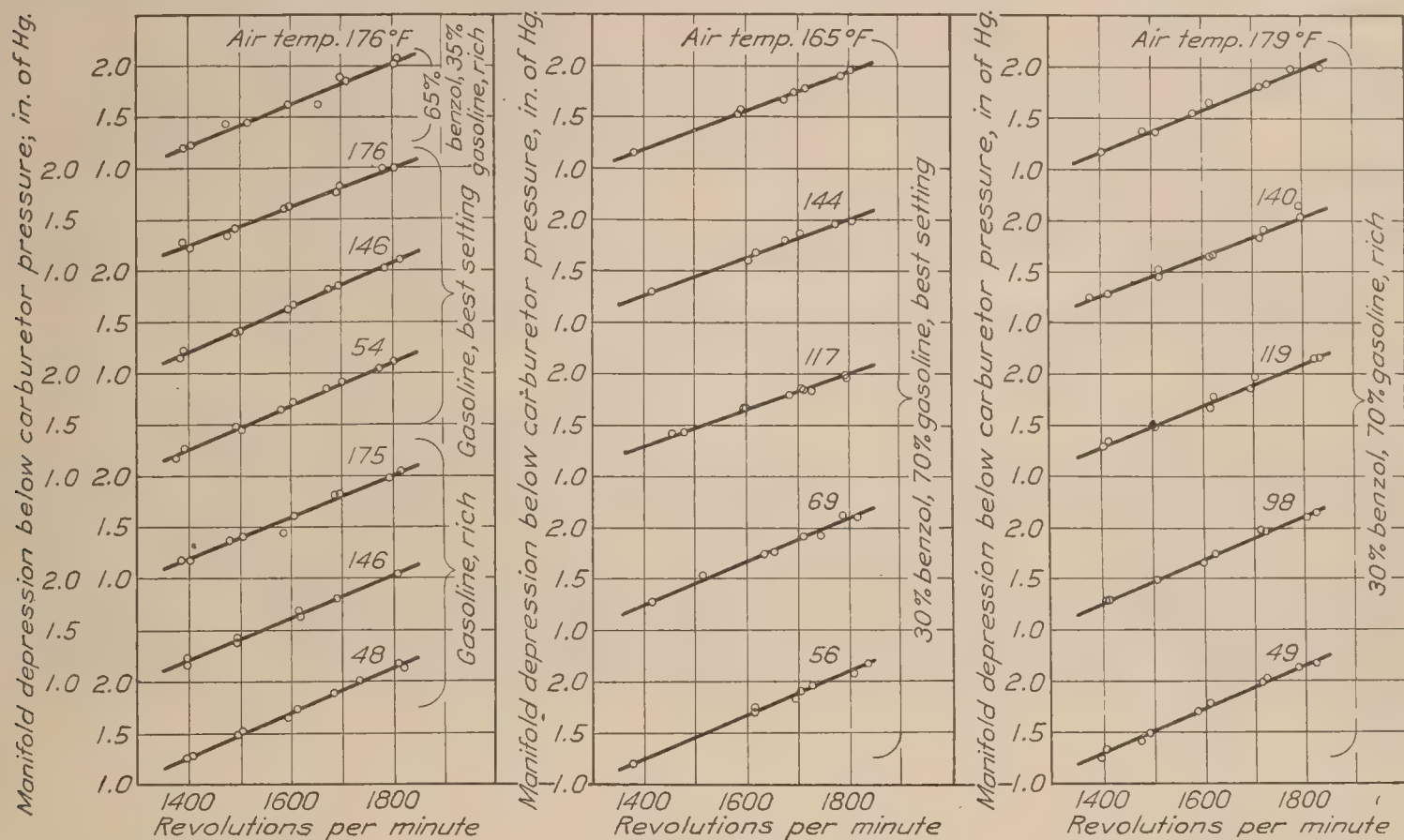


FIG. 12.—Liberty 12 engine. Depressions in manifold below existing pressure at entrance to carburetor for various air temperatures (average of front right and rear left manifolds)

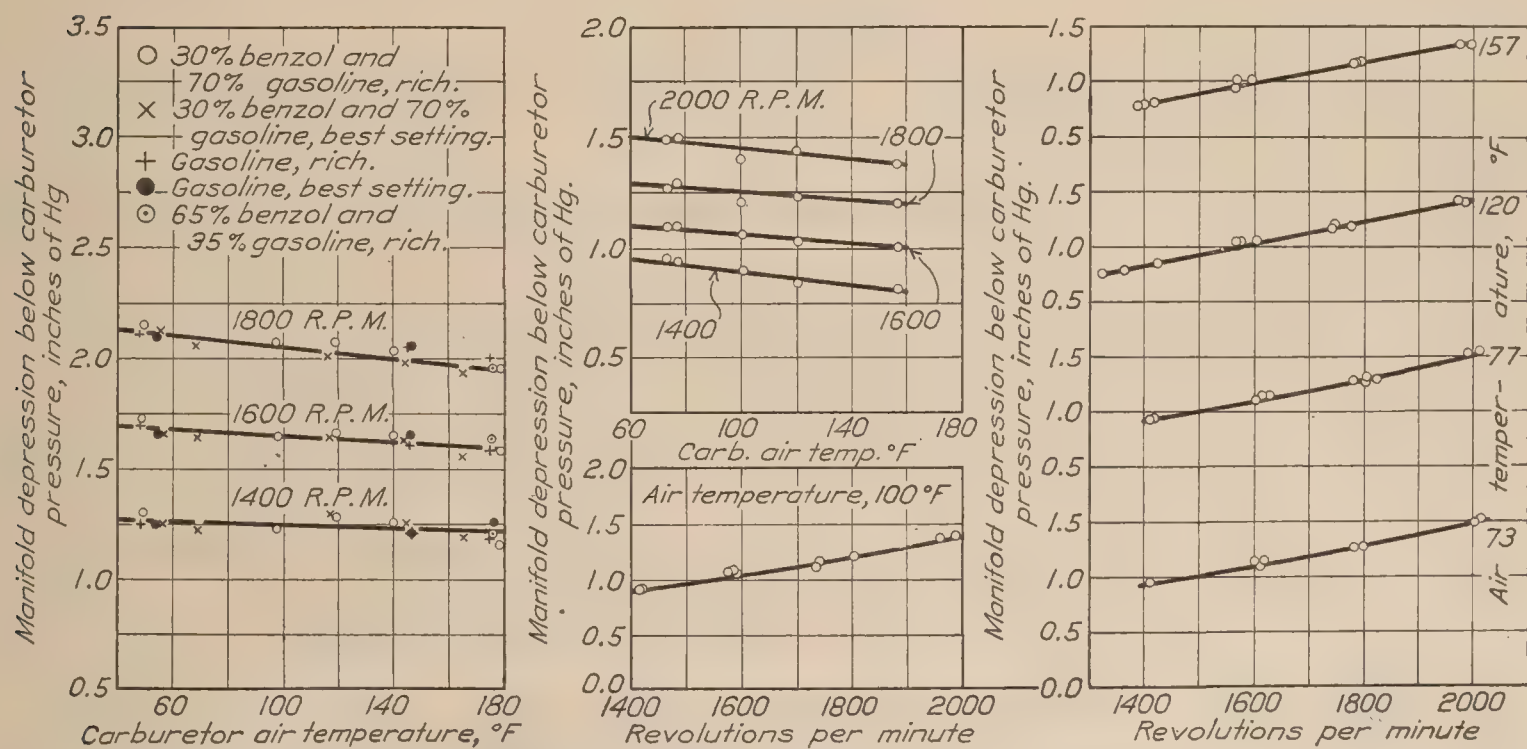


FIG. 13.—Liberty 12 engine. Variation in manifold depression with air temperature (cross plot of fig. 12)

FIG. 14.—Wright E-4 engine. Depressions in manifold below existing pressure at entrance to carburetor for various air temperatures (average of right and left manifolds) and variation in manifold depression with air temperature (cross plot of above curves)

increase, has a relatively negligible effect on power; but the information is pertinent as showing the direction of the change, and the constancy of the pressure head on the intake valves at high temperatures.

CONCLUSIONS

The present results show that a gain of 5 to 6 per cent in the full-throttle power of the Liberty 12 aviation engine (5.4 to 1 compression ratio) at speeds giving the maximum volumetric efficiency is obtained by using a fuel mixture consisting of 30 per cent of commercial benzol and 70 per cent aviation gasoline instead of plain aviation gasoline. This gain is practically the same for all air temperatures investigated. As the volumetric efficiency of the supercharged engine with free exhaust is greater than for any condition of the normal engine, and as, unlike the normal engine, the conditions inducing detonation when using plain gasoline are encountered at all altitudes, the gain from the use of this special benzol blend in the supercharged Liberty engine would be appreciable.

The relative increase in power obtained at high air temperatures by increasing the benzol content in the fuel mixture to 65 per cent is only 2 per cent.

For the conditions of test, both the brake and indicated power of the normal Liberty and Wright engines decrease at a faster rate with increase in air temperature than given by the generally accepted square root relation. With regard to brake power, the order of the difference is from 3 to 5 per cent for a temperature difference of 120° F. When using the 30-70 benzol blend, the relation between power and air temperature is found to be linear for both engines. Although these differences are noted, the theoretical square root relation may be considered as being generally applicable except where greater precision over a wide range of temperatures is desired, in which case it appears that the particular engine should be tested under the given conditions.

LANGLEY MEMORIAL AERONAUTICAL LABORATORY,
NATIONAL ADVISORY COMMITTEE FOR AERONAUTICS,
LANGLEY FIELD, VA., *February 11, 1927.*

REFERENCES

1. DICKINSON, H. C., JAMES, W. S., and ANDERSON, G. V. Effect of Compression Ratio, Pressure, Temperature, and Humidity on Power. N. A. C. A. Technical Report No. 45, Part III, 1918.
2. GAGE, V. R. Some Factors of Airplane Engine Performance. N. A. C. A. Technical Report No. 108, 1921.
3. WHITE, H. S. Investigation of the Effect of Air Conditions upon the Power of Aviation Engines. "The Armour Engineer," Vol. XII, No. 3, March, 1921.
4. SPARROW, S. W. Correcting Horsepower Measurements to a Standard Temperature. N. A. C. A. Technical Report No. 190, 1924.
5. BERRY, O. C. Standard of Carburetor Performance. "Transactions of the A. S. M. E.," Vol. 41, p. 348, 1919.
6. BROWN, G. G. A Chemically Controlled Automobile. "Journal of Industrial and Engineering Chemistry," Vol. 14, No. 1, p. 6, January, 1922.
7. SPARROW, S. W. Relation of Fuel-Air Ratio to Engine Performance. N. A. C. A. Technical Report No. 189, 1924.
8. GIBSON, A. H. The Relationship between Air Temperature and the Power of a Petrol Engine. Internal Combustion Engine Subcommittee of British Advisory Committee for Aeronautics. Report No. 19, 1917.

9. SPARROW, S. W., and WHITE, H. S. Performance of a Liberty 12 Airplane Engine. N. A. C. A. Technical Report No. 102, 1921.
10. Test of Stromberg Inverted Carburetor Model NA-L5 on the 12 Cylinder Liberty Aviation Engine. Air Service Information Circular No. 158, Vol. II, McCook Field Serial No. 1340, 1921.
11. KEGERREIS, C. S. The Effect of Mixture Ratio and Temperature on Power and Economy. "Automotive Industries," Vol. 45, No. 13, p. 610, September 29, 1921.
12. SPARROW, S. W. The Effect of Changes in Compression Ratio upon Engine Performance. N. A. C. A. Technical Report No. 205, 1925.
13. SPARROW, S. W. Fuels for High-Compression Engines. N. A. C. A. Technical Report No. 232, 1925.
14. KEGERREIS, C. S., and YOUNG, G. A. Survey of Gasoline and Kerosene Carburetion. "Transactions of the S. A. E.," Vol. 18, Part I, p. 169, 1923.
15. MOSS, H., and STERN, W. J. The Mechanical Efficiency of an Internal Combustion Engine. "Automobile Engineer," Vol. 15, No. 200, p. 78, March, 1925.

REPORT No. 278

**LIFT, DRAG, AND ELEVATOR HINGE MOMENTS OF
HANDLEY PAGE CONTROL SURFACES**

By R. H. SMITH

Aerodynamical Laboratory, Bureau of Construction and Repair, U. S. Navy

REPORT No. 278

LIFT, DRAG, AND ELEVATOR HINGE MOMENTS OF HANDLEY PAGE CONTROL SURFACES

By R. H. SMITH

INTRODUCTION

This report combines the wind-tunnel results of tests on four control surface models made in the two wind tunnels of the Navy aerodynamic laboratory, Washington Navy Yard, during the years 1922 and 1924, and submitted for publication to the National Advisory Committee for Aeronautics May 7, 1927. The purpose of the tests was to compare, first, the lifts and the aerodynamic efficiencies of the control surfaces from which their relative effectiveness as tail planes could be determined; then the elevator hinge moments upon which their relative ease of operation depended. The lift and drag forces on the control surface models were obtained for various stabilizer angles and elevator settings in the 8 by 8 foot tunnel by the writer in 1922; the corresponding hinge moments were found in the 4 by 4 foot tunnel by Mr. R. M. Bear in 1924.

DESCRIPTION OF MODELS

For all four models the over-all dimensions are 6 by 18 inches and the basic profile a twin cambered section of easy form known as the Martin M-1. One is provided with a plain flap elevator, three with Handley Page balanced elevators. The sizes of the elevators and the manner of hinging them, the main dimensions of the members, and the offsets of the cambered surfaces are given in the diagram and tables of Figure 2, which also defines the stabilizer angle of attack and elevator pitch. Figure 3 is a photograph of Model No. 4 mounted for the determination of the elevator hinge moments. The models were made of dry pine and varnished.

METHOD OF TEST

The lift and drag forces were measured on the six-component balance to which the models were attached by means of the standard 5-inch model holder, whose two thin streamlined prongs engaged the models at mid span. For zero degrees stabilizer angle and for each 5° increase to $+20^\circ$ the elevator was set at a succession of angles to the stabilizer, ranging from -20° to $+20^\circ$ by 5° increments for Models 1, 3, and 4 and from -25° to $+25^\circ$ by the same increments for Model 2. These limits to the elevator pitch were chosen to exceed the angles at which air leakage between the elevator and stabilizer begins. For Models 2, 3, and 4 the respective angles of incipient leak are $19^\circ-6'$, $13^\circ-29'$, and $10^\circ-40'$. Measurements were not made at negative stabilizer angles because they are inferable from symmetry.

The elevator hinge moments were measured in pound-inches on the 4 by 4 foot tunnel cross-arm balance, according to the usual procedure of finding the pitching moments on an aerofoil. The angles of stabilizer and elevator pitch corresponded in the tests on Models 1, 2, and 3, to those used in the lift and drag tests on these models, except for the inclusion of the symmetrical angles for negative stabilizer. In testing Model 4 the elevator angle range was again $\pm 20^\circ$, but the moment measurements, at zero stabilizer angle, showed an overbalance control condition, and in order to shorten a test of no apparant practical value the usual additional stabilizer angles were limited to $\pm 10^\circ$ and $\pm 20^\circ$.

RESULTS OF TESTS

The net lift and drag forces on the models and the derived coefficients are given without correction for model symmetry, Vl/ν or wall effect in Tables I to VII; the absolute coefficients are plotted in Figures 4 to 11. The engineering coefficients are tabulated but not plotted.

Elevator hinge moments are given in Table VIII corrected for model asymmetry by taking the mean of the moments for symmetrical stabilizer angles and elevator settings and subtracting or adding to all these mean moments the moment at zero angle of stabilizer and elevator setting. Figures 16 to 19, inclusive, give various direct and derived plots of the moments thus corrected.

LIFT COEFFICIENT

The following mathematical analysis of the lift coefficient plots, given in Figures 3 to 6, as well as that of the drag coefficient plots in the next section, was made by Doctor Zahm.

Each lift diagram presents a family of lines that are nearly straight for small values of the stabilizer angle α , and of the elevator setting δ . The equation for the rectilinear parts of each diagram may be written

$$C_L = m\alpha + n\delta \quad (1)$$

in which m and n are fairly constant, and have the respective values $m = \delta C_L / \delta \alpha$ and $n = \delta C_L / \delta \delta$.

Of these partial derivatives the first expresses the slope of the line; the second its vertical shift per degree turn of elevator, so that the intercept on the vertical axis is $n\delta$.

To find the relation of α and δ , differentiate (1), C_L constant, giving $n/m = \delta\alpha/\delta\delta = C/E$ where C and E are the distances from the trailing edge, respectively, to the pivot and to the leading edge, as shown in Figures 1 and 2. Writing $n = m C/E = mr$ the original equation becomes

$$C_L = \frac{m\alpha + m r \delta}{m (\alpha + \alpha')} \quad (2)$$

in which $r = C/E$, varies with shifting of the elevator pivot, and $\alpha' = r\delta$, is the virtual increase of

incidence contributed to α by the increase δ of the elevator setting.

On scaling the diagrams it is found that m has practically the same value for all; n is constant for each diagram, but declines successively from the first to the last with the shortening

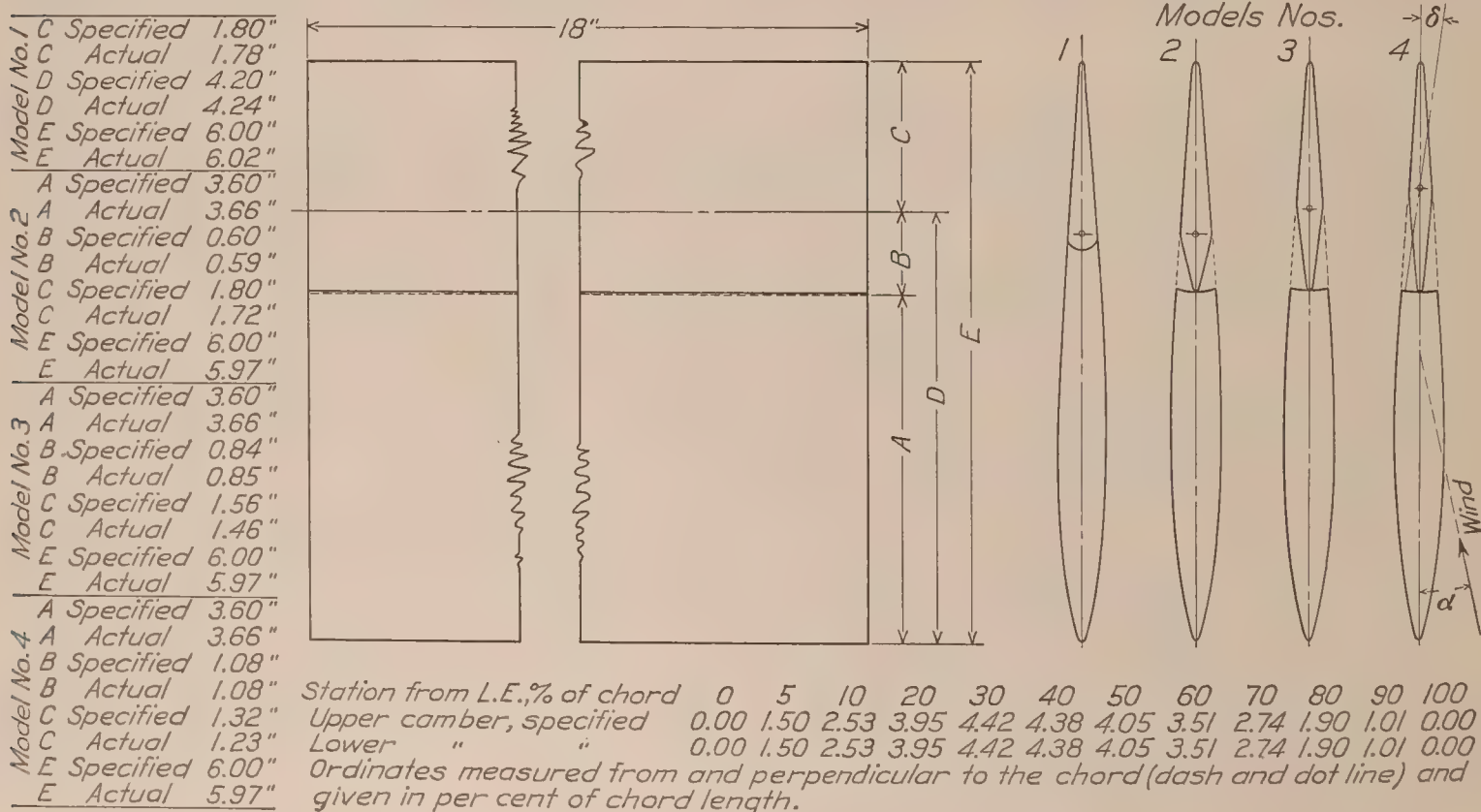


FIG. 2.—Dimensions of models used in tests on Handley Page control surfaces

of C . Owing to the constancy of $m = \delta C_L / \delta \alpha$, for all the diagrams, it follows that the increment of lift per unit change of the effective incidence $\alpha + \alpha'$, whether this change results from pitching the whole model or from pitching only the elevator, is the same for all four models. Its mean

value for angles ranging from 0 to ± 10 , as detailed in Table IX, is for the models in the order 1, 2, 3, 4.

$$m = \delta C_L / \delta \alpha = .0517 \quad .0472 \quad .0480 \quad .0514$$

The increment α' due to the elevator setting δ , is, of course, proportional to the linear displacement of the trailing edge, as shown in Figure 1, by which also one may derive the geometrical ratio already assumed $\delta \alpha / \delta \delta = C/E$.

It is noticeable that $\delta \alpha' / \delta \delta$ here derived is positive, but that $\delta \alpha / \delta \delta$ derived from (1) is negative. In taking this derivative C_L was assumed constant, which means that as the elevator setting δ is given a positive increment $+\delta \delta$, the model angle α must be given a negative increment $-\delta \alpha$, to preserve the constancy of the lift. The absolute value of the two derivatives is of course the same.

The maximum value of the lift coefficient, as should be expected, and as seen in all the diagrams, occurs at progressively lower angles of the stabilizer as the elevator is given increased setting angles. The greatest maximum, 1.15 is found for the fairest model with the stabilizer at about 13° angle of attack and the elevator at 20° setting. If the aspect ratio were increased twofold or more, the lift coefficient would be considerably increased, and would indicate a serviceable high-lift wing. Still higher values could be found with larger elevator settings, without prohibitive lift/drag ratios.

The effect of leakage of air between the elevator and stabilizer at large elevator settings is clearly manifest in Figures 4, 5, and 6. For the balanced elevator the lift drops sharply at settings beyond the leakage angle, while for the plain elevator the lift continues to rise with the setting up to angles known to be far beyond the ones here used, possibly extending beyond 60° .

Some of the lift relations of immediate practical interest may be summarized.

1. For elevator setting angles that cause no leakage between the stabilizer and elevator, all models exert the same lift at equal angles of the stabilizer and equal linear displacement of the trailing edge of the elevator.

2. The lift of each balanced control increases continuously with the elevator setting until leakage occurs, and for larger settings declines sharply, while the lift of the plain-elevator control continues to increase for still higher settings.

3. For all the particular controls here tested the lift coefficient is well expressed by the formula

$$C_L = 0.050 (\alpha + r\delta)$$

in which α and δ are respectively the stabilizer angle of attack and the elevator setting, in degrees, and r is the ratio of the distances from the elevator's rear edge respectively to the pivot and to the stabilizer's leading edge. The statement applies for α ranging from 0° to $\pm 10^\circ$.

DRAG COEFFICIENTS

The drag coefficients are plotted in Figures 8 to 11. For the smaller values of α and δ the graphs on each diagram form a family of upturned parabolas symmetrically grouped to right and left of the axis $\alpha = 0$. Rotating each actual plot 180° about the axis $\alpha = 0$ gives an extension to each graph which completes it for negative incidence.

The equation of each family has approximately the form

$$C_D = p(\alpha - a\delta)^2 + b\delta^2 + c \text{-----} (3)$$

in which $a\delta$ and $b\delta^2 + c$ are the coordinates of the vertex; p , a , b , and c being constants that can be found by scaling from the diagrams. The vertices of the parabolas are approximately on

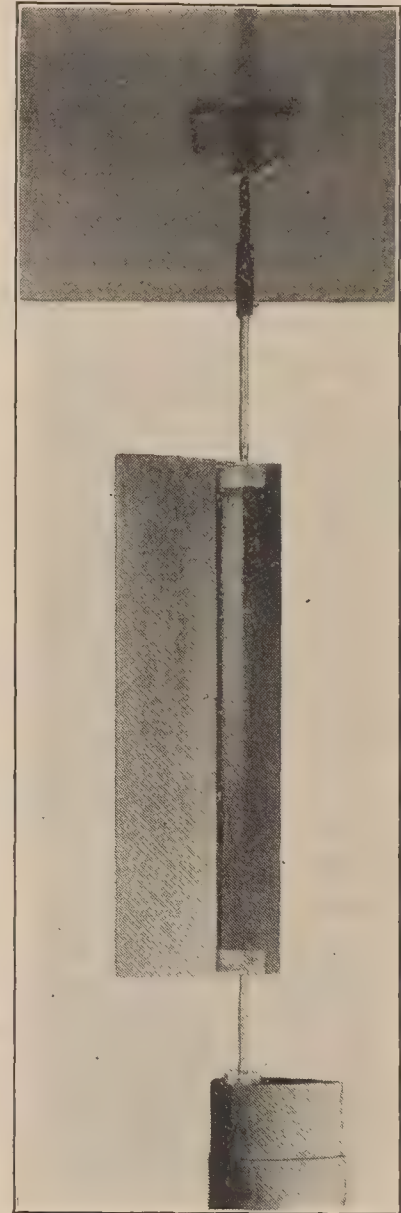


FIG. 3.—Model No. 4, mounted in 4 by 4 foot tunnel for measuring elevator hinge moments on Handley Page control surface

the locus—itself a parabola—whose parametric equations are $\alpha = a\delta$, $C_D = b\delta^2 + c$. The locus is a parabola because the drag is a quadratic function of the effective incidence $\alpha + \alpha'$, which is a linear function of the elevator setting δ . As the drag is of minor importance in the present study, the determination of the constants is omitted.

The leak effect, though manifest, is not so marked as for the lift.

LIFT/DRAG

The efficiency diagrams, Figures 12 to 15, call for little comment. The largest lift/drag for zero elevator setting is found with Model 1 as 10.5, at just under 5° angle of attack. For 5° to 10° elevator setting the maximum ratio is well above 12. For the other models the maximum is somewhat, though not greatly, less. The diagram for negative stabilizer angle of attack obviously can be derived by rotating the present one 180° about the axes $\alpha = 0, L/D = 0$.

HINGE MOMENTS

The elevator hinge moments of the four models, tabulated in Table VIII, are plotted against elevator setting, δ , in Figure 16 and against stabilizer angle, α , in Figure 17. Four diagrams derived from them are plotted in Figure 18. The values of α for the elevator and stabilizer angles of no-lift were read from Figures 4, 5, and 6. The no-lift curves of Figure 18 were obtained by plotting the moments of the dashed no-lift curves of Figure 17 against δ . The α vs. δ curves for complete elevator balance or for zero moment, of Figure 18, were plotted from data read from the curves of Figure 16. Figure 19 contains curves plotted from lift and hinge moment data and their ratios, for the controls with stabilizer angle, $\alpha = 0^\circ$.

The moment curves of Figures 16, 17, and 18 show that the elevator of Model 2 is the only one of the Handley Page types which is always underbalanced within the limits of the test. The elevator of Model 4 is completely overbalanced for the usual elevator setting range, and that of Model 3 exhibits uncertain conditions at settings of δ between -10° and -20° for stabilizer angles above 10° .

For a general comparison of the ease with which each elevator controls, the curves of Figure 18, for $L = 0$ and $\alpha = 0$, are useful, as each curve is typical of the family to which it belongs. A comparison of the moment versus δ curves for $\alpha = 0$, of Figure 18, shows the elevator hinge moments for Handley Page Model 2 to vary from two-thirds to one-half as much as for the conventional plain flap type. Also the hinge moments for Model 3 are seen to average about one-fifth as much as for the conventional type.

The relative lift values and the L/M ratios, where L = lift and M = hinge moment, may be seen, for $\alpha = 0^\circ$, in Figure 19. Although Model 3 shows a very much greater L/M ratio than Model 2, and for small elevator settings and stabilizer angles a superiority to the latter as a balanced control surface, the unstable conditions at higher elevator settings and stabilizer angles are objectionable.

AERODYNAMICAL LABORATORY,
BUREAU OF CONSTRUCTION AND REPAIR,
NAVY YARD, WASHINGTON, D. C., May 7, 1927.

REFERENCE

- Reference 1.—Irving, H. B., and Ower, E.: An Investigation of the Aerodynamic Properties of Wing Ailerons. Part II in Reports and Memoranda No. 615, Part III in Reports and Memoranda No. 651.

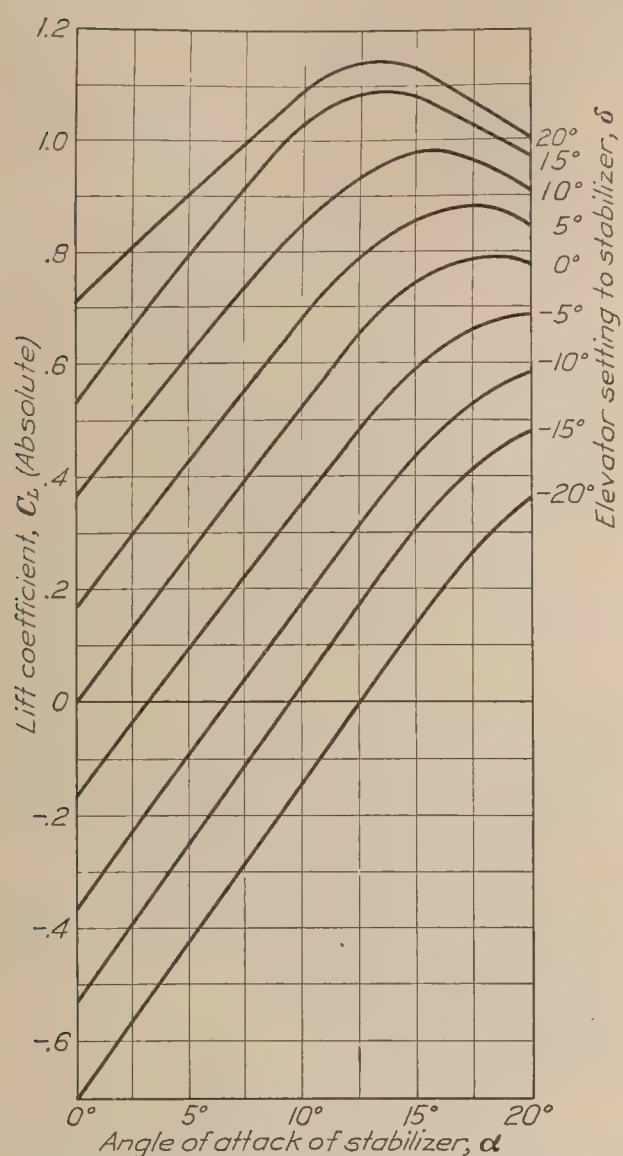


FIG. 4.—Lift coefficients for Model No. 1. Air speed, 40 M. P. H.

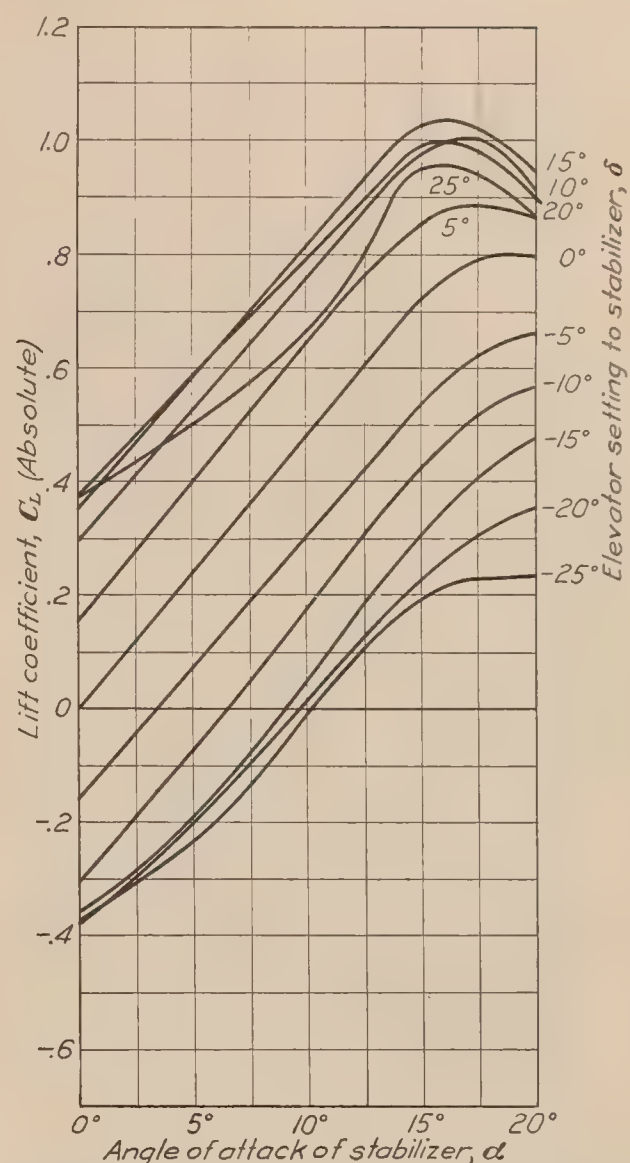


FIG. 5.—Lift coefficients for Model No. 2. Air speed, 40 M. P. H.

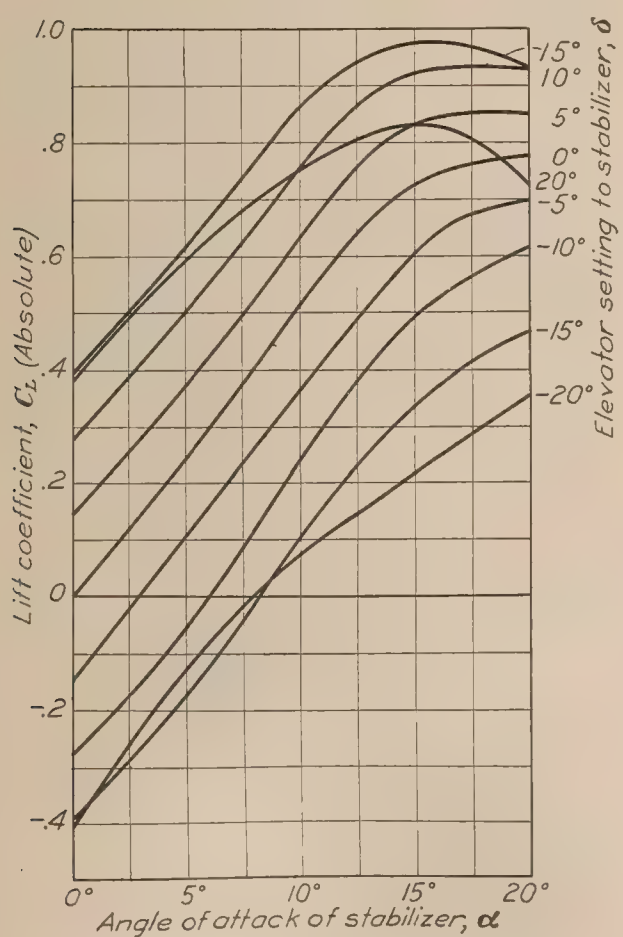


FIG. 6.—Lift coefficients for Model No. 3. Air speed, 40 M. P. H.

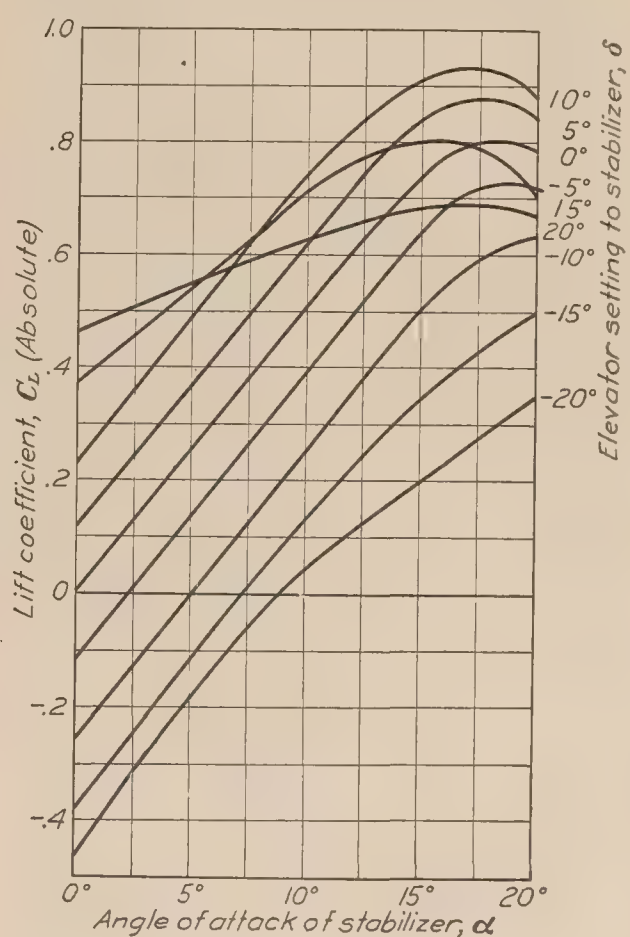


FIG. 7.—Lift coefficients for Model No. 4. Air speed, 40 M. P. H.

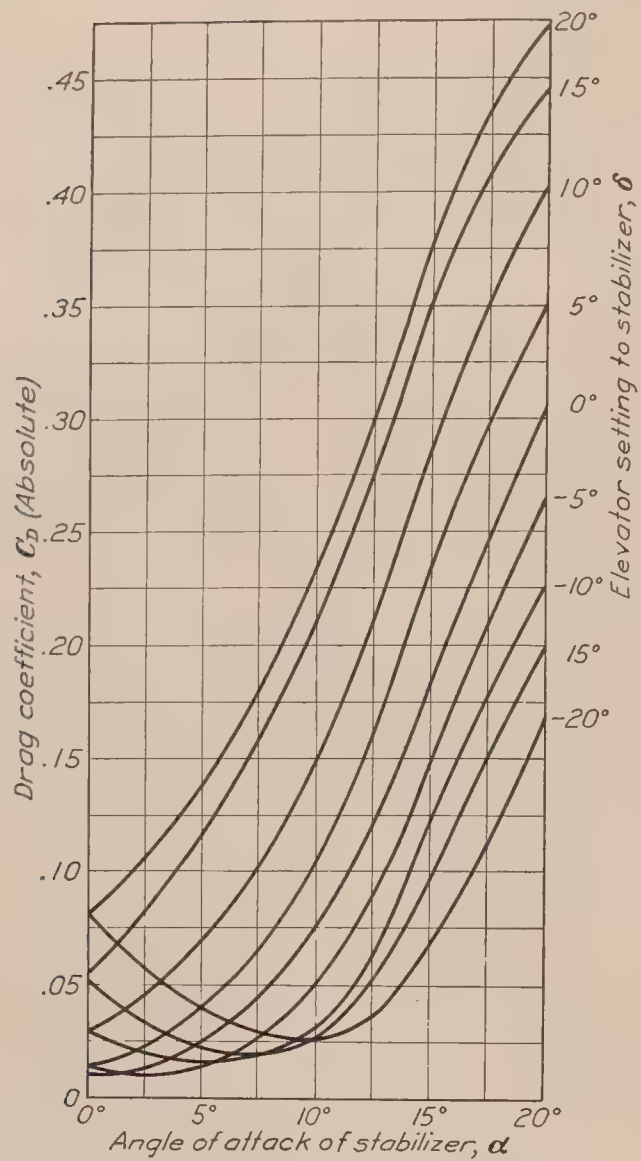


FIG. 8.—Drag coefficients for Model No. 1. Air speed, 40 M. P. H.

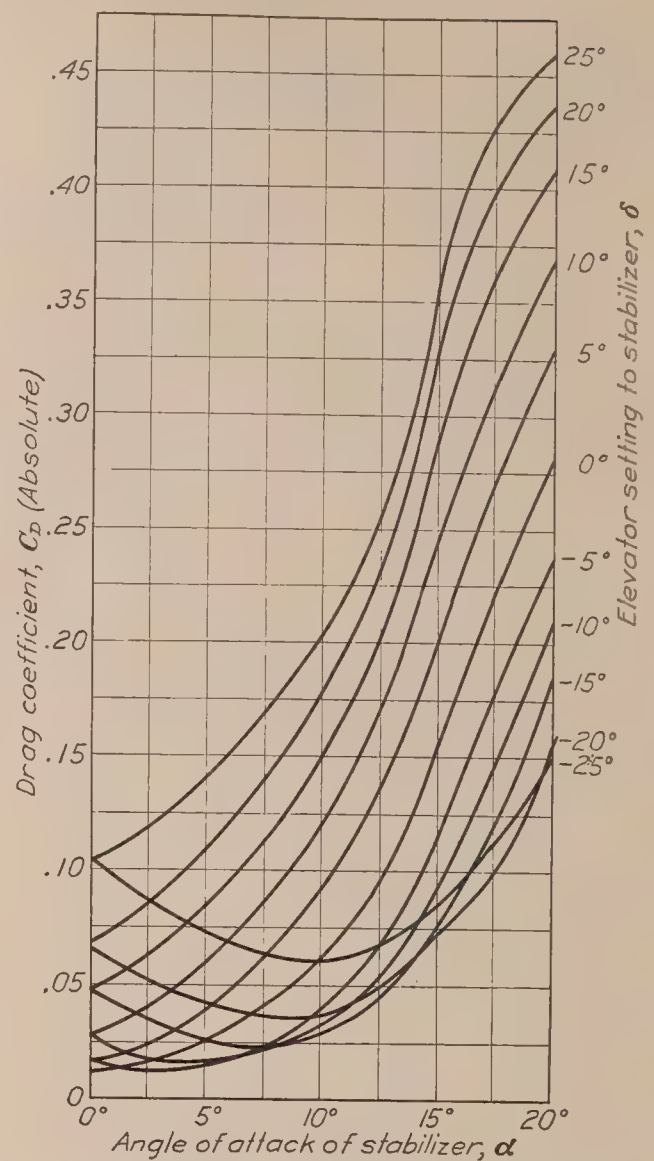


FIG. 9.—Drag coefficients for Model No. 2. Air speed, 40 M. P. H.

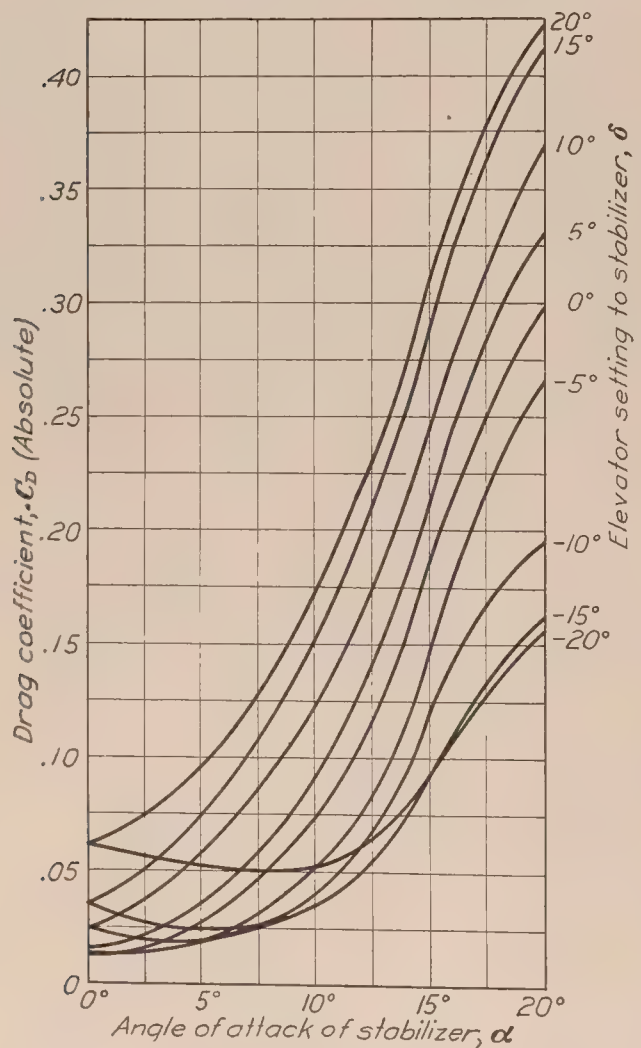


FIG. 10.—Drag coefficients for Model No. 3. Air speed, 40 M. P. H.

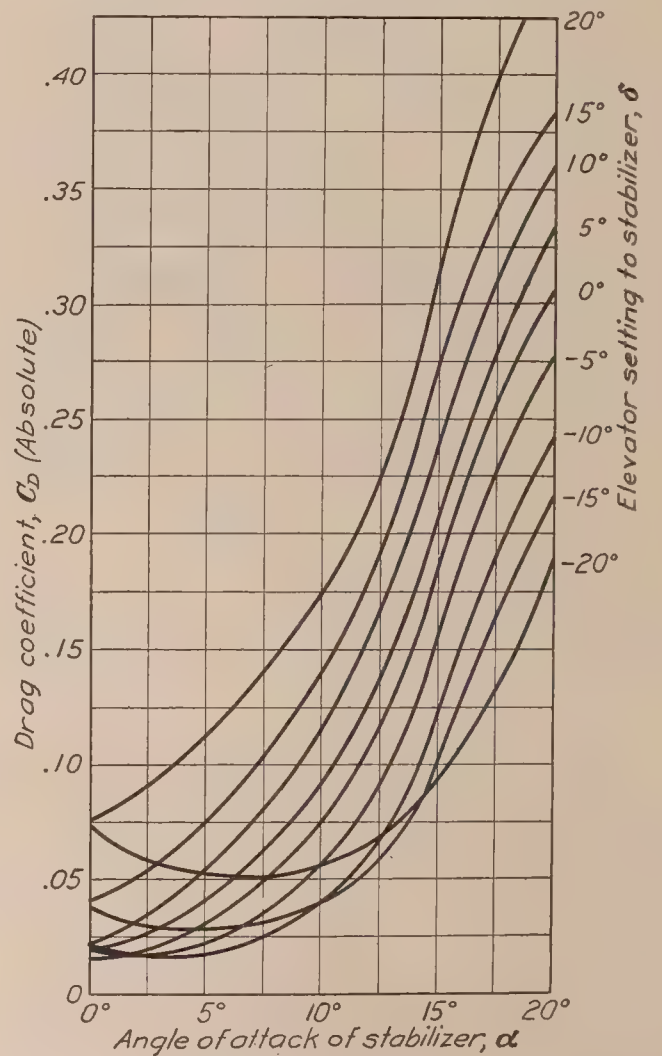


FIG. 11.—Drag coefficients for Model No. 4. Air speed, 40 M. P. H.

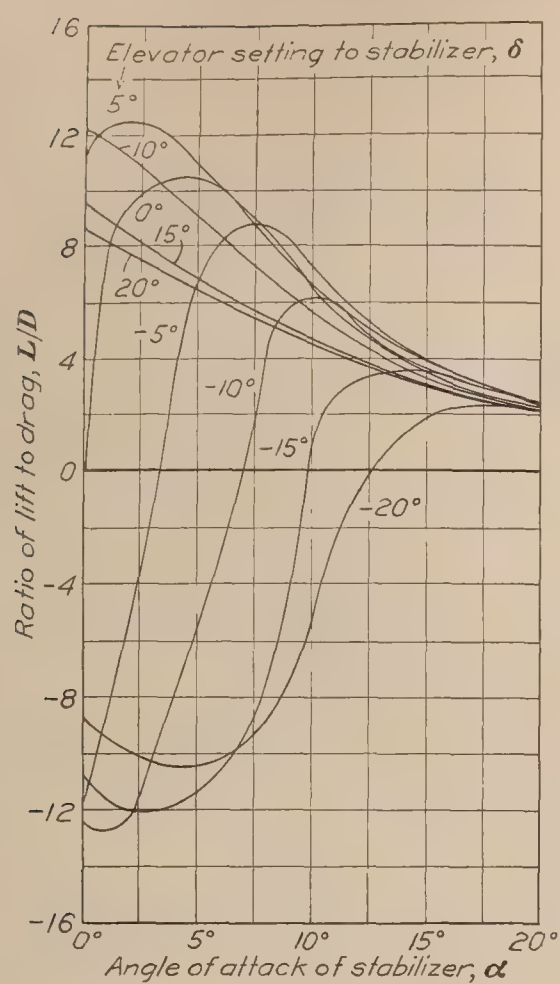


FIG. 12.—Ratio of lift to drag for Model No. 1.
Air speed, 40 M. P. H.

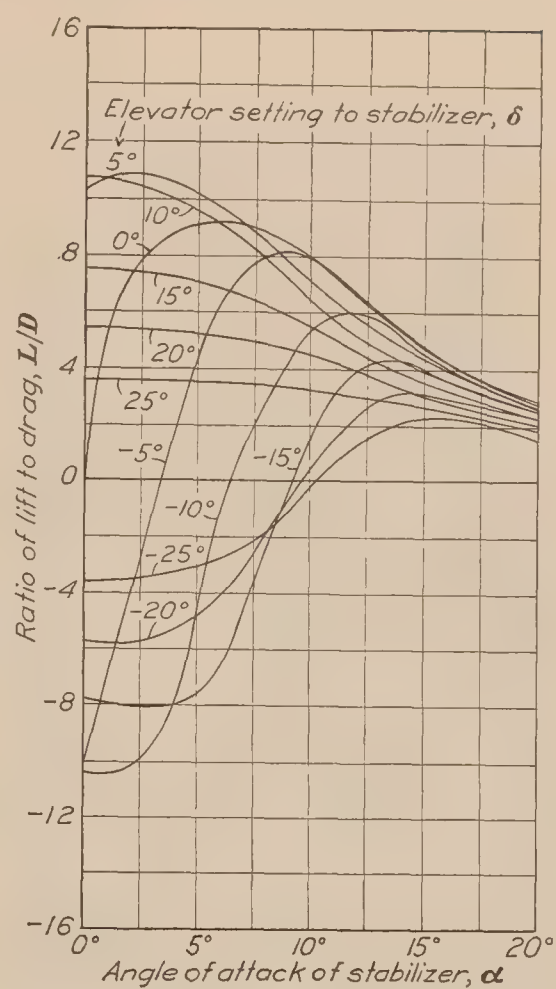


FIG. 13.—Ratio of lift to drag for Model No. 2
Air speed, 40 M. P. H.

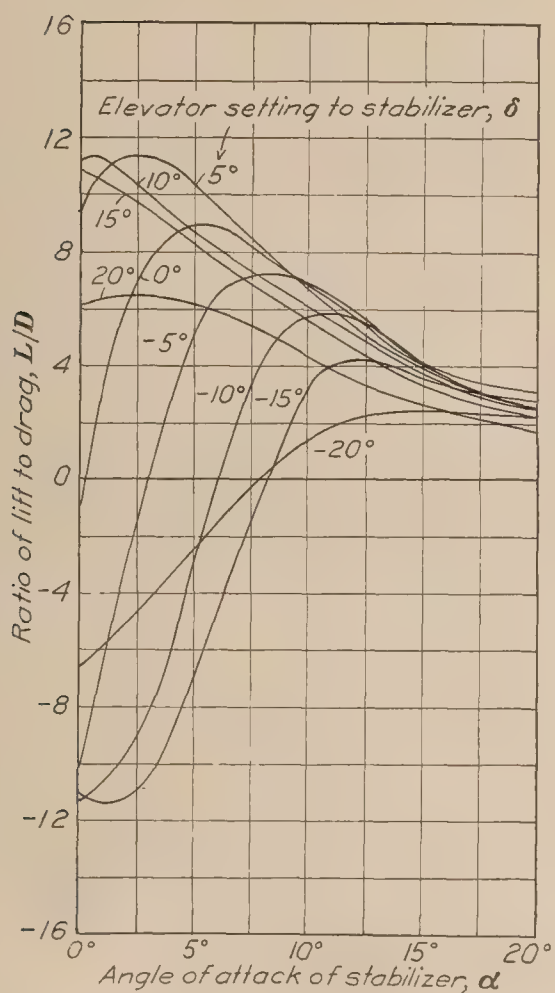


FIG. 14.—Ratio of lift to drag for Model No. 3.
Air speed, 40 M. P. H.

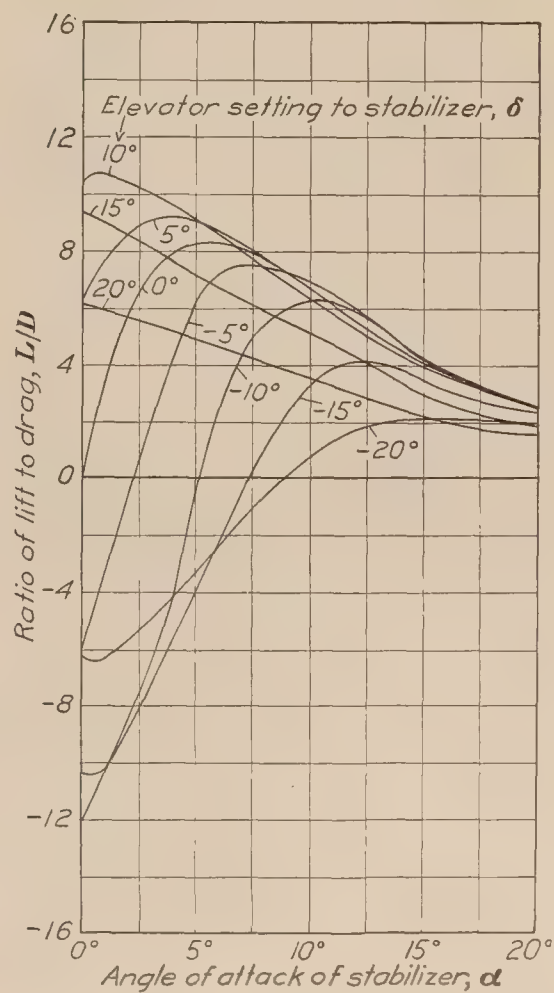
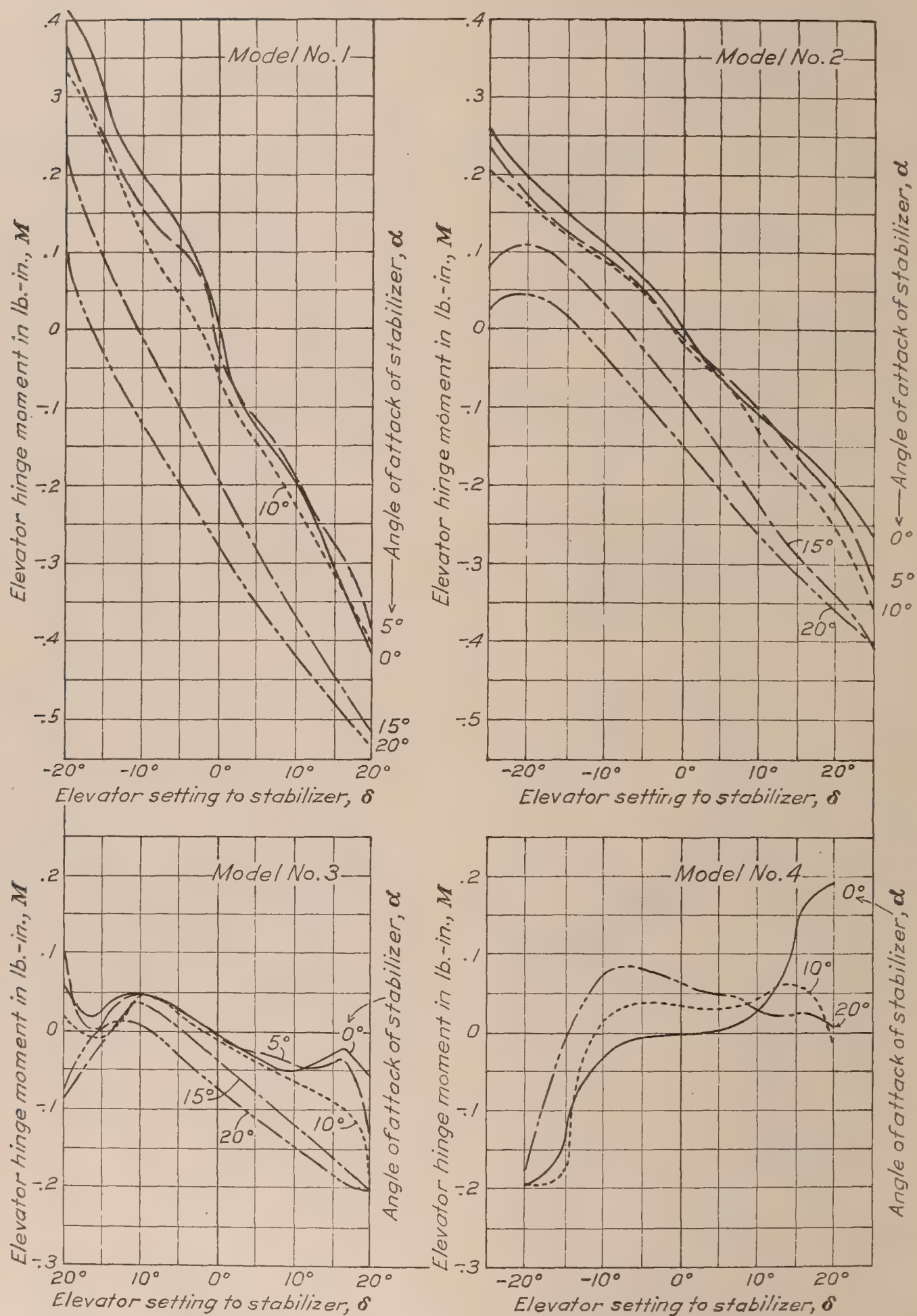
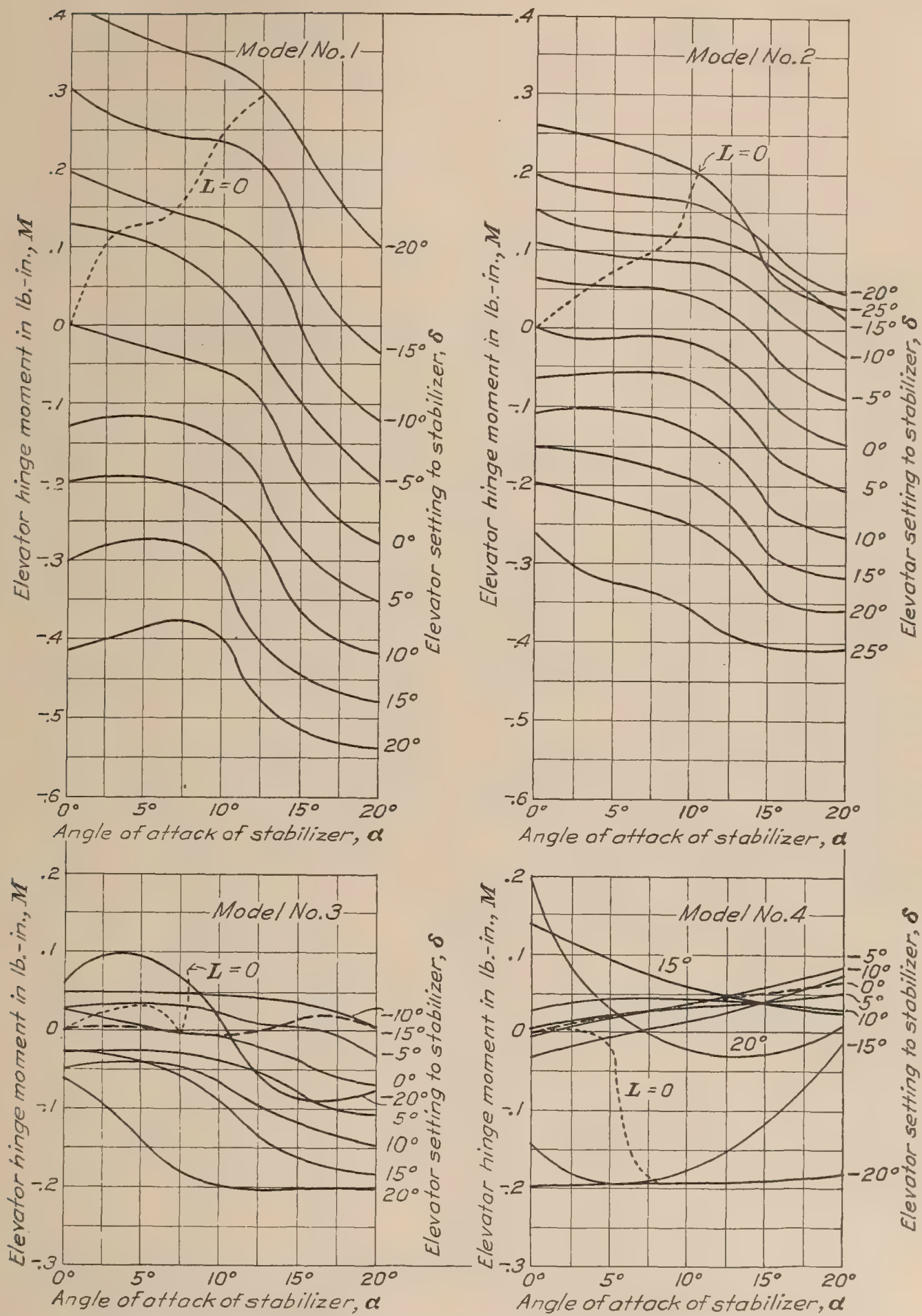
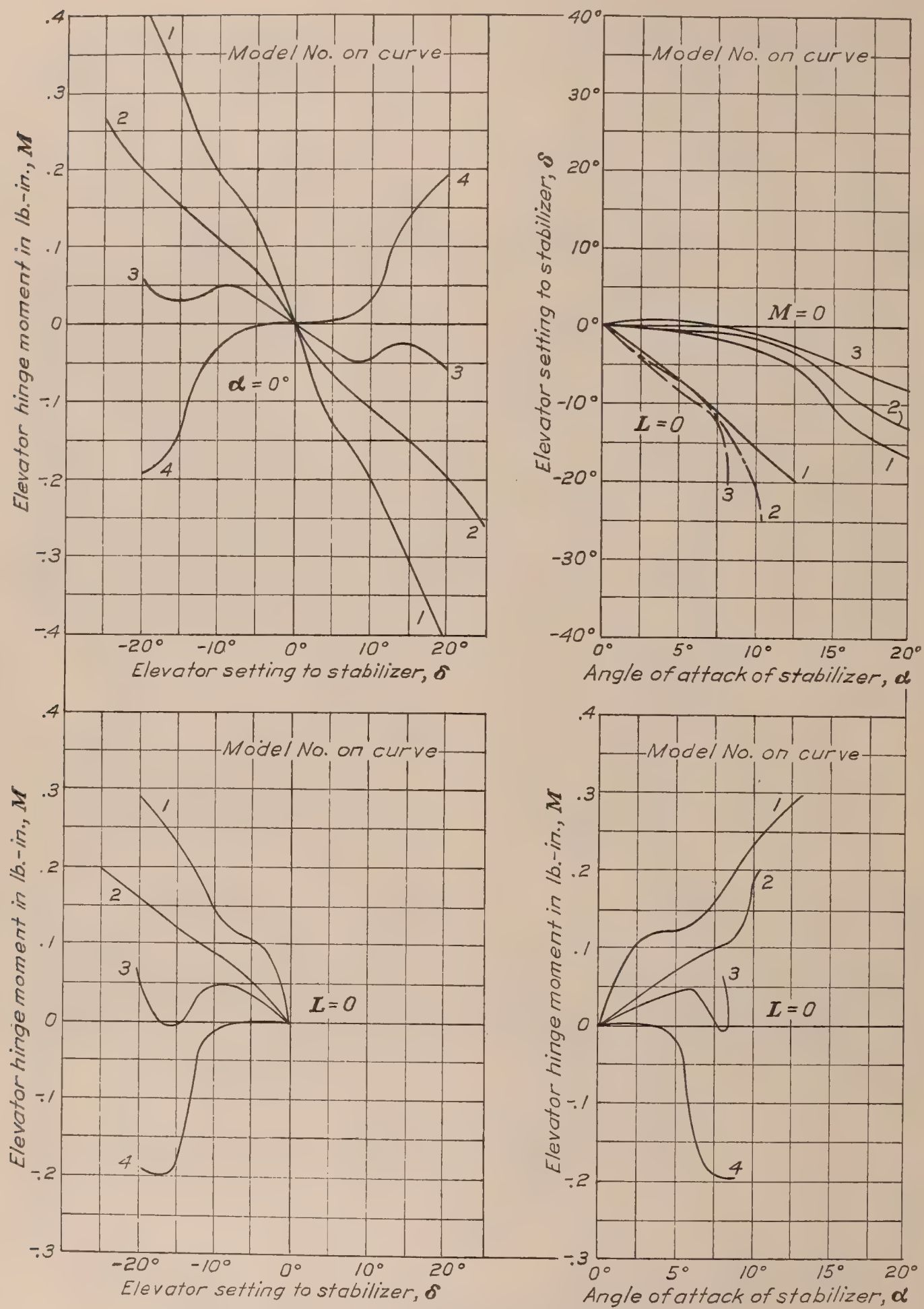


FIG. 15.—Ratio of lift to drag for Model No. 4.
Air speed, 40 M. P. H.

FIG. 16.—Elevator hinge moments, M vs. δ at different α for Models Nos. 1, 2, 3, and 4

FIG. 17.—Elevator hinge moments, M vs. α at different δ for Models Nos. 1, 2, 3, and 4

FIG. 18.—Moment and angle relations for α , L or $M=0$ for Models Nos. 1, 2, 3, and 4

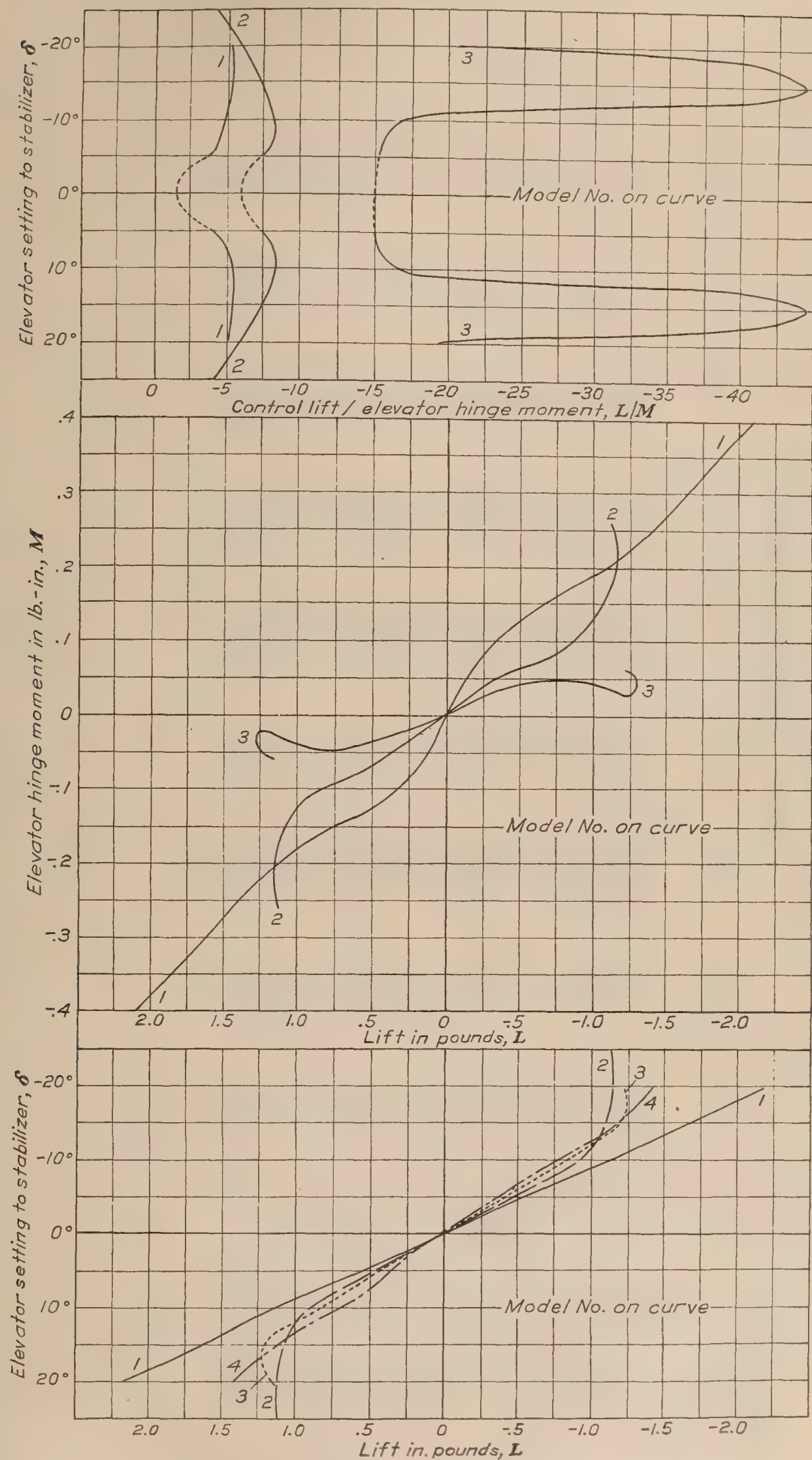
FIG. 19.—Lift and moment data for $\alpha=0$ at 40 M. P. H.

TABLE I
Lift of Handley Page stabilizer and elevator (pounds)
 (Air speed, 40 M. P. H.)

Angle of attack of stabilizer α (degrees)	Elevator setting to stabilizer (degrees) = δ										
	+25	+20	+15	+10	+5	0	-5	-10	-15	-20	-25
Model No. 1:											
0		+2.182	+1.639	+1.124	+0.505	-0.009	-0.511	-1.124	-1.644	-2.174	
+ 5		2.734	2.434	1.880	1.307	+ .809	+ .299	- .274	- .776	1.294	
10		3.368	3.198	2.621	2.086	1.598	1.090	+ .564	+ .095	- .457	
15		3.467	3.314	3.012	2.638	2.286	1.822	1.387	.972	+ .437	
+20		+3.045	+2.970	+2.795	+2.579	+2.374	+2.114	+1.802	+1.470	+1.104	
Model No. 2:											
0	+1.131	+1.149	+1.080	+ .916	+ .473	+ .001	- .481	- .921	-1.077	-1.157	-1.131
+ 5	1.529	1.811	1.794	1.602	1.231	.721	+ .204	- .231	- .556	- .610	.685
10	2.018	2.419	2.491	2.333	1.971	1.473	.926	+ .534	+ .135	+ .054	- .025
15	2.922	3.049	3.142	2.975	2.609	2.199	1.649	1.288	.920	.675	+ .608
20	+2.646	+2.736	+2.877	+2.798	+2.645	+2.448	+2.029	+1.717	+1.451	+1.083	+ .710
Model No. 3:											
0		+1.159	+1.200	+ .831	+ .434	- .003	- .443	- .829	-1.200	-1.221	
+ 5		1.798	1.865	1.536	1.142	+ .755	+ .325	- .159	- .519	- .376	
10		2.293	2.619	2.291	1.918	1.563	1.112	+ .740	+ .369	+ .238	
15		2.534	2.964	2.804	2.530	2.211	1.839	1.495	.991	.677	
20		+2.198	+2.835	+2.825	+2.588	+2.352	+2.125	+1.862	+1.410	+1.069	
Model No. 4:											
0		+1.407	+1.139	+ .702	+ .351	+ .003	- .354	- .783	-1.165	-1.418	
+ 5		1.672	1.641	1.498	1.135	.778	+ .426	.000	- .356	- .538	
10		1.907	2.183	2.269	1.893	1.551	1.212	+ .771	+ .398	+ .133	
15		2.097	2.468	2.793	2.565	2.275	1.968	1.548	1.066	.580	
+20		+2.043	+2.154	+2.678	+2.548	+2.390	+2.190	+1.901	+1.514	+1.062	

TABLE II

Drag of Handley Page stabilizer and elevator (pounds)

(Air speed, 40 M. P. H.)

Angle of attack of stabilizer α (degrees)	Elevator setting to stabilizer (degrees) = δ										
	+25	+20	+15	+10	+5	0	-5	-10	-15	-20	-25
Model No. 1:											
0		0. 254	0. 170	0. 092	0. 045	0. 028	0. 044	0. 090	0. 160	0. 247	
+ 5		. 426	. 356	. 210	. 123	. 077	. 045	. 052	. 068	. 124	
10		. 720	. 646	. 462	. 325	. 227	. 155	. 090	. 084	. 082	
15		1. 173	1. 096	. 892	. 737	. 567	. 463	. 378	. 298	. 217	
+20		1. 458	1. 373	1. 237	1. 078	. 940	. 819	. 699	. 624	. 520	
Model No. 2:											
0	0. 314	. 209	. 144	. 085	. 046	. 037	. 048	. 089	. 140	. 201	0. 317
+ 5	. 438	. 338	. 252	. 185	. 120	. 079	. 046	. 051	. 072	. 126	. 222
10	. 618	. 546	. 457	. 371	. 279	. 183	. 117	. 097	. 084	. 113	. 183
15	1. 091	. 994	. 880	. 752	. 615	. 478	. 352	. 287	. 233	. 225	. 263
+20	1. 398	1. 330	1. 241	1. 118	1. 003	. 855	. 723	. 636	. 559	. 483	. 458
Model No. 3:											
0		. 189	. 110	. 074	. 046	. 039	. 044	. 073	. 109	. 189	
+ 5		. 292	. 229	. 178	. 109	. 084	. 061	. 060	. 075	. 162	
10		. 532	. 467	. 371	. 286	. 229	. 158	. 128	. 103	. 159	
15		. 948	. 888	. 758	. 654	. 565	. 460	. 371	. 288	. 287	
+20		1. 287	1. 257	1. 126	1. 009	. 910	. 811	. 599	. 501	. 484	
Model No. 4:											
0		. 228	. 121	. 068	. 056	. 044	. 059	. 065	. 114	. 228	
+ 5		. 345	. 229	. 164	. 126	. 093	. 069	. 054	. 085	. 165	
10		. 531	. 426	. 357	. 285	. 230	. 174	. 121	. 119	. 169	
15		. 966	. 850	. 732	. 630	. 570	. 477	. 383	. 304	. 287	
+20		1. 371	1. 169	1. 100	1. 013	. 930	. 848	. 743	. 657	. 572	

TABLE III
Absolute lift coefficient, C_L , for Handley Page stabilizer and elevator
 (Air speed, 40 M. P. H.)

Angle of attack of stabilizer α (degrees)	Elevator setting to stabilizer (degrees) = δ										
	+25	+20	+15	+10	+5	0	-5	-10	-15	-20	-25
Model No. 1:											
0		+0. 7100	+0. 5333	+0. 3657	+0. 1643	-0. 0029	-0. 1663	-0. 3657	-0. 5350	-0. 7074	
+ 5		. 8896	. 7920	. 6118	. 4253	+ . 2632	+ . 0973	- . 0892	- . 2525	. 4211	
10		1. 0959	1. 0406	. 8529	. 6788	. 5200	. 3547	+ . 1835	+ . 0309	- . 1487	
15		1. 1282	1. 0784	. 9801	. 8584	. 7439	. 5929	. 4513	. 3163	+ . 1422	
+20		+ . 9908	+ . 9664	+ . 9095	+ . 8392	+ . 7725	+ . 6879	+ . 5864	+ . 4783	+ . 3592	
Model No. 2:											
0	+0. 3711	+ . 3770	+ . 3544	+ . 3006	+ . 1552	+ . 0003	- . 1578	- . 3022	- . 3534	- . 3796	-0. 3711
+ 5	. 5017	. 5942	. 5886	. 5256	. 4039	. 2366	+ . 0669	- . 0758	- . 1824	- . 2002	. 2248
10	. 6621	. 7937	. 8173	. 7655	. 6467	. 4833	. 3038	+ . 1752	+ . 0443	+ . 0177	- . 0082
15	. 9588	1. 0004	1. 0310	. 9762	. 8561	. 7215	. 5411	. 4226	. 3019	. 2215	+ . 1995
+20	+ . 8682	+ . 8977	+ . 9440	+ . 9181	+ . 8679	+ . 8032	+ . 6658	+ . 5634	+ . 4761	+ . 3554	+ . 2330
Model No. 3:											
0		+ . 3803	+ . 3937	+ . 2727	+ . 1424	- . 0010	- . 1454	- . 2720	- . 3937	- . 4006	
+ 5		. 5900	. 6119	. 5040	. 3747	+ . 2477	+ . 1066	- . 0522	- . 1703	- . 1234	
10		. 7524	. 8593	. 7517	. 6293	. 5129	. 3649	+ . 2428	+ . 1211	+ . 0781	
15		. 8315	. 9725	. 9200	. 8301	. 7255	. 6034	. 4905	. 3252	. 2221	
+20		+ . 7212	+ . 9302	+ . 9269	+ . 8492	+ . 7717	+ . 6973	+ . 6110	+ . 4626	+ . 3508	
Model No. 4:											
0		+ . 4617	+ . 3737	+ . 2303	+ . 1152	+ . 0010	- . 1162	- . 2569	- . 3823	- . 4653	
+ 5		. 5486	. 5384	. 4915	. 3724	. 2553	+ . 1398	. 0000	- . 1168	- . 1765	
10		. 6257	. 7163	. 7445	. 6211	. 5089	. 3977	+ . 2530	+ . 1306	+ . 0436	
15		. 6881	. 8098	. 9164	. 8416	. 7465	. 6457	. 5079	. 3498	. 1903	
+20		+ . 6703	+ . 7068	+ . 8787	+ . 8360	+ . 7842	+ . 7186	+ . 6238	+ . 4968	+ . 3485	

TABLE IV
Absolute drag coefficient, C_D , for Handley Page stabilizer and elevator
 (Air speed, 40 M. P. H.)

Angle of attack of stabilizer α (degrees)	Elevator setting to stabilizer (degrees) = δ										
	+25	+20	+15	+10	+5	0	-5	-10	-15	-20	-25
Model No. 1:											
0		0. 0827	0. 0553	0. 0299	0. 0146	0. 0091	0. 0143	0. 0293	0. 0521	0. 0804	
+ 5		. 1386	. 1158	. 0683	. 0400	. 0251	. 0146	. 0169	. 0221	. 0403	
10		. 2343	. 2102	. 1503	. 1058	. 0739	. 0504	. 0293	. 0273	. 0267	
15		. 3817	. 3566	. 2903	. 2398	. 1845	. 1507	. 1230	. 0970	. 0706	
+20		. 4744	. 4468	. 4025	. 3508	. 3059	. 2665	. 2275	. 2030	. 1692	
Model No. 2:											
0	0. 1030	. 0686	. 0472	. 0279	. 0151	. 0121	. 0157	. 0292	. 0459	. 0660	0. 1040
+ 5	. 1437	. 1109	. 0827	. 0607	. 0394	. 0259	. 0151	. 0167	. 0236	. 0413	. 0728
10	. 2028	. 1791	. 1500	. 1217	. 0915	. 0600	. 0384	. 0318	. 0276	. 0371	. 0600
15	. 3580	. 3261	. 2887	. 2467	. 2018	. 1568	. 1155	. 0942	. 0765	. 0738	. 0863
+20	. 4587	. 4364	. 4072	. 3668	. 3291	. 2805	. 2372	. 2087	. 1834	. 1585	. 1503
Model No. 3:											
0		. 0620	. 0361	. 0243	. 0151	. 0128	. 0144	. 0240	. 0358	. 0620	
+ 5		. 0958	. 0751	. 0584	. 0358	. 0276	. 0200	. 0197	. 0246	. 0532	
10		. 1746	. 1532	. 1217	. 0938	. 0751	. 0518	. 0420	. 0338	. 0522	
15		. 3111	. 2914	. 2487	. 2146	. 1854	. 1509	. 1217	. 0945	. 0942	
+20		. 4223	. 4124	. 3695	. 3311	. 2986	. 2661	. 1965	. 1644	. 1588	
Model No. 4:											
0		. 0748	. 0397	. 0223	. 0184	. 0144	. 0194	. 0213	. 0374	. 0748	
+ 5		. 1132	. 0751	. 0538	. 0413	. 0305	. 0226	. 0177	. 0279	. 0541	
10		. 1742	. 1398	. 1171	. 0935	. 0755	. 0571	. 0397	. 0390	. 0555	
15		. 3170	. 2789	. 2402	. 2067	. 1870	. 1565	. 1257	. 0997	. 0942	
+20		. 4499	. 3836	. 3609	. 3324	. 3052	. 2782	. 2438	. 2156	. 1877	

LIFT, DRAG, AND ELEVATOR HINGE MOMENTS

TABLE V
Lift/drag for Handley Page stabilizer and elevator
 (Air speed, 40 M. P. H.)

Angle of attack of stabilizer α (degrees)	Elevator setting to stabilizer (degrees) = δ										
	+25	+20	+15	+10	+5	0	-5	-10	-15	-20	-25
Model No. 1:											
0		+8.60	+9.64	+12.22	+11.22	-0.32	-11.61	-12.50	-10.27	-8.81	
+5		6.42	6.84	8.96	10.63	+10.51	+6.65	-5.27	-11.41	10.43	
10		4.68	4.95	5.68	6.42	7.04	7.04	+6.27	+1.13	-5.58	
15		2.96	3.02	3.38	3.58	4.03	3.94	3.67	3.26	+2.02	
+20		+2.09	+2.16	+2.26	+2.39	+2.53	+2.58	+2.58	+2.36	+2.12	
Model No. 2:											
0	+3.61	+5.50	+7.50	+10.78	+10.28	+0.03	-10.02	-10.35	-7.70	-5.76	-3.57
+5	3.49	5.36	7.12	8.66	10.25	9.13	+4.44	-4.53	-7.72	-4.84	3.09
10	3.27	4.43	5.46	6.30	7.07	8.06	7.91	+5.51	+1.61	+0.48	-0.14
15	2.68	3.07	3.57	3.96	4.24	4.60	4.69	4.49	3.95	3.00	+2.31
+20	+1.89	+2.06	+2.32	+2.50	+2.64	+2.86	+2.81	+2.70	+2.60	+2.24	+1.55
Model No. 3:											
0		+6.14	+10.91	+11.23	+9.44	-0.77	-10.06	-11.35	-11.00	-6.46	
+5		6.16	8.14	8.64	10.48	+8.99	+5.33	-2.65	-6.92	-2.32	
10		4.32	5.61	6.18	6.71	6.83	7.04	+5.78	+3.58	+1.50	
15		2.67	3.34	3.70	3.87	3.92	4.00	4.03	3.44	2.36	
+20		+1.71	+2.26	+2.51	+2.56	+2.59	+2.62	+3.11	+2.81	+2.21	
Model No. 4:											
0		+6.18	+9.42	+10.32	+6.28	+0.07	-6.00	-12.05	-10.22	-6.22	
+5		4.85	7.17	9.14	9.01	8.37	+6.18	0.00	-4.19	-3.26	
10		3.59	5.13	6.36	6.64	6.75	6.97	+6.37	+3.34	+0.79	
15		2.17	2.90	3.82	4.07	4.00	4.13	4.04	3.51	2.02	
+20		+1.49	+1.84	+2.43	+2.51	+2.57	+2.58	+2.56	+2.31	+1.86	

TABLE VI

Lift coefficient, K_u , for Handley Page stabilizer and elevator (lb./ft.³/mi.²/hr.²)

(Air speed 40 M. P. H.)

α^*	Elevator setting to stabilizer (degrees) = δ										
	+25	+20	+15	+10	+5	0	-5	-10	-15	-20	-25
Model No. 1:											
0		+0.001818	+0.001365	+0.000936	+0.000421	-0.000007	-0.000426	-0.000936	-0.001370	-0.001811	
+ 5		.002277	.002028	.001566	.001089	+0.000674	+0.000249	-0.000228	-0.000646	.001078	
10		.002806	.002664	.002183	.001738	.001331	.000908	+0.000470	+0.000079	-0.000381	
15		.002888	.002761	.002509	.002198	.001904	.001518	.001155	.000810	+0.000364	
+20		+0.002536	+0.002474	+0.002328	+0.002148	+0.001978	+0.001761	+0.001501	+0.001224	+0.000920	
Model No. 2:											
0	+0.000950	+0.000965	+0.000907	+0.000770	+0.000397	+0.000001	-0.000404	-0.000774	-0.000905	-0.000972	-0.000950
+ 5	.001284	.001521	.001507	.001346	.001034	.000606	+0.000171	-0.000194	-0.000467	-0.000513	.000575
10	.001695	.002032	.002092	.001960	.001656	.001237	.000778	+0.000449	+0.000113	+0.000045	-0.000021
15	.002455	.002561	.002639	.002499	.002192	.001847	.001385	.001082	.000773	.000567	+0.000511
+20	+0.002223	+0.002298	+0.002418	+0.002350	+0.002222	+0.002056	+0.001704	+0.001442	+0.001219	+0.000910	+0.000596
Model No. 3:											
0		+0.000974	+0.001008	+0.000698	+0.000365	-0.000003	-0.000372	-0.000696	-0.001008	-0.001026	
+ 5		.001510	.001566	.001290	.000959	+0.000634	+0.000273	-0.000134	-0.000436	-0.000316	
10		.001926	.002200	.001924	.001611	.001313	.000934	+0.000622	+0.000310	+0.000200	
15		.002129	.002490	.002355	.002125	.001857	.001545	.001256	.000833	.000569	
+20		+0.001846	+0.002381	+0.002373	+0.002174	+0.001976	+0.001785	+0.001564	+0.001184	+0.000898	
Model No. 4:											
0		+0.001182	+0.000957	+0.000590	+0.000295	+0.000003	-0.000297	-0.000658	-0.000979	-0.001191	
+ 5		.001404	.001378	.001258	.000953	.000654	+0.000358	.000000	-0.000299	-0.000452	
10		.001602	.001834	.001906	.001590	.001303	.001018	.000648	+0.000334	+0.000112	
15		.001762	.002073	.002346	.002154	.001911	.001653	.001300	.000895	.000487	
+20		+0.001716	+0.001809	+0.002249	+0.002140	+0.002008	+0.001840	+0.001597	+0.001272	+0.000892	

* α =angle of attack of stabilizer (degrees).

TABLE VII

Drag coefficient, K_x , for Handley Page stabilizer and elevator ($\text{lb./ft.}^2/\text{mi.}^2/\text{hr.}^2$)

(Air speed, 40 M. P. H.)

α^*	Elevator setting to stabilizer (degrees) = δ										
	+25	+20	+15	+10	+5	0	-5	-10	-15	-20	-25
Model No. 1:											
0		0. 0002117	0. 0001416	0. 0000765	0. 0000374	0. 0000233	0. 0000366	0. 0000750	0. 0001334	0. 0002058	
+ 5		. 0003548	. 0002964	. 0001748	. 0001024	. 0000643	. 0000374	. 0000433	. 0000566	. 0001032	
10		. 0005998	. 0005381	. 0003848	. 0002708	. 0001892	. 0001290	. 0000750	. 0000699	. 0000684	
15		. 0009772	. 0009129	. 0007431	. 0006139	. 0004723	. 0003858	. 0003149	. 0002483	. 0001807	
+20		. 0012145	. 0011438	. 0010304	. 0008980	. 0007831	. 0006822	. 0005824	. 0005197	. 0004332	
Model No. 2:											
0	0. 0002637	. 0001756	. 0001208	. 0000714	. 0000387	. 0000310	. 0000402	. 0000748	. 0001175	. 0001690	0. 0002662
+ 5	. 0003679	. 0002839	. 0002117	. 0001554	. 0001009	. 0000663	. 0000387	. 0000428	. 0000604	. 0001057	. 0001864
10	. 0005192	. 0004585	. 0003840	. 0003116	. 0002342	. 0001536	. 0000983	. 0000814	. 0000707	. 0000950	. 0001536
15	. 0009165	. 0008348	. 0007391	. 0006316	. 0005166	. 0004014	. 0002957	. 0002412	. 0001958	. 0001889	. 0002209
+20	. 0011743	. 0011172	. 0010424	. 0009390	. 0008425	. 0007181	. 0006072	. 0005343	. 0004695	. 0004058	. 0003848
Model No. 3:											
0		. 0001587	. 0000924	. 0000622	. 0000387	. 0000328	. 0000369	. 0000614	. 0000916	. 0001587	
+ 5		. 0002452	. 0001923	. 0001495	. 0000916	. 0000707	. 0000512	. 0000504	. 0000630	. 0001362	
10		. 0004470	. 0003922	. 0003116	. 0002401	. 0001923	. 0001326	. 0001075	. 0000865	. 0001336	
15		. 0007964	. 0007460	. 0006367	. 0005494	. 0004746	. 0003863	. 0003116	. 0002419	. 0002412	
+20		. 0010811	. 0010557	. 0009459	. 0008476	. 0007644	. 0006812	. 0005030	. 0004208	. 0004065	
Model No. 4:											
0		. 0001915	. 0001016	. 0000571	. 0000471	. 0000369	. 0000497	. 0000545	. 0000957	. 0001915	
+ 5		. 0002898	. 0001923	. 0001377	. 0001057	. 0000781	. 0000579	. 0000453	. 0000714	. 0001385	
10		. 0004460	. 0003579	. 0002998	. 0002394	. 0001933	. 0001462	. 0001016	. 0000998	. 0001421	
15		. 0008115	. 0007140	. 0006149	. 0005292	. 0004787	. 0004006	. 0003218	. 0002552	. 0002412	
+20		. 0011517	. 0009820	. 0009239	. 0008509	. 0007813	. 0007122	. 0006241	. 0005519	. 0004805	

* α = angle of attack of stabilizer (degrees).

TABLE VIII
Elevator hinge moments for Handley Page control surfaces (lb. in.)
 (Air speed, 40 M. P. H.)

Angle of attack of stabilizer α^1 (degrees)	Elevator setting to stabilizer (degrees) = δ										
	25°	20°	15°	10°	5°	0°	-5°	-10°	-15°	-20°	-25°
Model No. 1:											
0-----		-0. 412	-0. 301	-0. 199	-0. 129	0. 000	+0. 129	0. 199	0. 301	+0. 412	-----
5-----		-. 384	-. 272	-. 195	-. 116	-. 029	+ . 106	. 159	. 251	+ . 367	-----
10-----		-. 398	-. 310	-. 225	-. 143	-. 059	+ . 044	. 126	. 235	+ . 333	-----
15-----		-. 514	-. 444	-. 367	-. 284	-. 193	-. 100	-. 007	+ . 092	+ . 231	-----
20-----		-. 537	-. 478	-. 418	-. 350	-. 278	-. 199	-. 118	-. 033	+ . 102	-----
Model No. 2:											
0-----	-0. 260	-. 199	-. 151	-. 109	-. 064	. 000	+ . 064	. 109	. 151	. 199	+0. 260
5-----	-. 324	-. 220	-. 161	-. 105	-. 057	-. 011	+ . 055	. 093	. 123	. 173	+ . 240
10-----	-. 355	-. 251	-. 191	-. 129	-. 063	-. 017	+ . 044	. 088	. 120	. 163	+ . 205
15-----	-. 407	-. 339	-. 288	-. 223	-. 154	-. 088	-. 025	+ . 035	. 081	. 108	+ . 079
20-----	-. 407	-. 358	-. 317	-. 263	-. 204	-. 146	-. 089	-. 034	+ . 019	. 046	+ . 025
Model No. 3:											
0-----		-. 059	-. 027	-. 050	-. 029	. 000	. 029	. 050	. 027	+ . 059	-----
5-----		-. 137	-. 039	-. 039	-. 023	+ . 004	. 034	. 049	+ . 009	+ . 099	-----
10-----		-. 196	-. 087	-. 061	-. 035	-. 006	+ . 024	+ . 046	-. 006	+ . 022	-----
15-----		-. 201	-. 160	-. 117	-. 075	-. 034	+ . 006	. 039	+ . 015	-. 087	-----
20-----		-. 201	-. 181	-. 144	-. 107	-. 069	-. 029	+ . 011	+ . 007	-. 073	-----
Model No. 4:											
0-----		+ . 196	. 142	. 030	+ . 003	. 000	-. 003	-. 030	-. 142	-. 196	-----
5-----											-----
10-----		-. 019	+ . 062	. 045	. 033	. 038	. 039	+ . 016	-. 176	-. 190	-----
15-----											-----
20-----		+ . 010	. 028	. 031	. 052	. 067	. 087	+ . 075	-. 012	-. 181	-----

TABLE IX

Slope, m , of C_L curves for elevator settings between $+10^\circ$ and -10° for Handley Page stabilizer and elevator

$\Delta\alpha=5^\circ$ in each case. Air speed, 40 M. P. H.

Elevator setting to stabilizer δ (degrees)	Model No. 1		Model No. 2		Model No. 3		Model No. 4	
	ΔC_L	Slope $m = \frac{\Delta C_L}{\Delta \alpha}$	ΔC_L	Slope $m = \frac{\Delta C_L}{\Delta \alpha}$	ΔC_L	Slope $m = \frac{\Delta C_L}{\Delta \alpha}$	ΔC_L	Slope $m = \frac{\Delta C_L}{\Delta \alpha}$
+10 -----	0. 246	0. 0492	0. 232	0. 0464	0. 227	0. 0454	0. 260	0. 0520
+5 -----	. 255	. 0510	. 248	. 0496	. 230	. 0460	. 255	. 0510
0 -----	. 260	. 0520	. 241	. 0482	. 245	. 0490	. 258	. 0516
-5 -----	. 259	. 0518	. 228	. 0456	. 258	. 0516	. 256	. 0512
-10 -----	. 273	. 0546	. 232	. 0464	-----	-----	. 256	. 0512
Average slope -----	-----	. 0517	-----	. 0472	-----	. 0480	-----	. 0514

REPORT No. 279

**TESTS ON MODELS OF THREE BRITISH AIRPLANES
IN THE VARIABLE DENSITY WIND TUNNEL**

**By GEORGE J. HIGGINS and GEORGE L. DeFOE
Langley Memorial Aeronautical Laboratory**

**W. S. DIEHL
Bureau of Aeronautics, Navy Department**

REPORT No. 279

TESTS ON MODELS OF THREE BRITISH AIRPLANES IN THE VARIABLE DENSITY WIND TUNNEL

By GEORGE J. HIGGINS, W. S. DIEHL, and GEORGE L. DEFoe

SUMMARY

This report contains the results of tests made in the National Advisory Committee for Aeronautics variable density wind tunnel on three airplane models supplied by the British Aeronautical Research Committee. These models, the BE-2E with R. A. F. 19 wings, the Bristol Fighter with R. A. F. 15 wings, and the Bristol Fighter with R. A. F. 30 wings, were tested over a wide range in Reynolds Numbers in order to supply data desired by the Aeronautical Research Committee for scale effect studies.

The maximum lifts obtained in these tests are in excellent agreement with the published results of British tests, both model and full scale. No attempt is made to compare drag data, owing to the



FIG. 1.—BE-2E airplane model with special equipment as tested

omission of tail surfaces, radiator, etc., from the model, but it is shown that the scale effect observed on the drag coefficients in these tests is due to a large extent to the parts of the models other than the wings.

INTRODUCTION

At the request of the British Aeronautical Research Committee, nominal models of three British airplanes incorporating wing sections of widely different aerodynamic characteristics, have been tested in the variable density wind tunnel over a range in Reynolds Number extending from about 150,000 to more than 3,000,000. These models have been designated as "nominal," since no attempt was made to incorporate all details necessary for geometrical similarity; the omission of the tail surfaces and radiators being the most important deviations in this respect. The tests on such models may be expected to indicate the scale effect on lift with fair accuracy, but previous experience with the variable density wind tunnel has shown that the drag data are not reliable unless exact geometric similarity is obtained. (See Reference 1.) The foregoing limitations must be borne in mind in any interpretation of the test results.

The purpose of these tests was to supply data for comparative studies by the British Aeronautical Research Committee. The models had previously been tested very thoroughly in England, and comparisons made with full scale flight test data on the airplanes represented.

DESCRIPTION OF MODELS AND METHOD OF TESTING

The three models, consisting of a BE-2E to one-twelfth scale fitted with R. A. F. 19 wings, and two Bristol Fighters to one-fifteenth scale fitted with R. A. F. 15 and R. A. F. 30 wings, were tested as supplied by the British Aeronautical Research Committee. The constructional details of the models are clearly shown in Figures 1 to 5. It will be noted that the tail surfaces are omitted and that various other details do not conform to the requirements of geometrical similarity. For this reason it is desired to emphasize the fact that the test data are valid only in comparison with data obtained in other tests on the same or similar models.

The method of mounting the models during the tests is shown in Figures 2, 3, and 5. The model is supported by two vertical stream-line rods which are hinged at their point of attachment to the model and rigidly connected to the balance at their lower ends. A short horizontal yoke rigidly attached to the shielded vertical balance bar, extends upstream and is hinged to the rear of the model. The angle of attack is changed at the operating panel outside of the tunnel, through an electric drive which raises or lowers the vertical balance bar. A detailed explanation of the operation of the balance in measuring lift, drag, and pitching moments is given in reference 2. The interference between the shielded vertical balance bar and the model was carefully investigated in the tests on the Sperry Messenger model (Reference 1) and found to be negligible.

TEST RESULTS

Each model was tested at pressures of approximately 1, $2\frac{1}{2}$, 5, 10, and 20 atmospheres. In each test the dynamic pressure was held as nearly constant as practicable at a value corresponding to a velocity of about 22 meters per second. The coefficients are based on the true dynamic pressure which was determined for each observation. Drag coefficients and angles of attack have been corrected for tunnel wall effect by the Prandtl formulas,

$$\Delta C_D = \frac{C_L^2 S}{2\pi D^2},$$

and

$$\Delta \alpha = \frac{57.3 C_L S}{2\pi D^2}$$

where S is the model wing area, and D the tunnel diameter. In tabulating the test data, both corrected and uncorrected values of C_D and α have been given. The test data are given in Tables I to XV inclusive and the various plots of these data in Figures 6 to 26 inclusive.

The usual absolute coefficients have been used. These are defined by the relations:

$$\text{Lift} = C_L q S$$

$$\text{Drag} = C_D q S$$

$$\text{Pitching moment about reference axis} = C_M q S c$$

where q is the dynamic pressure $\frac{1}{2} \rho V^2$ and S the wing area.

The center of gravity locations for the three models were not given, so arbitrary reference axes have been taken. The location of these axes is given along with the model dimensions in Table XVI.

The following summary of tables and figures is included for convenience:
BE-2E with R. A. F. 19 wings:

Test data at 1, $2\frac{1}{2}$, 5, 10, and 20 atmospheres—Tables I to V, inclusive.

C_L vs. α —Figure 6.

C_D vs. α —Figure 7.

C_D vs. C_L —Figure 8.

L/D vs. C_L —Figure 9.

C_M vs. C_L —Figure 10.

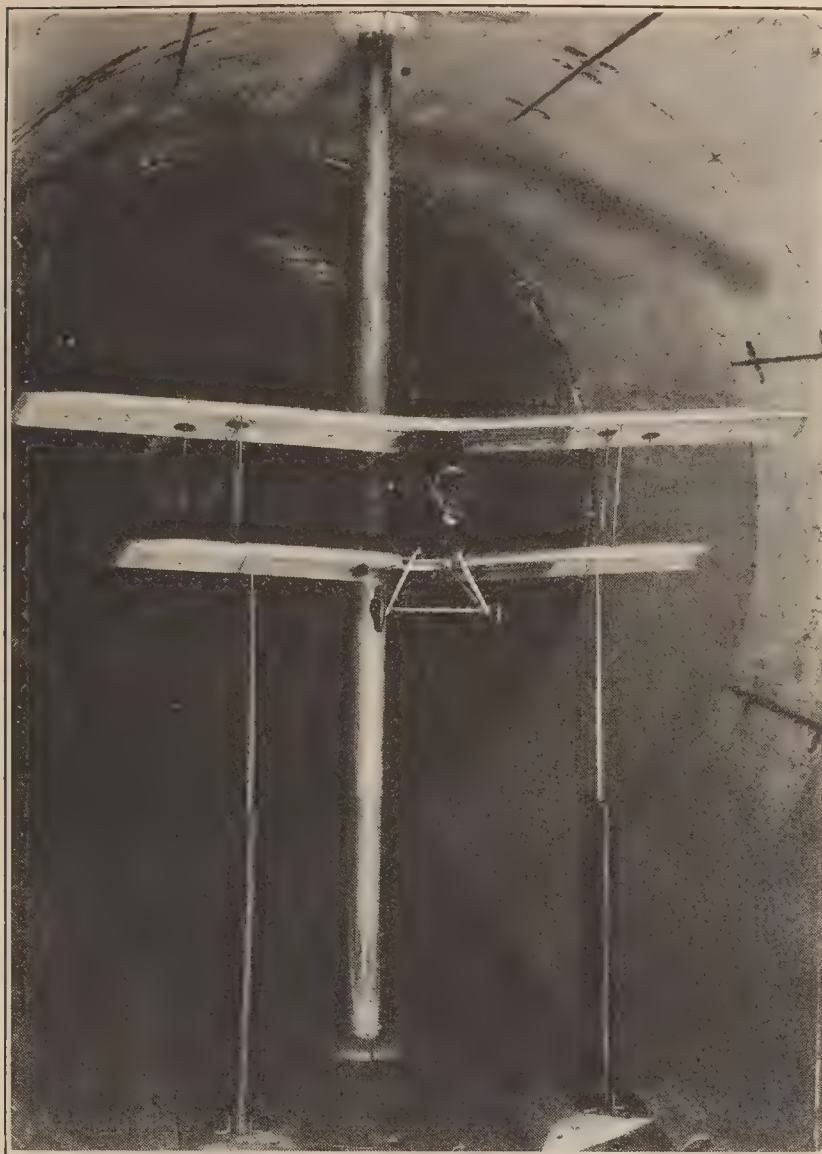


FIG. 2.—BE-2E airplane model mounted in tunnel

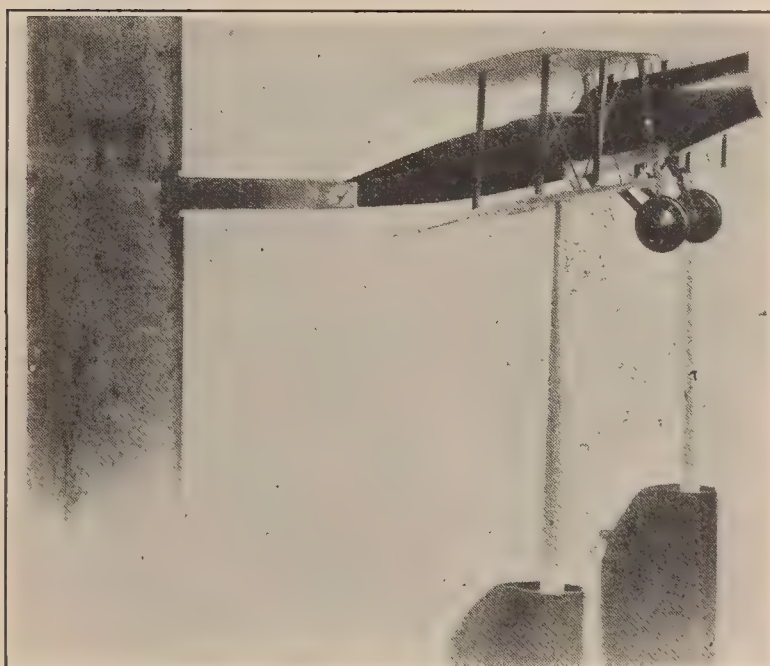


FIG. 3.—Bristol Fighter airplane model with R. A. F. 15 wings as mounted in tunnel



FIG. 4.—Bristol Fighter airplane model with R. A. F. 30 wings

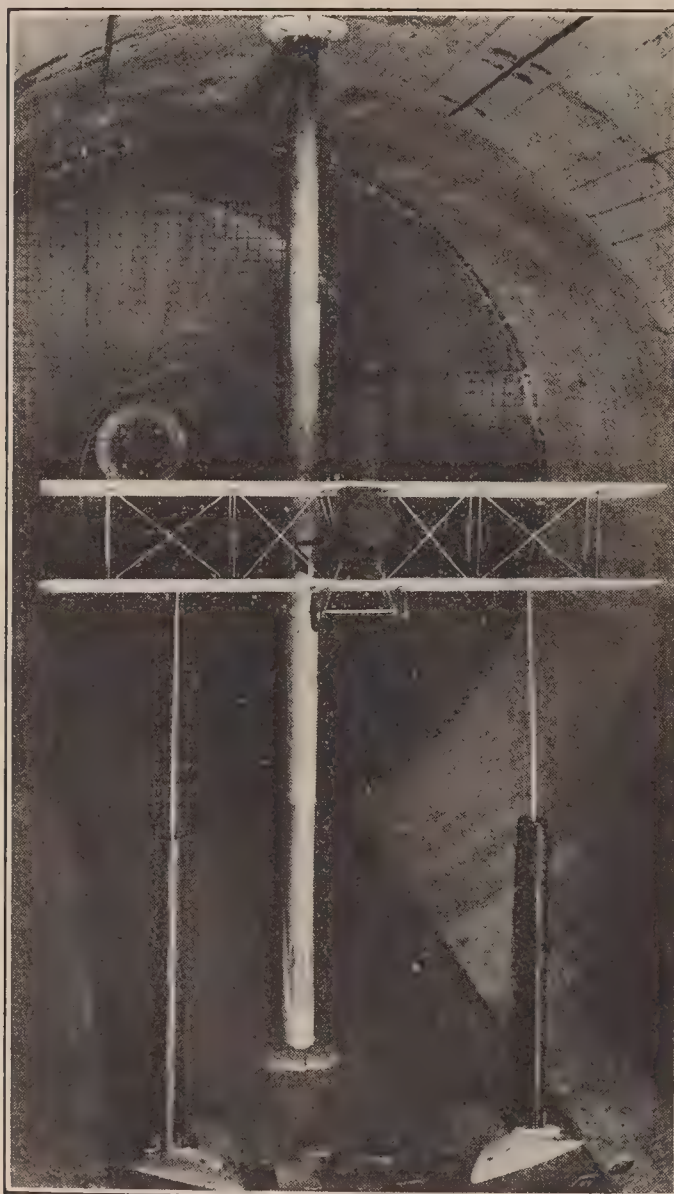


FIG. 5.—Bristol Fighter airplane model with R. A. F. 30 wings mounted in tunnel

BE-2E with R. A. F. 19 wings—Continued.

$C_{L_{max}}$ and α vs. Reynolds Number—Figure 11.

$C_{L_{max}}$ vs. Reynolds Number—Figure 12.

$C_{D_{min}}$ vs. Reynolds Number—Figure 13.

Dimensional data on model—Table XVI.

Bristol Fighter with R. A. F. 15 wings:

Test data at 1, 2½, 5, 10, and 20 atmospheres—Tables VI to X inclusive.

C_L vs. α —Figure 14.

C_D vs. α —Figure 15.

C_D vs. C_L —Figure 16.

L/D vs. C_L —Figure 17.

C_M vs. C_L —Figure 18.

$C_{L_{max}}$ vs. Reynolds Number—Figure 19.

$C_{D_{min}}$ vs. Reynolds Number—Figure 20.

Dimensional data on model—Table XVI.

Bristol Fighter with R. A. F. 30 wings:

Test data at 1, 2½, 5, 10, and 20 atmospheres—Tables XI to XV inclusive.

C_L vs. α —Figure 21.

C_D vs. α —Figure 22.

C_D vs. C_L —Figure 23.

L/D vs. C_L —Figure 24.

C_M vs. C_L —Figure 25.

$C_{L_{max}}$ vs. Reynolds Number—Figure 26.

$C_{D_{min}}$ vs. Reynolds Number—Figure 20.

Dimensional data on model—Table XVI.

Comparison of sections R. A. F. 30, Göttingen 459, N. A. C. A. 99—Figure 27.

DISCUSSION OF DATA

BE-2E model with R. A. F., 19 wings:

The variation in $C_{L_{max}}$ with Reynolds Number for this model is so great that it constitutes the most striking feature of the tests. The following tabulation of data selected from Tables I to V and Figures 6, 11, and 12, will assist in the study of the changes:

Tunnel pressure atmospheres.....	1	2½	5	10	20
Reynolds Number $\times 10^{-5}$	1.915	4.61	9.49	18.70	40.0
$C_{L_{max}}$	1.69	1.67	1.62	1.43	1.41
Angle of attack at $C_{L_{max}}$ α_m	21.0°	20.1°	19.3°	13.5°	12.4°
Angle of attack for $C_L=0$ α_o	-9.0°	-9.0°	-9.0°	-8.9°	-9.1°
$\alpha_m - \alpha_o$	30.0°	29.1°	28.3°	22.4°	21.5°

$C_{L_{max}}$ is greatest at 1 atmosphere and decreases gradually up to a tank pressure of 5 atmospheres. Between 5 and 10 atmospheres, or as shown by Figure 11, between Reynolds Numbers 1,000,000 and 1,800,000 there is rapid decrease in $C_{L_{max}}$. Increasing the Reynolds Number above this critical value causes $C_{L_{max}}$ to decrease slightly more but at such a slow rate that the change is negligible. It has been noted in previous tests in the variable density tunnel that all very thick and very highly cambered wing sections tend to show a decrease in $C_{L_{max}}$ if the Reynolds Number be made great enough. For example, the U. S. A., 35A section is of conventional form, similar to the Göttingen 387, but having a camber of 18.18% as compared with 15.2% for the R. A. F. 19. Tests on this section (reference 3) show that at 1 atmosphere $C_{L_{max}} = 1.57$ and at 20 atmospheres $C_{L_{max}} = 1.21$, with intermediate values closely parallel to those found for the R. A. F. 19. It therefore follows that very high lifts on highly cambered sections found in tests at moderate Reynolds Numbers should be viewed with suspicion since it is unlikely that they can be realized at full scale.

That these characteristics are inherent with the R. A. F. 19 section, and are not an interference effect, is clearly evident from the comparison in Figure 12 of the curves of $C_{L_{max}}$ against Reynolds Number for R. A. F. 19 section alone and for the BE-2E model. It is of interest to note in this connection that data on the R. A. F. 19 section have been obtained at very low Reynolds Numbers by operating the tunnel at subatmospheric pressures.

The effect of Reynolds Number on C_D is not as great as on C_L , but it is considerable, as shown by the following tabulation of $C_{D_{min}}$ from the data in Tables I to V and plotted in Figure 13:

Reynolds Number $\times 10^{-5}$ -----	1.915	4.61	9.49	18.70	40.00
$C_{D_{min}}$ -----	.0861	.0850	.0854	.0782	.0719

The most important feature seems to be the pronounced reduction in $C_{D_{min}}$ concurrent with the reduction in $C_{L_{max}}$ previously noted. By comparison with a similar curve obtained by testing the R. A. F. 19 airfoil section, it may be concluded that this scale effect is primarily due to the wings. There also seems to be a large scale effect in the second regime but inspection of the curves in Figure 7 shows that the curves may be too irregular to justify any definite conclusions. The irregularities in the curves for both C_L and C_D at low angles are probably due to the unstable nature of the flow over the lower surface near the leading edge.

The plot of C_D vs. C_L (fig. 8), brings out the scale effect on drag much better than plot of C_D vs. α . For values of C_D corresponding to values of C_L less than 1.0, there is a large scale effect on C_D , particularly noticeable for the higher Reynolds Numbers. This condition is also shown by the plotting of L/D vs. C_L , Figure 9.

The moment curves of Figure 10 are rather irregular and do not indicate any very definite tendency except that at the higher lift coefficients the 10 and 20 atmosphere curves are displaced very slightly towards the base line.

Bristol Fighter with R. A. F., 15 wings:

The curves of C_L vs. α for this model, Figure 14, show no unusual features except at angles of attack greater than 12° where a moderate scale effect is found. $C_{L_{max}}$ increases from 0.99 at 1 atmosphere to 1.11 at 2.5 atmospheres and then falls off gradually to 1.032 at 20 atmospheres, Figure 19. The constancy of the angle of attack for zero lift is again noticeable. Between $C_L=0$ and $C_L=0.9$ the divergencies of the C_L curves are small and rather inconclusive but a tendency may be observed for C_L to decrease when the Reynolds Number is increased.

The curves of C_D vs. α , Figure 15, indicate a considerable decrease in C_D as Reynolds Number is increased. If the curves for 1 and for 20 atmospheres be compared the decrease in C_D is comparatively uniform except at the critical angle range between 13° and 16° . This is shown quite clearly by the polar plot, Figure 16, which also indicates that the value of $C_{D_{min}}$ is less at 1 atmosphere than at $2\frac{1}{2}$ and 5 atmospheres. This condition is probably due to the experimental errors in reading the low drags at 1 atmosphere.

The improvement in L/D , shown by the plot of L/D vs. C_L on Figure 17, is about of the same order as that observed on the BE-2E model, Figure 9. A point of similarity is to be found in that the curves in each series fall into two groups: One containing the 1, $2\frac{1}{2}$, and 5 atmosphere data, the other containing the 10 and 20 atmosphere data. This would indicate a change in flow type between the 5 and 10 atmosphere conditions for both models. Another point of interest is that L/D_{max} for the various Reynolds Numbers tends to occur at the same value of C_L for the Bristol Fighter with R. A. F. 15 wings, while for the BE-2E model the value of C_L at L/D_{max} decreases as the Reynolds Number increases.

Figure 20 contains the plot against Reynolds Number of $C_{D_{min}}$ for the Bristol Fighter model, for the R. A. F. 15 airfoil, and for the difference between the two, representing the drag of the model less wings plus interference. It is apparent that the scale effects observed on this model are due almost entirely to parts other than the wings, and in all probability the struts account for a large proportion of the total effect.

The moment curves of Figure 18 show no well defined tendencies. The cause of the irregularity in the 10-atmosphere curve is not known and no indication of a change in flow type can be found in the remaining data at 10 atmospheres.

Bristol Fighter with R. A. F., 30 wings:

The curves of C_L vs. α for this model, Figure 21, show a very large scale effect on lift coefficients at angles of attack greater than 11° , but below this angle the effects of Reynolds Number are negligible. The angle of attack for zero lift appears to be practically unaffected by changes in Reynolds Number.

The following data have been abstracted from Tables XI to XV:

Tank pressure atmosphere-----	1	2½	5	10	20
Reynolds Number $\times 10^{-5}$ -----	1.52	4.04	7.60	15.00	30.50
$C_{L_{max}}$ -----	0.761	0.814	0.916	1.067	1.006
Angle of attack for $C_{L_{max}}$ ----- α_m -----	14.0°	14.0°	16.0°	20.0°	17.0°
Angle of attack for $C_L=0$ ----- α_o -----	-0.4°	-0.4°	-0.4°	-0.1°	-0.4°

Both $C_{L_{max}}$ and α_m increase with tank pressure up to 10 atmospheres, or to a Reynolds Number of about 1,800,000, above which they decrease slowly as Reynolds Number is increased. This characteristic appears to be a property of the moderately thick, double-cambered sections, as shown by the comparative plots, on Figure 26, of $C_{L_{max}}$ vs. Reynolds Number for the present model, for the N. A. C. A. 99 airfoil and the Göttingen 459 airfoil. The Göttingen 459 section differs very little from the R. A. F. 30 but the N. A. C. A. 99 is considerably thicker at points forward of the maximum ordinate. Figure 27 is a superposed plot of the three sections, for comparison.

It is of interest to note that the major scale effect on C_L for the R. A. F. 30 section is of the same type as that for the R. A. F. 15 and the R. A. F. 19, in that it consists of an expansion or contraction of the angular range between zero and maximum lift, without any marked changes in the angle of attack for zero lift or in the slope of the lift curves $\frac{dC_L}{d\alpha}$.

The scale effect on C_D for the Bristol Fighter with R. A. F. 30 wings is about the same as that observed for the R. A. F. 15 wings, and as shown by the curves of $C_{D_{min}}$ vs. Reynolds Number, Figure 20, it is also due to the same causes, that is, to parts other than the wings. Referring to Figure 4, it is quite apparent that the considerable length of small streamline struts and of large brace wires is responsible for the greater part of the effect observed. Consequently, it is rather difficult to apply a general interpretation to the curves of C_D or L/D .

The moment curves of Figure 25 are again erratic and show no well defined tendency. The only general conclusion justified is that the change of moment from model to full scale is probably of no great importance.

CONCLUSIONS

The following conclusions may be drawn from the present tests, due consideration being given to data previously accumulated in the variable density wind tunnel:

1. The scale effects depend on the airfoil section and are, in general, similar for similar sections.

2. All airfoil sections may be roughly divided into three general classes as follows:

(a) The highly cambered or very thick section having a very high lift at Reynolds Numbers within the testing range of the average wind tunnel. This class, of which the R. A. F. 19 is an example, usually shows a decrease in $C_{L_{max}}$ with increase in Reynolds Number.

(b) The moderately cambered, medium lift section, of which the R. A. F. 15 is an example. This class usually has a moderate, and favorable scale effect on C_L with a fairly low and favorable scale effect on C_D .

(c) The thin, to moderately thick, double-cambered section of low lift at normal test Reynolds Numbers. This class, of which the R. A. F. 30 is an example, usually shows a large increase in $C_{L_{max}}$ and a moderate decrease in $C_{D_{min}}$ with increase in Reynolds Number.

3. The scale effect on drag found in this investigation is caused to a large extent by the wing bracing used on the models.

4. The lift coefficients obtained in the variable density wind tunnel are in excellent agreement with those found in previous tests on the same models and also with the reported full-scale data.

LANGLEY MEMORIAL AERONAUTICAL LABORATORY,
NATIONAL ADVISORY COMMITTEE FOR AERONAUTICS,
LANGLEY FIELD, VA., *April 5, 1927.*

REFERENCES

1. MUNK, MAX M., and DIEHL, WALTER S.
"The Air Forces on a Model of the Sperry Messenger Airplane without Propeller." N. A. C. A., Technical Report No. 225. 1925.
2. MUNK, MAX M., and MILLER, ELTON W.
"The Variable Density Wind Tunnel of the National Advisory Committee for Aeronautics." N. A. C. A., Technical Report No. 227. 1926.
3. HIGGINS, GEORGE J.
"The Comparison of Well Known and New Wing Sections Tested in the Variable Density Wind Tunnel." N. A. C. A., Technical Note No. 219. 1925.
4. GARNER, H. M., and BRADFIELD, F. B.
"Lift and Drag of BE-2E with R. A. F., 19 Wings. Comparison of Full Scale and Model Results." British Aeronautical Research Committee Reports and Memoranda No. 763 (Ae. 24), August, 1921.
5. AERODYNAMICS STAFF.
"Lift and Drag of the Bristol Fighter with Wings of Three Aspect Ratios." British Aeronautical Research Committee Reports and Memoranda No. 859. (Ae. 99.) April, 1923.
6. AERODYNAMICS STAFF.
"Lift and Drag of Standard Bristol Fighter with R. A. F. 4D Engine. Comparative Full Scale and Model Tests." British Aeronautical Research Committee Reports and Memoranda No. 896. (Ae. 126.) November, 1923.
7. MUNK, MAX M.
"Preliminary Wing Model Tests in the Variable Density Wind Tunnel of the National Advisory Committee for Aeronautics." N. A. C. A., Technical Report No. 217. 1925.
8. WIESELSBERGER, C., BETZ, A., and PRANDTL, L.
"Ergebnisse der Aerodynamischen Versuchsanstalt zu Göttingen." (Results obtained in the Göttingen Aerodynamic Laboratory—Report I, 1921.)
9. BRADFIELD, F. B., and HARTSHORN, A. S.
"Test of Four Thick Aerofoils, R. A. F., 30, 31, 32, and 33." British Aeronautical Research Committee. Reports and Memoranda No. 928. (Ae. 150.) September, 1924.
10. NUTT, A. E. WOODWARD, HARRIS, R. G., and CAYGILL, L. E.
"Full Scale and Model Measurements of Lift and Drag of Bristol Fighter with R. A. F. 30 Wings." British Aeronautical Research Committee Reports and Memoranda No. 1052. August, 1926.

TABLE I

MODEL, BE-2E (R. A. F., 19 WINGS) AIRPLANE MODEL. AVERAGE TANK PRESSURE, 1 ATM.
AVERAGE DYNAMIC PRESSURE, 27.4 kg/m². AVERAGE REYNOLDS NUMBER, 191,500

Degrees α	C_L	C_D	L/D	C_M	¹ Degrees α	¹ C_D'
-11.57	-0.079	0.1575	-0.50	-0.016	-11.50	0.1574
-10.03	-.032	.1430	-.22	+.071	-10.00	.1430
-8.48	+.020	.1300	+.15	-.003	-8.50	.1300
-6.92	.088	.1185	.74	-.005	-7.00	.1184
-5.33	.183	.1044	1.75	+.012	-5.50	.1038
-3.74	.272	.0985	2.76	.012	-4.00	.0973
-2.13	.396	.0940	4.22	.048	-2.50	.0914
-1.50	.526	.0861	6.10	.063	-1.00	.0816
+1.12	.652	.0952	6.85	.085	+.50	.0882
2.75	.767	.1049	7.30	.099	2.00	.0952
4.35	.898	.1188	7.58	.106	3.50	.1055
5.95	1.007	.1324	7.64	.120	5.00	.1157
7.56	1.117	.1488	7.46	.141	6.50	.1283
9.14	1.207	.1669	7.25	.144	8.00	.1429
10.75	1.317	.1926	6.85	.136	9.50	.1640
12.32	1.391	.2145	6.50	.148	11.00	.1825
13.88	1.462	.2359	6.22	.144	12.50	.2006
15.46	1.548	.2619	5.92	.135	14.00	.2224
17.02	1.608	.2926	5.49	.148	15.50	.2500
18.52	1.659	.3215	5.16	.138	17.00	.2762
20.10	1.689	.3552	4.76	.117	18.50	.3082
21.60	1.689	.3950	4.28	.131	20.00	.3480
23.08	1.672	.4372	3.84	.111	21.50	.3911
24.56	1.653	.4825	3.43	.108	23.00	.4373
26.04	1.633	.5224	3.13	.097	24.50	.4784

¹ Uncorrected for tunnel wall effect.

TABLE II

MODEL, BE-2E (R. A. F., 19 WINGS) AIRPLANE MODEL. AVERAGE TANK PRESSURE, 2.47 ATM. AVERAGE DYNAMIC PRESSURE, 67.6 kg/m². AVERAGE REYNOLDS NUMBER, 461,000

Degrees α	C_L	C_D	L/D	C_M	¹ Degrees α	¹ C_D'
-11.57	-0.069	0.1512	-0.46	-0.004	-11.50	0.1511
-10.20	-.023	.1380	-.17	+.006	-10.00	.1380
-8.20	+.029	.1228	+.24	.009	-8.50	.1228
-6.91	.095	.1117	.85	.019	-7.00	.1116
-5.32	.190	.1011	1.88	.039	-5.50	.1005
-3.72	.296	.0967	3.06	.051	-4.00	.0953
-2.10	.421	.0901	4.67	.068	-2.50	.0872
-1.47	.559	.0850	6.58	.085	-1.00	.0798
+1.16	.695	.0949	7.30	.095	+.50	.0869
2.76	.799	.1036	7.70	.106	2.00	.0930
4.39	.942	.1160	8.14	.121	3.50	.1014
5.99	1.043	.1304	8.00	.131	5.00	.1124
7.58	1.148	.1469	7.82	.137	6.50	.1252
9.17	1.240	.1647	7.52	.139	8.00	.1394
10.77	1.339	.1991	6.72	.143	9.50	.1596
12.35	1.429	.2101	6.80	.130	11.00	.1764
13.93	1.514	.2355	6.42	.168	12.50	.1977
15.50	1.582	.2605	6.06	.156	14.00	.2192
17.05	1.633	.2890	5.65	.148	15.50	.2450
18.57	1.661	.3248	5.10	.118	17.00	.2792
20.07	1.664	.3717	4.47	.095	18.50	.3260
21.57	1.662	.4111	4.05	.085	20.00	.3655
23.06	1.645	.4543	3.62	.077	21.50	.4096
24.54	1.624	.4943	3.29	.060	23.00	.4508
26.00	1.591	.5999	2.66	.059	24.50	.5581

¹ Uncorrected for tunnel wall effect

TABLE III

MODEL, BE-2E (R. A. F., 19 WINGS) AIRPLANE MODEL. AVERAGE TANK PRESSURE, 5.1 ATM. AVERAGE DYNAMIC PRESSURE, 144.6 kg/m². AVERAGE REYNOLDS NUMBER, 949,000

Degrees α	C_L	C_D	L/D	C_M	¹ Degrees α	¹ C_D'
-11.57	-0.077	.1531	-0.50	-0.004	-11.50	0.1530
-10.03	-.032	.1370	-.23	-.002	-10.00	.1370
-8.47	+.026	.1249	+.21	+.004	-8.50	.1249
-6.91	.098	.1129	.87	.009	-7.00	.1127
-5.31	.197	.1027	1.92	.024	-5.50	.1021
-3.71	.310	.0946	3.28	.045	-4.00	.0930
-2.08	.449	.0880	5.11	.059	-2.50	.0847
-.45	.580	.0854	6.80	.069	-1.00	.0799
+1.16	.696	.0920	7.58	.093	+.50	.0840
2.77	.812	.1019	7.94	.104	2.00	.0910
4.39	.942	.1133	8.34	.106	3.50	.0987
5.99	1.045	.1292	8.07	.131	5.00	.1112
7.58	1.141	.1505	7.58	.134	6.50	.1290
9.17	1.241	.1675	7.41	.123	8.00	.1420
10.77	1.340	.1898	7.04	.138	9.50	.1602
12.35	1.427	.2128	6.72	.131	11.00	.1792
13.92	1.503	.2388	6.29	.134	12.50	.2015
15.47	1.553	.2685	5.78	.109	14.00	.2287
17.01	1.598	.3090	5.18	.105	15.50	.2670
18.53	1.621	.3546	4.57	.092	17.00	.3112
20.03	1.620	.3965	4.08	.073	18.50	.3531
21.52	1.608	.4376	3.68	.055	20.00	.3950
23.00	1.582	.4715	3.36	.072	21.50	.4301
24.44	1.525	.5008	3.05	.013	23.00	.4624
25.89	1.471	.5204	2.83	.009	24.50	.4847

¹ Uncorrected for tunnel wall effect.

TABLE IV

MODEL, BE-2E (R. A. F., 19 WINGS) AIRPLANE MODEL. AVERAGE TANK PRESSURE, 10.1 ATM. AVERAGE DYNAMIC PRESSURE, 291 kg/m². AVERAGE REYNOLDS NUMBER, 1,870,000

Degrees α	C_L	C_D	L/D	C_M	¹ Degrees α	¹ C_D'
-11.61	-0.117	0.1565	-0.75	-0.036	-11.5	0.1563
-10.05	-.055	.1409	-.39	-.035	-10.0	.1408
-8.48	+.018	.1318	.14	-.056	-8.5	.1318
-6.88	.128	.1057	1.21	-.017	-7.0	.1054
-5.26	.256	.0901	2.84	-.001	-5.5	.0891
-3.64	.376	.0788	4.76	+.016	-4.0	.0765
-2.03	.495	.0782	6.33	.040	-2.5	.0742
-.43	.604	.0795	7.57	.066	-1.0	.0735
+1.19	.730	.0859	8.48	.092	+.5	.0771
2.77	.825	.0929	8.85	.116	2.0	.0817
4.40	.948	.1139	8.34	.134	3.5	.0991
6.00	1.052	.1287	8.20	.103	5.0	.1104
7.58	1.139	.1436	7.94	.155	6.5	.1223
9.18	1.242	.1737	7.15	.118	8.0	.1482
10.76	1.332	.1899	7.00	.129	9.5	.1606
12.34	1.412				11.0	
13.84	1.411	.2565	5.50	.100	12.5	.2235
15.35	1.427	.2858	5.00	.082	14.0	.2522
16.87	1.412	.3321	4.26	.083	15.5	.2991
18.34	1.421	.3523	4.03	.058	17.0	.3190
19.84	1.416	.3949	3.59	.038	18.5	.3619
21.53	1.406	.4185	3.36	.038	20.0	.3859
22.82	1.398	.4485	3.12	.023	21.5	.4163
24.30	1.378	.4879	2.83	.002	23.0	.4566
25.80	1.375	.5143	2.68	.000	24.5	.4831

¹ Uncorrected for tunnel wall effect.

TABLE V

MODEL, BE-2E (R. A. F., 19 WINGS) AIRPLANE MODEL. AVERAGE TANK PRESSURE, 20.4 ATM.
AVERAGE DYNAMIC PRESSURE, 637 kg/m². AVERAGE REYNOLDS NUMBER, 4,000,000

Degrees α	C_L	C_D	L/D	C_M	¹ Degrees α	¹ $C_{D'}$
-11.58	-0.080	0.1416	-0.57	-0.002	-11.5	0.1415
-10.04	-.036	.1268	-.28	-.004	-10.0	.1268
-8.48	+.036	.1123	+.32	+.001	-8.5	.1123
-6.89	.114	.0994	1.15	.009	-7.0	.0992
-5.25	.260	.0896	2.90	.010	-5.5	.0885
-3.62	.403	.0719	5.59	.038	-4.0	.0692
-2.01	.522	.0698	7.46	.037	-2.5	.0653
-.40	.635	.0740	8.55	.064	-1.0	.0673
+1.21	.752	.0845	8.93	.075	+.5	.0752
2.80	.850	.0961	8.85	.083	2.0	.0889
4.41	.963	.1126	8.55	.099	3.5	.0973
6.00	1.058	.1286	8.20	.105	5.0	.1102
7.60	1.168	.1554	7.53	.116	6.5	.1329
9.18	1.247	.1703	7.30	.112	8.0	.1447
10.77	1.343	.1994	6.75	.121	9.5	.1696
12.34	1.413	.2290	6.18	.099	11.0	.1960
13.81	1.382	.2649	5.21	.068	12.5	.2334
15.30	1.374	.3012	4.57	.053	14.0	.2700

¹ Uncorrected for tunnel wall effect.

TABLE VI

MODEL, BRISTOL FIGHTER (R. A. F., 15) AIRPLANE MODEL. AVERAGE TANK PRESSURE, 1 ATM. AVERAGE DYNAMIC PRESSURE, 27.8 kg/m². AVERAGE REYNOLDS NUMBER, 157,000

Degrees α	C_L	C_D	L/D	C_M	¹ Degrees α	¹ $C_{D'}$
-4.58	-0.114	0.0616	-1.85	-0.075	-4.5	0.0614
-3.00	+.000	.0513	+.00	-.012	-3.0	.0513
-1.43	.106	.0502	2.12	+.001	-1.5	.0501
+.13	.199	.0500	3.99	.004	0	.0495
1.70	.296	.0534	5.53	.008	+1.5	.0524
3.26	.387	.0604	6.38	.022	3.0	.0587
4.82	.484	.0684	7.09	.054	4.5	.0657
6.37	.558	.0781	7.14	.013	6.0	.0745
7.94	.664	.0226	7.14	.068	7.5	.0875
9.50	.749	.1045	7.14	.070	9.0	.0980
11.06	.845	.1206	7.00	.092	10.5	.1123
12.62	.926	.1358	6.81	.102	12.0	.1258
14.15	.983	.1575	6.25	.083	13.5	.1463
15.66	.986	.2153	4.59	.080	15.0	.2040
17.16	.990	.2578	3.85	.081	16.5	.2464
18.64	.968	.2877	3.37	.065	18.0	.2768
20.14	.961	.3353	2.87	.049	19.5	.3246
21.62	.939	.3949	2.38	+.019	21.0	.3847
23.12	.930	.4373	2.13	-.004	22.5	.4273
24.60	.901	.4644	1.94	-.036	24.0	.4550
26.08	.877	.4920	1.78	-.047	25.5	.4831

¹ Uncorrected for tunnel wall effect.

TABLE VII

MODEL, BRISTOL FIGHTER (R. A. F., 15 WINGS) AIRPLANE MODEL. AVERAGE TANK PRESSURE, 2.58 ATM. AVERAGE DYNAMIC PRESSURE, 69.2 kg/m². AVERAGE REYNOLDS NUMBER, 390,000

Degrees α	C_L	C_D	L/D	C_M	¹ Degrees α	¹ C_D'
-4.55	-0.082	0.0545	-1.51	-0.051	-4.5	0.0544
-2.99	+.013	.0507	+.26	-.042	-3.0	.0507
-1.42	.114	.0497	2.29	-.024	-1.5	.0495
+.14	.204	.0513	3.97	-.009	0	.0508
1.70	.294	.0554	5.32	-.001	+1.5	.0544
3.26	.393	.0615	6.41	+.024	3.0	.0598
4.83	.491	.0685	7.14	.035	4.5	.0657
6.39	.585	.0793	7.41	.043	6.0	.0753
7.95	.682	.0909	7.52	.062	7.5	.0855
9.51	.770	.1040	7.41	.079	9.0	.0971
11.07	.863	.1178	7.30	.073	10.5	.1092
12.63	.951	.1336	7.14	.095	12.0	.1231
14.19	1.032	.1560	6.63	.104	13.5	.1436
15.72	1.067	.1940	5.50	.079	15.0	.1808
17.23	1.092	.2355	4.63	.085	16.5	.2217
18.74	1.110	.2858	3.89	.081	18.0	.2715
20.22	1.086	.3450	3.14	.065	19.5	.3313
21.69	1.041	.3960	2.63	.044	21.0	.3834
23.16	1.000	.4458	2.24	.015	22.5	.4342
24.64	.965	.4788	2.02	+.009	4.0	.4684
26.12	.934	.5078	1.84	-.031	25.5	.4977

¹Uncorrected for tunnel wall effect.

TABLE VIII

MODEL, BRISTOL FIGHTER (R. A. F., 15 WINGS) AIRPLANE MODEL. AVERAGE TANK PRESSURE, 5.1 ATM. AVERAGE DYNAMIC PRESSURE, 146 kg/m². AVERAGE REYNOLDS NUMBER, 780,000

Degrees α	C_L	C_D	L/D	C_M	¹ Degrees α	¹ C_D'
-4.55	-0.068	0.0502	-1.36	-0.051	-4.5	0.0501
-3.00	+.008	.0484	+.17	-.026	-3.0	.0484
-1.45	.108	.0478	2.26	-.024	-1.5	.0477
+.13	.199	.0500	3.99	-.006	0	.0495
1.69	.288	.0537	5.38	+.012	+1.5	.0527
3.26	.392	.0593	6.63	.032	3.0	.0575
4.82	.485	.0666	7.20	.047	4.5	.0639
6.38	.574	.0754	7.64	.059	6.0	.0716
7.95	.673	.0882	7.64	.085	7.5	.0829
9.51	.762	.1004	7.58	.089	9.0	.0937
11.07	.851	.1143	7.46	.108	10.5	.1059
12.62	.932	.1323	7.04	.104	12.0	.1223
14.18	1.024	.1549	6.63	.119	13.5	.1427
15.70	1.053	.2014	5.24	.111	15.0	.1885
17.21	1.072	.2270	4.46	.087	16.5	.1925
18.72	1.065	.2829	3.76	.091	18.0	.2697
20.20	1.059	.3385	3.13	.078	19.5	.3255
21.69	1.037	.3979	2.61	.039	21.0	.3854
23.18	1.017	.4365	2.33	.041	22.5	.4245
24.66	.986	.4745	2.08	+.004	24.0	.4632
26.13	.948	.5038	1.88	-.002	25.5	.4934

¹Uncorrected for tunnel wall effect.

TABLE IX

MODEL, BRISTOL FIGHTER (R. A. F., 15 WINGS) AIRPLANE MODEL. AVERAGE TANK PRESSURE, 10.5 ATM. AVERAGE DYNAMIC PRESSURE, 307 kg/m². AVERAGE REYNOLDS NUMBER, 1,580,000

Degrees α	C_L	C_D	L/D	C_M	¹ Degrees α	¹ C_D'
-4.56	-0.084	0.0434	-1.93	-0.048	-4.5	0.0433
-3.00	+.003	.0429	+.07	-.037	-3.0	.0429
-1.44	.096	.0428	2.24	-.043	-1.5	.0427
+.13	.193	.0441	4.37	-.006	0	.0437
1.68	.268	.0461	5.82	-.036	+1.5	.0453
3.24	.366	.0518	7.10	+.010	3.0	.0502
4.81	.463	.0627	7.41	.086	4.5	.0602
6.37	.558	.0679	8.20	.094	6.0	.0643
7.92	.639	.0744	8.63	.087	7.5	.0697
9.48	.729	.1026	7.10	.098	9.0	.0964
11.06	.848	.1080	7.88	.082	10.5	.0996
12.60	.905	.1202	7.52	.029	12.0	.1107
14.18	1.017	.1429	7.10	.084	13.5	.1309
15.68	1.021	.2006	5.11	.073	15.0	.1885
17.19	1.039	.2363	4.41	.057	16.5	.2237
18.68	1.022	.2733	3.74	.050	18.0	.2611
20.16	.999	.3257	3.07	.025	19.5	.3141
21.66	.997	.3639	2.72	+.016	21.0	.3524
23.16	.987	.4253	2.32	-.019	22.5	.4140
24.65	.978	.4549	2.15	-.010	24.0	.4438
26.14	.960	.5058	1.90	-.041	25.5	.4951

¹ Uncorrected for tunnel wall effect.

TABLE X

MODEL, BRISTOL FIGHTER (R. A. F., 15 WINGS) AIRPLANE MODEL. AVERAGE TANK PRESSURE, 20.6 ATM. AVERAGE DYNAMIC PRESSURE, 618 kg/m². AVERAGE REYNOLDS NUMBER, 3,120,000

Degrees α	C_L	C_D	L/D	C_M	¹ Degrees α	¹ C_D'
-4.56	-0.090	0.0436	-2.07	-0.053	-4.5	0.0435
-3.00	+.000	.0412	+.00	-.032	-3.0	.0412
-1.43	.099	.0414	2.40	-.025	-1.5	.0413
+.12	.180	.0427	4.22	-.021	0	.0423
1.68	.277	.0461	5.99	+.025	+1.5	.0452
3.25	.377	.0526	7.20	.016	3.0	.0510
4.81	.466	.0594	7.88	.030	4.5	.0569
6.37	.555	.0683	8.14	.053	6.0	.0647
7.93	.647	.0778	8.34	.062	7.5	.0730
9.49	.737	.0910	8.14	.082	9.0	.0847
11.06	.836	.1075	7.75	.052	10.5	.0994
12.61	.920	.1218	7.58	.102	12.0	.1120
14.17	1.004	.1391	7.20	.101	13.5	.1274
15.69	1.032	.1606	6.41	.100	15.0	.1482
17.17	1.013	.2305	4.39	.079	16.5	.2186
18.66	.997	.2737	3.64	.059	18.0	.2622
20.14	.964	.3145	3.07	.040	19.5	.3037
21.62	.931	.3581	2.60	.008	21.0	.3481
23.13	.943	.3972	2.37	.012	22.5	.3869

¹ Uncorrected for tunnel wall effect.

TABLE XI

MODEL, BRISTOL FIGHTER (R. A. F., 30 WINGS) AIRPLANE MODEL. AVERAGE TANK PRESSURE, 1 ATM. AVERAGE DYNAMIC PRESSURE, 27.2 kg/m². AVERAGE REYNOLDS NUMBER, 152,000

Degrees α	C_L	C_D	L/D	C_M	¹ Degrees α	¹ C_D'
-1.52	-0.067	0.0603	-1.11	+0.015	-1.48	0.0602
+ .01	+ .019	.0569	+ .33	- .003	0	.0569
1.56	.120	.0570	2.10	+ .020	+1.48	.0568
3.10	.211	.0601	3.51	.017	2.96	.0596
4.64	.301	.0652	4.63	.042	4.44	.0642
6.17	.400	.0726	5.50	.072	5.91	.0708
7.71	.492	.0827	5.95	.078	7.39	.0799
9.25	.584	.0938	6.21	.116	8.86	.0899
10.77	.662	.1071	6.18	.134	10.33	.1021
12.29	.726	.1228	5.92	.125	11.81	.1167
13.78	.761	.1524	5.00	.173	13.28	.1457
15.23	.745	.2084	3.57	.155	14.74	.2020
16.69	.733	.2537	2.89	.155	16.21	.2475
18.13	.712	.3005	2.37	.137	17.66	.2947
19.58	.696	.3341	2.08	.117	19.12	.3285
21.01	.687	.3670	1.87	.110	20.56	.3616

¹ Uncorrected for tunnel wall effect.

TABLE XII

MODEL, BRISTOL FIGHTER (R. A. F., 30 WINGS) AIRPLANE MODEL. AVERAGE TANK PRESSURE, 2.72 ATM. AVERAGE DYNAMIC PRESSURE, 72.8 kg/m². AVERAGE REYNOLDS NUMBER, 404,000

Degrees α	C_L	C_D	L/D	C_M	¹ Degrees α	¹ C_D'
-1.52	-0.066	0.0536	-1.23	-0.013	-1.48	0.0535
+ .02	+ .029	.0517	+ .56	- .005	0	.0517
1.57	.130	.0517	2.52	+ .017	+1.48	.0515
3.11	.221	.0557	3.97	.029	2.96	.0551
4.64	.304	.0606	5.03	.037	4.44	.0595
6.17	.397	.0690	5.75	.055	5.91	.0672
7.71	.487	.0769	6.33	.074	7.39	.0742
9.24	.579	.0872	6.62	.091	8.86	.0833
10.77	.665	.1003	6.62	.113	10.33	.0952
12.31	.751	.1139	6.58	.127	11.81	.1074
13.82	.814	.1280	6.37	.119	13.28	.1204
15.27	.809	.1922	4.21	.129	14.74	.1847
16.74	.798	.2368	3.37	.116	16.21	.2295
18.16	.755	.2868	2.63	.085	17.66	.2802
19.60	.730	.3274	2.23	.077	19.12	.3213
21.04	.721	.3621	1.99	.065	20.56	.3561

¹ Uncorrected for tunnel wall effect.

TABLE XIII

MODEL, BRISTOL FIGHTER (R. A. F., 30 WINGS) AIRPLANE MODEL. AVERAGE TANK PRESSURE, 5.27 ATM. AVERAGE DYNAMIC PRESSURE, 141 kg/m². AVERAGE REYNOLDS NUMBER, 760,000

Degrees α	C_L	C_D	L/D	C_M	¹ Degrees α	¹ C_D'
-1.52	-0.063	0.0522	-1.21	-0.022	-1.48	0.0522
+.02	+.033	.0508	.65	-.015	0	.0508
1.57	.131	.0524	2.50	+.003	+1.48	.0522
3.10	.218	.0557	3.91	.013	2.96	.0552
4.64	.306	.0605	5.05	.033	4.44	.0594
6.17	.396	.0672	5.89	.048	5.91	.0654
7.71	.485	.0763	6.37	.058	7.39	.0736
9.24	.576	.0870	6.63	.082	8.86	.0832
10.77	.666	.0986	6.76	.093	10.33	.0935
12.30	.750	.1113	6.76	.110	11.81	.1048
13.83	.831	.1232	6.76	.114	13.28	.1156
15.34	.913	.1392	6.54	.111	14.74	.1296
16.81	.916	.1877	4.88	.096	16.21	.1780
18.24	.883	.2338	3.78	.102	17.66	.2248
19.69	.870	.2946	2.95	.094	19.12	.2859
21.08	.783	.3613	2.17	.039	20.56	.3542

¹ Uncorrected for tunnel wall effect.

TABLE XIV

MODEL, BRISTOL FIGHTER (R. A. F., 30 WINGS) AIRPLANE MODEL. AVERAGE TANK PRESSURE, 10.33 ATM. AVERAGE DYNAMIC PRESSURE, 290 kg/m². AVERAGE REYNOLDS NUMBER, 1,500,000

Degrees α	C_L	C_D	L/D	C_M	¹ Degrees α	¹ C_D'
-1.52	-0.070	0.0471	-1.49	-0.040	-1.48	0.0470
+.00	-.005	.0461	-.11	-.094	0	.0461
1.55	+.103	.0468	+2.20	+.014	+1.48	.0467
3.09	.193	.0504	3.83	.029	2.96	.0500
4.62	.278	.0554	5.03	.052	4.44	.0545
6.16	.375	.0620	6.06	.076	5.91	.0604
7.68	.441	.0695	6.33	.046	7.39	.0673
9.23	.566	.0787	7.20	.104	8.86	.0750
10.76	.651	.0991	6.58	.114	10.33	.0942
12.30	.744	.1034	7.20	.065	11.81	.0970
13.84	.851	.1198	7.10	.120	13.28	.1115
15.36	.938	.1344	7.00	.119	14.74	.1242
16.87	1.002	.1528	6.58	.073	16.21	.1412
18.33	1.022	.1814	5.65	.111	17.66	.1694
19.83	1.067	.2225	4.81	.073	19.12	.2094
21.24	1.031	.2563	4.03	.099	20.56	.2441
22.66	.993	.3382	2.94	.038	22.00	.3268
24.05	+.941	.3693	2.55	.005	23.43	.3591

¹ Uncorrected for tunnel wall effect.

TABLE XV

MODEL, BRISTOL FIGHTER (R. A. F., 30 WINGS) AIRPLANE MODEL. AVERAGE TANK PRESSURE, 21.0 ATM. AVERAGE DYNAMIC PRESSURE, 620 kg/m². AVERAGE REYNOLDS NUMBER, 3,050,000

Degrees α	C_L	C_D	L/D	C_M	¹ Degrees α	¹ C_D'
-1.52	-0.059	0.0449	-1.31	-0.020	-1.48	0.0449
+ .02	+ .026	.0439	+ .59	- .012	0	.0439
1.57	.130	.0443	2.93	+ .017	+1.48	.0441
3.10	.213	.0472	4.51	.019	2.96	.0467
4.64	.297	.0509	5.85	.033	4.44	.0499
6.17	.398	.0592	6.72	.017	5.91	.0574
7.70	.476	.0669	7.10	.056	7.39	.0643
9.23	.562	.0771	7.30	.052	8.86	.0735
10.76	.650	.0849	7.64	.069	10.33	.0800
12.30	.747	.1051	7.10	.097	11.81	.0987
13.83	.832	.1145	7.25	.097	13.28	.1065
15.35	.927	.1316	7.05	.123	14.74	.1217
16.87	1.006	.1513	6.66	.137	16.21	.1397
18.32	.999	.1964	5.08	.107	17.66	.1849
19.76	.976	.2358	4.13	.084	19.12	.2249
21.14	.876	.3109	2.82	.032	20.56	.3021

¹ Uncorrected for tunnel wall effect.

TABLE XVI
DATA ON MODELS

Model	BE-2E	Bristol Fighter	Bristol Fighter
Wing section-----	R. A. F. 19-----	R. A. F. 15-----	R. A. F. 30.
Scale ratio-----	1:12-----	1:15-----	1:15.
Span upper wing---	40 in. (101.6 cm.)-----	31.50 in. (80 cm.)-----	30.54 in. (77.57 cm.).
Span lower wing---	30 in. (76.20 cm.)-----	31.50 in. (80 cm.)-----	30.54 in. (77.57 cm.).
Gap (average)-----	6.23 in. (15.82 cm.)-----	4.35 in. (11.05 cm.)-----	4.35 in. (11.05 cm.).
Chord upper wing---	5.50 in. (13.97 cm.)-----	4.40 in. (11.18 cm.)-----	4.38 in. (11.13 cm.).
Chord lower wing---	5.50 in. (13.97 cm.)-----	4.40 in. (11.18 cm.)-----	4.40 in. (11.18 cm.).
Area upper wing---	1.507 sq. ft. (0.1400 sq. m.)-	0.907 sq. ft. (0.0843 sq. m.)-	0.901 sq. ft. (0.0837 sq. m.).
Area lower wing---	1.019 sq. ft. (0.0947 sq. m.)-	0.907 sq. ft. (0.0843 sq. m.)-	0.907 sq. ft. (0.0843 sq. m.).
Area total-----	2.526 sq. ft. (0.2347 sq. m.)-	1.814 sq. ft. (0.1685 sq. m.)-	1.808 sq. ft. (0.1680 sq. m.).

PITCHING MOMENT AXIS

BE-2E (R. A. F., 19).—The axis, relative to the leading edge of the upper wing chord at root, is 3.46 inches behind and 4.72 inches below, parallel and perpendicular to the chord line.

Bristol Fighter (R. A. F., 15).—The axis, relative to the leading edge of the lower wing chord at root, is 1.125 inches behind and 2.06 inches above, parallel and perpendicular to the chord line.

Bristol Fighter (R. A. F., 30).—The axis, relative to the leading edge of the lower wing chord at root, is 1.125 inches behind and 2.03 inches above, parallel and perpendicular to the chord line.

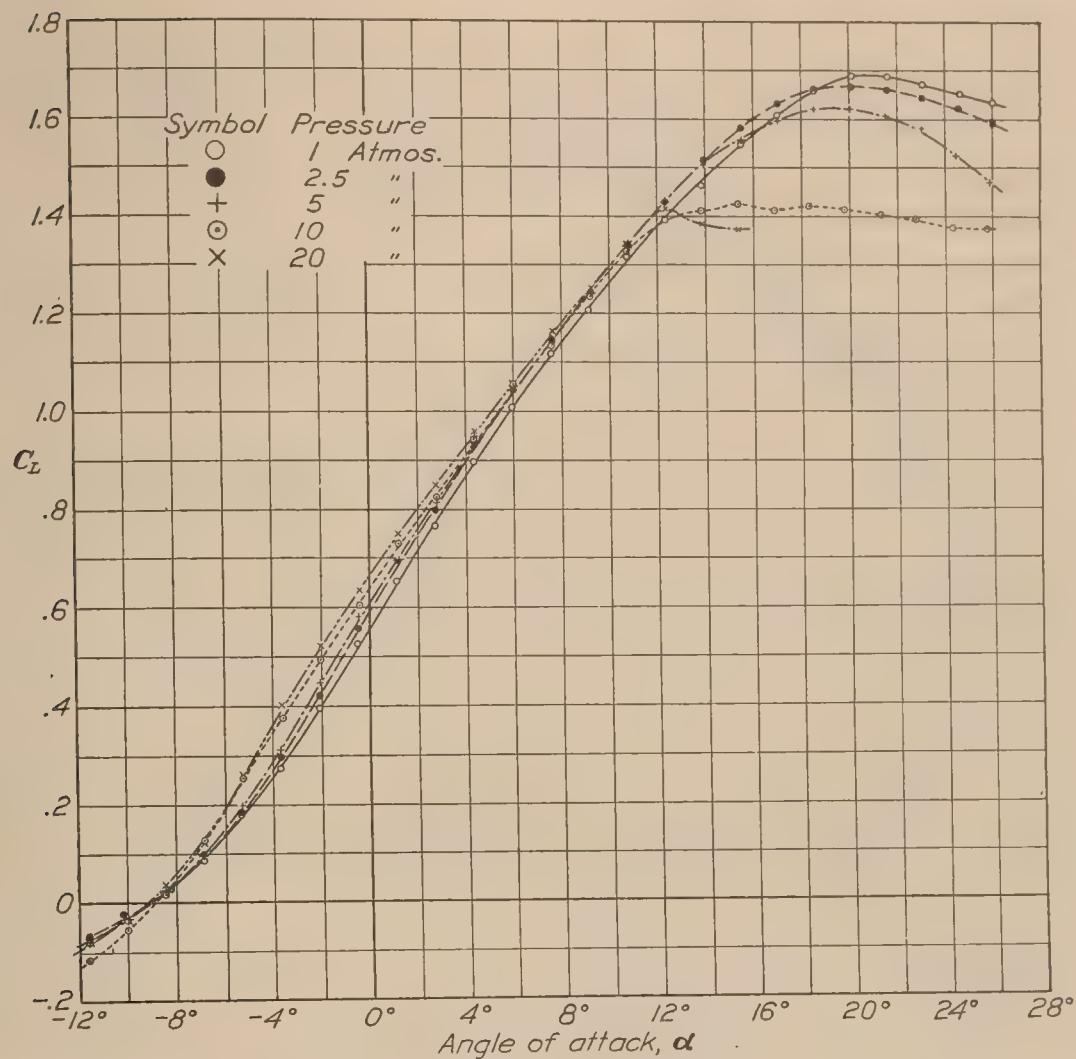


FIG. 6.—Lift coefficient vs. angle of attack. BE-2E airplane model with R. A. F. 19 wings

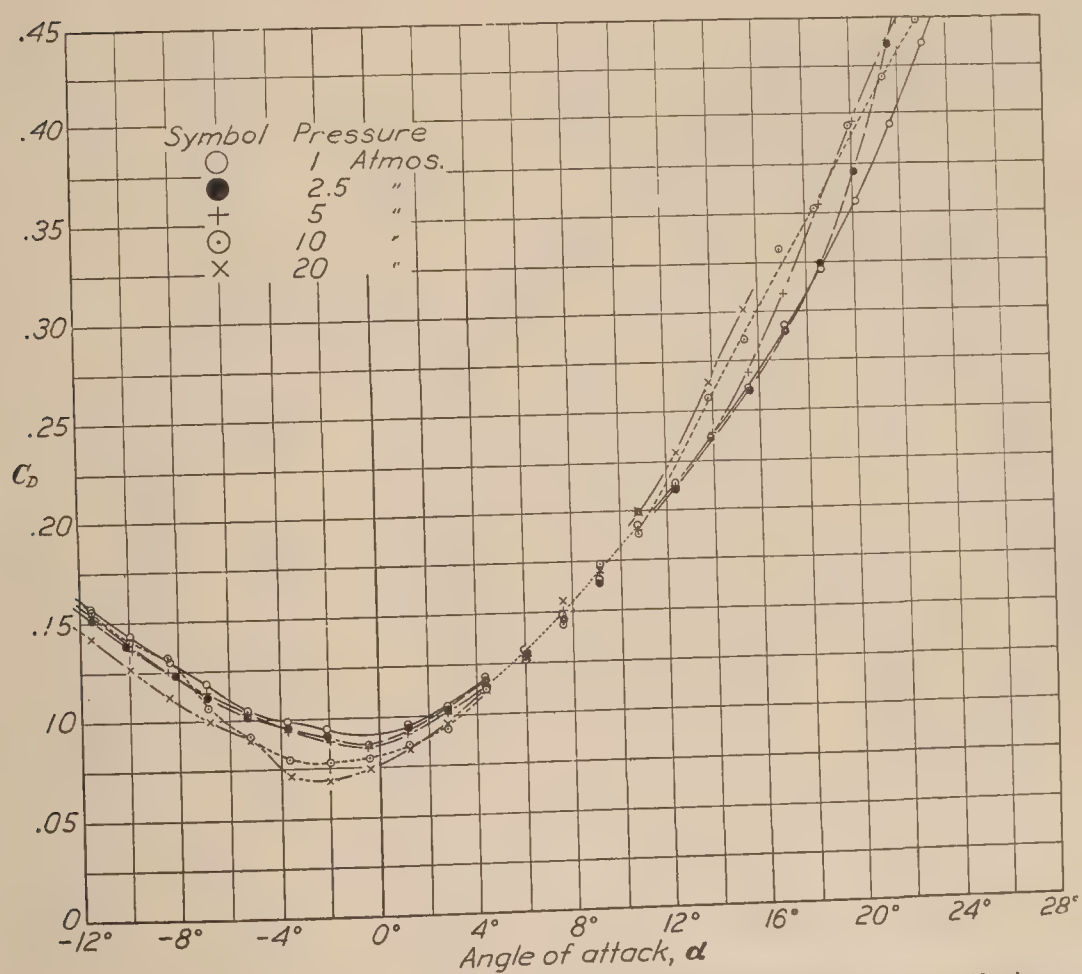


FIG. 7.—Drag coefficient vs. angle of attack. BE-2E airplane model with R. A. F. 19 wings

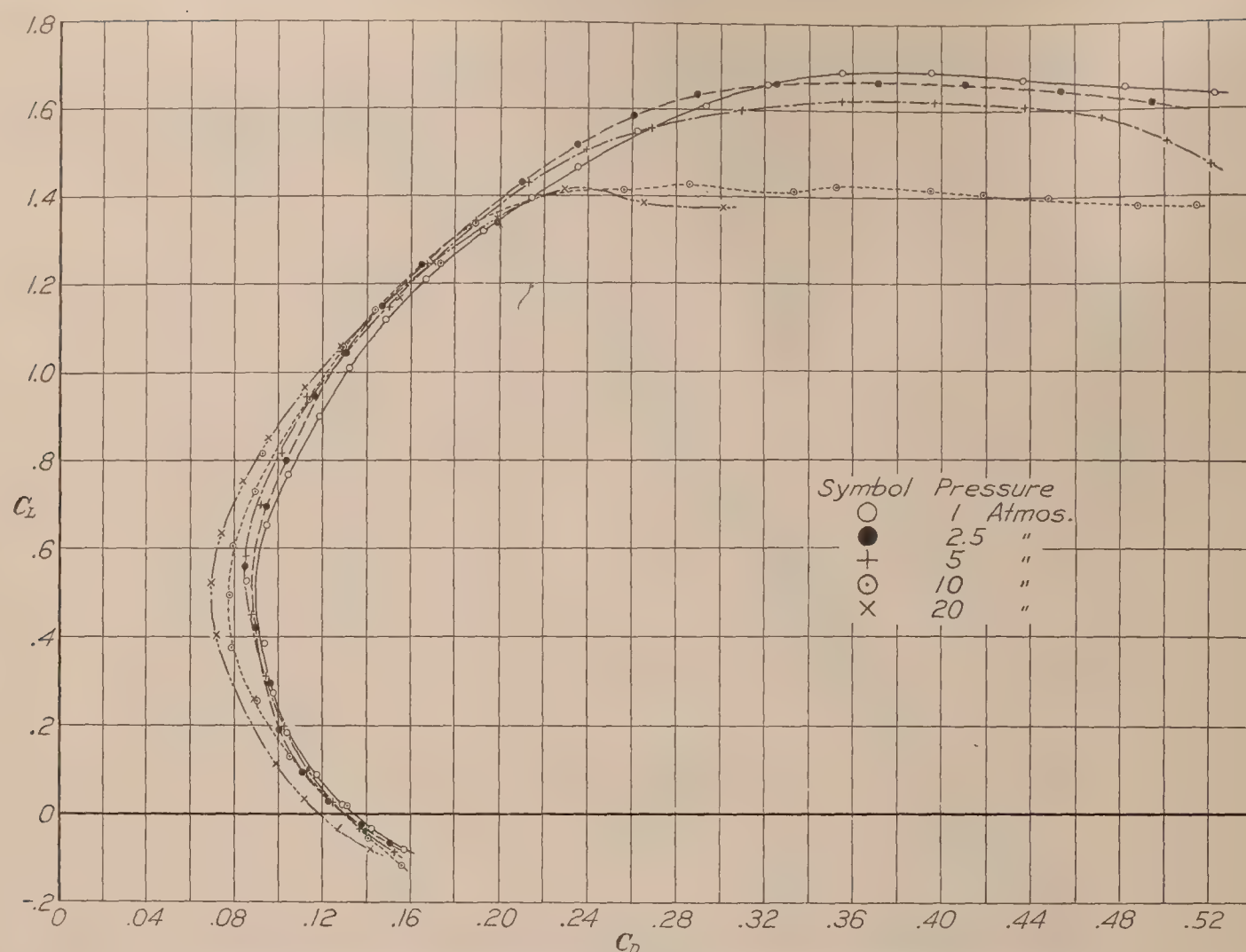


FIG. 8.—Lift coefficient vs. drag coefficient. BE-2E airplane model with R. A. F. 19 wings

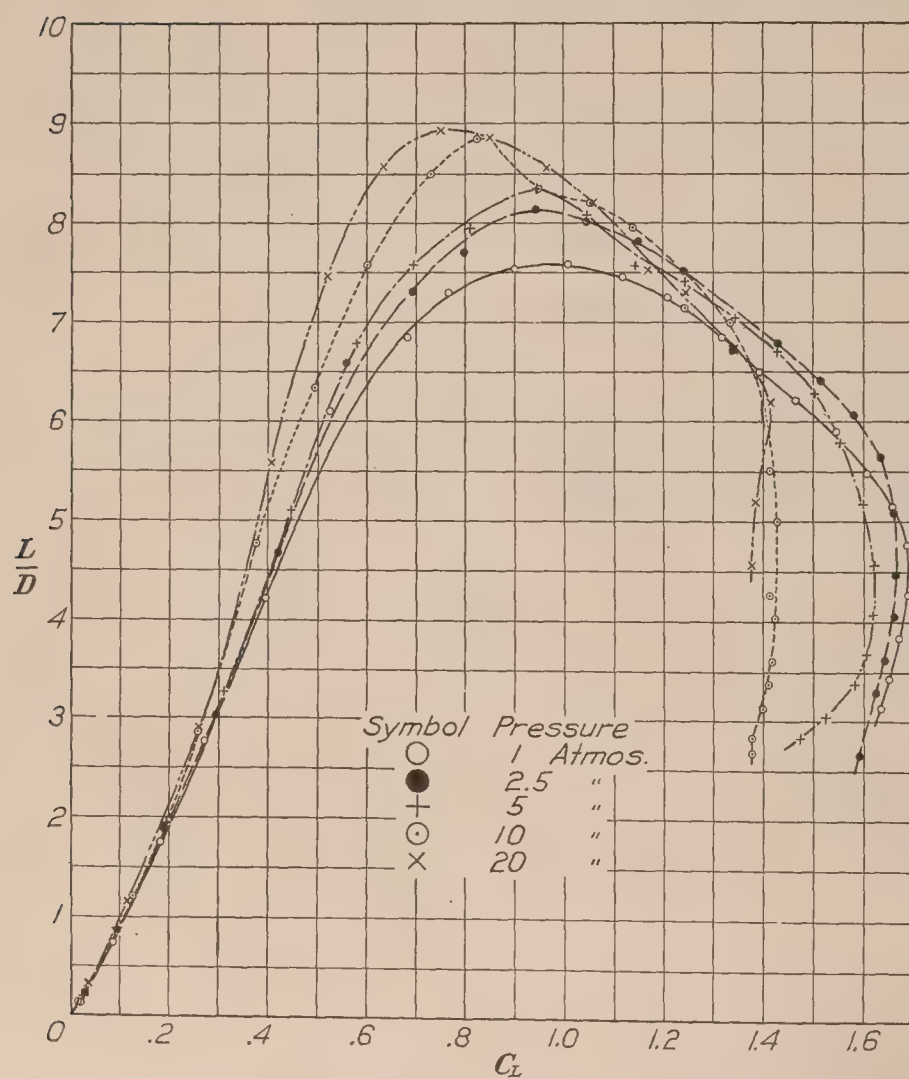


FIG. 9.—Lift/drag vs. lift coefficient. BE-2E airplane model with R. A. F. 19 wings

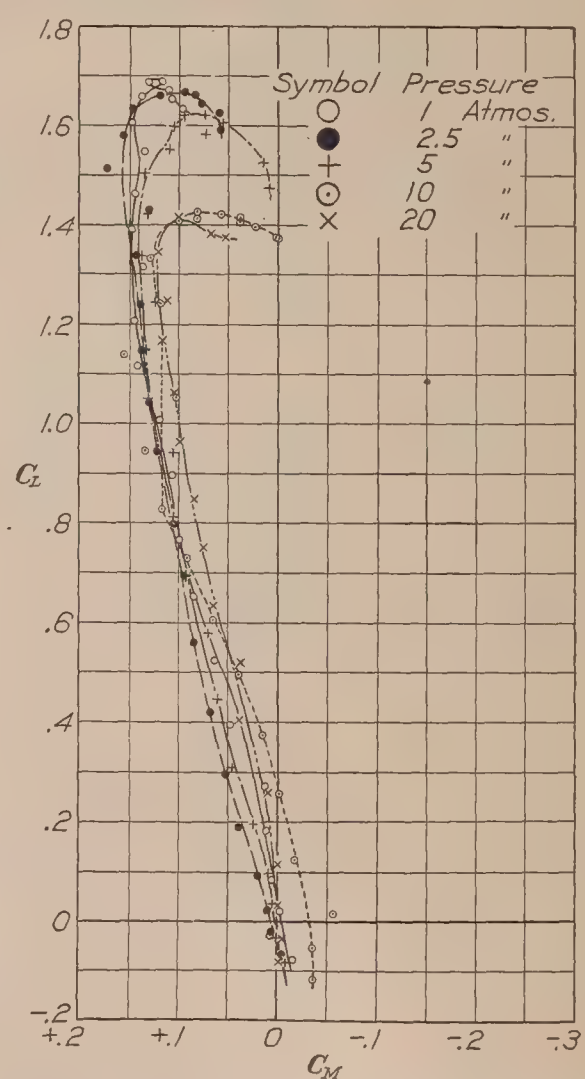


FIG. 10.—Lift coefficient vs. moment coefficient. BE-2E airplane model with R. A. F. 19 wings

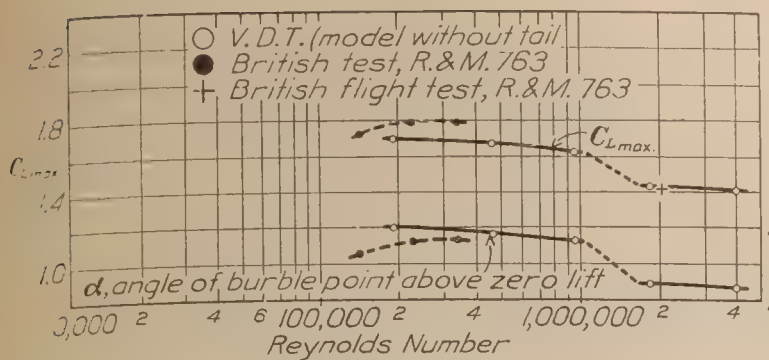


FIG. 11.—Scale effect on $C_{L_{max}}$. BE-2E airplane model with R. A. F. 19 wings

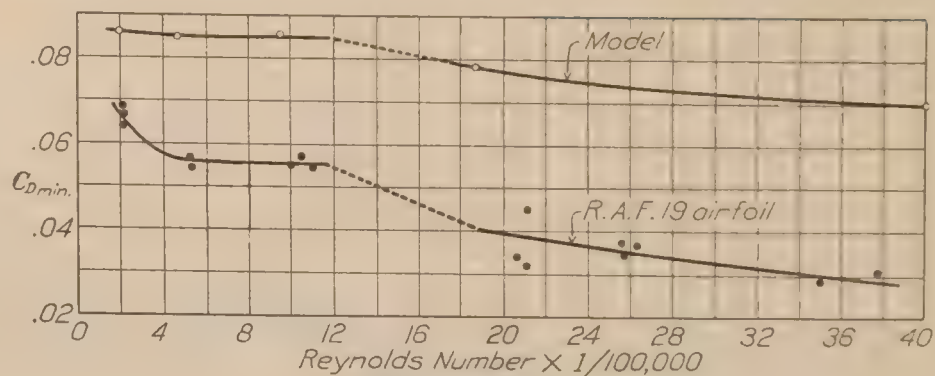


FIG. 13.—Scale effect on $C_{D_{min}}$. BE-2E airplane model with R. A. F. 19 wings and without tail group

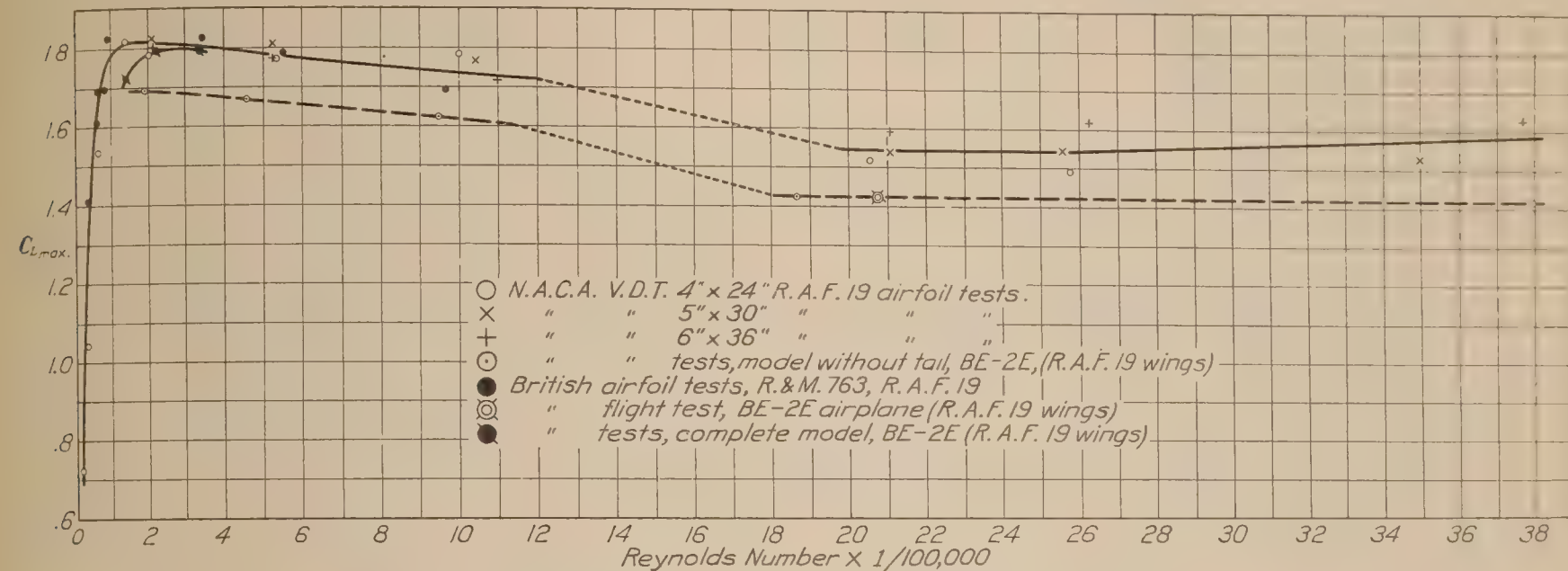


FIG. 12.—Scale effect on $C_{L_{max}}$. BE-2E airplane model with R. A. F. 19 wings

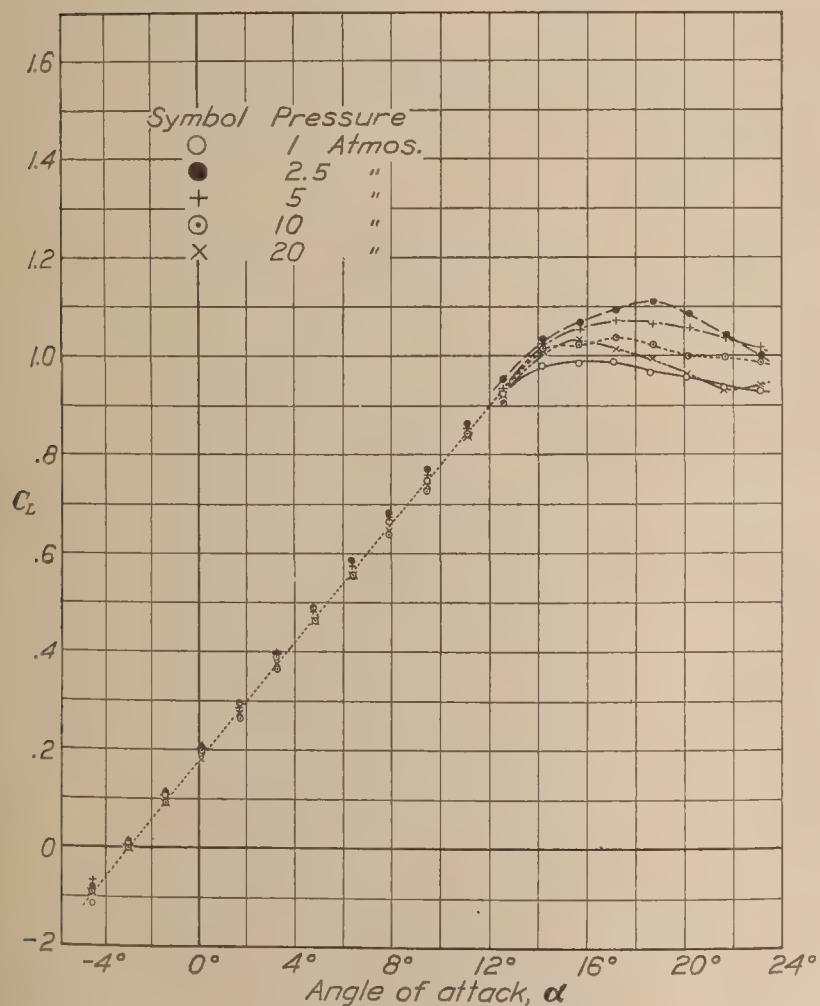


FIG. 14.—Lift coefficient vs. angle of attack. Bristol Fighter airplane model with R. A. F. 15 wings

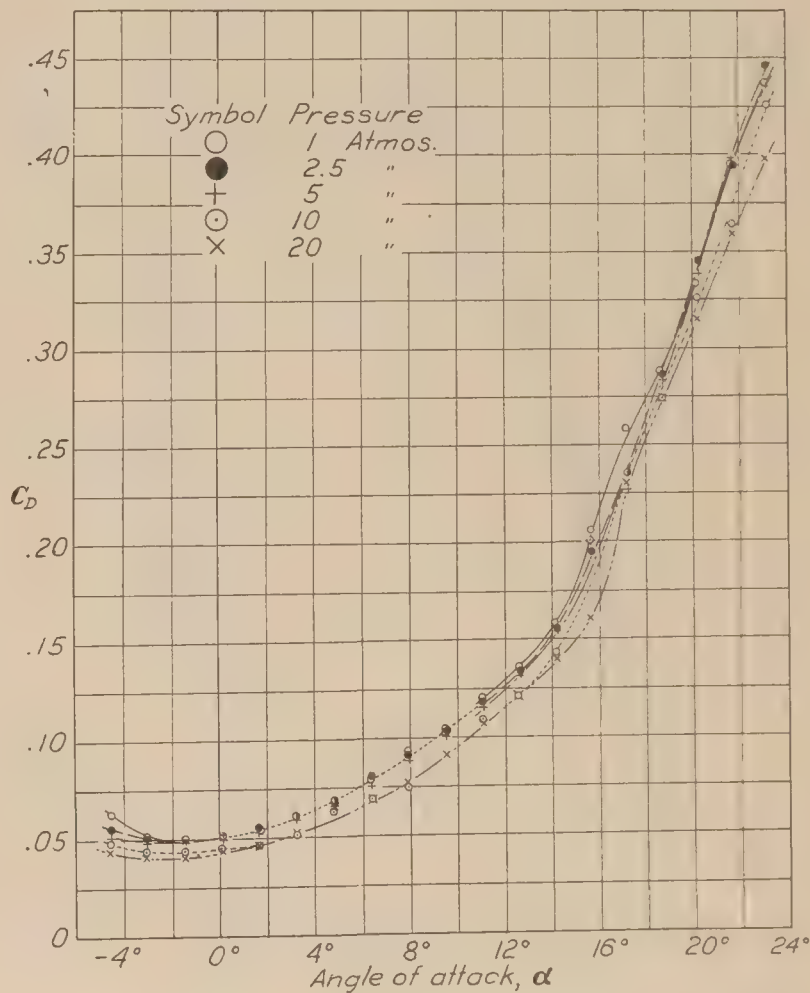


FIG. 15.—Drag coefficient vs. angle of attack. Bristol Fighter airplane model with R. A. F. 15 wings

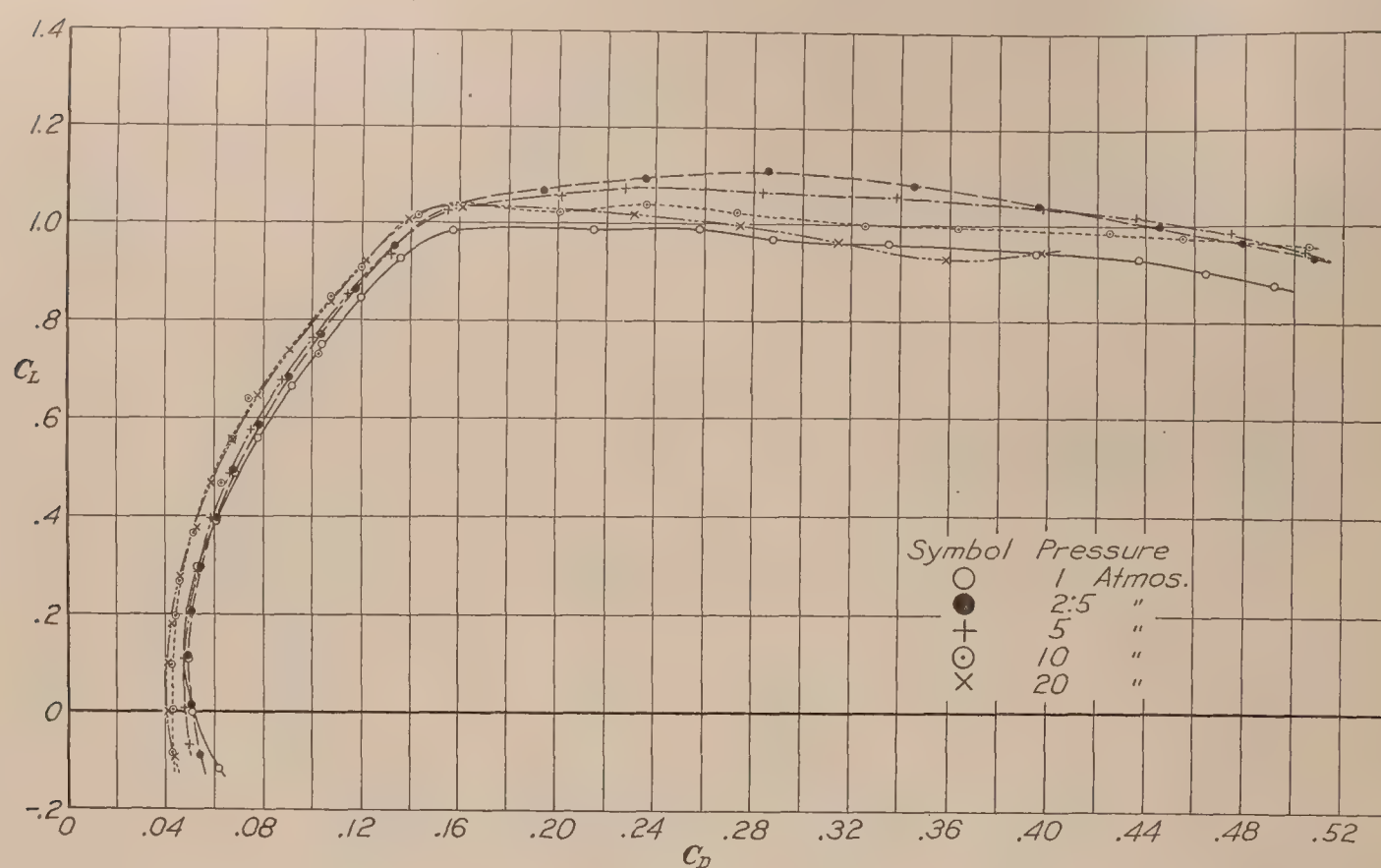


FIG. 16.—Lift coefficient vs. drag coefficient. Bristol Fighter airplane model with R. A. F. 15 wings

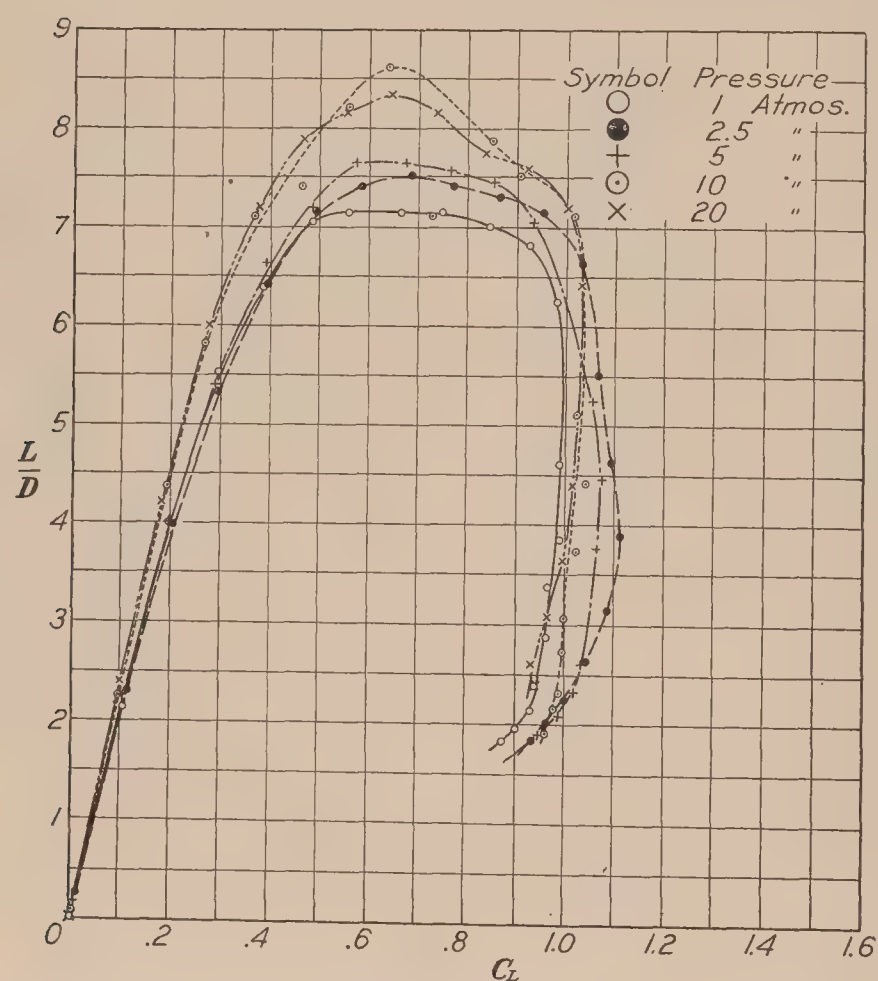


FIG. 17.—Lift/drag vs. lift coefficient. Bristol Fighter airplane model with R. A. F. 15 wings

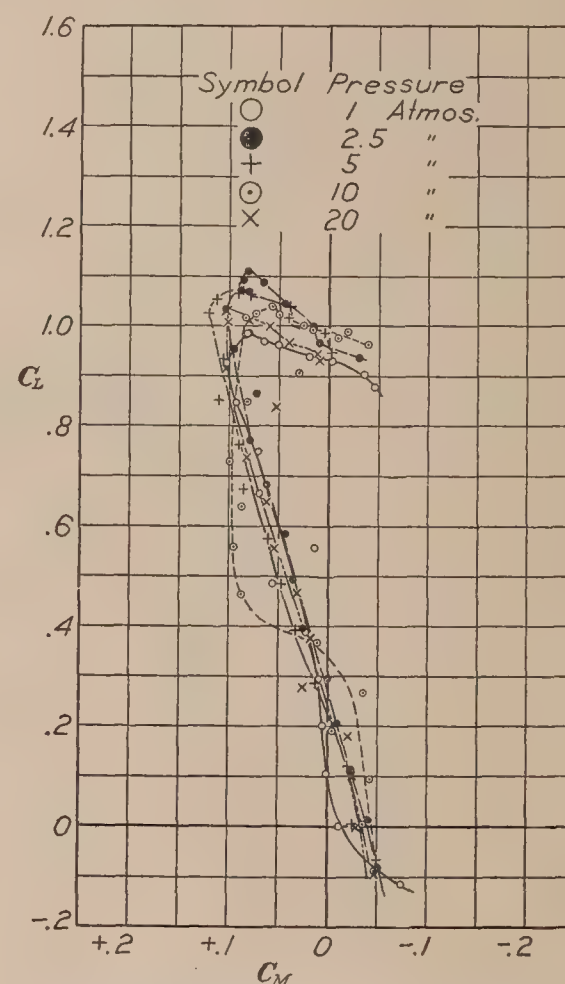


FIG. 18.—Lift coefficient vs. moment coefficient. Bristol Fighter airplane model with R. A. F. 15 wings

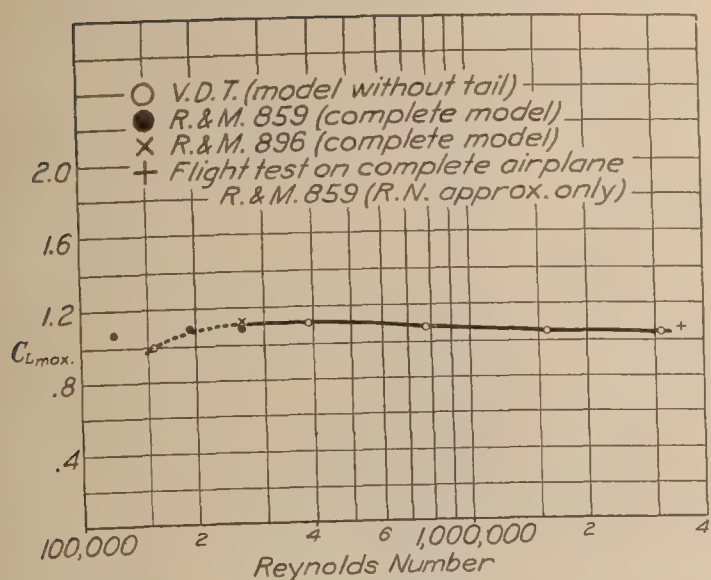


FIG. 19.—Scale effect on C_{Lmax} . Bristol Fighter airplane model with R. A. F. 15 wings

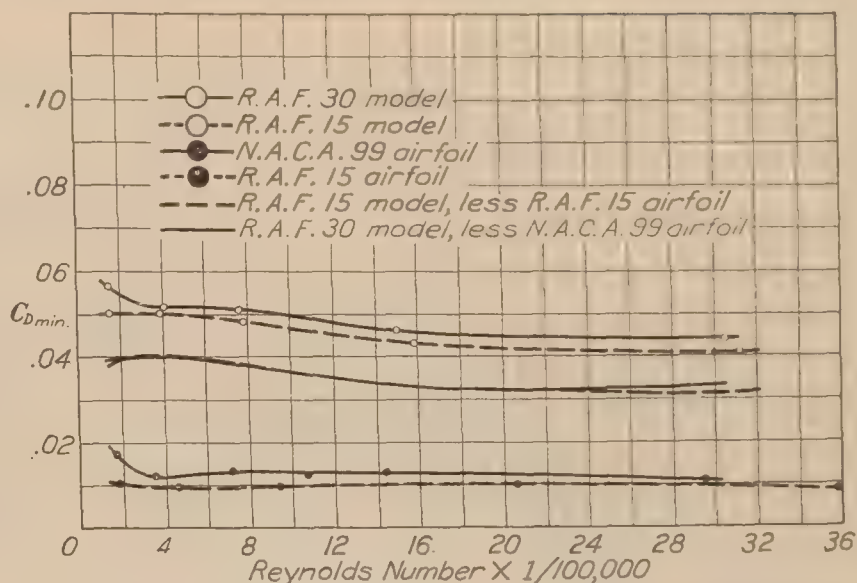


FIG. 20.—Scale effect on C_{Dmin} . Bristol Fighter airplane model without tail group

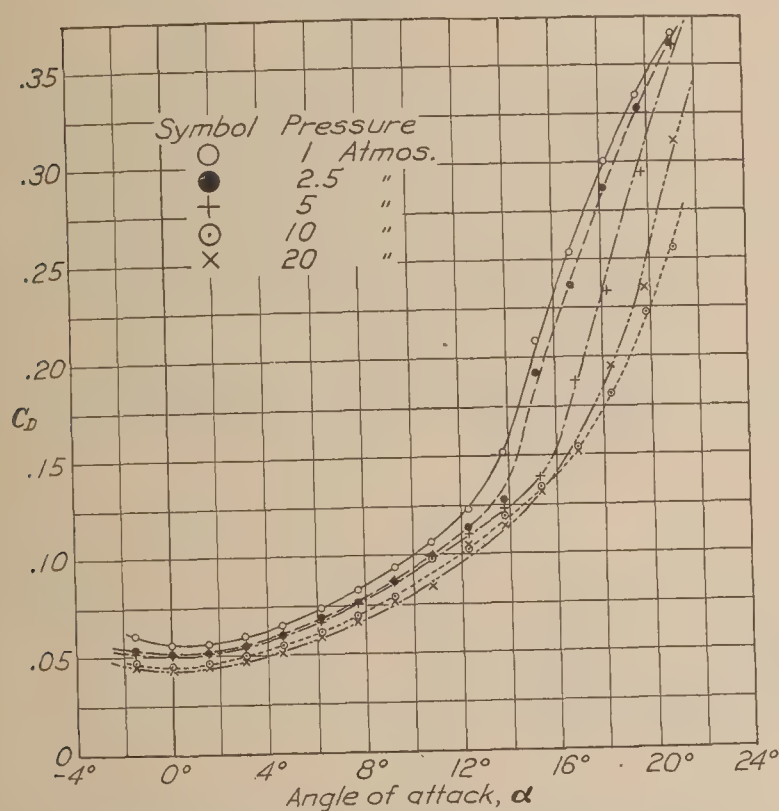


FIG. 21.—Lift coefficient vs. angle of attack. Bristol Fighter airplane model with R. A. F. 30 wings

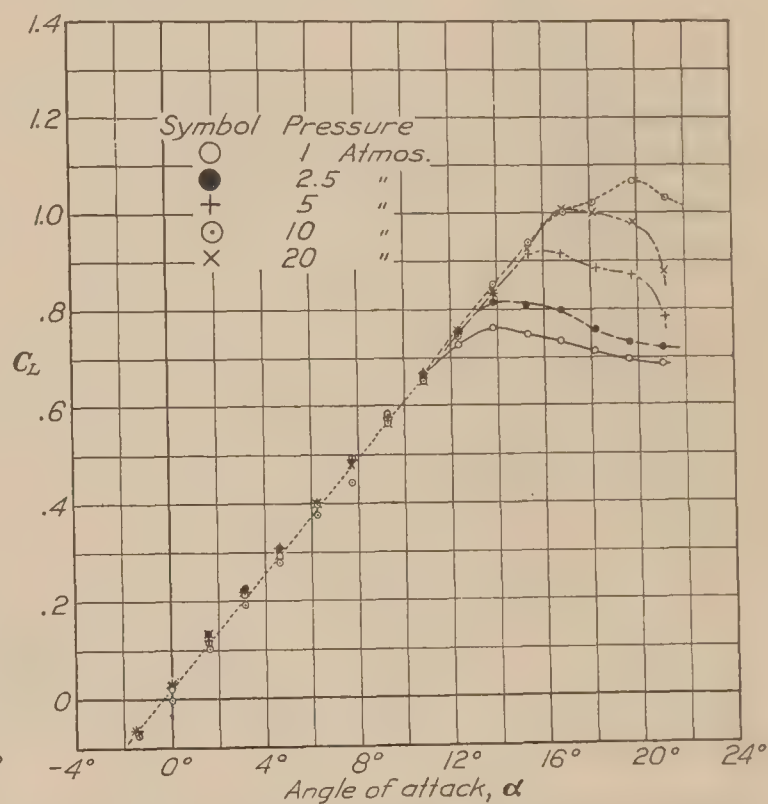


FIG. 22.—Drag coefficient vs. angle of attack. Bristol fighter airplane model with R. A. F. 30 wings

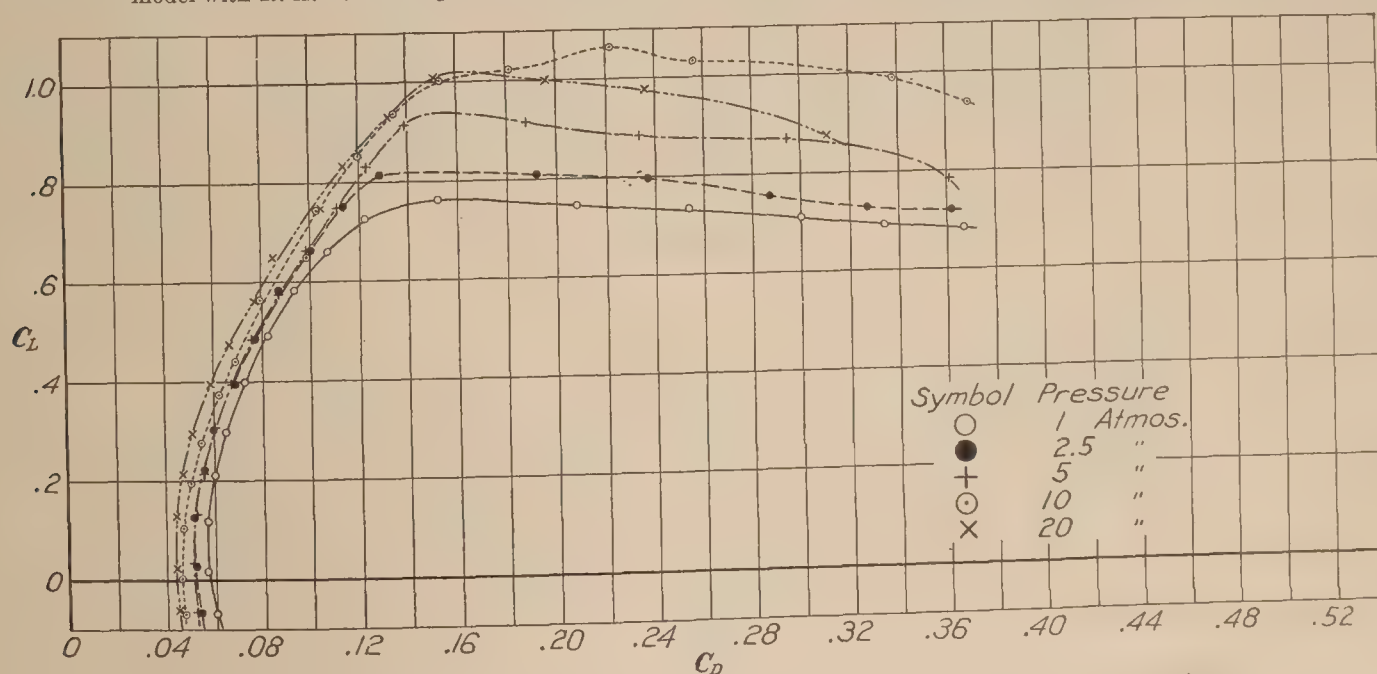


FIG. 23.—Lift coefficient vs. drag coefficient. Bristol Fighter airplane model with R. A. F. 30 wings

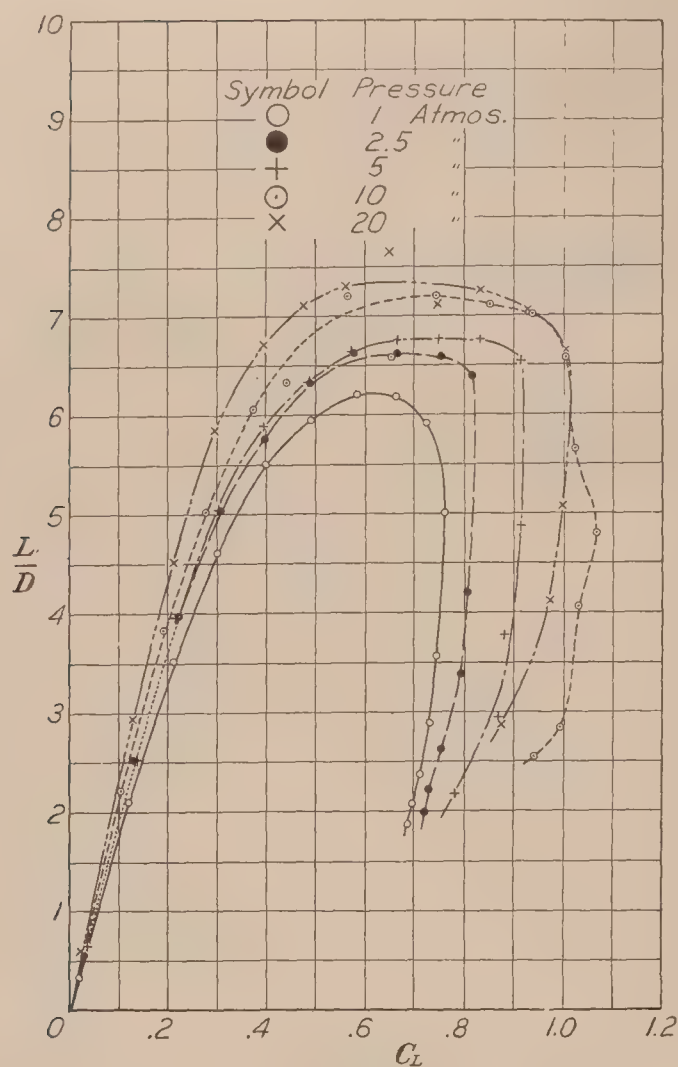


FIG. 24.—Lift/drag vs. lift coefficient. Bristol Fighter airplane model with R. A. F. 30 wings

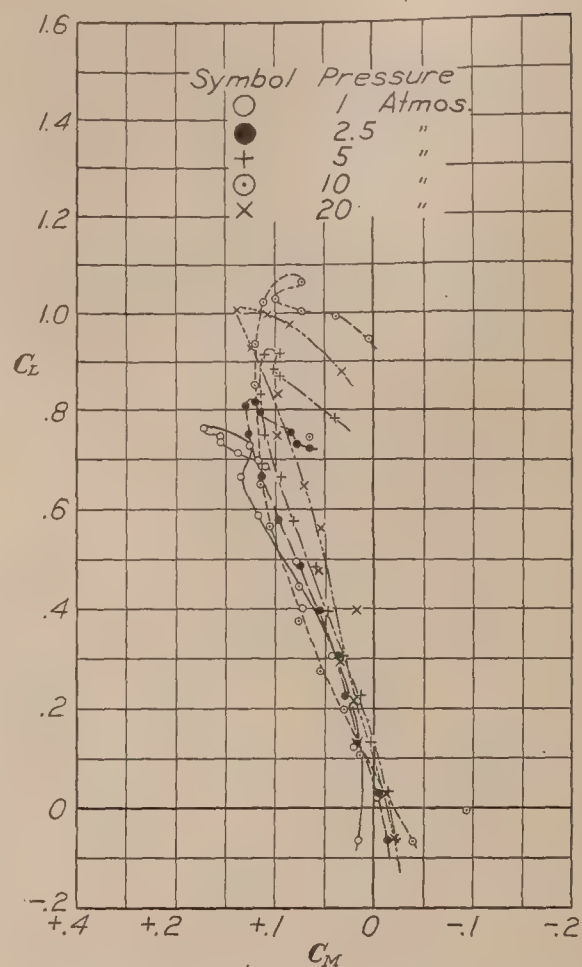


FIG. 25.—Lift coefficient vs. moment coefficient. Bristol Fighter airplane model with R. A. F. 30 wings

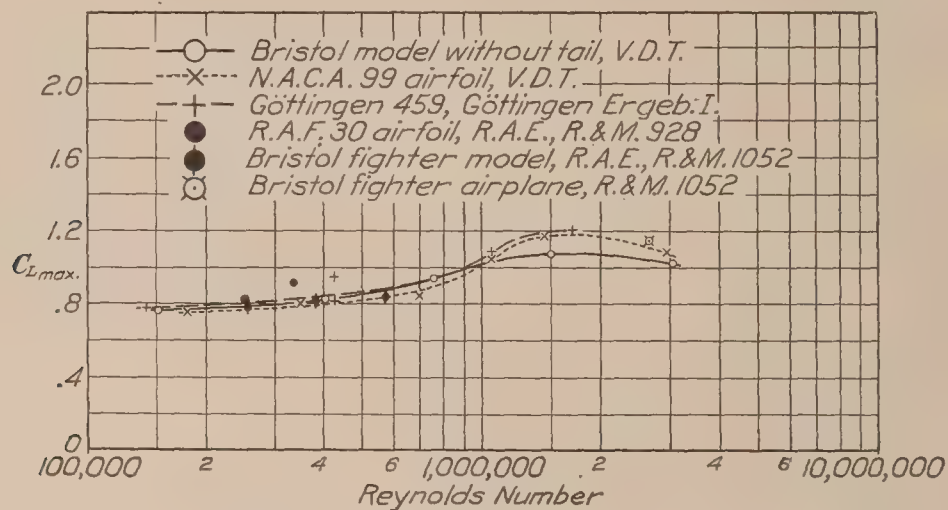


FIG. 26.—Scale effect on $C_{L_{max}}$. Bristol Fighter airplane model with R. A. F. 30 wings

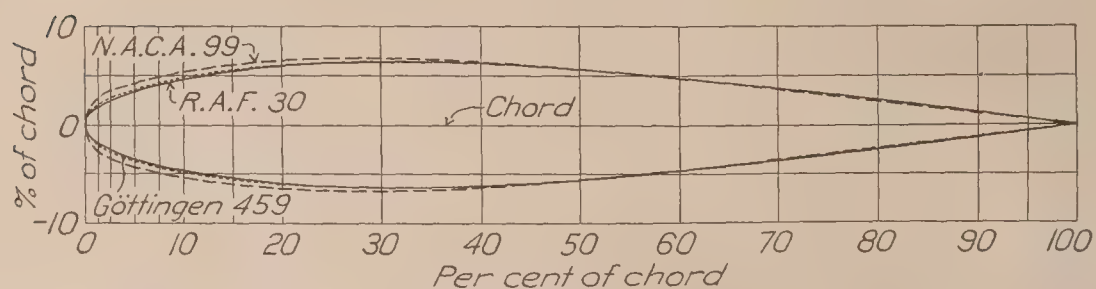


FIG. 27.—Superposed plot of airfoil sections R. A. F. 30, N. A. C. A. 99 and Göttingen 459 for comparison

APPENDIX

REPORT OF

AERODYNAMICS SUBCOMMITTEE

BRITISH AERONAUTICAL RESEARCH COMMITTEE

TESTS OF THREE AIRPLANE MODELS

By H. C. H. TOWNEND, B. Sc.

Tests have been made of models of BE2e with R. A. F. 19 wings, Bristol Fighter with R. A. F. 15 wings, and Bristol Fighter with R. A. F. 30 wings, for comparison with those obtained with the same models in the variable density tunnel of the National Advisory Committee for Aeronautics, America. Owing to lack of time it has not been possible to produce a complete report, and in consequence the absolute lift and drag coefficients only are given here, the moment coefficients being omitted for the present.

The wind velocity was adjusted in each case to give the same value of Vl/ν as in the corresponding test at atmospheric pressure in the N. A. C. A. tunnel. The particulars of the models as given in Table XVI of this report have been used in obtaining lift and drag coefficients.

The models were tested exactly as they were received, with the exception of the BE2e, which was found to be damaged on arrival. In addition to other minor defects, the lower wing was found to be slightly loose, yawed about 2° , displaced bodily about $\frac{3}{16}$ inch to starboard and bent at the root in such a way that its angle of attack was about $\frac{1}{3}^\circ$ in error. With the exception of the lateral displacement, the above defects were rectified before test.

Results.—The results have been corrected for effect of the tunnel walls. There is some doubt about the exact direction of the wind in the tunnel in which the models were tested which introduces some uncertainty in the value of minimum drag and it has not been possible to test for this yet.

The absolute lift and drag coefficients are plotted in Figures 28, 29, and 30. The agreement with the results in the variable density tunnel is very close for all the models. In the case of the BE2e with R. A. F. 19 wings the sharp fall in C_L above the maximum, which is characteristic of this wing section, does not occur in the N. A. C. A. tests, the results of which for this model are particularly smooth near the stall.

June, 1927.

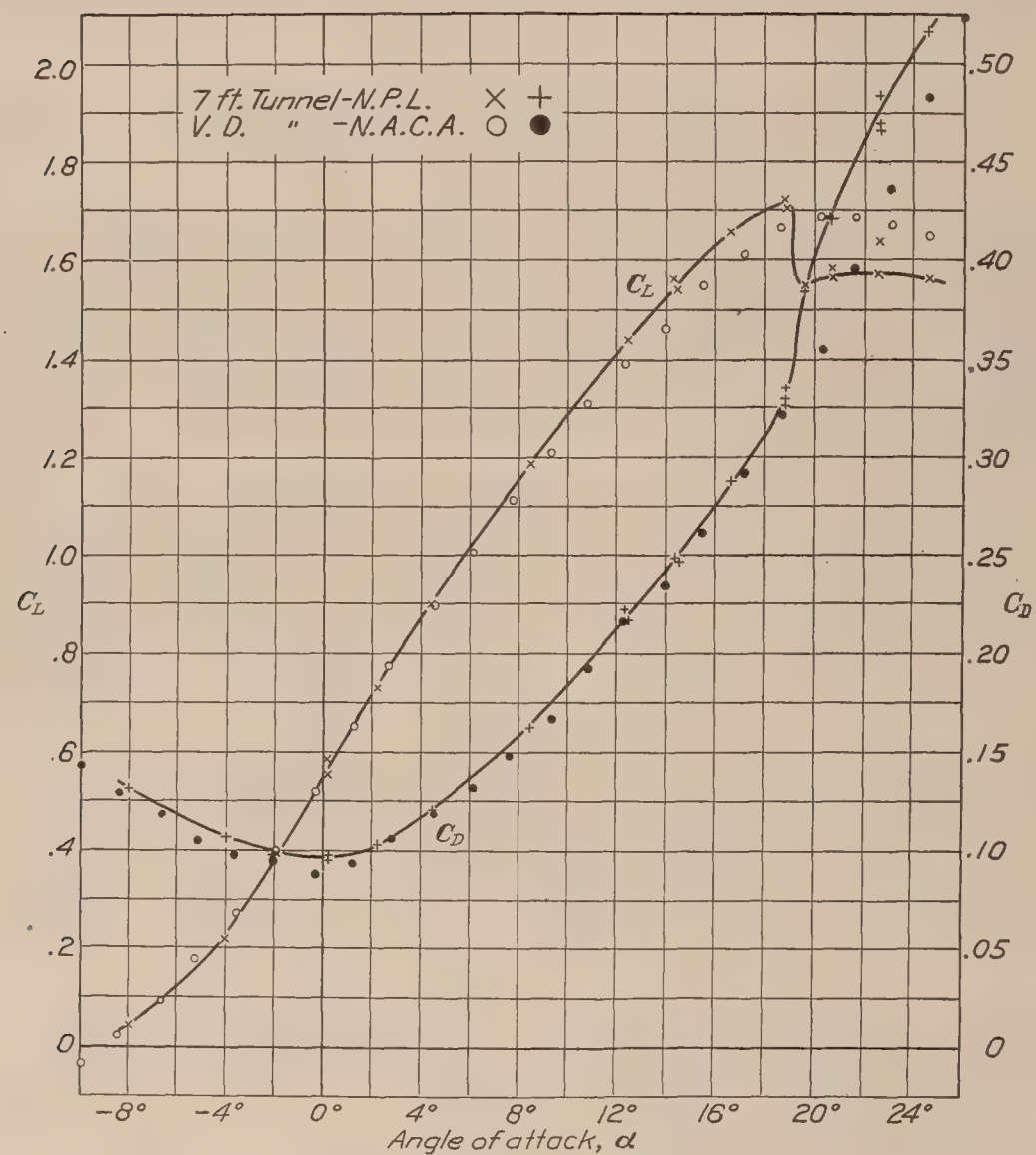


FIG. 28.—Lift and drag coefficients at $\frac{Vl}{\mu} = 191,500$ for BE2c model with R. A. F. 19 wings (without tail unit)

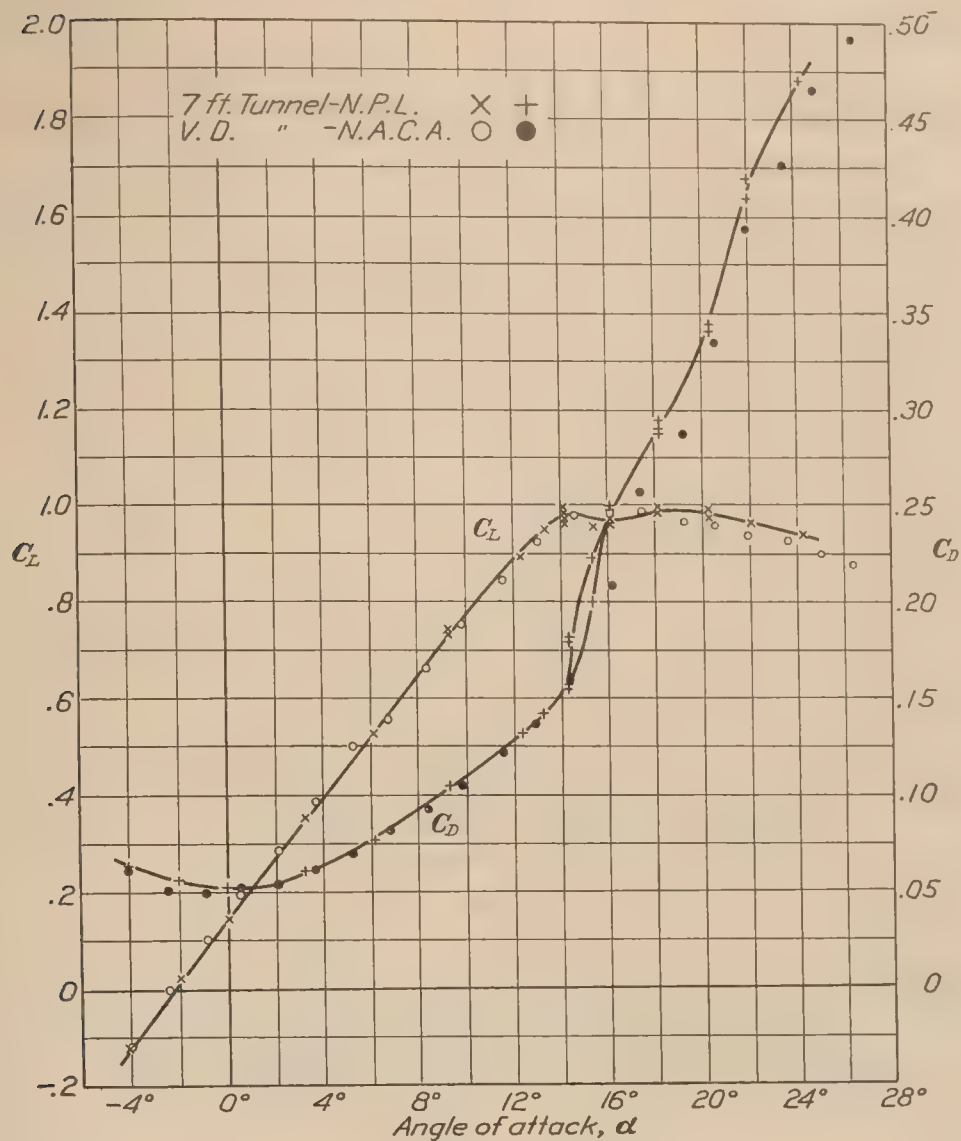


FIG. 29.—Lift and drag coefficients at $\frac{Vl}{\mu} = 157,000$ for Bristol Fighter model with R. A. F. 15 wings (without tail unit)

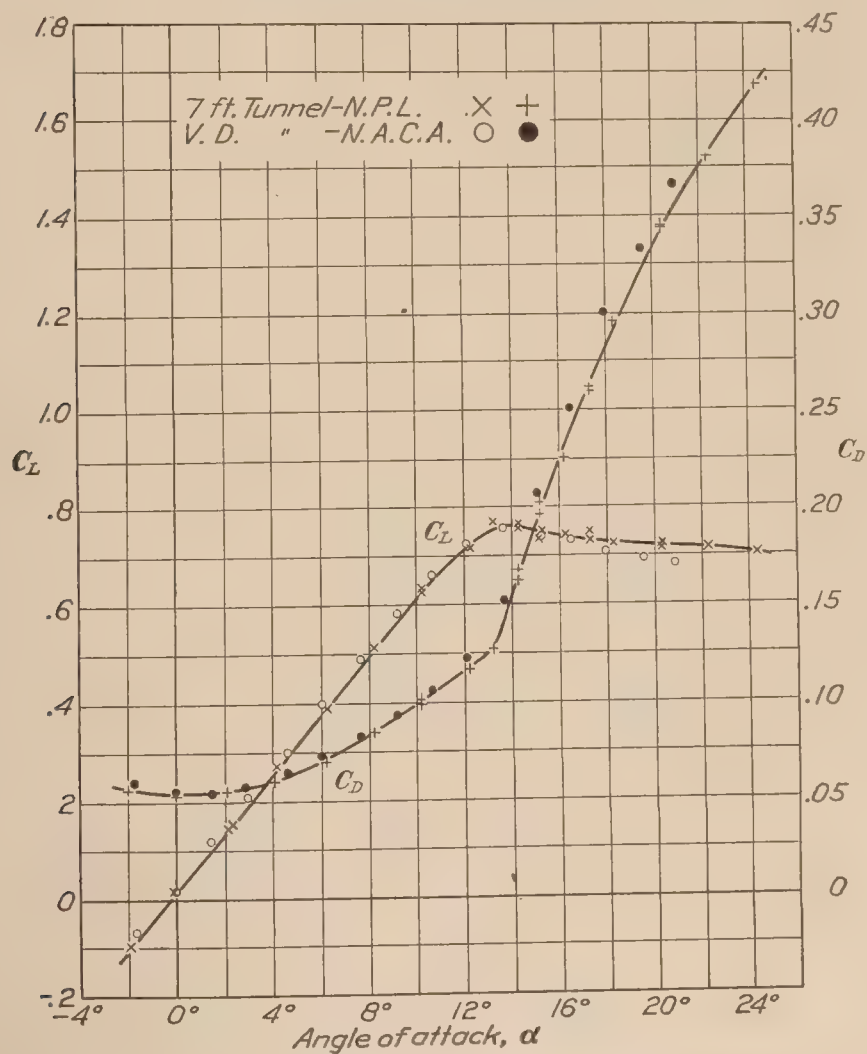


FIG. 30.—Lift and drag coefficients at $\frac{Vl}{\mu} = 152,000$ for Bristol Fighter model with R. A. F. 30 wings (without tail unit)

REPORT No. 280

**THE GASEOUS EXPLOSIVE REACTION
THE EFFECT OF INERT GASES**

**By F. W. STEVENS
Bureau of Standards**

REPORT No. 280

THE GASEOUS EXPLOSIVE REACTION—THE EFFECT OF INERT GASES

By F. W. STEVENS

SUMMARY

(1) Attention is called in the following paper to previous investigations of gaseous explosive reactions carried out under constant-volume conditions, where the effect of inert gases on the thermodynamic equilibrium was determined. The advantage of constant-pressure methods over those of constant volume as applied to studies of the gaseous explosive reaction is pointed out and the possibility of realizing for this purpose a constant-pressure bomb mentioned.

(2) The application of constant-pressure methods to the study of gaseous explosive reactions, made possible by the use of a constant-pressure bomb, led to the discovery of an important kinetic relation connecting the rate of propagation of the zone of explosive reaction within the active gases, with the initial concentrations of those gases:

$$s = k_1[A]^{n_1}[B]^{n_2}[C]^{n_3}\text{-----}$$

(3) By a method analogous to that followed in determining the effect of inert gases on the equilibrium constant, K , the present paper records an attempt to determine their kinetic effect upon the expression given above. It is found that this effect for the inert gases investigated, — N_2 , He , and CO_2 — may be expressed as

$$s = k_1[A]^{n_1}[B]^{n_2}[C]^{n_3}\text{-----} + \beta[G_i]$$

where $[G_i]$ represents the initial concentration of the inert gas. From results obtained it seems probable that the value of β depends upon the combined effect of the thermal properties of the inert gas on the heat distribution of the reaction; the property of heat conductivity being predominant.

(4) An example of the utility of the constant-pressure bomb for the study of the kinetics of the gaseous explosive reaction is offered in the results of the present paper.

THERMODYNAMICS

From the standpoint of thermodynamics the effect of inert gases upon the equilibrium of the gaseous explosive reaction has received extended consideration from Nernst and his pupils (References 1, 2, 3), who employed in their investigations a spherical bomb of constant volume fired from the center. This series of investigations extended to temperatures of over 3,000° Abs. and formed part of the most extensive investigation of a gaseous reaction involving the equilibrium products of combustion, carbon dioxide, and water vapor, that has yet been carried out. "No other chemical equilibrium has so far been investigated by so many methods which can also be controlled at the same time by thermodynamic calculations. * * * A specially high value must be attached to explosion methods, since, by suitable variations of the experimental conditions it enables both the specific heats and the equilibrium to be determined." (Reference 4.)

In a previous report (Reference 5), a simple device was described that was found to function as a bomb of constant pressure. This simple device—an ordinary soap film holding temporarily the active gases to be investigated—provides the complement to the bomb of constant volume in the relation

$$PV = nRT \tag{1}$$

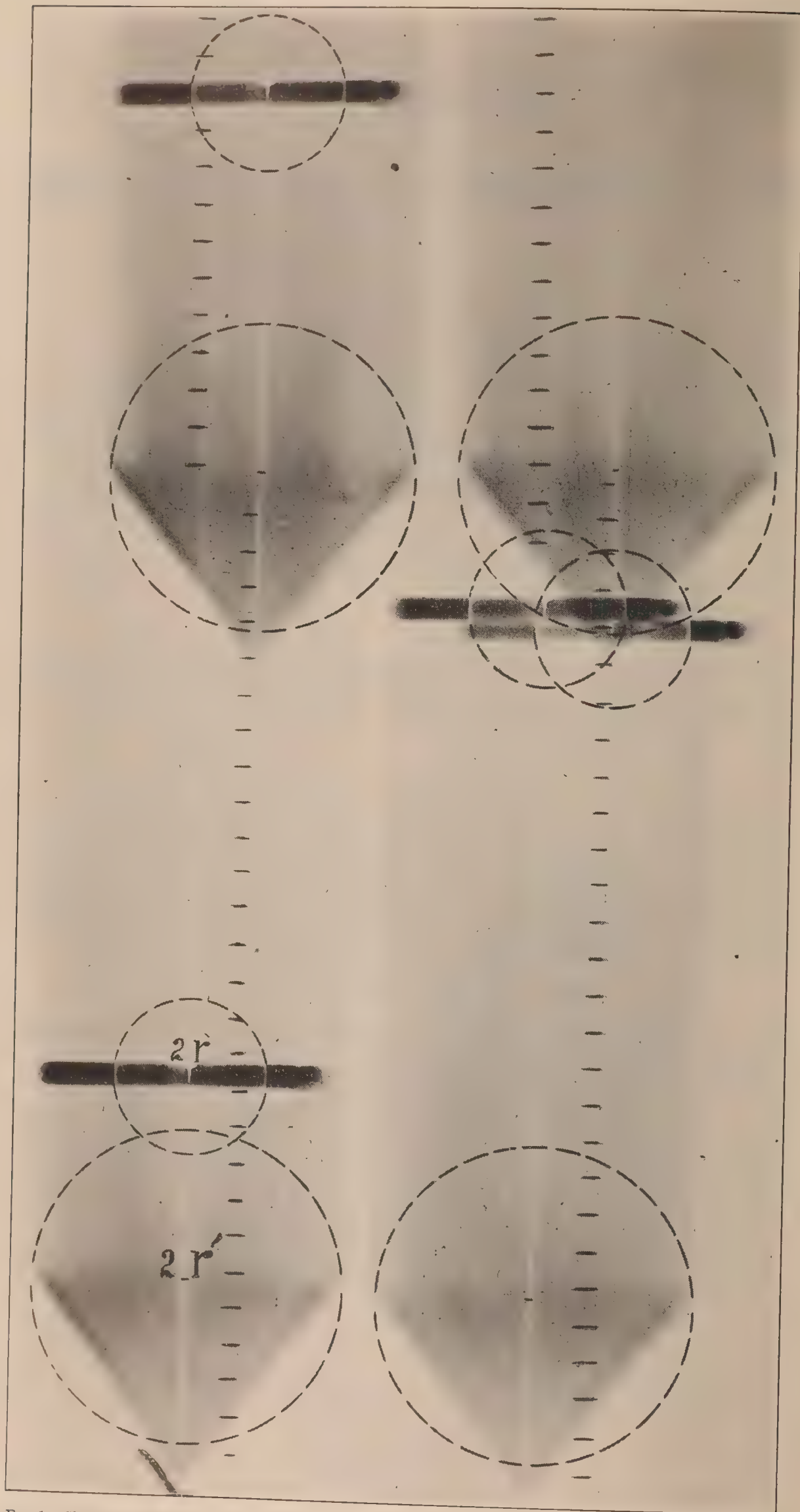


FIG. 1.—Shows a photographic time-volume record of four gaseous explosive reactions at constant pressure. The figures are $\frac{1}{4}$ actual size. $2r$ is the sphere of initial components considered. $2r'$ the sphere of its reaction products at the instant the reaction is complete

by expressing the initial and final condition of the reacting gases in terms of volume¹ at a constant pressure instead of pressure at a constant volume.

Besides the advantages attending the use of constant pressure methods as applied to thermodynamic studies of gaseous explosive reactions, the constant pressure bomb also offers unusual advantage in the study of an important kinetic phase of the reaction, namely, the rate at which the zone of explosive reaction is propagated within the active gases. The reason for this advantage both to thermodynamic and kinetic studies lies chiefly in the fact that at constant pressure the processes of the explosive reaction become automatically uniform, whereas, under the condition of constant volume and, to a much greater extent under conditions that only approach constant volume, they become unusually variable and complex. The possibility secured by a constant pressure bomb of so conditioning the reaction that it may run its course at a constant pressure (not necessarily atmospheric) thus greatly simplifies the course automatically taken by the transformation by eliminating a number of variables due to the effect of variable pressure upon the mass movement of the gases and upon their concentrations. The constant pressure bomb being transparent permits an accurate and continuous time-volume record of the reaction to be directly secured by photographic means. Such a record much reduced is shown at Figure 1. It gives the dimensions of the initial and final volumes of the reacting gases independent of the volume of the container and records the uniform progress by which a sphere r of initial components is transformed at a constant pressure into a sphere of equilibrium products, r' . This final volume represented by r' ,— as does the final pressure in the case of a constant volume bomb—corresponds to the equilibrium constant of the reaction,

$$K = \frac{[A']^{n'_1}[B']^{n'_2}[C']^{n'_3} \dots}{[A]^{n_1}[B]^{n_2}[C]^{n_3} \dots} \quad (2)$$

Pier has shown (Reference 1, p. 538) that the deviation from this constant due to the presence of an inert gas, permits the specific heat of that gas to be determined at the reaction temperature; and Siegel (Reference 3, p. 654), has shown that this expression allows the degree of dissociation of the combustion products to be found. For the case of the trimolecular reaction $2\text{CO} + \text{O}_2$, equation (2) may be written

$$K = \frac{[\text{CO}_2]^2}{[\text{CO}]^2[\text{O}_2]}$$

and if x is the degree of dissociation of CO_2 , then, for the case of the constant pressure bomb,

$$K_p = \frac{[\text{CO}_2]^2}{[\text{CO}]^2[\text{O}_2]} = \frac{(1-x)^2(2-x)}{x^3} \quad (3)$$

KINETICS

The photographic record (fig. 1) of the gross mechanism and progress of the reaction at constant pressure, upon which equal time intervals have been impressed, is a time-volume record of the reaction and hence may provide some general information as to the kinetics of the explosive transformation.

If the rate of flame movement is to be connected in any way with the rate of molecular transformation, it is obvious that its rate should be determined relative to the gases it is transforming and not relative to space, as is usually done. And it should likewise be recognized that

¹ It should be made clear that the term volume does not here refer to the actual volume of the temporary soap film container. The symmetry automatically assumed by the zone of reaction in the case of a homogeneous mixture of explosive gases fired from a point and under conditions of constant pressure, offers a much more accurate mode of procedure; for under these conditions the zone of reaction originating at the point of ignition advances in all directions from this point at a constant rate. It thus forms an expanding spherical shell of flame inclosing the products of combustion as they are formed by the passage of the initial active components through the zone of explosive reaction advancing at a constant rate. This sphere of reaction products is thus protected as well as may be from heat losses, during the reaction, due to conduction and convection. By reference to Figure 1 it will thus be seen that the initial volume of gases considered, is the volume of an ideal sphere $2r$ of the gases held by the temporary container, and not the volume of the container itself, for this is never a sphere. The final volume is the volume of the sphere $2r$ transformed into the sphere of reaction products, $2r'$. The conditions that determine uniform flame movement in a gaseous explosive reaction—whether for the slower reaction rates or for the more rapid rates of the explosive wave—are a homogeneous mixture of the explosive gases and a constant pressure; for under these conditions only is it possible for the mass movement of the gases and for their concentrations to remain constant during the reaction process.

unless the method employed makes it possible to follow the concentrations of the active gases which the zone of explosive reaction is entering, a kinetic relation connecting the movement of this region with the composition and concentration of the explosive gases, could hardly be expected to result from its use.

An examination of a great number of records similar to that shown at Figure 1, obtained with different gases at different concentration ratios, has shown that at constant pressure the rate of movement s of the zone of reaction, measured relative to the active gases, is proportional to the product of the initial partial pressures of those gases:

$$s = k_1 [A]^{n_1} [B]^{n_2} [C]^{n_3} \dots \dots \dots \quad (4)$$

In this expression, k_1 is a proportionality factor. The inclosed symbols refer to initial concentrations or partial pressures of the active components. s is the rate of propagation of the zone of reaction measured relative to the active gases it is entering.

It was of interest to examine the effect of inert gases on the rate of propagation of the zone of reaction in the light of the kinetic relation expressed in (4) and by a method suggested by that employed in the determination of their effect upon the thermodynamic equilibrium. It is the purpose of this report to record the results obtained in this endeavor.

EXPERIMENTAL PART

From the photographic figure of the progress of the reaction, it will be seen that the constant rate of flame movement s' , *in space*, may be determined at any instant during the transformation. At the instant the reaction is completed its value may be written

$$s' = \frac{r'}{t}$$

But this is not the rate at which the flame is entering the gases. The rate s , at which the flame is entering the gases, may be found for the case of a spherical shell of flame expanding at a uniform rate s' , as follows: Let m, m (fig. 2) be an element of the flame surface held at rest by the uniform rate of flow s , of the active gases against it; then s will be the rate at which the flame area enters the gases and s' will be the rate at which the transformed gases leave the flame area. If ρ and ρ' are the initial and final gas densities then from the equality of masses

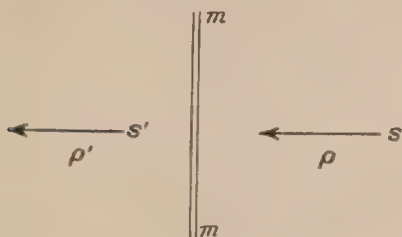


FIG. 2

$$\rho s = \rho' s'$$

For the case of the two spheres of radius r and r' , we also have from the equality of masses

$$\frac{4}{3\pi} \rho r^3 = \frac{4}{3\pi} \rho' r'^3;$$

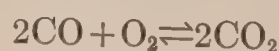
hence

$$\frac{s}{r^3} = \frac{s'}{r'^3}$$

and

$$s = s' \frac{r^3}{r'^3} = \frac{r^3}{r'^2 t} \quad (5)$$

For experimental purposes, the gaseous explosive reaction at water vapor saturation,



was selected. For this special case equation (4) may be written

$$s = k_1 [\text{CO}]^2 [\text{O}_2] \quad (6)$$

and including equation (5),

$$s = \frac{r^3}{r'^2 t} = k_1 [\text{CO}]^2 [\text{O}_2] \quad (7)$$

Since the sum of the partial pressures of the gaseous components present in the reaction at pressure p must equal p , equation (6) may be written for atmospheric pressure,

$$s = k_1 [\text{CO}]^2 [1 - \text{CO}]$$

without designating the composition of $1 - \text{CO}$ further than to indicate that the sum of the partial pressures of its components remains the same as the partial pressure of the component O_2 in equation (6) and that under the same circumstances both equations represent the same impact probability though not the same proportion of effective impacts nor the same potential energy. In case the component $1 - \text{CO}$ is made up of the fraction a of the active gas O_2 and the fraction $(1 - a)$ of an inactive gas, the partial pressure of this component may be expressed as

$$[1 - \text{CO}] = \underset{\text{active}}{[1 - \text{CO}] a} + \underset{\text{inert}}{[1 - \text{CO}] (1 - a)}$$

and equation (6) may then be written as

$$s = k_1 ([\text{CO}]^2 [1 - \text{CO}] a + [\text{CO}]^2 [1 - \text{CO}] (1 - a)).$$

If all of the impacts involving the inert gas are futile and the possible effect of its various physical properties as specific heat, heat conductivity, etc., on the course of a thermal reaction be disregarded, then the last term in the above expression may be neglected and the effect on reaction probability of replacing the fraction $(1 - a)$ of an active gas by an inactive one may be written

$$s = k_1 [\text{CO}]^2 [1 - \text{CO}] a \quad (8)$$

This mass law expression takes into account the effect of the remaining active components only; and this is the major effect to be expected; but while the inert gas introduced may take no part in the molecular transformation, its presence in the zone of explosive reaction and in the active gases adjacent to it, must necessarily affect the heat distribution in that region. If the effect of the thermal properties of the inert gas is a simple function of its concentration, then the deviation from the relation expressed in (8), due to its presence in the zone of reaction might be expressed as

$$s = \frac{r^3}{r'^2 t} = k_1 [\text{CO}]^2 [1 - \text{CO}] a + \beta [1 - \text{CO}] (1 - a). \quad (9)$$

From this relationship it will be seen that the maximum effect of the inert gas should be found for the minimum value of $[\text{CO}]$ and *vice versa*. In carrying out the observations, therefore, the effect of each successive increase in the partial pressure of each of the inert gases investigated, nitrogen, carbon dioxide, and helium,² was observed over the entire range of partial pressure ratios that would ignite. This procedure, which resulted in a very large number of observations and calculations, was necessary because the proportion of inert gas to the whole varies with each ratio of the partial pressures.

² Some of the thermal properties of the gases involved in the reaction are given in the following table:

Gas	C_p	Heat conductivity
N_2	6.75	566
CO_2	9.44	337
He	5.00	3,360
CO	6.75	542
O_2	6.75	570

For the purpose of comparison, Table I gives the results obtained when no inert gas was present:

TABLE I
FLAME SPEED AND VELOCITY COEFFICIENT FOR THE $2\text{CO} + \text{O}_2$ REACTION WITHOUT INERT GAS

Partial pressure (atmospheres)		$\Gamma = [\text{CO}]^2 [\text{O}_2]$	$s = \frac{r^3}{r'^2 t}$ cm/sec.	$k_1 = \frac{s}{[\text{CO}]^2 [\text{O}_2]}$
[CO]	[O ₂]			
0.25	0.75	0.0469	34.9	745
.30	.70	.0630	44.0	698
.35	.65	.0796	53.5	672
.39	.61	.0907	66.0	711
.435	.565	.1069	75.5	706
.45	.55	.1114	76.0	682
.47	.53	.1171	83.5	713
.48	.52	.1198	84.0	701
.50	.50	.1250	87.0	696
.505	.495	.1262	88.0	681
.532	.468	.1326	89.0	672
.55	.45	.1361	94.0	691
.56	.44	.1380	93.0	674
.585	.415	.1420	97.5	687
.60	.400	.1440	99.5	691
.61	.39	.1451	100.0	689
.63	.37	.1468	102.0	695
.67	.33	.1481	104.0	702
.69	.31	.1476	104.0	705
.70	.30	.1470	99.1	674
.75	.25	.1406	96.3	685
.80	.20	.1280	90.5	707
.825	.175	.1191	82.0	693
.84	.16	.1129	78.7	697
.86	.14	.1136	66.5	642
.894	.106	.1147	58.0	685
.94	.06	.0530	33.0	622
				Av. k_1 690

The results given in the above table may be expressed in graphic form by plotting the values of s as ordinates and either the corresponding partial pressures or the corresponding values for impact probability, $T = [\text{CO}]^2 [\text{O}_2]$, as abscissas. In Figure 3 and in the other figures to be given, the more familiar relation between rates and partial pressures will be used. The experimental values of s found are represented in Figure 3 by solid circles. Theoretical values corresponding to the relation $s = k_1 [\text{CO}]^2 [\text{O}_2]$ are represented by open circles connected by a continuous line. This curve will be reproduced for reference in the figures that follow that represent the effect of an inert gas on the rate of reaction.

In Figure 4 the upper curve represents results when no inert gas is present. The lower curve represented by a continuous line corresponds to equation (8), $s = k_1 [\text{CO}]^2 [1 - \text{CO}]^{0.9}$, for the case where 10 per cent of the component $1 - \text{CO}$ is made up of an inert gas. The experimental values found when 10 per cent of inert gas used was N_2 are indicated by the mark \times ; when the inert gas was CO_2 by the mark \blacksquare ; and when the inert gas was He by the mark \blacktriangle . When such small amounts as 10 per cent of the different inert gases are introduced, not much difference in their effect is to be noticed. Their thermal characteristics do not mask the effect of the active gases.

In like manner, Figure 5 represents results obtained when 20 per cent of the component $1 - \text{CO}$ consists of an inert gas. The lower continuous curve corresponds to equation (8) for this case, $s = k_1 [\text{CO}]^2 [1 - \text{CO}]^{.8}$. The observed values when this amount of the three inert gases N_2 , CO_2 , and He were successively used are indicated by the same symbols employed in Figure 4.

When 40 per cent of the component $1 - \text{CO}$ consists of an inert gas, the individual thermal characteristics of the different gases become more marked. When a somewhat greater amount than 40 per cent of CO_2 is employed at atmospheric pressure the range of ignition is much

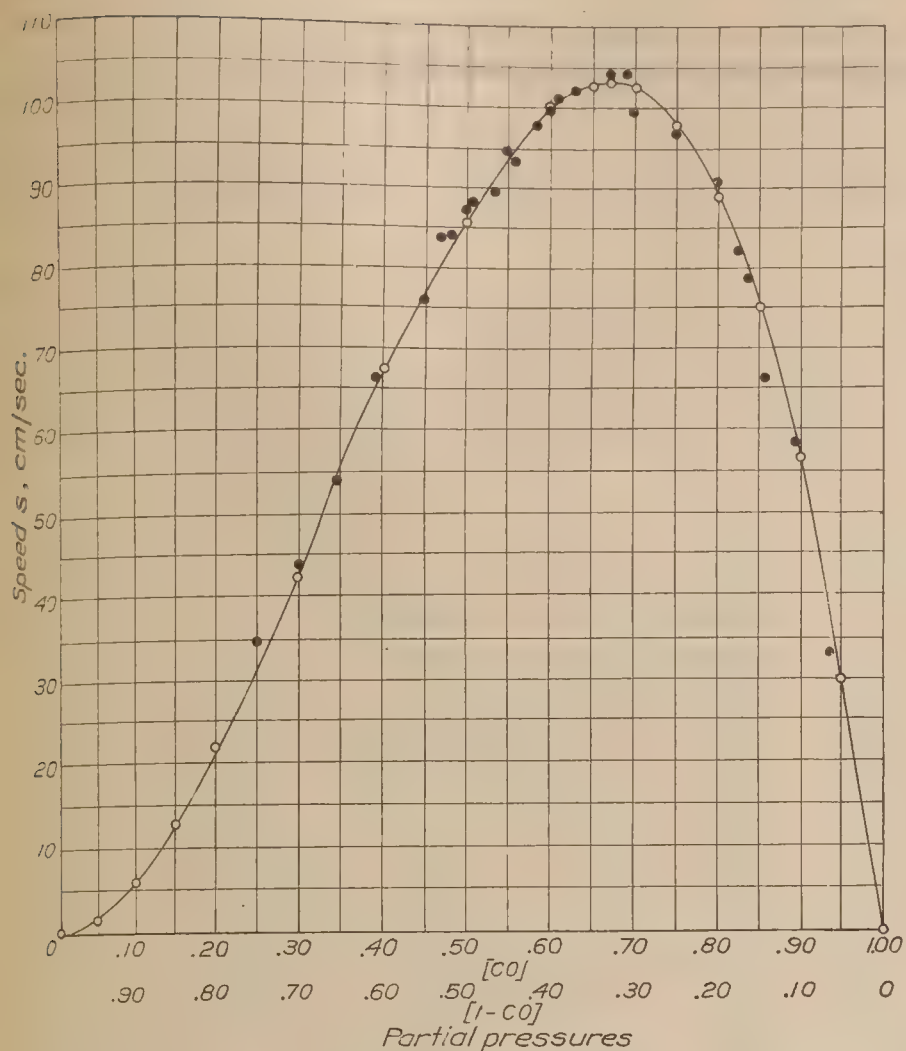


FIG. 3.—Shows the relation between the linear rate of propagation of the zone of reaction, relative to the active gases, and the partial pressures, $[]$, of those gases, CO and O_2 . The solid circles are the observed values, $\frac{s=r^3}{r^{1/2}t}$. The open circles, and the continuous line show calculated values, $s=k_1 [CO]^2 [O_2]$

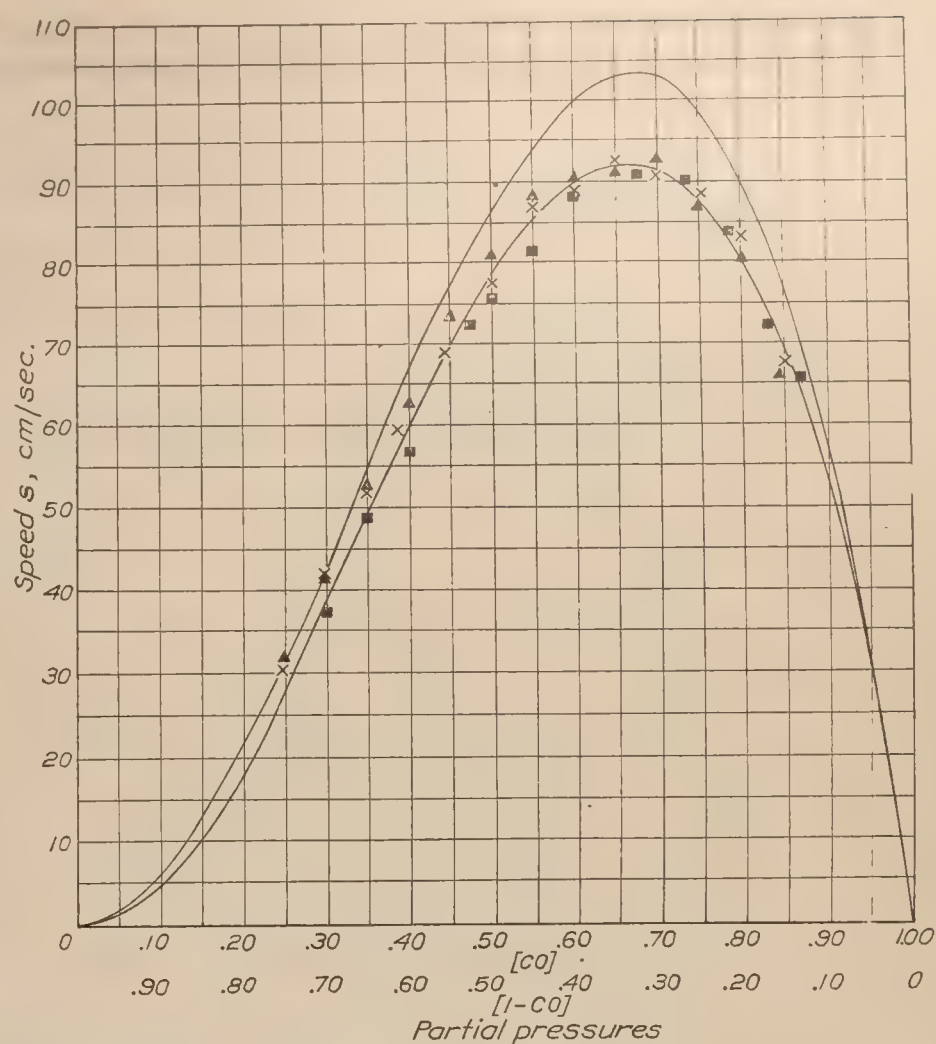


FIG. 4.—The upper curve corresponds to values found when no inert gas was present. The lower continuous curve corresponds to equation (8) for the case where 10% of the component $+1-CO$ consists of an inert gas: $s=k_1 [CO]^2 [1-CO].9$. The observed values when the inert gas used was N_2 are indicated by the mark X, CO_2 by the mark ■, and He by the mark ▲

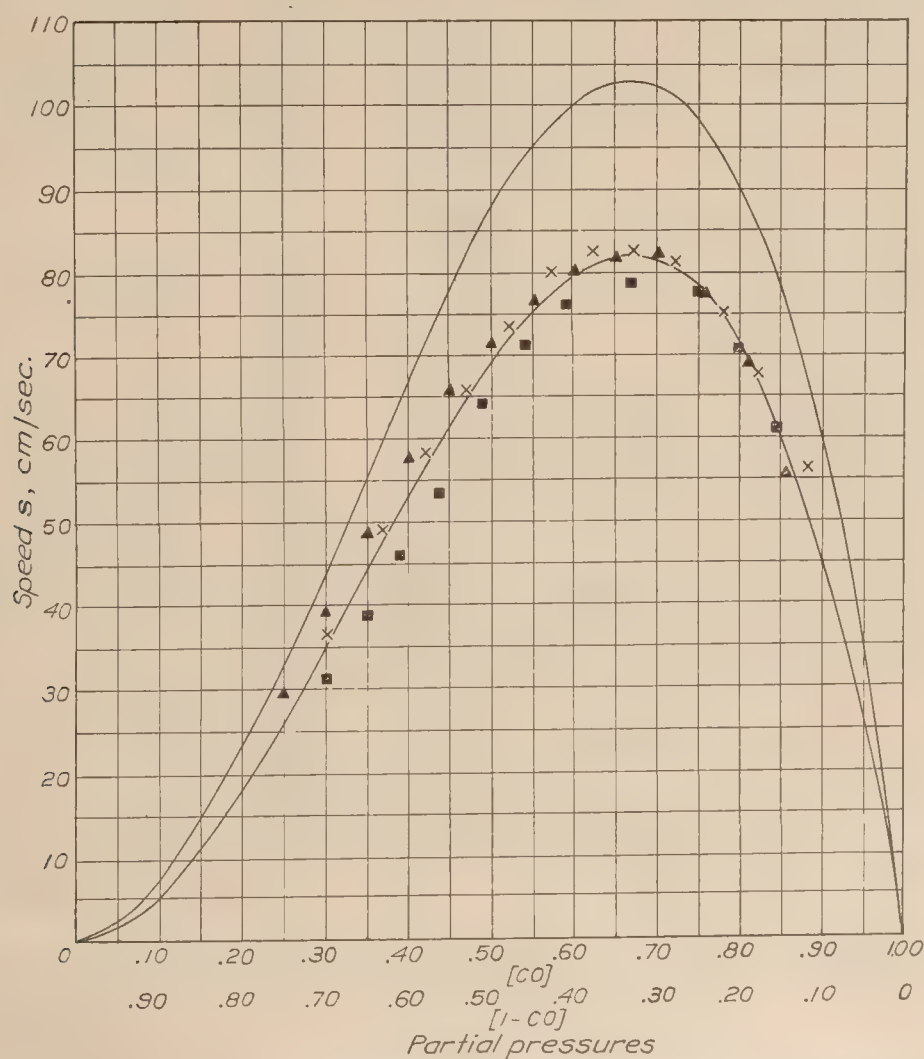


FIG. 5.—The upper curve corresponds to values found when no inert gas was present; the lower continuous curve corresponds to equation (8) for the case where 20% of the component $+1-CO$ consists of an inert gas: $s=k_1 [CO]^2 [1-CO].8$. The observed values when the inert gas used was N_2 are indicated by the mark X, CO_2 by the mark ■, and He by the mark ▲

reduced and the reaction rate becomes so slow that the few results obtainable with the gas are of little value—the sphere of heated reaction products starts to rise, like a hot-air balloon before the reaction is completed.

A tabulation of the results obtained with 40 per cent He is given below in Table II. Similar tabulations were made in all cases for the other inert gases used and for each successive increase in the amount introduced.

TABLE II

FLAME SPEED AND CONSTANT β FOR THE $2\text{CO} + \text{O}_2$ REACTION IN THE PRESENCE OF HELIUM

Partial pressure (atmospheres) [CO] [1-CO] [He]			$\Gamma = \frac{r}{[\text{CO}]^2[1-\text{CO}]}$	$s' = \frac{r'}{t}$ cm/sec.	$s = s' \frac{r^3}{r'^3}$ cm/sec.	η cm/sec.	$\beta = \frac{s - k_1 a [\text{CO}]^2 [1-\text{CO}]}{[\text{He}]}$
0.22	0.78	0.312	0.0377	256	48.3		
				266	50.2		
				267	50.4		
				261	49.2	49.5	112
.265	.735	.294	.0516	335	55.5		
				349	57.9		
				340	56.3		
				330	54.6	56.1	119
.30	.70	.280	.0630	368	58.6		
				393	62.7		
				359	57.1		
				384	61.2	59.9	119
.35	.65	.260	.0796	440	60.0		
				455	62.8		
				441	60.2		
				459	62.6	61.4	111
.40	.60	.240	.0960	512	70.0		
				470	64.3		
				498	68.0		
				511	69.8	68.0	117
.45	.55	.220	.1140	548	72.8		
				552	73.3		
				553	73.4		
				509	67.6	71.8	118
.50	.50	.200	.1250	566	72.1		
				563	71.7		
				573	73.0	72.3	99
.55	.45	.180	.1360	671	80.5		
				626	75.2		
				615	73.8		
				613	73.6	75.8	105
.60	.40	.160	.1440	635	79.1		
				590	73.6		
				610	76.1		
				618	77.0	76.5	101
.65	.35	.140	.1480	619	77.6		
				604	75.7		
				618	77.5		
				605	75.9	76.6	103
.70	.30	.120	.1470	588	73.5		
				591	73.9		
				582	72.8		
				604	75.5	73.9	108
.75	.25	.100	.1410	560	72.4		
				538	69.5		
				536	69.2		
				518	66.9	69.5	103
.80	.20	.080	.1280	480	69.1		
				439	62.5		
				421	59.8		
				445	61.9	63.3	104
.85	.15	.060	.1080	291	50.7		
				299	52.0		
				314	55.5		
				287	50.0	52.0	100
							Av. β 108

Figure 6 shows experimental results obtained when 40 per cent of the component 1-CO was made up of inert gas. The lower continuous curve corresponds to equation (8) for this case, $s = k_1 [\text{CO}]^2 [\text{O}_2] .6$. The deviations of the experimental values from this curve are well marked.

In the last column of Table II for helium is given the experimental value of β in equation (9).

$$\beta = \frac{s - k_1 a [\text{CO}]^2 [1 - \text{CO}]}{[\text{He}]}$$

When the average value of this factor, 108, is introduced into equation (9) and the values of s computed over the possible range of partial pressure ratios, the curve marked He results. In the same way there was obtained from the experimental values for 40 per cent CO_2 , $\beta = -41.8$ and for 40 per cent N_2 , $\beta = 42$. When these values are substituted in equation (9) the curves marked CO_2 and N_2 are determined. The constancy of these β -values indicate that the thermal effect of the inert gas on the rate of flame propagation is proportional to its concentration in the explosive mixture. That its value depends upon the additive effect its physical properties have on the heat distribution of the reaction seems reasonable. Of these properties, that of heat conductivity is expressible as a rate; that of its specific heat, being a thermodynamic factor, is expressible, as already pointed out (Reference 4) in terms of the thermodynamic equilibrium. The kinetic effect of the specific heat of the inert gas would be expressed as a temperature coefficient of the velocity constant k (Reference 6).

The effect of adding an inert gas of high heat conductivity to a gaseous explosive mixture may seem in some cases anomalous, for it may even increase the rate of flame propagation for some partial pressure ratios above those where no inert gas is present.

This may be seen by comparing the observed and theoretical values for the 40 per cent He mixtures with the observed and theoretical values for pure CO and O_2 mixtures. The presence of an inert gas of high heat conductivity also increases markedly the range of ignition; while a gas of low conductivity reduces it.

The mixture ratio for maximum flame velocity for the conditions expressed by equations (6) and (8) is the point $0.66+$ in the coordinate figures. But for equation (9) this point will be displaced to the left according to the positive magnitude of the last term, and to the right according to its negative magnitude. It will be seen that the experimental result confirms this deduction.

It is also of interest to note that it is possible to secure a mixture of two inert gases whose thermal effect upon the rate of reaction is in opposite sense, such that their effects balance each other and the last term in equation (9) becomes negligible. The conclusion could be

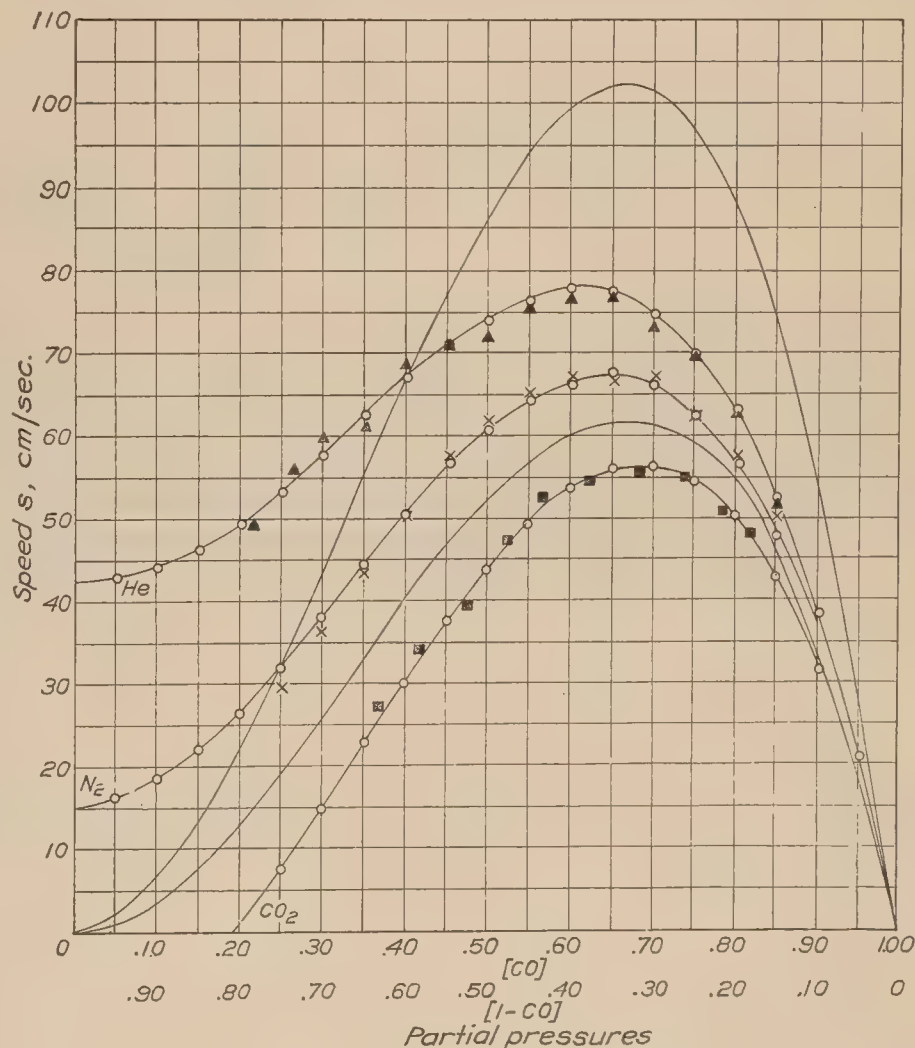


FIG. 6.—The upper curve corresponds to values found when no inert gas was present; the lower heavy continuous curve without other marks corresponds to equation (8) for the case where 40% of the component 1-CO consists of an inert gas: $s = k_1 [\text{CO}]^2 [1 - \text{CO}] .6$. The curves marked He, N_2 and CO_2 represented by the open circles and the solid line correspond to equation (9) when the respective experimental values for β are introduced. The observed values when the inert gas used was N_2 are indicated by the mark X, CO_2 by the mark ■, and He by the mark ▲.

drawn from such a case that the reaction velocity is dependent only on the concentrations of the active components. This conclusion might also seem warranted by the experimental results obtained when the inert gas is present in comparatively small amounts; Figures 4 and 5; and for all of the results where the value of $[\text{CO}]$ is large and the partial pressure of the inert gas small. It was therefore important to make use of inert gases whose thermal characteristics differed widely and to determine in each case the effect of the reaction of the same active components upon the same partial pressure of each of the inert gases and this for the inert gases over the entire range of partial pressure mixtures that would ignite. The complete tabulation of so large a number of observations is perhaps unnecessary to reproduce here. A specimen tabulation for 40 per cent He is given, Table II. The theoretical and observed results obtained for that gas and for CO_2 and N_2 are indicated graphically at Figure 6.

BUREAU OF STANDARDS,
WASHINGTON, D. C., *June 24, 1927.*

REFERENCES

1. Pier: "Zeitschrift Physikalische Chem." 15, 536, (1909).
2. Bjerrum: "Zeitschrift Physikalische Chem." 79, 513, (1912).
3. Siegel: "Zeitschrift Physikalische Chem." 87, 614, (1914).
4. Nernst: "Theoretical Chemistry," 10th Macmillan edition, (1923), p. 783.
5. Stevens, F. W.: A Constant Pressure Bomb. N. A. C. A. Technical Report No. 176 (1923).
6. Jouguet: Velocity of Reaction and Thermodynamics. "Ann. de Phys." V, 5-73 (1926).

REPORT No. 281

**THE EFFECTS OF
FUEL AND CYLINDER GAS DENSITIES
ON THE CHARACTERISTICS OF FUEL SPRAYS
FOR OIL ENGINES**

**By W. F. JOACHIM and EDWARD G. BEARDSLEY
Langley Memorial Aeronautical Laboratory**

REPORT No. 281

THE EFFECTS OF FUEL AND CYLINDER GAS DENSITIES ON THE CHARACTERISTICS OF FUEL SPRAYS FOR OIL ENGINES

By WM. F. JOACHIM and EDWARD G. BEARDSLEY

SUMMARY

This investigation was conducted at the Langley Memorial Aeronautical Laboratory as a part of a general research on fuel-injection engines for aircraft. The purpose of the investigation was to determine the effects of fuel and cylinder gas densities upon several characteristics of fuel sprays for oil engines.

The start, growth, and cut-off of single fuel sprays produced by automatic injection valves were recorded on photographic film by means of special high-speed motion-picture apparatus. This equipment, which has been described in previous reports, is capable of taking twenty-five consecutive pictures of the moving spray at the rate of 4,000 per second.

The penetrations of the fuel sprays increased and the cone angles and relative distributions decreased with increase in the specific gravity of the fuel. The density of the gas into which the fuel sprays were injected controlled their penetration. This was the only characteristic of the chamber gas that had a measurable effect upon the fuel sprays. Application of fuel-spray penetration data to the case of an engine, in which the pressure is rising during injection, indicated that fuel sprays may penetrate considerably farther than when injected into a gas at a density equal to that of the gas in an engine cylinder at top center.

INTRODUCTION

The fuels used by internal-combustion engines operating on the Otto cycle are practically limited thus far to the lighter and more volatile liquid hydrocarbons such as gasoline and kerosene. An outstanding advantage inherent in Diesel engines is that they may be operated on a wide variety of fuel oils. These oils range from those as light as kerosene to some so heavy that they are usually heated for delivery to the engine. In general the light distillates give somewhat better engine performance, but these fuels are more expensive.

The facility with which fuel oils may be atomized depends upon their physical characteristics, important among which are viscosity and specific gravity. Kuehn (Reference 1) gives information concerning the relative size of oil drops produced with kerosene, specific gravity 0.813, and gas oil, specific gravity 0.852. Somewhat smaller drops were obtained with kerosene, as might be expected. The effects of the physical characteristics of the fuel upon the penetration, general shape, and distribution of fuel sprays injected into the dense gases in an engine are important considerations in the successful operation of the engine. Some knowledge of these physical effects on oil sprays should lead to a more successful use of various grades of fuels in all classes of oil engines.

The question has been raised at various times whether it is the pressure or the density of the gases in the cylinder which controls oil-spray penetration and distribution in an engine. Investigation of these effects is important because injection of the fuel generally starts several degrees before top center, when the pressure in the cylinder is only 200 or 300 pounds per square inch, and usually continues up to and beyond top center, when the pressure due to compression may range from 350 to around 550 pounds per square inch, depending upon the engine design. After combustion starts the pressure may rise considerably higher. (References 2 and 3.) The density of the gases during compression and combustion, however, varies only with the position of the

piston and compression ratio. Thus while the cylinder gas pressures may increase several hundred per cent during injection of the fuel, the gas densities will usually vary less than 100 per cent.

The viscosity of the chamber gas may also affect oil spray characteristics. The viscosities of the gases in an engine cylinder are higher during injection of the fuel because of the high temperatures caused by the compression of gases. According to the kinetic theory of gases the viscosity of a gas increases in proportion to the square root of the absolute temperature. Actually the viscosity of a gas increases somewhat faster than this. (References 4 and 5.) An investigation of the effect of gas density and viscosity on spray characteristics is important, therefore, in order to provide data for the better application to engine conditions of results from researches on fuel sprays injected into gases at room temperature.

The object of this investigation, conducted at the Langley Memorial Aeronautical Laboratory at Langley Field, Va., was to determine the effects of some of the physical characteristics of the fuel, and the density and viscosity of the spray chamber gas, upon the penetration, general shape, and distribution of fuel sprays for various injection conditions.

Two injection valve assemblies were used in each test. One valve produced a noncentrifugal spray and the other a high-centrifugal spray. Tests were made with four different fuels having specific gravities ranging from 0.70 to 0.90. Each fuel was injected at 8,000 pounds per square inch pressure into a spray chamber containing nitrogen gas at atmospheric, 200, 400, or 600 pounds per square inch pressure in the tests on fuel characteristics. Nitrogen, carbon dioxide, helium, or air were used at these pressures in the spray chamber to determine the effects of gas density. Tests were also made with these different gases at pressures calculated to give constant gas densities in the spray chamber to determine the effects of gas viscosity.

METHODS AND APPARATUS

The general method employed to study the effects of fuel characteristics and spray chamber gas density and viscosity on fuel sprays was to record on photographic film the start, development, and cut-off of single sprays from an automatic injection valve. This was accomplished by injecting each of the fuels investigated into a spray chamber containing one of the gases under pressure and taking successive pictures, at high speed, of the moving spray with the N. A. C. A. fuel-spray photography apparatus. This equipment (References 3 and 6) is capable of taking 25 consecutive, well-defined pictures of a fuel spray at a rate of 4,000 per second. By measuring the fuel spray images recorded on photographic film, data were obtained on the penetrations, spray-cone angles, volumes and relative distributions of the sprays produced from the four fuels studied and the effect of injection into the various gases.

A diaphragm type injection valve was used in this investigation. It was fitted with two different stem and nozzle assemblies, one of which had 90-degree or axial fuel grooves and the other 23-degree helical fuel grooves near the end of the valve stem. The former produced a noncentrifugal spray and the latter a high-centrifugal spray. This injection valve has been described in N. A. C. A. Report No. 268 (Reference 7).

RESULTS AND DISCUSSION

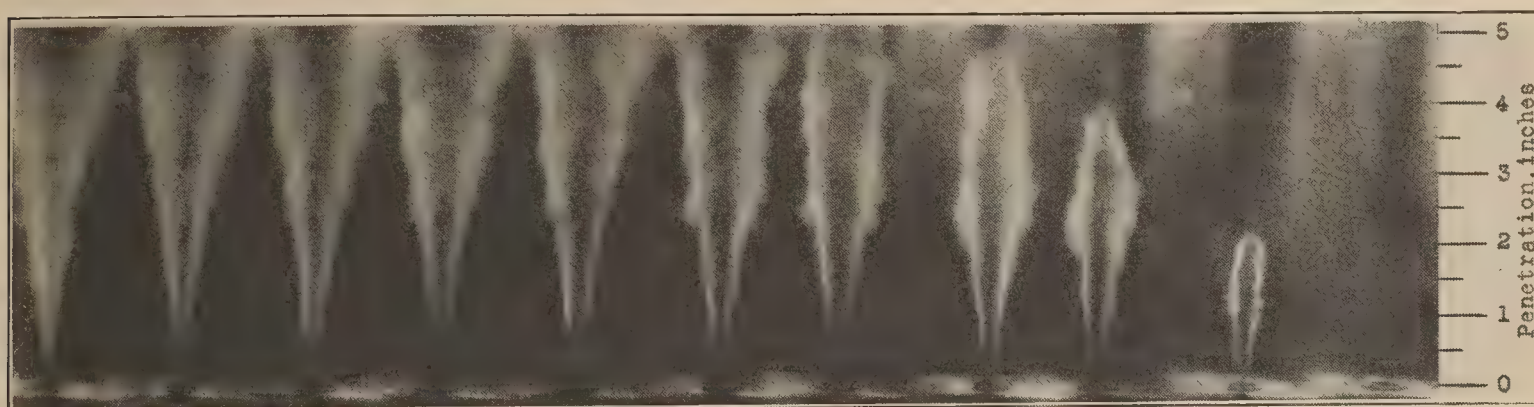
Figure 1 shows two series of pictures, one of a noncentrifugal spray and the other of a high-centrifugal spray. Diesel oil was injected from the automatic injection valve at 8,000 pounds per square inch pressure into the spray chamber containing air at 200 pounds per square inch pressure for these tests. These photographs illustrate the kind of spray records obtained throughout this investigation, similar photographic records being taken for each fuel, and spray chamber pressure and gas studied.

FUEL DENSITY

Fuel spray penetrations for various time intervals during and following injection for both non-centrifugal and high-centrifugal sprays similar to those shown in Figure 1 are presented in Figures 2 and 3. Diesel oil having a specific gravity of 0.85 at 80° F. was injected at 8,000 pounds per square inch into the spray chamber containing air at atmospheric, 200, 400 or 600 pounds per

square inch pressure. These penetration-time curves are representative of the results obtained with the various fuels investigated. These and similar curves for the other fuels form the basis from which crossplotted data on the effects of specific gravity were derived.

Figure 4 shows the results obtained when the penetrations, spray-cone angles, and distributions of both noncentrifugal and high-centrifugal sprays are plotted against the specific gravity of the fuels studied. The data is for injection at 8,000 pounds per square inch, a spray chamber pressure of 200 pounds per square inch using nitrogen, and a time interval after the beginning of injection of 0.003 second. It may be noted that the penetration increased and the spray-cone angle decreased with increase in the specific gravity of the fuel injected. With the high-centrifugal injection valve, having 23° helical fuel grooves, the spray-cone angle was decreased 20 per cent and the penetration was increased 16 per cent for an increase in the specific gravity of the fuel from 0.80 to 0.90. These data indicate that the heavy fuel is more difficult to atomize, and that the greater inertia of the large spray particles of the heavy fuel results in greater penetration.



Injection pressure, 8,000 pounds per square inch. Noncentrifugal spray Chamber pressure, 200 pounds per square inch. Diesel oil injected into air



Injection pressure, 8,000 pounds per square inch. High-centrifugal spray Chamber pressure, 200 pounds per square inch. Diesel oil injected into air

FIG. 1.—Effect of centrifugal force on fuel sprays

The curves in this figure emphasize the large differences in penetration and spray-cone angle that may be obtained under the same injection conditions with non-centrifugal and high-centrifugal injection valves.

The increase in volume which a drop of fuel undergoes when it is discharged from an injection valve in the form of a spray is a measure of both the ability of the injection valve to distribute and atomize the fuel and the fuel's adaptability for spray formation. The distribution value of a fuel spray produced by any injection valve or injection condition is obtained by calculating the ratio of the spray volume to the volume of the fuel in the spray. The spray volume is approximately determined by summation of the volumes of a number of disks into which the photographic spray images may be divided for volume calculations. The volume of the oil in the spray is calculated from weight determinations of many sprays injected under the same test conditions and caught in a special container.

Figure 4 also shows the spray distribution values of the four fuels investigated for both the noncentrifugal and the high-centrifugal injection valve. The decrease in distribution and

probably also in atomization with increase in specific gravity of the fuel for both types of injection valves are noteworthy, the heavy fuels being more difficult to distribute and atomize. The distribution values for the noncentrifugal injection valve range from 580 for gasoline to 460 for heavy fuel oil, a decrease in distribution of about 21 per cent. The distribution values for the high-centrifugal injection valve range from 1,080 for gasoline to 980 for heavy fuel oil, a decrease of only about 9 per cent. These data indicate the value of using centrifugal force to distribute and atomize heavy fuels.

GAS DENSITY AND VISCOSITY

The effect of injecting similar oil sprays into gases of different densities in the spray chamber is shown in Figure 5. Diesel oil was injected at 8,000 pounds per square inch pressure into helium, nitrogen, and carbon dioxide, each at a pressure of 200 pounds per square inch. All injection conditions were maintained constant. The difference in penetration obtained with these three gases at the same pressure definitely shows that the physical characteristics of the gases affect spray penetration.

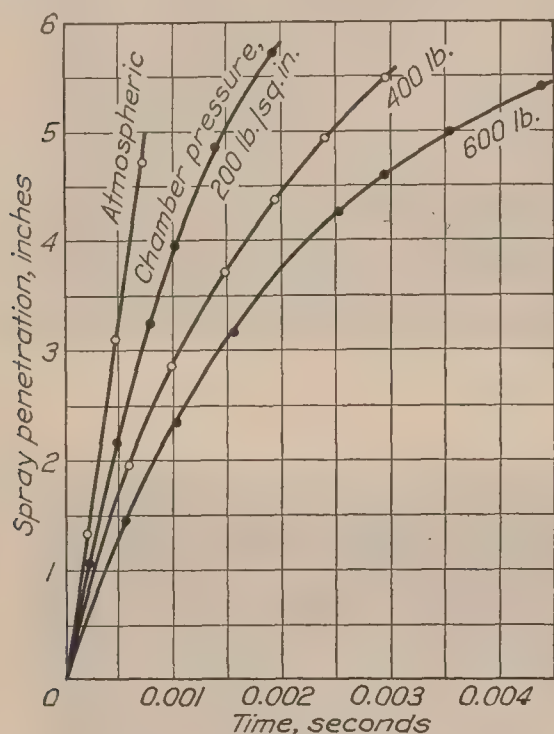


FIG. 2.—Effect of chamber pressure on spray penetration. Injection pressure, 8,000 pounds per square inch. Orifice diameter, 0.022 inch. Groove helix angle, 90°. Ratio of orifice length to orifice diameter, 2. Ratio of orifice area to groove area, 0.63

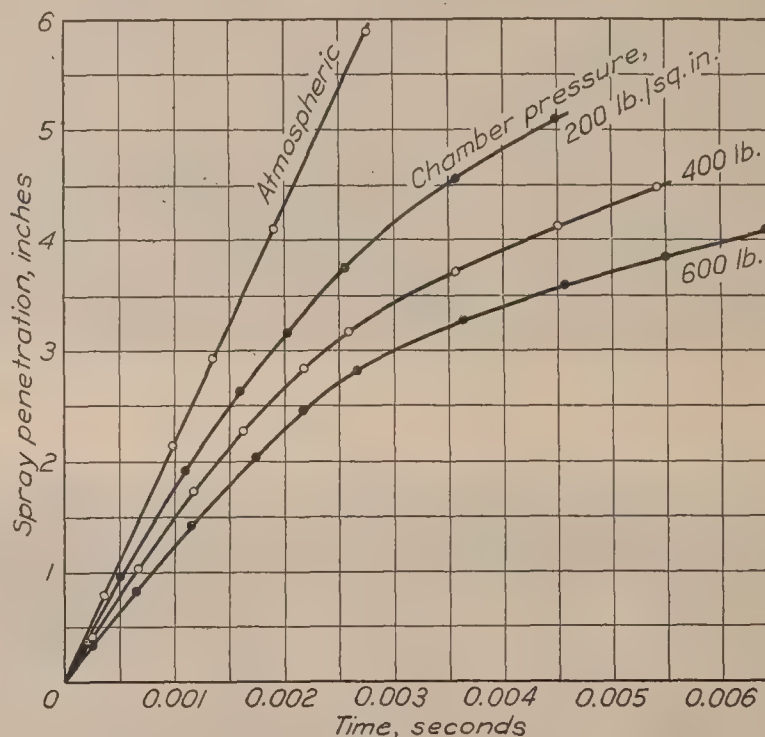


FIG. 3.—Effect of chamber pressure on spray penetration. Injection pressure, 8,000 pounds per square inch. Orifice diameter, 0.022 inch. Groove helix angle, 23°. Ratio of orifice area to groove area, 0.63. Ratio of orifice length to diameter, 2

Further tests were made using gas pressures in the spray chamber that were calculated to give the same density for each gas. The spray penetration was found to be the same for all gases under these conditions, thus showing that gas density rather than gas pressure controls spray penetration. The viscosities of the gases investigated vary from 148 to 202 (Reference 8), but this property of the gases produced no measurable effect upon either the appearance of these sprays or upon their penetration.

The effect of gas densities from 0.08 to 4.80 pounds per cubic foot upon spray penetration after 0.001, 0.002, and 0.003 second is shown in Figure 6. These curves were cross-plotted from results obtained by injecting similar Diesel oil sprays into the three different gases investigated at several different pressures. The abscissas give the gas density and the equivalent air pressure. Each point is labeled to show the gas used at that density. Since all the points lie on smooth curves, it may be again noted that the density and not the pressure or viscosity of the gas in the spray chamber controls spray penetration.

The effect of gas density on the spray tip velocity is shown in Figure 7. The rapid decrease in spray tip velocity with increase in gas densities up to about 1 pound per cubic foot is worthy of note, as this range covers the densities usually occurring in engine cylinders. The curves converge at zero density because the spray velocity will not diminish with time for injection into a vacuum except for the effects of vaporization.

The effect of spray chamber gas density upon the volume growth of centrifugal sprays, with time, is shown in Figure 8. The volume growth of these sprays is practically negligible for about 0.0005 second following the beginning of injection, after which it increases first at an accelerating rate and then, after about 0.0015 second, at practically a constant rate. These curves indicate that the spray is poorly distributed and probably little atomized during about the first 0.001 second. Under these conditions ignition of the fuel in an engine cylinder would probably be impossible in a time interval less than about 0.001 second after the beginning of injection because of the practically complete lack of atomization and, therefore, the prevention of vaporization by the highly heated cylinder air.

The data in Figure 8 show that large decreases in the volumes of similar sprays occur with increased gas densities. Since the density of the gas in an engine cylinder is proportional to the compression ratio, the volume growth of a fuel spray in an engine cylinder will depend upon the compression ratio. For the data given in Figure 8, the volume of these fuel sprays at various time intervals after the beginning of injection was found to vary as given in equations 1, 2, and 3.

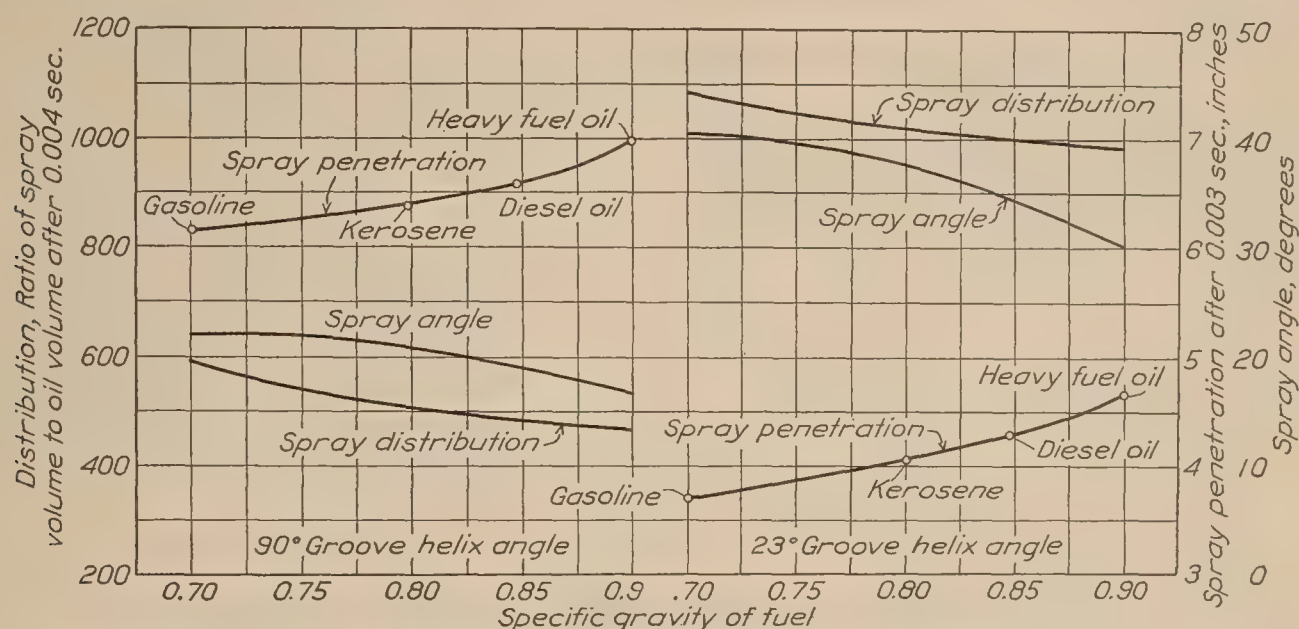


FIG. 4.—Effect of fuel on spray characteristics. Injection pressure, 8,000 pounds per square inch. Chamber pressure, 200 pounds per square inch. Orifice diameter, 0.022 inch. Ratio of orifice length to orifice diameter, 2. Ratio of orifice area to groove area, 0.63

- (1) $V = 1.85 - 2.0 \log_{10} D$. (Injection for 0.002 sec.)
 - (2) $V = 3.75 - 4.2 \log_{10} D$. (Injection for 0.003 sec.)
 - (3) $V = 5.90 - 6.4 \log_{10} D$. (Injection for 0.004 sec.)
- V = Spray volume in cubic inches.
 D = Density of spray chamber gas in pounds per cubic foot.

APPROXIMATE APPLICATION OF PENETRATION DATA TO ENGINE CONDITIONS

In the fuel spray investigations described thus far, the fuel sprays have been injected into a chamber containing gas at constant pressure. In actual engine operation, injection usually starts a short time before top center and therefore before maximum compression pressure has been reached, and continues while the compression pressure is rapidly increasing. In order to obtain approximately true spray penetration-time data, a composite curve has been drawn by cross-plotting from data obtained by injection into gases at various densities covering the range of cylinder gas densities occurring in an engine. Spray chamber gas pressures were used that were calculated to produce gas densities equal to those in an engine with a compression ratio of 10.3 for every 5° of crank travel after the start of injection. Injection of the fuel was assumed to start 30° before top center. Photographic records were taken of similar fuel sprays injected under each condition. The composite spray penetration curve, Curve I, in Figure 9, was obtained from these records. The second curve was obtained for a spray chamber gas density equal to that at engine top center. About 17 per cent greater spray penetration, after injection for 0.003 second, was obtained for injection into gases at densities varying as in an engine.

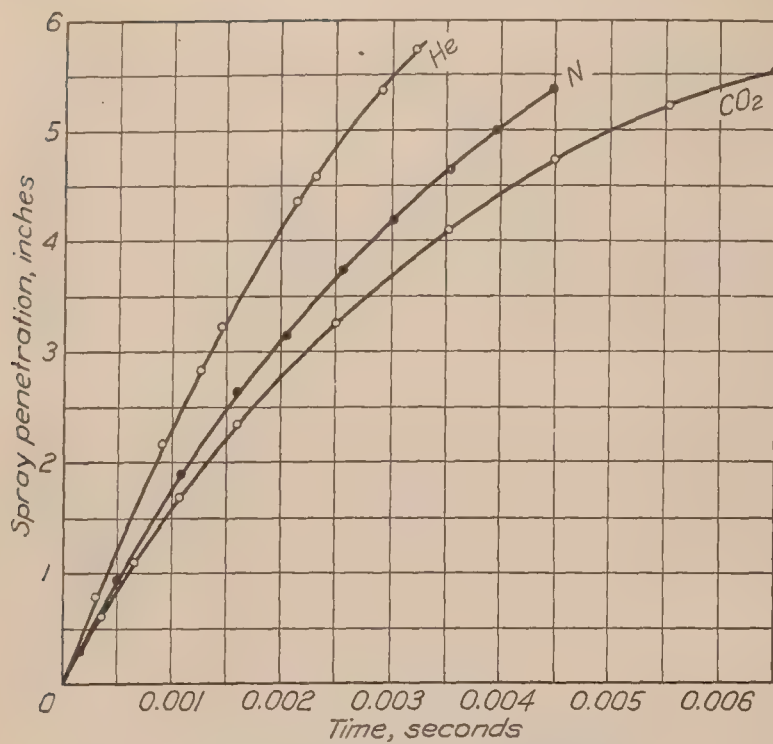


FIG. 5.—Effect of gas density on spray penetration. Injection pressure, 8,000 pounds per square inch. Chamber pressure, 200 pounds per square inch. Orifice diameter, 0.022 inch. Groove helix angle, 23°. Ratio of orifice length to orifice diameter, 2. Ratio of orifice area to groove area, 0.63.

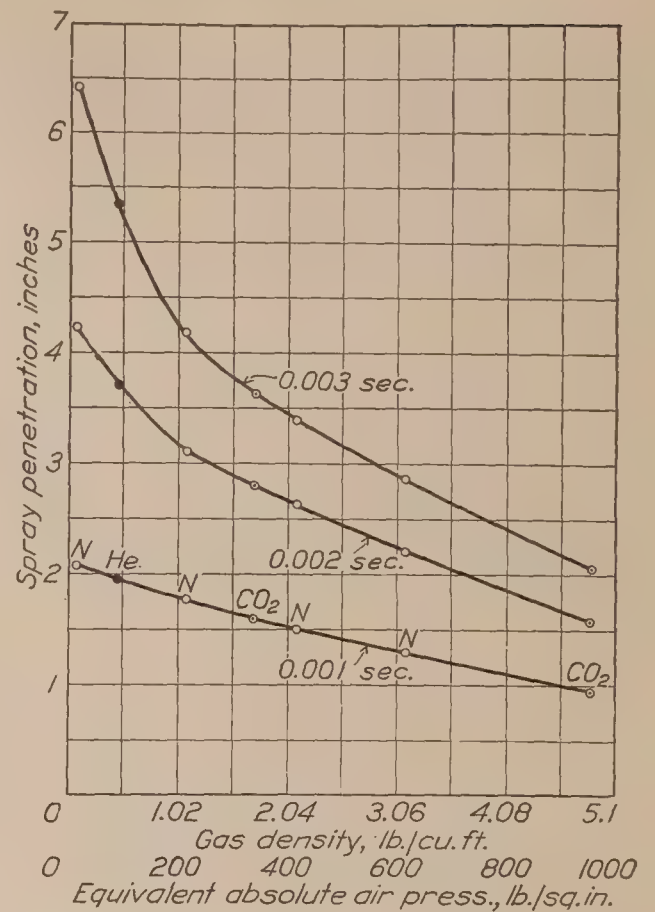


FIG. 6.—Effect of gas density on spray penetration. Injection pressure, 8,000 pounds per square inch. Orifice diameter, 0.022 inch. Groove helix angle, 23°. Ratio of orifice length to orifice diameter, 2. Ratio of orifice area to groove area, 0.63. Gas in spray chamber, nitrogen, carbon dioxide, or helium.

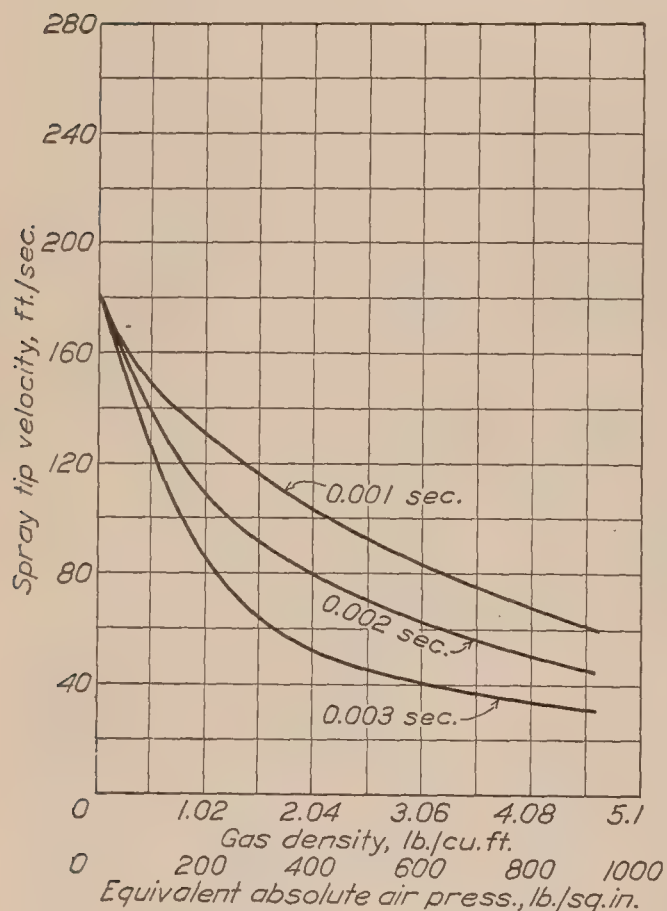


FIG. 7.—Effect of gas density on velocity of spray. Injection pressure, 8,000 pounds per square inch. Orifice diameter, 0.022 inch. Groove helix angle, 23°. Ratio of orifice length to orifice diameter, 2. Ratio of orifice area to groove area, 0.63.

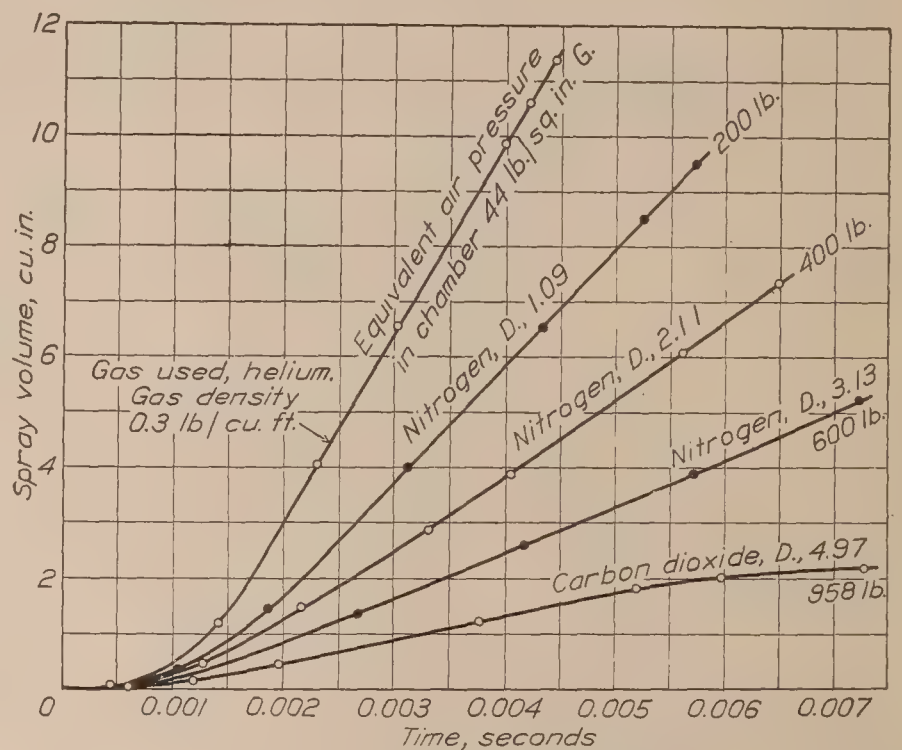


FIG. 8.—Effect of chamber pressure on the volumetric growth of centrifugal sprays. Injection pressure, 8,000 pounds per square inch. Orifice diameter, 0.022 inch. Groove helix angle, 23°.

In the case of a fuel spray injected into an engine cylinder, gas temperature and turbulence would have appreciable effects on all spray characteristics. These effects remain to be determined.

CONCLUSIONS

The results of this investigation show that the spray penetration increases and the spray distribution, cone angle, and atomization decrease with increase in the specific gravity of the fuel oil. The effects of applying centrifugal force to fuel sprays is pronounced. The use of centrifugal force to atomize and distribute a fuel is more important for heavy fuels than for light fuels.

The density of the chamber gas was found to control spray penetration rather than the gas pressure. The kind of gas used in the spray chamber for conditions of constant density had no measureable effect on the fuel sprays. The effect of gas viscosity was, therefore, negligible.

A composite curve for spray penetration for injection into gases varying in density as in an engine, showed about 17 per cent greater penetration after 0.003 second than did the curve for a constant gas density equal to that at maximum compression.

LANGLEY MEMORIAL AERONAUTICAL LABORATORY,
NATIONAL ADVISORY COMMITTEE FOR AERONAUTICS,
LANGLEY FIELD, VA., June 14, 1927.

REFERENCES

1. KUEHN, R.: Atomization of liquid fuels. N. A. C. A. Technical Memorandum No. 330, 1925. Figures 13 and 14.
2. JOACHIM, W. F.: Research on oil injection engines for aircraft. Mechanical Engineering, 1926. Vol. 48, pp. 1123-1128.
3. JOACHIM, W. F.: Oil spray investigation of the National Advisory Committee for Aeronautics. Paper presented April 24, 1927, before the Oil Power Conference at the Pennsylvania State College, State College, Pa.
4. PRESTON, THOMAS: Theory of heat. Third edition, 1919. xix + 840 pp. London. Macmillan & Co., Ltd.
5. GLAZEBROOK, SIR RICHARD: A dictionary of applied physics. Vol. I, 1922. ix + 1067 pp. London. Macmillan & Co., Ltd.
6. BEARDSLEY, E. G.: The N. A. C. A. fuel spray photography apparatus and test results from several researches. N. A. C. A. Technical Report No. 274, 1927.
7. JOACHIM, W. F., AND BEARDSLEY, E. G.: Factors in the design of centrifugal type injection valves for oil engines. N. A. C. A. Technical Report No. 268, 1927.
8. FOWLE, FREDERICK E.: Smithsonian physical tables. Reprint of seventh revised edition. 1921. xlv + 452 pp. Washington. Smithsonian Institution.

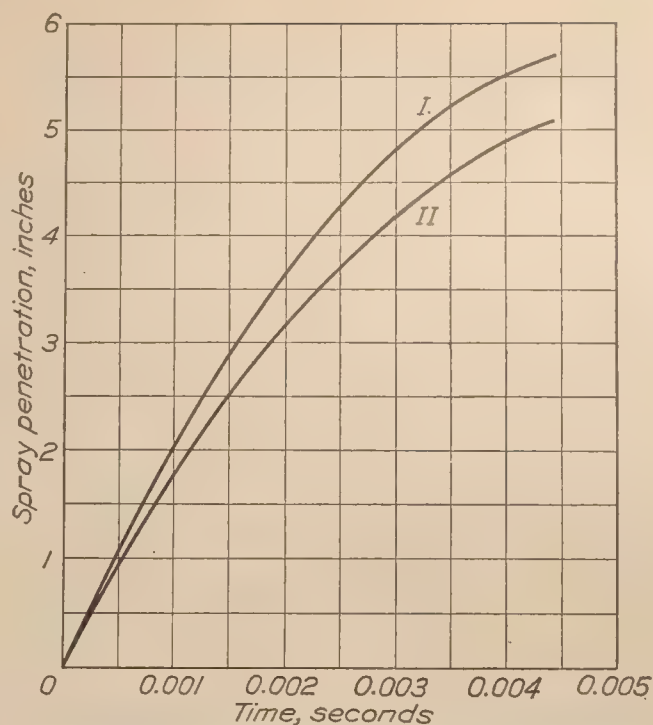


FIG. 9.—Approximate spray penetration in an engine cylinder
I. Approximate spray penetration in an engine cylinder: Compression ratio 10:3. Start of injection, 30° before top center.

II. Spray penetration in a gas at a density equal to that in an engine cylinder at top center. Injection pressure, 8,000 pounds per square inch. Orifice diameter, 0.022 inch. Groove helix angle, 23°

REPORT No. 282

**THE
PERFORMANCE OF SEVERAL COMBUSTION CHAMBERS
DESIGNED FOR AIRCRAFT OIL ENGINES**

**By WILLIAM F. JOACHIM and CARLTON KEMPER
Langley Memorial Aeronautical Laboratory**

REPORT No. 282

THE PERFORMANCE OF SEVERAL COMBUSTION CHAMBERS DESIGNED FOR AIRCRAFT OIL ENGINES

By WILLIAM F. JOACHIM and CARLTON KEMPER

SUMMARY

Several investigations have been made on single-cylinder test engines at the Langley Memorial Aeronautical Laboratory of the National Advisory Committee for Aeronautics to determine the performance characteristics of four types of combustion chambers designed for aircraft oil engines. Two of the combustion chambers studied were bulb-type precombustion chambers, the connecting orifice of one having been designed to produce high turbulence by tangential air flow in both the precombustion chamber and the cylinder. The other two were integral combustion chambers, one being dome-shaped and the other pent-roof shaped. The injection systems used included cam and eccentric driven fuel pumps, and diaphragm and spring-loaded fuel-injection valves. A diaphragm-type maximum cylinder pressure indicator was used in part of these investigations with which the cylinder pressures were controlled to definite values. The performance of the engines when equipped with each of the combustion chambers is discussed. The data presented show the performance for speeds from 600 to 1,800 R. P. M.

The results obtained indicate that aircraft-type oil engines with suitably designed combustion chambers and fuel-injection systems may be operated at speeds around 1,800 R. P. M. without encountering excessive explosion pressures. At a speed of 1,600 R. P. M. and with a fuel quantity giving 15 per cent excess air in the cylinder, a maximum I. M. E. P. of 119 pounds per square inch was obtained with a fuel consumption of 0.43 pound per I. HP. per hour. The maximum cylinder pressure was 740 pounds per square inch. A minimum fuel consumption of 0.26 pound per I. HP. per hour at an I. M. E. P. of 52 pounds per square inch and 1,600 R. P. M. was obtained with a cylinder head having a bulb-type precombustion chamber. The maximum cylinder pressure was 560 pounds per square inch.

It is concluded that an increase in the specific power output of the high-speed aircraft oil engine depends upon the ability to obtain higher mean effective pressures and an improvement in the mechanical efficiency of the engine. The best performance for the tests reported was obtained with a bulb-type combustion chamber designed to give a high degree of turbulence within the bulb and cylinder.

INTRODUCTION

The design of combustion chambers to meet the fundamental requirements of high-speed, fuel-injection engines is a part of the National Advisory Committee for Aeronautics research program for the development of the aircraft oil engine.

The essential requirements to be met in the design of combustion chambers for high-speed oil engines are, first, the fuel spray must be completely distributed throughout the combustion chamber; second, the degree of cylinder air turbulence must be sufficient to produce complete burning of the fuel in the short time available; and, third, the ignition and combustion of the fuel must take place early enough in the power stroke to give high mean effective pressures without excessive explosion pressures. (References 1 and 2.) Since November, 1924, reliable data have been obtained as to the behavior of fuel sprays when injected into gases under pressure.

The National Advisory Committee for Aeronautics, in its investigation of oil sprays for fuel-injection engines, has recorded the start, development, and cut-off of sprays by means of high-speed moving pictures. (References 2, 3, and 4.) The data obtained from the several researches conducted thus far enable the combustion chamber to be more efficiently designed to fit the fuel spray selected.

Other requirements for fuel-injection engine combustion chambers are the same as those for any type of engine. Thus, the combustion chamber must be strong enough to withstand the explosion pressures. It should also give a uniform dissipation of heat and prevent large temperature differences which may lead to cracking of the cylinder head. Particular attention should be given to the location of the inlet valve to provide an unobstructed flow of air into the engine cylinder.

If the oil-injection engine is to compete with present-day carburetor engines for aircraft, it is necessary that the weight per brake horsepower be reduced to approximately 3 pounds. This reduction in weight may be brought about by increasing the speed of the oil engine from the relatively slow speeds of around 300 R. P. M. to a speed of 1,800 R. P. M. The attainment of this engine speed, if good combustion and fuel economy with low maximum cylinder pressures are to be maintained, is complicated, however, by the problems of fuel injection, the degree of atomization, spray velocity, turbulence, and the short time available for vaporization and ignition of the fuel. For a four-stroke cycle engine running at 1,800 R. P. M. and having an injection interval of 30° , the corresponding injection time is approximately 0.003 second. The lag of autoignition, as determined for slow and medium speed engines, depends upon the compression ratio, the combustion chamber, and the fuel-injection system. An average value may be taken as approximately 0.020 second. If the performance of the fuel-injection engine is to be increased at high engine speeds without excessive cylinder pressures, it is necessary that the time lag of autoignition of the fuel be decreased or the entire fuel charge may be injected into the cylinder before ignition occurs. Under these conditions combustion will take place at practically constant volume, with resulting explosion pressures which may exceed 1,600 pounds per square inch.

In order to avoid these excessive explosion pressures, many engine designers use a pre-combustion chamber in which the small volume of air permits only partial combustion of the fuel charge, further combustion of the fuel taking place in the cylinder proper. The connecting orifice between the two chambers is usually designed to meter the products of the partial combustion in the precombustion chamber to obtain practically constant pressure combustion in the cylinder.

The use of the connecting orifice between the bulb and the cylinder results, at higher engine speeds, in the following losses: First, a friction or pumping loss due to forcing the gases through the orifice at high velocity; second, a loss in pressure on the piston caused by the lag of the gas pressure; and third, an increase in the heat loss to the jacket water due to the scrubbing action of the gases. These losses may be more than compensated for by the increase in combustion efficiency obtained by the higher degree of turbulence produced by the orifice.

DESCRIPTION OF APPARATUS

TEST ENGINES

The performance of a given design of combustion chamber is determined at the Langley Memorial Aeronautical Laboratory by tests made with single-cylinder test engines having a 5-inch bore and a 7-inch stroke. (References 5 and 6.) The engines are coupled to 50–75 horsepower electric cradle-type dynamometers. The cylinder heads are bolted to special steel cylinders which are bolted to the engine crankcase. Standard aircraft engine valves, pistons, and connecting rods are used. Arrangements are provided to maintain fuel, oil, and water temperatures at constant values. For the tests reported the water-outlet temperature and oil temperature were maintained, respectively, at 140° and 120° F. A general view of the single-cylinder Liberty test engine is shown in Figure 1.

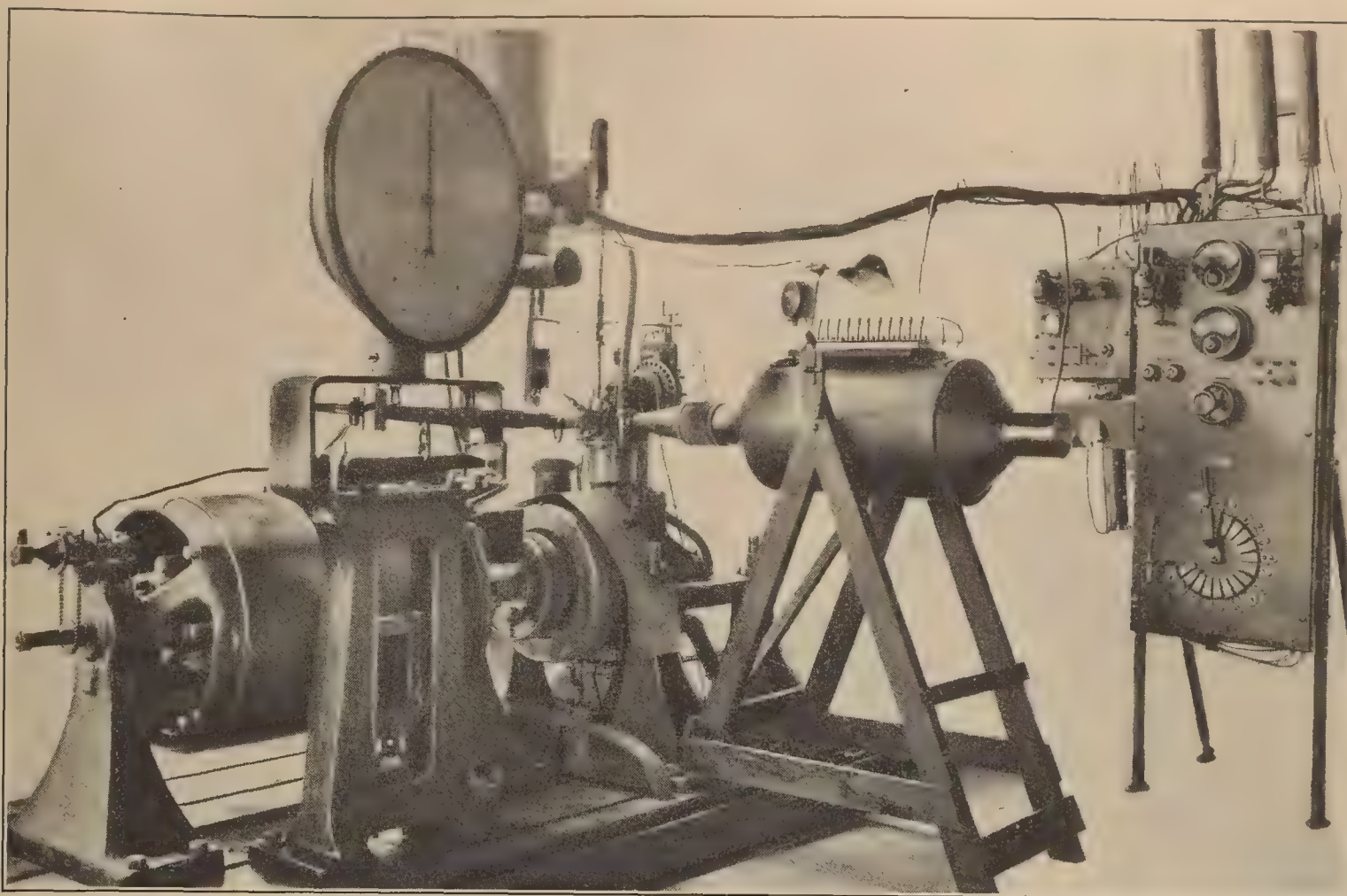


FIG. 1.—Arrangement of Liberty type test engine and apparatus

INJECTION SYSTEM

The fuel-injection systems for the tests reported on cylinder heads designated as Nos. 1 and 3 comprised a primary gear pump supplying oil at 90 pounds per square inch pressure to a cam-actuated impact-type injection pump, and an automatic fuel-injection valve. (Reference 6.) The opening pressure and design of the fuel-injection valve control the pressure at which the fuel is delivered by the injection pump. The type of injection valve determines the necessary opening pressure for maximum efficiency. For the investigation of cylinder head No. 3 a spring-loaded injection valve was used having a static opening pressure of 6,000 pounds per square inch. The design of this injection valve limits the maximum injection pressure to approximately 6,000 pounds per square inch.

CYLINDER HEAD NO. 1

The first combustion chamber designed for fuel-injection work is shown in Figure 2. The design was recommended for test because of its simple construction and uniform shape. Due to the Liberty type of valve mechanism used with this cylinder head it was impossible to locate a fuel valve centrally in the combustion chamber. The fuel-injection valve used with this combustion chamber was spring-loaded and fitted with an impact surface for producing a flat, fan-shaped spray. The fuel was injected from a point near the periphery of the combustion chamber. This cylinder head was tested with a standard Navy type Liberty piston and a compression ratio of 12.7.

CYLINDER HEAD NO. 2

Figure 4 shows the outline of the first type of combustion chamber used having a bulb-type precombustion chamber. The connecting orifice between the bulb and cylinder was 1 inch in diameter. This cylinder head was fitted with a standard Army type Liberty piston arranged to give a compression ratio of 9.9. The fuel system comprised an automatic diaphragm-type fuel-injection valve and an eccentric-driven fuel injection pump.

FIG. 3.—Fuel-injection performance, Liberty test engine. Combustion chamber No. 1, having directed flow of inlet air. Maximum explosion pressure 800 pounds gauge, 1,500 R. P. M.

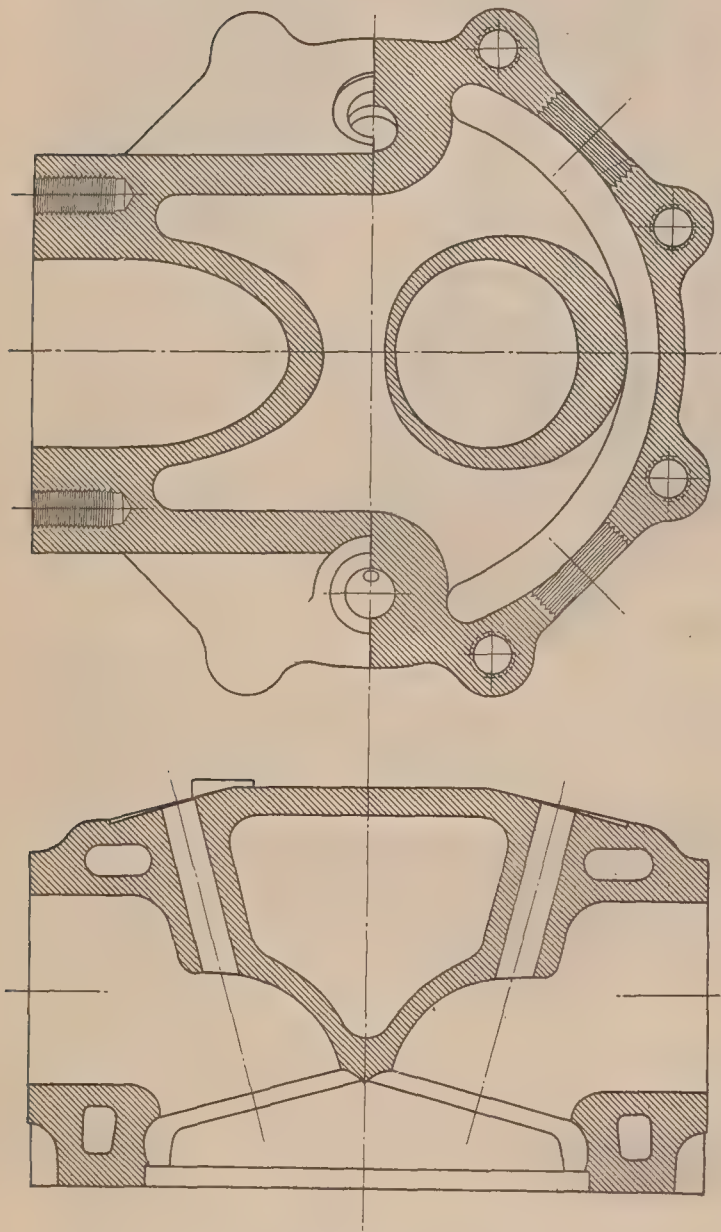
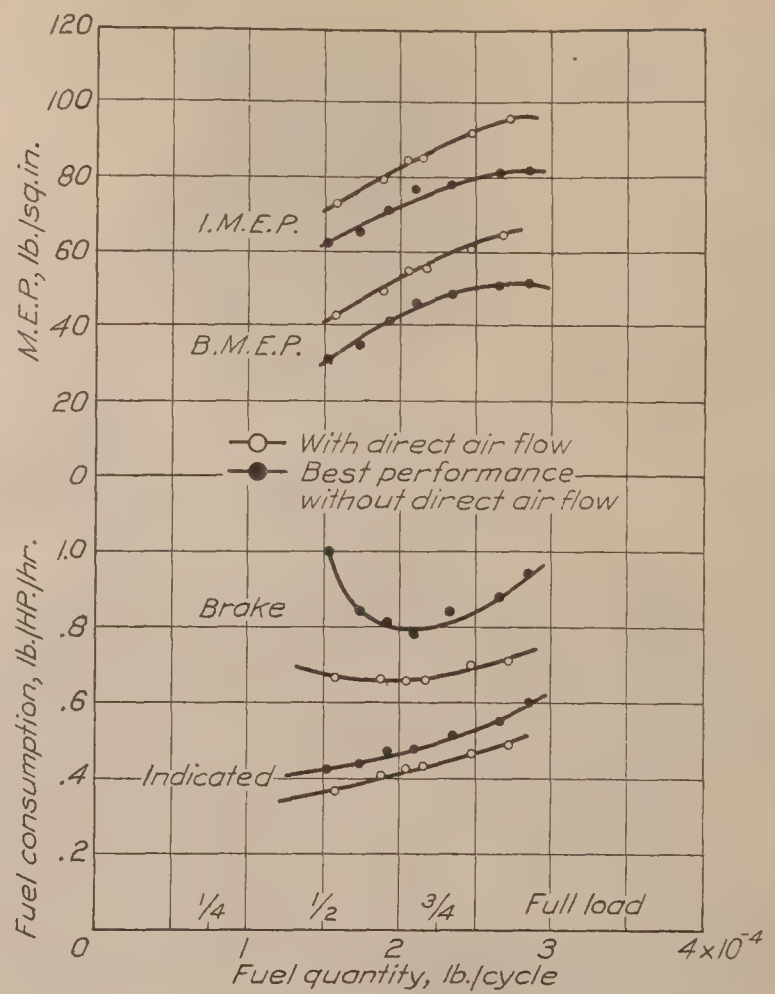


FIG. 2.—Combustion chamber design No. 1

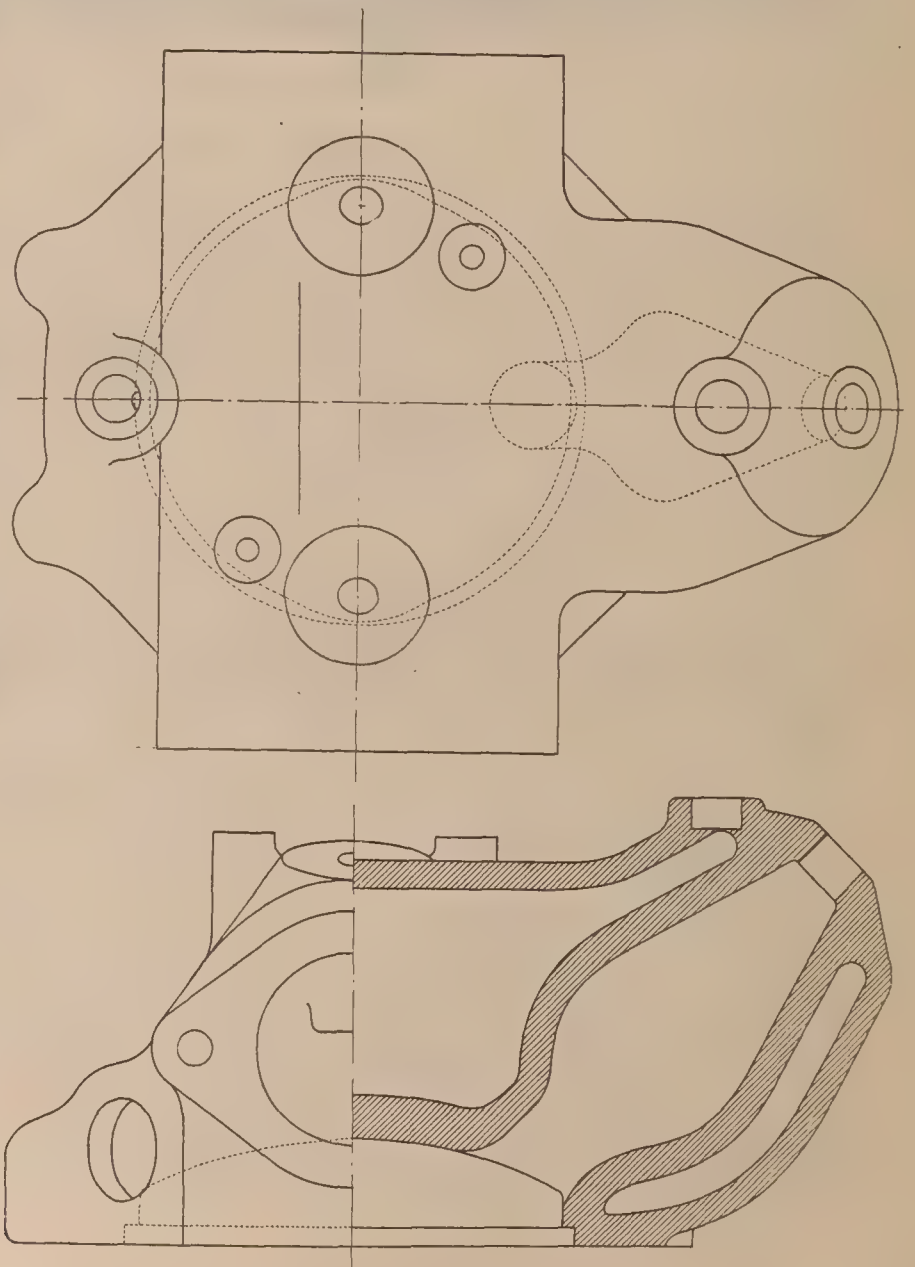


FIG. 4.—Combustion chamber design No. 2

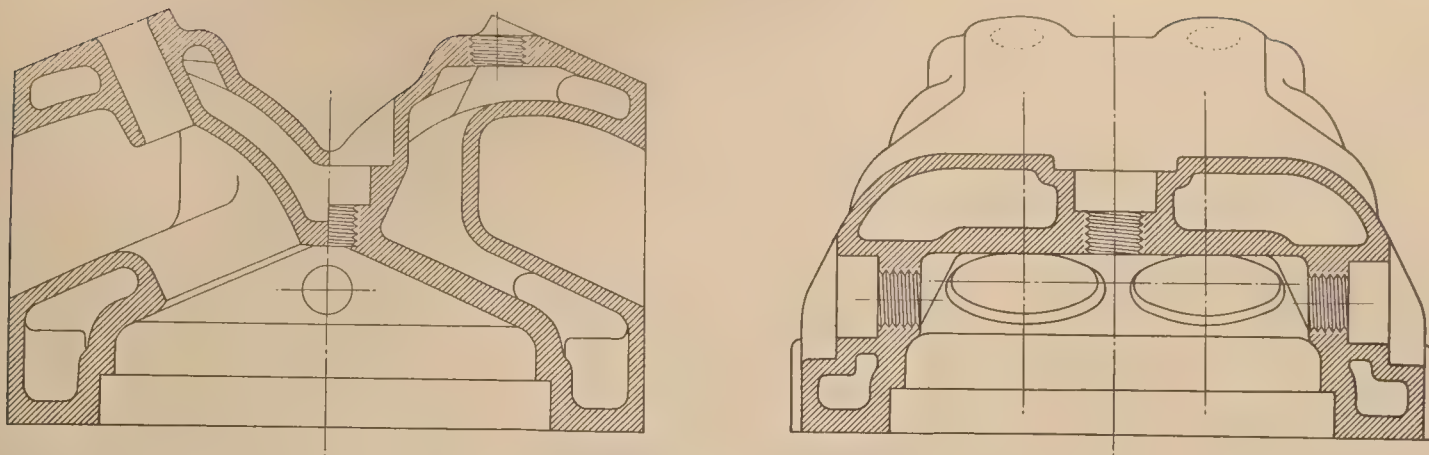


FIG. 6.—Combustion chamber of Universal test engine

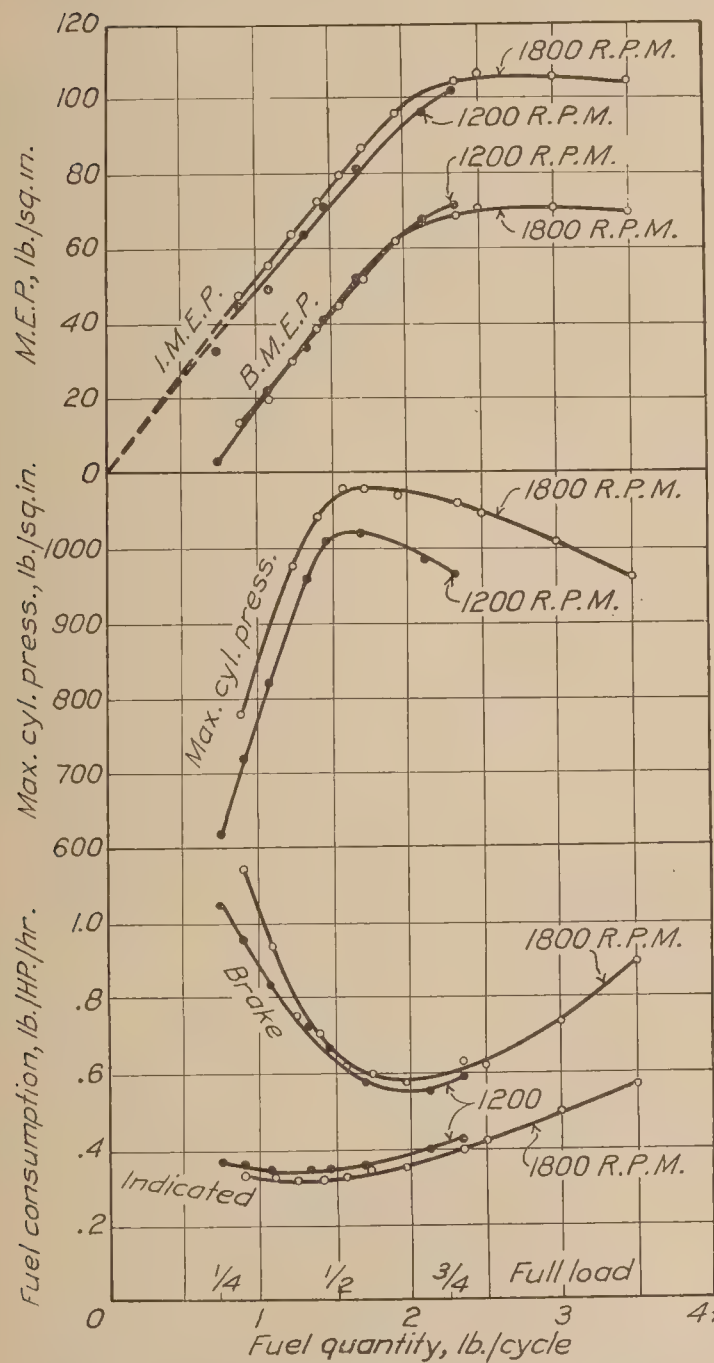


FIG. 5.—Effect of load on engine performance. Fuel-injection performance, cylinder head No. 2. Orifice, 1 inch; engine, S. C.-L. T. E.; compression ratio, 9.9; operating temperature, standard

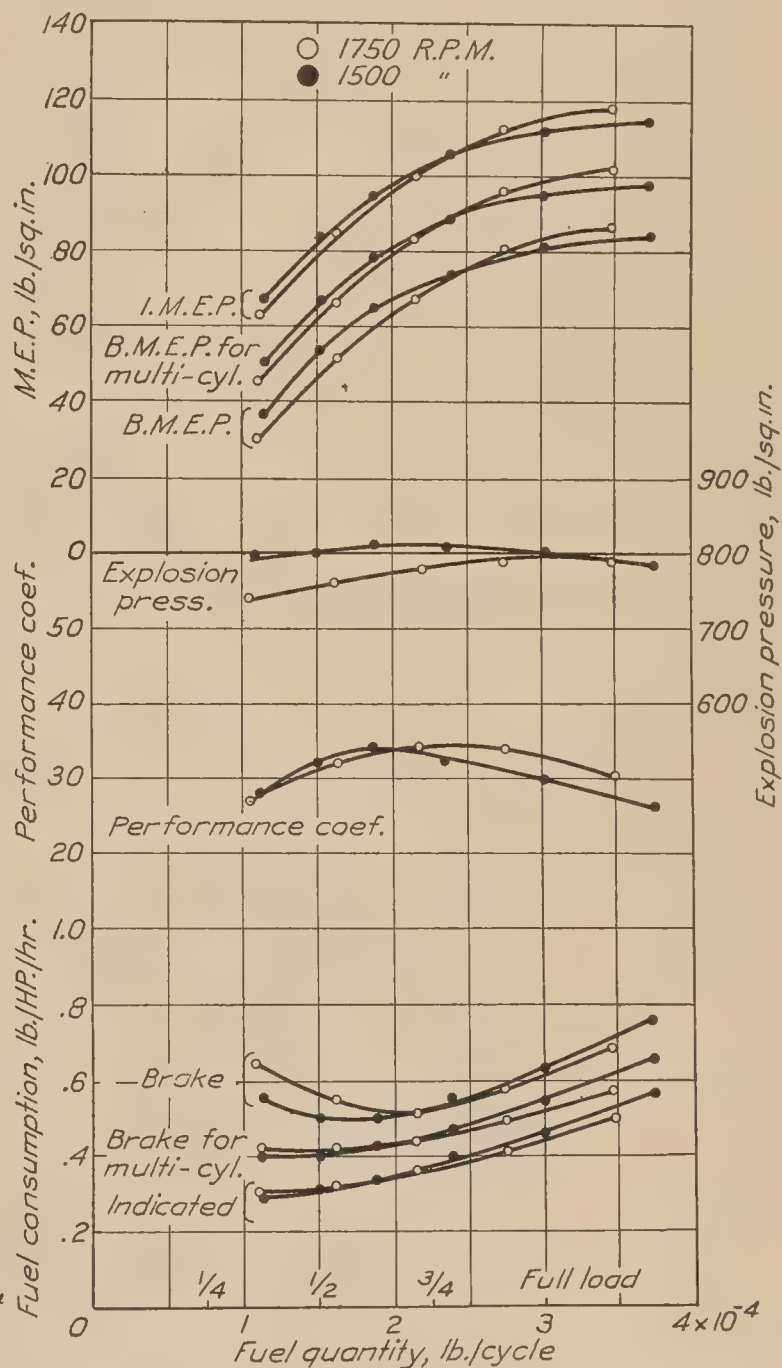


FIG. 7.—Fuel-injection performance, Universal test engine

CYLINDER HEAD OF UNIVERSAL TEST ENGINE

The type of combustion chamber shown in Figure 6 was designed for carburetor work on the N. A. C. A. Universal test engine. (Reference 5.) The cylinder head was tested using a diaphragm-type fuel-injection valve and an eccentric-driven fuel injection pump. The piston used was an Army type Liberty piston. The compression ratio of this engine was adjusted for the tests reported at 10.2.

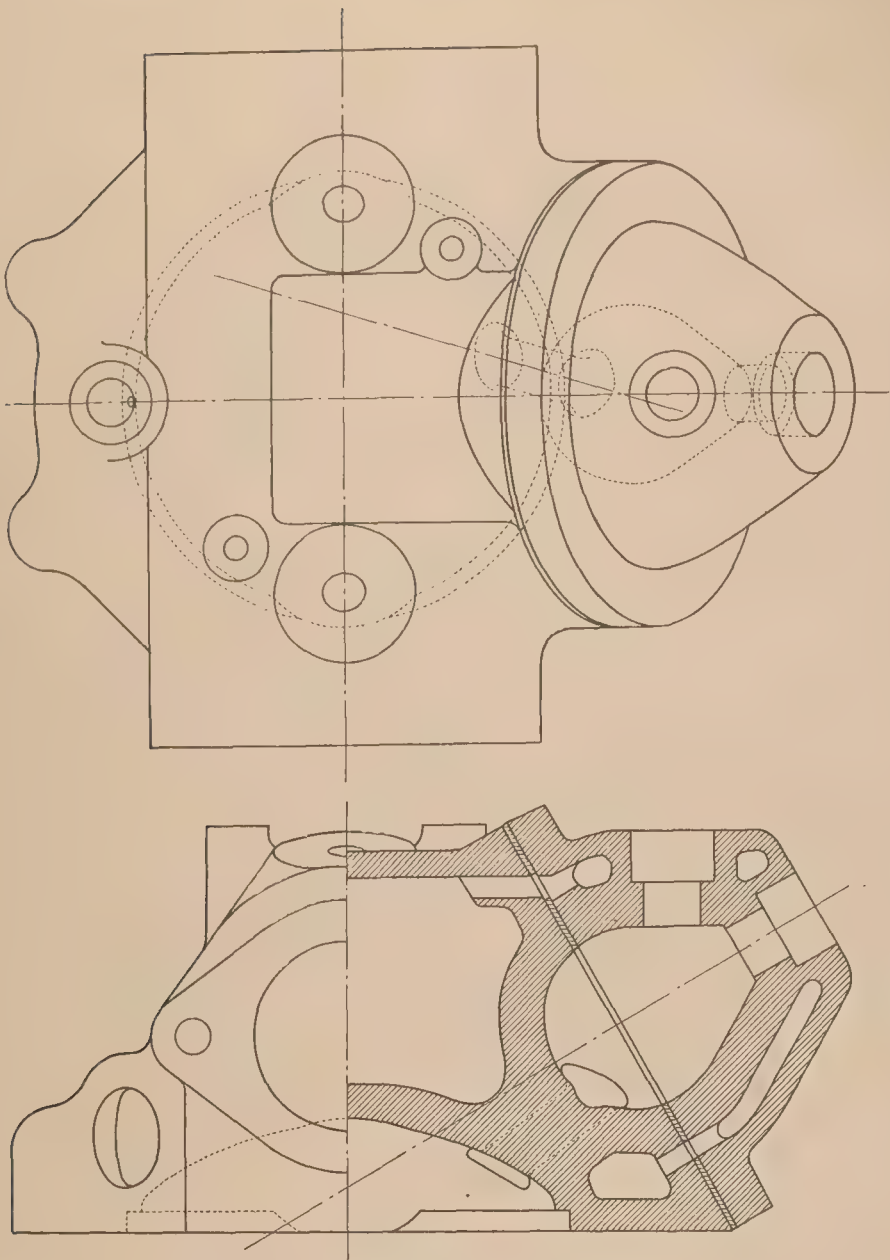


FIG. 8.—Combustion chamber design No. 3

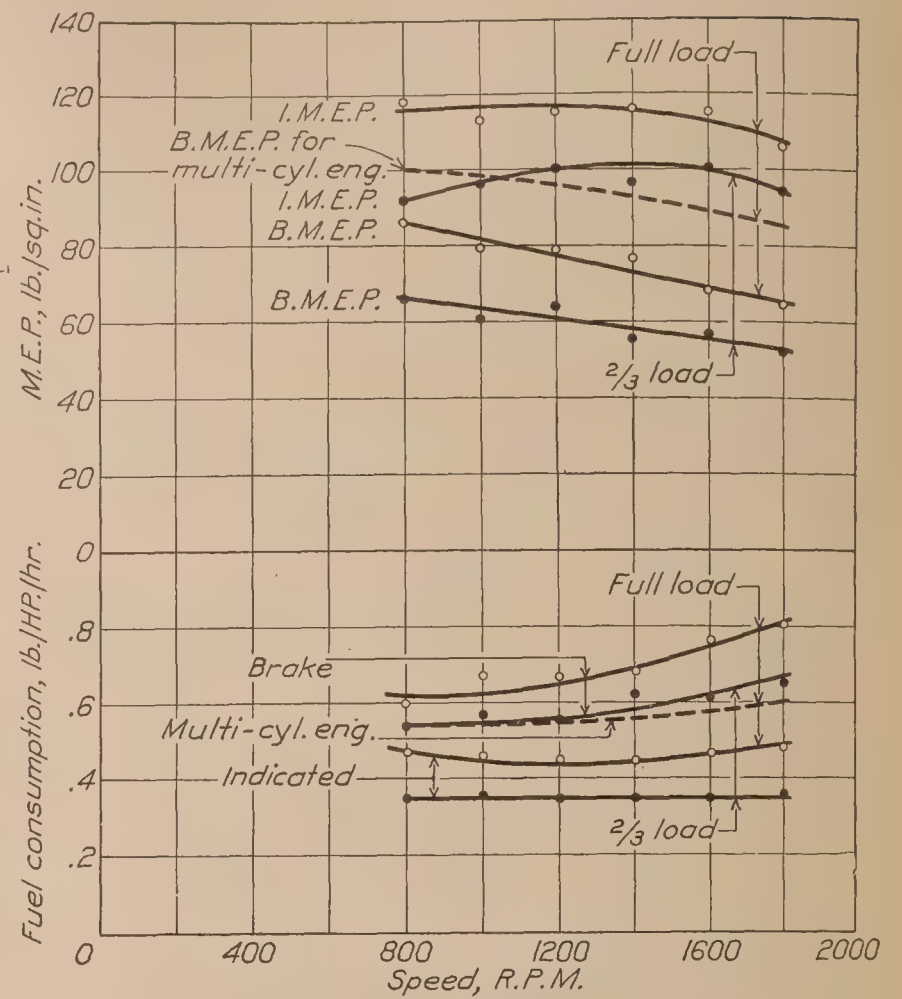


FIG. 10.—Fuel injection performance, Liberty test engine. Cylinder head No. 3

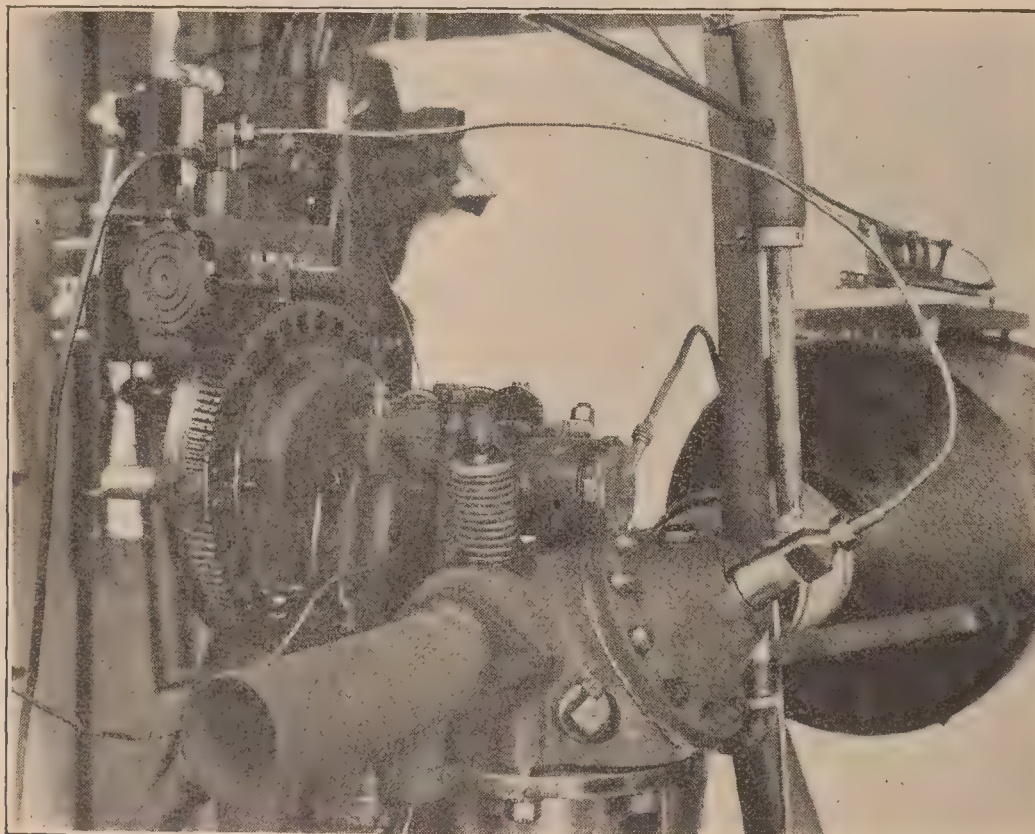


FIG. 9.—Cylinder head No. 3 assembled on Liberty test engine

CYLINDER HEAD NO. 3

The combustion chamber illustrated in Figures 8 and 9 was designed to give a high degree of turbulence within the pear-shaped bulb on the compression stroke and within the cylinder on the expansion stroke. This has been obtained by locating the $\frac{9}{16}$ -inch orifice to produce tangential air flow in both the bulb and cylinder. The ratio of the volume of air in the bulb to the volume of air in the cylinder is approximately one when the piston is on top center.

In order to determine the effects of variations in the degree of cylinder air turbulence on engine performance, provision was made in the design for progressively altering the orifice. The cylinder head has been tested with a $\frac{9}{16}$ -inch sharp-edge orifice, with the orifice edges rounded, and the orifice flared to discharge the burning gases from the bulb tangentially over one-half the piston area. The compression ratio used for the tests reported was 13.5 to 1, which gave a compression pressure of 450 pounds per square inch at 1,000 R. P. M.

PERFORMANCE MEASUREMENTS

FUEL

The fuel used in these tests was a commercial grade of Diesel-engine fuel oil having a Saybolt viscosity of 41 seconds and a specific gravity of 0.85 at 80° F.

ENGINE POWER

The engine power was determined by means of torque scales graduated to read in 0.2 pound intervals and a magnetically operated stop watch and counter.

The fuel consumption was determined by timing the flow of 200 cubic centimeters of fuel with a stop watch. The quantity of fuel delivered per cycle by the injection pump for any given pump adjustment was determined from the total number of engine cycles passed through during the consumption of the 200 cubic centimeters of fuel.

MAXIMUM CYLINDER PRESSURES

Maximum cylinder pressures have been determined by a gas balanced-valve type pressure indicator. This has been replaced, however, by a diaphragm-type indicator which is operated by the pressure of the gases within the engine cylinder. The pressure of the cylinder gases, trapped above the diaphragm, is indicated by a calibrated pressure gauge. Since the weight of the moving element of the indicator is 0.00044 pound, the exposed area 0.0767 square inch, the maximum lift 0.002 inch, and the seat width 0.005 inch, the error in the pressures recorded is probably small. Engine tests have shown that it is unnecessary to provide means for cooling the diaphragm of this type of maximum cylinder pressure indicator.

ENGINE PERFORMANCE AND DISCUSSION

CYLINDER HEAD NO. 1

The performance of cylinder head No. 1 was an improvement over that obtained with a standard Liberty aircraft engine cylinder and a special piston. (Reference 7.) The operation of the engine was smoother and no trouble was experienced with cracking of the standard aircraft aluminum pistons.

An improvement in combustion was obtained by directing the flow of the inlet air through the inlet valve to produce a definite kind of air flow within the cylinder. (Reference 8.) The curves of Figure 3 give the performance of this combustion chamber with and without directed air flow. It may be noted that in these tests the I. M. E. P. was increased from 82.0 to 96.0 pounds per square inch, with a corresponding decrease in the fuel consumption from 0.60 to 0.51 pound per I. HP. per hour. This increase in performance, obtained by directing the flow of the inlet air toward the fuel-injection valve, was thought to be caused by the better removal of the products of combustion surrounding the fuel valve. The fuel, therefore, was injected into a charge of relatively pure air, which improved the combustion.

CYLINDER HEAD NO. 2

The performance of cylinder head No. 2 for various loads and for speeds of 1,200 and 1,800 R. P. M. is shown in Figure 5. The B. M. E. P. at full load and 1,800 R. P. M. is 71.0 pounds per square inch. The full-load fuel quantity is considered as the fuel weight per cycle giving 15 per cent excess air. The corresponding I. M. E. P. is 106.0 pounds per square inch. This large difference in mean effective pressure is caused by the low mechanical efficiency of this single-

cylinder test engine. If a mechanical efficiency of 80 per cent is assumed as an average value for multiple-cylinder oil engines, the B. M. E. P. is increased to 84.8 pounds per square inch. This same factor of mechanical efficiency is responsible for the high fuel consumption when taken on a brake-horsepower basis. The linear portions of the I. M. E. P. and B. M. E. P. curves indicate that for fuel quantities less than 0.0002 pound per cycle combustion of the fuel is practically complete. For fuel quantities greater than this, however, the curves tend to flatten, which indicates that the fuel and air are not sufficiently well mixed to obtain efficient combustion. Data for the curve of maximum explosion pressures were obtained with a gas balanced-valve type of maximum explosion pressure indicator.

CYLINDER HEAD OF UNIVERSAL TEST ENGINE

The engine performance obtained with the Universal test engine for variable fuel quantity and speeds of 1,500 and 1,750 R. P. M. is shown in Figure 7. Due to the pent-roof type combustion chamber, it was impossible to distribute the fuel completely with a centrally located diaphragm-type injection valve. The results are of interest since they show the engine performance obtained with a design of combustion chamber unsuitable for fuel injection but with a fuel valve and pump designed to give a high degree of fuel atomization. This engine, due to its construction (Reference 5), has a higher mechanical efficiency than the Liberty test engine, which accounts, in part, for the higher B. M. E. P.

CYLINDER HEAD NO. 3

The curves in Figure 10 give the engine performance of cylinder head No. 3 with a sharp-edge orifice for the range of speeds from 800 to 1,800 R. P. M. and for two-thirds and full load.

The maximum value of 117.0 pounds per square inch I. M. E. P. is at 1,200 R. P. M. and full load. The fuel economy is 0.44 pound per I. HP. per hour. The corresponding B. M. E. P. values are 77.0 pounds per square inch and 0.65 pound per B. HP. per hour. If a mechanical efficiency of 80 per cent is assumed, as shown by the curve "Multicylinder engine," the performance values on a brake basis are, respectively, 96.0 pounds per square inch B. M. E. P. and 0.55 pound per B. HP. per hour. For two-thirds load the indicated fuel consumption curve has the average value, throughout the range of speeds, of 0.35 pound per I. HP. per hour.

The improvement in engine performance obtained by rounding the orifice edges is indicated in the curves of Figure 11. It may be noted that the I. M. E. P. at full load, 3×10^{-4} pound per cycle, was increased approximately 4.5 per cent by this alteration to the orifice. The maximum cylinder pressures as recorded with the diaphragm-type maximum cylinder pressure indicator were maintained constant for both series of tests. At a fuel quantity of 3.5×10^{-4} pound per cycle and zero per cent excess air, the maximum cylinder pressure was 755 pounds per square inch.

The engine performance coefficient, which is taken as the ratio

$$\frac{\text{I. M. E. P.}}{\text{cyl. pressure} \times \text{fuel consumption lb./I. HP./hr.}},$$

has a maximum value of 49.0 at a fuel quantity of 1.5×10^{-4} pound per cycle, which corresponds to approximately 130 per cent excess air in the cylinder. As the fuel quantity is increased above this value the performance coefficient decreases rapidly because of the decrease in the combustion efficiency of the combustion chamber.

After the edges of the orifice had been rounded the orifice on the cylinder side was flared to discharge the gases from the bulb tangentially over one-half the piston area. The curves in Figure 12 give the engine performances for this alteration to the orifice. The full-load I. M. E. P. was increased to 119 pounds per square inch, and the corresponding B. M. E. P. to 76 pounds per square inch. The low value of the mechanical efficiency, 63.8 per cent, accounts for the wide difference in values of the I. M. E. P. and B. M. E. P. curves. The fuel consumption, taken on an I. HP. basis, varies from 0.26 to 0.43 pound per HP. per hour for one-fourth to full-load fuel quantities, respectively. Flaring the orifice has not appreciably increased the maximum value of the performance coefficient over that shown in Figure 11, but the maximum value now appears at two-thirds load instead of one-half load, the corresponding percentages of excess air within the cylinder being approximately 72 and 132 per cent. This would indicate that flaring the orifice permitted the fuel from the bulb to reach more of the air in the cylinder.

The fuel consumption of 0.26 pound per I. HP. per hour at one-fourth load, one-fourth the fuel weight per cycle at full load, is worthy of note for an engine speed of 1,600 R. P. M.

Figure 13 shows the variation of engine performance with the bulb-to-cylinder orifice flared as noted above for speeds from 600 to 1,800 R. P. M. and for a constant fuel quantity of 2.5×10^{-4} pounds per cycle, which is approximately 83 per cent of the full-load fuel charge. The I. M. E. P. throughout the entire range of speeds is approximately 110 pounds per square inch and the fuel economy 0.39 pound per I. HP. per hour. The curves of F. M. E. P. (motoring) plotted against speed show the large difference between the indicated and brake power of this engine.

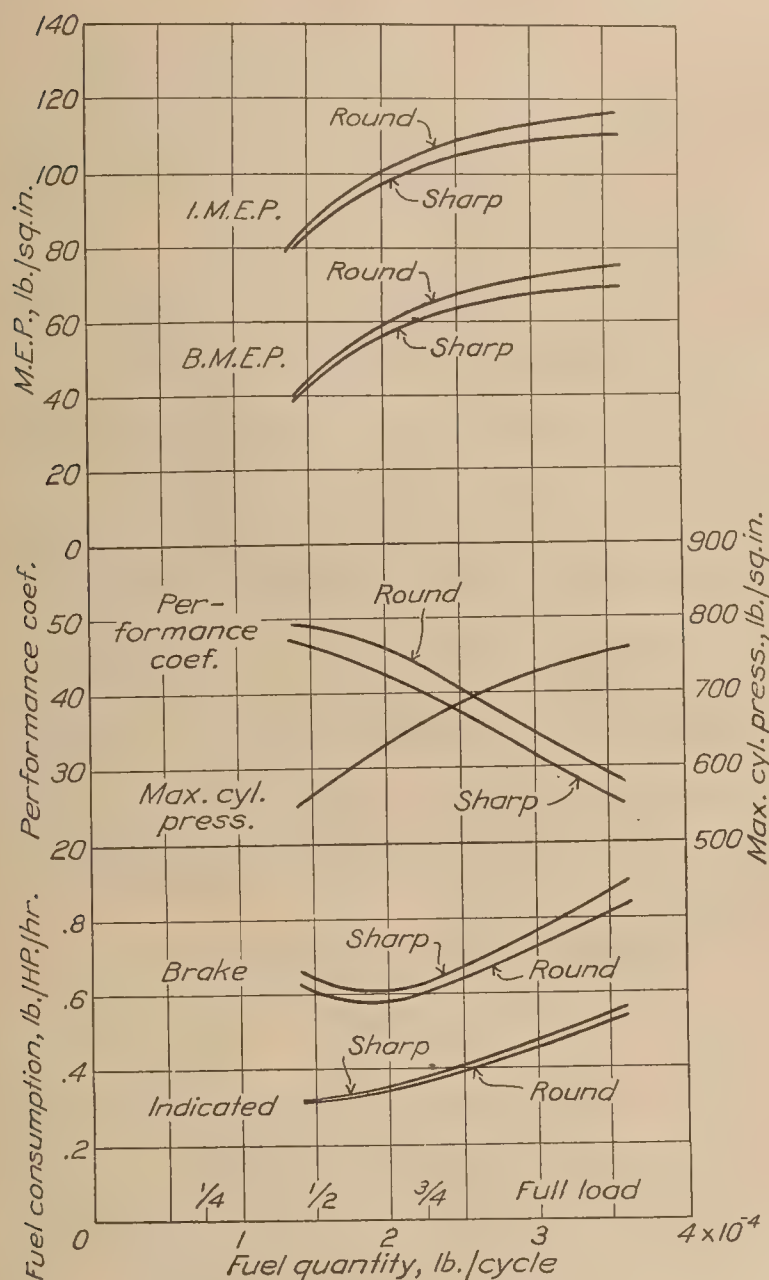


FIG. 11.—Comparison of sharp and rounded orifice edges. Engine, L.T.E. Cylinder head No. 3; engine parts, standard; compression ratio, 13.5; engine R. P. M., 1,600; operating temperature, standard; injection valve No. 3A-.048; injection pump No. 5.

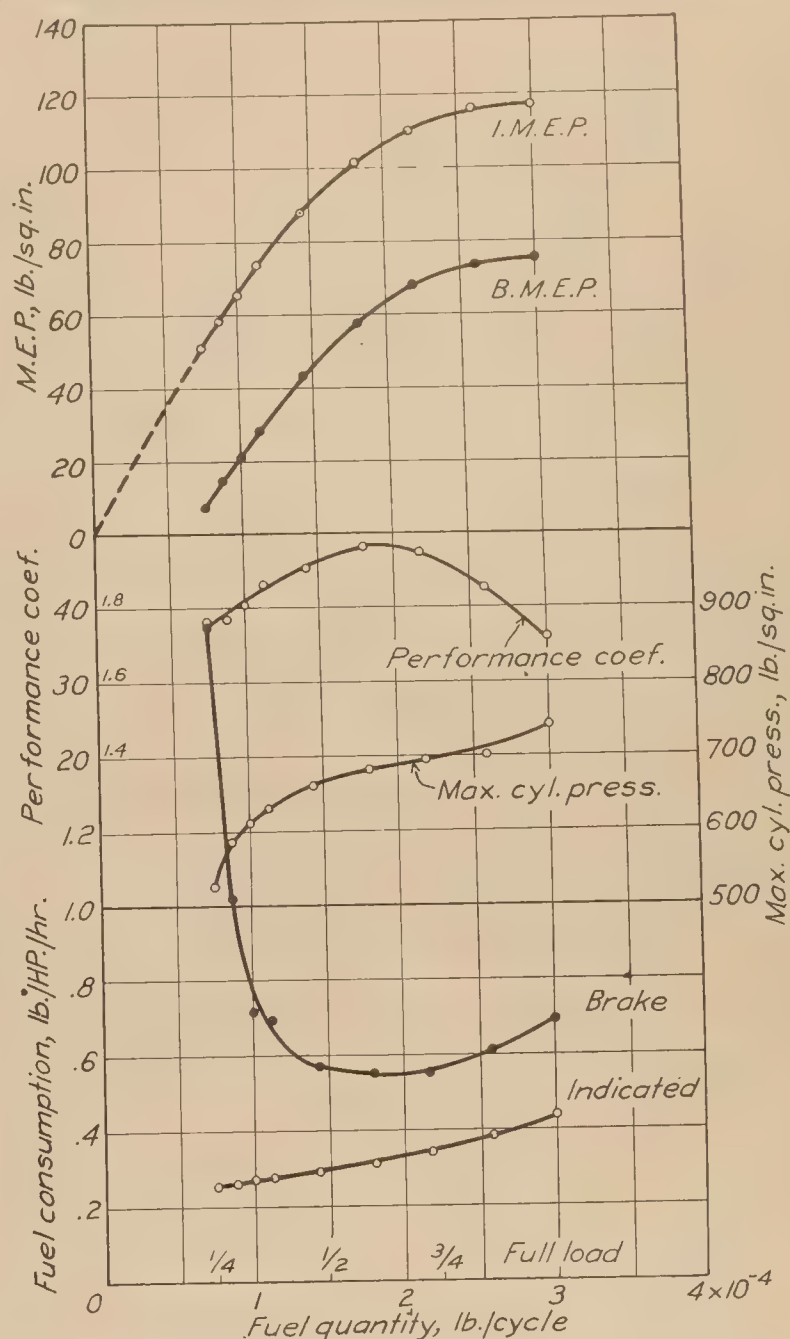


FIG. 12.—Effect of load on engine performance. Fuel-injection performance, cylinder head No. 3. Engine S. C.-L. T. E.; orifice, $\frac{1}{8}$ -inch; orifice flared to cover one-half piston area; compression ratio, 13.5; operating temperature, standard; static opening pressure, 6,000 lb./sq. in.; fuel, Diesel oil, sp. gr.=0.847

POSITION OF FUEL-VALVE NOZZLE

The effect on engine performance of extending the fuel nozzle into the bulb for distances of $\frac{1}{4}$ inch and $\frac{1}{2}$ inch has been determined for the full range of fuel quantities per cycle and a speed of 1,600 R. P. M. The tests indicate that the flush or $\frac{1}{4}$ -inch extension gave somewhat better performance than the $\frac{1}{2}$ -inch extension. An examination of the carbon deposits on the walls of the bulb after each engine test indicate that for the flush and $\frac{1}{4}$ -inch extensions part of the fuel was swept from the nozzle and thrown against the walls of the bulb. The $\frac{1}{2}$ -inch extension gave a uniform coat of carbon over the entire surface of the bulb. The engine performance data, however, showed that these short extensions did not result in any appreciable gain in combustion efficiency.

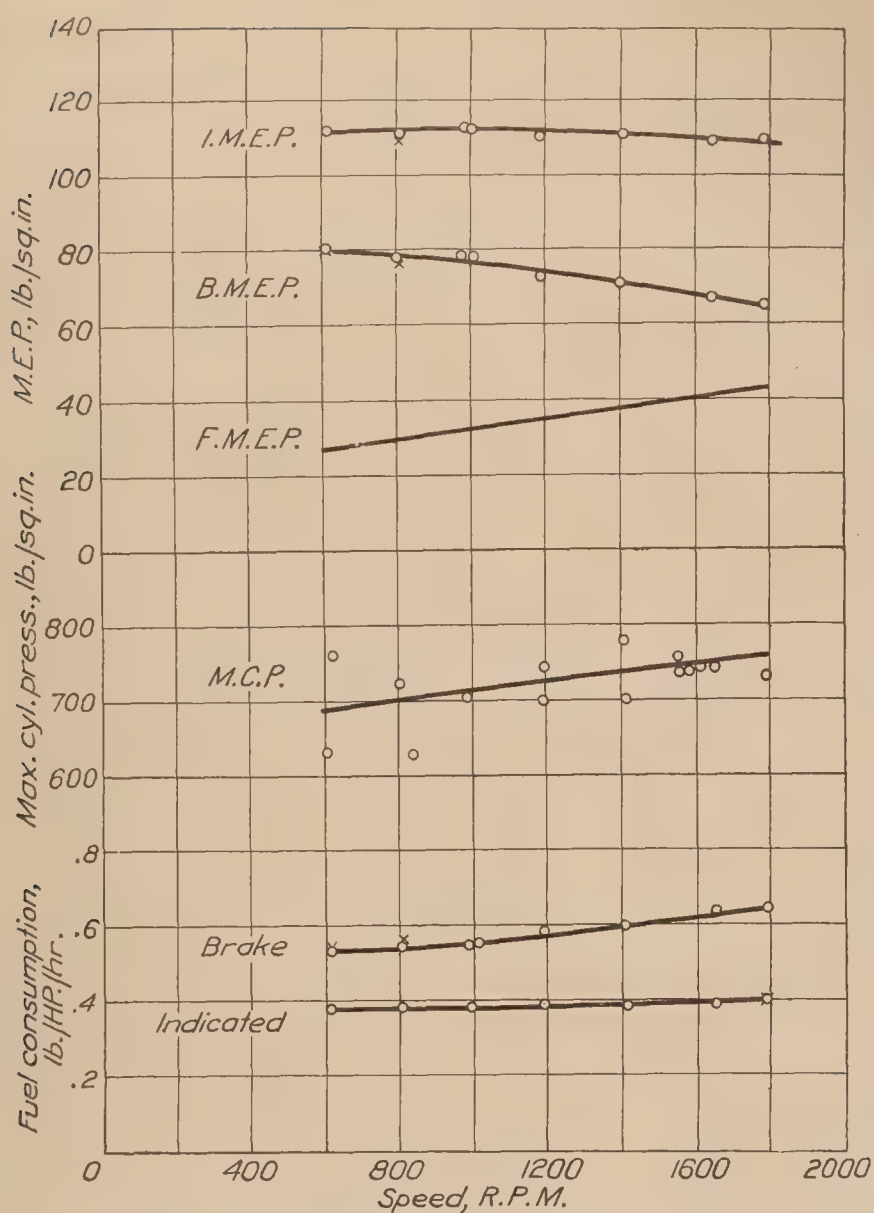


FIG. 13.—Effect of speed on engine performance. Engine, S. C. Liberty. Compression ratio, 13.5; operating temperature, standard; engine parts, standard; fuel, lb./cycle, 2.50×10^{-4} .

LANGLEY MEMORIAL AERONAUTICAL LABORATORY,
NATIONAL ADVISORY COMMITTEE FOR AERONAUTICS,
LANGLEY FIELD, VA., June 9, 1927.

REFERENCES

1. JOACHIM, WILLIAM F.: Oil Spray Investigation of the National Advisory Committee for Aeronautics. Paper presented before the Oil Power Conference at Pennsylvania State College, Pa., April 24, 1927.
2. JOACHIM, WILLIAM F.: Research on Oil Injection Engines for Aircraft. "Mechanical Engineering," November, 1926.
3. BEARDSLEY, E. G.: The N. A. C. A. Fuel Spray Photography Apparatus and Test Results from Several Researches. N. A. C. A. Technical Report No. 274 (1927).
4. BEARDSLEY, E. G.: Some Factors Affecting the Reproducibility of Penetration and the Cut-Off of Oil Sprays for Fuel Injection Engines. N. A. C. A. Technical Report No. 258 (1927).
5. WARE, MARSDEN: Description of the N. A. C. A. Universal Test Engine and Some Test Results. N. A. C. A. Technical Report No. 250 (1927).
6. PATON, C. R., and KEMPER, CARLTON: Power Output and Air Requirements of a Two-Stroke Cycle Engine. N. A. C. A. Technical Report No. 239 (1926).
7. GARDINER, A. W.: A Preliminary Study of Fuel Injection and Compression Ignition as Applied to an Aircraft Engine Cylinder. N. A. C. A. Technical Report No. 243 (1926).
8. KEMPER, CARLTON: Improving the Performance of a Compression Ignition Engine by Directing Flow of the Inlet Air. N. A. C. A. Technical Note No. 242 (July, 1926).

CONCLUSIONS

Comparison of the data presented shows that the precombustion chamber type cylinder head, arranged to provide controlled, high-velocity air turbulence as in cylinder head No. 3, gave the best engine performance. It is concluded that this type of cylinder head gave the highest indicated mean effective pressures and the lowest fuel consumptions per indicated horsepower hour with the lowest cylinder pressures at all loads and speeds in these tests, because the most thorough mixing of the fuel and air was obtained and high cylinder pressures were prevented by this cylinder head design.

Equal and even superior engine performance have been obtained with integral combustion chamber type cylinder heads, but the cylinder pressures were in excess of those for the precombustion chamber type cylinder head.

These tests indicate that improvement in the performance of aircraft oil engines depends primarily upon the complete mixing of well-atomized fuel with the air charge in precombustion chamber type cylinder heads and, in addition, upon the prompt ignition of the fuel in integral combustion chamber type cylinder heads.





SMITHSONIAN LIBRARIES



3 9088 01800 8649